

TAILINGS AND MINE WASTE '18

Sept. 30-Oct. 2, 2018
Keystone Resort
Keystone, Colorado



COLORADO STATE UNIVERSITY

TAILINGS AND MINE WASTE '18

PROCEEDINGS OF THE 22ND INTERNATIONAL CONFERENCE ON TAILINGS AND MINE WASTE
KEYSTONE, COLORADO, USA, SEPTEMBER 30–OCTOBER 2, 2018

©The copyright for all papers is retained by the authors

Published by: UBC Studios
University of British Columbia
110 – 2329 West Mall
Vancouver BC, V6T 1Z4

Preface

This proceedings includes 82 state-of-the-art papers. These papers address the important issues faced by the mining industry today and will provide a record of the discussions at the conference that will remain of value for many years.

The organizing committee wishes to thank all who have contributed to this year's conference including authors, presenters, keynote speakers, short course providers, sponsors, and exhibitors.

Organization

The Tailings and Mine Waste 2018 conference was organized by the Department of Civil and Environmental Engineering, Colorado State University, Fort Collins, Colorado in conjunction with the University of Alberta, Edmonton, Alberta and the University of British Columbia, Vancouver, British Columbia.

SPONSORS AND ORGANIZING COMMITTEE

Christopher Bareither	Colorado State University, Fort Collins, CO
Jason Hilgers	AECOM, Denver, CO
Kurt Schimpke	Barr Engineering Co., Minneapolis, MN
Mike Henderson	BGC Engineering, Montrose, CO
Andy Jung	CETCO, Evergreen, CO
Shawn Steiner	ConeTec, Inc., Salt Lake City, UT
Daniel D. Overton	Engineering Analytics, Fort Collins, CO
Dean Durkee	Gannett Fleming, Phoenix, AZ
Brent Bronson	Golder Associates, Inc., Lakewood, CO
Kate Patterson	Klohn Crippen Berger, Ltd., Vancouver, B.C.
Jim Cremeens	Knight Piésold Consulting, Denver, CO
Carlo Cooper	MineBridge Software Inc., Calgary, A.B.
Nicholas Rocco	NewFields, Denver, CO
Matt Bachman	Paterson & Cooke, Denver, CO
Jack Caldwell	Robertson GeoConsultants, Inc., Vancouver, B.C.
Larry Cope	SRK Consulting, Inc., Fort Collins, CO
Melanie Davis	Stantec, Denver, CO
Daryl Longwell	TetraTech, Fort Collins, CO
Matt Fuller	Tierra Group International, Ltd., Lakewood, CO
Brett Byler	Wood, Englewood, CO
Ward Wilson	University of Alberta, Edmonton, AB
Dirk van Zyl	University of British Columbia, Vancouver, BC

COMMUNITY SPONSORS

Anddes Asociados SAC

Table of Contents

iii PREFACE

v ORGANIZATION

1 CONFERENCES SUMMARY

KEYNOTE

3 TSFs, Risk, and the Human Element

J.F. Lupo

DESIGN AND OPERATION

9 Alternative Approaches to Management and Closure of Tailings Storage Facilities

D.J. Williams

17 Benefits of Rotational, Thin Layer, Air Dried Tailing Deposition after 25-Years of Operation of the Juniper Tailing Storage Facility

A.H. Gipson, Jr., J. Taylor, J. Chilson, B. Hutchings, and J. Gilbert

27 Changes to Tailings Dam Regulation in Brazil in the Aftermath of Failures

K.F. Morrison, H.G. Pedrosa, G.J.I. dos Santos, P.C.R. Gomide, and A.M. Ferreira

35 Design Considerations for Distributed Tailings Deposition Systems

J. Stowe, R. Cooke, I. Farrell, and R. Martinson

43 Guidance for the Safe and Optimized Operation of Waste Rock Facilities

J.A. Vides, L. Piciacchia, and V. Marefat

51 Leading versus Lagging Indicators of Tailings Dam Integrity

J. Boswell and J. Sobkowicz

63 Learnings from Real-time Pore Pressure Monitoring at a Platinum Tailings Facility

L. Boshoff, H.A.C. Meintjes, and M. Boroko

77 Lime as an Additive for Oil Sands Ore-Water Slurry Based Bitumen Extraction, Tailings Disposal and Fluid Fine Tailings Dewatering Processes

S. Arnipally, R. Burden, J.D. Scott, and B. Ozum

87 Mine Waste Rock Storage Facilities Design, Construction, and Operation as Engineered Structures

L. Piciacchia, J.A. Vides, and J. Mosquera

95 System Dynamics Approach to Tailings Management Simulation

T. Zheng and N. Beier

109 The Use of 3D Models and Analysis in Support of Waste Stockpile Design and Operations

L. Piciacchia, V. Marefat, and J. Mosquera

GEOTECHNICAL ENGINEERING

- 117 **Adjustments to Tailings Deposition with Thickened Tailings in Svappavaara**
S. Töyrä, P. Marthin, K. Jokinen, and D. Lundell
- 127 **Assessing Oil Sands Tailings Consolidation Parameters Relative to Long-term Reclamation**
H. Rourke and D. Hockley
- 139 **Characterization of Ancient Mine Wastes: An Approach for Environmental Management and Metals Recovery**
M.L. Dinis, A. Fiúza, A. Futuro, A. Leite, J. Figueiredo, J. Góis, M.C. Vila, and D. Martins
- 151 **Characterization and Field Performance of Long-Term Settlement Behavior of a Tailings Pile**
B.F.H. Foster, S.T. Parkhill, M.D. Moriarty, and B.N. Lingwall
- 163 **Compression Behavior of Filtered Tailings and Waste Rock Mixtures: GeoWaste**
C.A. Bareither, M.H. Gorakhki, J. Scalia, and M. Jacobs
- 175 **Creep Displacements Induced from Waste Rock Loading**
J. Kurylo, M. Rykaart, and A. Lizcano
- 187 **Desiccation of Tailings in an Instrumented Column under Laboratory and Atmospheric Conditions**
D.J. Williams, S. Quintero, C. Zhang, and X.Lei
- 201 **Essential Issues for Testing and Modeling of Tailings Exhibiting Creep**
D. Perić, G. Gjerapić, and D. Znidarčić
- 209 **Filter-Pressed Dry Stacking: Design Considerations Based on Practical Experience**
C. Crystal, C. Hore, and I. Ezama
- 221 **Fine Coal Refuse – 25 Years of Field and Laboratory Testing Data and Correlations**
B.E. Genes, G. Castro, T.O. Keller, and F. Ciloglu
- 233 **Frozen Core Tailings Dam: Part 1, Long-Term Thermal Performance**
M. Rykaart, P. Luedke, and C.W. Stevens
- 245 **Frozen Core Tailings Dam: Part 2, Long-Term Creep Deformation**
M. Rykaart, A. Barrero, and A. Lizcano
- 259 **Geotechnical Considerations to Reduce Adverse Impacts of Mine Waste Rock Dumps on the Environment**
R.B. Kaunda
- 267 **Improved Methodology for TSF Capacity Prediction**
G. Gjerapić and D. Znidarčić
- 277 **Investigating the Effect of Pre-shear Prior to Flocculation**
C. Torrez López, M.L. Catling, J. Bellwood, and L. Boxill
- 287 **Platinum Tailings – Field and Laboratory Investigation to Evaluate Geotechnical Behaviour**
A. Smith and H.A.C. Meintjes
- 301 **Practical Nomograms for Waste Rock Piles Design on Competent Foundations**
L. Piciacchia, V. Marefat, and A. Vides
- 309 **Review of Alternative Tailings Disposal Methods for Water Management**
C.L. Strachan

- 319 **Scale-effect Considerations for Shear Strength Assessment of Coal Mine Spoil**
L.R. Bradfield, S.G. Fityus, and J.V. Simmons
- 333 **Static Liquefaction of Tailings: A South African Perspective on Rate of Rise**
H.C. Ungerer and W. Kruger
- 347 **The Shear Strength of Filtered Tailings and Waste Rock Blends**
R. Burden, D.J. Williams, G.W. Wilson, and M. Jacobs
- 357 **Toward the Sensible Use of Tailings Filtering Technology**
B. Ulrich and J. Rogers
- 365 **Undrained Shear Strength Evolution with Loading on an Undisturbed Block Sample of Desiccated Gold Tailings**
D. Reid, A. Fourie, J. Castro, and J. Lupo

GEOCHEMISTRY

- 377 **Bench-Scale Nitrate and Sulphate Biochemical Reactor Case Study, Amulsar Mine, Armenia**
J.J. Gusek, G. Fattore, L.P. Josselyn, and A. Aghajanyan
- 387 **Impact of Calcium Hydroxide on the Equipment and Process of Oil Sands Tailings Treatment**
K. Rahal, J. Fox, J. Leikam, M. Tate, and N. Romaniuk
- 399 **Minimization, Treatment, and Monitoring of Acid Waters Generated in the Prometida Mine Waste Dump**
C. Del Castillo Macedo
- 409 **Mitigation and Treatment Options for Selenium Control in Minesite Runoff**
D. Jackson
- 419 **Passive Arsenic and Manganese Removal in Neutral Mining Influenced Water**
T. Wildeman and F. Vasconcelos
- 427 **Pile Scale Models for Acid Rock Drainage Prediction and Their Application**
L. Ma, C. Huang, Z-S Liu, and K.A. Morin
- 435 **Understanding Mineralogical Composition, Weathering, and Alteration to Manage ML/ARD in a Base-Metal Tailings Storage Facility**
J. Durocher and L. Robertson

GEOSYNTHETICS AND LINERS

- 451 **A New Safe and Sustainable Approach for Constructing Ballast Layers for Waste Containment Facility Liner Systems**
C. Cilliers and M. Briers
- 463 **Critical Strength of High Peel Strength Geosynthetic Clay Liners at Low Normal Stresses**
S. Ghazizadeh and C.A. Bareither
- 477 **Geotextile Dewatering of Acid Mine Drainage Precipitates**
K.J. Westhaver, K. Zimmermann, N. Devaere, D.R. Latulippe, R. Mafi, and E. Ausch
- 489 **Lessons Learned on the Performance of Multi-Linear Drainage Geocomposites for Mining Applications**
P. Saunier and E. Blond

- 503 **Vertical Expansion of a 41-m High Geosynthetic Reinforced Soil Slope**
F. Herrera, L. Chahua, E. Murrugarra, and D. Reaño

IMAGING AND SPATIAL ANALYSIS

- 519 **High Resolution Estimates of Tailings Facility Evaporation Using Landsat Data**
J. Keller, J. Hendrickx, M. Milczarek, F. Partey, and M. Geddis
- 527 **Satellite-based Repeat Surveying of Tailings: A Cost-effective Alternative to Aerial Surveying**
G. Mitchell, J. Turner, and J. Engels

MILL TAILINGS DESIGN

- 535 **Design of a Centerline Method Tailings Dam using Mine Waste Rockfill in Perú**
P.W. Ridlen, T.F. Kerr, G. Dominquez, J-B Varnier, and J. Toro
- 547 **Direct Extraction Lithium Processes: The Challenges of Spent Brine Disposal**
I. Ezama, C. de los Hoyos, P. Cortegoso, and T. Braun

RECLAMATION AND REMEDIATION

- 557 **Assessment of CCBE Performance with Climate Change: Case Study of the Lorraine Mine Site**
G. Hotton, É. Bresson, B. Bussière, I. Demers, P. Thomas, and R. Philippe
- 569 **Closure of Abandoned and Derelict Asbestos Mines: Design, Construction and Monitoring**
R. Mayne, W. Naidoo, and X. Adams
- 583 **Effectiveness of Oxygen Barriers under Climate Change: Definition of a Drought Index**
É. Bresson, I. Demers, Y. Chavaillaz, P. Roy, and T. Pabst
- 595 **Evaluation of Physical Parameters in Environmental Desulfurization by Flotation for Production of Reclamation Cover-suitable Desulfurized Tailings**
J. Guimond-Rousson, I. Demers, and C. Rocard
- 607 **Mine Waste Remediation as a Stepping Stone for New Contractors in Emerging Economies**
X. Adams, B. Engelsman, and R. Mayne
- 619 **Monitoring a Cover Performance Test Section on a Uranium Mill Tailings Management Cell**
M.M. Davis, C.H. Benson, E.F. Redente, and H.R. Roberts
- 631 **Remediation Design of a Uranium Mill Tailings Pond**
Y. Koitzsch, S. Metzker, A. Mühl, U. Barnekow, and M. Speer
- 643 **Repurposing Mine Sites – A Win for Owners, Colorado, and the Environment**
R.L. Almon and S.L. Borden
- 649 **Soil Health & Biotic Soils via 5 Fundamentals for Sustainable and Cost Effective Mine Rehabilitation**
M.D. Robeson and A. Jung
- 659 **Synergy between Operation and Closure of the Orcopampa Mine**
A.B. Fernandez Canchos
- 671 **Thermal Cover Design for Mine Waste Facilities in Cold Regions**
C.W. Stevens, T. Shapka-Fels, and M. Rykaart

REGULATIONS

- 685 **Update on Tailings Dam Safety and Regulation in the United States**
C.F. Cobb

RISK INFORMED DESIGN

- 699 **Assessment of Design and Operating Practices on the Risks Associated with Waste Rock Stockpiles**
L. Piciacchia, B. Lavoie, J. Mosquera, and Z. Bouazza
- 707 **Risk Informed Design of a Large Scale, Lined Tailings Storage Facility**
L.I. Boshoff, R.W. McNeill, and M. Boroko
- 721 **Risk Management by Tailings Storage Facility Dam Classification**
C. Johns and D. Hasanloo
- 733 **Tailings Facility Performance: 2017 & 2018**
C. Strachan and J.A. Caldwell

SITE CHARACTERIZATION AND MONITORING

- 739 **A Geotechnical Monitoring System to Support Implementation of the Observational Method at Teck Highland Valley Copper**
G. Afriyie, B. Bale, and C. Anderson
- 747 **Comparing CPT and Vs Liquefaction Triggering Methods for Mine Tailings**
R. Moghaddam, Y. Mao, and S. Kam
- 757 **EGT – Innovative Fine Granular Material Sampling Technique**
J-F. St-Laurent
- 767 **Geotechnical and Structural Monitoring System Deployment for the Spillway of a Dam at Padcal Mine in the Philippines**
V. Le Borgne, A. Cosentino, S.-É. Thivierge, and J.-M. Br  h  
- 775 **Magnetometric Resistivity as an Effective Tool for Leakage Detection and Monitoring**
M. Jessop, V. Kofoed, K. Wall, A. Revil, and A. Jardani
- 781 **Non-Invasive Geophysics for Active Mining Sites**
S. Calendine and D. Rucker
- 791 **Site Characterization throughout the Tailings Facility Life Cycle**
M. Malgesini, L. Aubone, R. Hunsaker, and W. Boyd

WATER MANAGEMENT

- 799 **Assessing Mine Site or Tailings Facility Water Management Risks by Integrating Tailings Deposition and Water Balance Modeling**
K. Patterson, M. Liew, and R.W. Chambers
- 811 **Geochemical Behavior of Different Waste Rock Configurations from the Lac Tio Mine: Comparison between Column Tests and Experimental Waste Rock Pile Results**
B. Poaty, B. Plante, B. Bussiere, M. Benzaazoua, T. Pabst, V. Martin, M. Th  riault, and P. Nadeau
- 823 **How Plant Water Use Efficiency Can Inform Evapo-transpirative Cover Design**
R. Murphy and J. Dillon

- 829 Impact of Changes in Water Use Policy and Legislation on Mine Waste Water Management Infrastructure – A Case Study of In-Line Attenuation Ponds**
W. Naidoo and P. Janse van Rensburg
- 841 Improving Water Management in the Orcopampa Mine**
J.C. Gabriel Espinoza
- 853 Mine Tailings Drainage: A Bottoms Up Approach Using HDD Well Installation Methods**
J. Gallagher and D. Bardsley
- 861 Operational Improvements through Installation of Seepage Cutoff Wall using Soil Mixing**
I. Contreras and G.K. Bryant
- 873 Optimizing Tailings Deposition and Water Management for a Mine in Ontario, Canada**
R. Couto and P. Merry
- 883 AUTHOR INDEX**

The Conferences

The first conference in the series was on Uranium Mill Tailings Management and was held in 1978. It was organized by the Geotechnical Engineering Program of the Civil Engineering Department of Colorado State University, Fort Collins, Colorado. The organizing committee consisted of John Nelson, Thomas Shepherd, Steven Abt, Wayne Charlie, and John Welsh. The series of conferences on uranium mill tailings continued through 1985. The nine volumes of proceedings were published totaling some 3,700 pages. By 1984, the Uranium Mill Tailings Remedial Action (UMTRA) Project was well underway. The development of new uranium mines had declined and interest in uranium tailings was no longer wide-spread. Thus in 1984 and 1985, the conference title was expanded to Management of Uranium Mill Tailings, Low-level Waste and Hazardous Waste.

In 1986, the organizing committee, this time consisting of Steve Abt, John Nelson, Richard Wardwell, and Dirk van Zyl, changed the title and focus to Geotechnical and Geohydrological Aspects of Waste Management. They noted the following reasons for this change in the preface: “The first five annual symposia focused on the design, construction, and operation of uranium tailings impoundments. The sixth and seventh were of broader scope, and included low-level and hazardous waste management. This eighth symposium continues the process of technology transfer but focuses more precisely on the geotechnical and geohydrological aspects of waste management: the two engineering areas of prime importance in the design and operation of waste disposal facilities.” This symposium attracted about fifty-five papers with the proceedings being 558 pages. This same focus was maintained for the 1987 conference.

By 1988 the uranium market had declined, uranium mills had closed, and support for a symposium on uranium mill tailings, hazardous waste, or most any topic associated with mine waste had declined. Thus the conference was not held from 1988 until 1994. In 1994, Colorado State University, the sponsor of the uranium mill tailings conferences, resuscitated the conference series as Tailings and Mine Waste, the title by which the series goes today. The proceedings of 1994 contain twenty-seven papers. The proceedings from 1995 contain a mere fourteen. By 2003, the paper count was up to sixty and the venue was Vail, Colorado. In 2004 the paper count and attendance reduced leading to a negative financial situation for the conference and reluctance on the part of the management of the Department of Civil Engineering at Colorado State University to support the conference series, thus the conference was not held from 2005 until 2008.

In late 2007 an organizational committee was established in Colorado and through the support of a number of consulting engineering companies, Engineering Analytics, Golder, Knight Piésold, MWH Global, Robertson GeoConsultants, Inc., SRK Consulting, Inc. Tetra Tech, Inc. and URS Corporation, a stable financial basis was established for the conferences in Colorado. It was also decided to rotate the conference series between Colorado State University and two Canadian Universities. The following sequence was established: even years, Colorado State University, odd years alternating between University of Alberta and University of British Columbia.

There now are specialty conferences on mine closure, paste tailings, and many other focus topics that were once part of this series. In spite of the specialty meetings, this series remains the best attended and provides the most overall focus of tailings and mine waste.

Table 1: Conference proceedings details, 1978 to 2017

Year	Title	Date and Location	Pages	Papers	Publisher
1978	Uranium Mill Tailings Management	Fort Collins, CO., November 20 - 21	172	11	Geotechnical Engineering Program, Colorado State University
1978	Uranium Mill Tailings Management, Volume II	Fort Collins, CO., November 20 - 21	126	9	Geotechnical Engineering Program, Colorado State University
1979	Uranium Mill Tailings Management	Fort Collins, CO., November 19 - 20	308	26	Geotechnical Engineering Program, Colorado State University
1980	Uranium Mill Tailings Management	Fort Collins, CO., November 24 - 25	573	30	Geotechnical Engineering Program, Colorado State University
1981	Uranium Mill Tailings Management	Fort Collins, CO., October 26 - 27	727	43	Geotechnical Engineering Program, Colorado State University
1982	Uranium Mill Tailings Management	Fort Collins, CO, December 9 - 10	556	38	Geotechnical Engineering Program, Colorado State University
1984	Management of Uranium Tailings, Low- Level Waste and Hazardous Waste	Fort Collins, CO, February 1 to 3	670	66	Geotechnical Engineering Program, Colorado State University
1985	Management of Uranium Tailings, Low- Level Waste and Hazardous Waste, Volume I	Fort Collins, CO, February 6 to 8	252	60	Geotechnical Engineering Program, Colorado State University
1985	Management of Uranium Tailings, Low- Level Waste and Hazardous Waste, Volume II	Fort Collins, CO, February 6 to 8	334	34	Geotechnical Engineering Program, Colorado State University
1986	Geotechnical and Geohydrological Aspects of Waste Management	Fort Collins, CO, February 5 to 7	558	55	A.A. Balkema, Rotterdam
1987	Geotechnical and Geohydrological Aspects of Waste Management	Fort Collins, CO, February 1 to 6	312	26	Lewis Publishers, Inc.
1994	Tailings and Mine Waste '94	Fort Collins, CO, January 19 to 21	259	27	A.A. Balkema, Rotterdam
1995	Tailings and Mine Waste '95	Fort Collins, CO, January 17 to 20	131	14	A.A. Balkema, Rotterdam
1996	Tailings and Mine Waste '96	Fort Collins, CO, January 16 to 19	664	69	A.A. Balkema, Rotterdam
1997	Tailings and Mine Waste '97	Fort Collins, CO, January 13 to 17	788	83	A.A. Balkema, Rotterdam
1998	Tailings and Mine Waste '98	Fort Collins, CO, January 26 to 28	968	99	A.A. Balkema, Rotterdam
1999	Tailings and Mine Waste '99	Fort Collins, CO, January 24 to 27	808	88	A.A. Balkema, Rotterdam
2000	Tailings and Mine Waste '00	Fort Collins, CO, January 23 to 26	566	61	A.A. Balkema, Rotterdam
2001	Tailings and Mine Waste '01	Fort Collins, CO, January 16 to 19	472	52	A.A. Balkema, Rotterdam
2002	Tailings and Mine Waste '02	Fort Collins, CO, January 27 to 30	520	64	A.A. Balkema, Rotterdam
2003	Tailings and Mine Waste '03	Vail, CO, October 12 to 15	526	63	A.A. Balkema, Lisse
2004	Tailings and Mine Waste '04	Vail, CO, October 10 to 13	428	48	A.A. Balkema, Leiden
2008	Tailings and Mine Waste '08	Vail, CO, October 19 to 22	449	41	Taylor and Francis Group, London
2009	Tailings and Mine Waste '09	Banff, Alberta, November 1 to 4	901	79	University of Alberta Geotechnical Center, University of Alberta
2010	Tailings and Mine Waste '10	Vail, CO, October 17 to 20	471	46	Taylor and Francis Group, London
2011	Tailings and Mine Waste '11	Vancouver, British Columbia November 6 to 9	861	72	University of British Columbia Available on-line: https://circle.ubc.ca/
2012	Tailings and Mine Waste '12	Keystone, CO, October 14 to 17	666	58	University of British Columbia
2013	Tailings and Mine Waste '13	Banff, Alberta November 3 to 6	663	64	University of Alberta Geotechnical Center, University of Alberta
2014	Tailings and Mine Waste '14	Keystone, CO, October 5 to 8	566	51	University of British Columbia
2015	Tailings and Mine Waste '15	Vancouver, British Columbia October 25 to 28	699	61	University of British Columbia
2016	Tailings and Mine Waste '16	Keystone, CO October 2 to 4	939	86	University of British Columbia
2017	Tailings and Mine Waste '17	Banff, Alberta November 5 to 8	780	75	University of Alberta Geotechnical Center, University of Alberta

TSFs, Risk, and the Human Element

J.F. Lupo

Newmont Mining Corporation, Denver, Colorado USA

ABSTRACT: The risks associated with tailings storage facilities (TSFs) are often thought of technical issues, which for the most part is true (although there are social, environmental, and financial risks to be considered). However, the way we approach and manage risks requires us to adopt less prescriptive methods in favor of risk-based processes for the design, construction, and operation of TSFs. Intuitively, risk-based approaches should be more rigorous than their prescriptive counterparts; however, adopting risk-based processes introduces the human element in the form of biases. These biases can complicate the risk-based processes resulting in a potentially flawed risk assessment.

1 INTRODUCTION

For some time now, risk and risk management have been part of the lexis when discussing tailings storage facilities (TSFs). The events of Mt. Polley in 2014 and Samarco in 2015 (and other less known events) have refocused risk discussions emphasizing governance on the design, construction, and operation of TSFs. Risk, risk management, and the role of governance are prominently discussed in TSF guidelines presented by MAC (2017), ANCOLD (2012), and ICOLD (2011). Risk is also highlighted in the 2016 Position Statement from the International Council on Mining and Metals (ICMM) with regard to tailings management and governance.

Traditionally, TSFs have been designed, constructed, and operated based a set of prescriptive criteria (e.g., design criteria, construction technical specifications, and operational criteria). Prescriptive criteria provide an unambiguous set of numerical values or limits to be achieved, and are often preferred by engineers. Yet these criteria do not convey any information regarding risk to the design, construction, nor operation of the TSF. Governance programs also often rely on these criteria to assess operation and performance of the TSF, despite lacking its association with risk. As an example, consider an embankment for a TSF that is to be designed to have a minimum Factor of Safety (FoS) of 1.5, which is commonly an acceptable value in the industry for static loading. The value of 1.5, by itself, says nothing about whether this value is acceptable from a risk or risk management perspective. It's simply a number that is being assumed as being appropriate for the design, based on its broad acceptance in the industry. Now let's assume the embankment has been designed to that FoS, meeting the stated criterion, how do we know, other than it meets a stated criteria, that the facility will be stable? In the context just presented, the short answer is you can't be sure the facility is stable as no information regarding uncertainty, design assumptions, nor variability in material properties has been provided.

While this example just considered the FoS, the same issues apply to other design criteria, such as:

- Tailings dry and bulk density,
- Tailings void ratio/porosity,
- Tailings deposition beach slope,
- Design storm event for containment
- Design storm event for spillway operation,
- Minimum freeboard,
- Seismic design events (Operational Basis Earthquake, Maximum Credible Earthquake, and Maximum Design Earthquake),
- TSF lining system (if needed),
- Drainage element capacity (underdrains, embankment/dam internal drains, etc.), and
- Minimum embankment/dam crest width.

Operating criteria are also often defined in a prescriptive manner, yet convey no information on risk or risk management. Typical operating criteria include:

- Tailings delivery rate,
- Tailings percent solids,
- Tailings rheological parameters,
- Maximum allowable rate of rise,
- Maximum reclaim pool extent,
- Minimum beach widths,
- Pore pressure or piezometric level threshold,
- Embankment/dam acceptable deformation threshold,
- Seepage collection rate and threshold,
- Decant operating criteria (maximum height, water level thresholds, structural thresholds), and
- Hydraulic conveyance maximum pressures and flow rates.

From a risk and risk management point-of-view, it does not appear reasonable to rely solely on prescriptive criteria. Risk concepts should and can be integrated into design criteria, construction specifications, and operating criteria. This is particularly important when uncertainties and variabilities are present, as they always in the geotechnical field.

2 RISK BASED DESIGN/RISK INFORMED DECISION MAKING

Recently, terms such as “risk-based design (RBD)” and “risk-informed decision making (RIDM)” are being used in association with TSFs as an alternative to prescriptive approaches. The reasoning being that RBD and RIDM processes provide the means to interweave risk considerations directly into the engineering process.

Zio and Pedroni (2012) define RBD as a decision-making process that provides a technically defensible basis for making decisions and helps to identify the greatest risks and prioritize efforts to minimize or eliminate them. It is based primarily on a narrow set of model-based risk metrics, and generally does not leave much space for interpretation. Considerations of cost, feasibility and stakeholder concerns are generally not a part of risk-based decision-making, which is typically conducted by technical experts, without public consultation or stakeholder involvement. In contrast RIDM is a process that uses a set of performance measures, together with other considerations, to “inform” decision-making. The RIDM process acknowledges that human judgment has a relevant role in decisions, and that technical information cannot be the unique basis for decision-making. This is because of inevitable gaps in the technical information, and also because decision-making is an intrinsically subjective, value-based task. In tackling complex decision-making problems involving multiple, competing objectives, the cumulative knowledge provided by experienced personnel is essential for integrating technical and nontechnical elements to produce dependable decisions.

Both RBD and RIDM processes have been widely used in other industries (aerospace, chemical, shipping, water storage dams, etc) but are relatively new to the mining industry, and in particular tailings facilities. Some general guidance (non-mining related) on the RBD and RIDM processes are provided by Ven Gelder, et al (2001), Olsson and Frantzich (2018), FERC (2016), Zio and Pedroni (2012) and others. In a general sense, RBD is embedded within the RIDM process, while RIDM provides further consideration to technical experience and judgement (the human element, but more on that later). Figure 1 presents a graphic prepared by the author summarizing the RIDM process for TSFs. This figure was derived from the information presented in FERC (2016) for water dams, but modified for TSFs. It's important to note that RIDM does not only apply to the TSF design, the same process can and should be applied in construction, operation, and closure. The vast majority of guidance on RIDM focuses primarily on design with some operational aspects (monitoring). None consider risk associated with construction, which is particularly important for TSFs where an outside contractor is typically hired to construct the facility, sometimes without an owner's or designer's representative at the site.

As illustrated in Figure 1, a key component of the RIDM processes is a Risk Assessment; however, other tools such as Failure Modes Effects Analysis (FMEA), Fault Tree Analysis (FTA), and Event Tree Analysis (ETA) are also often employed. At this point, it is important to recognize that the RIDM process is not a rigid process. RIDM can be made as simple or as complicated as needed, depending on the project requirements. The RBD and/or RIDM process should not be thought of as a cumbersome program (though it can be made that way). The process does not necessarily need more data or information as the traditional, prescriptive approach, but it does need experience and judgment (the human element) to get the full benefits of the method.

2.1 The Dilemma of Likelihood vs Probability

The equation of Risk = Likelihood x Consequence is used quite extensively to define the overall concept of risk. When it comes to risk, Consequences (like the failure of a facility) tend to be easily understood; whereas Likelihood is less understood or perhaps less intuitive. While likelihood and probability are sometimes used synonymously in risk, they are actually quite different. Likelihood refers to the possibility of an occurrence in a qualitative measure, such as low, medium, and high. Probability is a quantitative measure of occurrence (e.g. 70% chance of something occurring). For well constrained problems a probability of occurrence may be calculated. For example, the probability of a 1 in 100 year storm event occurring is exactly one percent in any one year. For less constrained problems, a probability may not be possible to calculate and only likelihood can be estimated. An example of this would be assessing the potential for internal erosion (piping) through an embankment. Since piping is not only a function of hydraulic gradients (seepage), material properties (embankment fill and filters), and construction quality, it does not lend itself to a quantitative measure, therefore likelihood may be used.

As engineers, we often feel more comfortable with numerical values (with two or more decimal places!). Numerical values tend to imply a level of accuracy, though that often is not the case. We feel less comfortable with giving qualitative answers. Yet in the assessment of risk, a qualitative approach may be of more value to a project than a quantitative (probability based) one, as not all things can be quantified.

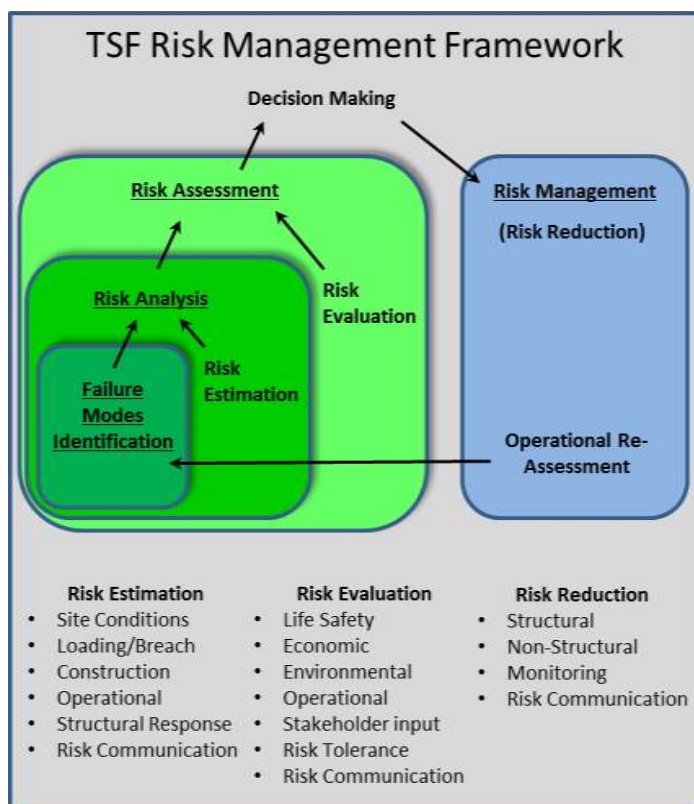


Figure 1 TSF Risk Management Framework (based after FERC, 2016)

2.2 The Human Element

When assessing risks with respect to design, construction, and operation, a qualitative measure of likelihood is commonly adopted due to the presence of natural uncertainty and variability with geomaterials. Uncertainty arises from our lack of perfect knowledge of a system, while variability reflects real differences in space and time of system variables (like shear strength). As qualitative measures of risk are employed, it is inevitable that the human element of judgement will be required to assign an appropriate level of likelihood. NRC (1994) suggests that uncertainty forces decision makers to judge how *likely* risks will be underestimated or overestimated, whereas variability forces a decision maker to cope with the *certainty* that differences exist. This leads us to conclude that the judgement (e.g., experience and bias) of the decision maker(s) can have a significant influence when managing risks for TSFs.

Siefert (2007) explains that humans are the sum of their experiences and education, as well as their emotional or non-rational reaction to circumstances. Researchers in human behavior have shown that judgements and decisions of people are subject to numerous biases (Montibeller and von Winterfeldt, 2015), termed cognitive biases. Cognitive biases are those that lead to judgments and decisions that violate commonly accepted normative processes. In other words, we may make judgments or decisions that do not fully take into account all of the information from a neutral point of view. Biases are present and shape our everyday lives. Some biases we are aware of, but most of the time we are unaware of our biases (Siefert, 2007). With respect to risk, our cognitive biases influence our perception and tolerance to risk.

Surprisingly, well over one-hundred cognitive biases have been identified (see Figure 2). At this point, it's not important to understand all cognitive biases, although they are informative. What is important is to recognize that all of us have biases that shape our judgement and risk perception. What one person considers a high likelihood risk, another person may see as a low likelihood risk. In this context, it is easy to see how cognitive biases can shape the outcome of risk assessments, and ultimately our perception of risk to a TSF. Note that if cognitive biases are not challenged, a flaw could be introduced during the risk assessment process with significant negative consequences. For example, a risk assessment may suggest that foundation failure is a low-likelihood risk due to the belief (bias) that the geotechnical investigation and interpretations are correct, when in fact several gaps in geotechnical knowledge exist. As a result, the mode of foundation failure will be understated.

Anytime judgement and experience are used in the risk process, recognize that biases may present that are dominating the process. Challenging the biases can be an effective tool for managing their influence, resulting in a more neutral or well supported risk assessment.

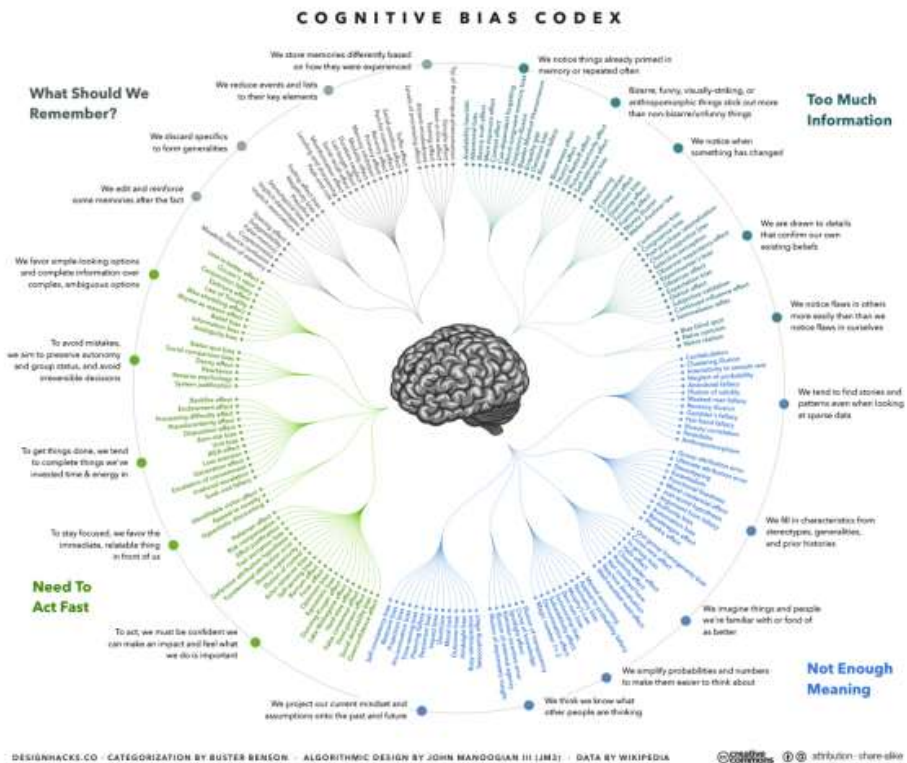


Figure 2 Cognitive Biases (source: Jm3 - Own work, CC BY-SA 4.0, <https://commons.wikimedia.org/w/index.php?curid=57942404>)

2.3 What Does RIDM Look Like?

So what do the outcomes of the RIDM process look like? The short answer here is RIDM outcomes can be anything you would like to effectively communicate risk to stakeholders. The key here is communication, not some pre-conceived format. If the background of the stakeholders is very broad, then the RIDM outcomes could be presented in a few different

formats, tailored to a specific audience. At a minimum, the RIDM outcomes should identify potential risks with a discussion on how the risk is being mitigated through design, construction, and/or operation. For example, overtopping of a TSF is a risk often identified in risk assessments. The RIDM process would discuss the overtopping risk to the TSF and describe what measures are being implemented in the design, construction, and operation to mitigate this risk. This may include more freeboard or an operational spillway, use of non-erodible materials in certain parts of the construction, managing the reclaim pool to a certain level, or all of the above. The RIDM outcomes should also include a discussion on uncertainty (how well are material properties known? can the pool management concept be implemented? how well is the water balance understood?).

3 CONCLUSIONS

By applying risk-based approaches (either RBD or RIDM) to the design, construction, and operation of our TSFs, we will be moving closer managing risks in a rational way. TSF risks can be managed, but to do so we need to recognize not only the technical aspects, but also the human element. In all levels of assessing risk, the human element, in terms of bias, is present (for better or for worse). Recognizing and challenging these biases is an important step in the application of RIDM.

RIDM can be a very effective process when applied in a practical framework. The outcome of the RIDM process is not only identification of risks, but also the mitigative measures to be implemented. RIDM should not be only used for design, but should be applied to construction and operation (as well as closure). Perhaps the most important aspect of RIDM is communication of outcomes. Effective communication is perhaps more important than the RIDM process itself. Afterall, communication is just one more aspect of the human element.

4 REFERENCES

- ANCOLD, 2012. Guidelines on Tailings Dams – Planning, Design, Construction, Operation and Closure, Australian National Committee on Large Dams.
- ICOLD, 2011. Improving Tailings Dam Safety – Critical Aspects of Management, Design, Operation and Closure, International Committee of Large Dams.
- FERC, 2016. FERC Risk-Informed Decision Making Guidelines, Federal Energy Commission, USA
- MAC, 2017. A guide to the management of tailings facilities – 3rd edition, Mining Association of Canada.
- Montibeller, G. and von Winterfeldt, D., 2015. Cognitive and Motivational Biases in Decision and Risk Analysis, *Risk Analysis*, Vo. 35, No. 7, pp 1230 - 1251
- National Research Council (NRC) (1994), *Science and Judgment in Risk Assessment*. Washington, DC: National Academy Press.
- Olsson, F. and Frantzich, H. 2018. An Approach towards a Simple Risk Based Design Method From:
https://www.researchgate.net/publication/267544703_An_Approach_towards_a_Simple_Risk_Based_Design_Method, Department of Fire Safety Eng., Lund University, Sweden
- Siefert, W.T. 2007. Cognitive Biases in Risk Management, Master Theses 4590,
http://scholarsmine.mst.edu/masters_theses/4590
- Ven Gelder, P., Roos, A., and Vrijling, H., 2001. Risk Based Design of Civil Structures. Communications on hydraulic and geotechnical engineering, No. 2001-01, TU Delft.
- Zio, E. and Pedroni, N. 2012. Risk-Informed Decision-Making Processes – An Overview, Foundation for an Industrial Safety Culture, France.

Alternative Approaches to Management and Closure of Tailings Storage Facilities

D.J. Williams

The University of Queensland, Brisbane, Queensland, Australia

ABSTRACT: The financing of mining projects is promoted using a Net Present Value accounting approach, with a high Discount Factor. This is extended to tailings disposal, resulting in the minimisation of short-term capital costs, with rehabilitation costs discounted. As a result, tailings are disposed as a slurry using inexpensive and robust centrifugal pumps to initially too small surface facilities, with high rates of rise, creating wet and soft tailings deposits storing excessive amounts of water. Operating costs tend to blow out, and the risk of tailings run-out on loss of containment increases. The wet and soft tailings are also difficult and expensive to rehabilitate, at a stage when the operator is least able to fund work, discouraging rehabilitation. The paper describes alternative approaches to tailings management and closure, in which larger initial tailings footprints may enable the optimal cycling of tailings disposal to improve tailings dewatering, density and shear strength, and subsequent rehabilitation.

1 INTRODUCTION

Large-scale mining projects are high cost. In order to facilitate the financing of new mining projects, the Net Present Value (NPV) accounting approach is applied, with a high Discount Factor of typically 6 to 10%, several times the inflation rate. At a 10% Discount Factor, a 10-year delay in expenditure is discounted by 61%. The NPV approach is extended to tailings disposal, resulting in the minimisation of short-term capital costs, with rehabilitation costs discounted by the same high Discount Factor. This results in:

- An increased risk of tailings dam failure.
- Initially inexpensive but too small surface tailings facilities storing slurry tailings delivered by robust and inexpensive centrifugal pumps and pipelines.
- Wet and soft tailings deposits, excessive stored water, and an ever-increasing tailings stored volume and footprint.
- A blow out in operating and capital costs.
- Difficult and costly rehabilitation, at a time when revenues cease, discouraging rehabilitation and leading to poor land use potential and ecological function.

2 CONVENTIONAL APPROACH TO TAILINGS DISPOSAL AND STORAGE

The conventional approach to tailings disposal and storage is the pumping of tailings slurry using robust and inexpensive centrifugal pumps by pipeline to a surface tailings storage facility (TSF), where the tailings are deposited sub-aerially forming a beach. The tailings containment and method of construction and dam raising varies from region to region. Upstream construc-

tion, using tailings where possible, is widely employed in South Africa, Australia and the south-west of the USA, which share a dry climate. Downstream construction is employed in wet regions. Sand dams, cycloned and/or compacted, are widely employed in South America, usually raised by the centreline method. Roller compacted concrete dams are finding favour for high tailings dams in the deep valleys of the Andes in South America. While the necessity for downstream construction is understandable in wet climates, the choice between upstream construction and sand dams is not so obvious. It seems that it is more a function of past experience and established regional practices.

Figure 1 (adapted from Davies & Rice, 2004) describes the NPV (capital expenditure, CapEx and operational expenditure, OpEx) and tailings material drivers of tailings management. There is a commonly held perception, supported by the NPV approach, that transporting tailings as a slurry to a dam is the most economic approach. The cost of closing and rehabilitating the resulting TSF is discounted and not considered to be significant. However, few TSFs have been rehabilitated, due to the difficulty of capping a “slurry-like” (wet and soft) tailings deposit and the excessive cost involved, particularly at a time when the mine is no longer producing revenue. Dewatering tailings to a paste or by filtration is perceived to be too capital intensive upfront due to the capital and operating costs of the dewatering equipment and the need for expensive piston pumps or conveyors/trucks to transport the paste or filter cake, respectively. The reduced storage volume occupied by tailings paste or filter cake, and the relative ease of capping “soil-like” tailings are discounted, as is the potential for a higher level future land use and/or ecological function.

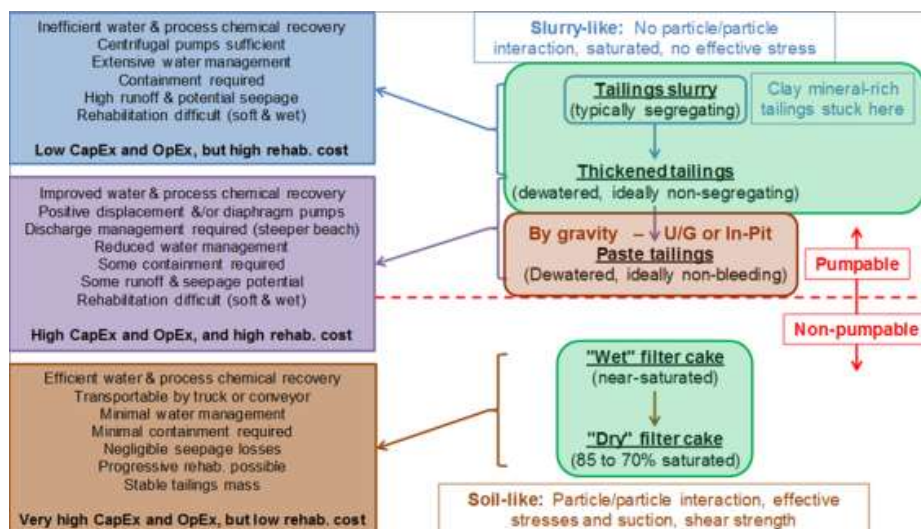


Figure 1. Tailings continuum (adapted from Davies & Rice, 2004).

Most tailings can be thickened mechanically, some to a paste consistency. However, clay mineral-rich tailings, such as coal tailings, mineral sands tailings, tailings from some oxide ores, and residue from the processing of bauxite and nickel laterite, are difficult to dewater mechanically, particularly where sodium smectite is present. Where tailings are to be transported by pumping, thickening is often limited to a consistency that can be pumped by robust and inexpensive centrifugal pumps, which results in a shallow tailings beach. Pumping more thickened or paste tailings would require piston pumps, which are about an order of magnitude more expensive than centrifugal pumps, cost more to operate, and are more sensitive to variable input feeds. Also, piston pumps discharge a “toothpaste-like” consistency, which requires that the discharge point be constantly moved. However, tailings paste can be delivered under gravity as underground backfill or into a pit if the dewatering facility is located close to the discharge

point, possibly on a mobile skid that can be moved. Underground tailings paste backfill will generally reach its intended destination under gravity provided that the angle between the discharge and final points is steeper than 45 degrees. If a consistency greater than is readily pumpable by centrifugal pumps is desirable, it is often best to jump to filtration. Centrifuges or belt press filters can produce a “wet” filter cake, while plate and frame or screw filtration can produce a “dry” filter cake. The filter cake can then be transported by truck or conveyor. Centrifuged filter cake may still flow, while dry filter cake can be compacted.

3 TAILINGS DAM FAILURE RATES

Recent years have seen a number of tailings dam failures in developed countries and involving global mining companies that have attracted much adverse publicity globally. In particular, these include tailings dam failures at Mount Polley, Canada in 2014, and at Samarco, Brazil in 2015. Other recent tailings dam failures include Luoyang, China in 2016, Southern Judean Desert, Israel in 2017, and Cadia, Australia and Cieneguita, Mexico in 2018. The risk of another tailings dam failure worldwide is certain.

In their paper on tailings dam failures, Rico et al. (2008) collated data on 147 historical worldwide tailings dam failures, including their location, construction, actual or presumed failure cause, tailings characteristics, and the socio-economic consequences and environmental impacts of the failures. They found that the USA had reported the highest number of tailings dam failures of any country, with 39% of the 147 failures, with 18% located in Europe, 12% in Chile, and 5% in the Philippines. Most of the tailings dams that failed were of moderate height, in the range from 5 to 20 m high.

In many of the tailings dam failures considered (39%), the failure was caused by a combination of factors. The main cause identified was extreme rainfall or snowfall, accounting for 25% of worldwide cases where a single cause was identified. Unknown causes accounted for a surprisingly high 15% of failures worldwide. The next most significant single cause was earthquakes, accounting for 14% worldwide, although such failures were concentrated in earthquake-prone countries such as Chile. Poor tailings management accounted for 10% of failures worldwide. Tailings dam foundation failure accounted for 6% of cases worldwide, but a high 12% of the failures in Europe. Other single causes included seepage leading to piping, overtopping, and mine subsidence.

Unknown dam construction accounted for almost 50% of the tailings dam failures worldwide, while dams constructed by the upstream method were by far the most frequent to fail of those whose construction was known, at about 35% of the total worldwide.

Azam & Li (2010) reviewed 218 tailings dam failures worldwide over the last 100 years, including the 147 studied by Rico et al. (2008) that were better documented, and identified the following vulnerabilities to failure:

- Dam construction using mine wastes.
- Sequential dam raises together with an increase in tailings production.
- The lack of regulations on design criteria, particularly in developing countries.
- High maintenance costs post-closure.

For a world inventory of 18,401 mine sites, the average tailings dam failure rate over the last 100 years is 1.2% or 2.2/year, which is more than two orders of magnitude higher than that reported for water retention dams of 0.01%. The peak rate of tailings dam failures occurred in the 1960s, with five failures per year on average. Azam & Li (2010) found that North America had the highest number of tailings dam failures over the last 100 years with 77, at a failure rate of 0.9%. The corresponding number and rates of failure for South America, Europe, Asia, Africa, and Australia were 40 and 2.2%, 58 and 5.0%, 23 and 1.5%, 13 and 0.8%, and 7 and 0.2%, respectively. Azam & Li (2010) identified the causes of failures in order from most to least frequent as extreme precipitation, poor management, seepage, unknown causes, structural defects, slope instability, foundation subsidence, and overtopping. Most of the failed tailings dams were less than 30 m high, and contained small to intermediate volumes of tailings up to 5 Mm³. The volume of tailings released typically varied from 30 to 40% of the stored tailings. Environmental pollution was the most common impact, followed by loss of life, infrastructure damage and impact on public health.

Responses to the recent high profile tailings dam failures include:

- Reviews of:
 - Existing tailings dams by major mining companies.
 - Existing tailings dams, required by Regulators.
- Little consideration of abandoned tailings dams.
- More conservative tailings dam designs, including the adoption of lowest bound design parameters in some cases, implying that previous designs may not have been safe.
- Changes in tailings containment practices:
 - Sometimes certain practices are outlawed by Regulators.
 - For example, upstream tailings dam construction was outlawed in Chile following earthquake-induced failures of upstream dams in the 1960s, although sand dams constructed using the centreline method with flattening and compaction of the downstream face has not eliminated earthquake-induced damage.
- Increased liability of the “Engineer of Record” or design engineer.
- Concern about personal liability/prosecution of senior executives, driving tailings management.
- Regulators seeking to increase Security Bonds and Guarantees for TSFs.

Responses to tailings dam failures have not (yet) included a major shift in the methods of tailings disposal and containment, or in the method of tailings dam construction, at existing mines. More tangible drivers for change in tailings disposal and containment are conditions imposed on new mining projects.

4 ALTERNATIVE APPROACHES TO TAILINGS MANAGEMENT

The use of NPV and an artificially high Discount Factor result in apparent cost savings in tailings management in the short-term, with increasing operational and capital costs, and unintended cumulative detrimental impacts, over time, and ever-increasing closure and rehabilitation risks and costs in the long-term. To illustrate this, simple NPV analyses are applied to alternative management and closure approaches for coal tailings from open pit mining operations in the relatively flat terrain of the Eastern Australian Coalfields. A mine life of 20 years is assumed.

4.1 *Operational phase*

Figure 2 illustrates NPV capital and operating cost comparisons for Discount Factors of 2.5% (close to the Consumer Price Index), 5% and 10%, applied to: (i) a series of surface TSFs, (ii) an in-pit TSF, (iii) on-off temporary surface tailings cells in which the tailings are desiccated and harvested periodically and dumped with coarse-grained wastes, (iv) pressure filtration and “dry” disposal of the tailings filter cake with coarse-grained wastes, and (v) a surface TSF until a completed pit becomes available for tailings disposal. These comparisons do not include closure and rehabilitation costs.

The high costs of the series of surface TSFs would surprise many, but arise from the flat terrain of the Eastern Australian coalfields providing limited “free” storage for tailings and requiring an ever-increasing perimeter dam for a surface TSF. This limits the height of each TSF due to the excessive cost of dam raising, forcing a new surface TSF to be constructed. An in-pit TSF is the least expensive option, but this assumes that a pit is available from the start, which is unlikely. The other three options attract similar capital and operating costs. The costs of on-off temporary tailings cells are dominated by high re-handling costs, although drying by the sun and wind is relatively robust, with high rainfall affecting less than 30 days per year on average. The costs of pressure filtration are dominated by the high up-front cost of the equipment, which will be sensitive to the variable input stream. The initial use of a surface TSF until a completed pit becomes available for tailings disposal appears to be marginally the best option.

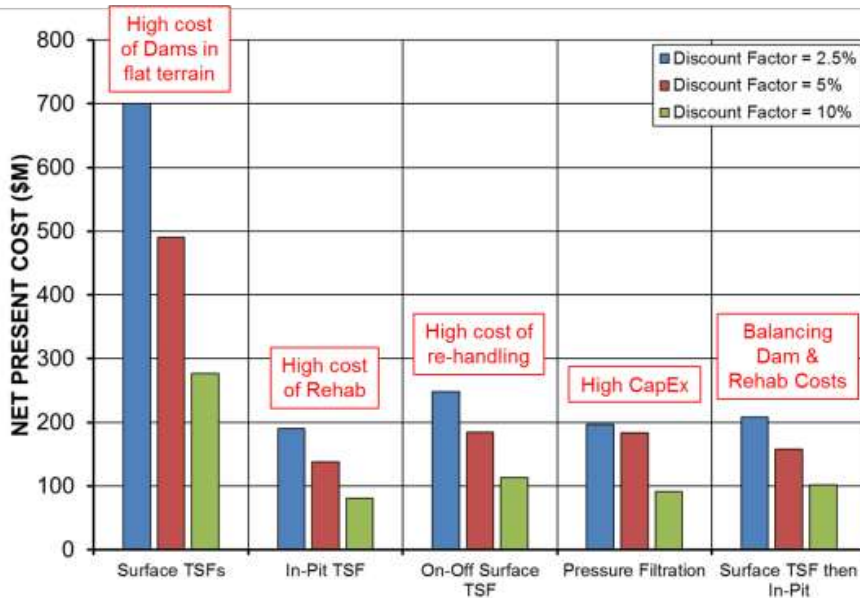


Figure 2. NPV comparisons of alternative operational tailings storage scenarios.

4.2 Including closure and rehabilitation

Figures 3 and 4 show, respectively, NPV comparisons at Discount Factors of 10% and 2.5%, for a series of surface TSFs, including operational and rehabilitation costs. Three surface TSFs are operated during the 20-year life of the coal mine, the first to year 7, the second from year 7 to year 15, and the last from year 15 to year 20. Rehabilitation of the TSFs is carried out progressively, the first in year 7, the second in year 15 and the last in year 20. A 10% Discount Factor obscures the cost of TSF rehabilitation, which is by far the major cost impost in undiscounted terms, while a more realistic 2.5% Discount Factor better reflects the real and substantial cost of rehabilitation. Leaving the rehabilitation of all three TSFs to the end of the mine life would reduce the heavily discounted cost of rehabilitation further, while likely to raise the actual cost.

4.3 Rehabilitation security deposit

The New South Wales Mining Act 1992 and Environment Planning and Assessment Act 1979 (updated in June 2017), and the Queensland Mineral Resources Act 1989 and Environmental Protection Act 1994 (also updated in 2015), require coal mine operators to assess and submit a Security Deposit against future mine site rehabilitation. Security Deposit discounts can apply to mining companies that demonstrate sound financial health and a budgetary provision for rehabilitation, progressive rehabilitation, or waste minimisation. Both the New South Wales Rehabilitation Cost Estimation Tool (www.resourcesandenergy.nsw.gov.au/miners-and-explorers/rules-and-forms/pgf/environmental-guidelines), and the Queensland Mining Financial Assurance Calculator (www.business.qld.gov.au/running-business/environment/licences-permits/rehabilitation/security-deposit) provide the same indicative costs for reshaping, capping/sealing tailings:

- AUD170000/ha for tailings likely to present considerable difficulties due to reactive and/or soft tailings.
- AUD108000/ha for tailings likely to present moderate difficulties due to reactive and/or soft tailings.

- AUD81000/ha for benign and strong tailings.

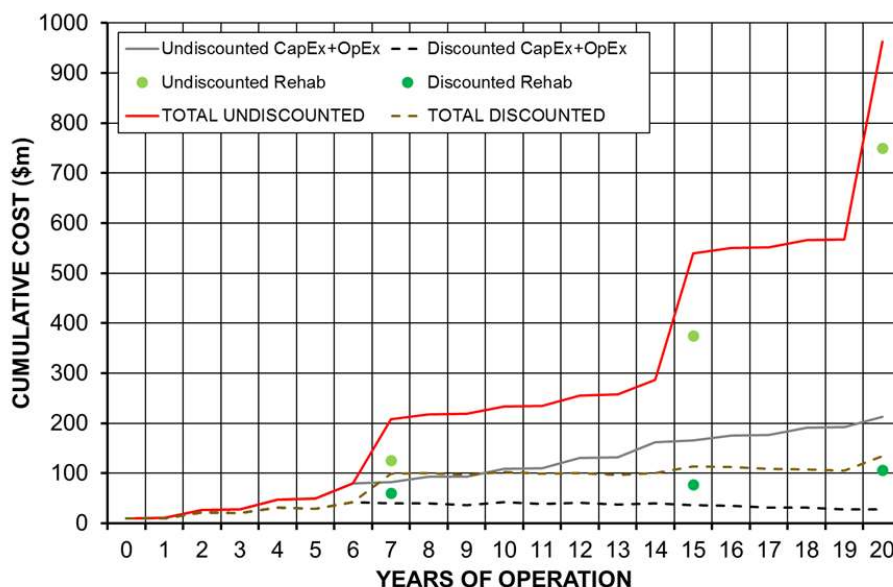


Figure 3. NPV comparisons at a Discount Factor of 10%, for a series of surface TSFs, including operational and rehabilitation costs.

In addition, indicative unit costs are provided for land preparation and revegetation of AUD4000 to 5000/ha, plus maintenance of rehabilitated tailings of AUD300 to 40000/ha, increasing with decreasing rehabilitation performance from successful rehabilitation to total rehabilitation failure. Hence, the total Security Deposit ranges from AUD85300 to 215000/ha, while the actual rehabilitation costs could be far lower, under favourable conditions, presenting a large potential for cost savings. The Security Deposit can be submitted in the form of a Bank Guarantee, cash, Bond, or Insurance Policy. The cost of the favoured Bank Guarantee varies with the financial strength of the mining company, and over time. It is based on a benchmark such as the London Interbank Offered Rate (LIBOR), plus a premium of around 0.3% per annum of its value, and its duration, and would be expected to be 1.5 to 3% pa of the Security Deposit. While this rate is of a similar order to the inflation rate, the Bank Guarantee and budget to cover the Security Deposit tie up funds that could be used more productively. The cost of a Bank Guarantee could range from about AUD1300 to 6500/ha per annum, which would be a lesser driver for cost savings.

The actual cost of rehabilitating coal tailings will depend on the difficulties presented by the tailings and the storage, and the availability and cost of suitable capping materials. It could take advantage of reduced costs for material supply and haulage during operations, to be as low as perhaps AUD50000/ha. The cost of a Bank Guarantee could amount to AUD50000/ha over 7.5 to 40 years, not accounting for inflation. Effectively encapsulating potentially contaminating coal tailings, accommodating or improving their poor bearing capacity, and progressive rehabilitation using capping materials available during operations, will translate to substantial cost savings and greater certainty about the rehabilitation of coal tailings.

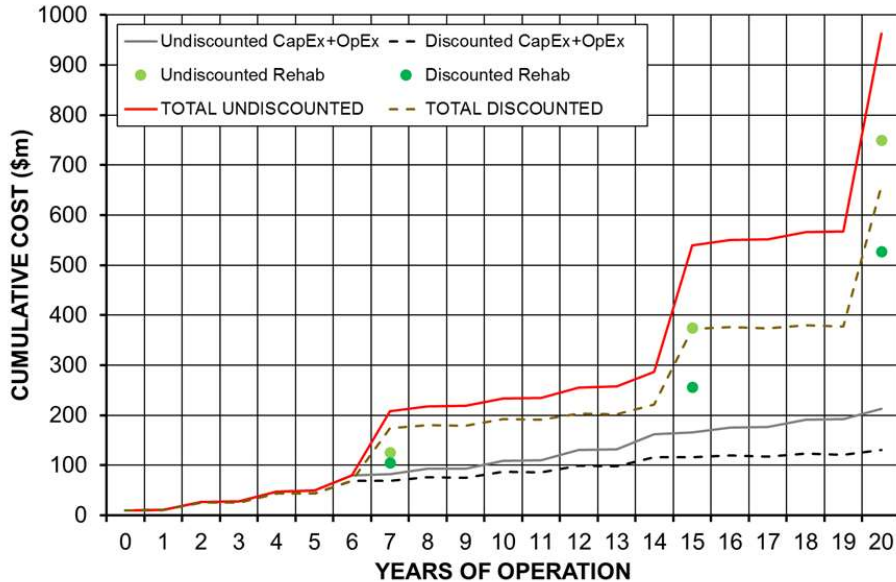


Figure 4. NPV comparisons at a Discount Factor of 2.5%, for a series of surface TSFs, including operational and rehabilitation costs.

5 CONCLUSIONS

While high costs of large-scale mining projects may necessitate NPV with a high Discount Factor to secure financing, it is best not applied to tailings operations and closure since it:

- Increases the risk of tailings dam failures.
- Threatens the mining industry's financial and social licence to operate.
- Entrains excessive process water; storing water rather than solids and taking up more volume.
- Leads to wet and soft tailings deposits.
- Potentially leads to unintended cumulative impacts that are difficult and expensive to rectify.
- Leads to difficult and high cost tailings rehabilitation.
- Discourages tailings rehabilitation.
- Limits post-closure land use and ecological function of tailings storages.
- Distorts and increases actual Life-of-Mine costs.

6 REFERENCES

- Azam, S. & Li, Q. 2010. Tailings dam failures: a review of the last one hundred years. *Geotechnical News*, 28(4): 50–53.
- Davies, M.P. & Rice, S. 2004. An alternative to conventional tailing management – “dry stack” filtered tailings. *Proceedings of Tailings and Mine Waste 2004, Vail, Colorado, USA, 10-13 October 2004*, 411–422. Amsterdam: A.A. Balkema.
- Rico, M., Benito, G., Salgueiro, A.R., Díez-Herrero, A. & Pereira, H.G. 2008. Reported tailings dam failures. *Journal of Hazardous Materials*, 152(2): 846–852.

Benefits of Rotational, Thin Layer, Air Dried Tailing Deposition after 25-Years of Operation of the Juniper Tailing Storage Facility

A.H. Gipson, Jr., J. Taylor, J. Chilson, and B. Hutchings
Knight Piésold Consulting, Inc., Denver, Colorado, U.S.A

J. Gilbert
Newmont USA Limited, Twin Creeks Mine, Golconda, Nevada, U.S.A.

ABSTRACT: From inception in the late 1980s, the Juniper Tailings Storage Facility has been constructed in stages as a massive, compacted, rock fill, modified centerline embankment to retain fine grained predominately silt tailing. The initial cells were designed to contain 8 million tons. Three horizontal expansions and numerous staged raises have been made to the initial facility bringing the planned storage to 150 million tons at a height of 225 feet. Currently additional expansions are being considered. The initial stages of each basin were constructed as downstream embankments and the basins of each initial stage were lined with a 12-inch thick layer of low permeability soils overlain by a 12-inch thick drain layer containing a series of corrugated, slotted HDPE drain pipes. A drain/transition layer was included in the upstream face of the raises so that the fine-grained tailing did not migrate into the rock fill and any seepage was contained within the upstream side of the initial lined embankment where it was collected in the lined basin. Thus, no lining was needed above the initial embankment. This paper discusses the design, construction and operation of the facility including a summary of the benefits realized by the type of embankment constructed and the use of rotational, thin layered, air dried deposition. The features discussed could be considered for inclusion in other projects to provide safety and security, reduce costs and provide efficient operations.

1 INTRODUCTION

1.1 General

Newmont USA Limited (Newmont) owns and operates the Twin Creeks gold mining and processing facility located in Humboldt County, Nevada, approximately 35 miles northeast of Golconda. The Juniper Tailing Storage Facility (TSF) provides storage for tailing produced by the processing operations. The current planned storage for the facility is 150 million tons. The TSF currently has a footprint covering 770 acres and a planned height of 225 feet. Additional raises are being evaluated.

1.2 Topography, Drainage, and Vegetation

The site itself is plainer and overall it slopes gently to the southeast. The Juniper TSF presently comprises one cell that is the combination of the previous Cells 1, 2, and 3. It has been constructed in numerous stages including both vertical and horizontal expansions. A plan view of the one cell, current configuration, TSF is shown in Figure 1 and the older two cell facility in Figure 2.

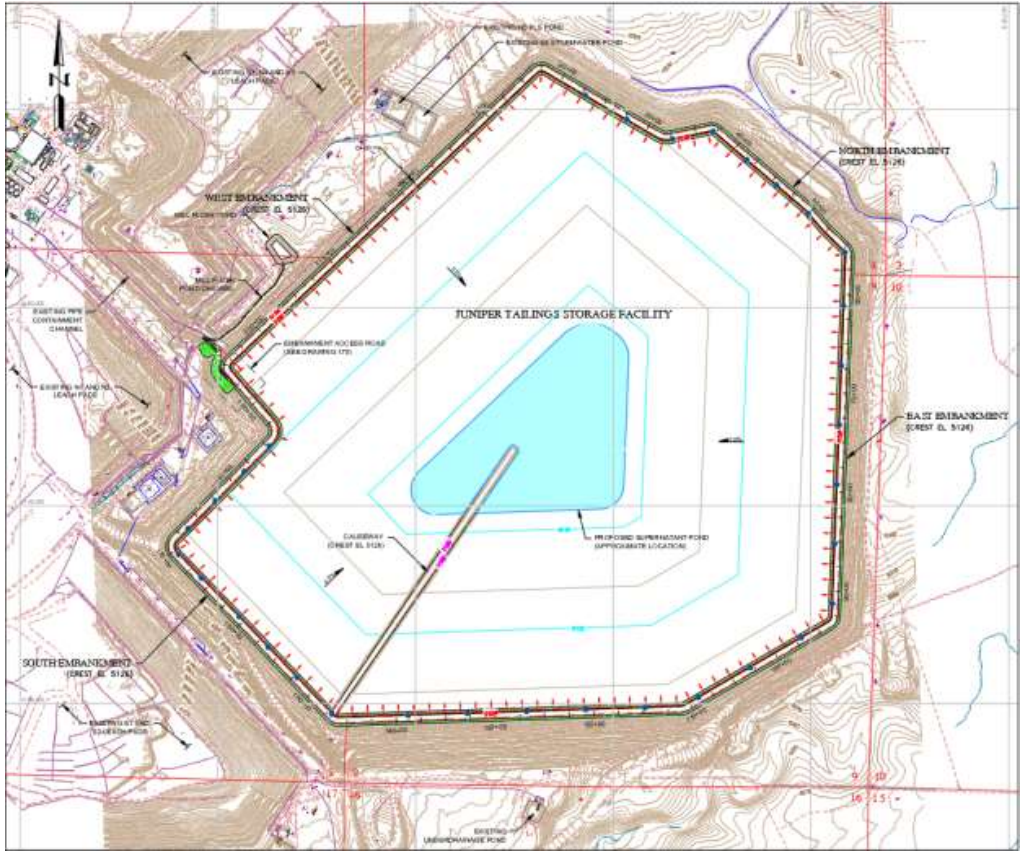


Figure 1. Plan view of current configuration. Combined Cells 1, 2, and 3.

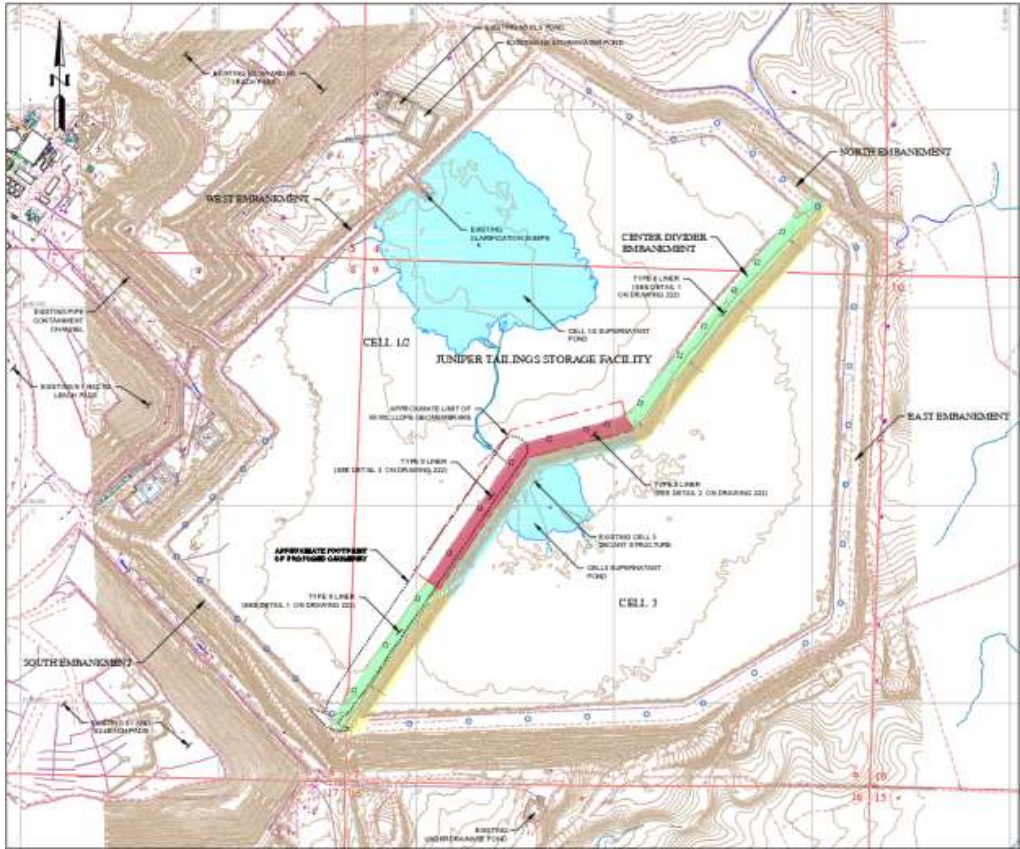


Figure 2. Plan view of Cell 1/2 and Cell 3 configuration.

The primary area wide drainage is generally to the south through Kelly Creek, which flows into the Humboldt River. A secondary drainage tributary to Kelly Creek, which is Rabbit Creek, emanates from numerous small canyons in the Osgood Mountains located to the west and flows to the southeast toward Kelly Creek. Rabbit Creek was diverted around the northeast corner of the TSF prior to joining Kelly Creek as part of the Cell 2 construction. These water courses are generally dry.

The natural vegetation is typical sagebrush and is characterized by Thurber needlegrass, Wyoming big sagebrush, blue bunch wheatgrass, Indian ricegrass, Sandberg bluegrass, and Webber ricegrass. The agricultural potential is low.

1.3 Project History

The starter facility was designed in early 1987. It consisted of a two-celled facility comprising a southern Cell A and northern Cell B with impounding embankments and a fully-lined basin with an underdrainage system. When the facility was first commissioned, tailings from oxide ore pulp processed through the Juniper Mill were deposited in Cells A and B that were later combined to form Cell 1 that was constructed in 1988. In the summer of 1989 the Stage 2 expansion was designed. The Stage 2 expansion consisted of raising the embankments using upstream construction methods and expanding the liner and the drainage system in the basin. It was constructed in 1990. The Stage 3 expansion was designed in 1991 and constructed in 1992 to provide storage until the end of 1996. The Stage 3 expansion included an upstream raise to the existing embankment and expansion of the liner and the drainage systems in the basin. Both the Stage 2 and 3 expansions maintained the initial Cell A and B configuration. This portion of the facility had a capacity of 8 million tons.

After construction of Stage 3, plans for a sulfide project were developed, which prompted evaluating the existing facility to estimate the expansion required to adequately store an additional 50 million tons. It was determined that combining Cells A and B into a single cell and construction of an additional cell was necessary to store a total of 58 million tons in the facility. The new cells were denoted as Cell 1, the old Cells A and B, and Cell 2. These components were incorporated into expansions covering Stages 4 through 8.

Stage 4 Cell 1 expansion was constructed during the summer of 1996. Stage 4 Cell 2 was constructed in the spring and summer of 1997 and was the first lateral expansion of the facility. The expansion was to the northeast. The locations of Cells 1/2 and 3 are shown on Figure 2.

In November 1996, tailings from sulfide ore pulp processed in the new Sage Mill and autoclaves were first produced and added to the existing oxide millstream and deposited in Cell 1. Soon afterwards, in May 1997, Newmont commenced processing ore from the Mule Canyon Mine through the Sage Mill. The Mule Canyon ore comprised about 5-10 percent of the sulfide stream. In September 1997, Cell 2 was commissioned using tailings comprised of oxide ore through the Juniper Mill and sulfide and Mule Canyon ore through the Sage Mill. Deposition of this tailings blend continued through February 1999 when processing of Mule Canyon ore ceased. Late in 1997 a change in the tailings behavior was observed, resulting in a significant increase in the time required for solids in the slurry to settle and a decrease in the density of the tailings mass. This led to pulling solids with the solution from the supernatant reclaim system and a more rapid filling rate of the facility than originally envisioned. The addition of Cell 2 and expansion of the supernatant pool in the early stage of filling Cell 2 alleviated pulling solids with the solution from the supernatant reclaim system. Construction of Stage 5 Cells 1 and 2 commenced in October 1997 and was completed at the end of September 1998.

In 1999 the price of gold was low and Newmont wanted to consider viable options for expanding the facility considering two options including (1) a vertical expansion if the price remained low and (2) a horizontal and vertical option if the gold price increased. The price remained low, so Newmont proceeded with the vertical expansion. By 2005 the gold price had increased, Newmont requested the designs be revised to include the Cell 3 horizontal expansion. Cell 3 construction was undertaken in 2004. The plan view of the Cell 1/2 and Cell 3 configuration is shown on Figure 2. The Cell 3 expansion increased the storage capacity to about 115 million tons off tailing.

In 2014 Newmont requested the design of three additional vertical expansions to store an additional 35 million tons bringing the number of stages for vertical raises to 12 and storage capacity to about 150 million tons.

1.4 Regulatory Considerations

The designs were completed in accordance with the appropriate State of Nevada regulations. The facility is permitted by the Nevada Division of Environmental Protection (NDEP) and Division of Water Resources (NDWR).

2 EMBANKMENT CONSTRUCTION

2.0 Foundation

The facility is founded on a sequence of very dense, permeable, alluvial sands and gravels. The alluvial sequence is hundreds of feet thick and the water level in the alluvium is generally deep, typically on the order of 100 feet below ground surface. This provides a very stable foundation for the facility.

2.1 Embankment

From inception of the Juniper tailings storage facility in the late 1980's, the facility has been constructed in stages, with a massive exterior compacted rockfill embankment comprised of predominately rock fill or granular alluvium placed in 4-foot-thick lifts compacted to high density by controlled routing of the large haul trucks to retain the fine-grained (predominately silt) tailing. The rockfill is high strength and highly permeable. The rockfill embankment is designed to be dry. A face drain constructed on the upstream face of the rockfill provides a controlled pathway to safely remove water from the tailing placed adjacent to the rock fill and direct it to the base drain, as described below, to collect the seepage and prevent flow into the rock fill and discharges from the facility into the environment. The face drain is also designed as a filter to prevent the fine-grained, very-low-permeability tailing from infiltrating into the rockfill. These key design features maintain the phreatic surface or water level inboard or upstream of the tailing/rock fill interface, thus keeping the rockfill dry to further enhance the stability and safety of the perimeter embankment. Since dry, dense rockfill is not susceptible to liquefaction or strength loss from earthquake loading, it is inherently the most stable type of embankment.

The design of the embankment staging was an intricate process that considered balancing storage needs, mine rock availability, construction timing and costs to develop a cost-effective design. Figure 3 shows the staging for the south embankment. Note that the first major expansion, Stage 4, required starting the embankment on natural ground that greatly increased the needed volume of rock fill compared to that used in Stages 2 and 3. Also note that Stage 5 construction was split into two phases to provide for construction of the base with the mine waste rock available at the time and then the raise later when additional mine waste rock was available.

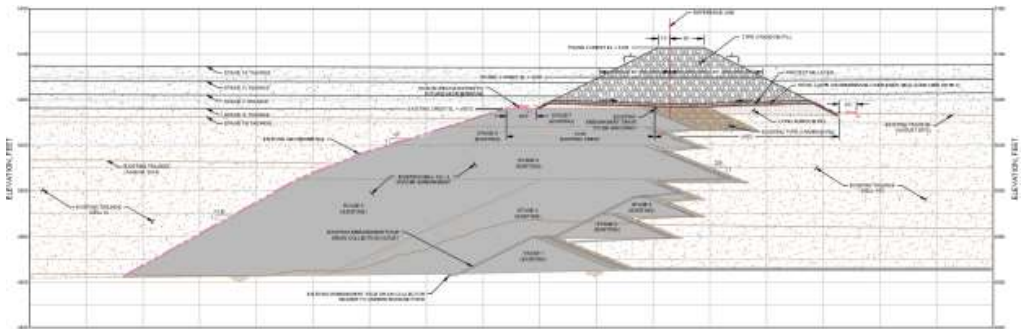


Figure 3. South embankment section showing overall embankment and individual raises.

2.2 Basin Liner and Underdrains

A 12-inch thick layer of compacted, low permeability soils was constructed over the alluvium throughout the basin and upstream slope of the initial stage to provide a hydraulic barrier to reduce seepage losses from the tailings basin. This layer is overlain by a 12-inch-thick sand and gravel drain layer, base drain, containing a series of corrugated, slotted, HDPE drain pipes to remove seepage and reduce the hydraulic head on the liner. Collected seepage is conveyed to the underdrain seepage collection pond by double contained HDPE pipes. An HDPE liner has been included in the liner system beneath the areas of the supernatant pond.

2.3 Foundation Preparation for Upstream Shell Construction on Tailings

Foundation preparation and placement of the initial and subsequent lifts of rockfill beneath the upstream portion of the embankment raises extending over the tailing surface has been ongoing since the late 1980's. Approximately 20 miles of foundation surface has been prepared successfully. The drier denser tailing resulting from the depositional procedure provides a stable base for the raises. The procedure used is as follows:

- Once the tailing surface has reached the desired foundation elevation, it is allowed to drain and air dry, to the extent practical, to gain strength prior to placement of the initial lift of rock fill.
- The first lift of rockfill is placed in about a 4 to 6-foot thickness. In wetter areas it displaces several feet of tailing. The lift is allowed to rest and stabilize, as needed, prior to the placement of subsequent fill. The lift thickness may need to be varied based on observation of performance during the actual construction.
- Thicker lifts are not desirable as they create additional load to the tailings surface.
- Some experimentation may be needed in the selection of the dozer model used to push the initial lift of rockfill over the tailing. If the available dozers cause excessive deformation, it may be necessary to use smaller equipment with wider tracks.
- The lift is placed by dozing the rockfill dumped on previously prepared foundation onto the tailing surface. On the advance, the dozer should push a full load and not push the entire load over the working face. The amount of material left should be small enough that it can be moved on the subsequent push out. It should also serve as a safety berm. Care needs to be taken to operate the dozer normal to the working face. Likewise, haul truck traffic should avoid travel adjacent and parallel to the working face and always maintain a safe distance from the working face. The trucks should turn and back toward the working face, dumping the load so that the toe of the dumped pile is about 20 feet from the working face.
- Subsequent lifts should be placed in the same manner for any working face adjacent to a slope.
- For rock being placed in a single lift over a previously placed lift of rockfill, a safety berm should be constructed at the crest of the advancing face and the haul truck backed toward the safety berm for dumping normal to the advancing face.
- Safety berms are maintained along each working or advancing face in keeping with mine safety protocol.

Also, as with any project, the construction is continuously observed to identify any abnormal soft areas, cracking, deformations at the toe of the slope, on the slope or at the crest or “waves” made as the haul trucks or other equipment travel on the fill surface.

3 ROTATOINAL, THIN-LAYER, AIR-DRIED TAILING DEPOSITION

The tailing is being placed by rotational, air-dried, thin-layer deposition to produce a denser, drier tailings deposit that increases the amount of tailing that can be contained within a given volume and increases the strength of the tailings deposit. The tailings distribution system is designed to accommodate up to 15,500 tpd at a 40 percent solids content. The tailing distribution system includes a tailing delivery pipeline around the perimeter of the facility with valves and drop bars at 125-foot centers. The drop bars extend from the discharge valves to the tailing surface. The drop bars are 6-inch-diameter pipes with a series of 4-inch-diameter holes drilled in the top of the pipe, through which the tailings slurry is deposited on the surface of the facility. This distribution system produces laminar flow of tailings over the surface of the facility. The tailing is deposited by sequentially rotating the point of deposition around the facility so that as the depth of deposited tailing reaches 4- to 6-inches in thickness, the point of deposition is moved or rotated to the next area of deposition. Usually about 8 to 10 of the drop bars are in use at any one time.

The surface area of the facility and tailing production rate are such that the most recently-deposited lift of tailing, preferably, will have a month or more to air dry and consolidate prior to placement of the next tailing layer. As the tailing dries, drying cracks form on the tailing surface, which indicate that the tailing is consolidating and increasing in density. The net result is a denser, drier, more stable tailing deposit, as demonstrated by indications that the pore pressures in the tailing facility, outside the limits of the water pool, are less than hydrostatic. This condition reduces the potential for loss of strength in the event of

earthquake loading, as supported by the measured in-situ densities. The current tailing density near the point of deposition that has the most opportunity to dry averages 76 pcf, whereas near the supernatant pond, the density averages 69 pcf.

It should also be noted that the benefits of rotational, air-dried, thin-layer deposition are enhanced by the crew operating the tailing facility. Based on our observations made during the annual inspections, the crew clearly understands the deposition procedures and accordingly implements them. This develops the beneficial attributes in the deposited tailing described above. The facility is generally operated by a one operator, occasionally supported by one or two others.

4 TAILING PROPERTIES

4.0 *Tailings Gradation and Density History*

When the facility was commissioned, tailings from oxide ore pulp processed through the Juniper Mill were deposited in Cells A and B at a density of 90 pcf compared to the predicted drained and air dried density of 85 pcf. For comparison the predicted undrained density was 60 pcf. In November 1996, tailings from sulfide ore pulp processed in the new Sage Mill and autoclaves were first produced and added to the existing oxide millstream and deposited in Cell 1. The predicted undrained density was 45 pcf and the predicted drained and air-dried density was 80 pcf.

Based on the above it can be seen that the predicted densities compared fairly well with the in-situ densities and that there was a significant variance in the densities that was basically a function of the amount of fines and nature of the fines.

4.1 *Recently Deposited Tailing Classification and Density*

Based on index test results of the recently deposited tailing, there was no discernable difference in the tailings gradation based on samples from the beach near the point of deposition or near the supernatant pond or with depth. However, as would be expected, variations in average moisture contents and average dry density were noted between materials from near the supernatant pond with an average moisture content of about 51 percent and average dry density of about 69 pcf and materials in the tailings beach areas with an average moisture content of about 36 percent and average dry density of about 76 pcf.

4.2 *Permeability*

The consolidation test data was used to develop a hydraulic conductivity vs. effective stress profile, which estimated an average hydraulic conductivity of 2.5×10^{-7} centimeters per second (cm/s) (1×10^{-7} inches per second [in/s]). This value was used as input for the seepage analyses. Additionally, this testing indicates that at the end of consolidation the tailings are anticipated to reduce in hydraulic conductivity with increasing effective confining stress (i.e., increased depth of burial); however, the average was used for analyses presented herein to represent the vertical hydraulic conductivity of the tailings.

5 STABILITY ANALYSES

Slope stability for both the static and earthquake loading conditions were considered. The minimum static, drained, factor of safety considering steady-state conditions found for the downstream slope was 2.0 and upstream slope, prior to any tailing placement, was 1.9 for the raises evaluated versus the minimum of 1.4 required by Nevada Dam Safety. It should be noted that most other agencies, international design guidelines for tailings dams, and practitioners use 1.5 as the minimum factor of safety for these cases. The level of conservatism indicated by the factors of safety is reasonable. It is recommended that factors of safety in the range of 1.8 to 2.0 be used in the initial design as there are often changes in the materials or construction or operations that tend to reduce the factor of safety. If one has designed for the minimum value and there is a change, as there often is, the resulting factor of safety will be below the minimum. In this case additional raises are being considered so the factors of safety being above the minimums are supportive of the potential for significant raises. If the factor of safety used for the initial design was near the minimum value a new facility would likely have been needed that would have greatly increased the cost of tailing disposal.

Analyses of the upstream slope stability for selected embankment raises, prior to any tailing being deposited against the slope, under post-earthquake conditions was considered for both the Operating Based Earthquake (OBE), representing the 475-year probabilistic event, and Maximum Design Earthquake (MDE), representing the 2,475-year probabilistic event. Generally, the OBE is selected with input from the operator to estimate a level of damage and cost to repair the damage that is acceptable to the operator. The MDE is the earthquake that the structure can tolerate without the release of tailing or supernatant fluid.

The CPT data indicated that the tailings in the area on which the upstream raise is to be constructed should not liquefy under either the OBE or MDE. The other three sets of CPT data evaluated were adjacent to or near the supernatant pond. The analyses indicate that liquefaction would be unlikely under the OBE and that the top 5 to 15 feet of tailings might liquefy under the MDE. These results are reasonable as the tailing deposited around the perimeter gets the full benefit of densification created by the rotational, thin layer, air dried deposition and the drainage provided by the proximity to permeable rock fill embankment. The tailing near the supernatant pool is continually wet so does not gain the advantage. The average densities measured in the test work support this: the average density of the tailing near the crest was 76 pounds per cubic foot and near the water pond was 69 pounds per cubic foot.

For the downstream slope, assuming the tailing liquefied, the minimum factor of safety found was 1.9, which is well above the minimum commonly accepted value of 1.1. This high factor of safety is attributed to the massive compacted rockfill perimeter embankment and very dense alluvial foundation. The deformation analyses indicated there would be negligible deformation for both the OBE and MDE. This is also consistent with the massive compacted rockfill perimeter embankment and very dense alluvial foundation.

Consequently, the risk of significant damage to the upstream slope of the facility from the earthquakes evaluated appears to be low or nil given the following considerations:

- The OBE can be thought of as occurring on average about once every 475 years (i.e., a 10% probability of occurrence in a 50-year period) and the MDE about once every 2,475 years (i.e., a 2% probability of occurrence in a 50-year period).
- The level of damage to the upstream slope would be nil on the evaluation of the CPT data described above.

6 WATER MANAGEMENT

General

This section discusses the three areas of interest related to water management including (1) surface water diversion, (2) the supernatant pond and (3) under seepage. Hydrologic analyses for design of storm water management facilities were based on the regulatory criteria that indicate the primary fluid management system must be designed to be able to remain fully functional and fully contain all process fluids including accumulations resulting from a 24-hour storm event with a 25-year recurrence interval and to withstand the runoff from a 24-hour storm event with a 100-year recurrence interval. For this site, the 25-year storm has a rainfall of 2.1 inches and the 100-year storm 2.6 inches (Knight Piésold, 1996). Given that the difference in the storm events is small the 100 year 24 hour storm event was used as the design storm.

Surface Water Diversion.

The primary drainage crossing the site is Rabbit Creek. As part of the Cell 2 construction Rabbit Creek was diverted around the northeast side of the facility in a channel designed to pass the 24-hour 100-year storm event. The area around the northeast corner is such that if the 24-hour 100-year channel overflowed the natural topography is such that it can safely pass storms much larger than the design storm. The drainage areas on the other sides of the facility are small and the runoff diversion is provided by constructed channels.

Supernatant Pond

Water falling directly on the surface of the tailing will in part infiltrate into the tailing or runoff to the supernatant pond. The limits of the supernatant pond are set to provide a minimum of 3 feet of freeboard while containing the 24-hour 100-year storm.

Under Seepage

In 1999 as part of the evaluation of the Cell 3 expansion, a seepage analysis was performed to predict estimated seepage from each of the cells. Collected seepage reports to the underdrain seepage collection pond at the downstream side of the facility where underflow quantities are monitored.

It was estimated that flows from Cell 1/2 would be on the order of 430 gpm and from Cell 3 510 gpm. The average flows from Cell 1/2 from 2004 to 2013 were 231 gpm and the average for 2012 and 2013 was 128 gpm. For Cell 3 from 2004 to 2013 the average flow was 379 gpm and for 2012 and 2013 198 gpm. During the 2017 annual inspection the flow from Cell 1/2 was 137 gpm and Cell 3 131 gpm. This information is summarized in the following table.

Table 1. Estimated versus Measured Underseepage

Period	Cell 1/2 Seepage (gpm)	Cell 3 Seepage (gpm)
1999 Estimated Seepage Rates	430	510
2004 to 2013 Average	231	379
2012 and 2013 Average	128	198
September 25, 2017	137	131

The estimated seepage values compare well with the measured values. The measured seepage is reducing with time as would be expected as the vertical load on the lower tailing is increasing thus reducing the permeability and flow.

7 INSPECTIONS AND PERFORMANCE

7.1 General

The inspections and monitoring systems include:

- Daily observations by the operations personnel
- Periodic inspections by the site geotechnical group
- Annual inspections by the designers
- Groundwater monitoring wells
- Basin underdrain pore water pressure piezometers
- Flow-measuring flumes at the underdrainage pond
- Overflow alarm at the underdrainage pond
- Tailings distribution delivery pipeline pressure sensor

7.2 Performance

Juniper tailings storage facility is performing very well and in conformance with the design intent. A few key observations from the inspections related to seepage and stability are worthy of note. There is little, if any, indication of significant settlement of the embankment. There have been no indications of slope or foundation instability. For a structure of this size, there was remarkably little cracking in the crest associated with settlement of the tailing beneath the upstream portion of the embankment constructed over the tailings beach.

This is consistent with the expected performance of a well-compacted rockfill embankment founded on a dense alluvial deposit and an indication that the tailing itself had gained density and strength from the deposition method used and the procedures used to prepare the tailing surface for construction of the upstream portion of the embankment extending onto the tailing surface.

Additionally, the estimated seepage from the facility compares very closely with the seepage monitored and collected at the underdrain seepage collection pond indicating the underdrain system is performing as designed. There has been no indication of seepage in the area of the downstream slopes or the natural ground adjacent to the downstream slopes.

8 RECLAMATION

For ease of reclamation, the drained and air dried tailing deposition scheme has distinct benefits in comparison to other methods. It is the only slurry deposition method that the authors are currently aware of that is currently in use that leaves a consolidated tailing deposit for ease of reclamation. Usually, construction equipment can be operated on the tailing surface a few months after deposition has stopped up to near the limits of the supernatant pond. With subaqueous deposition the resulting deposits are generally saturated and low density subject to considerable long term consolidation after deposition ceases. The long term consolidation presents considerable challenges to design of a reclamation system.

For example, reclamation of the surface of the Big Springs subaerial tailings facility was accomplished with scrapers and low ground pressure dozers to grade the surface of the facility for drainage and placement of the cover system. Scrapers were able to operate directly on the graded surface to place the cover materials.

9 CLOSING - PERFORMANCE AND BENEFIT SUMMARY

There are a number of notable benefits associated with the design and construction of this facility that have made this a safe and secure structure, as well as, a well performing and cost-effective structure including the following:

- As is often the case, the initial facility was expanded to provide storage for additional tailing. In the initial design consideration should be given to opportunities to expand the facility.
- The facility location and design have been compatible with two major horizontal expansions and numerous vertical raises. This has provided a facility that has been able to be safely, and cost effectively expanded to provide additional tailing storage well beyond the storage need that was initially envisioned.
- Use of higher than minimum factors of safety for slope stability has proven beneficial for providing safe and secure facility expansions.
- Use of mine waste rock for embankment construction provided a low cost yet robust embankment.
- Modified centerline construction minimized the amount of material in the embankment and thus cost. Also, as additional stages were constructed the outer limits of tailing were moved inside the facility and over the basin and liner system constructed throughout the basin and on the upstream face of the initial stage negating the need for lining raises. This simplified construction and reduced costs.
- The rotational deposition system yielded cost savings with the increased storage created by air drying and hence compaction of the newly deposited tailing.
- Rotational deposition provided a stable foundation for the upstream slopes of the embankment raise.
- Under normal operating conditions only one operator is needed to operate the facility.
- The operators understand the general engineering concepts related to the TSF construction and tailing deposition leading to a well-managed and monitored facility.
- The facility design and size provided flexibility or ability to retain varying types of fine grained tailings ranging from silts to clayey silts.
- Comparison of the estimated seepage rate to measured seepage rates indicates that the underdrain system and liner are performing as designed.

Reclamation costs should be considerably lower with the use of air dried deposition in comparison to subaqueous or thicker layer deposition.

10 REFERENCES

- Gipson, A.H. (1998). Tailing Disposal – The last 10 years and future trends, Tailings and Mine Waste '98, 127-135, A.A. Balkema/Rotterdam/Brookfield.
- Reisinger, R.W., East, D.R., Gipson, A.H., Valera, J.E., Gorman, J.A, 2001. Reclamation of the Big Springs subaerial tailings facility, Nevada. Tailings and Mine Waste 2001, 423-433, A.A. Balkema/Rotterdam/Brookfield.

Changes to Tailings Dam Regulation in Brazil in the Aftermath of Failures

K.F. Morrison

CMOC International, Phoenix, Arizona, USA

H.G. Pedrosa and G.J.I dos Santos

CMOC Brasil, Catalão, Goiás, Brasil

P.C.R. Gomide

CMOC Brasil, Belo Horizonte, Minas Gerais, Brasil

Alexandre M. Ferreira

ABSTRACT: On November 5, 2015, the Fundão tailings dam at the Samarco iron ore mine in the state of Minas Gerais (Brazil) failed with catastrophic consequences. By now, nearly three years later, most persons working in the mining industry are aware of this failure; however, few outside of Brazil know of the further reaching effects that this event (or previous tailings dam failures) has had on tailings management within the country. Failures and incidents are often the catalyst for change, with the Samarco failure effecting significant changes to the regulations and requirements surrounding tailings management in Brazil. This paper outlines recent important changes to the regulations surrounding tailings dam safety in the country.

1 MINING IN BRAZIL

Brazil is the world's third largest country with respect to geographical area and possesses rich reserves of important commodities such as bauxite, iron ore, niobium, kaolin and nickel, also producing other commodities such as gold, coal and phosphates (Invest In Brazil, 2018). Since Portuguese settlers first arrived in Brazil in the 1500s, a desire to find precious metals and gems prevailed; however, abundant mineral deposits were not located until about two centuries later (Machado & Figueirôa, 2001). At the end of the seventeenth century, gold was discovered in rich alluvial deposits in the state of Minas Gerais (near the city of Ouro Preto), and some believe that Brazil contributed 50% of the world production of gold and diamonds in the seventeenth and eighteenth centuries, promoting the prosperity and luxury of the Portuguese crown (Machado & Figueirôa, 2001).

The country supported the Allies by supplying manganese in the First World War and, during World War II, supplied manganese, iron ore, tungsten and other strategic minerals (Machado & Figueirôa, 2001). Machado & Figueirôa (2001) states that though Brazil had the strongest economy within the whole of Latin America, their economy was so diversified that, at the end of the twentieth century, the value of mineral production (including oil and gas) accounted for a mere 2% of the GDP (Gross Domestic Product).

In 2016, Brazil ranked as the third largest global producer of both iron ore and bauxite (Brown et al., 2018). With respect to niobium, Brazil's production far exceeds that of any other country as the entire world's supply comes from only three operating mines, two of which are in Brazil (Ronald, 2016). In fact, Companhia Brasileira de Metalurgia e Mineração (CBMM) operates the Araxá mine, which is the world's largest and highest-grade niobium operation, providing approximately 85% of the global niobium production (Ronald, 2016). Clearly, Brazil ranks among the largest non-fuel mineral producers in the world today.

2 TAILINGS DAM FAILURES IN BRAZIL

Brazil has an estimated 839 tailings dams, with approximately 44% located in the state of Minas Gerais (ANM, 2018), the most important Brazilian state for mining. Most tailings dams are understood to have been developed for conventional tailings management and were typically constructed using the upstream or centerline methods.

Given Brazil’s global importance with respect to mining, it is not surprising that the country has experienced several notable tailings dam failures. In fact, at least eight notable tailings dam failures have been documented since 1986, many having severe consequences and the majority having occurred before the advent of Brazilian legislation applicable to tailings dams. Figure 1 presents a timeline of major tailings dam failures in Brazil and implementation of key dam safety regulation.

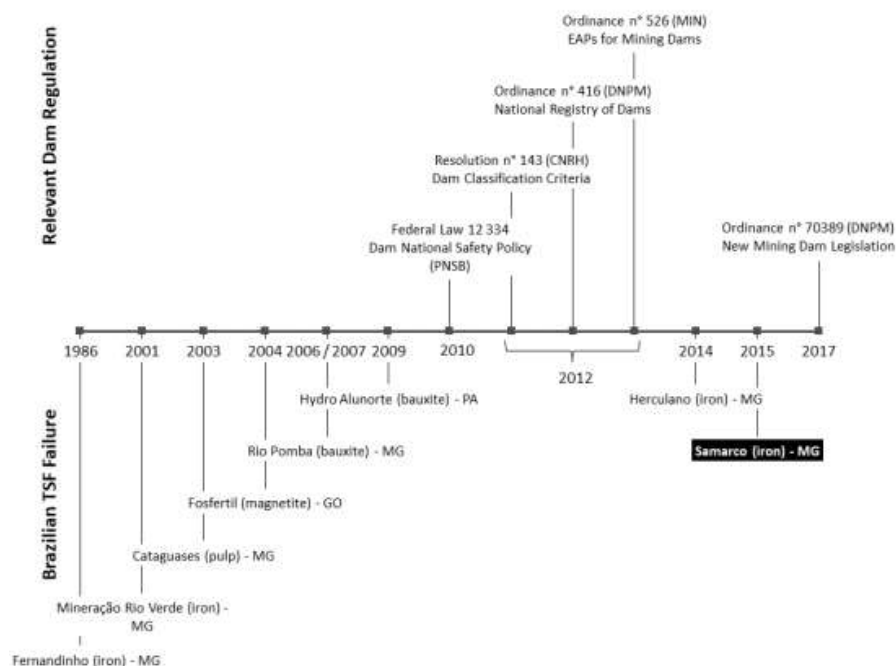


Figure 1. Chronological sequence of reported tailings dam failures in Brazil and notable changes in regulation (created using data from Barbosa, 2015, and WISE Uranium Project, 2018).

The first documented tailings dam failure in Brazil occurred in the central region of Minas Gerais in 1986 at the Fernandinho iron ore mine, leaving seven dead (Barbosa, 2015). No other documented tailings dam failures occurred until 2001 when a tailings dam owned by Mineração Rio Verde ruptured in Macacos, a district in the municipality of Nova Lima in the metropolitan area of Belo Horizonte, resulting in five fatalities and significant environmental damage (Barbosa, 2015).

In 2007, the Rio Pomba bauxite mine in Minas Gerais was shut down after heavy rains caused the tailings dam to break releasing approximately two million cubic meters of red mud into the nearby river compromising the water supply in cities in the states of Minas Gerais and Rio de Janeiro, partially burying streets and houses in two neighboring villages, and leaving about 4,000

residents homeless (WISE Uranium Project, 2018). Remarkably, this failure resulted in no fatalities, which the authors understand to be the result of an effective emergency action plan. Notably, the 2007 tailings dam failure at Rio Pomba followed a leakage event that occurred at the same tailings dam in March 2006 (Reuters, 2010). Though the public was informed that the mud flow was non-toxic, the mining company was forced to shut down (Reuters, 2010).

On November 5, 2015, the Fundão tailings dam at the Samarco iron ore mine in the state of Minas Gerais suddenly failed, releasing an estimated 43 million cubic meters of tailings (80% of the total contained volume), polluting 668 kilometers of watercourses extending from the Doce River to the Atlantic Ocean, and killing 19 people (Carmo et al., 2017). Carmo et al. (2017) stated that “the collapse of Fundão was the biggest environmental disaster of the world mining industry, both in terms of the volume of tailings dumped and the magnitude of the damage.”

3 BRAZILIAN TAILINGS REGULATION

Despite a long history of mining in Brazil, including enactment of the Mining Code in 1967 and associated regulations in 1968, regulation pertaining to tailings dam safety is a relatively fresh concept in the country. The first law pertaining to dam safety went into effect in 2010, while the first one specific to tailings dams went into effect in 2012. Recently, after the Fundão tailings dam failure, significant changes to regulations pertaining to tailings dam safety have been enacted in the country. It is important to note that only tailings storage facilities (TSFs) that employ dams fall under the Brazilian dam safety regulations, and therefore the term tailings dam is used in the following sections. Specifically, TSFs developed without retention dams such as in-pit facilities or dry stack facilities do not fall under the Brazilian dam safety regulations.

3.1 Dam National Safety Policy

Though Brazil had published guidelines for dam safety since at least the 1990s (e.g., CRSB, 1999), the first dam safety policy was published in September 2010 via Federal Law No. 12,334 (Presidência de República, 2010). This law established the Dam National Safety Policy (PNSB), which applies to any dam intended to accumulate water and/or waste for any use meeting one or more of the following: (i) dam height greater than or equal 15 meters; (ii) reservoir capacity greater than or equal three million cubic meters; (iii) reservoir containing hazardous solids (according to Brazilian standards); and/or (iv) classification of medium or high with respect to associated potential damage.

Three new duties were also established as part of this law (ANA, 2018), including: organizing the National Dam Safety Information System (SNISB); promoting coordination among regulatory state dam agencies; and coordinating elaboration of a report on dam safety submitted annually to the National Council of Water Resources (CNRH).

The policy delegated supervision to various agencies based on the purpose, function and location of the dam. Table 1 summarizes the agencies responsible for dam regulation in Brazil.

Table 1. Brazilian dam regulatory agencies.

Agency Acronym	Regulatory Organization	Type of Dam
ANA	National Water Agency (<i>Agência Nacional de Águas</i>)	Water dams in national rivers
ANM*	National Mining Agency (<i>Agência Nacional de Mineração</i>)	Mine tailings dams
ANEEL	National Electric Energy Agency (<i>Agência Nacional de Energia Elétrica</i>)	Dams for power generation
Varies	State Environmental Agencies	Industrial waste dams

*Recent regulations created ANM to replace the National Department of Mineral Production (DNPM) (Jamasmie, 2017).

Law No. 12,334 set out general requirements for dam owners with respect to dam safety, including classifying dams based on risk, development of dam safety plans, and dam safety inspections and reviews. Owners had two years within the date of publication to abide by the new law.

As Law No. 12,334 was general in nature, subsequent regulation was developed to provide necessary detail. Resolution No. 143 was published by CNRH (2012) in July 2012 to establish criteria for dam classification based on risk category and potential associated damage in accordance with Article 7 of the law. In September 2012, the National Mining Agency (ANM), formerly the National Department of Mineral Production (DNPM, 2012), published Ordinance No. 416 that created the National Mining Dams Registry in accordance with Article 16 of the law. As of December 2016, 54% of the estimated 839 tailings dams located within Brazil are framed by the law (e.g., height of 15 meters or greater) and hence registered (ANM, 2018). Ordinance No. 416 also provided requirements for periodic safety reviews and regular and special safety inspections. Also, in September 2012, the law received additional complementation with publishing of Ordinance No. 526 (MIN, 2012), which specifically addresses the emergency action plan (PAE) for mining dams.

3.2 *Regulatory Changes After Samarco*

After failure of Samarco’s Fundão Dam, safety legislation for Brazilian tailings dams underwent substantial redesign. In May 2017, ANM (DNPM, 2017) published Ordinance No. 70,389, which replaced Ordinance Nos. 416 and 526.

Ordinance No. 70,389 modified the National Mining Dams Registry; revised the classification criteria for tailings dams; overhauled the emergency action plan requirements; established requirements for periodic dam safety review; and included various other modifications. Owners have until May 2019 to comply fully with the new law, but some portions required earlier action. The following sections discuss the main changes that this ordinance has regarding tailings dam safety in Brazil.

3.2.1 *Modifications to the National Mining Dams Registry*

Though the National Mining Dams Registry was established in 2012 through Ordinance No. 416, Ordinance No. 70,389 established an integrated management system for the safety of mining dams called SIGBM. SIGBM is a unique online database that provides the Brazilian mining agency (i.e., ANM) with access to key information on each registered tailings dam in the country. Owners were required to have tailings dams registered in SIGBM within 60 days after publishing of the new ordinance. Within SIGBM, each mine must designate a technical manager for their tailings dams, whose role is to:

- Register the structure, including pertinent technical data;
- Provide dam safety plan information (i.e., design, construction as-builts, operational monitoring, and audits);
- Perform inspections of the tailings dam every two weeks;
- State whether the dam is undergoing raise construction;
- Report budgetary and actual spend information; and
- Confirm stability of the structure(s) along with a third-party.

Data is uploaded into SIGBM by the mine’s designated technical manager every two weeks, upon completion of the bi-weekly dam inspections.

3.2.2 *Revisions to Tailings Dam Classification Criteria*

Since Resolution No. 143 (CNRH), a classification matrix for tailings dams has been employed in Brazil. This matrix considers two parameters, each of which are scored separately: (i) risk category (CRI); and (ii) associated potential damage (DPA).

The CRI is developed based on the technical characteristics of the facility (e.g., dam height, dam length, storm storage capacity); performance of the structure (e.g., identified structural or seepage issues); and the dam safety plan for the facility (e.g., project documentation, mine organizational structure, operating manual, emergency action plan).

The DPA addresses the potential consequences of an unwanted event, accounting for the total volume of tailings and water stored; population at risk in the downstream areas; environmental

impacts; and socio-economic impacts. Unlike other risk-based criteria that consider the population at risk in the downstream area as a function of numbers (e.g., CDA, 2013), DPA only considers whether a population exists (any number), and whether the population is temporary or permanent. Each of these parameters (i.e., CRI and DPA) are considered separately using a scorecard, resulting in classifications of “low”, “medium” or “high.” The final classification considers both parameters, as demonstrated in Table 2, whereby Class A is the highest hazard and Class E is the lowest when considering both parameters.

Table 2. Classification matrix based on risk category and associated potential damage category.

Risk Category (CRI)	Associated Potential Damage Category (DPA)		
	High	Medium	Low
High	A	B	C
Medium	B	C	D
Low	B	C	E

Of the 449 registered tailings dams in Brazil, approximately 50% are classified as high and 32% are classified as medium based on associated potential damage (DPA); however, regarding technical characteristics, a large majority (84%) classify as low risk (CRI). This relationship is illustrated in Figure 2. Currently, approximately 50% of the tailings dams registered in Brazil are Class C structures, as defined using the criteria in Table 2, with a small percentage (6% total) classifying as higher risk (Figure 3).

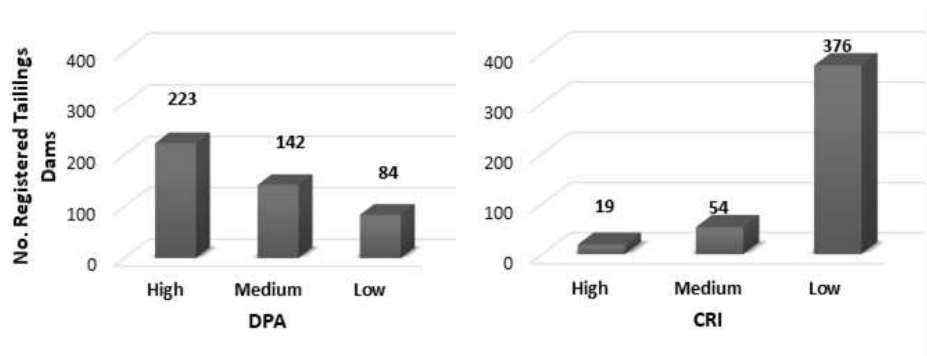


Figure 2. Tailings dam classifications in Brazil based on associated potential damage, DPA (left), and risk category, CRI (right) (created using data as of December 2016 from ANM, 2018).

As part of Ordinance No. 70,389, two additional criteria are now considered in development of the CRI category, namely dam construction method and monitoring instrumentation. Specifically, construction of a tailings dam using the upstream method (or an unknown method) penalizes the classification score as compared to downstream or single-stage dam construction, while lack of (or insufficient) instrumentation on a tailings dam also impacts the score with respect to risk. Though rumblings of banning upstream construction of tailings dams in Brazil occurred after failure of the Fundão Dam, upstream dam construction remains a permitted activity (Eisenhammer & Nogueira, 2016).

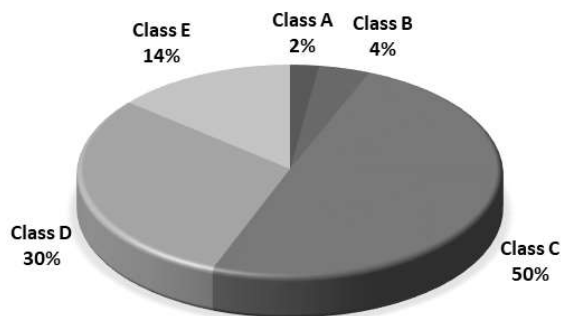


Figure 3. Brazil tailings dam overall classification (created using data as of December 2016 from ANM, 2018).

3.2.3 Enhancements to Emergency Action Planning Requirements

An emergency action plan (PAEBM) is mandatory based on the DPA category of a tailings dam and/or considering either the existence of a downstream population or if failure would result in significant environmental impact. For tailings dams with a DPA of high, a PAEBM is required; however, tailings dams that classify with a DPA of medium require a PAEBM if the score with respect to downstream population or environmental impacts is sufficiently high.

Based on dam breach analysis (i.e., a study of the hypothetical rupture of a dam) and the resulting inundation maps, a self-rescue zone (ZAS) and a secondary security zone (ZSS) is defined. The ZAS is defined as the region downstream of the dam within 10 kilometers or where the time of arrival of the flood wave is equal to 30 minutes, whichever is greater. The ZSS is the remainder of the area within the inundation zone where more time is anticipated for notification. The revised law defines the following requirements and owner responsibilities:

- Maintenance of physical copies of the plan on-site in the dam safety team office (or nearest to the structure), and at the nearby municipalities and civil defense agencies;
- When updates to the plan are required, and frequency for review;
- Training of the internal emergency action plan team at a maximum six-month interval, including maintaining relevant records of the training activities;
- Support and participation in simulated emergency situations in conjunction with neighboring municipalities, civil defense, population within the ZAS, and others involved;
- Formal designation of a PAEBM coordinator and replacement thereof;
- Definition of alert strategies, communication, and guidance to the population contained within the ZAS; and
- Deployment of an early warning system, including sirens and other appropriate mechanisms, for warning the population within the ZAS.

With the requirement for an early warning system comes the inherent obligation of the owner to not only employ staff capable of identifying an impending failure, but the responsibility to trigger the alarm.

3.2.4 Periodic Dam Safety Review Requirements

The new law mandated performance of periodic dam safety reviews (RPSBs). The RPSB is to be performed by a third-party multidisciplinary team with expertise in the disciplines associated with tailings dam safety and design. The mandated frequency for performing RPSBs is based on the DPA classification, as outlined in Table 3. Owners were obliged to complete the first RPSB by the end of May 2018.

Table 3. Frequency for dam safety review (RPSB) based on DPA classification.

Associated Potential Damage Category (DPA)	Dam Safety Review Frequency*
High	3 years
Medium	5 years
Low	7 years

*RPSBs are to be conducted at an increased frequency for tailings dams with continuous dam raising regardless of DPA.

Periodic third-party dam safety reviews (or DSRs) are considered standard practice in Canada with the frequency of review dependent on the consequence of failure of the dam. However, the Canadian Dam Association (CDA) suggests that DSRs be performed at a lesser frequency, every five years for very high to extreme consequence dams to every 10 years for significant consequence dams. After the Mount Polley tailings failure in British Columbia in August 2014, the British Columbia Ministry of Energy and Mines (BCMEM, 2017) revised their mining code to include more stringent requirements for tailings management, with DSRs to be performed at least every five years, regardless of failure consequence.

In addition to the higher frequency of third-party review as compared to Canadian guidance and British Columbia legislation, Brazilian regulation requires that even more frequent reviews be performed for tailings dams that undergo continuous construction. Such tailings dams are required to have RPSBs performed at a minimum frequency of every two years, or for every 10 meters of height increase, regardless of the DPA category.

The RPSB requires thorough review of the tailings dam, including design, construction and operations. Updated stability analyses are to be presented in the RPSB based on the as-built condition, which consider the historical time series of monitoring instrumentation (i.e., piezometric levels), hydraulic storage (e.g., flood storage), and evaluation of concurrence between design and as-built conditions. The result of the RPSB is a statement of the condition of stability (termed the Declaração da Condição de Estabilidade, DCE), which must also be declared in SIGBM.

3.2.5 Other New Requirements

With the new 2017 law, additional requirements placed on tailings dams include the following, among others:

- Real-time monitoring of installed dam instrumentation including continuous (24/7) video monitoring;
- Establishment of instrumentation alert or action levels;
- Requirement for “as built” or “as is” documentation; and
- Performance of semi-annual audits, whereby the first half audit may be performed by a company representative and the second half audit should be performed by a third-party.

The semi-annual audits also should be followed with the statement of the condition of stability (i.e., DCE) and this document must be declared in SIGBM. Without acceptable stability, the owner is required to cease use of the tailings dam until mitigation or remediation is complete. Many of the above requirements are generally considered good practice, merely formalized into regulation, such as development of as-built documentation for tailings dams and establishment of threshold levels for monitoring instrumentation. However, the requirement for real-time monitoring and continuous video goes above and beyond good practice, moving toward state-of-the-art.

4 CONCLUSIONS

Failures and incidents are often the catalyst for change, and this is particularly true as it pertains to regulation. The Samarco failure effected significant change to the regulations pertaining to tailings dam safety in Brazil. Recently, the authors had the opportunity to observe, first-hand, the state-of-the-art dam monitoring and downstream notification program that Samarco has developed, which includes such features as real-time monitoring (including video cameras), a fully-staffed control room dedicated to around-the-clock tailings dam monitoring, and an early warning system for downstream areas. In many ways, recent legislation in Brazil has followed Samarco’s

lead, adopting the same state-of-the-art measures for tailings dam monitoring that Samarco has willingly employed to ensure future dam safety and obtain the permits required to restart operations. It is important to note that state-of-the-art does not reflect state-of-practice, with Brazilian regulations including measures for tailings management that exceed that of current state-of-practice elsewhere in the world.

REFERENCES

- Agência Nacional de Águas (ANA). 2018. “The Granting of Rights to the Use of Water Resources.” Retrieved June 9, 2018, from <http://www3.ana.gov.br/portal/ANA/portal-ingles/Regulation>
- Agência Nacional de Mineração (ANM). 2018. “Classificação de Barragens de Mineração.” Database Dezembro de 2016. Retrieved June 9, 2018, from <http://www.anm.gov.br/assuntos/barragens/plano-de-seguranca-de-barragens>
- Associação Brasileira de Normas Técnicas (ABNT). 2017. *Mining – Preparation and presentation of design of tailings, sediments and/or water dams – Requirements*. ABNT NBR 13028:2017. 20 pp.
- Barbosa, F. 2015. “Worst dam accidents in Brazil’s Minas Gerais.” In Business News Americas. November 13, 2015. Retrieved June 9, 2018, from <https://www.bnamericas.com/en/features/mining/worst-dam-accidents-in-brazils-minas-gerais-state/?position=1921463>
- British Columbia Ministry of Energy and Mines (BCMÉM). 2017. *Health, Safety and Reclamation Code for Mines in British Columbia*. Revised June 2017. 365 pp.
- Brown, T.J., Idoine, N.E., Raycraft, E.R., Shaw, R.A., Hobbs, S.F., Everett, P., Deady, E.A. & Bide, T. 2018. *World Mineral Production, 2012-16*. British Geological Survey, Keyworth, Nottingham.
- Canadian Dam Association (CDA). 2013. *Dam Safety Guidelines 2007*. 2013 Edition. 88 pp.
- Carmo, F.F., Kamino, L.H.Y., Junior, R.T., Campos, I.C., Carmo, F.F., Silvino, G., Castro, K.J.S.X., Mauro, M.L., Rodrigues, N.U.A., Miranda, M.P.S. & Pinto, C.E.F. 2017. “Fundão tailings dam failures: the environment tragedy of the largest technological disaster of Brazilian mining in global context.” In *Perspectives in Ecology and Conservation*. 15. 145-151.
- Conselho Nacional de Recursos Hídricos (CNRH). 2012. “Resolução N° 143, de 10 Julho de 2012.”
- Comissão Regional de Segurança de Barragens (CRSB). 1999. *Guia Básico de Segurança de Barragens*. Núcleo Regional de São Paulo.
- Departamento Nacional de Produção Mineral (DNPM). 2001. “Portaria N° 237, de 18 de Outubro de 2001.” Adopting regulatory standards contemplated in Article 97 of Law N° 227 dated 28 February 1967.
- Departamento Nacional de Produção Mineral (DNPM). 2012. “Portaria N° 416, de 03 de Setembro de 2012.” Revoked and replaced with Portaria N° 70.389.
- Departamento Nacional de Produção Mineral (DNPM). 2017. “Portaria N° 70.389, de 17 de Maio de 2017.”
- Eisenhammer, S. & Nogueira, M. 2016. “Brazil mining dam reforms unsettle companies, do little for safety.” May 11, 2016. In Reuters. Retrieved June 9, 2018, from <https://www.reuters.com/article/us-brazil-damburst-safety-idUSKCN0Y21PH>
- Invest In Brazil. 2018. Mining Industry. Retrieved June 9, 2018, from <http://www.investinbrazil.biz/industry/mining/mining-industry>
- Jamasmie, C. 2017. “Changes to Brazil mining law to bring mostly higher taxes, cost – experts.” In MINING.com. August 18, 2017. Retrieved June 9, 2018, from <http://www.mining.com/changes-to-brazil-mining-law-to-bring-mostly-higher-taxes-costs-experts/>
- Jamasmie, C. 2018. “Brazil’s President to change mining regulations as early as next week.” In MINING.com. June 7, 2018. Retrieved June 9, 2018, from <http://www.mining.com/brazils-president-to-change-mining-regulations-as-early-as-next-week/>
- Machado, I.F. & Figueirôa, S.F.M. 2001. “500 years of mining in Brazil: a brief review.” In *Resources Policy*. 27. 9-24.
- Ministério da Integração Nacional (MIN). 2012. “Portaria N° 526, de 6 de Setembro de 2012.”
- Presidência de República. 2010. “Lei N° 12.334, de 20 de Setembro de 2010.”
- Reuters, 2010. “Brazil bauxite mine closed after dam burst.” January 21, 2007. Retrieved June 9, 2018, from <https://www.reuters.com/article/idUSN10315283>
- Ronald, E. 2016. “Niobium in a Nutshell.” In Mining Geology. May 28, 2016. Retrieved June 9, 2018, from <http://www.mininggeologyhq.com/niobium-in-a-nutshell/>
- WISE Uranium Project. 2018. *Chronology of major tailings dam failures*. Retrieved June 9, 2018, from <http://www.wise-uranium.org/mdaf.html>

Design Considerations for Distributed Tailings Deposition Systems

J. Stowe, R. Cooke & I. Farrell
Paterson & Cooke USA, Golden, CO, USA

R. Martinson
Paterson & Cooke Chile, Santiago, Chile

ABSTRACT: High-density thickened tailings applications are becoming more prevalent in the interest of water savings to mitigate environmental concerns and meet corresponding increasing regulations. Among the many challenges with high density thickened tailings is the delivery and subsequent distribution within the tailings storage facility to meet geotechnical requirements related to storage capacity optimization and beach slope formation.

Achieving evenly distributed discharge, often over long distances, is needed to meet geotechnical requirements while also accommodating process variability. These criteria present unique hydraulic design challenges for tailings distribution systems. Due to the typical rheological nature of high density thickened tailings, inadequate design of these systems can result in laminar pipeline flow conditions and coarse-particle segregation leading to pipeline blockage. This paper summarizes the challenges, proposed hydraulic design approach and operational issues for distributed tailings deposition systems. Two case studies of recently implemented systems are discussed.

1 INTRODUCTION

High-density thickened tailings systems are often targeted in design to achieve water savings goals such as minimizing make-up water costs and to satisfy associated regulations. These types of systems, generally, are in the 60% to 70% solids concentration range and the fully-sheared slurry yield stress range of 30 to 60 Pa (Bazan, et al 2017). Often these high-density thickened tailings systems are associated with the objective of increasing the tailings beach slopes in the tailings storage facility (TSF) to increase storage capacity and reduce water losses.

The targeted beach slopes are best achieved using a distributed tailings deposition system comprising multiple simultaneously operating discharges which are spaced sufficiently far apart to ensure the individual discharges do not combine on the beach (McPhail, 2018). The system must accommodate the inherent variability in process conditions and tailings properties (Martinson, et al 2015). A typical flow diagram of a distributed tailings deposition system is shown in Figure 1. The system features are the primary delivery pipeline, the distribution pipelines and widely spaced, simultaneously operating discharge spigots. A typical arrangement is provided in Figure 2. The system achieves the required beach slopes for tailings slurries with moderate rheologies reducing the degree to which the tailings must be dewatered. While the system has been developed for high-density tailings, it also has application for moderately thickened tailings where beach slopes of around 2% can be achieved.

This paper describes the design challenges and proposed approach to the hydraulic design of distributed tailings deposition systems including two case studies where the approach has been successfully implemented for high-density tailings applications.

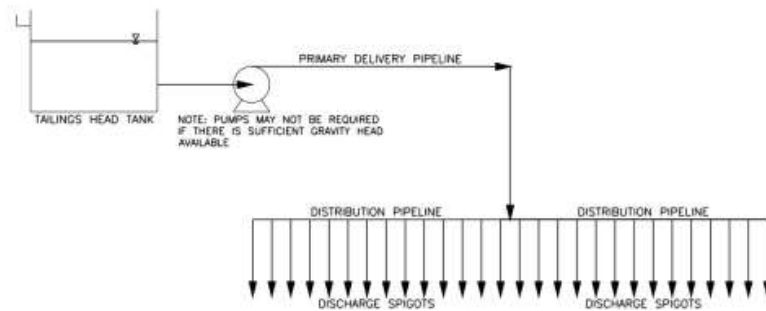


Figure 1. Typical distributed tailings deposition system.



Figure 2. Typical arrangement, with widely spaced, simultaneously operating discharges.

2 HYDRAULIC DESIGN CHALLENGES AND APPROACH

The hydraulic design of a distributed tailings deposition system needs to consider the following factors:

- Achieving approximately equal flow rates through the simultaneously operating spigots,
- Ensuring the operating velocities are high enough to minimize particle settling and the consequent risk of pipeline blockage,
- Accommodating variable process conditions (throughput, solids concentration and slurry rheology).

2.1 Equal Flow Rate Over Spaced Discharges

A key requirement of the system is to achieve equal flow rates through multiple simultaneously operating spigot discharges. The methods to determine the target flow rate per spigot and discharge spacing is dependent on the geotechnical requirements of the TSF (McPhail, 2018). Depending on the topography and design of the TSF, these operating discharges may span relatively long distances, on the order of one to two kilometers.

In a typical spigot discharge arrangement, assuming equally sized spigots with no other appurtenances, the flow rate through the spigots decreases from the furthest upstream discharge to the last as the head (energy) in the distribution line decreases. To equalize the spigot discharge flow rates, flow control in the form of a localized head loss is required upstream of the spigot. The required head loss for each spigot is established by applying an energy balance along the distribution line as shown in Figure 3.

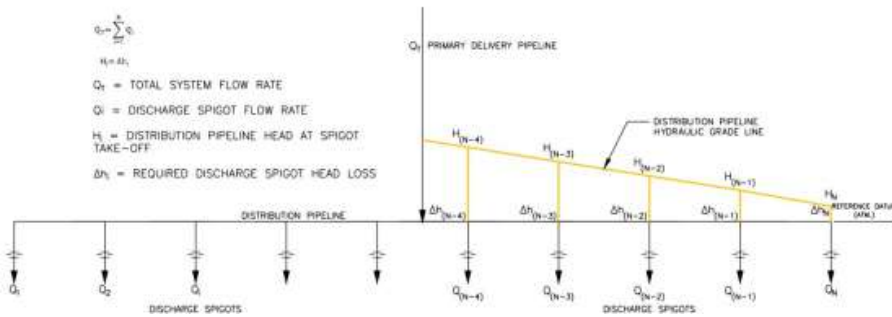


Figure 3. Example to determine flow control requirements for each spigot.

Once the head loss requirements are known for each spigot the control element can be selected and sized. There are several options available to provide flow control for each spigot including:

- Modulating slurry-rated valves, such as pinch valves,
- Small bore orifice plates, and
- Using small diameter spigot piping of varying lengths to act as a “choke”.

Each of the above alternatives has advantages and disadvantages. Consideration should be given to the capital and operating costs, maintenance requirements, potential component wear and preferred level of operator interaction.

2.2 Maintaining Sufficient Operating Velocities

As with most slurry pipeline designs, the operating velocity should be greater than the velocity at which deposition will occur to avoid the risk of pipeline blockage. This minimum required velocity is based on either the turbulent deposition velocity or laminar-turbulent transition velocity. A typical slurry pipeline operating envelope plot is shown in Figure 4 which highlights:

- Minimum velocity requirements over a range of concentrations and process conditions for a single pipe size,
- The acceptable operating region above minimum required velocity, and
- How the reduction in flow rate from upstream to downstream spigots can violate the velocity requirement if the header is a single pipe size.

While operating tailings pipelines below turbulent deposition velocity is becoming more common (Cooke, 2018), laminar flow operation of tailings is not well understood and consid-

ered high risk due to the potential of laminar flow coarse particle segregation (Cooke, 2002). To achieve sufficient velocities, the distribution pipeline size is reduced along the length.

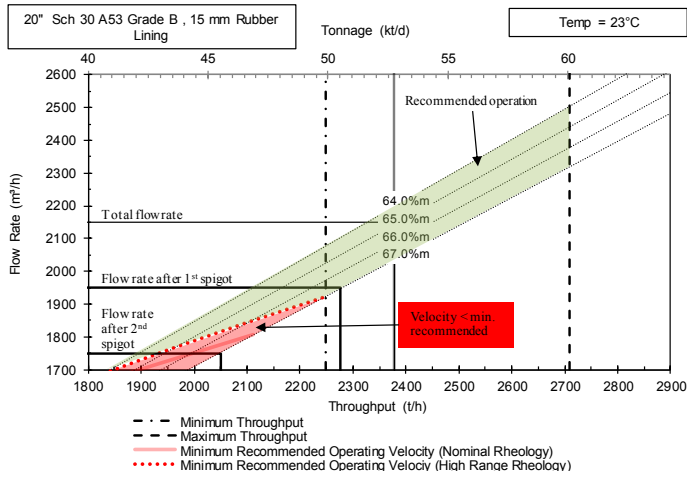


Figure 4. Typical pipeline operating envelope illustrating reduction in flow rate in single pipe size.

2.3 Variability in Process Conditions and Tailings Rheology

Tailings delivery and distribution systems are subject to inherent throughput and solids concentration ranges. A robust system design must account for and accommodate this variability. Slurry rheology, specifically yield stress, is an important property for the design of high-density thickened tailings systems as it, along with slurry density or concentration, determines laminar-turbulent transition velocity. For slurry transport in the yield stress range typical of high-density thickened tailings, laminar-turbulent transition velocity is the often the limiting minimum velocity. Figure 5 provides an example for the range of slurry yield stress as a function of both concentration and source of tailings. In this example, the slurry yield stress can vary from 11 Pa to 32 Pa in the range of 64%*m* to 67%*m*. The resulting laminar-turbulent transition velocity range is 1.6 m/s to 2.7 m/s. This variability presents a challenge in terms of sizing the flow control elements and distribution pipelines. Due to the process and slurry property variability some tolerance must be given to the equal flow rate criterion.

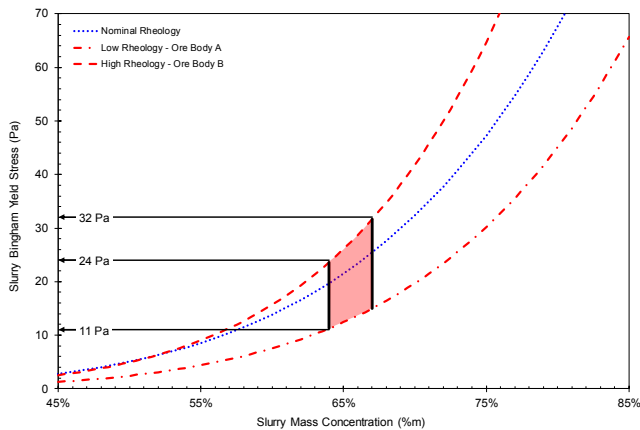


Figure 5. Example of ore body-based slurry rheology variability.

3 IMPLEMENTATION (CASE STUDIES)

The following case studies provide examples of full-scale implementation of the proposed approach. The two case studies were designed to ultimately assist in improving the tailings deposition beach slope to increase tailings storage capacity. The pipelines were designed to achieve near-equal flow rate through multiple simultaneously operated discharges, over lengths of greater than one kilometer.

3.1 Case Study 1

Case Study 1 is a 105,000 t/d copper mine in South America. High-density thickened tailings are delivered via a pumped pipeline system with a solids concentration range of 64% to 67%_m (Martinson, 2015). The distribution pipeline length needed to meet the geotechnical requirements was 1620 m and with 28 discharges spaced at 60 m. The distribution pipeline was designed with pipes ranging from 355 mm to 125 mm selected to ensure turbulent flow along the entire length. The use of orifice plates as the flow control element was preferred in this case due to capital and operating costs, as well as requiring less operator interaction. The orifice bore diameters ranged from 70 mm to 88 mm. Figure 6 shows one of the fabricated orifice plates prior to installation in the 125 mm spigot piping.

Knife gate valves were selected to isolate each spigot, with the orifice plates installed immediately downstream as illustrated in Figure 7. During startup and commissioning of Case Study 1, flow distribution issues were encountered. The cause of this issue was discovered when one of the installed spigot configurations was unbolted. Tramp material from the plant was being transported in the tailings system. Because the orifice bore diameters are relatively small, this tramp material was partially blocking the orifice bore and influencing the flow control characteristics. Grizzly screens were installed upstream of the tailings pumps to remove this material as shown in Figure 8. Following this modification, the system achieved its targets and the beach slope increased from 0.5% pre-implementation to 2.0% to 3.6% post-implementation.



Figure 6. Typical orifice plate for spigot installation at Case Study 1.

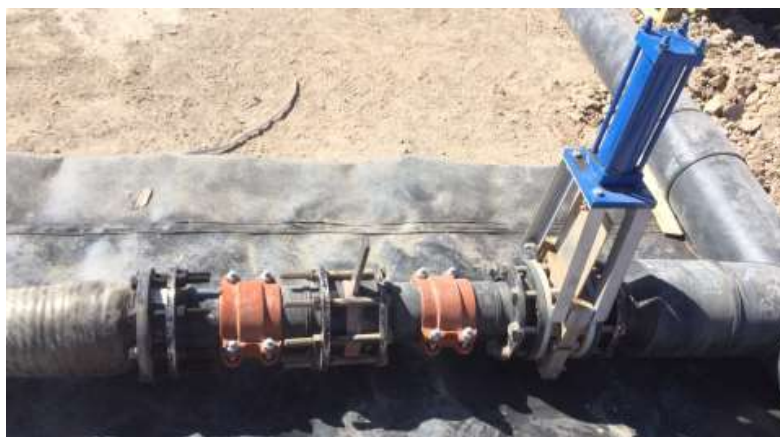


Figure 7. Typical spigot arrangement for Case Study 1.



Figure 8. Examples of tramp material at installed grizzly screen that was previously causing partial orifice bore blockage.

3.2 Case Study 2

Case Study 2 is a 114,000 t/d copper mine in South America. Tailings are delivered via a gravity fed, pressurized, pipeline system with a solids concentration range of 58% to 62%*m*. The distribution pipeline length needed to meet the geotechnical requirements was 1265 m and with 28 discharges spaced at 55 m. The distribution pipeline was designed with pipes ranging from 450 mm to 280 mm selected to ensure turbulent flow along the entire length. The use of orifice plates as the flow control element was also preferred in this case due to capital and operating costs, as well as needing less operator interaction. The orifice bore diameters ranged from 73 mm to 108 mm.

Knife gate valves were selected to isolate each spigot, with the orifice plates installed immediately downstream as illustrated in Figure 9. Drain valves were added to the spigot arrangement to assist maintenance operations, also shown in Figure 9. On a portion of the installed distribution pipeline, pressure transmitters were installed to assist operations and the engineers validate the system and orifice plate performance over time, shown in Figure 10. The system achieved its targets and the beach slope increased from 0.5% pre-implementation to 2.6% to 3.3% post-implementation.

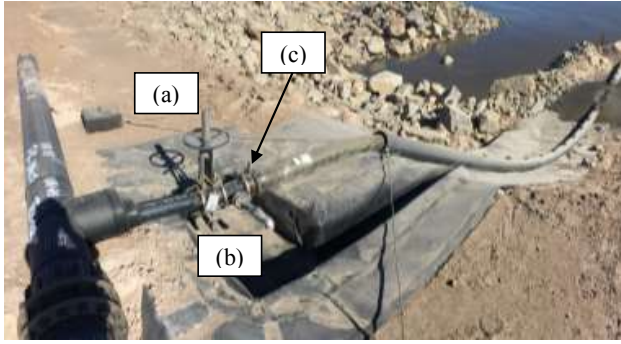


Figure 9. Typical spigot arrangement at Case Study 2 showing (a) spigot isolation, (b) spigot drain and (c) spigot orifice plate.



Figure 10. Typical spigot arrangement at Case Study 2 showing pressure instrumentation upstream and downstream of take-off.

3.3 Summary

The two case studies illustrate the implementation of the proposed design approach in full-scale applications. The use of the proposed approach has allowed the operations to achieve the objectives of near-equal flow through the widely spaced discharge spigots while maintaining the minimum requirements for robust slurry transport over a range of slurry properties and process conditions. This approach has helped to enable the operations to improve the tailings beach slope and increase the facility storage capacities. Table 1 below provides a summary of the two applications, including the approximate change in tailings beach slope achieved.

Table 1. Case Studies Summary

Item	Case Study 1	Case Study 2
Nominal throughput (t/d)	105,000	114,000
Delivered tailings concentration (%m)	64% to 67%	58% to 62%
Slurry yield stress (Pa)	35 to 55	11 to 17
Distribution pipeline length (m)	1620	1265
Number of simultaneous discharges	28	28
Discharge spacing (m)	60	55
Distribution pipe size range (mm)	355 to 125	450 to 280
Spigot pipe size (mm)	125	280
Delivery system type	Pumped	Gravity pressure
Pre-implementation tailings beach slope	0.5%	0.5%

Post-implementation tailings beach slope 2.0% to 3.6% 2.6% to 3.3%

4 CONCLUSIONS

Distributed tailings deposition systems allow for the development of reasonably steep beach slopes without incurring the high cost of dewatering and transporting tailings with high yield stresses. This paper presents a design approach which addresses the challenges of near-equal flow rate from widely spaced, simultaneously operating spigot discharges, maintaining turbulent flow over a wide range of pipeline conditions, slurry properties and rheology variability. The proposed design of this type of high-density thickened tailings system has been successfully implemented at the two case studies presented.

REFERENCES

- Bazan, I., Eriz, G., Martinson, R. & Bello, F. 2017. Tailings Distribution Systems Operating with Spigots Discharges: Design and Practical Considerations. *4th International Seminar on Tailings Management, Santiago, 12-14 July 2017*.
- Cooke, R. 2002. Laminar Flow Settling: The Potential for Unexpected Problems. *Hydrotransport Seminar HT15, Banff, Canada*.
- Cooke, R. & Stowe, J. 2018. Developments in Tailings Pipeline Transportation. *5th International Seminar on Tailings Management, Santiago, 11-13 July 2018*.
- Martinson, R., Engels, J. & McPhail, G.I. 2015. High Density Thickened Tailings - New Design Challenges in Transportation and Deposition. *3rd International Seminar on Tailings Management, Santiago, 19-21 August 2015*.
- McPhail, G.I. 2018. Beach prediction experience to date: further development and review of the stream power-entropy approach. *21st International Seminar on Paste and Thickened Tailings, Perth, 11-13 April 2018*.

Guidance for the Safe and Optimized Operation of Waste Rock Facilities

J.A. Vides, L. Piciacchia, and V. Marefat

BBA Inc., Mine Waste Management and Environment, Montreal, Quebec, Canada

ABSTRACT: Failure of Waste Rock Facilities (WRF) can be a major concern because it can put human life and surrounding environment at extreme risk. As such, waste rock piles should be considered structures, and rigorous attention should be afforded in design and operation of WRF. Selecting an appropriate operational strategy can greatly lessen the risks involved. The important aspects in the operational phase of a WRF, which impact the stability, include the use of appropriate design criteria, waste material segregation, and rate of deposition, operational load, operational manual, deposition plan and instrumentation. This paper discusses, in detail, the importance of operational parameters and how these can be controlled to reduce the overall risk associated with such facilities. It further discusses the importance of integrating design into deposition plans, the use of operational manuals to document good operating practices and the supervision of ongoing operations.

1 INTRODUCTION

Waste rock storage facilities (WRSF) are large, massive structures constructed over the course of the life of a mining project. These structures are part of mining environments, landscaping, and layouts; instabilities in these structures can impact critical nearby mining infrastructure, equipment and personnel as well as the surrounding environments including lakes, streams and rivers.

Despite the significance of these structures it is common practise to treat them as dumps, with very little effort allocated to design, engineering, construction, supervision and monitoring, stockpiles deposition planning, site characterization or operations. Those typically charged with the operations of these facilities are also held accountable for the economical and profitable exploitation of the mining operation, thus these facilities risk being treated as cost generators with little focus on the long term liabilities that these WRSF can represent to the mining company.

The result of this type of approach and philosophy towards wasterock facilities has resulted in numerous failures. Between 1968 and 2005 in excess of 200 incidents of wasterock facility failures were recorded in BC (Canada) alone. The magnitude of these failures is variable from minor runouts and up to 30Mm³ of material (Cunning and Hawley, 2017). This data is based on a commissioned study in BC and represents a mere sampling of the number of failures that could be expected across Canada and the rest of the mining community.

Despite the compelling reported data, which has been know and documented as far back as the early nineties, not all operators acknowledge the need to treat these facilities as structures. Thankfully some jurisdictions have adopted design criteria which will compel operators to design and operate these facilities as structures.

If one considers, WRSF as structures, standardization of procedures will be required. This will include design, construction, operation and monitoring. This paper discusses some of the key elements which need to be incorporated in standardized procedures.

2 STANDARD PROCEDURES

2.1 *Design criteria*

WRSF that are considered and operated as simple dumps, do not required any form of design. In a best case scenario, a factor of safety of 1.0 will most certainly be achieved (on a competent foundation) with descending construction methods. Any variability in the material properties or an increase in water table elevation within the pile can give rise to instability. Operating in this manner can put WRSF at risk and outside of compliance.

Regulators have already recognized WRSF as structures and have applied the same level of regulation as those governing tailings management facilities, which include design criteria for bearing capacity, short and long term local stability, and short and long-term static and pseudo-static overall stability.

Factors of safety as defined by regulators accounts for risk and uncertainty, as such it is more stringent than just attempting to maintain equilibrium, relying solely on material properties to avoid instabilities. The design of stockpile needs to be based on long-term facility closure requirements rather than short term operational conditions.

2.2 *Rate of advancement*

In many operations the common practice is to operate WRSF based on cycle's times between waste stockpiles and pit operations. This practice continues until the mining operation moves to a new area of the pit or a failure occurs, and only then will the deposition proceed in a different sector.

This trial and error approach is not acceptable for ensuring short-term stability of structures. For example, the rate of rise when building a dam over soft clay is strictly controlled, to account for increases in pore water pressure; the same principles need to be applied when advancing a waste stockpile. The common practice described, for WRSF, is not consistent with the concept or philosophy that WRSF are considered structures by operators.

The rate of advance can affect stability both of the foundation and the pile itself. With respect to the foundation, the example given above with the rate of loading of a clay layer during dam construction applies equally to the advance of a stockpile over the same stratigraphic unit. Advance too quickly and you risk failure in the foundation clay layer.

It is noted that granular materials also need time to settle when being deposited, if such settlement occurs too quickly failure and instability can ensue. Several cases of failures have reportedly occurred as result excess of rate of advance regardless of the foundation condition.

Incorporating rate of advance within the operation of a WRSF can be logistically challenging. Mine sites will often be operating more than one pit within the same site and multiple waste stockpiles simultaneously. Some waste stockpiles are dedicated to specific pits, while others are shared between pits, thus increasing the level of complexity, as illustrated in Figure 1. The complexity is further increased if a decision is made to segregate wastes (e.g. fine and coarse), creating additional waste streams.

The stability of a waste rock pile is influenced by several parameters such as the geometry of the pile, the quality of the materials, the climatic conditions and the materials comprising the foundations. However, several cases of historical failures show that they are closely related to the height and rate of advance of the pile. During deposition of waste rock, it is important to evenly distribute the materials on the crest, allowing materials (foundation and/or stockpile) to settle and consolidate naturally.

On sloping ground the rate of advance will change over time as the height of the pile increases. Proper intervals for reassessment of the rate of advance should be established for each pile. The length of the deposition front can be varied to compensate for a reduction on rate of advance should the volume to deposition remain constant. This is illustrated in Figure 2.

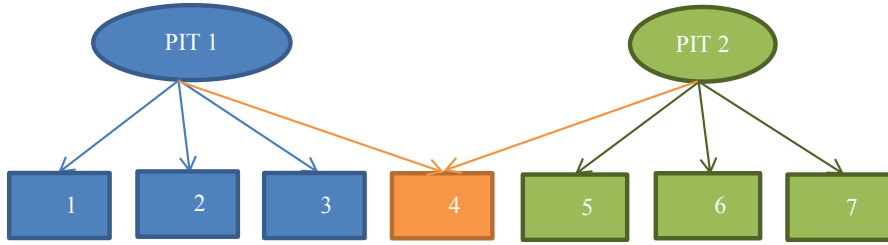


Figure 1. Scheme of a mine operation considering 2 pits and 7 deposition areas

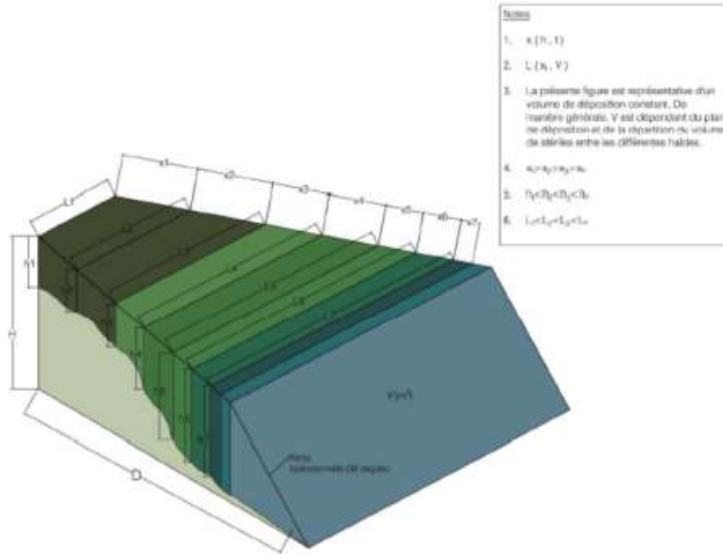


Figure 2. WRSF construction parameters and advancement rate (figure to be translated)

As an example, a multi-variable graph was prepared for a coarse waste material deposited on a medium quality foundation. The graph is shown Figure 3, and provides a rate of advance and resulting volume per linear meter at the deposition front, for a range of heights between 70m and 250m.

When managing multiples stockpiles, with one or multiple waste streams, taking into account the rate of advance, can be logistically challenging. Equation 1 below can be used for each of the waste streams. The total volume (Vt) should be balanced to the overall volume being handled at a particular time. In the mine scheme shown at Figure 1, if a rate of advance is a constraint to placing the required volumes at a particular time, the length of the deposition front should be increased.

$$Vt = \sum_{x=1}^n Vx * Lx \tag{1}$$

Where:

- H_x = Height (m) of a particular pile
- n = number of stockpile in construction at a given time, t
- V_x = Volume per linear meter of deposition front advance (m³ / lm)

L_x = Length of the deposition front crest (m) of a particular stockpile advanced at a given period, t

V_t = total volume of material to be deposited per day for a given period, t

n, L_x and V_t are time dependent and, as such, become the key parameters required to establish an operational deposition plan.

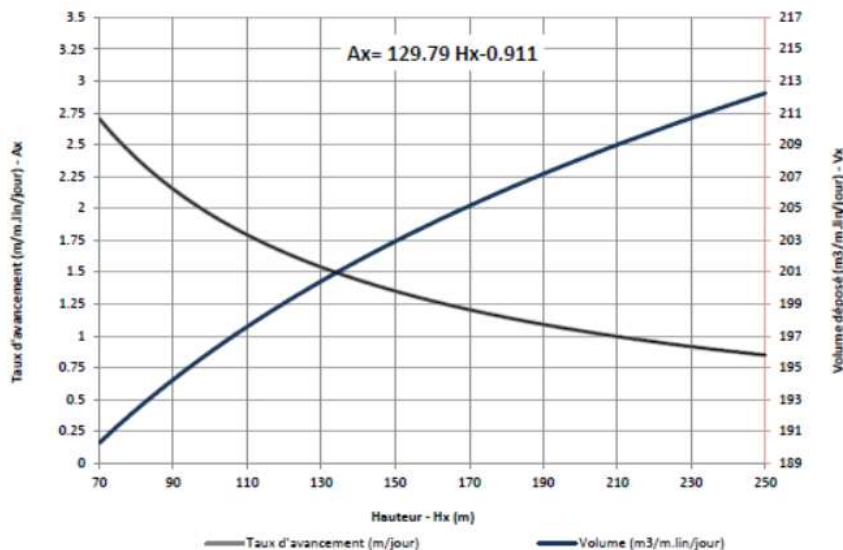


Figure 3. Coarse WRSF – Relation between stockpile height and advancement rate (to be translated)

2.3 Segregation

Material types entering the WRF can vary over time. Given the marked difference between the angle of internal friction of fine and coarse waste rock, it is generally recommended to deposit these materials in separate stockpiles. From a design perspective this will eliminate or reduce input design parameter variability.

Experience has shown that at times (i.e. during a push-back on a pit wall) larger quantities of fine grained waste will likely be generated. If these materials are placed over the face of a coarse grained waste, which are also free draining, water levels within the stockpile will rise. The rising water levels can initiate a failure, particularly in the finer material. This has been modeled, and shown in Figure 4.

Where smaller quantities of fine grained material are produced alternatives using free dumping techniques remain a possibility. The management of fine materials can be accomplished by various means. They can continue to be managed in separate stockpiles or by a designed co-deposition. Managing the fine material in separate stockpiles may not be cost effective if small quantities are involved. A proper co-deposition method offers some advantages with respect to cycle times and overall simplification to planning and coordination. It can also ensure the stability of the stockpile. In this example, we present a co-deposition method in which the fine materials are deposited in separate layers within the stockpile body between coarse materials and maintaining setbacks from the slope crest. Figure 5 shows a possible configuration using free dumping of fine material within a coarse stockpile. Figure 6 illustrates the resulting 3D seepage model of the configuration and shows that will proper design the water table within the stockpile can be kept low.

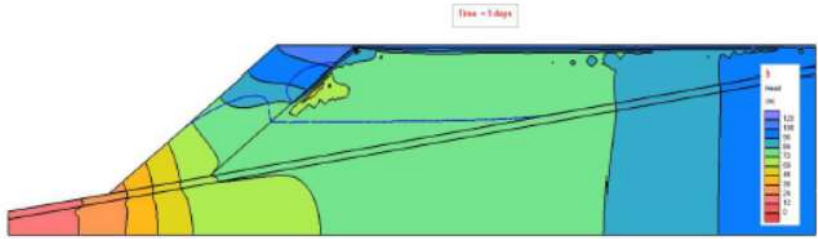


Figure 29. Nappe phréatique dans une HSG ($k_{sat}=1 \times 10^{-4}$ m/s) avec une face en matériaux fins ($k_{sat}=1 \times 10^{-7}$ m/s)

Figure 4. 2D Seepage model- Fine grained material over the face of a coarse grained stockpile (Piciacchia et al., 2018a)

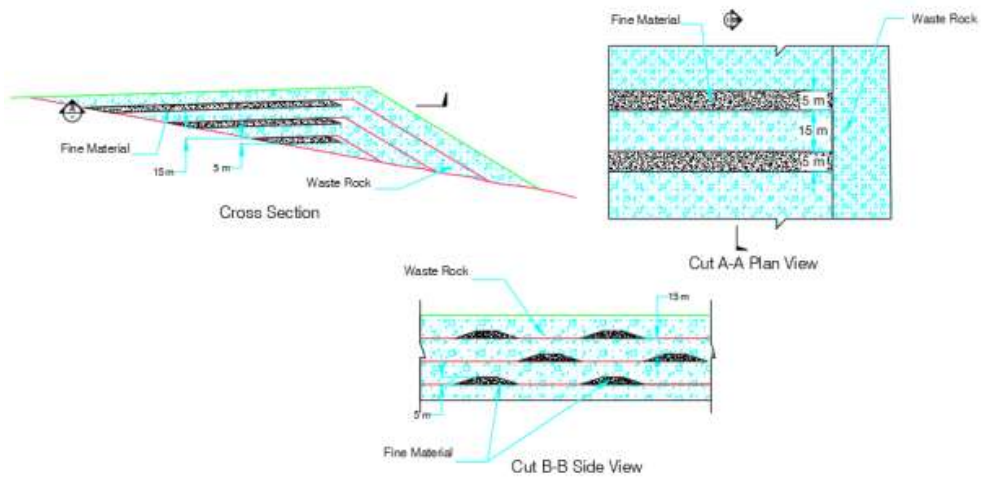


Figure 5: Cross-section, plan and side view for the proposed co-deposition method (Piciacchia et al., 2018a)

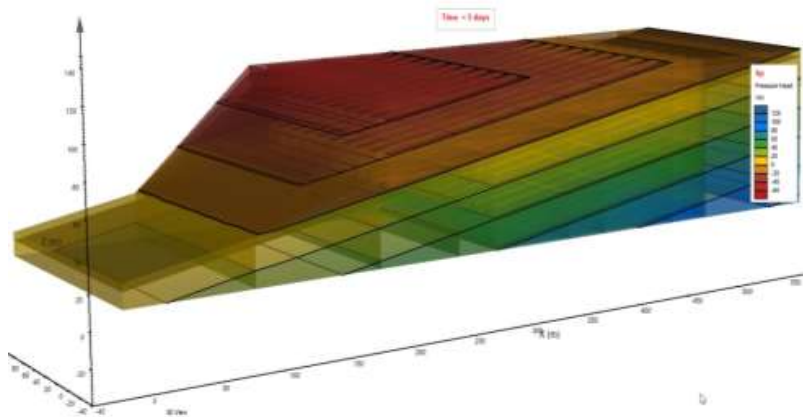


Figure 6: 3D seepage analysis result (Piciacchia et al., 2018a) (Figure to be upgraded)

2.4 *Depositions plans*

WRSF are complex structures whose operating criteria change over time, including the quantity and quality of materials to be managed at a specific time. In addition, the construction of these structures must be harmonized with all other mining and engineering activities. As such, waste rock deposition plans are essential management tools that orient mining operations. They allow operators to evaluate and prioritize, proactively, the design and construction needs aligned with the mine plan.

It is recommended to prepare deposition plan, for various stages of the mine life. These plans should be updated in a regular basis as recommended below:

- Long term considering closure prediction: updated each 5 years;
- Short-term (5 years horizon) considering global planning: updated annually;
- Immediate-term (1-2 years horizon) for operational purposes: updated annually.

Should significant changes occur in the operation, the impact on the deposition plans must be evaluated at that time. This process is similar to that which is undertaken for TMF.

2.5 *Operation Manual*

The Operation, Management and Safety (OMS) manual allows for the clarification of individual responsibilities, decision-making processes, guidelines for design and possible modifications, instrumentation, monitoring and the development of environmental protection measures and emergency plans for the WRF. Operational guidelines must take into account both long-term and short-term operational needs. The operating manual is a master document that standardizes the operating procedures at the mine and should be updated to include any changes in the operation. The implementation and application of an OMS manual has a direct impact on the long term continuity and performance of the WRF overtime. An OMS manual should cover as a minimum the following management categories:

- Roles and responsibilities: the organisational structure should be described with the overall responsibility being clearly identified. The level and frequency of training required for individuals entrusted with the facilities should also be documented. Personnel turnover and revised staff assignments will require this section of the document to be updated on a regular basis. This section may also include the nomination of an engineer of record to ensure compliance with design criteria and operating standards;
- Facility description: this section of the manual aims to put a framework for the WRSF. A detailed description of the facility, as well as maps, layouts, and plans showing detailed information of the facility are required. Historic data with regards to topography, environment, and other baseline information must be recorded and organized in such a document. Design reports, construction drawings, as-built drawings, construction reports, and all documents related to the development of the facility must be maintained.
- Construction and operation: this section should include a description of the mine plan under which the WRSF is to be operated, including the details of the deposition plans, aligned with the exploitation plan. In addition, it should include chapters which cover environmental protection, risk management, health and safety, snow management (if applicable) instrumentation and inspection, foundation preparation, waste classification and management, and water management. This provides a brief list of some of the key element that should be include, mine operators should tailor the list of operational KPIs which they deem most appropriated for their operation.

3 CONCLUSION

This paper has attempted to demonstrate some key changes that need to be implemented as WRSF go from being considered simple dumps to engineered structures. Regulation established by legislators demonstrates their recognition that WRSF are in fact structures. Thus they need to be designed and managed as such.

WRSF are by the nature of the waste streams, which vary in quantity and quality over time, are more complex, from a management perspective, than TMF. In addition, the number of failures, albeit less consequential, which had been recorded during the past 40 years in BC alone far surpasses the high profile failures in tailings facilities over the same period. Yet the amount of rigor presently employed in the design and operation of WRSF is significantly less than with TMF design. Recognition of these facilities as structures will change the approach to their design, planning and operation.

4 REFERENCES

- Hawley, Mark, and John Cuning 2017. Guidelines for Mine Waste Dump and Stockpile Design.
- Piciacchia, Luciano, Marefat, Vahid and Mosquera, Jenyfer, 2018. The use of 3D models and analysis in support of waste stockpile design and operations. *18th Tailing and Mine Waste Conference, The Department of Civil and Environmental Engineering at Colorado State University.*

Leading versus Lagging Indicators of Tailings Dam Integrity

J. Boswell and J. Sobkowicz

Thurber Engineering Ltd., Calgary, Alberta, Canada

ABSTRACT: Despite the best efforts of the international tailings community, experience over the past decades and in the last five years in particular, has shown that tailings dam failures continue to occur. The consequences of these failures and the likelihood of future failure do not show an improving trend. Those owners, operators, engineers, regulators and reviewers tasked with the responsibility of monitoring, surveillance and review of tailings dam integrity can benefit from the introduction of alternative tools for tracking dam safety: the use of leading rather than lagging indicators of dam integrity. Alternatively, is it possible to predict failure, rather than waiting for it to happen? Could we be more forward looking and anticipative in our vigilance, and if so how? This is particularly important for those structures where the risk profile increases with time. This paper proposes a shift in emphasis for tailings engineering practice to place more weight on leading indicators of dam structural integrity.

1 INTRODUCTION

Over the past four years three significant dam incidents have served to highlight new attention to dam integrity: the Mount Polley tailings breach on August 4, 2014 in British Columbia (Morgenstern et al, 2015); the failure of the Fundão tailings dam which resulted in the loss of 19 lives in Brazil on November 5, 2015 (Morgenstern et al, 2016); and the evacuation of nearly 200,000 people in response to a spillway failure of the largest water dam in the USA, Oroville Dam, California, in February 2017 (Wikipedia, 2017).

These incidents and other dam and tailings breaches have led to a substantial revision of legislation and regulation (such as in British Columbia, BC MEM 2017, 2016; EGBC, 2016a and in preparation in Alberta, Canada), and dam safety guidelines and bulletins, (CDA 2016, MAC 2017). Standards of leading practice in the design, construction and operation of tailings facilities have also improved. Increased attention and vigilance is being focused and there is no doubt that published standards of dam safety are rising.

However, despite the best efforts of the international tailings community, experience over the past decades and in the last five years in particular, has shown that tailings dam failures continue to occur. The consequences of these failures, and the likelihood of future failure do not show an improving trend – at least not sufficiently, or fast enough. Over the past 12 months we have witnessed two more dam failures involving fatalities in Mexico (Reuters, 2018 - La Cieneguita Mine tailings failure - 7 fatalities) and Kenya (CBC, 2018 - Patel water dam, Kenya - 47 fatalities).

This is not acceptable at a societal level and should not be acceptable within the engineering profession. Senior professionals must exert leadership to effect change.

2 WHY ARE FAILURES STILL OCCURRING?

Based on a reading of published accounts of recent failures and industry experience, the following factors appear to be relevant:

2.1 *Unregistered dams*

On May 9, 2018 an unregistered water dam in Kenya failed (CBC, 2018), with disastrous consequences. In all, 47 lives were lost. The tailings failure which occurred at Obed Coal Mine on October 31, 2013 (Wikipedia, 2018) was from an unregistered dam, from which 600,000 m³ of coal tailings slurry entered the Athabasca river.

2.2 *Poorly informed dam owners and management*

As a result of concern about small dam owners and single dam owners in Canada, over the past year the presidential theme for the Canadian Dam Association has been to promote and broaden the awareness of dam safety and risks to all owners of dams. At the CDA annual conference in Kelowna, B.C. in October 2017, an entire parallel stream of conference technical sessions raised awareness among small dam owners and single dam owners.

2.3 *Insufficient professional engineering involvement*

The Merriespruit tailings failure in 1994 in South Africa (Wagener et al, 1997) led to the loss of 17 lives from a supposedly dormant tailings dam into which unsupervised tailings deposition had continued to occur. The dam was not licensed, not under the supervision of a professional engineer, and not actively monitored.

While the efforts of professional engineering institutions and regulators continue to raise standards in this regard, failures of dams with little or no engineering involvement continue to occur.

Leading jurisdictions now specify requisite levels of qualification for the Engineer of Record (EOR), Designer of Record (DOR) and other positions of dam safety leadership (Boswell and Martens, 2017).

2.4 *Absent or insufficient dam safety laws and regulations*

At the two-day workshop held in San Antonio, Texas in October 2017, “Lessons Learned from Recent Tailings Failures” convened by the US Society on Dams and the Association of State Dam Safety Officials (USSD, 2017), it was concluded that the regulation of tailings facilities across the USA was insufficient and inconsistent between states, and that more attention was needed in order to avert future tailings dam failures in the USA.

After the Mount Polley Failure, new legislation was introduced in British Columbia, (BC MEM 2017, 2016; EGBC, 2016a; MFLNRO, 2010) which in the opinion of the authors of this paper now represents the highest published standard of tailings dam regulation in current practice, worldwide.

In Alberta, Canada the existing Water Act is being strengthened in regard to dam safety (Boswell and Martens, 2017).

In the aftermath of the Merriespruit tailings breach in 1994, a South African mining guideline for mine waste disposal was substantially updated (Chamber of Mines, 1996), and a code of practice was introduced for tailings management (SABS, 1998).

However, many countries and regions continue to allow mining with insufficient regulation of tailings dam safety.

2.5 *Insufficient or untrained regulators and inspectors*

In Alberta it has now been recognized that inspection of dams with a higher safety consequence classification requires more advanced skills of regulatory inspectors (Eaton, 2017). In particular, dams with a classification of High or more, as classified by the Canadian Dam Association

(CDA 2007, 2013), now require inspection by a professional engineer with relevant dam experience.

2.6 *A checklist-only approach to dam safety*

Cost pressures and over-competitive pricing of a dam safety review (DSR) may have the effect of consigning a DSR to the mere completion of a checklist. As a result, there appears to be an increasing demand for QA/QC procedures for dam integrity activities such as DSRs, dam safety inspections (DSIs), and annual performance reviews (APRs), to ensure that dam safety is actually assessed.

There is of course no substitute for professional engineers following the duty of care expected of them in the execution of their work in assessing dam safety and identifying and managing dam safety risks (Boswell and Sobkowicz, 2011).

2.7 *Rising risk profiles*

A significant distinguishing feature of tailings dams is that left unchecked, tailings dams, may be expected to follow a rising risk profile, since their construction continues over many years.

This characteristic has implications for dam safety activities:

- Inspections and risk assessments such as Failure Modes and Effects Analysis (FMEA), should be regularly revisited upon any significant change in a structure, including moving from one phase of the project life cycle to another (from design, to construction, operation or closure).
- Operation, Maintenance and Surveillance (OMS) plans and actions must target active risks and credible failure modes.

2.8 *Lulled into instrumented apathy*

The mere existence of instrumentation such as vibrating wire piezometers, slope inclinometers and automated data loggers is no guarantee of dam safety. The safest dams are not necessarily those with the most number of instruments. Care should be taken to ensure that instruments continue to target actual risks and failure modes, that instruments are in working order, that engineers are still physically inspecting the structure, that the data and risks are being actively analyzed and interpreted and that corrective action is taken in a timely manner.

2.9 *Normalization of deviance*

Steven Vick has produced excellent work (Vick, 2017a, 2017b, 2014) which clearly demonstrates the consequences of the normalization of deviance for dam safety. Quoting from Vaughan (1996) in his paper *Dam Safety Risk—From Deviance to Diligence* (Vick, 2017a), Vick used as his departure point the failure analysis for the Challenger Space Shuttle which exploded in January 1986, and which introduced the term normalization of deviance. The paper makes for fascinating but worrying reading. He further illustrates the folly of normalization of deviance with examples drawn from the tailings industry.

There were strong indications of the normalization of deviance in the months and years before the Fundão tailings failure – warning signals which should have been picked up from incidents and events in the years before, which contributed to the failure (Morgenstern, 2016). The same normalization of deviance applied to Mount Polley (Morgenstern, 2015), Merriespruit (Wagener et al, 1997) and many others. Hindsight of course provides a much clearer view than foresight, but recent lessons should not be ignored.

2.10 *Normalization of imponderable consequences*

Overarching all of the above factors is the deep understanding, at the conceptual stages of a proposed project, of the “what if” consequences of failure. What if the steep valley below the Stava dam became densely populated? What if a planned mining village was relocated to the toe of the Merriespruit dam?

At this Colorado based conference two years ago, Boswell and Sobkowicz (2016) argued that structures with extremely high i.e., imponderable consequences of failure should simply be avoided – that no low level of probability could reduce the risk to an acceptable level. In other words, in the event that a catastrophic tailings failure would lead to imponderable consequences, then no matter how infinitesimal the likelihood was calculated to be, the level of risk would be unacceptable, and the design should be reconceived to avoid the consequence altogether.

At Tailings and Mine Waste 2015 in Vancouver, the same authors (Boswell and Sobkowicz 2015), warned three weeks before the Samarco tailings failure that: *“we should not be building tailings facilities with imponderable consequences. If the consequences of a catastrophic failure would repeat a Stava or an El Cobre, then no matter how small the probabilities of actual failure are, the design should be completely revisited.”*

3 LEADING INDICATORS

In the light of ongoing failures described above, and notwithstanding the increase in published standards and attention, what more could be done?

3.1 *Looking forward rather than backward*

Those owners, operators, engineers, regulators and reviewers tasked with the responsibility of monitoring, surveillance and review of tailings dam integrity may benefit from the introduction of alternative tools for not just tracking dam safety, but actually predicting it: the use of leading rather than lagging indicators of dam integrity. Is it possible to predict failure, rather than waiting for it to happen? Could we be more forward looking and anticipative in our vigilance, and if so how? This is particularly important for those structures where the risk profile increases with time (usually a result of increases in height of tailings facilities and contained volume of tailings and fluid and/or ageing of dams). This paper suggests a revised vigilance through focusing on leading indicators of dam integrity.

3.2 *A definition*

What are leading indicators, and how do they differ from lagging indicators?

Van der Poel (2012) has described the difference between leading and lagging indicators in performance management as follows:

“In performance management we often talk about “lagging” and “leading” indicators. But what do they mean exactly?”

Lagging indicators are typically “output” oriented, easy to measure but hard to improve or influence while leading indicators are typically input oriented, hard to measure and easy to influence.

Let me illustrate this with a simple example: For many of us a personal goal is weight loss. A clear lagging indicator that is easy to measure. You step on a scale and you have your answer. But how do you actually reach your goal? For weight loss there are 2 “leading” indicators: 1. Calories taken in and 2. Calories burned. These 2 indicators are easy to influence but very hard to measure. When you order lunch in a restaurant the number of calories is not listed on the menu. And if you are me, you have no clue how many calories you burn on a given day.”

Similarly, in tailings failure analysis, tracking fatalities per year or millions of cubic metres of escaped tailings slurry may be straightforward, but these lagging indicators are unhelpful in improving future performance. They are simply reminders of underperformance.

What are some of the key indicators which are able to give advance warning of risk – that we might describe as leading indicators, rather than lagging indicators?

4 STRUCTURAL PERFORMANCE INDICATORS

There are many leading indicators of good performance which provide assurance of sound tailings disposal practice. Some of the general indicators are summarized in Sections 5 below.

However, the focus of this paper is centered on the performance indicators which may be described as structural. These leading indicators of sound structural performance are described in the section immediately below.

4.1 *Leading indicators which forewarned of catastrophe*

Several good lists of tailings failures are described in other papers and websites as included in the references to this paper, but are not reproduced in further detail here. This paper considers many of the failures which have taken place over the past 50 years, and selects seven published examples:

- Buffalo Creek, 1972 (Blight and Fourie, 2003).
- Bafokeng, 1974 (Blight and Fourie, 2003).
- Stava, 1985 (Morgenstern, 2000).
- Merriespruit, 1994 (Wagener, Craig, Blight and Strydom, 1997).
- Los Frailes, 1998 (Alonso and Gens, 2006).
- Mount Polley, 2014 (Morgenstern et al, 2015).
- Samarco, 2015 (Morgenstern et al, 2016).

These well documented tailings failures show how certain leading indicators point specific attention, warning of impending catastrophe.

From these papers, a list of key leading indicators was drawn up, and referenced back to the examples, in Table 1 below. Clearly there could be many more indicators selected (and some are further listed in Section 5 below), but in the authors' view these were the most reliable structural indicators of tailings dam risk.

Table 1. Leading indicators of impending failure.

Historical Tailings Failure, Date Reference	Buffalo Creek, 1972 Blight et al (03)	Bafokeng, 1974 Blight et al (03)	Stava, 1985 Morgenstern (2000)	Merriespruit, 1994 Wagener et al (97)	Los Frailes, 1998 Alonso & Gens (06)	Mt. Polley, 2014 Morgenstern et al(15)	Samarco, 2015 Morgenstern et al(16)
Leading Indicator							
Rate of rise	x		x	x	x	x	x
Beach freeboard	x	x	x	x	x	x	x
Height of dam	x	x	x	x	x	x	x
Contained volume of fluid	x	x	x	x	x	x	x
Changes in water level	x	x	x	x	x	x	x
Slope steepening		x			x	x	
Recycle water capacity	x	x	x	x	x	x	x
Foundation geotechnics					x	x	

As illustrated in the demarcated cells above, it is interesting to note just how many of the leading indicators were present just before each of the failures occurred. Each of the leading indicators is discussed in detail in the following sub-sections.

4.2 *Rate of rise*

In the authors' experience, the measurement of rate of rise has been used as a benchmark indicator for tailings dam performance for at least 50 years. However, our experience as an industry over the past 50 years has also continued to demonstrate through failure upon failure, the belief

that some operators hold that somehow, they might be immune to the risk of excessive rates of rise - until it actually happens to them, of course.

Morgenstern et al (2016) describe very high incremental monthly and annualized rates of rise that immediately preceded the Fundão tailings failure, in some cases up to an annualized rate of rise of 35 metres per year (Figure 1). It is no coincidence that upon breaching, the entire contents of the Fundão tailings facility were lost, a most unusual tailings failure characteristic.

Pollock, Mettananda and MacGowan (2014) show that oil sands tailings beach above water (BAW) deposition at annual rates of rise in excess of 10 metres per year, which is not track-packed, is liquefiable.

One of the authors of this paper showed in a series of papers at T&MW conferences (Boswell, 2009, 2011, 2015, 2017) the benefits which accrue from consistent adherence to rate of rise controls and limits in tailings deposition practice. Advice included the following:

- Calculation of allowable rates of rise for each deposit and each material.
- Establishment of allowable limits for rate of rise, and maximum height, based on the de-watering and consolidation characteristics of the tailings material.
- Measurement of incremental and average rates of rise.
- Strict compliance with seasonal, annual and overall rate of rise limitations.
- Adjustment of trigger levels and limits to cater for unseasonal or extreme precipitation.

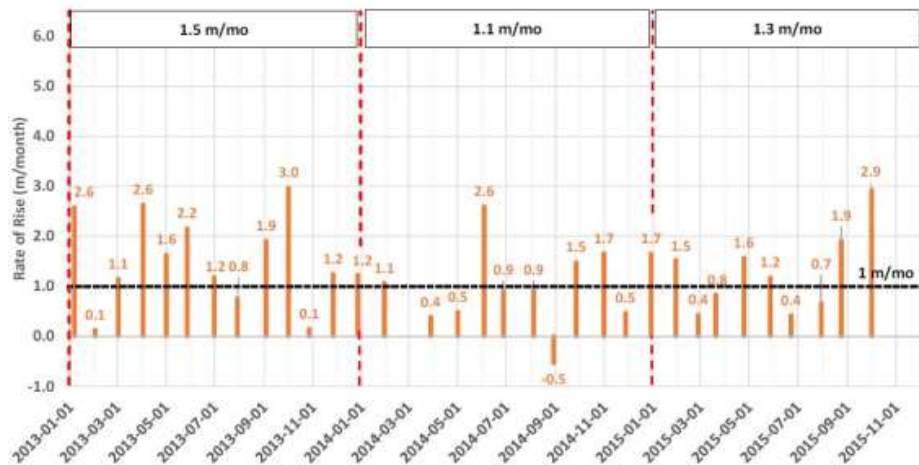


Figure 1. Rate of dam crest rise at Fundão left abutment setback (from page 49, Morgenstern et al, 2016)

4.3 Beach freeboard

A distinction should be made at the outset, between total freeboard and beach freeboard. As the name implies, beach freeboard is the amount of freeboard provided by the beach alone.

As illustrated in Figure 2, total freeboard provides the (as-measured) overall defense against overtopping, and may be rapidly improved by elevating the crest of the dam. Beach freeboard is much harder won but provides a number of additional benefits:

4.3.1 An additional defense against liquefaction

Tailings deposited on a subaerial beach, or beach above water (BAW), is usually not liquefiable, whereas tailings deposited sub-aqueously or beach below water (BBW) is usually liquefiable. There are exceptions to this rule, depending on climate, mineral type, particle size distribution, slurry specific gravity, mechanical compaction, but the trend is valid.

4.3.2 *Improved slope stability*

Existence of a long beach provides greater separation between the outer embankment and the pond, and consequently improved control of phreatic surface within the tailings and resulting embankment slope stability.

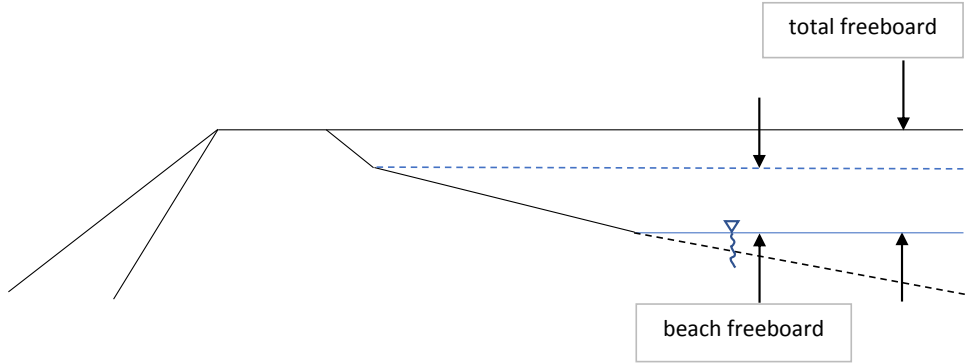


Figure 2. An illustration of the meaning of beach freeboard (vertical scale exaggerated)

4.3.3 *Better pond control*

A long beach also provides better pond control through the establishment of improved deposition basin geometry. In one of the author’s experience, on one large platinum tailings dam, beach freeboard of over 15 metres in vertical height was achieved, providing substantial margins of safety against overtopping, flooding, pore pressure rise and slope instability.

The clearest illustration of the value of beach freeboard in defense against catastrophic failure, may be found in a photograph of the Cadia tailings failure (Cadia, 2018) in Australia, in May of this year, shown in Figure 3 below.



Figure 3. Slope failure in upper compartment at Cadia, Australia (Cadia press release, 2018)

Without the added protection of the significant beach freeboard shown in the photograph, the local slope failure shown in the upper compartment would not have been contained, but instead

would likely have become a catastrophic tailings flow failure, cascading into the lower compartment and adding to the flow volume with multiplied severity of downstream consequences.

4.4 Height of dam

Robertson (2011) argued that tailings dam risk is very closely tied to absolute height of the structure. He also presented a thought provoking case for the rising risk profile of dam designs over the last decades. It is difficult to disagree with him.

He advanced an argument as shown below.

“Each 1/3 century:

Volume of waste increases by ~10 fold

Area of waste increases by ~ 5 fold

Heights of dams/dumps increase by ~ 2 fold

Max. Dam heights in 1900 ~ 15 m

Max. Dam heights in 1930's ~ 60 m

Max. Dam heights in 1960's ~ 120 m

Max. Dam heights in 2000's ~ 240 m

Max. Dam heights in 2030's ~ 480 m

Risk = Likelihood x Consequences

For dams: Likelihood ~ ‘somewhat’ proportional to height

Consequences ~ ‘somewhat’ proportional to volume

Increase in ‘potential risk’ per 1/3 century is ~ 2 X 10 = 20 fold”

Existing mine and tailings planning, design and risk management tools are demonstrably capable of taking these factors into account in order to manage risk proactively.

However, as noted in Section 2.10, the authors of this paper have argued that tailings dams which present inoperable risks to society should be reconceived (Boswell and Sobkowicz, 2015; 2016).

4.5 Contained volume of fluid and liquefiable material

While Robertson (2011) proposed that absolute volume of contained waste is an indicator of risk, there may be a better leading indicator. An extremely large dam like that at Chuquicamata Copper Mine in northern Chile now contains well over 1 billion m³ of tailings and covers 52 km² (Vogt, 2006), but the tailings are safely contained.

A better indicator of risk would be volume of fluid and liquefiable (by static or seismic means) material. An increasing trend in contained liquid volume is a reliable indicator of rising risk profile and should trigger additional precautions, in order to be safely managed.

Without the fluid and liquefiable material contained within the tailings dams, the catastrophic failures referred to in this paper would not have occurred.

Contained volume of fluid and liquefiable material is thus a reliable leading indicator.

4.6 Changes in water levels

Changes in supernatant water levels, in groundwater levels or within the phreatic surface of a tailings dam are usually very good indicators of reducing stability and/or increasingly severe consequences of failure.

Leading industry practice has employed piezometers and other instrumentation for many decades, for good reason. However, the mere existence of instrumentation is no guarantee of dam safety, as cautioned earlier in section 2.8 above.

4.7 Slope steepening

Many tailings failures have been preceded by the steepening of embankment side slopes: Mount Polley (Morgenstern et al, 2015), Los Frailes (Alonso and Gens, 2006) and Bafokeng (Blight and Fourie, 2003) are well published examples.

Slope steepening is often a desperate remedial measure, sometimes introduced to contain increasingly large amounts of fluid and to maintain sufficient freeboard. It is a poor choice of defense, often proved so with disastrous results, as shown in the references immediately above.

The use of beach freeboard as described in section 4.2 while not a quick fix by any manner of means, is a far more reliable remedy for freeboard problems. Sufficient capacity in recycle water storage is also a sound defense (Section 4.8 below).

4.8 Recycle water capacity

Catastrophic tailings failure is seldom possible without the presence of water or fluid. By the same token, the maintenance of a “zero pond” hydraulic fill dam is not achievable without the provision of adequate recycle water capacity, in a separate water dam.

Many large valley fill dams hold very large quantities of supernatant and precipitation. This is an ongoing risk which demands very close attention.

Reduced capacity for recycle water or water containment, or rising water inventories are usually reliable indicators of risk. This is especially true for poorly managed or unmonitored facilities, such as the Merriespruit failure (Wagener et al, 1997).

4.9 Foundation geotechnics

The Los Frailes failure in 1998 (Alonso and Gens, 2006) was a clear message to the international tailings community of the importance of deep-seated weak foundation layers and how they could contribute to catastrophe.

However, no-one really took any notice, until 16 years later an almost identical failure mechanism caused the Mount Polley failure in 2014 (Morgenstern et al, 2015). This failure introduced widespread awareness of the risks of deep-seated weak clay layers, the importance of understanding of the engineering geology of the region, and the importance of sufficient geotechnical investigation.

Soon after the Mount Polley failure, the BC government immediately addressed letters to every owner of a tailings dam, whether operational or not in BC, demanding immediate confirmation of the existence of (and appropriate consideration of) weak clay foundation layers below tailings dams. Similar letters were addressed to other dam owners by regulators elsewhere in Canada.

Engineers and Geoscientists BC (EGBC, formerly APEGBC) published a useful technical guideline in 2016 entitled Site Characterization for Dam Foundations in BC (EGBC, 2016b). This document provides substantial and detailed requirements for consideration of dam foundation geotechnics.

5 GENERAL LEADING INDICATORS

Time and space does not allow for further detailed consideration in this paper of other leading indicators which although not necessarily structural in nature, are nevertheless most useful in identifying and managing dam safety risks.

5.1 Human performance indicators

These include:

- Management commitment to dam integrity.
- Dam safety leadership.

- Documented roles and responsibilities for Engineer of Record (EOR) and Designer of Record (DOR).
- Up to date OMS, EPP and ERP manuals.
- Documented procedures for design changes, including “management of change”.
- Key staff turnover.
- Changes in contractor or operator.

There is an excellent recent publication, *Guide to the Management of Tailings Facilities Third Edition*, by the Mining Association of Canada (MAC, 2017), which is essential reading in this regard, compliance with which is in any case required for any member of MAC. The guide itemizes system essentials and organizational requirements for a sound tailings management team.

Boswell and Martens (2017) summarize the roles and responsibilities required of all personnel associated with dam safety, including the EOR and DOR. In addition, there has been work in the USA in 2017 and 2018 on a document by the GBA entitled *Tailings Engineer of Record Task Force* (GBA, 2017). This is intended to be a US National Practice Guideline for the Tailings Storage Facility (TSF) Engineer of Record, but has not been published yet.

5.2 Other leading indicators

These include:

- Mine profitability.
- Commodity price.
- Changes in production and storage capacities.
- Changes in the regulatory domain.
- Changes in environmental milieu.
- Stakeholder influences and changes.

Davies and Martin (2011) provide thought provoking insight into the direct correlation between adverse commodity price cycles and tailings dam failures.

6 CONCLUSION

For every failed tailings dam, there exists a large number of stable, well managed tailings facilities around the world. These structures do not achieve stability by chance, coincidence or serendipity. Their stability is the result of sustained effort over many years by the engineers that design and build them.

Nevertheless, there is an unacceptable rate of failure of tailings dams, worldwide and in our own countries. Many of these failures occurred under the watch of reputable engineers and consultants, working for responsible dam owners. A step-change improvement in engineering practice is urgently needed.

This paper outlines one path forward: placing more weight on leading indicators of dam structural integrity. It is hoped that the ideas herein will initiate a conversation in the dam engineering community and an evolution in dam engineering practice.

We have the ability to enact appropriate regulations. We also have the tools and the expertise to manage dams safely. However, if we do not engage top management in a culture of integrity management then we will continue to have failures like the ones we have seen.

We have to have the will to effect change. Senior professionals must exert leadership to effect this change.

7 ACKNOWLEDGMENTS

The support offered by our colleagues at Thurber Engineering Ltd. and in the Alberta Dam Integrity Advisory Committee (DIAC) is gratefully acknowledged.

8 REFERENCES

- Alonso and Gens, 2006. Los Frailes Anzacollar dam failure part 1 field observations and material properties. *Geotechnique* 56, No. 3, 165–183.
- BC MEM, 2017. HSRC. 2017. *Health Safety and Reclamation Code (HSRC) for Mines in British Columbia and accompanying HSRC Guidance Document*. BC Ministry of Energy and Mines, June 2017.
- BC MEM, 2016. *British Columbia Dam Safety Regulation*. B.C. Reg. 40/2016. http://www.bclaws.ca/civix/document/id/complete/statreg/40_2016
- Blight & Fourie, 2003. *A Review of Catastrophic Flow Failures of Deposits of Mine Waste and Municipal Refuse*. Int. Workshop, Sorrento, Italy: IW-Flows2003, May 14-16, 2003.
- Boswell, J.E.S. and Gidley, I.D.C. (2017). *Strategic Developments in the Next Decade for Tailings*. T&MW 2017. Banff, AB. Nov 2017.
- Boswell, J.E.S. and Martens, S. 2017. *The Engineer of Record for Tailings Dams: Recent Dam Safety Perspectives from the Alberta Oil Sands*. CDA 2017, Oct. 2017.
- Boswell, J.E.S. and Sobkowicz, J.C. 2016. *The Avoidance of Imponderable Consequences in Tailings*. T&MW 2016. Keystone, CO, USA, October 2016.
- Boswell, J.E.S. and Sobkowicz, J.C. 2015. *International Tailings Failures and Best Available Technology*. T&MW 2015. Vancouver, October 25-28, 2015.
- Boswell, J.E.S. & Sobkowicz, J.C. 2011. *Duty of Care in Tailings Operations*. T&MW 2011, Vancouver, Canada.
- Boswell, J.E.S. 2009. *Strategies for Dealing with Fine Fluid Tailings and Suspended Fines: Some International Perspectives*. T&MW 2009 Tailings and Mine Waste Conference, Banff, Alberta, November 2009.
- Cadia, 2018. Cadia Press Release March 12, 2018. *Cadia Northern Tailings Dam*. Newcrest Mining Ltd. www.newcrest.com.au
- CBC, 2018. 'It was a sea of water': Dam on Kenya rose farm bursts, killing 47. May 10, 2018. <http://www.cbc.ca/news/world/kenya-dam-bursts-1.4656484>
- CDA. 2007. *Dam Safety Guidelines*. Canadian Dam Association.
- CDA. 2013. *Dam Safety Guidelines. Revision of Sections 6.1, 6.2 and 6.3*. Canadian Dam Association.
- CDA, 2016. *Technical Bulletin – Dam Safety Reviews*.
- Chamber of Mines of South Africa, 1996. *Guidelines for Environmental Protection. The Engineering Design, Operation and Closure of Metalliferous, Diamond and Coal Residue Deposits*. March 1996.
- Davies, M. and Martin, T., 2009. *Mining Market Cycles and Tailings Dam Incidents* T&MW 2009, Banff, AB, Canada. November 2009.
- EGBC, 2016a. Engineers and Geoscientists, BC (EGBC formerly APEGBC) *Professional Practice Guidelines – Legislated Dam Safety Reviews in BC*. Version 3.0. Oct. 2016.
- EGBC, 2016b. *Site Characterization for Dam Foundations in BC*. V1.2. Engineers and Geoscientists, BC (EGBC formerly APEGBC).
- Eaton, T., 2017. Presentation by Alberta Energy Regulator to Alberta Dam Integrity Advisory Committee. 2017.
- Fourie A.B., Blight G.E. and Papageorgiou G., 2001. *Static liquefaction as a possible explanation for the Merriespruit tailings dam failure*. *Can. Geotech. J.* Vol. 38, 2001.
- GBA, 2017. Tailings Engineer of Record Task Force 2017. *Unpublished draft. National Practice Guideline for the Tailings Storage Facility (TSF) Engineer of Record (EoR)*. GBA, 2017.
- MAC. 2017. *Guide to the Management of Tailings Facilities. Third Edition*. Mining Association of Canada, Oct. 2017.
- Mettananda, D.C.A., Pollock, G.W. and MacGowan, T. 2014. *Construction of Suncor's first tailings sand structure under tailings reduction operation – Sand Dump 8*. T&MW 2014. Keystone, CO, Oct. 2014.
- MFLNRO, 2010. Ministry of Forests, Lands and Natural Resource Operations, Water Stewardship Division. 2010. *Dam Safety Inspection Checklist – for Dam Safety Reviews* (Excel file) [web]
- Morgenstern, N., Vick, S., Viotti, C., and Watts, B. 2016. *Report on the Immediate Causes of the Failure of the Fundão Dam*. Fundão Tailings Dam Review Panel. <http://fundaoinvestigation.com/the-report/>
- Morgenstern, N.R., Vick, S. and van Zyl, D. 2015. *Report on Mount Polley Tailings Storage Facility Breach*, Independent Expert Investigation and Review Panel. Victoria, Province of British Columbia. <https://www.mountpolleyreviewpanel.ca/final-report>
- Pollock, G.W., Mettananda, D.C.A., MacGowan, T., 2014. *Design of Suncor's first tailings sand structure under tailings reduction operation*. T&MW 2014. Keystone, Colorado, USA.
- Reuters, 2018. *Seven mine workers missing after accident in northern Mexico*. La Cieneguita, Mexico, June 6, 2018. <https://www.reuters.com/article/us-mexico-mining-accident/seven-mine-workers-missing-after-accident-in-northern-mexico-idUSKCN1J2355?i=0>

- Robertson, A.M. 2011 *Top Ten Things that go wrong with Plans for Mine Closure*. 6th Int. Conf. on Mine Closure, Lake Louise, Sept 2011.
- SABS, 1998. *Code of Practice. Mine Residue*. South African Bureau of Standards.
- USSD, 2017. Two-day workshop held in San Antonio, Texas in October 2017, “*Lessons Learned from Recent Tailings Failures*” convened by the US Society on Dams and the Association of State Dam Safety Officials (ASDSO)
https://ussdams.wildapricot.org/resources/Pictures/Preliminary%20Agenda_Tailings%20Workshop.pdf
- Van der Poel, K. 2012. Quote accessed from <https://kpilibrary.com/topics/lagging-and-leading-indicators>.
- Vick, S. G. 2017a. *Dam Safety Risk—From Deviance to Diligence*. Geo-Risk Denver 2017 GSP 282.
- Vick, S.G. 2017b. Presentation to CDA Dam Safety Seminar. *Risk Analysis. How Did We Get Here and Where Are We Going? Marriott Hotel*, Calgary International Airport. April 2017.
- Vick, S.G. 2014. *The use and abuse of risk analysis. FMEA*. T&MW 2014 Keystone CO. October 2014.
- Vogt, M.L., 2006. *The tailings impoundment of Talabre (Chuquicamata, Chile)* accessed June 26, 2018 at [https://www.unil.ch/files/live/sites/iste/files/shared/X.Library/Master%20theses%20%26%20DEA/Vogt%20Marie-Louise%20\(2006\).pdf](https://www.unil.ch/files/live/sites/iste/files/shared/X.Library/Master%20theses%20%26%20DEA/Vogt%20Marie-Louise%20(2006).pdf)
- Wagener F., Craig H., Blight, G. and Strydom, K. 1997. *Merriespruit Tailings Dam Flow Failure: Causes and Consequences*. T&MW 1997.
- Wikipedia, 2018. *Obed Coal Mine spill*. https://en.wikipedia.org/wiki/Obed_Mountain_coal_mine_spill
- Wikipedia 2017. URL accessed on Aug 14, 2017 https://en.wikipedia.org/wiki/Oroville_Dam_crisis.
- Useful websites re tailings failures:
<http://www.tailings.info/casestudies>
<http://www.infomine.com/library/publications/docs/>
<http://www.wise-uranium.org>
http://en.wikipedia.org/wiki/Dam_failure

Learnings from Real-time Pore Pressure Monitoring at a Platinum Tailings Facility

L Boshoff

SRK Consulting, Pietermaritzburg, KwaZulu Natal, South Africa

HAC Meintjes

SRK Consulting, Johannesburg, Gauteng, South Africa

M Boroko

Anglo American Platinum, Mototolo JV Concentrator, Lydenburg, Mpumalanga, South Africa

ABSTRACT: Following the major failure of the Fundão Tailings Storage Facility of the Samarco Mine in Brazil, outcomes of the post failure review prompted the industry to reassess their approach to tailings facility risk evaluation, design and operational management. In particular, vulnerability of Tailings Storage Facility (TSF) that contain materials displaying high static liquefaction potential was of concern. Based on a defined risk profile review of typical liquefaction triggers and their relevance to Anglo American Platinum sites, the particular facility forming the subject of this paper was identified as having a potentially high risk. Piezocone testing with pressure measurement (CPTu) investigations were initiated to confirm the material properties, existing pore pressure regime and extent of possible excess pore water pressure development. At a time of steadily increasing rate of rise on this facility, seepage was also observed on one of the flanks, adding additional urgency to understanding the prevalent conditions. Assessments culminated in a recommended risk management approach to stabilize the TSF by means of a waste rock buttress and enhanced monitoring capability. This included, amongst other measures, the installation of a network of Vibrating Wire Piezometers (VWP) to track and analyze pore pressure responses within the facility. This paper presents the learnings from the data gathered via this network before and during construction activities and active tailings deposition.

1 INTRODUCTION

1.1 Background

The major tailings facility failure (Fundão TSF) that occurred at the Samarco Mine in Brazil late in 2015, prompted many in the TSF industry to review their tailings facility risk evaluation approach, design and management standards. This included focus on the vulnerability to slope failure of tailings facilities, particularly under undrained loading conditions in tailings materials that may have a high static liquefaction potential.

In response to these concerns, the Anglo-American Group engaged with its various operations and consulting teams across the world to initiate a screening analysis of all facilities in their portfolios, specifically those being constructed using upstream deposition methods.

The screening analyses included evaluation of existing monitoring data to rank each facility based on a defined risk profile, considering the prevalence of typical liquefaction triggers such as high rates of rise (RoR) of the tailings embankment and beach, highly elevated phreatic surfaces, excess pore pressure build up, foundation materials prone to deformation, etc.

This was followed by stability reviews on high risk facilities and identification of facilities where more data would be required to complete a thorough assessment of vulnerability to possibly static liquefaction events.

Subsequently, the Helena TSF in South Africa was identified as one of the facilities having a high vulnerability should undrained shear strength be mobilized.

Confirmation of vertical hydraulic flow gradients achieved and the extent of possible excess pore water pressure development (considering the steadily increasing RoR maintained on the Helena TSF at the time) was of particular interest.

As the investigations were progressing in April 2017, seepage was observed on the south-east flank of the Helena TSF. The occurrence of this seepage added additional urgency to the process of data gathering and understanding of current conditions.

The location of this facility is shown in Figure 1.

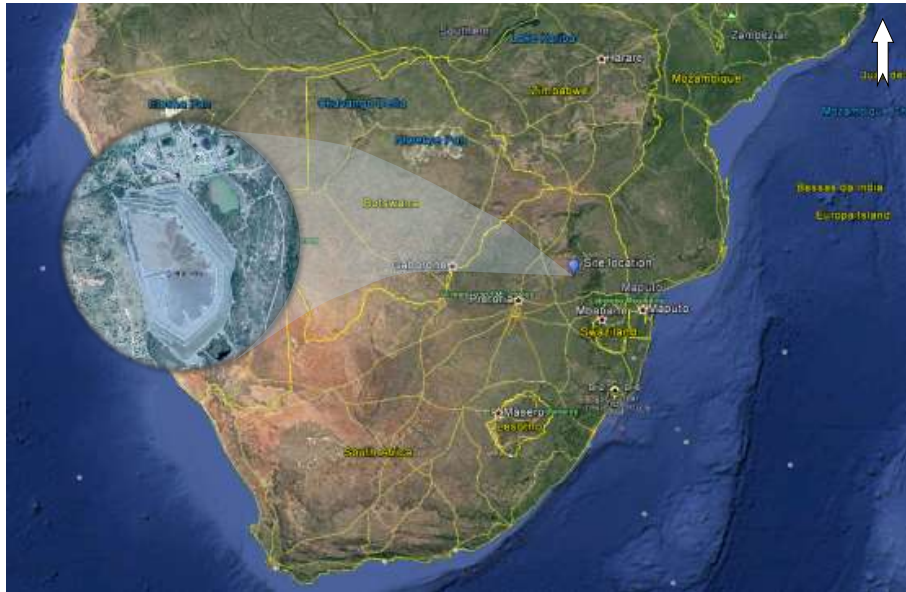


Figure 1. Site location.

1.2 Risks evaluation and mitigation approach

From May 2017 to July 2017 investigations continued and the scope of the analyses was expanded to address the issues arising. The outcome of various analyses and risk assessments at the time culminated in a recommend risk mitigation approach including temporarily shutting down the production plant, stabilizing the TSF by means of implementation of a Phase 1 and Phase 2 waste rock buttress and putting into place a more advanced monitoring system at the facility to monitor response to construction and continued deposition.

The implementation of a vibrating wire piezometer (VWP) network within the facility formed an essential component of critical controls required as part of the risk reduction strategy. This network allowed monitoring and assessment of increased risk of triggering and mobilization of the undrained shear strength that can typically lead to flow liquefaction.

Although not a new technology, the installation of such real-time monitoring devices, until very recently, has been a rare occurrence within the South African mining context. The risk of excess pore pressure build-up has always been managed by cautiously considering the TSF site location, size and deposition rate requirements. Subsequently the design and restriction of the facility RoR combined with operational management via routine CPTu monitoring have long been the accepted standard means of identifying and managing instances of excess pore pressure development within tailings facilities. However, it is now being acknowledged, following various events that a renewed focus on this phenomenon, especially in the presence of tailings materials in a potentially liquefiable state, is required. Especially when considering that it is very difficult to quantify the type and size or combination of trigger events required to lead to an undrained response. In general, it is accepted that risk evaluation and associated design and monitoring have to become

even more robust to prevent repeat incidents like the Fundão TSF failure. The more understanding that is gained on the response of your materials to any external events, the more informed your risk mitigation approach can be.

The authors consider any learnings gained beneficial and of significance not only within the South African context but in general.

2 VIBRATING PIEZOMETER NETWORK

2.1 *Monitoring rationale*

Readings from vibrating wire piezometers show a quick response to changes in pore pressures because of a short lag time. Short lag time could be seconds or at most minutes compared with other piezometers such as stand pipe piezometers where the lag time could be several weeks. This allows vibrating wire piezometers to be used for real-time monitoring of pore pressures in a variety of applications from:

- pore pressures related to dynamic loading applications, to
- construction (excavations and fills) related pore pressures, to
- long term monitoring of changes in pore pressures specifically in very fine-grained materials such as clays.

In the case of Helena TSF, the main purpose of the vibrating wire piezometers is to evaluate changes in pore pressures related to seepage flow within the body of the TSF, the rate of construction of the buttress and the rate of the tailings deposition construction of the TSF. The impact of seepage flow within the body of the TSF is specifically monitored to establish the response to deposition and whether the rate of rise affects the seepage flow regime in the body of the TSF, and/or excess pore pressures develop in the body of the TSF as a result of too high a rate of rise.

Secondly, the VWP monitoring is used to monitor the development and thereby allow management of excess pore pressures resulting from the construction of the buttress to the TSF.

2.2 *Layout and configurations*

There are approximately 11 main monitoring lines located in the areas that are of main concern along the east, north-east and south-eastern perimeter of the TSF. In these areas, the facility is currently more than 50 m in height (at its highest location) and will be about 65 m in height when it reaches the approved terminal elevation. The monitoring lines are equipped with conventional standpipe piezometers on selected bench locations and additional piezometers are added as the facility is raised.

As a first phase, VWP clusters were installed along six (6) of these lines to enable continuous tracking of pore pressures. Piezometer locations and depths were selected based on the most recent interpretation of data collected during a 2017 CPTu test campaign. A layout of the currently installed VWP cluster locations is given in Figure 2.

The VWP tip locations were chosen, where possible, to coincide with CPTu test locations to enable baseline data comparison. The exact correlation of CPTu data to an installed tip location is unlikely to be completely accurate but serves as reasonable correlation within the general variability noted in profile.

Of the six lines where VWP tips were installed, data collected from three of these monitoring line locations (Line D, E and G) have been chosen for further evaluation and discussion as part of this paper. The areas chosen for further discussion have been exposed to slightly different buttress construction, deposition sequencing timelines and other pre and post installation events.

Figures 3 to Figure 5 illustrate the section lines and location of the VWP tips and clusters installed along Line D, E and G which form the topic of discussion. These Figures also show the Phase 1 and Phase 2 buttress design geometry, the inferred phreatic surface as interpreted using 2017 CPTu and piezometer monitoring data as well as current Phase 2 buttress progress as surveyed during April 2018 and May 2018.

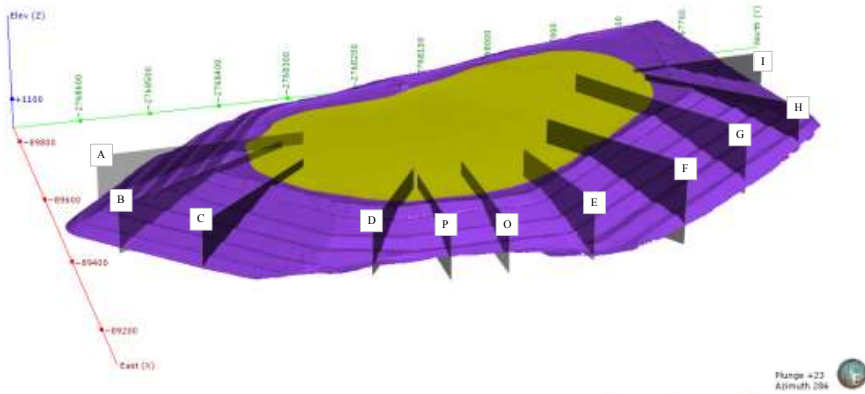


Figure 2. 3D representation of Helena TSF main monitoring Lines.

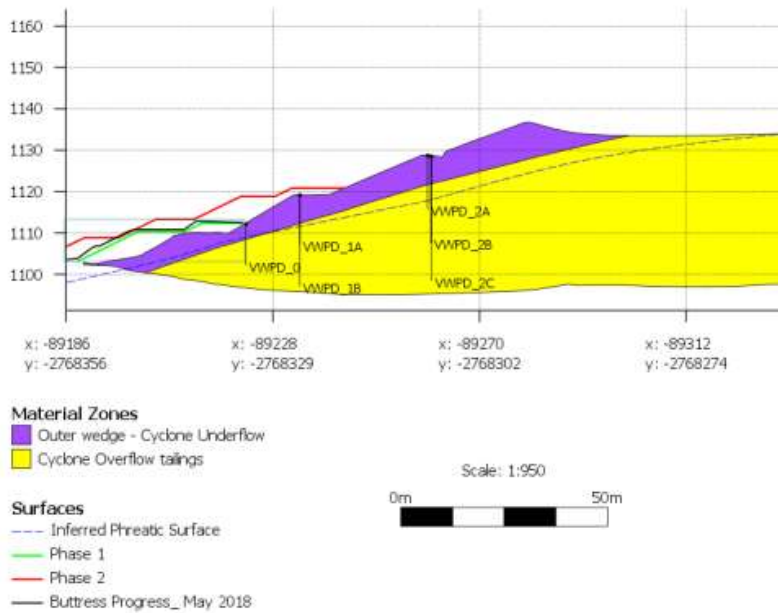


Figure 3. Section of Line D illustrating VWP cluster locations, TSF and buttress geometry.

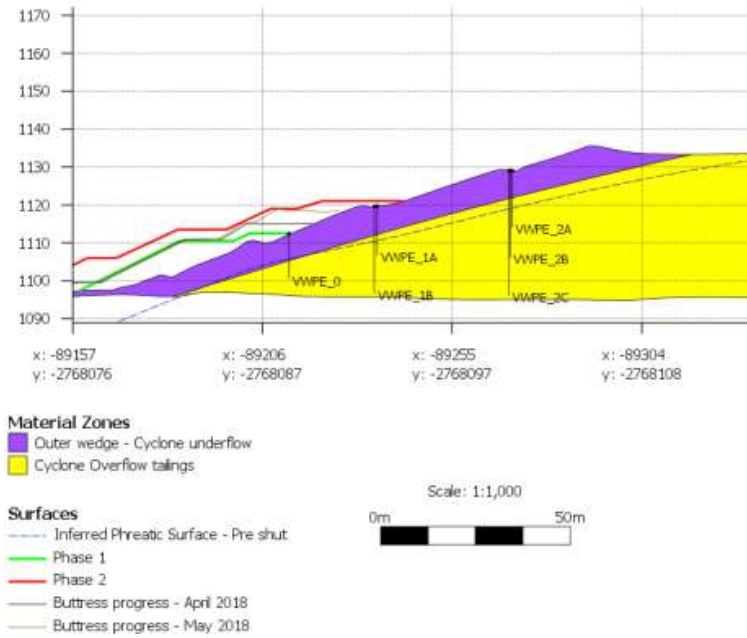


Figure 4. Section of Line E illustrating VWP cluster locations, TSF and buttress geometry.

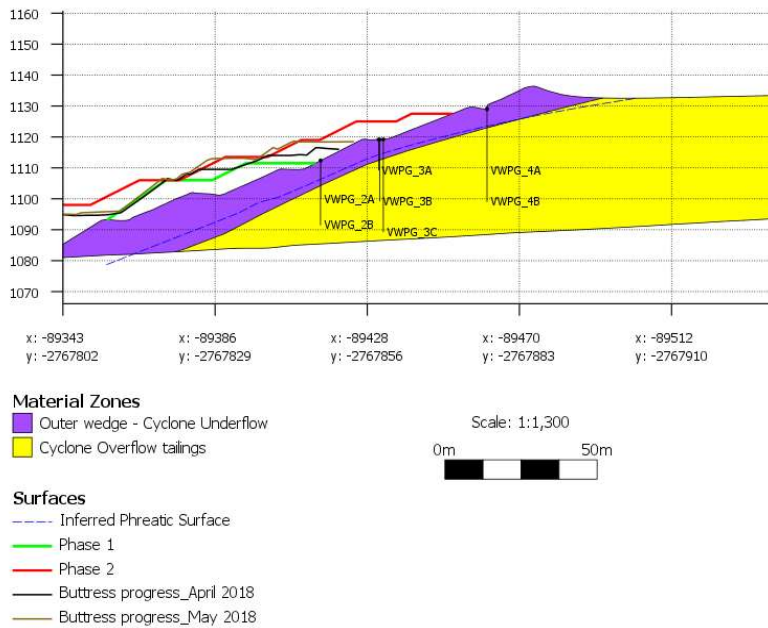


Figure 5. Section of Line G illustrating VWP cluster locations, TSF and buttress geometry.

3 DATA REVIEW AND DISCUSSION

3.1 Baseline pore pressure conditions

Phreatic conditions interpreted from CPTu pore pressure dissipation testing completed in 2017 pre – plan shut down and pre-buttress construction was used as a baseline. Where applicable, this information could be used for correlation, to evaluate changes in the flow regime and to identify where excess pore pressures are developing.

Table 1 below summarizes the estimated phreatic surface depth below tailings level and local vertical flow gradients interpreted for the relevant VWP cluster locations, at locations where correlations were appropriate.

The general flow regime, as indicated by the CPTu pore pressure dissipation test interpretations shows consistent sub-hydrostatic pore pressure flow conditions. In most locations well-conditioned basal drainage is taking place, however, basin conditions in the vicinity of Line E to D, straddling the south-eastern area where seepage was observed, is underlain by less permeable basin conditions, consequently allowing closer to hydrostatic seepage flow conditions and contributing to the observed seepage and high phreatic levels in this area.

An increase in excess pore pressures have been noted in locations affected by buttress construction, phreatic levels in the upper regions of the slope have dropped following the process plant shut down, but at the time of compiling this paper had started recovering and exceeding pre-shutdown levels. This could be due to a steady increase in the rate of rise combined with the impact of increased loading resulting from buttress construction.

The following sections elaborate on the detailed real-time trends in pore pressure measured at selected tip locations along Line D, E and G correlated with specific activities that occurred in these locations.

Table 1. Summary of baseline phreatic levels and local vertical flow gradients along Section Lines D, E and G for comparison to current interpretations from relevant VWP cluster installations.

		Baseline - Pre Plant shut and Construction			Status - May 2018		
Monitoring Section Line	Piezocene Test	Test date	Interpreted Depth to Phreatic surface (m)	Local Pore pressure build up (kPa/m)	Correlating VWP cluster	Interpreted Depth to Phreatic surface (m)	Local Pore pressure build up (kPa/m)
D	PC13		2.0		N/A		
	PC14		11.0	3.7	VWPD_2	10.4	6.8
E	PC11	Jun-17	6.8	5.8	VWPE_1	7.5	7.9
	PC11_Q3	Aug-17	5.8	7.6			
	PC12	Jun-17	7.8	6.8	VWPE_2	10.5	7.2
	PC12_Q3	Aug-17	6.8	5.5			
G	PC5	Jun-17	Not encountered	N/A	VWPG_2	3	4.5
	PC6	Jun-17	5.2	3.6	VWPG_3	5.7	6.9
	PC7	Jun-17	9.5	5.4	VWPG_4	10.0	6.0

*Indicative of vertical flow/drainage where < 9.81 kPa/m

3.2 Trends and events

To provide context to the data and trends gathered by the VWP along each line, a schematic representation of the general timelines and order of events that unfolded at the Helena TSF site is provided in Table 2.

The datasets reviewed and presented as part of this paper include data gathered up to the end of May 2018.

Table 2. Schematic representation of site events and timeline.

	Apr-17	May-17	Jun-17	Jul-17	Aug-17	Sep-17	Oct-17	Nov-17	Dec-17	Jan-18	Feb-18	Mar-18	Apr-18	May-18	
Other	Seepage noted along South-eastern flank										Gully wash away incident and repair				
Deposition	Active deposition				PLANT SHUT				Active deposition						
Construction				Phase 1 commences, production ramp up from July to 15 December 2017					Second phase construction -ongoing						
Monitoring	Piezocone testing of baseline conditions and stability reviews				Preliminary VWP data collection selected areas				Formal VWP network installed and data collection						

As noted in Section 1 of this paper, the observations of seepage in the south-eastern flank (in close proximity to Lines D, P and O, Fig. 2) initiated various investigations and risk assessments and as indicated in Table 2, the decision to shut down the process plant for approximately four months until construction of the first phase of buttressing could be completed. Upon completion of the first buttress construction phase (which was monitored by VWP surveillance monitoring at a few locations) the process plant resumed deposition in early December 2017. Key VWP installations were completed as part of the mitigation works during this phase and started logging data at the start of December 2017.

3.2.1 Data trends and events at specific areas of interest

The specific VWP lines chosen for discussion were each exposed to relatively unique conditions. As pore pressure within the tailings materials can be impacted by the seepage flow effects of the extended plant shut down, recovery following restart and also simultaneous construction it was necessary to review these impacts separately, if and where possible.

Other events of interest, and the resulting impact on pore pressures were also evaluated where applicable. A summary of the unique conditions that occurred along each monitoring line chosen for further discussion is provided below.

3.2.1.1 Section D

Figure 6 provides graphical output of the typical data trends observed at selected VWP tip/cluster location along Section D (Fig. 3). Recorded rainfall data are superimposed on the lower bench location trend graph and deposition events and surveyed TSF beach head (BH) elevations are noted on the upper bench location trend graph as reference.

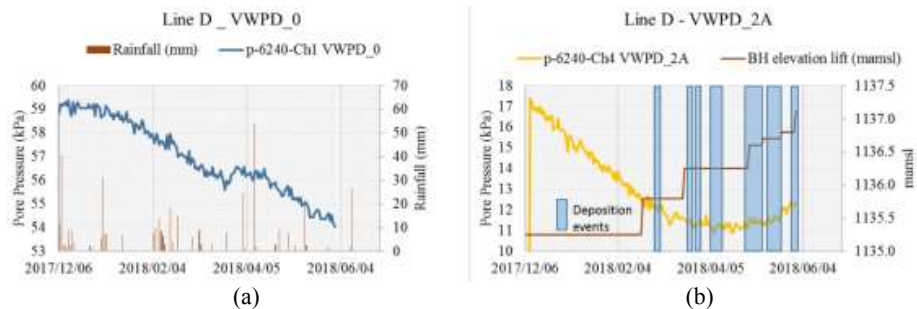


Figure 6. Example of typical pore pressure trend at lower bench installation vs. upper bench installations along Section Line D (Fig. 3 refers).

Section D was chosen as an example where a relatively isolated response of the tailings body to the four month shut and resulting recovery following the deposition restart can be observed. Although Phase 1 of buttress construction would have impacted on the measured pore pressures at the start of monitoring, baseline conditions prior to the first construction phase could be evaluated from CPTu data.

No construction activities had taken place in this specific area since December 2017, and all pore pressure changes in this location from December would be almost purely due to a response

to tailings deposition loading and associated seepage flow and recovery of the phreatic levels. The increased rate of rise due to a gradual decrease in the top surface tailings deposition area as the TSF is being raised, may result in a gradual increase in the rate of pore pressure build up in the tailings.

It is noted that the VWP tips installed on the upper benches (Fig. 6b) have shown steady decline in pore pressures, this is believed to still be related to a return to original pore pressures following Phase 1 of buttress construction (especially within VWPD_0 locations). Although tailings deposition recommenced in December 2017, deposition within the vicinity of Section Line D only occurred on a more regular basis from February 2018.

3.2.1.2 Section E

Figure 7 illustrates trends measured within the lower bench installation VWPE_0 impacted directly by buttress material placement from mid-March to mid-May 2018 from levels around 1112.5 mamsl to just below 1119 mamsl. Strong correlation with the buttress activity was observed in the piezometer tip installations just above where active construction took place (Cluster VWPE_1, Fig. 4).

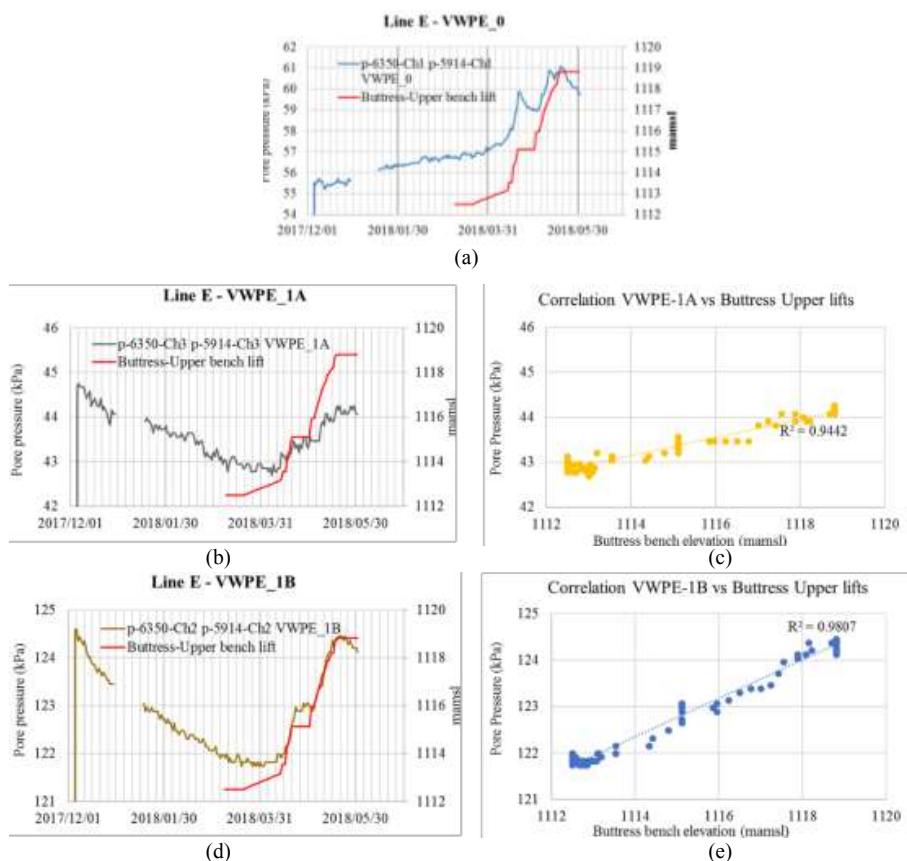


Figure 7. Graphical representations of typical pore pressure trends measured in lower bench piezometer installations VWPE0 7(a) and Cluster VWPE1 7(b) and 7(d) and selected correlations shown in 7(c) and 7(e), along Section Line E (Fig. 4).

Section E data trends also provide insight into the response to seepage flow impacts. In this regard it has also been considered that responses observed in the upper benches may not be solely

impacted by tailings loading, but also to some degree influenced by overall buttress works – especially in the deeper installations, where looser tailings materials possibly associated with stronger pore pressure response, reside.

3.2.1.3 Section G

Figures 8 and Figure 9 provide graphical summary of selected VWP trends along Section G.

General response to buttress construction and seepage flow was evaluated based on Figure 8 and 9 respectively in Section 3.3.

The dataset for Line G plotted in Figure 9 provides data on the VWP responses related to a gully wash out incident and repair. The incident occurred early in January 2018 in close proximity (60 to 120 m north) to installed piezometer tips VWPG_4A and 4B, on the upper bench at Section G. The decrease in pore pressures is related to the erosion taking place i.e. the unloading of this area; and the reloading of this area during repairs is related to the subsequent increase in pore pressures

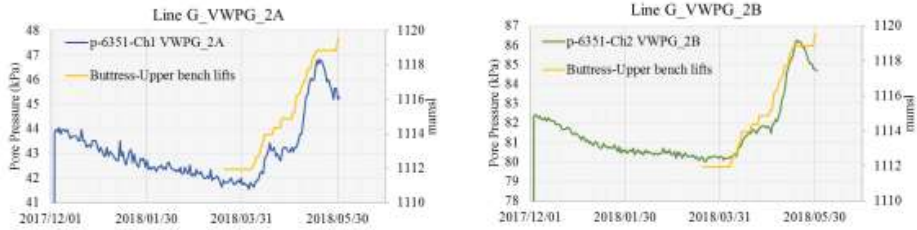


Figure 8. Example of typical pore pressure trends in lower bench installations along Section Line G (Fig. 5 refers).



Figure 9. Example of typical pore pressure trends in upper bench installations along Section Line G exposed to gully wash away and expedited backfill event and TSF deposition in general (Fig. 5 refers).

The repair of this gully took place intermittently over a 3 week period, where continued deposition of underflow tailings to backfill the erosion gully was required. Backfill commenced on 24 January 2018. The distinct upturn in pore pressure was noted to coincide with the start of the backfill operations, but little response prior to this. A drop off in pore pressures followed completion of repairs followed by an increase in the pore pressures likely associated with a period of regular tailings deposition that took place along this area around the end of March 2018.

3.3 Pore pressure coefficients- Pore pressure response in context

3.3.1 Laboratory determined pore pressure parameters

Pore pressure coefficients are used to express the response of pore water pressure to changes in total stress under undrained conditions. Typical pore pressure coefficients can be determined for specific materials experimentally in the laboratory and can be used to predict pore water pressures in the field under similar stress conditions (Craig, 1997).

Skempton’s pore pressure coefficient formula (Skempton, 1954) in its general form can be written as follows:

$$\Delta u = B[\Delta\sigma_3 + A(\Delta\sigma_1 - \Delta\sigma_3)] \tag{1}$$

Where A (pore pressure coefficient for any given increment of principal stress difference ($\Delta\sigma_1 - \Delta\sigma_3$), and B is the pore pressure response to a change in $\Delta\sigma_3$. A can be determined experimentally and AB can also be written as \bar{A} as:

$$\bar{A} = AB \tag{2}$$

and in the case of a fully saturated soil $B = 1$ and $\Delta\sigma_3 = 0$, then:

$$\bar{A} = AB = \frac{\Delta u_1}{\Delta\sigma_1} \tag{3}$$

The value of \bar{A} for a fully saturated soil can be determined in the laboratory from equation (3) during the undrained triaxial test by measuring and relating the pore pressure changes to the applied incremental changes in major principal stress at any stage of the test. The value of \bar{A} at failure (\bar{A}_f) is however of more interest.

Tests were conducted on tailings materials representing typical underflow (UF) and Overflow (OF) tailings. Samples were prepared at various densities, ranging from loose through to dense of the typical in-situ measured density. From these tests the typical pore pressure response at the point of mobilization of the peak undrained shear strength could be interpreted.

The typical \bar{A} and \bar{A}_f pore pressure coefficients calculated ranged between 0.0 to 0.5, typical of loose to medium dense sandy materials, which display similar behaviour to slightly over-consolidated clay. Dense sands will typically display values similar to heavily over-consolidated clays and have \bar{A} and \bar{A}_f pore pressure coefficients ranging from -0.5 to 0; i.e. showing dilative behaviour.

The typical \bar{A}_f parameter interpreted from the triaxial test work is summarized in Figure 10a and 10b below. Figure 10c provides a graphical idealization of the stress path direction associated with these typical pore pressure responses during triaxial testing.

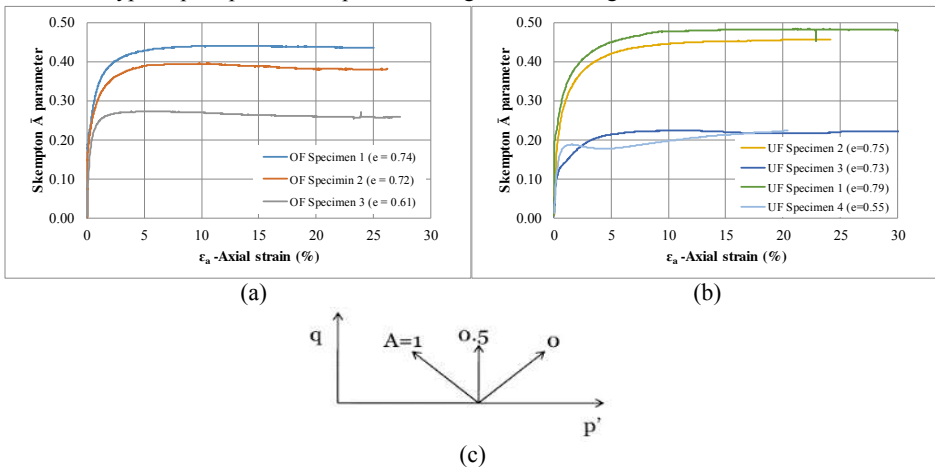


Figure 10. Summary of experimentally determined pore pressure coefficient \bar{A}_f for (a) Overflow tailings samples and (b) Underflow tailings samples tested under consolidated undrained conditions at different void ratios, and (c) providing idealized general stress path directions in q and p' space typically associated with the \bar{A} pore pressure coefficient determined.

3.3.2 Pore pressure parameter quantification – Field behaviour

Trend graphs discussed in Section 3.2 can be used to evaluate the field behaviour observed. One way to quantify and evaluate the pore pressure response of the materials in the field to changing stress conditions would be to relate changing pore pressures to the rate of buttress construction. The simplest way to do this is to relate the change in pore pressure to the increased loads induced by the height of buttress and/or TSF construction.

The height of construction of any buttress increment can be expressed as a vertical stress value or as an inclined stress value, i.e. to consider that the buttress is constructed on an inclined surface by applying a factor to the height of the buttress similar to the sin of the angle of construction. A stress analysis would be required to determine the exact applied load impacting on a soil element at any point in-situ, but translating the vertical height into a vertically applied load was considered a good enough approximation for the initial assessment presented with this paper.

The overall pore pressure coefficient to an isotropic stress increase $\Delta\sigma_3$ together with an axial stress increase ($\Delta\sigma_1 - \Delta\sigma_3$) as in a triaxial test, the following equation is relevant:

$$\bar{B} = \frac{\Delta u}{\Delta\sigma_1} \quad (4)$$

In this case, for $\Delta\sigma_3=0$, \bar{B} from Equation 1, defaults to:

$$\bar{B} = AB \quad (5)$$

As noted above, \bar{B} is a parameter used to describe the overall pore pressure response coefficient to an applied total stress difference, and below the phreatic surface B should be close to 1 (if there is no dissolved air within the pore water) and thus essentially in this instance, for field responses equation (4) can be written as.

$$\bar{B} = \frac{\Delta u}{\Delta\sigma_v} \quad (6)$$

Where:

Δu is total change (increase) in measured pore pressure (as measured by the piezometers over a day or over a chosen period for which the response needs to be evaluated) and,

$\Delta\sigma_v$ is the estimated change in vertical total load due to the addition of a vertical load increment of buttress materials and/or tailings material over that same period – the applicable load will depend on the location evaluated. The assumption is made that the lateral change in load as a result of an increase in vertical load is not significant for the purposes of this paper. In this case the magnitude of the A parameter portion of \bar{B} will dominate as discussed above.

Examples of pore pressure responses are:

$\bar{B} = 1$ typical of a strong pore pressure response to changing stress.

$\bar{B} = 0$ for no pore pressure response; fully drained behaviour.

Where lower calculated coefficients are associated to the denser samples compared to the higher coefficients associated with response of the looser prepared samples.

Using the VWP data trends the pore pressure response could be considered in the context of the recorded buttress and TSF lift activities and, in so doing, a better understanding of the field behaviour can be gained.

It is of significance to note that during early buttress construction works, based on initial responses measured within the first VWP installations along Line F (not discussed specifically within this paper), a buttress layer lift restriction was introduced where any placed vertical lift increment was not to exceed 0.6 m on a daily basis and no more than 2.1 m could be placed in any given area on a weekly basis. This restriction was intended to ensure the development of excess pore water pressure within the tailings remain within acceptable limits. The review of the monitoring data would provide confirmation of whether this restriction was adequate or needed adjustment. During monitoring the authors considered any Δu signifying interpreted $\bar{B} \geq 0.2$ (derived as noted above) to constitute reason for concern. This type of response would trigger steps to manage and re-prioritize construction activities, in order to control the generation of significant excess pore pressures and rates of pore pressure changes that would move towards an undrained type response.

3.3.2.1 Response quantification – Line D

Based on the levels surveyed, the average rate of rise (of tailings) in the vicinity Line D was approximately 4 m/annum, or effectively 0.01 m/day translating to theoretical vertical load of 0.2 kPa per day (Fig. 6). The rate of decrease in pore pressures measured up to the date of the first deposition event was approximately 0.1 kPa/day. This would imply that at some point pore pressures would start increasing at this rate of deposition.

The Δu from the turning point in the pore pressure trends, beginning April 2018, up to May 2018 was approximately 1.24 kPa. If the Δu was exclusively associated with the total vertical TSF lift in this area of 0.85 m (equivalent to an estimated load of 17 kPa over the period and/or 0.2 kPa/day) the pore pressure coefficient (\bar{B}) associated with this type of response is approximately 0.1. The Δu could also be associated with a rising phreatic level of approximately 180 mm from April 2018 levels.

3.3.2.2 Response quantification – Line E

Along Section E, \bar{B} was evaluated for the response measured at VWPE_0 between 20 March to 20 April where the effective buttress lift over this period in close proximity and directly over the installed tip location was approximately 2.6 m (estimated $\Delta\sigma_v = 63$ kPa). This translates to a \bar{B} of 0.05.

Based on pore pressure responses measured at VWPE_1A and 1B, over the period of 20 March to 20 May (overall buttress lift increment of 6.3 m and $\Delta\sigma_v = 152$ kPa) the interpreted \bar{B} value was 0.01 and 0.02 respectively. Overall during this period, the daily average Δu of 0.024 kPa was associated with a daily $\Delta\sigma_v$ of 2.6 kPa and thus a \bar{B} of 0.01.

3.3.2.3 Response quantification – Line G

The trends along Section G were characteristic of close by activities as discussed above. Specifically, during the infill and repair of an erosion gully. The response to gully fill was related back to the 0.55 m beach head lift (Fig. 9) that occurred during this time. It is believed that the loading as well as seepage flow/temporary rise in the local phreatic surface could have impacted on the pore pressures observed. If only accounting for the impact of the placed tailings in this area a \bar{B} of 0.14 can be interpreted. If pore pressures responded solely to a fluctuating phreatic level, the 1.72 kPa increase would have signified an upward shift in phreatic level of approximately 300 mm during this time, as the local vertical gradient measured at this time was associated with an increase in pore pressure with depth of approximately 6 kPa/m. The \bar{B} of 0.14 interpreted for this event was markedly higher, as the area was subject to continuous stress and seepage flow changes during the repair period. It is, however, of significance that pore pressure coefficients remained below 0.2.

Considering trends observed in Figure 8 at locations VWPG_2A and VWPG_2B, the overall pore pressure coefficient \bar{B} interpreted, during the period where buttress placement in this vicinity took place directly on the location of the installed tips, was <0.03 . During this period the $\Delta\sigma_v = 180$ kPa and $\Delta u = 4$ to 5 kPa. Therefore, it can be observed that there was almost full pore pressure dissipation in the available time.

4 CONCLUSIONS

The interpretation of an overall pore pressure coefficient \bar{B} can serve as a simplified approach to contextualize real time pore pressure responses observed and measured in-situ. For the Helena TSF, the typical response of materials to the current changing stress conditions could be observed and more insight has been gained in the impact of construction and deposition activities on pore pressures within the facility. The pore pressure coefficients interpreted for the VWP tip locations discussed in this paper confirmed that the current buttress lift restriction (0.6 m/day and 2.1m/week) and tailings RoR limit of 6.0 m/a being enforced at the facility, is effective at controlling pore pressure increases to ensure a close to drained response within the tailings material. The assessments further show, on average, that materials behave in line with densely prepared samples ($e < 0.7$) and pore pressure coefficients noted at low axial strain.

It is however always important to note that, irrespective of the fact that increasing load results in a close to a drained response, the transition to undrained behaviour and mobilization of the peak

/ yield undrained shear strength and potential flow liquefaction can possibly be near instantaneous given a sufficiently large trigger event.

Further application of the in-situ information could include applying the measured pore pressure responses to calibrate appropriate deformation models, which can assist in evaluating and simulating the response of the materials to various loading conditions. These models can be used to evaluate the loading conditions under which instantaneous flow failures will occur, which will assist in the design of appropriate mitigation measures or operational controls to guard against the detrimental effects of such load conditions. Given a thorough review of the in-situ material properties and all relevant trigger events/conditions applicable to the facility, a fit for purpose mitigation design and/or monitoring and risk management system can be implemented.

ACKNOWLEDGEMENT

The collection and sharing of the data provided as part of this paper was made possible by Anglo American Platinum and the relevant operation. The authors would like to thank all affiliated parties involved in this process.

REFERENCES

- Craig, R.F. Soil Mechanics (Sixth edition). 1998. *Pore pressure coefficients*: 142–149. Department of Civil Engineering, Dundee UK: E & FN Spon.
- Skempton, A.W. 1954. The pore pressure coefficients A and B, *Geotechnique, Volume 4, Issue 4*: 143-147.

Lime as an Additive for Oil Sands Ore-Water Slurry Based Bitumen Extraction, Tailings Disposal and Fluid Fine Tailings Dewatering Processes

S. Arnipally, R. Burden^(*), J.D. Scott^(*) and B. Ozum

Apex Engineering Inc., Edmonton, AB, Canada

^(*) *University of Alberta, Edmonton, AB, Canada*

ABSTRACT: Since 1967, bitumen is commercially produced in Alberta, Canada by surface mining of Athabasca oil sands followed by ore-water slurry-based extraction processes, over 1.3×10^6 barrels/day current production capacity. Clark Hot Water Extraction (CHWE) process of 1930s is used at all plants, which uses caustic *NaOH* additive to achieve an acceptable bitumen extraction efficiency; however, *NaOH* is also detrimental to process water chemistry, promotes production of fluid fine tailings (FFT) and causes issues for long-term operating sustainability of oil sands plants. Our research shows that all of these problems would be solved by suppressing silt-clay size particles dispersion in the extraction process slurry and disposing of tailings as non-segregating tailings materials, while simultaneously eliminating or reducing Na^+ accumulation in recycled process water. These fundamental operating objectives could be accomplished simply by using lime (*CaO*) as the additive. For the extraction process, *CaO* would be added at dosages ranging from 100-300 mg-*CaO*/kg-ore. For the whole tailings treatment before cyclones, *CaO* would be added at dosages ranging from 1,000-1,500 mg-*CaO*/m³-tailings. For production of non-segregating tailings (NST) from the blend of cyclone underflow, thickener underflow and existing FFT, *CaO* would be added at dosages ranging from 800-1,500 mg-*CaO*/m³-NST. Our extensive research shows that lime could also be used as an effective additive for FFT dewatering processes at 1,000 – 10,000 mg-*CaO*/kg-FFT dosages, such as in-situ treatment of FFT followed by capping with sand or NST, or treatment of FFT followed by blending with overburden soil. Recently generated data, specifically on NST production, FFT dewatering and bitumen extraction processes using lime as an additive will be presented. Our research findings conclude that use of lime as an additive at oil sands plant operations reduces environmental impacts and improves long terms sustainability of oil sands plants, in a simple and cost-effective manner.

1 BACKGROUND

1.1 Bitumen Production, Environmental and Long-Term Sustainability Challenges of Oil Sands Plants

Bitumen has been commercially produced in Alberta for five decades by surface mining of the Athabasca oil sands ores followed by ore-water slurry-based extraction processes. All oil sands plants are using some version of the Clark Hot Water Extraction (CHWE) process developed in the 1930s (Clark 1944 & 1939, Clark and Pasterneck 1932). The CHWE process uses *NaOH* as an extraction process additive, which increases the *pH* of the extraction process, reduces water surface tension (γ_W) and bitumen-water interfacial tension ($\gamma_{B/W}$), promotes liberation of bitumen from the oil sands ore matrix and provides acceptable bitumen extraction efficiency (Kasperski, 2001, Speight and Moschopedis, 1980 & 1977/78).

The CHWE process provides acceptable bitumen recovery efficiency; however, it is the source of many problems too. Reduction of γ_W promotes dispersion of clay in the extraction process slurry ore-water slurry and promotes production of FFT with poor settling and consolidation characteristics. Reduction of $\gamma_{B/W}$ promotes liberation of bitumen from oil sands matrix; however, suppresses kinetics of bitumen droplets coalescence and aeration processes in the extraction process slurry (Liu et al. 2005; Pan et al. 2012; Pan and Yoon 2010). Because of suppressed bitumen droplets coalescence and aeration kinetics, oil sands plants demanded large process vessels and large capital investment.

Since the oil sands plants are permitted to operate on a no-discharge policy, released water from the CHWE process tailings accumulated in tailings disposal ponds are recycled to the extraction process. By this process the water chemistry is harmed by a steady increase in salinity, specifically bicarbonate (HCO_3^-) and sodium (Na^+) concentrations. This steady increase in process water Na^+ concentration harms the efficiency of the bitumen extraction and tailings disposal processes.

In summary, use of CHWE process, more specifically the use of $NaOH$ as an extraction process additive, is the source of high capital and operating costs, bitumen extraction efficiency, tailings disposal properties, mature FFT tailings dewatering, process water chemistry and long term operating sustainability challenges of the oil sands plants.

Oil sands players have spent sincere effort, over the five decades, for the development of low temperature, non-additive extraction processes to improve thermal efficiency oil sands plants and to reduce production of matured FFT. These processes could not provide acceptable bitumen production efficiency and gradually converted to other versions of the CHWE process.

Sincere effort was also devoted for the development of tailings disposal processes to reduce mature FFT production. For this purpose, production of composite tailings (CT) or nonsegregating tailings (NST), tailings reduction operation (TRO), atmospheric drying, coke capping, in-line thickening and dewatering of mature FFT by centrifuging technologies were developed (Wells et al. 2010; Jeeravipoolvarn, 2010; Mikula, 2014). Some of these technologies showed limited commercial success.

Mature FFT is one of the major challenges of oil sands plants, inventory of which is exceeding 10^9 m³ and increasing exponentially as the capacity of existing plants are increased and new plants are commissioned. Centrifuging and pressure filtering of FFT, which are high capital and operating costs processes, are being selected by the oil sands players for their commercial implementations.

As of today, novel technologies to improve oil sands plants efficiency, to reduce FFT production, dewater existing mature FFT inventory, to improve process water chemistry and long-term sustainability of oil sands plants are needed.

2 *Use of Lime as an Additive for Bitumen Extraction, Tailings Disposal and FFT Dewatering Processes*

Any novel technology to reduce environmental impacts and to improve long-term sustainability of oil sands plant should be founded on three principles:

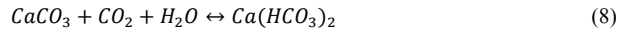
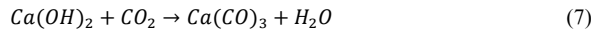
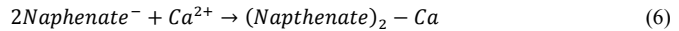
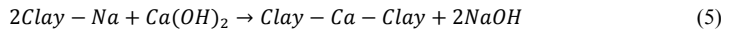
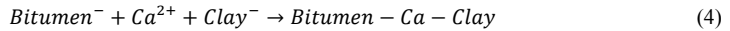
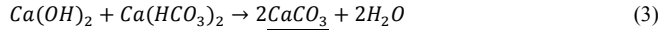
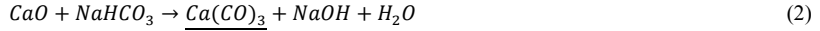
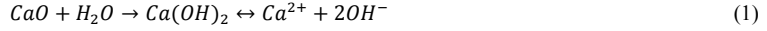
- (i) suppress dispersion of silt-clay size particles in the extraction process slurry;
- (ii) dispose oil sands tailings material as a non-segregating tailings material; and
- (iii) convert *Na-Clay* to *Ca-Clay* before the implementation of any mature FFT dewatering processes.

While focusing on these process principles, process water chemistry, simplicity, integration to the existing plants, health and environmental safety, capital and operating costs must be considered as constraints. Our research findings showed that existing challenges of the oil sands plants could be solved or reduced in simple and cost-effective manners by using CaO as an additive for the following processes:

- (i) bitumen extraction process: improves bitumen recovery efficiency, suppresses silt-clay size particles dispersion, produces tailings with improved settling and consolidation properties and reduces Na^+ accumulation in the process water. These processes improve the long-term sustainability of oil sands plants;
- (ii) whole tailings treatment: which could be implemented before cyclones or direct deposition of the whole tailings into the tailings ponds;
- (iii) dispose the tailings as a non-segregating tailings (NST) material; and,
- (iv) treat mature FFT with a calcium-based additive before the implementation of commercially available or novel dewatering processes.

2.1 Benefits offered by CaO Chemistry

Our research findings suggest that *CaO* could be used as an additive for oil sands unit operations because of the unique characteristics of *CaO* chemistry, which increases the *pH* of the oil sands ore-water slurry and provides Ca^{2+} ions simultaneously. Because of these characteristics of the *CaO* additive, the following parallel and consecutive chemical reactions could take place between the species contained in oil sands ore-water slurry and atmospheric CO_2 :



Equilibrium attained in aqueous oil sands ore-water slurry systems by adding *CaO* at selected dosages could improve the performance of bitumen extraction or tailings disposal processes, simultaneously improving the process affected water chemistry and long-term sustainability of oil sands plants.

2.2 Use of CaO as an Extraction Process Additive

Our in-house, and jointly with Shell Canada Ltd., research on the use of *CaO* as an additive for the bitumen extraction process showed highly promising bitumen extraction process efficiency and process water chemistry (Babadagli, et al. 2008; Ozum and Scott, 2010). Further tests made using *CaO* as an extraction process additive jointly with Shell Canada Ltd. and third-party verification tests made at NAIT-NARCOSS as requested by COSIA, also showed similar results; it provided higher bitumen extraction efficiency, reduced slit-clay size particles dispersion in the extraction process slurry and suppressed-eliminated Na^+ accumulation in the process water (COSIA, 2013; Ozum and Scott, 2009). In these tests Five-Lock Cycles were made by recycling the water recovered from *CaO* additive extraction tests and using it for the next *CaO* additive extraction test consecutively, without importing any fresh water.

The advantages of the use of *CaO* as an extraction process additive compared to that of *NaOH* additive in the CHWE process evolves from the unique characteristics of *CaO* chemistry, as mentioned in Section 2.1. When *CaO* is used as an additive, it increases *pH* of the slurry by the chemical reaction expressed in Equation 1, without increasing the Na^+ concentration of the ore-water slurry. An increase in ore-water slurry *pH* activates naphthenic acids contained in the bitumen, which acts as a surfactant and reduces water surface tension (γ_W), which promotes dispersion of clays in the slurry and bitumen-water interfacial tension ($\gamma_{B/W}$), which promotes liberation of bitumen from the oil sands ore matrix. However, Ca^{2+} ions introduced by *CaO* addition reduces surfactant activities of water soluble naphthenic acids salts (chemical reaction, Equation 6) and gradually increases both γ_W and $\gamma_{B/W}$. An increase in γ_W reduces attraction between water and clay, which suppresses dispersion of clays and an increase in $\gamma_{B/W}$ promotes hydrophobic characteristics of bitumen droplets and promotes coalescence and aeration of bitumen droplets in the extraction process slurry, as depicted in Figure 1 (Ozum et al, 2014).

As discussed in Section 2.1, when *CaO* is used as an extraction process additive, several reactions would take place in parallel and/or consecutive fashion. Therefore, a fraction of the *CaO* added into the extraction process slurry could react with clay, bitumen and bicarbonates too. All experimental studies show that when *CaO* is used at dosages which could maintain the extraction process slurry *pH* in the range of 8.0 to 8.4, it increases bitumen extraction efficiency and

extraction process kinetics, suppresses silt-clay size dispersion and eliminates an increase in Na^+ concentration.

These observations suggest that when CaO is used as an additive it does not promote attractions between negatively charged clay and bitumen species and does not suppress bitumen extraction efficiency, which contradicts the observations made on the role of Ca^{2+} on the attractions between the clay and bitumen species using $CaCl_2$ as an additive (Masliyah et al. 2004). Discrepancy between the two research findings could be attributed to the differences in the chemistry of CaO , which increases the pH (increase alkalinity) of the slurry and $CaCl_2$, which decreases the pH (increases acidity) of the slurry.

Oil sands operators are concerned that alterations made in the bitumen extraction process could cause an increase in Ca^{2+} incorporated in bitumen. Our preliminary bitumen extraction tests showed that soluble Ca^{2+} measured in bitumen produced by using $NaOH$ and CaO additives are better correlated by the pH of the process slurry, rather than the dosages of $NaOH$ or CaO used in the extraction process, as shown in Figure 2.

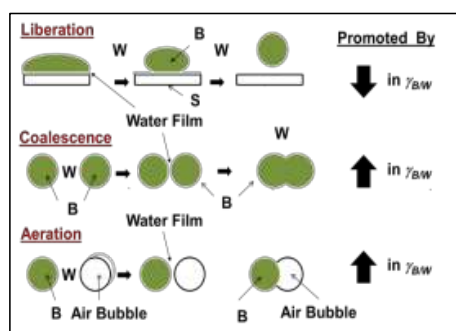


Figure 1. Mechanism of bitumen liberation, Coalescence and Aeration (Ozum et al, 2014)

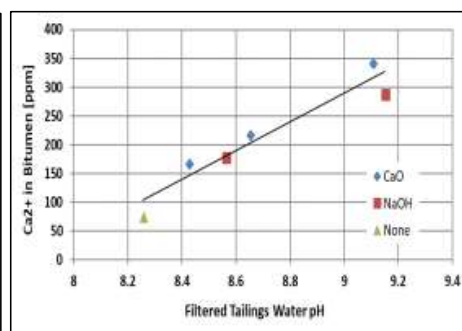


Figure 2. Concentration of Ca^{2+} in bitumen versus filtered tailings water pH

In summary, use of CaO as an extraction process additive would have great impacts on solving the existing challenges of oil sands plants in a simple and cost effected manner.

2.3 Use of CaO as an Additive for Non-segregating Tailings Production

Disposal of oil sands tailings as a non-segregating tailings material is one of the methods to suppress or eliminate production of mature FFT. Unfortunately, oil sands tailings produced by CHWE process has poor settling and consolidation properties. Upon the deposition of the tailings to the ponds, coarse sand particles segregate quickly and form a beach, the remaining fine tails of 6 to 10 w % solids accumulate in the tailing ponds, quickly settles to 20 w % solids content and over a few years to about 30 w % solids (86 % by volume water) and 1-2 w % residual bitumen contents, with a stable slurry structure. This tailings material is called mature FFT, which will remain in a fluid state for centuries because of their very slow consolidation rate (Kasperski, 1992).

Since 1967, mature FFT has accumulated in the tailings ponds and existing volume is estimated to be over 10^9 m³, which is a serious environmental liability. To reduce mature FFT inventory, non-segregating composite tailings (CT) production technology was developed and implemented commercially. This process is based on the treatment of the blend of Cyclone Underflow and existing mature FFT with gypsum ($CaSO_4$) additive (Caughill et al, 1993 & 1994).

In fact, commercial implementation of the CT production process could not provide long term solutions to reduce the existing mature FFT inventory, since additional mature FFT is also produced from the Cyclone Overflow tailings. Also, the CT process could not improve the energy efficiency of the oil sands plants, because of the discharge of warm tailings slurry into the tailings ponds. Continuous accumulation of Ca^{2+} and SO_4^{2-} ions detrimentally affects recycled release water chemistry, potentially promotes scaling in process vessels and pipes, and may cause

H_2S emissions from the tailings ponds by anaerobic reduction of SO_4^{2-} by the residual bitumen in the tailings. Furthermore, performance of the CT production process would be harmed by a steady increase in process water Na^+ concentration because of the use of the CHWE process in the first place. An increase in Na^+ concentration increases the sodium adsorption ratio (SAR) in the tailings slurry, which suppresses the ion exchange reaction between clay Ca^{2+} and clay which detrimentally affects the performance of the CT process (Miller et al, 2010; Dawson et al. 1999).

As an alternative to the CT process, our laboratory has been working on the production of non-segregating tailings (NST) by treating the blend of Cyclone Underflow, Thickener Underflow (thickened Cyclone Overflow) and/or existing mature FFT with CaO or CaO and CO_2 .

Shell Canada Ltd., Canadian Natural Resources Ltd. (CNRL) and Alberta Energy Research Institute (AERI) were interested in the production of non-segregating tailings (NST) from the Albion Sands Muskeg River mine tailings material. NST production test results were summarized in seven reports and shared with AERI and the oil sands industry (Apex, 2004-2005; Scott et al, 2007). Test results demonstration that NST with 59% solids content and SFR (sand-to-fines ratio) of 4 and 5 could be produced by using CaO additive at 0.6 and 0.8 kg- CaO/m^3 -NST dosages respectively.

Test made on the production of NST from Syncrude's Aurora Mine tailings material also showed similar results; NST could be produced at 60% and 55% solids contents, SFR of 5, by using CaO additive at 0.6 and 0.4 kg/ m^3 -NST dosages respectively (Donahue et al, 2012; Apex, 2005).

It was observed that NST production using CaO additive reduced process affected water Na^+ concentration. NST produced from the Albion Sands Muskeg River Mine tailings material by CaO additive at 0.6 to 0.8 kg/ m^3 -NST dosages, when the plant was operating in a non-additive extraction process mode, Na^+ concentration was reduced from about 130 to 110 mg/L. It was also observed that process water Na^+ concentration was reduced from 625 to 515 mg/L by NST production from Syncrude Canada Ltd.'s Aurora Mine tailings material, also using CaO at 0.6 to 0.8 kg/ m^3 -NST dosages.

A steady increase in process water Na^+ concentration detrimentally affects performance of NST production, because of an increase in SAR in the process water. Recent NST production tests made at our laboratory on selected oil sands tailings samples showed that the required dosage of CaO additive is increased by 50% to 100% compared to that of the dosages required to produce NST a decade ago.

In summary, disposal of oil sands tailings effluent as a non-segregating tailings material reduces or eliminates the steady increase in the existing FFT inventory. Use of CaO as an additive to produce NST provides additional advantages; improves process water chemistry by reducing bicarbonates (reduces scaling in process vessels and pipes) and Na^+ concentrations in process water. Our research findings suggest that NST production using CaO as an additive offers great advantages to oil sands tailings disposal practices, especially when it could be implemented coupled with the use of CaO as an additive in bitumen extraction and/or whole tailings treatment processes.

2.4 Use of CaO as an Additive for Mature FFT Dewatering

Recently, oil sands players are interested in dewatering of existing mature FFT by treating it with flocculants followed by centrifuging and pressure filtering (Mikula, 2014). At our laboratory, use of CaO as an additive for dewatering of existing mature FFT is being investigated for two purposes: (i) as a pretreatment of mature FFT before its centrifuging or pressure filtration; and, (ii) in-situ treatment followed by sand capping or blending with overburden soils, which could be implemented after treating the water layer of the mature FFT ponds with CaO at about 400-1,000 g/ m^3 -water and recycling it to the extraction plant.

In this study, two mature FFT samples produced at two oil sands plants were treated with CaO at 500 g to 100,000 g/kg-FFT (500 to 100,000 ppm based on FFT mass). Dosages and alterations in FFT characteristics, such as the yield stress, Atterberg and hydraulic conductivity are measured as a function of time.

The interaction and chemical reactions between CaO and clay soils are complex; they are generally considered to be two distinct processes; clay modification, which is usually complete

within 24 to 72 hours and clay stabilization, which are long term changes brought about by pozzolanic reactions, where silica and alumina within the clay minerals react with lime to produce calcium silicate hydrate (*CSH*) and calcium aluminate hydrate (*CAH*) gels which have a cementation effect. This has a dramatic influence on the stress-strain behavior; increasing the strength and brittleness of the material. To achieve full stabilization both moisture content and degree of compaction must be tightly controlled, and the dosage of lime addition must be greater than the lime fixation point. The amount of lime required to bring about full modification is known as the fixation point. Studies show that the progress of the lime modification reactions can be observed by measuring the Atterberg limits (Craig, 2004; Rogers & Glendinning 1996; Rogers et al. 1997; Boardman et al. 2001).

In this study, mature FFT samples are treated with *CaO* in the range of 500 g to 100,000 g/kg-FFT (500 to 100,000 ppm based on MFT mass) dosages and alterations in FFT characteristics, such as the yield stress, Atterberg limits and hydraulic conductivity are measured as a function of time.

Atterberg limit tests were carried out to evaluate soil plasticity of two mature FFT samples, identified as Mature FFT Operator 1 and Mature FFT Operator 2, by treating with *CaO* (quick lime) at 1,000 to 100,000 g/kg-FFT (1,000 to 100,000 ppm) dosages. Atterberg limit measurements made after 28 days curing time for Operator 1 and Operator 2 mature FFT samples as a function of *CaO* dosage are presented in Table 1 and 2. Atterberg limit measurements made as a function of curing time on the same mature FFT samples treated with *CaO* at 7,000 g/kg-FFT (7,000 ppm) dosage are presented in Table 3 and 4.

Table 1. Atterberg limits at 28 days curing time, as a function of *CaO* dosage, Mature FFT Operator 1.

Lime Dosage (ppm)	Plastic Limit (%w)	Liquid Limit (%w)	Plastic Index (%w)
0	34.2	79.2	45.0
1,000	34.2	82.7	48.4
3,000	39.4	74.9	35.5
7,000	43.5	69.5	25.9
10,000	42.1	66.2	23.0
30,000	41.8	61.8	20.0
50,000	39.9	54.4	14.5
100,000	41.8	49.0	7.2

w is mass of water/dry mass

Table 4. Atterberg limits at 28 days curing time, as a function of *CaO* dosage, Mature FFT Operator 2.

Lime Dosage (ppm)	Plastic Limit (%w)	Liquid Limit (%w)	Plastic Index (%w)
0	35.1	108.0	45.0
1,000	31.0	102.2	48.4
3,000	41.3	69.3	35.5
7,000	41.2	65.0	25.9
10,000	38.6	70.0	23.0
30,000	39.0	60.5	20.0
50,000	39.6	58.5	14.5
100,000	39.7	41.9	7.2

w is mass of water/dry mass

Table 3. Atterberg limits as a function of curing time, 7,000 ppm *CaO* dosage, Mature FFT Operator 2.

Curing Time (day)	Plastic Limit (%w)	Liquid Limit (%w)	Plastic Index (%w)
1	40.7	73.1	32.4
3	41.3	68.9	27.6
7	42.8	66.8	24.1
28	43.5	69.5	25.9
56	42.5	64.8	22.2

w is mass of water/dry mass

Table 2. Atterberg limits as a function of curing time, 7,000 ppm *CaO* dosage, Mature FFT Operator 1.

Curing Time (day)	Plastic Limit (%w)	Liquid Limit (%w)	Plastic Index (%w)
1	40.8	92.0	51.2
3	40.0	83.6	43.6
7	42.6	82.5	39.8
28	41.2	65.0	23.8
56	43.0	68.0	25.0

w is mass of water/dry mass

It was observed that at the higher lime addition dosages, around 10,000 ppm and above, unreacted lime was evident in the sample upon testing. This suggests that at these concentrations the moisture content at the plastic limit is not sufficient to cause all the lime to react; which may cause the results of the tests at higher lime addition dosages to underestimate the degree of lime modification, especially with respect to the plastic limit. Similar tests are planned for mature FFT treated with high dosages of *CaO* followed by capping with sand and/or blending with overburden soils, along with the large strain consolidation and permeability tests, such as those developed by at a range of different lime addition dosages (Suthaker & Scott 1996).

2.5 Treatment of Whole Tailings with Lime

Initial research into tailings treatment with calcium compounds, including lime (CaO), focused on the whole tailings treatment to reduce the environmental impacts of oil sands tailings disposal, as well recovering $NaOH$ produced by ion exchange reaction between $Ca(OH)_2$ and sodium-clay, the chemical reaction expressed in Equation 5 in Section 2.1 (Kessick, 1983). Whole tailings treatment with CaO additive was studied for the disposal of the whole tailings as an environmentally acceptable tailings disposal practice (Hamza et al, 1996; Lane et al, 19984; Lane, 1983; C-H Synfuels, 1984).

Previous studies made on treating oil sands tailings with chemical additives, including CaO , focused on the coagulation and flocculation of clay particles, without considering segregation of fines from coarse sand particles. Treatment of the whole tailings produced at Syncrude Canada Ltd. with CaO was studied on tailings with nine different solids and fines contents (Ozum et al, 2004). This study showed that by using CaO additive at 1,000 to 1,300 g/m^3 -whole tailings dosages, whole tailings could be deposited with over 95% fines capture efficiency for most of the tailings over 50% solids and 15% fines contents.

Whole tailings treatment with CaO could be implemented for commercial practices before the cyclones, or direct deposition of the whole tailings. Treatment of the whole tailings alters the bitumen-water interfacial tension and reduces the stability of bitumen-in-water emulsions; by which the residual bitumen trapped in the tailings slurry could be removed by a flotation process (Romaniuk et al, 2015).

At our laboratory, the incorporation of CaO as an additive was explored for the treatment of a whole tailings sample with 37.5% solids, 92.3% fines and 1.2% bitumen composition, which is a typical tailings material recovered from cyclone overflow. The tailings sample was pressure filtered; water chemistry tests were made on two filtered water (process water-PW) samples.

The results of the water chemistry analyses are provided in Table 5. The total alkalinity of the tailings decreased when CaO was added at 1,000 ppm dosage (by chemical reactions of Equation 2 and Equation 3, Section 2.1); however, it increased on further increase in CaO addition dosages.

Table 5. Water chemistry results of the filtrate water from tailings samples.

Sample ID	CaO		Cond. mS/cm	Total Alkal. $CaCO_3$ (mg/L)	Cations				Anions	
	(ppm)	pH			Ca^{2+} mg/L	Mg^{2+} mg/L	Na^+ mg/L	K^+ mg/L	Cl^- mg/L	SO_4^{2-} mg/L
Tailings	0	8.4	1.9	429	50	20	280	18	145	265
Tailings	1,000	9.4	1.4	108	21	1	219	11	155	240
Tailings	3,000	11.8	6.7	1401	316	<DL	353	23	146	187
PW-1	0	8.4	1.7	401	45	20	276	15	147	234
PW-2	0	8.4	1.7	402	44	20	274	15	145	235

PW: Process Water

The yield stress values of the tailings samples were measured using a Brookfield viscometer and reported in Table 6. The yield stress values of the samples increased with increase in CaO dosage except for the 1,000 ppm dosage; which also implies that CaO is consumed by the bicarbonates (by chemical reactions of Equation 2 and Equation 3, Section 2.1) and Ca^{2+} ions and clay particle binding was better facilitated with the increase in CaO dosage.

Table 6. Yield stress of whole tailings samples with various dosages of CaO .

Sample ID	CaO (ppm)	Secondary Position Spindle No.	Shear Rate (RPM)	Static Yield Stress (Pa)
Tailings	0	71	0.1	24.3
Tailings	1,000	71	0.1	15.8
Tailings	3,000	73	0.1	162.9
Tailings	5,000	73	0.1	241.8

Effect of CaO additive on the hydraulic conductivity of the tailings sample was also measured by the constant head hydraulic conductivity measurement; results of which are presented in Figure 3. Increase in both yield stress and hydraulic conductivity of the tailings sample by CaO treatment is encouraging that whole tailings treatment before the cyclones and/or direct deposition could provide significant benefits in tailings disposal practices.

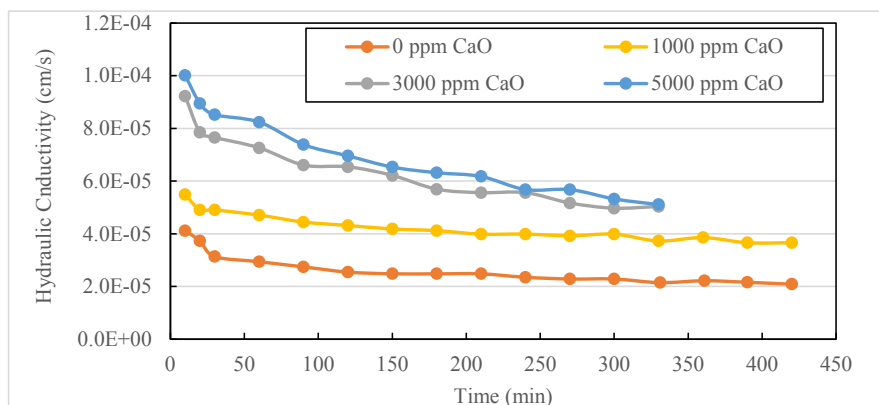


Figure 1. Constant hydraulic conductivity measurements.

3 SUMMARY

The CHWE process provides acceptable bitumen recovery efficiency; however, it is the source of many problems too. Reduction of the water surface tension (γ_w) promotes dispersion of clay in the extraction process slurry ore-water slurry and promotes production of FFT with poor settling and consolidation characteristics. Reduction of the bitumen-water interfacial tension ($\gamma_{B/W}$) promotes liberation of bitumen from oil sands matrix; however, suppresses kinetics of bitumen droplets coalescence and aeration processes in the extraction process slurry. Because of suppressed bitumen droplets coalescence and aeration kinetics, oil sand plants require large process vessels and large capital investment.

Any novel technology to reduce environmental impacts and to improve long-term sustainability of oil sands plant should be founded on three principles:

- (i) suppress dispersion of silt-clay size particles in the extraction process slurry;
- (ii) dispose oil sands tailings material as a non-segregating tailings material; and,
- (iii) convert *Na-Clay* to *Ca-Clay* before the implementation of any mature FFT dewatering processes.

While focusing on these process principles, process water chemistry, simplicity, integration to the existing plants, health and environmental safety, capital and operating costs must be considered as constraints. Our research findings showed that existing challenges of the oil sands plants could be solved or reduced in simple and cost-effective manners by using CaO as an additive for the following processes:

- (i) bitumen extraction process: improves bitumen recovery efficiency, suppresses silt-clay size particles dispersion, produces tailings with improved settling and consolidation properties and reduces Na^+ accumulation in the process water. These processes improve the long-term sustainability of oil sands plants;
- (ii) whole tailings treatment: which could be implemented before cyclones or direct deposition of the whole tailings into the tailings ponds;
- (iii) dispose the tailings as a non-segregating tailings (NST) material; and,
- (iv) treat mature FFT with a calcium-based additive before the implementation of commercially available or novel dewatering processes.

4 FUTURE STUDIES

Recently, oil sands players are interested in dewatering of existing mature FFT by treating it with flocculants followed by centrifuging and pressure filtering. At our laboratory, use of *CaO* as an additive for dewatering of existing mature FFT is being investigated for two purposes: (i) as a pretreatment of mature FFT before its centrifuging or pressure filtration; and, (ii) in-situ treatment followed by sand capping or blending with overburden soils, which could be implemented after treating the water layer of the mature FFT ponds with *CaO* at about 400-1,000 g/m³-water and recycling it to the extraction plant.

It was observed that at the higher lime addition dosages, around 10,000 ppm and above, unreacted lime was evident in the sample upon testing. This suggests that at these concentrations the moisture content at the plastic limit is not sufficient to cause all the lime to react; which may cause the results of the tests at higher lime addition dosages to underestimate the degree of lime modification, especially with respect to the plastic limit. Similar tests are planned for mature FFT treated with high dosages of *CaO* followed by capping with sand and/or blending with overburden soils, along with the large strain consolidation and permeability tests, such as those developed by at a range of different lime addition dosages.

REFERENCES

- Apex Engineering Inc. 2005. Production of Nonsegregating Tailings (NST) from Syncrude's Aurora Mine Tailings. *Report produced for Syncrude Canada Ltd., November 2005, Edmonton, AB, Canada.*
- Apex Engineering Inc. 2004-2005. NST production from Albion Sands Muskeg River Mine tailings material using CaO additive. *Seven reports produced for Shell Canada Ltd., Canadian Natural Resources Limited and Alberta Energy Research Institute, Edmonton, AB, Canada.*
- Babadagli, T., Burkus, Z., Moschopedis, S.E. and Ozum, B. 2008. Bitumen Extraction from Oil Sands Ore-Water Slurry Using CaO (Lime) and/or Ozone, *SPE 117677, SPE International Thermal Operations and Heavy Oil Symposium, 20-23 October, Calgary, AB, Canada.*
- Boardman, D. I., Glendinning, S. and Rogers, C. D. F. 2001. Development of stabilisation and solidification in lime-clay mixes. *Géotechnique 51(6): 533-543.*
- Caughill, D.L., N.R. Morgenstern and J.D. Scott. 1993. Geotechnics of nonsegregating oil sands tailings, *Can. Geotechnical Journal, 30(5): 801-811.*
- Caughill, D.L., Scott, J.D., Liu, Y., Burns, R. & Shaw, W.H. 1994. Field Program on Nonsegregating Tailings at Suncor Inc. *Proceedings of the 47-th Canadian Geotechnical Conference, Halifax, September, 1993.*
- C-H Synfuel. 1983. Dry Tailings Disposal from Oil Sands Mining, Oil, Gas and Energy Division, Industrial Programs Division, Environmental Protection Service, Environment Canada. Ottawa, ON, Canada K1A 1C8.
- Clark, K.A. 1944. Hot-Water separation of Alberta bituminous sands, *Trans. Can. Inst. Min. Met. (47): 257-274.*
- Clark, K.A. 1939. The Hot Water Method for Recovering Bitumen from Bituminous sand, *Report on Sulivan Concentrator, Alberta Research Council, Edmonton, Alberta, Canada.*
- Clark, K.A. and Pasternack, D.S. 1932. Hot water separation of bitumen from Alberta bituminous sand. *Ind. & Eng. Chem. 24, 1410-1416.*
- COSIA, 2014. Apex Project Report, *Prepared by NAIT-NARCOSS, January 31, Calgary, AB, Canada.*
- Craig, R. F. 2004. *Craig's Soil Mechanics, Seventh Edition, Taylor & Francis.*
- Dawson, R. F., Sego, D. C., & Pollock, G. W. 1999. *Freeze-thaw dewatering of oil sands fine tails. Canadian Geotechnical Journal, 36: 587-598*
- Donahue, R., Jeeravipoolvarn, S., Scott, J.D. and Ozum, B. 2012. Properties of Nonsegregating Tailings Produced from the Aurora Oil Sands Mine Tailings, *Proceedings of IOSTC-2012, pp. 143-152, December 7-10, Edmonton, AB, Canada.*
- Hamza, H.A., Stanonick, D.J. and Kessick, M.A. 1996. Flocculation of lime-treated oil sands tailings, *Fuel, 75(3): 280-284.*
- Jeeravipoolvarn, S. 2010. Geotechnical behavior of in-line thickened oil sands tailings, *Ph.D. Thesis, January 2010, University of Alberta, Edmonton, AB, Canada.*

- Kasperski, K.L. 1992. A Review of Properties and Treatment of Oil Sands Tailings, *AOSTRA Journal of Research*, 8:11-53.
- Kasperski, K.L. 2001. Review of Research on Aqueous Extraction of Bitumen from Mined Oil Sands. Report, *CONRAD Extraction TPG, Division Report CWRC 01-17 (CF)*, CANMET, Devon, AB, Canada.
- Kessick, M.A. 1983. Recovery of water and alkali used in oil sands and heavy oil extraction, *Fuel*, 62(11), 296-1298.
- Lane, S.J., Khan, F.Z. and Tonelli, F.A. 1984. Dry Tailings Disposal from Oil Sands Mining, Report to Environmental Protection Service, *Environment Canada and Department of Supply and Services Canada*.
- Lane, S. 1983. Lime Coagulation and Stabilization of Total Oil Sands Tailings. *Petroleum Society of Canada Annual Technical Meeting, May 10-13. Banff, AB, Canada*.
- Liu, J., Xu, Z. and Masliyah, J. 2005. Interaction forces in bitumen extraction from oil sands, *Journal of Colloid and Interface Science* 287: 507–520.
- Masliyah, J., Zhou, Z.J., Xu, Z, Czarniecki, J. and Hamza, H. 2004. Understanding Water-based Bitumen Extraction from Athabasca Oil Sands, *Can. J. Chem. Eng.*, 82: 628-654.
- Mikula, R. 2014. Tailings Answers *New Technology Magazine*, April 2014, pp. 26-29.
- Miller, W.G., Scott, J.D. & Segó, D.C. 2010. Influence of the extraction process on the characteristics of oil sands fine tailings, *CIM Journal*, 1(2):93-112.
- Pan, L., Jung, S. and Yoon, R.H. 2012. A fundamental study on the role of collector in the kinetics of bubble-particle interaction, *International Journal of Mineral Processing*, 106-109, 37-41.
- Romaniuk, N. Tate, M.J., Scott, J.D., Mehranfar, M., Selani, H. & Ozum, B. 2015. Residual bitumen recovery from oil sand tailings with lime, *T&MW Conference, 25-28 October, Vancouver, BC, Canada*.
- Ozum, B, Rick J. Chalaturnyk, R.J. and Scott, J.D. 2004. Production of Nonsegregating Slurry from Whole Tailings, *CIM Edmonton 2004 Conference, May 9-12, Edmonton, AB, Canada*.
- Ozum, B., Romaniuk, N., Sorta, A., Feland, B. and Scott, J.D. 2014. A Paradigm Change Needed in Oil Sands Industry: CaO as Additives for Bitumen Extraction and Nonsegregating Tailings Production Processes, *SPE 170174-MS, SPE Heavy Oil Conference-Canada, 10-12 June, Calgary, AB, Canada.-Canada, 10-12 June, Calgary, Alberta, Canada*.
- Ozum, B., Romaniuk, N.A., Sorta, A. and Scott, J.D. 2012. *Oil Sands Mature Fine Tailings and Bitumen Extraction, Proceedings of IOSTC-2012, December 2-5, Edmonton, AB, Canada*.
- Ozum, B. and Scott, J.D. 2010. Methods to Reduce Production of Oil Sands Fluid Tailings, *2-nd IOSTC, December 5-8, Edmonton, AB, Canada*.
- Ozum, B. and Scott, J.D. 2009. Reduction of Oil Sands Fine Tailings, *Proceedings of T&MW Conference, pp. 383-395, November 1-4, Banff, AB, Canada*.
- Pan, L., Jung, S. and Yoon, R.H. 2012. A fundamental study on the role of collector in the kinetics of bubble-particle interaction, *International Journal of Mineral Processing*, 106-109, 37-41.
- Pan, L. and Yoon, R.H. 2010. Hydrophobic Forces in Wetting Films, *Faraday Discussion*, 146: 325-340.
- Rogers, C. D. F., Glendinning, S. and Roff, T. E. J. 1997. Lime Modification of Clay Soils for Construction Expediency, *Proceedings of the Institution of Civil Engineers - Geotechnical Engineering* 125(4): 242-249.
- Rogers, C. D. F. and S. Glendinning, S. 1996. Modification of Clay Soils Using Lime, Lime Stabilisation, *proceedings of the seminar held at Loughborough University Civil & Building Engineering Department, 25 September, Thomas Telford*. 99-114.
- Scott, J.D., Donahue, R., Blum, J.G., Paradis, T.G., Komishke, B. and Ozum, B. 2007. *Production of Nonsegregating Tailings with CaO or CaO and CO₂ for Improved Recycle Water Quality. CONRAD's Water Usage Workshop, November 21-22, Calgary, AB, Canada*.
- Speight, J.D. and Moschopedis, S.E. 1980. Surface and Interfacial Phenomena Related to the Hot Water Processing of Athabasca Oil Sands, *Information Series 86, Alberta Research Council, Edmonton, AB, Canada*.
- Speight, J. G. and Moschopedis, S.E. 1977/78. Factors Affecting Bitumen Recovery by Hot Water Processes, *Fuel Technology*, 1: 261-268.
- Suthaker, N. N. and Scott, J.D. 1996. Measurement of hydraulic conductivity in oil sand tailings slurries, *Canadian Geotechnical Journal* 33(4): 642-653.
- Wells, P.S., Coldwell, J. and Fournier, J. 2010. Suncor pond 5 coke cap - The story of its conception testing and advance to full-scale construction, *Proceedings of 14-th T&MW Conference, pp. 341-346, 17-20 October, Vail, CO, USA*.

Mine Waste Rock Storage Facilities Design, Construction, and Operation as Engineered Structures

L. Piciacchia, J.A. Vides, and J. Mosquera

BBA Inc., Mine Waste Management and Environment, Montreal, Quebec, Canada

ABSTRACT: Waste rock storage facilities (WRSF) are massive structures that make part of mining environments, landscape, and layouts. Instabilities in these structures can impact nearby mining infrastructure, equipment and personnel as well as the surrounding environment including lakes, streams and rivers. Despite the significance of these structures it is common practise to treat them as dumps, with very little effort allocated to design, engineered construction, supervision and monitoring, stockpile deposition planning, site characterization or operations. It is only when we look at the long-term that the increased apparent costs of planning, design, construction and operation of a WRSF is put into perspective. It is therefore important that the current mindset regarding WRSFs evolves and becomes more holistic by considering not only short term needs but include proper fit to purpose engineering and construction of these structures. This paper provides an example of an optimized design along with consideration for constructability where existing stockpiles need to be brought to code for long term stability.

1 INTRODUCTION

Waste rock is an important waste stream generated in all open pit and underground mining operations. The amount of waste rock produced depends on the commodity being mined, the mining method employed, and the geometric orientation of the orebody. Waste rock needs to be managed according to the type, quantity, geochemical and geotechnical characteristics of the waste material being produced, as well as of the geotechnical characteristics of the foundation on which the WRSF will be deposited.

Typical methods for managing mining waste, which may include rock altered to varying degrees, sand, till and organics materials, are deposited directly on natural ground. The materials are normally transported by truck and deposited by one of three methods:

- *End dumping:* consist on depositing waste rock over the face of an existing waste rock pile or from the crest of a natural ridge. This method usually results in particle size segregation down slope towards the toe of the waste rock pile. Particle size generally increases from the top to the bottom. The end dumping method might be beneficial for coarse waste rock as larger fragments accumulating at the toe will form a natural drain, making the waste rock pile self-draining.
- *Push dumping:* consists of depositing waste rock from trucks onto the waste rock pile platform, followed by leveling and pushing by tractors and shovels over the waste rock pile face. This method also results in particle size segregation, with finer waste rock at the top and coarser waste rock at the toe of the waste rock pile. Push dumping has a similar self-draining effect at the base of the waste rock pile as that described for the end dumping method. However, push dumping has the added benefit of providing an extra degree of safety to workers as large trucks do not approach the crest of the waste rock pile during waste rock placement.

- *Free dumping*: this method is similar to push dumping, but instead of pushing waste rock over the slope of the existing pile, the material is spread over the platform with tractors and shovels. The result is a better graded in place waste rock material with minimal particle size segregation. This is an ideal method for ascending waste rock pile construction or for co-deposition of fine and coarse waste rock.

Mine waste rock piles configurations tend to take advantage of the topography in which they are situated. Common classification for such configurations has been described by Hawley and Cuning (2017), as follows: valley-fill, cross-valley, side-hill, ridge, or heaped. Within a particular topography the method of deposition and construction are typically governed by economic aspects of the project and often result in either an ascending or descending configuration.

Where topography permits, descending construction method tends to be the most cost-effective. It is important to note that by using a descending construction method, the platform elevation remains constant and the deposition front advances towards the final footprint. On sloping ground the slope height increases with the waste rock pile advancement. As such, the factor of safety associated with the pile will decrease with the advancing front. For granular materials, the theoretical factor of safety will never be less than one (1) if the WRSF is built on a competent foundation (Piciacchia et al., 2018a). However, the regulatory requirements for waste rock piles design specifies that an overall factor of safety 1.5 should be maintained for long term stability (MERN, 2017). Within limiting heights, using descending construction methods alone will result in waste rock piles that do not conform to legislation.

On sites where foundations conditions are considered to be less than ideal or where the overall pile height are the driving factors for stability, the ascending construction method should be considered. This method offers the potential to control the incremental loads placed on non-competent foundations. It further offers a means of controlling the geometry of large waste rock piles and therefore the overall factor of safety. However, ascending construction is a more costly method.

2 MATERIAL CONSIDERATIONS IN THE DESIGN OF WASTE ROCK PILES

Overburden and blasted rock (waste rock) are the two primary waste streams generated during orebody exploitation before any milling and grinding processes occurs. The overburden portion usually consists of organic material followed by coarse grained soils such as sand and till, and/or fine-grained and cohesive materials such silt and/or clay. Waste rock grain size, shape, and degree of fragmentation varies from coarse to fine depending on the type of rock and the method used for its extraction (blasting and ripping).

These two waste streams have drastically different design properties. Parameters such as permeability, water retention capacity, angle on internal friction (ϕ) and cohesion (c) can vary significantly for the various waste streams. If the overburden and waste rock are to be managed within the same waste rock pile, the degree of heterogeneity will be proportional to the amount of each type of material in the pile at any given time. Spatial and temporal uncertainty of mine waste rock properties are the biggest management challenges for mine operators and designers. These challenges can be mitigated, in part, by adopting good practices such as material sorting at the point of origin and by managing the waste streams in separate piles (Vides et al., 2018).

The properties of soil in the foundation are also governing factors in waste rock stability assessment. The result of conventional geotechnical investigations of the foundation is a basic input that must be integrated into the waste rock design. Three dimensional numerical modelling is useful tool for a more realistic identification of critical sections within a waste rock pile, (Piciacchia et al., 2018b), as it helps visualize materials interactions in different directions.

3 DESIGN CRITERIA

Waste rock pile guidelines and regulations such as the one proposed by MERN, 2017, requires that different factors of safety need to be maintained under varying operating conditions including the closure stage of a WRSF. Table 1 presents factors of safety used in WRSF design.

Table 1. Stability analysis - Minimum values for factor of safety

Condition	Factor of Safety (FS)
Bearing capacity of the foundation under WRF	1.5 to 2.0
Local stability of the piles (for each bench)	
Short term static analysis*	1.0 to 1.1
Long term static analysis	1.2
Overall stability, for deep failures or failures pass through Foundation	
Short term static analysis *	1.3 to 1.5
Long term static analysis	1.5
Pseudo-static analysis	1.1 to 1.3

* According to risk and uncertainty

Factors of safety as defined by regulators account for risk and uncertainty, as such it is more stringent than just designing to maintaining equilibrium between restraining and driving forces acting in a waste stockpile (i.e. F.S of 1.0); which is acceptable under legislation for short term or operational conditions.

The design of the ultimate stockpile needs to be based on long term facility closure requirements rather than short term operational conditions. Proper economical design should incorporate both the requirement to optimize the overall construction of a waste rock stockpile and those of stability at closure. The construction approach and sequencing described herein is based on a mine plan which will be executed to closure.

4 CASE STUDY

4.1 Description

A practical example of implementing a proper design approach for an existing WRSF is summarized below. The WRSF closure configuration has an overall strike length in excess of 10 km and measures between 200m to 300 m in height. The WRSF has a width of 2 km and will store over 2 billion m³ of coarse waste rock at closure.

This facility operates a number of open pits in a synchronized fashion. Deposition areas are built and operated in sequence. The main criterion for defining areas of deposition is transportation distance between the pit and the waste rock stockpile. End dumping and push dumping methods account for the majority of the deposition methodology. Stockpile development proceeds using descending construction.

Over the years, some geotechnical characterisation has been performed at the site of the study area. Foundation could be described as competent, and are characterised by shallow deposits of glacial till to a maximum depth of 6m, overlaying bedrock. The overall waste rock deposition can be considered a side hill fill configuration, on a moderated sloping topography (about 15 degrees). The stockpiles currently under construction are mainly composed of coarse material; this includes gravels, cobbles and boulders with less than 5% of fines. Stockpiles in place appear to be in equilibrium, with angles of repose equal to the angle of internal friction of approximately 35-37 degrees. The factor of safety evaluated for the current operation and stockpile configuration is 1.0.

In order for the facility to meet regulatory requirements, a generalized overall slope of 26 degrees will be required at closure. In addition, bench heights and widths will need to be designed in order to meet local stability design criteria (Piciacchia et al., 2018). Descending construction method alone can therefore not be used to meet closure configurations. The facility has advanced to this point, meeting regulatory requirements for short term stability.

Looking ahead plans needed to be developed in order for the operators to meet long term regulatory requirements. Figure 1 summarizes the most important features of the current operation.

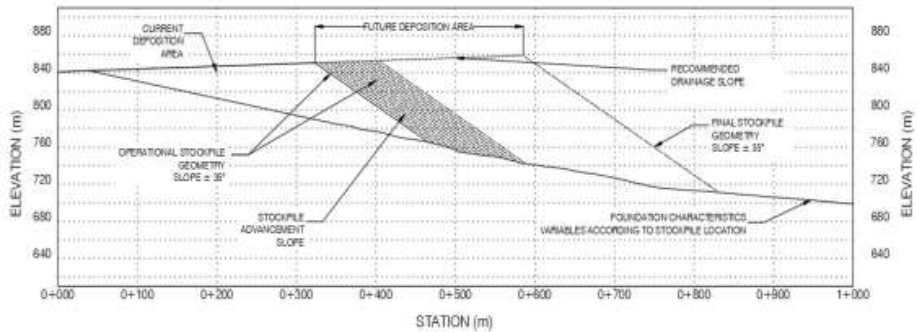


Figure 1. Typical waste rock pile of the study area

4.2 Configuration approach and design

The final configuration required for the pile can be met by different construction approaches. Figure 2 presents one of the proposed construction alternatives required to attain a long term factor of safety equal to 1.5. This option is essentially an ascending construction method commencing from the final toe of the proposed waste rock pile and built in lifts.

As shown in figure 2, the first level of the pile is built to the prescribed elevation and then backfilled to natural terrain. Subsequent benches are built maintaining a design setback.

The number of benches built in this fashion would be governed by the final elevation of the existing waste rock pile and the design bench height. In essence this approach would require mine operators to move completely away from a descending construction method in favour of ascending construction method. It was determined that such a drastic modification would not only be disruptive to operations, but would be extremely costly due to a significant increase in truck cycle times. This cost increase would impact both the capital and operational costs of the project as the current fleet of trucks would need to be increased.

An alternate approach to construction is shown in Figure 3. This option maximizes the use of the descending construction method and limits ascending construction to a minimum limiting such construction to the containment structure (buttress) located at the final foot of the waste rock pile. This confinement structure is built before the current deposition front comes in proximity to the footprint of the designed buttress structure. The construction sequence also allows for the confinement structure to be built safely and reduces the volume of ascending construction required, from 100% in the first option to about 25% in the construction of the buttress.

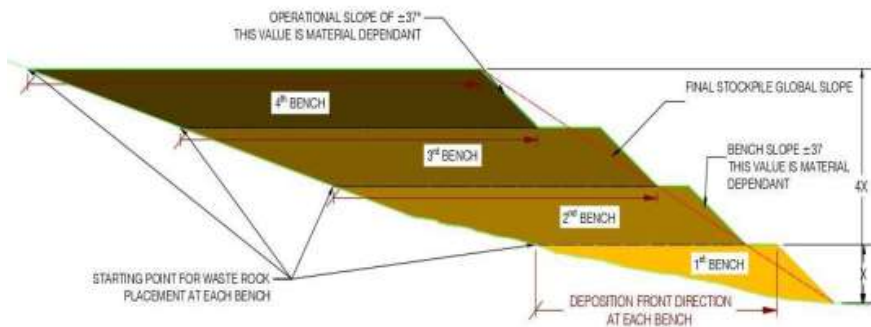


Figure 2. Waste rock pile construction Method – Alternative 1

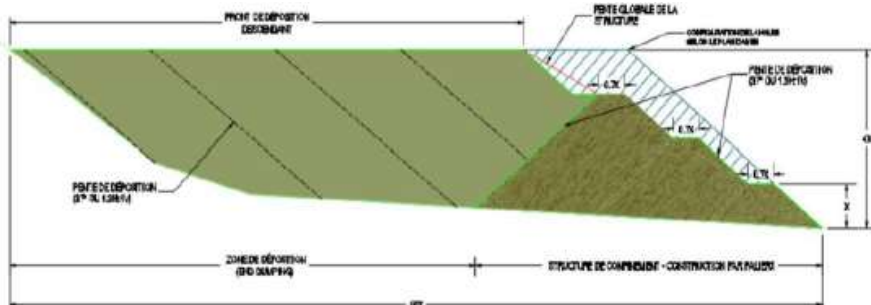


Figure 3. Waste rock pile construction method – Alternative 2

In order to reduce the volume required for the construction of the confinement structure, a maximum bench height for the recommended configuration was defined. Bench width was determined using analytical calculations and the safety factor was validated using 2D and 3D numerical models. The maximum height for a bench comprising a waste rock with an ϕ of 36° is 50 m, as developed by Piciacchia et al. (2018). This geometry required a bench width of 35 m in order to attain an overall FS=1.5, and a local FS=1.2. Figure 4 presents a typical cross section applied along the strike on the entire deposition area. Figure 5 presents a plan view of the resulting 3D application of the typical cross section.

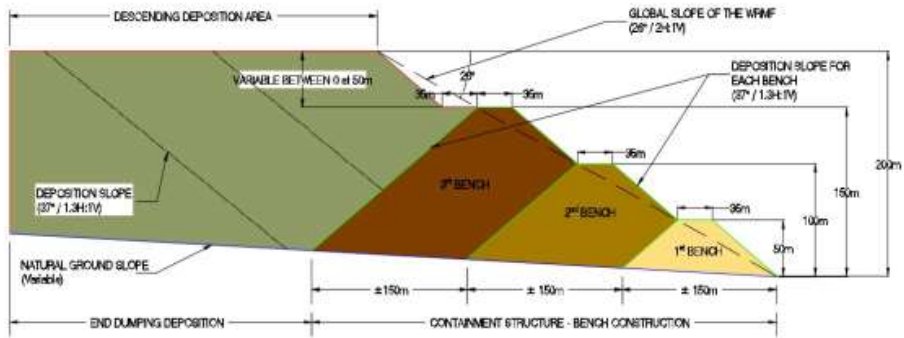


Figure 4. Typical design cross section applied on the deposition area

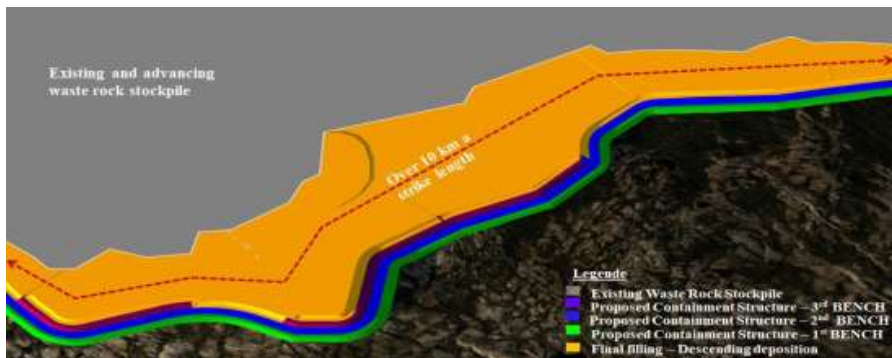


Figure 5. Resulting 3D model of the recommended solution

A verification of interferences between the proposed final configuration and existing infrastructure and environmental constraints was conducted to ensure feasibility of the construction method and configuration proposed. Hybrid solutions are often needed in cases where interferences cannot be mitigated in the short term. The hybrid solutions should be aligned with the needs of the mine development plan.

4.3 Constructability

Constructability entails assuring access to the construction site, availability of the quantity and quality of materials required for construction, assessment of construction drawings, preparation of a construction schedule in alignment with operational needs, and a detailed sequence of each construction stage. The availability of the construction material can be ensured by developing deposition plans which are synchronized with the mine development plan including the volumes and material specifications required for buttress construction.

Options for access to the construction site of the confinement buttress have been considered including a ring road at the toe of the WRSF. However, such roads would not only be costly to build, but will increase truck cycle times. As such, access roads were incorporated into the confinement structures themselves. Figure 6 illustrates the resulting configuration of such an approach.

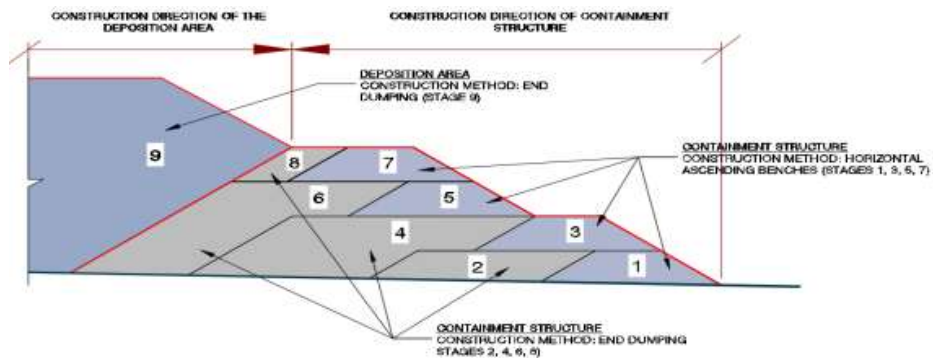


Figure 6. Access roads and containment structure approach

With the construction of each bench the platform area should be extended beyond the design bench width in order to accommodate the base of the following bench. The construction of individual benches could be achieved by one or multiple lifts depending on overall dimensions and degree of compaction required. Figure 7 illustrates a sequence in which each bench is built in two lifts.

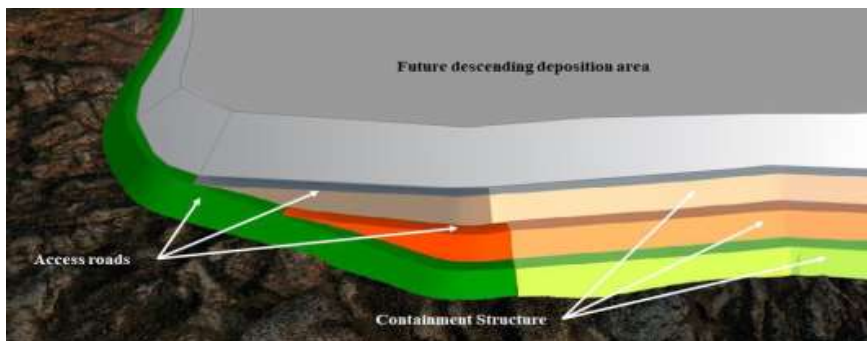


Figure 7. Construction sequence for benches of the containment structure

The construction phases shown in Figure 7 can be undertaken using ascending or descending construction methods. For this particular, stages 1,3,5,7 were recommended to be done using ascending construction, while 2, 4, 6, 8 and 9 using descending construction method.

5 CONCLUSION

This paper has presented a design approach which attempts to find the balance between operational needs, constructability, safety and compliance. WRSF should be considered as engineered structures instead of dumps and should be given the attention that structures of this size, magnitude and importance demand. This paper provides an example of the complex nature of WRSF design and the need to adapt to changing design input parameters. Flexibility in design is essential and needs to account for operating constraints as well as regulatory requirements. Special attention should be given to the design nuance between the operational factor of safety and the factor of safety required at closure.

Given the long life of WRSF, it is essential to conduct proper planning, scheduling and sequencing of the construction. Likewise, waste rock deposition plans are important management tools that aid in the planning, operation and construction of WRFS. Planning should be done to varying levels of precision accounting for the special and temporal variability of the waste rock properties.

REFERENCES

- Hawley, Mark, and John Cunning 2017. *Guidelines for Mine Waste Dump and Pile Design*. CSIRO Publishing
- Ministère de l'Énergie et des Ressources Naturelles (MERN) du Québec, Direction de la restauration des sites miniers 201. *Guidelines for preparing mine Closure plans in Québec*.
- Piciacchia, L., Marefat, V., & Vides, A. 2018. Practical Nomograms for Waste Rock Piles Design on Competent Foundations. *18th Tailing and Mine Waste Conference. Department of Civil and Environmental Engineering at Colorado State University*.
- Piciacchia, Luciano, Marefat, Vahid and Mosquera, Jenyfer, 2018. The use of 3D models and analysis in support of waste pile design and operations. *18th Tailing and Mine Waste Conference. Department of Civil and Environmental Engineering at Colorado State University*.
- Vides, José Antonio, Piciacchia, Luciano and Marefat, Vahid, 2018. Guidance for the safe and optimized operation of waste rock facilities. *18th Tailing and Mine Waste Conference. Department of Civil and Environmental Engineering at Colorado State University*.

System Dynamics Approach to Tailings Management Simulation

T. Zheng and N. Beier

University of Alberta, Edmonton, Alberta, Canada

ABSTRACT: Tailings Management System (TMS) consists of a web of inter-related sub-systems across disciplinary and organizational boundaries. Conventional predictive models simulate physical processes in each discipline with great details. In contrast, simulation based on System Dynamics (SD) focuses on overall behavior of the system over time rather than the typical mechanistic predictions seen in conventional numerical models. SD technique has been widely used in the field of business, ecology, public health, and environmental studies. However, despite the adoption of various SD-based tools in mine water balance and water quality studies, the identification and formulation of causal loop diagrams and feedback structures are rarely practiced in the management of tailings and mine waste. This paper builds on the foundation of a previously developed dynamic simulation tool, Tailings Management Simulator (TMSim) to demonstrate how SD can be used as a framework for inter-disciplinary collaboration and stakeholder communication. Advantages and limitation of SD-based modeling approach will also be discussed.

1 INTRODUCTION

This paper provides an overview of the SD philosophy and how it can be applied in the tailings management context. SD-based modelling process consists of two major parts: qualitative stage and quantitative stage. The paper will focus on the qualitative process while serving as a companion paper to future modeling of soil water dynamics between reclamation covers and underlying tailings substrate.

1.1 History of System Dynamics

Originated from the development of feedback control mechanisms for military radars and gun mounts during World War II (Forrester, 1994), System Dynamics is a modelling technique that deals with complex inter-relationships between components within a system or multiple systems. Jay Forrester first applied the methodology in the mid-1950s to the field of business and operations research at the newly created Sloan School of Management at MIT. The first application of SD was a dynamic model, created in late 1950s, to explain poor business performance at General Electric where the employment instability was later discovered to come from internal structures rather than external forces such as economic cycles. In the 1970s, the use of SD gradually shifted from business modelling to urban planning due to the proliferation of low-cost housing initiatives. Over the years, the application of SD has found its way into a variety of fields such as public health, ecology and engineering. (Lane and Sterman, 2017). Today, SD has become a full-fledged academic field so matured that an association named System Dynamics

Society and its affiliated academic journal, System Dynamics Review, are solely dedicated to its advancement and promotion.

1.2 The Big Picture

Despite its wide applications in business and social sciences, SD has not been widely used in tailings management and mine closure planning. Based on a preliminary keyword review of the bibliography database in System Dynamics Journal, Table 1 showed that only 12% of the total articles in the bibliography database from System Dynamics Society is related to technical fields most relevant to the mining industry. A quick search in other literatures has also yielded very few applications of SD in mining-related fields. Li and Simonovic (2002) successfully used SD to model hydrological processes in groundwater flow. Subsequently, Elshorbagy et al (2005) expanded the SD approach to study flow regime in un-saturated soil cover. More recently, King et al (2017) adopted SD in the evaluation of hydro-power dam safety from a system perspective. Despite potential publication bias in the System Dynamics Review journal, the mining industry at large and certainly niches like tailings and closure management may have benefited very little from this modelling paradigm.

The lack of case studies related to SD in tailings management can be attributed to the unique gap between numerical models and our mental models. Conventional numerical models are based on extensive experimental and empirical evidence. In contrast, mental models are built upon heuristics and intuition. In Figure 1, different types of models are located inside an inverted triangle formed by three axes of scale. The diagram puts the traditional numerical models at the bottom since they provide the foundation on which other types of models are built. At the top of the inverted triangle are the mental and conceptual models, which strive for simplicity and maximum degree of horizontal integration. In the middle of the graph, the intermediate models strive for balance between breadth and comprehensiveness.

Ford (2010) argued that to study climate change, SD models are the most powerful when designed to fit in the conceptual model category at the top. For topics as broad as climate change and evolutionary ecology, maximum horizontal integration across different disciplines is not only productive but sometimes also necessary. However, over-simplification and absence of key physical processes in a model will inevitably pose challenges during calibration and validation process. Furthermore, endogenous variables in climate systems such as precipitation and daily temperatures become exogenous in a tailings management context due to the much smaller system boundary. Therefore, SD-based models in tailings management should aim for the middle ground between conceptual models and traditional numerical models.

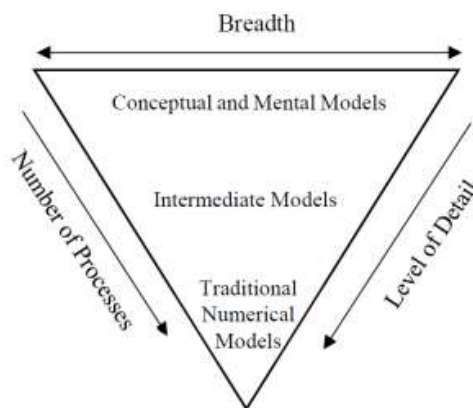


Figure 1. Classification of models

Table 1. Keyword search of System Dynamics Review bibliography database.

Keyword	Number of Articles	Proportion*
Mining	88	<1%
Water	972	8%
Construction	500	4%
Dam	17	<1%

*Based on a total number of 12,412 articles.

2 SD MODELLING PROCESS

2.1 Qualitative Stage

Stocks and flows, feedback structures are the three basic building blocks of any SD-based models. Stocks are state variables that track accumulation of quantities at any given time. Flows are variables that add or subtract quantities per unit of time step. Feedback structures are closed-form relationships that either reinforce or balance each other. Auxiliary variables in the form of mathematical equations are often required to explain Flows.

The qualitative stage of model development involves the following steps: i) familiarization with the system and background studies; ii) construction of specific questions that need to be answered by the model; iii) identification of variables, stocks and flows; iv) formulation of causal loop diagrams; and v) iterative revision of causal loop diagrams through learning, debate and discussion. It should be noted that, though anything qualitative tends to be perceived as being conceptual, the qualitative stage in SD modelling is a rigorous process with its own set of syntax, clear-defined rules and best practices. During this stage of model development, general patterns are more important than precise numbers (Ford, 2010).

Feedback structures are represented by causal loop diagrams which are drawn by the Vensim software in this paper. Figure 2 is a popular case study used in many SD literature to explain the basics of causal loop diagrams. Here, population is treated as a stock. Variables are connected by one-way arrows which represent causal relationships. Either positive (+) or negative (-) polarity is assigned to the arrowhead based on how the dependent variable changes in response to changes in the independent variables. Positive causal link means that the linked variables change in the same direction. All else being equal, a higher birth rate will increase population which in turn drives up the birth rate. Negative causal link means that variables change in the opposite direction. A higher death rate will decrease population which in turn reduces death rate. It should be noted that, as a good practice, polarity is assigned by testing the effect of positive polarity on variables at the arrowhead.

If the number of negative polarities in a loop is odd, the feedback loop is classified as negative. If the number of negative polarities is even, the feedback loop is identified as positive. Negative feedback loop balances the system while positive feedback loop gives rise to run-away behavior or amplified system response to any changes in variables (Richardson, 1997).

In Figure 2, the parallel lines at the top and bottom of the loop denote the concept of delay. There are two types of delay: material delay and information delay. For the material delay, the effect of increasing population will not be reflected in the birth rate since family formation and pregnancy take time. For the information delay, even though the effect of rising birth rate is instantaneously reflected in the population, modelers will not be aware of this information due to time interval between censuses. The same rationale can also be applied to the delay effect shown in Figure 2b.

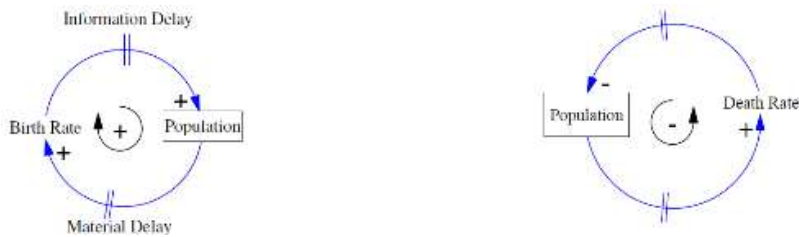


Figure 2. a) Causal loop diagram for population growth b) Causal loop diagram for population decline

The methodology used for constructing Figure 2a and 2b can be applied to examining the one-dimensional consolidation behavior of foundation soil under a rising tailings storage facility. In Figure 3, excess pore pressure is modelled as a stock element with construction rate as inflow and dissipation rate as outflow. Assuming that Darcy’s Law is valid and that the principle stress in the foundation soil can be approximated by the vertical stress, an increase in construction rate will trigger a series of chain reactions and lead to a negative feedback structure, which makes sense since the consolidation process brings the system back into balance. The counter-clockwise loop symbol is also given a name to communicate the major theme of the feedback structure. Alternatively, a numeric value can be assigned to keep track of multiple feedback loops.

Variables outside the feedback loop are considered exogenous while those from inside are considered endogenous. In this case, construction rate, hydrostatic pore pressure and existing total stress are all considered exogenous or external to the system. Exogenous variables can become endogenous and vice versa depending on how the boundary of the system changes. For example, construction rate becomes endogenous when additional feedback loops are used to incorporate the observational method and contingency plans. It is the endogenous variables that give rise to interesting behaviors in the system (Richardson, 2011).

The causal loop diagram in Figure 3 does not contain enough information for quantitative modelling since additional feedbacks, delays and auxiliary variables are absent. Spatial arrangement, level of confining stress, principle stress rotation, and in-situ soil properties are also not explicitly considered in Figure 3. However, the systematic process of creating the diagram builds a robust foundation on which further revision of the model can be communicated across disciplinary boundaries.

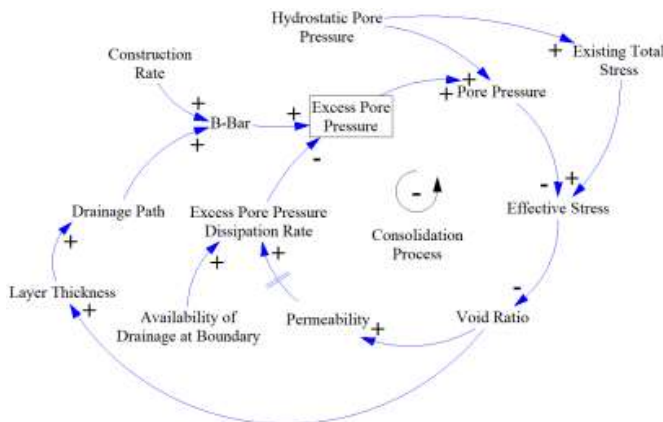


Figure 3. Causal loop diagram for consolidation of foundation layer under fully saturated condition (Zheng and Beier, 2018)

2.2 Quantitative Stage

The quantitative stage of SD consists of the following major steps: i) conversion of causal loop diagrams to runnable models; ii) parameter estimation; iii) sensitivity analysis; iv) analysis of varying parameter input and model structures; and v) continued model maintenance based on new information and insights. The quantitative process in SD is similar to that of conventional numerical modelling except in a few areas that require new ways of thinking. These areas of differences are discussed in Section 2.3 and further addressed in Section 3.1 and 3.2. Case studies and SD-based tailings management models will be presented in a separate paper.

2.3 Model Maintenance

SD models are not pre-made packages off the shelf. Building models from scratch is the norm rather than the exception in SD modelling (Homer, 1996). Since it is possible to incorporate tentative knowledge and personal beliefs in SD models, continuous improvement of the model is necessary, especially when key parameters transition from being soft to hard as a result of new data becoming available.

Mine plans and tailings plans keep evolving through multiple feedback structures. At the beginning of mine development, mine planners provide input parameters to tailings planners in a one-way manner. Over time, mine plan will have to be continuously adjusted as the performance of tailings system becomes available and lessons-learned is shared. This dynamic nature of planning cycles requires constant questioning of underlying assumptions in SD models.

3 WHY SYSTEM DYNAMICS?

3.1 Advantages and Benefits

a) Transparency

In a SD simulation environment, all elements and functional relationships are exposed, visual and transparent through causal loop diagrams and stock-and-flow figures. Modelers and users can also explore the underlying empirical relationships and numerical schemes that are used to explain inter-relationships between elements. There should be no black boxes and hidden components in a SD simulation environment (Nicolson et al, 2002). In Figure 4, additional visualization is used in GoldSim to enhance clarity for dynamically simulating volumes of Fluid Fine Tailings (FFT), further demonstrating the communicative power of SD.

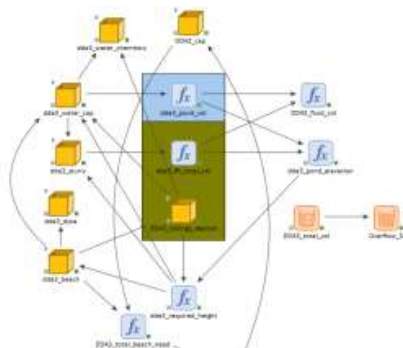


Figure 4. Elements of a sub-model in GoldSim (Modified from Beier, 2015)

b) *Flexibility and Expandability*

As part of top-down approach, simplified “child” models can first be developed prior to creating time-consuming larger models. The nature of object-oriented programming allows for scalability of those “child” model elements, saving time and preventing accumulation of errors in the future. This is particularly true for spatial components since SD-based tools can intrinsically handle time but not space (Kossik and Miller, 2004). In case greater spatial accuracy is required, SD model can be easily expanded if elements in each “child” models follow the same structure and naming convention.

Figure 5 shows a consolidation “child” model for tailings deposits developed in the GoldSim software. In Figure 5a, all elements of the calculation process and their respective influence directions are exposed and visible to the user. The numerical scheme is linearized based on an explicit, non-iterative finite difference method. In Figure 5b, each red-colored box or container denotes a discretized layer which stores the elements in Figure 5a with identical format and naming conventions. A total of 12 containers were specified for this model. However, should greater accuracy be needed, the user can easily add more containers by duplication without creating new mathematical relationships.

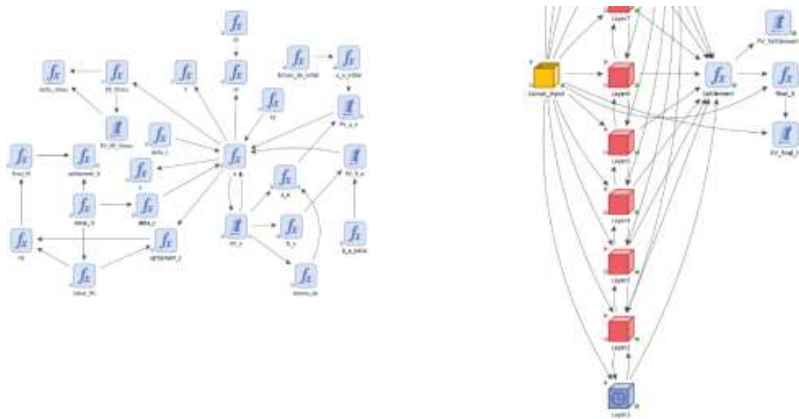


Figure 5. a) Exposed components of the “child” consolidation module; b) Parental setup of all the “child” consolidation modules with 7 spatial layers visible. (Zheng and Beier, 2018)

The causal loop diagram in Figure 6 is constructed using the methodology described in Section 2.1. As the name of the feedback loop suggests, the diagram focuses on 1D un-saturated flow mechanism in a soil layer. Figure 6 may be sufficient if the goal is to understand the run-away behavior of the system under climatic forces. However, if the objective of the model is to evaluate the state of water storage and soil water content over time, Figure 6 needs to be expanded to include additional pieces of physics.

As shown in Figure 7, flexibility and expandability inherent in causal loop diagrams allow for the incorporation of evapotranspiration process and effect of volume change to the unsaturated flow mechanism. As expected, evapotranspiration is a negative feedback loop, providing checks and balances to regulate the run-away behavior of unsaturated flow and volume change. There are still rooms for expansion since Figure 7 assumes the absence of bottom boundary conditions, surface run-off and inter-flow between adjacent layers.

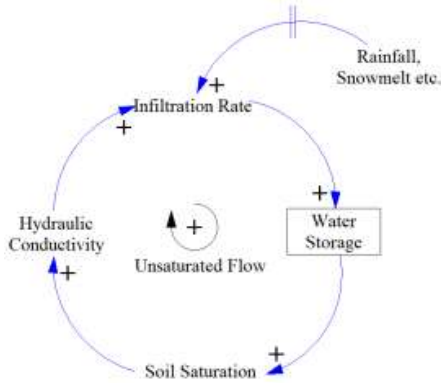


Figure 6. Causal loop diagram for un-saturated flow in soil cover (Modified from Elshorbagy et al, 2005).

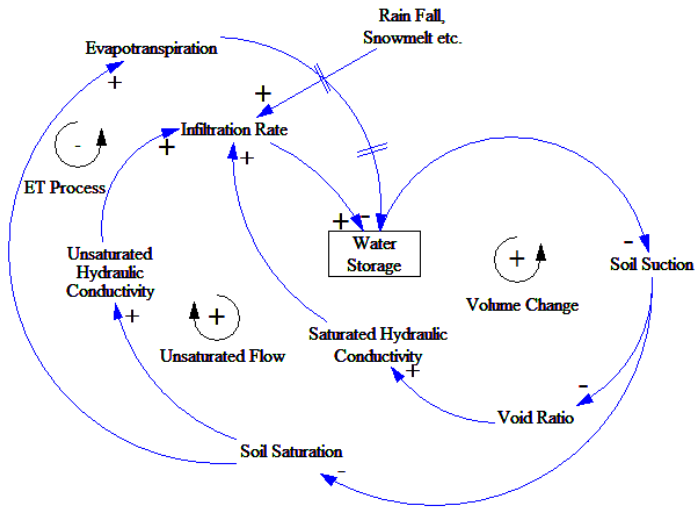


Figure 7. Expanded causal loop diagram from Figure 6.

c) *Stakeholder Participation*

Due to the extensive qualitative process prior to quantification of model parameters, the modelling process itself, rather than the end-product, offers the greatest insights. This view is supported by publications on the philosophy of SD modelling (Richmond, 1993; Forrester, 1994; Sternman, 1994 and Meadows, 2008) as well as on case histories of SD (Hovmand, 2014 and ElSawah et al, 2017). Beier (2015) also echoed the same view in the conclusion for simulating the Cross-Flow Filtration (CFF) tailings dewatering technology that failed simulation runs and the process of gathering input data itself provided insights into underlying mine planning assumptions.

Haraldsson et al (2006) had some success in the use of SD and Causal Loop Diagrams in engineering education. This is equally true for non-technical stakeholders. Hovmand (2014) and Cavana and Maani (2000) demonstrated that stakeholders without in-depth knowledge of differential equations are able to contribute to model conceptualization, formulation and simulation

through causal loop diagramming exercises in a group workshop setting. Minimum expertise in coding is required for participants to actively engage in the modelling process. In fact, this type of modelling workshop is feasible even without any basic knowledge of SD from the participants.

Hager et al (2015) described a case study where researchers attempted to use qualitative measures from SD to equip small-scale village farmers in Zambia with short-term and long-term strategies to increase their food security and economic stability. In addition to the tactical objectives, a more strategic goal of the study was to improve the shared learning experiences in preparation for changing environment and adaptive policies. In Figure 8, stock and flow elements were represented by tangible objects familiar to the village farmers. Variable names were simply written on the white board. Model facilitators used water glasses to show effects of changing variables and devised intuitive terms such as “draining the glasses” and “filling the glasses”. The end results were encouraging, according to Hager et al (2015), despite participants’ lack of formal training in SD.

In the tailings planning context, participatory modelling is expected to be less challenging than the above case study given the multi-disciplinary nature of the mining industry and a well-trained workforce at major mining operations. Causal loop diagram can be an effective communication tool through which different disciplines can communicate with each other under a formalized framework.



Figure 8. Community-based modelling workshop in Zambia (Hager et al, 2015)

d) Structural Sensitivity

Numerical sensitivity analysis studies the impact of varying specific parameter input with other parameters being held constant. In contrast, the emphasis of structural sensitivity is no longer the variation of numerical values but instead the structural uncertainty and behavioral assumptions of the model. As Ford (2010) pointed out, both input and output can change if the fundamental structure of the model is altered. For example, a different model time step is required if the dominant groundwater transport mechanism changes from advection-based to diffusion-based process. Sterman (2004) also recommends the modeler to examine the sensitivity of results to alternative structural assumptions, such as changing key performance indicators and how boundary conditions of the system are treated.

e) *The “Intangibles”*

TMS is a complex system of inter-related “intangible” components outside the technical realms. Primary organizational and human components of TMS consist of: in-house operation staff, Engineer-of-Records, Independent Technical Review Board, consultants, research institutes, advisory associations, regulatory bodies and community stakeholders (MAC, 2017). In addition to the adoption of Best Available Technology (BAT) and Best Available Practice (BAP), understanding the dynamic interaction between those organizational and human components plays an equally important role in successfully managing TMS.

The qualitative and quantitative framework of SD provide opportunities for integration between the construction side and design aspects of TMS. Figure 9 illustrated a causal loop diagram for a typical scenario related to construction Quality Control and Quality Assurance (QA/QC) of a tailings storage facility. For simplicity, only three feedback structures most critical to the process were shown, and it should be noted that they do not depict a complete picture of the construction QA/QC process. As described in Section 2.1, each feedback loop is classified as either positive or negative and given a name to reflect its major theme.

For large-scale tailings dams that stretch over several kilometers in length, it is not uncommon to open multiple work fronts far apart and construct the dam structure simultaneously from different locations. It is also desirable, from a financial perspective, to maintain high rate of construction to meet aggressive deadlines and save on equipment and labor costs.

In Figure 9, the original student-assignment model from Sterman (2004) was revised to better fit in the tailings construction context. At a fixed staffing level, backlogs are created by an increase in the number of work fronts and construction rate. Mathematically, “Tasks Backlog” is equal to rate of new tasks subtracted by “Task Completion Rate”. Work pressure depends on the number of backlogged tasks and inspection interval assigned to each task. The shorter the time interval between inspection, the longer work hours are required to complete all the QA/QC tasks.

For management, the first intuitive reaction to increasing backlogs is to demand overtime and longer work hours. The positive feedback loop “QA/QC Staff Burnout” operates as a vicious cycle – increasing work hours to combat backlogs leads to more backlogs being generated.

The negative loop in “Staff Feedback” balances the vicious cycle in “Staff Burnout”. As work pressure is increased, QA/QC staff may submit additional requests for extension of time between each inspection. In response, construction managers will extend inspection intervals based on the frequency of requests from QA/QC staff. With more time to travel between each work front, QA/QC staff now has less work pressure, which will work through the positive feedback loop to reduce the backlog of tasks.

The negative feedback loop of “Corner Cutting” also balances the vicious cycle in “Staff Burnout”. One way to reduce backlogs is to spend less effort on each task, which in turn increases task completion rate. Since both “Productivity” and “Efforts Devoted to Each Task” work together to affect “Task Completion Rate”, their combined effect on “Tasks Backlog” depends on which feedback loop structure would dominate the other over time.

Elements from both design and construction can be combined into one causal loop diagram through shared variables (i.e. construction rate). A more extensive causal loop diagram is possible by incorporating more feedback processes such as the observational method and budget control. The combination of causal loop diagrams from different perspectives promotes interdisciplinary understanding. However, as causal loops are combined and expanded, it is important to strike the right balance between over-simplification and over-complexity of the system boundary.

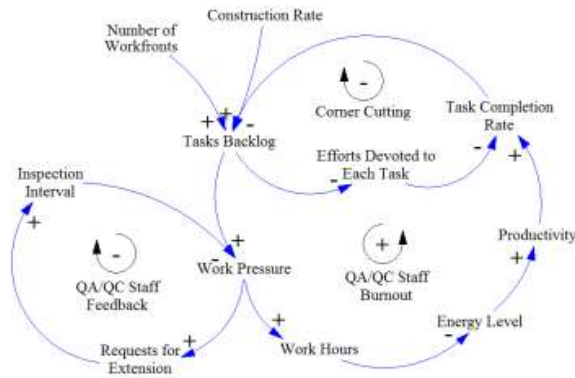


Figure 9. Causal loop diagram for staff fatigue and burnout (Modified from Sterman, 2004)

3.2 Discussions

a) Predictive Power

SD models are constructed to help us gain a big-picture understanding of system behaviors and why they follow certain patterns (Forrester, 1980). The process of simplification and linearization of key physical processes inevitably reduce their predictive powers in terms of absolute numeric values. SD models may provide satisfactory prediction in exchange for larger model size and increased computational time. However, since SD models are lumped models that only provide the average state of the system, traditional numerical models are better suited for precise prediction over time.

On the other hand, predictive models focus on a singular objective that is to provide the most accurate forecast of the future state of the system. Reconciling the difference between predictive models and SD-based models continues to be a challenge partly due to heavy emphasis on discipline-based, narrowly-defined numerical modelling methods taught in the engineering curriculum (Saito et al., 2007). Furthermore, SD models are often misunderstood as predictive models, further deepening the suspicion from end users (Ford, 2010).

b) Validation

Validation of predictive models is straightforward. Matching model results with historical and experimental data gives confidence in the model provided that the same underlying assumptions and boundary conditions are used during the validation process.

Validation of SD-based models is similar to that of predictive models based on matching historical behavior and measured data if available (Elshorbagy et al, 2005 and Huang et al, 2011). Difficulties arise when little to no measured data exists, as in the case of farm villagers in Zambia in Figure 8 and staff fatigue and burnout model in Figure 9. In this case, alternative validation approaches must be adopted. Various practitioners and theorists of SD have advocated for a soft approach to validation: building confidence in the model through debate, education, critique and qualitatively matching behaviors based on expert opinion and well-established fundamental physical processes. Adding more controversy is the notion that validation and verification are impossible, and that all models are ultimately wrong since models are considered simplifications of the reality (Forrester, 1961). Sterman (2004) noted that validation in a SD context is an iterative process where modelers and users continuously question the model's ability to qualitatively replicate expected behavior based on critiques, discussion, known empirical relationships, tentative knowledge and expert opinions. These un-settled validation techniques have become a point of contention and heavy criticisms for the SD modelling paradigm.

c) Causality vs Correlation

Causality should not be confused with correlation. The arrow linking variables and stocks in Causal Loop Diagrams must represent strong causal relationships without ambiguity.

Sometimes, the difference between causality and correlation is obvious. For example, in Alberta, the amount of precipitation correlates well with the level of construction activities. However, higher rate of construction activities is not caused by greater amount of precipitation during summer but instead by the availability of favorable weather condition.

Modelers need to pay close attention to differences between causality and correlation. In tailings dam construction, for instance, it can be tempting to draw a causal link between frequency of dam foundation movement and number of construction workforce. The modeler must critically debate the strength of the causal link by asking what other factors stand in between foundation movement and number of construction workforce. As shown in Figure 10, causality is improved by breaking up the original link and adding another variable that has strong causal polarity to the other two variables.

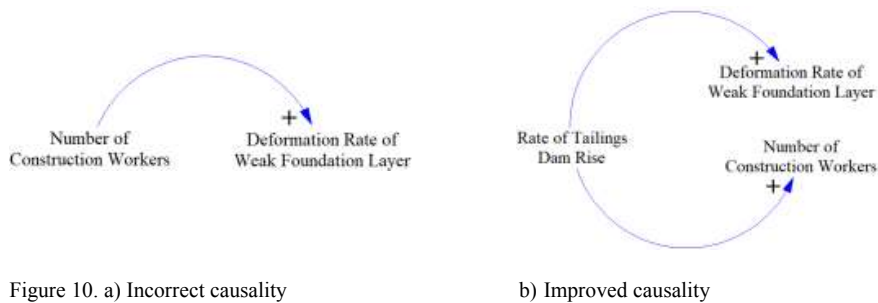


Figure 10. a) Incorrect causality

b) Improved causality

d) Resistance vs Over-reliance

When SD is employed in a participatory modeling environment, resistance to adopting SD can come from specialists who tend to concentrate on the detail with which they are most familiar. (Nicolson et al, 2002). To be successful in inter-disciplinary modelling exercises, Cockerill et al (2007) suggested that participants need to have a sense of humility and accept the fact that they need to learn new languages and concepts from other disciplines as well as general principles of SD modeling. Nicolson et al. (2002) further warned that there will be steep learning curves for participants even though they may be experts in their respective fields.

At the other end of the spectrum is over-reliance on SD models which seem to have the ability of integrating multiple disciplines. Limitations in the predictive power of SD models cannot be ignored. Over-emphasis on causal loop diagramming can also erode sound scientific basis and exaggerate the usefulness of conceptual models. Homer (1996) reported an alarming trend that the ease with which causal loop diagrams can be created may have exacerbated the belief that SD is mainly conceptual instead of empirical, and that creativity takes precedence over thoroughness.

4 CONCLUSIONS

SD allows for coupling of multiple processes and systems across disciplinary boundaries. Figure 3 and Figure 9 demonstrated the potential marriage between technical and business models through causal loop diagrams. Figure 6 and Figure 7 showed how SD techniques can be applied to model multiple physical processes that can also interact with each other. Figure 8 provided an example of how a complex model can be communicated and conceptualized by stakeholders without knowledge of differential equations.

Furthermore, the qualitative stage of the SD modeling is a rigorous process with its own syntax, well-established rules, and best practices. The qualitative stage of SD modeling process also emphasizes transparency, simplicity and flexibility. The process of constructing causal loop diagrams provide further insights into the tailings management process and serve as a vehicle for inter-disciplinary communication.

However, causal loop diagrams constructed above are not inclusive and may not contain enough information for subsequent quantitative modeling exercises. As research and stakeholder participation progress, additional causal loop diagrams, variables and processes need to be identified and incorporated. At the same time, redundant components and insignificant processes may be discarded. Historical data and empirical evidence are also required for validation purposes.

5 ACKNOWLEDGEMENTS

The authors would like to thank the Natural Sciences and Engineering Research Council of Canada (NSERC), Canada's Oil Sands Innovation Alliance (COSIA) and Alberta Innovates – Energy and Environment Solutions for their financial support.

6 REFERENCES

- Beier, N., 2015. *Development of a Tailings Management Simulation and Technology Evaluation Tool*, Edmonton, AB: University of Alberta.
- Cavana, R. & Maani, K., 2000. *A Methodological Framework for Integrating Systems Thinking and System Dynamics*. Bergen, Norway, 18th International Conference of System Dynamics Society.
- Cockerill, K. V., Tidwell, H. P. & Malczynski, L., 2007. Cooperative modeling lessons for environmental management. *Environmental Practice*, 9(1), pp. 28-41.
- Elsawah, S. et al., 2017. An overview of the system dynamics process for intergrated modelling of socio-ecological systems: Lessons on good modelling practice from five case studies. *Environmental Modelling & Software*, Volume 93, pp. 127-145.
- Elshorbagy, A., Julta, A., Barbour, L. & Kells, J., 2005. System dynamics approach to assess the sustainability of reclamation of disturbed watersheds. *Canadian Journal of Civil Engineering*, pp. 32: 144-158.
- Ford, A., 2010. *Modelling the Environment*. Washington, D.C.: Island Press.
- Forrester, J., 1961. *Industrial Dynamics*. Portland, Ore: Productivity Press.
- Forrester, J., 1994. System dynamics, systems thinking, and soft OR. *System Dynamics Review*, 10(2-3), pp. 245-256.
- Forrester, J. W., 1980. System dynamics - future opportunities. *TIMS studies in Management Sciences*, pp. 14: 7-21.
- Hager, G. M., Kopainsky, B. & Nyanga, P. H., 2015. *Learning as conceptual change during community based group interventions. A case study with smallholder farmers in Zambia*. Cambridge, MA, s.n.
- Haraldsson, H., Belyazid, S. & Sverdrup, H., 2006. *Causal Loop Diagrams - promoting deep learning of complex systems in engineering education*. Lund, Sweden, 4th Pedagogical Inspiration Conference.
- Homer, J. B., 1996. Why we iterate: scientific modeling in theory and practice. *System Dynamics Review*, 12(1), pp. 1-19.
- Hovmand, P. S., 2014. *Community Based System Dynamics*. St Louis: Springer.
- Huang, M. et al., 2011. System dynamics modeling of infiltration and drainage in layered coarse soil. *Canadian Journal of Soil Science*, Volume 91, pp. 185-197.
- King, L. M., Simonovic, S. P. & Hartford, D. D., 2017. Using system dynamics simulation for assessment of hydropower system safety. *Water Resources Research*, Volume 53, pp. 7148-7174.
- Kossik, R. & Miller, I., 2004. *A probabilistic total system approach to the simulation of complex environmental systems*. Washington, D.C., Proceedings of the 2004 Winter Simulation Conference.
- Lane, D. C. & Sterman, J. D., 2017. A model simulator: The lives of Jay Forrester. *Journal of Simulation*.
- Li, L. & Simonovic, S., 2002. System dynamics model for predicting flood from snowmelt in North American prairie watersheds. *Hydrological Processes*, Volume 16, pp. 2645-2666.

- Meadows, D. H., 2008. *Thinking in systems: a primer*. s.l.:Chelsea Green Publishing.
- Mining Association of Canada, 2017. *A Guide to the Management of Tailings Facilities*, s.l.: s.n.
- Nicolson, C. A., Starfield, G. K. & Kruse, J., 2002. Ten heuristics for interdisciplinary modeling projects. *Ecosystems*, Volume 5, pp. 376-384.
- Richardson, G. P., 1997. Problems in causal loop diagrams revisited. *System Dynamics Review*, 13(3), pp. 247-252.
- Richardson, G. P., 2011. Reflections on the foundations of system dynamics. *System Dynamics Review*, 27(3), pp. 219-243.
- Richmond, B., 1993. Systems thinking: critical thinking skills for the 1990s and beyond. *System Dynamics Review*, 9(2), pp. 113-133.
- Saito, L., Segale, H. M., DeAngelis, D. L. & Jenkins, S. H., 2007. Developing an Interdisciplinary Curriculum Framework for Aquatic-Ecosystem Modeling. *Journal of College Science Teaching*, pp. 46-52.
- Sterman, J., 2004. *Business Dynamics: System Thinking and Modeling for a Complex World*.. Boson: McGraw-Hill.
- Sterman, J. D., 1994. Learning in and about complex systems. *System Dynamics Review*, 10(2-3), pp. 291-330.
- Zheng, T. & Beier, N. A., 2018. *Stochastic Simulation of Tailings Consolidation Process*. Edmonton, AB, 71st Canadian Geotechnical Conference.

The Use of 3D Models and Analysis in Support of Waste Stockpile Design and Operations

L. Piciacchia, V. Marefat, and J. Mosquera

BBA Inc., Mine Waste Management and Environment, Montreal, Quebec, Canada

ABSTRACT: The complexities of waste rock stockpiles are often underestimated. Slope stability analysis for such earth structures is usually carried out using two-dimensional (2D) slope stability methods. Furthermore the sections used in the analysis are often idealized. Selecting a typical or critical section is left to the designer. Given the number of parameters that can affect stability this approach may not always bring focus to those areas of the waste stock pile which are most critical. As such, three-dimensional (3D) slope stability analysis offers a more complete screening tool which assists the designer in identifying the most critical areas. Mining projects, in which complex co-deposition schemes are employed, using both fine and coarse material, coupled 3D seepage and slope stability analysis can prove useful. This allows modelling the impact of various co-deposition methods on the waste rock pile's hydraulic regime and its effect on stability. Some complex co-deposition configurations modelling cannot be carried out with 2D analysis.

1 INTRODUCTION

Slope stability analyses are typically performed using two dimensional (2D) methods. The 2D analysis assumes an infinitely wide failure surface. As such, the influence of shear resistance and force on the 3rd dimension is negligible compared to the overall driving and resisting forces (Akhtar, 2011). However, most slopes are finite and have 3D geometry. For example, waste rock piles and tailing dams on mine sites generally have definite 3D geometries. Conducting 2D slope stability analysis for such cases is thought to be conservative for engineering applications, because the influence of shear resistance along the 3rd dimension is ignored. For slope design, the conservative result of 2D analysis might be accepted, but for the case of back-calculation analysis of a slope failure, 2D slope analysis can overestimate shear strength by about 30% (Stark and Eid 1998).

Three dimensional slope stability analyses take into account the influence of topography, internal stratigraphy in the 3rd dimension, and groundwater level change within the model. Furthermore, 3D slope stability analysis is an important screening tool to identify the most critical section for further 2D slope stability and seepage analyses.

In common engineering applications, slope stability analysis is mostly conducted by limit equilibrium (LE) method rather than finite element (FE) or finite difference (FD) strength reduction methods. The LE methods are worldwide accepted, easy to handle, require less computational effort and are preferred for routine engineering analyses. On the other hand, LE methods do not take into account constitutive stress-deformation relationships. As such, the stability result provided by LE methods for high risk projects needs to be validated by FE or FD strength reduction procedures (Akhtar, 2011).

This paper puts emphasis on using 3D slope stability and seepage analysis in mine waste applications. The LE method was applied in the 3D slope stability analysis described in this paper.

Two general examples were analysed. The first example presents the use of 3D slope stability analysis as a screening tool to identify the critical sections. The second example illustrates the use of 3D seepage analysis to model the groundwater surface for a complex co-deposition method where the geometry changes in the 3rd dimension.

2 EXAMPLES AND APPLICATIONS

2.1 3D slope stability analysis of a homogenous stockpile

In 3D slope stability analysis, contrary to 2D analysis, some additional aspects need to be taken into consideration. The most important aspects are slip surface shape, aspect ratio and the slip direction. This example focused on the application of 3D slope stability analysis as a screening tool to identify the critical locations through a stockpile model which is founded partly on competent and partly on clay foundation.

To create a 3D geometry of the stockpile, AutoCAD DXF files of the original topography, various internal strata and stockpile contours were used. Figure 1 shows the geometry of the model. In this example, where the foundation is clay, the failure can occur either in the foundation or within the deposited material itself.

The stockpile has a variable height ranging between 90 m and 70 m on the left and right sides, respectively. The waste rock pile's slope angle is variable. The waste rock pile contains 4 benches on the left and 3 benches on the right sides (Figure 1). The two first benches are steeper than the others. In general, there is a slope angle of about 29 degrees. The waste rock is deposited on a clay foundation on the right side. However, its foundation on the left side is competent bedrock.

The pile contains waste rock material with an angle of internal friction of 38 degrees. The material is considered self-draining. Therefore, the slope stability analysis was conducted under dry conditions. The groundwater is within the foundation with no water within the waste rock pile. The material strength type was characterized as Mohr-Coulomb for the waste rock and depth depended undrained shear strength for the clay layer. The bedrock was assumed to comprise a competent foundation. Table 1 summarises the material properties and strength type used in this simulation.

The stockpiles are commonly constructed by end or push dumping method. The failure can occur in the foundation soil or within the deposited material itself. For a stockpile comprising a material with an angle of internal friction of 38 and benches with a height of less than 55 meters (m) a minimum local factor of safety of 1.2 is expected (Piciacchia et al., 2018). This example focuses only on the global slope stability based on the requirement of attaining a factor of safety (FS) = 1.5. Global stability here is defined as a failure surface that extended into more than one bench.

As shown in Figure 1, the left side of the stockpile has a higher exposed slope than the right side. On the other hand, the right side has a weaker foundation condition with a varying thickness of clay. In the absence of a 3D analysis it is left to the user to choose the most critical cross section for the 2D slope stability analysis. At first glance, the user might focus on that portion of stockpile with the weaker clay foundation. If so, where within the waste rock pile is the critical section? Where the clay is thickest or where the pile is highest? Conducting a 3D slope stability analysis screens the critical sections and helps users to analyse a problem with a comprehensive understanding of a location and mechanism of the failure. For the geometry illustrated in Figure 1, the 3D slope stability analysis focused only on the front exposed face.

Table 1: Material properties used for 3D slope stability analysis in this paper.

Material	Strength Characterization	γ (kN/m ³)	\emptyset (degree)	Min Shear Strength (kPa)	Undrained Strength Ratio
Waste Rock	Mohr Coulomb	19	38	NA	NA
Clay	Undrained strength ratio	17.5	0	40	0.23
Bedrock	NA	NA	NA	NA	NA

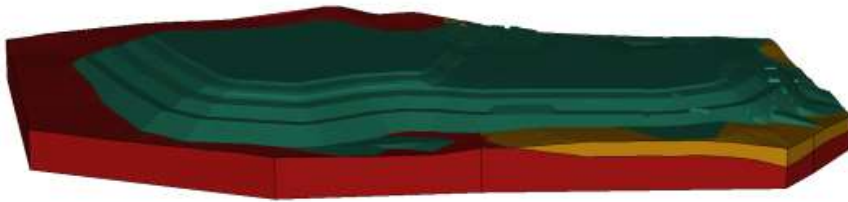


Figure 1 : geometry for the 3D slope stability model

The 3D slope stability model was performed based on the following criteria:

- Slip surface shape: ellipsoid;
- Ellipsoid aspect ratio: between 0.7 and 3.0;
- Slip Surface search method: Slope search;
- Number of surfaces: 20000;
- Direction of the slip: perpendicular to the principal axis.

Figure 2 presents the result of the 3D slope stability analysis.

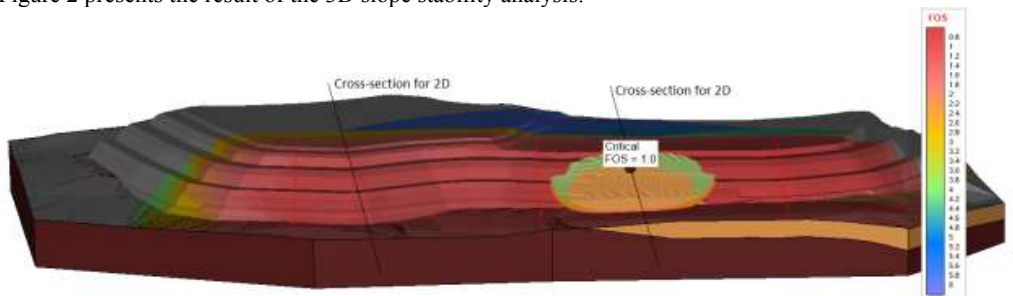


Figure 2 : 3D slope stability result

As expected the critical section passes through the clay foundation on the right side of the stockpile. However, this does not occur where the clay is thickest, rather where the pile is the highest and the clay is closer to the surface. However, on the left side of the stockpile, there are some locations that are critical as well (having a factor of safety less than 1.5), as shown by the isocontours for factor of safety (Figure 2). Based on the 3D analysis, two critical sections were selected for detailed evaluation. Figure 3 presents the results of 2D analysis.

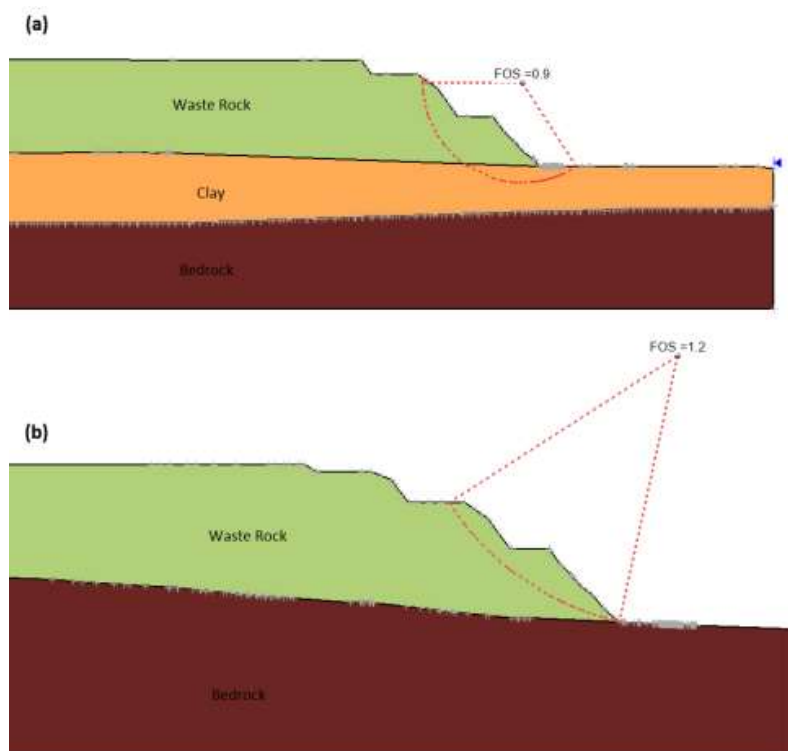


Figure 3 : 2D slope stability analysis: a) right side with clay foundation and b) left side with rock foundation

The 2D slope stability analysis confirms the results of 3D analysis. The right side where the stockpile is constructed on the clay foundation is the most critical. The 2D slope stability analysis resulted in a lower FS value than 3D analysis showing that the 2D analysis is more conservative. This is consistent with previous findings (Akhtar, 2011; Chaudhary et al., 2016). The lower calculated factor of safety for the 2D analysis is due to the geometry aspect of the slope in the 3rd dimension. Therefore, the 3D factor of safety is slightly higher. The 2D section presented in Figure 3b exhibits that the setback distance for the second bench is not properly designed. The stockpile's global slope for the 2 first benches is about 7 degrees steeper than the pile's global slope. This resulted in a global FS of less than 1.5.

2.2 3D seepage analysis for a co-deposition method

The waste materials produced from mining activities can have a vast grainsize distribution and angle of internal friction. These materials should be separated and deposited with a proper strategy. There are several methods that are commonly followed by mining companies: a) fine and coarse materials are mixed and deposited together; b) fine materials are deposited in successive layers in front of previously deposited coarse materials; and c) fine and coarse material are separated and the fine materials are deposited as a single stockpile.

In the case of mixing fine and coarse materials, the waste rock pile stability can be affected by a possible rise in the phreatic surface. Mixing of fine and coarse materials decrease the local

and global hydraulic conductivity of the pile and can potentially increase pore water pressure within the waste rock pile. If fine material is deposited in successive layers in front of previously deposited coarse material, a failure of this new layer of fine material could occur. The fine material blocks the drainage of the waste rock pile, which results in a pore water pressure build up and failure of the pile. For these reasons, it is strongly recommended that fine and coarse materials be managed separately where possible.

The management of fine materials can be conducted by various means: as a single pile or co-deposition of fine and coarse materials. Managing the fine material as a single pile may create drainage problems, safety issues and depending on haulage distances may be cost intensive. A proper co-deposition method help resolve some of these issues. The evaluation of particular co-deposition scheme must first consider the effect that the deposition plan will have on the phreatic surface within the combined waste rock stockpile. In this example, a co-deposition method in which the fine materials are deposited in separate layers within the body of a coarse stockpile is presented. In this example the focus is on the 3D seepage analysis for the proposed co-deposition method, which could not be modelled in 2D due to the fact that fine material is not continuous parallel to the pile crest, as shown in the cross-sections of Figure 4. If 2D modelling of this configuration was attempted, it would likely result in perched water conditions above and within the fine grained material. Figure 4 presents a plan view and cross sections for the proposed co-deposition method.

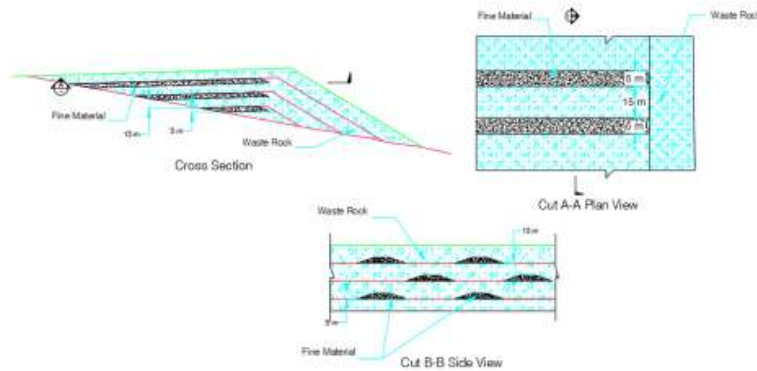


Figure 4 : Cross-section, plan and side view for the proposed co-deposition method

To investigate the impact of fine material on the pore water pressure condition in the proposed co-deposition method, an idealized 3D seepage model was performed. The model was constructed based on the geometries presented in Figure 4. The dimensions presented in Figure 4 are not the optimised dimensions and are used only for the purpose of seepage analysis in this example. The model length and width were 600 m and 200 m respectively. The pile was constructed on a ground with a natural slope of about 8 degrees. The foundation material is saturated silt material with a hydraulic conductivity on the order of 1×10^{-7} m/s. The construction comprised 4 lifts with heights of 20 m. The fine material was placed with a setback of 30 m from the slope crest. The fine material had a width of 5 m and placed at 15 m intervals from the crest setback. The length of the fine material was variable from each lift, depending on the original ground slope. The percentage of fine to coarse material for this model was about 5%.

The fine and coarse material are initially considered as unsaturated materials in the seepage analysis. Hydro-geotechnical characterization of waste material plays a crucial role in the long- and short-term stability of the waste rock piles. One of the most important hydro-geotechnical parameters of waste material is the water retention capacity, which is associated with the material grain size distribution and in-situ condition. Coarse waste materials are usually considered as a self-draining. However, fine waste material has a high capacity to retain water. As such, this type of material is able to quickly build up pore pressure (e.g. during a high intense precipitation event), which may endanger the stockpile's stability.

The unsaturated properties of material are presented in water retention curve (volumetric water content versus matric suction). There are theoretical methods to estimate the unsaturated hydraulic conductivity of materials based on the water retention capacity of the material. This example used modified Campbell method to estimate the unsaturated hydraulic conductivity of the fine and coarse material. Figure 5 presents the water retention curve for the fine and coarse material used in this analysis. These properties were taken from the literature (e.g., SoilVision data base).

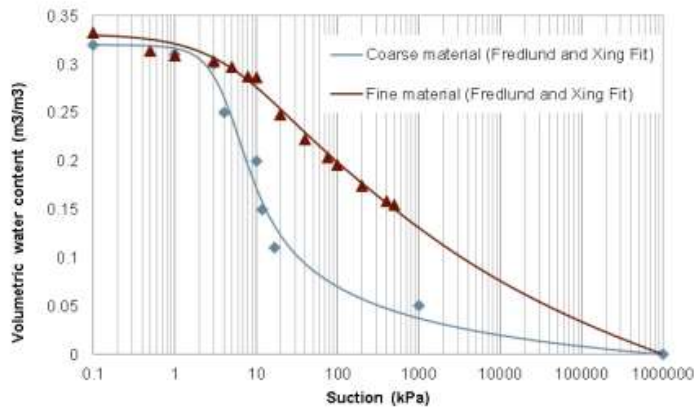


Figure 5 : Water retention curves for coarse and fine materials

The seepage analysis was conducted in 2 phases. First, a steady state model was performed as an initial condition for the subsequent transient seepage analysis. The steady state seepage was performed by setting hydraulic head boundary conditions to the natural ground elevation. For the transient analysis, a climate boundary condition considering an intense precipitation of 100 millimeters per day for 5 days was modelled. Figure 6 presents the isocontour for pore water pressure within the stockpile.

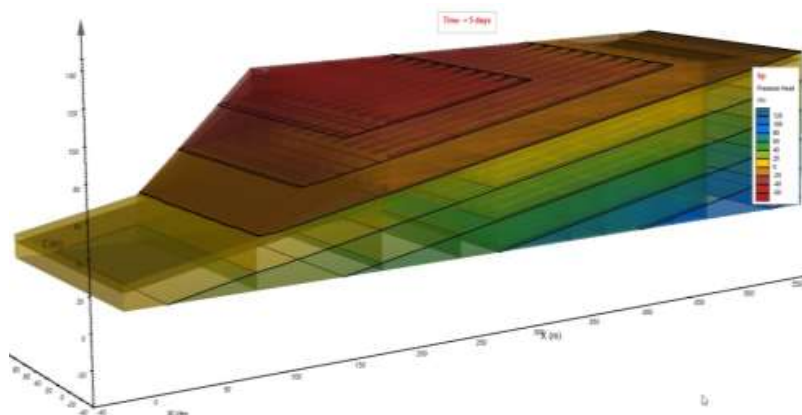


Figure 6 : 3D seepage analysis result (pore water pressure isocontour)

The 3D seepage analysis showed that for the idealised model the coarse material was free drainage and did not become saturated. It is noteworthy that the 3D seepage analysis performed

here only represents the result for the geometry and dimensions presented in Figure 4. Any other layout than that of modelled herein needs a further numerical analysis.

3 CONCLUSION

This paper presented the importance of 3D analysis in mining application through two practical examples. The 3D slope stability analysis was successfully used as a screening tool to identify the critical sections through the model. The 3D slope stability analysis provided slightly higher FS than 2D analysis. For the case in which the actual shear strength is applied for the slope stability, the 2D slope stability analysis would be conservative. Quebec regulations require a minimum FS values based on 2D slope stability analysis for man-made slope design. However, the results of this paper, which is aligned with the pervious findings on 3D slope stability analysis, shows that the 2D slope stability analysis is conservative.

The need for 3D seepage analysis was illustrated using a complex co-deposition layout, which could not be modelled otherwise. The analysis performed in this study indicated that for the proposed co-deposition method the coarse materials was free drainage and did not become saturated. This co-deposition method needs further investigation in order to evaluate various combinations of the fine and coarse material and geometry of the model. These combinations can only be modelled using 3D analysis.

4 REFERENCES

- Akhtar, K. 2011. Three Dimensional Slope Stability Analysis for Natural and Manmade Slopes. *PhD Thesis*, Civil Engineering Department, University of Illinois at Urbana-Champaign.
- Chaudhary, K., Honorato D. V., Gitirana, G., Fredlund, M., & Lu, H. 2016. Three-Dimensional Slope Stability: Geometry Effects. *16th Tailing and Mine Waste Conference, at Keystone Colorado*.
- Piciacchia, L., Marefat, V., & Vides, A. 2018. Practical Nomograms for Waste Rock Piles Design on Competent Foundations. *18th Tailing and Mine Waste Conference, The Department of Civil and Environmental Engineering at Colorado State University*.
- SoilVision Systems Ltd. 2017. SVSLOPE Theory Manual (SVOFFICE 2017). Saskatoon, Saskatchewan, Canada.
- Stark, T. D., and Eid, H. T. 1998. Performance of three-dimensional slope stability methods in practice. *Journal of Geotechnical Engineering Division, ASCE, 124(11), 1049-1060*.

Adjustments to Tailings Deposition with Thickened Tailings in Svappavaara

S. Töyrä

LKAB, Kiruna, Sweden

P. Marthin

LKAB, Malmberget, Sweden

K. Jokinen

LKAB, Svappavaara, Sweden

D. Lundell

Tailings Consultants Scandinavia, Stockholm, Sweden

ABSTRACT: Difficulties with adapting an existing tailings storage facility, TSF, to become suitable for deposition with thickened tailings, are presented in this case study.

The Svappavaara iron ore mine is one of three mine sites of LKAB. Svappavaara is located in the far north of Sweden in the sub arctic climate zone. The tailing storage facility, TSF, was originally built in 1967 as a conventional impermeable dam between natural heights. The tailings were deposited into the TSF by hydraulic deposition with a low solids content and the TSF had large volumes of stored water. To optimize the storage capacity the deposition was changed into thickened tailings with the intention to obtain a steeper slope of the tailings. Significant changes were also introduced in the design of the embankments, to optimize the positive effects of the thickened tailings.

1 SVAPPAVAARA OPERATION

1.1 Background

The majority of the Swedish mine sites have been in operation for a long time and the Swedish tailings management has a legacy and a great influence from the hydropower sector. Most of the mine sites are, or has been, going through a transition from an older approach with storage of significant volumes of water, to systems with more optimized tailings deposition schemes. Initially the embankments of the tailings storage facilities were designed with impermeable embankments and large volumes of free water in circulations, combined with one or few slurry discharge points (the latter usually as an alternating single discharge point). The Swedish dam safety legalization and the mining organization's guidelines are also greatly influenced by the hydropower sector.

The driving force for the mentioned transition has often been to reduce the cost for raises and not the enhancement of dam safety. Usually the transition has been made to tailings depositing by spigots and raises with the upstream method, but this is not the case for the Svappavaara TSF. In Svappavaara the transition started with filling out excessive water volumes with tailings and then installing a deep cone thickener to be able to store tailings with a greater inclination of the tailings surface and thereby be able to postpone the need of raises of the embankments.

The purpose of this paper is to give an example of the problems that may arise in this process and how the design was adjusted to the older approach and still optimized to fit the new choice of depositing of the tailings.

1.2 Introduction to LKAB and the Svappavaara site

Svappavaara is a small mining village in Kiruna municipality in the northern most part of Sweden located 120 km north of the arctic circle. The average annual temperature is -1°C (30.2 °F) and the region has approximately 200 days of snow cover per year. About 40% of the annual precipitation comes as snow.

The mining findings of iron ore has been known since mid-17th century. Copper ore has been mined in small scale around mid-17th century but the big scale mining of iron ore started in the first open pit, Leveäniemi, 1965 and continued until 1983 when production ceased and the open pit started to fill up with water. Even though there were no iron ore production at the site the concentration plant and pelletizing plant were still running after 1983 fed with ore from the Kirunavaara mine, meaning that the TSF was also still in use.

As the iron ore price was climbing LKAB opened up a new open pit, Gruvberget, in 2010 and it was in operation until February 2018. In 2014 the Leveäniemi open pit was emptied of water and reopened. There is also a third open pit mine, Mertainen, that has been started up but is not currently in operation.

Today the Leveäniemi open pit is in operation as well as one fine crusher, a concentrating plant and a pelletizing plant. The plants are running on a mixture of ore from the site as well as ore from the Kirunavvara mine that is brought in to the site by train. The pellets are transported by train to the harbor in Narvik, Norway, then shipped worldwide.

2 THE TAILING STORAGE FACILITY IN SVAPPAVAARA

The TSF in Svappavaara is located in the north-west part of the mine site on the west side of the Gruvberget hill, which partly is converted to an open pit, see **Figure 1**. The plants are located in between the Leveäniemi open pit and Gruvberget. The area in the south is used for waste rock and till deposits.

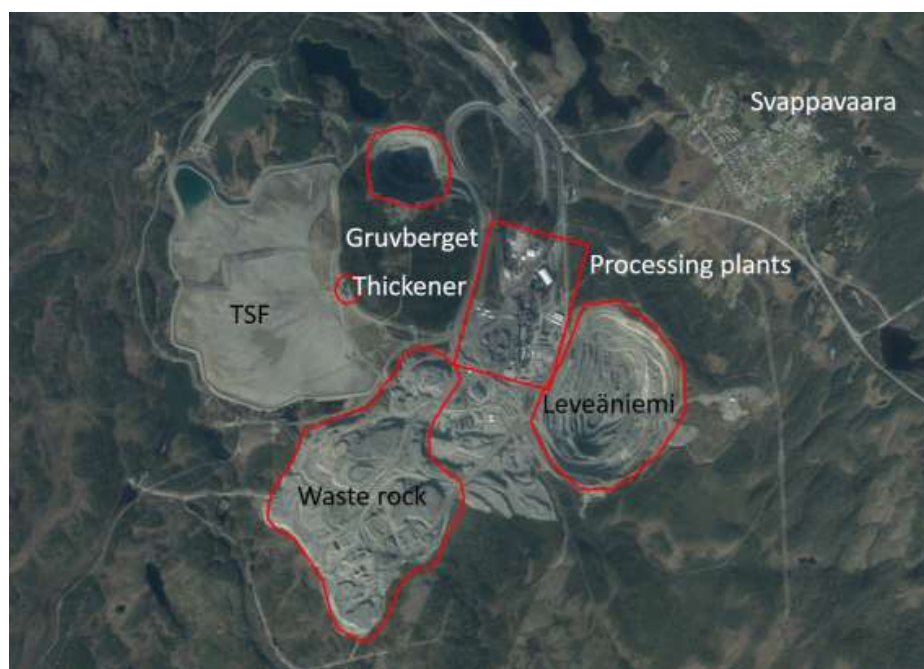


Figure 1 Overview of the Svappavaara mine site.

On the west side of the TSF, on the hillside of Gruvberget, two deep cone thickeners are located, the first one installed in 2012 and the second one in 2016. The tailings are pumped up to the thickener from the concentrating plant. After the thickener the tailings consist of approximately 70 % solids by weight and are deposited into the TSF at different points along the hillside, usually by a single outlet point at a time.

Before the thickeners were installed the tailings were pumped to the TSF and discharged by one single outlet point in the south part of the TSF, near A in **Figure 2**. The solids content of the tailings was around 7% by weight. It formed a flat well segregate tailings surface, meaning that the finer particles were deposited in the northern part of the TSF close to the spillway.

The overflow from the thickener flows by gravity into the recipient pond that is used as a clarification pond. During winter a small stream of the warm water (ca 20 °C) is directed through the spillway of the TSF to ensure that it is kept free of ice. The process water is pumped from the recipient pond via the small natural lake Metträsk back to the plants. Since there is a surplus of water in the system 4-5 Mm³ is discharged every year. The water is discharged to a fairly small creek that runs off to the Torne river and finally ends up in the Baltic sea.

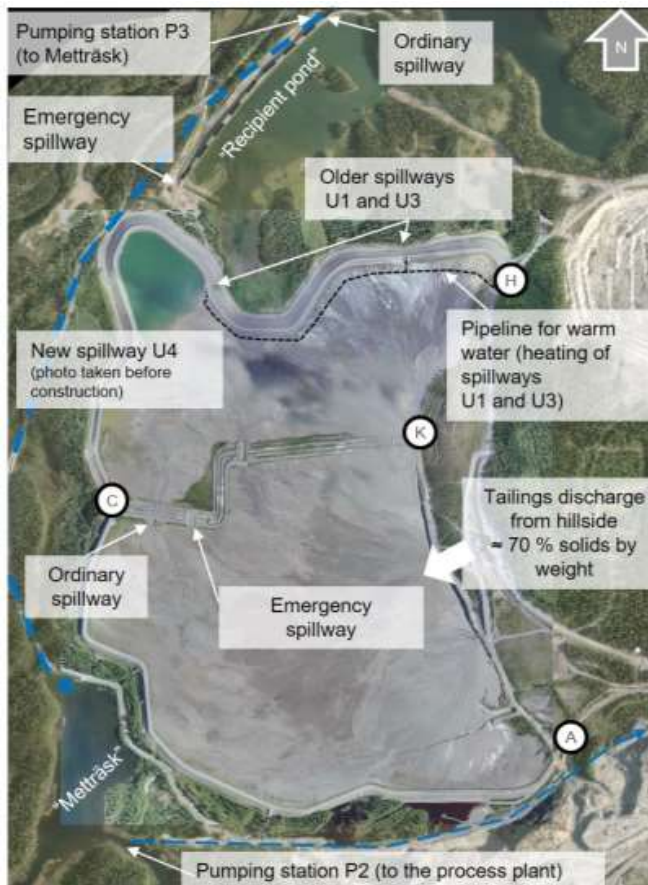


Figure 2 Overview of the Svappavaara tailing storage facility and recirculation of process water.

3 DEVELOPMENT OF A NEW DEPOSITION STRATEGY

The Svappavaara Tailings Storage Facility (TSF) was operated using the same strategy for deposition of tailings for almost 50 years (1964 - 2012). The principle was simple: deposition of tailings at one end of the facility, using a natural valley to create a pond, and then aiming at creating a flat slope (approx. 1:300) to form a TSF with a beach close to the outlet (in the south) and free water along the northern embankment, **Figure 3**. All perimeter dams were originally designed with an impermeable till core or as homogeneous till dams, which basically allowed free water around the whole perimeter. Over the years some minor adjustment was made, using internal embankments and also, at a few occasions, moving the outlet (however, the very low solids content in the tailings – approximately 7 % solids by weight – resulted in a high flow and therefore a very low flexibility regarding moving outlets), but basically, during the period 1964 – 2012, the deposition strategy remained the same.

As the TSF was filled up, the embankments were raised, finally reaching a point where the combination of growing embankments and increased awareness of limitations in the older embankment design, led to discussions about alternative strategies, to create more volume with less need of raising the embankments.

Beginning in mid-2000 an alternative strategy was being developed. The idea of a thickener was introduced, with the target to create a sloping tailings surface from the natural hill, Gruvberget, in the east, allowing for a greater volume with less need of raising the embankments. A sloping surface (targeting an overall slope of $\approx 3\%$) would generate a large volume and basically postpone the need of raising the embankments with several years. At the same time a decision was made to decrease the water volume in the north part of the pond and fill the majority of the volume with tailings. With these factors combined, an extended life span of almost 20 years without raising the embankments was obtained, according to the initial estimate. In 2012 operations with a thickener was started and further raises of the embankments were postponed.



Figure 3 Photo of Svappavaara TSF from 1989.

3.1 *Need to raise embankments*

Jumping to 2015, the following observations could be made. The start of operation of the thickeners had encounter several minor difficulties, which in the end lead to major deviations in the outcome of the tailings surface. One of the problems with the thickener was that it was designed for a lower throughput since the production rate at site had increased when both the Gruvberget open pit as well as the Leveäniemi open pit was in operation. Since the thickener was not running as intended (long periods of time when the thickener was by passed and the deposition was carried out with solids content less than 7 % by weight, which was the ordinary solids content before introducing the thickener), the overall tailings slope created was not reaching the target slope. As a consequence of the deviation from the strategy, major problems started to arise in the TSF – the available volumes at the abutments were almost completely filled out, the water surface was shrinking quickly and one of the spillways (required to meet the necessary capacity for the design flood) was going to be completely cut off from the free water surface if more tailings where filled out in the area. The tailings flow towards the outer dams also led to local impounded water, leading to issues regarding the freeboard and pore pressure above desired levels. There were also significant periods of time with low solids flow (both unthickened tailings, overflow from the thickener and excess water from the plant) that were led through the TSF and interfered with the strategy to build up the sand cone.

To avoid problems that would potentially lead to insufficient capacity, it was decided to take immediate actions in the TSF to postpone problems related to deviation from the deposition strategy. This included internal walls and excavation of tailings to compensate for the flatter overall slope, and to concentrate flow with low solids content to outside the intended cone area. In addition to these actions it was decided to install a new thickener, to better meet the demands at site.

Finally, it was also decided that the embankments should be raised to allow for more time with deviation from the intended deposition strategy and to create more volume according to the intended strategy, but taking into account that the overall slope may range from 2 % to 3 % and that the surface may become concave (not flat). In addition to this it was assumed that approximately 10 % of the tailings would not be thickened, and instead be deposited at a solids content of 7 % by weight. The choice of design slope was based on an overall slope of 2 % almost being reached in parts of the TSF, even when the thickener was only partly operational, combined with an expected better performance of the new thickener. The second thickener was designed to meet the demands of an increased production at site with all three open pits in operation at the same time.

3.2 *Transforming the embankments*

The current situation 2015 included:

- Embankments surrounding the valley constructed to be impermeable (till core).
- A foundation that, in earlier years had been a significant problem, because of a much greater seepage than anticipated.
- The sloping tailings surface leading to the free water surface being pushed into the north west corner of the facility, where the surrounding older embankments were already rather high (≈ 20 m) and partially damaged from frost penetration in the till core.
- Only one of two spillways placed close to the free water (the second being placed in area where the tailings surface is intended to be raised several meters).
- An internal embankment allowing for a difference of approximately 8 meters in crest level of the perimeter embankment (upstream and downstream the internal wall).

The design target was to keep a free water surface in the north west part of the pond, change the profile of the embankments to better suit the intended buildup of a sloping cone and to allow drainage in the tailings placed in the future (in addition to the now favorable drainage already taking place in the very permeable foundation). To meet this target the north western embankment was kept as impermeable, with the design mainly focusing on avoiding frost penetration damage in the future, through increasing the freeboard to allow for better insulation of the till

core. For the rest of the embankments, a downstream raise was designed with basically only a filter zone and rock fill, with the goal to allow for drainage over the older till core **Figure 4** and **Figure 5**. Due to the rather low permeability of the tailings and no free water upstream these embankments, the seepage is predicted to be limited and no major phreatic pressure build up is anticipated in the draining part of the embankments.

The profile of the embankments is changed so that the embankments close to the abutments, close to the hill in the east, are raised significantly more than the embankments along the west-ern side of the TSF, creating more room for the build up of the tailings cone, **Figure 6**.

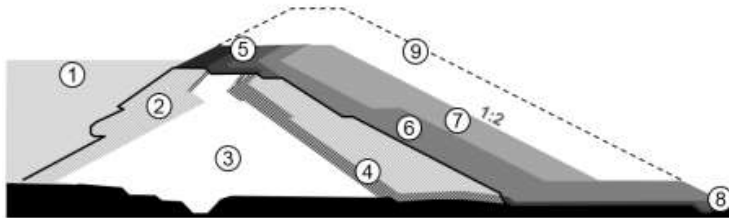


Figure 4 Cross section of southern embankment – section changed to allow for drainage of tailings placed in the future. The solid black line state out the original embankments before the raise in 2017. 1) Deposited tailings 2) Older erosion protection and filters 3) Homogenous till embankment 4) Older support buttress with filters 5) Filter layers 6) Sorted rock fill for drainage 7) Unsorted rock fill 8) Filters and toe drainage 9) Intended future raise

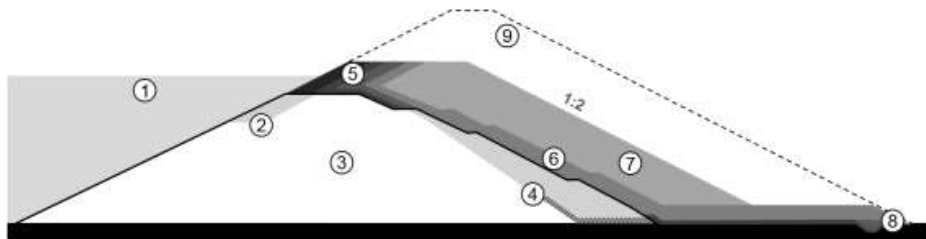


Figure 5 Cross section of northern embankment – section changed to allow for drainage of tailings placed in the future. The solid black line state out the original embankment before the raise in 2017. 1) Deposited tailings 2) Older erosion protection and filters 3) Homogenous till embankment 4) Older support buttress with filters 5) Filter layers 6) Sorted rock fill for drainage 7) Unsorted rock fill 8) Filters and toe drainage 9) Intended future raise

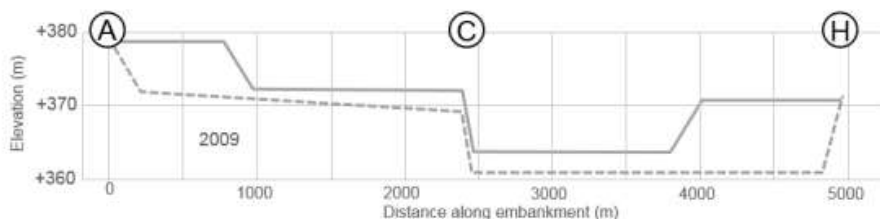


Figure 6 Schematic comparison of crest levels before the change of design (dotted line) and after intended raises (solid line). Letters A, C and H are specified points on the embankments (see Figure 2). The crest levels are raised significantly close to the abutments (A and H), allowing for buildup of the tailings cone along the hill in the east.

3.3 Major challenges

A new spillway was required and needed to be installed in the lower part of the facility where there will still be free water. This meant construction of a spillway through the rather high embankments in the north west (where the foundation levels are low). The design includes pipelines running on the downstream slope of the embankment. The inlet consists of two open pipes, that allows for a limited peak outflow in case of an extreme flood (compared to an overflow weir), which is preferred since there is a bigger challenge in avoiding erosion along the downstream slope, due to the height of the embankment, than to actually release the rather limited design flood.

Furthermore, the buildup of a tailings cone on partially saturated tailings has led to questions on the overall stability of the tailings. Special attention has been given to the effect of freeze and thaw of the sloping surface, where pore pressure builds up the upper part of the tailings surface, during thaw, was assumed to potentially generate an instable surface (Knutsson, Viklander, Knutsson, 2016-04-29). This has been concluded not be a risk in Svappavaara, given the current tailings slopes and coefficient of consolidation. However, it remains to follow up on the pore pressure build up in the older tailings where drainage is limited. High pressure in the older tailings has been noted close to the point of deposition, where the new tailings surface at times has been raised quickly. It remains to control that a similar buildup will not take place closer to the embankments when the buildup of the tailings cone reaches the embankments.

Finally, the method of raising the embankments downstream requires a lot of placed fill, and the additional volume per raise increases with increased height of the embankment (since the foundation becomes wider).

3.4 Current situation

As of 2018, the potential problems identified in 2015 have been avoided. The immediate actions in the TSF (internal embankments and excavation of tailings) gave sufficient volume to allow for enough time for design, permitting and construction of a raise of the embankments (first phase being built 2017). In addition to this the new thickener generates a slurry that meets the initial target of a slope of 3 % with no major concavity, se **Figure 7**, monitored both through areal scans every 6 months as well as a regular observation of the cone perimeter (since the tailings cone doesn't yet reach the embankments, a given slope gives an expected perimeter of the cone, that may easily be controlled visually, se **Figure 8**). This means that, at the moment, the buildup of the tailings cone follows the initially intended strategy, and the now raised embankments have created room for a large volume and also additional margin in case of further deviations from the intended deposition strategy. The solids content in the deposited tailings is approximately 70 % by weight.

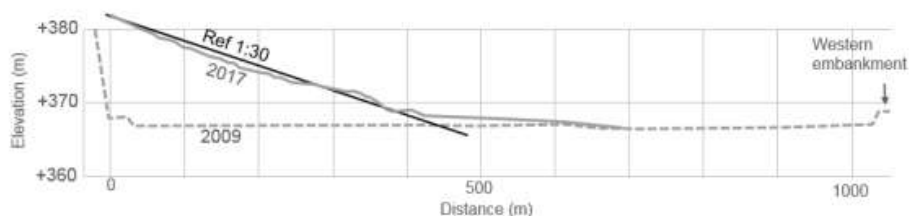


Figure 7 Cross section of the tailings cone - from the hill in the east to the western embankment. Levels measured 2017 compared with tailings surface 2009 and a reference line showing the target slope (1:30).



Figure 8 The outer perimeter of the thickened tailing cone.

3.5 *Moving forward*

The approach to raise the embankments downstream requires a large amount of placed fill material. However, there are reasons to believe that the significant seepage in the foundation will allow for drainage of the older tailings. Combined with allowing for drainage in the upper part of the older impermeable embankments, allowing tailings placed in the cone to be drained, it might be possible to achieve a foundation that will be suitable for future upstream raises.

4 CONCLUSIONS – WHAT TO LEARN FROM THE SVAPPAVAARA CASE

In the Svappavaara case the focus on creating more volume somewhat resulted in water management being partly overlooked. When faced with the need of raising the embankments, it had been assumed that installing new spillways would not be a challenge. However, the design and construction of a spillway through the highest part of the embankments turned out to be the major challenge when transforming the TSF to better suit the new deposition strategy.

Furthermore, the startup of the thickener – to obtain the target slope – took a lot longer time than anticipated. Connected to this it should be stressed that one great challenge, that should not be overlooked, is the organization's expectations on tailings management. When, after almost 50 years of deposition in an TSF that has basically been built up as an artificial lake with no requirements on the placed tailings, moving into a situation where the tailings slurry becomes an engineered product, the view of tailings management within the organization needs to be completely changed.

The implementation of a new deposition strategy requires close follow up – in this case both on the behavior of the thickener, the behavior of the placed tailings as well as the tailings cone being built. The organization monitoring the deposition needs to have sufficient capacity to perform required monitoring activities, required knowledge on what to measure, how to measure and how to interpret the results, as well as a mandate to make necessary changes in direct response to observations made. This type of organization needs to be created – and takes a lot of

time to build – since after 50 years of rather successful deposition following a simple strategy, follow up activities related to tailings placement will naturally have been reduced to an absolute minimum, and there will most likely not be such capacity already available within the organization.

5 REFERENCES

Knutsson, R. Viklander, P. Knutsson, S. 2016-04-29, Stability considerations on thickened tailings due to freezing and thawing, Paper presented at the 19th International seminar on paste and thickened tailings.

Assessing Oil Sands Tailings Consolidation Parameters Relative to Long-term Reclamation

H. Rourke and D. Hockley
SRK Consulting, Vancouver, BC, Canada

ABSTRACT: The reclamation of tailings deposits is dependent upon long-term consolidation, which determines both the final storage volume and ultimate deposit strength. Very soft materials like flocculated mature fine tailings undergo large deformations during consolidation. Describing this “large strain consolidation” requires non-linear equations for compressibility and hydraulic conductivity as functions of void ratio or effective stress. Typically, these equations are input to a finite strain consolidation model to estimate overall consolidation rates. This paper presents a robust sensitivity analysis to examine the effects of material property functions and design variables on consolidation model results. The tested variables included compressibility constants, hydraulic conductivity constants, years of deposition, rate of rise, specific gravity, initial solids content, and surcharge load application. Interpretation of the results identified clear patterns and dimensionless groupings that can be used as indicators of ultimate consolidation performance.

1 INTRODUCTION

The large inventory of mature fine tailings and the need to reclaim tailings deposits is a major challenge for the oil sands industry. Reclamation plans commonly include capping and revegetating tailings surfaces, which requires the tailings to develop sufficient strength to support construction equipment. Oil sands operators currently apply a variety of methods to treat fluid tailings. Initial water removal is achieved through flocculant addition followed by thickening, centrifugation or air drying. Further dewatering and strength gain is governed by the material’s consolidation behavior. Factors affecting consolidation include the hydraulic conductivity and compressibility properties of the tailings, as well as design variables such as deposition rates (rate of rise) and ultimate depth. But the interactions among these variables are non-linear, making it difficult to know exactly which variable should be changed in order to achieve “better” consolidation. The objective of this study is to understand how the interaction of material properties and design variables affect the consolidation of flocculated mature fine tailings. The hope is that such an understanding will help focus research efforts and operational strategies for creating reclaimable deposits within reasonable timeframes.

2 METHOD

2.1 Overview of consolidation theory

The classic one-dimensional Terzaghi consolidation theory was published in 1925 and is represented by Equation 1:

$$\frac{c_v \partial^2 u}{\partial z^2} = \frac{\partial u}{\partial t} \quad (1)$$

Where:

- c_v = coefficient of consolidation
- u = pore pressure
- z = depth
- t = time

The Terzaghi relationship assumes that compressibility and hydraulic conductivity are constant and not affected by changes in void ratio. This is appropriate for small-strain applications common in foundation design, but not for soft tailings deposits that can undergo large deformations and very significant changes in void ratio. For these applications, finite strain theory is needed. The Gibson finite strain theory (Gibson 1967 and 1981) is shown in Equation 2.

$$\pm \left(\frac{\rho_s}{\rho_f} - 1 \right) \frac{d}{de} \left[\frac{k(e)}{1+e} \right] \frac{\partial e}{\partial z} + \frac{\partial}{\partial z} \left[\frac{k(e)}{\rho_f(1+e)} \frac{d\sigma'}{de} \frac{\partial e}{\partial z} \right] + \frac{\partial e}{\partial t} = 0 \quad (2)$$

Where:

- ρ_s = solids density
- ρ_f = fluid density
- k = hydraulic conductivity
- e = void ratio
- σ' = effective stress
- z = depth
- t = time

Two constitutive relationships, describing the changes in compressibility and hydraulic conductivity as the material consolidates, are needed to solve the equation (2). There is continued debate and research about the most appropriate compressibility-void ratio relationship (e - $\log \sigma'$). Proposed representative relationships vary from power law, to modified power law, to Weibull functions. For the purposes of this paper, a widely-used power law function is applied:

$$e = A\sigma'^B \quad (3)$$

Where:

- e = void ratio
- σ = effective stress
- A = unique material constant
- B = unique material constant

The hydraulic conductivity-void ratio relationship (k - e) is also commonly modelled using a power function:

$$k = C e^D \quad (4)$$

Where:

- k = hydraulic conductivity
- C = unique material constant
- D = unique material constant

Before looking at how these functions interact, a good starting point is to look at the constitutive relationships on their own. The effect of the A and B values on the shape of the compressibility function is shown in Figure 1. The effect of the C and D values on the shape of the hydraulic conductivity function is shown in Figure 2.

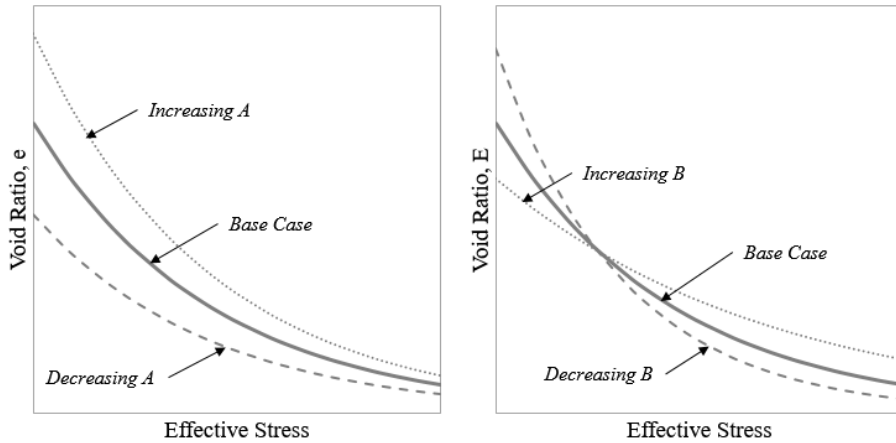


Figure 1. Effect of A and B values on compressibility

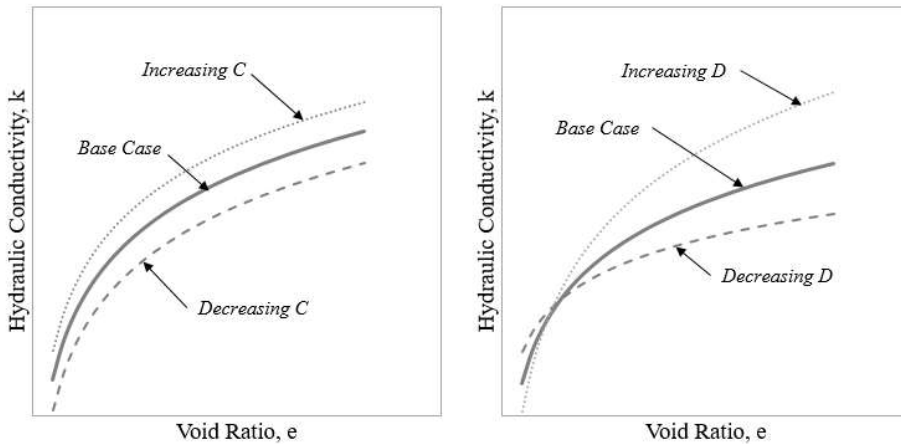


Figure 2. Effect of C and D values on hydraulic conductivity

2.2 Modeling Approach

To understand the combined effects of the hydraulic conductivity and compressibility functions, it is necessary to run a full consolidation model that also considers stresses associated with tailings deposition, porewater pressure, and physical characteristics such as specific gravity and initial solids content. This study used the one-dimensional finite strain program FSConsol© (Version 3.49; GWP Software 1996).

The model was run in a sensitivity analysis mode, allowing the influence of each input parameter on final outcomes, such as the time to 90% consolidation, to be tested. A Python script was written and used to automate the modelling process. This allowed the authors to run the hundreds of models required to perform a complete parametric analysis. Over 700 models were run in total, and each model was run for a 1000 year simulation period.

The key input parameters and ranges tested in the sensitivity runs are summarized in Table 1. Compressibility and hydraulic conductivity data sources include both laboratory and field measurements of flocculated mature fine tailings. While laboratory compressibility estimates are generally representative of field behavior, laboratory hydraulic conductivity results commonly underestimate field scale values by 3-10 times (COSIA 2014, Masala et al. 2014, Hockley 2017). To account for this, laboratory hydraulic conductivity estimates were increased by a factor of 5 to develop the ranges shown in Table 1.

Table 1. Typical ranges of consolidation inputs found in literature

Parameter	Base Case	Min	Max	Reference
Rate of rise (m/year)	5	1.5	10	Experience
Years of deposition	20	10	50	Experience
Applied surcharge (kPa) ⁽¹⁾	36	0	90	Experience
Compressibility (kPa) constants				Masala <i>et al.</i> 2010,
• A	3.2	2.8	3.5	Jeeravipoolvarn 2010,
• B	-0.25	-0.30	-0.18	Znidarcic 2016
Hydraulic conductivity (m/s) constants ⁽²⁾				Masala <i>et al.</i> 2010,
• C	2.5E-10	5.0E-11	5.0E-10	Jeeravipoolvarn 2010,
• D	4.0	3.3	6.0	Znidarcic 2016
Specific gravity (SG)	2.50	2.45	2.65	Masala <i>et al.</i> 2010,
				Jeeravipoolvarn 2010,
				Znidarcic 2016
Solids content (SC)	35%	20%	50%	COSIA 2014

⁽¹⁾ Base case surcharge of 36 kPa represents an approximate 2 m soil cap; maximum surcharge represents a 5 m soil cap

⁽²⁾ Laboratory hydraulic conductivity have been increased by a factor of 5 to account for the difference between laboratory and field-scale measurements

Sensitivity analyses were first run by varying each input parameter individually. Next the following multiple parameters scenarios were run to understand the combined effects:

- A and B to assess combined compressibility effects
- C and D to assess combined hydraulic conductivity effects
- A, B, C, D to assess combined consolidation effects
- Years of deposition and rate of rise to assess combined operational effects

Three results of each model run were recorded and used in the further analysis:

- Time to reach 90% consolidation, as an indicator of reclamation timeframes;
- Height after 1000 years, as an indicator of volume reduction; and
- Solids content after 1000 years, as an indicator of shear strength.

3 RESULTS

3.1 Overall Ranges

Results of all the sensitivity runs are summarized in Table 2. The first two columns indicate the tested parameter and range of values, and the next six columns show the range of model results. For each result, the corresponding parameter value is shown underneath in parentheses.

Table 2. Summarized Results Over 1000 Year Simulation Period

Parameter	Tested Values	Time to 90% Consolidation (years)		Minimum Height (m) after 1000 years		Maximum Solids Content (% Solids) after 1000 years	
		Best	Worst	Best	Worst	Best	Worst
Base Case	See Table 1	197		33.8		73.3%	
Individual-variable runs							
Rate of rise (m/year)	1.5 to 10	85 (1.5)	409 (10)	10.6 (1.5)	70.3 (10)	73.3% (1.5)	71.4% (10)
Years of deposition	10 to 50	126 (10)	488 (50)	17.3 (10)	90.5 (50)	73.3% (20)	70.6% (50)
Surcharge (kPa)	0 to 90	243 (90)	302 (0)	32.2 (90)	36.9 (0)	75.3% (90)	69.8% (0)
A (kPa)	2.8 to 3.5	254 (3.5)	309 (2.8)	32.4 (2.8)	35.0 (3.5)	75.0% (2.8)	71.9% (3.5)
B	-0.18 to -0.32	152 (-0.18)	352 (-0.32)	31.2 (-0.32)	40.1 (-0.18)	76.6% (-0.32)	66.5% (-0.18)
C (m/s)	5E-10 to 5E-11	192 (5E-10)	564 (5E-11)	33.3 (5E-10)	41.5 (5E-11)	73.9% (5E-10)	65.1% (5E-11)
D	3.25 to 6	278 (4)	360 (3.25)	33.6 (6)	34.2 (3.25)	73.6% (6)	72.9% (3.25)
Specific Gravity	2.45 to 2.65	258 (2.65)	287 (2.45)	32.0 (2.65)	34.5 (2.45)	74.8% (2.65)	72.8% (2.45)
Initial % Solids	20% to 50%	159 (20%)	558 (50%)	17.8 (20%)	55.5 (50%)	73.3% (35%)	72.4% (20%)
Multiple-variable runs							
A and B		132 (A=3.5 B=0.18)	357 (A=2.8 B=-0.3)	31.4 (A=3 B=-0.3)	42.1 (A=3.5 B=-0.18)	77.2 (A=2.8 B=-0.3)	64.5 (A=3.5 B=-0.18)
C and D		182 (C=5E-10 D=3.5)	699 (C=5E-11 D=3.5)	33.3 (C=5E-10 D=5)	45.6 (C=5E-11 D=3.5)	73.9 (C=5E-10 D=5)	61.3 (C=5E-11 D=3.5)
A, B, C, D		35 (A=3.5 B=-0.18 C=5E-10 D=6)	708 (A=2.8 B=-0.3 C=5E-11 D=3.5)	29.1 (A=2.8 B=-0.3 C=5E-10 D=3.5)	47.2 (A=3.5 B=-0.18 C=5E-11 D=3.5)	79.6 (A=2.8 B=-0.3 C=5E-10 D=3.5)	60.0 (A=3.5 B=-0.18 C=5E-11 D=3.5)
Rate of Rise and Years of Deposition		45 (2 m/yr 10 years)	578 (10 m/yr 50 years)	5.4 (1.5 m/yr 10 years)	205.5 (10 m/yr 50 years)	73.3 (10 m/yr 10 years)	65.4 (10 m/yr 50 years)

3.2 Time for 90% consolidation

It is possible to plot results of the 700 sensitivity runs in many ways. As a simple example, Figure 3 illustrates the effects of the model inputs on the range of time to reach 90% consolidation. The first two rows are unsurprising. Varying all of the consolidation parameters A, B, C and D creates a very wide range in results. Rate of rise and years of depositions together determine the overall depth of the deposit, and therefore also have a strong effect on consolidation times.

The remaining rows are more informative. They show that the hydraulic conductivity parameters C and D are very influential, and that C is more influential than D, at least over the ranges tested here. The compressibility parameters A and B are less influential, in part because the 90% consolidation endpoint partially accounts for the compressibility curve. Initial solids content has a predictably strong effect, but the surcharge loading has very little effect.

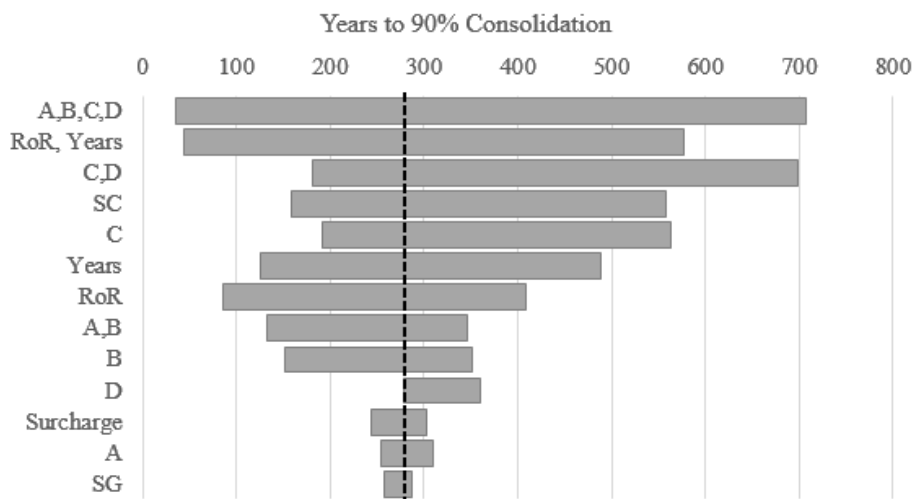


Figure 3. Years to 90% consolidation

3.3 Combined effect of hydraulic conductivity and compressibility parameters

Figures 4 and 5 show another way to plot the sensitivity results. Figure 4 shows the combined influence of the compressibility parameters A and B on reclamation times. The “bubbles” on the plot show the number of years required to reach an average solids content of 65%, with larger bubbles representing longer times.

The smallest bubble, indicating the fastest consolidation time, is at the top right-hand corner of the graph when A and B are at their highest values of 3.5 and -0.18, respectively. The trends clearly show that increasing either A or B, or both, improves consolidation times.

Looking at the first column, for a constant B value of -0.3, the consolidation time varies from 357 years when A is 2.8 to 324 years when A is 3.5. Looking at the bottom row, for a constant A value of 2.8, the consolidation times vary from 357 years when B is -0.3 to 188 years when B is -0.18. Clearly changes to B have a much greater effect on consolidation times than changes to A, over the ranges tested here.

Figure 5 uses a similar format to show the effects of the hydraulic conductivity constants C and D on the time to reach an average solids content of 65%. By following the same line of reasoning as presented above, it is clear that C is more influential than D. Interestingly, the effect of D depends on C. For example, when C is high (in the top row) increasing D leads to increasing consolidation times, but when C is low (bottom row) increasing D leads to reduced consolidation times. The underlying reasons for this are apparent from a close inspection of Figure 2.

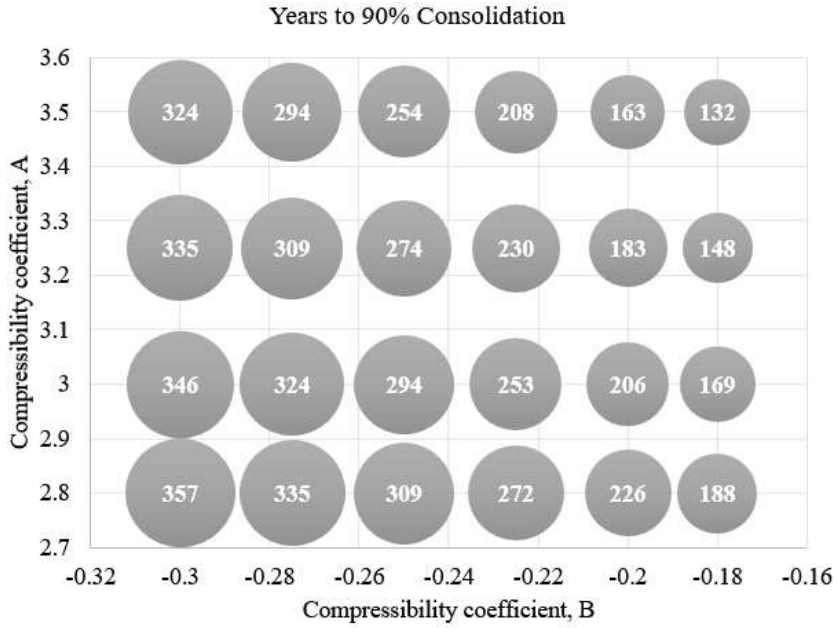


Figure 4. Effects of compressibility parameters on time to reach 90% consolidation

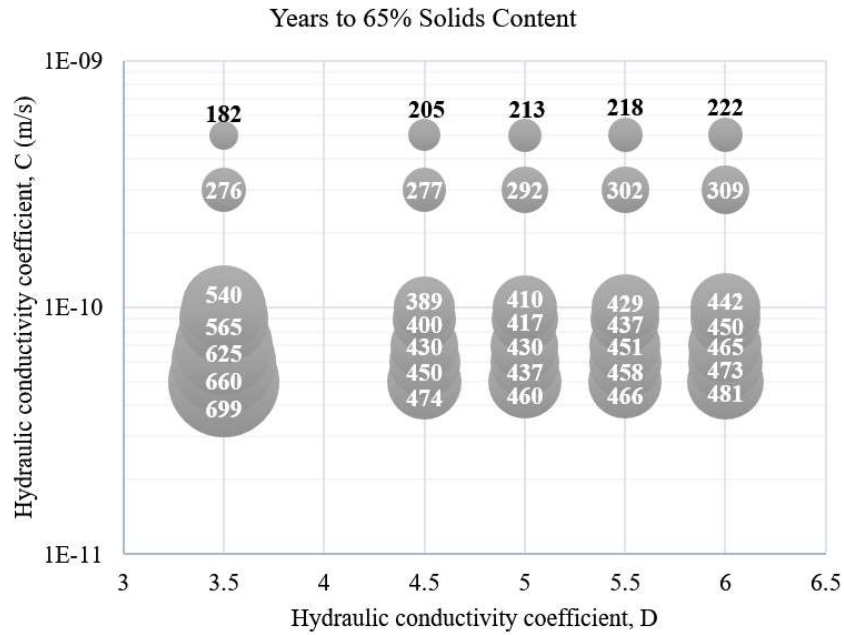


Figure 5. Effects of hydraulic conductivity parameters of time to reach 65% solids

4 DISCUSSION

4.1 Dimensionless Rate of Rise

Deriving further insights from the sensitivity analyses requires that the 700 sets of results be collapsed to simpler forms. One method to look for underlying patterns in complex information is dimensional analysis (Cimbala and Cengel, 2006). Briefly, the method consists of defining dimensionless combinations of parameters, and then converting results to those dimensionless forms in the hopes that “universal” patterns become more evident.

Figure 6 shows an example. It converts the rate of rise and hydraulic conductivity to a “dimensionless rate of rise” on the x-axis. (The plot shows the case where hydraulic conductivity is calculated at a void ratio of 3.0, but a similar plot is obtained with other void ratios.) The y-axis is another dimensionless quantity obtained by dividing the deposit height reached at the end of tailings deposition to the product of rate of rise times years of deposition. The product is in fact the height that would be reached if there were no consolidation during deposition. The resulting dimensionless quantity varies between 0.4 and 1 over the ranges of inputs tested, with higher values indicating that there has been less removal of pore water during the deposition period. Inspection of the curve shows that, when the dimensionless rate of rise on the x-axis exceeds about 10, there is little or no consolidation during deposition. In other words, when actual rates of rise are more than 10 times the hydraulic conductivity, all of the excess water is trapped in the initial deposit. Consolidation times and settlement depths would be correspondingly high.

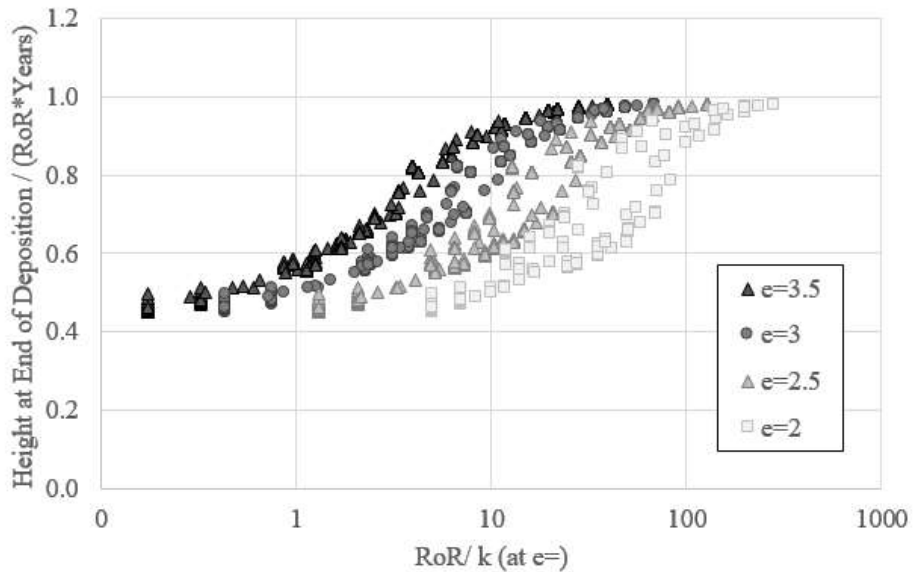


Figure 6. Dimensionless rate of rise vs dimensionless deposit height

4.2 Coefficient of consolidation

In Terzaghi theory, the coefficient of consolidation, c_v , is used to represent the combined effect of hydraulic conductivity and compressibility and allow dimensionless solutions of the consolidation equation. The coefficient of consolidation c_v is calculated as:

$$c_v = \frac{k(1+e)}{a_v \gamma_w} \tag{7}$$

Where:

- k = hydraulic conductivity
- e = void ratio
- a_v = coefficient of compressibility
- γ_w = unit weight of water

The same concept can be used in large-strain theory but c_v becomes a function of effective stress (or void ratio) rather than a constant. Figure 7 illustrates the value of c_v as a predictor of consolidation time. The x-axis in this case has also been “dimensioned” by dividing c_v by the square of the initial deposit height. That seems arbitrary but in reality, it simply adjusts for the effect of the different initial conditions. (The c_v value in Figure 7 were all calculated at $e=2.5$, which is entirely arbitrary, but a similar figure is obtained with other choices.)

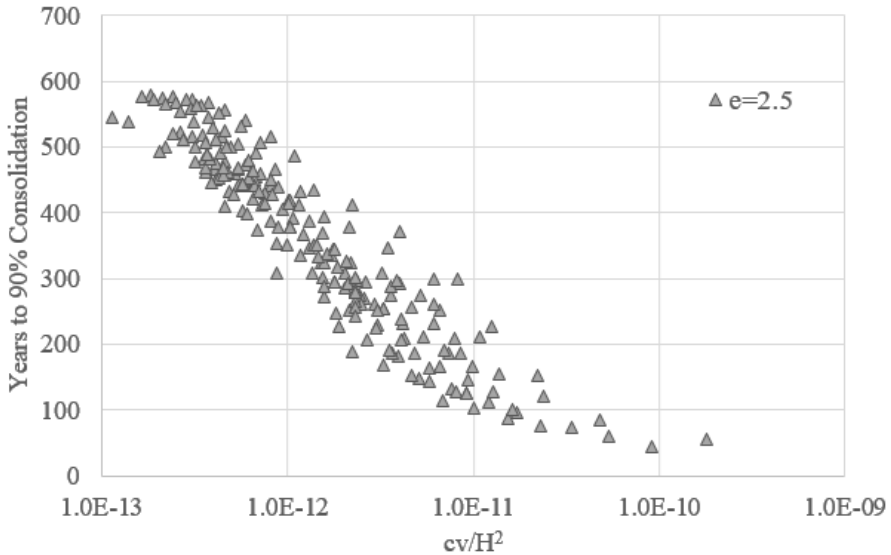


Figure 7. Consolidation time versus c_v/H^2 ¹

All of the c_v functions resulting from the sensitivity runs are plotted against effective stress in Figure 8. The results show a wide range of c_v values. More surprising perhaps is the diversity in how the c_v values change with increasing effective stress: some plots increase by orders of magnitude, some decrease by orders of magnitude, and some stay constant. Determining the significance for consolidation times takes some further thought. Clearly the best case is a constant high c_v such as shown on the bottom right plot in Figure 8. Cases where the c_v function slopes upward indicate that c_v values will increase as consolidation proceeds, (i.e. consolidation will accelerate)

¹ Note: D values were kept constant to reduce scatter in Figure 7.

and are likely to lead to overall faster consolidation than cases where the c_v function slopes downward.

In terms of the input parameters, there a clear relationship between B and D values and the slope of the c_v functions in Figure 8. Increasing (less negative) B values result in upward sloping c_v functions. Increasing D values lead to initially high c_v functions, but with strongly negative slopes. The differences within the family of curves shown in each plot represent the effects of the A and C coefficients. Changing the C coefficient shifts the c_v function upward by up to an order of magnitude, whereas changing A less than half an order of magnitude effect.

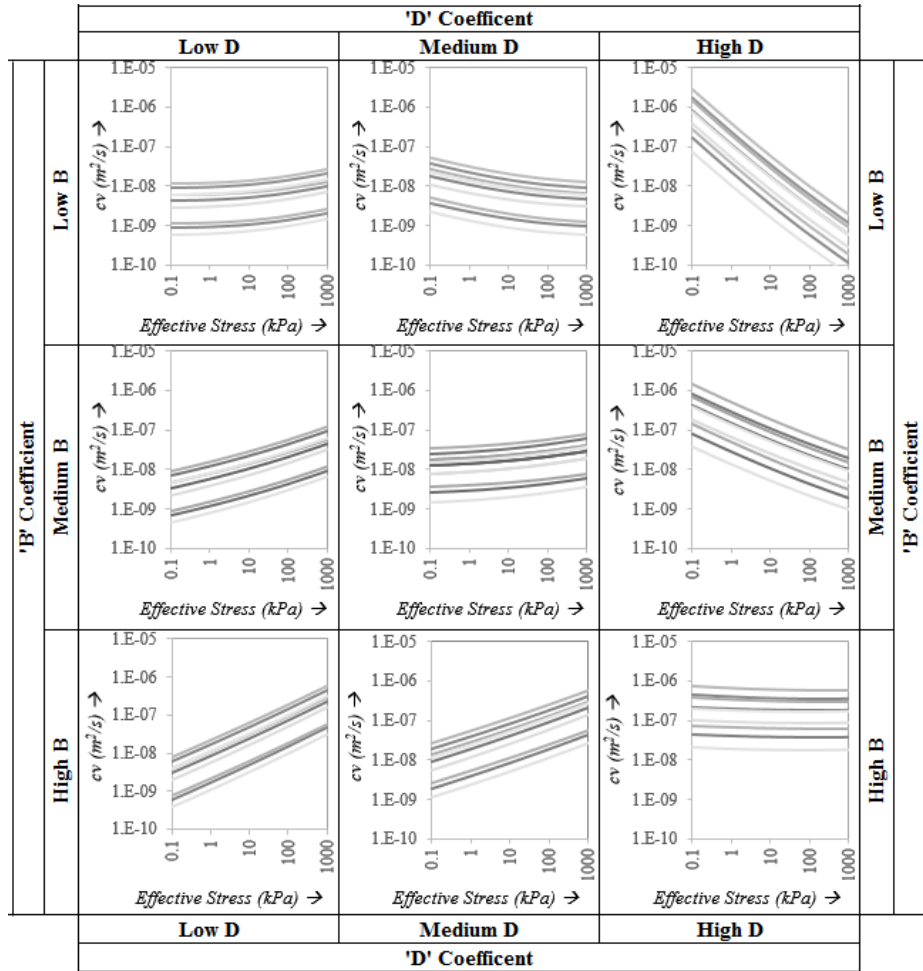


Figure 8. Coefficient of consolidation (c_v) functions from 700 sensitivity runs

4.3 Practical implications

There are three key performance issues associated with the successful reclamation of oil sands tailings deposits:

1. transforming mature fine tailings deposit into sustainable dry closure landscapes requires the tailings to have sufficient strengths to support construction equipment and allow cover construction ;
2. there is currently a large inventory of mature fine tailings stored in above-ground tailings facilities that require volume reduction; and
3. reclamation times are currently very slow with deep deposits requiring hundreds to thousands of years to reach desired closure strengths and/or volumes.

If the primary goal is to develop high shear strengths, a key performance indicator is the solids content achieved at a point in time. Table 2 shows that material properties are more influential than operational practices in increasing the 1000-year solids content of the deposit. For this case, increasing compressibility is more important than increasing hydraulic conductivity.

If the primary goal is to reduce overall deposit volumes, a key performance indicator is the height of the deposit at a point in time. Table 2 shows that operational practices are most important and that 1000-year heights can be greatly reduced by depositing less material at a slower rate. Initial solids content also has a significant effect, as does increasing compressibility.

Increasing shear strengths and reducing volumes has little benefit if it requires hundreds or thousands of years to do so. Therefore, the primary goal is often reducing reclamation timeframes. Both improving material properties (such as consolidation parameters) and operational practices (such as the rate of rise) are important. The most influential parameters are the initial solids content, hydraulic conductivity constant, C , the number of years of deposition, and rate of rise. For this case, increasing the hydraulic conductivity is most important and the compressibility has a lesser effect.

An important use that the authors see for these patterns is to direct development of new mature fine tailings treatments toward material properties that have the greatest influence on desired outcomes. A very practical example would be the pattern showing the importance of the hydraulic conductivity constants. Given that lab scale methods have difficulty measuring representative hydraulic conductivities, this finding might indicate a much greater need for field scale testing.

5 SUMMARY AND CONCLUSIONS

This study undertook a parametric sensitivity analysis to examine the effect of material properties and design variables on tailings consolidation. The material properties tested covered the range of flocculated mature fine tailings in the oil sands literature. Findings to date include the importance of the hydraulic conductivity function for determining consolidation times, relationships between rate of rise and the extent of initial consolidation, and the complex influence of both compressibility and hydraulic conductivity inputs on coefficients of consolidation.

Limitations of this study and possible avenues for further work include the following:

- Only one compressibility function was tested in the analyses. Further work could test the influence of alternative functions, such as the Weibull or modified power law relationships.
- Compressibility and hydraulic conductivity inputs only included ranges found in publicly available literature for flocculated mature fine tailings.
- Only four multiple-variable scenarios were tested as described earlier. Given that there were 5 to 7 values tested for each of the nine input variables, thousands of runs would be required to test every combination of multiple-variable scenarios. The results of this work could be used to identify key combinations of variables that warrant testing in future analyses.

6 REFERENCES

- Alberta Energy Regulator (AER) Directive 085 October 12 2017 Fluid Tailings Management for Oil Sands Mining Projects. <https://www.aer.ca/documents/directives/Directive085.pdf>
- Cimbala, J.M. and Cengel, Y.A.. (2006) *Fluid Mechanics: Fundamentals and Applications*, Boston,

- McGraw-Hill Higher Education
- COSIA (2014) Guidelines for Performance Management of Oil Sands Fluid Fine Tailings Deposits to Meet Closure Commitments. *Canadian Oil Sands Innovation Alliance*, February, 2014, 19 pp.
- Gibson, R.E., English, G.L., and Hussey, M.J., (1967) The Theory of One Dimensional Consolidation of Saturated Clays. *Geotechnique*, 17, 2, pp.261-273
- Gibson, R.E., Shiffman, R.L., and Cargill, K.W., (1981) The Theory of One-Dimensional Consolidation of Saturated Clays II. *Can Geotech Journal*, 18, 2, pp.280-293
- GWP Software Inc (1996). FSConsol Computer Software, Version 3.49. Retrieved from: <http://www.fsconsol.com/>
- Hockley, D., (2017) Clay effects on tailings geotechnical properties. In: *Clay in Oil Sands (O. Omotoso and D. Hockley, editors). Workshop Lecture Series, 22*, The Clay Minerals Society, Chantilly, Virginia, USA.
- Jeeravipoolvarn, S. (2010) *Geotechnical behaviour of in-line thickened oil sands tailings*. PhD thesis, Geotechnical Engineering, University of Alberta, Edmonton, AB, 431 pp.
- Locat, J., and Demers, D. (1988) Viscosity, yield stress, remolded strength, and liquidity index relationships for sensitive clays. *Canadian Geotechnical Journal*, 24, 4, pp. 799-806.
- Masala, S., Nik, R.M., Freeman, G., and Mahood, R. (2014) Geotechnical insights into deposition, dewatering and strength performance of thickened and paste tailings deposits at Shell Canada's tailings test facility. Pp. 277-288 in: *Fourth International Oil Sands Tailings Conference (IOSTC), 7-10 December 2014, Lake Louise AB (D.C. Segó, W. Wilson and N.A. Beier, editors)*. University of Alberta, Edmonton, AB.
- McKenna, G., Mooder, B., Burton, B., and Jamieson, A. (2016) Shear strength and density of oil sands fine tailings for reclamation to a boreal forest landscape. Pp. 130–153 in: *Fifth International Oil Sands Tailings Conference (IOSTC) (D.C. Segó, W. Wilson, and N.A. Beier, editors)*. University of Alberta, Edmonton, Alberta, Canada.
- Miller, W.G, Scott, J.D., and Segó, D.C. (2010a) Effect of extraction water chemistry on the consolidation of oil sands fine tailings. *CIM Journal*, 1, 2, pp. 113-129.
- Miller, W.G, Scott, J.D., and Segó, D.C. (2010b) Effect of the extraction process on the characteristics of oil sands fine tailings. *CIM Journal*, 1, 2, pp. 93-112.
- Wood, D.M. (1990) *Soil Behaviour and Critical State Soil Mechanics*, Cambridge University Press, Cambridge
- Znidarcic, D., Van Zyl, D., Ramirez, M., Mittal, K., and Kaminsky, H. (2016) Consolidation characteristics of flocculated MFT – Experimental column and SICT data. Pp. 408-415 in: *Fifth International Oil Sands Tailings Conference (IOSTC), Lake Louise Alberta, Canada (D.C. Segó, W. Wilson, and N.A. Beier, editors)*. University of Alberta, Edmonton, Alberta, Canada.

Characterization of Ancient Mine Wastes: An Approach for Environmental Management and Metals Recovery

M.L. Dinis, A. Fiúza, A. Futuro, A. Leite, J. Figueiredo, J. Góis, and M.C. Vila
Centre for Natural Resources and the Environment (CERENA-FEUP), Faculty of Engineering, University of Porto (FEUP), Porto, Portugal

D. Martins
Faculty of Engineering, University of Porto (FEUP), Porto, Portugal

ABSTRACT: The characterization of ancient mine wastes provides important information for land-management decisions, in particular when considering potential reprocessing activities or the development of an environmental protection programme. In addition, outcomes from such characterization may define the scope for more detailed investigations. The present work describes the characterization of tailings from the Cabeço do Pião tailings impoundment performed within the project: Improve Resource Efficiency and Minimize Environmental Footprint (ReMinE). The study involved the collection of 41 samples at different locations at two different depths, physical and chemical characterization of the wastes, natural leaching tests and potential for acid generation. The results showed that, apart from the potential instability of the dyke (slope of 35°), the drained solutions flowing by percolation contain very small particles with high arsenic content that is incorporated into the river sediments. This data is fundamental for economic and environmental assessment of the two main alternatives, reprocessing or removal.

1 INTRODUCTION

Industrial and mining wastes still represent a challenge for many countries where mining activities were, or still are, in place. In particular, ancient mine wastes can constitute a threat or an opportunity for local communities. They become a threat when they are simply abandoned and measures are not taken to reduce the risks to the environment; they can also represent an interesting resource of critical and valuable metals with potential economic benefits.

In many cases, the deposits of ancient mine wastes, derived from past mining and metallurgical activities, reflect the absence of efficient extraction methods or a low economic value at that time and they often contain significant amounts of potentially valuable metals. In addition, waste reprocessing may reduce environmental liabilities for public and private stakeholders. Therefore, any new extractive waste treatment process should be accompanied by information about the physical and chemical characteristics of the waste in order to provide the required useful information to the authorities and to the companies that are intending to begin with potential reprocessing activities or with an environmental protection programme. The mitigation of the environmental impacts resulting from mine wastes, and the remediation options, will depend on the waste properties and its behavior in the environment.

Mine wastes primarily consist of waste rock and mine tailings. In particular, mine tailings are finely ground rock particles resulting from ore processing which may be highly reactive due to their small particle size and content of reactive minerals, such as pyrite (FeS_2). Other metals that may be present include base transition metals such as iron, copper, nickel and zinc, in rela-

tively high concentrations and occasionally precious metals such as gold and silver. Toxic elements, such as arsenic, may also be present in high concentrations.

The exposure of reactive mine tailings to both oxygen and water can generate acidic effluents and runoff waters containing high concentrations of dissolved metals and sulfates. Acid mine drainage (AMD) is a widely reported environmental impact at mine sites throughout the world. For historical mining waste deposits, the geotechnical stability and the potential release of dissolved metals, acidity or suspended particles can also be a serious and long-lasting problem.

The Cabeço do Pião tailings impoundment was considered as a case study of historical mining wastes for the present work. The interest in reprocessing the tailings coexists with the necessity to solve the environmental problems caused by the potential instability of the unconfined tailings if left exposed during severe meteorological conditions. The impoundment is located on a bank of the Zêzere River and has an average arsenic content of 15%. Other metals (e.g. Cu, Zn and W) are present with significant concentrations.

The present work describes the characterization of tailings from Cabeço do Pião performed within the project: Improve Resource Efficiency and Minimize Environmental Footprint (ReMinE). The study involved the collection of 41 samples at different locations at two different depths, physical and chemical characterization of the wastes, natural leaching tests and screening tests for acid generation potential.

2 METHODS AND MATERIALS

2.1 Area of study

The Cabeço do Pião tailings impoundment belonged to the Industrial Complex of Panasqueira mine (Fig. 1), which is one of the largest operating tungsten mines in the Market Economy Countries (MEC). The Panasqueira mine started operating in 1896 focusing mainly on wolframite exploitation with cassiterite and chalcopyrite exploitation as by-products (Candeias et al., 2014).



Figure 1. Panasqueira mine and Cabeço do Pião tailings deposit.

The geology of the Panasqueira mine was extensively studied and described by several authors (D'Orey, 1967; Bloot & de Wolf, 1973; Kelly & Rye, 1979; Noronha et al., 1992; Ávila et al., 2008). The ore deposit is considered one of the biggest W-Sn deposits of Western Europe and it is located in the Central Iberian Zone (CIZ). The deposit is a classic example of a W-Sn hydrothermal mineralization associated with the Hercynian plutonism. The present minerals include quartz, wolframite, pyrite, pyrrhotite, arsenopyrite, chalcopyrite, cassiterite, beryl, mica, and fluorite (Candeias et al., 2014; Grangeia et al., 2011). Additionally, many rare minerals were identified, including sulfides, sulphosalts, oxides, carbonates, silicates, phosphates, and tungsten minerals (Kelly and Rye, 1979).

The first area where wolframite ore was processed in a large scale was located in Cabeço do Pião. The main processing plant later moved to the Panasqueira village, treating ores from several orebodies in the area. The resulting tailings were disposed of at the Cabeço do Pião site, in an impoundment around a hill on the edge of the Zêzere River, starting in 1927 and continuing for 90 years. The slope of the crest and supporting bedrock is 35° and the average height is approximately 90 m, draining directly to the Zêzere River (Fig. 2).



Figure 2. Slope of the Cabeço do Pião tailings deposit.

The estimated volume of the tailings is $1.32 \times 10^6 \text{ m}^3$. The tailings are exposed to atmospheric conditions and altered by chemical, mineralogical, physical and geotechnical factors. An arsenopyrite stockpile (9400 m^3) was deposited near the former processing plant and remained exposed until 2006, when it was capped with geotextile and layers of clay (Candeias et al., 2014).

The altitude in the region ranges from 350 to 1080 m forming deep valleys. The Zêzere River is the main watercourse in the area. The climatic conditions can be very extreme, with rainy and windy winters and very dry and hot summers. The average annual precipitation is 1600 mm and snows events occur frequently above the altitude of 700 m. The average temperature ranges between 0° C in the winter and about 30° C in the summer (Candeias et al., 2015).

Collecting representative samples of mine waste material can be challenging due to the high heterogeneity of the chemical and mineralogical composition of the tailings. Different origins of the ores that were processed, as well as different production techniques over time and different deposition strategies influenced the characteristics of the tailings such as the particle size distribution, type of the secondary minerals and concentration in heavy metals (Martin et al., 2016).



Figure 3. Cabeço do Pião sampling grid (adapted from Google earth, 2016).

The tailings from Cabeço do Pião were sampled at 41 sampling points for surface samples (50 to 60 cm depth) and for deep samples (approximately 2 m). Surface samples are most relevant for wind-borne transport, exposure and direct contact with precipitation and surface runoff.

The sampling events took place between November 2016 and January 2017. A rectangular grid of 40 x 20 m (Fig. 3) was defined for the collection of samples. The samples were identified with letters from A to F followed by a numbering sequence from the right to the left side of the figure. In addition, the samples were geo-referenced and identified as 'S' for the surface samples and as 'P' for the deep samples.

2.2 Experimental methods

The experimental methods included determination of particle size distribution, chemical composition, pH, density and porosity.

Tailing samples were oven dried at 50° C until constant weight, homogenized and sieved through a 200-mesh screen. The grain size distribution of the undersize fraction was analyzed with a laser diffraction particle size analyzer (Malvern Mastersizer 2000).

The bulk chemical composition was determined by X-ray fluorescence (XRF) with an Oxford XRF Analyzer (X-MET 7500). The pH of the tailings was determined in an aqueous solution by two different methods, with distilled water in a 1:1 solid-liquid ratio and with 0.01 M CaCl₂ in a 1:2 solid-liquid solution ratio (Black, 1965). Particles density were determined by the Pycnometric method described in the standard CEN ISO/TS 17892-3:2004.

Natural leaching tests were performed with representative tailing samples. The leaching process was simulated with distilled water in batch cells with constant stirring for a maximum period of 24 hours. The tests were stopped at 1, 3, 12 and 24 hours to measure the pH, dissolved oxygen, salinity, total dissolved solids, conductivity and temperature. The standard method DIN 38414-S4 was followed to set up the experimental phase in the laboratory. The leached solid samples were dried and then analyzed for chemical composition by XRF. The results were compared with the chemical composition of the unleached samples.

The acid generation capacity was also tested using two acid generation prediction methods: the Net Acid Generation test (NAG) and the modified Acid Base Accounting (ABA) method for neutralization potential (Lawrence & Wang, 1997). Ancient mine wastes are weathered material and therefore a method that incorporates the potential acid production of secondary and tertiary minerals and the potential acid-consuming capacity of host rock minerals (e.g. carbonates, aluminosilicates and silicates) should be adopted (Smith et al., 2006).

The Net Acid Generation (NAG) test determines the balance between the acid producing and acid consuming components of tailings/waste rock samples. NAG results provide the acid rock drainage characteristics based on the complete oxidation of the sulfide content of the samples (as well as ferrous iron from siderite dissolution). Acid that is produced by oxidation is consumed by carbonates and/or other acid consuming components of the material. The pH of the solution is measured (NAG pH). The acid remaining after the reaction is titrated with standardized NaOH to determine the net acid generated.

The modified acid-base accounting (ABA) (Lawrence, 1990) determines the maximum potential for acid production (Acid Production Potential or APP) and acid neutralization (Neutralization Potential or NP). The procedure involves a laboratory static test that compares the maximum APP of a sample with its maximum NP. The APP is based on sulfur analysis, and the NP is determined by the amount of acid neutralized when the sample is in contact with a solution in the approximate pH range of 1 to 3.5. The potential of a mine waste to produce acidic drainage is determined by the difference (net NP) or ratio (NP/APP) of these values (Lapakko, 1992).

3 RESULTS AND DISCUSSION

3.1 Characterization of tailings samples

3.1.1 Physical properties

Figure 4 presents the grain size distributions of mine tailings collected at two different depths (0–2 m) and designated as surface (S) and deep samples (P).

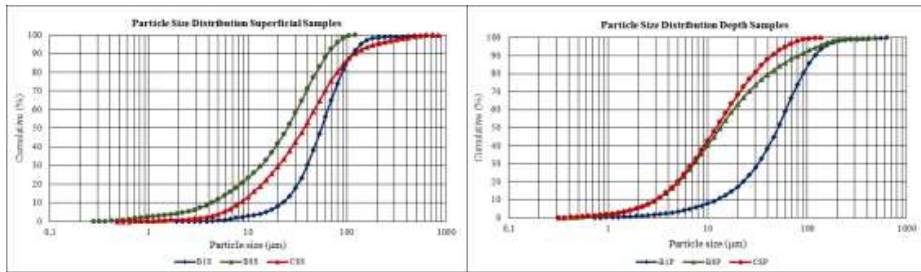


Figure 4. Particle size distribution of tailings samples from Cabeço do Pião impoundment.

The mine tailings are composed of particles ranging in size from 0.25 to 900 μm for surface samples and particles ranging in size from 0.3 to 700 μm for deep samples. The overall composition includes sand-sized particles ranging in size from 62 to 1000 μm , silt-sized particles ranging in size from 4 to 62 μm and clay sized particles < 4 μm . The following observations emerge from the grain size analyses for the surface and deep tailings samples.

The surface samples are very heterogeneous with regard to grain size. The silt fraction represents the highest content: 65%, 84% and 73% for B1S, B8S and C8S, respectively. The sand content is 34%, 8% and 24% for samples B1S, B8S and C8S, respectively. The D-values (D10, D50 & D90) are as follows: B1S (4 μm , 25 μm , 70 μm), B8S (8 μm , 35 μm , 100 μm) and C8S (2 μm , 65 μm , 100 μm).

For the depth samples, the silt fraction presents the higher content: 57%, 73% and 82% for B1P, B8P and C8P, respectively. The sand content is 41%, 16% and 7% for samples B1P, B8P and C8P, respectively. The D-values (D10, D50 & D90) are as follows: B1P (13 μm , 52 μm & 102 μm), B8P (3 μm , 13 μm & 80 μm) and C8P (3 μm , 12 μm & 46 μm), respectively.

The tendency of the sand fraction to increase with depth and that of the silt fraction to decrease with depth is presumed to arise from the preferred sedimentation of the coarse sand particles upon disposal of the slurry. In addition, the oxidation and weathering of tailings on the surface would cause a significant decrease of the grain size with depth. However, what was observed from the grain size analysis was that some surface samples present a coarser grain size than deeper samples taken from the same sampling location and therefore there are grain size variations in the tailings throughout the impoundment. These variations are related to the distance from the tailings discharge pipe where the tailings were discharged as slurry; the coarser grains settled closer to the pipe, while the finer grains settled further away. In addition, the re-deposited tailings in some areas of the impoundment are also the cause of this variation.

For surface samples, the loose bulk density ranged from 1.10 to 1.54 g/cm^3 and the compacted bulk density ranged between 1.83 and 2.50 g/cm^3 , the particle density ranged from 3.16 to 3.76 g/cm^3 and the voids percentage ranged from 35% to 41%. For the deep samples, the loose bulk density ranged between 1.07 and 1.46 g/cm^3 and the compacted bulk density ranged between 2.14 and 2.44 g/cm^3 , the particle density ranged between 3.58 and 3.89 g/cm^3 and the voids percentage ranged from 37% to 41%. The tailings exhibit low bulk densities and there is no significant variation with depth; the same pattern was verified for the variation of particle density with depth. Nevertheless, the void percentage slightly decreased for deeper samples evidencing some consolidation. An effective porosity of the tailings in depth will limit the infiltration of water and oxygen.

3.1.2 Environmental properties

The pH of the tailings measured in solution with distilled water and CaCl_2 is presented in Figure 5. The difference of the results between the two methods can be neglected.

All samples show acidic pH values ranging from 1.4 to 3.6. However, the surface samples (S) present a lower pH than deep samples (P). The higher acidic pH observed at the surface is apparently a consequence of atmospheric oxidation of the exposed pyrite minerals in the tailings deposit that produces sulfuric acid (acid mine drainage).

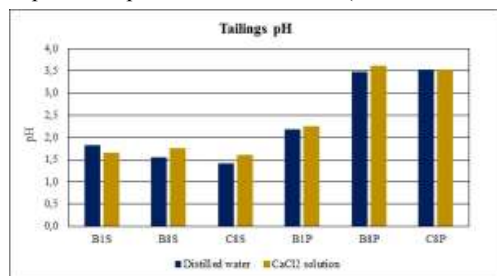


Figure 5. Tailings pH determined in solution with distilled water and CaCl₂ solution.

3.1.3 Chemical composition

A summary of the element chemical composition of the tailings samples is presented in Table 1.

Table 1. Elemental content in tailings samples from Cabeço do Pião impoundment

Element	B1S	B8S	C8S	B1P	B8P	C8P
	(%)	(%)	(%)	(%)	(%)	(%)
As	13.10	17.87	12.81	18.75	14.17	12.39
Cu	0.36	0.09	0.70	0.79	0.51	0.56
Fe	24.11	20.98	21.22	27.25	27.03	26.13
Hg	0.03	0.06	0.04	0.04	0.04	0.05
K	0.55	0.34	0.64	-	-	-
Mn	-	-	-	0.01	0.21	0.21
Sb	-	-	-	-	0.01	0.01
Sn	0.05	0.10	0.07	0.08	0.09	0.08
S	9.90	2.50	10.10	10.40	7.40	7.50
W	0.06	0.25	0.23	0.15	0.47	0.50
Zn	0.82	0.05	0.64	1.26	1.63	1.56

The results show the prevalence of Fe ($\cong 25\%$) and As (12-20%), followed by Zn (0.99%), Cu (0.5%) and W (0.28%). There is an observed increase in Fe, Mn, Zn and W content with depth and a decrease in K content with depth for all samples. As content increases with depth for samples B1 and B8 but decreases for sample C8, while Sn content increases with depth for samples B1 and C8 and decreases for sample B8. The results show that the major environmental concern is the high As content present in the tailings. The oxidation of sulfide minerals exposed to atmospheric oxygen can generate acidic drainage when in contact with water. The overall results are presented in Figure 6.

In previous studies, the materials from the Cabeço do Pião impoundment were characterized from selected samples from drill cores (Grangeias et al., 2011). For all cores samples, As is enriched from the surface down to a depth of 13 m, with a concentration ranging between 8.7 and 24%. From this depth, arsenic content decreases to values near or below 1%. Results from X-ray diffraction (XRD) analyses described in Grangeia et al. (2011) showed the presence of quartz, mica, feldspar, illite-vermiculite, arsenopyrite, marcasite, pyrite, pyrrhotite and chalcopyrite. Others minerals, like scorodite and natrojarosite are also present and enriched in As, Cu, Mn, Pb and Zn.

The fine-grained nature of these materials with high As content are the most immediate environmental concerns both due to the potential transport and dispersion by the wind and the proximity to the Zêzere River. Moreover, other elements are present at high concentration in parti-

cles that are readily mobilized during ongoing removal and processing. The material from the arsenopyrite stockpile that was deposited on the top of the tailings contains high concentrations of Ag (124 mg/kg), As (210,000 mg/kg), Cd (3057 mg/kg), Cu (1426 mg/kg), Fe (19.8%), W (5166 mg/kg) and Zn (460 mg/kg) (Candeias et al., 2014; Avila et al., 2008).

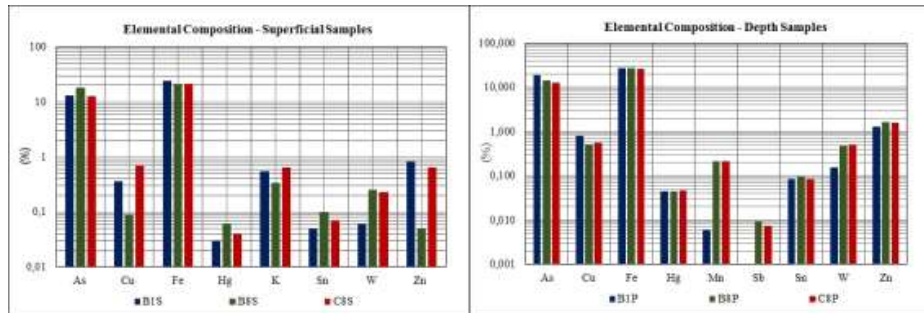


Figure 6. Elemental composition of tailings samples from Cabeço do Pião impoundment.

3.2 Natural leaching tests

Natural leaching tests are one of the commonly used worldwide procedures to evaluate, characterize and prioritize mine wastes. These tests allow identifying and estimating the amount of soluble constituents that can be released from waste rock materials and tailings during natural climatic conditions, which may include severe rainstorms and snow melt events. Using this test, it is possible to determine the concentration of contaminant(s) that are present in the solidified/stabilized (S/S) waste form, and more importantly, their likely mobility.

For the collected samples, natural leaching tests were carried out as short-term extraction tests (24-hour batch extraction tests using distilled water). These tests provide information on the short-term metal leaching potential, although in natural conditions (under the influence of atmospheric conditions and the presence of microorganisms) there are several physical, chemical and biological processes that are not possible to reproduce in batch laboratory tests. The variation of leachate parameters over time was also assessed.

3.2.1 Variation of pH over time

The pH of the leachate solution as a function of weathering (leaching) time in hours is presented in Figure 7. At the beginning, the pH of the distilled water used to leach the samples was 6.6 for surface samples and 7.2 for deep samples.

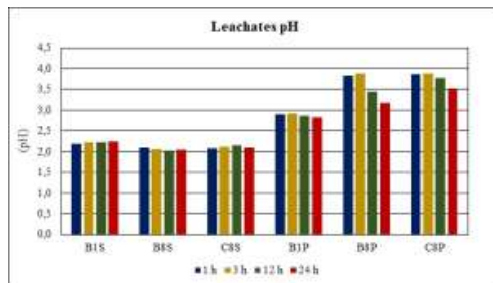


Figure 7. Variation of leachates' pH over time.

The test results show a significant decrease in the pH of the leaching solutions (6.55 and 7.25) to values similar to those of the collected samples' pH range (1.98-2.32). These are typical pH values of impacted waters resulting from the percolation of rainwater through the tailings, causing the weathering of the sulfide-rich minerals. During the sampling events, it was

possible to observe the occurrence of acid drainage at the base of the tailings embankment, and the consequent development of iron coating and ferruginous crust. The chemical composition of these waters present high concentrations of dissolved sulfates, Al, As, Cd, Co, Cu, Fe, Mn, Ni, and Zn which are indicative of the oxidation and dissolution of sulfides (pyrite, chalcocopyrite, sphalerite and arsenopyrite) (Grangeia et al., 2011). In addition, for pH values below 5, it is assumed a potential aquatic toxicity exists from cationic metals (Al, Cd, Cu, Ni, Pb and Zn) as in this condition metals are generally dissolved and minimally complexed with organic or inorganic ligands (Smith et al., 2006).

3.2.2 Variation of salinity over time

The measured values for salinity during the leaching test are presented in Figure 8.

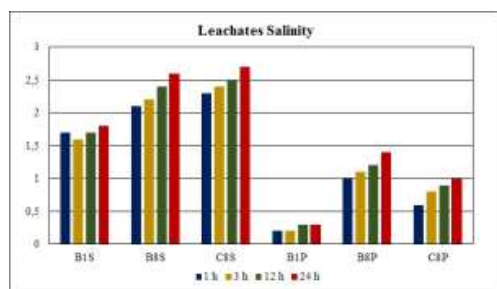


Figure 8. Variation of leachates' salinity over time.

The dynamics of salinity in tailings is very important for future revegetation of the disposed tailings, as high salinity is one of the major constraints to revegetation in many tailings impoundments (Gozzart et al., 2009; Huang et al., 2012). Pyrite oxidation is a major factor responsible for the acidification of mine wastes, causing extreme salinity and metal toxicity (Evangelou & Zhang, 1995). In general, areas requiring reclamation will be affected by high salinity of the generated leachates and therefore, when considering this option, an assessment of the tolerance of plants to salinity in runoff/seepage water is made by calculating the average root zone salinity (DITR, 2007).

For the samples from the Cabeço do Pião tailings impoundment, the salinity increases over time. This results from the weathering of reactive tailings' minerals, which acidifies the pore water and increases the release of saline ions and toxic elements. The tailings leachate drains directly to the Zêzere River.

3.2.3 Variation of electrical conductivity over time

The results obtained for electrical conductivity (EC) during the leaching tests are presented in Figure 9. As expected, both parameters, electrical conductivity and salinity, show a similar behavior over time. The values increase and are higher for surface samples (more oxidizing environment) than for deep samples. The increase in electrical conductivity, as well as the decrease in pH, indicate the tailings oxidation activity.

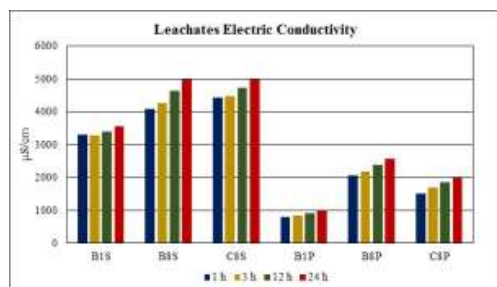


Figure 9. Variation of leachates' electric conductivity over time.

3.2.4 Chemical composition of the solid leached samples

The leached solid samples were dried at 60°C for 24 hours and analyzed on X-ray fluorescence for element composition. The results are presented in Figure 10.

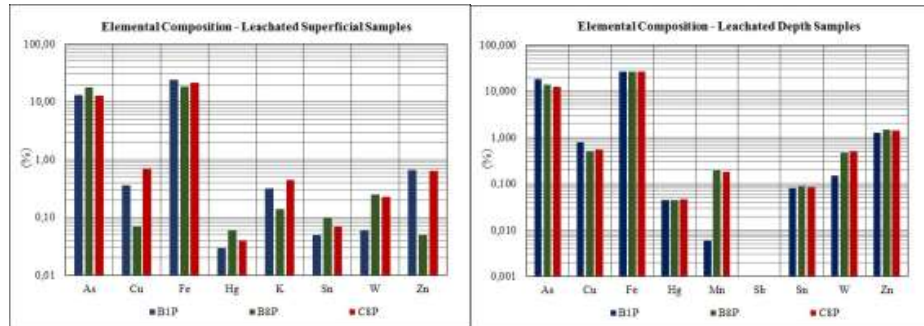


Figure 10. Elemental composition of the leached solid samples.

Apart from a few exceptions (Cu, Fe: B8S, C8S samples; K: B1S, B8S, C8S; Zn: B1S, B8P C8P), the chemical composition of the solid phase after the natural leaching test is similar to the chemical composition before the natural leaching test. Although the leachate presents an extremely acidic pH and the EC and salinity increase over time as well, which means high concentrations of dissolved sulfates, Al, As, Cd, Co, Cu, Fe, Mn, Ni, and Zn (Grangeia et al., 2011), it appears that there are some mechanisms that limit the effects of the acid drainage since the crusts and clays efficiently fixate some of the contaminant elements, especially the iron oxides (Ávila et al., 2008).

On the other hand, the mine tailings used in this study were sampled from historical mine tailings which means that the surface of the uncovered mine tailings had been allowed to be in contact with oxygen. This condition resulted in the oxidation of sulfide minerals. The oxidation of sulfide, which combine with As or heavy metals, results in the dissolution of As and heavy metals by water (Kim & Jung, 2004). Based on the presence of sulfide minerals, high contents of As and heavy metals, potential of oxygen contact, and high sulfate concentration in the mine tailings, the dissolution of iron and arsenic, as an example, could have already occurred in the mine tailings. Heavy metals released by oxidation can be re-adsorbed onto the surface of ferric hydroxide and adsorbed heavy metals can be separated from the surface of ferric hydroxide by water (Holmstrom et al., 2004). The low leaching concentration in the test may also indicate that the more soluble fraction of As and heavy metals might have already been released by the oxidation of sulfide minerals with air and water for a long period at the tailings deposition site. Based on this, investigations on the status of contaminants in nearby soils and groundwater are needed.

3.3 Acid generation potential

The static geochemical tests, NAG and modified ABA (Lawrence), were performed to determine the total acid generating and total acid neutralizing potential of the collected samples. Individually, each test has limitations in how accurately it can predict AP and NP and therefore it is a good practice to use a combination of methods to define NPR (Neutralization Potential Ratio: NP/AP) and identify samples requiring further investigation (Smith et al., 2006).

3.3.1 Net Acid Generation Test (NAG)

The NAG test was performed on 2.5 g of pulverized sample (less than 75 µm); however, as the obtained NAG values were above 25 kg H₂SO₄/t (tons of acidity per ton of rock) for all samples, the test was repeated with 1 g of material as shown in Table 2.

In this test, hydrogen peroxide is used to accelerate the oxidation of sulfide (Lawrence et al. 1988). The reaction generates acid which in turn reacts with the buffering minerals in the sam-

ple. One potential limitation of this test is that if the extent of oxidation in the field setting is greater than in the test, the potential exists for the test to underestimate acid production, creating the possibility that some acid producing waste may be incorrectly classified as non-acid-producing (EPA, 1994). This is not the case, as the results indicate that these samples have high risk of acid generating and therefore are classified as “Potentially Acid Forming – PAF) according to the Geochemical Classification Criteria based on NAG value and NAG pH (DITR, 2007).

Table 2. NAG test results

Sample	NAG pH	NaOH (ml)	NAG values (kg H ₂ SO ₄ /t)
B1S	2.12	22.6	58.21
B1P	2.22	20.1	44.69
B8S	1.98	23.0	91.14
B8P	2.32	22.5	54.88
C8S	2.10	20.0	61.94
C8P	2.24	25.0	52.14

3.3.2 Modified Acid-Base Accounting Test (modified ABA)

In this test, the acid production potential (APP) is determined from the sulfide sulfur content as follows: 31.25 x percent S = APP (modified ABA: the sulfur contribution from non-sulfide sources is not included) and assumes that two moles of acid will be produced for each mole of sulfur. Units for APP are tons of acidity per ton of rock. Neutralization Potential (NP) is determined first by a simple fizz test to select the acid strength to use in the next step to insure the addition of sufficient acid to react all the calcium carbonate present.

For the modified ABA test, 0.5 g of sample was first used to determine the fizz rating and then 2.0 g of sample (less than 250 µm) to determine the NP in order to calculate the NNP and NPR (Lawrence et al., 1988; Lawrence, 1990; Miller et al., 1997). The fizz rating was classified as “none” for all samples. The results of the modified ABA test are presented in Table 3.

Table 3. Modified ABA test results

Sample	pH	NaOH (ml)	NP (kg CaCO ₃ /t)	SO ₃ (%)	S (%)	AP (kg CaCO ₃ /t)	NNP (kg CaCO ₃ /t)
B1S	8.51	21.6	-53.25	24.6	9.9	3.08	-56.33
B1P	8.40	12.8	-31.95	26.0	10.4	3.25	-34.75
B8S	8.36	23.1	-57.00	6.1	2.5	0.77	-57.77
B8P	8.30	20.4	-50.90	18.6	7.4	2.33	-52.33
C8S	8.33	21.1	-52.00	25.1	10.1	3.14	-55.14
C8P	8.34	20.9	-52.15	18.7	7.5	2.34	-53.59

The modified method assumes that sulfur present as sulfate is not acid producing and therefore may underestimate available APP if jarosite or other acid producing sulfate minerals are present. Conducting the acid digestion at standard temperature may reduce the contribution of iron carbonate minerals when determining the NP.

Assumptions of the test are that all the sulfur in the sample is reactive. This assumption does not take into account the presence of gypsum and other non-reactive sulfur minerals. A shortcoming of the technique is the potential to overestimate NP.

Tests conducted by Ferguson (reported by Lapakko 1993) indicate that NNP values less than -20 (kg CaCO₃/t) are likely to form acid. Those with NNP values greater than 20 were not likely to form acid. For NNP values between -20 and 20 it was difficult to determine the acid potential (samples are classified as “uncertain”). In this case, all samples are likely to form acid, as the NNP is less than -20 (kg CaCO₃/t). Also, a sample is classified as “possibly” or “likely acid generating” if the NPR of the samples are less than 1, which seems to be the case.

The modified ABA results, along with NAG results, indicated that these samples would produce acidity (PAF) and therefore these historical mine wastes are a source of potential acidity that can be generated under natural oxidation processes.

The discharge of acid mine drainage with low pH and high dissolved metals content will seriously affect the aquatic environment (Grangeia et al., 2011).

3.4 *Reprocessing investigations and environmental alternatives*

The reprocessing of zinc from the tailings of Cabeço do Pião deposit could represent a promising solution to the depletion of zinc ores worldwide. Zinc ores can be concentrated by acidic leaching processes, but this treatment presents the disadvantage of dissolving other metals, such as Fe, Ca, Mg and Si. Several leaching tests were already performed with sulfuric acid and hydrochloric acid-oxygen leaching. The process of zinc concentration was limited by the content of iron and arsenic in samples material. Leaching tests were more effective when performed with sulfuric acid but the recovery was only up to 50%. Alkaline extraction tests are ongoing.

The main issues from the reprocessing process comes from the low tonnage of W, Cu and Zn content in the tailings, high capital costs and foreseen high processing costs. An uncertainty remains with regards to the As problem and if it will be solved with reprocessing.

The alternatives to minimize environmental impacts include: i) Cover the tailings on-site, avoiding leaching and weathering. However, the topographical issues will imply a complete reshape of the disposal and a large movement of ground in a difficult topography; ii) Excavation and transport of the tailings to other location for final confinement. The main advantage is the effective possibility of sealing the tailings. However, a large volume of materials will need to be transported and the reshape of the actual facility after the removal of the tailings as well. The selection of a new site to deposit the tailings with an impervious bottom will need to be considered; iii) Ex-situ inertization, meaning excavation of the tailings and transport to a new location also. In this case, several solutions are possible: cementation, solidification and polymeric resins. The main advantage is the inertization of the tailings, but large volume of materials will still need to be transported to a new location, apart from the cost of the process; iv) In-situ inertization has the main advantage of avoiding transport, however, the feasibility of this alternative is not certain although there are several possible variations: cement, clays, polymeric resins, geochemical immobilization.

4 CONCLUSIONS

Historical mine tailings were characterized for particle size, elemental composition, natural leaching behavior and potential for acid mine drainage generation. The mitigation of the environmental impacts resulting from mine wastes, and the remediation options, will depend on wastes characteristics and behavior on the environment.

The results were analyzed through two different approaches based on the economic and environmental assessment of the two main alternatives, reprocessing or removal. The high As content along with the fine-grained nature of these materials are the most immediate environmental concerns both due to the potential transport and dispersion by the wind and the proximity to the Zêzere River. In addition, both modified ABA and NAG test results classified the tailings samples as “potentially acid forming”. On the other hand, the high grades in W, Cu and Zn represent a possibility for profitable reprocessing of the tailings.

Several alternatives have already been considered for the Cabeço do Pião tailings deposit, but not without some drawbacks. With regard to reprocessing the tailings, the low tonnage of valuable metals in the tailings and the cost of the recovery process are the main constraints. For the environmental solutions, all alternatives will have advantages and disadvantages but the ones avoiding excavation and transport will be preferable.

After the characterization of the tailings and the reprocessing optimization process, it is necessary to go through a decision-making process, determining the pros and cons of each alternative and perform a cost- benefit analysis for each alternative.

ACKNOWLEDGMENT

This work is part of the project REMinE that was funded with public national funds from FCT under the programme for International Cooperation ERA-NET, supported by ERA-MIN (2011-2015) funded under the EU 7th Framework Programme FP7-NMP.

REFERENCES

- Ávila, P., Ferreira da Silva, E., Salgueiro, A., & Farinha, J.A. 2008. Geochemistry and mineralogy of mill tailings impoundments from the Panasqueira mine (Portugal): implications for the surrounding environment. *Mine Water and the Environment*, 27(3), 210–224.
- Black C.A. 1965. *Methods of Soil Analysis: Part II Chemical and Biological Properties*, Nº. 9 (Part 2), Second Edition, American Society of Agronomy, Madison, Wisconsin, USA, 914-926.
- Blout C. & Wolf L.C.M. 1953. Geological features of the Panasqueira tin-tungsten ore occurrence.
- Candeias C., Ávila P.F., Ferreira da Silva, E., & Teixeira, J.P. 2015. Integrated approach to assess the environmental impact of mining activities: estimation of the spatial distribution of soil contamination (Panasqueira mining area), *Environ Monit Assess* (187) 135.
- Candeias, C., Ávila, P.F., Ferreira da Silva, E., Ferreira, A., Salgueiro, A. & Teixeira, J.P. 2014. Acid mine drainage from the Panasqueira mine and its influence on Zêzere river (Central Portugal). *Journal of African Earth Sciences* (99) 705-712.
- DITR, 2007. Department of Industry, Tourism and Resources of Australia.
- D'Orey, F.C. 1967. Tungsten-tin mineralization and paragenesis in the Panasqueira and Vale da Ermida Mining Districts, Portugal, *Comunicações dos Serviços Geológicos de Portugal* (52) 117-167.
- Evangelou, V.P. & Zhang, Y.L. 1995. A review: pyrite oxidation mechanisms and acid mine drainage prevention. *Crit Rev Env Sci Technol* (25) 141-199.
- Gozzard, E., Vink S., Nanjappa, V. & Moran, C.J. 2009. Salt dissolution dynamics on surface mine spoils, *Proc. of Water in Mining*, Perth, Australia, 233-240.
- Grangeia, C., Ávila, P.F., Matias, M. & Ferreira da Silva, E. 2011. Mine tailings integrated investigations: the case of Rio tailings (Panasqueira Mine-Centre Portugal), *Eng Geol* 123 (4), 359-372.
- Holmstrom, H., Ljungberg, J., Ekstrom, M. & Ohlander, B. 1999. Secondary copper enrichment in tailings at the Laver mine, northern Sweden. *Environ. Geol* (38) 327-342.
- Huang L., Baumgartl T. & Mulligan D. 2012. Is rhizosphere remediation sufficient for sustainable revegetation of mine tailings? *Ann Bot-London* (110) 223-238.
- Kelly, W.C. & Rye, R.O. (1979). Geologic, fluid inclusion and stable isotope studies of the tin-tungsten deposits of Panasqueira, Portugal. *Economic Geology* (74) 1721-1822.
- Kim, M. & Jung, Y. 2004. Vertical distribution and mobility of arsenic and heavy metals in and around mine tailings of an abandoned mine, *J. Environ. Sci. Health*, Part A, (39) 203-222.
- Lapakko, K.A. 1992. Recent literature on static predictive tests. *Technologies for a cleaner environment*, Phoenix, AZ, February 24-27, Metallurgy, and Exploration, Inc., Littleton, CO., 109-119.
- Lapakko, K. 1993. Evaluation of Tests for Predicting Mine Waste Drainage pH. *Report to the Western Governors' Association by the Minnesota Department of Natural Resources*.
- Lawrence, R.W., Jaffe, S. & Broughton, L.M. 1988. In-House Development of the Net Acid Production Test Method, Coastech Research.
- Lawrence, R.W. 1990. Prediction of the behaviour of mining and processing wastes in the environment, in F. Doyle (ed.), *Proceedings Western Regional Symposium on Mining and Mineral Processing Wastes*. Society for Mining, Metallurgy, and Exploration, Inc., Littleton, CO., 115- 121.
- Lawrence, R.W. & Wang, Y. 1997. Determination of Neutralization Potential in the Prediction of Acid Rock Drainage, *Proc. 4th International Conference on Acid Rock Drainage*, Vancouver, BC, 449-464.
- Martin R., Dowling, K., Pearce, D.C., Florentine S., Bennet, J.W. & Stopic, A. 2016. Size-dependent characterization of historical gold mine wastes to examine human pathways of exposure to arsenic and other potentially toxic elements. *Environ Geochem Health* (38) 1097-1114.
- Miller, S., Robertson, A. & Donahue, T. 1997. Advances in Acid Drainage Prediction using the Net Acid Generation Test, *Proc. 4th Inter. Conference on Acid Rock Drainage*, Vancouver, BC, 533-549.
- Noronha, F. Doria, A., Dubessy, J. & Charoy, B. 1992. Characterization and riming of the different types of fluids present in the barren and ore veins of the W-Sn deposit of Panasqueira, Central Portugal, *Mineralium Deposita* (27) 72-79.
- Smith, K. Hageman P.L., Ramsey, C.H., Wildeman, T.R. & Ranville, F. (2006). Reconnaissance sampling and characterization of mine-waste material, *US EPA Hard Rock Mine 2006 Conference*, Tucson, Arizona, November 14-16.
- US EPA, 1994. Technical Document: *Acid Mine Drainage. Prediction*, EPA 530-R-94-036.

Characterization and Field Performance of Long-Term Settlement Behavior of a Tailings Pile

B.F.H. Foster, S.T. Parkhill, and M.D. Moriarty
Kleinfelder, Salt Lake City, Utah, USA

B.N. Lingwall
South Dakota School of Mines and Technology, Rapid City, SD, USA

ABSTRACT: This paper presents a case history describing the long-term settlement characteristics of a tailings pile being studied for potential development. As undeveloped land in urban areas becomes increasingly expensive, it is attractive to remediate and develop mine tailings piles in urban areas. One of the risks to development on tailings is the long-term settlement behavior of the tailings material as it undergoes 1) self-weight consolidation, 2) compression from desaturation, 3) micro-mechanical creep and secondary compression as the tailings age, and 4) elastic consolidation and secondary compression of the tailings material beneath new surface loads. The long-term settlement characteristics of the site were evaluated using laboratory testing, cone penetration tests, multichannel analysis of surface waves geophysical surveys, and measured settlement beneath test fills and footing load tests. The results from this investigation show tailings material exhibits complex settlement behavior and provides additional insight into the long-term compression characteristics of granular and fine-grained soils.

1 INTRODUCTION

A 270-acre site in a central location in the Salt Lake Valley, presented a great opportunity for development. The catch – the property had terrible soil conditions, with 15m of mine tailings (soft clays and loose sands) that were expected to be prone to slope failures, and large liquefaction and static settlements. Adding to these challenges, the site had serious contamination issues, a Superfund designation and major constraints that came from the capping of the site. Previous development attempts had shown this site to be un-economical for development. Building on this site was going to require a very unconventional approach.

The site (Figures 1 and 2) consists of a 270-acre Superfund site in the Salt Lake Valley, specifically in Midvale, Utah. As described by the Bureau of Reclamation (1999), Between 1906 and 1971, milling and smelting operations extracted lead, copper and zinc from crushed rock, which was then deposited as waste tailings, slurried from the mill into an evolving series of tailings ponds. The tailings and surrounding berms were extended to the west until they reached the Jordan River. At completion, the waste pile contained about 8 million cubic meters of tailings, ranging up to an 18.3m-depth along the banks of the rerouted Jordan River.

Environmental problems were first noted in 1982, when it was discovered that tailings with elevated levels of heavy metals had left the site in both windblown dust and erosion of the tailings pile by the Jordan River. In 1988, the U.S. Bureau of Reclamation (BOR) conducted studies for the Environmental Protection Agency (EPA), which resulted in the listing of the site on the National Priorities List under CERCLA. Following additional studies at the tailings site, the EPA decided to consolidate and cap the tailings. The capping solution was completed by the BOR in the fall of 1997. The goal of the cap was to prevent contact with the contaminated soils (especially arsenic and lead) and to reduce the leaching of metals into the groundwater. The tailings and contaminated soils at the 270-acre site were excavated and relocated below a combination earthfill

and three-layer geosynthetic cap. Precipitation is collected and controlled by the cap and a sub-surface drainage system. Slopes were also stabilized to prevent failures into the adjacent Jordan River. Water entering the site from the east as groundwater is collected and managed by a 7m deep interceptor trench and drain that runs along the eastern edge of the capped portion of the site. The multi-layer cap consists of soil cover, a drainage layer, a PVC liner layer and a geosynthetic clay liner (GCL).



Figure 1. The Jordan Bluffs tailing pile. Imagery copyright ©Google 2017.

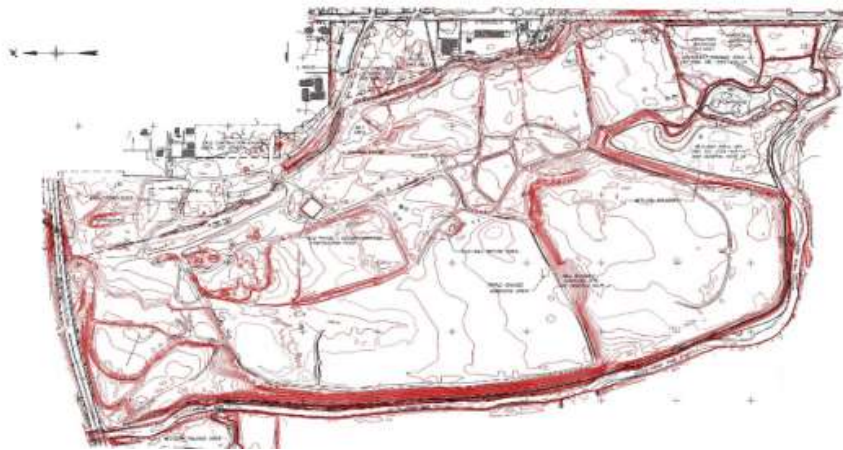


Figure 2. Layout of the ponds at the pile circa 1999 prior to capping

The requirement to preserve this cap system has combined with the geotechnical challenges on this site to make subsequent redevelopment very difficult. The nature of the tailings presents a series of geotechnical challenges, which are summarized in Figure 3. With these challenges, past attempts to re-develop the site had concluded that development was not economically feasible.

While all of these challenges are being studied and addressed, this paper will explore only the static settlement challenges.

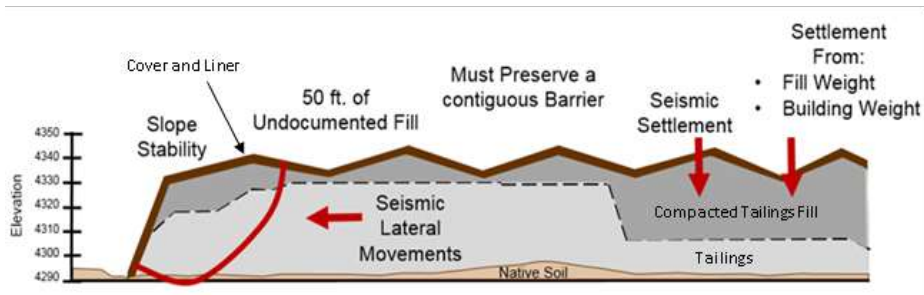


Figure 3. Typical east-west section across the pile showing various geotechnical hazards.

2 FIELD SITE CHARACTERIZATION

Explorations were conducted for a previous development attempt in 2004, consisting of limited hollow-stem auger borings, test pits, and cone penetrometer testing (CPT). Settlement calculations conducted after these explorations determined that static settlement would be a very significant issue on the site. Additional explorations, consisting of more than 50 borings and CPT were conducted on the site between 2016 and 2018. Figure 4 shows a typical north-south section within the pile, with variable soils and surface topography.

The native soils exposed near the site have been mapped as consisting primarily of lacustrine deposits to the east and alluvial deposits to the north, south, and west. The lacustrine deposits are mapped as consisting of clays and silts and the alluvial deposits are mapped as consisting of fine-grained sands and silts (Davis, 2000). The tailings consist of fine crushed rock ranging in size from medium sand to clay size. While clay minerals were generally not present, much of the finer tailings material would be classified geotechnically (Atterberg Limits and CPT) as clay. Although some of the tailings materials may be classified as clay, they have additional properties and behavior that are not typical for the local clays. These differences are very significant. For example, the tailings appear to have generated a hard, desiccated crust prior to the capping in the 1990s. Above this tailings crust in most of the site, the BOR placed compacted tailings fill, compacted to 92% Standard Proctor.

The very challenging site conditions and variability of the tailings also caused the project to investigate the use of multichannel analyses of surface waves (MASW) geophysical investigation, and ground penetrating radar (GPR). The GPR work did not prove effective, as changes in density between soft clays and loose sands were too small to provide contrasts on GPR returns. Likewise, the water contents were too similar for a difference in sounding. However, the MASW geophysical work proved very useful and has become a key element of both investigation and design.

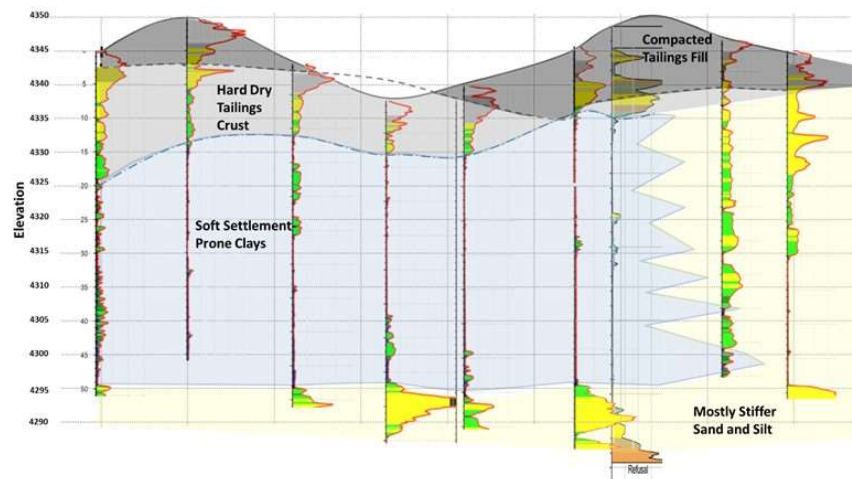


Figure 4. Typical variation in surface topography and subsurface conditions at the pile showing CPT soundings and major units.

3 LABORATORY TESTING

An initial program of geotechnical laboratory tests was performed on selected soil samples to estimate their engineering properties. Tests included conventional tests such as: Moisture Content; Minus 200 Wash; Sieve Analysis; Atterberg Limits; One-Dimensional Consolidation; Direct Shear, and Direct Simple Shear. Since the explorations and initial geotechnical laboratory testing program showed soft soil conditions where large post site fill settlements could occur, surcharging to reduce long term settlements became a leading design option for the site. To explore the potential benefits of surcharging for settlement reduction, special consolidation tests were also conducted. Special tests were needed as mine tailings are not conventional soft sediments that have deposited naturally and aged for hundreds to tens of thousands of years. Due to their young age, mine tailings undergo relatively large self-weight consolidation and creep settlements that can take decades to reach equilibrium. Additionally, as super-saturated tailings age, they drain, changing the effective stresses within the tailings which can cause additional settlements. The tailings had several decades for these various processes to occur; however, it was likely that the addition of loads from site fills would induce new settlements that would occur simultaneously with the ongoing self-weight settlement processes. Therefore, the second phase laboratory tests required very long secondary compression hold times of up to one week and multiple small unload/reload cycles to measure post-surge secondary compression using methods described in Saye et al. (2001).

Phase 2 laboratory consolidation tests showed that the Coefficient of Secondary Compression (C_{α}) of the clayey soils in the field could be greatly reduced by surcharging as long as surcharging was held to a time of 90% primary consolidation settlement (t_{90}) or greater. Laboratory tests showed that if the surcharge was held to t_{90} , a reduced post-surge coefficient is induced (C'_{α}), details are shown in Table 1. However, the laboratory testing was not able to constrain the self-weight compression or load induced creep settlements of the sandy mine tailings materials, as no undisturbed sandy tailings samples could be obtained for testing at the state the materials were deposited in. This deficiency was a prime motivation for test fills at the site. Another motivation for test fills was the fact that a small number of laboratory tests is insufficient to deal with uncertainties of the magnitude for a site of this size. In Table 1 AAOS is the Adjusted Amount of Surcharge method from Saye et al. 2001, and MPP indicated the Maximum Past Pressure (i.e., preconsolidation stress). In Table 1, OC and NC represent over and normally consolidated conditions, respectively.

Table 1. AAOS secondary compression laboratory test summary

Sample	PI	LL	w	LOG(t _s /t _r)	AAOS MMP In- crease	OC C _a /C _r	NC C _a /C _c	OC C' _a /C _a	NC C' _a /C _a
-----	%	%	%	-----	%	-----	-----	-----	-----
1	42	63	31.5	0.5	12.5	0.09	0.01	0.80	0.40
2	42	63	31.5	0.5	12.5	0.09	0.01	0.80	0.40
3	30	49	24.9	0.5	5.0	0.08	0.02	0.62	0.24
4	30	49	24.9	0.5	6.3	0.08	0.01	0.62	0.40
5	27	48	36.8	0.5	12.5	0.05	0.02	1.00	0.26
6	27	48	36.8	0.5	12.5	0.11	0.02	0.56	0.26
7	23	42	36.8	0.5	2.5	0.09	0.02	0.71	0.40
8	23	42	36.8	0.5	12.5	0.09	0.02	0.53	0.31
9	26	44	33.9	0.5	12.5	0.09	0.02	0.72	0.33
10	26	44	33.9	0.5	12.5	0.09	0.02	0.71	0.30
11	29	50	41.7	0.5	17.5	0.09	0.02	1.00	0.35
12	29	50	41.7	0.5	12.5	0.12	0.03	0.63	0.30

4 TEST FILLS

The known uncertain behaviors of mine tailings from previous project experience and the geotechnical literature, the variability seen in the geotechnical explorations and variable measurements in geotechnical laboratory testing left the engineers and owners with considerable doubt about the ability to build on the site with spread footing foundations and conventional site fills. Deep foundations were not expected to be economically viable due to the added costs associated with the environmental issues on the site (i.e. penetrating the capping liner system is expensive)..

Additionally, while the BOR has indicated that they had monitored the placement of the compacted tailings, the compaction was only to 92% Standard Proctor, and the thicknesses of the compacted tailings above the uncompacted tailings was highly variable and not clearly defined. As such, these partially compacted tailings fills (and the loose tailings below) would typically be characterized as “undocumented fill”. On most projects, this material would be removed and replaced or would be bypassed with deep foundations or ground improvement. However, on this site, deep foundations would significantly raise the cost of construction, and neither deep foundations nor 16.8m of excavate and replace would be economically viable from a development perspective.

To build on these undocumented tailings fills, observational approach based on full scale footing load tests for structures and large test fills for site grading and surcharging was required. This observational approach was performed in three phases. Phase 1 of the observational approach field test program consisted of monitoring of 4 test fills for a period of 12 years. Phase 2 consisted of constructing additional test fills at the site, and phase 3 removal of the initial (2004) test fills, and re-placing test fills at the initial (2004) test fill locations to observe reloading behaviors. Figure 5 presents a graphic detailing the concept and results of the test fill program along with the later footing load test program.

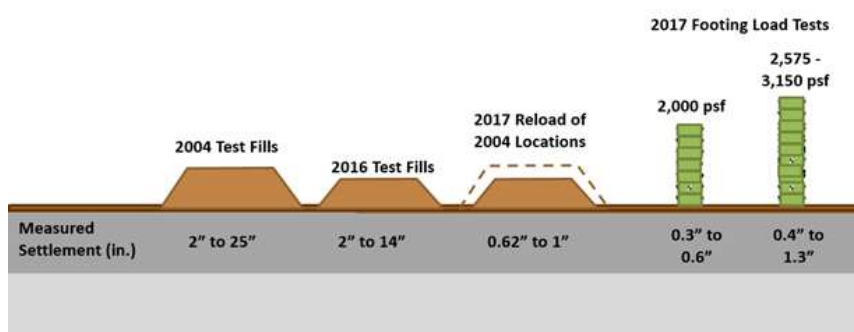


Figure 5. Timing and relative sizes of the test fills and footing load tests.

The first phase of the observational field test program began in 2004 when four test fills were constructed and monitored. These test fills were roughly 27m by 27m by 5m high. Following the end of the 2004 development attempt, these test fills remained on site until 2016, providing 12 years of settlement data and an excellent window into the static site settlement challenges. Settlements were monitored by optical surveys using benchmarks set off-site. The measured maximum settlement of the four test fills (Test Fill 2004-1, Test Fill 2004-2, Test Fill 2004-3/5, and Test Fill 2004-4) ranged from 75 to 635 mm over the 12-year monitoring period.

As pore pressure measurements were not made in any clay layers, the breakdown of settlement from self-weight processes, consolidation, elastic, and secondary compression is not known. However, the measured total settlement from these sources appears to be approximately linear on a logarithmic time scale beyond about 20 days from the time of initial load application. From this observation, we concluded that it should be possible to predict with reasonable accuracy the amount of long-term settlement that may occur from placing large fills on the site. Figure presented later in Figure 9.

For this particular site, we were interested in the settlement that would occur over a period of 30 years, which is the proposed warranty period of structures by the developer. The projected settlement of about 500 mm in 30 years is unacceptably high for any structure that would be built at this site. Therefore, we needed to consider options for reducing settlement and, if possible, reducing the amount of time required for the majority of settlement to occur. Given the undocumented nature of the fill at the site, we decided surcharging may be a viable option for both reducing settlement from fill and building foundation loads as well as reducing the spatial variability of the compression characteristics of the fill.

In addition to the large total settlements observed over 12 years in the 2004 test fills, there were two other challenges associated with settlement on the site. First, conventional settlement analyses did not provide settlement estimates that were in satisfactory agreement with measured settlement from the 2004 test fills. Also, while the CPT and lab testing described some of the soils as having clay-like behavior, an unusually large portion of the test fill settlements were atypical linear log-time creep settlements. With potential for very large long-term creep (secondary compression) settlement, the conventional approach of addressing settlement with surcharges would be difficult. Additionally, we suspected that some of the observed settlements in the 2004 test fills might have been due to site-wide self-weight processes, and thus it was possible that new surcharges would show smaller settlements.

To address these issues, Phase 2 of the exploration program was designed to evaluate settlement for the current site conditions, i.e. after the tailings had undergone an additional 12 years of consolidation and secondary compression under self-weight of the fill, and to evaluate settlement that occurs after surcharging is performed. Beginning in December of 2016, the 2004 test fills were removed. The soil from these test fills was used to construct the 4 additional test fills (Test Fill 2016-1 through -4). From the results of the 2004 test fills, we anticipated a similar log-time linear settlement trend would start to develop approximately 3 weeks after placement of the test fills and that this trend could be defined after a period of about 2 to 3 months of settlement monitoring. As such, settlement of these test fills was monitored for approximately 2 to 3 months to obtain the

trend of the linear portion of the settlement curve. Table 2 shows the measured and projected settlements from the 2016 test fills that were applied to areas not previously loaded. Soil conditions for both sets of test fills were similar.

Table 2. Test fill summary

Test Fill	Date Placed	Average Height (m)	Approximate Bearing Pressure (kPa)	Projected 30-year Settlement (mm)
2004-1	5-2004	4.39	79	305 – 635
2004-2	5-2004	4.42	80	330 – 605
2004-3/5	6-2004	4.51	81	200 – 250
2004-4	6-2004	4.60	83	50 – 75
2016-1	12-2016	3.99	79	140 – 165
2016-2	2-2017	2.68	51	50
2016-3	2-2017	3.54	65	280 – 355
2016-4	2-2017	3.55	61	75 – 100
2017-1	4-2017	3.32	60	18
2017-2	4-2017	2.44	44	25
2017-3	4-2017	2.80	50	15
2017-4	5-2017	2.87	52	25

Test Fill 2016-1 showed a maximum 12-year projected settlement of about 140 mm, which is approximately 300 mm less than the 12-year measured settlement from Test Fill 2004-1. This reduced settlement behavior was similar in all 2016 test fills near 2004 test fills. This suggests that a considerable amount of settlement measured at the 2004 test fills was composed of self-weight settlements, independent of the test fill loading and/or that the reduction in water in the tailings has changed their settlement behavior. Still, settlements observed in the 2016 test fills were excessively high for a structure that would be built at this site. After the 2016 test fills were completed, a portion of the soil was moved back to their original 2004 locations. Test fills placed in the original locations (Test Fill 2017-1 through -4 shown in Figure 9) were 1.5 to 2.5m shorter than the original test fills to ensure that the returned 2017 test fills would apply less stress than the original test fill. This was done to observe the effects surcharging would have on long-term settlement resulting from site fill and building loads. (surcharging is pre-loading an area of the site to stresses larger than the stresses resulting from final fill and footing loads)

5 FOOTING LOAD TESTS

Given the presence of the stiff tailings crust and partially compacted tailings fills, it was suspected that settlements of footings would be lower than the settlements of the test fills. With conventional settlement analyses proving unreliable, and the large site variability, would there be a way to reliably predict and confirm future footing settlements? Footing load tests (FLT) were also performed initially at eight locations across the site to answer that question. Half of the footing load tests were conducted in areas where the test fills had been placed and removed (surcharged areas) and the other half were placed in areas where no test fills had been placed. The footing load tests were conducted using 2 by 2.5 m footings, initially with a bearing pressure of 96 kPa. After stable long-term creep settlement (secondary compression) rates were obtained, the concrete blocks were moved to increase the bearing pressures to either 125 or 150 kPa. The footings were loaded using 0.6 by 0.6 by 2 m concrete blocks stacked vertically to reach the desired loading conditions. As shown in Figure 7, horizontal inclinometers were used to measure settlements. Optical survey of points on each side of the footings were used as a backup method. Figure 6 shows two of these footing load tests. Since completion of these 13 tests listed in Table 3, an additional 12 footing load tests have been conducted on other portions of the site. Very similar results were observed.

The very low settlements observed in the footing load tests suggested that it would be possible to support structures on this site with spread footings, assuming that the structure loads, bearing pressures and footing sizes were small enough to keep the loads in the site’s stiff crust (compacted tailings and/or desiccated and cemented tailings.) However, given the acknowledged difficulty in predicting settlement on this site, an alternate design method would be required.



Figure 6. Two footing load tests.

Table 3. Footing load test summary

Footing Load Test	Date Placed	Load (kPa)	Projected 30-year Settlement (mm)
FLT-1	5-2017	96	0
FLT-2	5-2017	96	10
FLT-3	6-2017	96	9
FLT-4	6-2017	96	15
FLT-5	12-2016	96	12
FLT-6	2-2017	96	13
FLT-7	2-2017	96	10
FLT-8	2-2017	96	10
FLT-5a	12-2016	125	13
FLT-7a	2-2017	125	12
FLT-8a	2-2017	125	19
FLT-1a	2-2017	150	11
FLT-6a	2-2017	150	32

6 SYNTHESIS OF THE LONG-TERM SETTLEMENT DATA

It was thought that if we could develop a method of identifying the softest areas within each building, that we might be able to test those soft areas with footing load tests, and if the settlements in all of the soft areas were small, that we might have enough confidence to use the footing load test results as the methodology to establish allowable bearing pressure in each building. Thus immediate settlement, consolidation settlements, and long-term secondary and creep settlement could all be accounted for at each building location reliably. To identify soft spots, we compared geophysical test results (shear wave velocity profiles from MASW surveys conducted with closely spaced geophones) with CPT testing and the footing load test results. MASW and CPT testing was conducted at each FLT location, as shown in Figure 7. A sample comparison is shown in Figure 8. As can be seen, there was a good correlation between material behavior soil classifications from the CPT and the shear wave velocities measured by the MASW testing.

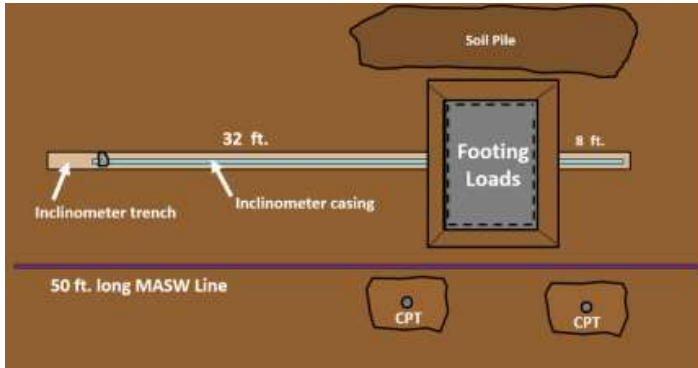


Figure 7. Layout of instrumentation, subsurface explorations, and footing load tests.

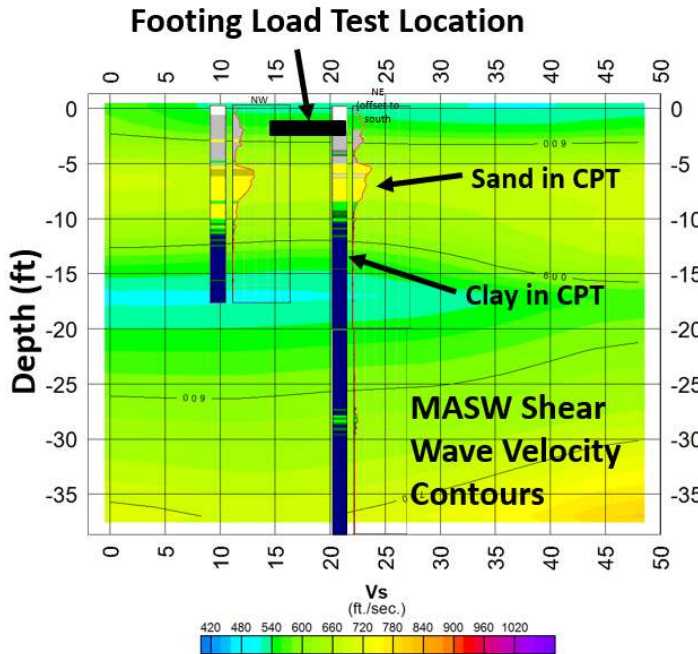


Figure 8. Comparison of CPT and MASW Testing at Footing Load Test #3.

We also compared the footing load test settlement behavior with the CPT and MASW test results. We believed that shear wave velocity might be an indication the stiffness of the crust, and therefore relate to the settlements of footings on the crust. As shown in Figure 9, there was a good relationship between the MASW indication of subgrade stiffness (V_s) and load test performance. That is, increases in loading on low shear wave velocity soils resulted in greater settlements, and lower settlements were observed when the upper part of the crust demonstrated high shear wave velocities.

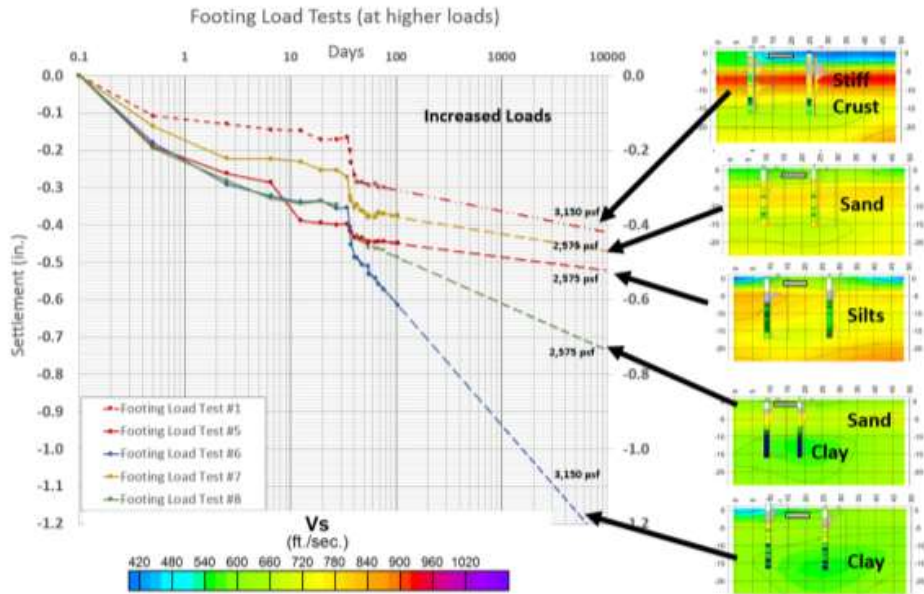


Figure 9. Footing Load Test settlement data for select footing tests along with MASW contours of Shear Wave Velocity at the location of the respective footing load tests.

To control settlements to acceptable levels, a variety of measures have been proposed. These measures include surcharging and minimizing grade raises through careful site planning. Based on site history and soil explorations, the site was zoned into areas of low to highest risk (Figure 10). Locations with minimal clay tailings are examples of low risk, while areas with 50-feet or more of clay tailings are categorized with high to very high risk. Areas of highest risk will likely receive no structures or have structures founded on deep foundations if economically viable.

Level of Risk/Challenge	Lowest	Lower	Moderate	High	Higher	Highest
Soil Support	24' to 38' of Compacted Tailings	8' to 32' Compacted Tailings	5' to 20' of Compacted Tailings and Stiff Soils over Alternating Sands/silts/clays	5' to 20' of Compacted Tailings and Stiff Soils over Alternating Sands/silts/clays (more clay)	5' to 20' of Compacted Tailings and Stiff Soils over Thick Clays	Thick uncompacted Tailings, 50' or more of clay tailings
Challenge	Potential Buried Trees	No Explorations	Settlement of Tailings From Grade Raises			Varies. Example: buried trees
Potential Mitigation	Site Standard *	Site Standard *	Site Standard *	<ul style="list-style-type: none"> - Taller and longer surcharge, - Reduce grade raises further, - Office buildings on piles - Site Standard* 	<ul style="list-style-type: none"> - Pile Support, - Warehouses w. adjustable structural features, - Site Standard* 	

* Site Standard Mitigation: Minimize grade raises, keep footings up in stiffer crust, surcharge.

Figure 10. Risk matrix to be used in conjunction with building specific CPT and MASW.

7 CONCLUSIONS

Successful (economically viable) development of this 270-acre mine tailings Superfund site has required breaking with traditional design approaches. That is, since traditional test borings/lab testing/settlement prediction and design was not producing accurate estimates of site behavior, an alternate approach needed to be developed.

We have found that a site that was once very soft and prone to large settlements at the ground surface is now covered by a crust composed of stiff tailings and tailings fill. It is thought that the stiff tailings and tailings fill are a result of self-weight consolidation, desiccation, and cementation of the tailings from the calcium and magnesium carbonate components in the tailings material.

Contrary to conventional wisdom, we have found that conventional spread footing foundations can be used for development of this site without generating unacceptably large settlements. We also found that MASW shear wave velocity profiles can be used to identify relatively soft areas within a building footprint and to help predict footing settlement behavior.

The results of this investigation suggest that test fills and footing load tests could be used efficiently on other similar projects. While the initial cost of obtaining the concrete dead weight blocks was relatively high, reuse of these blocks greatly reduces costs of subsequent tests.

8 REFERENCES

- Bureau of Reclamation (BOR), 1999, Sharon Steel/ Midvale Tailings Operational Unit No. 1, Remedial Action.
- Davis, D.D. 2000. Geologic Map of the Midvale Quadrangle, Salt Lake County, Utah, UGS Map 177, Scale 1:24,000
- Saye, S.R., Ladd, C.C., Gerhardt, P.C., Pilz, J., and Volk, J.C. 2001. Embankment Construction in and Urban Environment: the Interstate I15 Experience, in Foundations and Ground Improvement, *ASCE Geotechnical Specialty Publication No. 113*, Virginia Tech, 842-857.

Compression Behavior of Filtered Tailings and Waste Rock Mixtures: GeoWaste

C.A. Bareither, M.H. Gorakhki, and J. Scalia
Colorado State University, Fort Collins, Colorado, USA

M. Jacobs
Goldcorp Inc., Vancouver, BC, Canada

ABSTRACT: The focus of this study was to evaluate the compression behavior of fast-filtered tailings and waste rock mixtures (i.e., GeoWaste). Tailings and waste rock were collected from two hard rock mines; one-dimensional (1D) compression tests were conducted on unsaturated tailings and GeoWaste, and 1D consolidation tests were conducted on inundated tailings and GeoWaste. GeoWaste was prepared to mixture ratios of 0.4 and 1.0 (R_t = total mass of waste rock / total mass of tailings), which represented tailings-dominated mixtures with waste rock acting as inclusions. In general, compressibility of GeoWaste was lower than pure tailings. However, compressibility of the tailings fraction in GeoWaste was comparable to pure tailings. Unsaturated GeoWaste evaluated in constant strain rate (CSR) compression tests (strain rate \approx 3 mm/hr) did not exhibit positive pore pressure until the vertical stress surpassed 400 kPa for the mixture prepared at $R_t = 0.4$ and no positive pore pressure was measured for the $R_t = 1.0$ mixture up to a vertical stress of 1630 kPa (maximum applied). Measurements from CSR compression tests were used to estimate stacking heights of GeoWaste in potential full-scale operations considering continuous material deposition. Stress conditions at the end of the CSR compression tests corresponded to stack heights of approximately 73 m for GeoWaste prepared at $R_t = 0.4$ and 75 m for GeoWaste prepared at $R_t = 1.0$.

1 INTRODUCTION

Standard mine waste management corresponds to storing tailings and waste rock in separate locations. Although this practice has a proven track record, waste rock piles can be susceptible to acid rock drainage (ARD) and tailings storage facilities (TSFs) are susceptible to failure (Blight 2009). The high-permeability of waste rock allows ingress of atmospheric oxygen and precipitation, which can lead to ARD when sulfide-rich minerals are present in the waste rock. The loose, contractive, nature of slurry-deposited mine tailings can lead to low shear strength and potentially liquefiable materials under rapid vertical loading (static liquefaction) and/or seismic loading (dynamic liquefaction), which has resulted in an unacceptable number of TSF failures over the last century (Azam and Li 2010). Co-disposal of waste rock and tailings (WR&T) has been evaluated as an alternative mine waste management technique to address ARD concerns in waste rock piles and low shear strength / liquefaction concerns in TSFs. Although various WR&T co-disposal techniques have been considered and evaluated at the research level (Williams et al. 2003; Wickland et al. 2006; Bussi re 2007), the challenge of scaling mixture processes from laboratory to the field has hindered subsequent development.

Blending of fast-filtered tailings (i.e., water content \approx 3% higher, by weight, than common filtration processes) and waste rock in a tailings-dominated mixture, referred to as GeoWaste, is an innovative co-disposal approach to mine waste management. The vision of GeoWaste is to

create a material that facilitates placement in deposits that are geotechnically and geochemically stable, and does not require dams or embankments necessary in TSFs constructed for slurry-deposited tailings. The addition of waste rock to fast-filtered tailings is anticipated to improve shear strength and reduce liquefaction potential of the tailings, which promotes geotechnical stability. Blending GeoWaste as a tailings-dominated mixture is envisioned to encapsulate potentially acid-generating waste rock in tailings to inhibit the ingress of oxygen and mitigate ARD potential, which promotes geochemical stability.

A key benefit to GeoWaste is the potential to blend and transport the material on conventional conveyor systems, which allows scaling-up the technology to mines with high generation rates of waste rock and tailings (e.g., > 100,000 Mg/d). Placement of GeoWaste is envisioned as aggrading stacks, constructed via direct disposal at the end of the conveyor system. Thus, an important geotechnical consideration for GeoWaste is compressibility. The stacking process will rapidly increase vertical stress via continuous material placement, and the construction of subsequent lifts will increase vertical stress on previously deposited material.

The goal of this study was to evaluate the compressibility of GeoWaste. Key objectives of the laboratory testing carried out for this study were to (1) compare compressibility of tailings and GeoWaste, (ii) evaluate pore water pressure development during continuous compression, and (iii) estimate potential stress, pore pressure, and unit weight within a GeoWaste deposit. The first objective was assessed via compression tests on pure tailings and GeoWaste mixtures. The second objective was assessed via constant strain rate compression tests on GeoWaste. Results from the constant strain rate compression tests were used to estimate potential stress, pore pressure, and unit weight profiles for full-scale GeoWaste deposits.

2 BACKGROUND

The mixture ratio (R_t) of WR&T is defined as the ratio of total mass of waste rock over total mass of tailings. Schematics of particle arrangements in pure waste rock, pure tailings, and potential WR&T mixtures are shown in Figure 1. A waste rock-dominated mixture corresponds to waste rock particles that are in contact and not all void space between waste rock particles are filled with tailings (Figure 1-b). At the opposite end of the spectrum, a tailings-dominated mixture (e.g., GeoWaste) corresponds to waste rock particles that act as inclusions (i.e., are floating) in a tailings matrix (Figure 1-d). The mixture ratio corresponding to a state in which waste rock particles retain particle-to-particle contacts and all void space between waste rock particles are filled with tailings is called the optimum mixture ratio ($R_{t,opt}$, Figure 1-c). In general, strength and compressibility of mixtures at $R_t \geq R_{t,opt}$ are controlled by the waste rock, whereas hydraulic behavior of mixtures at $R_t \leq R_{t,opt}$ are controlled by the tailings (e.g., Wickland et al. 2006). Furthermore, the presence of waste rock particles in tailings-dominated mixtures ($R_t \leq R_{t,opt}$) has been shown to enhance shear strength and aid in transitioning shear behavior from contractive to dilative tendencies (e.g., Jehring and Bareither 2016; Hamade and Bareither 2018).

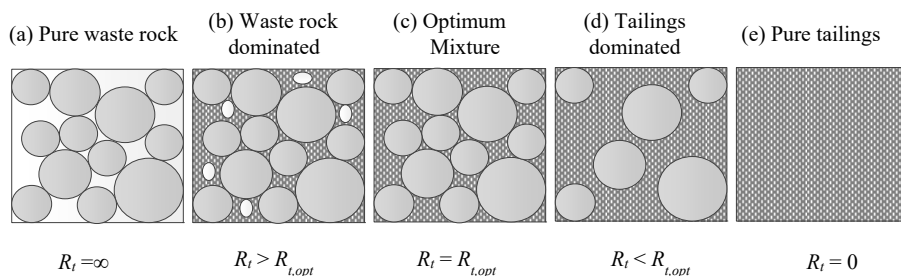


Figure 1. Schematics of waste rock and tailings mixture at different mixture ratios (R_t) (adapted from Wickland et al. 2006).

The compressibility of WR&T mixtures was evaluated in Wickland et al. (2006) and Wickland and Wilson (2005). Wickland et al. (2006) compared the compressibility of slurry mine tailings (fines content = 96%, liquid limit = 50.2%, and water content = 95% to 107%), waste rock (gravel content = 80%, maximum particle diameter, $d_{max} = 50$ mm), and WR&T mixtures prepared at R_t . Test specimens were 300 mm in diameter and 180 mm in height and compressed to stresses ranging from 10 to 320 kPa. The compression indices (C_c) of tailings ranged between 0.53 and 1.87 and the C_c of waste rock ranged between 0.005 and 0.090. The C_c of WR&T mixtures at R_t ranged between 0.016 and 0.073, which indicated that WR&T compression behavior was controlled by the waste rock.

Wickland and Wilson (2005) evaluated the compressibility of WR&T mixtures under self-weight in 1-m-diameter by 6-m-tall columns. Mixtures of WR&T were prepared at three different mixture ratios with $R_t > R_{t,opt}$. A total settlement of approximately 5% was reported for WR&T mixtures after 100 days, which was comparable to settlement measured in a column with pure waste rock (7.5%) and less than settlement predicted in pure tailings ($\approx 20\%$). Moreover, they reported that the coefficient of consolidation in WR&T mixtures was one order of magnitude larger than pure tailings, which suggested that WR&T mixtures settled faster due to more rapid dissipation of excess pore water pressure compared to pure tailings. These past studies focused on compressibility of WR&T mixtures at $R_t > R_{t,opt}$ indicate that compression behavior was controlled by the waste rock.

3 METHODS AND MATERIALS

3.1 Materials

Mine tailings (T) and waste rock (WR) were collected from two mines: Mine P and Mine M. Specific materials evaluated included Mine P tailings (P-T), Mine M tailings (M-T), Mine P GeoWaste (P-GW), and Mine M GeoWaste (M-GW). GeoWaste was prepared at $R_t = 0.4$ for Mine M mine waste and $R_t = 0.4$ and $R_t = 1.0$ for Mine P mine waste. These GeoWaste mixtures both coincided with $R_t < R_{t,opt}$ (Figure 1-d), which were tailings-dominated mixtures with waste rock particles acting as inclusions within the tailings matrix.

3.1.1 Mine Tailings

Geotechnical characterization of mine tailings included mechanical sieve and hydrometer (ASTM D422), Atterberg limits (ASTM D4318), and standard-effort compaction (ASTM D698). Characteristics of M-T and P-T are summarized in Table 1. The higher fines content and clay-size content (particle size < 0.002 mm) of M-T relative to P-T coincided with higher plasticity (liquid limit, LL , and plasticity index, PI). Tailings from Mine M classified as low plasticity clay (CL), whereas tailings from Mine P classified as low plasticity silt (ML).

Compaction tests were conducted on tailings in a 101.6-mm-diameter mold to determine the optimum water content (w_{opt}) and maximum dry density (ρ_{d-max}). The w_{opt} and ρ_{d-max} for M-T and P-T are reported in Table 1. Mine M and Mine P tailings were sealed in buckets at the mine sites after a fast-filtration process, which removed water under a more rapid process than in a typical filter plant that generates filtered tailings. The higher w_{opt} and as-received water content for M-T compared to P-T were attributed to the higher plasticity of M-T that corresponded to a higher propensity for moisture retention. In addition, the as-received water contents of both materials reflect the fast-filtering process, which produces filtered tailings with higher water contents than conventional filtration procedures (e.g., $\approx 3\%$ higher water content, by weight).

3.1.2 Waste Rock

Geotechnical characteristics of M-WR and P-WR are summarized in Table 1. All waste rock samples were passed through a 76.2-mm screen during sampling at the mines. Mine M waste rock contained 40% sand and fines, whereas, the sand and fines content was negligible in P-WR ($< 3\%$). The M-WR classified as gravel with silt (GM), whereas P-WR classified as poorly

graded gravel (GP). The as-received water content of M-WR was 5.8% and P-WR was 2.2%. The higher as-received water content for Mine M waste rock was attributed to the higher fines content of the material (Table 1) and wetter climate of the mine.

3.2 Methods

One-dimensional compression tests were performed in conventional fixed-ring consolidation cells on pure tailings in accordance with ASTM D2435. All tailings specimens were prepared at the as-received water content (Table 1) in consolidation rings with an inside diameter of 63.5 mm and height of 25 mm. Specimens were compacted in three equal layers to obtain a uniform density, and subsequently inundated with tap water, which yielded saturation > 95%. Consolidation rings containing the tailings specimens were placed in oedometers and low-weight porous disks were placed on top of the specimens. Vertical deformation was recorded using linear potentiometers and pore water pressure was measured using pressure transducers. Vertical loads were applied incrementally every 24 hr following Method A in ASTM D2435.

Table 1. Summary of physical characteristics for tailings and waste rock from Mine M and Mine P.

Material	M-T	P-T	M-WR	P-WR
Liquid limit, LL (%)	30.1	20.9	NA	NA
Plasticity index, PI (%)	9.2	1.3	NA	NA
Unified soil classification	CL	ML	GM	GW
Gravel content (%)	0	0	59.1	95.1
Sand content (%)	14.3	35.8	26.5	2.8
Fines content (%)	85.7	64.2	14.4	2.1
Clay-size content ($d_{max} < 2$ mm) (%)	23.6	17.4	NA	NA
As-Received Water Content (%)	21.5	20.3	5.8	2.2
Optimum water content, w_{opt} (%)	15.8	14.2	NM	NM
Maximum dry density, ρ_{d-max} (Mg/m ³)	1.69	1.82	NM	NM

Notes: NA = not applicable; NM = not measured

Constant stress consolidation tests were performed on P-GW and M-GW at $R_t = 1.0$. The GeoWaste specimens were prepared by hand-mixing tailings and waste rock at the as-received water contents. GeoWaste specimens were 300 mm in diameter and 150 mm tall, and were compacted in the consolidation cell to a target total density of 1.9 Mg/m³ in five layers. Waste rock was sieved to $d_{max} \leq 50$ mm such that the specimen diameter to maximum particle size ratio was six. Tap water was permeated through the specimen (from the bottom up) prior to loading until the ratio of outflow volume to inflow volume ranged between 0.9 and 1.1. During vertical loading, drainage was allowed at the top of the specimen, whereas drainage was prevented at the bottom of the specimen as drainage lines were connected to a pressure transducer. Loading was applied incrementally using a 300-mm diameter air cylinder to a maximum load of 50 kN. The vertical load was measured using an S-type load cell and deformation was measured using a linear potentiometer connected to a PC with LabVIEW software. Although the pressure transducer indicated that pore pressure dissipated within the first few minutes, specimens were allowed to compress under each vertical load for 24 hr.

Constant strain rate (CSR) compression tests were performed on GeoWaste in a 380-mm-diameter compression cell with a constant rate of vertical strain ≈ 3 mm/hr. Waste rock was sieved to $d_{max} \leq 64$ mm and mixed with mine tailings in a concrete mixer for 30 min. GeoWaste specimens were compacted in five, 30-mm-thick layers to obtain a uniform density. The ratio of specimen diameter to height was kept constant ($D/H = 2.5$) between the large-scale compression tests and conventional oedometer tests. High strength porous disks that did not deform under loading were used on the top and bottom of specimen. Load was applied with an Applied Test

System load frame to maximum vertical load of 200 kN. Three pressure transducers were installed at the bottom of the compression cell. Two pressure transducers had a maximum pressure rating of 700 kPa and one pressure transducers had a maximum pressure rating of 200 kPa to obtain more accurate measurements at lower pressures.

4 RESULTS

4.1 Tailings Consolidation

Relationships of void ratio (e) versus vertical effective stress (σ'_v) for pure tailings are shown in Figure 2. Tailings from Mine P were prepared at dry densities (ρ_d) of 1.24 and 1.48 g/cm³ and tailings from Mine M were prepared at $\rho_d = 1.22$ g/cm³. The compression indices (C_c) of pure tailings ranged between 0.20 and 0.31, which were within the range of C_c ($0.06 < C_c < 0.40$) reported for tailings by Qiu and Sego (2001). In general, M-T was more compressible compared to P-T, which was due to the higher fines content, clay content, and plasticity of M-T (Table 1).

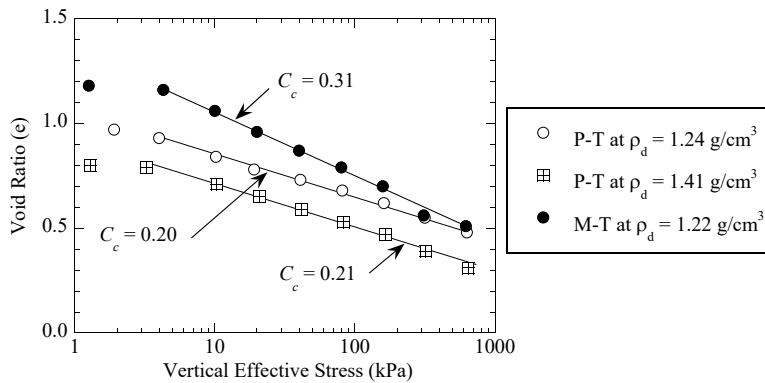


Figure 2. Relationships of void ratio versus vertical effective stress for consolidation tests conducted on pure tailings. Compression indices (C_c) were determined via least squares regression though all data points except the lowest value of effective stress.

4.2 GeoWaste Consolidation

Relationships of e versus σ'_v for M-GW and P-GW at $R_t = 1.0$ are shown in Figure 3. Void ratios for the bulk GeoWaste specimens were computed as a global void ratio, which was the ratio of void volume to total solid volume (i.e., waste rock + tailings solid volume). The e - σ'_v relationships from M-T and P-T are reproduced in Figure 3 for comparison. The C_c of GeoWaste were 0.06 for M-GW and 0.11 for P-GW, which were smaller than C_c of pure tailings. This comparison suggests that the addition of waste rock to tailings in a tailings-dominated structure ($R_t < R_{t,opt}$) reduced compressibility of the mixture. These results are in agreement with findings by Wickland et al. (2006) on co-mixed WR&T; however, Wickland et al. (2006) reported approximately one order of magnitude lower C_c for WR&T in comparison with pure tailings. The more pronounced difference in C_c reported by Wickland et al. (2006) was attributed to WR&T mixed at $R_t = R_{t,opt}$, whereby waste rock particles were in contact with each other to create a more rigid waste rock skeleton throughout the waste mixture. Thus, the extent of reduced compressibility of waste rock and tailings mixtures (e.g., GeoWaste) depends on the amount of waste rock inclusions within the mixture.

Two possible mechanisms were identified that could reduce compressibility of GeoWaste in comparison with pure tailings: (i) the inclusion of waste rock particles reduced the volume of compressible material in the mixture (i.e., tailings); or (ii) contacts existed between waste rock

particles to create pockets of tailings surrounded by a waste rock skeleton that prevented compression of trapped tailings. To investigate these potential mechanisms and the compression behavior of GeoWaste, the tailings fraction within the GeoWaste was isolated and assessed. The tailings fraction void ratio (e_t) in GeoWaste was computed as

$$e_t = \frac{V_V}{V_{S-T} - V_{S-R}} \quad (1)$$

where V_V is the void volume, V_{S-T} is the total solid volume (i.e., tailings and waste rock), and V_{S-R} is the volume of waste rock solid particles.

Relationships of e_t in the GeoWaste specimens versus σ'_v are shown in Figure 3. The C_c of GeoWaste, pure tailings, and tailings fraction in the GeoWaste were 0.11, 0.20, and 0.25, respectively, for mine waste from Mine P (Figure 3-a). The C_c of GeoWaste, pure tailings, and tailings fraction in the GeoWaste were 0.06, 0.27, and 0.19, respectively, for mine waste from Mine M (Figure 3-b). The C_c for pure tailings and the tailings fraction within GeoWaste were more comparable relative to the correlation between pure tailings and the global void ratio of GeoWaste. Closer comparison between C_c of pure tailings and the tailings fraction in GeoWaste suggests the waste rock particles acted as inclusions within the tailings matrix such that compression behavior of GeoWaste was controlled by the tailings fraction. In addition, the close comparison of e for pure tailings and e_t (Figure 3) implies that loose pockets of tailings within the GeoWaste specimens did not exist. Loose pockets of tailings in GeoWaste would lead to abnormally high e_t and e_t - σ'_v relationships that do not agree with e or e - σ'_v for pure tailings, neither of which was observed in compression data shown in Figure 3.

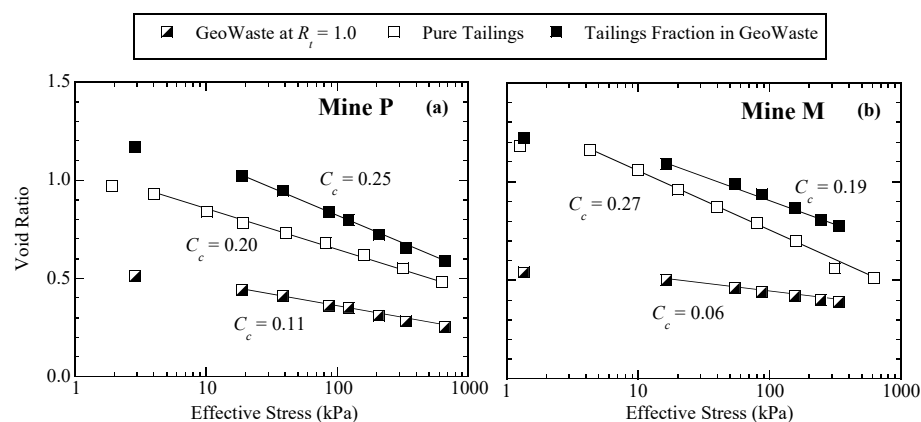


Figure 3. Relationships of void ratio versus vertical effective stress for GeoWaste specimens at $R_f = 1.0$, pure tailings, and tailings fraction in the GeoWaste for (a) Mine P and (b) Mine M.

4.3 GeoWaste Unsaturated Compression

Results from the CSR compression tests on unsaturated GeoWaste from Mine P are shown in Figure 4 as relationships of vertical strain, degree of saturation, and bulk density versus total vertical stress (σ'_v). The σ'_v was not plotted because specimens were prepared at their as-received water content such that saturation initially was less than 100% and suction was not measured. Thus, the actual magnitude of σ'_v was not known for the unsaturated GeoWaste specimens. However, σ'_v could be estimated as the equivalent of σ_v prior to saturation, and once specimens reached 100% saturation as σ_v less the measured pore pressure.

Minor vertical deformation was measured in the GeoWaste specimen prepared at $R_f = 0.4$ for $\sigma_v < 10$ kPa and for the GeoWaste specimen prepared at $R_f = 1.0$ for $\sigma_v < 50$ kPa. The limited compression at low σ_v was attributed to compaction-induced over consolidation developed during specimen preparation. Subsequent increase in σ_v for both GeoWaste specimens resulted in a

nearly constant rate of vertical strain as a function of logarithm of σ_v (Figures 4-a and 4-b). During the constant accumulation of vertical strain, porosity decreased and bulk density increased in both GeoWaste specimens (Figures 4-e and 4-f).

The relationships of saturation in Figures 4-c and 4-d indicate that 100% saturation was reached in the $R_t = 0.4$ GeoWaste at $\sigma_v \approx 155$ kPa, whereas 100% saturation was reached in the $R_t = 1.0$ GeoWaste at $\sigma_v \approx 1190$ kPa. Saturation in both specimens was computed based on weight-volume relationships under the assumption that all vertical compression corresponded to void volume reduction of the air phase prior to 100% saturation. A higher degree of saturation was achieved in the $R_t = 0.4$ GeoWaste since the initial water content of that specimen was higher based on the larger tailings fraction and preparing the mixtures at the as-received water contents of each fraction (Table 1). Furthermore, the lower waste rock content of the $R_t = 0.4$ GeoWaste led to a more compressible material relative to the $R_t = 1.0$ GeoWaste, which coincided with larger vertical strain and higher bulk density at lower σ_v . Regardless of variations in compressibility, at the end of loading both specimens were 100% saturated with similar bulk density (≈ 2.32 Mg/m³).

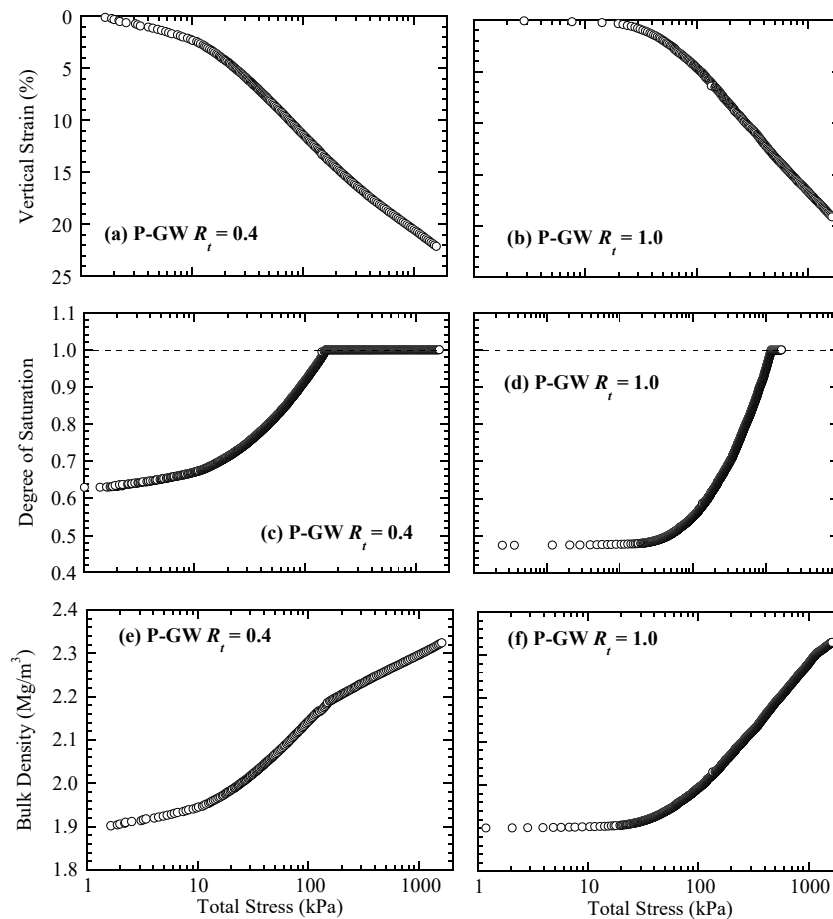


Figure 4. Constant strain rate compression relationships for Mine P GeoWaste: vertical strain versus total stress for (a) $R_t = 0.4$ and (b) $R_t = 1.0$, degree of saturation versus total stress for (c) $R_t = 0.4$ and (d) $R_t = 1.0$, and bulk density versus total stress for (e) $R_t = 0.4$ and (f) $R_t = 1.0$.

Temporal relationships of σ_v and pore water pressure measured during the CSR compression tests on both GeoWaste specimens are shown in Figure 5. Pore pressure monitored by all three pressure transducers was plotted for both compression specimens. A pore water pressure measurement of zero was recorded for the GeoWaste specimen prepared at $R_t = 1.0$ during the entire compression test as σ_v increased to ≈ 1630 kPa, which indicated that positive pore pressure did not develop during compression. The GeoWaste specimen prepared at $R_t = 0.4$ exhibited positive pore pressure when σ_v reached and exceeded approximately 400 kPa. The saturation trend in Figure 4-c indicated 100% saturation was reached at $\sigma_v \approx 155$ kPa in the $R_t = 0.4$ GeoWaste. The 100% saturation and lack of positive pore pressure measured between $\sigma_v \approx 155$ kPa and 400 kPa could be attributed to a combination of factors: (i) drainage occurred at the top of the specimen to dissipate pore pressure; (ii) additional void space existed at boundaries between the specimen and compression cell that occupied water; and/or (iii) minor errors existed in the weight-volume calculations. Regardless of the factors contributing to the difference between saturation and pore water pressure, the positive pore pressure in the $R_t = 0.4$ GeoWaste at the end of the CSR experiment indicated that the specimen was completely saturated.

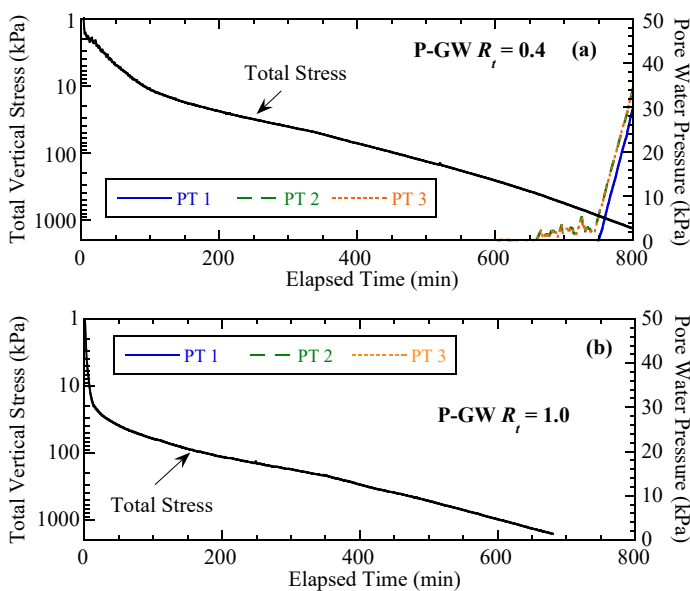


Figure 5. Temporal relationships of total vertical stress and pore water pressure from constant strain rate compression tests on Mine P GeoWaste specimens prepared to mixture ratios of (a) $R_t = 0.4$ and (b) $R_t = 1.0$. Note: PT = pressure transducer.

4.4 Assessment of Stress and Unit Weight in a GeoWaste Stack

A critical attribute to the full-scale viability of GeoWaste is the ability to blend and transport the material on a conveyor system. Placement of GeoWaste is envisioned to occur via direct disposal at the end of the conveyor system such that the material is placed to designed stack heights. An assessment of σ_v , pore pressure, and total unit weight (γ_t) as a function of depth within a potential GeoWaste stack was conducted via vertical deformation, σ_v , and pore pressure measurements made in the CSR tests.

The total unit weight of GeoWaste (γ_{ti}) corresponding to a given increment of applied total stress (σ_{vi}) in the CSR test was computed as

$$\gamma_{ti} = \frac{W_T}{V_T - (\Delta H_i \cdot A)} \tag{2}$$

where W_T = total initial specimen weight, V_T = total initial specimen volume, A = cross-sectional area of the specimen, ΔH_i = incremental vertical settlement, and i corresponds to σ_{vi} computed between subsequent measurements made during the CSR test. An assumption made in Eq. 2 was that W_T of the GeoWaste remained constant during the CSR test (i.e., there was no loss of solid or liquid mass). The depth in a GeoWaste deposit during continuous stacking at the end of a conveyor system was then computed as

$$Depth = \sum_{i=1}^n \frac{\Delta \sigma_{vi}}{\gamma_{ti}} \tag{3}$$

where n corresponds to the number of measurements made during the test. The laboratory CSR data were used to estimate depth in a GeoWaste stack based on the assumption that the relationship between σ_v and ρ (or γ) determined from the CSR test (e.g., Figure 4-e and 4-f) was representative of the anticipated relationship between σ_v and ρ (or γ) in a full-scale GeoWaste deposit. Thus, vertical layers in a full-scale GeoWaste deposit were represented by incremental stress and unit weight in the CSR tests (i.e., n combinations of σ_{vi} and γ_{ti}). Finally, pore pressure measured in the CSR test corresponding to a given value of applied σ_v were connected to specific depths in the GeoWaste stack that corresponded to the same σ_v .

Vertical profiles of σ_v , γ_t , and pore pressure as a function of depth in GeoWaste during continuous stacking are shown for GeoWaste from Mine P prepared at $R_t = 0.4$ and $R_t = 1.0$ in Figure 6. Total thickness of the GeoWaste stack at the end of the CSR test was estimated to be 73 m for $R_t = 0.4$ and 75 m for $R_t = 1.0$. Considering that positive pore pressure was not measured in the CSR test on the $R_t = 1.0$ GeoWaste, no pore pressure profile is shown in Figure 6-b. The average pore water pressure measured from the three pressure transducers in the CSR test on the $R_t = 0.4$ GeoWaste was plotted in Figure 6-a. The first positive pore pressure measurement was 0.01 kPa and is plotted at a depth of 18.8 m, which corresponds to $\sigma_v \approx 400$ kPa. The pore pressure at the maximum depth of the GeoWaste stack (73 m) was approximately 45 kPa and corresponded to $\sigma_v \approx 1630$ kPa.

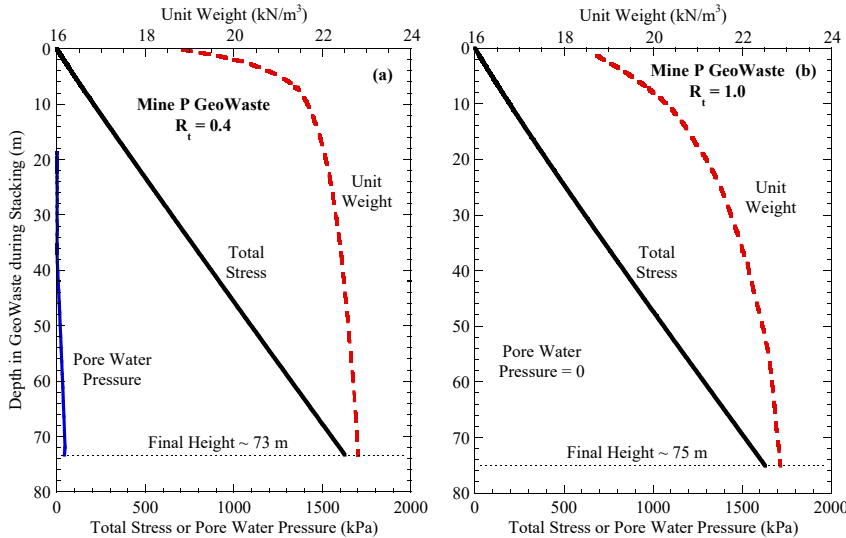


Figure 6. Estimated vertical profiles of unit weight, total stress, and pore pressure as a function of depth in a GeoWaste deposit during continuous stacking based on results from constant strain rate compression tests on GeoWaste from Mine P prepared at mixture ratios of (a) $R_t = 0.4$ and (b) $R_t = 1.0$.

The pore pressures plotted in Figure 6-a for the $R_t = 0.4$ GeoWaste are low, but indicate that a considerable portion of the GeoWaste deposit would be 100% saturated during continuous material placement. The magnitude of saturation and pore pressure within the CSR tests were a function of the tailings water content, which may vary (lower or higher) during field operations. The CSR tests appear to be a useful tool to extrapolate laboratory measurements to potential field conditions, but need to be validated via stress and pore pressure measurements made during actual material deposition.

5 SUMMARY AND CONCLUSIONS

The overall objective of this study was to evaluate the compressibility of GeoWaste, which is a mixture of fast-filtered mine tailings (i.e., $\approx 3\%$ higher water content, by weight, compared to conventional filtration processes) and waste rock prepared as a tailings-dominated mixture. Incremental loading compression tests were conducted on tailings and GeoWaste to compare compressibility of the two materials. Constant strain rate (CSR) compression tests were conducted on GeoWaste to assess pore water pressure development during continuous compression and estimate potential profiles of total vertical stress (σ_v), pore pressure, and total unit weight (γ_t) as a function of depth within a full-scale GeoWaste deposit. The following observations and conclusions were drawn from this study.

- The compression index (C_c) of GeoWaste was less than the C_c of pure tailings when C_c for GeoWaste was computed as a function of the global void ratio. However, when C_c was computed based on void ratio of the tailings fraction within GeoWaste, the C_c of GeoWaste was comparable to the C_c of pure tailings. The lower compressibility of GeoWaste relative to pure tailings was attributed to the presence of non-compressible waste rock particles that acted as inclusions in the mixture (i.e., adding waste rock decreased compressibility).
- Saturation of GeoWaste in the CSR compression tests was computed based on weight-volume relationships and revealed that 100% saturation was reached in GeoWaste prepared at $R_t = 0.4$ at $\sigma_v \approx 155$ kPa, whereas 100% saturation was reached in GeoWaste prepared at $R_t = 1.0$ at $\sigma_v \approx 1190$ kPa. Weight-volume relationships for both specimens indicated similar bulk densities were reached at the end of loading (≈ 2.32 Mg/m³).
- Positive pore pressure was not measured in the CSR test on GeoWaste prepared at $R_t = 1.0$ when σ_v increased to 1630 kPa. However, positive pore pressure was measured in the CSR test on GeoWaste prepared at $R_t = 0.4$ when σ_v reached and exceeded ≈ 400 kPa.
- A GeoWaste stacking assessment was conducted on results from the CSR tests to assess potential depth profiles of σ_v , pore pressure, and γ_t based on anticipated continuous material deposition for full-scale implementation. End-state conditions of the CSR test on GeoWaste prepared at $R_t = 0.4$ corresponded to a stack height of approximately 73 m, whereas a stack height of approximately 75 m was computed for GeoWaste prepared at $R_t = 1.0$.

ACKNOWLEDGMENTS

Financial support for this study was provided to Colorado State University by Goldcorp Inc. and the National Science Foundation (CMMI #1538344). The opinions, findings, conclusions, or recommendations expressed herein are those of the authors and do not necessarily represent the views of the Goldcorp Inc., National Science Foundation, or Colorado State University.

REFERENCES

- ASTM D422-63e2. (2007). *Standard Test Method for Particle-Size Analysis of Soils* (Withdrawn 2016), ASTM International, West Conshohocken, PA.

- ASTM D698-12e2. (2012). *Standard Test Methods for Laboratory Compaction Characteristics of Soil Using Standard Effort* (12 400 ft-lbf/ft³ (600 kN-m/m³)), ASTM International, West Conshohocken, PA.
- ASTM D2435-11 (2011). *Standard Test Methods for One-Dimensional Consolidation Properties of Soils Using Incremental Loading*, ASTM International, West Conshohocken, PA
- ASTM D4318-17e1. (2017). *Standard Test Methods for Liquid Limit, Plastic Limit, and Plasticity Index of Soils*, ASTM International, West Conshohocken, PA.
- Azam, S., and Li, Q. (2010). Tailings dam failures: a review of the last one hundred years. *Geotechnical News*, 28(4), 50-54.
- Blight, G. (2009). *Geotechnical engineering for mine waste storage facilities*, CRC Press, London.
- Bussière, B. (2007). Hydro-geotechnical properties of hard rock tailings from metal mines and emerging geo-environmental disposal approaches, *Canadian Geotechnical Journal*, 44(9), 1019-1052.
- Hamade, M.M.P. and Bareither, C.A. (2018). Consolidate undrained shear behavior of synthetic waste rock and synthetic tailings mixtures, *Geotechnical Testing Journal*, in press.
- Jehring, M.M. and Bareither, C.A. (2016). Tailings composition effects on shear strength behavior of co-mixed mine waste rock and tailings, *Acta Geotechnica*, 11(5), 1147-1166.
- Qiu, Y. and Sego, D. C. (2001). Lab properties of mine tailings, *Canadian Geotechnical Journal*, 38(1), 183-190.
- Wickland, B.E., and Wilson, G.W. (2005). Self-weight consolidation of mixtures of mine waste rock and tailings, *Canadian Geotechnical Journal*, 42(2), 327-339.
- Wickland, B.E., Wilson, G.W., Wijewickreme, D., and Klein B. (2006). Design and evaluation of mixtures of mine waste rock and tailings, *Canadian Geotechnical Journal*, 43, 928-945.
- Williams, D.J., Wilson, G.W., and Panidis, C. (2003). Waste rock and tailings mixtures as a possible seal for potentially acid forming waste rock, *Proc. 6th International Conference on Acid Rock Drainage, Cairns, QLD*, 427-435.

Creep Displacements Induced from Waste Rock Loading

J. Kurylo, M. Rykaart, & A. Lizcano

SRK Consulting (Canada) Inc, Vancouver, BC, Canada

ABSTRACT: Waste rock deformations were measured on a high altitude dump using survey prisms and inclinometers. Rates of downslope advancement of about 0.2 to 0.5 m/day (70 to 180 m/year) were measured. This waste dump is founded on very thick (greater than 40 m), warm (approximately -0.5°C) ice-rich permafrost moraine deposits.

From satellite observations and site displacement measurements, it was concluded that the observed displacement was a result of both movement on the ground surface (sliding at the interface of the waste rock dump and foundation) and movement on a shear strain localization surface within the foundation (i.e. creep). This paper describes how the observational data were used to determine the deformation processes and offers potential mitigation solutions for stopping the continued movement of this waste rock dump.

1 INTRODUCTION

Lisiy Glacier is a high altitude glacier (over 4,000 masl) located in a remote area of the Tian-Shan mountain range in Kyrgyzstan. This glacier is in the Kumtor mine project area, which is located about 350 km southeast of the capital of Bishkek and 80 km south of Lake Issyk-Kul, near the border with China (Fig. 1). Prior to mining, the Lisiy Glacier (which includes the Lisiy Cirque Glacier and the Lisiy Valley Glacier) was retreating. When mining started in the region, waste rock and ice was dumped onto the Lisiy Cirque Glacier; the glacier stopped retreating and then started advancing. By the time the glacier started to advance, the original Lisiy Glacier had become more of a rock-glacier due to dumping practices. Because of the glacier advancement, mining operations moved waste placement and started to construct the North-East Valley Waste Rock Dump (NEV-WRD). This waste rock dump (NEV-WRD) was constructed on ice-rich moraine immediately adjacent to the glacier. Moving the location of waste rock placement allowed the cessation of dumping rock onto the Lisiy Glacier area, however the practice of dumping ice mined from various areas of the site onto the glacier was maintained. In time, it was evident that the NEV-WRD was also moving downslope and creep was postulated to be the driving movement mechanism. The collective name for all waste rock dumped in the Lisiy Valley, including the Cirque Rock Glacier and the NEV-WRD, is termed the Lisiy Valley Dump (LV Dump) or “the Dump”, for ease of reference in this paper. Figure 1 shows a layout of the Kumtor mine site and the location of the LV Dump.

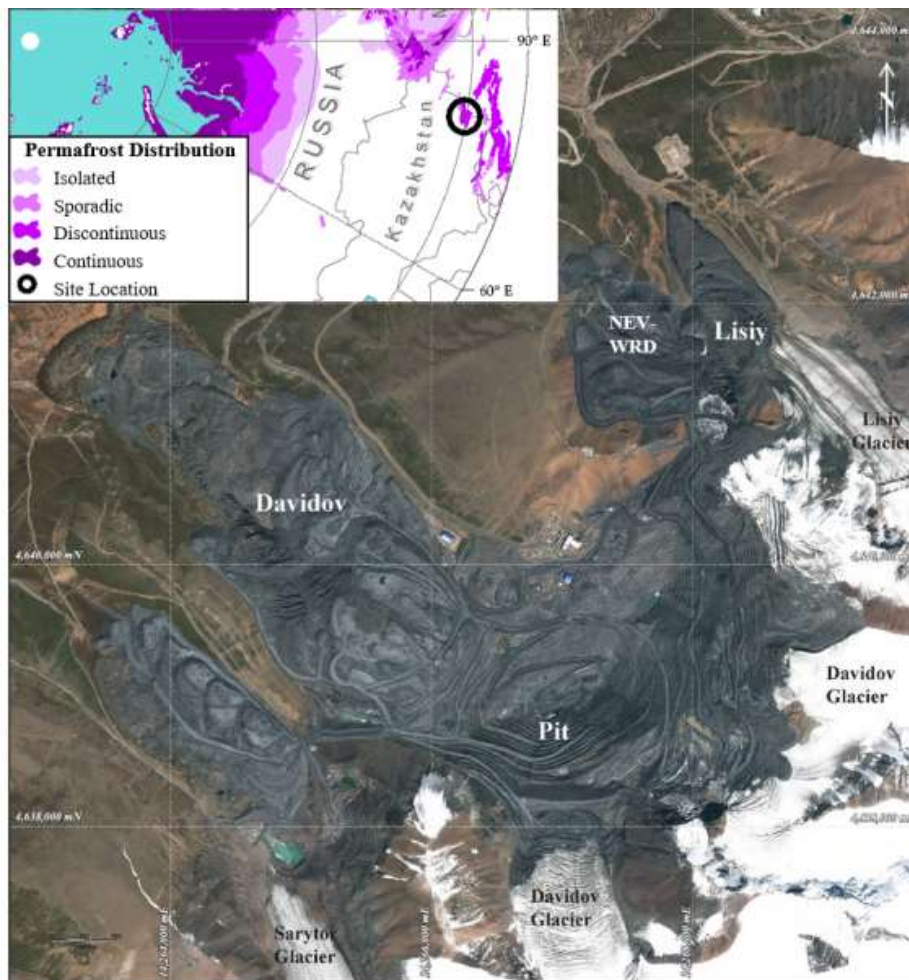


Figure 1. Site study location / location map of the Kumtor mine (in 2016) and surrounding glaciers (some covered in waste rock).

The LV Dump continues to advance downslope, with the rate dependent on the rate of loading. The rock glacier is moving downstream in the direction of Lisiy Creek, which is the same direction as the meltwater channel of Lisiy Glacier. The adjacent NEV-WRD is moving perpendicular to Lisiy Creek and is slowly cutting off flow in the creek.

Continued mine life, at least up to 2023, requires continued expansion of the LV Dump. If the LV Dump continues to advance, Lisiy Creek will be blocked off resulting in the potential of a moraine (soil and rock) blockage/dam and a subsequent flooding hazard. In addition, if the LV Dump continues to advance downstream, important surface infrastructure would have to be relocated prior to the planned end of mine life.

The objective of this study was to develop technically and economically viable options that could slow down the LV Dump long enough to preclude the need to relocate important surface infrastructure prior to 2023, while also demonstrating control with regard to management of glacier movement. Mitigation options also required that flow be maintained in Lisiy Creek (which is fed in part by glacial meltwater).

2 LISIY VALLEY DUMP MOVEMENT (KINEMATICS)

2.1 *Lisy Cirque Glacier (Rock Glacier) Displacement*

2.1.1 *Displacement History (1998–2016)*

Movement of the Lisy Glacier with the LV Dump on its surface is a consequence of the waste rock and ice load dumped on the Lisy Glacier. Jamieson et al. (2015) reconstructed the advancement history of the Lisy Cirque Glacier with the LV Dump on the surface over a period of 15 years (from 1999 to 2014) based on interpretation of satellite images (Fig. 2). During this period, the terminus of the Cirque Glacier advanced around 1.2 km. Much of the movement occurred in the first 6 years (Fig. 3). The main features related to the movements reported by Jamieson et al. (2015), and reproduced in Figures 2 and 3, can be summarized as follows:

- 1998–2002: The Cirque Glacier (and the Valley Glacier) was retreating;
- 1999: Most of the Cirque Glacier was covered with waste rock, including the Cirque Glacier's accumulation zone (i.e. the area above the glacier firm line, above which is characterized by glacial material left from previous years that has properties or is at an intermediate stage between snow and ice);
- 1999–2002: The covered portion of the Cirque Glacier accelerated downhill, forming a terminus of advancing ice-covered waste rock;
- 2003: The Cirque Glacier (covered with waste rock) progressed downslope and connected to the main body of the Lisy Valley Glacier. As a result, the terminus began to advance;
- 2004: The advance/movement of the Cirque Glacier terminus was around 700 m by 2004. This movement occurred at a relatively constant rate of around 230 m/year (around 0.64 m/day);
- 2004–2009: As the Cirque Glacier continued to move and overcome the Valley Glacier, the rate of the Cirque Glacier decreased to a very low and relatively constant value;
- 2010: The volume of mined ice (from the pit) began to increase steadily as this material was placed with the waste rock on and around the historic Cirque Glacier area.
- 2012–2013: Both glaciers advanced. The Cirque Glacier portion covered with waste rock advanced much faster and moved ahead of the Valley Glacier;
- 2013–2014: The whole terminus became covered with waste rock, as was the trunk of the Cirque Glacier.

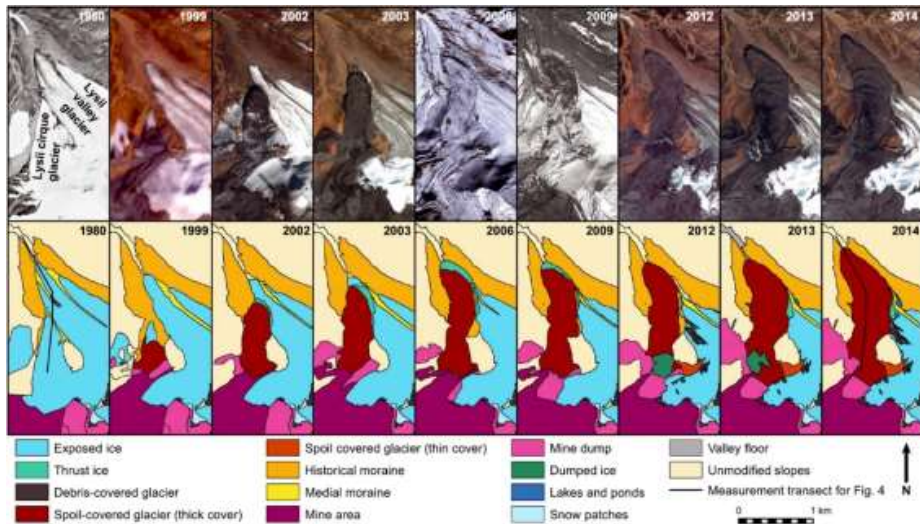


Figure 2. Select time series of glacier and landcover changed for the Lisy Glacier between 1999 and 2014. Top: high-resolution satellite imagery. Bottom: classification of surficial geology and glacier ice/debris cover. Extracted from Jamieson et al. (2015).

Although the volume of waste rock and ice loaded onto the glacier was not quantified, Jamieson et al. (2015) assumed, based on satellite imaging, continuous waste rock and ice loading at the head of the Lisiy Cirque Glacier during their observation period.

Topographical mapping from Kumtor mine of the LV Dump between 1999 and 2014 suggest that between 2004 and 2010, no waste rock or ice was loaded at the head of the Lisiy Cirque Glacier. These maps confirm loading resumed in 2011. This could therefore be an alternative explanation for the cessation of movement between 2004 and 2010 (Fig. 3).

Available displacement data between 2014 and 2016 was reviewed and found to be focused around the nearby but not immediately adjacent Davidov Glacier area (with limited data around the LV Dump). The primary sources of pre-2016 data around the LV Dump area (primarily boreholes with inclinometers and piezometers installed in them) are shown on Figure 9.

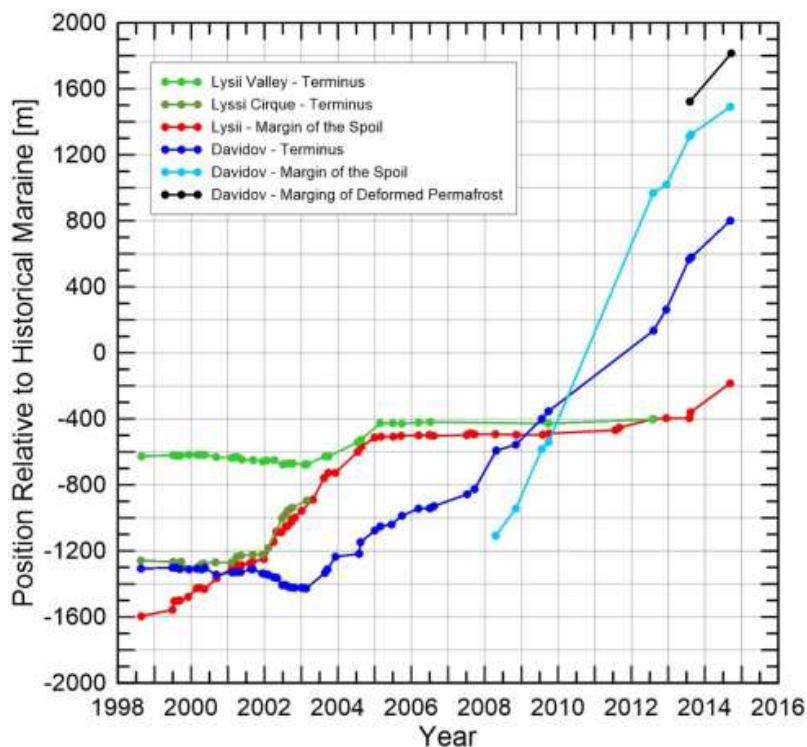


Figure 3. Glacier terminus and spoil margin position for the Lisiy and Davidov Glaciers. Positions are measured relative to the fronts of the most prominent historical moraines in the respective valleys. Extracted from Jamieson et al. (2015).

2.1.2 Lisiy Rock Glacier – 2017 Displacements

Topographical mapping of the Lisiy Cirque Glacier, now covered with waste rock (*aka* Lisiy Rock Glacier), at the end of October 2017 suggest that the glacier is moving in two directions (Fig. 4). Cross sections A and B in Figures 4 and 5 coincide with these movement directions.

Measurements carried out between August and October 2017 at surface monitoring points located approximately along cross sections A and B (Fig. 5) showed that the Lisiy Rock Glacier moved almost in the same North-West direction following the alignment of Lisiy Creek. For the purposes of interpreting the data, it is assumed that waste rock and ice were not discharged onto the Rock Glacier during this period.

Between August and October 2017, the Lisy Rock Glacier moved with a relative constant average velocity of approximately 0.22 m/day. The average thickness of the Lisy Rock Glacier in October 2017 was 40 m, varying between 41 m and 48 m along section A and between 31 m and 45 m along section B (Fig. 5).

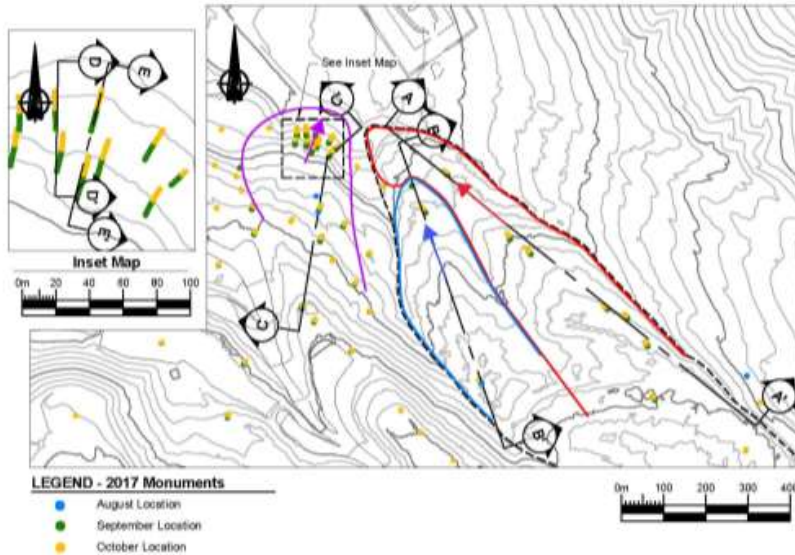


Figure 4. General movement directions of the Lisy Valley Dump (blue and red) and the North-East Valley Waste Rock Dump (purple) as of October 2017.

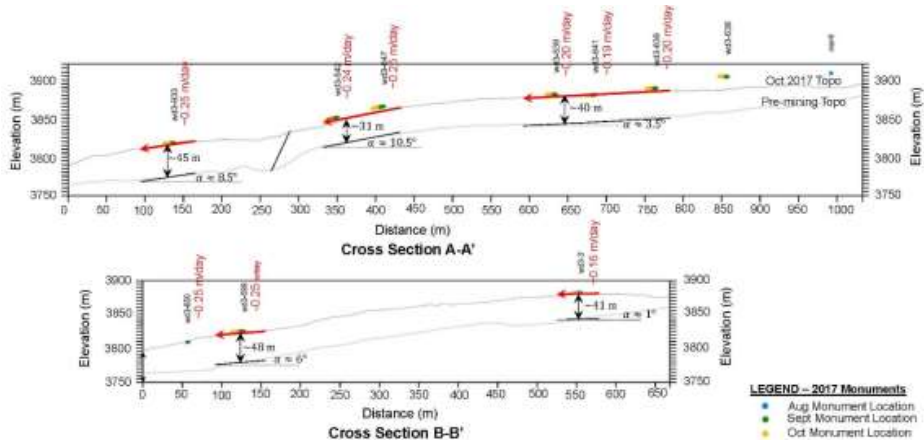


Figure 5. Movements of the Lisy Rock Glacier along section A and B

2.1.3 North-East Valley Waste Rock Dump (NEV-WRD) – 2017 Displacements

There is no data available on the slope displacement of the NEV-WRD toward Lisy Creek before August 2017. Between August and October 2017, the displacement of the NEV-WRD slope were measured at surficial monitoring points.

For purposes of interpreting the data, again it is assumed that there was no discharge of waste rock in the NEV-WRD during the period of surficial monitoring. Cross sections through the NEV-WRD aligned with the measured North-East displacements are shown in Figure 6 (cross section C, D and E).

Like the movements of the Lisiy Rock Glacier, the monitoring points on the NEV-WRD displaced almost parallel to the ground surface, and their rates correlate to the slope of the ground surface. Along cross section C, approximately 40 m in waste rock thickness, movement was variable with rates between 0.24 and 0.36 m/day between August and October 2017. In the same period, the NEV-WRD moved at a rate between 0.41 m/d and 0.55 m/d along cross sections D and E, with higher rates at the steeper upper sections of the slope. The measurements at the nearby available inclinometer (locations shown in Figure 9) also showed that the NEV-WRD moved toward Lisiy Creek like a rigid body on the surface of the ice-rich moraine with a velocity of 0.75 m/day. After two days of observations, the borehole for the aforementioned inclinometer was sheared off.

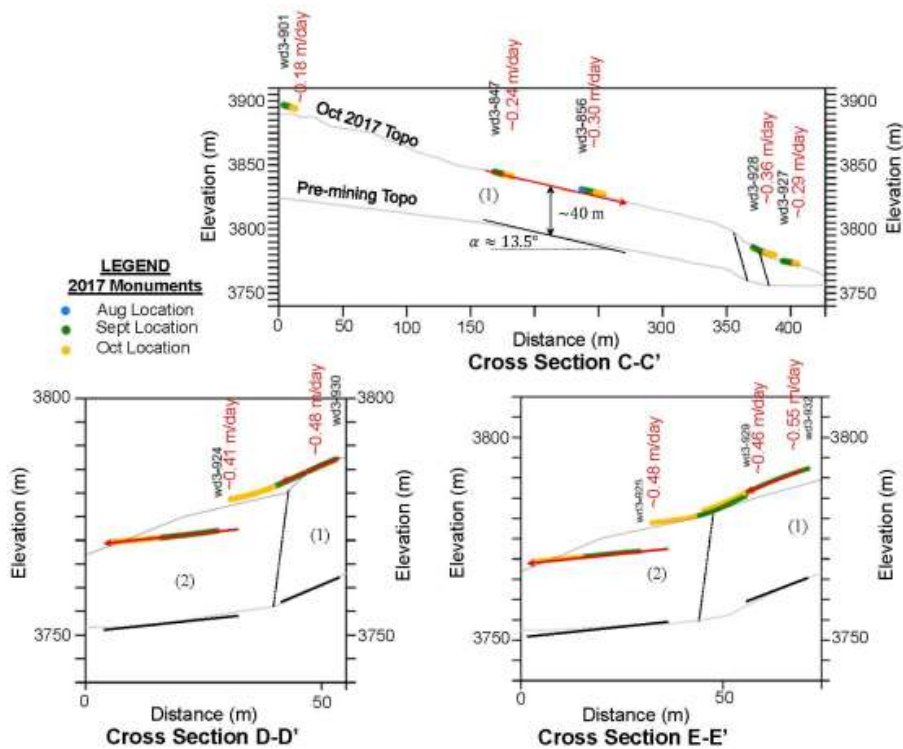


Figure 6. Movements of the NEV-WRD along section C, D and E.

2.2 Movement Mechanism (Kinematics)

Measurements suggest, in the relative short period between August and October 2017, that the Lisiy Rock Glacier and the NEV-WRD were displaced through a translational movement mechanism. The mechanism is compounded of several distinct, almost rigid bodies with internal sliding surfaces. The movement (direction and rate) is dictated by the natural topography. The rigid body translational movement mechanism was confirmed by three days of measurements at one inclinometer located at the NEV-WRD. From satellite observations and displacement measurements at surficial monitoring points, it is not possible to infer whether the Lisiy Rock Glacier and NEV-WRD move:

- on the ground surface (sliding at interface of the glacier-foundation and dump-foundation), or
- on a shear strain localization surface within the foundation, or
- because of shear deformation of the foundation caused by the weights of the Lisiy Rock Glacier and the NEV-WRD.

However, the mode of movement can be inferred from inclinometer measurements. Since there were no inclinometer measurements available in the vicinity of the Lisiy Rock Glacier, inclinometer measurements of the Davidov Glacier (approximately 4 km away) were used to infer the movement mode of the Lisiy Rock Glacier based on the similarity of movements and characteristics of the foundations (translational movement, constant rate, slope of the ground surface, and foundation soil type). While the measurements of additional inclinometers (Fig. 9) in this nearby Davidov glacier indicate a movement due to the shear deformation of the foundation, the measurements at the available inclinometer at the NEV-WRD shows that movement is on the original ground surface. These modes of movement are strongly dependent on the slope of the ground surface. The average slope of the ground surface underneath the Lisiy Rock Glacier is constant and around 4° . The ground surface slope underneath of the NEV-WRD vary between 15° and 20° . The greater the ground surface slope, the greater the shear stress at the base, and the movement can explain the influence of the shear strength at the interface between the NEV-WRD and the moraine. For a gentle ground surface slope, such as 4° , movement of the glacier on the foundation surface is less likely to occur, since the shear stress is much smaller than the expected shear strength at the Rock Glacier-foundation interface.

3 DISPLACEMENT MODEL

A displacement model was developed to study engineering solutions to slow down the movement of the LV Dump along the Lisiy Creek alignment. The main components of the LV Dump that were considered included the permafrost foundation, the glacial ice, and the waste rock material on top of the glacial ice.

The site foundation condition comprises warm permafrost with an average temperature of -0.5°C (to a maximum of approximately -1.2°C at 10 m depth below existing ground). The foundation material contains fine-grained, ice-rich till (i.e., glacial moraine). Considering there is no temperature data available from the glacial ice, it is assumed that the ice temperature across the Lisiy Rock Glacier is lower than the temperature of the ice-rich soils in the foundation. As generally stated in the description of glacier movements (Ingólfsson et al. 2016), meltwater from the glacier interacting with the foundation was not considered in the model as it was unable to be separated out of the data set. Therefore, the potential impact of this meltwater on the movement was not assessed in detail. Consideration of meltwater however was incorporated into the final proposed mitigation in terms of allowing meltwater to flow down the existing Lisiy Creek, and through stability and sliding analysis.

As discussed in Section 2, it is not possible to definitively confirm the displacement mode from displacement measurements at surficial monitoring points, and therefore the measurement results are used to infer the following for development of the displacement model:

- The occurrence of deformation at approximately constant rates under a constant stress state (no rock and ice loaded in the zones of the monitoring points) would suggest that the observed displacements are due more to creep strains than movements on the ground surface. The latter would show undefined deformation rates, like in a failure state, since the strength in the LV Dump foundation interface should be exceeded to allow movement of the LV Dump on the ground surface;
- Creep shear strains are not expected in the waste rock material; the movements should have been due to constant creep strain rates in the ice-rich till in the foundation and ice in the Lisiy Rock Glacier;
- Considering temperature-dependent creep properties of ice and ice-rich till, with temperatures in the foundation near the phase change, the movements were very likely due to constant creep strain rates in the ice-rich foundation soil; and,

- The influence that meltwater from the glacier and/or unfrozen water in the foundation may have influenced the displacements. However, it is difficult to quantify this with the available data set, therefore it has not been considered in the development of the model.

Figure 7 presents the model developed taking as reference basal motion modes of rapid ice-glacier flows (extracted from Ingólfsson et al. 2016). In general, the model considers that the movement of the LV Dump is due to:

- Creep deformation of the ice-rich till in the foundation
- Basal displacement (sliding at the glacier-foundation interface)
- Creep deformation of the glacial ice

Engineering solutions to slow down the movement consider creep deformations (i) and (iii) only, as it is unlikely that sliding at the glacier-foundation interface occurs, and if so, it was not possible to estimate with the available data.

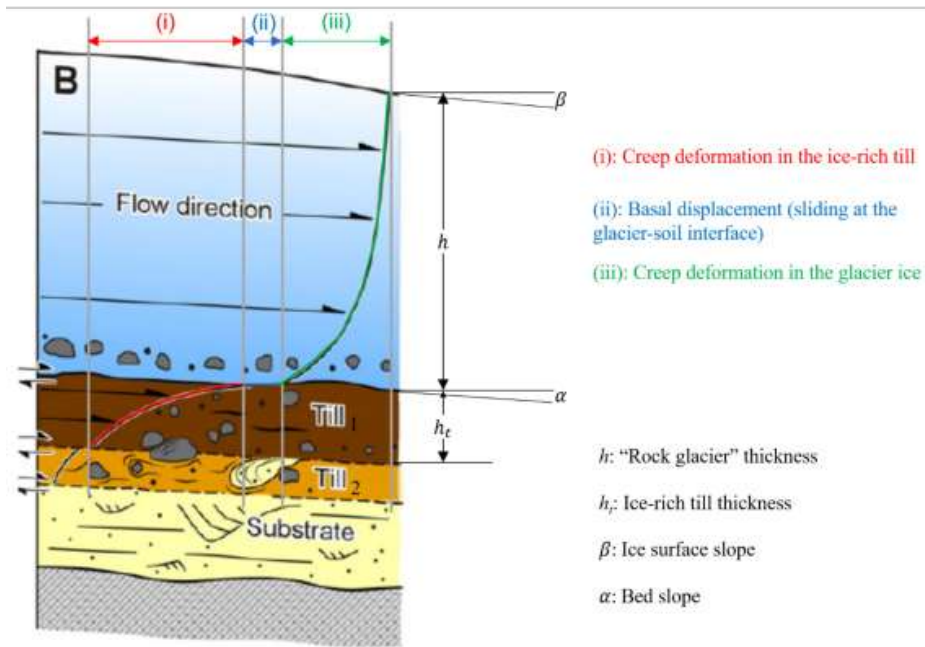


Figure 7. Displacement model. Deforming bed model graphic extracted from Ingólfsson et. al (2016) and further annotated.

4 CREEP PARAMETER OF THE ICE-RICH TILL

Figure 3 includes long-term total displacements measured for the Lisiy Cirque and Davidov Glaciers using high-resolution satellite Landsat and Aster imagery (Jamieson et al. 2015). To determine the creep parameter A of the ice-rich till in the foundation of the LV Dump, the total displacement of the nearby Davidov Glacier was used, since that data set was the most complete and offers the greatest certainty. Sufficient similarity in flow mass and foundation conditions makes the Davidov data suitable to estimate the creep parameter A for use in the foundation of Lisiy Glacier.

In accordance with the model in Figure 7, total displacement is the sum of both the creep displacements in the foundation (i) and in the glacial ice (iii), neglecting the basal displacement (ii), and the total displacement can be determined from the Davidov data in Figure 3. The deformation flow velocity v_i due to creep strains in the glacial ice is determined by the creep equation (Cuffey and Paterson 2010):

$$v_i = \frac{2nA_i}{n+1} (\tau_b)^n \quad (1)$$

Where:

- h is the Davidov Rock Glacier thickness¹ (glacier + waste rock),
¹ The shear strain occurs throughout the height of the Rock Glacier
- A_i is the temperature-dependent creep parameter of the glacial ice,
- n is a model parameter ($n = 3$ for ice and ice-rich soils), and,
- τ_b is the shear stress at the base of the glacier, considering rigid body movement of the rock glacier.

The creep parameter A_i changes with the annual change in the temperature of the ice-glacier. For an assumed average annual temperature of -5°C in the ice-glacier $A_i = 2.9\text{E-}08 \text{ kPa}^{-3}\text{year}^{-1}$.

Considering rigid body movement for the Davidov Rock Glacier, τ_b in Equation (1) is determined by:

$$\tau_b = (\gamma_{wr}h_{wr} + \gamma_i h_i) \sin \alpha \quad (2)$$

with

- $\gamma_{wr} = 24 \text{ kN/m}^3$: Unit weight of the waste rock;
- $\gamma_i = 9 \text{ kN/m}^3$: Unit weight of the glacial ice;
- h_{wr} : Waste rock thickness,
- h_i : Glacier thickness, and
- α : Slope of the ground surface.

The deformation velocity due to creep strains in the foundation ice-rich till is:

$$v_t = v - v_i \quad (3)$$

based on the displacement model in Figure 7, with v as the total displacement velocity of the Davidov Rock Glacier according to Figure 3.

The strain rate $\dot{\gamma}_t$ due to creep strains in the ice-rich till with the thickness h_t will be:

$$\dot{\gamma}_t = \frac{v_t}{h_t} \quad (4)$$

The creep parameter A of the of the ice-rich till is determined by:

$$A = \frac{\dot{\gamma}_t}{(\tau_t)^n} \quad (5)$$

Assuming shear deformation in the till parallel to the to the ground surface, the shear stress τ_t in the till layer will be

$$\tau_t = \gamma_t h_t \sin \alpha \quad (6)$$

with the unit weight γ_t of the ice-rich till in the foundation.

Table 1 includes the calculations of the creep parameter A for the Davidov Glacier thickness $h_i = 120 \text{ m}$, an average ground surface slope of $\alpha = 5^\circ$, an average glacial ice temperature of -5°C and some waste rock thicknesses h_{wr} as reported in Jamieson et al. (2015).

The thickness of the ice rich till was assumed to be $h_t = 15$ m based on the measurements at the Davidov inclinometers. Finally, the unit weight of the ice-rich till was assumed to be $\gamma_t = 20$ kN/m³. Based on this analysis, the average value of the creep parameter for the site ice-rich low salinity till is $3.5 \text{ E-}04 \text{ year}^{-1} \text{ kPa}^{-3}$.

Table 1: Calculation of Creep Parameter A of the Ice-Rich Till

Component	Sym- bol	Units	Calculation Period			Source
			23/03/ 2006	26/09/ 2009	29/07 /2012	
Waste rock thickness	h_{wr}	m	63	55	113	Jamieson et al. (2015)
Shear stress base of the glacier	τ_b	kPa	226	209	330	Equation (2)
Flow velocity of glacial ice (-5°C)	v_i	m/year	30.9	23.5	123.3	Equation (1)
Total velocity	v	m/year	108.0	158.0	185.0	Jamieson et al. (2015)
Deformation velocity due to creep strains in the ice-rich till	v_t	m/year	77.1	134.5	61.7	Equation (3)
Shear strain rate in the till	$\dot{\gamma}_t$	sec-1	1.63E-07	2.84E-07	1.30E-07	Equation (4)
Creep Parameter of the till	A	kPa-3 year-1	2.87E-04	5.02E-04	2.30E-04	Equation (5)

At warmer temperatures (above -3°C), the creep parameter A is very sensitive, and tends toward high values. In addition, the A creep parameter is also sensitive to salinity. The A parameter is not well constrained in the literature for ice-rich soils at temperatures between -3°C and 0°C. Since the temperature of the site permafrost foundation is -0.5°C, the site creep parameter presents considerable uncertainty.

Figure 8 presents a sensitivity calculation for two values of A that vary by one order of magnitude. The figures show the significant impact that values of A have on the creep strain rates, when structures (e.g., embankments, waste rock dumps, etc.) of different heights are placed on creep-susceptible layers of different thicknesses.

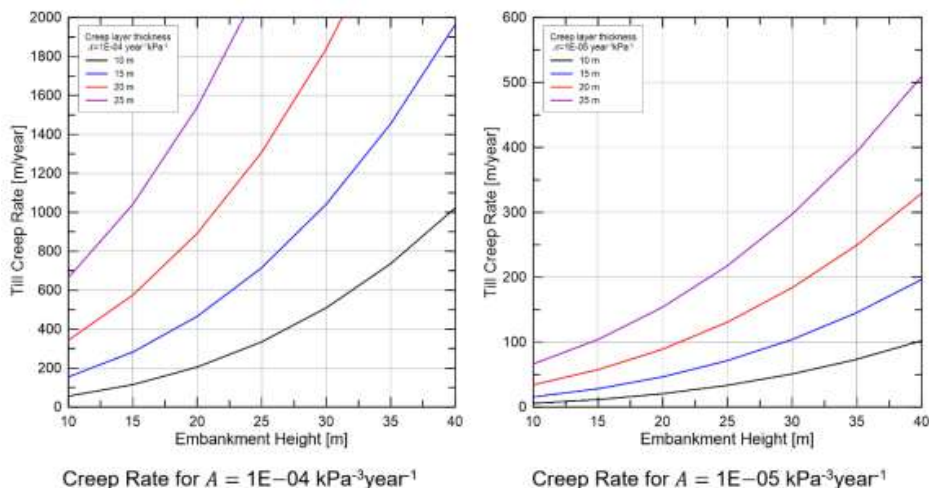


Figure 8. Glacial till creep rates as a function of creep parameter, till thickness and embankment height (rock loading).

5 ALTERNATIVES TO SLOW DOWN THE GLACIER MOVEMENT

The outlined movement mechanism, displacement mode, and calculated creep strains confirmed that unless dumping is ceased, the only way to slow down movement of the LV Dump was to provide a resisting force within the upper 15 m of the foundation soil, or to remove and replace that material with ice-poor soil. Subsequently four alternatives were studied to achieve these goals; (1) piles, (2) ground freezing, (3) conventional buttress, and (4) Glacier Retention Structure (GRS):

Both piles and ground freezing are technically feasible alternatives to slow down the movement of the LV Dump. However, they were found to be not economically feasible. More importantly, the time to implement these alternatives would be in the order of many years, which in itself is not considered a practical solution.

A conventional buttress founded on ice-rich till will significantly increase the shear stress in the till due to its weight. High shear stresses will activate creep deformations in the till, which in turn will cause large movement of the buttress. Therefore, a conventional buttress founded on ice-rich till is not technically feasible.

A GRS, designed and constructed according to specific design principles, especially those related to removing and replacing the ice-rich till in the foundation, is the least expensive, and is a technically feasible solution to slow down the movement of the LV Dump. After confirmation of initial sliding and stability analysis, this alternative was determined to be well suited to the activity and experience of the site. The GRS would need to be constructed downstream of the current LV Dump, and after it has been constructed the flow-through system would need to be connected to the terminus of the Lisiy Galcier. Figure 9 presents a plan view, and Figure 10 is a cross section of the conceptual GRS design.

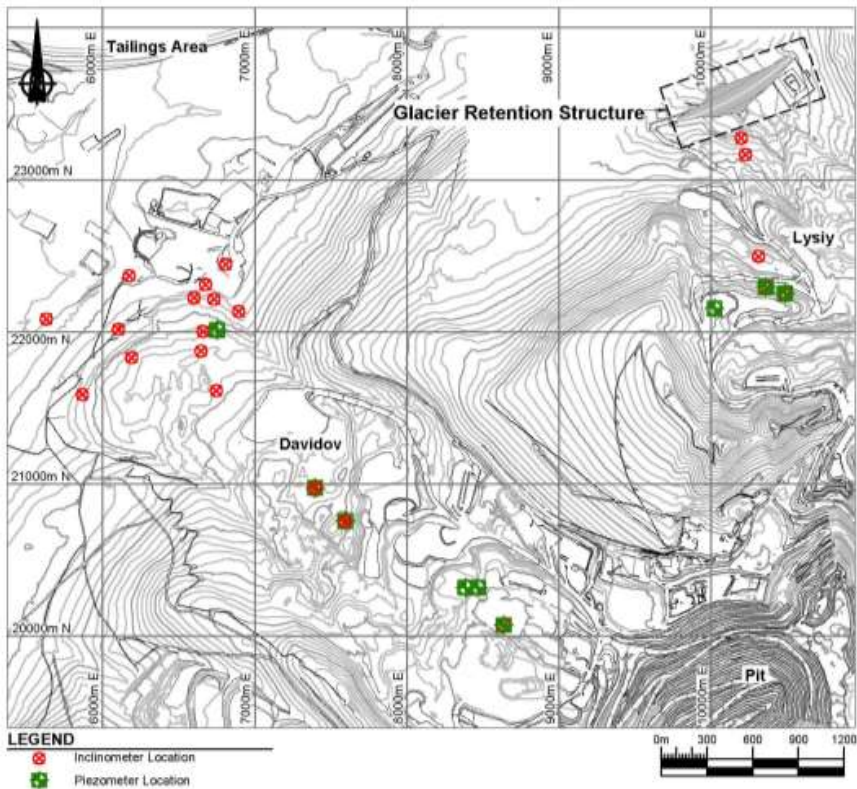


Figure 9. Glacier Retention Structure location and available inclinometer and piezometer data locations.

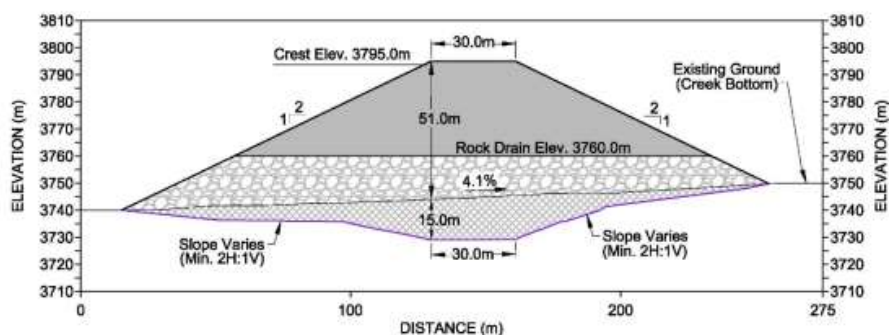


Figure 10. Typical cross sections through center of the conceptual Glacier Retention Structure

6 CONCLUSION

This paper presents a practical example of how monitoring data (satellite imagery and surficial monument surveying), coupled with laboratory test data, can be used to back-analyze and confirm movement mechanisms for waste rock placed on ice and ice-rich till material. The case study confirmed that, to slow down the movement of the Lisiy Valley Dump, a resisting force within the upper ice-rich till layer must be provided, temperature dependent creep properties of the ice-rich till must be modified, or the ice-rich till must be removed and replaced by ice-poor soil (such as waste rock). Performance and monitoring data of the proposed mitigation measures were unavailable at the time of writing this paper. If the proposed Glacier Retention Structure (GRS) is constructed, then the performance of the GRS would be the subject of a future / subsequent paper.

ACKNOWLEDGEMENT

The authors are grateful to Kumtor Gold Company, Centerra Gold Inc., for the opportunity to work on the Lisiy Valley Dump project and for permission to publish this material. Finally, the authors could not have presented this material were it not for the tireless efforts of their colleagues at SRK Consulting (Canada) Inc., who were involved throughout this assessment.

REFERENCES

- Cuffey K, Paterson, W.S.B. 2010. The physics of glaciers. 4th edition. Academic Press (Elsevier). ISBN 9780123694614.
- Ingólfsson, Ó., Benediktsson Í. Ö., Schomacker, A., Kjær, K.H., Brynjólfsson, S., Jónsson, S.A., Korsgaard, N.J., & Johnson, M.D. 2016. Glacial geological studies of surge-type glaciers in Iceland — Research status and future challenges. *Earth-Science Reviews* 152, 37–69. January 2016.
- Jamieson, S.S.R., Ewertowski, M.W., & Evans, D.J.A. 2015. Rapid advance of two mountain glaciers in response to mine-related debris loading. *Journal of Geophysical Research: Earth Surface* 120, 1418–1435. DOI 10.1002/2015JF003504
- Leinenkugel, J.H. 1976. Deformation and strength behavior of cohesive soils. Experimental Results and their Physical Interpretation (in German). PhD. Dissertation. Institute for Soil Mechanics and Rock Mechanics, KIT. Heft No. 66.
- LLC Technology. 2016. Results of geophysical explorations to determine the areas of high ice content in soils of the Kichi-Sarytor, the Chon-Sarytor (Centralnaya) Valleys and the Lysyi Glacier Valley. Report prepared by LLC Geotechnology. 2016.
- Schwarz, W. 1987. Dowels in clayey soils (in German). PhD. Dissertation. Institute for Soil Mechanics and Rock Mechanics, KIT. Heft No. 105.

Desiccation of Tailings in an Instrumented Column Under Laboratory and Atmospheric Conditions

D.J. Williams, S. Quintero, C. Zhang and X.Lei
The University of Queensland, Brisbane, Queensland, Australia

ABSTRACT: A purpose-built, instrumented column has been constructed to test the settling, self-weight consolidation and desiccation of tailings from a slurry state. The column has a usable height of 1,200 mm and an internal diameter of 200 mm, and was instrumented with dielectric moisture, and thermal suction and temperature sensors developed at The University of Queensland and used to test tailings. The sensor data are recorded using a purpose-built data logger, to which all sensors are connected, and the data are uploaded to a webpage for easy access. The column can be deployed under controlled conditions in the laboratory, or under atmospheric conditions monitored by a weather station. The column is placed on load cells for recording the water balance during the test. The paper describes the column, the design of the sensors, their calibration, and the desiccation of iron ore sand tailings and slimes under controlled laboratory and atmospheric conditions.

1 INTRODUCTION

On deposition in a surface tailings storage facility (TSF), tailings slurry will undergo beaching, hydraulic sorting, settling, consolidation and desiccation on exposure. The settling and consolidation of tailings have the most profound effect on the volume that the deposited tailings occupy (Shokouhi & Williams, 2015; Shokouhi et al., 2016). These processes are particularly important where the rate of rise is rapid and/or deposition is under water. Settling occurs in the upper part of the recently deposited tailings layer, while consolidation occurs simultaneously towards the base of the layer. During the initial rapid settling of tailings slurry, there is limited particle contact and essentially no development of excess pore water pressure (PWP). As the tailings form a sediment, particles come into contact, excess PWPs develop and, on drainage and consolidation, these transfer to effective stress. The magnitude of consolidation is far less than the reduction in volume on settling, and consolidation is a far slower process than settling.

Desiccation occurs when the surface of the tailings becomes exposed to the sun and wind and has most effect on the shear strength of the tailings, with limited densification, particularly once the shrinkage limit is reached at which pore water is replaced by air. The effect of the sun and the wind drops off exponentially with depth, as does the strengthening effect (Zhang et al., 2016). The three processes of settling, consolidation and desiccation are conventionally tested separately in the laboratory; settling in a column, consolidation in a consolidometer, and desiccation in a drying tray and/or a Tempe cell or desiccator. The tailings sediment formed in a settling column cannot be transferred to a consolidometer, and neither the tailings sediment nor consolidated tailings can be transferred to a drying tray or Tempe cell. As a result, there are disconnects between the three laboratory tests.

Laboratory devices have been developed within the Geotechnical Engineering Centre (GEC) at The University of Queensland (UQ) capable of the continuous testing of tailings from their initial slurry-like state to a soil-like state. These devices include a purpose-built, instrumented column in which tailings slurry is allowed to settle, undergo self-weight consolidation, and surface desiccation and re-wetting cycles. Desiccation is simulated in the laboratory using a heat lamp and/or a fan, with wetting-up by flooding. The column can be subjected to weather-induced desiccation and re-wetting cycles outdoors.

In the conventional pumping of tailings slurry using robust and inexpensive centrifugal pumps by pipeline to a surface TSF, the main focus is on the design of the dam to contain the tailings to limit the risk of dam failure and the potential run-out of flowable or liquefiable tailings. However, tailings dam failures continue to occur at an unacceptably high rate. Further, the incremental construction and raising of tailings dams to delay capital expenditure results in tailings slurry deposits that continue to contain excessive amounts of entrained water, occupying larger storage volumes and ultimately covering larger footprints than could be achieved with initially larger storage footprints. This adds to operational costs and to the capital costs of the necessary dam raises, although these appear to be reduced by discounting over time. It also results in wet and soft tailings deposits that are difficult and expensive to close and rehabilitate.

Compared with the greater attention paid to the design of the dam to contain the tailings, less attention is paid to the “design” of the tailings deposit to be more soil-like, although attention is increasingly being paid to the management of the tailings discharge. Tailings are more consistently being deposited in thin layers from around the dam, to form an even beach, to control the location of the slimes and decant pond away from the dam, and to facilitate desiccation in a dry climate. If the resulting tailings dry density, shear strength and hydraulic conductivity (rate of drainage) are better known, the tailings footprint and deposition layer thickness required for a given tailings production and tailings type can be optimised to produce the desired soil-like tailings consistency. This then minimises the tailings storage volume required, reduces the need and/or frequency of dam raises required, facilitates upstream raising of the dam (possibly using harvested desiccated tailings) where this is feasible, and facilitates closure and rehabilitation of the tailings deposit to a high level of future land use and/or ecological function. In turn, this approach offers the potential to greatly reduce the whole-of-life cost of tailings storage.

2 INSTRUMENTED TAILINGS COLUMN

The instrumented column was purpose-built in the GEC at UQ following a trial column described in Zhang et al. (2016). The intended purpose of the instrumented column is to simulate settling, self-weight consolidation and desiccation of a given tailings to assist in optimising the tailings deposition layer thickness and deposition cycle time. The results of the instrumented column test, together with the given tailings production rate, enable the optimal tailings footprint to be determined to maximise dewatering, densification, and shear strength gain by desiccation. The instrumented column was designed to be robust and cost-effective to manufacture and instrument, to encourage its widespread deployment in laboratories and at mine sites.

The column dimensions are an internal diameter of 200 mm, comprising Perspex or PVC tubing that is readily and cheaply available commercially, and a working height of 1.2 m. For ease of filling, emptying and re-use, the column is manufactured in three lengths of 400 mm, or two lengths of 600 mm, with flanges and O-ring seals between the lengths. The column can also be made in a single length for ease of use at mine sites. The column can be instrumented with moisture, suction, temperature and salinity sensors, plus four base load cells to monitor the water balance of the column, which are specifically and cost-effectively developed by the GEC.

2.1 Sensors and data logging

The sensors are mounted through the wall of the column, at appropriate intervals up its height, with up to 10 of each sensor type installed at quarter points around the column. The sensors are designed to be robust, inexpensive, and capable of long-term use in the chemically aggressive environments that often exist in tailings, such as highly acidic, highly alkaline and/or highly saline conditions. This has involved designs that prevent, where possible, direct contact between

the measuring element and chemically aggressive tailings water. For example, some measurements are based on humidified air generated by tailings water and passed through a ceramic of high air entry. Further, the sensors are specifically designed for testing tailings from a slurry to the desiccated state. A camera is added to capture the surface desiccation cracking. All sensors, plus the weather station and camera, are connected to a single data logger that is also specifically and cost-effectively developed in-house, and is driven by open-source software that enables data collection via the internet in real time. Further, the data logger powers each sensor individually before powering each one down in turn. This not only dramatically reduces the power demand, but also avoids sensor drift due to heating of the leads and sensors. The in-house development of the sensors and data logger has enabled costs to be dramatically reduced (by between 70% and 90%) from those of sensors and data loggers available commercially.

Some of the sensors developed in-house are shown in Figure 1 (Williams & Zhang, 2017). The moisture sensor developed in-house measures the volumetric water content of tailings indirectly from its dielectric permittivity, relying on the much higher dielectric constant of water (55 to 90, depending on salinity and temperature) than that of dry soil (4 to 20, depending on soil mineralogy and temperature). Although the readings from dielectric permittivity-based moisture sensors are somewhat affected by salt and temperature, these impacts can be compensated by measuring salinity and temperature at the same location using other sensors. Dielectric permittivity-based moisture sensors are much less effected by salinity and temperature than the more conventional time domain reflectometry-based moisture sensors available commercially, which are affected substantially by attenuation in saline pore water (Hook et al., 2004).

Two suction sensors have been developed in-house: (i) a dielectric permittivity-based suction sensor that measures the dielectric permittivity of a porous ceramic when it comes into equilibrium with the surrounding unsaturated tailings, and (ii) a heat dissipation-based suction sensor that measures the unsaturated soil suction via a temperature rise on heating, and also provides a measure of temperature. The thermal suction sensor is preferred, since it is more stable, is unaffected by salinity, and it also monitors temperature.

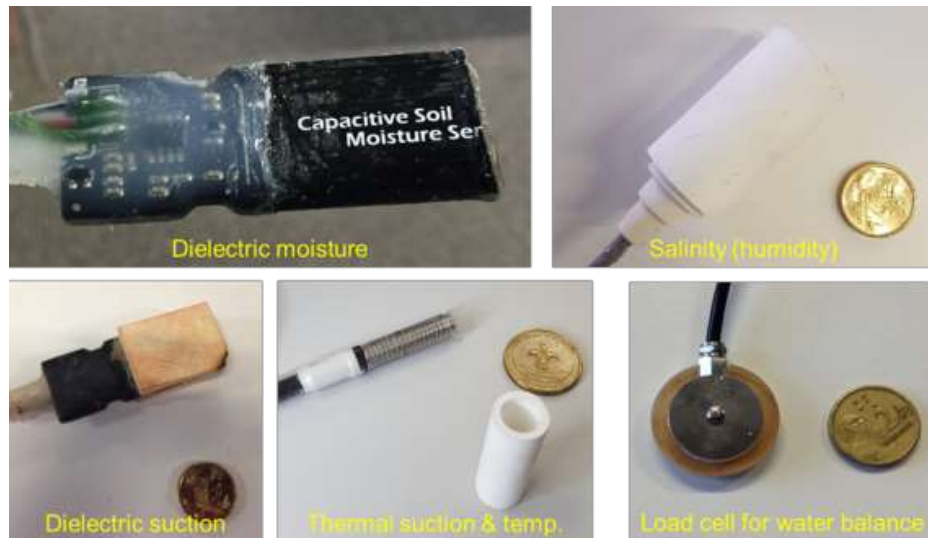


Figure 1. Sensors developed and manufactured by GEC for use in instrumented column.

The salinity sensor developed in-house measures the relative humidity of the pore air in the surrounding unsaturated tailings, and is capable of measuring salinity over the entire range from fresh to the solubility limit (up to 265 ppt), although it is most sensitive above the salinity of seawater (35 ppt). If the pore water is fresh, the sensor can also measure suctions up to high values.

2.2 Tailings column test methodology

The various sensors developed in-house are subjected to calibration and reliability testing in a purpose-built drying/wetting cycle test, as shown in Figure 2. It is essential to carry out sensor calibration in the tailings in which the sensors will be embedded, rather than relying on the calibration supplied for the particular sensor. Sensor durability and reliability is essential in the harsh conditions many tailings exist under, including high salinity, and highly acidic or highly alkaline pH. For the purposes of calibration, a 4 cm deep layer of settled tailings is allowed to dry, followed by wetting and drying cycles, which is what the tailings will undergo. This depth of settled tailings was selected to ensure reasonably uniform conditions with depth, and the sensors are embedded in the middle of the layer. Drying is simulated using a fan, to eliminate the heating that would occur using heat lamps, while wetting is achieved by flooding the desiccated tailings. The in-house sensors have been found to perform well and to demonstrate high reliability.

Tailings slurry is added to the column in a series of layers, much as it is deposited in a TSF, with each layer allowed to settle and the supernatant water removed, before the next layer of slurry is added. An extra 200 mm length is added to the top of the column to enable the last layer of tailings slurry to be added, and this is removed once the tailings has settled to an overall height of 1.2 m.

When the instrumented column is deployed in a laboratory, a heat lamp and/or fan are used to simulate solar and wind drying, with re-wetting by flooding. The instrumented column can also be deployed in the field, in combination with a climate station to monitor actual climatic conditions.

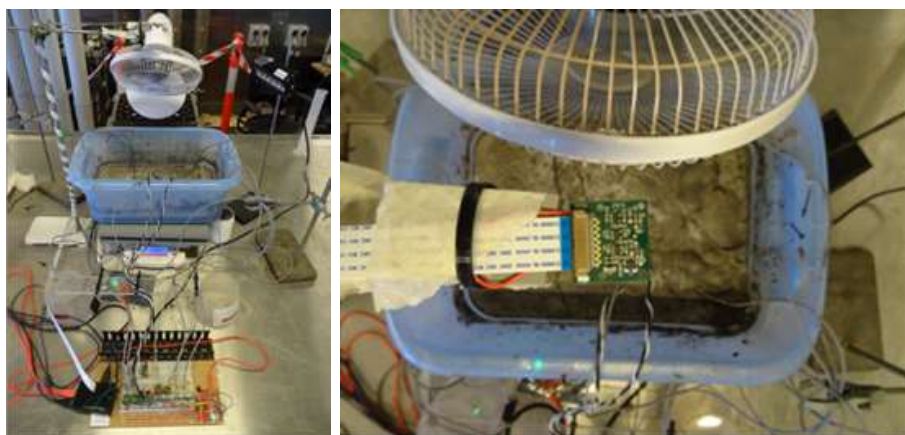


Figure 2. Calibration and durability testing of in-house sensors.

3 COLUMN TESTING OF IRON ORE SAND TAILINGS AND SLIMES

The results of instrumented column testing of iron ore sand tailings and slimes are described in the following sections. The sand tailings comprised about 50% fine to medium-grained sand-sized particles (0.06 to 1 mm in size), 48% silt-sized particles (0.002 to 0.06 mm in size) and 2% clay-sized particles (finer than 0.002 mm), classifying them as a Silty SAND (SM). The slimes comprised about 75% silt-sized particles and 25% clay-sized particles, with a Liquid limit of 28.1%, a Plastic Limit of 13.5%, a Plasticity Index of 14.6%, and a Linear Shrinkage of 5.0%, classifying them as a Clayey SILT of low plasticity (ML). The specific gravity of the sand tailings is 2.85 and that of the slimes is 3.86. Both slurries have a pH of about 7.6, and an electrical conductivity of about 500 $\mu\text{S}/\text{cm}$.

The sand tailings and slimes are discharged into the TSF at solids concentrations of 40% and 25% by mass, respectively. On settling in a 1,000 cc measuring cylinder, the sand tailings and

slimes achieved 71% (gravimetric moisture content of about 40% and dry density of 1.33 t/m^3) and 60% solids by mass (gravimetric moisture content of about 65% and dry density of 1.10 t/m^3), almost instantaneously and in about 24 hours, respectively.

Samples of sand tailings and slimes were prepared at 40% and 25% by mass, respectively, and added in 24 layers to separate instrumented columns (two for the sand tailings and two for the slimes) at a high rate of rise equivalent to 16 m/year . Each layer was left to settle and consolidate for 24 hours, and the supernatant water removed, before the subsequent layer of slurry was placed. All columns were instrumented with a series of dielectric moisture, and thermal and temperature sensors. Two of the columns, one filled with sand tailings and the other with slimes, were tested in the laboratory, with desiccation simulated using a 375 watt infrared lamp mounted above the top of the column (see Figure 3(a)). The other two columns were tested on a rooftop at UQ and exposed to ambient weather conditions that were monitored using a full weather station (see Figure 3(b)), assembled in-house. The weather station recorded rainfall, temperature, humidity, atmospheric pressure, wind direction and intensity, and solar radiation, from which potential evaporation was calculated using the Penman-Monteith equation (Monteith, 1981).

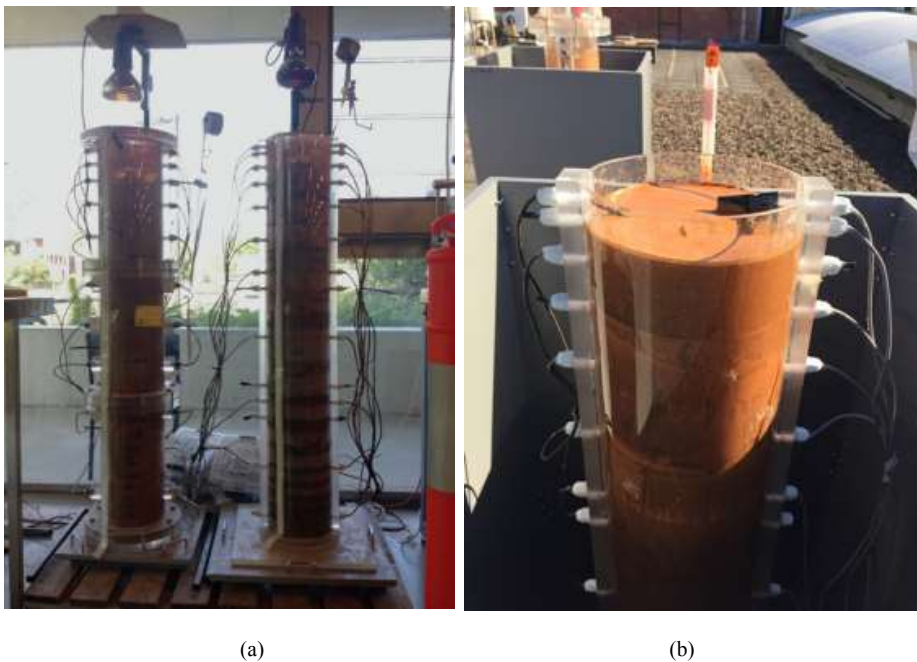


Figure 3. Instrumented columns: (a) laboratory columns, and (b) rooftop columns.

3.1 Sand tailings laboratory column test

The laboratory columns have been monitored for over 120 days. The results for the sand tailings are shown in Figures 4 and 5. Three desiccation stages are evident from the evaporation rates shown in Figure 4(a), and no surface desiccation cracking was observed. An initial constant evaporation rate of about 4.7 mm/day lasted for about 10 days. The evaporation rate decreased from days 10 to 70, and the last stage beyond day 70 showed a roughly constant evaporation rate of only about 0.3 mm/day . Hence, desiccation of the sand tailings is largely complete after 70 days of drying using a 375 watt infrared lamp in the laboratory. Figure 4(b) shows that a significant temperature gradient developed towards the surface. Figure 4(c) shows that after 120 days of desiccation, the top 30 cm of the sand tailings was dry, and some desaturation had

reached a depth of 70 cm. The cumulative water loss was about 18 cm, indicating an average gravimetric moisture content for the desaturated upper 70 cm layer of 22.0%.

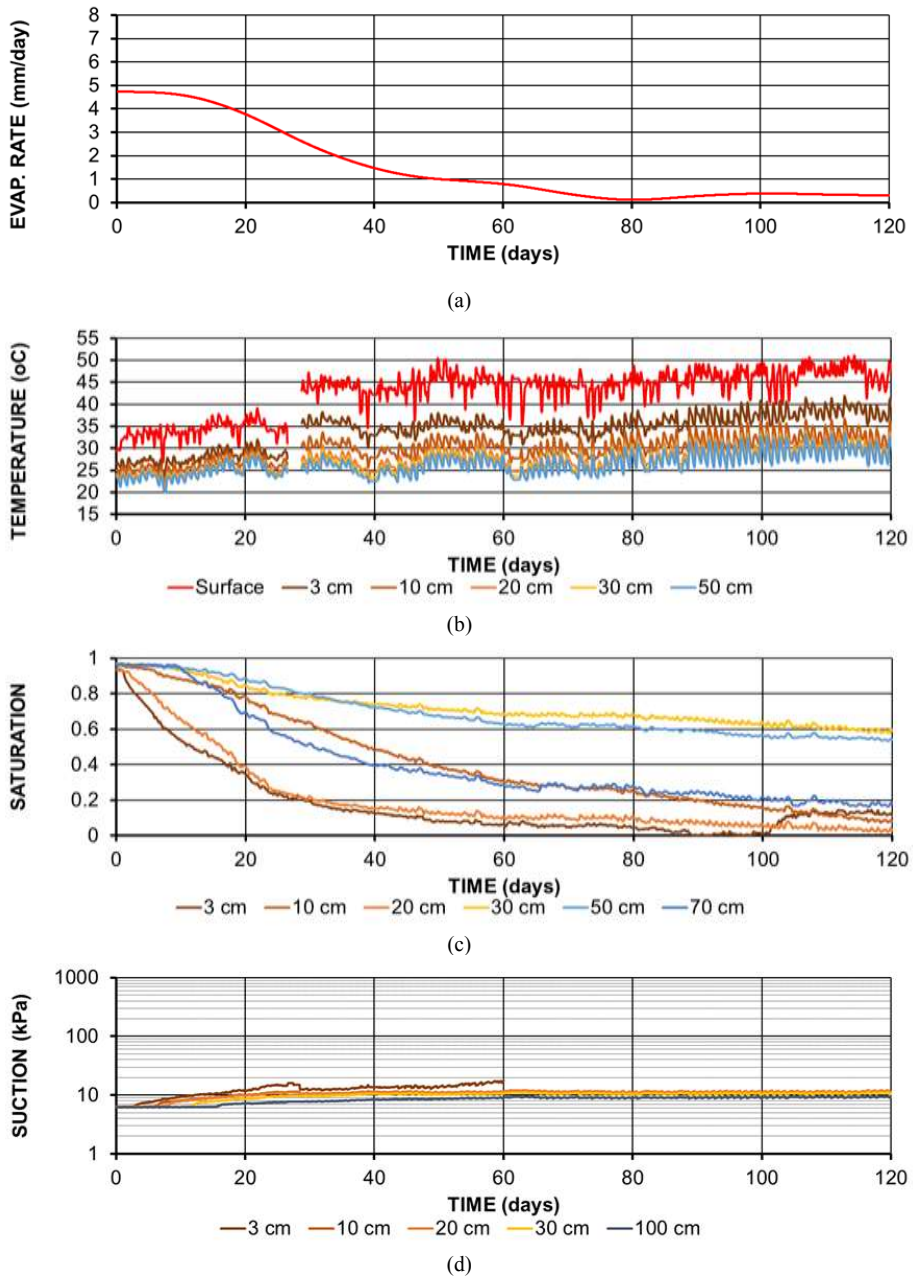


Figure 4. Sand tailings laboratory column test results: (a) actual evaporation rate, (b) temperature, (c) degree of saturation, and (d) suction versus time at various depths.

Accompanying desiccation, the surface of the sand tailings shrunk about 9.5 cm, indicating an average dry density for the desaturated layer of 1.67 t/m^3 . Figure 4(d) shows that only minor matric suctions developed in the sand tailings, limited by the inability of the dry sand tailings to maintain matric suction.

Profiles of degree of saturation with depth at 20-day intervals during the sand tailings laboratory column test are shown in Figure 5. These profiles suggest that flow is occurring in two directions: (i) upwards flow driven by evaporation, which diminished with time and depth, and (ii) substantial downwards flow below a depth of about 0.4 m driven by gravity drainage towards the sealed base of the column, which also diminished with time.

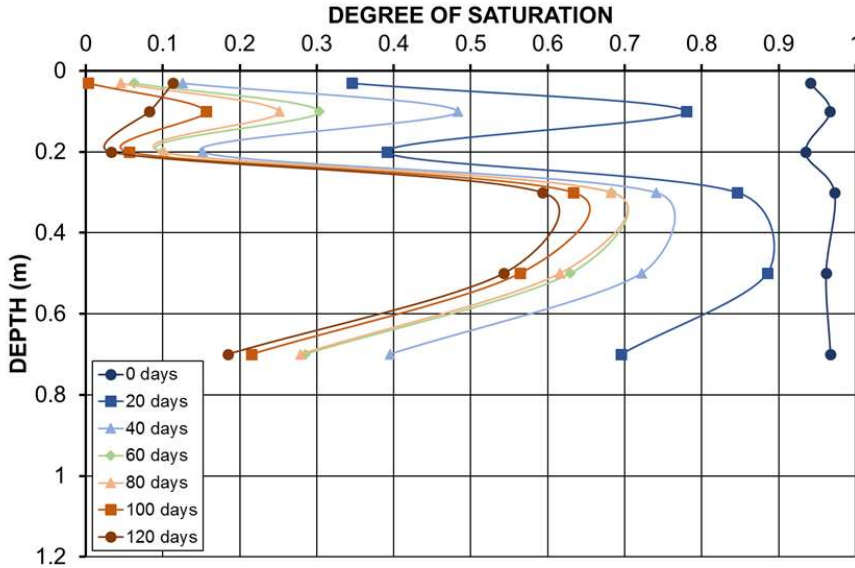
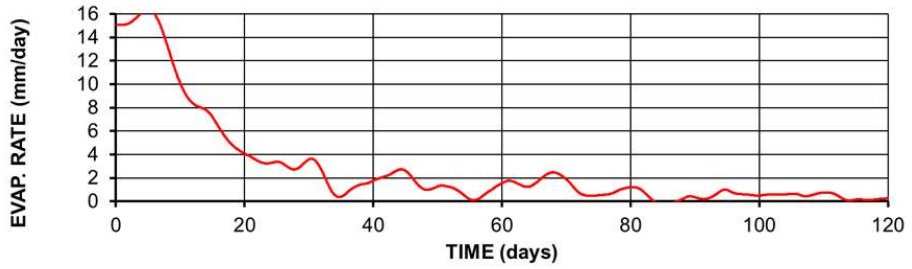


Figure 5. Profiles of degree of saturation with depth at 20-day intervals during sand tailings laboratory column test.

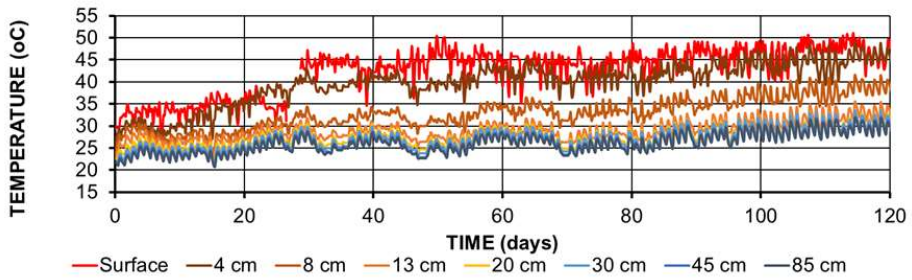
3.2 Slimes laboratory column test

The results for the slimes laboratory column are shown in Figures 6 and 7. Three desiccation stages are again evident from the evaporation rates shown in Figure 6(a). An initially very high evaporation rate of about 16 mm/day (three times the rate observed in the sand tailings) lasted for about 5 days, until the surface started to crack and the slimes underwent significant shrinkage. The evaporation rate decreased rapidly from days 5 to 70, and beyond day 70 was near-zero. Hence, desiccation of the slimes is complete after 70 days of drying using a 375 watt infrared lamp in the laboratory. Figure 6(b) shows that a significant temperature gradient developed towards the surface. Figure 6(c) shows that after 120 days of desiccation, the top 13 cm of the slimes was dry, and some desaturation had reached a depth of 60 cm. Cumulative water loss was about 35 cm, indicating an average gravimetric moisture content for the desaturated upper 60 cm layer of 30.5%. Accompanying desiccation, the surface of the slimes shrunk about 15 cm, indicating an average dry density for the desaturated upper layer of 2.25 t/m^3 . Figure 6(d) shows that high matric suctions were measured in the slimes to 60 cm depth.

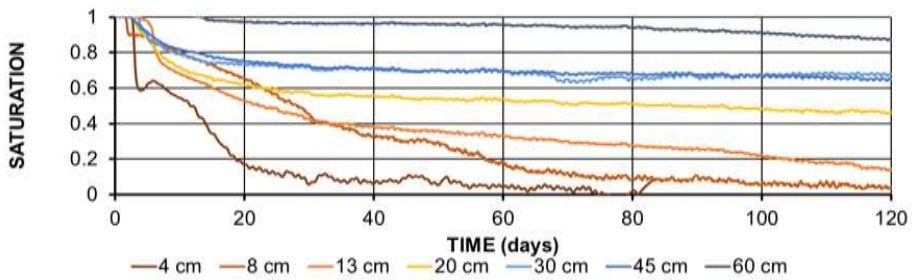
Profiles of degree of saturation with depth at 20-day intervals during the slimes laboratory column test are shown in Figure 7. These profiles again suggest that flow is occurring in two directions: (i) dominant upwards flow driven by evaporation, which diminished with time and depth, and (ii) minor downwards flow below a depth of about 0.4 m driven by gravity drainage, limited by the low hydraulic conductivity of the slimes.



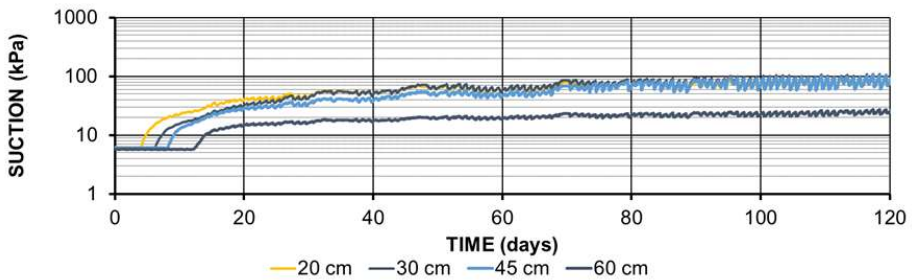
(a)



(b)



(c)



(d)

Figure 6. Slimes laboratory column test results: (a) actual evaporation rate, (b) temperature, (c) degree of saturation, and (d) suction versus time at various depths.

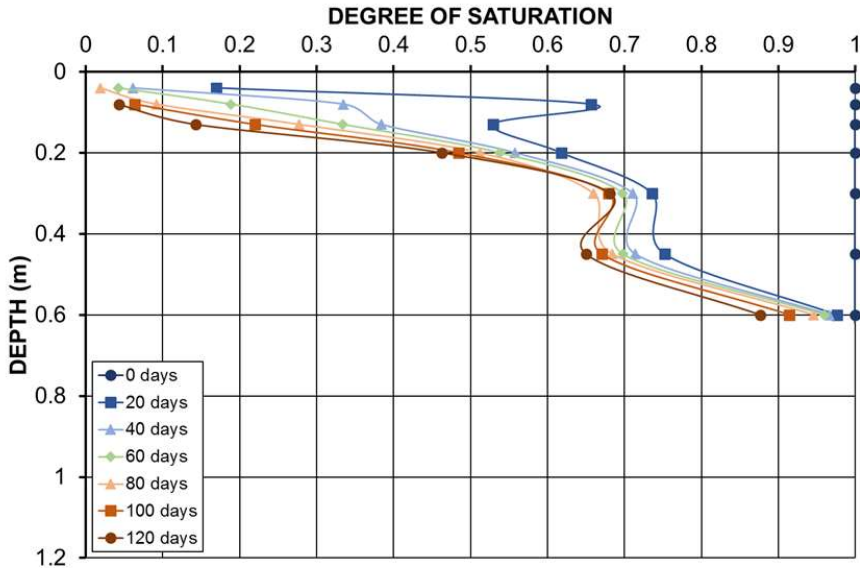


Figure 7. Profiles of degree of saturation with depth at 20-day intervals during slimes laboratory column test.

3.3 Sand tailings rooftop column test

Monitoring of the rooftop columns began on 22 August 2017 (in the middle of the sub-tropical dry season in Brisbane). The results for the sand tailings for the first 45 days or so are shown in Figures 8 and 9. Figure 8(a) shows potential evaporation rates having daily fluctuations, of up to 8 mm/day during daylight hours (almost twice that produced by the infrared lamp in the laboratory), dropping to zero during the night due to condensation. Figure 8(b) shows daily ambient temperatures fluctuating between about 10°C and 35°C, increasing over time as summer approaches. Greater daily temperature fluctuations are seen within the sand tailings. Desiccation started at day 11 when the surface water had evaporated, as seen in Figure 8(c). Desiccation was largely limited to the upper 6 cm, and was initially most pronounced at 1 cm depth. It was largely complete after about 30 days of dry conditions (less than half the 70 days indicated by the laboratory simulated desiccation column test on the sand tailings). After 40 days of desiccation, only the top 1 cm of the sand tailings was dry, and some desaturation had reached a depth of only 6 cm. Cumulative water loss was negligible, since drying was limited to very shallow depth. Accompanying desiccation, the surface of the sand tailings shrunk only 2.75 cm, indicating an average dry density for this very thin desaturated upper layer of 2.50 t/m³. Matric suction in the sand tailings were negligible, due to the inability of the dry sand tailings to sustain matric suction. Rainfall events occurred at days 40 (about 40 mm) and 44 (minor rainfall), which temporarily wet-up the desiccated surficial sand tailings.

Profiles of degree of saturation with depth at 10-day intervals during the sand tailings rooftop column test are shown in Figure 9. These profiles again suggest that flow is occurring in two directions: (i) dominant upwards flow driven by evaporation, which diminished with time and depth, and (ii) minor downwards flow below a depth of about 0.06 m driven by gravity drainage, which appears to continue over time.

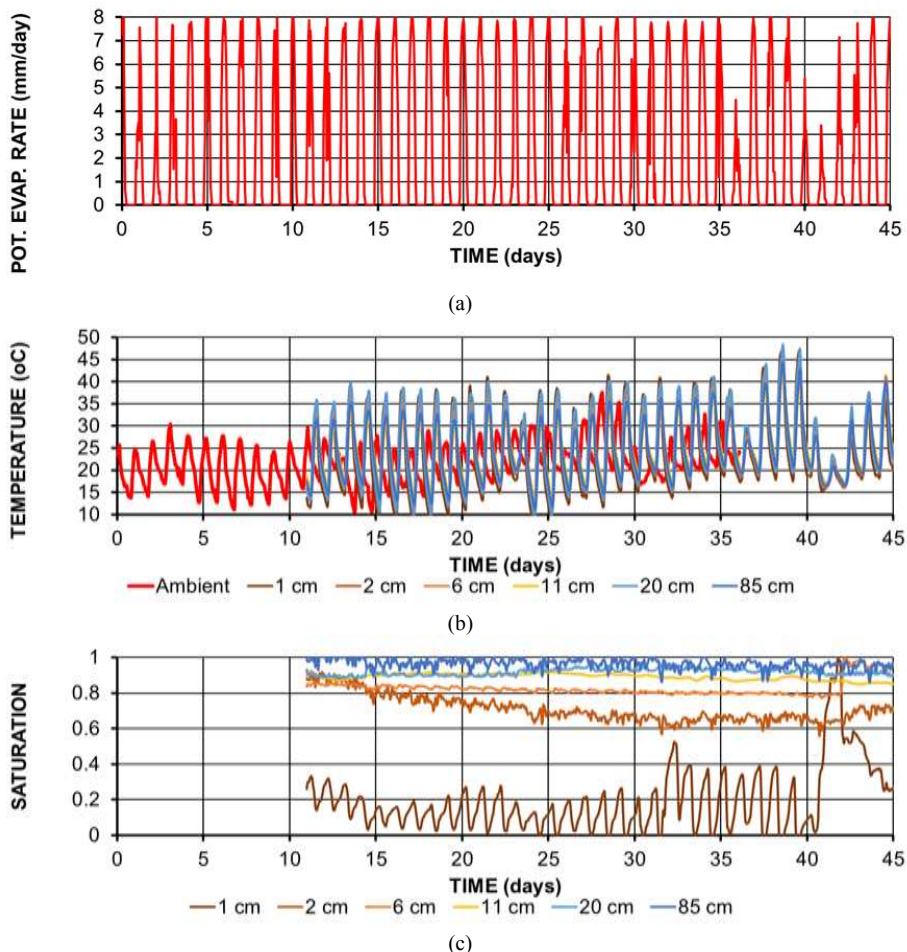


Figure 8. Sand tailings rooftop column test results: (a) potential evaporation rate, (b) temperature, and (c) degree of saturation versus time at various depths.

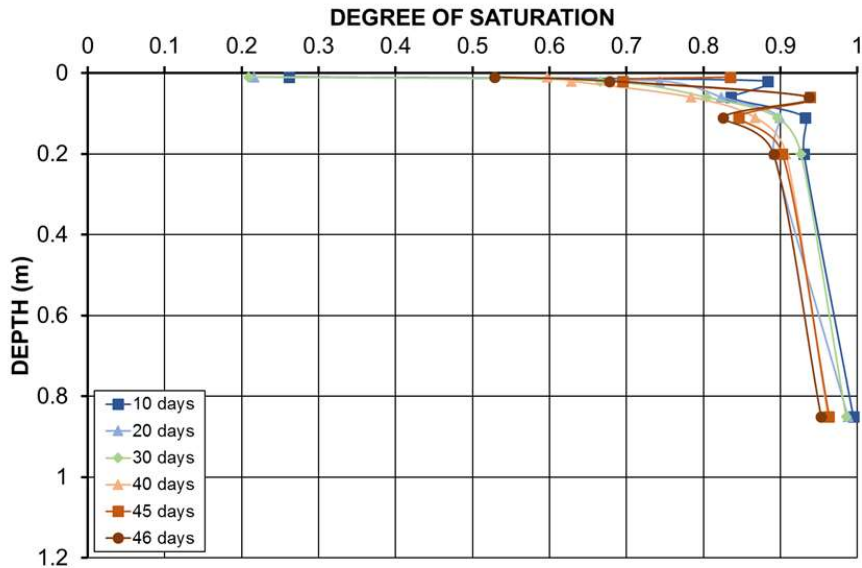


Figure 9. Profiles of degree of saturation with depth at 10-day intervals during sand tailings rooftop column test.

3.4 Slimes rooftop column test

The results for the slimes rooftop column are shown in Figures 10 and 11. Desiccation was largely limited to the upper 30 cm, and was initially most pronounced at 1 cm depth, as shown in Figure 10(b). It was largely complete after about 25 days, when the top 30 cm of the slimes was dry, and some desaturation reached a depth of 60 cm. Desiccation was essentially complete after about 25 days of dry conditions (less than half the 70 days indicated by the laboratory simulated desiccation column test on the slimes). Cumulative water loss was about 15 cm, indicating an average gravimetric moisture content for the desaturated upper layer of 50.0%. Accompanying desiccation, the surface of the slimes shrunk about 14 cm, indicating an average dry density for the desaturated upper layer of 2.18 t/m^3 . Figure 10(c) shows that matric suctions in the slimes were high, varying with daily fluctuations in evaporation rate and saturation, and rainfall events, and reached 60 cm depth. The rainfall event at day 40 wet-up the desiccated slimes to a depth of about 30 cm.

Profiles of degree of saturation with depth at 10-day intervals during the slimes laboratory column test are shown in Figure 11. These profiles again suggest that flow is occurring in two directions: (i) upwards flow driven by evaporation, which diminished with time and depth, and (ii) downwards flow below a depth of about 0.4 m driven by gravity drainage, which diminished over time as the slimes desaturated and lost permeability.

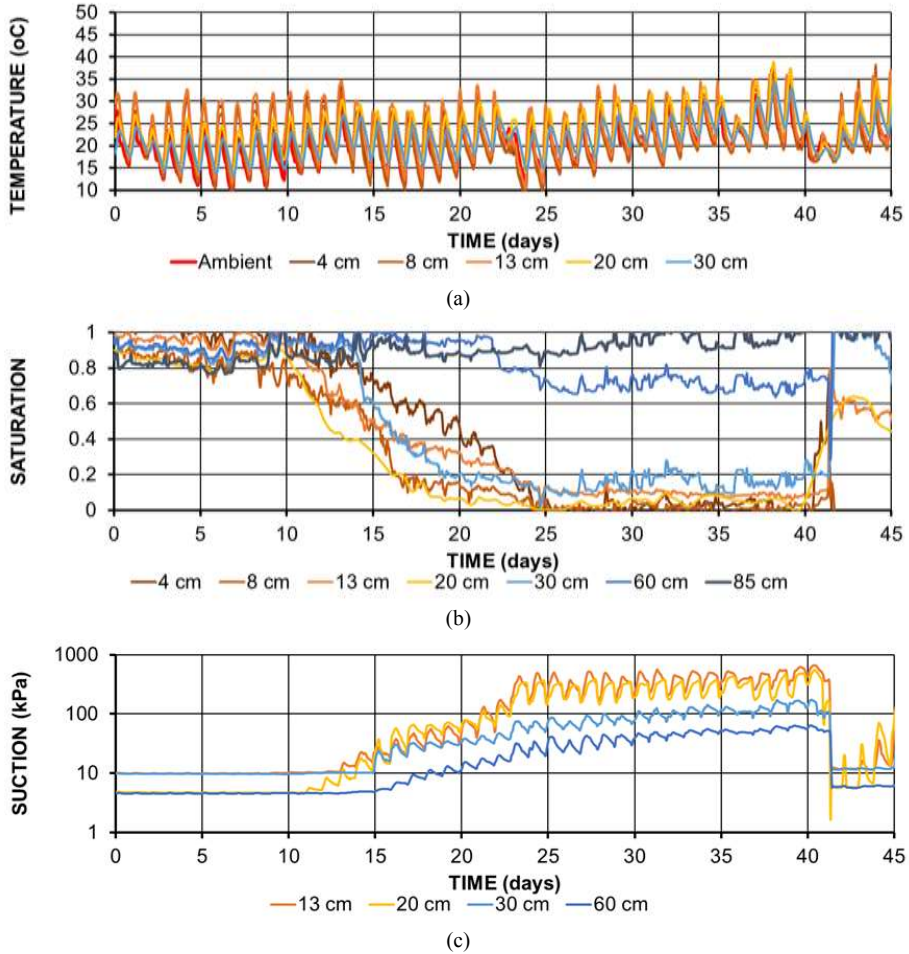


Figure 10. Slimes rooftop column test results: (a) temperature, (b) degree of saturation, and (c) matric suction versus time at various depths.

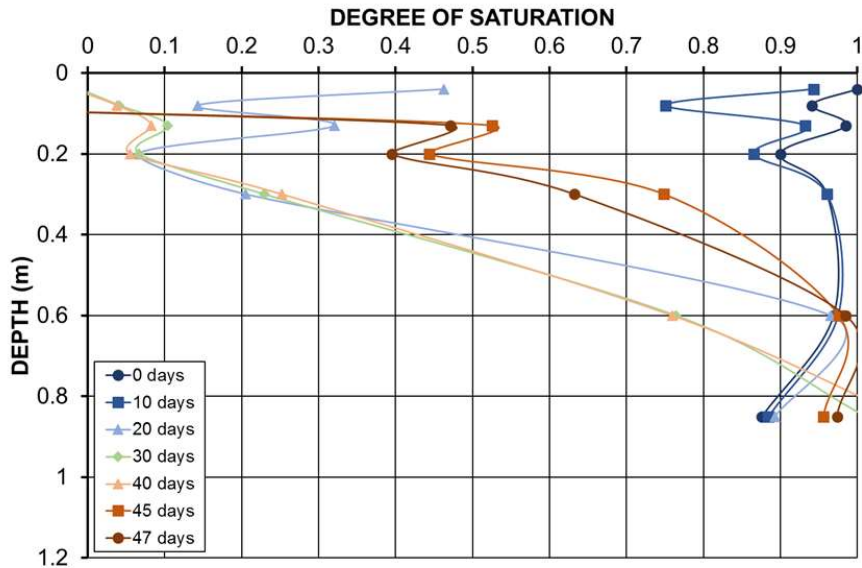


Figure 11. Profiles of degree of saturation with depth at 10-day intervals during slimes rooftop column test.

3.5 Summary of instrumented column test results

In summary, the instrumented column tests on the iron ore sand tailings and slimes showed the following results:

- All of the column test results suggested flow in two directions:
 - Upwards flow, driven by evaporation, which diminished with time and depth, and ceased due to sealing by the surface crust that formed.
 - Downwards flow below a certain depth, driven by gravity drainage towards the sealed base of the column, which also diminished with time and depth.
- Simulated desaturation in the laboratory using a heat lamp was complete after about 70 days for both the iron ore sand tailings and slimes.
- Desaturation under prevailing dry weather conditions was complete after about 30 days for the sand tailings and about 25 days for the slimes, indicating that natural drying is over twice as intense as simulated drying.
- Desaturation dropped off approximately exponentially with depth, and reached depths of approximately:
 - 70 cm for the sand tailings in the laboratory column test, causing a water loss of about 18 cm, a surface settlement of about 9.5 cm, and reducing the gravimetric moisture content of this layer from the settled value of about 40% (dry density of 1.33 t/m^3) to an average desaturated value of 22.0% (average dry density of 1.67 t/m^3).
 - 60 cm for the slimes in the laboratory column test, causing a water loss of about 35 cm, a surface settlement of about 15 cm, and reducing the gravimetric moisture content of this layer from the settled value of about 65% (dry density of 1.10 t/m^3) to an average desaturated value of 30.5% (average dry density of 2.25 t/m^3).
 - Only 6 cm for the sand tailings in the rooftop column test, resulting in negligible water loss, a surface settlement of only 2.75 cm, and an average dry density for this very thin desaturated upper layer of 2.50 t/m^3 . The drying intensity of the sun and wind appears to have closed off desiccation.

- 60 cm for the slimes in the rooftop column test (the same depth as in the laboratory column, causing a water loss of about 15 cm, a surface settlement of about 14 cm, and reducing the gravimetric moisture content of this layer to an average desaturated value of 50.5% (average dry density of 2.18 t/m³). This result was similar to that obtained in the laboratory, except that it occurred in less than half the time.

4 CONCLUSIONS

The results of instrumented column tests on iron ore sand tailings and slimes from a slurry state, carried out under simulated desiccation using a heat lamp in the laboratory and under atmospheric conditions, have been described. The laboratory column test results show that desaturation of the tailings by a combination of evaporation and gravity drainage occurs to relatively shallow depth of 60 to 70 cm and takes about 70 days. Atmospheric drying was found to be over twice as rapid as drying under a heat lamp in the laboratory, taking 25 to 30 days. Under atmospheric drying, the sand tailings underwent minimal desaturation to a very limited depth of about 6 cm, apparently due to the more intense atmospheric drying closing off desiccation. The slimes subjected to atmospheric drying demonstrated similar desaturation to that obtained in the laboratory, except that it occurred in less than half the time.

For the sand tailings, the results of the rooftop instrumented column tests suggest that there is little to be gained from atmospheric drying. However, the sand tailings would be expected to settle rapidly to a relatively high dry density of about 1.33 t/m³, which would increase further under the loading imposed by further sand tailings being deposited.

For the slimes, an optimal layer thickness for desaturation of the order of 60 cm is suggested, requiring about a month to achieve under the atmospheric conditions prevailing at the time of the test. This would result in settlement of about 15 cm (25% of the layer thickness), and a doubling of the dry density of the slimes from a settled value of about 1.1 to about 2.2 t/m³ on desaturation.

5 REFERENCES

- Hook, W.R., Ferré, T.P.A. & Livingston, N.J. 2004. The effects of salinity on the accuracy and uncertainty of water content measurement. *Soil Science Society of America Journal*, 68(1): 47–56.
- Shokouhi, A. & Williams, D.J. 2015. Settling and consolidation behaviour of coal tailings slurry under continuous loading. *Proceedings of Tailings and Mine Waste 2015, Vancouver, Canada, 25-28 October 2015*, 263–274. Vancouver: University of British Columbia.
- Shokouhi, A., Williams, D.J. & Ridgway, T.H. 2016. Settling and consolidation behaviour of red mud slurry under constant rate and incremental loading. *Proceedings of Tailings and Mine Waste 2016, Keystone, CO, USA, 2-5 October 2016*, 85–94. Fort Collins: Colorado State University.
- Williams, D.J. & Zhang, C. 2017. A suite of tests for designing slurried tailings deposition. *Proceedings of 4th International Seminar on Tailings Management, Santiago, Chile, 12-14 July 2017*, 9p. Santiago: Gecamin.
- Zhang, C., Williams, D.J. & Shokouhi, A. 2016. Settling, self-weight consolidation and desiccation of coal mine tailings in a laboratory column. *Proceedings of Tailings and Mine Waste 2016, Keystone, CO, USA, 2-5 October 2016*, 95–104. Fort Collins: Colorado State University.

Essential Issues for Testing and Modeling of Tailings Exhibiting Creep

D. Perić

Kansas State University, Manhattan, Kansas, USA

G. Gjerapić

Golder Associates Inc., Denver, Colorado, USA

D. Znidarčić

University of Colorado, Boulder, Colorado, USA

ABSTRACT: One of the main objectives in management of mine waste and tailings is development of reliable predictions of settlement with time to allow accurate prediction of storage capacity. For tailing materials for which settlement rates are controlled by both hydraulic conductivity and creep behavior, reliable predictions need to account for both of these processes. During the phase of settlement dominated by the dissipation of excess pore pressures, which is also known as primary consolidation, these processes may occur simultaneously and it may not be possible to separate them from each other. Consequently, creep effects are often considered negligible or non-existent when estimating primary consolidation settlements in engineering practice. The phase of the settlement process referred to as the secondary compression is dominated by creep effects and is assumed to start when excess pore pressures become relatively small or negligible by most engineering practitioners.

To address the creep component that develops during primary consolidation, most of the existing creep models effectively extrapolate laboratory creep measurements backwards in time. To address non-uniqueness of the void ratio – effective stress relationship, these creep models often require definition of the reference void ratio – effective stress relationship for predicting settlements in the field.

This paper discusses several currently employed approaches for modeling creep effects and evaluates their applicability to predicting rate of settlement in tailing ponds. Both, the laboratory testing and numerical modeling requirements specific to tailings consolidation and creep are examined. A new model is proposed along with the material testing and model calibration procedures.

1 INTRODUCTION

1.1 Background

One of the main objectives in management of mine waste and tailings is development of reliable predictions of settlement progression that are necessary for a proper design of tailings disposal facilities. Settlement rate is primarily controlled by hydraulic conductivity but some tailings may also exhibit significant creep effects. It has been well established through applications in the engineering practice that the finite strain consolidation theory (Gibson et al., 1967) provides reliable settlement predictions for tailings that do not exhibit a significant creep. Nevertheless, there is a growing number of indications that some tailings are likely to manifest a significant creep, especially polymer treated materials. For these materials, primary consolidation and creep occur simultaneously during the initial phase of settlement and they cannot be separated from each other. The subsequent phase of settlement, also known as secondary compression, begins at the time when the settlement rate controlled by creep becomes larger than the settlement rate controlled by

hydraulic conductivity. Consequently, a reliable settlement prediction for tailings that exhibit significant creep requires an augmentation of the finite strain consolidation theory that accounts for creep. The required modification needs to be based on a sound theoretical background and validated against laboratory experiments and field observations.

To this end, a literature overview is provided covering the presently available models for prediction of creep. A new model is proposed along with the corresponding material testing and model calibration procedures.

1.2 Overview of Creep Models

A void ratio (e) - vertical effective stress (σ') relationship for 1D compression of fine grained soils is typically obtained from either 24-hour incremental loading (24HR) or multi-step incremental loading (MSL) oedometer tests that are conducted on thin laboratory samples. In the former case, a new load increment is applied every 24 hours while in the latter case a new load increment is applied only after the tested material has reached a so-called end of primary consolidation (EOP) for the previous load increment. While different authors have defined the EOP differently, it should ideally correspond to the state at which the rate of creep-induced settlement becomes larger than the rate of the settlement controlled by hydraulic conductivity. To this end, we propose the term Reference Compressibility Relationship (RCR) for the void ratio-vertical effective stress relationship obtained for such state noting that, theoretically, the primary consolidation never ends and that the EOP condition is not reached at the same time at all points within the consolidating layer. Thus, RCR is introduced to avoid any ambiguity as to what the void ratio effective stress relationship represents. This is especially important when modeling field conditions where the EOP may or may not include any creep as advocated by various authors. Due to the 1D nature of the experiment, vertical effective stress will be referred to as effective stress while vertical strain will be simply referred to as strain.

In a material that does not exhibit any creep, RCR obtained from MSL test and $e-\sigma'$ relationship obtained from 24HR test should be equal to each other provided that 24 hours is sufficient time to reach the end of the hydraulic conductivity controlled consolidation. Consequently, the $e-\sigma'$ relationship given by RCR is unique for these materials. In contrast, if a material exhibits creep, the amount of creep deformation that has accumulated by the end of each load step in 24HR and MSL tests will be different. As a result, the $e-\sigma'$ relationships from these two tests will be different, implying non-uniqueness of the void ratio-effective stress relationship. For example, Been and Sills (1981) observed time-dependence of void ratio-effective stress relationships at low effective stresses. Sills (1998) attributed the observed non-uniqueness of these $e-\sigma'$ relationships to creep effects.

For modeling purposes, the non-uniqueness of $e-\sigma'$ relationships can be resolved by introducing additional variable related to time. Most recent models use the time rate of change of void ratio (\dot{e}) or strain ($\dot{\epsilon}$), thus enabling the definition of a unique relationship between the void ratio, time rate of change of void ratio (or strain), and effective stress. This relationship represents a creep law allowing for augmentation of consolidation settlements beyond those controlled solely by hydraulic conductivity (i.e. controlled by dissipation of excess pore pressures).

An example of a unique relationship between σ' , e and \dot{e} is depicted graphically in the form of set of parallel lines in the void ratio - logarithm of effective stress coordinate system shown in Figure 1. The rate of change of void ratio is constant for effective stress void ratio pairs that are located on a given line. These lines were first introduced by Šuklje (1957) and have been known as isotaches since then. The top line corresponds to the highest rate of change while the bottom line corresponds to the lowest rate of change of void ratio, i.e. the infinitesimally small change of void ratio with time. A superscript “ ir ” associated with the rate of change of void ratio (\dot{e}) in Figure 1 denotes the fact that an isotache represents visco-plastic, and therefore irreversible, deformation of the soil matrix. Furthermore, this deformation is analogous to delayed compression defined by Bjerrum (1967) denoting change in void ratio at constant effective stress for a given duration of sustained loading, e.g., the change in void ratio from point A to B in Figure 1 indicates deformation at constant effective stress during the period of time for which the rate of change of void ratio decreases from \dot{e}_1^{ir} (point A) to \dot{e}_3^{ir} (point B). The isotaches are not necessarily straight lines. For example Watabe et al. (2008) and Watabe et al. (2012) presented experimental data that indicate that they are curves in $e - \log \sigma'$ coordinate system.

Degago et al. (2011) pointed out that early researchers who studied creep including Šuklje (1957), Bjerrum (1967) and Janbu (1969) assumed that any combination of void ratio (or strain), effective stress and rate of change of void ratio (or strain) is unique throughout both, the primary and secondary consolidation phases. Bjerrum (1967) introduced decomposition of the total settlement into the instant compression and delayed compression. While the latter was clearly defined to occur at the constant effective stress the former appears to correspond to the compression that would occur in case that pore water pressures were incapable of slowing down the compression, thus resulting in the instant transfer of the externally applied pressure onto the effective stress. Bjerrum (1967) also referred to instant compression as compression during sedimentation. Garlanger (1972) referred to any combination of effective stress and void ratio that would be located at the outer most or the top most line or so called instant line as the state in which the soil structure is just capable of supporting the applied pressure. If a soil could dissipate the load induced excess pore pressure instantaneously, the instant line would be located above the RCR as depicted by the dashed line with the rate of change of void ratio, \dot{e}_0^{lr} , in Figure 1. Christie and Tonks (1985) argued that the physical basis for instant line, which limits the rate of delayed settlement, is not clear. They defined the limit time line using the $\log e - \log \sigma'$ coordinate system implying a single value of instant compressibility, which is elastic in nature. Christie and Tonks (1985) also defined the time associated with their limit time line by extrapolation of $\log e - \log t$ data whereby t denotes time. Watabe et al. (2012) limited the set of isotaches from the bottom by associating the most bottom isotache with the infinitesimally small strain rate. It is noted that in soils that do not exhibit creep all isotaches coalesce into a single line or curve that defines the unique void ratio effective stress relationship.

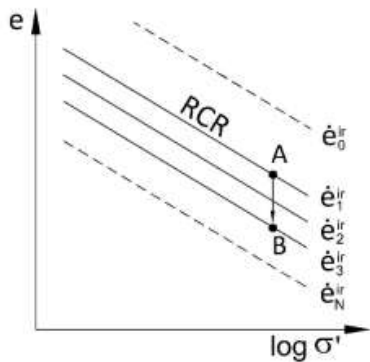


Figure 1. Illustration of time-dependent change of void ratio – “isotache” model

In summary, the authors that advocate simultaneous occurrence of primary consolidation and creep have extrapolated isotaches above RCR into the primary consolidation range. e.g., Szavits-Nossan (1988) and Hawlader et al. (2003) used this approach. Results from Watabe and Leroueil (2015) indicate the use of a similar methodology, however, it is difficult to provide a definite conclusion as they did not present details of their finite element analysis.

A new approach, not relying on extrapolation of isotaches into the range of hydraulic conductivity controlled consolidation, is presented herein. Nevertheless, accompanying calibration of the constitutive model accounts for occurrence of creep during the hydraulic conductivity controlled consolidation.

2 CREEP MODELING FOR SOFT TAILINGS SLURRIES

Modeling of soft tailings slurries often requires capturing relatively large differences in surface void ratio during the sedimentation/consolidation process, i.e. it requires incorporation of soil

creep (Sills 1998). For general engineering problems, the use of a reference time parameter that corresponds to the end of primary consolidation process is often considered impractical. Hence, the proposed approach adopts the relationship in the form $e = f(\sigma', \dot{\epsilon})$ commonly suggested in the literature (see e.g., Leroueil et al. 1985).

The proposed approach and the corresponding numerical implementation is similar to the methodology proposed by Szavits-Nossan (1988) and Imai (1995), who developed models based on the assumed: 1) linear e -log σ' relationship (using the compression index C_c , the initial void ratio, e_0 , and the initial effective stress, σ'_0 , to describe referent compressibility curve), 2) linear e -log k relationship (i.e. using the hydraulic conductivity parameter C_k and the referent permeability value, k_0 , to define functional dependence between the hydraulic conductivity and the void ratio), and 3) linear e -log t relationship (using the secondary compression parameter C_α to describe irreversible changes in void ratio with time). The proposed model was developed with the primary goal to analyze experimental data for which permeability and creep-controlled phenomena cannot be distinguished in a consolidation experiment. The model allows for a more flexible treatment of input parameters and underlying physical mechanisms based on the following changes:

- Characteristic (“yield”) function can be replaced by the arbitrary $e = f(\sigma', \dot{\epsilon})$ relationship determined from experimental data. The model allows for a non-linear e -log t (or e -log $\dot{\epsilon}$) relationships, i.e. it avoids reliance on a single parameter, C_α , to define the time-dependent change of void ratio at constant value of effective stress.
- The model allows for the conventional consolidation approach if tailings settlements are dominated by the dissipation of excess pore pressures (i.e. if tailings deformation is governed by hydraulic conductivity values). Creep mechanism is activated at some threshold value determined from laboratory data.
- Implemented numerical model allows for the input of general compressibility and permeability relationships, i.e. the model is not constrained by a pre-defined constitutive relationships with a constant compression index.

Validation of the proposed model is illustrated in Figure 2 depicting the numerical predictions of the pore pressure at the bottom of the sample according to the well documented creep model adopted by Yuan and Whittle (2013), i.e. the model using linear $e - \log t$ relationship to describe time-dependent change of void ratio, and the model proposed herein. The magnitude of corresponding maximum strain is approximately 12 percent.

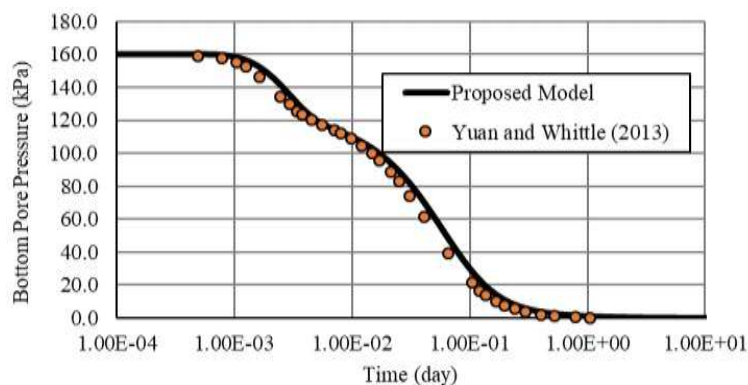


Figure 2. Proposed model vs. Yuan and Whittle (2013) results – excess pore pressure

Comparison of the predicted void ratio change with time according to both of the above models is presented in Figure 3.

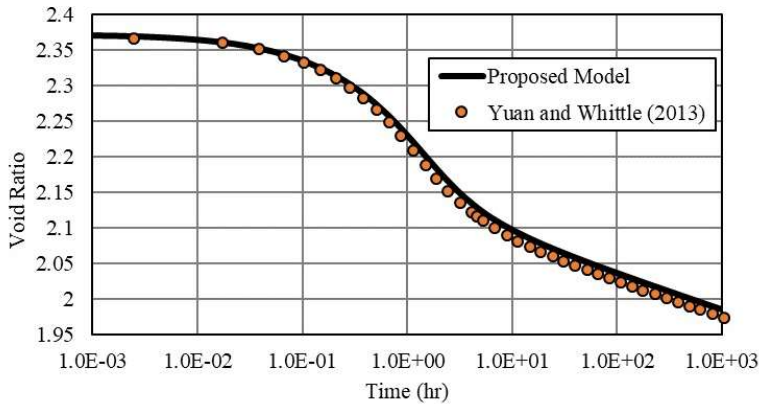


Figure 3. Proposed model vs. Yuan and Whittle (2013) results – average void ratio

The model was also validated using the large-strain consolidation results for phosphatic clays (Mc Vay et al. 1986 and Fox and Berles 1997), i.e. using results for the tailings exhibiting deformation in excess of 40 percent. A comparison between the performance of the proposed model and the benchmark large-strain consolidation model is presented in Figure 4.

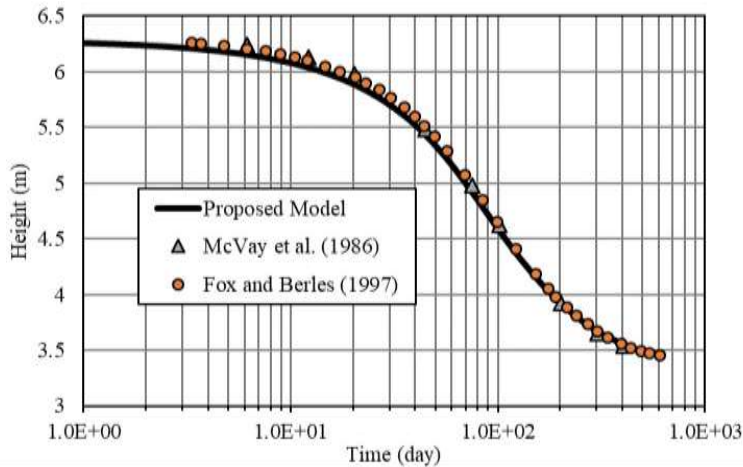


Figure 4. Proposed model vs. large-strain consolidation results (Mc Vay et al. 1986 and Fox and Berles 1997) for phosphatic clay sample

Results in Figure 4 demonstrate favorable match between the proposed model and the benchmark large-strain consolidation results for “soft” phosphatic clays reported in the literature. In addition, the proposed model is capable of capturing time-dependent deformations as illustrated in Figures 2 and 3. Therefore, the implemented numerical scheme provides flexibility to model behavior of soft tailings slurries while distinguishing the permeability controlled deformation rate from the creep controlled deformation rate. The model was developed with the primary goal to analyze experimental data for which permeability and creep-controlled phenomena cannot be distinguished in a consolidation experiment conducted on an individual soil sample, e.g. data reported by Sills (1998), which are shown in Figure 5. Figure 5 demonstrates the discrepancy between the observed creep behavior for a soft tailings deposit (bauxite mining waste) and the

theoretical behavior predicted by conventional creep models such as the model illustrated in Figure 1.

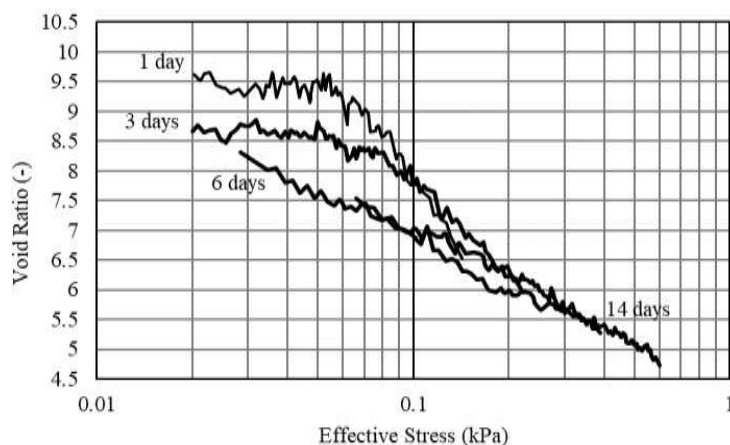


Figure 5. Time-dependent change of void ratio for bauxite mining waste – after Sills (1998)

The work on advancing the model to capture general creep behavior of soft tailings slurry, such as observed for bauxite mining waste and oil sand tailings, is on-going.

3 PARAMETER DETERMINATION FROM LABORATORY TESTS

The parameters required for creep modeling need to be determined from laboratory tests on tailing samples that capture both consolidation and creep behavior of the material. The following procedure is proposed to establish the $e = f(\sigma', \dot{e})$ relationship. The sample is subjected to a minimal seating load of say 0.01 kPa (though for practical purposes a value of 0.1 kPa is likely to be sufficiently low) and the resulting settlement is recorded for the duration of about a week. In some cases, longer periods of time might be warranted. The hydraulic conductivity is measured at that time under very low gradient to minimize the void ratio variation along the height of the sample. The Seepage Induced Consolidation Test Analysis might be necessary to properly account for the void ratio variation within the sample during the test (Abu-Hejleh et al. 1996).

The sample is then loaded to the subsequent loads of the desired magnitude (say 1, 10, 100 and 1000 kPa) to cover the stress range of interest in the field. Again, the settlement is recorded for each increment over a week or longer and the hydraulic conductivity is measured at the end of each settlement monitoring period.

The final points for each load provide the initial estimate of the void ratio - effective stress and void ratio - hydraulic conductivity relationships for the material. These relationships are used in analyses in which each load increment is simulated using a nonlinear finite strain consolidation model and the settlement with time from the model is compared to the recorded data from the experiment. For materials not exhibiting measurable creep in the time frame of the experiments, a good agreement between the settlement predictions and measured values should be expected. For materials exhibiting creep, the predicted settlement curves will indicate an earlier end of settlement than observed in the laboratory (with predicted/model settlements controlled by hydraulic conductivity of the material) and any recorded settlement after that time (when hydraulic conductivity settlement rate becomes negligible) is attributed to creep.

In order to define the RCR the void ratio effective stress relationship is reformulated by pairing the applied effective stress with the void ratio calculated from sample height at the time when the hydraulic conductivity controlled settlement rate becomes negligible. The test analyses can be repeated with the new void ratio – effective stress relationship as needed until a consistent RCR is obtained. The initial creep rate is then calculated from the collected data at the time when the

hydraulic conductivity controlled settlement rate ceases and its change with time obtained using data from the subsequent available record. A creep model can then be fitted to the data (e.g., a single creep parameter, C_α model) and used for the extrapolation of creep rates beyond the available experimental times. Note that for each load level a different initial value of C_α might be observed and the subsequent observed settlement rates could justify the adoption of a more complex nonlinear creep model (e. g. Watabe and Leroueil 2015).

Two important observations should be made. First, any creep model predicts the change in creep rates with time based on limited test duration in the lab. Selected testing time in the lab depends on the duration of the hydraulic conductivity controlled consolidation and the amount of time that can be allotted to creep monitoring. For most engineering problems, test duration of several days to weeks, and in some circumstances few months, is possible. However, in order to predict settlement rates at field scale, extrapolation of the observed behavior is necessary. Second, the RCR defined in this section incorporates void ratio changes due to changes in the effective stress as well as due to creep accumulated during the hydraulic conductivity controlled settlement. Thus, RCRs obtained from the tests on identical samples of varying height will be different and should not be considered unique for the material. The RCR is simply a “reference” relationship for modeling purposes and as such it is used in the model being developed. A synergy between the model and the testing procedure is essential for any engineering model to be realistic.

4 CONCLUSIONS

Currently used creep models have been developed for soils undergoing time-dependent deformations at relatively large effective stresses and are not capable of capturing time-dependent void ratio changes for soft tailings deposits.

The proposed numerical model utilizes the large strain consolidation approach developed by Gibson et al. (1967) with the addition of reference creep function describing time dependent void ratio changes as a function of void ratio and effective stress based on experimental data. Time-dependent consolidation model parameters require definition of the compressibility, permeability and creep parameters. Compressibility parameters are defined using the RCR determined from compression data at the end of the loading test when the hydraulic conductivity settlement rate becomes negligible. Permeability parameters are determined at the end of loading periods using low hydraulic gradients to minimize sample (void ratio profile) disturbance. Initial estimates of creep parameters are determined from the measured rate of change of void ratio when the hydraulic conductivity controlled settlement ceases and from the subsequent available record.

A synergy between the time-dependent consolidation model and the testing procedure is required to develop a realistic engineering model for soft tailings materials exhibiting creep.

5 REFERENCES

- Abu-Hejleh, A. N., Znidarcic, D., and Barnes, B.L., 1996, Consolidation Characteristics of Phosphatic Clays, *J. of Geotech. Eng.*, ASCE, Vol. 122, No. 4:295-301.
- Been, K., and Sills, G.C. 1981. Self-weight consolidation of soft soils: and experimental and theoretical study. *Géotechnique*, Vol. 31, No. 4:519-535.
- Bjerrum, L. 1967. Engineering geology of Norwegian normallyconsolidated marine clays as related to settlements of buildings. *Géotechnique*, Vol. 17, No. 2:81-118.
- Christie, I.F., and Tonks, D.M. 1985. Developments in time lines theory of consolidation. *Proc. 11th ICSMFE, San Francisco*, Vol. 2, 423-426.
- Degago, S.A., Grimstad, G., Jostad, H.P., Nordal, S., and Olsson, M. 2011. Use and misuse of the isotache concept with respect to creep hypotheses A and B. *Géotechnique*, Vol. 61, No. 10:897-908.
- Fox, P. J., and Berles, J. D. 1997. “CS2: A piecewise-linear model for large strain consolidation.” *Int. J. Numer. Anal. Methods Geomech.*, 21(7), 453–475
- Garlanger, J. 1972. The consolidation of soils exhibiting creep under constant effective stress. *Géotechnique*, Vol. 22, No.1: 71-78.
- Gibson, R.E., England, G.L. and Hussey, M.J.L. 1967. The theory of one-dimensional consolidation of saturated clays. 1. Finite Non-linear Consolidation of Thin Homogeneous Layers. *Géotechnique*, Vol. 17, 261-273.

- Hawladar, B.C., Muhunthan, B., and Imai, G. 2003. Viscosity Effects on One-Dimensional Consolidation of Clay, *Int. J. Geomech.*, Vol. 3, No. 1: 99-110.
- Imai, G. 1995. Analytical examination of the foundation to formulate consolidation phenomena with inherent time dependence. *Keynote lecture on Compression and Consolidation of Clayey Soil, IS-Hiroshima, Japan*, Balkema, Rotterdam, The Netherlands, 891-935.
- Janbu, N. 1969. The resistance concept applied to deformation of soils. *Proc. 7th ICSMFE, Mexico City*, Vol. 1, 191-196.
- Leroueil, S., Kabbaj, M., Tavenas, F., and Bouchard, R. (1985). Stress-strain-strain rate relation for the compressibility of sensitive natural clays. *Géotechnique*, Vol. 35, No. 2:159-180.
- McVay, M., Townsend, F. and Bloomquist, D. 1986. Quiescent consolidation of phosphatic waste clays, *J. Geotech. Eng. ASCE* 112, pp. 1033-1049.
- Sills, G.C. 1998. Development of structure in sedimenting soils. *Philos. T. R. Soc. A*, Vol. 356, 2515-2534.
- Szavits-Nossan, V. 1988. Intrinsic Time Behavior of Cohesive Soils during Consolidation, Ph.D. thesis, University of Colorado at Boulder.
- Šuklje, L. 1957. The analysis of the consolidation process by the isotaches method. *Proc. 4th ISMFE, London*, Vol. 1, 200-206.
- Watabe, Y., Udaka, K., and Morikawa, Y. 2008. Strain rate effect on long-term consolidation of Osaka Bay clay. *Soils Found.*, The Japanese Geotechnical Society, Vol. 48, No. 4: 495-509.
- Watabe, Y., Udaka, K., Nakatani Y., and Leroueil, S. 2012. Long term consolidation behavior interpreted with isotache concept for worldwide clays. *Soils Found.*, The Japanese Geotechnical Society, Vol. 53, No. 3: 449-464.
- Watabe, Y., and Leroueil, S. 2015. Modeling and Implementation of the Isotache Concept for Long-Term Consolidation Behavior. *Int. J. Geomech.*, Vol. 15, No. 5: A4014006.
- Yuan, Y. and Whittle, A.J. 2013 Examination of Time Dependent Soil Models in One-Dimensional Consolidation, Constitutive Modeling of Geomaterials – Advances and New Applications, Yang, Q., Zhang, J.-M., Zheng, H., Yao, Y. (Eds.), *Proceedings from 2nd Int. Symp. On Const. Modeling of Geomaterials, Beijing, China*, Oct 15-16-, 2012, Springer, pp. 159-166.

Filter-Pressed Dry Stacking: Design Considerations Based on Practical Experience

C. Crystal and C. Hore

SRK Consulting, Vancouver, British Columbia, Canada

I. Ezama

SRK Consulting, Salta, Salta, Argentina

ABSTRACT: Filter pressing is a viable and proven tailings management alternative. Building on the experience at successful dry-stack operations, operating at production rates of up to 30,000 tonnes per day, filter-pressed dry-stacking can be (and is being) considered as an economically feasible tailings management alternative for even higher production rates. The paper presents a discussion of design basis and operational approaches based on the author's direct experience on operational projects in a variety of climatic conditions as well as ongoing feasibility studies for much higher throughputs currently planned. The paper considers limitations of currently available filtering technologies (in particular filterability of various types and grinds of tailings streams and target and achievable moisture contents of the resulting filter cake) as well as geotechnical and geomechanical properties of the filtered tailings relative to design, operations and overall performance of the dry-stack. The paper further describes mechanical conveying equipment and placement (or stacking plan) strategies including considerations with respect to lift thickness, rate of rise and pore pressure generation considerations. The paper highlights the author's experience with successful dry-stacking strategies and addresses some common misconceptions and constraints with respect to geotechnical and hydraulic performance of dry stack tailings, based on actual lab and field data presented. While not necessarily "dry" filter-pressed tailings may be conveyed or transported by trucks and are amenable to stacking and compaction (for structural zones) or placement via conveyor to angle of repose (for non-structural zones) in various stacking approaches. The advantages with respect to water consumption, reduced and/or flexible stack footprints and geometries, seepage control requirements, closure/reclamation costs and public perception of risk can result in dry-stacking being selected as an economically beneficial alternative, particularly if life of mine risks and costs are appropriately considered. As with any conventional tailings management approach, careful and diligent planning, engineering and operational controls, QA/QC; instrumentation and monitoring, is required to manage risks and uncertainties.

1 INTRODUCTION

Filter-pressed dry-stacking (or filtered tailings) has been proven as tailings management alternative for currently operating facilities at production rates of 2,500 to up to 30,000 tpd. A sample of currently operating dry-stack tailings facilities are identified, by daily tonnage, in Figure 1. There are many studies and proposed projects considering significantly higher production rates in the order of 100,000 tpd.

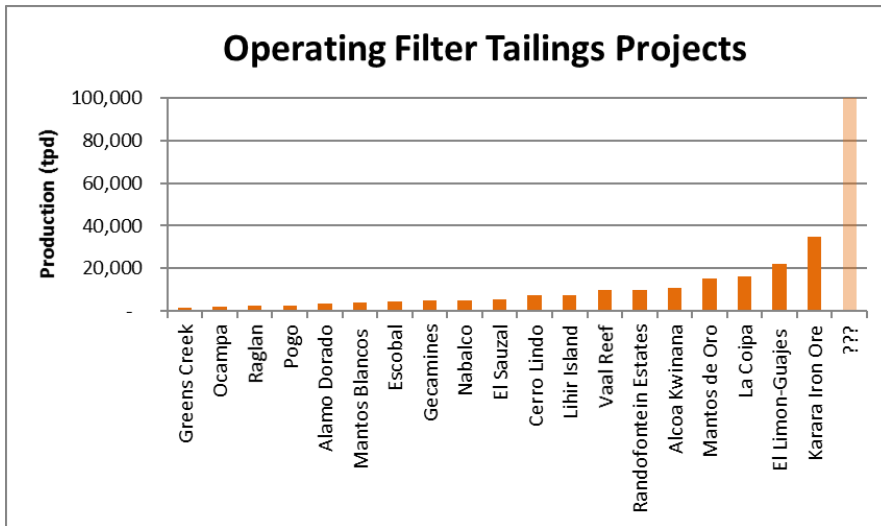


Figure 1. Operating Filter Tailings Project (dry stacks)

However, there remains significant industry uncertainty related to achieving economically viable filtration and stacking at high throughputs (on the order of 50,000 to 100,000 tpd, or more). Concerns related to filtration efficiency (and cost), efficient material handling and placement at high throughputs, operational controls and high operating costs to achieve physical stability are among the challenges to be addressed. The physical stability of 100 to 200 m high planned stacks—a consequence of the planned production volumes on the order of 50,000 to 100,000 tpd or more—warrants careful consideration with respect to design basis assumptions and achievable strength and density of stacked materials, affecting overall performance. Capital (CAPEX) costs for a high production rate dry-stacking operation may be of the same order of magnitude as conventional approaches, but managing operating (OPEX) costs and ultimately closing the gap on cost differential between dry-stacking and conventional slurry and alternative (paste, thickened and cyclone) tailings management alternatives is highly dependent on selected stacking approaches and strategies for managing these identified risks and uncertainties. Haul distance, placement strategy and compactive effort in structural zones, as well as re-handling of off-spec materials can significantly increase the unit cost of a dry stack facility in comparison with a more conventional impoundment. To reduce the risks and uncertainties associated with potentially high OPEX costs requires close interface between owners, designers, operators and equipment vendors in planning and execution stages. Tight constraints and maintaining cost-effective operational controls (including QA/QC, instrumentation and monitoring) for high production rates are also a challenge, but no more than for conventional facilities of similar heights and volumes.

2 FILTRATION

2.1 Filterability

Plate and frame filter-press may be increasing in size (from 2x2 and 2.5x2.5 m to 4x4 and 5x5 m plates), but the fundamental underlying technology has not advanced significantly in the last 20 years. Current advancements in the actual filtration technology seem to be primarily focused on reducing OPEX costs (e.g., more durable filter cloths and process efficiencies with respect to cycle time, air blow, wash cycles, etc.). Nevertheless, almost all tailings are filterable. The question remains at what efficiency (cost) to achieve the desired target moisture contents and whether stacking strategies can overcome the inevitable gap between desired (target) and actually achievable filter cake moisture content. It has been the authors' experience that only some unique residues (e.g., from rare earth metal mines, containing significant amounts of gypsum and other process chemicals) result in material that is truly not filterable. Some typical gradation curves for

a range of dry-stack projects (in which the authors have been involved) are plotted in Figure 2. The percent fines (silt-sized fraction passing the #200 sieve) and clay-sized fraction (< 2 microns) affect the efficiency of the filtration process and the required filter pressures and cycle times, and the resulting consistently achievable filter cake moisture contents, but all have been filterable. The potential for true clay mineralogy as opposed to rock flour with clay sized fraction is important to distinguish when considering filter-pressing efficiency. Significant challenges including clogging of filters can occur, if the clay-sized fraction is truly a clay mineralogy and present in a significant portion of the tailings.

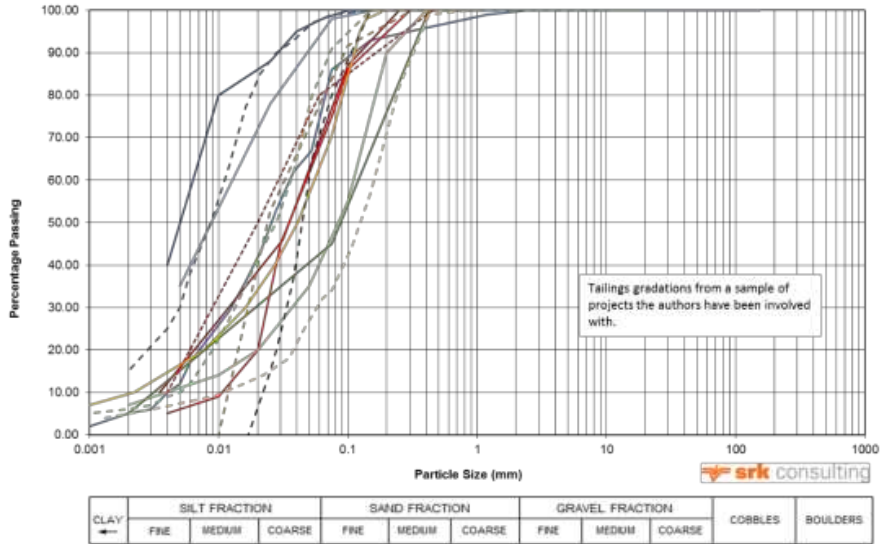


Figure 2. Typical gradation curves, filtered tailings

The tailings engineer has no control over the desired grind for recovery (or gradation of the tailings) or the production processes that may result in tailings stream with significantly different gradations. Nor do engineers and operators have significant control over the variability of the ore which may be the controlling factor in achieving consistently economical filter-pressing. Often, clay mineralogy zones are generally short-lived in terms of life of mine and if this variability is anticipated and accounted for, placement strategies to manage high moisture content (less efficiently filter-pressed) filter cake over relatively short durations can help manage this risk.

Consideration of the potential for variability in the tailings gradation and or percent solids by weight feed to the filter presses are key factors to be considered. Tailings variation has always been present in mining operations but filtration and dry stacking is more sensitive to these variations than conventional storage methods. Often the filter pressing operations can handle short-lived variability in clay content, as long as it's not also compounded by a significant and potentially longer duration variability in the solids feed due to rheological constraints at the thickeners. Engineers and designers should not focus solely on a single or average particle size distribution from a limited pre-production metallurgical or pilot testing tailings sample for planning and design. The range of particle size distributions in Figure 2 could just as easily be considered a range in variability of ore and grind over a number of years (life-of-mine) and this should be kept in mind when considering the potential variability during operations. Often the designer is provided with limited and potentially unrepresentative samples of tailings in the early stages of a project, and it is therefore important that consideration be given to the mine plan and ore body geological information in considering the likelihood for variation in ore properties.

With respect sensitivity to grind variability and/or the variation in particle size distribution from various process streams —where a process stream may result in a much finer gradation and/or represent a greater risk of low efficiency overall than other streams—there is a benefit to filtering the challenging waste streams separately and accepting a lower efficiency of pressure filtration for this single stream, only. Combining the filter cake after the fact, rather than the combined waste streams before filtering, may be more cost effective. Lower efficiency (higher moisture content) streams can be managed by placing in the off-spec (or non-structural zones) of the dry stack. Separate filtering and handling of potentially acid generating tailings streams may also prove to be more effective. These streams may similarly be filtered separately and co-disposed or encapsulated within designated zones of the dry-stack.

2.2 Achievable vs. Target Moisture Contents

When discussing filterability, it is a common misconception that the tailings material can and must be filtered to a specific target moisture content (often cited as 15% in technical literature and by vendors). Three key points are made: 1) an average target moisture content of 15% is just that, a target, and the consistently achievable moisture content is often significantly higher; 2) the volumetric moisture content is several percent higher than the geotechnical (or gravimetric) moisture content; and 3) the “target” moisture content from the filter press (whether defined as volumetric or gravimetric) should be in line with the required facility design criteria, stacking plan and performance and can therefore vary significantly between various facility zones (structural and non-structural) and facilities, depending on location, climate, stack geometry and other factors. For example, the Alcoa Operations in Kwinana, Western Australia, operate a filtered tailings facility with a target moisture content of 30%. This was determined to be the acceptable filter cake moisture content, based on deposition strategy and the arid environment. The Karara operation in Western Australia (see Figure 3) considers the more typical average target moisture content of 15% and average achievable of 18% acceptable, again based on environment, deposition strategy and stack geometry. The Escobal Mine operation in Guatemala has a similar target moisture content of 15% and average achieved moisture content of 18%, however based on high seismic risk and stack geometries an additional target moisture content on the order of 12-13% has been specified as part of stringent compaction requirements in structural zones.

Commonly, projects are specifying (or promising) a target filter-cake moisture at the limit of the filter performance (including at the limit of the thickener’s ability to deliver feed at the required solids ratio). This has caused numerous examples where the operating performance does not consistently meet the target. The authors’ have consistently seen results similar to those presented from the Karara project in Figure 3, with respect to achieved versus target moisture contents. Essentially, irrespective of site, ore body type, or filter press manufacturer, a 15% moisture content remains a typical target, while tracking of day-in and day-out moisture contents of filter cakes demonstrate that achievable moisture contents are often in the range of 17 to 18% when things are running smoothly and can be up to 20 to 23% when off-spec.

The authors suspect this difference in target versus achieved moisture content, irrespective of ore body type, has to do with a variety of limiting factors in combination with specifying the target moisture at the limit of the filter performance: (a) tailings gradation and mineralogy variation; (b) limitations on thickening and rheology controlling the solids content feed to the filter presses; (c) limitations of efficient and cost-effective cycle times with higher fines/lower permeability tailings, and (d) degradation of filter cloths resulting in varied performance for the same tailings material.

Notably, this is also evident in the long term and not just during commissioning. As can be seen in Figure 3 the scatter of the moisture content results reduces with time but the overall trends remain.

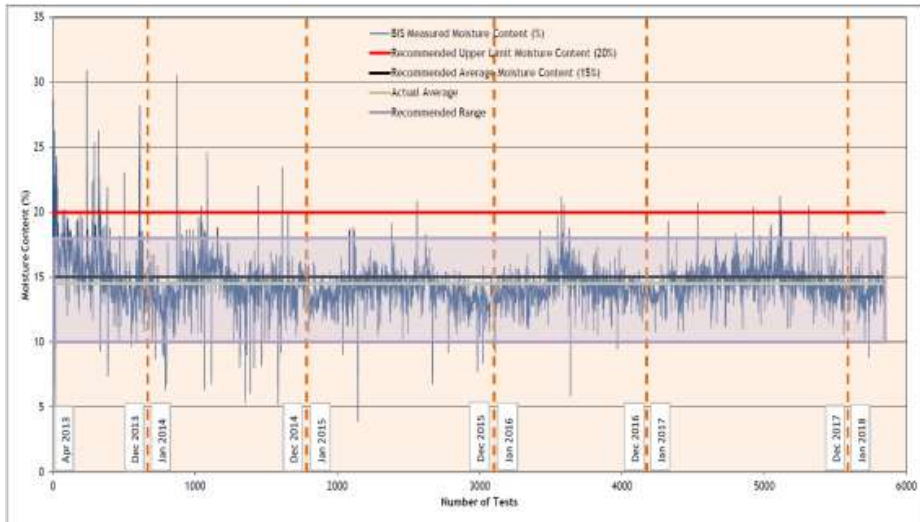


Figure 3. Anticipated target vs. actual range of achievable moisture contents (image source: Nelson Amoah, published materials, April 2018)

Coarser tailings overall will be more efficiently filter pressed and will usually be able to produce filter cakes at moisture contents at or near optimum for compaction, but in general in the range of anticipated grinds achievable moisture contents, at current state of the technology, are generally higher (and often significantly higher) than the optimum required of structural zones. See Figure 4 for definition of structural zones after Lupo, 2010.

As illustrated by Figure 3, “targets” may be cited or promised, but achievable filter cake moisture contents and the variability of the process are not generally within the tailings engineer’s control. The tailings engineer can, however, specify acceptable moisture contents for different areas of the dry stack, depending on stacking strategies. For example, external structural zones may have more stringent criteria than non-structural zones, for which reduced constraints may be allowed. The author’s approach more typically specify target moisture contents at the operating deck, considering conveyance and stacking approaches for achieving specific performance objectives for the overall geotechnical and physical stability of the landform, considering both static and potential seismic loading conditions, drainage, rate of rise, consolidation, and overall stack height and geometries.

2.3 Off-spec tailings

During operations the requirement for off-spec tailings storage is reduced (but not eliminated) after start-up as the processing systems are optimized and stabilized and effective stacking approaches are refined. If the filter plant is set up with multiple presses and redundancies or spares, the likelihood that all the presses going down together are low, and the need for a separate conventional impoundment for off-spec materials (un-filtered tailings) is generally not a requirement during operations, but may be during commissioning. During commissioning, the dewatering systems can commonly underperform. This can be exacerbated with operational efforts often concentrated on the ore processing and mineral recovery systems during this period.

As noted, off-spec materials are commonly defined as materials having moisture contents above 18 percent (or on the order of 20-22 percent), depending on the target moisture content for the facility. What is typically required for managing these materials is an emergency radial stacker and sufficient stacker pad area to provide for temporary storage piles of filter cake. Providing for both a large stacker pad and large operational deck is also of great value to maintain operational flexibility. A temporary storage area(s) of filter cake material placed for 8 to 10 days (at least) via an emergency radial stacker near to the filter building area is recommended for operations, with larger potentially required at commissioning. Operational flexibility on-deck should also be

provided with back-up plans for truck transport and dozer pushes if mobile stacker and conveyor systems do not have sufficient redundancy. For conveyor transport systems, it is more likely that the conveyor system and mobile stackers would need a back-up plan.

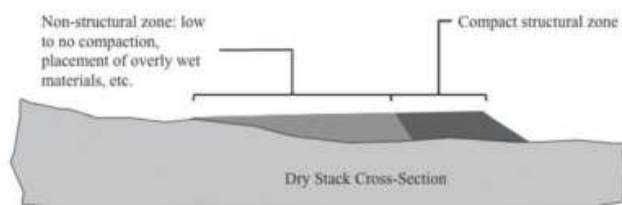


Figure 4 Consideration of a Structural (Compacted) Stability Zone (Davies, Lupo et al 2010)

3 STACK / LANDFORM PLANNING, DESIGN AND CONSTRUCTION

3.1 Climate

Achieving a physically stable landform in wet and cold environments will not be accomplished in the same way (i.e. with the same disposal strategy and operational requirements) as in an arid locale. Moreover, scalability of solutions may become highly non-economical if the approach for achieving a physically stable landform becomes operationally demanding. Therefore, as any other type of tailings facility design, climatic conditions and production scale will have a great impact on the design and operational approaches to dry-stacking.

Arid climates have been the first to embrace higher production rate dry stacking projects, typically driven by the economics and scarcity of water for processing, but also due to permitting and land acquisition constraints. Dry stacks in these climates can utilize the high evaporation potential to further enhance the dewatering process and ensure the stack will remain unsaturated. Deposition in thin lifts/faces over large areas can result in significant additional drying of the tailings. However, it should be noted that transport and deposition by trucking and compaction will limit impact and effectiveness of evaporative drying. Facilities with conveyor stacking arrangements placing loose material in thin faces will achieve higher evaporative drying, but this may still be limited to the outer few centimeters depending on stacking cycle time.

Wet climates face additional challenges with surface water management and typically must employ active management of the operating deck to facilitate high run-off. Radial stackers, stacking filtered materials in relatively steep piles that readily shed water during intense storms is also one operational approach that has been implemented.

Cold climates—defined here as climates where freeze back of tailings can be expected in the short or long term—can and do successfully employ dry stacking technology. The Raglan Project (Quebec, Canada) and Pogo Project (Alaska, USA) are two examples of operational facilities in cold climates. In addition, the Hope Bay Project (Nunavut, Canada) has a designed dry-stack facility undergoing final permitting and expected to be developed in the next few years. Freeze back of the tailings can be advantageously used in these environments to improve stability and minimize seepage potential. A common industry concern is the freezing of tailings prior to placement causing issues with equipment and post placement density. This is a balance of transport method and time with climatic conditions. The authors have found that this is typically not an issue even in the high arctic when transporting with trucks. Thermal modelling for conveyor transport can be undertaken to determine the maximum exposure period for the tailings at a given climatic conditions. It is also noted that freezing of the tailings, post placement and compaction, will result in a reduction in dry density of the placed tailings and an active layer will develop in the stacked landform. The freeze-thaw impacts and associated density reduction should be considered in stability analyses of the stacked landform.

3.2 Conveyance and Transport and Deposition

Either trucking or conveying can be used effectively for filtered tailings. The decision is typically driven by the economics of the project. Typically, the authors have found that trucking as the primary transport methodology is only cost effective for production rates below 10,000 tpd. For higher production rate operations, conveyance, including mobile stackers and innovative stacking approaches utilizing long-reach radial stackers, is typically required to minimize placement and handling (including re-handling) costs.

The filter cake is generally amenable to conveyance and transport at higher moisture contents than are acceptable for stability zones. As such, alternative methods of materials drying and handling (including solar and wind evaporation) of thin lifts may be required to achieve desired moisture contents and densities for the overall physical stability of the stack. Target density can be achieved by compaction of structural zones, but several approaches have been used for reduction of moisture content post filtering including thin lift deposition when advance stacking (such as at Karara, as illustrated in Figure 5). Similarly long-reach, retreating mobile radial stackers are being considered for several planned large tonnage facilities.

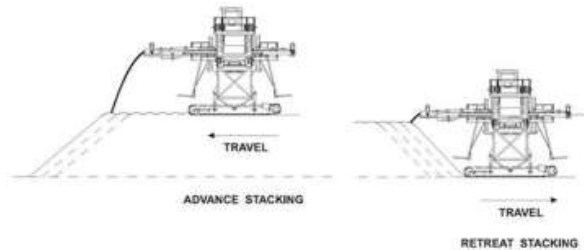


Figure 5 Alternative Stacking Approaches (Luppnow and Hore, 2014)

3.3 Rate of Rise and Pore Pressure Generation

Depending on efficiency of the filters, the variability of the ore, other operational constraints, and poor operational control there is a very reasonable risk that low-density, high-moisture content filtered tailings will be placed within the dry stack. Figure 6, illustrates that at the range of typical target and achievable moisture contents, it is more likely than not that the tailings will behave as a saturated material unless arid conditions prevail and/or other moisture conditioning measures are not taken during placement.

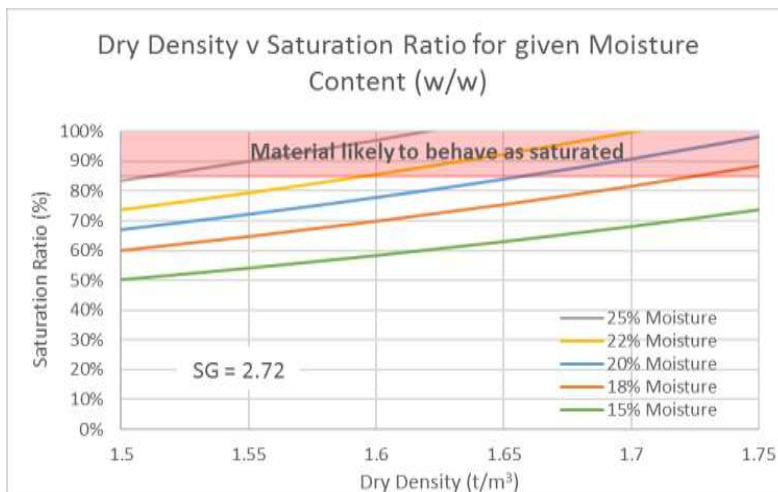


Figure 6 Dry Density vs. Saturation Ratio for given Moisture Contents

As with conventional tailings facilities, managing the rate of rise over critical areas is also particularly important to allow time for consolidation and drainage to occur and for any developed excess pore pressures to dissipate, particularly if the filter cake is placed significantly wet of optimum.

Pore pressures may increase in localized zones, but if the rate of rise is adequately managed to ensure that mobilized stresses are less than the in-situ and/or residual strength of the materials, it is the author's experience that localized excess pore pressures within the stack generally dissipate within a few weeks or months of initial placement of a given lift. Balancing the rate of rise with rigorous instrumentation and monitoring to verify the actual dissipation of pressures once stacked can be a key part of the overall engineering and operational control of the dry stack to minimize and/or mitigate risk, particularly at high placement/production rates. If the tailings become and/or remain saturated, they can be susceptible to pore pressure increases and associated strength reductions as well as static and seismic liquefaction.

Special attention will need to be paid to the drainage conditions base of the stack, as dry stacks are not "dry" and lower layers may become saturated during stacking of subsequent lifts. The basal layer can often be the layer with the most off-spec, high moisture content material as it is placed during commissioning when the operation of the filters are being optimized. This reinforces the need to have adequate off-spec and QA/QC during operations over the entire life of mine to create and maintain a geotechnically stable landform.

3.4 Stacking Height and Overall Physical Stability Performance

Stack heights upwards of 100 m may be pushing the boundaries of the state of empirically based knowledge of the application of this technology, with respect to the stress states and strengths within the stack, particularly if compared with more conventional earthen embankment or dam heights. But this is no more or less true than the heights being pushed with more conventional facilities and cyclone sand dams. These are challenges and do represent risks and uncertainties, but these challenges are within our ability as engineers to evaluate and monitor.

Application of critical state soil mechanics can help us understand the limitations for stacking height (and the response of a given lift to subsequent lifts) with respect to the stacked tailings moisture content and density. Dense materials dilate while loose materials contract during shear to reach a common void ratio at large distortional strain (i.e. the critical void ratio). With respect to filtered tailings, individual lift thicknesses exceeding conventional earthworks compacted lift thickness (on the order 12–18 inches or 0.2 to 0.3 m) will result in stacked tailings that are contractive, regardless of climatic or other stacking conditions.

If filtered tailings are placed in excessive lifts and/or at angle of repose (i.e. not compacted to a dilatant state), they can exhibit contractive behavior under future loading (whether static loading under subsequent lifts, or seismic loading due to earthquake events). Even if dry (unsaturated), low-density lifts on the order of 20 to 30 meters placed with advancing or retreating mobile stackers are still at risk of being contractive in response to subsequent loading (including by the next 30 meter lift). Under shear, contractive tailings could lead to very low static undrained shear strengths, even under static conditions, within the dry stack. Liquefaction of stack can be avoided if the stack (including basal zones) are placed and remain unsaturated and/or the structural zones are placed (and compacted) to an adequately dense (dilative) state. To preclude this, and associated strength loss and excessive deformation of the stack whether static or seismic, key structural stability zones must be compacted to a dilative state, typically requiring mechanical compaction at moisture contents at or slightly dry of optimum.

3.4.1 Co-mingling/Co-disposal

There always remains the alternatives of co-mingling (mixing filtered materials with dryer coarser materials) or buttressing (with amended tailings zones or borrow or waste rock co-disposal) which can significantly reduce the filtering constraints on all or a large portion of the tailings across the life of mine.

These co-mingling/co-disposal and buttressing approaches have their own challenges, risks, and associated operational cost considerations. However, they may offer needed operational flexibility and present a toolbox of approaches when handling increased production, increased

heights, potential for changing conditions and challenging climates (as already demonstrated at several operating stacks), and a number of bench and field-scale pilot studies.

4 SOME ADDITIONAL RISK CONSIDERATIONS

4.1 Infiltration and Seepage

Limiting the potential for excess pore pressures development may also be managed by limiting infiltration or subsequent rewetting of any given lift once placed. In general, if the permeability of the placed filtered tailings is low (on the order of 10^{-6} cm/s or less) the tailings mass can be highly resistant to infiltration and saturation and, in general, seepage within the stack is governed by unsaturated hydraulic conductivities (AMEC 2008).

Operational controls on the upper surface can also manage infiltration and surface water run-on, run-off and ponding to also minimize infiltration to the overall stack. Safety berms around the edges of dry stack need to be carefully placed with adequate outflow points along with grading of the upper surface to ensure ponding and infiltration does not occur at the outer edges. This can be an issue even in arid climates as has been seen at Karara.

Moisture retention and unsaturated hydraulic conductivity characteristics of the filtered and stacked tailings can be established relative to seepage potential. However, in general, there is a finite and limited (transient) volume of entrained water remaining in the filter tailings available to seep (as illustrated in Figure 7) governed by unsaturated flow as compared to significantly higher volumes governed by saturated flow of more conventional facilities.

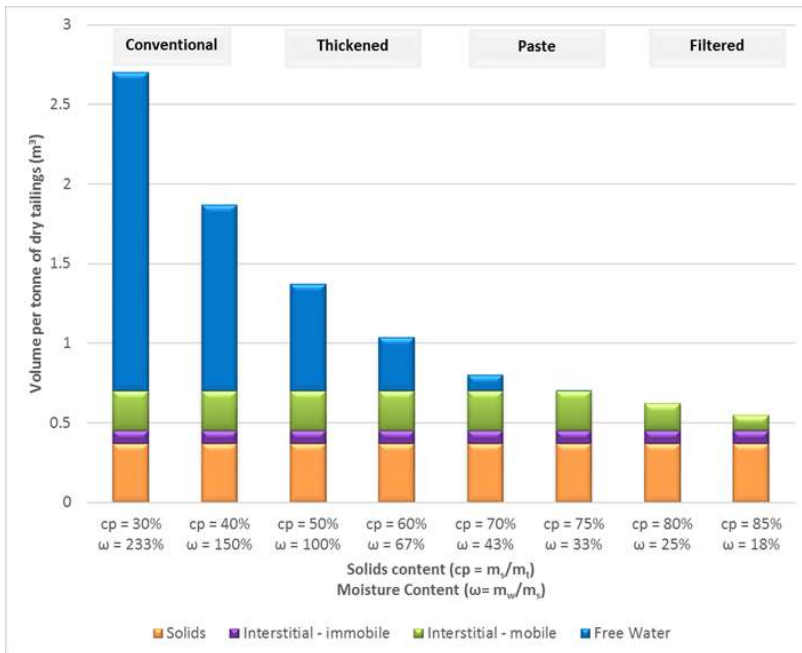


Figure 7 Free vs. Interstitial (mobile and immobile) Water Comparison – Alternative Tailings Technologies

For generally fine grained tailings of relatively low permeability, it has been the author’s experience as previously concluded by Davies and Rice (2001) that with respect to infiltration and seepage:

“If there is proper compaction and maintenance of target moisture contents, seepage is negligible, and instead of creating a complex system to capture seepage that will likely never appear, spend those resources more appropriately on surface water management measures

that include a collection pond downgradient of the dry stack. Resaturation of properly placed and compacted filtered tailings is extremely difficult and not the concern many presume.”

Instrumentation and monitoring for both infiltration and seepage will serve to help manage and mitigate risks and uncertainties.

5 COST AND COST RISK CONSIDERATIONS

Haul distance, placement strategy, and compaction effort in structural zones, as well as re-handling of off-spec materials, can significantly increase the unit cost of a dry stack facility in comparison with conventional storage facilities. To reduce the risks and uncertainties associated with potentially high OPEX costs, a risk management plan including close and ongoing interface between owners, designers, operators, and equipment vendors in planning, design and execution stages is required. Not unlike conventional facilities.

Based on the authors experience on operating dry stacks and engineering estimates performed for current prefeasibility and feasibility dry-stack projects of various production scales, it is our finding that CAPEX costs for dry-stacking do not generally represent a significant increase over conventional tailings CAPEX—at least they are not the determining factor. OPEX, however, for dry stacking approaches can represent a significant differential that may or may not be offset if project wide and life-of-mine costs are appropriately considered. The OPEX for conventional facilities is on the order of \$1.00 tonne. By comparison the OPEX for dry stacking can in the order of \$2.00 to \$3.50 per tonne of dry tailings in the authors’ experience. This range of OPEX dry-stacking is lower than previously published guidance based on older databases and which presumably reflects technologies, operational constraints and potential re-handling considerations of early projects. On the basis of the experience of the operating facilities, constraints are continually being evaluated and optimized as the industry works hard to plan and demonstrate the economic viability of higher production rate dry-stack facilities. More recent preliminary economic assessments have reported lower projected OPEX costs per tonne for planned high tonnage dry-stack projects as reflected above. Further development of the method has and will likely continue to narrow the differential in the range of OPEX costs between conventional and dry-stacking, but the differential is likely to remain at least \$1.00 to \$1.50 per tonne higher than the currently estimated cost of slurry disposal, for the time being.

Offsetting this OPEX differential requires careful, project-specific consideration of all costs and risks, particularly those key cost differentiators that have a very real potential to make up cost differentials over the life-of-mine. These may include land acquisition, water makeup, borrow, liner, reclamation costs, and costs of delays to the project based on permitting and stakeholder perceptions of risk. The risk costs associated with conventional facilities with significantly higher consequences of failure relative to dry stack facilities should be incorporated into the economic assessments.

6 CONCLUSIONS

Filter press tailings facilities have been in successful operation for over 30 years. More and more mines are using or considering the approach. There are limitations and challenges. However, the filter press manufacturers, the design engineers, and the mine operators are rising to the challenges and we can expect more advancements to come. The argument of scale alone should not be used to eliminate dry-stacking as a tailings management alternative.

With the appropriate management of costs and risks, dry stacking is an appropriate technology for tailings management. With a shifting industry, public and regulatory level of risk tolerance, dry stacking will likely continue to become more favorable.

With respect to operational cost differentials (as compared to conventional slurry or cyclone sand dam facilities), it is the authors’ experience that appropriate and holistic consideration of the true life-of-mine costs and risks, as well as appropriate planning and execution of engineering and administrative controls has the potential to further reduce the current differential in OPEX as compared to conventional facilities. The result is the filter-pressed dry stack will more and more be considered an economically viable—and even preferred—option when considering higher tonnage projects.

7 REFERENCES

- AMEC, 2008 " Rosemont Copper Company Filtered Tailings Dry Stacks Current State of Practice Final Report" November, 2008
- Davies, M.P., and S. Rice (2001). An alternative to conventional tailing management — "dry stack" filtered tailings. In proceedings of Tailings and Mine Waste '01, Balkema.
- Davies, Lupo et al 2010, Davies, M.P, & Lupo, J. & Martin, T. & McRoberts, E. & Musse, M. & Ritchie, D., 2010, Dewatered Tailings Practice – Trends and Observations. In proceedings of Tailings and Mine Waste '2010, Balkema.
- DJ Luppnow & CJ Hore, 2014, Karara Iron Ore TSF – design considerations for a unique large scale dry stack facility. Tailings and Mine Waste, 2014

Fine Coal Refuse – 25 Years of Field and Laboratory Testing Data and Correlations

B.E. Genes

GAI Consultants, Inc., Export, Pennsylvania

G. Castro

GEI Consultants, Woburn, Massachusetts

T.O. Keller

GEI Consultants, Carlsbad, California

F. Ciloglu,

GAI Consultants, Inc., Homestead, Pennsylvania

ABSTRACT: A significant quantity of high quality field and laboratory testing data has been amassed over the past 25 years as part of evaluations of liquefaction triggering and post-earthquake slope stability of fine coal refuse (FCR) at numerous high-hazard, coal refuse disposal facilities in West Virginia (WV), Kentucky (KY) and Illinois (IL). Field testing of FCR typically included performing Piezo-Seismic Cone Penetration Testing (PSCPT) with concurrent field sampling by obtaining high quality, fixed-piston undisturbed samples of FCR for subsequent laboratory testing. Estimates of peak (S_{up}) and steady-state (S_{ss}) undrained shear strength at in-situ effective stress (σ'_v) conditions from 15 sites throughout WV, KY and IL are presented, as well as normalized PSCPT tip resistance (Q) and friction ratio (F), shear wave velocity (V_s), and other PSCPT data correlations. The correlations can be used for comparison in parametric static- and seismic-related liquefaction analyses of coal refuse upstream pushouts where a lack of data may exist.

1. INTRODUCTION

Tailings dams are among the largest earth structures in the world and consequently receive intense regulatory and public scrutiny. Upstream-constructed coal refuse impoundments have unique characteristics compared to other engineered structures, as the hydraulically-deposited FCR is used as the foundation for subsequent embankment stages. Coal refuse disposal facilities, their design, construction and operation are regulated by the U.S. Department of Labor, Mine Safety and Health Administration (MSHA). The concern for refuse disposal safety and environmental control has led to the development of design procedures, which are presented in the updated MSHA Engineering Design Manual (2009). This manual presents a consensus of information on many design aspects, including data summaries from multiple reference sources pertinent to the development of undrained shear strength properties, and the evaluation of stage construction, liquefaction, and post-earthquake seismic stability.

A typical high hazard, upstream-constructed coal refuse disposal facility is constructed over long periods of time, can reach heights of 400-plus feet, and include multiple upstream stages “pushed out” into the previous stage’s tailings pond. Fine coal refuse consolidated under upstream stages typically is loose, silty sand to sandy silt- and clay-sized particles, saturated, and usually highly contractive. Thus, the potential exists for excess pore pressure generation and loss of strength following a rapid (dynamic) loading event such as an earthquake, or rapid construction loading (static) event.

Numerous comprehensive site evaluation and exploration programs of the upstream-constructed facilities have been performed, and typically included both in-situ field testing and laboratory testing to obtain information on the character of FCR, especially under undrained loading conditions. The type and extent of the various explorations depended on the size, geometric complexity, foundation materials, and impounding function of the facility. Field testing

techniques have evolved over the years, increasing the maximum in-situ testing and sampling depths at FCR facilities and thus allowing data to be obtained for higher effective stress conditions. Field testing in FCR has included performing PSCPT to obtain tip stress (q_c), sleeve friction (f_s), pore-pressure measurements (u), and shear wave velocity (V_s), and a myriad of correlated geotechnical parameters. High quality, fixed-piston undisturbed samples of FCR were obtained, and sample volume change and in-situ void ratio estimates made to judge the quality of the samples and correct laboratory strength data as necessary to account for changes in void ratio from in-situ conditions. Based on the field and laboratory testing results at the 15 coal refuse disposal sites, correlation of laboratory peak (S_{up}) and steady-state (S_{us}) undrained shear strength to various PSCPT data and in-situ effective stress (σ'_v) were made. The results of the field and laboratory data correlations presented below can be used parametrically at early stages, and/or for comparison at later stages of a disposal facility testing and design cycle.

2. DATABASE

A database of FCR field and laboratory testing data has been compiled from the evaluation of numerous coal refuse disposal facilities sites throughout WV, KY and IL. These evaluations were performed from 1991 to 2017. Field and laboratory testing results from a total of 15 high hazard sites comprise the database of information presented herein. Sites 1, 2, 3, 4, 5, 6, 7, 8, 9 and 15 are in WV, Sites 10 and 12 are in KY, and Sites 11, 13 and 14 are in IL.

The database of field testing included data from approximately 10,000 feet of PSCPT, over 5,000 feet in FCR, and in excess of 3,500 V_s tests to a maximum depth of 344 feet below the ground surface. A total of about 120 high quality, fixed-piston undisturbed samples of FCR were obtained at various depths up to 320 feet, with volume changes during sampling generally about 4 percent or less.

The laboratory testing database of high quality FCR samples includes approximately 100 suites of moisture content, grain-size distribution, Atterberg limits and specific gravity index tests. Strength testing results comprising the database are from approximately 80 isotropically consolidated, monotonically loaded, undrained triaxial (R-bar) tests on high quality undisturbed samples of FCR, as well as the results from about 60 R-bar triaxial tests on remolded and slurry FCR samples. The raw data is too voluminous to present in this paper, therefore tables were prepared to summarize the average, minimum, maximum and standard deviation of laboratory testing results and PSCPT data geotechnical correlations. Tables 1 and 2 present a summary of FCR laboratory and field testing data, respectively.

Additionally, PSCPT soundings and undisturbed sample borings were drilled adjacent to each other (typically within about 8 – 10 feet). For purposes of data comparison, the Table 2 PSCPT data intervals in FCR generally included an approximate \pm 1-foot data overlap above and below the laboratory testing sample depth range. For the oldest five (5) sites, PSCPT data is not digitally available and thus not included in the database. However, V_s data from two of the oldest five sites were more easily interpreted at the depths of laboratory strength test samples, and are thus included in Table 2.

3. ANALYTICAL APPROACH

The database of field and laboratory testing data from 15 high-hazard, upstream-constructed facilities was evaluated mainly for material characterization and undrained shear strength estimation. The methodology by Poulos, Castro, and France (1985) was implemented to estimate in-situ void ratio, and peak (S_{up}) and steady-state (S_{us}) undrained shear strength of FCR. PSCPT data was interpreted using the methods presented by P.K. Robertson (2009), among other similarly authored references, and for material characterization. Finally, the MSHA (2009) Engineering Design Manual, particularly Chapter 7, provides the basis for the development of undrained shear strength properties specific to FCR, and the results of field and laboratory testing data presented herein supplements the manual's database of pertinent information.

Table 1. Summary of Fine Coal Refuse Laboratory Testing Data – WV, KY and IL Sites.

	Depth to Top of Sample, feet	In-Situ Vertical Effective Stress, ksc	Passing No. 200 Sieve (Fines) %	Water Content, %	Liquid Limit, %	Plastic Limit, %	Plasticity Index, %	Liquidity Index, %	Specific Gravity
Num	94	94	102	72	41	41	42	36	100
Avg.	126	5.05	61.8	34.3	37	23	14	1.2	1.8
Min.	10	0.52	15.7	13.1	22	9	4	0.2	1.2
Max.	343	11.62	98.1	94.4	47	32	28	4.4	2.4
Std Dev.	83	3.55	22.4	14.7	6	4	7	0.9	0.3

	Void Ratio In-Situ (Sampled)	Void Ratio in Tube /Mold	Void Ratio During Shear	Lab Effective Consol Stress, ksc	Equiv. Vertical Effect Stress in Field, ksc	Shear Stress at Peak, q, ksc	Shear Strain, %	Peak Friction Angle, degrees	Shear Stress at Steady State (SS), q, ksc
Num	94	149	139	141	141	120	120	120	133
Avg	0.58	0.71	0.53	6.37	9.55	2.83	21.9	34.1	2.72
Min.	0.32	0.36	0.32	0.34	0.51	0.21	1.8	23.2	0.03
Max.	0.98	2.33	1.56	16.20	24.30	6.57	35.1	45.9	6.57
Std Dev.	0.12	0.36	0.20	4.33	6.50	1.77	7.1	3.4	1.72

	Steady-State Shear Strain, %	Undrained SS Strength S_{us} , ksc	SS Friction Angle, degrees	S_{us} at In-Situ Void Ratio, ksc	S_{up}/σ'_v
Num	134	140	134	60	94
Avg.	27.9	2.19	33.9	1.26	0.28
Min.	6.0	0.01	26.8	0.06	0.18
Max.	39.9	5.47	40.4	5.03	0.78
Std Dev.	5.6	1.49	2.6	1.25	0.11

	S_{up}/σ'_v 2/3-1/3 Sup Ratio	S_{us}/σ'_v	S_{us}/σ'_v 2/3-1/3 S_{us} Ratio	SS Shear Strength In-Situ S_{us} , ksc	Slope of Steady State Line	Peak Shear Strength In-Situ S_{up} , ksc
Num	14	59	12	65	13	82
Avg.	0.24	0.23	0.16	1.01	0.13	1.37
Min.	0.19	0.09	0.03	0.05	0.11	0.19
Max.	0.35	1.18	0.27	3.14	0.53	4.80
Std Dev.	0.04	0.15	0.08	0.91	0.12	0.94

Table 2. Summary of Fine Coal Refuse PSCPT Field Testing Data – WV, KY and IL Sites.

	Normalized Tip Resistance Q	Normalized Friction Ratio F	Soil Behavior Index I_c	Corrected Blow Count $N_{1,60}$, bpf	Fines Content FC, %	Corrected Tip Resistance q_{c1} Mpa	Undrained Strength S_u , ksc	Shear Wave Velocity V_s , m/s
Num	50	50	50	50	47	39	50	60
Avg.	4.8	3.1	3.4	5	80	1.14	1.06	256
Min.	0.0	0.0	2.5	1	30	0.11	0.00	91
Max.	20.8	12.5	4.5	39	100	4.58	4.14	794
Std Dev.	5.0	2.2	0.5	6	21	1.14	1.10	135

4. MATERIAL CHARACTERIZATIONS

For many aspects of undrained strength analyses, static or dynamic, coal refuse materials are characterized as sand-like or clay-like depending on whether they exhibit monotonic and cyclic undrained shear loading behavior that is fundamentally more similar to that of either sand or clay. This differentiation is significant primarily if the material is loose enough (for sands) or soft enough (for clays) relative to the material being potentially susceptible to strength loss. Coal refuse materials, particularly FCR, typically yield field and laboratory testing results that characterize the material as either or both sand-like and clay-like. Based on extensive field data and experience, it is possible to estimate grain characteristics directly from PSCPT results using the Soil Behavior Type, Zones 2 – 7 as shown in Figure 1 from Robertson and Wride (1998). The boundary separating sand-like and clay-like material corresponds to Soil Behavior Type Index (I_c) of 2.6, which is a function of normalized tip resistance (Q), normalized friction ratio (F), and effective stress conditions. PSCPT data correlations of FCR include estimating Q , F , I_c and fines content (FC), which are used to characterize the FCR as sand-like and/or clay-like. Figure 1 presents average Q and F values for the noted FCR sites included in the database. As presented in Figure 1 most of the Q and F values are in Soil Behavior Type (SBT) Zones 2, 3 and 4, with I_c greater than 2.6, and thus characterized as clay-like. Additionally, the noted sites with PSCPT data fall within liquefaction potential Zones B and C. From Robertson and Wride (1998), Zone B indicates clay-like material where a significant strength loss is unlikely, and Zone C indicate potentially highly sensitive clay-like material that may be susceptible to strength loss. Zones A_1 and A_2 indicate sand-like material with I_c values less than 2.6; however, none of the average PSCPT data fall with Zones A_1 or A_2 .

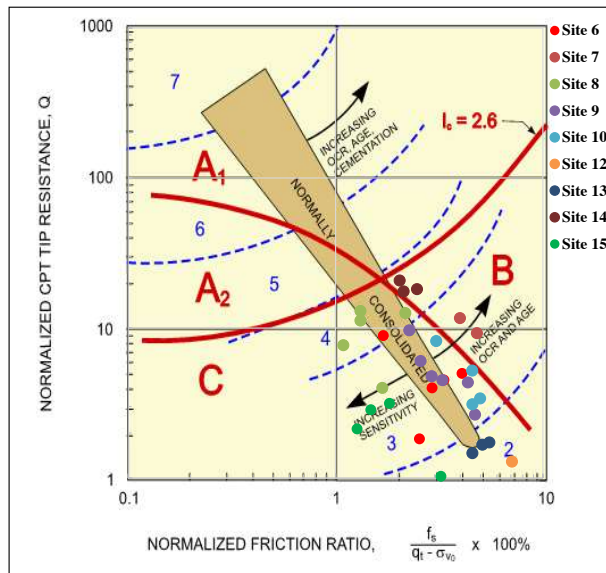


Figure 1. Normalized Tip Resistance (Q) and Friction (F) Ratio for FCR Materials/Sites

Plots of I_c versus average fines content (FC) for field-derived and laboratory-derived fines content are presented in Figures 2 and 3, respectively. FC and I_c correlations can be used for material characterization, and it can be seen from Figures 2 and 3 that field and laboratory derived FC were generally comparable. Figures 2 and 3 further indicate that I_c values are generally greater than 2.6 and FC are greater than 30 percent. Based on these data, most of the

tested FCR tends to behave more clay-like, confirming the characterizations provided in Figure 1. I_c values greater than 2.6 generally are considered as clay-like material.

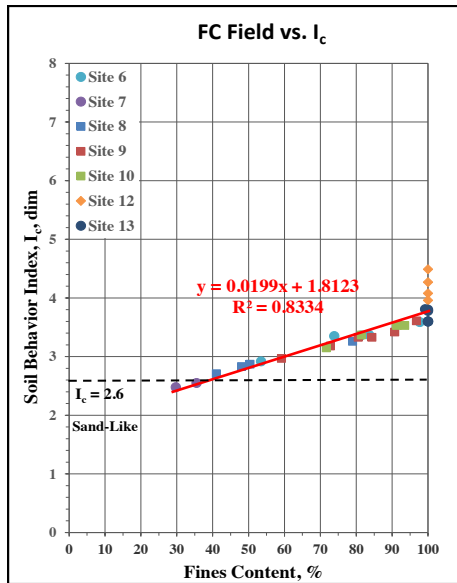


Figure 2. Fines Content Field vs SBT I_c

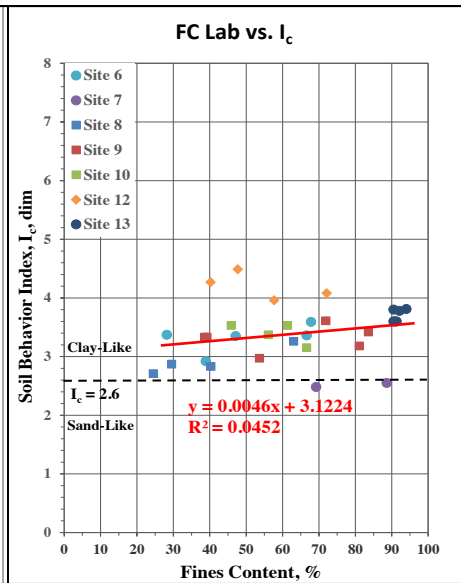


Figure 3. Fines Content Lab vs SBT I_c

The laboratory testing data were used to characterize the coal refuse materials. As presented in Table 1, the average fines content was 62 percent and the average plasticity index (PI) was 14, indicative of clay-like material. Another key factor in differentiating loose sand-like material from soft or medium clay-like material, for the purposes of seismic stability and deformation analyses, are the strain at peak undrained strength and the abruptness of the drop-off in shearing resistance as strains increase beyond the strain at peak. Loose sands and highly sensitive clays can reach peak undrained shear strength (S_{up}) at small shear strains (less than about 2 percent), and experience abrupt drop-off in resistance at higher strains. Most clays tend to reach S_{up} at higher shear strains (more than about 5 percent), and tend to experience more gradual and limited drop-off in shearing resistance at higher strains. Material with stress-strain behavior falling between that described above is considered borderline, and, to be conservative, is generally analyzed as sand-like. Fine coal refuse deposits often include materials falling within both classifications, and near the boundary of these two types of behavior.

Based on 120 R-bar triaxial laboratory strength tests of FCR conducted, 100 percent of the results presented in Figure 4 have shear strains above 5 percent. The shear strain was derived by multiplying the axial strain in the triaxial test by 1.5. This data overwhelming suggests that FCR is behaving predominately clay-like in undrained loading conditions.

The results of the laboratory and field testing data presented in Tables 1 and 2, respectively, suggest that the FCR behaves primarily as a clay-like material. The sand-like material characterization is based on several samples being non-plastic (NP) based on Atterberg limits tests, and a small percentage of the triaxial strains at peak strength being at or near 5 percent. Therefore, based on these results, the fine coal refuse is dually characterized as having both sand-like and clay-like behavior; however, FCR has a much higher tendency to behave more clay-like.

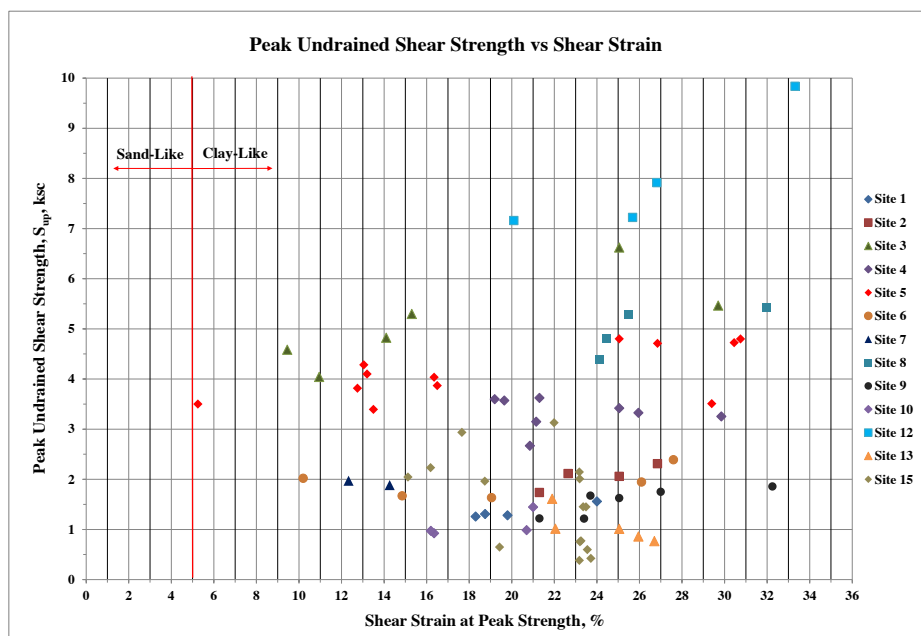


Figure 4. Summary of Shear Strain Range for Laboratory Tested FCR Samples

5. UNDRAINED SHEAR STRENGTH

Undrained shear strength of FCR has been estimated by laboratory testing and field testing data correlations. The database presented in this paper includes 80 R-bar triaxial compression tests performed on high quality undisturbed samples of FCR, and 60 R-bar tests performed on remolded batch samples of FCR from the various sites to determine peak (S_{up}) and steady-state (S_{us}) undrained shear strengths, and corresponding strength-to-effective stress ratios. Undisturbed FCR samples were isotropically consolidated in the laboratory to a range of vertical effective stresses of about 0.34 to 16.2 kilogram per square centimeter (ksc). Batch mix samples were consolidated to a range of vertical effective stresses of 0.34 to 12.0 ksc. In general, specimens exhibited contractive behavior when sheared under undrained conditions.

Distribution of laboratory measured S_{us} of the undisturbed coal refuse samples versus vertical effective stress (σ'_v) is presented in Figure 5. A 2/3 - 1/3 relationship of the data (i.e., 2/3 of data points have lower strength) for each site was employed and yielded an average S_{us} -to- σ'_v relationship of $S_{us}/\sigma'_v = 0.16$ with a lower bound ratio of 0.03 and an upper bound ratio of 0.27. This ratio was obtained by correcting measured undrained shear strength to the in-situ void ratios representing in-situ undrained shear strength in accordance with the methods presented in Poulos, Castro and France (1985). Case histories presented in MSHA (2009) indicate a ratio of S_{us}/σ'_v in the range of 0.03 to 0.22, which is comparable to relationships developed from this database.

Similarly, a plot of the peak undrained shear strength (S_{up}) of the undisturbed samples versus vertical effective stress (σ'_v) is presented in Figure 6. A 2/3 - 1/3 relationship of the data for each site yielded an average S_{up} -to- σ'_v relationship of $S_{up}/\sigma'_v = 0.24$ with a lower bound ratio of 0.19 and upper bound ratio of 0.35.

Undrained steady-state shear strength versus in-situ void ratio for 60 remolded batch samples of FCR is presented in Figure 7. The steady-state lines (SSLs), or ratio of $\Delta e/\Delta \log S_{us}$ are

presented in Figure 8 for the various sites in WV, KY and IL. Figure 8 indicates that slope of steady-state lines $\Delta e/\Delta \log S_{us}$ are in the range of 0.11 to 0.14 for remolded FCR samples from WV and KY sites. Slopes of the SSL $\Delta e/\Delta \log S_{us}$ ratio for sites in IL are in the range of 0.24 to 0.53, which are attributed to the much higher clay content, higher void ratio, and lower degree of consolidation of the IL site samples. MSHA (2009) notes Genes et al. (2000) and GEI (2007) reported slopes of the steady-state line $\Delta e/\Delta \log S_{us}$ for sites in WV and KY to be in the range 0.09 and 0.14, which is consistent with the findings of this paper.

The database was evaluated to develop relationships of laboratory measured S_{up} and S_{us} versus PSCPT normalized tip stress (q_{c1}) in kilogram per square centimeter (ksc), correlated standard penetration test ($N_{1,60}$) in blows per foot (bpf), I_c , FC (%), and V_s (meters per second, m/s) and are presented in Figures 9 to 16. $N_{1,60}$ versus S_{us} and S_{up} in Figures 11 and 12, respectively present comparisons to literature data, particularly lower bound Seed & Harder, and GEI data relationships (both presented in MSHA, 2009). FCR strength values with $N_{1,60}$ are higher than the soil strengths, which is likely the result of clay-like FCR compared to the literature relationships developed for sand-like material.

The various relationships presented in this paper can provide a comparative basis for undrained strength analysis of future placement of FCR stages and limited in-situ testing data. Similarly, the data and relationships can form the basis for the initial development of undrained strength engineering properties in the early stages of a site design where parametric analyses are performed to initially evaluate the feasibility of various embankment geometries and staging.

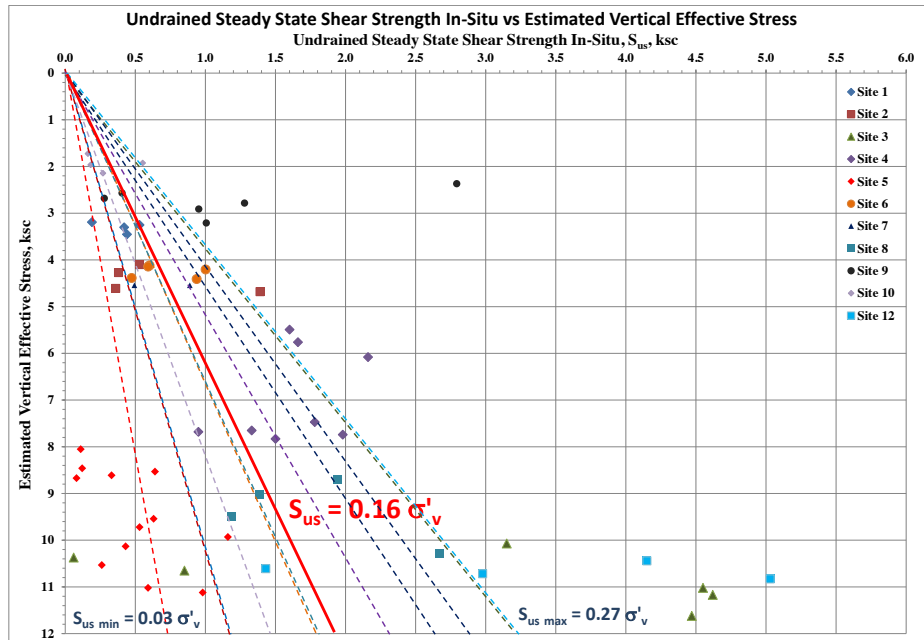


Figure 5. Undrained Steady-State Shear Strength to Effective Stress Strength Ratio

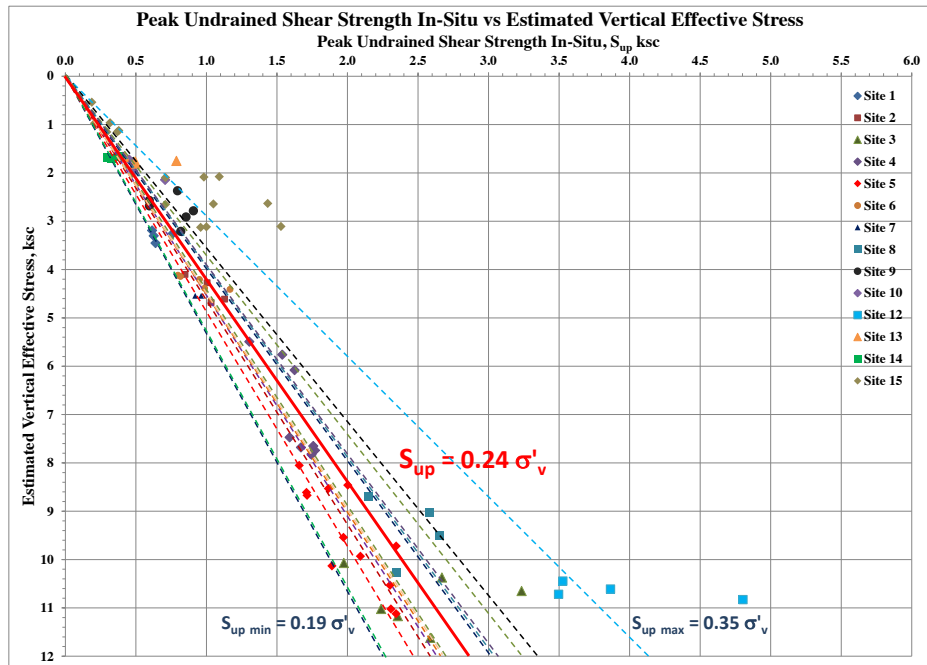


Figure 6. Peak Undrained Shear Strength to Effective Stress Strength Ratio

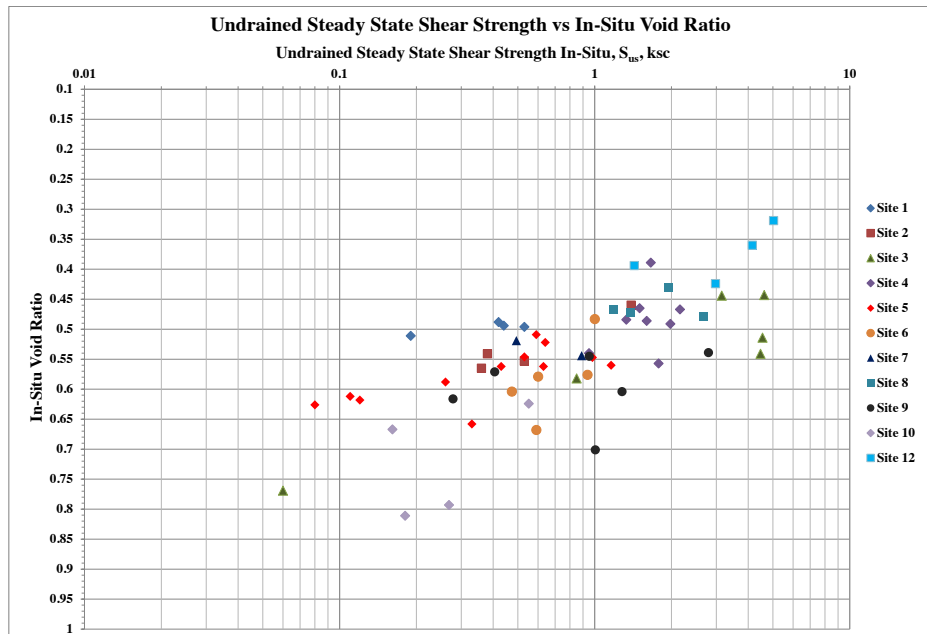


Figure 7. Undrained Steady-State Shear Strength vs. In-Situ Void Ratio

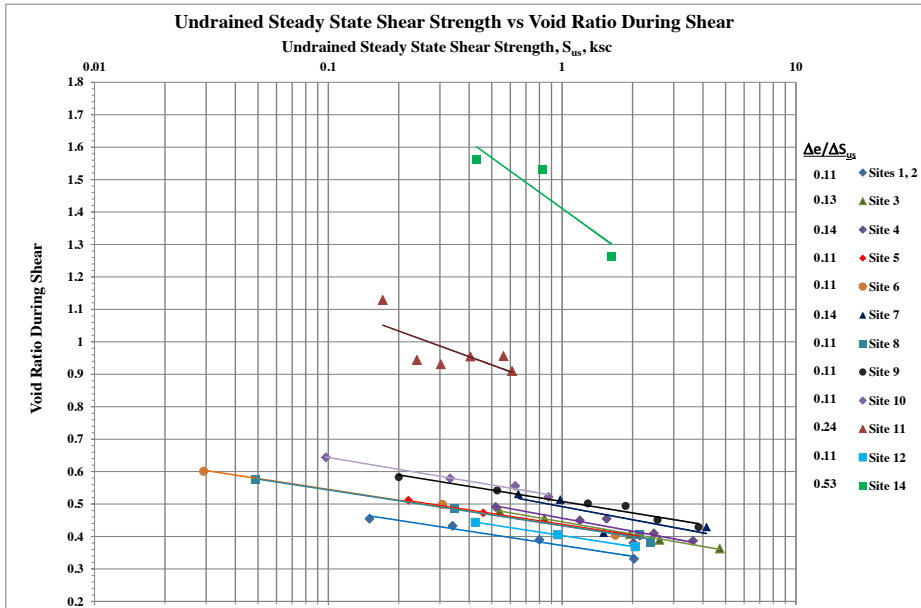


Figure 8. Steady-State Line – WV, KY and IL Sites

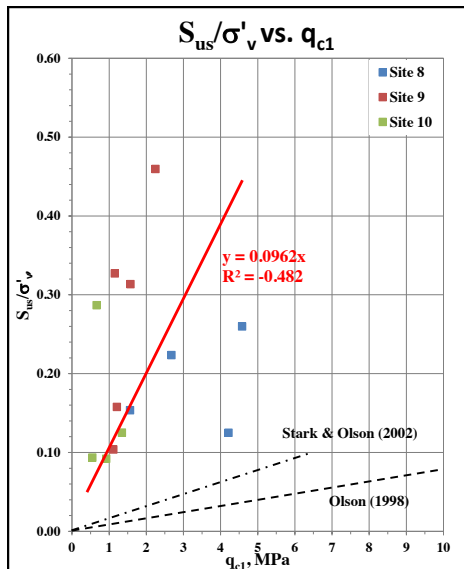


Figure 9. S_{us}/σ'_v vs. q_{c1} Relationship

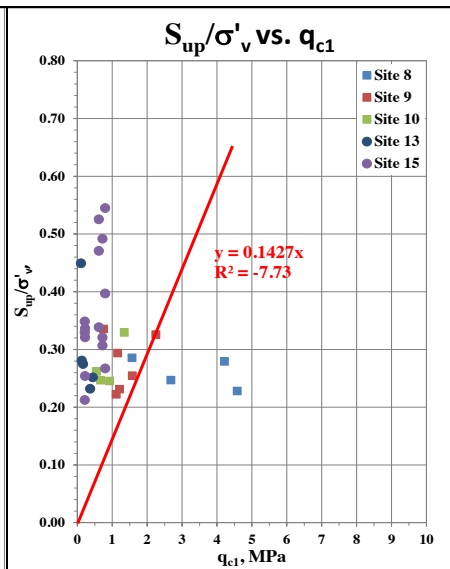


Figure 10. S_{up}/σ'_v vs. q_{c1} Relationship

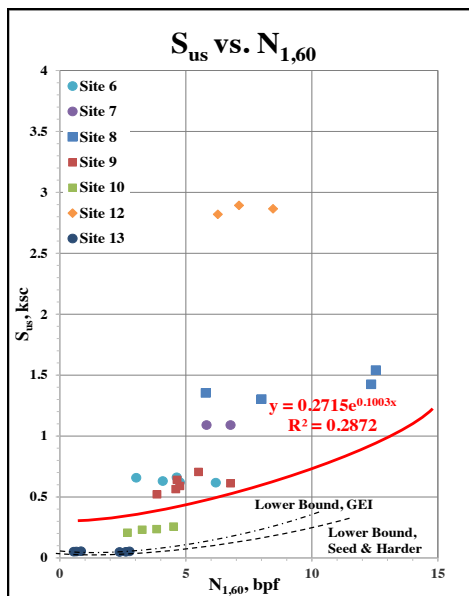


Figure 11. S_{us} vs. $N_{1,60}$ Relationship

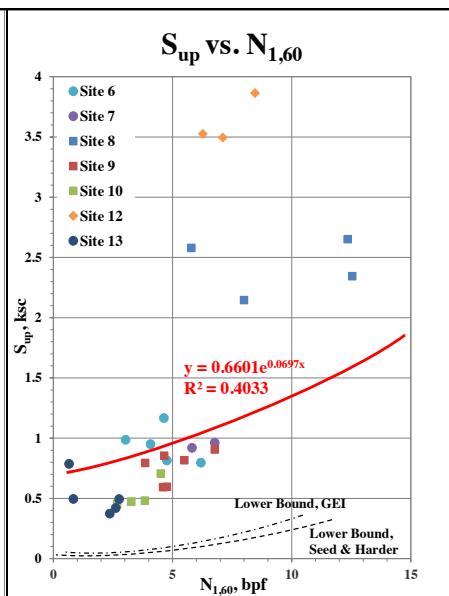


Figure 12. S_{up} vs. $N_{1,60}$ Relationship

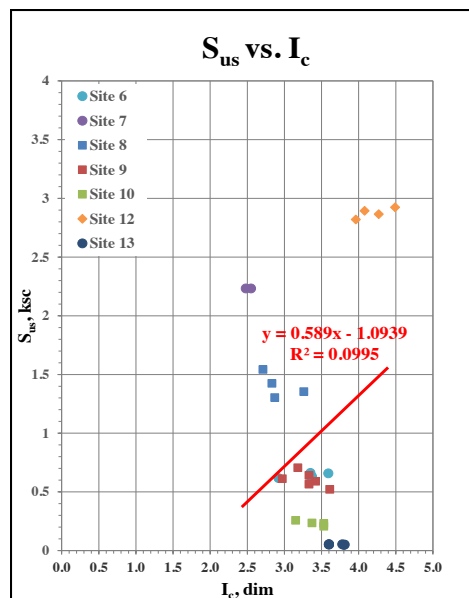


Figure 13. S_{us} vs. Soil Behavior Index, I_c

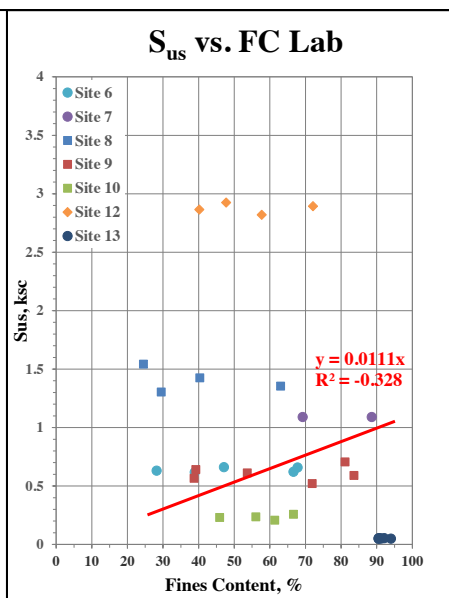


Figure 14. S_{us} vs. Laboratory Fines Content

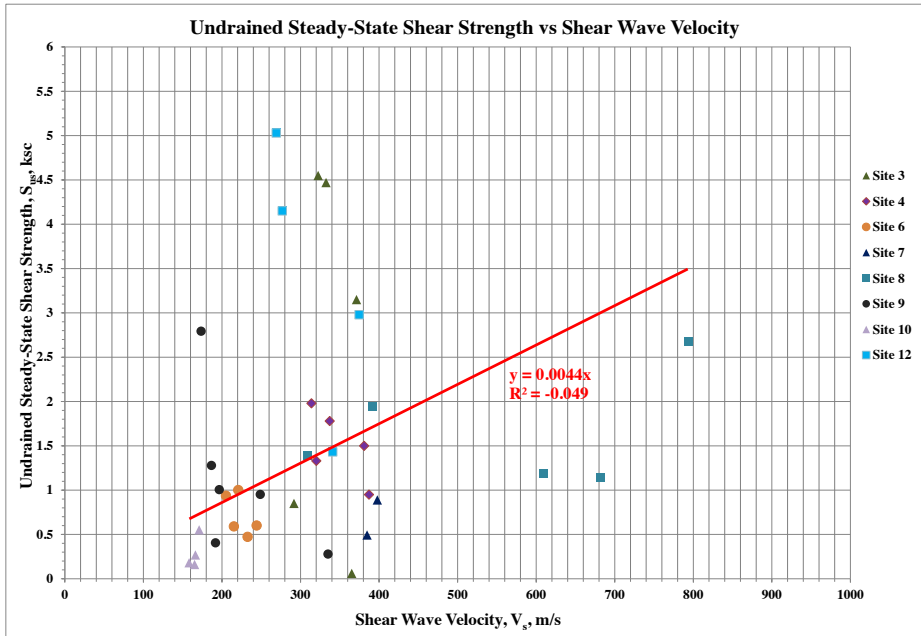


Figure 15. Undrained Steady-State Shear Strength, S_{us} vs. Shear Wave Velocity, V_s

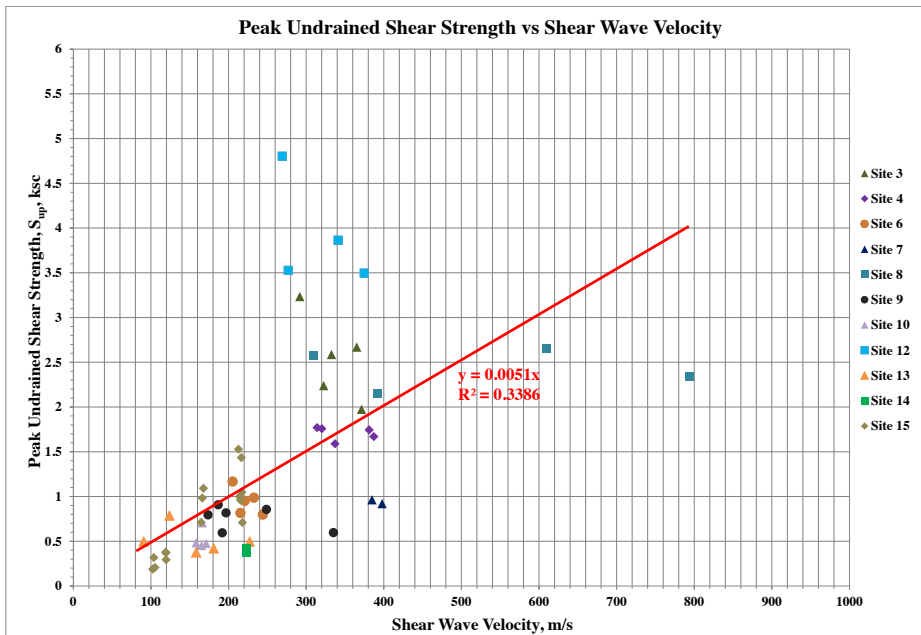


Figure 16. Peak Undrained Shear Strength, S_{up} vs. Shear Wave Velocity, V_s

6. CONCLUSIONS

Seismic stability evaluations of 15 high-hazard, upstream-constructed FCR facilities in WV, KY, and IL performed in the period 1991 to 2017 were used to generate a database of field and laboratory testing data of FCR. Tables 1 and 2 present a summary of laboratory and field testing data, respectively; these data were used to develop the correlations presented in this paper. Field testing in FCR has included performing PSCPT to obtain tip stress (q_c), sleeve friction (f_s), pore-pressure measurements (u), and shear wave velocity (V_s). Concurrent field sampling included obtaining high quality, fixed-piston undisturbed samples of FCR for subsequent laboratory testing, and to estimate in-situ void ratio and void ratios changes that occurred during and after sampling. Based on the testing results, characterization of the FCR as sand-like and/or clay-like were made, with a predominately clay-like behavior observed. Laboratory peak and steady-state undrained shear strength-to-effective stress ratios were determined for the WV, KY and IL sites, with average values of 0.24 and 0.16 estimated, respectively. The average, and range of strength ratios of S_{up}/σ'_v and S_{us}/σ'_v are consistent with similar data presented in MSHA (2009). Data relationships of S_{us} and S_{up} versus PSCPT normalized q_{c1} , correlated $N_{1,60}$, I_c , FC , and V_s were made, and presented in numerous figures presented above.

These relationships can be used in parametric staged construction, post-earthquake stability and liquefaction analyses of upstream-constructed coal refuse disposal facilities in the absence of, or where limited FCR data may exist. Ultimately, site specific data should be obtained to evaluate material characteristics as either sand-like or clay-like, and undrained shear strength determined from both field and laboratory testing methods, as described in MSHA (2009), and necessary to perform realistic undrained strength analyses.

Future efforts should include expanding the database of information and useful relationships, as well as evaluating the effect of the parameter boundary conditions on loading rate- and liquefaction-related undrained strength analyses. Future evaluation of instrumentation performance data on model refinement and undrained strength properties/parameter calibration are seen as furthering our understanding of the behavior of fine coal refuse under rapid loading conditions.

REFERENCES:

- Boulanger, R. W. and Idriss, I. M. 2007. Evaluation of Cyclic Softening in Silts and Clays. *Journal of Geotechnical and Geoenvironmental Engineering, ASCE, Vol. 133, No. 6, pp. 641-652.*
- Castro, G. 1987. On the Behavior of Soils during Earthquakes – Liquefaction. *Soil Dynamics and Liquefaction,* A. S. Cakmak, Editor, Elsevier.
- Genes, B. E., Keller, T. O. and Laird, J. P. 2000. Steady-State Liquefaction Susceptibility of High Hazard Upstream-Constructed Coal Refuse Disposal Facilities. *Association of State Dam Safety Officials, U.S. Committee on Large Dams, March 28-30, 2000.*
- Poulos, S. J., Castro, G., and France, J. W. 1985. Liquefaction Evaluation Procedure. *Journal of the Geotechnical Engineering Division, ASCE, Vol. 111, No. GT6, pp. 772-792.*
- Robertson, P. K. 2009. Interpretation of Cone Penetration Tests – A Unified Approach. *Canadian Geotechnical Journal, Vol. 46, November, pp. 1337-1355.*
- Robertson, P. K. and Wride, C.E. 1998. Evaluating Cyclic Liquefaction Potential Using the Cone Penetration Test. *Canadian Geotechnical Journal, Vol. 35, No. 3, June, pp. 442-459.*
- Seed, R. B. and Harder, L.F., Jr. 1990. SPT-Based Analysis of Cyclic Pore Pressure Generation and Undrained Residual Strength. *H.B. Seed Memorial Symposium, Bi-Tech Publishing Ltd., Vol. 2, pp. 351-376.*
- Stark, T. D. and Olson, S.M. 2002. Liquefied Strength Ratio from Liquefaction Flow Failure Case Histories. *Canadian Geotechnical Journal, Vol. 39, pp. 629-647.*
- United States Department of Labor, Mine Safety and Health Administration. Engineering and Design Manual, Coal Refuse Disposal Facilities, Chapter 7 Seismic Design: Stability and Deformation Analyses. *May 2009.*
- Youd, T. L. and Idriss, I. M. 2001. Liquefaction Resistance of Soils: Summary Report from the 1996 NCEER and 1998 NCEER/NSF Workshops on Evaluation of Liquefaction Resistance of Soils. *Journal of Geotechnical and Geoenvironmental Engineering, ASCE, Volume 127, No. 10, pp. 817-833.*

Frozen Core Tailings Dam: Part 1, Long-Term Thermal Performance

M. Rykaart and P. Luedke

SRK Consulting (Canada) Inc., Vancouver, British Columbia, Canada

C.W. Stevens

SRK Consulting (U.S.) Inc., Anchorage, Alaska, USA

ABSTRACT: Tailings management at the Hope Bay Project in Nunavut, Canada, includes reliance on an innovative frozen core dam. This dam does not have a tailings beach against it, and has been designed as a water retaining dam with a 30-year design life. Successful performance of the dam relies on both the core and the underlying foundation maintaining specific target temperatures throughout its service life. This paper, which is the first in a two-part series, describes the dam performance six years post construction, and compares modelled thermal response with field performance data collected from multiple ground temperature cables. The data and modelling confirm that the dam has performed in accordance with expectations and that it is on track to meet long-term performance targets, including for conservative climate change scenarios. The second paper in this series describes creep deformation of the dam, which uses the thermal response as a key parameter.

1 INTRODUCTION

The tailings management system for the Hope Bay Project, in Nunavut, Canada, includes sub-aerial tailings deposition into the Doris tailings impoundment area (Doris TIA). The Doris TIA is located in the basin of the former Tail Lake, a shallow lake which has been delisted in accordance with Schedule II of the Metal Mining Effluent Regulations. To provide containment, a frozen core water retaining dam (North Dam) was designed (SRK 2007, 2017a), and constructed over the winter seasons of 2011 and 2012 (SRK 2012). Following six years of monitoring, conclusions regarding dam performance can be made, both with respect to thermal response and creep deformation. This paper, which is Part 1 of a two-part series, describes the thermal performance monitoring and associated modeling, while Part 2 (Rykaart et al. 2018) describes the creep deformation monitoring and associated modeling. Section 1 through 6 of Part 1 and Part 2 is identical to allow the papers to be read independently.

2 TAILINGS MANAGEMENT SYSTEM

The Doris TIA, when fully developed, will consist of one frozen core water retaining dam (North Dam), and two frozen foundation dams (South Dam and West Dam). Tailings will be discharged from the South and West Dams, as well as select locations around the perimeter of the facility. The North Dam will provide water containment for the Reclaim Pond, and no tailings will be in contact with the dam during its 30-year design life. At closure, the Reclaim Pond will be drained, and the North Dam breached, with no need for a permanent water retaining dam (SRK 2017a).

3 FOUNDATION CONDITIONS

The project is located within the continuous permafrost region of Canada, approximately 140 km north of the Arctic Circle. Site measurements indicate that permafrost in the area is approximately 570 m thick, with an active layer of 0.9 m to 1.7 m, depending on the material type. The ground temperature at the depth of zero annual amplitude is -8°C , and the geothermal gradient is 0.021°C/m (SRK 2017b).

Numerous geotechnical characterization programs have been completed within the alignment of the North Dam, to characterize the foundation conditions. Programs included boreholes, test pits, in-situ hydraulic conductivity testing, installation of ground temperature cables (GTCs), long-term ground temperature monitoring (starting in 2002), percolation testing, geophysics, and both undisturbed and disturbed sample collection and laboratory testing (SRK 2017b).

The North Dam is located in a narrow valley approximately 200 m downstream of the northernmost extent of the former Tail Lake. The stratigraphy under the dam has two distinct zones; the southwest abutment is dominated by ice-saturated sand deposits 10 m to 15 m thick, overlain by up to 3 m of silt and clay, while the northeast abutment is dominated by ice-saturated marine clayey silt with a maximum thickness of 15 m. Excess ground ice, averaging 10 % to 30% by volume, occasionally as high as 50%, is also present on both abutments.

A thin layer of sand and gravel overlies the bedrock surface in the upper portions of the valley, and a peat unit was encountered near the center of the dam, in the area of the lake outflow. The average pore water salinity is 39 parts per thousand (ppt), with a freezing point depression of -2.2°C (SRK 2017c). During construction, an isolated hypersaline zone, with salinity values in excess of 90 ppt, was also encountered within the key trench (SRK 2012). Bedrock is generally competent basalt.

Figure 1 provides a generalized longitudinal section of the North Dam foundation conditions, as understood prior to percolation testing and key trench excavation.

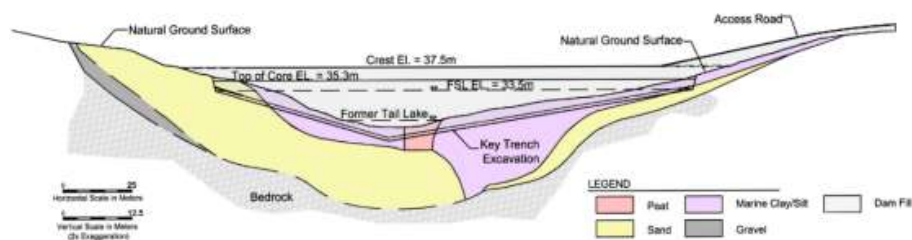


Figure 1. Longitudinal section of the North Dam showing generalized foundation conditions.

4 DAM DESIGN

A conventional unfrozen dam was not suitable for this location due to the thick ice-rich overburden foundation, remote site location, and lack of suitable low-permeability borrow material (Miller et al. 2013). Additionally, the thick overburden meant a frozen core dam founded on bedrock, similar to those constructed at other Canadian mines (Miller et al. 2013) was not feasible. Therefore, an innovative frozen core dam was designed to accommodate these challenging foundation conditions.

The North Dam is approximately 200 m long, with a maximum overall height of 10 m. The frozen ice-saturated core, keyed-in to the frozen foundation are designed to ensure water retention properties and containment. A geosynthetic clay liner (GCL) was installed along the upstream side of the frozen core to provide secondary water-retaining capability in case cracks develop in the core caused by thermal expansion, thermal erosion, differential settlement, or creep deformation. Thermal design to ensure primary containment requires that the frozen core maintains a

temperature at or below -2°C , at a width that is at least twice the head of water impounded against the dam. In addition, the saline foundation needs to maintain a temperature at or below -8°C for the same width, extending to bedrock under normal operating conditions (SRK 2007).

The dam was uniquely designed for the saline ice-rich foundation that is particularly susceptible to creep deformation. Therefore, the dam was designed to accommodate long-term shear strains in the core and foundation approaching 2% and 10%, respectively, and maximum shear strain rates at or below $1.0\text{E}-05 \text{ sec}^{-1}$ ($3.2\text{E}+02 \text{ year}^{-1}$) (SRK 2007).

The dam design included a key trench ranging from 2 m to 5 m deep to allow complete bonding of the core to the permafrost foundation (SRK 2012). Twelve sloped thermosyphons, six extending from each abutment of the dam, were installed at the base of the key trench to adequately cool the core and foundation over the design life assuming water permanently impounded against the upstream face to full supply level, and with consideration for climate change. The typical design cross section for the North Dam is illustrated in Figure 2, and the equivalent as-built cross section is illustrated in Figure 3 for comparison.

The core material is comprised of sand-sized crushed basalt, placed in a near saturated state and allowed to freeze during construction. The core is surrounded by a transition layer, consisting of jaw crusher run rock that acts as a filter, should the dam thaw. An outer shell constructed of run-of-quarry rock acts as a thermal protection layer for the frozen core, provides buttressing against creep deformation, and provides ice and wave run-up protection.

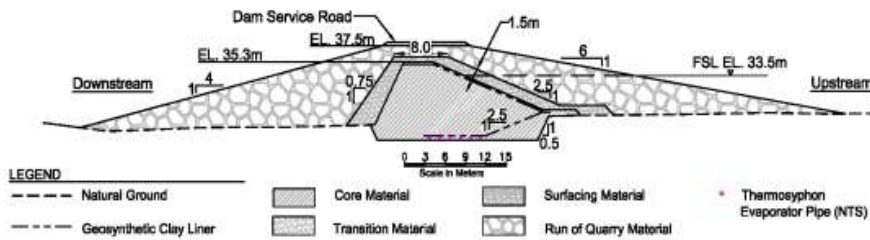


Figure 2. Typical design cross-section of the North Dam.

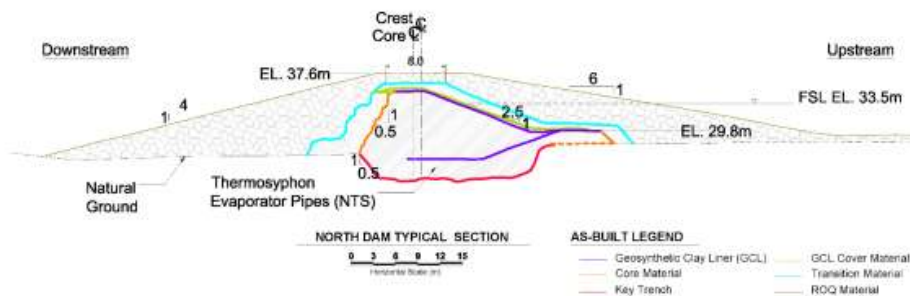


Figure 3. Typical as-built cross section of the North Dam.

5 CONSTRUCTION

The North Dam was designed to be constructed using construction techniques similar to those employed for the frozen core dams constructed at other Canadian mines (Miller et al. 2013). However, the site climate, available quarry rock material, and foundation conditions necessitated adaptations to the construction method (SRK 2012); some of which are summarized in Kurylo et al. (2013). Details on lessons learned from the North Dam construction are presented in Miller et al. (2013).

Drilling and blasting were used to excavate the key trench. Key trench excavation included the removal of all peat from the center portion of the dam, and over-excavation of the hypersaline zone. Following completion of the key trench excavation, the frozen core was constructed by placing and compacting 0.2 m to 0.3 m thick lifts of core material. Core material was produced in a modified asphalt plant by mixing and heating crushed rock and water. The lifts of saturated hot core material were then left to freeze back to target temperature (at or below -2°C) prior to the placement of the next lift.

Core placement required stringent quality control and quality assurance to ensure that saturation, freeze-back, density, and material specification requirements were met. Quality control and quality assurance included continuous material testing (laboratory and field), visual inspections, and constant and open communication with the client and contractor. These procedures ensured freeze-back, saturation (average 85% or greater, with no test below 80%), and compaction requirements (90% or greater of standard Proctor) were met. Between each lift, loose material and snow was cleared. To ensure that the lifts would freeze within a reasonable timeframe, frozen core placement was not attempted when ambient air temperatures were warmer than -10°C .

Due to the larger than expected excavation required to remove the peat and hypersaline soils, and a warm spring, the dam could not be completed in one winter season as originally planned. At the end of the 2011 construction season, the lower GCL and horizontal thermosyphons were installed and covered. However, the frozen core was not completed. To protect the core during the subsequent summer, a temporary 2 m thick run-of-quarry cover was placed over the partially constructed core. Work recommenced in the winter of 2012, and the dam was substantially complete by April 2012. The last remaining instrumentation on the downstream side of the dam was installed in August 2012 (SRK 2012).

6 INSTRUMENTATION

Performance of the North Dam is dependent on the core and foundation maintaining design temperatures, and the long-term strains, and strain rates remaining below target limits (SRK 2012, 2018a). Thermal performance of the dam is monitored with a series of thirteen horizontal GTCs, and eleven vertical GTCs. Figure 4 provides a typical dam cross section, including the location of these GTCs. Three horizontal GTCs are positioned at the top, middle and base of the core, while vertical GTCs are positioned along the foundation on the upstream side, in the center of the dam (key trench) and on the downstream side.

The working condition of each thermosyphon unit is confirmed using a single bead thermistor attached to the radiator riser pipe and compared with ambient air temperature measurements collected over the same period of time.

Deformations are monitored by a series of surficial, shallow, and deep settlement points and six inclinometers. Eighteen surficial settlement points are located on the downstream face of the dam, to monitor deformation of the dam shell in the location of the greatest expected deformation. Three deep settlement points are used to monitor deformation of foundation soils, again at the location of the greatest expected deformation. Fourteen shallow settlement monitoring points were installed on the crest of the dam to monitor crest deformation and differential settlement. The inclinometers are installed along the location of the greatest expected deformation and monitor deformation of both the dam shell and foundation. The instrumentation layout at the area of greatest expected deformation can be seen in Figure 4.

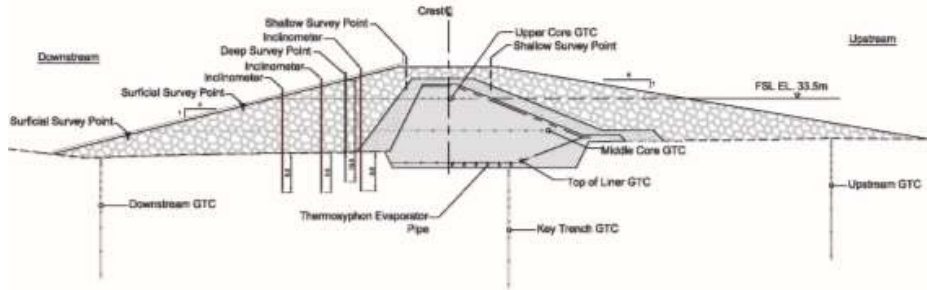


Figure 4: North Dam typical instrumentation.

7 THERMAL MONITORING DATA

North Dam monitoring includes ground temperature measurements recorded every six hours with data loggers, and monthly manual deformation measurements (i.e. survey settlement and inclinometers). Additionally, ongoing visual inspection of the dam structure by Project staff, and a formal annual geotechnical inspection by a Professional Geotechnical Engineer, who is also the engineer-of-record, is conducted (SRK 2018a).

Annual inspections (SRK 2018b), and review of monitoring data, suggest the dam is performing in accordance with the design expectations. The North Dam has had impounded water since the first winter of construction in 2011. The operating water level impounded against the upstream face of the dam has averaged 29.8 m, with a maximum level of 30.2 m over the period from May 2011 to June 2018. The original water level of Tail Lake prior to construction of the North Dam was 28.3 m, and the design full supply level is 33.5 m. Deformation measurements suggest movements less than predicted at this point in time (Rykaart et al. 2018).

Since the dam was commissioned in 2012, the GTC measurements have been recorded every six hours, using two separate data loggers and are manually downloaded by site staff monthly. During that time over 2150 days of monitoring data have been collected with minimal interruption from instrument malfunction or human error with the exception of 215 days of data lost from one of the GTCs becoming disconnected by unknown means, and 169 days of data lost following vehicle damage to one of the GTCs. During recalibration of the dataloggers in early 2018, no data was recorded for 70 days. This scheduled recalibration (every 5 years) was intentionally completed during the cooling cycle to limit data loss during the critical thaw period.

A few GTC beads (e.g. thermistor sensors) from select GTCs have recorded erroneous readings, and prior to June 16, 2014 two GTCs at chainage 0+175 m were incorrectly connected to the data logger, and consequently the three bottom beads of GTC #ND-VTS-175-KT were not recorded. None of these errors or data losses are considered material, as there is sufficient redundancy built into the monitoring system, and the overall trends in ground temperatures can still be observed with confidence.

Since completion of construction, all core GTC measurements are well below the required design temperature of -2°C , with the warmest temperature measured to be about -4.5°C , over the most recent year of monitoring. The colder than expected temperatures, when compared to what was originally predicted by thermal modeling, are explained by the lower water level presently impounded against the upstream face of the dam. Impoundment started in 2011 and tailings deposition began in 2016, and over this period the water level in the impoundment has on average been about 1.5 m above the original lake water level as opposed to having total head of 5.2 m at full supply level as it was modelled. The lower water level has resulted in greater exposure of the upstream face to atmospheric cooling during the winter, limited saturation and latent heat effects of the material upstream of the liner, and limited heat gain to the core that would normally result from the impounded water.

Figures 5a, 5b and 5c presents an example of the core temperatures recorded at chainage 0+130 m. Figure 5a shows the uppermost horizontal GTC (ND-HTS-130-33.5), Figure 5b the middle GTC (ND-HTS-130-31.0), and Figure 5c the lower GTC (ND-HTS-130-28.8), located immediately above the thermosyphons. The uppermost GTC, located 1.8 m below the dam crest at the top of the core, not surprisingly shows the greatest seasonal range as compared to the middle and lower GTCs. Similarly, the outermost beads on the middle and lower GTCs shows the greatest seasonal range. The apparent erratic response on some of the beads in the lowest GTC is not an error, but rather clearly shows the effect of the thermosyphons which act to significantly cool the core and associated foundation.

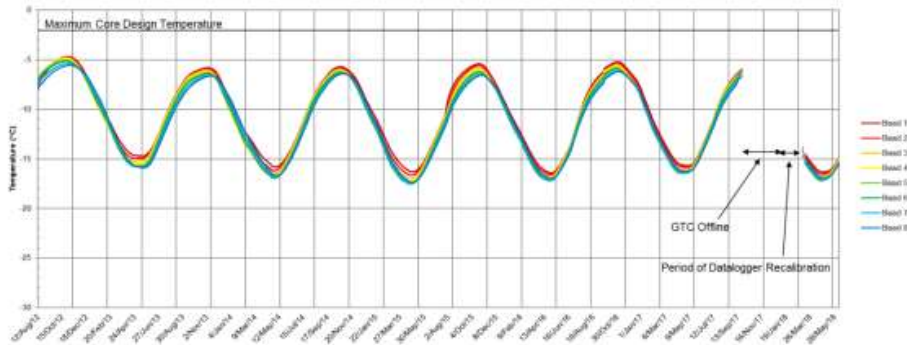


Figure 5a. Upper horizontal GTC at chainage 0+130 m, located at elevation 33.5 m (ND-HTS-130-33.5).

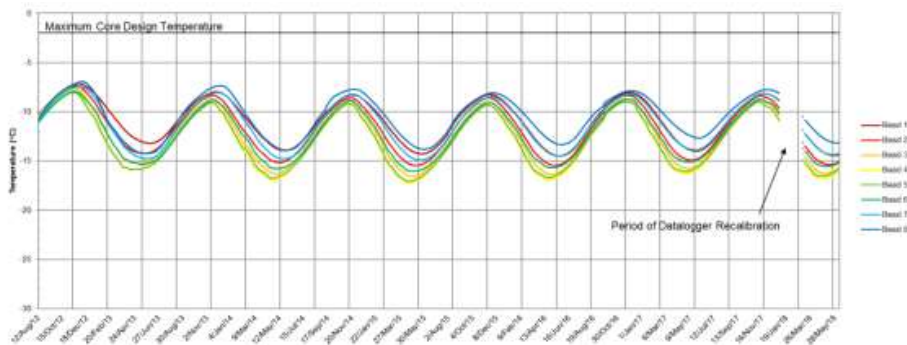


Figure 5b. Middle horizontal GTC at chainage 0+130 m, located at elevation 31.0 m (ND-HTS-130-31.0).

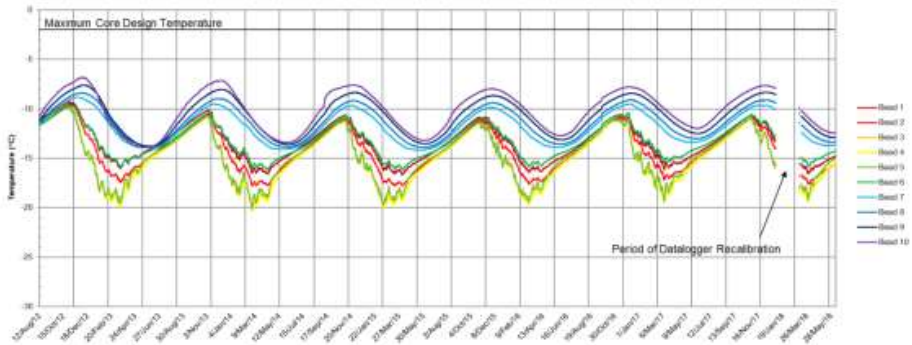


Figure 5c. Lower horizontal GTC at chainage 0+130 m, located at elevation 28.8 m (ND-HTS-130-28.8).

Measured foundation temperatures for the North Dam are all at or below design temperatures, except for three beads of one vertical GTC in the key trench at chainage 0+175 m (ND-VTS-175-KT). This GTC has remained stable, at or below -6.7°C .

Key trench foundation temperature measurements indicate that after construction the foundation temperatures in a few places were warmer than design temperatures. In 2012, the vertical key trench GTCs at chainage 0+040 m, 0+085 m, and 0+175 m (ND-VTS-175-KT, ND-VTS-085-KT and ND-VTS-040-KT) had some foundation measurements warmer than the design temperature of -8°C , at shallower depths, with no areas warmer than -5.7°C . Since 2012, a cooling trend has been observed and all foundation measurements for both GTCs ND-VTS-040-KT and ND-VTS-085-KT, which are now below -8°C (Figures 6a and 6b). GTC ND-VTS-175-KT has consistently had two beads with measurements peaking above the design temperature for a maximum of 60 days during the warmest period of each year as shown in Figure 6c. In the last monitoring year, the maximum temperature was -6.8°C , more than 1°C cooler than after construction in 2012.

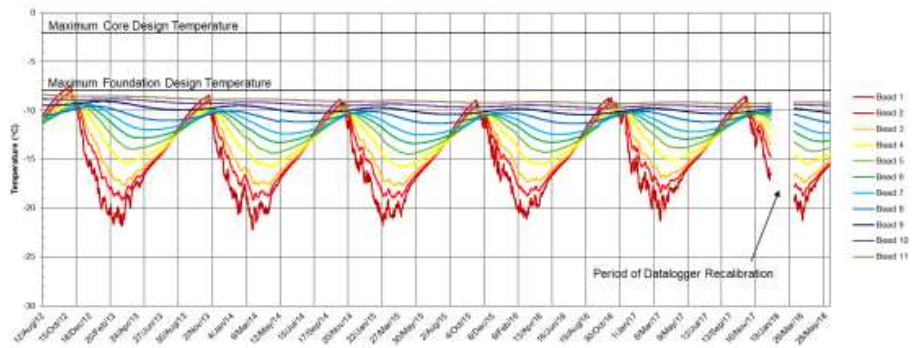


Figure 6a. Time series data for the key trench vertical GTC at chainage 0+040 m (ND-VTS-040-KT).

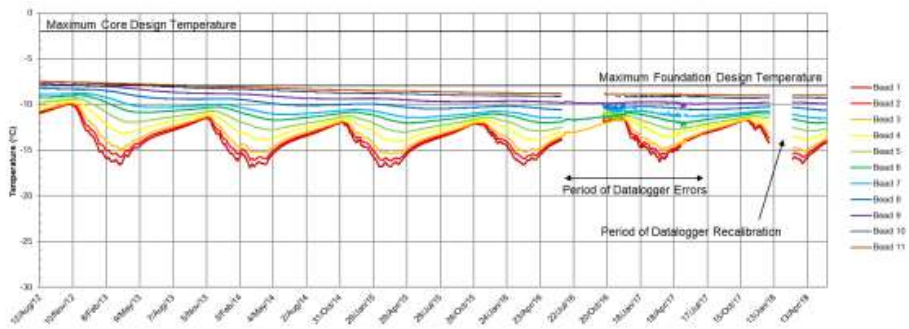


Figure 6b. Time series data for the key trench vertical GTC at chainage 0+085 m (ND-VTS-085-KT).

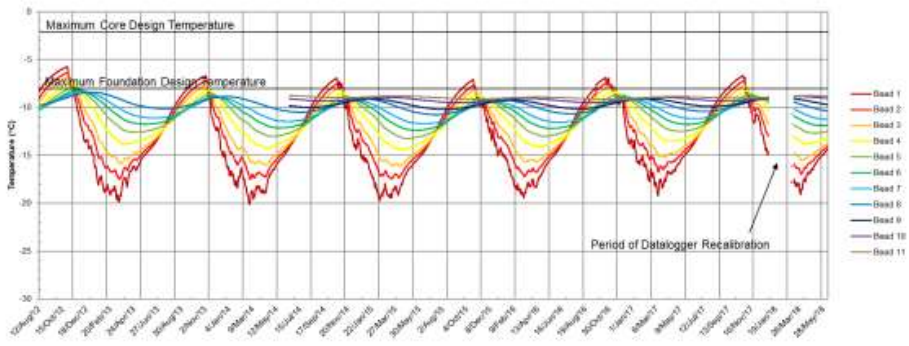


Figure 6c. Time series data for the key trench vertical GTC at chainage 0+175 m (ND-VTS-175-KT).

The maximum measured temperature of the near surface beads for vertical GTCs upstream and downstream of the key trench have been between 0°C and -3°C since 2015. These warmer temperatures are consistent with the design thermal modeling, and are a function of the ambient conditions. Figure 7a shows an example of the thermal behavior for the upstream (ND-VTS-130-US), and Figure 7b, the key trench (ND-VTS-130-KT) vertical GTCs at chainage 0+130 m. Because there is not much head of water behind the dam, there is currently no discernable difference between the ground temperature profiles in the upstream and downstream CTGs.

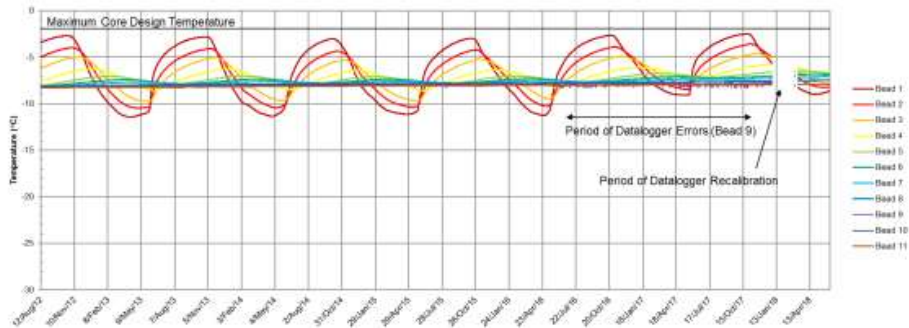


Figure 7a. Time series data for the upstream vertical GTC at chainage 0+130 m (ND-VTS-130-US).

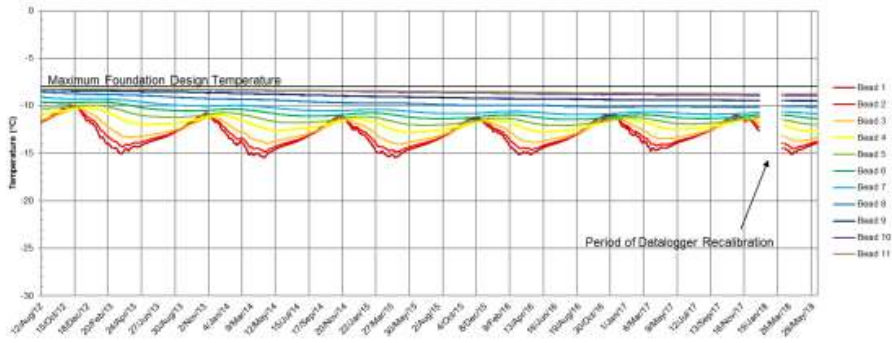


Figure 7b. Time series data for the key trench vertical GTC at chainage 0+130 m (ND-VTS-130-KT).

8 LONG-TERM THERMAL PERFORMANCE

As part of the design for the Phase 2 Doris TIA, additional North Dam thermal modeling was completed to determine if the current configuration of the North Dam is suitable to maintain the thermal design criteria over the intended design life of 30 years. The existing GTC monitoring data, water levels, and climate data were used to calibrate and validate the thermal model to observed conditions. The validated model was then used to model long-term performance over an extended 40-year design life (10 years beyond the planned 30-year design life) with consideration for climate change.

Figures 8a, 8b and 8c shows select calibration model results for chainage 0+085 m. The modeled temperatures at the thermosyphon evaporator pipe closely matches the measured temperature at an equivalent position, and are conservatively warmer during the winter heat extraction period (Figure 8a). The modeled evaporator pipe temperature agrees with the timing of heat extraction from the thermosyphon evaporator pipe which is observed as a rapid decrease in temperature, and the timing of warm and maximum temperature are reached when the thermosyphons are seasonally inactive.

Figures 8b and 8c show calibration model temperatures for the middle of the frozen core and the foundation below the key trench, respectively. The frozen core and foundation temperature also shows good agreement with measured temperature over the calibration period. The combined agreement between the measured and modelled results confirms the model surface boundary conditions, thermosyphon heat extraction, and material thermal properties input to the model are reasonable.

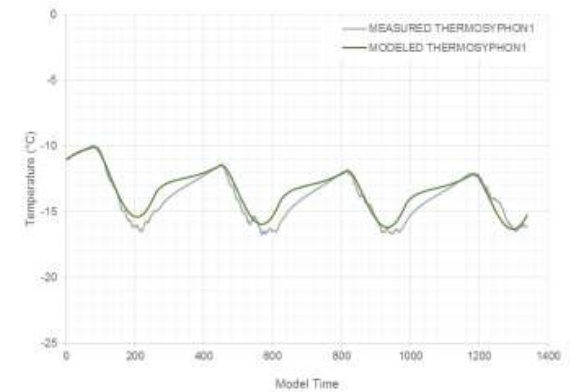


Figure 8a: Thermosyphon evaporator pipe temperature calibration model at chainage 0+085 m.

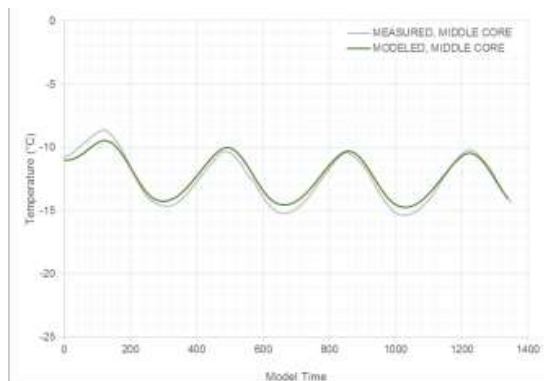


Figure 8b: Middle core temperature calibration model at chainage 0+085 m.

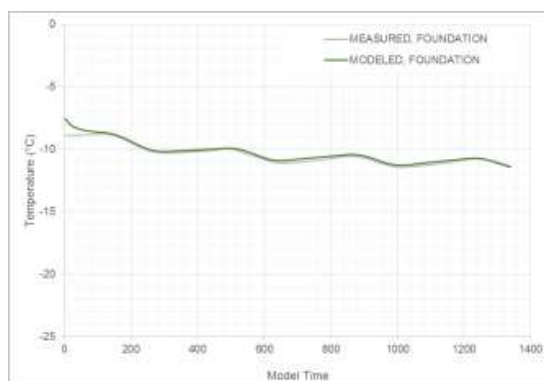


Figure 8c: Foundation temperature calibration model at chainage 0+085 m.

Figure 9 shows the long-term model results for chainage 0+85 m, at the end of the 30-year design life. The critical section of the dam used to assess performance is shown as a yellow bounding box in Figure 9. The results over the critical section indicate the frozen core and foundation will remain below -2°C and -8°C , respectively.

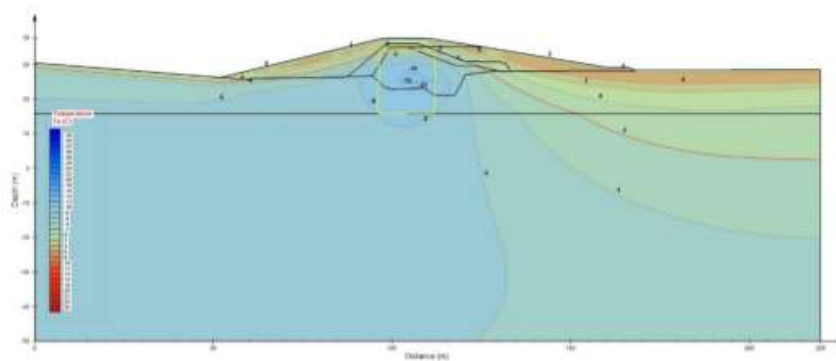


Figure 9. Long-term thermal model results for chainage 0+85 m.

Additional modeling completed for smaller sections of the dam indicate the core temperature over the critical section remains below -2°C for the design life and most, but not all, of the foundation remains at or below -8°C . A smaller portion of the foundation (approximately 8%) is warmer than -8°C at the end of 30 years. The increase in ground temperature outside the critical section of the foundation will result in a higher fraction of unfrozen water and a greater potential for creep deformation (Rykaart et al. 2018).

9 CONCLUSIONS

The frozen core North Dam of the Doris TIA has been designed to retain water at its full supply level over the 30-year design life. Based on thermal modelling and observational monitoring data, the core and foundation are expected to meet the overall thermal design requirements of -2°C and -8°C respectively. Following construction over two winter seasons, six years of monitoring data has been collected and suggests the dam is performing within the design expectations.

While the modelling and monitoring data validates the design, the deep, ice-rich saline marine silts and clays in the foundation will result in long-term creep deformation, and therefore the design geometry has been specified to accommodate large deformations.

The observed and long-term modelled performance of the North Dam continues to exemplify the advantages of prudent design, comprehensive monitoring and observational validation in advancing the state of practice in the challenging conditions of cold regions dam design.

10 ACKNOWLEDGEMENTS

The authors are grateful to TMAC Resources Inc. for allowing the material presented on the North Dam to be published in this paper. The authors would also like to kindly acknowledge their colleagues at SRK Consulting (Canada) Inc. who assisted with design, construction, and on-going monitoring and analysis of the North Dam.

REFERENCES

- Kurylo J., Rykaart M., Wade L. 2013. Engineering challenges for tailings management facilities in permafrost regions. Proceedings of Tailings 2013, Santiago, Chile, August 28-30.
- Miller M., Kurylo J.B., Rykaart M. 2013. Frozen dams in permafrost regions. Proceedings of Mine Water Solutions, Lima, Peru, April 15-17.
- Rykaart M., Barrero A., Lizcano A. 2018. Frozen Core Tailings Dam: Part 2, Long-Term Creep Deformation. Proceedings of Tailings and Mine Waste 2018, Colorado, USA, September 30 – October 2.
- SRK Consulting (Canada) Inc. 2007. Design of the tailings containment area, Doris North Project, Hope Bay, Nunavut Canada, Report prepared for Miramar Hope Bay Ltd. 326 p.
- SRK Consulting (Canada) Inc. 2012. Hope Bay Project, North Dam As-built Report, Report prepared for Hope Bay Mining Ltd. 41 p.
- SRK Consulting (Canada) Inc. 2017a. Doris Tailings Management System Phase 2 Design, Hope Bay Project. Report prepared for TMAC Resources Inc., November.
- SRK Consulting (Canada) Inc. 2017b. Hope Bay Project, Geotechnical Design Parameters and Overburden Summary Report. Report prepared for TMAC Resources Inc., November.
- SRK Consulting (Canada) Inc. 2017c. Hope Bay Project: Doris Tailings Impoundment Area North Dam Thermal Modeling. Memo prepared for TMAC Resources Inc., November 30.
- SRK Consulting (Canada) Inc. 2018a. Hope Bay Project, North Dam Monitoring: Standard Operating Procedures – Revision 2. Report prepared for TMAC Resources Inc., May.
- SRK Consulting (Canada) Inc. 2018b. 2017 Annual Geotechnical Inspection Tailings Impoundment Area Doris Project, Hope Bay, Nunavut. Report prepared for TMAC Resources Inc., March.

Frozen Core Tailings Dam: Part 2, Long-Term Creep Deformation

M. Rykaart, A. Barrero, and A. Lizcano

SRK Consulting (Canada) Inc., Vancouver, British Columbia, Canada

ABSTRACT: Tailings management at the Hope Bay Project in Nunavut, Canada, includes reliance on an innovative frozen core dam. This dam does not have a tailings beach against it, and has been designed as a water retaining dam with a 30-year design life. The dam foundation is subject to significant long-term creep deformation. This paper, which is the second in a two-part series, describe the dam performance six years post construction, and compares modelled creep deformation with field performance data collected from shallow and deep settlement monitors, and inclinometers. The data and modelling confirm that creep deformation is less than originally anticipated during the design stage, and that continued long-term creep deformation of the dam will not result in excessive long-term strains that could impact the structure's performance. The first paper in this series describes the thermal performance of the dam, which is a key parameter driving creep deformation.

1 INTRODUCTION

The tailings management system for the Hope Bay Project, in Nunavut, Canada, includes sub-aerial tailings deposition into the Doris tailings impoundment area (Doris TIA). The Doris TIA is located in the basin of the former Tail Lake, a shallow lake which has been delisted in accordance with Schedule II of the Metal Mining Effluent Regulations. To provide containment, a frozen core water retaining dam (North Dam) was designed (SRK 2007, 2017a), and constructed over the winter seasons of 2011 and 2012 (SRK 2012). Following six years of monitoring, conclusions regarding dam performance can be made, both with respect to thermal response and creep deformation. This paper, which is Part 2 of a two-part series, describes measured deformation data, and associated updated creep deformation modeling, while Part 1 (Rykaart et al. 2018) describes the thermal performance monitoring and associated modeling. Section 1 through 6 of Part 1 and Part 2 is identical to allow the papers to be read independently.

2 TAILINGS MANAGEMENT SYSTEM

The Doris TIA, when fully developed, will consist of one frozen core water retaining dam (North Dam), and two frozen foundation dams (South Dam and West Dam). Tailings will be discharged from the South and West Dams, as well as select locations around the perimeter of the facility. The North Dam will provide water containment for the Reclaim Pond, and no tailings will be in contact with the dam during its 30-year design life. At closure, the Reclaim Pond will be drained, and the North Dam breached, with no need for a permanent water retaining dam (SRK 2017a).

3 FOUNDATION CONDITIONS

The project is located within the continuous permafrost region of Canada, approximately 140 km north of the Arctic Circle. Site measurements indicate that permafrost in the area is approximately 570 m thick, with an active layer of 0.9 m to 1.7 m, depending on the material type. The ground temperature at the depth of zero annual amplitude is -8°C , and the geothermal gradient is $0.021^{\circ}\text{C}/\text{m}$ (SRK 2017b).

Numerous geotechnical characterization programs have been performed within the alignment of the North Dam, to characterize the foundation conditions. Programs included boreholes, test pits, in-situ hydraulic conductivity testing, installation of ground temperature cables (GTCs), long-term ground temperature monitoring (starting in 2002), percolation testing, geophysics, and both undisturbed and disturbed sample collection and laboratory testing (SRK 2017b).

The North Dam is located in a narrow valley approximately 200 m downstream of the northernmost extent of the former Tail Lake. The stratigraphy under the dam has two distinct zones; the southwest abutment is dominated by ice-saturated sand deposits 10 m to 15 m thick, overlain by up to 3 m of silt and clay, while the northeast abutment is dominated by ice-saturated marine clayey silt with a maximum thickness of 15 m. Excess ground ice, averaging 10 % to 30% by volume, occasionally as high as 50%, is also present on both abutments.

A thin layer of sand and gravel overlies the bedrock surface in the upper portions of the valley, and a peat unit was encountered near the center of the dam, in the area of the lake outflow. The average pore water salinity is 39 parts per thousand (ppt), with a freezing point depression of -2.2°C (SRK 2017c). During construction, an isolated hypersaline zone, with salinity values in excess of 90 ppt, was also encountered within the key trench (SRK 2012). Bedrock is generally competent basalt.

Figure 1 provides a generalized longitudinal section of the North Dam foundation conditions, as understood prior to percolation testing and key trench excavation.

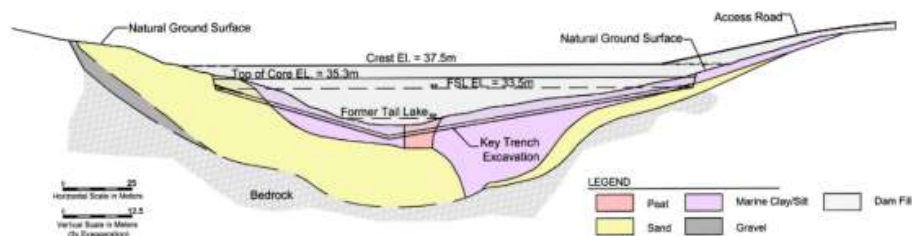


Figure 1. Longitudinal section of the North Dam showing generalized foundation conditions.

4 DAM DESIGN

A conventional unfrozen dam was not suitable for this location due to the thick ice-rich overburden foundation, remote site location, and lack of suitable low-permeability borrow material (Miller et al. 2013). Additionally, the thick overburden meant a frozen core dam founded on bedrock, similar to those constructed at other Canadian mines (Miller et al. 2013), was not feasible. Therefore, an innovative frozen core dam was designed to accommodate these challenging foundation conditions.

The North Dam is approximately 200 m long, with a maximum overall height of 10 m. The frozen ice-saturated core, keyed-in to the frozen foundation are designed to ensure water retention properties and containment. A geosynthetic clay liner (GCL) was installed along the upstream side of the frozen core to provide secondary water-retaining capability in case cracks develop in the core caused by thermal expansion, thermal erosion, differential settlement, or creep deformation. Thermal design to ensure primary containment requires that the frozen core maintains a

temperature at or below -2°C , at a width that is at least twice the head of water impounded against the dam. In addition, the saline foundation needs to maintain a temperature at or below -8°C for the same width, extending to bedrock under normal operating conditions (SRK 2007).

The dam was uniquely designed for the saline ice-rich foundation that is particularly susceptible to creep deformation. Therefore, the dam was designed to accommodate long-term shear strains in the core and foundation approaching 2% and 10%, respectively, and maximum shear strain rates at or below $1.0\text{E}-05 \text{ sec}^{-1}$ ($3.2\text{E}+02 \text{ year}^{-1}$) (SRK 2007).

The dam design included a key trench ranging from 2 m to 5 m deep, to allow complete bonding of the core to the permafrost foundation (SRK 2012). Twelve sloped thermosyphons, six extending from each abutment of the dam, were installed at the base of the key trench to adequately cool the core and foundation over the design life, assuming water permanently impounded against the upstream face to full supply level, and with consideration for climate change. The typical design cross section for the North Dam is illustrated in Figure 2, and the equivalent as-built cross section is illustrated in Figure 3 for comparison.

The core material is comprised of sand-sized crushed basalt, placed in a near saturated state and allowed to freeze during construction. The core is surrounded by a transition layer, consisting of jaw crusher run rock that acts as a filter, should the dam thaw. An outer shell constructed of run-of-quarry rock acts as a thermal protection layer for the frozen core, provides buttressing against creep deformation, and provides ice and wave run-up protection.

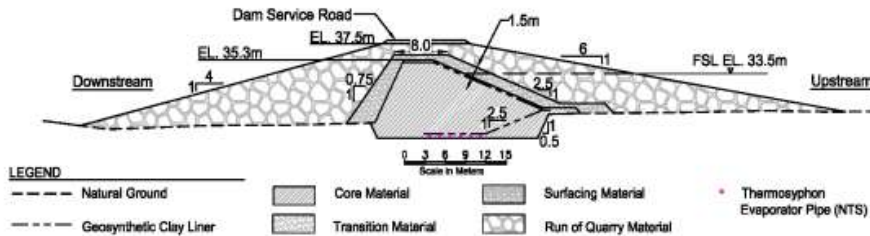


Figure 2. Typical design cross-section of the North Dam.

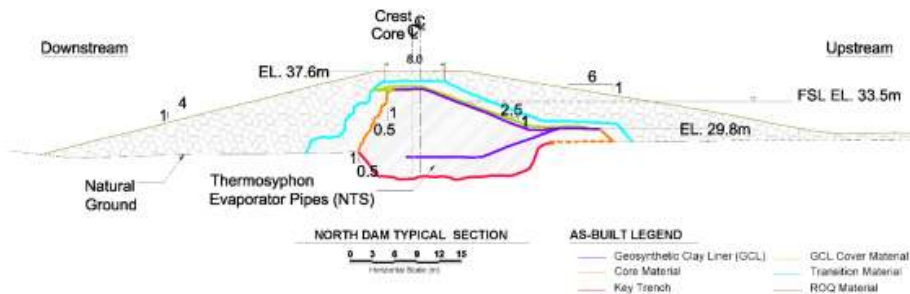


Figure 3. Typical as-built cross section of the North Dam.

5 CONSTRUCTION

The North Dam was designed to be constructed using construction techniques similar to those employed for the frozen core dams constructed at other Canadian mines (Miller et al. 2013). However, the site climate, available construction material, and foundation conditions necessitated adaptations to the construction method (SRK 2012); some of which are summarized in Kurylo et

al. (2013). Details on lessons learned from the North Dam construction are presented in Miller et al. (2013).

Drilling and blasting were used to excavate the key trench. Key trench excavation included the removal of all peat from the center portion of the dam, and over-excavation of the hypersaline zone. Following completion of the key trench excavation, the frozen core was constructed by placing and compacting 0.2 m to 0.3 m thick lifts of core material. Core material was produced in a modified asphalt plant by mixing and heating crushed rock and water. The lifts of saturated hot core material were then left to freeze back to target temperature (at or below -2°C) prior to the placement of the next lift.

Core placement required stringent quality control and quality assurance to ensure that saturation, freeze-back, density, and material specification requirements were met. Quality control and quality assurance included continuous material testing (laboratory and field), visual inspections, and constant and open communication with the client and contractor. These procedures ensured freeze-back, saturation (average 85% or greater, with no test below 80%), and compaction requirements (90% or greater of standard Proctor) were met. Between each lift, loose material and snow was cleared. To ensure that the lifts would freeze within a reasonable timeframe, frozen core placement was not attempted when ambient air temperatures were warmer than -10°C .

Due to the larger than expected excavation required to remove the peat and hypersaline soils, and a warm spring, the dam could not be completed in one winter season as originally planned. At the end of the 2011 construction season, the lower GCL and horizontal thermosyphons were installed and covered; however, the frozen core was not completed. To protect the core during the subsequent summer, a temporary 2 m thick run-of-quarry cover was placed over the partially constructed core. Work recommenced in the winter of 2012, and the dam was substantially complete by April 2012. The last remaining instrumentation on the downstream side of the dam was installed in August 2012 (SRK 2012).

6 INSTRUMENTATION

Performance of the North Dam is dependent on the core and foundation maintaining design temperatures, and the long-term strains, and strain rates remaining below target limits (SRK 2012, 2018a). Thermal performance of the dam is monitored with a series of thirteen horizontal GTCs, and eleven vertical GTCs. Figure 4 provides a typical dam cross section, including the location of these GTCs. Three horizontal GTCs are positioned at the top, middle and base of the core; while vertical GTCs are positioned along the foundation on the upstream side, in the center of the dam (key trench) and on the downstream side.

The working condition of each thermosyphon unit is confirmed using a single bead thermistor attached to the radiator riser pipe and compared with ambient air temperature measurements collected over the same period of time.

Deformations are monitored by a series of surficial, shallow, and deep settlement points and six inclinometers. Eighteen surficial settlement points are located on the downstream face of the dam, to monitor deformation of the dam shell in the location of the greatest expected deformation. Three deep settlement points are used to monitor deformation of foundation soils, again at the location of the greatest expected deformation. Fourteen shallow settlement monitoring points were installed on the crest of the dam to monitor crest deformation and differential settlement. The inclinometers are installed along the location of the greatest expected deformation and monitor deformation of both the dam shell and foundation. The instrumentation layout at the area of greatest expected deformation can be seen in Figure 4.

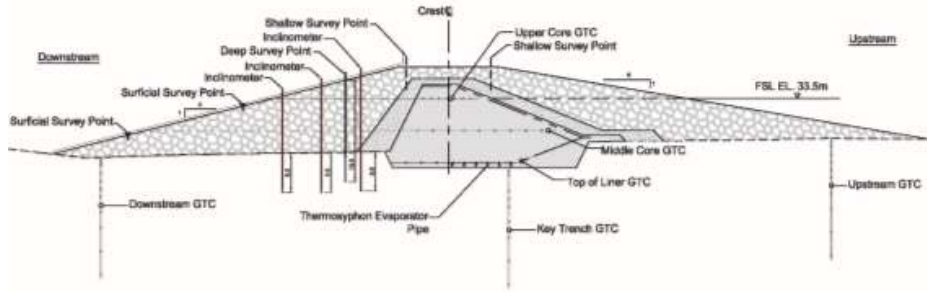


Figure 4. North Dam typical instrumentation.

7 DEFORMATION MONITORING DATA

North Dam monitoring include ground temperature measurements recorded every six hours with data loggers, and monthly manual deformation measurements (i.e. survey settlement and inclinometers). Additionally, ongoing visual inspection of the dam structure by Project staff, and a formal annual geotechnical inspection by a Professional geotechnical engineer, who is also the engineer-of-record, is conducted (SRK 2018a).

Annual inspections (SRK 2018b), and review of monitoring data, suggest the dam is performing in accordance with the design expectations. The North Dam has had impounded water since the first winter of construction in 2011. The operating water level impounded against the upstream face of the dam has averaged 29.8 m, with a maximum level of 30.2 m over the period from May 2011 to June 2018. The original water level of Tail Lake prior to construction of the North Dam was 28.3 m, and the design full supply level is 33.5 m. Core and foundation temperatures have been below the design temperatures of -2°C and -8°C, respectively (Rykaart et al. 2018).

Tables 1 and 2 summarize displacement and deformation data collected between August 2012 and June 2018. Surficial settlement as measured by the downstream dam shell settlement points (Table 1) show the greatest overall displacement. However, much of this occurred soon after construction and this probably largely reflects natural consolidation settlement of the run-of-quarry dam fill material used to construct the dam shell.

Both vertical and horizontal settlement of the dam crest (Table 1) is similar, ranging between 0.02 m and 0.08 m, with the data suggesting no real change over the most recent two years of monitoring. The deep settlement points (Table 1), which provides an indicator of foundation settlement, shows similar overall horizontal deformation as the crest but approximately half of the vertical displacement as compared to the crest.

The inclinometer measurements (Table 2) show similar deformations as measured by the deep and crest-settlement points (Table 1) and confirm that the most deformation occurred in the upper part of the dam shell. Foundation deformation as determined by the lower sections of the inclinometers show very little movement at this point in time, suggesting minimal foundation creep has occurred.

Table 1. Overall vertical (downward) and horizontal displacements measured with settlement points (August 2012 through September 2017).

Location	No. of stations	Vertical Displacement (m)			Horizontal Displacement (m)		
		Min.	Max.	Avg.	Min.	Max.	Avg.
Deep settlement points	3	0.02	0.04	0.03	0.01	0.08	0.05
Crest settlement points	14	0.03	0.08	0.05	0.02	0.07	0.04
Downstream dam shell settlement points	18	0.03	0.21	0.11	0.01	0.25	0.07

Table 2. Maximum deformation measured with inclinometers (August 2012 through June 2018).

Inclinometer	Overall Maximum Deformation (m)	Depth Below Dam Surface (m)	Height Above Foundation (m)	Maximum Foundation Deformation (m)
070-1	0.023	1.0	8.5	0.002
070-2	0.026	2.5	6.5	0.017
070-3	0.013	3.5	4.0	0.002
120-1	0.011	0.5	6.5	0.009
120-2	0.022	0.5	5.5	0.005
120-3	0.017	0.5	2.7	0.002

8 CREEP DEFORMATION ANALYSIS

8.1 Model Setup

Creep deformations were re-assessed post-construction (SRK 2017d) by plane strain conditions using the two-dimensional nonlinear finite difference code, Fast Lagrangian Analysis of Continua (FLAC 2-D), by Itasca (2012). The analysis was carried out along the thickest as-built cross section of the dam (Figure 2). Thermal modelling was completed for the same cross section (SRK 2017c, Rykaart et al. 2018). Five material regions were considered in the deformation model: shell, transition zone, core, foundation, and bedrock. The GCL liner was not represented in the model as it has no structural significance.

8.2 Assessment Approach

The ice-saturated granular material in the frozen core is a dense material with a void ratio around 0.35 (SRK 2017b). The deviatoric strength (peak or residual) of the frozen core material is expected to be above 1 MPa based on published results from laboratory tests conducted on frozen sand samples under constant temperatures around -5°C , and constant strain rates around $1\text{E-}07 \text{ sec}^{-1}$ (Bragg and Andersland 1981, Arenson 2002). Considering the height of the North Dam, the level of deviatoric stresses within the frozen core is anticipated to be low relative to the expected deviatoric strength of the frozen material in the core. According to Andersland and Ladanyi (2004), medium to high-density ice-saturated sands under low stress levels exhibit only primary creep (i.e. decreasing strain rates). Therefore, the creep deformation analysis assumed the frozen core will exhibit only primary creep.

Secondary creep (i.e. constant creep strain rate) was assumed for the frozen marine clayey silt in the foundation. These type of soils exhibits a short primary-creep period, and a prolonged secondary-creep phase (Andersland and Ladanyi 2004).

Based on the Bailey-Norton law (Norton 1929, Bailey 1935), creep strain rates ($\dot{\epsilon}$) of frozen soils due to deviatoric stresses ($\bar{\sigma}$) can be described by the following general equation:

$$\dot{\epsilon} = (A\bar{\sigma}^n) \cdot mt^{m-1} \quad (1)$$

where A is a creep parameter that depends on soil type and temperature, n and m can be considered temperature independent parameters, and t is the elapsed time after load application.

Secondary creep is commonly described by Equation 1, with $m = 1$. In this case, the equation can be rewritten as:

$$\dot{\epsilon} = A\bar{\sigma}^n \quad (2)$$

With Equation 2, frozen soils are always predicted to creep for any given deviatoric stresses. Even for very small stresses, frozen soil is predicted to creep. This may lead to overestimating

actual long-term displacements. A threshold stress (σ_{th}) for frozen soils likely exists, as for metals (Norton 1929), below which creep cannot be measured and Equation 2 no longer applies. Equation 2, as most constitutive equations for creep, is however formulated without a threshold stress.

In the performed analysis, creep strains were evaluated using a constitutive relation represented by Equation 2 implemented in FLAC, described as “The Two-Components Power Law” (Itasca 2012). For the analysis, a temperature independent threshold stress of 30 kPa was selected for all frozen materials, based on published laboratory testing results (Ladanyi 1971, Nixon and Lem 1984, Wijeweera and Joshi 1991, Arenson 2002) and engineering judgment. No creep strains were predicted ($\dot{\epsilon} = 0$) for $\bar{\sigma} < \sigma_{th} = 30$ kPa. This stress is considered to be low, relative to the expected peak deviatoric strength. The assumed stress was not a threshold for the deviatoric stresses as introduced by Norton (1929). In this latter case, the deviatoric stresses ($\bar{\sigma}$) in Equation 2 is reduced by σ_{th} , or $\dot{\epsilon} = (\bar{\sigma} - \sigma_{th})^n$. Likely thresholds for other creep mechanisms in frozen soil (e.g. temperature) were not considered in the analysis. Equation 2 can therefore be written as follows:

$$\frac{\dot{\epsilon}}{\dot{\epsilon}_r} = \left(\frac{\bar{\sigma}}{\sigma_r}\right)^n \quad (3)$$

where $\dot{\epsilon}_r$ and σ_r are reference values for the strain rate and stress. According to Equation 3, the creep parameter A in Equation 2 is:

$$A = \frac{\dot{\epsilon}_r}{(\sigma_r)^n} \quad (4)$$

Based on the experimental work from Nixon and Lem (1984) on saline fine grained frozen soils, Andersland and Ladanyi (2004) proposed the following empirical expression for σ_r in kPa as a function of temperature and salinity:

$$\sigma_r = 0.323(1 - T)^2 \left(\frac{59.505 - S}{8.425 + S}\right) \quad (5)$$

where T is the temperature in Celsius degrees, and S is the salinity in ppt.

The parameter A ($\text{kPa}^{-n} \cdot \text{year}^{-1}$) can be then calculated with Equation 4 as a function of temperature and salinity, using Equation 5 for σ_r , and a reference strain rate of $\dot{\epsilon}_r = 10^{-4} \text{ year}^{-1}$ (Anderson and Ladanyi 2004). For the analysis, the parameter A was determined with Equation 4 at different temperatures for the reported average salinity of 39 ppt.

8.3 Methodology

The creep analysis used the ground thermal conditions predicted through thermal modelling (SRK 2017c, Rykaart et al. 2018). It is expected that the creep behavior of the frozen core and foundation changes as the temperature changes over the dam design life. An accurate prediction of long-term creep deformations therefore requires a thermomechanical coupled constitutive model. However, an efficiently implemented coupled thermo-mechanical model is not available in commercial codes. Hence, long-term creep behavior was evaluated for the ground temperature distribution predicted ten years after dam construction. This time interval is considered as representative for the long-term creep deformation in the North Dam. Subsequently the analysis steps, as described in Table 3, were followed.

Table 3. Creep deformation analysis process.

Step	Procedure
Initial State	The initial stresses of the dam embankment and foundation was obtained in the model by using elastic properties for all materials and turning gravity on.
Elasto-plastic Phase	Dam shell, transition zone, and foundation zone (thawed clayey silt) over the -2°C isotherm was changed from elastic to Mohr-Coulomb materials, and the model was again brought to equilibrium.
Creep Phase	Temperature dependent elastic and creep properties were assigned to the frozen core and foundation, based on the predicted temperature ten years after dam construction. The model was allowed to deform for 30 years.

8.4 Material Properties

Elastic and creep material properties from laboratory tests are not available and were estimated based on previous site-specific studies (EBA 2006), published literature, and engineering judgment. Initial state elastic and shear strength properties were taken from EBA (2006). However, the frozen foundation elastic modulus was adjusted. Table 4 summarizes the elastic and shear strength properties used for obtaining the initial state in the model.

 Table 4. Elastic and shear strength properties used for obtaining the initial state¹.

Model Region	Material	Unit Weight (kN/m ³)	Elastic Modulus (kPa)	Poisson's Ratio (-)	Cohesion (kN/m ²)	Friction Angle (°)
Shell	Run-of-quarry	22	1.0E+05	0.35	-	40
Transition	150 mm minus	21	1.0E+05	0.30	-	35
Core	20 mm minus: 5 mm minus (2:3 blend by volume)	22	1.0E+05	0.25	-	-
Foundation	Thawed clayey silt	17	6.4E+05 ²	0.35	40	-
Bedrock	Basalt	26	1.0E+08	0.25	1000	-

Notes:

1. EBA (2006).
2. Adjusted; EBA (2006) Elastic Modulus was 5×10^{-4} kPa.

Table 5 summarizes the parameters used for the creep phase of the analysis. Parameters n , m , and A (Equation 1) for the frozen core were estimated based on the laboratory test results from Ottawa sand (Sayles 1968) and an average temperature of -9°C in the core ten years after dam construction (Rykaart et al. 2018). For the frozen foundation, n , (Equation 2) was estimated based on published laboratory testing results from saline fine-grained soils (Nixon and Lem 1984, Wijeweera and Joshi 1993). Temperature dependent A values for the frozen foundation were calculated with Equations 3 and 4 for a constant salinity of 39 ppt. For reference, Figure 5 plots Equations 3 and 4 for different temperatures and salinities. The figure includes values from Nixon and Lem (1984) for a salinity of 35 ppt, and those used by EBA (2006) for a salinity of 45 ppt.

Table 5 includes the estimated temperature dependent elastic moduli of the frozen core and foundation required for the elastic strains. Since creep is considered to be a constant volume process, the analysis used a Poisson's ratio of 0.5 for the frozen core and foundation.

Table 5. Creep and elastic properties of the frozen core and foundation¹.

Model Region	b (-)	n (-)	A (kPa ⁻ⁿ ·year ^{-b})	Elastic Modulus (kPa)
Core (-9 ^o C)	0.26	1.32	2.0E-07	3.0E+05
Foundation ²	-3 ^o C	1	9.6E-05	1.0E+04
	-4 ^o C	1	2.5E-05	3.2E+04
	-5 ^o C	1	8.4E-06	6.6E+04
	-6 ^o C	1	3.3E-06	1.4E+05
	-7 ^o C	1	1.5E-06	2.8E+05
	-8 ^o C	1	7.4E-07	5.7E+05
	-9 ^o C	1	3.9E-07	1.2E+06
-10 ^o C	1	3	2.2E-07	2.4E+06

Notes:

1. Constant volume deformation; Poisson's ratio $\nu = 0.5$.
2. Salinity 35 ppt.

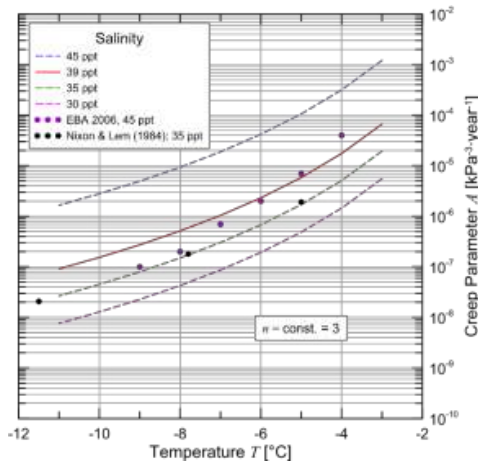


Figure 5: Creep parameter A for the marine clayey silt foundation material.

9 RESULTS

Table 6 summarizes the predicted creep strains and stresses as well as the displacements in the frozen core and underlying frozen foundation, 10 and 30 years post dam construction. Displacements are also listed for the core crest.

Table 6. Creep strains, stresses and displacements in the frozen core and foundation.

Period	Location	Maximum Shear Strain Rate (year ⁻¹)	Maximum Shear Strain (m/m)	Maximum Deviatoric Stress (kPa)	Shear Stress (kPa)	Displacement (m)	
						Max. Horizontal	Max. Vertical
10 years post construction	Core crest	-	-	100 ³	-	-	0.2
	Core ¹	5.0E-08	5.0E-02	300 ⁴ 400 ⁵	20 50 ⁵	0.4	0.6
	Foundation ²	1.0E-07	~1.0E-01	50	20	0.4	0.6
30 years post construction	Core crest	-	-	50 ³	-	-	1.0
	Core ¹	2.0E-08	1.0E-01	300 ⁴ 450 ⁵	20 70 ⁵	0.8	1.0
	Foundation ²	4.0E-08	~2.0E-02	50	20	0.6	1.0

Notes:

1. Within the frozen core.
2. Underneath the frozen core.
3. At the top of the frozen core.
4. At the bottom of the frozen core.
5. Localized at the upstream lower corner of the core.

9.1 Shear Strain Rates and Shear Strains

The analysis predicts shear strain localization mainly at the downstream side of the dam. The shear localization zone is almost circular and goes along the transition zone and through the saline frozen foundation. This surface can be considered as a likely failure surface in the event that the material strength is mobilized along this surface.

In general, the predicted shear strain rates are very low in all zones of the dam and foundation compared with strain rates usually used in laboratory tests with frozen soils (Sayles 1968, Wijeweera and Joshi 1991, Arenson 2002). The maximum shear strain rates are 3.5E-07 year⁻¹ and 1.E-07 year⁻¹, 10 and 30 years after dam completion, respectively. The maximum shear strains are 4.0E-01 m/m (40%) and 6.0E-01 m/m (60%) for the same periods of time. Maximum shear strain rates and shear strains are predicted to occur in points within the shear localization zone (i.e. outside the frozen core and underlying foundation).

In the frozen core and underlying foundation (Table 6), the maximum rate of shear strain meets the design criteria for ductile material behavior (Section 4), while the shear strains themselves exceed the criteria. However, for the frozen core, ductile material behavior is expected because the maximum rate of shear strain is predicted to be very low (~ 1E-08 year⁻¹). Based on Bragg and Andersland (1981), and Arenson (2002), a brittle mode of failure can be excluded in frozen sands that deform under a shear strain rate below < 1E-05 sec⁻¹ (3.2E+02 year⁻¹).

9.2 Principal Stresses Difference

Creep strain rates were evaluated as a response to induced deviatoric stresses by the dam weight. Maximum principal stresses differences of around 75 and 300 kPa are predicted to be almost constant at the crest and bottom of the frozen core, respectively, throughout the dam design life (Table 6). In the frozen saline foundation, an almost constant principal stress difference below 50 kPa is predicted over the design life.

The predicted stress differences at the bottom of the frozen core can be considered as intermediate, compared with the expected peak deviatoric stresses. In the remaining areas of the frozen core and underlying foundation, low stresses difference will prevail.

9.3 Shear Stresses

In general, the shear stresses in the frozen core and foundation are predicted to be relatively low over the design life of the dam, compared with the expected shear strengths of these materials.

9.4 Displacements

Based on the thermal modelling, a greater frozen area is predicted in the foundation at the downstream side than at the upstream side (SRK 2017c, Rykaart et al. 2018). Therefore, the maximum creep displacements due to the frozen foundation will be expected at the downstream side of the dam.

Maximum horizontal displacements of 2.8 and 4.2 m are predicted to occur 10 and 30 years after dam construction, respectively, in a small zone of the foundation at the downstream side. Within and underneath the frozen core, the horizontal displacements remain under 0.8 m over the design life of the dam (Table 6).

Figure 6 shows the vertical displacement history of a point located on the frozen core crest determined for a threshold stress of 30 kPa and pore water salinity of 30 ppt. At the end of the planned design life, the core crest is predicted to settle around 1.0 m.

As a reference for the predicted vertical displacements, Figure 6 includes the maximum measured vertical displacements. These displacements were measured at the downstream part of the dam crest in station 1+20 m, over the first four years after dam completion (although data since then shows a consistent trend).

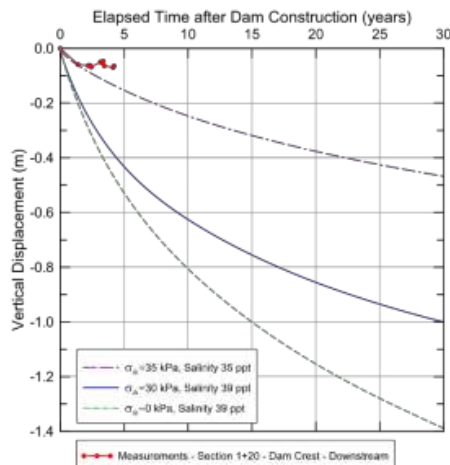


Figure 6: Vertical displacement history of the core crest.

To show the impact of threshold stresses and salinities on the creep deformation analysis, Figure 6 also includes predictions of core crest settlements obtained with thresholds stresses of 0 and 35 kPa, and salinities of 39 ppt and 35 ppt. The lower the threshold stress and higher the salinity, the greater the core crest settlement will be. For a salinity of 39 ppt, and without threshold stress ($\sigma_{th} = 0$ kPa), the core crest is predicted to settle around 1.4 m at the end of the dam design life, i.e. the core crest will settle up to the water full supply level of 33.5 m. However, this result is considered an overestimation of vertical displacements for the reasons outlined in Section 8.2.

10 CONCLUSIONS

The innovative 30-year design life water retaining North Dam constructed in Nunavut, Canada has challenging foundation conditions consisting of thick, saline, ice-rich permafrost, marine

clayey silts, and is highly susceptible to creep deformation. Rigorous thermal and deformation monitoring data has been collected to monitor the dam performance since its completion in 2012.

Rykaart et al. (2018) presents the results of six years of thermal performance monitoring data which demonstrates that the dam is meeting its required thermal design criteria, and updated thermal modeling confirms that this is expected to be maintained for the design life of the structure.

This paper similarly presents six years of deformation monitoring data and updated numerical creep deformation analysis that confirms that the measured deformations in the dam are less than predicted, but even the predicted deformations would not subject the dam to stresses and strain rates outside of the deformation design criteria.

Long-term performance of the frozen core is not expected to be compromised throughout the dam design life. Thirty years after dam construction, the total settlement of the core will be around 1.0 m, i.e. 0.5 m above the full supply level (33.5 m).

11 ACKNOWLEDGEMENTS

The authors are grateful to TMAC Resources Inc. for allowing the material presented on the North Dam to be published in this paper. The authors would also like to kindly acknowledge their colleagues at SRK Consulting (Canada) Inc. who assisted with design, construction, and on-going monitoring and analysis of the North Dam.

REFERENCES

- Andersland O.B., Ladanyi B. 2004. *Frozen Ground Engineering* 2nd Edition. John Wiley and Sons, Inc. Hoboken, New Jersey.
- Arenson L.U. 2002. *Unstable Alpine Permafrost: A Potentially Important Natural Hazard – Variations of Geotechnical Behavior with Time and Temperature*. PhD Thesis, Swiss Federal Institute of Technology (ETH), Zurich.
- Bailey R.W. 1935. *The Utilization of Creep Test Data in Engineering Design*, Proceedings of the Institution of Mechanical Engineers, pp. 131-260.
- Bragg R.A., Andersland O.B. 1981. Strain rate, temperature, and sample size effects on compression and tensile properties of frozen sand. *Engineering Geology* 18: 35-46.
- EBA Engineering Consultants Ltd. 2006. *Thermal Design of Tailings Dams Doris North Project*, NU. Report prepared for SRK Consulting (Canada) Inc.
- Itasca 2012. *Fast Lagrangian Analysis of Continua*. Version 7.0. Itasca Consulting Group, Inc. Minneapolis.
- Kurylo J., Rykaart M., Wade L. 2013. *Engineering challenges for tailings management facilities in permafrost regions*. Proceedings of Tailings 2013, Santiago, Chile, August 28-30.
- Ladanyi B. 1971. *An Engineering Theory of Frozen Soils*. *Geotechnical Journal*, Vol. 9, 63-80.
- Miller M., Kurylo J.B., Rykaart M. 2013. *Frozen dams in permafrost regions*. Proceedings of Mine Water Solutions, Lima, Peru, April 15-17.
- Nixon J.F., Lem G. 1984. *Creep and Strength Testing of Frozen Saline Fine-Grained Soils*. *Canadian Geotechnical Journal*, Vol. 21, 518-529.
- Norton F.H. 1929. *Creep of steel at high temperatures*, New York, Mc Graw-Hill.
- Rykaart M., Luedke P., Stevens, C.W. 2018. *Frozen Core Tailings Dam: Part 1, Long-Term Thermal Performance*. Proceedings of Tailings and Mine Waste 2018, Colorado, USA, September 30 – October 2.
- Sayles F.H., 1968. *Creep of Frozen Sands*. CRREL Technical Report 190, 60p.
- SRK Consulting (Canada) Inc. 2007. *Design of the tailings containment area, Doris North Project, Hope Bay, Nunavut Canada*, Report prepared for Miramar Hope Bay Ltd. 326 p.
- SRK Consulting (Canada) Inc. 2012. *Hope Bay Project, North Dam As-built Report*, Report prepared for Hope Bay Mining Ltd. 41 p.
- SRK Consulting (Canada) Inc. 2017a. *Doris Tailings Management System Phase 2 Design*, Hope Bay Project. Report prepared for TMAC Resources Inc., November.
- SRK Consulting (Canada) Inc. 2017b. *Hope Bay Project, Geotechnical Design Parameters and Overburden Summary Report*. Report prepared for TMAC Resources Inc., November.
- SRK Consulting (Canada) Inc. 2017c. *Hope Bay Project: Doris Tailings Impoundment Area North Dam Thermal Modeling*. Memo prepared for TMAC Resources Inc., November 30.

- SRK Consulting (Canada) Inc. 2017d. Hope Bay Project: Doris Tailings Impoundment Area North Dam Creep Deformation Analysis. Memo prepared for TMAC Resources Inc., November 30.
- SRK Consulting (Canada) Inc. 2018a. Hope Bay Project, North Dam Monitoring: Standard Operating Procedures – Revision 2. Report prepared for TMAC Resources Inc., May.
- SRK Consulting (Canada) Inc. 2018b. 2017 Annual Geotechnical Inspection Tailings Impoundment Area Doris Project, Hope Bay, Nunavut. Report prepared for TMAC Resources Inc., March.
- Wijeweera H., Joshi R.C. 1991. Creep Behavior of Fine-Grained Frozen Soils. Canadian Geotechnical Journal, Vol. 28, 489-502.

Geotechnical Considerations to Reduce Adverse Impacts of Mine Waste Rock Dumps on the Environment

R.B. Kaunda

Colorado School of Mines, Golden, Colorado, USA

ABSTRACT: The shear strength envelope for coarse mine waste rock dumps is nonlinear at low confining stress near the surface. On the other hand, the rock particles buried below the surface are under high confinement and therefore the friction angles decrease with increasing normal stress. Further, at very low confinement, the rock particles have relatively higher mobility with respect to each other and can dilate leading to increased friction angles. As the normal stress increases with depth within the waste rock dump, dilatancy effects grow minimal due to inter-particle crushing. Consequently, this leads to significantly reduced friction angles and reduced rock shear strength and a risk for instability. Using principal component analysis, this study shows that accounting for the rock particle size gradation, fineness modulus, gradation modulus, material hardness, relative density, and confinement can preliminarily assist in evaluation of the shear strength and stability of waste rock dumps and stock piles.

1 INTRODUCTION

1.1 Engineering design of mine waste rock dumps

The failure of a mine waste rock dump can have adverse impacts on the surrounding environment. To prevent failure it is important that dumps are properly designed and constructed. There are seven main components to detailed engineering design of stable mine waste rock dumps and stock piles including site-specific investigations, characterization of foundation conditions, geotechnical characterization of the waste rock materials, static and kinetic geochemical characterization of waste rock materials, hydrogeological characterization, modeling, and the establishment of detailed monitoring systems and Trigger Action Response Plans (TARPS) (Hawley, 2017). In certain cases, however, detailed engineering or characterization of the waste rock is not feasible due to a variety of reasons. For instance, a mine operator may inherit historical, legacy waste dumps whose structural stability is questionable. The geographical location, planned dump dimensions or site specific constraints could also introduce material behavior not anticipated during laboratory testing of waste rock materials. Ideally, it is important to undertake geotechnical considerations accounting for the in-place behavior and stability of the waste rock dump. However establishing the in-place shear strength of a waste rock dump is not always practical in the mining industry.

1.2 Shear strength of mine waste rock dumps

The shear strength of coarse mine waste rock material within a dump can be estimated using back analysis of failures and correlations with penetration rates (Dorador et al., 2017) artificial neural network modeling (Kaunda 2015), and upscaling of small-scale laboratory testing using the matrix method (Siddiqi 1984), scalping method (Al-Hussaini 1983) and parallel gradation (Lowe 1964, Verdugo & de la Hoz 2007). In cases where waste rock dumps are not adequately designed, there are risks of instability and failure.

Blight (2010) has documented several example failure cases of dry waste rock dumps which were end-tipped from the top of a ramp and which failed in shear. Such cases of waste rock dump failures can lead to adverse impacts on the environment if they are chemically reactive (which often mine waste materials are) and escape sequestration or come in contact with the elements. The objective of this paper is to identify key parameters influencing the shear strength of dry waste rock dumps for preliminary geotechnical analysis when available field data is limited. A global geotechnical database involving laboratory and field tests was compiled from more than 10 sites where material properties and shear strengths were characterized. Particle size distribution coefficients are calculated and applied in principal component analysis to investigate their relationships with reported shear strength properties of the waste rock. In this paper, the term waste rock is broadly used to even include coarse types of rock fill used in the mining context, because there are relatively less data on waste rock materials.

2.1 Geotechnical characterization

Outside the integrity of the foundation, regional tectonics and external factors such as precipitation, the shear strength envelope of the rock fill materials is one of the most important considerations during the evaluation of waste dump slope stability. A geotechnical characterization of the shear strength envelope of the fill materials is essential to establishing their shearing resistance. It should be noted, however, that in addition to the shearing resistance, the design of waste dumps also requires information about the deformation and permeability.

2.2 Shear strength envelopes

Geotechnical characterization of shear strength envelopes for waste rock is often compounded by the envelopes' non-linearity. The nonlinearity is a function of waste rock particle size distribution. If the particles are well graded, there is high inter-granular contact between the large and small particles leading to a high density and consequential shear strength. Conversely, if the rock particles are poorly graded, there is relatively low density and consequential shear strength. In cases of very high waste dumps, there is a non-uniform distribution of stress and confinement within the dump. As a result, the rock particles near the bottom of the pile are subjected to relatively greater vertical stress and confinement. The increased vertical stress and confinement near the bottom of the dump induces particle crushing and a subsequent reduction in the internal angle of friction (Valstad & Strøm 1975, Linero et al. 2007, Soroush & Jannatiaghdam 2012, Barton 2013, Fityus & Imre, 2017). In addition, the type of ore, parent rock, degree angularity/roundness, moisture, roughness, porosity, construction method and transportation all have significant bearing on the shear strength envelope of the waste rock. Whereas in hydro-dams rockfill is typically placed in lifts and compacted systematically, it is not uncommon for mine waste rock dumps to be "constructed" by simply overturning truckloads of waste rock leading to low initial densities and void ratios of the in-place material. However, the use of rubber-tired vehicles in some construction methods such as end-dumping, layer-dumping or multi-piling may add a degree of compaction to the structure.

3 METHODOLOGY

In light of the influence of rock particle size distribution on the resulting shear strength envelope, a large database consisting of 120 data points with different size distributions for rock fill materials from around the world was compiled (Table 1).

Table 1. Compiled global database.

Parameter*	D10 (mm)	D30 (mm)	D60 (mm)	D90 (mm)	Cc	Cu	GM	FM	Hardness (R.)	Min UCS (Mpa)	Max UCS (Mpa)	Dry unit wt (kN/m ³)	Confining Stress (Mpa)	Shear Stress (Mpa)
Min	0.02	0.92	3.2	10	0.42	1.36	0.2	3.94	1	1	5	9.32	0.002	0.0065
Max	33.9	42.4	80.1	100	22.3	220	5	8.8	6	250	400	38.9	4.21	3.92
Mean	5.49	9.25	20.4	42.7	2.27	33.7	2.72	6.35	4	73.4	166.6	20.6	0.67	0.63
STDEV	10.05	11.56	15.92	24.14	3.6	46.73	1.26	1.27	1	41.84	92.17	5.44	0.76	0.66

(N = 120)

*D10, D30, D60, and D90 = 10%, 30%, 60% and 90% percent passing sieve sizes respectively; cu = coefficients of uniformity; cc = curvature; GM = gradation modulus; FM = fineness modulus; R = ISRM hardness rating; “min UCS” = minimum uniaxial compression strength of group; “max UCS” = maximum uniaxial compression strength of group; “dry unit wt” = dry unit weight at corresponding confining stress.

In addition the database included fill material hardness, relative density, confining stress and shear strength. From the particle size distributions, the coefficient of uniformity was calculated as shown in Equation 1:

$$C_u = (D_{30})^2 / (D_{10})(D_{60}) \quad (1)$$

where D_{10} , D_{30} and D_{60} are the percent passing sieve sizes corresponding to 10%, 30%, 60% respectively.

Next the coefficient of curvature was calculated from the particle size distributions using Equation 2:

$$C_c = (D_{60}) / (D_{10}) \quad (2)$$

The “fineness” Modulus used in aggregate/concrete applications was calculated according to Equation 3:

$$FM = \sum(\text{Cumulative percentage retained on specified sieves}) / 100 \quad (3)$$

where specified sieves are typically #4 (4.75 mm), #8 (2.36 mm), #16 (1.18 mm), #30 (600 μ m), #50 (300 μ m), and #100(150 μ m).

In addition, the Gradation Modulus (GM) was calculated as expressed by Equation 4:

$$GM = \sum(\text{Cumulative percentage passing sizes through specified sieves}) / 100 \quad (4)$$

where specified sieves are typically 1 1/2 in. (37.5 mm), 3/4 in. (19 mm), 3/8 in. (9.5 mm), #4(4.75 mm), #8(2.36 mm), #16(1.18 mm), #30(600 μ m), #50(300 μ m), #100(150 μ m), and #200 (75 μ m). The higher the GM the greater the content of fines in the waste rock or rock fill.

The compiled database is also comprised of descriptions of fill-material hardness based on International Society of Rock Mechanics (ISRM) ratings (Table 2) (Brown, 1981), minimum uniaxial compressive strength (UCS) and maximum UCS determined from laboratory tests.

Table 2. ISRM rock hardness ratings (modified from Brown, 1981)

Typical Range of Point Load Index (Mpa)	Typical Range of UCS (Mpa)	Hardness, R-Rating
>10	>250	6
4 - 10	100 - 250	5
2 - 4	50 - 100	4
1 - 2	25 - 50	3
-	5 - 25	2
-	1 - 5	1
-	0.25 - 1	0

Next, principal component analysis (PCA) was applied to the database to reduce the dimensionality of the data. The main objective of the dimensionality reduction is cluster isolation of similar variables, essentially responding to a single or similar phenomenon. In the current study, PCA helps indirectly identify the key parameters from the compiled database most affecting the shear strength behavior of the rock fill by transforming the original set of variables to a new set of principal components, in decreasing order of importance. Equation 5 summarizes the transformation applied to obtain the principal components from the dataset:

$$C_Y = 1/(n - 1)P(XX^T)P^T \tag{5}$$

where C_Y is the covariance matrix, n is the total number of variables, P is the transformation matrix of $m \times m$ dimensions, X is the $m \times n$ matrix of the scaled initial data, and P^T is the transpose of P . The principal components are represented by the Eigen values and Eigen vectors of XX^T . The results of the PCA are summarized in Table 3 and discussed in Section 4.

Table 3. Loading coefficients (weights) from principal component analysis of variables from Table 1.

*Principal Component	Parameter														Variance	Cum. Proportion
	A	B	C	D	E	F	G	H	I	J	K	L	M	N		
PC(1)	0.305	0.344	0.359	0.264	0.200	0.130	0.366	0.362	0.284	0.287	0.284	0.141	0.037	0.060	6.09	43.5%
PC(2)	0.280	0.205	0.063	0.282	0.086	0.017	0.019	0.042	0.055	0.076	0.014	0.216	0.600	0.608	2.45	61.0%
PC(3)	0.207	0.237	0.207	0.274	0.344	0.172	0.238	0.212	0.428	0.334	0.365	0.321	0.042	0.018	2.07	75.7%
PC(4)	-0.041	0.020	0.116	0.063	0.474	0.592	0.091	0.123	0.180	0.372	0.350	0.276	0.096	0.053	1.40	85.8%
PC(5)	0.014	0.031	0.091	0.104	0.035	0.613	0.028	0.115	0.115	0.193	0.187	0.690	0.127	0.107	0.76	91.1%
PC(6)	0.460	0.284	0.162	0.588	0.277	0.050	0.061	0.052	0.058	0.017	0.124	0.074	0.371	0.296	0.47	94.5%
PC(7)	-0.295	0.115	0.199	0.081	0.601	0.388	0.014	0.111	0.246	0.177	0.076	0.480	0.012	0.033	0.34	96.9%
PC(8)	0.151	0.236	0.476	0.104	0.255	0.065	0.435	0.461	0.337	0.230	0.131	0.160	0.023	0.050	0.18	98.2%
PC(9)	-0.348	0.082	0.417	0.603	0.188	0.201	0.169	0.331	0.127	0.209	0.212	0.082	0.069	0.061	0.12	99.1%
PC(10)	-0.065	0.177	0.234	0.076	0.258	0.158	0.019	0.231	0.677	0.069	0.536	0.027	0.065	0.045	0.05	99.4%

PC(11)	-0.119	0.082	0.000	0.022	0.006	0.005	0.476	0.476	0.049	0.010	0.058	0.074	0.498	0.516	0.04	99.7%
PC(12)	-0.103	0.003	0.077	0.135	0.040	0.050	0.533	0.411	0.107	0.157	0.167	0.059	0.450	0.488	0.03	99.9%
PC(13)	0.270	0.232	0.343	0.080	0.005	0.006	0.258	0.049	0.118	0.656	0.472	0.012	0.096	0.067	0.01	100.0%
PC(14)	-0.489	0.730	0.397	0.053	0.043	0.039	0.039	0.066	0.088	0.191	0.061	0.013	0.063	0.076	0.01	100.0%

*Parameter A=D10, B=D30, C=D60, D=D90, E=coefficient of uniformity, F=coefficient of curvature, G=gradation modulus, H= fineness modulus, I= ISRM hardness rating, J= minimum uniaxial compression strength, K= maximum uniaxial compression, L= dry unit weight, M=confining stress, N=shear stress.

4 DISCUSSION

Table 3 shows the coefficients for the fourteen principal components. In addition, the variance and the percent of variance attributed to each principal component are shown in descending order. This implies that the first principal component has the largest variance, while the fourteenth principal component has the least variance. Given that the first five principle components account for more than 90% of the total variance, they can be assessed to contain most of the predictive information about the system behavior (i.e. shear strength). For example, the results reveal that the first principal component is mainly weighted on the GM, the FM, and the D60 based on the largest absolute coefficient values. The second principal component is mainly weighted on confining stress, and the third principal component on material hardness, maximum UCS, coefficient of curvature, minimum UCS and dry unit weight. Figure 3 shows how the particle size distribution parameters are correlated with the shear strength.

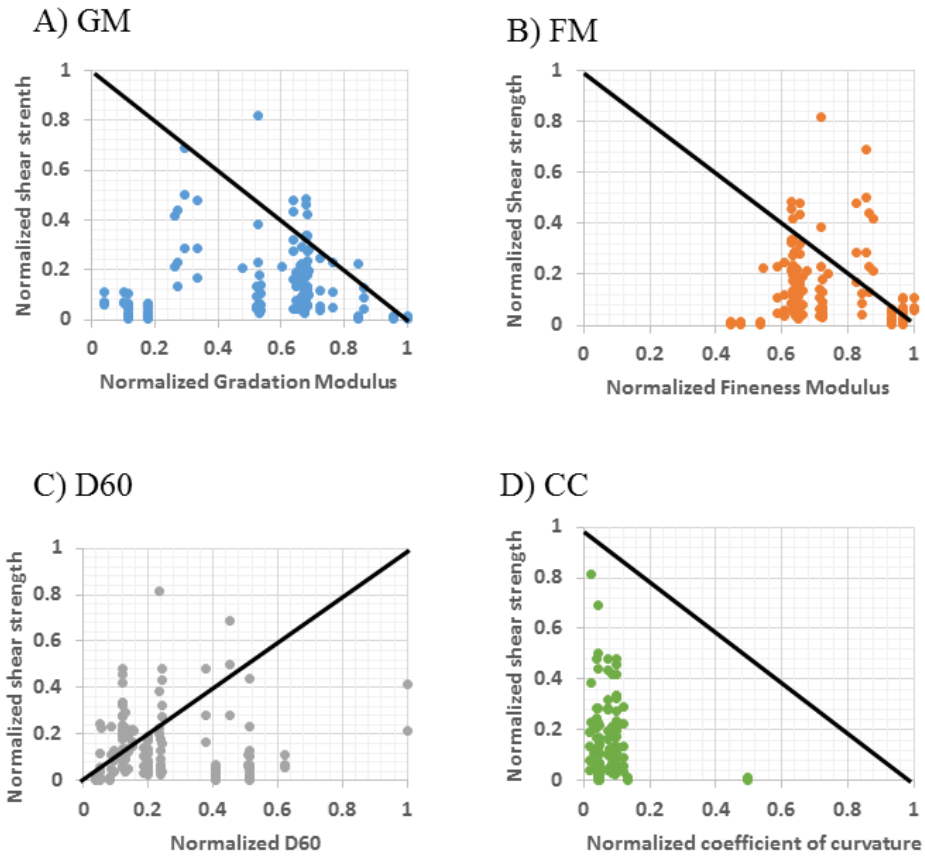


Figure 3. Scatter plots of normalized particle size distribution parameters and normalized shear strength: a) gradation modulus b) fineness modulus c) D60% passing size and d) coefficient of curvature

The implication of the principal component analysis results is that if the particle size distribution for a waste dump can be derived (e.g. through drone photogrammetry and digital image processing) the GM, FM, D60 and coefficient of curvature can provide useful information about the shear strength in conjunction with the confining stress, unit weight, and minimum and maximum particle intact strength. The particle size distribution will also be a function of dump height, transportation, and emplacement method due to material crushing and progressive degradation. This in turn has direct effects on in-place density, void ratio, porosity and internal angles of friction which can be expected to be non-uniform throughout the waste dump. Therefore, the shear strength of a waste rock dump is not static and is highly dependent on its environment and time. As a result, there should be continued ongoing monitoring and stability analysis of mine waste dumps, including those which have been historically stable. Additional factors not covered in this study on shear strength characterization such as deformation analysis and hydrogeological characterization should also be considered.

5 CONCLUSIONS

The characterization of coarse granular materials in mine waste rock dumps is significantly more challenging than in rock-fill dams. Many previous studies have recognized the correlation between rock particle size distribution and shear strength in waste rock dumps. This preliminary study has identified and ranked key geotechnical parameters in terms of their influence on the shear strength of waste rock, based on a compiled global database and principal component analysis. The study indicates that the gradation modulus, the fineness modulus and the D₆₀% passing size have a significant influence on the shear strength of drained waste rock piles. Other equally important considerations are the in situ confining stress, rock particle hardness, maximum and minimum UCS of intact particles, and the dry unit weight. Where site-specific data is unavailable or limited, all efforts should be expended to acquire an estimation of these listed parameters for preliminary geotechnical assessment of the shear strength of the waste rock dump. It should be noted, however, that the current findings are preliminary, and that further research is required by expanding the utilized multi-site database and resolving its limitations. The present study provides encouraging support that parameters derived from particle size distribution curves, which can be obtained from emerging technologies such as drone photogrammetry and digital image processing, can be highly useful in preliminary estimation of the shear strength of mine waste rock dumps.

REFERENCES

- Al-Hussaini, M. 1983. Effect of particle size and strain conditions on the strength of crushed basalt. *Canadian Geotechnical Journal* 20(4): 706-717.
- Araei, A.A., Soroush, A., & Rayhani, M. 2010. Large scale triaxial testing and numerical modeling of rounded and angular rockfill materials. *Scientia Iranica Transaction A Civil Engineering* 17(3): 169-183.
- Azam, S., Wilson, G.W., Fredlund, D.G., & Van Zyl D. 2009. Geotechnical characterization of mine waste rock. *Proc. 17th Intern. Conf. Soil Mech. Geotech. Eng., Alexandria, Egypt, October 5 – 9.*
- Barton, N. 2013. Shear strength criteria for rock, rock joints, rockfill and rock masses: problems and some solutions. *Journal of Rock Mechanics Geotechnical Engineering* 5(4): 249-261.
- Brauns, J. 1993. *Laboratory Tests Report on Materials of Masjed Soleyman Dam*, Division of Earth Dam and Landfill Technology, University of Karlsruhe, Karlsruhe, Germany.
- Brown, E.T. 1981. *Rock characterization, testing and monitoring, ISRM suggested methods*, Oxford: Pergamon Press.
- Charles, J.A. & Watts, K.S. 1980. The influence of confining pressure on the shear strength of compacted rockfill. *Geotechnique* 30(4): 353-367.
- Dorador, L., Cunning, J., Junqueira, F., & Hawley, M. 2017. Material Characterization. In: Hawley, M., & Cunning, J. (eds.), *Guidelines for Mine Waste Dump and Stockpile Design*: 13-27. The Netherlands: CSIRO PUBLISHING/Balkema.
- Fityus, S., & Imre, E. 2017. The significance of relative density for particle damage in loaded and sheared gravels. In EPJ Web of Conferences 140: 07011.
- Gharavy, M. 1996. Experimental and numerical Investigations into the mechanical characteristics of rockfill materials, Ph.D. thesis, University of Newcastle Upon Tyne, U.K.
- Hawley, M. 2017. Basic design Considerations. In: Hawley, M., & Cunning, J. (eds.), *Guidelines for Mine Waste Dump and Stockpile Design*: 13-27. The Netherlands: CSIRO PUBLISHING/Balkema.
- Indraratna, B., Ionescu, D., & Christie, H.D. 1998. Shear behavior of railway ballast based on large-scale triaxial tests. *Journal of Geotechnical and Geoenvironmental Engineering* 124(5): 439-49.
- Kaunda, R. 2015. Predicting shear strengths of mine waste rock dumps and rock fill dams using artificial neural networks. *International Journal of Mining and Mineral Engineering* 6(2): 139-171.
- Linero, S., Palma, C., & Apablaza, R. 2007. Geotechnical characterization of waste material in very high dumps with large scale triaxial testing. In Y. Potvin, (ed): *Proc. intern. symp. on rock slope stability in open pit mining & civil eng.*, Australian Center for Geomechanics, Perth, Australia, pp. 12-14.
- Low, J. 1964. Shear strength of coarse embankment dam materials. In Proc., 8th Int. Congress on Large Dams 3: 745-761. Paris: International Commission on Large Dams.
- Marsal, R.J. 1972. *Mechanical Properties of Rockfill in Embankment Dam Engineering*, Casagrande Volume, New York: Wiley and Sons.

- Rayhani, M.H.T. 2000. Investigation of the behavior of earth and rockfill dam shell materials based on triaxial and direct shear tests. MS thesis, Tarbiat Moallem University, Iran.
- Siddiqi, F. H. 1984. Strength evaluation of cohesionless soils with oversized particles. PhD thesis, University of California, Davis, California.
- Soroush, A. & Jannatiaghdam, R. 2012. Behavior of rockfill materials in triaxial compression testing. *International Journal of Civil Engineering* 10(2):153 – 161.
- Valstad, and T. Strøm E. 1975. Investigation of the mechanical properties of rockfill for the Svartevann Dam, using triaxial, oedometer and plate bearing tests. *Norwegian Geotechnical Institute Publication* 110:3-8.
- Varadarajan, A., Sharma, K.G., Venkatachalam, K., & Gupata, A. K. 2003. Testing and Modeling Two Rockfill Materials', *Journal of Geotechnical and Geoenvironmental Engineering* 129 (3): 206-218.
- Verdugo, R., & de la Hoz, K. 2007. Strength and stiffness of coarse granular soils. In *Soil stress-strain behavior: Measurement, modeling and analysis*: 243-252. Dordrecht: Springer.
- Yamaguchi, Y., Satoh, H., Hayashi, N., & Yoshinaga, H. 2008. Strength Evaluation of Rockfill Materials Considering Confining Pressure Dependency. *Journal of Japan Society of Dam Engineers* 18(3): 166-181.

Improved Methodology for TSF Capacity Prediction

G. Gjerapic

Golder Associates Inc., Denver, Colorado, USA

D. Znidarcic

University of Colorado, Boulder, Colorado, USA

ABSTRACT: Design of tailings storage facilities (TSFs) often requires three-dimensional considerations of seepage and consolidation behavior for accurate predictions of storage capacity. Current industry practice to estimate TSF capacity is commonly based on the use of one-dimensional consolidation models accounting for large strain deformations of tailings during the deposition process. This approach, however, often fails to accurately account for three-dimensional effects and has the potential for excessive water and mass balance errors, especially when considering TSF configurations exhibiting significant changes in the depositional area and variable production rates during the life-time of the facility.

This paper presents an upper and lower bound solutions that can be implemented to rapidly assess potential range of the average tailings densities during operation and closure. In addition, the paper presents the methodology to account for variable production rates using a three-dimensional consolidation TSF model based on a series of one-dimensional soil-columns and compares the proposed model to an equivalent approach commonly used in the industry.

Analyzed TSF filling scenarios with the production rates varying from zero to 30,000 tonnes/day, indicate the potential mass balance error between different modeling methodologies of approximately 50 percent. The paper demonstrates that the available analytical solutions can be applied to perform initial screening between different numerical methods for TSF capacity predictions while avoiding constraints typically associated with complex geometries and variable filling conditions.

1 INTRODUCTION

The deposition of soft soil materials has been successfully modeled by utilizing large strain consolidation theory proposed by Gibson et al (1967). For TSF capacity predictions, complexities in the numerical implementation and convergence issues when modeling large strain consolidation of tailings materials has largely restricted engineering practitioners to using one-dimensional models. Some of the available computer programs capable of solving the one-dimensional Gibson's equation are ACCUMV (Schiffman et al. 1992), CONDES (Yao and Znidarcic1997), FSConsol (GWP Software 1999) and CS2 (Fox and Berles 1997, Fox and Pu 2012).

Gjerapic et al. (2008) proposed the model for TSF capacity prediction based on a series of one-dimensional tailings columns with the approach automated by Coffin (2010). This paper presents a modification of Gjerapic et al. (2008) methodology to illustrate the impact of variable production rates and the importance of evaluating mass balance errors when assessing performance of different numerical schemes for modeling of the TSF filling process.

2 APPROACH AND INPUT PARAMETERS

2.1 Analytical Models for TSF Capacity Prediction

The upper and lower TSF capacity limits can be found by considering analytical solutions for:

- 1) Tailings exhibiting negligible vertical strains during the filling process. For TSF filling scenarios featuring relatively high filling rates and low hydraulic conductivities of deposited tailings, the filling process may cease while the average degree of consolidation remains at relatively low values. For the design purposes, these tailings may be assumed to remain incompressible (i.e., the consolidation model can be simplified assuming that the tailings remain at zero percent consolidation throughout the filling process). In practice, this type of modeling can be often applied to determine TSF capacity estimates for the deposition of thickened mature fine tailings (MFT) or kimberlite tailings deposited in mining raises and stopes.
- 2) Fully consolidated tailings. For TSF filling scenarios with a relatively low rate of rise and/or high tailings hydraulic conductivity, tailings may exhibit the degree of consolidation close to 100 percent. This scenario applies to tailings that are readily expelling pore water during the deposition process (i.e., the magnitude of excess pore water pressures during the deposition process remains negligible). Consequently, the deposition process for these tailings may be modeled by successively applying the steady-state solution for instantaneous consolidation (e.g., the analytical relationship proposed by Gjerapic and Znidarcic 2007) as it allows for accurate integration of the tailings void ratio profile with depth.

The above solutions considering incompressible tailings and tailings undergoing instantaneous consolidation can be readily applied to determine physical limits for any TSF modeling scenario evaluated by numerical models, i.e. these analytical solutions can be used as a “sanity check” when assessing validity of numerical consolidation models in engineering practice.

2.2 Model Geometry

In an earlier paper (Gjerapic et al 2008), a rigorous discretization for the creation of model stage storage curve was developed. For simplicity, the model stage storage curve can be also constructed based on the requirement that the incremental and cumulative tailings volumes at pre-defined elevation points correspond to their respective design values. While this model is preserving volume equivalence, it does not strictly enforce the equivalence between the design and the model areas at pre-defined heights as shown in Figure 1.

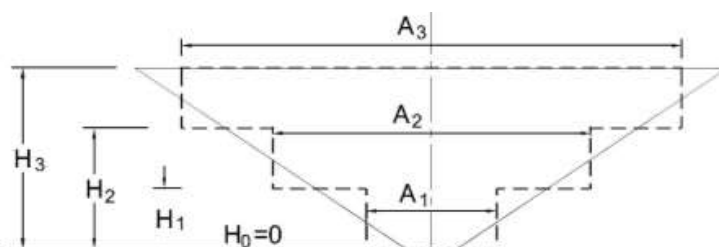


Figure 1. Model discretization of the design stage storage relationship based on the incremental and cumulative volume equivalence at pre-defined heights

The approach to discretize design stage-storage curves based on the equivalence between incremental and cumulative volumes is commonly used in practice and often provides sufficient accu-

racy for engineering calculations. The total TSF impoundment volume in this case can be expressed as:

$$V_{\text{total}} = \sum_{i=1}^n (H_i - H_{i-1}) A_i, \tag{1}$$

where A_i denotes the model TSF area for the i -th stage ($i=1, 2, 3, \dots, n$).

2.3 Numerical Models for TSF Capacity Prediction

One can now construct the three-dimensional consolidation model using the staged filling approach. The i -th stage of the model represents filling of the horizontal layer between heights H_{i-1} and H_i while the model area, A_i , remains constant. For the constant tailings production rate, Q_s , one can calculate the step-wise constant rate of rise, q_i , at every stage as:

$$q_i = \frac{Q_s}{G_s \rho_w A_i} (1 + e_0) \tag{2}$$

where G_s denotes the specific gravity of tailings solids, ρ_w is the density of water and e_0 is the initial tailings void ratio. This type of the consolidation model implicitly assumes that the impoundment sides are undergoing the same deformation as the tailings at the deepest portion of the impoundment. Hence, Gjerapic et al. (2008) noted that the TSF capacity prediction based on such a model is essentially “the upper bound solution”, i.e. this type of consolidation model tends to overpredict the TSF impoundment capacity.

Gjerapic et al. (2008) developed the “lower bound solution” to estimate the TSF capacity. Their approach proposes the development of a three-dimensional consolidation model as an assembly of n one-dimensional columns with the areas $A_{LBi} = A_i - A_{i-1}$ ($i = 1, 2, \dots, n$) where $A_0 = 0$ as shown in Figure 2.

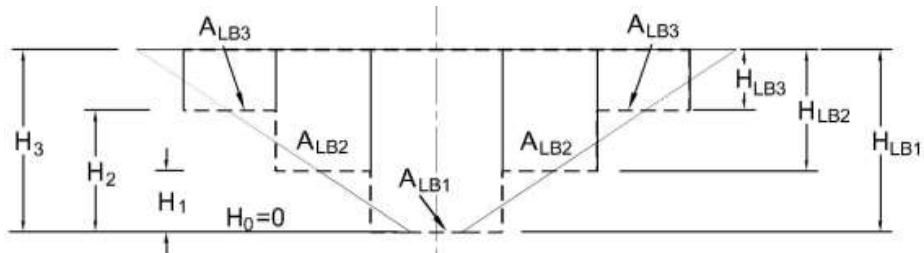


Figure 2. Model discretization as an assembly of one-dimensional columns used for “lower bound” TSF capacity estimates.

The maximum height of individual columns is defined as $H_{LBi} = H_n - H_{i-1}$ where $H_0 = 0$. This approach assumes that the sides of the tailings impoundment are incompressible and therefore provides a conservative (lower bound) estimate of the impoundment capacity which is better suited for use in engineering practice.

2.4 Input Parameters

In this paper, numerical simulations were conducted using stage-storage relationship for discretized TSF geometry as presented in Table 1.

Table 1. Model discretization parameters.

Layer/Column Number, i	H_i (m)	A_i (m ²)	A_{LBi} (m ²)	Cumulative Volume (m ³)
1	30	8.771E+04	8.771E+04	2.631E+06
2	45	8.170E+05	7.293E+05	1.489E+07
3	60	2.406E+06	1.589E+06	5.097E+07
4	75	3.603E+06	1.197E+06	1.050E+08
5	90	4.532E+06	9.293E+05	1.730E+08

All presented TSF simulations were conducted using the following compressibility and permeability relationships (see e.g. Liu and Znidarcic 1991 and Abu-Hejleh and Znidarcic 1996):

$$e = A(\sigma' + Z)^B \quad (3)$$

and

$$k = Ce^D, \quad (4)$$

where e denotes the void ratio, σ' is the effective stress and k stands for the hydraulic conductivity. A , B , C , D and Z are material parameters typically determined from laboratory measurements. Material parameters defining compressibility and permeability relationships in this study are modified from Estepho et al. (2013) by increasing saturated hydraulic values by a factor of one hundred as illustrated in Table 2. If the original hydraulic conductivity values were used, the filling example would produce virtually no consolidation in the 20 years modeling period and would not highlight the differences between different modeling approaches.

Table 2. Material parameters

Gs (-)	A (kPa ^{1/B})	B (-)	Z (kPa)	C (m/day)	D (-)
2.65	3.000	-0.177	0.204	1.21e-4	3.550

For the production rate, $Q_s = 30,000$ t/day, the maximum TSF capacity assuming unconsolidated tailings material can be determined as

$$V_{U=0\%} = \frac{Q_s t_{\max}}{G_s \rho_w} (1 + e_0) \quad (5)$$

Similarly, one can determine the TSF capacity for the fully consolidated tailings as

$$V_{U=100\%} = \sum_{i=1}^n A_{LBi} H_{LB}(H_{si}) \quad (6)$$

where $H_{LB}(H_{si})$ denotes the height of the i -th column expressed as a function of the height of solids contained within the TSF impoundment area A_{LBi} :

$$H_{LBi} = H_{si} + \frac{A\{[(G_s - 1)\gamma_w H_{si} + Z]^{B+1} - Z^{B+1}\}}{\gamma_w (B+1)(G_s - 1)} \quad (7)$$

For the known tailings throughput, the TSF capacity for fully consolidated tailings ($U=100\%$) conditions can be calculated iteratively based on the following mass conservation requirement

$$\int_0^t Q_s(\tau) d\tau = G_s \rho_w \sum_{i=1}^n A_{LBi} H_{si}^*, \quad n^* \leq n \quad (8)$$

i.e., for the known amount of tailings in the impoundment, one can adjust the current height of the tailings surface, H^* by utilizing Equation (7) and the relationship, $H_{LBi}^* = H^* - H_{i-1}$, until matching the required impoundment capacity defined by Equation (8).

Equation (8) can be also used to develop a generalized three-dimensional model based on a series of one-dimensional columns that allows for the TSF filling scenario with variable filling rates. I.e., the production rate, Q_s , in this model can be expressed as a function of time. After noting that the left hand side of Equation (8) denotes the total amount of tailings in the impoundment, the filling scheme (specifically, the duration of the corresponding filling rates) in the numerical model needs to be adjusted until the mass conservation statement represented by Equation (8) is satisfied.

This paper presents the performance of different numerical schemes used to model three-dimensional tailings deposition, namely upper and lower bound solution discussed in Gjerapic et al. (2008), for scenarios considering variable filling rates. The upper bound evaluations were conducted using FSConsol (GWP Software 1999). The lower bound simulations were conducted by

utilizing program FILLCON. Numerical simulations in FILLCON are conducted by successive iterations using a series of one-dimensional tailings columns.

3 EXAMPLES

3.1 Case Scenarios

All models presented in this study are based on the production rate of 30,000 t/day and the total tailings throughput of 109.5 Mt. The following scenarios were considered:

- Case 1 - TSF filling with the constant production rate ($Q_s = 30,000$ t/day) for the duration of 10 years. The filling period is followed by a quiescent/inactive period for additional 10 years. Case 1 model duration is 20 years.
- Case 2 – On-off filling schedule based on the sequence consisting of active TSF filling for 1-year followed by a quiescent period with the 1-year duration. Total duration for the Case 2 model simulation is 20 years.

Filling rates used for the considered model simulations are shown in Figure 3.

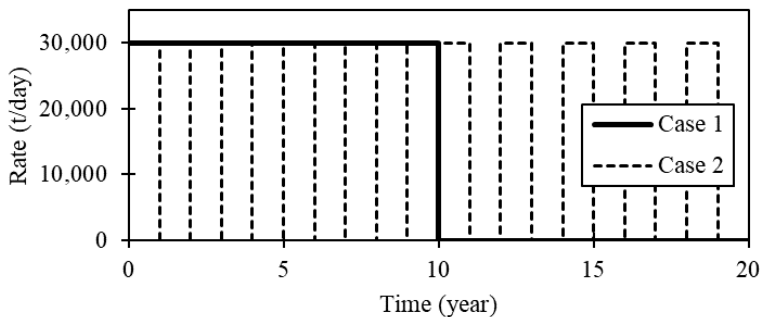


Figure 3. Production rates used for Case 1 and Case 2 model scenarios

Cumulative tailings mass for Case 1 and Case 2 model simulations is presented in Figure 4.

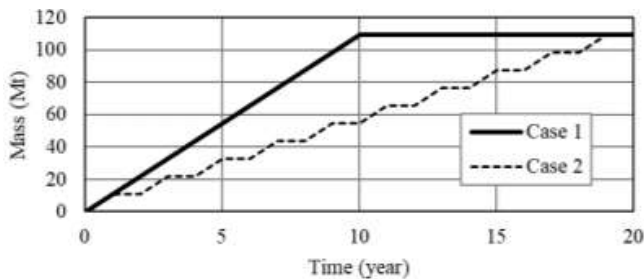


Figure 4. Cumulative tailings mass for Case 1 and Case 2 model scenarios

For the known cumulative production of 109.5 Mt, one can utilize analytical solution for a fully consolidated material to calculate the TSF capacity as shown in Table 3. Results in Table 3 illustrate the capacity demand of 99.8 million cubic meters, i.e. if one assumes that the tailings are fully consolidated, the average tailings density of approximately 1.1 t/m^3 can be used for the tailings impoundment design. The analytical estimate of 99.8 million cubic meters represents the minimum (optimistic) TSF capacity requirement as it assumes that no excess pore pressures are generated during the deposition process. On the other hand, if no consolidation is assumed during the filling process the average tailings density remains at its initial value of 0.53 t/m^3 , requiring

the maximum (pessimistic) TSF capacity of 205.6 million cubic meters. The corresponding tailings depths for the specified geometry would be 73.6 and 95.9 meters, respectively.

Table 3. TSF Capacity for Instantaneous Consolidation – Fully Consolidated Tailings

Column ID	Height (m)	Height of Solids, Hs (m)	Vol. of Solids (m ³)	Mass of Solids (t)	Volume (m ³)	Avg. Dry Density (t/m ³)
1	73.55	33.51	2.940E+06	7.790E+06	6.451E+06	1.21
2	43.55	18.75	1.367E+07	3.623E+07	3.176E+07	1.14
3	28.55	11.72	1.861E+07	4.933E+07	4.536E+07	1.09
4	13.55	5.09	6.096E+06	1.616E+07	1.622E+07	1.00

3.2 Results

Modeling results from FSConsol simulations are summarized in Table 4. For a given tailings height, the total amount of tailings (total tailings mass) is determined from the calculated average solid content and the TSF volume. The calculated model mass is then compared to the actual tailings mass determined from the tailings production rate and the cumulative throughput shown in Figures 3 and 4.

Table 4. FSConsol Results

Case Scenario	Tailings Height (m)	TSF Capacity (m ³)	Avg. Void Ratio (-)	Avg. Dry Density (t/m ³)	Mass Error dM=Model – Actual (tonne)	Relative Error dM/Cum. Production (%)
Case 1 – 10 yr	82.58	1.39E+08	3.02	0.66	-1.76E+07	-16.10%
Case 1 – 16 yr	71.06	9.08E+07	2.46	0.77	-3.99E+07	-36.47%
Case 1 – 20 yr	65.54	7.09E+07	2.19	0.83	-5.06E+07	-46.20%
Case 2 – 20 yr	70.77	8.98E+07	2.26	0.81	-3.64E+07	-33.26%

Modeling results from FILLCON simulations for Case 1 scenario after 10-years are summarized in Table 5.

Table 5. FILLCON Results – Case 1 after 10 years

Column	Tailings Height (m)	Capacity (m ³)	Avg. Void Ratio (-)	Avg. Dry Density (t/m ³)	Model Mass (tonne)	Mass Error dM=Model – Actual (tonne)	Relative Error dM/Cum. Production (%)
1	83.48	7.32E+06	3.03	0.66	4.82E+06		
2	53.60	3.91E+07	2.65	0.73	2.83E+07		
3	38.58	6.13E+07	2.43	0.77	4.74E+07		
4	23.59	2.82E+07	2.32	0.80	2.26E+07		
5	8.58	7.97E+06	2.38	0.78	6.24E+06		
Total		1.439E+08			1.094E+08	-9.974E+04	-0.091%

Modeling results from FILLCON simulations for Case 1 scenario at the end of model simulation are summarized in Table 6.

Table 6. FILLCON Results – Case 1 after 16 years

Column	Tailings Height (m)	TSF Capacity (m ³)	Avg. Void Ratio (-)	Avg. Dry Density (t/m ³)	Model Mass (tonne)	Mass Error dM=Model – Actual (tonne)	Relative Error dM/Cum. Production (%)
1	73.74	6.47E+06	2.56	0.75	4.82E+06		
2	46.15	3.37E+07	2.16	0.84	2.82E+07		
3	33.28	5.29E+07	1.97	0.89	4.72E+07		
4	20.11	2.41E+07	1.84	0.93	2.24E+07		
5	7.31	6.80E+06	1.90	0.91	6.22E+06		
Total		1.239E+08			1.089E+08	-6.411E+05	-0.585%

Results in Table 5 and Table 6 demonstrate the potential for the “lower bound” solution to reduce or eliminate mass balance errors commonly encountered when applying the “upper bound” approach. A comparison between different consolidation models for Case 1 conditions is illustrated in Figure 5.

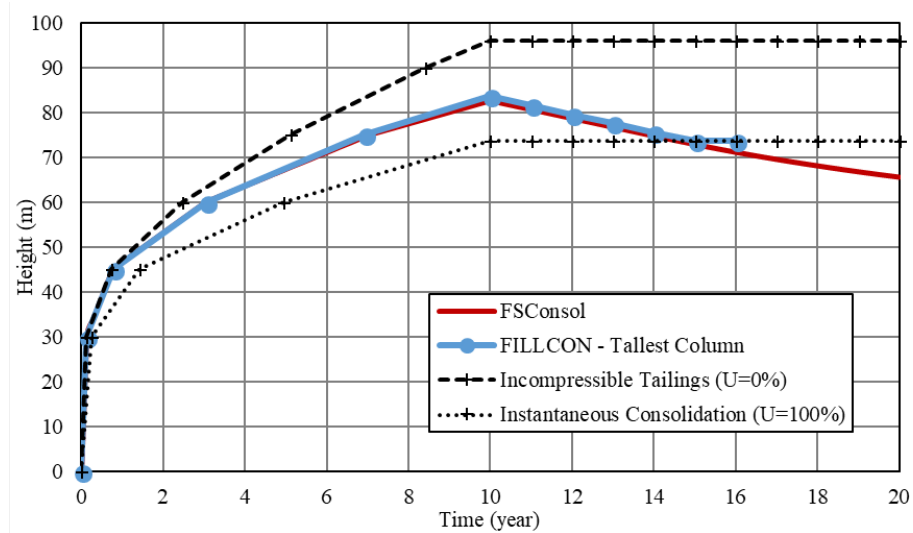


Figure 5. Time settlement curve for Case 1 model scenarios

FSConsol (“upper bound”) results in Figure 5 indicate physically inadmissible conditions, i.e. the maximum tailings height determined from the analytical solution assuming fully consolidated tailings ($U=100\%$) is larger than the tailings height determined by the “upper bound” consolidation model. The numerical error in the model is cumulative in a sense that it increases with time. As noted previously, the ill-conditioned model performance is due to assumption that the sides of the tailings impoundment are undergoing the same deformation as the tailings in the part of the TSF with the tallest tailings height. Results in Table 4 demonstrate that the continuously increasing dry density values result in continuous increases in the mass balance error. The amount of tailings mass in the model is determined by multiplying the TSF volume (determined from the model height-area-volume relationship for a given tailings height) and the average tailings density. The “apparent” loss of mass is significantly smaller for “lower bound” simulations conducted in FILLCON (see Tables 5 and 6) because this model does not allow for deformations at the bottom of individual tailings columns. Void ratio profiles for Case 1 simulations are presented in Figures 6 and 7. Analytical solutions in Figures 6 and 7 assume fully consolidated tailings and were determined based on input parameters summarized in Table 3.

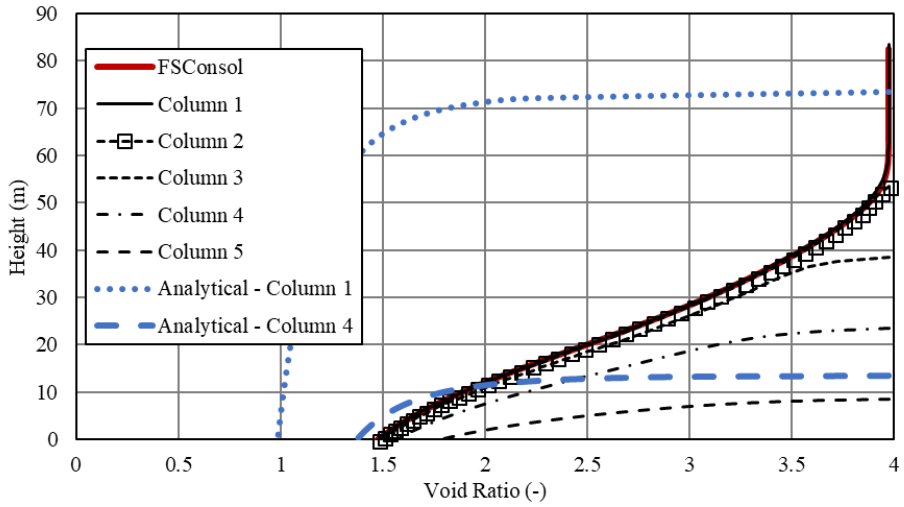


Figure 6. Void ratio profiles for Case 1 model scenarios at the end of filling, time = 10 years.

Results in Figure 6 demonstrate that the tailings are not fully consolidated at the end of the deposition process. Void ratio profiles determined by FSConsol and FILLCON for Column 1 indicate that the degree of consolidation is negligible for more than 25 percent of tailings in the deepest part of the impoundment.

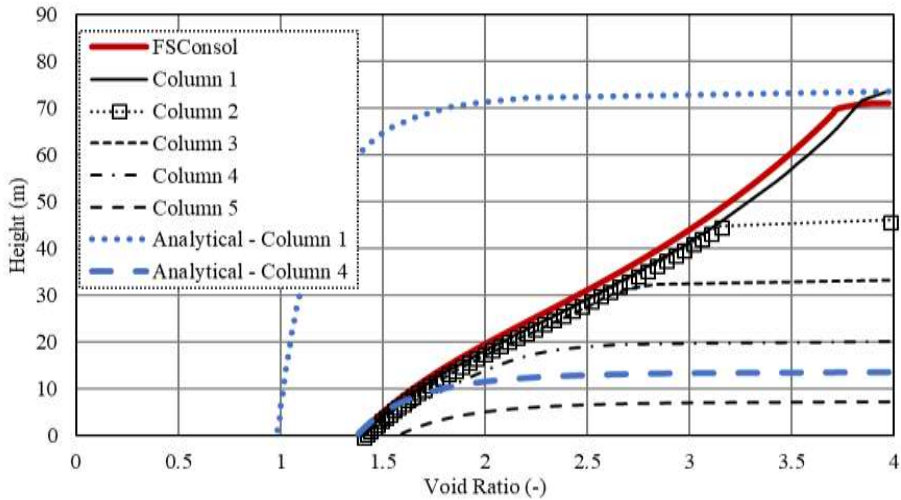


Figure 7. Void ratio profiles for Case 1 model scenarios 6 years after closure, time = 16 years.

To investigate sensitivity of the developed “lower bound” numerical scheme to variable production rates, FSConsol and FILLCON models were evaluated for the sequential on-off filling, Case 2, scenario. This scenario is illustrated by production curves in Figures 3 and 4. Case 2 model results after 20-years from the beginning of deposition are summarized in Table 7.

Table 7. FILLCON Results – Case 2 after 20 years

Column	Tailings Height (m)	TSF Capacity (m ³)	Avg. Void Ratio (-)	Avg. Dry Density (t/m ³)	Model Mass (tonne)	Mass Error dM=Model – Actual (tonne)	Relative Error dM/Cum. Production (%)
1	74.15	6.50E+06	2.30	0.80	5.23E+06		
2	44.68	3.26E+07	1.93	0.90	2.95E+07		
3	29.92	4.75E+07	1.81	0.94	4.48E+07		
4	15.11	1.81E+07	1.87	0.92	1.67E+07		
5	0.66	2.87E+00	1.90	0.91	2.63E+00		
Total		1.047E+08			9.618E+07	-1.332E+07	-12.165%

A comparison between different consolidation methodologies evaluated for Case 2 conditions is shown in Figure 8 in terms of time-settlement curves.

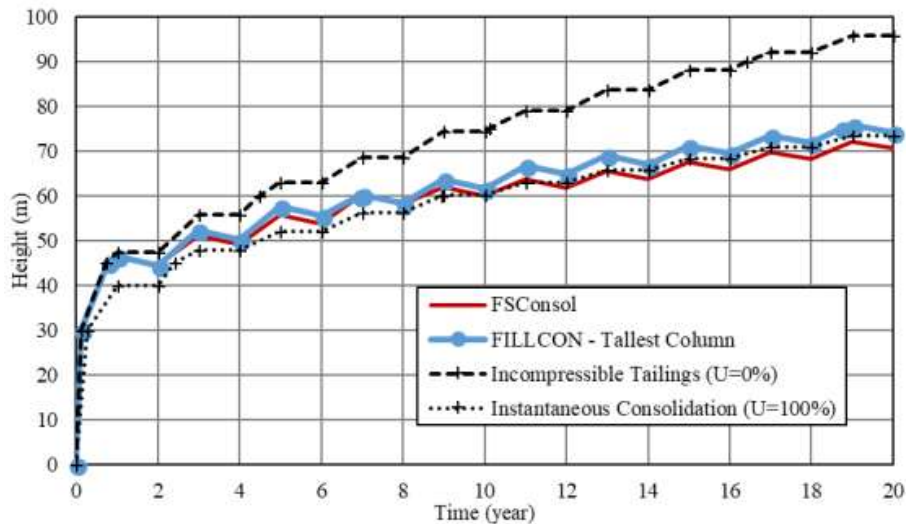


Figure 8. Time settlement curve for Case 2 model scenarios

Similar to trends observed for Case 1 conditions, Figure 8 indicates that the maximum tailings height for fully consolidated tailings ($U=100\%$) is larger than the tailings height determined by the “upper bound” consolidation model. While the FILLCON (“lower bound”) solution performance is better than the performance of the “upper bound model”, results in Table 7 indicate that the currently implemented deposition algorithm requires improvements (i.e., the iterative scheme currently used in FILLCON to solve Equation (8) will be modified in future versions of the model to enforce stricter mass balance criteria).

4 CONCLUSIONS

This paper presents results of different numerical models for TSF capacity predictions that are commonly used in today’s engineering practice. The paper demonstrates that three-dimensional consolidation models using the representation of TSF geometry as a series of horizontal layers may lead to significant mass-balance errors.

The three-dimensional consolidation model using a series of one-dimensional columns, the “lower bound” solution, presents realistic representation of actual TSF conditions and, consequently, results in significantly lower mass-balance errors.

A three-dimensional consolidation model FILLCON was developed to demonstrate that the “lower bound” solution model can be applied to TSF scenarios with variable tailings production rates.

Upper and lower TSF limits can be determined by using analytical solution for incompressible tailings and tailings exhibiting instantaneous consolidation.

5 REFERENCES

- Abu-Hejleh, A.N. and Znidarcic, D., 1994, Estimation of the Consolidation Constitutive Reactions, Computer Methods and Advances in Geomechanics, Siriwardane & Zaman (eds) Balkema, Rotterdam, pp. 499-504.
- Abu-Hejleh, A. N., Znidarcic, D., and Barnes, B.L., 1996, Consolidation Characteristics of Phosphatic Clays, Journal of Geotechnical Engineering, ASCE, New-York, Vol. 122, No. 4, pp. 295-301.
- Coffin, J.G. 2010. *A three-dimensional model for slurry storage facilities*, Ph.D. Dissertation, Department of Civil Engineering, University of Colorado, Boulder, Colorado.
- Estepho, M., van Zyl, D., Znidarcic, D. and Revington, A. Seepage induced consolidation testing of mature fine tailings, Proceedings of Tailings & Mine Waste 2013 Conference, November 3-6, 2013, Banff, Alberta, Canada, pp. 101-109.
- Fox, P. J., and Berles, J. D. 1997. CS2 : A piecewise-linear model for large strain consolidation. *Int. J. Numer. Anal. Methods Geomech.*, Vol. 21, No. 7, pp. 453 – 475.
- Fox, P. J., and Pu, H. 2012. Enhanced CS2 Model for Large Strain Consolidation, International Journal of Geomechanics, Vol. 12, No. 5, pp. 574-583.
- Gibson, R.E., England, G.L., and Hussey, M.J.L. 1967. The theory of one-dimensional consolidation of saturated clays. 1. Finite Non-linear Consolidation of Thin Homogeneous Layers. *Géotechnique*, Vol. 17, 261-273
- Gjerapic, G. and Znidarcic, D., 2007. A Mass-Conservative Numerical Solution for Finite-Strain Consolidation during Continuous Soil Deposition. In: Siegel, T.C., Luna, R., Hueckel, T. & Laloui, L., eds. Geo-Denver 2007: Computer Applications in Geotechnical Engineering: New Peaks in Geotechnics (GSP 157) conference proceedings. Denver, CO, CD-ROM.
- Gjerapic, G., Johnson, J., Coffin, J. and Znidarcic, D., 2008. Determination of Tailings Impoundment Capacity via Finite-Strain Consolidation Models. In: Alshawabkeh, A.N., Reddy, K.R. & Khire, M.V. eds. GeoCongress 2008: Characterization, Monitoring, and Modeling of GeoSystems (GSP 179) conference proceedings. New Orleans, LA, 798-805.
- GWP Software 1999. FSConsol User’s Manual.
- Liu, J.C., and Znidarcic, D., 1991. Modeling One-Dimensional Compression Characteristics of Soils. Journal of Geotechnical Engineering, ASCE, 117, No. 1, pp. 164-171.
- Schiffman R.L. Szavitz-Nossan, V., McArthur, J.M. 1992. “ACCUMV — Non-linear Large Strain Consolidation”, Computer Code Manual, Department of Civil Engineering, University of Colorado at Boulder.
- Yao, D.T.C. and Znidarcic, D. 1997. “Crust Formation and Desiccation Characteristics for Phosphatic Clays - Users’ Manual for Computer Program CONDES0”, *Florida Institute of Phosphate Research (FIPR)* Publication No. 04-055-134.

Investigating the Effect of Pre-shear Prior to Flocculation

C. Torrez López and M.L. Catling

BASF Corporation, Tucson, Arizona, United States of America

J. Bellwood

BASF PLC, Low Moor, Bradford, Great Britain

L. Boxill

BASF Canada, Calgary, Alberta, Canada

ABSTRACT: The dewatering of high clay, high solids slurries via the use of anionic copolymers is known to be a challenge, often requiring high quantities of polymer for improvements in the overall strength of the deposit. This is particularly true in applications where secondary flocculation follows primary treatment of a tailings stream. Treatment of thickener underflow or secondary treatment of material that has been dredged from a tailings storage facility and initially treated are examples of secondary flocculation. This paper describes the improvement in dewatering performance that can be achieved by controlling shear prior to flocculation. Pre-shearing maximizes the dewatering of a substrate whilst minimizes the dose of polymer required. This study uses tailings from several mineral sources with varying clay and solids content. The paper also investigates if it is possible to “overly pre-shear” the slurry of interest, and whether this hinders the dewatering performance of the flocculant being used to treat the substrate.

1 INTRODUCTION

1.1 *Background*

Typically, mining operations produce high quantities of waste, called tailings, leading to an increase in the number/volume of tailings storage facilities (TSF) required, as more product is mined. Much work has been done for the remediation and management of the tailings, as these facilities pose environmental and public hazards. That is why it is very important to employ an efficient method of treatment and disposal. Several methods have been applied to their treatment, but the use of synthetic chemicals is helping to lead towards to better disposal of tailings. Since their discovery, the use of chemical flocculants has improved the treatment of tailings by accelerating the settlement of fine particles and the tailings dewatering, making them very effective at solid-liquid separation in a reasonable amount of time (Stocks, 2006).

Tailings contain a variety of components such as sand, clays, chemicals, and water. Nevertheless, the fine solids present in the tailings are the component which mainly governs the tailings’ physicochemical and rheological properties. Clays are very fine particles with less than 2 μm diameter which have a sheet-like structure and are a sub-group of the fine solids (< 44 μm) fraction in tailings (Sanford, 1983, Kotlyar et al. 1995, Masliyah et al. 2004). It is known that clays entrap water in their structure, making this a problem when trying to dewater tails (Van Olphen, 1986, Hogg, 2000). The water present in the tailings interacts with the surface of the clay through strong interactions like hydrogen bonding.

This is one of the reasons why dewatering may be less efficient if clay particles are aggregated together. Figure 1 shows how clay can assume a stacked or “house of cards” arrangement and a dispersed configuration (Johnson et al. 2000).

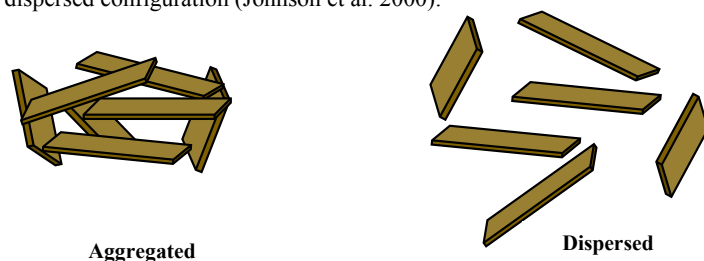


Figure 1. Different arrangements of clay particles in aqueous suspension. The picture on the left displays a aggregated configuration of the clay particles, which is the preferred arrangement if left to consolidate. The picture on the right shows physically dispersed clay platelets.

One method of breaking up clay particle aggregates is by using a shear force, which was investigated in this study. Therefore, shearing the tails would rupture the interparticle interactions between the clay platelets releasing the trapped water and making the clay surface available for flocculation. However, over-shearing may be detrimental, if it leads to an increase in the number of primary particles in the system.

1.2 Objective

The primary objective of this study was to investigate if pre-shear prior to flocculation improves the dewatering on two different types of mine tailings while decreasing the amount of polymer required. This was completed by shearing a tailings substrate for different amounts of time before treating with the flocculant. Investigating different lengths of time of pre-shearing provided insight on the amount of time needed to achieve maximum dewatering of the tailings. Sieves were used to evaluate the free drainage dewatering and to quantify the amount of water released during different time frames. Secondly, the study investigated if it was possible to “overly pre-shear” the slurry of interest and whether this hindered the dewatering performance achieved by the flocculant being used. If proven to be successful, optimal pre-shear could be utilized to minimize flocculant dose needed to optimize dewatering. This would be a more cost-effective solution for companies, reducing the amount of flocculant needed to achieve the same dewatering performance.

2 EXPERIMENTAL

2.1 Materials

2.1.1 Mine Tailings Samples

Two different substrates were utilized in this study: (1) oil sands mature fine tailings (MFT) and (2) tailings thickener underflow from a copper mine. The oil sands sample was obtained from Alberta, Canada and the thickener underflow sample was obtained from a copper mine in Arizona, United States.

2.1.2 Polymers used

For this study anionic polymers from BASF were used as flocculants. Table 1 includes characteristics of these conventional polymers.

Table 1. Characteristics of polymers used in this study

Flocculant	Molecular Weight	Anionic Charge Density (% wt.)
Polymer A	high	23
Polymer B	low – medium	30

Polymer A and Polymer B were chosen to treat the thickener underflow from the copper mine and the oil sands MFT, respectively. Polymers were prepared as 0.5% w/v solutions from a dry polymer powder in process water (PW). Polymer A was made in PW sourced from the copper mine while Polymer B was hydrated with synthetic PW of similar chemical composition to a recycle PW sourced from an oil sands operation. The hydrated polymer solutions were initially mixed by hand for approximately 1 minute, then for 1 hour in a tumble wheel set at 30 RPM. Polymer solutions were prepared and used on the day each experiment was completed.

2.1.3 Instruments

The IKA RW 20 digital and SCILOGEX OS40-Pro overhead mixers were used to pre-shear the slurry samples. The IKA Eurostar 60 Control overhead mixer was used to condition the oil sands MFT with Polymer B. Yield stress data was obtained using a DV3T Brookfield Rheometer. Particle size distribution (PSD) data was conducted using a Beckman Coulter LS I3 320 Laser Diffraction Particle Size Analyzer. A pHTestr 30 pH meter was used to obtain the pH of tailings. A Brookfield LVT Viscometer was used to measure viscosity of the different tailings samples.

2.2 Tailings Characterization

Characterization of tailings included density, pH, solids content, clay content, and PSD. These characteristics are summarized in Table 2.

Table 2. Characterization Data for Tailings

Tailings	Oil Sands	Copper Thickener Underflow
pH	7.9	11.2
Density (g/mL)	1.27	1.45
Solids Content (w/w%)	35.6	48.5
Clay Content (w/w%)	63.0	11.9
PSD		
Mean (μm)	16.6	188.6
Median (μm)	9.3	130.1
Mode (μm)	14.9	269.2
d_{10} (μm)	1.8	6.8
d_{50} (μm)	9.3	130.1
d_{90} (μm)	38.7	462.7

2.3 Experimental Procedure

A representative MFT sample of 300 g was measured and placed in a plastic beaker. The sample container was covered and its contents sheared at 500 RPM using an overhead mixer with a flat blade impeller. For this study, different shearing times were set at 1, 5, and 60 minutes. Control samples were not pre-sheared.

The overhead mixing method was used to condition the oil sands MFT with Polymer B, where the mixer was set at 250 RPM. The desired amount of the polymer was added approximately 1 to 2 cm above the surface of the slurry and approximately 2 cm from the outside edge of the beaker. The sample was mixed until optimum structure was defined by the visual point of optimum net

water release observed. The beaker containing the polymer-treated slurry was removed from the overhead mixer and any material remaining on the impeller was scraped into the beaker.

The beaker-pour mixing method was used for conditioning copper tailings with Polymer A. Polymer was added at the bottom of an empty beaker and the optimum structure was obtained by pouring the tailings back and forwards between the beaker with sample and beaker with polymer.

Immediately after conditioning the samples, the yield stress of the treated slurry was taken using the V-72 half-vane method. The mass of the beaker with treated material was recorded and the sample was transferred into a 1 mm mesh sieve fitted with a base through a 2-inch plastic collar on top of the sieve. The beaker was scraped clean to add any remaining solids to the sample already on the sieve. The collar was removed, a stopwatch was started to record the time, and the mass of the empty beaker was recorded. The mass of the sieve with treated material and the mass of base with released water at 10, 60, and 1440 minutes after the polymer treated slurry was placed in the sieve. These mass values were used to calculate the net water release by free drainage at each timepoint, as shown in Equation 1. For the copper tailings, the data for the 1440 minutes timepoint was not measured.

$$NWR (\%) = \left(\frac{(Total\ volume\ of\ water\ released\ (mL) - Volume\ of\ Product\ Added\ (mL)) * Density\ of\ water\ released\ (\frac{g}{mL})}{Mass\ of\ slurry\ used\ (g) * \left(1 - \left(\frac{Slurry\ Solids\ Content\ (\%w/w)}{100}\right)\right)} \right) * 100 \quad (1)$$

The yield stress of the material was also taken at each time interval (described earlier) using the V-73 half-vane method. To minimize water loss caused by evaporation, the sieve was covered after 60 minutes. After the last time point measurement, the water released in the base beneath the sieve was removed using a syringe and transferred to a Nalgene bottle. The bottle was inverted and allowed to rest for 60 minutes prior to collecting the water from the top and analyzed for dry solids content Equation 2. Water samples were then left to dry overnight in an oven at 110°C.

$$Solids\ Content\ (\%w/w) = \left(\frac{\left(\frac{Slurry\ Solids\ Content\ (\%w/w)}{100}\right) * Mass\ of\ Slurry\ Used\ (g)}{Mass\ of\ Solids\ Deposited\ on\ Sieve\ (g)} \right) * 100 \quad (2)$$

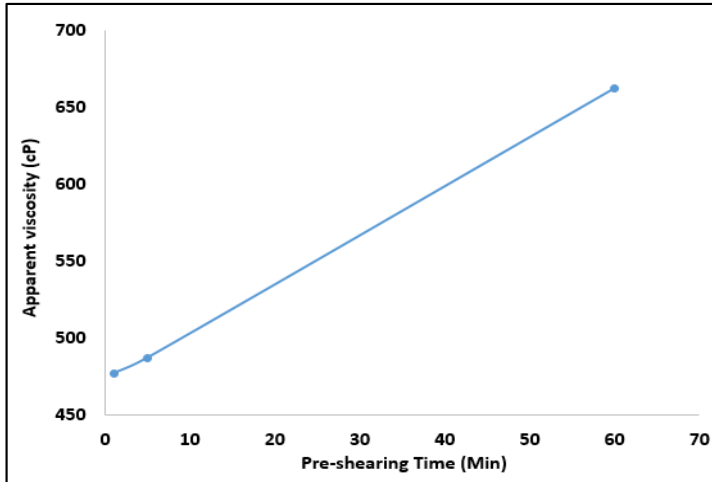
This procedure was repeated six times for each polymer dose at the different pre-shearing times.

3 RESULTS AND DISCUSSION

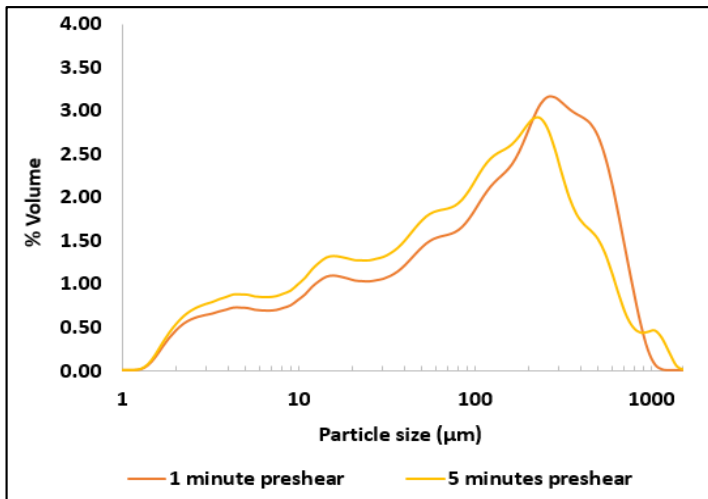
3.1 Copper Thickener Underflow

3.1.1 Viscosity Profiles

Apparent viscosities were taken for the 1, 5, and 60 minutes pre-sheared underflow copper tailings samples (Graph 1). Tailings apparent viscosity increased with longer pre-shearing time, categorizing this substrate as a shear thickening material with dilatant behavior. The increase in apparent viscosity can be due to the formation of smaller particles as the coarser particles are exposed to additional shear. Graph 2 shows PSD data for the samples that were pre-sheared for 1 and 5 minutes.



Graph 1. Apparent viscosity of copper tailings from thickener underflow at different shearing times.

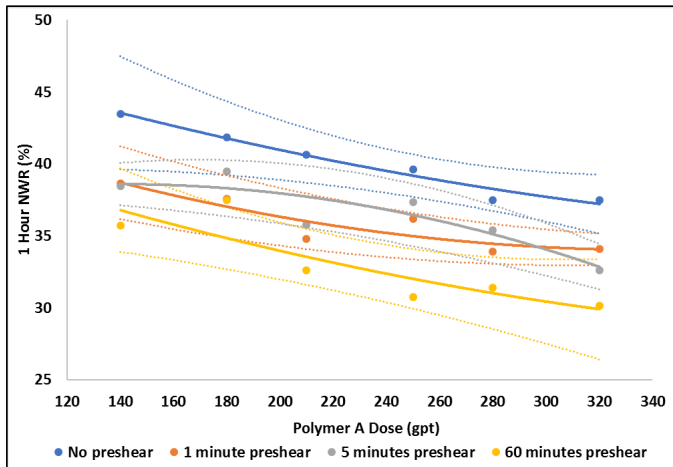


Graph 2. PSD for the copper thickener underflow samples pre-sheared for 1 minute and 5 minutes.

There was a decrease on the average size from the 1 minute and the 5 minutes pre-sheared samples, with mean values of 211.4 µm to 171 µm, respectively. Also, percentages of fine particles (less than 44 µm) differed between samples, as the value for the 1 minute pre-shear had 30.04 % of fine particles and the 5 minutes pre-shear sample had 36.47 %. This trend was expected to continue with additional shear.

3.2.1 Free Drainage Dewatering of Treated Tailings

The dewatering of the copper underflow tailings was quantified by net water release and taken at 10 minutes and 1 hour after treating with Polymer A. Graph 3 shows the amount of dewatering at 1 hour for material pre-sheared for differing amounts of time.



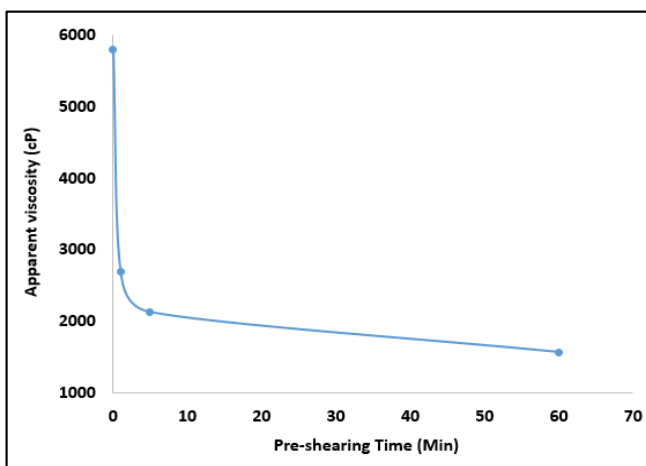
Graph 3. Net water release after dewatering for 1 hour for different pre-sheared thickener underflow copper tailings. Data points are an average of 6 tests and dotted lines represent the 95% confidence error of the data set.

The results show that the dewatering of the material was negatively affected the longer it was pre-sheared. The samples that did not undergo pre-shearing had better overall dewatering than any of the pre-sheared samples. Comparable values were obtained between the samples that were pre-sheared for 1 minute and 5 minutes. Lower dewatering values were obtained by the samples that were pre-sheared for 1 hour. As shown in Graph 1, the viscosity of the sample increases the longer the shear force was applied. This hindered the effectiveness of the interaction between the particles and the polymer. This may be due to the increased disorder in the system.

3.2 Oil Sands MFT

3.2.1 Viscosity Profiles

Apparent viscosity readings were taken for the same pre-shear time intervals used with the copper tailings. Graph 4 shows the results of the testing. The viscosity of the MFT decreased the longer it was pre-sheared, indicating that the material is shear thinning or is pseudoplastic in nature.

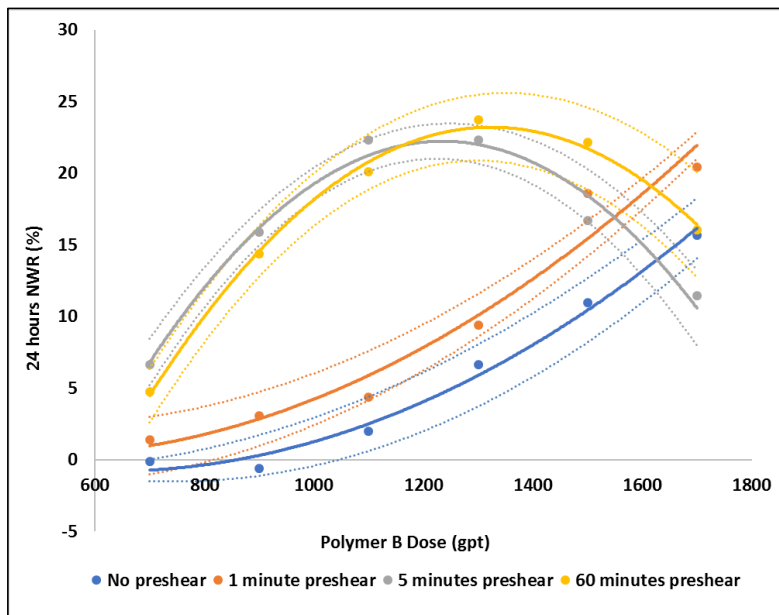


Graph 4. Apparent viscosity of oil sands MFT at different shearing times

There was a significant decrease in apparent viscosity when the sample was pre-sheared for just 1 minute, where the viscosity dropped from 5800 cP to 2690 cP. From this point, the viscosity decreased at a much slower rate. With shearing, the interactions between the clay network are broken and the particles are mixed through the medium, thus the immediate drop in viscosity. Once the particles were already dispersed, continued shearing of the sample then had negligible effect on its viscosity.

3.2.2 Free Drainage Dewatering of Tailings Over Time

The dewatering of the material was calculated by the net water release and taken at the same time intervals as the copper samples and at 24 hours after treating with Polymer B. Graphs 5 show the progression of dewatering through 24 hours.

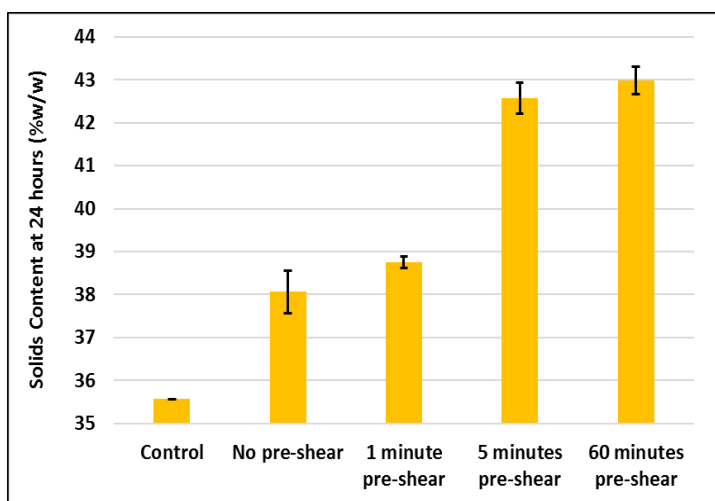


Graph 5. Net water release after dewatering for 24 hours for different pre-sheared times on oil sands MFT. Data points are an average of 6 tests and dotted lines represent the 95% confidence error of the data set.

During the period of the study, the samples that were not pre-sheared exhibited limited dewatering performance at low doses of polymer, but performance increased as more polymer was added to treat the MFT. It is important to note that within the polymer dose range studied, these samples did not reach optimal dewatering and required incrementally higher doses of polymer to improve dewatering. This is not a cost-effective solution for mine operators, as more polymer is needed to achieve good dewatering. When the sample is not pre-sheared, the interactions between the clay particles in the MFT are not broken. Clay platelets agglomerate with each other while retaining water in the structure, increasing water retention (Van Olphen, 1986). Because of the nature of their inter-particle interactions, when not physically dispersed, the flocculant will not interact with the particles in an efficient manner. Dewatering of non-pre-sheared material was hindered by the clay particle-to-clay particle interactions, such as hydrogen bonding.

A small increase in dewatering at each dose was observed when the sample was pre-sheared for 1 minute. This followed the same overall trend as the samples that were not pre-sheared. This amount of shear was not enough to achieve maximum dewatering, but it proved that pre-shear

before flocculation had a beneficial effect in the dewatering performance of the treated substrate. The use of pre-shear for at least 5 minutes significantly improved the dewatering of the material, while the dose of polymer required was decreased to achieve maximum dewatering. It appears that with this amount of shearing there was an inverse parabolic relationship with the dose range chosen and the dewatering. Doses of 700 grams per ton (gpt) and 900 gpt did not achieve good dewatering, meaning that the amount of polymer used was not enough to obtain optimal structure nor optimal dewatering. It reached maximum dewatering of 22.3 % between 1100 gpt and 1300 gpt. As mentioned in Table 2, the solids content of the MFT was 35.6 %w/w. At this amount of dewatering, the solids content of the material increased to approximately 42.6 %w/w. Then dewatering of the substrate decreased when overdosing with polymer, due to water retention by the polymer (Vedoy and Soares, 2015). The inversed parabolic trend also was seen when the MFT was pre-sheared for 1 hour. The data suggests that “over pre-shearing” the MFT for 1 hour does not hinder the dewatering performance of the treated substrate during the period of the study. Results are comparable to those obtained when the MFT was pre-sheared for 5 minutes, where under dosing and over dosing with flocculant hindered the amount of water released by the material. At 24 hours of free drainage dewatering, the solids content of the material was comparable to the 5 minutes pre-sheared sample as these values were 42.6 %w/w (5 minutes pre-shear) and 43 %w/w (1 hour pre-shear). Graph 6 shows progression of the solids content when 1300 gpt of polymer was added to the MFT. The data shows that the dewatering performance increased when the material was pre-sheared for longer times.

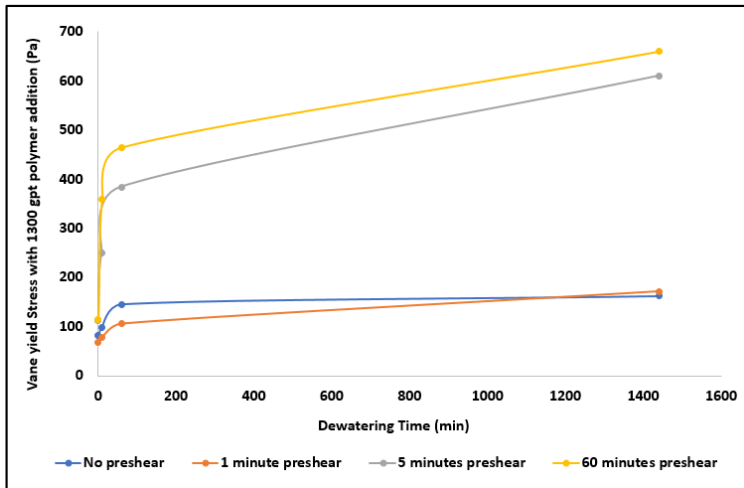


Graph 6. Solids content of material after 24 hours of drainage and treated with 1300 gpt of polymer. Control sample was MFT without polymer treatment. Data points are an average of 6 tests and error bars represent the 95% confidence error of the data set.

In summary, for this oil sands substrate, at least 5 minutes of pre-shear was needed to obtain maximum amount of free water release, and a treated material with a higher solids content.

3.2.2 Relationships Between Solids Content, Dewatering Time, and Vane Yield Stress

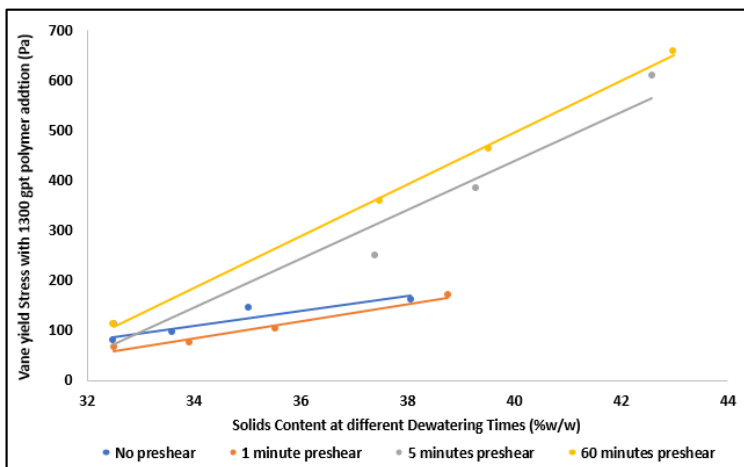
The vane yield stress of the treated material was measured immediately after treatment with the flocculant and after 10 minutes, 1 hour, and 24 hours of initial dewatering. Graph 7 shows the yield stress of the treated material when 1300 gpt of polymer was added to the different pre-sheared samples. The data can be separated into two groups. The material that was not pre-sheared and pre-sheared for 1 minute are quite similar compared to the 5 minutes and 60 minutes pre-sheared samples.



Graph 7. Vane yield stress at different dewatering times of the different pre-sheared oil sands substrate when 1300 gpt of Polymer B was added to the material. Each data point represents an average of 6 test results.

Higher yield stress was observed for the same dose due to improved dewatering. With addition of 1300 gpt of polymer, maximum dewatering was achieved at the higher pre-shearing times of 5 and 60 minutes. This graph illustrates how yield stress varies with pre-shearing time when polymer dose remains constant showing that higher yield stress can be achieved with increasing pre-shear. It was observed that most of the dewatering occurred in the first hour, which resulted in a faster increase in yield stress, as the material becomes more plastic.

As the material dewatered over time (reducing water content), the yield stress and solids content increased. Graph 8 illustrates the relationship between the yield stress and the solids content of the samples when dosed at 1300 gpt of polymer. Higher solids contents were achieved in samples pre-sheared for 5 and 60 minutes, which are the samples that achieved maximum dewatering.



Graph 8. Relationship between the vane yield stress and the solids content at different dewatering times for the oil sands MFT when 1300 gpt of Polymer B was added to the material. Each data point represents an average of 6 test results.

4 CONCLUSIONS

Pre-shearing increases the dewatering performance for the oil sands MFT, but has the opposite effect on the copper tailings tested. As the copper tailings naturally segregate due to the higher particle size, the apparent viscosities at any shearing time were much lower than the oil sands MFT. Nevertheless, when exposed to shear, the copper tailings increased in apparent viscosity while apparent viscosity decreased for the oil sands tailings. This affected the interactions between the particles and the polymer for both samples investigated. The particles in the slurry must be physically dispersed enough to facilitate effective interaction with the flocculant. This dispersion happened in the oil sands MFT when it was pre-sheared, allowing the polymer to effectively interact with the substrate.

As for the second objective of this study, the results suggested that “over pre-shearing” the substrate does not hinder dewatering performance for the oil sands sample tested. The data showed decreasing dewatering performance when the copper tailings thickener underflow was pre-sheared for longer durations. For the oil sands substrate, maximum dewatering data was similar to the data obtained when the sample was pre-sheared for 5 minutes. This showed that longer shearing times may not be necessary beyond an optimal shearing point, as the structure of the particle aggregates has been sufficiently broken down. Consequently, saving both energy and time.

As shown with this study, pre-shearing does not work for all tailings. Each tailings substrate has its own physicochemical makeup and rheology. Therefore, understanding the characteristics of the slurry is essential to identifying how to optimize material treatment based on the performance criteria specified.

5 ACKNOWLEDGEMENTS

The authors would like to thank BASF Corporation for allowing us the permission to publish this work. Also, special thanks to Carlos D. Silva Gaxiola and Ava J. Hopkinson for their participation in this project.

REFERENCES

- Hogg, R. 2000. Flocculation and dewatering. *International Journal of Mineral Processing* 58: 223–236.
- Johnson, S.B., Franks, G.V., Scales, P.J., Boger, D.V., Healy, T.W. 2000. Surface chemistry rheology relationships in concentrated mineral suspensions. *International Journal of Mineral Processing* 58: 267-304.
- Kotlyar, L.S., Sparks, B.D., Woods, J., Capes, C.E. and Schutte, R. 1995. Biwetted ultrafine solids and structure formation in oil sands fine tailings. *Fuel* 74(8): 1146-1149.
- Masliyah, J.; Zhou, Z. J.; Xu, Z.; Czarnecki, J. & Hamza, H. 2004. Understanding Water-Base-Bitumen Extraction from Athabasca Oil Sands. *Canadian Journal of Chemical Engineering*, 82: 628–654.
- Stocks, P. Reagents. In *Paste and thickened tailings-A guide* (2nd ed.), 2006. Nedlands: Australian Centre of Geomechanics, The University of Western Australia.
- Van Olphen, H. 1986. *An introduction to clay colloid chemistry, 1977*. National Academy of Sciences, Washington, DC.
- Vedoy, D. R. L. & Soares, J. B. P. 2015. Water-soluble polymers for oil sands tailing treatment: A review. *The Canadian Journal of Chemical Engineering* 93: 888-904.

Platinum Tailings – Field and Laboratory Investigation to Evaluate Geotechnical Behaviour

A Smith and H.A.C. Meintjies

SRK Consulting (SA) (Pty) Ltd., Johannesburg, Gauteng, South Africa

ABSTRACT: An extensive site investigation and laboratory testing sub-project is currently being carried out for one of the major platinum producers in South Africa. This sub-project forms part of the main project comprising the design of new lined tailings dams and associated works for the client. Results from the field and laboratory test work are crucial from a design perspective. The sub-project comprises piezocone testing at specific positions on two operational tailings dams at the mine, followed by geotechnical drilling at the same positions. Surface samples were also obtained at these positions. Extensive laboratory testing, including a wide spectrum of specialized geotechnical test work, was carried out on the samples. The main objective of this paper is to analyze and compare selected geotechnical properties obtained through piezocone testing with those results obtained through laboratory testing of the geotechnical drilled and surface samples as to evaluate the geotechnical behaviour of platinum tailings. The main findings include that the average effective stress friction angle values determined through CPTu probing and from the laboratory testing of the geotechnical drilled tailings samples, compare reasonably well. The average permeability values calculated for the geotechnical drilled samples, obtained at the respective tailings dams, are similar. Tailings material that behave in a contractive as well as a dilative manner, was encountered at the two tailings dams. Specific void ratio and undrained shear strength ratio values are associated with the aforementioned behaviour. The average effective stress friction angle values determined for Tailings Dams No's 1 and 2, utilizing all triaxial test (consolidated undrained) results, are 36.1 degrees and 37 degrees respectively. For both tailings dams outer wall building material with peak undrained shear strength ratio values higher than 0.6 was determined through CPTu probing.

1 INTRODUCTION

1.1 Background

SRK was requested by one of the main platinum producers in South Africa to carry out the design of new lined tailings dams and associated works to accommodate increased tailings deposition tonnages as a result of a planned expansion project.

To ensure that the new tailings dam complex can be operated as a safe and stable facility, reliable geotechnical data on the tailings material to be deposited, is required for design purposes. The proposed tailings deposition method is spigotting, which is currently being implemented successfully at the other upstream constructed operational tailings dams on the mine.

After consultation with the mine, it was agreed to embark on an extensive CPTu probing, geotechnical drilling and laboratory testing investigation at the two operational tailings dams, namely Tailings Dam No.1 and Tailings Dam No.2, to obtain a more accurate indication of the applicable geotechnical strength parameters to be implemented for design purposes. Refer to Figures 1 and 2 below for a visual interpretation of the layouts of the respective tailings dams. Strength parameter results obtained from the geotechnical drilled samples would be used to verify similar results obtained from the CPTu probing.

The applicable orebodies comprise Merensky and UG2 reefs. Tailings from underground and opencast mining activities report to Tailings Dam No.1. This tailings dam initially re-

ceived tailings containing chrome. Subsequently a chrome extraction plant was implemented to extract chrome from the tailings streams. Tailings from underground mining activities report to Tailings Dam No.2. Tailings (with chrome extracted) containing slag is currently being deposited on this tailings dam.

Furthermore, milling techniques have improved over time resulting in much finer tailings material reporting to these tailings dams. Typical during the initial operational phases for Tailings Dams No's 1 and 2, between 55% and 65% of the tailings particles would have passed the 75 micron sieve size. Currently as much as 75% to 85% of the particles passes the 75 micron sieve size. The respective tailings products have no plasticity and can be classified as a sandy silt (ML) according to the Unified Soil Classification System (USCS).

1.2 CPTu probing, geotechnical drilling and laboratory testing details

CPTu probing by an international based geotechnical drilling company utilizing a crawler, was carried out at ten positions at Tailings Dam No.1 and at nine positions at Tailings Dam No.2. Refer to Figures 1 and 2 below for a visual interpretation of the probing lines and locations at the respective tailings dams. The respective probing lines were selected in such a way that they firstly cover the critical flanks of each tailings dam. In terms of the three probing positions as part of a probing line, the first probing position is located downstream of the curtain drain, with the second and third probing positions (both located upstream of the curtain drain) located in the outer upper basin area and the inner upper basin area, respectively. Probing was carried out for the full depth at each position for both tailings dams, which varies between five meters (shallowest) and 26 meters (deepest). The total probing depth at Tailings Dam No.1 is equal to 191 meters and the total probing depth at Tailings Dam No.2 is equal to 111 meters.

Geotechnical drilling for sampling purposes was carried out at the same positions where CPTu probing was undertaken. These samples were extracted using the PQ3 sampling system initially, to obtain undisturbed samples, and later on Shelby tubes (75 mm diameter) when difficulties were experienced due to saturated material and hard layers. Geotechnical drilling was carried out to the full depth of the two tailings dams. At Tailings Dam No.1 a total of 143 No. samples were removed and at Tailings Dam No.2 a total of 121 No. samples were removed. Surface (block / undisturbed) samples were also manually obtained at the same positions where the geotechnical drilling occurred. In total 8 No. and 6 No. surface samples were obtained at Tailings Dam No.1 and at Tailings Dam No.2 respectively.

In terms of the Tailings Dam No.1 geotechnical drilled and surface samples, moisture content, dry density, foundation indicators (sieve analysis to 75 micron and hydrometer to 2 micron), Atterberg limits and SG determination were carried out. On 24 No. samples triaxial testing (consolidated undrained) as well as flexible wall permeability testing were carried out. On 4 No. of the surface samples, consolidated drained triaxial tests were carried out too. In terms of the Tailings Dam No.2 geotechnical drilled and surface samples, moisture content, dry density, foundation indicators (sieve analysis to 75 micron and hydrometer to 2 micron), Atterberg limits and SG determination were carried out. On 24 No. samples triaxial testing (consolidated undrained) as well as flexible wall permeability testing were carried out. On 3 No. of the surface samples, consolidated drained triaxial tests were carried out too. In terms of the triaxial testing (consolidated undrained), the British Standards (BS 1377-8, 1990) are applicable.

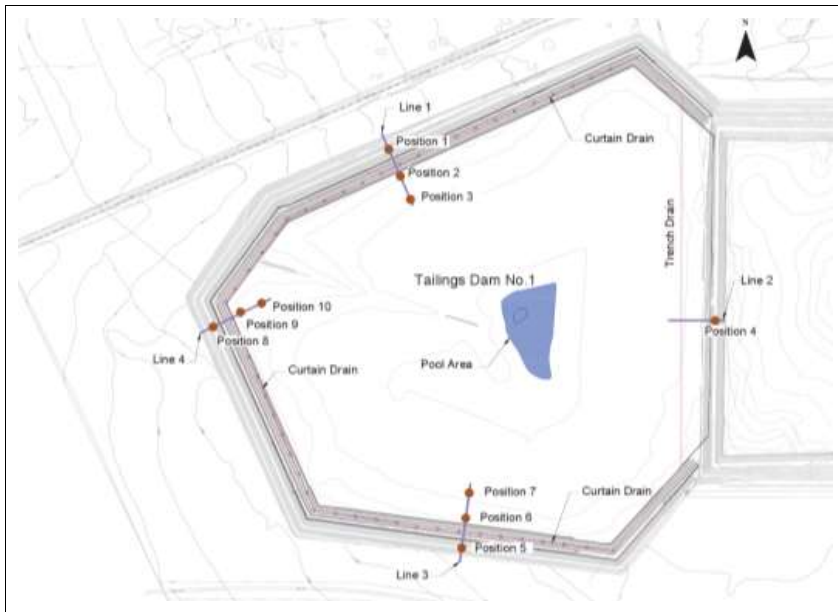


Figure 1. Tailings Dam No.1 - Probing lines and positions.

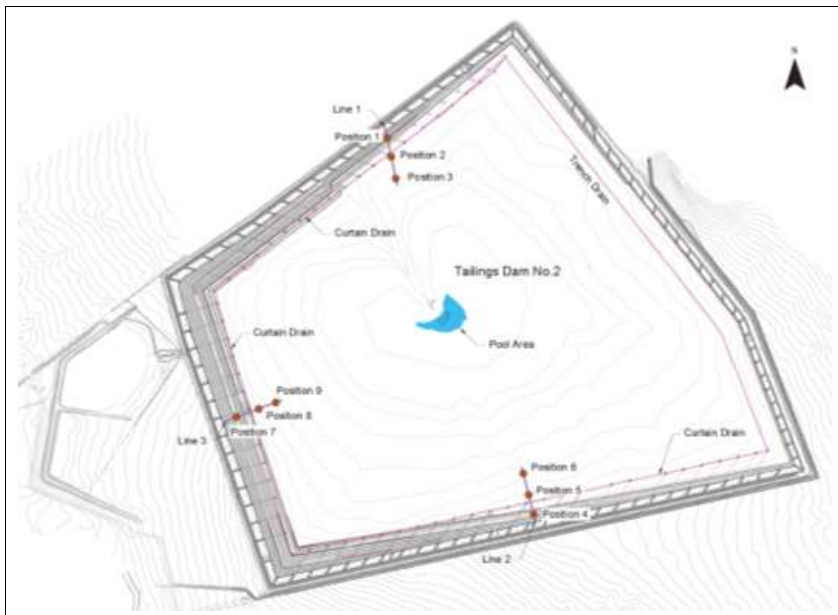


Figure 2. Tailings Dam No.2 – Probing lines and positions.

2 PIEZOCONE TESTING AND GEOTECHNICAL DRILLED SAMPLES RESULTS

2.1 Tailings Dam No.1

Table 1 below summarizes the geotechnical results obtained through CPTu probing at the ten positions and specifically with regard to the depths indicated. Note that the chosen

depths coincide with the depths at which geotechnical drilled samples were obtained for tri-axial testing (consolidated undrained) purposes. Seventeen geotechnical drilled samples refer. Note that at certain positions more than one depth is applicable. In this paper reference will be made to undrained shear strength ratio which can be defined as the ratio of undrained shear strength, c_u , to the vertical effective stress, σ_v' . In tailings dam engineering, this undrained shear strength ratio allows the undrained shear strength, c_u of tailings at various depths to be directly compared.

Table 2 summarizes the geotechnical results obtained from the laboratory testing of the geotechnical drilled samples.

Table 1. Tailings Dam No.1 – Piezocone testing - Geotechnical material properties.

Position	Depth (meters)	Friction angle (ϕ')	Peak shear strength ratio*	Contractive/Dilative**	Permeability (m/s)
1	0.90 – 1.40	33.38	0.66	dilative	1.32E-05
2	1.75 – 3.15	34.78	0.69	dilative	3.11E-06
2	3.00 – 3.50	35.03	0.70	dilative	2.89E-06
2	13.75 – 15.25	33.06	0.64	contractive	2.60E-07
3	2.00 – 2.50	33.97	0.66	dilative	3.39E-07
3	3.90 – 5.40	27.58	0.42	contractive	3.65E-08
4	5.00 – 5.50	34.91	0.70	dilative	3.47E-06
4	11.50 – 12.00	36.34	0.74	dilative	5.73E-07
5	2.40 – 3.90	34.10	0.68	dilative	1.25E-05
6	3.00 – 3.50	34.58	0.69	dilative	6.69E-06
6	6.00 – 6.50	36.33	0.74	dilative	8.24E-07
7	0.00 – 1.50	34.01	0.68	dilative	1.05E-05
8	3.50 – 4.05	34.01	0.67	dilative	5.98E-06
9	5.60 – 6.10	34.32	0.67	dilative	9.83E-07
9	8.60 – 9.10	31.09	0.56	dilative	1.53E-07
10	2.40 – 2.90	33.77	0.66	dilative	1.36E-07
10	3.90 – 5.40	33.77	0.64	dilative	4.31E-07
Average		33.83	0.66		3.65E-06

*Peak undrained shear strength ratio (Robertson & Cabal, 2014).

**Dilative / contractive (Jefferies & Been, 2016).

Table 2. Tailings Dam No.1 – Geotechnical drilled samples - Geotechnical material properties.

Position	Depth (meters)	Friction angle (ϕ')	Undrained shear strength ratio (c_u/σ_v')	Contractive/Dilative*	Permeability (m/s)
1	0.90 – 1.40	30.10	0.36	contractive	4.50E-07
2	1.75 – 3.15	36.80	0.58	dilative	4.38E-07
2	3.00 – 3.50	36.20	0.56	dilative	6.11E-08
2	13.75 – 15.25	35.80	0.41	dilative	4.78E-07
3	2.00 – 2.50	40.70	0.50	dilative	-
3	3.90 – 5.40	38.50	0.50	dilative	1.53E-07
4	5.00 – 5.50	33.30	0.41	contractive	4.95E-07
4	11.50 – 12.00	36.30	0.44	dilative	4.21E-07
5	2.40 – 3.90	36.80	0.63	dilative	3.65E-07
6	3.00 – 3.50	34.40	0.30	contractive	4.78E-07
6	6.00 – 6.50	30.10	0.25	contractive	2.63E-07
7	0.00 – 1.50	37.80	0.78	dilative	6.84E-07
8	3.50 – 4.05	29.10	0.14	contractive	4.52E-07
9	5.60 – 6.10	36.30	0.25	contractive	2.44E-07
9	8.60 – 9.10	37.30	0.50	dilative	3.13E-07
10	2.40 – 2.90	37.30	0.44	dilative	1.07E-07
10	3.90 – 5.40	35.80	0.29	dilative	5.09E-07
Average		35.45	0.43		3.69E-07

Comparing the geotechnical material properties summarized in Tables 1 and 2, the following is observed:

- The average effective stress friction angle values are similar.
- The average peak shear strength ratio and average undrained shear strength ratio values do not compare well.

- More of the laboratory test results for the geotechnical drilled samples indicate a contractive behavior compared to the results obtained through the CPTu probing.
- The average permeability value obtained through the CPTu probing is tenfold higher than the average permeability value calculated for the geotechnical drilled samples.

2.2 Tailings Dam No.2

Table 3 below summarizes the geotechnical results obtained through CPTu probing at the nine positions and specifically with regard to the depths indicated. The chosen depths coincide with the depths at which geotechnical drilled samples were obtained for triaxial testing (consolidated undrained) purposes. Fourteen geotechnical drilled samples refer. Note that at certain positions more than one depth is applicable.

Table 4 summarizes the geotechnical results obtained from the laboratory testing of the geotechnical drilled samples.

Table 3. Tailings Dam No.2 – Piezocone testing - Geotechnical material properties.

Position	Depth (meters)	Friction angle (ϕ')	Peak shear strength ratio*	Contractive/Dilative**	Permeability (m/s)
1	3.00 – 3.50	31.51	0.61	dilative	1.77E-04
2	5.00 – 5.50	34.16	0.68	dilative	1.90E-05
2	10.00 – 10.50	35.12	0.70	dilative	2.17E-04
3	2.50 – 3.00	29.88	0.57	dilative	7.01E-04
3	6.00 – 6.50	28.56	0.44	contractive/dilative	1.39E-07
4	2.50 – 3.00	30.68	0.59	dilative	2.72E-04
4	4.50 – 5.00	34.76	0.69	dilative	9.18E-06
5	5.00 – 5.60	31.04	0.60	dilative	5.21E-04
5	9.80 – 10.90	32.10	0.60	contractive/dilative	6.10E-07
6	5.65 – 6.17	32.36	0.63	dilative	9.41E-05
7	5.50 – 6.00	31.20	0.61	contractive/dilative	3.28E-05
8	9.80 – 10.30	35.07	0.70	dilative	2.59E-05
9	10.50 – 11.00	35.33	0.71	dilative	6.73E-06
9	12.30 – 12.80	36.27	0.73	dilative	6.71E-07
Average		32.72	0.63		1.48E-04

*Peak undrained shear strength ratio (Robertson & Cabal, 2014).

**Dilative / contractive (Jefferies & Been, 2016).

Table 4. Tailings Dam No.2 – Geotechnical drilled samples - Geotechnical material properties.

Position	Depth (meters)	Friction angle (ϕ')	Undrained shear strength ratio (c_u/σ_v')	Contractive/Dilative	Permeability (m/s)
1	3.00 – 3.50	40.00	0.84	contractive	5.62E-07
2	5.00 – 5.50	37.20	0.43	contractive	8.26E-07
2	10.00 – 10.50	40.60	0.19	dilative	-
3	2.50 – 3.00	38.30	0.58	dilative	6.39E-07
3	6.00 – 6.50	36.30	0.37	dilative	4.12E-07
4	2.50 – 3.00	34.50	0.69	contractive	1.11E-06
4	4.50 – 5.00	34.40	0.47	contractive	-
5	5.00 – 5.60	36.80	0.23	contractive	5.76E-07
5	9.80 – 10.90	40.20	0.41	dilative	5.76E-07
6	5.65 – 6.17	37.40	0.65	dilative	3.83E-07
7	5.50 – 6.00	35.40	0.58	contractive/dilative	5.61E-07
8	9.80 – 10.30	33.30	0.14	contractive	4.92E-07
9	10.50 – 11.00	34.10	0.67	contractive	8.97E-07
9	12.30 – 12.80	36.30	0.26	contractive	6.84E-07
Average		36.77	0.47		6.43E-07

Comparing the geotechnical material properties summarized in Tables 3 and 4, the following is observed:

- The average effective stress friction angle values compare reasonably well, with the average effective stress friction angle value obtained from the laboratory testing of the geotechnical drilled samples, again the higher of the two average values, as per the Tailings

Dam No.1 tailings.

- The average peak shear strength ratio and average undrained shear strength ratio values do not compare well, similar to the Tailings Dam No.1 tailings.
- As for the Tailings Dam No.1 tailings, more of the laboratory test results for the geotechnical drilled samples indicate a contractive behavior compared to the results obtained through the CPTu probing.
- The average permeability value obtained through the CPTu probing, indicates two orders of magnitude difference to the average permeability value measured for the geotechnical drilled samples.
- Also note that the average permeability values calculated for the geotechnical drilled samples are similar.

3 CONTRACTIVE AND DILATIVE BEHAVIOUR

3.1 Tailings Dam No.1

As indicated under Section 2, the respective tailings samples can either behave in a contractive or a dilative manner when loaded. Furthermore, tailings samples behaving in a contractive manner, has a high void ratio (e) value, typical in the order of 1.0. Tailings samples behaving in a dilative manner, have void ratio (e) values below 0.8. For illustrative purposes, the following tailings samples were selected:

- Position 4, depth 5.00 meters to 5.50 meters – contractive (Sample 7).
- Position 4, depth 11.50 meters to 12.00 meters – dilative (Sample 8).

Figures 3 to 6 (extracts from the original triaxial results) to follow provide a visual interpretation of the aforementioned behavioural aspects.

Figures 3 and 4 below provide a graphical interpretation of the behaviour of tailings samples that can be described as contractive whilst undergoing triaxial testing.

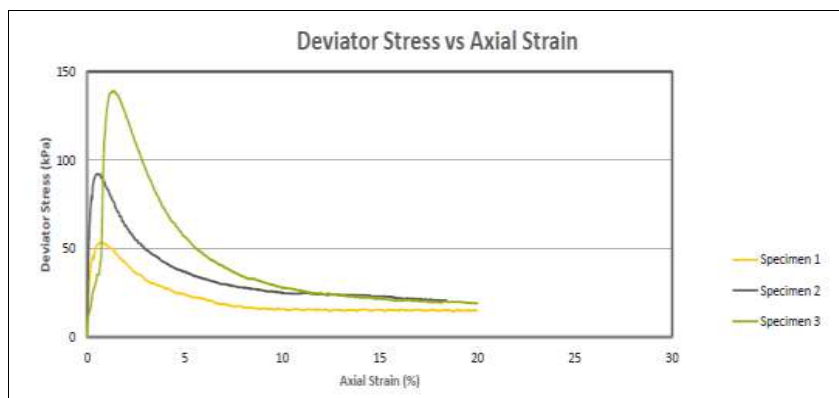


Figure 3. Sample 7 – Deviator stress versus axial strain.

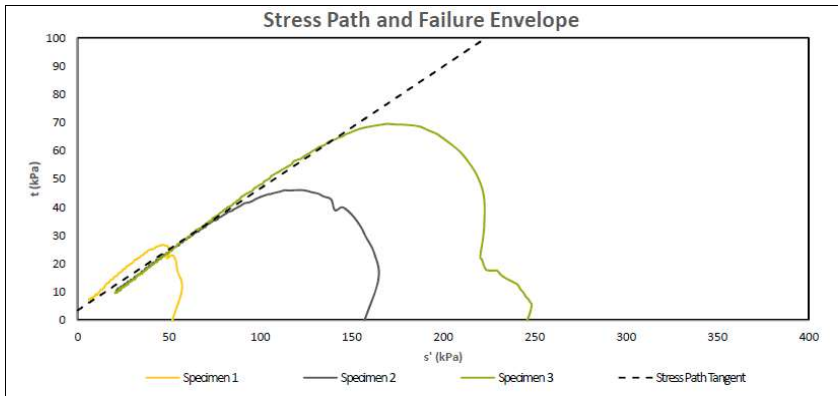


Figure 4. Sample 7 – Stress path and failure envelope.

Figures 5 and 6 below provide a graphical interpretation of the behaviour of tailings samples that can be described as dilative whilst undergoing triaxial testing.

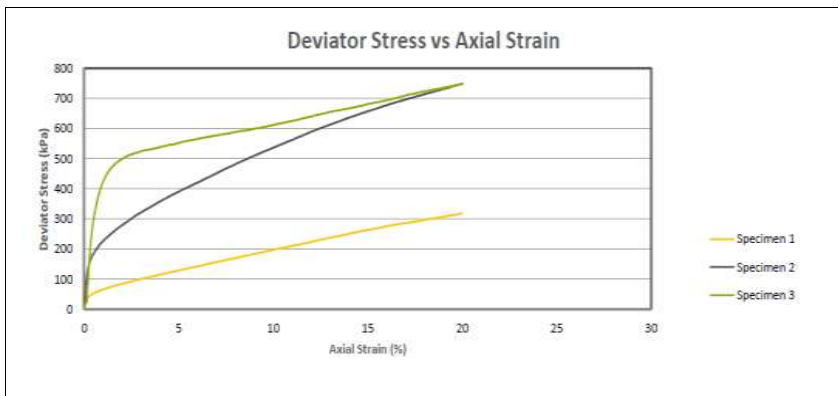


Figure 5. Sample 8 – Deviator stress versus axial strain.

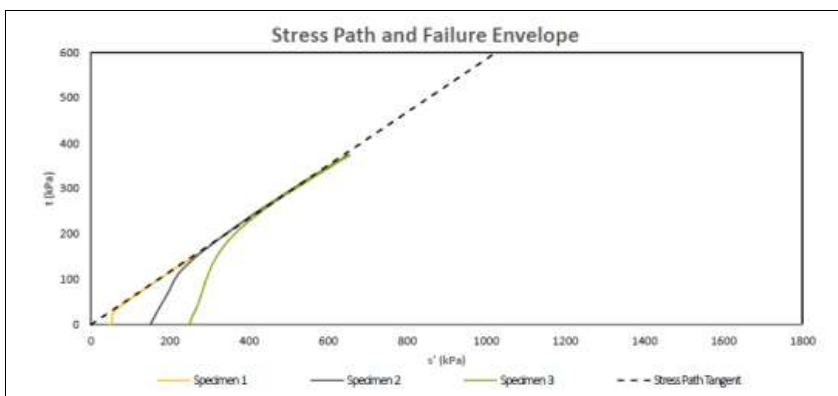


Figure 6. Sample 8 – Stress path and failure envelope.

Similar behaviour, as illustrated in Figures 3 to 6 above, was observed for the Tailings Dam No.2 samples.

4 EFFECTIVE STRESS FRICTION ANGLE

4.1 Tailings Dam No.1

Effective stress friction angle values were determined through triaxial testing on 24 No. tailings samples, comprising geotechnical drilled samples (16 No.) as well as surface samples (8 No.). The average effective stress friction angle value is equal to 36.1°, with a standard deviation value equal to 2.9.

Figure 7 below provides a visual interpretation of the cumulative distribution applicable to the calculated effective stress friction angle values.

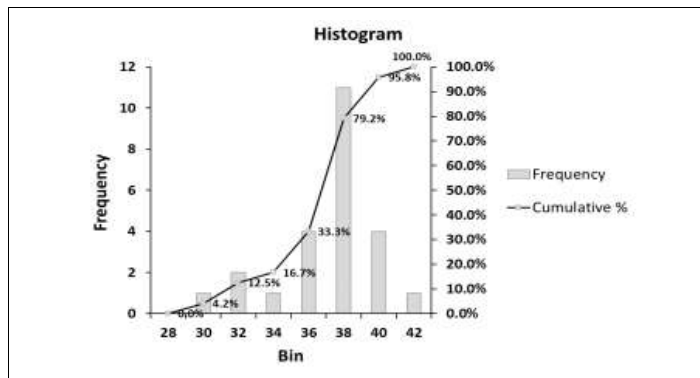


Figure 7. Tailings Dam No.1 – Effective stress friction angle – Cumulative distribution.

The above figure confirms that 45.8% of the calculated effective stress friction angle values fall within the 36% to 38% category.

4.2 Tailings Dam No.2

Effective stress friction angle values were determined through triaxial testing on 24 No. tailings samples, comprising geotechnical drilled samples (18 No.) as well as surface samples (6 No.). The average effective stress friction angle value is equal to 37°, with a standard deviation value equal to 2.4.

Figure 8 below provides a visual interpretation of the cumulative distribution applicable to the calculated effective stress friction angle values.

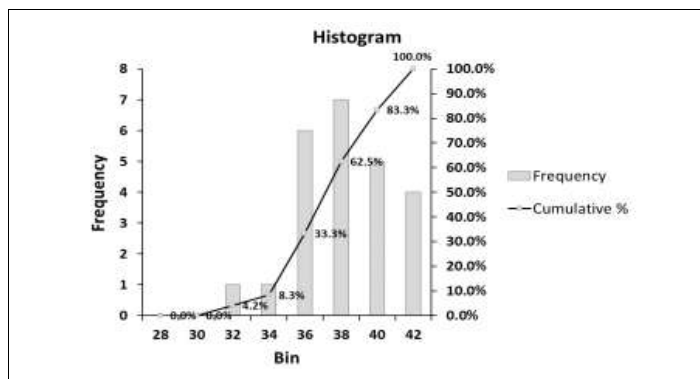


Figure 8. Tailings Dam No.2 – Effective stress friction angle – Cumulative distribution.

The above figure confirms that 29.2% of the calculated effective stress friction angle values fall within the 36% to 38% category.

5 EFFECTIVE STRESS FRICTION ANGLE VERSUS VOID RATIO BEHAVIOUR

5.1 Tailings Dam No.1

Figure 9 below provides a visual interpretation of the applicable effective stress friction angles and their corresponding void ratio values applicable to the Tailings Dam No.1 samples. Note that these are the final, average (three specimens per sample) void ratio values per samples tested.

Also indicated is the contractive or dilative behaviour for each sample. This figure indicates that most of the samples with a dilative behaviour, have e-values below 0.87 and effective stress friction angle values above 35°. In terms of the samples with a contractive behaviour, the e-values are above 0.87 and the effective stress friction angle values below 37°. Some outliers are also observed.

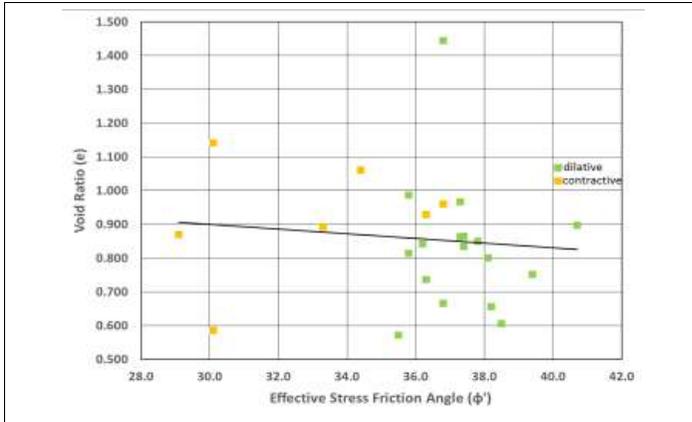


Figure 9. Tailings Dam No.1 – Effective stress friction angle versus void ratio behaviour.

5.2 Tailings Dam No.2

Figure 10 below provides a visual interpretation of the applicable effective stress friction angles and their corresponding void ratio values applicable to the Tailings Dam No.2 samples.

The samples with a dilative behaviour have e-values below 0.9 and effective stress friction angle values larger than 35°. The samples with a contractive behaviour have e-values above 0.82 and effective stress friction angle values below 35°. Outliers are noticed too.

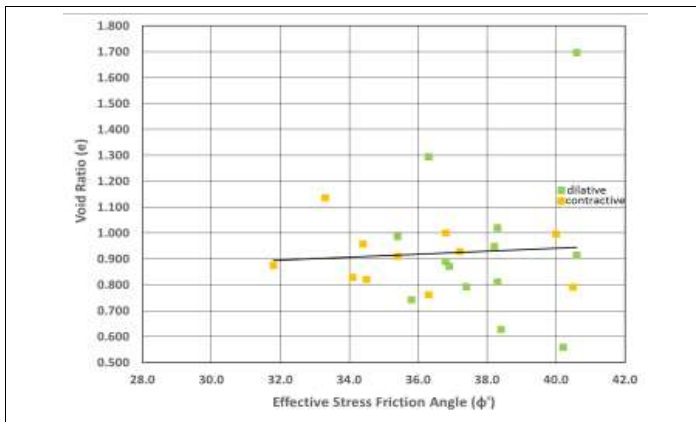


Figure 10. Tailings Dam No.2 – Effective stress friction angle versus void ratio behaviour.

6 VOID RATIO VERSUS UNDRAINED SHEAR STRENGTH BEHAVIOUR

6.1 Tailings Dam No.1

Figure 11 below provides a visual interpretation of the void ratios versus undrained shear strength behaviour of the Tailings Dam No.1 samples. Note that the outliers were removed prior to the compilation of this figure.

It appears that the samples with a void ratio lower than 0.85 and an undrained shear strength ratio value larger than 0.3, have a dilative nature and that the samples with a void ratio larger than 0.85 and an undrained shear strength ratio value smaller than 0.3, have a contractive behavior. Note that these findings correspond with the findings made under Section 5 for this tailings dam and with specific reference to the void ratio values.

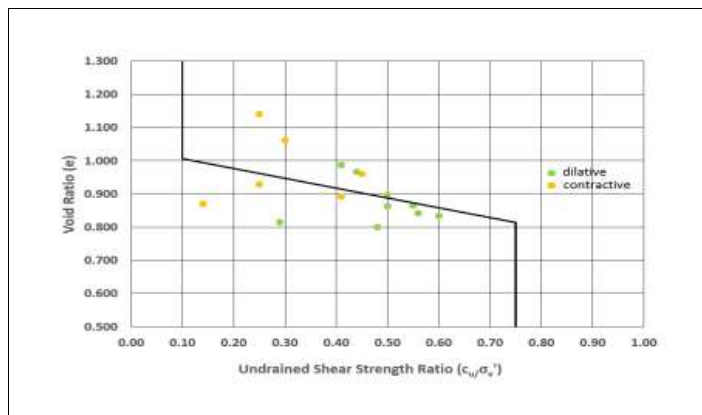


Figure 11. Tailings Dam No.1 – Void ratio versus undrained shear strength behaviour.

6.2 Tailings Dam No.2

Figure 12 below provides a visual interpretation of the void ratios versus undrained shear strength behaviour of the Tailings Dam No.2 samples. Note that the outliers were removed first before the compilation of this figure.

From this figure it appears that samples with a void ratio below 0.9 and an undrained shear strength ratio value larger than 0.55, have a dilative nature and that samples with a void ratio larger than 0.9 and an undrained shear strength ratio value smaller than 0.55, have a contractive behavior. Note that the aforementioned findings correspond with the findings made under Section 5 for this tailings dam and with specific reference to the void ratio values.

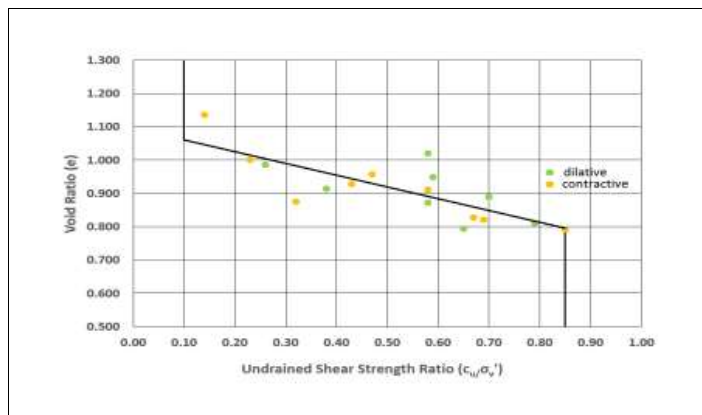


Figure 12. Tailings Dam No.2 – Void ratio versus undrained shear strength behaviour.

7 MOISTURE CONTENT VERSUS DEPTH BEHAVIOUR

7.1 Tailings Dam No.1

Figure 13 provides a visual interpretation of the moisture content versus depth information for Tailings Dam No.1. Note that the laboratory test results received for the geotechnical drilled samples specifically were implemented.

This figure indicates an average moisture content value equal to 10.2%. Note that the average value is not representative of a saturated tailings behaviour.

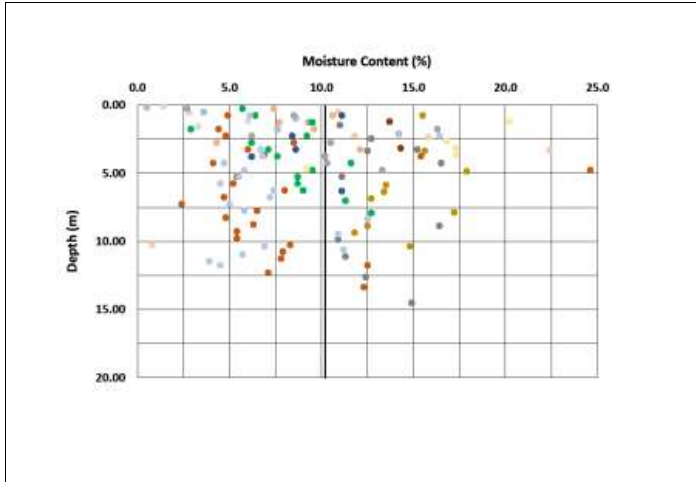


Figure 13. Tailings Dam No.1 – Moisture content versus depth plot.

7.2 Tailings Dam No.2

Figure 14 provides a visual interpretation of the moisture content versus depth information for Tailings Dam No.2. The laboratory test results received for the geotechnical drilled samples specifically were implemented.

From the figure the average moisture content is equal to 9.1%. The average value is not representative of a saturated tailings behaviour.

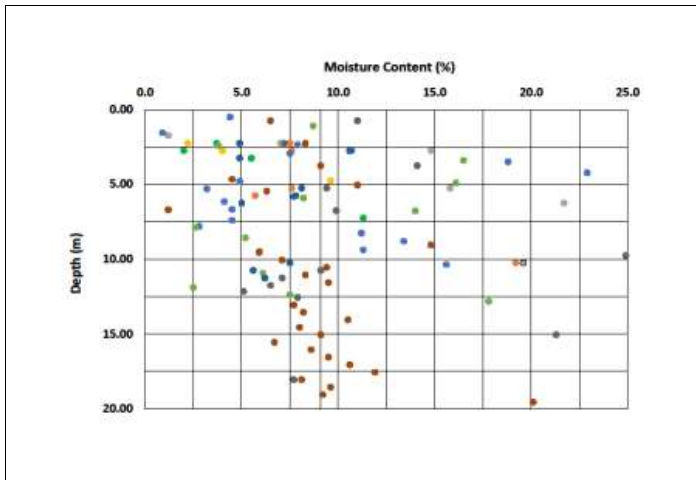


Figure 14. Tailings Dam No.2 – Moisture content versus depth plot.

8 WALL VERSUS BASIN MATERIAL

8.1 Tailings Dam No.1

From an overall stability point of view it is crucial that a large enough portion of the outer wall of Tailings Dam No.1 comprise quality wall building material, typical with an undrained shear strength ratio equal to 0.6 or higher. Figure 15 below confirms this requirement based on the peak shear strength ratio values (0.66 and 0.68) obtained through the CPTu probing carried out at line 4 (highest flank of this tailings dam). Also note the lower peak shear strength ratios (0.52 and 0.42) recorded along the basin area of the tailings dam.

In terms of the other three flanks of the tailings dam, average peak shear strength ratio values equal to 0.65, 0.69 and 0.65 for lines 1, 2 and 3 respectively, were recorded. The curtain drain assists with the overall drawdown of the phreatic surface of the tailings dam, which further assists with the overall stability of the tailings dam.

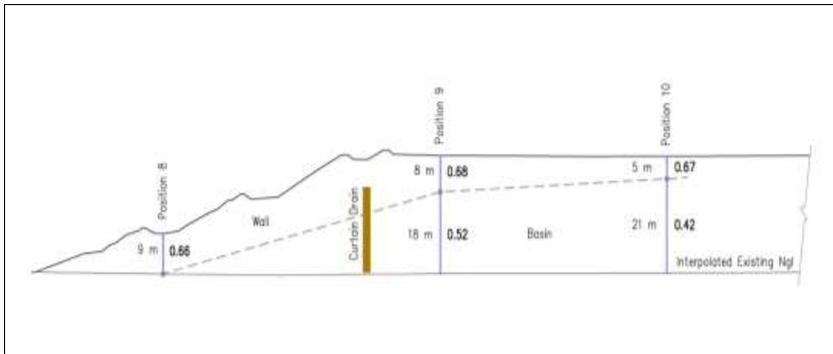


Figure 15. Tailings Dam No.1 – Line 4 – Peak shear strength ratios.

8.2 Tailings Dam No.2

Figure 16 below confirms acceptable peak shear strength ratio values (0.63 and 0.67) obtained through the CPTu probing carried out at line 3 (highest flank of the tailings dam). Even along the basin area a good peak shear strength ratio (0.71) was recorded. This can most probably be ascribed to slag that is co-disposed on this tailings dam.

In terms of two of the other three flanks of the tailings dam, average peak shear strength ratio values equal to 0.62 and 0.63 for lines 1 and 2 respectively, were recorded. As indicated, a curtain drain is also installed at this tailings dam.

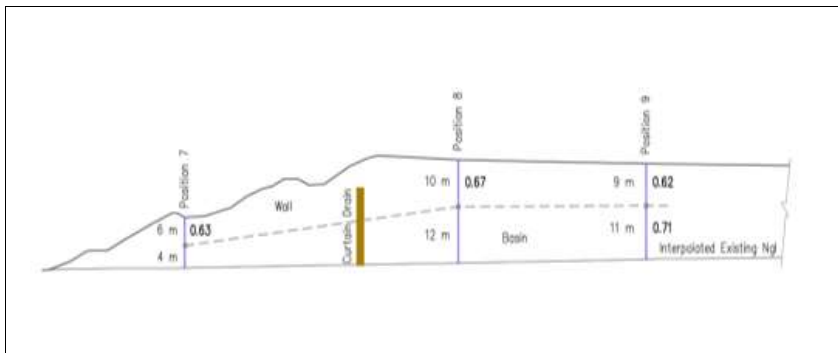


Figure 16. Tailings Dam No.2 – Line 3 – Peak shear strength ratios.

9 CONCLUSIONS

From the laboratory and site investigations the following can be concluded:

- The average effective stress friction angle values determined through CPTu probing and from the laboratory testing of the geotechnical drilled tailings samples, compare reasonably well. For both Tailings Dams No's 1 and 2 the respective average effective stress friction angle values obtained from the laboratory testing of the geotechnical drilled samples are higher than the respective effective stress friction angle values determined through CPTu testing.
- The average permeability values calculated for the geotechnical drilled samples, obtained at the respective tailings dams, are similar.
- Tailings material that behave in a contractive as well as a dilative manner, was encountered at the two tailings dams.
- For contractive tailings samples the axial strain increases further after the deviator stress has reached a maximum. For dilative tailings samples the axial strain increases as the deviator stress increases.
- The average effective stress friction angle values determined for Tailings Dams No's 1 and 2, utilizing all triaxial test (consolidated undrained) results, are 36.1 degrees and 37 degrees respectively.
- For Tailings Dam No.1 the samples with a void ratio lower than 0.85 and an undrained shear strength ratio larger than 0.3, have a dilative behaviour. Samples with a void ratio larger than 0.85 and an undrained shear strength ratio smaller than 0.3, have a contractive behaviour.
- For Tailings Dam No.2 the indications are that samples with a void ratio below 0.9 and an undrained shear strength ratio larger than 0.55, have a dilative nature. Samples with a void ratio above 0.9 and an undrained shear strength ratio smaller than 0.55, have a contractive behaviour.
- For Tailings Dam No.1 the average moisture content value is equal to 10.2%. For Tailings Dam No.2 the average moisture content values is equal to 9.1%. For both tailings dams the respective average moisture content values are not representative of a saturated tailings behaviour.
- For both tailings dams, outer wall building material with peak shear strength ratio values higher than 0.6, was determined through CPTu probing. Average peak shear strength ratio values above 0.6 were also determined at the respective remaining flanks of the two tailings dams.
- It is recommended that the various geotechnical parameters determined through CPTu probing and the laboratory testing of the various samples be implemented with the design of the new lined tailings dams.

10 REFERENCES

- BS 1377-8: 1990 Part 8: Shear strength tests (effective stress) triaxial compression test.
- Head, K.H. 1998. *Manual of Soil Laboratory Testing - Volume 3 - Effective stress tests*, Wiley.
- Jefferies, M. & Been, K. 2016. *Soil liquefaction: A critical state approach*. 2nd Edition, CRC Press.
- Lade, P.V. 2016. *Triaxial Testing of Soils*. Wiley Blackwell.
- Lunne, T., Robertson, P.K. & Powell, J.J.M. 1997. *Cone penetration testing in geotechnical practice*. Blackie Academic & Professional.
- Robertson, P.K. & Cabal, K.L. 2014. *Guide to cone penetration testing for geotechnical engineering*. 6th Edition, Gregg

Practical Nomograms for Waste Rock Piles Design on Competent Foundations

L. Piciacchia, V. Marefat, and A. Vides

BBA Inc., Mine Waste Management and Environment, Montreal, Quebec, Canada

ABSTRACT: Waste Rock Piles can measure hundreds of meters in height and their failure can put life and property at extreme risk as well as significantly impact the surrounding environment. As such, waste rock piles should be considered structures, rather than dumps. Waste rock piles geometry and height is site-specific and govern the level of risk associated to its construction, operation and management. However, the design of these structures does not always garner the rigorous attention that they should be afforded. This paper provides practical nomograms for designing waste rock piles on solid competent foundations. In cohesionless soils, commonly placed using end-dumping methods, the stability of the stockpile slope depends on the angle of internal friction (ϕ), slope angle and the height, for a given depth of critical slip failure. The nomograms presented herein are based on the requirement of attaining an overall factor of safety of 1.5 and a local factor of safety of 1.2.

1 INTRODUCTION

Failure in Waste Roc Facilities (WRF) can occur in the foundation soils or within the deposited material itself. As such, an evaluation of both materials is required to properly assess their overall stability and risk. Regardless, of where failure may occur, proper design can be used to mitigate such failure and reduce risk. For purposes of developing the practical nomograms presented in this paper, the regulatory requirements of the Quebec Ministry of the Environment and Natural Resources (MERN) have been used. Table 1, outlines these requirements.

Table 1: Stability analysis - Minimum values for factor of safety (MERN)

Condition	Factor of safety
Bearing capacity of the foundation under WRF	1.5 to 2.0
Local stability of the piles (for each bench)	
Short term static analysis*	1.0 to 1.1
Long term static analysis	1.2
Overall stability, for deep failures or failures pass through Foundation	
Short term static analysis *	1.3 to 1.5
Long term static analysis	1.5
Pseudo-static analysis	1.1 to 1.3

* According to risk and uncertainty

The nomograms presented in this paper are intended for WRF where the foundation is deemed to be competent (i.e., rock and/or shallow deposit of till) and the deposited material is self-draining.

A common method for deposition of waste rock disposal facilities is end-dumping or push-dumping. In both deposition methods, the overall waste rock pile slope angle follows the angle of internal friction of the materials that compose it. In other words, materials repose on their angle of internal friction. For instance, an angle of repose approaching 37° is a result of end dumping for a material with an ϕ value of around 37° . The deposited mass in these types of slopes is always in a state of equilibrium. In the other words, a FS of unity is always expected for these types of slope, except in dynamic condition or change pore water pressure conditions.

In this type of material the critical failure mechanism is usually shallow sliding. The depth for critical slip failure not only considers a serious failure but also eliminates the shallow (insignificant) failures, which may occur on the slope surface. The methodologies to define the appropriate depth of failure for the critical slip circle and nomograms to design waste rock piles that will meet MERN regulatory requirements are presented herein.

2 METHODOLOGY

2.1 Critical slip surface depth (D_{cf}).

The most common failure mechanism of cohesionless soils is shallow sliding. As such, an appropriate depth for the critical slip failure needs to be defined in order to conduct more realistic slope stability analyses. A question may arise: what depth should be considered for the critical slip failure when conducting slope stability analysis? The depth of the critical slip failure is related to the angle of internal friction of the material in the waste rock pile. Consider two slopes similar in height but containing two different materials. The first slope is comprised of fine sandy material and the second contains oversized coarse rock and boulders. It is certain that the depths of critical slip failure will not be similar for these materials. What is known is that a slope angle which corresponds to ϕ will have a FS of 1, for a stockpile with infinite height. As such, a depth of failure (D_{cf}) which would yield a FS=1 is considered appropriate.

To define the depth for critical slip surface, a number of 2D slope stability analyses were conducted using the limit equilibrium (LE) method. An idealized cross section of a waste rock pile with a fixed height of 150 m was considered. The waste rock pile was considered to be resting on a competent foundation. As a result, all of the slip failures pass through the waste rock pile and not the foundation. The waste rock pile is made of various cohesionless materials with an angle of internal friction ranging between 32 and 42 degrees. The slope angle (α) in the model was maintained at an angle equal to ϕ . Figure 1 presents a general sketch of the 2D slope stability model used in this study.

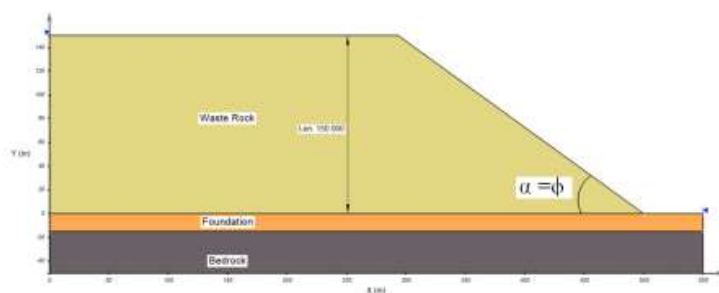


Figure 1: sketch of 2D slope stability model

The depth of critical slip failure was determined based on the premise of attaining a FS=1. To do so, a number of depths were assigned in the LE slope stability analysis. The maximum depth D_{cf} was defined when the obtained FS was equal to 1. This depth not only represents a serious slip failure with a FS = 1, but also eliminates the shallow slip failures along the slope.

The exercise was repeated for a range of materials with angle of internal friction between 32 and 42 degrees. The resulting D_{cf} are represented in Figure 2.

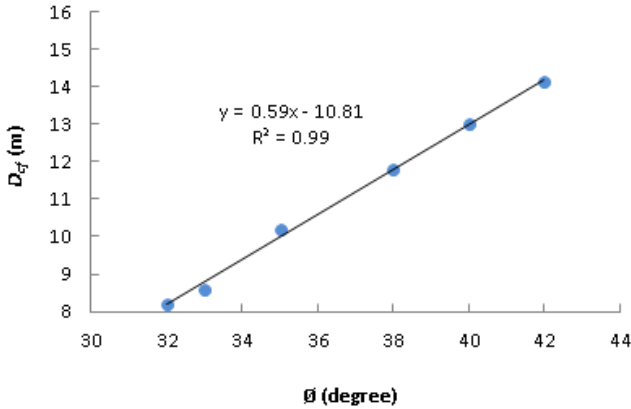


Figure 2: Angle of internal friction versus depth of critical slip failure

2.2 Maximum bench height (h_{max})

For an infinite slope and a defined D_{cf} yielding $FS=1$, the FS can be increased by reducing the slope height. In this way, a maximum exposed slope height can be determined, which will yield a $FS=1.2$. This height, called the maximum bench height (h_{max}) in this paper, was also found by means of LE slope stability analysis for a bench comprising various waste rock materials with an ϕ ranging from 32 to 42 degrees.

To determine the maximum bench height of a bench comprising a material with a given ϕ and a given D_{cf} , various heights were assigned for the bench in the slope stability analysis. The height at which a local FS of 1.2 was obtained is considered as the maximum bench height, for a given material.

2.3 Minimum bench width (W)

For a waste rock pile with a general configuration, shown in Figure 3, the minimum bench width (W) was calculated based on the requirement of attaining an overall FS of 1.5.

As shown in Figure 3, W can be obtained as follows:

$$W = X_2 - X_1 = \frac{h}{\tan \beta} - \frac{h}{\tan \phi_1} \quad (2.1)$$

In which, h is the bench height and β is the angle of the waste rock pile's overall slope. The angle (β) represents the overall slope angle corresponding to a global $FS=1.5$. The global FS is defined as the ratio of available shear strength to strength required to maintain stability:

$$FS = \tan \phi / \tan \beta \quad (2.2)$$

For an overall $FS=1.5$, the overall slope angle can be calculated as follows:

$$\beta = \tan^{-1}(\tan \phi / 1.5) \quad (2.3)$$

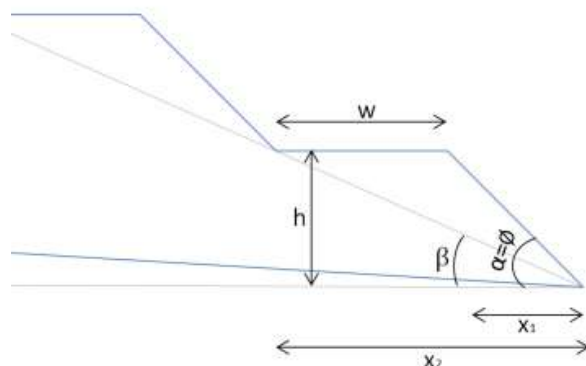


Figure 3: sketch for general configuration of a waste rock pile

Replacing Eq. (2.3) into Eq. (2.1) yields:

$$W = h / \tan(\tan^{-1}(\tan \phi / 1.5)) - h / \tan \phi \quad (2.4)$$

3 RESULT AND DISCUSSION

The relationship between the angle of internal friction and the depth of critical slip failure (D_{cf}) for waste rock materials with an ϕ ranging between 32° and 42° has previously been defined in section 2.1. The resulting relationship between ϕ and D_{cf} was found to be linear and is represented by Equation 3.1.

$$D_{cf} = 0.59\phi - 10.81 \quad (3.1)$$

For example, for a material with an angle of internal friction of 36 degrees, the critical slip failure depth is about 10 m. The obtained D_{cf} , for various materials in this study ($\phi = 32 - 42$ degrees), was then used in the slope stability analysis to determine the maximum height for the bench (h_{max}) considering a FS=1.2. The relationship between the maximum bench height and ϕ was also found to be linear and is represented in Figure 4 and Equation 3.2.

$$h_{max} = 3.22\phi - 65.46 \quad (3.2)$$

The obtained h_{max} can then be used to determine the minimum bench width using Eq. (2.4) attaining an overall FS of 1.5. Figure 4 also provides a nomogram showing the relationship between h_{max} and W .

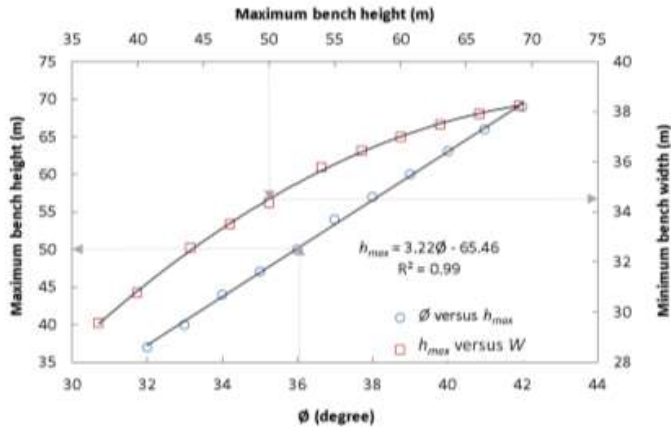


Figure 4: Relationship between ϕ , h_{max} and W attaining a local FS of 1.2 and an overall FS of 1.5.

An example is given herein to guide the users when using the nomogram presented in Figure 4. For a material with an angle of internal friction (ϕ) of 36 degrees, the maximum height for each bench is 50 m. which can be found from the linear graph representing the relationship between ϕ and h_{max} . After having determined the maximum bench height, the minimum bench width (of 34.5 m) can be found by the non-linear graph in Figure 4 representing the relationship between h_{max} and W . The minimum bench width can also be calculated by means of Eq. (2.4).

The nomogram presented in Figure 4 provides only the design parameters based on the maximum bench height (h_{max}). For the cases in which the bench height is not as high as h_{max} , an optimised nomogram is needed to assist the designers. Figure 5 presents another nomogram, which is developed based on the requirements of attaining an overall FS of 1.5. For various waste materials with an ϕ between 32 degrees and 42 degrees, the nomogram was developed based on Eq. (2.4). For a given material, the nomogram provides a bench width associated with a proposed bench height achieving an overall FS of 1.5.

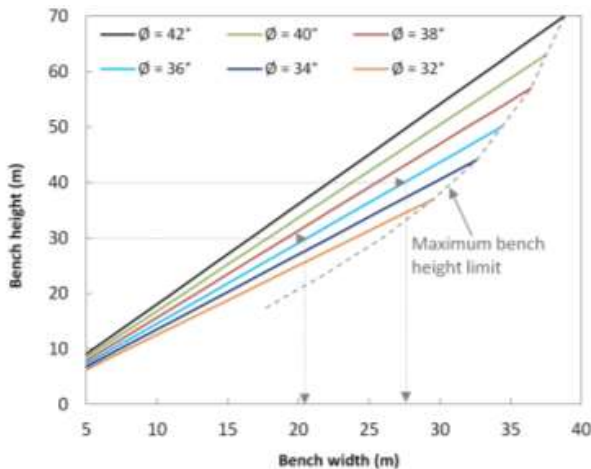


Figure 5: Waste rock pile design nomogram, achieving an overall FS of 1.5.

As mentioned, the maximum height for a bench comprising a waste rock with an ϕ of 36 degrees is 50 m, which needs a minimum bench width of 34.5 m attaining an overall FS=1.5. For bench heights of less than h_{max} corresponding bench widths should be designed in order to optimize volume and maintain overall slope. This will ensure that an FS=1.5 is achieved. For example, 40 m and 30 m of bench heights for a pile comprising a waste rock with an $\phi=36$ degrees would have the minimum bench widths of 27.5 m and 20.5 m respectively.

The results and analysis provided herein can be used to design the waste rock piles comprising dry/unsaturated waste material constructed on unyielding competent foundation. The effect of pore water pressure on the pile stability is not considered in this study as the material to be considered self-draining. In piles comprising fine waste material, the phreatic level may rise during wet seasons, which may greatly affect the stability of the pile. These nomograms are not intended to be used in such cases.

4 APPLICATION

As such, if we apply this approach to a material having an $\phi=40$ degrees and an overall height of 200 m. The maximum bench height of 63 m with a corresponding width of 37 m should be considered for the design. Alternately, should the operator decide to limit bench height to 50 m, the bench width could be reduced to 30 m based on the nomogram presented in Figure 5. Both configurations would yield an overall FS of 1.5 and a local FS=1.2. The slope stability analysis presented in Figures 6 and 7 validates this application.

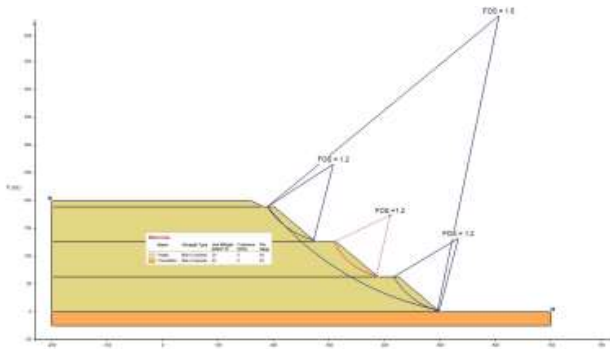


Figure 6: Slope stability simulation for maximum bench height.

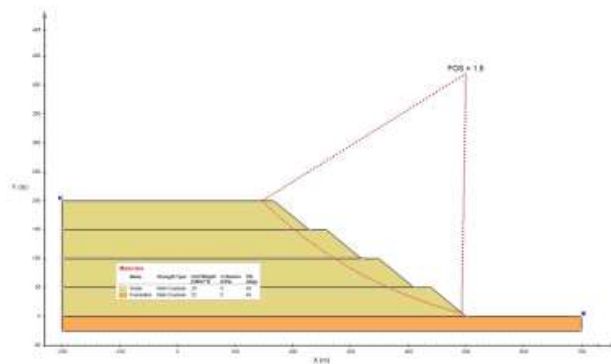


Figure 7: Slope stability simulation for the reduced bench height.

5 CONCLUSION

Waste rock piles geometry is site-specific and governs the level of risk associated to its construction, operation and management. As such, waste rock piles should be considered structures, rather than dumps. Therefore, rigorous attention should be afforded for the design of these structures. Several slope stability analyses were conducted to define the parameters for designing local and overall geometry of the waste rock piles. The stability results showed that maximum bench height should be limited in order to attain a local FS=1.2. The results showed that maximum bench height is linearly related to the bench material angle of internal friction.

The overall stability of a waste rock pile is controlled by its global slope angle (β). To achieve an overall FS=1.5 the method of construction becomes critical variable. It is not possible to simply end dump and anticipate satisfactory configuration. An analytic solution for a range of bench heights and material types was developed to calculate minimum bench width. The analytic solution provided a non-linear relationship between bench maximum height and bench width. For a case in which the bench height is less than the maximum bench height, this paper presented another nomogram to design optimum geometry for waste rock piles.

The results obtained in this paper can be used to design waste rock piles comprising self-draining waste material on unyielding competent foundations.

6 REFERENCES

SoilVision Systems Ltd. 2017. *SVSLOPE Theory Manual (SVOFFICE 2017)*. Saskatoon, Saskatchewan, Canada.

Review of Alternative Tailings Disposal Methods for Water Management

C.L. Strachan

Stantec Consulting Services Inc., Fort Collins CO USA

ABSTRACT: This paper presents a review of alternative tailings disposal methods (methods that involve reducing the percentage of process water with tailings discharge). These methods include thickened, paste, and filtered tailings disposal.

This review is based on published information, and identifies where and at what production capacity these alternative methods are used. Observations from this information include: (1) the reasoning for use of filtered, paste, or filtered tailings disposal; (2) the differences in process water recovery compared with conventional slurry disposal; and (3) the potential savings in cost and time to close or reclaim these facilities. With the operating experience of these alternative methods, key elements of technology are being developed, resulting in use of these methods at higher production capacity and at lower operating cost.

1 INTRODUCTION

This paper presents a current review of alternative methods of tailings disposal. These are methods that involve reducing the percentage of process water with tailings discharge from the percentage that is discharged with a typical tailings slurry. These methods include thickened, paste, and filtered tailings disposal.

While there is significant consideration of these alternative methods in the industry, and thickened and filtered tailings process technology is rapidly developing, this review is based on published information. This review identifies the location, production capacity, and operational details of the alternative methods are in operation.

2 BACKGROUND

Tailings comprise the residue from a hydrometallurgical or hydraulic separation process for recovery of metals, diamonds, or other materials of value.

The tailings particle-size distribution depends on the crushing and grinding circuit as well as the mineralogical composition of the material that is processed. A general overview of the physical tailings characteristics from various types of processing is provided in Vick (1990). Tailings are typically of sand and silt-sized gradation, produced by mechanical crushing and grinding. Clay-sized particles in tailings are derived from alteration and weathering of the original ore.

The tailings process solution chemistry is dictated by the specific hydrometallurgical process used for recovery. These range from low-pH conditions in an acid-leach process to near-neutral pH for a flotation process to high-pH conditions for a cyanide-leach process. Tailings chemistry is also influenced by the mineralogy and alteration of the original ore and its degree of oxidation during and after milling.

Due to the water required for processing, tailings are discharged from the mill or processing facility as a slurry at a relatively low solids content (10 to 20 percent solids; ten percent solids is equivalent to 1 kg solids in 9 kg of water). The tailings may be directed through a thickener to recycle a portion of the process solutions prior to discharge.

Alternative tailings transport and disposal methods (that differ from conventional slurried methods) have been used since the 1970s. Paste thickening has been used for processing tailings for mine backfill, and thickened tailings have been utilized in surface disposal in varying climates world-wide for over 20 years. Sites in North America (such as Greens Creek in Alaska, and Jardine in Montana) have utilized filtered tailings due to area constraints. Sites in South America (such as La Coipa and Mantos Blancos in Chile) have utilized filtered tailings due to costs of fresh water.

2.1 Slurried Tailings Disposal

Tailings from conventional methods of milling and separation have commonly been discharged from the mill as a slurry, typically at 30 to 50 percent solids (50 percent solids is equivalent to 1 kg solids in 1 kg of water). Tailings are typically transported to the tailings storage facility or impoundment by gravity through a pipeline or open channel or by pumping through a pipeline. Conventional slurried tailings disposal has been used at mine sites world-wide since the early 1900s, for a wide range of production rates.

The operational objectives of slurried tailings management are to contain the discharged slurry to allow settlement of tailings solids and recycling of process water. The ultimate objective is to allow the tailings solids to consolidate to sufficient density and shear strength for final environmental reclamation.

2.2 Thickened Tailings Disposal

Thickened tailings was first developed in Canada and used at Kidd Creek, Ontario in the 1970s (Robinsky, 1975), and at a number of sites in Australia (Seddon and Williams, 2010) and Canada (Kam et. al, 2011) since the 1980s. Additional background on the history and development of surface disposal of thickened tailings is given by Fitton and Seddon (2013), Williams et. al (2008), Brzezinski (2001), and Boswell et. al (2014).

Thickened tailings disposal uses high-density or deep-cone thickeners to increase tailings slurry densities. The higher slurry density has a higher viscosity yield strength and reduces particle segregation upon discharge. Thickened tailings slurry (typically 55 to 70 percent solids) is generally amenable to transport with centrifugal pumps.

Thickened tailings disposal has advantages over conventional tailings disposal where the impoundments have a large surface area, and the steeper thickened tailings beach slope and higher tailings density provide additional tailings storage capacity. Recovery of process water through the thickeners also reduces evaporation losses, where water is scarce and costly.

2.3 Paste Tailings Disposal

Paste tailings disposal typically requires thickening to approximately 70 to 75 percent solids, and is primarily used for underground mine backfill. Paste tailings backfill is typically mixed with cement, with transport and placement aided by gravity.

Due to the limited throughput of paste thickeners and relatively high operating costs, the use of paste thickening for surface disposal offers limited advantages, and generally occurs at mines with low production rates and short transport distances.

2.4 Filtered Tailings Disposal

Filtered tailings are “dewatered” using drum, disc, or belt filters (by vacuum) or with filter presses (using pressure) to solids contents typically greater than 80 percent. The resulting “dry cake” or “filter cake” requires transportation to the tailings storage facility by truck or conveyor. The tailings are dropped by a conveyor and stacker or placed and spread in lifts of selected thickness and compacted to a specified density. In some cases, lime or cement is added to the filtered tailings to bind with tailings porewater and increase tailings shear strength for placement of subsequent lifts of tailings. Construction equipment can typically work directly on the filtered tailings after deposition.

Filtered disposal requires a smaller impoundment area than other disposal methods because the resulting tailings density is higher and a confining embankment may not be necessary. The final slopes of a filtered

tailings disposal facility are dictated by closure requirements and cover characteristics (typically horizontal to vertical slopes of up to 3 to 1).

2.5 Alternative Tailings Disposal Methods Summary

Some of the key factors with conventional slurried and alternative methods of tailings disposal are summarized in Table 1.

Table 1. Tailings Management Characteristics of Alternate Tailings Disposal Methods.

Factor	Conventional	Thickened	Paste	Filtered
Typical solids content (%)	35-55	55-70	70-75	>80
Typical yield stress range on discharge (kPa)	0-20	20-150	150-400	>1000
Delivery to impoundment	As a slurry by gravity or centrifugal pump	As a slurry by centrifugal pump	As a high slump paste by positive-displacement pumping	As a "cake" by truck or conveyor
Storage in impoundment	Requires embankment containment	Requires toe containment	Requires low toe containment	Containment not necessary
Disposal space	Capacity for low-density tailings and area for settlement of solids	Capacity for medium-density tailings and area for thin layer deposition and air drying	Capacity for high-slump tailings and area for drying of thicker layers	Capacity for cake tailings placement and compaction
Settled tailings characteristics	Consolidation and settlement necessary	Consolidation and air drying necessary	Near shrinkage limit	At shrinkage limit
Amenability for covering at closure	Removal of ponded water and consolidation necessary	Generally amenable if air dried	Generally amenable if air dried	Ready for covering
Water recovery	Reclaim from supernatant pool	Reclaim from thickener and run-off from collection pond	Recovery from paste thickener and run-off from collection pond	Recovery from thickeners and filtration equipment
Major energy requirements	Reclaim water pumpback	Reclaim water pumpback	Paste thickener and displacement pumping	Filtration equipment and tailings transport

3 WATER CONSERVATION

The percent solids values mentioned above for the slurried and alternative disposal methods are shown graphically in Figure 1. The chart on the right shows the ranges of solids content values (at discharge) for the methods listed in Table 1. The chart on the left shows the equivalent range of values, in terms of water volume per unit weight of solids (at discharge) for the same ranges in tailings solids content values.

Both charts show the increase in solids content (and decrease in water content due to consolidation and drying) necessary to reach tailings closure conditions. These conditions would be where the tailings have sufficient density to preclude liquefaction and sufficient bearing capacity to support cover placement. These charts show the additional water reduction necessary for slurried tailings to reach conditions for closure.

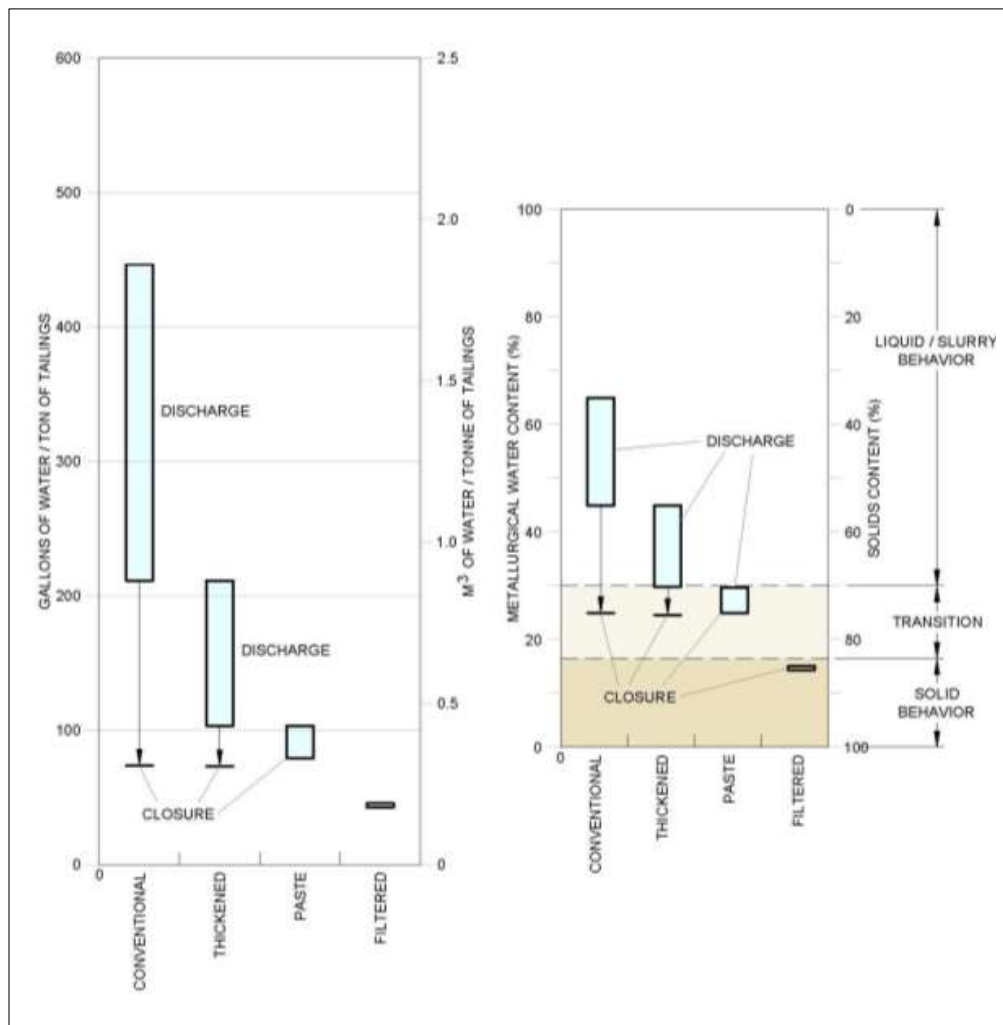


Figure 1. Comparison of Process Water Requirements with Tailings Solids Content

4 ALTERNATIVE TAILINGS OPERATION INFORMATION

Table 2 lists mines and processing facilities (from published information) where paste or thickened tailings are produced. Several facilities have production rates over 100,000 tonnes per day. Several lower production rate facilities are achieving solids contents above 70 percent (some as high as 77 percent).

Table 2. Operational Information for Thickened or Paste Tailings Disposal Facilities

Project	Location	Mineral	Approx. Prod. Rate (tonnes/day)	Solids Content at Discharge (%)	Fines (%)	Clay Content (%)	Data Source	Processing	Transport
Century Zinc	Australia	Zn	12,000	52-58	-----	-----	Williams et al. (2008)	One high-rate thickener, 45 m dia.	Down-valley discharge
Ellendale	Australia	Diamond	10,000	47-49	-----	-----	Williams et al. (2008)	One high-rate thickener, 34 m dia.	Down-valley discharge
Ernest Henry	Australia	Cu	20,000	75	-----	-----	Williams et al. (2008)	One high-compression thickener, 35 m dia.	Central discharge
Kwinana	Australia	Al	12,000	47-51, 60	-----	-----	MWH (2009a)	Fine and coarse tailings streams	-----
Mt. Keith	Australia	Ni	30,000	44-55	-----	-----	Williams et al. (2008), MWH (2009a)	Fine and coarse tailings streams; 1.2 tonne/m ³ density	-----
Murrin Murrin	Australia	Ni, Co	-----	30-32	-----	-----	MWH (2009a)	-----	-----
Osborne	Australia	Cu, Au	3,500	72-76	-----	-----	Williams et al. (2008)	One high-rate thickener, 9 m dia.	Central discharge
Pajingo	Australia	Au	2,000	59-61	-----	-----	Williams et al. (2008)	One paste thickener, 14 m dia.	In-pit discharge
Peak Mine	Australia	Cu	1,200	55-62	-----	-----	Williams et al. (2008), MWH (2009a)	One high-rate thickener, 8 m dia.; 1.65 tonne/m ³ density	Central discharge
Sunrise Dam	Australia	Au	10,000	62-67	-----	-----	Williams et al. (2008), MWH (2009a)	One high-rate thickener, 24 m dia.	Down-valley discharge
Alcan Vaudreuil Alumina Refinery	Canada	Al ₂ O ₃	2,465	50	86	30	KCB (2017)	Deep cone thickener	Positive displacement pump
Canadian Malartic	Canada	Au	55,000	-----	-----	-----	KCB (2017)	65-m-high wall thickeners	Centrifugal pump
Ekati	Canada	Diamond	4,600	40	-----	-----	Williams et al. (2008)	Two high-rate deep cone thickeners, 12 m dia.	-----

Project	Location	Mineral	Approx. Prod. Rate (tonnes/day)	Solids Content at Discharge (%)	Fines (%)	Clay Content (%)	Data Source	Processing	Transport
Kidd Creek	Canada	Cu, Zn	8,000	63	85	10	Williams et al. (2008)	One high-compression thickener; 70 m dia.	Central discharge
Musselwhite	Canada	Au	4,500	68	70	----	Kam et al. (2011)	One deep cone thickener	Perimeter discharge
Myra Falls	Canada	Zn, Pb, Cu	3,600	-----	98	20	KCB (2017)	One high-rate thickener, 25 m dia; disc filter	Positive displacement pump
Snap Lake	Canada	Diamond	3,150	73	-----	-----	KCB (2017)	Deep cone thickener	-----
Strathcona	Canada	Ni	1,400	45	-----	-----	Williams et al. (2008)	One high-rate deep cone thickener, 10 m dia.	-----
Sudbury Integrated Nickel Operations	Canada	Ni, Cu, Co, Pt	6,027	-----	-----	-----	KCB (2017)	-----	-----
Candelaria	Chile	Cu, Au, Ag	70,000	50	-----	-----	KCB (2017)	Two conventional thickeners, 122 m dia.	Centrifugal pump
Chuquibambata	Chile	Cu	182,000	55	-----	-----	KCB (2017)	-----	-----
Collahuasi	Chile	Cu	66,500	52	-----	-----	KCB (2017)	-----	-----
Miduk	Iran	Cu	13,700	57	72	15	Williams et al. (2008)	Four paste thickeners, 16 m dia.	Down-valley discharge
Sar Cheshmeh	Iran	Cu	60,000	-----	-----	-----	KCB (2017)	-----	-----
Aughinish Alumina	Ireland	Al ₂ O ₃	3,288	58	-----	35	KCB (2017)	Vacuum filtration	Central discharge
Oyu Tolgoi	Mongolia	Cu, Au	100,000	59	55	11	KCB (2017)	Two 80 m thickeners	Centrifugal pump
Cerro Verde	Peru	Cu	120,000	58	68	-----	KCB (2017)	Two 75 m thickeners	Gravity flow
Cobriza	Peru	Cu	1,484	77	-----	-----	Williams et al. (2008)	14 m dia. Paste thickener	Positive displacement pump
Neves Corvo	Portugal	Cu, Zn	4,800	-----	94	13	KCB (2017)	Deep cone thickener	-----
Bulyanhulu	Tanzania	Au	3,300	73	74	10	KCB (2017)	Two high rate thickeners, vacuum disc filters	Positive displacement pump

Project	Location	Mineral	Approx. Prod. Rate (tonnes/day)	Solids Content at Discharge (%)	Fines (%)	Clay Content (%)	Data Source	Processing	Transport
Toromocho	Peru	Cu	117,000	69-70	60	-----	Lara (2012)	-----	-----
El Brocal	Peru	Pb, Zn, Cu	18,000	62-63	82	-----	Lara (2012)	-----	-----
Cobriza	Peru	Cu	7,000	75-77	81	-----	Lara (2012)	-----	-----
Huanca	Peru	Cu	100,000	63-65	55	-----	Lara (2012)	-----	-----
Magistral	Peru	Cu, Mo	20,000	70-74	53	-----	Lara (2012)	-----	-----
Hilarion	Peru	Pb, Zn, Ag	5,000	72-74	63	-----	Lara (2012)	-----	-----
La Quinua	Peru	Au	14,000	69	-----	-----	Williams et al. (2008)	One high-rate thickener, 32 m dia.	Down valley discharge
San Rafael	Peru	Sn	4,000	60-62	90	-----	Lara (2012)	-----	-----
Collahuasi	Chile	Cu	66,500	52	-----	-----	MWH (2009b)	-----	-----
EKAPA	S. Africa	Diamond	2,300	53-57	-----	-----	Williams et al. (2008)	One paste thickener, 15 m dia.	In-pit discharge
Kimberley	S. Africa	Diamond	25,000	44-57	-----	-----	Williams et al. (2008)	Five paste thickeners; 15 m dia.	Central discharge

Table 3 lists the mines and processing facilities (from published information) where filtered tailings are produced. Several facilities have production rates over 5,000 tonnes per day, with Kakara, La Coipa, and Mantos Blancos having the largest reported production rates. Most filtration facilities are pressure plate systems, all of which are reportedly achieving over 80 percent solids.

Table 3. Operational Information for Filtered Tailings Disposal Facilities

Project	Location	Mineral	Approx. Prod. Rate (tonnes/day)	Solids Content at Discharge (%)	Fines (%)	Clay Content (%)	Data Source	Processing	Transport
Greens Creek	Alaska	Pb, Zn, Ag, Au	750	88	80	3	KGCMC (2004)	Three 32 plate filter presses	Truck
Pogo	Alaska	Au	1,360	87	80	7	KCB (2017)	Pressure filtration	Truck
Karara	Australia	Fe	35,000	87	----	----	KCB (2017)	Fine fraction - pressure filtration; Coarse fraction - dewatering screens	Stacking conveyor
Bellekeno	Canada	Ag	188	----	----	----	KCB (2017)	Filter press	Truck
Éléonore	Canada	Au	4,000	----	----	----	KCB (2017)	Pressure filtration	----
Minto	Canada	Cu	3,800	86	----	----	KCB (2017)	Five 1.5-m by 1.5-m pressure filters	----
El Penon	Chile	Au, Ag	4,200	83	63	----	Lara (2012)	Vacuum belt filtration	Truck
La Coipa	Chile	Ag, Au	18,000	81	54	----	MWH (2009b)	Thickeners, vacuum belt filtration	Stacking conveyor
Mantos Blancos	Chile	Cu	12,000	83	38	----	KCB (2017)	Belt filters, dewatering screens, 0.5 m ² /tonne makeup water	Stacking conveyor
Escobal	Guatemala	Ag	1,528	84	----	----	KCB (2017)	Pressure filtration	Truck
Marlin	Guatemala	Au	4,000	84	80	18	KCB (2017)	Plate pressure filters	Conveyor, truck
Alamo Dorado	Mexico	Au, Ag	4,000	82	----	----	KCB (2017)	Two belt filters at 160 m ²	Conveyor, truck
San Dimas	Mexico	Au, Ag	2,500	----	----	----	KCB (2017)	Vacuum belt filter	----
Skorpion Zinc	Namibia	Zn	5,040	60	75	13	KCB (2017)	Vacuum belt filter	Stacking conveyor
Catalina	Peru	Au	1,000	80-82	57	----	Lara (2012)	Tailings contained in dam	----
Catalina Huanca	Peru	Zn, Ag, Pb	2,000	----	----	----	KCB (2017)	Filtered	Truck
Cerro Lindo	Peru	Zn, Pb, Cu	6,480	88	57	----	KCB (2017)	30 m high compression thickener, belt filter;	Truck
Efemçukuru	Turkey	Au	700	----	----	----	KCB (2017)	Plate pressure filtration	Truck

5 CONCLUSIONS

The selection of a tailings disposal method depends on site-specific factors, which are discussed below.

5.1 Topography

Steep topography typically requires larger embankments and smaller ratios of storage capacity to embankment volume, resulting in relatively higher costs for conventional disposal. At some sites, limitations on area for conventional disposal result in filtered tailings disposal selection. Sites for filtered tailings disposal, however, require some areas flatter than the final reclaimed facility slope (such as 3:1) for operation and tailings storage capacity. For sites with flat topography and low seismicity, conventional, thickened, or paste disposal are often selected due to lower costs than filtered disposal.

5.2 Climate

For sites where precipitation exceeds evaporation (and there is a net gain of meteoric water), limitation of the impoundment area that is exposed to precipitation is desired, to reduce the volume of collected water requiring treatment and discharge. While this could result in a preference for filtered tailings disposal, sites with high precipitation may limit the ability to place filtered tailings.

For sites where evaporation exceeds precipitation, accumulation of excess meteoric water may not be an issue, resulting in a preference for conventional or thickened disposal. For sites where water supply is limited and recycling of process water is desired, thickened or filtered tailings may be preferred.

5.3 Geology and Construction Materials

The underlying geology of a specific site dictates the type of containment necessary for tailings and process water (whether a “natural” liner or containment system can be used, or a constructed liner system is necessary). If the tailings are unsaturated, the level of secondary containment and leak detection monitoring may be reduced. Country and/or local regulations may also dictate what liner types and hydraulic conductivity properties are admissible.

The area geology also dictates the suitability and volume of borrow sources for embankment and containment materials. The area geology affects whether mined materials can be used for construction, or if materials from other on-site borrow sources or off-site sources are necessary.

5.4 Seismicity

For areas of low seismicity, embankments raised by the upstream method and founded on drained tailings have been operated successfully. For areas of moderate to high seismicity, the potential for seismic liquefaction of saturated tailings requires containment by an embankment design that can withstand the loading of the tailings under seismic conditions with acceptable deformations. The other remedy for areas of moderate to high seismicity would be developing an impoundment with filtered, unsaturated tailings.

5.5 Production Rate

The mill production rate affects alternative selection. Current filtered tailings operations range from 1,000 to over 20,000 tonnes/day (Table 3). Current thickened operations have capacities of over 100,000 tonnes/day. For large mill production rates, conventional tailings disposal is typically used, but alternate methods are being considered with improvements in thickener and filter throughput capacity.

5.6 Closure

The closure costs of a tailings storage facility generally show that a conventional facility requires the highest cost due to (1) the period of time of monitoring and maintenance required for the tailings to reach an acceptable solids content, and (2) the requirement for treatment of excess process water.

5.7 Risk

The tailings disposal method affects the Hazard Classification Rating of the tailings storage facility, and subsequent seismic and meteoric design parameters. Dam break analyses and downstream inundation mapping show significantly larger impacts from a conventional slurried impoundment than facilities with unsaturated or denser tailings. A conventional slurried tailings impoundment also poses the longest duration risk, due to the time that the impoundment is susceptible to overtopping, instability, and erosion.

REFERENCES

- Boswell, J.E.S., I.D.C. Gidley, S. Jeeravipoolvarn, and K.D.O. Pellerin, 2014. “Thickened tailings deposition – operational challenges and remedies,” *Proceedings, Tailings and Mine Waste 2014*, Keystone, Colorado, October 5-8, pp 355-376.
- Brzezinski, L.S., 2001. “Surface Disposal of Thickened Tailings,” *Mining Environmental Management*, Volume 9, Number 5, September, pp 7-12.
- Fitton, T.G., and K.D. Seddon, 2013. “Paste and thickened tailings – myth busting and clarification,” *Paste 2013*, Belo Horizonte, Brazil, June.
- Kam, S, J. Girard, N. Hmidi, Y. Mao, and S. Longo, 2011. “Thickened tailings disposal at Musselwhite Mine,” *Paste 2011*, Australian Centre for Geomechanics, Perth, Australia, pp. 225-236.
- Kennecott Greens Creek Mining Company (KGC/MC), 2004. “General Plan of Operations, Appendix 3, Tailings Impoundment,” April 23.
- Klohn Krippen Berger (KCB), 2017. Study of Tailings Management Technologies, MEND Report 2.50.1, sponsored by the Mine Environmental Neutral Drainage (MEND) Program and the Mining Association of Canada, September.
- Lara, J.L., E. Pornillos, and C. Loayza, 2012. “The application of highly dewatered tailings in the design of tailings storage facilities – Experience in mining projects in Peru,” *Tailings and Mine Waste 2012*, pp 29-41.
- MWH Americas, Inc. (MWH), 2009a. “Report of Site Visit, Western Australia Alternative Tailings Disposal Initiative,” (November 2008 site visit), Draft for Internal Review, January.
- MWH Americas, Inc. (MWH), 2009b. “Report of Site Visit, Latin America Alternative Tailings Disposal Initiative,” (December 2008 site visit), Draft for Internal Review, January.
- Robinsky, E.I., 1975. “Thickened discharge – a new approach to tailings disposal,” *CIM Bulletin*, Vol. 68, No. 764, pp 47-53.
- Seddon, K.D., and M.P.A. Williams, 2010. “The development and design of thickened tailings discharge methods – a review,” *Mine Waste 2010*, Australian Centre for Geomechanics, Perth, pp 487-498.
- Vick, S. G., 1990. *Planning, Design, and Analysis of Tailings Dams*, BiTech Publishers.
- Williams, M.P.A., K.D. Seddon, and T.G. Fitton, 2008. “Surface Disposal of Paste and Thickened Tailings – A Brief History and Current Confronting Issues,” *Proceedings of the Eleventh International Seminar on Paste and Thickened Tailings*, Kasane, Botswana, May, pp. 143-164.

Scale-effect Considerations for Shear Strength Assessment of Coal Mine Spoil

L.R. Bradfield

Thiess Pty Ltd, Brisbane, Queensland, Australia

The University of Newcastle, Newcastle, New South Wales, Australia

S.G. Fityus

The University of Newcastle, Newcastle, New South Wales, Australia

J.V. Simmons

Sherwood Geotechnical and Research Services, Peregian Beach, Queensland, Australia

The University of Newcastle, Newcastle, New South Wales, Australia

ABSTRACT: One of the most debated subjects among mine geotechnical practitioners is the degree to which shear strength measurements obtained from conventional geotechnical laboratory equipment can be confidently relied upon to predict the shearing behaviour of actual spoil dumps. The reluctance of practicing engineers to apply shear strength parameters determined from standard laboratory testing equipment relates to uncertainty regarding the significance of scale-effects. This is particularly relevant in current times as spoil dumps approach uncharted heights, and load limitations of standard geotechnical testing equipment often results in the extrapolation of Mohr-failure envelopes well beyond their intended stress range. There are two scale-effects of note: The first relates to the degree to which the grading of a spoil sample must be down-scaled to comply with device capacity, such that the influence of prototype-sized particles on shear strength is not anomalous. The second relates to the normal stress limits of the test apparatus; and whether the failure envelope developed from measured strengths can be reliably extrapolated out to the “much higher” stress ranges to simulate field conditions. Scale effects on shear strength have been studied in the literature for soils and rockfills, however, the influence of scale on the shear strength of coal-measures spoil specifically has received little attention. This paper presents the results of an experimental study into the significance of scale effects by comparing shear strength data for a silica sand, considered to be immune to scale effects, with an Australian coal mine spoil tested in standard-sized direct shear machines (100mm, 300mm) and in a large direct shear machine (720mm) which was purpose-built to replicate a large-scale field condition for spoil dumps up to 400m in height. Spoil shear strength is shown to be strongly scale-dependent, both in terms of specimen size and magnitude of normal stress. Furthermore, it is demonstrated that adoption of shear strength measurements obtained from standard laboratory equipment will overestimate the available shear strength of coal mine spoil dumps with height-equivalent stresses ranging between 450kPa-4600kPa.

1 INTRODUCTION

Currently in Australia there are black coal open cut spoil dump heights of more than 350m, and plans for “very high” dumps in excess of 400m, which far exceeds the scale ($\leq 120\text{m}$) for which reliable design experience exists. For more than two decades, shear strength estimation for spoil dumps has been based either on infrequent, very small-scale tests, or on published guidelines such as the BMA Coal (BMAC) strength framework (Simmons and McManus, 2004). The BMAC framework strengths are expressed as linear Mohr-Coulomb envelopes, derived from small-scale test data and verified in practice by successful design and back analysis of instability for dumps with heights up to 120m.

The use of small-scale test data for reliable shear strength estimation of mine spoils has been the subject of debate among geotechnical practitioners for decades. The reluctance of practicing engineers to apply shear strength parameters determined from standard laboratory equipment ($\sim 100\text{mm}$ specimen size) relates to uncertainty regarding the significance of scale-effects. This is particularly relevant in current times, as spoil dumps approach unprecedented heights.

Standard 60 to 100 mm sized shear boxes are suitable for testing the majority of soils for civil engineering applications, and 300 mm shear boxes are routinely used for handling more gravelly granular materials such as reinforced earth wall backfill (QTMR Q181C-2002) and rockfill. For soils tested in boxes up to 300 mm in size, a maximum normal stress of around 1000kPa is the norm for ‘off-the-shelf’ equipment and scalping of oversize particles is usually not required. These standard laboratory equipment can provide reliable shear strength data for soils and stress ranges comparable to field conditions, in most civil engineering applications.

The reliability of the data is questionable when materials tested contain “oversize” particles, or particles deemed to be too big for the equipment being used. In such cases, samples require scalping to be performed to meet particle size restrictions of test standards. The reliability of data is also questionable when tests are performed under non-representative stress ranges. For coal mine spoils, to comply with equipment size limitations, a sample often needs to be scalped back to a fine fraction that is distinctly dissimilar to its original material. In addition to this, the effective vertical stress near the base of even a 200m-high dump (common in modern times) is likely to be far greater than the 1000kPa load capacity of standard test equipment.

There are two scale effects of note:

- A. The first relates to the degree to which the grading of a spoil sample must be down-scaled to comply with device size limitations, so that the influence of prototype-sized particles on shear strength is not anomalous.
- B. The second relates to the normal stress limits of the test apparatus; and whether or not the failure envelope developed from measured strengths can be reliably extrapolated out to the ‘much-higher’ stress ranges to simulate field-conditions for dumps of modern and future heights (>350m).

In the literature, the term ‘scale’ is traditionally associated only with physical size, rather than stress. This is possibly because standard direct shear testing apparatus can facilitate a range of different particle or specimen sizes but have a fixed load capacity which translates to a fixed upper stress limit for a specific specimen dimension. In this work, the term scale is extended to include stresses, as stresses in the context of mine waste are directly related to spoil pile heights.

2 BACKGROUND

The scale effects on shear strength suggests that there will be a minimum test specimen size, and a minimum test normal stress, that can be considered technically acceptable for simulating a shear surface within a high dump constructed of mine spoil.

Scale effects on shear strength have been studied in the literature for soils, rockfills, and some hard-rock spoils, however, the influence of scale on the shear strength of coal-measures spoil specifically has received little attention. This is possibly because of the significant costs and time associated with the design, construction and operation of equipment that is large enough and robust enough to test characteristic spoil samples at very high stresses, and the willingness to accept slightly higher risks for temporary slopes in the coal mining environment.

Most of the experimental studies in the literature concede that shear strength as defined by the friction angle, ϕ' , is a strongly scale-dependent variable; both in terms of physical size (particle size and specimen size) and magnitude of normal stress. These studies report a decrease in ϕ' with increasing particle or specimen size, and/or a reduction in ϕ' with increasing normal stress (Marachi et al., 1972; Marsal, 1967; Brown and Gonano, 1976; Barton and Kjaernsli, 1981; Hribar et al. 1986; Barton, 2008; Cerato and Lutenegeger, 2006; Wu et al., 2007; Frossard et al., 2012)

A review of the literature also revealed a significant deficiency in high-stress ($\sigma'_n > 1000\text{kPa}$) shear strength tests performed on characteristic samples of coal-mine spoil. However, studies relating to soils, rock joints, rockfills and hard-rock spoils, indicate that shear strength (as defined by the friction angle, ϕ') is scale-dependent, with non-linearity being most pronounced at very low and

very high stress ranges. (Marsal, 1967; Leps, 1970; Barton, 1976; Barton and Choubey, 1977; Hoek and Brown, 1980; Barton and Kjaernsli, 1981; Barton and Bandis, 1982; Charles and Soares, 1984; Linero et al., 2006; Bard et al., 2007; Valenzuela, et al.; 2008; Barton, 2008; Barton 2012). It follows that shear strength for coal mine spoils may also be stress-dependent, and failure envelopes may demonstrate a departure from linearity at very low and very high normal stresses.

Linear failure envelopes are embedded in the methods adopted by practicing mine-geotechnical engineers for characterizing coal mine spoils. One reason for this may be because the BMA Coal (BMAC) strength framework (Simmons and McManus, 2004), which provides linear Mohr-Coulomb shear strength parameters, has proven to be a convenient and reliable tool for shear strength estimation for several decades. However, because the BMAC framework is a linear fit to data which has long been believed to be non-linear, its appropriateness for shear strength estimation of very-high dumps needs to be validated.

3 EVALUATING THE SIGNIFICANCE OF SCALE EFFECTS ON SHEAR STRENGTH FOR MINE SPOIL

3.1 Large Direct Shear Machine (LDSM)

Recognition of the potential limitations of using test data obtained from standard-sized laboratory apparatus, has led researchers at the University of Newcastle to develop a large direct shear machine (LDSM), shown in Figure 1.

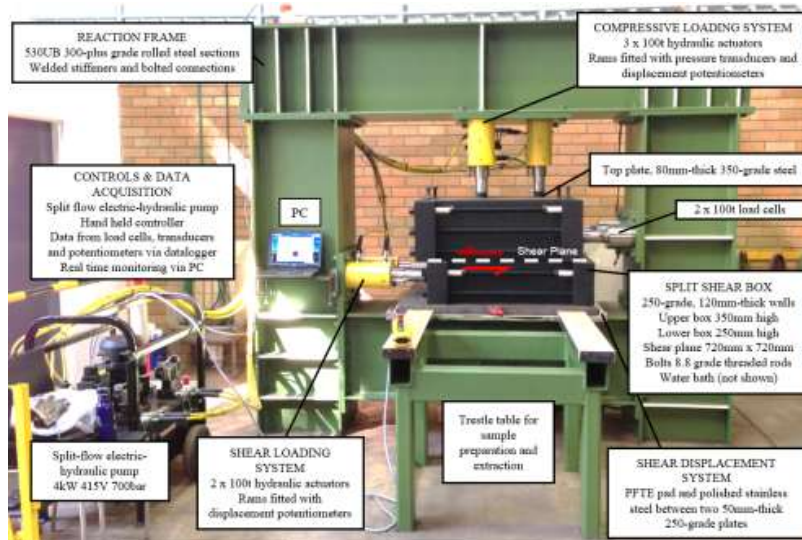


Figure 1. Photograph of the LDSM and main design components

The LDSM consists of a split-shear box with 120mm-thick solid steel walls, mounted to a large self-reacting steel frame. It can test saturated and unsaturated specimens with dimensions 720mm x 720mm x 600mm (L x W x H) over a wide normal stress range; up to 4600kPa. The large specimen volume allows typical mine spoil samples to be tested with minimal requirement for scalping, by accommodating a maximum particle size of ~100mm. This complies with the ASTM D 3080M-11 recommendation for a maximum particle diameter (D_{max}) to specimen thickness (T) ratio of 6:1. The 4600kPa normal stress capacity is sufficient to simulate field-stress conditions for spoil dumps

more than 400m in height (Bradfield *et al.*, 2013, 2014, 2015.a., 2015.b., 2018). Maximum horizontal shear displacements of 150mm (equivalent to 21% relative displacement) can be achieved using the LDSM.

3.2 Approach

The significance of the scale effects was evaluated by comparing shear strength data measured by small (60-100mm), medium (300mm), and large (720mm) direct shear machines (DSMs) for an inconsistently graded, Permian coal mine spoil containing fine and coarse-grained particles in a range of different proportions, and a consistently-graded, fine-grained, dry silica sand.

The tests performed on silica sand were used to confirm that the LDSM can give comparable results with smaller, standard-sized DSMs. These “calibration” tests were performed on sand rather than mine spoil for the following reasons:

1. The material had to be fine-grained enough to ensure that there were no particle size effects at any scale, and, satisfy the maximum particle size to specimen thickness ratio ($D_{max}:T$) of 1:6 for the smallest shear box of 60mm.
2. The material had to be consistently graded. Mine spoil is commonly highly variable, and therefore unsuitable.
3. A cohesionless material was required so that shear strength could be defined according to just one shear strength parameter, ϕ' . This made for relatively straightforward data interpretation and comparisons to be made between boxes.
4. The material had to be of mechanical strong grains so that grain crushing effects were not relevant.

The results of the direct shear tests performed on coarse mine spoil were then compared with the tests on sand, so that the significance of scale effects for direct shear testing of mine spoil could be evaluated.

Direct shear tests for this investigation generally followed the procedures outlined in ASTM D 3080M-11 and QTMR Q181C-2002. However, some aspects of sample preparation and testing were changed to reflect the conditions specific to the nature of coal-measures spoil piles. Table 1 summarizes the DSM specimen dimensions, stress capacity and material tested for each DSM size.

Table 1. Direct shear machine (DSM) specimen dimensions and stress capacity.

DSM size	Material Tested		Specimen dimension (mm)			Approximate Maximum Test Normal Stress (kPa)
	Silica sand	Coal mine spoil	Length	Width	Thickness	
Very small*	✓	×	60	60	45	500
Small	✓	✓	100	100	40	1000
Medium	✓	✓	300	300	190	1000
Large	✓	✓	720	720	600	4600

* Data obtained from previous study conducted by Ajalloeian *et al.* (1996)

4 DSM TESTS ON DRY SILICA SAND

Direct shear tests (DSTs) were performed on a locally well-known and consistently-graded, dry silica sand from the Stockton sand beds in small, medium and large DSMs (Table 1) and the results were compared (Table 2). For additional comparison, results from a 60mm-sized shear box were sourced from a detailed investigation at the University of Newcastle by Ajalloeian *et al.* (1996) who performed DSTs on the same silica sand prepared to loose (average $\rho_0=1.52t/m^3$), medium (average $\rho_0=1.61t/m^3$), and dense (average $\rho_0=1.72t/m^3$) states. The 100mm, 300mm and 720mm DSTs performed for the project used a target density of $1.5t/m^3$ to coincide with the loose sand tests in the Ajalloeian *et al.* (1996) study. Tests in the 300mm shear box could achieved a target density of $\rho_0=1.48t/m^3$.

Tests were conducted under constant normal effective stress (σ'_n) and constant rates of horizontal displacement (d). For all DSM sizes, stress vs. horizontal displacement data for initially loose specimens exhibited normally-consolidated behavior. Critical state strength (equivalent to peak strength loose specimens) was reached at relative horizontal displacements (δ_p) of between 8 and 9% for the 60mm DSM, between 9-10% for the 100mm DSM, 6.6-7.8% for the 300mm DSM, and between 8.4-9.9% for the 720mm LDSM.

Table 2. Comparison of test parameters and results for small, medium and large shear boxes.

DSM size	ρ_0 range {average} (t/m ³)	σ'_n range (kPa)	δ_p range (%)	ϕ'_s range (°)	ϕ' (°) ($c'=0kPa$)
60mm (very small)	1.52-1.54 {1.52}	38-379	8-9*	30.4-31.6	31.1
100mm (small)	1.50-1.52 {1.51}	249-998	9-10**	30.5-31.3	30.9
300mm (medium)	1.47-1.49 {1.48}	504-1108	6.6-7.8	28.6-30.0	29.5
720mm (large)	1.50-1.51 {1.50}	627-1247	8.4-9.9	31.0-31.8	31.4
	1.48-1.51 {1.50}	627-3379	8.4-9.9	30.5-31.8	31.1

*Interpreted by the writer from a chart published by Ajalloeian et al. (1996)

** Interpreted from a chart output because raw data not available

Critical state friction angles of 31.4° and 31.1° were measured by the 720mm LDSM for σ'_n ranges of 627 - 1247kPa, and 627 - 3379kPa respectively (Figures 2-3). Friction angles of 29.5°, 30.9° and 31.1° were similarly measured for the same loose sand using the 300mm, 100mm and 60mm DSMs respectively (Figures 2-3). Note that the slightly lower friction angle measured in the 300mm DSM is consistent with the slightly lower initial density of the specimens, or may be due to some configuration or operational feature of that particular device. The 300mm tests were performed for the project over the σ'_n range of 504 - 1108kPa; the 100mm tests were performed over the σ'_n range of 249- 998kPa, and separate 60mm tests by Ajalloeian et al. (1996) had previously been performed on similar sand for the σ'_n range of 38 - 379kPa. Plots of the secant friction angle (ϕ'_s) vs. test normal effective stress (ϕ'_n) for $\sigma'_n < 1400kPa$ (Figure 3) demonstrate that for each of the DSMs, there is no systematic increase or decrease in ϕ'_s with increasing σ'_n . Furthermore, when the 720mm LDSM data is considered over a much wider stress range (Figure 4), there is no relationship between ϕ'_s and σ'_n that would be revealing of a scale effect related to normal stress.

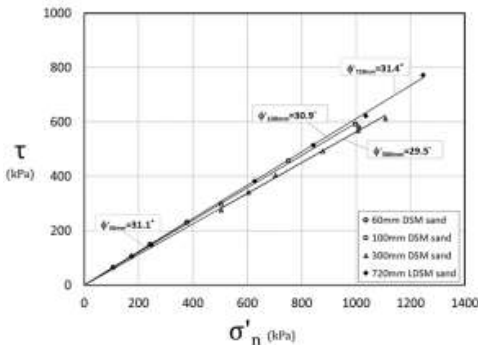


Figure 2. Plot of shear stress (τ) vs. test normal effective stress (σ'_n) for sand tests performed using 60mm, 100mm, 300mm, and 720mm DSMs for the σ'_n range of 0-1250kPa

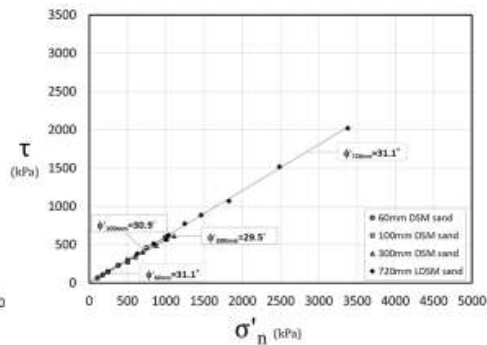


Figure 3. Plot of shear stress (τ) vs. test normal effective stress (σ'_n) for sand tests performed using 60mm, 100mm, 300mm, and 720mm DSMs for the σ'_n range of 0-3400kPa

The primary objective for the calibration testing on silica sand was to assess the reliability LDSM data prior to conducting tests on coal mine spoil. The calibration tests performed on the sand alone are not useful for evaluation of the scale effects described in Scale effect A and Scale effect B because particle size effects and shear box/specimen size effects at any scale are removed due to the fine-grained nature of the sand; and the sand grains are mechanically strong such that crushing effects on shear strength are not relevant for the range of stress offered by the DSMs and LDSM (i.e. scale effects related to normal stress will not occur because the shearing mechanism does not change within the LDSM stress range). The sand tests do, however, confirm that the LDSM is capable of giving comparable results with smaller scale, standard laboratory equipment, and so confirms that there are no significant performance anomalies in the LDSM.

The tests on sand are also useful for comparison with the tests on mine spoil, because although scale effects are irrelevant for sand, there is uncertainty regarding the significance of scale effects for mine spoil. The results of the DSM tests on coal mine spoil, and associated scale effects are discussed below.

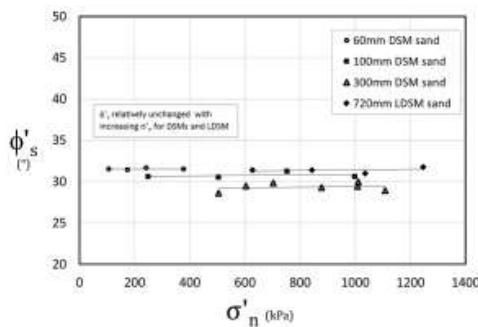


Figure 4. Plot of secant friction angle (ϕ'_s) vs. test normal effective stress (σ'_n) for sand tests performed using 60mm, 100mm, 300mm, and 720mm DSMs for the σ'_n range of 0-1250kPa

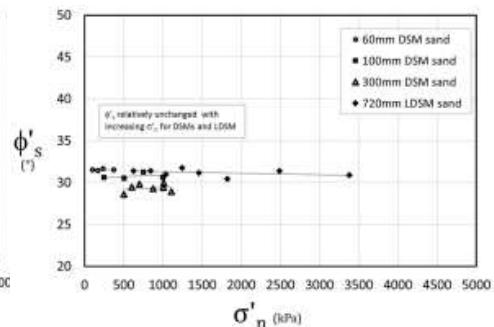


Figure 5. Plot of secant friction angle (ϕ'_s) vs. test normal effective stress (σ'_n) for sand tests performed using 60mm, 100mm, 300mm, and 720mm LDSMs for the σ'_n range of 0-3400kPa

5 DSM TESTS ON COAL MINE SPOIL

The spoil used for this study was sourced from a coal mine in the Hunter Coalfields, Australia. The sample was derived from Late Permian coal measures, and the lithology comprised predominantly siltstone and fine-to medium-grained sandstone with small amounts of claystone, shale, tuff, laminate and conglomerate (Figure 6). The particles are sub-angular to angular, and their strength (CoalLog – Larkin and Green, 2012) ranges from low-high. In the moist condition the fine fraction has low plasticity, feels gritty and is only slightly cohesive.

Direct shear tests were performed on air-dried spoil specimens in 100mm (small), 300mm (medium) and 720mm (large) DSMs, and the results were compared (Table 3). Testing generally followed the procedures outlined in ASTM D 3080M-11, and QTMR Q181C-2002, however, some aspects of sample preparation and testing were changed to reflect the conditions specific to the nature of coal-measures spoil piles.

Bulk samples were placed onto a tarpaulin on the floor, raked to a uniform thickness, and left to dry-back by evaporation for 12-24 hours prior to testing. A $D_{max}:T$ ratio of 6:1 allowed maximum particle sizes of 4.75mm, 26.5mm, and 85mm for the 100mm DSM, 300mm DSM and 720mm LDSM, respectively. Particles that exceeded these allowances were broken with a hand-held rock breaker to compliant-sized fragments and placed back into the specimen.



Figure 6. Photograph of spoil tested. Each colored bar on the ruler represents a 100mm interval.

ASTM D 3080M-11 provides instructions for preparing soil specimens to a nominal density or void ratio, compacted in layers of a specified thickness. This preparation method was not adopted as it does not effectively simulate the relatively looser condition of spoil emplaced by dragline or end-dumping by haul truck. For all DSMs, samples were instead raised above, and poured into the split boxes. This process was adopted to closely replicate the mechanisms of spoil emplacement in the field.

Tests were conducted under constant normal effective stress (σ'_n) and constant rate of horizontal displacement (d). Displacement rates to ensure drained conditions were 0.5mm/min. Peak shear stress was interpreted from plots of shear stress (τ) vs. relative horizontal displacements (δ_p) as the maximum recorded shear stress value. The 100mm and 300mm DSMs were load-limited to a maximum normal stress of approximately 1000kPa and 1100kPa respectively, whilst the LDSM could apply compressive loads of more than 4600kPa to the specimen.

Stress vs. relative horizontal displacements data for the 100mm, 300mm and 720mm specimens all exhibited behavior consistent with normally-consolidated materials. For a comparable σ'_n range of ~250kPa-1100kPa, peak shear strength was reached at relative horizontal displacements, δ_p , of between 11.2 and 14.5% for the 100mm DSM, between 10.3 and 16.0% for the 300mm DSM, and between 8.6 and 11.4% for the 720mm LDSM.

5.1 Comparison of secant friction angles

Secant friction angles (ϕ'_s) for all DSMs decreased systematically with increasing σ'_n for a comparable normal stress range of approximately 250kPa-1100kPa (Figure 7). This behavior is in general agreement with the soil mechanics literature that reports a decrease in ϕ'_s with increasing σ'_n as the shearing mechanism transitions from particle rearrangement, to particle sliding, and eventually to particle crushing at high stress.

Table 3. Comparison of test parameters and results for small, medium and large DSM tests on air-dried Permian spoil

DSM size	σ'_n range (kPa)	δ_p range (%)	ϕ'_s range (°)
100mm (small)	250-1000	11.0-14.0	36.1-40.1
300mm (medium)	250-1100	10.3-16.0	38.5-45.1*
720mm (large)	450-1050	9.7-11.2	30.0-33.1
	450-4600	8.6-11.4	27.8-35.0

*outlier: value likely to be closer to 43°: see Figure 7.

Consistent with the reviewed literature for soils and rockfills, it was anticipated that shear strength, defined by the friction angle, ϕ'_s , would decrease with increasing particle size and/or specimen size. It was therefore expected that the 100mm DSTs would generate higher values of ϕ'_s than the 300mm DSTs, followed then by the 720mm LDSTs. However, this was not the case for the small DSMs, with the 300mm DSM measuring higher secant friction angles (38.5–43°) than the 100mm DSM (36.1–40.1°). However, friction angles measured from the 720mm LDSM (30.0–33.1°) were lower than both the 100mm and 300mm DSMs, confirming the apparatus size scale effect reported in the literature.

When these test results for spoil (Figure 7) are compared with the test results for sand (Figure 5), it is evident that the ϕ'_s data for the 300mm DSM are also consistently lower than for the other two DSMs. This suggests there may exist some machine-intrinsic property that is unique to the 300mm DSM. However, in addition to this difference, the spoil ϕ'_s results exhibit a stress-dependence whereas the sand results do not. It is considered that there is a stress-related scale effect whereby measured friction angle decreases in spoil as the normal strength increases. It would seem that this stress-related scale effect is complex, potentially arising from the lower strength of the spoil particles, and their response to the applied normal stress.

Bradfield et al. (2015.b.) adopt a trilinear shear strength envelope to describe this stress-related scale effect for the same LDSM mine spoil test data presented and discussed here. Bradfield et al. (2015.b.) attribute the trilinear failure envelope for the stress range of ~450–4600kPa to differences in the shearing mechanisms that arise from the structure of the spoil specimen and its response to the level of compression applied. These three trilinear “zones” are summarized for ease of reference in Table 4.

Table 4. Trilinear shear strength zones and corresponding shearing mechanism for coal mine spoil; after Bradfield et al. (2015.b.)

Trilinear Zone	σ'_n range (kPa)	ϕ'_s trend	Spoil fabric appearance	Prevailing shearing mechanism
Zone 1	500-1600	Decrease	Rockfill	Particle rearrangement and interparticle contact sliding on a large scale
Zone 2	1600-3600	Increase	Shattered rock	Significant breakage of embedded clasts
Zone 3	3600-4600	Decrease	Compact, fine-grained mass	As per Zone 1, but on a much finer scale as a result of the extensive crushing and damage to large particles during the application of the very high compressive loads

Figure 8 shows secant friction angle (ϕ'_s) vs. test normal effective stress (σ'_n) for spoil tests performed using 100mm, 300mm, and 720mm DSMs, over the fully investigated range of ~250kPa–4600kPa, with the zones of the LDSM trilinear envelope displayed.

The systematic trend where ϕ'_s decreases with increasing normal stress, observed for all DSMs, corresponds only to Zone 1 of the trilinear envelope. There is no data within the “high” and “very-high” normal stress ranges that correspond to Zone 2 or 3 of the trilinear envelope for the 100mm DSM or the 300mm DSM, due to the normal stress-limits of those test apparatus. It is possible that the same ϕ'_s trends observed in the 720mm LDSM data could occur for 100mm and 300mm DSM tests if they had sufficient capacity to test up to the same “very high” stresses as the LDSM, however without data, this assertion cannot be tested.

When the data from Figure 8 for mine spoil is compared with the sand test data shown in Figure 5, it is evident that a scale effect related to the magnitude of normal stress (as per NOTE 2) is non-existent for the sand, because its grain strength is much higher than the stress-capacity of the LDSM: i.e. the shearing mechanism does not change within the stress range offered by the LDSM, and ϕ'_s remains relatively unchanged, even when the stress range is extended to ~500–3400kPa.

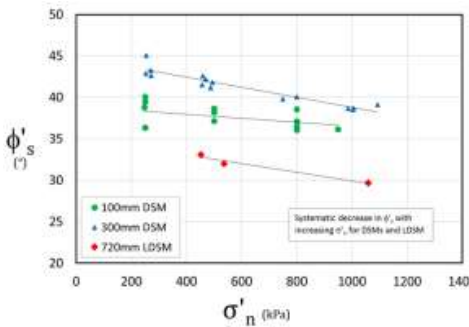


Figure 7. Plot of secant friction angle (ϕ'_s) vs. test normal effective stress (σ'_n) for spoil tests performed using 100mm, 300mm, and 720mm DSMs for the σ'_n range of ~250kPa-1100kPa.

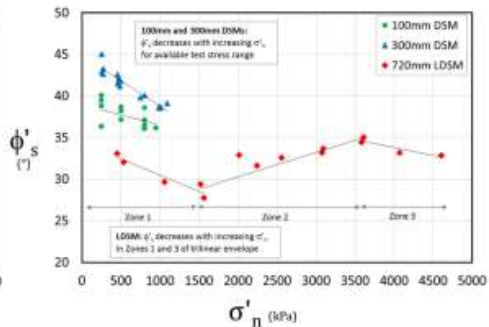


Figure 8. Plot of secant friction angle (ϕ'_s) vs. test normal effective stress (σ'_n) for spoil tests performed using 100mm, 300mm, and 720mm DSMs for the σ'_n range of ~250kPa-4600kPa.

However, the trilinear behavior interpreted from the LDSM tests on mine spoil is essentially a scale effect that is related to the magnitude of normal stress. What is different for the spoil, is that this scale effect occurs because the test material contains particles of sufficiently low strength to enable changes in the shearing mechanism to occur with increasing normal stress (e.g. from particle pushing and shoving at low stress, to particle sliding at medium stress, and particle crushing at high stress). Furthermore, the magnitude of this observed scale-effect will not only be a function of clast or particle strength, but also of the grading of the material.

6 SCALE EFFECTS ON SHEAR STRENGTH FOR COAL MINE SPOIL

6.1 Scale effects associated with scalping

In current practice, it is conventional for industry to adopt linear shear strength criteria for coal measures spoils. Spoil-specific shear strength testing is seldom performed, and published guidelines such as the BMA Coal (BMAC) strength framework (Simmons and McManus, 2004) are adopted in the absence of, or in preference to, obtaining laboratory data. The BMAC framework strengths are expressed as linear Mohr-Coulomb envelopes which were derived from small-medium-scale testing (up to 300mm DSM), and adjusted by back-analysis of failed dumps up to 120m in height.

Consistent with this practice, linear Mohr-failure envelopes have been developed from the test data measured in this study using the small, medium and large DSMs. These are displayed in Figure 9. Table 5 summarizes the corresponding linear effective stress parameters, cohesion (c') and friction angle (ϕ'_s) determined for these failure envelopes. Over a comparable range of normal stress (e.g. σ'_n range of ~250kPa-1100kPa) the failure envelopes are useful for understanding the extent to which scalping (selective removal of oversize, Figure 9) influences shear strength (as per scale effect A in section 1).

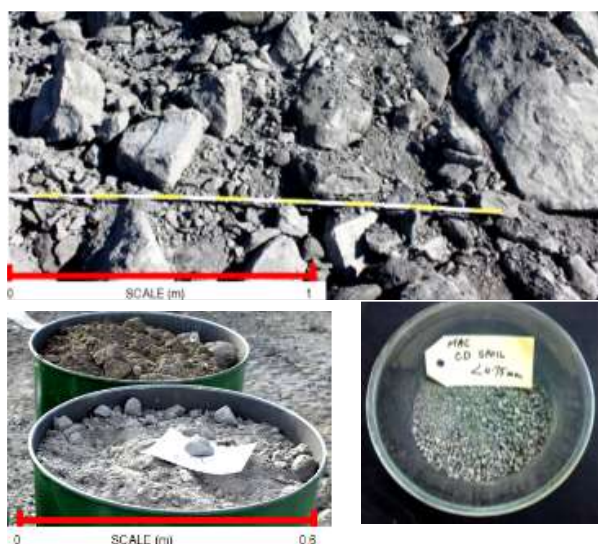


Figure 9. Photographs showing the extent that spoil samples are scalped to accommodate the conventional direct shear test equipment: (top) shows spoil prior to bulk sampling; (bottom left) shows spoil that has been scalped to remove large boulders at the time of sampling; and (bottom right) shows the sample is further scalped to sub-4.75mm to accommodate the 100mm shear box

It has been demonstrated (Bradfield et al., 2015.b.); Bradfield, 2018) that the 720mm LDSM data for the mine spoil tested in this study within the stress range of ~450kPa-1060kPa are comparable to the BMAC framework strengths for a type 2 Category spoil (Simmons and McManus, 2004), and on this basis, the LDSM data are considered likely to be reliable.

The data in Figure 10 shows that measured strengths are the highest for the 300mm DSM, followed by the 100mm DSM, and then the 720mm LDSM. Furthermore, the rate of increase in τ with increasing σ'_n for the 100mm and 300mm DSMs are similarly higher than for the 720mm LDSM. Noting that the 720mm LDSM data closely matches BMAC framework strengths, it is considered that the 100mm and 300mm DSMs overestimate shear strength for this type of spoil (BMAC: Category 2 spoil). Additionally, the 300mm DSM data plots slightly higher than the 100mm DSM data which is consistent with the test results for sand (Figure 4).

From the available data, it is concluded that scalping to match the constraints of standard-sized laboratory equipment for a typical coal-rock spoil, will result in an overestimation of shear strength. Figure 10 (for the normal stress range up to 1000kPa) shows the potential overestimation of shear strength for mine spoil associated with the 100mm and 300mm DSMs.

Table 5. Comparison of Mohr-Coulomb effective stress parameters developed from small, medium and large direct shear tests on mine spoil for the σ'_n range of ~250- 1100kPa.

DSM size	σ'_n range (kPa)	Mohr-Coulomb effective stress parameters	
		c' (kPa)	ϕ' (°)
100mm (small)	247-949	15.1	36.3
300mm (medium)	253-1092	60.4	36.9
720mm (large)	453-1059	62.6	27.0

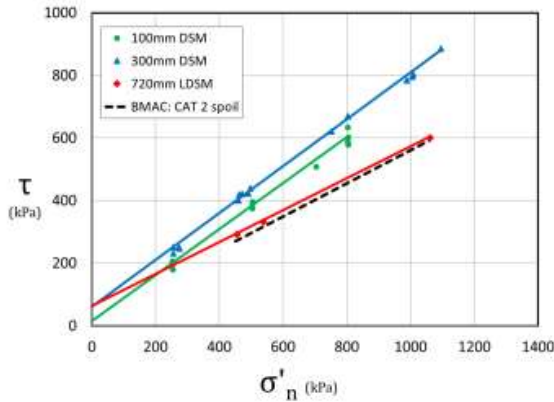


Figure 10. Plot of shear stress (τ) vs. test normal effective stress (σ'_n) for tests on mine spoil using 100mm, 300mm, and 720mm DSMs for the σ'_n range of ~250kPa-1100kPa. The BMA Coal shear strength envelope for Category 2 spoil is shown for the σ'_n range of ~450kPa-1060kPa.

6.2 Scale effects associated with normal stress

The reluctance of practicing engineers to apply shear strength parameters developed from small laboratory equipment, load-limited to around ~1000kPa, to full-scale spoil dump problems; or similarly, to apply the BMA Coal strength framework to spoil dumps that far exceed the stress limit for which the strength has been verified, is related to perceptions that the scale effect described in NOTE 2 could make such extrapolations unreliable.

The true significance of this scale effect is assessed by comparing extrapolated Mohr-failure envelopes for the 100mm and 300mm DSM tests with the 720mm LDSM data. Figure 11 shows the actual measured data, together with the corresponding failure envelopes, for the 100mm, 300mm, and 720mm DSMs. Figure 12 compares failure envelopes for the 100mm and 300mm DSMs that have been extrapolated out to the “very-high” stress capacity of the LDSM.

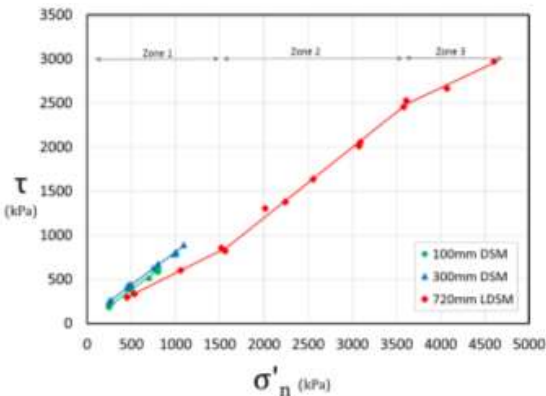


Figure 11. Plot of shear stress (τ) vs. test normal effective stress (σ'_n) for mine spoil tests using 100mm, 300mm, and 720mm DSMs for the σ'_n range of ~250kPa-4600kPa. Linear Mohr-Coulomb failure envelopes for the 100mm and 300mm data are shown. The trilinear failure envelope, together with corresponding “zones” of normal stress for the mine spoil are shown.

From Figure 12 it is evident that extrapolated failure envelopes will overestimate shear strength, assuming the trilinear failure envelope reflects the shear strength in spoil dumps under high stresses. Figure 13 shows the percentage by which the shear strength of the spoil (as measured by the LDSM) is overestimated when Mohr-failure envelopes developed from standard laboratory equipment (small and medium DSMs) is extrapolated out to “very-high” values of normal stress. The degree to which shear strength is overestimated is also stress-dependent, and it reflects the slope trends observed for the trilinear envelope. For example, shear strength overestimation increases with increasing normal stress in Zones 1 and 3, and decreases with increasing normal stress in Zone 2, for both the 100mm and 300mm DSMs.

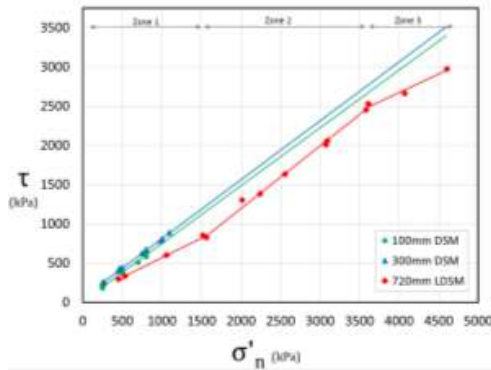


Figure 12. Trilinear failure envelope for mine spoil compared with extrapolated Mohr-failure envelopes developed from the 100mm and 300mm DSM data, for the σ'_n range of ~250kPa-4600kPa.

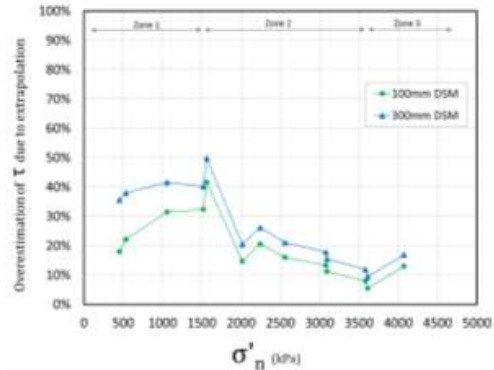


Figure 13. Percentage by which the shear strength of mine spoil (as measured by the LDSM) is overestimated when failure envelopes are developed from small (100mm) and medium (300mm) DSMs and extrapolated to the LDSM stress range.

7 CONCLUSIONS

The scale effect on shear strength implies that there will be a minimum DSM size, in terms of both specimen/shear box volume and load capacity, that can be considered technically acceptable for simulating a shear surface within a mine spoil dump.

For the mine spoil tests, shear strength as defined by the friction angle was found to be a strongly scale-dependent variable in terms of the physical size of the specimen tested. Secant friction angles were found to decrease with increasing box size for the 100mm and 720mm DSMs, consistent with reports in the literature. However, values of ϕ'_s for the 300mm DSM were higher than those for the 100mm DSM. A similar finding was noted for the 300mm DSTs on sand, in that higher friction angles were recorded for this device than the other devices. Hence, it is concluded that some machine-intrinsic characteristic, unique to the 300mm DSM, is responsible for the higher measured shearing resistance.

The secant friction angles (ϕ') measured by all DSTs on mine spoil were found to decrease systematically with increasing normal stress, for a σ'_n range of approximately 250kPa-1100kPa (which corresponds to Zone 1 of the trilinear failure envelope described by Bradfield et al. (2015.a)). This behavior is consistent with the literature, which reports a decrease in ϕ'_s with increasing σ'_n as the shearing mechanism transitions from particle rearrangement, to particle sliding, and eventually to particle crushing at high stress.

In this work, the term ‘scale’ has been extended to include stresses, rather than just physical size, because stresses in the context of mine spoil are directly related to spoil dump heights. Significant changes in the trend of the stress-strength relationship (σ'_n vs. ϕ'_s) observed for the mine spoil tested in the 720mm LDSM over a much wider stress range (~250kPa-4600kPa) are attributed to this stress-related scale effect. It is possible that the same three ϕ'_s trends observed in the 720mm LDSM data could exist in the smaller DSMs if they were able to test up to the same “very high” normal stresses as the LDSM, but limited small DSM machine capacity prevents acquisition of data to support this assertion.

For spoils like the one tested here, adoption of shear strength parameters measured from standard-sized DSMs (100mm and 300mm) will overestimate the available shear strength of dumps with height-equivalent stresses ranging between 450kPa-4600kPa. The degree to which shear strength is overestimated is stress-dependent and is consistent with the ϕ'_s trends observed for the trilinear envelope. The overestimation of shear strength when using the 100mm shear box is the largest at the transition point between Zone 1 and Zone 2 of the trilinear envelope (42%), and lowest at the transition point between Zone 2 and Zone 3 (6%).

Within the standard stress range of conventional DSM equipment (i.e. up to around 1000kPa), shear strength is overestimated by up to 30%.

From the available data, it is evident that scale effects are material-type dependent, and that adoption of a simple scaling factor based on specimen size alone (for $D_{max}:T$ compliant specimens) cannot be developed for predictions of spoil strength more generally. This is because (in this work) the most prominent indication of a scale-strength association occurs when the shearing mechanism changes (e.g. the trilinear envelope for mine spoil), and so any scaling factor must be considered in the broader context of other material-specific factors, such as particle strength and overall grading. Furthermore, the data also demonstrates that exceptions to the (shear box) size-strength relations described in the literature may be attributed to some unexplained operational or configurational feature for a given test device (as shown by the data measured in the 300mm box).

For coal mine spoils like the one in this study (i.e. coarse-sized material derived from fresh sandstone/siltstone, low-high clast strength) scale effects are significant in the context of spoil dumps of current and future heights. This is because DSTs performed on heavily-scalped specimens in 100mm or 300mm shear boxes that are load-limited to 1000kPa do not capture the influence of prototype-sized particles on shear strength, nor do they capture the changes in shearing mechanisms that occur under different stress conditions as a function of the original particle/clast strength and grading.

8 REFERENCES

- Ajalloeian, R., Yu, H. S., Allman, M. A. 1996. Physical and Mechanical Properties of Stockton Beach Sand. *Geomechanics in a Changing World: Proceedings, 7th Australia New Zealand Conference on Geomechanics*: 60-65.
- ASTM. 2011. D3080/3080M-11, Standard test method for direct shear testing of soils under consolidated drained conditions. *American Society for Testing and Materials*.
- Bard, E., Campana, J., Anabalón, M. E., Apablaza, R. 2007. Waste Rock Behaviour at high pressures, *Proceedings, XIII Pan-American Conference on Soil Mechanics and Geotechnical Engineering*: 348-353.
- Barton, N. 1976. The shear strength of rock and rock joints. *International Journal of Rock Mechanics and Mining Sciences and Geomechanics Abstracts Rock Mechanics Review*, 13: 255-79.
- Barton, N. 2008. Shear strength of rockfill, interfaces and rock joints, and their points of contact in rock dump design. *Keynote lecture, proceedings, Rock Dumps 2008, Perth*.
- Barton, N. 2012. Shear strength criteria for rock, rock joints, rock fill and rock masses: problems and some solutions. *Journal of Rock Mechanics and Geotechnical Engineering*, 5: 249-261.

- Barton, N., Bandis, S. 1982. Effect of block size on the shear behaviour of jointed rock. *Keynote lecture, proceedings, 23rd US symposium on rock mechanics*:739-760.
- Barton, N., Choubrey, V. 1977. The shear strength of rock joints in theory and practice. *Rock Mechanics*, 10:1-54.
- Barton, N., Kjaernli, B., 1981. Shear strength of rockfill. *Journal of the Geotechnical Engineering Division*, 107 :873-891.
- Bradfield, L.R., 2018. Reliable shear strength estimation for very-high spoil dumps. *Doctoral dissertation, University of Newcastle, Newcastle, Australia*, 463p.
- Bradfield, L., Simmons, J., Fityus, S., 2013. Issues related to stability design of very high spoil dumps, *Proceedings of the 13th Coal Operators' Conference*, Woollongong: 376-386.
- Bradfield, L.R, Fityus, S.G., Simmons, J.V., 2015. a. Large scale testing of mine spoil. *Proceedings of the 12th Australia New Zealand Conference on Geomechanics*, Wellington, New Zealand, 22-25 February 2015.
- Bradfield, L.R, Fityus, S.G., Simmons, J.V., 2015. b. A trilinear shear strength envelope for coal mine spoil. *Proceedings of the International Symposium on Slope Stability in Open Pit Mining and Civil Engineering, South African Institute of Mining and Metallurgy*, Cape Town, 12-14 October 2015.
- Bradfield, L., Koosmen, K., Fityus, S., Simmons, J., 2014. Practical considerations for direct shear testing of mine spoils. *Proceedings, 10YGPC: The 10th ANZ Young Geotechnical Professional's Conference. Queensland*: 123-130.
- Brown, E.T., Gonano, L.P. 1975. An analysis of size effect behaviour in brittle rock. *Proceedings, 2nd Australia-New Zealand Conference on Geomechanics, Brisbane*: 139-143.
- Cerato, A.B., Lutenegeger, A.J. 2006. Specimen size and scale effects of direct shear box tests of sands. *Geotechnical Testing Journal*, 29(6).
- Charles, J.A. and Soares, M.M. 1984. Stability of compacted rockfill slopes. *Géotechnique*, 34: 61-70.
- Hoek, E., Brown, E.T. 1980. Empirical strength criterion for rock masses. *Journal of Geotechnical Engineering*, 106:1013-1035.
- Hribar, J.H., Dougherty, M., Ventura, J., Yavorsky, P. 1986. Large scale direct shear tests on surface mine spoil. *Proceedings, International Symposium on Geotechnical Stability in Surface Mining, Calgary, USA*.
- Larkin, B.J., Green, D.R., 2012. Borehole Data Standard for the Australian Coal Industry: CoalLog Manual Version 1.1, ACARP Project C21003. Australian Coal Association Research Program (ACARP), 128p.
- Leps, T. M., 1970. Review of Shearing Strength of Rockfill. *Journal of the Soil Mechanics and Foundations Division*, 96:1159-1170.
- Linero, S., Palma, C. Apablaza, R. 2006. Geotechnical Characterisation of Waste Material in Very High Dumps with Large Scale Triaxial Testing. *Proceedings, International Symposium on Rock Slope Stability in Open Pit Mining and Civil Engineering 2007, Perth*: 59-75.
- Marachi, N.D., Chan, C.K., Seed, H.B. 1972. Evaluation of properties of rockfill materials. *Journal of the Soil Mechanics and Foundations Division*, 98: 95-114.
- Marsal, R.J. 1967. Large-scale testing of rockfills materials. *Journal of the Soil Mechanics and Foundations Division*, 93: 27-44.
- QTMR.2002. Q181C, Effective angle of internal friction at constant volume conditions for granular materials. Queensland Transport and Main Roads, Materials Testing Method.
- Simmons, J.V., McManus, D.A. 2004. Shear Strength Framework for Design of Dumped Spoil Slopes for Open Pit Coal Mines. *Proceedings, Advances in Geotechnical Engineering: The Skempton Conference*, 2: 981-991.
- Valenzuela, L., Bard, E., Campana, J., Anabalón, M.E. 2008. High Waste Rock Dumps - Challenges and Developments. *Proceedings, Rock Dumps 2008, Perth*: 65-78.
- Wu, P., Matsushima, K., Tatsuoka, F. 2007. Effects of specimen size and some other factors on the strength and deformation of granular soil in direct shear tests. *Geotechnical Testing Journal*, 31:1-20.

Static Liquefaction of Tailings: A South African Perspective on Rate of Rise

H.C. Ungerer and W. Kruger

SRK Consulting (Pty) Ltd, Johannesburg, Gauteng, South Africa

ABSTRACT: Soil liquefaction is a concern for tailings storage facilities as it can cause a flow slide failure that can travel for many kilometres and result in large scale environmental devastation, loss of life and destruction of property. This paper only considers static liquefaction potential of upstream constructed tailings embankments (in which subsequent wall raises are constructed from deposited tailings in an upstream direction). The main focus will be on the monotonic loading trigger, where the embankment is loaded relatively rapidly, so that excess pore water pressures are generated within the tailings deposit, and the loading condition can therefore be considered undrained. Specific field data is provided and discussed where excess pore water pressures have been, or may be generated due to a rapid rate of construction. Discussion also focusses on what South African engineers have adopted in their design approach to try and avoid the trigger ever occurring.

1 INTRODUCTION AND BACKGROUND

Soil liquefaction is a concern for tailings storage facilities (TSFs) as this can cause a flow slide failure that can travel for many kilometres and cause large scale environmental devastation, loss of life and destruction of property. Distinction is usually made between static and cyclic liquefaction (commonly caused by vibrations or seismic events). The recent Fundão TSF failure (5 November 2015) has generated renewed international interest in static liquefaction of TSFs. South Africa has had two well reported (static) liquefaction flow slides which occurred, after overtopping, that caused significant environmental and property damage and loss of human life – the Bafokeng failure (1974), a platinum TSF, and the Merriespruit failure (1994), a gold TSF. Both were upstream constructed tailings embankments.

1.1 Background to South African Practice

Contemporary tailings disposal in South Africa goes back to the start of diamond mining in the Kimberley diamond fields in the 1870s and has been developing ever since. Gold mining started on the Reef (Witwatersrand, Johannesburg area) in 1885. Originally mine tailings (slimes) were allowed to flow away across the open or uncultivated land (referred to as the veld in South Africa) or into streams. This practice would however not continue due to land constraints (Gowan 2012) and led to the practice of upstream construction of TSFs in South Africa.

Upstream constructed TSFs entail construction of subsequent wall raises in an upstream direction using previously deposited tailings as the foundation for each wall raise (the crest centre line

is moved progressively upstream as it is raised). The outer wall can be constructed using spigotting, cycloning or paddocking methods, although spigotting is the most common method of construction for platinum TSFs in South Africa. South Africa is uniquely suited for upstream construction due to the water deficit climate (evaporation greatly exceeds rainfall), the relatively flat ground (where sites for valley impoundments are also not always available), and the relatively low natural seismic risks (Gowan, 2012). It is therefore unsurprising that upstream construction is the most common construction method in South Africa.

Initially TSFs were raised at a high rate of construction (henceforth referred to as rate of rise) as the mines wanted to limit the amount of land space used. Rates of rise were about 0.6 m per month (7.2 m/year) and many TSFs failed before they reached a height of 10 m. The earliest significant failure occurred at the Simmer and Jack Mine in 1937, where a liquefaction flow slide killed people in nearby mine houses and took a steam engine off its rails (Gowan 2012). The realisation that occurred was that the rate of rise is important and “rule of thumb” criteria were developed for the sizing and operation of TSFs.

Along with technological advances in processing and TSF construction, progress was also made regarding the design of TSFs. George Donaldson investigated seepage problems at gold TSFs in South Africa’s East Rand in 1953 to 1959, where he considered seepage, underdrainage design and stability. Following this, a book was published by Donaldson on the geotechnical aspects of the design of TSFs. Main innovations were, inter alia, the introduction of planned underdrainage, flattening of the overall outer slope to 18 degrees (V:H = 1:3) in order to reduce the risk of foundation failure and aid in rehabilitation after the cessation of deposition, and limiting the rate of rise through thin lift deposition and allowance for drying (Gowan, 2012). Donaldson (1960) also commented on the importance of desiccation to maintain the stability of the dam and noted the importance of keeping the tailings as dry as possible by providing sufficient underdrainage, by decanting excess surface water as quickly as possible and by applying thin lift deposition to allow for drying. Further interesting comments by Donaldson (1960) considered liquefaction and resulting flow slides. It was commented that only the well dried-out tailings material provides sufficient strength to ensure stability and that this material is normally encountered in the outer wall zone. It was recommended that this zone be wide enough relative to the height of the TSF so that the critical failure surface does not pass through the looser inner material. Donaldson (1960) considered 250 ft (approximately 76 m) to be sufficient to this end. Although empirically developed and likely not fully understood at the time, these industry standards have been followed by South African engineers and have stood the test of time.

Design practice has also developed further with the foundations of South African good practice and guidelines summarized as follows (although not exhaustive):

1. In upstream constructed platinum TSFs where spigot deposition is employed the rate of rise is limited to 2.5 to 3.0 m/year (mostly limited to 2.5 m/year during the bulk of the TSFs life, with 3.0 m/year being reached just before closure). Where cyclone deposition is employed and sufficient quality underflow is present for wall building, the limit on rate of rise is kept to 4.0 to 5.0 m/year. For gold TSFs constructed via paddocking, the limit of the rate of rise is kept to 1.5 to 2.0 m/year. These limits apply where the tailings product is ground rock flour emanating from mining of hard rock, unweathered ore bodies (tailings material is finely ground rock and contains no clay minerals). Where deposits originate from weathered rock or weathered ore bodies, or where mining is opencast, where other materials can enter the tailings stream, these limits must be carefully considered and are often reduced, as the tailings stream may contain clay minerals which can impact on the hydraulic conductivity and consolidation characteristics of the tailings product.
2. Control the pool to have a centrally located and small pool (i.e. storage of supernatant water would generally be considered bad practice). Return water dams are provided adjacent to the TSFs in order to store decanted water to be returned to the process plant.
3. Strict control of the available freeboard to limit risk of overtopping.
4. Perform regular inspections by management teams and the involvement of a professional civil/geotechnical engineer.
5. Thin lift deposition and cycle time to allow for desiccation of tailings and assist in strength gain.

6. Monitoring and surveillance against design intent, and implement remedial measures if the intent is not met. This generally includes the regular use cone penetration testing with pore pressure measurement (CPTu) to reconcile piezometric level with phreatic surface and determine pore water pressure profiles, as well as to determine the strength of the tailings material.
7. Ensuring a minimum factor of safety (FoS) of more than 1.5 using effective stress strength parameters, where a lower FoS indicates an upset condition that has to be remedied to maintain a minimum FoS of 1.5.

1.2 Liquefaction Triggers

Before liquefaction triggers can be discussed, some of the concepts and definitions discussed herein should be clarified first.

Total stress is used to define the applied stress on a soil, due to self-weight and external applied loads, and is supported by the soil through a combination of inter-particle forces and pore water pressure in the voids (Knappett & Craig 2012). Should the pore water pressure increase to be equal to, or close to the total stress i.e. the overburden pressure, inter-particle forces reduce (effective stress reduces) and the soil acts like a liquid. This condition is known as liquefaction (Knappett & Craig 2012). Increases in the pore water pressure can be due excess pore pressures developing through contraction of the soil or tailings under loading, or high pore pressures can result from seepage (such as was the case with the Aberfan failure that occurred on 21 October 1966). Liquefaction can therefore be, generally, defined as a phenomenon in which a loose, saturated soil or tailings loses much of its shear strength and stiffness due to a significant reduction in the effective stress to close to zero, and behaves as a liquid. Liquefaction is therefore largely associated with excess pore water pressure development. Triggers for liquefaction can be cyclic, static or hydraulic (Jefferies & Been, 2016).

Density affects the behaviour of soils. Because a soil can exist over a wide range of densities, it is unreasonable to treat a certain density as having its own properties (Jefferies and Been, 2016). Therefore, a framework (Critical State Soil Mechanics (CSSM)) that explains why a soil at a particular density behaves in a particular way is essential (i.e. a function of the soils true properties and state). The critical state locus is the relationship between the critical void ratio, e_c , and the mean effective stress (p') (therefore the density at a specific state) and is an intrinsic soil property. The state parameter (ψ) is provided by Equation 1 and gives the relationship between the current void ratio (e) and e_c at a specific stress state, p' . Generally, a ψ limit of smaller or equal to -0.05 is defined to ensure that shear dilation dominates volumetric compression (Jefferies and Been, 2016). This deals with the definition of “loose enough”.

$$\psi = e_c - e \quad (1)$$

where e is the current void ratio of the soil and e_c is the void ratio of the critical state at the current mean stress state.

For liquefaction to be triggered, the saturated material must be loose enough, and the stress ratio (η) provided in Equation 2, must increase towards the critical friction ratio (M).

$$\eta = \frac{q}{p'} \quad (2)$$

where q is the deviatoric stress and p' is the mean effective stress.

Having discussed the concepts and definitions above, a list of the most probable and most often recorded ways in which static liquefaction is actually triggered can be developed; these are:

1. High pore water pressures developing from seepage (reduction in mean effective stress).
2. Rapid static (monotonic) unloading of the slope of the embankment or other parts of the embankment. This can be caused by erosion of the toe, overtopping events, seepage erosion, piping, unchecked erosion, sloughing etc.
3. Straining and deformation of the embankment and slope failure.
4. Failure of the foundation.
5. Deformation of the foundation.
6. Undermining collapse.

7. Failure of softer layers within embankment and/or deformation extrusion of softer layers (basal extrusion).
8. Rapid, monotonic loading through loading the top of the slope i.e. through embankment construction (rate of rise-related trigger).

It should be noted that these triggers listed are direct triggers and static liquefaction is not necessarily, and is often not, the cause of a failure but rather induced as a result of a failure, or large strain, event (direct trigger) occurring. Oftentimes mismanagement, negligence, diverging from the design intent and inadequate surveillance and monitoring can lead to these triggers developing. The Bafokeng failure (1974) of an upstream constructed platinum TSF and the Merriespruit failure (1994) of an upstream constructed gold TSF case histories can be considered. In both cases the overtopping erosion (loss of confinement) led to fatal liquefaction flow slides. In both instances pool control was inadequate, with the pool being large and non-centrally located close to the outer wall crest with the available freeboard also being inadequate. The active tailings deposition management was not focussed on addressing the freeboard and pool control problems. A large portion of what was supposed to be the relatively densely packed outer “wall” region, would have been in a looser state, though consolidated, with some of the impounded fines probably not being completely consolidated.

Blight (2010) discussed the Saaiplaats TSF failures of a gold TSF that occurred, where liquefaction was predominately triggered by the safe rate of rise being exceeded. This consisted of two failures between 18 and 19 March 1993 and a third failure on 22 March 1993. Originally the Mine was considered on the brink of closure and an old TSF, that was being re-mined, was recommissioned during 1981, with the idea to accommodate tailings for the few remaining months prior to closure. No effective underdrainage had been installed. The dam height was limited to 20 m and the rate of rise to 1.5 m/year. The mine however, did not close and the TSF reached a height of 28 m by late 1992, with the average rate of rise reaching 2.57 m/year in the previous year and 2.83 m/year in February 1993. Blight (2010) mentioned that the tailings had been remined and remilled, and an appropriate coefficient of consolidation, c_v , of 50 m²/year was proposed. In the absence of pore pressure readings, Blight (2010) estimated the degree of consolidation to be at about 65 percent, using Gibson’s (1958) extension to Terzaghi’s theory that takes account of the effects of continual deposition. The estimated resulting shear strength was then 32 kPa, which was inadequate for the TSF’s stability. The high rate of rise and lack of effective underdrainage had resulted in an insufficiently consolidated outer wall, with insufficient strength. These failures were primarily rotational slope failures, although flow slides followed as result. As very little water was contained on the dam (the pool was small), the flow slide didn’t travel very far and was ultimately contained by adjacent structures. No fatalities or injuries occurred and damage was only limited to mine property. The failure therefore did not garner any public and media attention at the time.

2 CASE STUDIES

The authors are primarily experienced in the design and management of platinum TSFs, to which they have the greatest access to readily available and relatively high-quality data and therefore, three, case studies on actual operational platinum TSFs are presented.

2.1 Piezocone tests and interpretation

Most of the data is presented in the form of piezocone probing results. Relevant laboratory results are also provided, if available, to provide further context. All the piezocone probing, unless otherwise noted, was carried out by pushing a 10 cm , 60 degree cone into the tailings at a constant rate of advancement.

Additionally, dissipation tests were also carried out in conjunction with piezocone probing to establish the ambient/initial pore water pressure. The correlations used to obtain soil parameters discussed herein are briefly declared below.

2.1.1 Coefficient of consolidation and Hydraulic Conductivity Permeability

The coefficient of consolidation presented in this paper was derived from CPTu dissipation test data that were based on the correlation in Equation 3 suggested by Jones & Rust (1995):

$$c_v = \frac{150}{t_{50}} \quad (3)$$

where t_{50} is the time required to dissipate 50 percent of an excess pore pressure induced by probing in minutes.

2.1.2 Hydraulic conductivity (Permeability)

The hydraulic conductivity (or permeability) of a soil mass is a function of the soil's modulus of volume compressibility (m_v). The m_v values of the soil are inferred from the shear phase of the piezocone probing and the c_v values are determined from the dissipation phase of the testing and is given by:

$$k = c_v \cdot m_v \cdot \gamma_w \quad (4)$$

where c_v is the coefficient of consolidation, m_v is the modulus of volume compressibility ($m_v = 1/(q_c \cdot \alpha_m)$, where α_m is predominantly taken to be 2.55) and γ_w the unit weight of water.

2.1.3 Undrained shear strength and undrained shear strength ratio

At this point the authors would like to note that the undrained shear strength of a soil is not a unique parameter and depends significantly on the mode of shearing, the rate of strain and the orientation of failure planes. Estimates of the undrained shear strength (c_u) can however be made from the cone resistance using the following empirical equation from Lunne et. al. (1997).

$$c_u = \frac{q_t - \sigma_{vo}}{N_{kt}} \quad (5)$$

where σ_{vo} is the total vertical stress at that point, N_{kt} is the cone factor (15 was used) and q_t is the cone tip resistance.

The undrained shear strength ratio can be obtained by dividing Equation 5 by the initial vertical effective stress (σ_{v0}'). Empirical correlations for estimating the peak undrained yield strength are also available and are based on back analysis of past field liquefaction flow failures and are based on work done by Olson & Stark (2002) and Sadrekarimi (2014).

2.1.4 State parameter

Where adequate laboratory tests (triaxial tests) were available and Norsand material parameters could be obtained, a Norsand model (a generalised constitutive critical state model, based on the state parameter, ψ , that captures the salient aspects of liquefaction, see Jefferies & Been (2016)) was calibrated and general trend lines were plotted for k and m (interpretation parameters that are a function of soil rigidity). This was done using the procedure as detailed also by Jefferies & Been (2016). Where insufficient or no laboratory results were available then ψ values were directly calculated using the Soil Behaviour Type Index, I_c , which is also detailed in Jefferies & Been (2016).

2.2 Case No.1: Good Practice

The first case study represents an upstream TSF, which is, in the opinion of the authors, a well operated and designed facility where good practice is applied. The TSF in this case was constructed in 2003 and operation commenced in February 2004. The TSF was designed for a maximum rate of rise of 2.5 m/year. Due to the limited initial deposition area, as influenced by the topography, the deposited tailings are contained behind a starter embankment until such a time that the available deposition area became large enough and rate of rise stabilized to below 2.5 m/year, where after upstream construction continued. The TSF is currently being operated at a rate of rise approaching 2.5 m/year. The TSF is located in a semi-arid climatic zone.

A geotechnical investigation was performed during the latter part of 2017 and the start of 2018 comprising of 37 CPTu probes and complementary laboratory testing. The resulting information provides some useful insight and shows how thick enough wall wedges constructed slowly enough can be used to safely construct upstream TSFs.

Figure 1 shows selected measurements and correlations of a CPTu probe that was done near the crest of the TSF's embankment and Figure 2 shows the selected measurements and correlations of another CPTu probe that was done approximately 100 m from the crest into the basin. The TSF is approximately 30 m high at this point on the crest and the overall downstream slope of the wall is 1:3 (V: H).

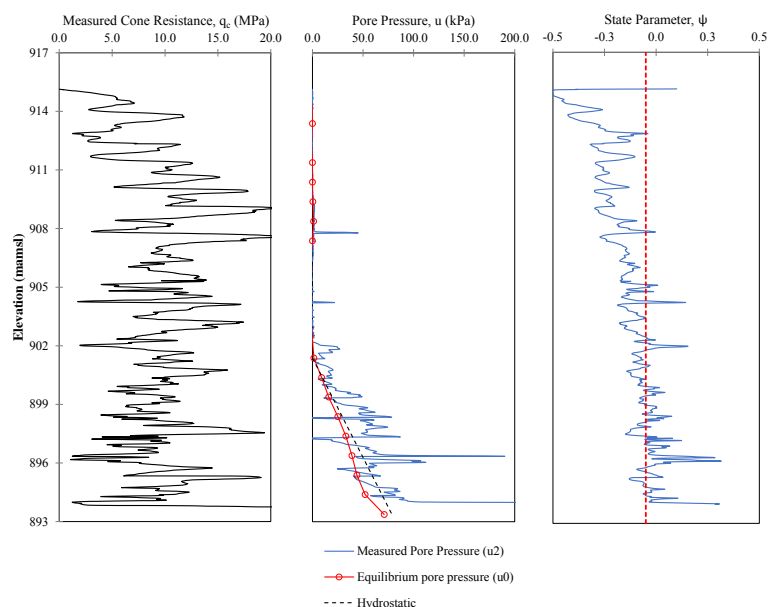


Figure 1. CPTu probe results for Case No.1 - Crest

The following points are noted:

1. Penetration was drained in the outer wall zone below the water table (the excess pore pressure ratio, B_q , was predominantly close to 0).
2. For some of the outer wall positions on the higher downstream side of the TSF and this section, it appears the material that was initially deposited behind the starter wall (crest elevation 902 mamsl) consists of thicker layers of slightly finer and looser tailings than the overlying material. This was most likely due to the initial deposition behind the starter wall, where the rate of rise was much higher due to the smaller deposition area, thus inhibiting desiccation and segregation.
3. There is a decrease in the measured cone resistance (q_c) with an increase of distance from the point of deposition. Measured cone resistances are typically in the order of 5 to 15 MPa and even as high as 20 MPa nearer to the outer wall. Typical q_c values from a distance of approximately 100 m from the outer crest was 2.5 to 5 MPa. The state parameter also tends more towards the $\psi = -0.05$ limit for dilative behaviour, although the material is generally still dilative. This indicates slightly looser, siltier material, as would be expected.
4. The outer wall material is medium dense to dense and dilatant, and although there is not enough data to define the exact extent of the outer wall zone, it can be deduced that the thickness of the outer wall was at least 50 m (taking into consideration other CPTu probes not reported here the outer wall thickness was on average 80 m thick).

- In this case effective stress parameters can be used with confidence in limit equilibrium stability analysis as excess (or unpredictably high) pore pressures have not been observed and are also unlikely to occur as the outer wall is dilatant and the rate of rise is limited.

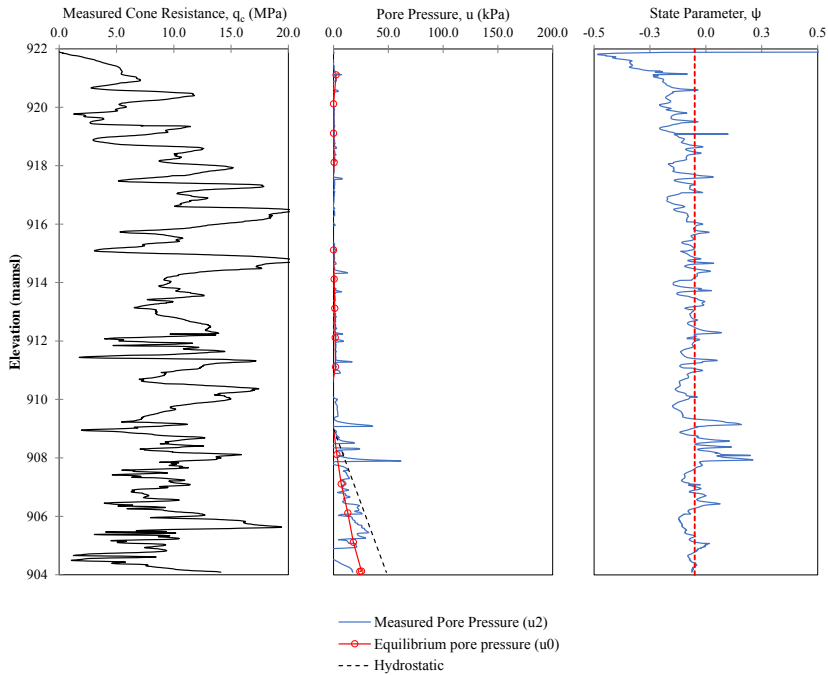


Figure 2. CPTu probe results for Case No.1 – Basin

2.3 Case No.2: Low Strength Soft/Loose material in outer wall

This case study presents a TSF where soft/loose material is present in the lower regions of the outer wall, where during the early phases of deposition the material exhibited “toothpaste” behaviour and the strength gain was poor (such as in the case of Saaiplaats TSF) and upstream construction above the starter wall elevation proved problematic.

The TSF was designed on the basis that the tailings material will be from processing of underground hard rock (unweathered ore). However, initial mining was opencast and the resulting tailings was found to be finer than conventional platinum tailings and it contained clay minerals. The Unified Soil Classification System (USCS) classification of the material was found to be of a silt to clayey silt with low plasticity (CL-ML) with a plasticity index (PI) of between 8 and 10. The specific gravity (G_s) of the solids was 3.47. The initial rate of rise was in excess of 4 m/year, reducing down to 2.5 m/year at the starter wall crest elevation. After a period, the amount of opencast tailings material deposited decreased. The TSF was also placed on “care and maintenance” from the period between June 2012 and November 2015, whereby no further deposition took place. During the initial period, circa 2004, when problems were occurring a round of CPTu probes were completed. Figure 3 shows CPTu probe results a typical soil profile then. During 2017 another round of CPTu probes were undertaken, by this time the TSF had raised by approximately 10 m and the typical results are presented in Figure 4. Figure 3 and Figure 4 present the measured tip resistance, the measured pore pressure, the equilibrium pore pressure from dissipation and the hydrostatic pore pressure gradient for reference.

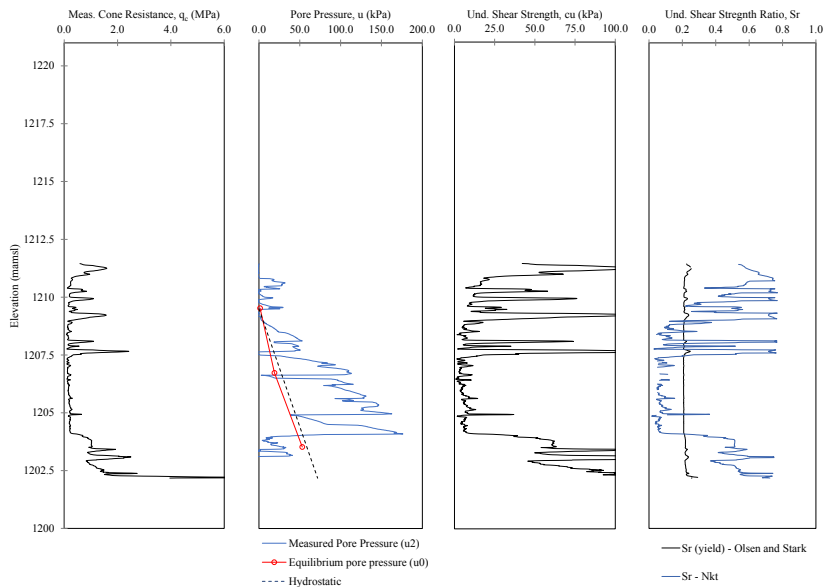


Figure 3. CPTu probe results for Case No.2 - 2004

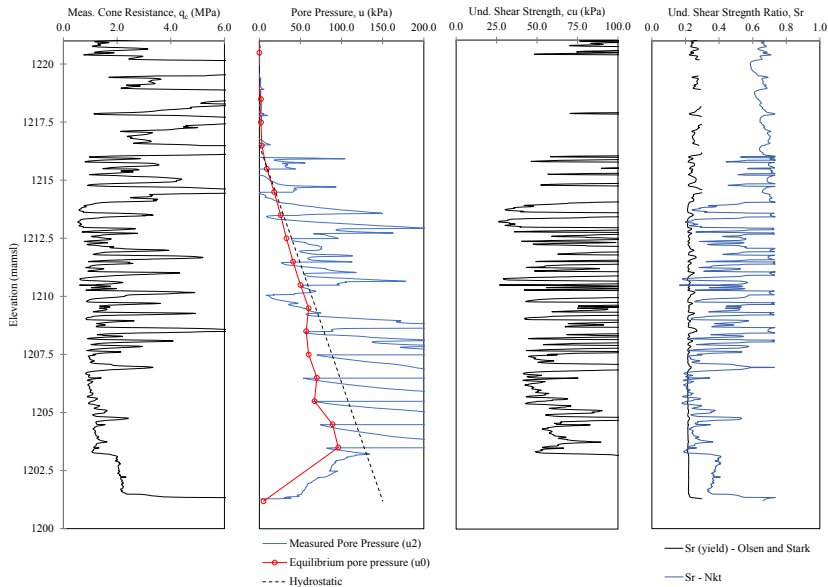


Figure 4. CPTu probe results for Case No.2 – 2017

The following points are noted:

1. Figure 3: The piezocone cone pressure shows that the material to be very soft or loose with average q_c values of 0.2 MPa. This would normally be considered being very low for platinum tailings forming part of the outer wall. The corresponding undrained shear strength is approximately 10 kPa.
2. Figure 4: The piezocone cone pressure shows the material, measured between 1208 mamsl and 1204 mamsl to be very soft or loose with average q_c values of 0.8 to 1.3 MPa. Although a higher cone resistance was measured than in 2004 these results would, again, normally be considered being very low for platinum tailings forming part of the outer wall. The corresponding undrained shear strengths are between 50 and 100 kPa.
3. Whilst it seems some strength gain had occurred in the soft material (apparently due to consolidation) it is unfortunately not clear exactly how much consolidation actually took place.
4. Evaluation of the coefficient of consolidation of the lower soft material yielded values as low as 12 to 40 $m^2/year$. Values like this are typically associated with clayey material. The corresponding, hydraulic conductivity values are $2.75 \times 10^{-9} m/s$ to $5.0 \times 10^{-9} m/s$. These values are about two orders of magnitude lower than typical hydraulic conductivity values of platinum tailings specifically in the outer wall. Generally, as a rule of thumb, when the hydraulic conductivity value, when converted to $m/year$, is lower than the rate of rise in $m/year$, more careful evaluation is required as problem this type of material could behave in an undrained manner during loading.
5. At the time of the 2004 investigations, it was judged that that the rate of strength gain was unlikely to occur under the present conditions at the then current deposition rate. As a result of this and the subsequent stability analyses using total stress strength parameters, a recommendation was put forward (and subsequently followed) in which a buttress was constructed for the TSF.
6. Figure 4: No excess pore pressures were observed in the lower soft materials. The rate of rise of the TSF at the time was approximately 1.1 $m/year$. An increase in the rate of rise may still however result in excess pore pressures.

7. It can be seen from Figure 3 and Figure 4 that the undrained shear strength ratio from the N_{kt} derivation are lower or coincide with those derived from Olsen & Stark (2002) in the loose/soft zone.
8. This case bears resemblance to that of the Fundão TSF failure and development of a constitutive model may be warranted as a limit equilibrium does not deal with the strain incompatibility.

2.4 Case No.3: Excess pore pressures measured in typical platinum tailings

This case study demonstrates a case in which actual excess pore pressures were measured due to relatively rapid construction and in which case the loading condition could therefore be considered truly undrained (potential monotonic loading trigger).

This project considers a platinum TSF where the tailings can be considered as rock flour emanating from the grinding and milling of unweathered hard rock.

In this project, a causeway was constructed to provide working foundation upon which a penstock decant pipeline would be constructed. The causeway was constructed using cyclone underflow material. The causeway was advanced at a rate of 3 m per day and the height of 2-3 m above the existing tailings level, although a significant amount of material settled into the existing tailings material. Time for construction was limited and the causeway was constructed as fast as reasonably possible, under the supervision of a geotechnical engineer. The cyclone vortex-finder was set so that the outer slopes were between 12 and 14 degrees (a slope of 1:4.7 – 1:4) to avoid failure.

The TSF was, and still is, constructed upstream and tailings are sub-aerially deposited through spigotting. The basin material is therefore finer than the wall quality material, but is however still classified as a silt (ML) according to the USCS, with non-plastic fines, indicating that the material is essentially a rock flour.

It is important to note that the piezocone testing could only be undertaken 20 days after the section of the causeway under consideration was fully constructed and no specific detailed knowledge of the development of excess pore pressures were recorded as the load was applied. Figure 5 illustrates the CPTu measures tip resistance (q_c), the measured pore pressure (u_2), the equilibrium pore pressure from dissipations (u_0), the hydrostatic pore pressure gradient for reference, the derived coefficient of consolidation (c_v) and hydraulic conductivity (k) for the wall quality material (underflow) and the basin material. The in-situ state parameter (ψ), derived using the screening procedure detailed by Jefferies & Been (2016) is also plotted in Figure 5.

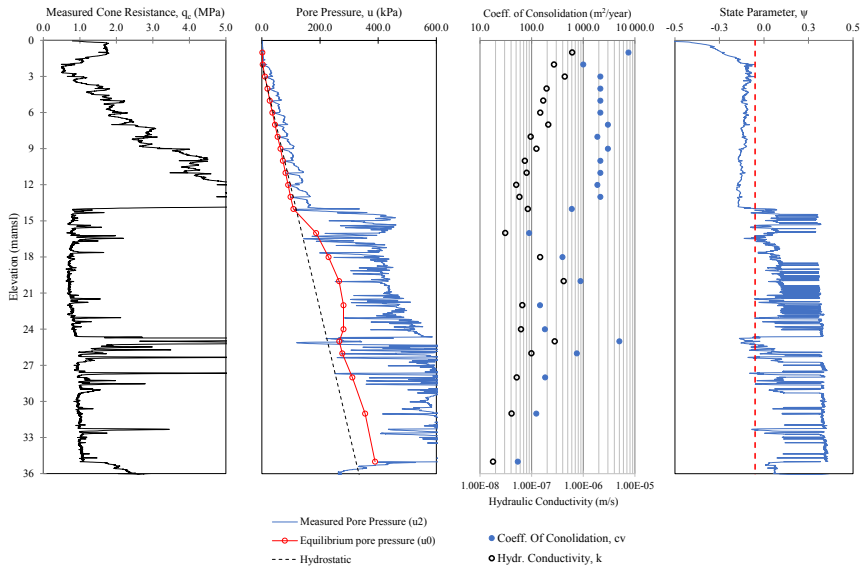


Figure 5. CPTu probe results for Case No.3

The average hydraulic conductivity of the basin material is 7.8×10^{-8} m/s (2.46 m/year). Considering Figure 5, it can be seen that the cyclone underflow penetrated about 11 m into the slimes (basin tailings). Excess pore pressures are present with the maximum excess pore pressure, of 88.67 kPa, occurring at a depth of 20 m. It seems that the sandier layer located at 25 m provides a more permeable drainage layer, with the excess pore pressure reducing to 40.68 kPa. The dimensionless time factor (T_v) for Terzaghi's theory of one-dimensional consolidation is represented by Equation 6:

$$T_v = \frac{c_v t}{d^2} \tag{6}$$

where t is the time in years and d is the length of the longest drainage path.

From T_v the degree of consolidation (U_z) can then be determined from isochrones showing the variation of U_z with depth for various T_v values, the form of which depends on the initial excess pore pressure distribution and drainage boundary conditions. The initial excess pore pressure (u_i) can be calculated using the following equation:

$$U_z = 1 - \frac{u_e}{u_i} \tag{7}$$

where u_e is the current excess pore pressure.

Using Equation 6 with $d = 5.5$ m and $t = 0.0548$ years (20 days), and a CPTu derived c_v of $89 \text{ m}^2/\text{year}$ for the centre of the layer, T_v is calculated to be 0.16.

To calculate u_i , two types of excess pore pressure diagrams have to be considered, and combined, in the calculation of U_z , a linear distribution with $u_e = 0$ at a depth of 14 m below the surface, or $z = 0$ m in terms of the excess pore pressure zone, and $u_e = 40.68$ kPa at a depth of 25 m, or $z = 2d$ in terms of the excess pore pressure zone, and a sinusoidal distribution with a maximum u_e of 68.33 kPa at a depth of 20 m. Using published isochrones from Das, (2008), the degree of consolidation is then calculated as 52 percent for the linear portion and 25 percent for the sinusoidal portion (average degree of consolidation of 34 percent) and the associated u_i , calculated using Equation 6, at a depth of 20 m below the surface is 133.45 kPa. Assigning a unit weight of 20 kN/m^3 to the underflow (γ_{UF}) and 14 kN/m to the slimes (γ_{SL}), the vertical loading

that caused the excess pore pressure is calculated to be 138 kPa. This provides a reasonable correspondence to u_i , which indicates that the consolidation calculation is acceptable.

From this the following points can be made:

1. If this causeway was in the outer wall, limit equilibrium analysis will have to be undertaken using either effective stress parameters with excess pore pressures calculated using the B-bar method. Alternatively, total stress strength parameters (undrained parameters) can be used.
2. The rate of loading far exceeded the hydraulic conductivity of the material of 2.46 m/year. Should the rate of construction have been limited to 2.5 m/year, excess pore pressures would likely not have been generated.
3. In this case, flattening the causeway outer slopes to 12 to 14 degrees ensured stability.

3 CONCLUSIONS

It is important to recognise that it is possible to generate excess pore pressures during static monotonic loading for specific site conditions and loading rates. This is illustrated via Case No.3, where excess pore pressures were generated in rock flour platinum tailings. This can trigger liquefaction (rapid monotonic loading trigger). It is however possible to design and operate the TSF in such a way to mitigate the risk.

From Case No. 1 it can be seen that for upstream construction under suitable climatic conditions, where evaporation largely exceeds rainfall (semi-arid climate), and where the tailings product is rock flour, that limiting the rate of rise to 2.5 m/year and applying thin lift deposition is beneficial in terms of the desiccation of the tailings material, thus ensuring an adequately thick outer wall consisting of dilative tailings. This mitigates against the risk of (large) excess pore pressures ever developing and liquefaction trigger through monotonic loading occurring. Ensuring adequate underdrainage and decanting excess surface water also improves the stability and strength gain.

Caution must however still be applied, as was witnessed considering Case No. 2, where a tailings product emanating from opencast mining (which typically yields high amounts of clay minerals in the tails) was deposited. It is therefore equally important to have an adequate knowledge of the mining processes involved and to understand the geotechnical behaviour of the tailings product reporting to the TSF. For this case study the initial rate of rise was too high to allow desiccation and strength gain, and should the rate of rise increase in the future, liquefaction may become a concern as excess pore pressures may be generated. Straining and deformation of this material may also trigger liquefaction via lateral extrusion, as was the case with the Fundão TSF failure. Rate of rise considerations should therefore be site-specific.

It is therefore quite possible to engineer against static liquefaction via rapid monotonic loading for upstream constructed TSFs, if the climatic conditions are suitable, enough land is available to allow for sufficient depositional space to limit the rate of rise.

Considering the two major TSF flow failures of Merriespruit and Bafokeng in South Africa, lack of proper water management is a common denominator and poses the greatest risk for liquefaction. It is therefore of utmost importance to maintain adequate freeboard, to keep the pool as small as possible and centrally located at the penstock, decant excess surface water as soon as possible and not store supernatant water on the TSF. The amount of water present on the TSF also dominates the consequence of failure, as can be seen considering the Saaiplaats failure, where very little water was contained on the dam (pool was small) and the liquefaction flow didn't travel very far and was ultimately contained by nearby structures.

The case studies discussed herein do not claim to solve all or even most of the problems related to liquefaction but have hopefully provided some insight into some of the techniques that South African engineers have learnt to employ with upstream constructed tailings dams and have served relatively well in helping avoid at least one of the (what used to be frequent) triggers of liquefaction of TSFs in South Africa even though the method of construction used has been shunned by others.

4 REFERENCES

- Blight, G.E 2009. *Geotechnical Engineering for Mine Waste Storage*. United Kingdom: CRC Press.
- Das, B. M. 2008. *Advanced Soil Mechanics, 3rd ed.* New York: Taylor and Francis
- Donaldson, G. W. 1960. The stability of slimes dams in the gold mining industry. *Journal of the South African Institute of Mining and Metallurgy*. 183-199
- Gibson R.E., 1958. The progress of consolidation in a clay layer increasing in thickness with time. *Géotechnique* Vol. 8: 171-182.
- Gowen, M. 2012. The Future of Tailings Disposal in South Africa [Presentation]. *Mine Tailings Africa Conference*.
- Jefferies, M. & Been, K. 2016. *Soil liquefaction A Critical State Approach, 2nd ed.* Boca Raton: CRC Press/Taylor & Francis Group.
- Jones, G. A., and E. Rust. Piezocone Settlement Prediction Parameters for Embankments on Alluvium, *Proc. International Symposium on Penetration Testing, CPT 95, Linköping, Sweden, Vol. 2, Swedish Geotechnical Society, Linköping*: 501–508.
- Knappett, J.A. & Craig R.F. 2012. *Craig's Soil Mechanics, 8th ed.* Spon Press. Abingdon.
- Lunne, T., Robertson & P.K., & Powell, J.J.M. 1997. *Cone Penetration Testing in Geotechnical Practice*. New York: Routledge & London: Blackie Academic
- Olsen, S.M. & Stark, T.D. 2002. Liquefied strength ratio from liquefaction flow failure case histories. *Canadian Geotechnical Journal* Vol. 39 : 629-647.
- Sadrekarami A, 2014. Effect of the Mode of Shear on Static Liquefaction Analysis. *Journal of Geotechnical and Geoenvironmental Engineering* Vol. 140 Issue 12 : 04014069.

The Shear Strength of Filtered Tailings and Waste Rock Blends

R. Burden, and G.W. Wilson

University of Alberta, Edmonton, Alberta, Canada

D.J. Williams

University of Queensland, Brisbane, Queensland, Australia

M. Jacobs

Goldcorp, Vancouver, British Columbia, Canada

ABSTRACT: Filtered tailings stacking is becoming an increasingly common practice in the mining industry. Co-mingling of waste rock and filtered tailings is an emerging technology that has the potential to offer several advantages over stacking tailings alone, namely increased density and improved stability. This paper investigates the relationship between mix ratio and shear strength for filtered tailings – waste rock blends. Blends of waste rock and filtered tailings were prepared at a range of mix ratios. Large scale direct shear tests were carried out using a 300 x 300 mm shear box. The results show that shear strength increases with increased rock content, and that even a small amount of rock in a tailings dominated matrix significantly increases the shear strength. At high stresses, shear strength of co-mingled blends was found to be higher than waste rock alone.

1 INTRODUCTION

Almost all mines produce fluid tailings as a by-product from the mineral extraction process. Conventionally these are stored behind dams, which in many cases are constructed from the tailings themselves (Vick 1990). These structures can present a challenge for reclamation and closure, and are a long-term risk and liability. As large, high-profile failures continue to happen (Morgenstern, Vick et al. 2015, Morgenstern, Vick et al. 2016), tailings dams are increasingly being seen as unacceptable by many stakeholders. To address this problem, an increasing trend in the industry is depositing tailings in self-supporting “dry stacks”, typically using pressure or vacuum filtration to rapidly de-water the tailings before stacking. Another technology that is gaining traction in dry-stacking is waste rock and tailings co-disposal; both approaches have now seen practical application (Habte and Bocking 2017, Wickland and Longo 2017). Combining these techniques offers an attractive solution to mine waste management. Adding co-mingled waste rock to a filtered tailings stack may improve stability, as well as reduce overall waste volumes. Since the stacks are self-supporting and not impounded by dams, the shear strength of the blend is an important design parameter. Whilst several researchers have investigated the geotechnical properties of waste rock and fine tailings blends, there is no published work in this field relating to filtered tailings. The objective of the study presented herein was to investigate the

shear strength of waste rock and filtered tailings blends, specifically the relationship between strength and mix ratio.

2 BACKGROUND

Co-disposal is certainly not a new idea and has been applied in many forms over the years, including underground backfills (Brawner and Argall 1978), the Canadian oil sands (Lord and Isaac 1989) and pumped co-disposal of coal wastes (Williams 1997). Wickland (2006) introduced the concept of blending waste rock and tailings to create a new, engineered material with favorable properties, termed “Paste Rock”. At an optimum mix ratio, the void spaces in the waste rock skeleton are “just filled” with fine tailings, giving a blend that combines the high strength and low compressibility of the rock with the low permeability and water retention properties of the tailings. Subsequently, several researchers have investigated the shear strength of “Paste Rock”-style blends. Khalili, Wijewickreme et al. (2010) carried out tri-axial testing on a blend of CIP (Carbon In Pulp) gold tailings and waste rock, prepared at the optimum mix ratio. It was found that shear strength of the blend was almost as high as with rock alone. Jehring and Bareither (2016) performed tri-axial tests on blends of crushed gravel and 4 different tailings types. The project was focused on cover design; consequently, the maximum confining stress used was 40 kPa. Blends were prepared at mix ratios close to the optimum. Similarly to the previous study, it was found that that friction angles measured for the blends were almost as high as those measured for rock alone. Neither of the previous studies comprehensively investigated the shear strength of blends with mix ratios significantly below optimum, i.e. blends in the “floating” condition. It was generally supposed that these blends would have a strength similar to the tailings themselves. With the emergence of filtered tailing - waste rock blends, where a waste rock “skeleton” is no longer a necessity for a stable stack, there is a clear need to revisit this question. In the mainstream geotechnical literature, “floating” rock particles have been generally shown to improve the stability of slopes (Iannacchione and Vallejo 2000).

Direct shear testing is widely used in geotechnical practice for determination of shear strength parameters in granular materials (ASTM D3080). An advantage of this test is that the shear box can readily be scaled up to permit testing on large grained materials. Selecting a test method that allows the largest possible particle size is critical; it has been shown that removing large particles can significantly affect the shear strength parameters measured in the direct shear test (Xu, Williams et al. 2017). Large scale shear boxes up to 300 x 300 mm are widely available, and have been used for measuring the shear strength of rockfills, coarse aggregates and geomembranes (Bauer and Zhao 1993, Alfaro, Miura et al. 1995, Yu, Ji et al. 2006).

3 BLEND CHARACTERISATION AND INDEX PROPERTIES

3.1 Material tested

The materials used in this study are filtered gold tailings and waste rock provided by Goldcorp Inc. The tailings were filtered using a pilot-scale filter plant. Prior to filtering, tailings are thickened to approximately 50 % solids. The thickened tailings are then de-watered using pressure filtration, with the pressure provided by the feed pump. Waste rock was screened by hand on site and particles larger than 100 mm were removed. Particle size distribution curves are shown below in Figure 1. Average moisture content and specific gravity of solids are given in Table 1.

Table 1: Moisture content and specific gravity

	w (%)	Gs
Filtered tailings	19.3	2.76
Waste rock	2.1	2.73

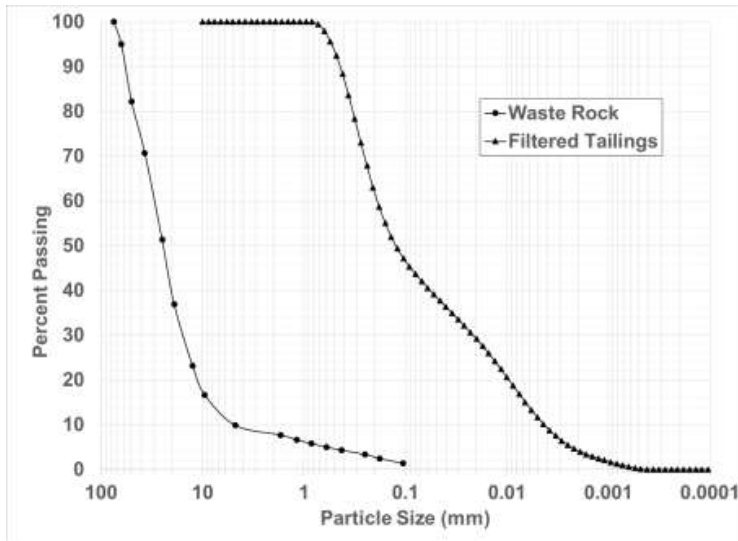


Figure 1: Particle size distributions

3.2 Mixture ratio

All mix ratios are given by dry mass, defined, after Wickland, Wilson et al. (2006):

$$R = \frac{\text{Mass of rock solids}}{\text{Mass of tailings solids}} \quad (1)$$

Co-mingled moisture content can be predicted using the following equation, where w_r and w_t are geotechnical moisture contents (mass of water / mass of solids) of the rock and tailings respectively:

$$w = \frac{w_r + R w_t}{1 + R} \quad (2)$$

Tests were carried out on tailings only, waste rock only and 3 different mix ratios: 0.4, 1 and 1.8. For the materials tested, 1.8 is approximately the “just filled” point.

3.3 Particle scalping

Waste rock particles larger than 37 mm were removed prior to blending. Removing large rock particles alters the mix ratio. Effective (after scalping) mix ratios, and measured and predicted moisture contents for the blends, are given below in Table 2.

Table 2: Effective dry mix ratios

Dry mix ratio (R) Before scalping	Effective dry mix ratio After scalping	Moisture content Predicted %	Moisture content Measured %
0.4	0.28	15.54	15.93
1	0.71	12.16	13.83
1.8	1.27	9.68	12.33

It should be noted that the scalped blends are consistently wetter than predicted, and this effect increases with increasing rock content since the majority of the water in the waste rock is contained in the finer (<37 mm) fraction.

3.4 *Blending procedure*

To account for material drying in transit, water was added to the materials to bring them up to their field moisture contents (given in section 2.1). The material was blended using a cement mixer. For laboratory-scale trials, as close as possible to perfect blending is preferable, to produce repeatable results. Photos below show an R=1.8 blend.





Figure 2: Blending Procedure

4 TEST METHOD

Large-scale direct shear tests were carried out at the University of Queensland using a shear box manufactured by Wille Geotechnik. The box dimensions were 300 x 300 x 205mm. Each mix ratio was tested at confining stresses of 250, 500 and 1000 kPa, consolidated in one load step at a rate of 100 kPa/minute. Materials were tested at the blended water contents. The tests were carried out at a slow shear strain rate of 0.1 mm/min to ensure fully drained conditions. To assess particle breakage effects, particle size distributions were taken after shearing the waste rock samples. Figure 3 shows the shear box containing a sample with a mix ratio (R) of 0.4.



Figure 3: Large-scale direct shear box containing R=0.4 sample

5 RESULTS AND DISCUSSION

5.1 *Shear Strength*

Peak shear stresses measured for each mix ratio are summarized below in Table 3 and plotted in Figure 4.

Table 3: Peak shear stress

Vertical stress (kPa)	Peak shear stress (kPa)					
	Filtered Tailings	R=0.4	R=1	R=1.8	Rock	
250	171.20	212.19	230.87	223.60	292.64	
500	351.68	393.18	439.05	442.68	554.34	
1000	712.09	805.48	851.32	850.49	797.43	

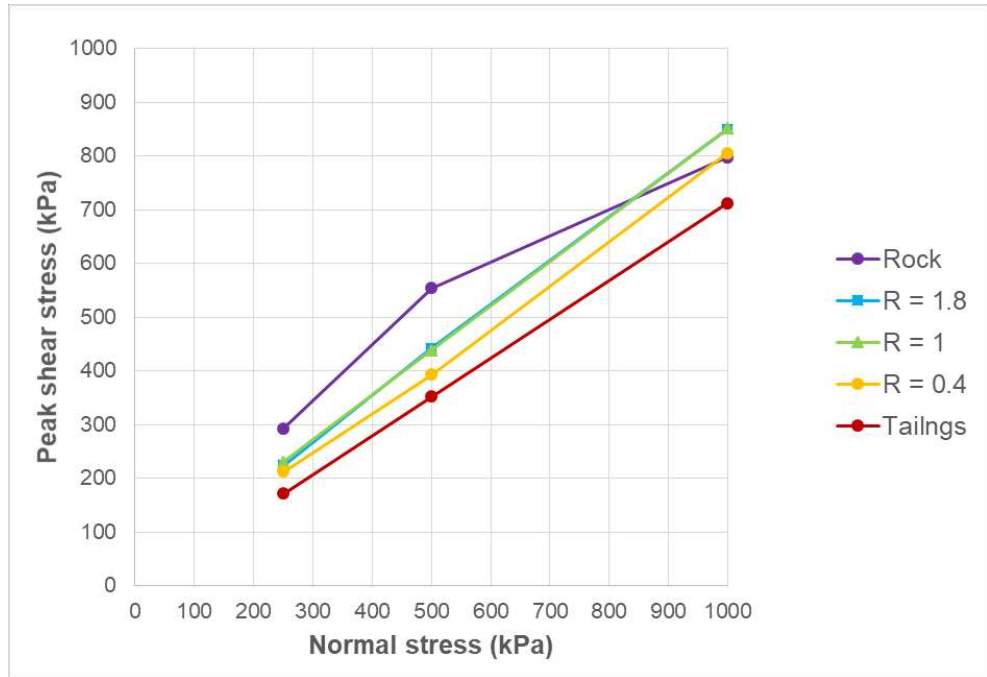


Figure 4: Peak shear stress against normal stress for blended filtered tailings and waste rock at a range of mix ratios

In general terms, the results show that the adding rock to filtered tailings results in increased shear strength; co-mingled waste rock and filtered tailings are always stronger than tailings alone. The shear strength appears to increase with higher rock content up to a limiting value of around 1:1 rock:tailings by dry mass.

Waste rock porosities measured at confining stresses at 250, 500 and 1000 kPa were 40, 43 and 48 % respectively. Using the approach given by Wickland, Wilson et al. (2006), this gives optimum mix ratios of approximately 1.8 – 2.5. This suggests that the blends tested consist of floating waste rock particles in a tailings dominated matrix. At lower stresses, the shear band is forced to go around the rocks, or occurs on the interface between the rock and the tailings. At higher stresses, some rock breakage was observed. One drawback of the direct shear test is that the sample is forced to shear on the interface between the two halves of the box. In materials that have considerable structure, such as blends containing large rock particles, this may not represent the path of least resistance. This could result in higher shear strength being measured in the lab than that would occur in the field. The problem can be mitigated by scaling up the box or removing larger particles. However, scalping large particles may result in measurements that are over conservative (Xu, Williams et al. 2017). Scalping to 37mm was considered to be a reasonable compromise. Other shear tests, such as tri-axial or simple shear, do not have this drawback.

However, most widely available equipment is limited to small sample sizes, so even more scalping would be required.

The results suggest that at higher stresses, above 1 MPa or approximately 50 m of fill, the blended materials have higher strength than waste rock alone. Rock strength reduction at higher stresses is most likely due to particle breakage at clast to clast contacts. When tailings occupy the void spaces between rock particles, this results in more contact points between particles, and consequently lower stress at each contact, resulting in less particle breakage. To test this hypothesis, grain size distributions were taken of the sheared waste rock samples, shown in Figure 5.

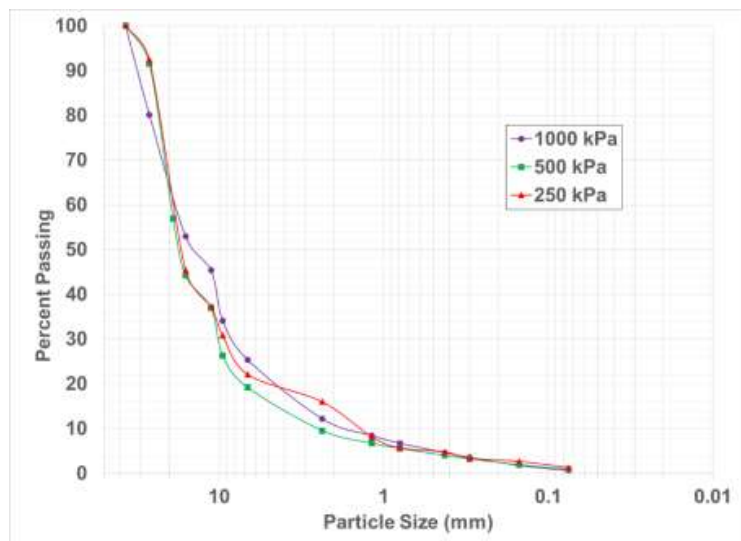


Figure 5: Particle size distributions of sheared waste rock samples

Figure 5 shows a significant amount of particle breakage at 1000 kPa. It should be noted that the particle size distributions were taken for the entire sample. Particle breakage along the shear band is likely to be much more extensive than implied by the results presented.

6 CONCLUSIONS

The results show that addition of even a relatively small amount of rock to a filtered tailings dry stack can significantly increase the shear strength. Shear strength increases with increasing mix ratio up to a limiting value of around 1:1 by dry mass. At higher stresses, comingled rock and filtered tailings have higher shear strength than rock alone, because the tailings prevent breakage of rock particles. The stress above which this occurs will depend upon the strength of the rock, and but can easily be determined by testing on the rock alone.

REFERENCES

- Alfaro, M., N. Miura and D. Bergado (1995). "Soil-Geogrid Reinforcement Interaction by Pullout and Direct Shear Tests."
- Bauer, G. and Y. Zhao (1993). "Shear Strength Tests for Coarse Granular Backfill and Reinforced Soils."
- Brawner, C. and J. Argall, GA (1978). Concepts and experience for subsurface storage of tailings. Proceedings of the 2nd International Tailings Symposium, Tailings Disposal Today, Denver, Colo.
- Habte, K. and K. Bocking (2017). Co-disposal practice in mine waste management. Tailings and Mine Waste '17. Banff, Alberta, Canada.

- Iannacchione, A. T. and L. E. Vallejo (2000). Shear Strength Evaluation of Clay-Rock Mixtures. Slope Stability 2000.
- Jehring, M. M. and C. A. Bareither (2016). "Tailings composition effects on shear strength behavior of co-mixed mine waste rock and tailings." Acta Geotechnica **11**(5): 1147-1166.
- Khalili, A., D. Wijewickreme and G. W. Wilson (2010). "Mechanical response of highly gap-graded mixtures of waste rock and tailings. Part I: Monotonic shear response." Canadian Geotechnical Journal **47**(5): 552-565.
- Lord, E. R. F. and B. A. A. Isaac (1989). "Geotechnical investigations of dredged overburden at the Syncrude oil sand mine in northern Alberta, Canada." Canadian Geotechnical Journal **26**(1): 132-153.
- Morgenstern, N., S. Vick and D. Van Zyl (2015). "Report on Mount Polley tailings storage facility breach." Report of independent expert engineering investigation and review panel. Prepared on behalf of the Government of British Columbia and the Williams Lake and Soda Creek Indian Bands.
- Morgenstern, N., S. Vick and B. Watts (2016). Fundão Tailings Dam Review Panel Report on the Immediate Causes of the Failure of the Fundão Dam.
- Vick, S. G. (1990). Planning, design, and analysis of tailings dams, BiTech.
- Wickland, B. and S. Longo (2017). Mine waste case examples of stacked tailings and co-disposal. Tailings and Mine Waste '17. Banff, Alberta, Canada.
- Wickland, B. E. (2006). Volume change and permeability of mixtures of waste rock and fine tailings, PhD Thesis, University of British Columbia.
- Wickland, B. E., G. W. Wilson, D. Wijewickreme and B. Klein (2006). "Design and evaluation of mixtures of mine waste rock and tailings." Canadian Geotechnical Journal **43**(9): 928-945.
- Williams, D. (1997). Effectiveness of co-disposing coal washery wastes. Proceedings of the 4th International Conference on Tailings and Mine Waste.
- Wilson, G., B. Wickland and J. Miskolczi (2008). Design and performance of paste rock systems for improved mine waste management. Proceedings of the 1st International Seminar on Management of Rock Dumps, Stockpiles and Heap Leach Pads, Perth, Australia.
- Xu, Y., D. J. Williams and M. Serati (2017). Effect of Scalping on Shear Strength of Aggregate. 51st U.S. Rock Mechanics/Geomechanics Symposium. San Francisco, California, USA, American Rock Mechanics Association.
- Yu, X., S. Ji and K. D. Janoyan (2006). "Direct Shear Testing of Rockfill Material." Soil and Rock Behavior and Modeling.

Toward the Sensible Use of Tailings Filtering Technology

B. Ulrich

Stantec Consulting Services, Inc., Denver, Colorado, USA

J. Rogers

Stantec Consulting Services, Ltd., Burnaby, BC, Canada

ABSTRACT: To date, filtered tailings technology has only been successfully implemented at a limited number of relatively low production-rate mining operations. However, the technology may be poised to make a dramatic leap forward as it is proposed for use at a number of high production-rate mines. Pressures ranging from increasing regulatory scrutiny to decreasing water availability are likely to drive further adoption of the technology. Considering the current state of the industry, how should tailings professionals view filtered tailings and the selection of a disposal technology? This paper presents a recommended approach to select a tailings disposal method and summarizes several filtered tailings design concepts and considerations that the authors have found useful in their practical experience.

1 INTRODUCTION

Historically, conventional slurried tailings have been produced as a byproduct of mineral processing and engineering and operational approaches were then applied to engineer a tailings storage facility (TSF) capable of safely storing the tailings. More recently, alternatives to conventional slurried tailings (thickened, paste, and filtered tailings) have been developed and implemented in the mining industry. These alternatives present the possibility of engineering the properties of the tailings themselves to address site conditions or limitations.

The delineation between these alternative technologies is often vague with various classification systems and terminology in use. The authors have found a performance-oriented classification system based on yield stress, rather than solids content, to be useful (such as the one presented in Table 1).

Table 1. Tailings Classification System (After Cooke, 2010)

Tailings Classification	Yield Stress (Pa)*	Typical Solids Content (%)
Conventional Slurried Tailings	<5 to 20	<50
Thickened Tailings**	20 to 100	50 to 70
Paste Tailings	100 to 800	70 to 85
Filtered Tailings	>800	>85

*Yield stress as measured at the point of deposition using a shear vane device.

**Also differentiated from conventional slurried tailings as being non-segregating at deposition

The application of filtered tailings technology appears poised to make a dramatic leap forward, moving from use at a limited number of relatively low production-rate operations (6,000 tonnes per day (tpd) or less) to greater adoption and use at relatively high production-rate facilities

(>50,000 tpd). Filtered tailings are proposed for use at high production-rate mines such as the planned Metates and Rosemont Mines (both with proposed production rates of 90,000 tpd). Filtered tailings are also currently undergoing proof-of-concept testing for use as part of the EcoTails system at the Penasquito Mine (M3, 2016; Hudbay, 2017; Mining Magazine, 2017). The successful implementation of this technology at one of these projects would represent a significant precedent in the industry.

There are a number of external pressures likely to drive further adoption of the technology. These include regulatory and internal corporate scrutiny, which is especially heightened in the post-Mt. Polley and Fundao TSF failure environment and the designation of filtered tailings as a best available technology (BAT) for tailings storage (IEEIRP, 2015). Another key pressure is increasing water scarcity worldwide, which may intensify concerns regarding a mine's social license to operate if an operation is seen to be competing with local users for water.

2 SELECTING A PREFERRED DISPOSAL ALTERNATIVE

Considering this momentum for the technology, how should practitioners view filtered tailings and how should they select a preferred tailings management solution?

Ulrich wrote that there are no universal remedies for tailings storage and that every tailings facility should be designed based on project-specific requirements (2013). Watson wrote that alternative tailing disposal practices have been viewed as a “silver bullet” that will solve all tailings management issues, yet misconceptions abound (2010). Davies wrote that each project should be assessed for the potential applicability of filtered tailings based upon technical, economical, and regulatory constraints (2011).

Davies continued that filtered tailings are not a “panacea” for mine waste management: they should be appropriately viewed as a potential alternative form of tailings placement and a part of the overall tailings continuum of options. Similarly, the 2014 Elko Roundtable proceedings stated that “properly designed, constructed and operated filtered tailings facilities may offer the closest application the industry has in attaining a truly walkaway tailings facility. It was noted that there is no one-size-fits-all technology that are suitable for all applications. This applies to filtered tailings. Each project should be approached individually and technologies chosen, or discarded, based on their merits for the specific site” (Ulrich, 2015). Furthermore, filtered tailings operations can be equally as susceptible to performance challenges as those using other tailings disposal technologies. Wilson and Robertson alluded to two filtered tailings facilities where “the design, operating and site conditions have [led] to an urgent need for remedial modifications to avoid failure conditions” (Wilson and Robertson, 2015).

There appears to be broad agreement in the industry that no one technology provides a “universal” solution for tailings management. However, there is growing concurrence that filtered tailings can offer significant advantages and should be considered for new tailings storage facilities. It is recommended that an alternatives assessment be performed as a part of the development or expansion of tailings storage facilities to aid in the selection of the most appropriate tailings management solution. The assessment should include not only an evaluation of various tailings storage locations, but should also include various tailings disposal methods, including the use of conventional slurried, paste, thickened, and filtered tailings in various storage locations including surface deposits, surface impoundments, underground workings, and open pits. While typically not considered acceptable based on regulatory and corporate policies, the consideration of lacustrine and marine disposal alternatives may also be warranted.

While alternatives are often considered during initial scoping studies, the completion of a more formal alternatives assessment can be valuable. The methodology developed by Environment and Climate Change Canada (ECCC) in their *Guidelines for the Assessment of Alternatives for Mine Waste Disposal* (the Guidelines) is a helpful framework for performing alternatives analyses (2016). The methodology presented in the Guidelines includes the identification of all possible mine waste disposal alternatives, a pre-screening stage to remove alternatives with clear fatal flaws, and a quantitative assessment of the remaining alternatives using a Multiple Accounts Analysis (MAA) approach which considers environmental, technical, economic, and socio-economic impacts, building on the method described by Robertson and Shaw (1999).

The identification and consideration of all possible alternatives encourages the designer and owner to think beyond their typical experience and pre-conceptions for the site while the MAA methodology facilitates the incorporation of value judgements from various stakeholders regarding the impacts of the alternatives. Even if the assessment is only being completed for internal use, the MAA can incorporate input from the members of the design team and mining company with differing areas of focus and responsibility.

3 DESIGN CONSIDERATIONS

Selecting the tailings deposition technology is merely the first step in implementing the tailings storage solution, next the practitioner will need to develop the facility design. The following summarizes selected design concepts and considerations that the authors have found beneficial in their practical experience.

2.1 Target Moisture Content for Clayey Tailings

All too often, the moisture content of the filter cake is based solely on filter plant production considerations, economics or other drivers, and not on geotechnical requirements. Davies (2011) wrote that one of the most misunderstood design parameters for a filtered tailings operation is the target moisture content for the filter cake. The goal should be to achieve a moisture content that eases construction and meets slope stability criteria. A rule of thumb is to target the moisture content equivalent to the standard Proctor (ASTM D-698) optimum moisture content. This is often modified to account for the climate (slightly drier for wetter climates, and slightly wetter for drier climates) and for higher throughput operations where filtered tailings stacks employ larger compaction equipment (where it may be more appropriate to reference the modified Proctor (ASTM D-1557) optimum moisture content (Davies, 2011)).

However, as the clay content of the tailings increases, the necessary filter plant cycle times and the resulting capital and operating costs to produce a filter cake near the optimum moisture content typically increase significantly and it can be impractical to specify a Proctor-based target moisture content. Thus, for higher clay content tailings (such as those with a saturated hydraulic conductivity of 1×10^{-4} centimeters per second (cm/s) or less), a constructability-based target should be considered, where the moisture content is targeted to allow for a trafficable tailings surface.

In order to achieve a trafficable surface, the filtered tailings should provide adequate bearing capacity for the equipment that will be accessing the filtered tailings. At a scoping level, this can be estimated based on literature relationships and published construction equipment ground pressures, as discussed below.

Based on a database of 641 fall cone test results from 101 cohesive soil samples, Vardanega and Haigh (2014) developed an updated correlation between the undrained shear strength of a soil (C_u) in kilopascals and its liquidity index (LI), as follows in Equation 1:

$$C_u = 1.7 * 35^{(1-LI)} \quad \text{kPa} \quad \text{for } 0.2 < LI < 1.1 \quad (1)$$

Where:

$$LI = (\omega - PL) / (LL - PL) \quad (2)$$

And:

ω is the moisture content of the soil,
 PL is the moisture content at the soil's plastic limit, and
 LL is the moisture content at the soil's liquid limit.

If $\omega = LL$, then $LI = 1$
 And if $\omega = PL$, then $LI = 0$

Note that Vardanega and Haigh suggest that their relationship is only applicable to LI values between 0.2 and 1.1 as their data set below 0.2 is limited and there is considerable curvature in

the data above LI values of 1.1. Further, the moisture content used in the equation is as defined by a geotechnical engineer (mass of water divided by mass of solids), not as would be defined by a metallurgist (mass of water divided by total mass), which can be a point of confusion, as discussed elsewhere (such as Ulrich and Coffin, 2013).

Figure 1 presents plotted results from Equation 1 for soils with varying LLs and PLs within the range of LI values suggested by Vardanega and Haigh. Two conclusions are immediately obvious:

- The strength increases significantly for soils that are drier than the liquid limit and nearer to the plastic limit; and,
- The significantly greater impact of moisture content on undrained shear strength for soils with a lower plasticity index ($PI = LL - PL$).

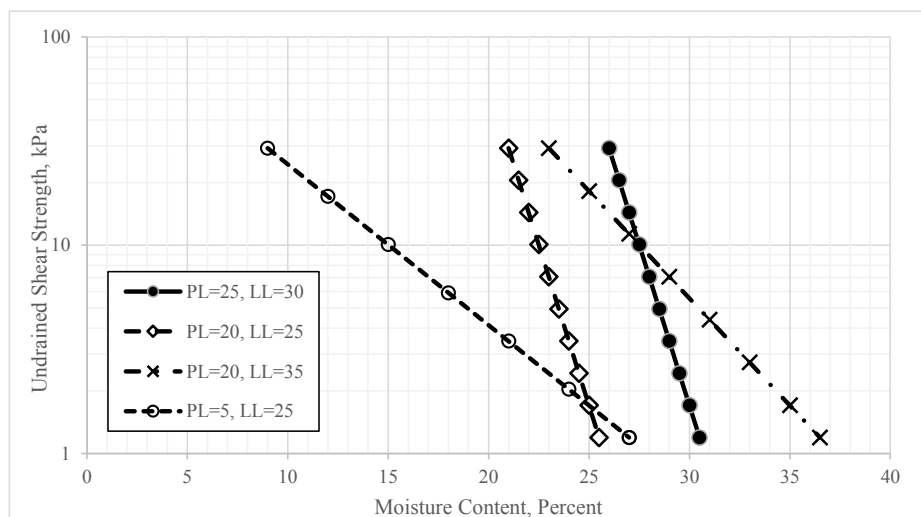


Figure 1. Estimated Undrained Shear Strength Results for Various Moisture Content Ranges

Per Equation 1, the undrained shear strength of a soil can be estimated as 60 and 2 kPa when the moisture content is at its PL and LL, respectively. Using Terzaghi’s bearing capacity equation for a square footing bearing on a cohesive soil with these strengths (refer to Sivakugan and Das, 2010, for example), the ultimate bearing capacity (q_{ult}) is about 260 and 20 kPa, respectively. Assuming a factor of safety of 3 to account for uncertainty (typical for spread footings), these ultimate bearing capacities are reduced to allowable bearing capacities (q_{all}) of about 90 and 7 kPa for a soil is at its PL and LL, respectively. This information is summarized in Table 2.

Table 2. Summary of Bearing Capacities

Moisture Content	Bearing Capacity	
	q_{ult}	q_{all}
$\omega = LL$	260	90
$\omega = PL$	20	7

To be trafficable by equipment, the bearing capacity of the filtered tailings should generally be greater than the ground pressure applied by the equipment working on the filter stack surface (although, it is likely possible to traffic areas while some limited amount of bearing capacity failures occur).

A typical person walking slowly may exert a ground pressure of about 40 kPa. Approximate ground pressures for various earth-moving equipment (Caterpillar, 2012) are as follows:

- D6 Low Ground Pressure Dozer: 30 kPa
- 320D Excavator: 40 kPa

- Articulated Trucks: 400 kPa

Whether Terzaghi's bearing capacity equation is entirely applicable for moving equipment is debatable, but the guidance provided by the relation still holds merit as a rule of thumb. It is considered applicable for initial assessments of the required production moisture content and may be useful guidance in reviewing the results from filter testing results.

Adjustments to the target moisture content values may then be made to account for variations in the moisture content due to conditions at the project site. These include:

- Site climate – In arid climates, additional drying would occur naturally during transport and placement in the filter stack.
- Tailings conveyance and placement method – Further drying of the filtered tailings may result due to the conveyance and placement method used. For example, significant reductions in moisture content may occur on a long conveyor belt in an arid climate and at operations which use long dozer pushes to spread and place the tailings.

Consideration of the material strengths represent a first step in defining the moisture content requirements for a clayier tailings and other considerations such as global slope stability criteria or the potential for saturation or seepage may eventually govern the target moisture content selection.

2.2 *Designing to Accommodate Varying Tailings Characteristics*

One common difficulty in the operation of filtered tailings stacks is accounting for excessively wet tailings. This may occur as a result of high intensity precipitation, long duration precipitation (such as during wet seasons), variations in the characteristics of the incoming ore, or operational and maintenance problems with the filtration equipment. Mines using filtered tailings disposal often include a conventional slurried tailings impoundment to allow for emergency deposition of tailings during periods of filter maintenance or when significantly out of specification filtered tailings are produced. However, limiting tailings deposition into the emergency facility to minimize the facility size and maximize the benefits of filtered tailings is always preferred. As such, designers commonly need to develop a filtered tailings stack design that can accommodate tailings with a wider range of moisture contents.

The most common way to address out of specification, or wet season tailings, is to include a defined area in the 'inner' zone of the stack (away from the outer perimeter, the 'structural' zone) where these higher moisture content tailings are to be placed. This 'inner' zone may receive limited, or no, mechanical compaction. The zone must be designed to provide environmental protection and to satisfy overall slope stability criteria. Furthermore, in cases where this zone is anticipated to be used for long durations during the wet season, the design should consider material balance requirements to ensure that the zone has sufficient capacity to carry operations through the end of the season. Consideration should also be given to incorporating decant facilities in this zone to allow precipitation and bleed water from the tailings to be removed from the facility.

The zoning can be developed using several design approaches, but typical approaches mimic conventional tailings dam designs, in a form of the following:

- Downstream construction - The outer structural filtered tailings are first placed and compacted (if required) in a zone that is similar to a starter dam. Inner tailings are impounded by this dam. The dam is expanded in the downstream direction and sized to accommodate the wet season placement of tailings. Developing staging for this approach requires careful material balance calculations.
- Centerline construction - Similar to the downstream construction approach, but the crest of the dam rises vertically as the facility is expanded.
- Upstream construction - The crest of the dam shifts upstream for raises above a starter dam. The degree of upstream shift may vary, from a significant upstream shift (an upstream raise) to a raise with a reduced upstream shift (sometimes described as "modified centerline" (Haile and Brouwer, n.d.)). In either case, while the dam may appear wide, it only comprises a structural shell above the starter dam and relies on the strength of the underlying inner zone tailings to a greater extent than the other two approaches for stability. This method requires more careful consideration of material strengths than the other two approaches and may present higher risks overall.

There are several hybrid forms of each of these designs.

2.3 Loading Rate and Liquefaction

Filtered tailings facilities are often referred to informally as ‘dry stacks’. This could lead a designer to overlook the possibility of liquefaction or the generation of excess pore pressures during operations. However, as discussed by Ulrich and Coffin (2013), saturation and problematic pore pressures can develop in a filter stack.

The insitu moisture content of the filtered tailings are a function of the production moisture content, climatic factors, hydraulic conductivity, suction, stiffness, and rate of loading. Recall that the optimum moisture content from Proctor testing is often selected as a target moisture content. In many cases, the optimum moisture content is near the zero air void curve, indicating the relatively close proximity to saturation in initially placed conditions. As the dry stack continues to rise, the air voids are compressed and the moisture content will increase, as long as the amount of water is not decreasing. Construction-induced loading from subsequent tailings placement can lead to saturation and the formation of excess pore pressures which can result in slope stability risks and the potential for liquefaction. This is further exacerbated if the filtered tailings are produced at a higher moisture content than was assumed in the design.

The loading rate should be considered in the facility design and may require the construction of a facility with a larger footprint area to reduce the rate of loading. If zones of saturated tailings may occur, and the potential for liquefaction exists, additional compaction of the filtered tailings may be required (if achievable), or the facility may require a substantial earthen or rockfill perimeter embankment (similar, perhaps, to a centerline-constructed dam) to protect against slope failure. For this case, it may be preferable to design a filter plant, and/or tailings conveyance and placement system, to produce a lower moisture content filter cake that will allow for embankment construction within tolerable pore pressure limits.

2.4 Underdrainage

If zones of saturation may develop within the stack, or if drain down is likely to develop, the designer should consider incorporating a network of engineered underdrains for the facility. This should be considered even if the tailings are benign and the facility is not constructed with a liner, as a way to mitigate the potential for pore pressure generation and resulting slope stability issues within the stack. The size and extent of the drainage system should be designed based on calculations of drain down and should include ample redundancy to account for pipe crushing or blockage. The quality of construction of these drains is of considerable importance and the designer should remain involved throughout the process with the construction oversight team.

4 CONCLUSIONS

There is no universal tailings management solution and there is no substitute for careful consideration of project-specific details in developing a tailings management design. An alternatives analysis should be performed to select a preferred tailings management option and demonstrate that potentially advantageous alternatives have not been overlooked. The Guidelines developed by Environment and Climate Change Canada are a valuable framework for performing such an assessment.

Good tailings facility design practice includes designs that accommodate tailings with varying properties and accounts for potential saturation and the resulting risks of excess pore-pressure generation and liquefaction. Further, selecting a target moisture content range for filtered tailings is a key step in the design process. For tailings with increased clay contents, constructability-related criteria present a convenient basis for selecting target moisture contents. Tailings facility designers are reminded that a filtered tailings facility design requires the same level and focus on design as other tailings management options.

5 ACKNOWLEDGEMENTS

The authors would like to thank our colleague Jason M. Cumbers, PE for his technical review of this paper and for his helpful comments.

REFERENCES

- Environment and Climate Change Canada (ECCC), 2016, Guidelines for the Assessment of Alternatives for Mine Waste Disposal, the government of Canada, <https://www.canada.ca/en/environment-climate-change/services/managing-pollution/publications/guidelines-alternatives-mine-waste-disposal.html>, accessed 6/1/2018, last modified 12/23/2016.
- Caterpillar, 2012, Caterpillar Performance Handbook, a publication by Caterpillar Inc., Peoria, Illinois, U.S.A. January.
- Cooke, R. 2010. MWH Short Course: Improved Water Recovery through Implementation of Alternative Tailing Disposal Methods. Short Course for the 2010 Tailings and Mine Waste Conference. Vail, Colorado.
- Davies, M., 2011, Filtered Dry Stacked Tailings: The Fundamentals, *Proc.: Tailings and Mine Waste*, University of British Columbia, November 30, 2011.
- Haile, J., Brouwer, K., n.d., Modified Centreline Construction of Tailings Embankments, Undated.
- Hudbay, 2017, Rosemont Project - NI 43-101 Technical Report – Feasibility Study, March 30, 2017.
- Independent Expert Engineering Investigation and Review Panel (IEEIRP), 2015, Report on Mount Polley Tailings Storage Facility Breach. January 30, 2015.
- M3, 2016, Metates Gold-Silver Project – NI 43-101 Technical Report – Updated Preliminary Feasibility Study, April 29, 2016.
- Mining Magazine, 2017, Goldcorp Trials new EcoTails technology, <http://www.miningmagazine.com/sustainability/news/1264248/goldcorp-trials-ecotails-technology>, accessed 6/1/2018.
- Robertson A. MacG, Shaw, S., 1999, A Multiple Accounts Analysis for Tailings Site Selection, *Proc. Sudbury '99 Mining and the Environment*, 3: 883 – 892.
- Sivakugan, N., and B.M. Das, 2010, Geotechnical Engineering, A Practical Problem Solving Approach, J. Ross Publishing, Inc.
- Ulrich, B., 2003, Toward a Sensible Use of Paste Tailings, *Mining Environmental Magazine*, The Mining Journal Limited: 21–23. May 2003. London.
- Ulrich, B., 2015, Innovations in Heap Leaching and, Mine Waste Discussed at 2014 Elko Roundtable, Mining Engineering Magazine, January, http://www.knightpiesold.com/en/assets/File/Article%20-%20Innovations%20in%20Heap%20Leaching%20and%20Mine%20Waste_January%202015.pdf, accessed 2/8/2017.
- Ulrich, B. and J. Coffin, 2013, Considerations for Tailings Facility Design and Operation Using Filtered Tailings, *Proc: Paste 2013*, R.J. Jewell, A.B. Fourie, J. Caldwell and J. Pimenta (eds), Belo Horizonte, Brazil.
- Ulrich, B. and T. Kerr, 2011, Elko Roundtable 2011: High-density Tailings, Paste and Filtered Tailings, *Mining Engineering Magazine*, November 2011.
- Vardanega, P.J. and S.K. Haigh, 2014, The Undrained Strength – Liquidity Index Relationship, *Canadian Geotechnical Journal*, 51: 1073–1086.
- Watson, A., 2010, Alternative Tailing Disposal - Fact and Fiction, *International Mining*, Paste Supplement, April. http://www.mwhglobal.com/wp-content/uploads/2010/04/International_Mining_April2010.pdf accessed 5/9/2018.
- Wilson, G. Ward and Andrew MacG. Robertson, 2015, The Value of Failure, *Geotechnical News*, 33 (2), June 2015.

Undrained Shear Strength Evolution with Loading on an Undisturbed Block Sample of Desiccated Gold Tailings

D. Reid, A. Fourie, and J. Castro

University of Western Australia, Crawley, WA, Australia

J. Lupo

Newmont Mining Corporation, Denver, CO, United States

ABSTRACT: A series of direct simple shear (DSS) tests were carried out on samples trimmed from blocks of desiccated surficial gold tailings. The testing was carried out to assess the effects of desiccation on subsequent shear strength and liquefaction susceptibility of the material. The testing indicated that peak undrained shear strength ratio tended to decrease up to approximately 250 kPa, beyond which the strength ratios consistently ranged from about 0.23 to 0.33. At low stresses, the material exhibited minimal contraction during shear. The implied preconsolidation pressure from desiccation - i.e. between approximately 100 and 250 kPa - is consistent with an effective stress interpretation of the stresses induced by suction on the desiccating tailings. Owing to visual indications of layering within the block sample, additional discrete samples were taken for wet sieving. These indicated significant gradation variation across distances less than 30 mm.

1 INTRODUCTION

It is common in arid and semi-arid regions for tailings to be cyclically deposited around a tailings storage facility, thus allowing desiccation to occur in fallow portions of the beach. This process can result in significant densification of the tailings compared to their behaviour when consolidated from a slurry without drying (e.g. Blight 1988). This desiccation process not only increases the density of the material at surface, but can also result in desaturation should drying continue such that suctions within the material exceed the air entry value (AEV). These processes enable construction works to take place on the material (i.e., improve local bearing capacity), but may also result in an overconsolidated material following placement of additional tailings above - to at least some depth. If this is achieved, it will reduce the propensity for the tailings in this condition to undergo flow liquefaction, as significant overconsolidation is likely to produce a dilative material state.

Despite the benefits of cyclic deposition and desiccation, there are currently relatively limited quantitative data available on the effects of this process on tailings after further loading, inundation, and potential resaturation. This is partly owing to some specific difficulties associated with characterising materials that have been dried in this manner. For example, the piezocone penetration test (CPTu) forms the basis of much in situ characterisation of tailings. However, currently-available CPTu interpretation methods are not well suited to characterising unsaturated soils (e.g. Pournaghiazar et al. 2013) - indeed, CPTu results generally indicate inaccurate, excessively dense conditions when probing a material in an unsaturated state. As mate-

rial that has been desiccated at surface may be unsaturated to some depth prior to eventual re-saturation, this means that a CPTu investigation that probes such materials will not provide a realistic assessment of their engineering properties should they later become saturated.

Laboratory element testing provides an alternative to CPTu probing, particularly in allowing assessment of the effects of different factors in controlled conditions. Perhaps the first examination of the effects of desiccation on subsequent material behaviour in the laboratory was that of Donaldson (1965), who assessed the preconsolidation pressure of dried South African gold tailings. Both in situ and laboratory-prepared specimens indicated significant preconsolidation pressures from desiccation. Similar results were later provided by Blight (1988).

A recent investigation was later carried out by a team at Carleton University (e.g. Al-Tarhouni et al. 2011; Daliri et al. 2014), primarily using direct simple shear (DSS) testing. Samples were prepared from a slurry and either tested directly (without drying), or dried to various gravimetric water contents (GWCs) at and above the Shrinkage Limit. Attempts were made to account for the overconsolidation induced by desiccation in a Bishop-type effective stress framework (e.g. Khalili et al. 2004). As would be typically expected in tailings practice, the results showed an increase in strength for dried tailings in the testing (at up to 500 kPa vertical stress), and therefore a reduced liquefaction susceptibility. However, the dried specimens showed looser densities than slurry-prepared specimens at a given vertical effective stress - a result inconsistent with the expected outcome of an overconsolidation process from desiccation-induced stresses, at least when considered analogous to mechanical overconsolidation.

While this program of work at Carleton University provides the most comprehensive laboratory-based study available on the effects of desiccation on subsequent tailing strength, two important points on this work are highlighted:

- The dried samples were rewetted without any bedding load (i.e. “free swelling” conditions). Given that many TSFs in arid regions are unsaturated to significant depths, this suggests that in many cases the resaturation process occurs under a significant load, and/or that cyclic rewetting and drying may occur. This may affect subsequent behaviour (e.g. Estabragh et al. 2015).
- The samples were prepared from a slurry deposited into moulds in a laboratory setting. Available evidence (Høeg et al. 2000; Chang et al. 2011) suggests that slurry deposition (or any other laboratory preparation method) does not produce a fabric consistent with actual field-scale deposition of silty materials.

To further assess some of the effects of desiccation on subsequent tailings behaviour – particularly undrained strength, contractive or dilative behaviour, and brittleness – a block sample obtained from a dried tailings beach during a recent site investigation was used to carry out DSS tests. The testing program was designed to investigate the effects of drying on the tailings strength, contractive/dilative tendency, and liquefaction susceptibility under a range of different vertical effective stresses from 50 to 500 kPa. As the samples were trimmed intact from a relatively undisturbed block sample, they likely provide the best practicable assessment of the in situ fabric created by hydraulic placement and subsequent drying that is practical using current technology. The implications of significant layering seen in the block sample were also investigated in a preliminary manner as part of the study.

2 TEST METHODS

2.1 Sampling and sample preparation

Testing outlined herein was all carried out on small samples trimmed intact from a block sample. A number of block samples were collected from a gold TSF as part of a sampling program that included large-scale bulk samples to supply calibration chamber test material. The block samples were collected as part of this program to enable assessment of in-situ layering and fabric, and therefore to provide input to works carried out on reconstituted samples. The block sampling process is illustrated in Figure 1.



Figure 1. Block sampling process

Owing to the visibly-evident layering in the sample (refer Figure 1), the authors decided to focus first on DSS testing as this device requires samples with a height of about 20- 30 mm. As these are much shorter than a triaxial specimen, it was hoped they would provide some ability to isolate different layers within the block. Specimens for testing were obtained by slowly advancing stainless steel cutting rings into the block, while at the same time trimming around the cutting ring with a scalpel, as shown in Figure 2. The block was divided into four layers in this process, with five or six rings used on each layer. The depth of each sample layer from the TSF surface was tracked during the sample preparation process. Trimmings created from each layer were saved for index testing and potential future reconstituted testing. A summary of each layer is provided in Table 1.

Although unlikely to be identical to any particular layer in the block given the layering observed, a mixed bulk sample of material from around the blocks had a Specific Gravity of 2.78, and Liquid, Limit, Plastic Limit, and Plasticity Index of 23%, 17%, and 6%, respectively.



Figure 2. Trimming samples from the block

Table 2. The number of officially reported plaque cases in the world.

Layer	Depth of layer from surface (mm)		Number of tests	%<75 μ m	Average in situ GWC (%)
	Top	Btm.			
1	168	198	6	53	16
2	106	136	6	55	11
3	49	79	5	54	13
4	0 (surface)	30	1	64	17

As noted in Table 2, only a single specimen from Layer 4 was tested. This was a result of the generally poor quality of this layer's specimens, likely a result of the brittle nature of the ~5 mm thick surficial crust of tailings that was included within the Layer 4 depth range.

2.2 DSS testing methods

DSS testing in the study was carried out under constant volume shearing conditions, within a membrane and stacked ring arrangement (i.e. SGI-type) apparatus. The bottom and top platens included "dead zones" of approximately 3.5 mm depth to prevent sliding of the specimen on the platens during shearing.

Specimens within the stainless steel rings (after trimming) were placed onto the bottom platen, and slowly extruded from the ring by placing a filter stone above the sample and pulling the stainless steel ring upwards. The samples were self-supporting owing to their initially unsaturated condition. A membrane and O-ring were then placed around the sample and platen, followed by the stack of Teflon-coated rings. The sample was then placed within the DSS device and a bedding load of 25 kPa was applied.

The specimen was then flooded with site decant water from the bottom to the top for two hours, after which time water had clearly flooded the sample and was evident above the top platen. There are two important considerations with respect to the flooding and saturation of DSS samples in the context of the current study:

- It has been shown that constant-volume DSS testing, on clean sands, carried out under dry conditions will give similar results as a saturated sample at the same density (Finn et al. 1978). However, this is unlikely to be the case for a silty tailings - silty materials exhibit suction hardening, resulting in a modification of the critical state line when unsaturate (Wang et al. 2002), and are generally more affected by the suction acting under partially-saturated conditions. For example, the effects of partial saturation on constant-volume DSS tests on a material with 55% < 75 μ m were evident in the results presented as part of the Fundão investigation (Morgenstern et al. 2016). As such, flooding to remove suctions is likely to be required to produce reasonable DSS results that represent saturated in situ conditions (Al-Tarhouni et al. 2011).
- It could be argued that the bedding load applied to the specimen during the flooding process may affect subsequent geotechnical behaviour. For example, some unsaturated soils, when under small (or no) bedding loads, can exhibit significant swelling. This may not be realistic compared to in situ behaviour should a sample only resaturate under significant load. Therefore, flooding of the sample in this study was carried out under a 25 kPa bedding load to minimise swelling. It is acknowledged that this was an arbitrary selection, and resaturation could actually occur under a range of conceivable vertical loads.

2.3 DSS test results

The results of the consolidation stage of the testing are outlined in Figure 3, where the consolidation dry density for each sample at final vertical effective stress is indicated. Dry density is used rather than void ratio as Specific Gravity of the individual layers has not yet been measured, and could conceivably vary slightly with gradation. While each layer shows a fairly consistent trend of increasing density with stress, not all layers align. Layer 2, for example, is significantly denser than the other layers across the range of vertical effective stresses. The potential explanation for this different range of densities for Layer 2 is discussed later in this paper.

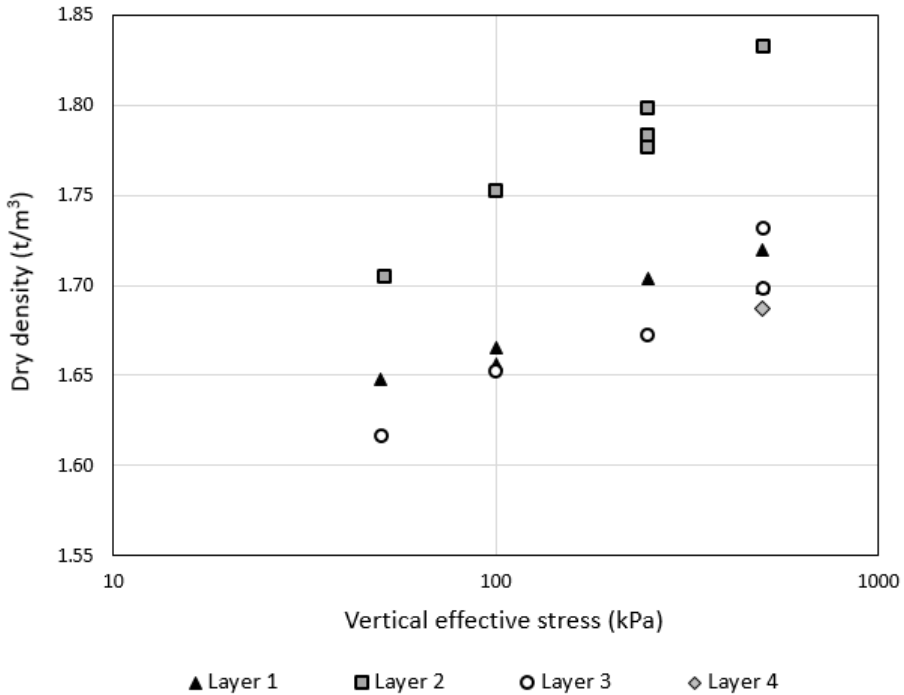


Figure 3. Consolidated densities

The DSS shearing stage results for Layer 1 are summarised in Figure 4, as undrained strength ratio (s_u / σ'_{vc}) vs. shear strain and as undrained strength ratio vs. normalised vertical effective stress (σ'_v / σ'_{vc}). Some duplicate tests sheared from the same consolidated stress are not included in Figure 4 for clarity (although they provided similar results). All the tests exhibited initial contraction, with varying degrees of subsequent dilation for the 50 and 100 kPa tests, resulting in higher strengths. A generally consistent trend of decreasing strength with increasing consolidated vertical effective stress was evident. Negligible post-peak brittleness was seen in any of the tests carried out in this study – an important consideration when considering the susceptibility of the material to static liquefaction. However, it is acknowledged that brittleness is likely to be greater if consolidated with a static bias.

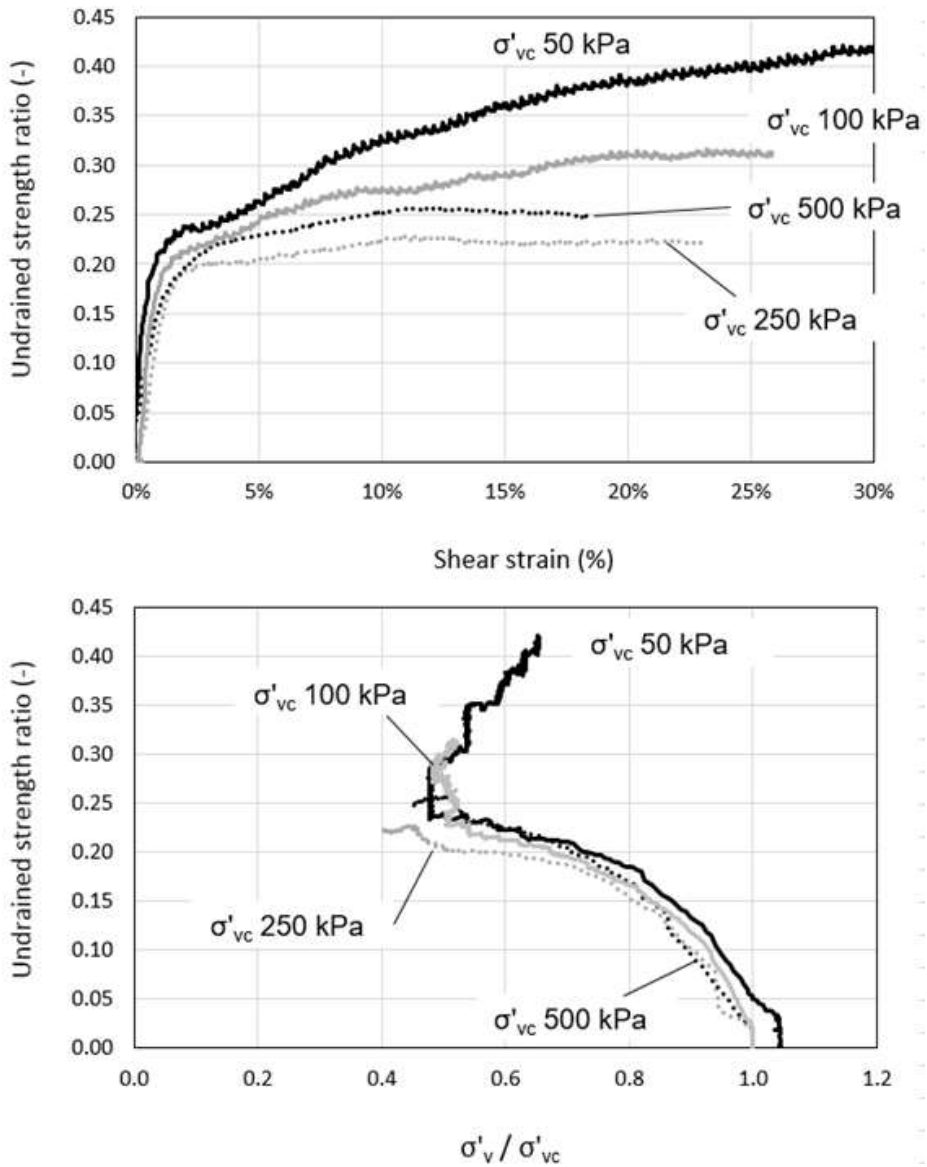


Figure 4. Layer 1 DSS results

The strength results from all the tests carried out in the study are summarised in Figure 5 as peak undrained shear strength ratio for the test against pre-shear (i.e. consolidated) vertical effective stress. Some of the tests at 50 kPa vertical effective stress were still dilating at the end of the strain limits of the DSS device. Where this occurred, it is indicated by an arrow on the test result in Figure 5.

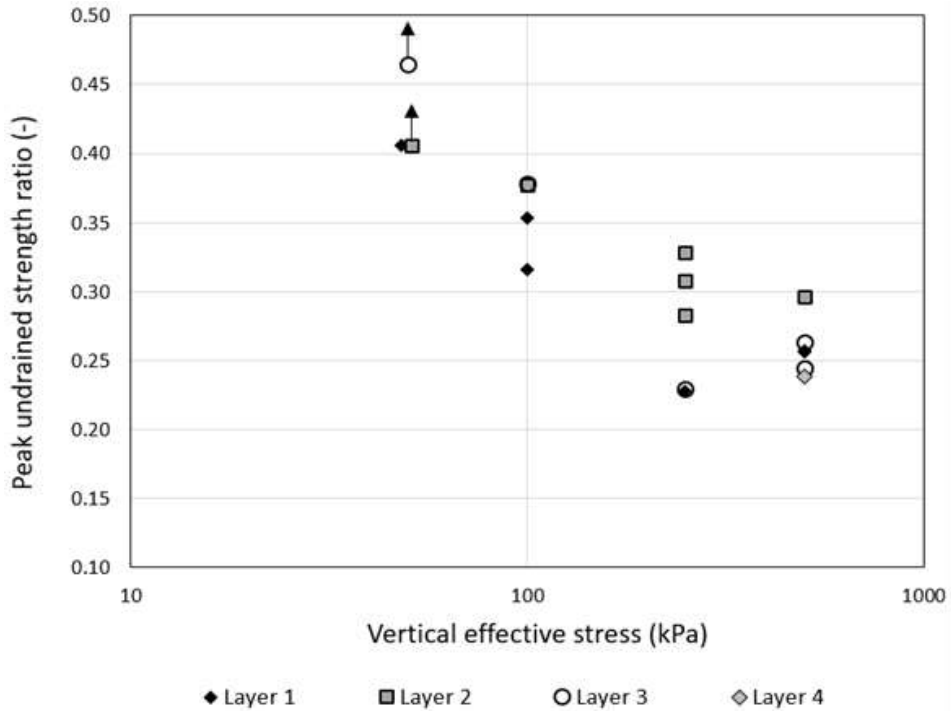


Figure 5. DSS result synthesis

Increased consolidation stress is generally associated with a reduction in peak undrained strength ratio. This is particularly evident from 50 to 250 kPa consolidation stresses. At 250 kPa and beyond, the results appear to be more consistent with experimental and sample variation rather than a physically meaningful trend. It is noted that a preconsolidation pressure induced by drying of 100 to 250 kPa, as suggested by these test results, is generally consistent with the effective stresses that would be implied in a desiccated tailings using Bishop-type effective stresses, particularly those that develop the weighting factor χ on the basis of *effective* saturation (e.g. Alonso et al. 2010)

The reduction in peak undrained strength ratio with increasing consolidation stress appears to be consistent with a reduction in the effects of desiccation-induced overconsolidation. It is noted that there should be no expectation of fully “normalised” behaviour across a range of vertical effective stresses for a sandy silt or silty sand (e.g. Bobei et al. 2009) - that is, a constant undrained strength ratio, which is typically consistent with parallel CSL and NCL’s. However, the variation seen in the results presented here is more substantial than could be accounted for simply through different CSL and NCL slopes. Therefore, the increased strengths at lower effective stresses appear to be a result of an overconsolidation effect.

3 LAYERING ASSESSMENT

3.1 *In situ* layering

As noted previously, it was apparent from visual inspection of the blocks that significant layering was present. Indeed, the layering was such that the ~30 mm DSS sample height was unlikely to have isolated individual layers - i.e., the intact specimens would have non-uniform gradations. This unlikely to be fully capture by wet sieving of the trimmings from each layer - these only varied from 53 to 64% < 75 μm as noted previously, perhaps implying a “smearing” effect within the layers, as the visual differences within the various layers appeared more significant than implied by the trimming gradations.

To assess the variation in gradation in finer detail, a block taken from the TSF surface adjacent to that used for the DSS testing was used to obtain small, discrete samples at a closer interval than the four layers of trimmings produced from DSS testing. Each of the small sub-samples taken was then wet sieved to measure the % < 75 μm. The results of this process are illustrated in Figure 6, with a visual indication of the layering presented in Figure 7. Clear zones of higher silt content are evident, at a smaller scale than the ~30 mm DSS sample layers could isolate. This result may also provide an indication as to the higher densities observed in Layer 2, as it seems possible that Layer 2 may have better isolated a zone of material at about ~55% < 75 μm, a gradation that is likely to result in a better packing efficiency if uniform throughout the specimen (e.g. Zuo and Baudet 2015). It is also noted that gradation correlated well to the in situ GWC of the discrete sub samples - higher silt content corresponded consistently with a higher GWC. This could imply a near-constant value of suction through the block, with the different GWCs being an indication of different soil water characteristics curves for the different gradations present.

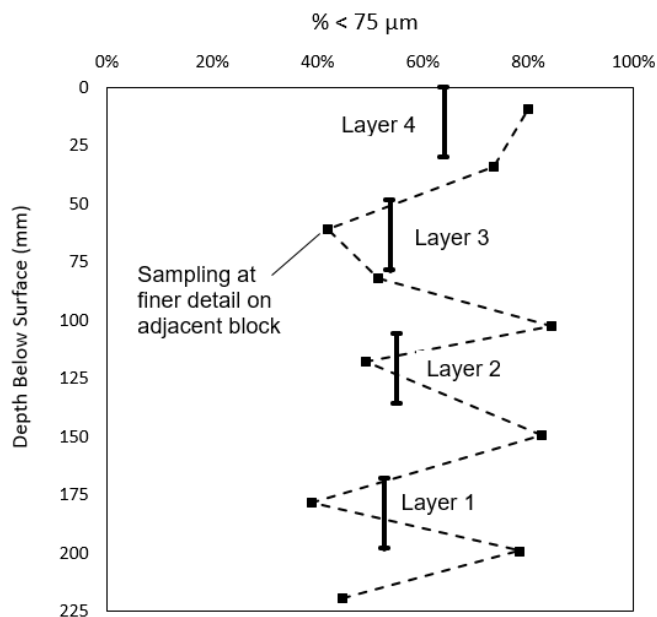


Figure 6. Gradation profile of block samples

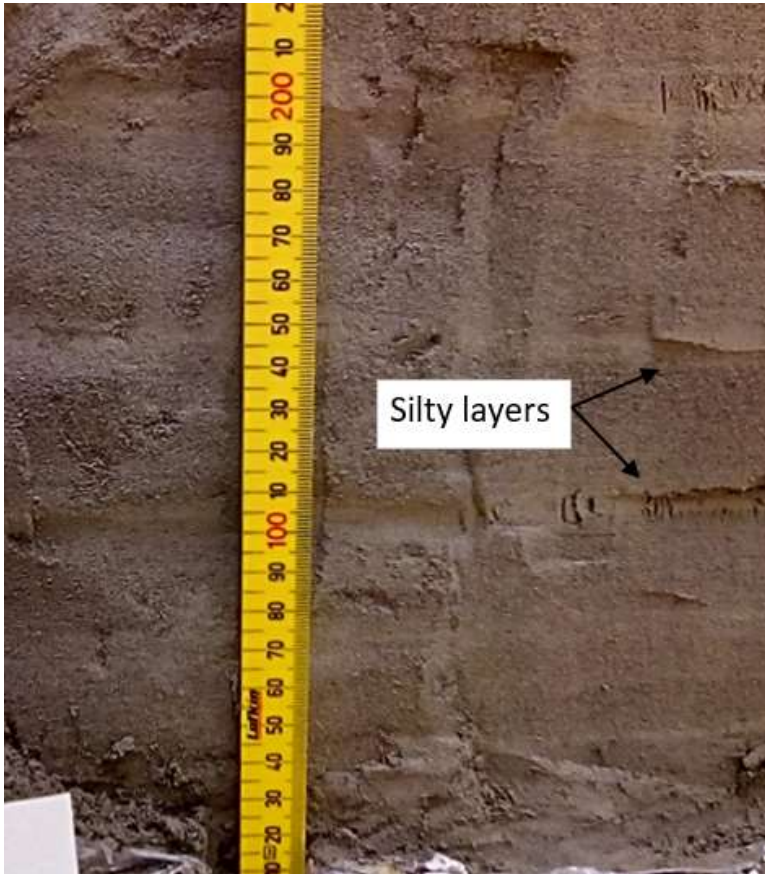


Figure 7. Visual indication of layering

3.2 Other examples

It is interesting to compare the in situ layering observed in the tested block samples in this study to some other examples presented in the literature for TSFs and hydraulic fills:

- Investigations at the Lower San Fernando Dam (LSFD) failure indicated significant small-scale layering (Baziar & Dobry 1995). This is consistent with the hydraulic fill construction method used at that facility, where segregation was promoted to attempt to develop a zoned embankment. In attempting to reconstitute specimens in the laboratory, it was found that homogenising the material resulted in denser states than observed in situ in some cases, as a result of the improved packing efficiency when homogenised (i.e. mixed sandier and siltier layers)
- Høeg et al. (2000) in their assessment of the fabric of remoulded and intact specimens noted layering present within the tailings tested. They note, qualitatively, that this layering may have played “some role” in the significantly different behaviour seen in remoulded and intact specimens.
- Chang et al. (2011) carried out testing on both block and remoulded specimens. While they state “only layers with a minimum thickness of 200 mm were sampled for testing”,

no quantitative confirmation of the homogeneity of the samples was made. Further, the photographs of the blocks tested as presented by (Chang 2009) appear to indicate visually apparent layering - qualitatively of a similar magnitude to that seen in the blocks tested in this study.

- Samples obtained during the CANLEX project (Robertson et al. 2000) often showed appreciable gradation variation across relatively small depth intervals. For example, at the Mildred Lake site at Syncrude, % < 75 μm varied between 1 and 12 in samples from the depth range from 30 to 37 m (refer Figure 8), including significant variation across depth intervals less than 100 mm (Wride and Robertson 1997). While seemingly a relatively small gradation range, such variation would have significant effects with respect to the CSL elevation and/or slope (Been & Jefferies 1985; Zuo & Baudet 2015).

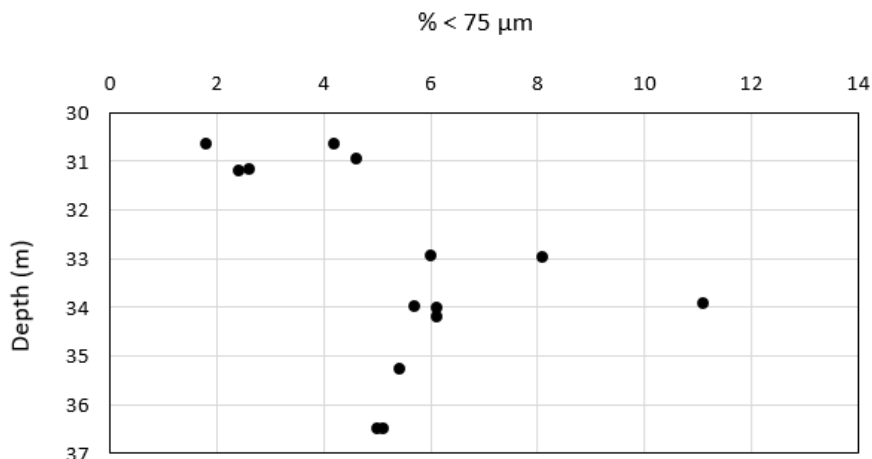


Figure 7. Mildred Lake gradation results, after Wride and Robertson (1997)

The results of this study, and other examinations of in situ layering, suggest that the use of homogenised remoulded specimens would be expected to exhibit different response to intact specimens at the same overall void ratio - exactly as was reported in much of the testing previously cited (Høeg et al. 2000; Chang et al. 2011). Particularly when viewed in light of the LSF D work (Baziar & Dobry 1995), these observations suggest that it may not be different sample preparation techniques per se, but small-scale in situ layering, that is the primary source of the differences often seen between intact and remoulded specimen behaviour. For example, a triaxial test carried out on an intact specimen from the blocks discussed in this study would have a range of gradations from 39 to 84 % < 75 μm . Each layer could have a unique CSL elevation and slope, with a significant range of both, given the gradation variation (e.g. Zuo and Baudet 2015). Clearly, fabric studies of remoulded and intact specimens must include greater cognisance of the potential importance of layering than has occurred up until now. This is of great importance to tailings practice, as the significant differences seen in intact and remoulded soils presents a fundamental challenge to widespread adoption of critical state soil mechanics, which has emerged as the dominant framework for assessing tailings liquefaction risk (Jefferies and Been 2015; Morgenstern et al. 2016).

4 FUTURE STUDY

Clearly, desiccation can have significant effects on undrained strength and liquefaction susceptibility of tailings. While laboratory elements of the type outlined herein provide further evidence on these effects, it would still be difficult to infer such conditions at various depths of the TSF. Therefore, future work being planned includes further element tests with wetting, drying, and rewetting under a wider range of confining pressures than surface blocks. Calibration chamber tests to improve the ability of the CPT to estimate liquefaction susceptibility of desiccated zones, should they later rewet, are also to be carried out.

5 CONCLUSIONS

A series of DSS tests were carried out on a block sample of desiccated gold tailings obtained from the surface of a gold TSF. The block sample was trimmed to produce samples for DSS tests on the material at a range of vertical effective stresses, to assess the effects of desiccation on subsequent shear strength and liquefaction susceptibility. The samples were resaturated as part of the DSS testing to assess their condition should they resaturate in the future at depth within the TSF. The results of the DSS testing indicated a general decrease in peak undrained shear strength, and increasing contractive tendency, with increasing vertical effective stress. The reduction in strength with vertical stress implied a preconsolidation pressure induced from drying in the order of 100 to 250 kPa. The results were generally consistent with expectations as to what effects could be envisaged from drying based on previous testing at Carleton.

An assessment of the variation in gradation within the blocks was also made, based on visual evidence of layering and the differences in consolidated densities seen in some of the layers. This assessment suggested significant variation in gradation across distances less than 20 mm. The implications of such layering on fabric studies may be greater than typically considered, as the layered in situ specimen would be quite different to a reconstituted sample prepared from trimmings from the block that were homogenized.

ACKNOWLEDGEMENTS

This work forms part of TAILLIQ (Tailings Liquefaction), which is an Australian Research Council (ARC) Linkage Project supported by financial and in-kind contributions from Anglo American, BHP, Freeport-McMoRan, Newmont, Rio Tinto, and Teck. The TAILLIQ project is being carried out at The University of New South Wales (UNSW), The University of South Australia, The University of Western Australia (lead university), and The University of Wollongong. We acknowledge the support and contributions of project personnel at each of the supporting organisations. We thank the mine site personnel who assisted in the block sampling process.

REFERENCES

- Alonso, E.E., Pereira, J.-M., Vaunat, J. and Olivella, S. 2010. A microstructurally based effective stress for unsaturated soils. *Geotechnique*, 60(12): 913–925.
- Al-Tarhouni, M., Simms, P. & Sivathayalan, S., 2011. Cyclic behaviour of reconstituted and desiccated-rewet thickened gold tailings in simple shear. *Canadian Geotechnical Journal*, 48(7): 1044–1060.
- Baziar, M.H. & Dobry, R., 1995. Residual Strength and Large-Deformation Potential of Loose Silty Sands. *Journal of Geotechnical Engineering* 121(12): 896–906.
- Been, K. & Jefferies, M.G., 1985. A state parameter for sands. *Geotechnique* 35(2), pp.99–112.
- Blight, G.E., 1988. Some less familiar aspects of hydraulic fill structures. In D. J. A. Van Zyl, ed. *Hydraulic Fill Structures*, ASCE Geotechnical Special Publication No. 21. ASCE, pp. 1000–1027.

- Bobei, D.C., Lo, S.R., Wanatowski, D., Gnanendran, T., & Rahman, M.M., 2009. Modified state parameter for characterizing static liquefaction of sand with fines. *Canadian Geotechnical Journal* 46(3), pp.281–295.
- Chang, N., Heymann, G. & Clayton, C., 2011. The effect of fabric on the behaviour of gold tailings. *Géotechnique* 61(3): 187–197.
- Daliri, F, Kim, H., Simms, P., and Sivathayalan, S., 2014. Impact of Desiccation on Monotonic and Cyclic Shear Strength of Thickened Gold Tailings. *Journal of Geotechnical and Geoenvironmental Engineering* 140(9).
- Donaldson, G.W., 1965. The effects of capillary action on the consolidation and shear strength of silt in a hydraulic fill dam. In Proc. 6th International Conference on Soil Mechanics and Foundation Engineering, Vol II, pp. 459–463.
- Estabragh, A.R., Parsaei, B. & Javadi, A.A., 2015. Laboratory investigation of the effect of cyclic wetting and drying on the behaviour of an expansive soil. *Soils and Foundations* 55(2) : 304–314.
- Finn, W D, Vaid, Y P & Bhatia, S K, 1978. Constant volume cyclic simple shear testing. In 2nd International Conference on Microzonation for Safer Construction - Research and Applications, Volume 2. pp. 839–851.
- Høeg, K., Dyvik, R. & Sandbækken, G., 2000. Strength of Undisturbed versus Reconstituted Silt and Silty Sand Specimens. *Journal of Geotechnical and Geoenvironmental Engineering* 126(7): 606–617.
- Jefferies, M.G. & Been, K., 2015. *Soil Liquefaction: A Critical State Approach, Second Edition*. CRC Press, Boca Raton, Florida.
- Khalili N., Geiser F. & Blight G. E., 2004. Effective Stress in Unsaturated Soils: Review with New Evidence. *International Journal of Geomechanics* 4(2): 115–126.
- Morgenstern, N.R. et al., 2016. Fundão Tailings Dam Review Panel: Report in the immediate causes of the failure of the Fundão Dam.
- Pournaghiazar, M., Russell, A.R., & Khalili, N., 2013. The cone penetration test in unsaturated sands. *Géotechnique* 63(14), pp. 1209-1220.
- Robertson, P.K. et al., 2000. The Canadian Liquefaction Experiment: an overview. *Canadian Geotechnical Journal* 37(3): 499–504.
- Wang, Q., Pufahl, D.E. & Fredlund, D.G., 2002. A study of critical state on an unsaturated silty soil. *Canadian Geotechnical Journal* 39(1): 213–218.
- Wride CE & Robertson PK, 1997. CANLEX - Phases I and III Data Review Report. Volume I - Data Report.
- Zuo, L. & Baudet, B.A., 2015. Determination of the transitional fines content of sand-non plastic fines mixtures. *Soils and Foundations* 55(1): 213–219.

Bench-Scale Nitrate and Sulphate Biochemical Reactor Case Study, Amulsar Mine, Armenia

J. J. Gusek, G. Fattore, L.P. Josselyn,
Sovereign Consulting, Lakewood, CO, USA

A. Aghajanyan
Lydian International, Yerevan, Armenia

ABSTRACT: Bench-scale biochemical reactors (BCRs) filled with organic media successfully removed nitrate and sulphate in a laboratory setting in advance of field testing. The Armenian treatment goals are strict: 2.5 mg-L⁻¹ (nitrate as N) and 16 mg-L⁻¹ sulphate. Barrels filled with media were connected in series; three sets of barrels were tested simultaneously. Each barrel set included a denitrifying BCR, intermediate mechanical aeration and settling, and a sulphate-reducing BCR, which fed a sulphide scrubber. One stand-alone BCR was tested to determine if nitrate and sulphate could be removed simultaneously. Water pumped into the barrel sets contained 50 mg-L⁻¹ nitrate, up to 150 mg-L⁻¹ sulphate, and exhibited a pH of 3.6. The sulphide scrubbers contained different inorganic reactive media. The test results exceeded expectations; the effluents from two barrel sets satisfied the Armenian standards throughout 26 weeks of operation. The stand-alone BCR met the nitrate standard but was unable to fully treat sulphate.

1 INTRODUCTION

Sovereign Consulting Inc., Global Resource Engineering, and Lydian International conducted bench-scale tests at the Amulsar Mine in Armenia to evaluate the efficacy of selected treatment technologies in the removal of sulphate and nitrate from a low-metals content mining influenced water (MIW) to sulphate concentrations less than 16 mg-L⁻¹ and nitrate concentrations less than 2.5 mg-L⁻¹ as N, respectively. While chemical-, labor-, and power-intensive active treatment technologies may be appropriate for treating the Amulsar MIW, the bench testing focused on the passive biochemical reactor (BCR) technology coupled with sulphide scrubbing with various reactive media. If the test results were promising, that is, the nitrate and sulphate standards could be met, the passive technology could be implemented to address MIW at the site once the mine is fully developed. While the mine intends to implement MIW prevention measures (which are also being tested), active treatment technologies could be implemented if passive technologies fall short of the mark.

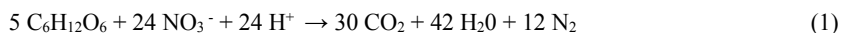
The primary objective of the bench-scale test was to identify regionally-available organic materials and mixtures that would be suitable for use in a future phase of testing: a pilot-scale nitrate and sulphate BCR. Three organic mixtures containing different ratios of straw, wood chips, wine pressings, and biochar were tested; manure provided the microbial inoculum. The inorganic fraction of the three mixtures included agricultural quality limestone. Additionally, three inorganic materials were evaluated for scrubbing excess hydrogen sulphide/sulphide ion from the BCR effluents. The scrubber reactors (SCRs) were charged with:

- a commercially available red iron oxide powder (thought to be hematite),
- scrap metal (zero valent iron [ZVI]), and
- upper volcanic rock from the site.

Each SCR received effluent from the same individual sulphate reducing BCR throughout the test.

Nitrate removal from water/wastewater can be achieved by a biological process, most commonly known as biological denitrification; it is an anaerobic biological process in which nitrate (NO_3^-) is ultimately reduced to nitrogen gas (N_2).

The anaerobic conditions in a typical BCR can lead to the formation of ammonium (NH_4^+). The conditions can also produce nitrogen gas (N_2), according to Equation 1: (Reynolds & Richards, 1982).



This reaction will result in an increase in alkalinity due to the removal of nitrate and hydrogen ion.

Sulphate reduction is a microbiological reaction that also occurs under anaerobic conditions. Sulphate is reduced to hydrogen sulphide and bicarbonate ion by a group of sulphate reducing bacteria (*Desulfovibrio*, for example), which utilize short chain organic acids and alcohols as carbon sources and sulphate as an oxidant (Equation 2). The general reactions, which have been cited in numerous publications and are considered conventional wisdom, can be represented as:



The hydrogen sulphide reacts with metals in solution (Me^{+2}) to form insoluble metal sulphide (MeS) precipitates (Equation 3). Me^{+2} is a divalent metal and MeS is the metal precipitate.



The reaction kinetics favor denitrification over sulphate reduction. Therefore, most of the nitrate needs to be removed from the MIW before sulphate reduction reactions can dominate. In other words, nitrate can interfere with biological sulphate removal.

The carbon source is generally provided by a mixture of solid substrates (e.g., wine pressings, straw, and wood chips) to provide both short-term and long-term carbon sources that insure a quick start up as well as steady prolonged treatment. BCR substrates also typically contain a crushed limestone component (even for net alkaline MIW) to suppress fermenting bacteria that can lower the pH. The limestone component can also protect the bacterial community against pH or acidity excursions (ITRC, 2013).

The secondary objective of the study was to determine which of the three sulphide-sequestering materials (iron oxide, scrap metal, upper volcanic rock) in the SCRs were more efficient at removing residual H_2S . Dissolved iron (generated by anaerobic corrosion of iron released from the scrap metal (zero valent iron, or ZVI) will remove dissolved sulphide from the water by precipitating iron sulphide (ITRC, 2013). Upper volcanic rock and iron oxide were also assessed as a source of sacrificial metal to scrub dissolved sulphide from a BCR. Each material was evaluated in an individual SCR. The results of using various organic/inorganic material blends in the BCRs and of coupling these reactors to the SCRs are presented here.

2 MATERIALS AND METHODS

MIW used in the bench testing was acidic (pH around 3.6 s.u.) and contained from 50 to 150 $\text{mg}\cdot\text{L}^{-1}$ of sulphate, around 50 $\text{mg}\cdot\text{L}^{-1}$ of nitrate, and very low concentrations of metals. The Amulsar Mine was being developed and actual MIW was unavailable at the start of the test. Consequently, a surrogate MIW water was prepared using tap water from the mine laboratory spiked with nitrate to 50 $\text{mg}\cdot\text{L}^{-1}$, sulphate to 50 $\text{mg}\cdot\text{L}^{-1}$, and pH-adjusted to 3.8 s.u. with sulphuric acid. This surrogate MIW was initially fed to the bench-scale barrel sets. Once water from a source of “natural” acid rock drainage was identified in a stream ~2 km from the mine, it was used to formulate the surrogate MIW that was fed to the test barrel sets. This natural water source exhibited a sulphate concentration of 150 $\text{mg}\cdot\text{L}^{-1}$ and a pH of 3.6 s.u., so sulphate spiking and pH adjustment were no longer necessary. Still, a nitrate spike was still required to mimic the predicted MIW chemistry.

The seven BCR material mixtures are shown in Table 1. The materials were selected based on their availability in bulk nearby the mine. This procurement policy, even for the bench testing, acknowledges the importance of favorable economics when the large quantities required for full scale construction are considered. Also, material substitutions are inevitable in large construction projects so the mixtures selected reflect the likely possibility that a material's availability or unit price might change by the time the system is constructed. The three SCR materials and their respective quantities and sources are provided in Table 2.

Table 1. Bench Scale Sulphate BCRs Mixture Proportions of Components by Weight.

Material	NBCR1	NBCR2	NBCR3	N/SBCR4	SBCR1	SBCR2	SBCR3
Biochar	9%	7%	18%	12%	13%	18%	10%
Wood Chips	4%	20%	26%	23%	0%	26%	24%
Limestone	9%	20%	17%	12%	13%	17%	10%
Wine Pressings	4%	8%	7%	17%	13%	7%	10%
Straw	62%	43%	31%	35%	60%	31%	44%
Animal Manure	12%	2%	1%	2%	2%	%	1%
Total	100%	100%	100%	100%	100%	100%	100%
Mass (kg)	25.2	15.2	26.5	18.8	27.2	24.0	23.9

Materials were locally procured (Armenia).

The limestone component was included to suppress substrate fermentation reactions and was not expected to be consumed faster than the organic materials in the alkaline influent MIW.

As limestone dissolution rates were inconsequential to the results of the test, the limestone was not characterized in any detail (e.g., Ca, Mg, Si, and CO₂ analyses).

Table 2. SCR Component Masses

Material	SCR	Quantity (kg)	Sand (kg)
Iron Oxide	SCR1	1.02	21.14
Scrap Metal	SCR2	5.44	18.94
Upper Volcanic Rock	SCR3	16.34	none

Each BCR apparatus consisted of a 200 L open-top barrel. They were configured for up flow (bottom to top). The floor of each barrel was fitted with a flow distribution layer consisting of a grid of perforated PVC pipes surrounded by pea-sized gravel. The MIW feed water was introduced at the bottom of each barrel to flow uniformly up through the media mixtures. Treated MIW exited through an overflow pipe installed near the top of the barrel. A photograph of the Bench-Scale test system as constructed is provided in Figure 1. A schematic of the bench-scale passive treatment system, showing all three treatment barrel sets and the stand-alone BCR unit, is shown in Figure 2. While the tiered test arrangement in Figure 1 suggests gravity flow, all MIW was pump-fed to the various process units.



Figure 1. Photo of the Bench-Scale Treatment Barrel Sets at the Amulsar Mine Lab

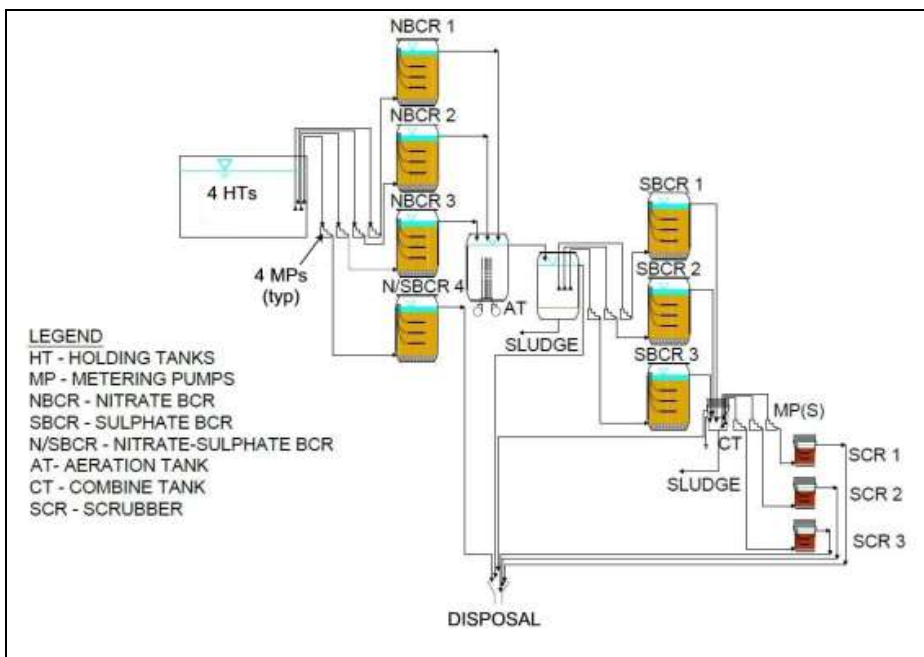


Figure 2. Bench-Scale Process Flow Diagram

The SCRs were comprised of 20 L wide mouth plastic containers. They too operated in an up-flow fashion. The bottom of each unit was also fitted with a flow distribution system consisting of a grid of perforated PVC pipes surrounded by gravel. Each SCR had an overflow tube positioned near the top of the unit for sampling and for directing the final treated MIW for disposal. The SCRs were fitted with sealed lids.

Weekly samples were collected for measurement of field parameters: pH, oxidation-reduction potential (ORP), and conductivity at which time flow rates from the head tank then in use were also measured. Sulphate and nitrate were also measured at the site laboratory using a HACH Col-

orimeter DR900. However, due to very low concentrations of these two parameters and interferences with biochemical oxygen demand (BOD), the tests were discontinued at the site and conducted at a certified laboratory by ion chromatography (IC).

Monthly water samples, collected for metals analysis, were filtered through a 0.45 µm filter and preserved with concentrated nitric acid to pH < 2. The major metals (e.g. Al, Fe, Mn, and Zn) were analyzed by inductively coupled plasma atomic mass spectrometry (ICP-MS) at an accredited laboratory in the Czech Republic. Total organic carbon (TOC) was also analyzed at this laboratory, giving insight into the release and use of organic carbon in the BCRs. As the influent metals were inconsequential to the study, the data is not presented in this paper.

3 RESULTS AND DISCUSSION

3.1 Nitrate (Only) Biochemical Reactors (NBCRs)

Initially, surrogate MIW used to fill the NBCRs was prepared using tap water to which aluminum sulphate, iron sulphate, and potassium nitrate were added. This incubation phase focused on growing a healthy denitrifying bacteria population. Sulphate reducing bacteria (SRB) were likely to grow as well. The flow through the NBCRs commenced at an initial average hydraulic retention time (HRT) of 5.9 days. The HRT in the NBCRs was variable (Figures 3 and 4). Due to increases in the oxidation-reduction potential (ORP) observed in the first few weeks of testing, the HRT was increased (i.e., the flow rate to each NBCR was decreased).

The study focused on nitrate and sulphate removal to relatively low concentration limits. The pH was raised from an average of 3.6 s.u. to an average of 6.2 s.u. (average of all three NBCRs) for the duration of the testing (26 weeks). Calcium and magnesium data suggest that most of this increase could be attributable to limestone dissolution. Figure 3 indicates that the concentration of nitrate was lowered to below the method detection limit (BDL) since the first month of testing in all the NBCRs. Sulphate concentration also decreased in the NBCRs. NBCR-3 sulphate performance was typically better than NBCR-1 and NBCR-2; the sulphate concentration was BDL in month 1 and 5. It is noteworthy that NBCR-3 contained more biochar, a catalytic media amendment that has shown to behave as an electron “shuttle” in anoxic electron donor-receptor situations (Xu, *et al.*, 2016).

MIW flow to NBCR-1 was suspended for about four weeks due to elevated positive values of ORP and depressed pH, which were not conducive to nitrate removal. It was suspected that fermentation bacteria may have prospered at the expense of denitrifying bacteria due to the large portion of straw and lack of buffering alkalinity in the media. NBCR-1 was “resuscitated” by increasing the amount of limestone in the upper 15 cm of media to a value similar to the other NBCRs and reversing the flow direction to down-flow. Following about three weeks of incubation, NBCR-1 again received raw MIW feed. Subsequently, it continued to achieve the BDL of nitrate concentration in concert with acceptable ORP and pH values. NBCR-1 was also able to decrease sulphate to a concentration even lower than NBCR-2 and NBCR-3 in the final month of testing.

While somewhat successful at removing sulphate, the NBCRs were incapable of consistently achieving and maintaining the target sulphate concentration. This condition was anticipated at the outset of the test, so the NBCRs were connected in series (since the beginning of the test) with the SBCRs to further increase the effective “barrel set” HRT after the nitrate was removed.

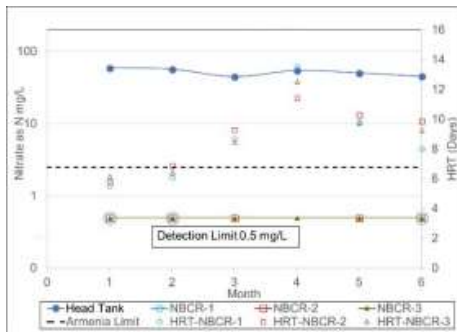


Figure 3. Nitrate and HRT in NBCRs

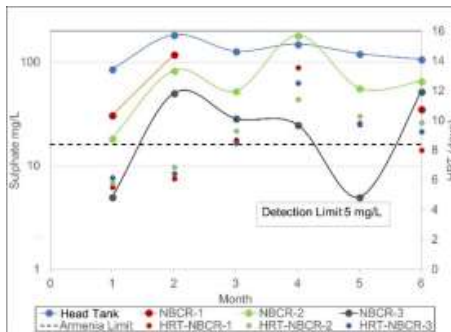


Figure 4. Sulphate and HRT in NBCRs

Please note that the trend lines shown in Figures 3 through 10 are provided to facilitate comparing data and/or interpreting it; direct interpolation between the data points is not intended or inferred.

3.2 Nitrate/Sulphate Biochemical Reactor (N/SBCR)

The MIW that was added to the N/SBCR for incubation was identical to that which was added to the NBCRs as previously described. This incubation phase focused on growing both a healthy denitrifying bacteria population and an SRB population. The initial HRT through the single N/SBCR test unit was adjusted to 5.7 days. The HRT in the N/SBCR was varied intentionally (Figures 5 and 6) to observe the performance response to this primary design parameter.

The pH of the MIW rose from an average of 3.6 s.u. [influent] to an average of 6.6 s.u. in the N/SBCR effluent for the entire 26 weeks of testing. The N/SBCR was able to lower the nitrate concentration to BDL for the duration of the test (Figure 5). The concentration of sulphate in the N/SBCR decreased to BDL in the first and fifth months of testing. Sulphate removal in the interval after the first month appears to plateau near or above the Armenia standard even though the HRT was lengthening. Sulphate removal efficiency appeared to suffer in the final sampling event, perhaps in response to shortening of the HRT to about eight days.

N/SBCR was configured to evaluate if nitrate and sulphate would be removed in the same BCR. However, the results indicate that a SBCR would likely be required to remove sulphate to the required Armenia sulphate standard. However, future pilot testing may still include an N/SBCR with a slightly longer HRT to fully resolve the issue.

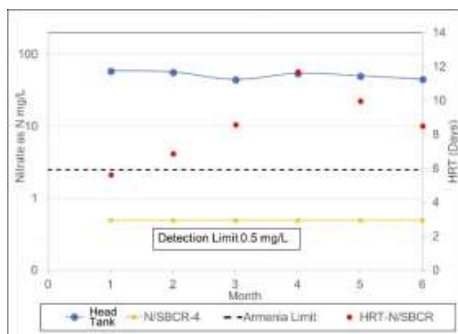


Figure 5. Nitrate and HRT in N/SBCR

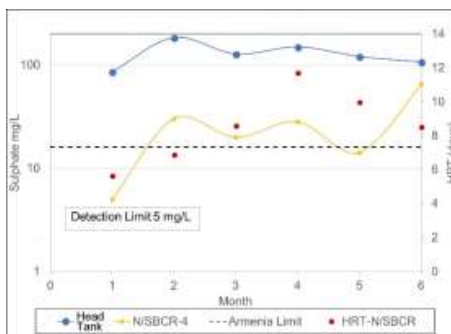


Figure 6. Sulphate and HRT in N/SBCR

3.3 Sulphate (Only) Biochemical Reactors (SBCRs)

Initially, surrogate MIW used to fill the SBCRs was prepared using tap water to which aluminum sulphate and iron sulphate were added; nitrate was not added to this water. This incubation phase focused on growing a healthy population of SRBs only. The flow through the SBCRs commenced at an initial average HRT of 6.3 days. It should be noted that the effluents from the NBCRs were mixed in the aeration tank (AT in Figure 2) and the flow was evenly distributed to all three SBCRs. As with the NBCRs, the HRT in the SBCRs varied (Figures 7 and 8). Since the NBCRs and the SBCRs were connected in series, HRT changes (e.g., increases) in the NBCRs were by default reflected in the SBCRs HRTs.

During the six-month test, the SBCR effluents typically exhibited a pH of about 6.7 s.u. Most of the pH improvement occurred in the NBCRs whose effluent pH averaged 6.2 s.u. The slight pH improvement in the SBCR could be attributable to either limestone dissolution or bicarbonate production coincident to SRB activity. However, since the sulphate concentration was relatively low (~150 mg-L⁻¹), it is likely that limestone dissolution was primarily responsible for the pH improvement in the SBCRs. This assumption was somewhat confirmed by typical increases observed in calcium and magnesium concentrations in the SBCR effluent samples compared to the calcium and magnesium concentrations reported in the SBCR influent samples. These design parameters will be further assessed in the next phase of testing.

Figure 7 indicates that the SBCRs were able to maintain the concentration of nitrate at levels below the detection limit during the test. The SBCRs decreased the residual sulphate contained in the combined NBCR effluents to BDL with few spikes. SBCR-2 and SBCR-3 sulphate removal performance was typically better than SBCR-1 which contained mostly straw (60% by weight) and no wood chips. Regardless, all SBCRs achieved the required Armenia sulphate concentration (Figure 8).

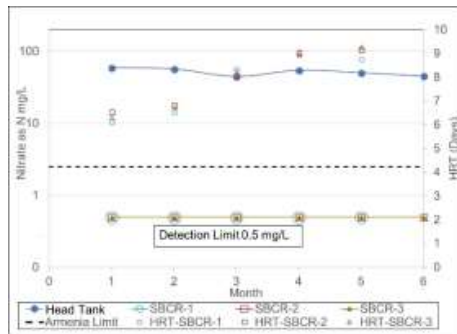


Figure 7. Nitrate and HRT in SBCRs

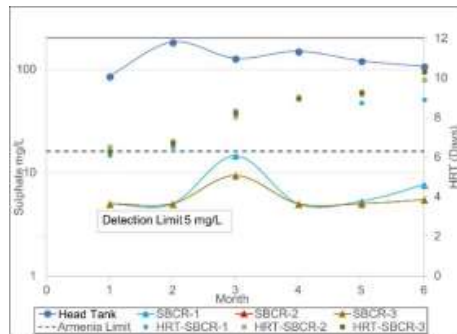


Figure 8. Sulphate and HRT in SBCRs

3.4 Sulphide Scrubbers (SCRs)

Untreated MIW was not added to the SCRs at their commissioning. Rather, they were filled with the effluent of the SBCRs once the flow was started. The SCRs received flow at the initial average value of 16.3 mL·min⁻¹ which was the combined flow from the three SBCRs evenly distributed among the three SCRs.

The average pH in the SCRs was 6.8 s.u. (average of all three SCRs) throughout the test interval. Data shown in Figure 9 indicates that the SCRs consistently maintained the concentration of nitrate BDL and below the Armenia limit. In addition, the SCRs were able to maintain the concentration of sulphate BDL. Some SCR effluent samples exhibited sulphate levels above the detection limit but every SCR effluent sample was still below the required Armenia sulphate concentration (Figure 10).

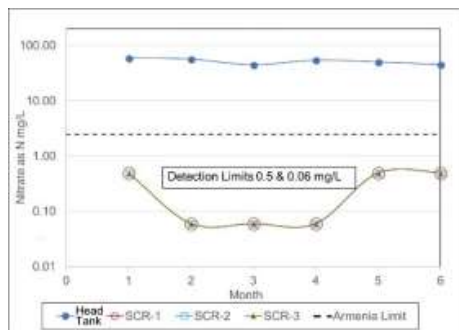


Figure 9. Nitrate Concentration in SCRs

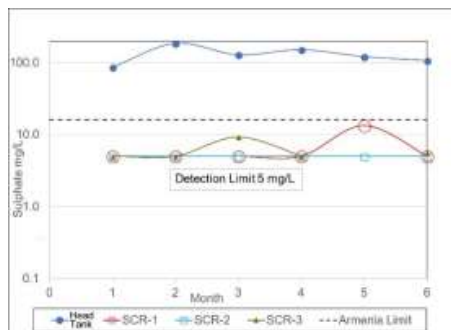


Figure 10. Sulphate Concentration in SCRs

Sulphide concentration ranged from 0.1 to 0.5 mg-L⁻¹ in SCR-1 and BDL to 0.7 mg-L⁻¹ in SCR-2. If this sulphide was allowed to oxidize, it will become sulphate. These low numbers represent very favorable overall sulphide removal rates. So, even if the sulphide in these SCRs is converted to sulphate, the final sulphate concentration in the individual barrel set effluents would comply with the standards.

SCR-3 sulphide concentration was elevated in month 4 and month 6 samples (13.7 mg-L⁻¹ and 8 mg-L⁻¹, respectively). If this sulphide was allowed to oxidize it would generate sulphate concentrations that would not comply with the Armenia standards. However, these were only two elevated values, the other four sulphide values were comparatively low and they would have complied with the standards if converted to sulphate. This aspect of final effluent polishing will be assessed in further testing.

Other design parameters not considered in this paper will be addressed in future test work at the mine site. For example, the aeration tank and settling tanks could be replaced with a more passive aerobic wetland zone and the final SCR effluents would also be polished in an aerobic wetland or similar process unit.

4 CONCLUSIONS

The six-month performance of the test units is encouraging enough to suggest that passive treatment methods should be capable of producing effluents that meet the Armenian nitrate and sulphate standards for the site.

The NBCR test results (i.e., NBCR-3) mildly suggest that the inclusion of “electron-shuttling” biochar in the media mixture could improve performance.

A relative lack of limestone (as seen in NBCR-1) could negatively affect ORP and pH. Due to the overabundance of straw and relative lack of limestone in the media, pH-depressing fermenting bacteria may have overpowered the denitrifying population. Adding limestone appeared to correct this imbalance. Calcium and magnesium data suggest that pH improvements in a BCR cells could be attributed to dissolution of the limestone component that was common to all media mixtures.

The lack of wood chips and an overabundance of straw (i.e., SBCR-1) in an SBCR may affect sulphate removal performance. The reason or reasons for this observation are undetermined at this time. But the apparent importance of wood chips in an SBCR media mixture appears to have been demonstrated.

N/SBCR-4 appeared to remove both nitrate and sulphate in a single treatment unit; this too is encouraging. However, the HRT's were not sufficiently long to allow sulphate removal to achieve discharge goals. If the optimal HRT could be determined, perhaps in a dedicated pilot cell, this finding could lead to a redesign of the full-scale passive treatment system into a smaller, more-compact footprint. This could eliminate the aeration step provided by the aeration tank and settling tank units in the bench scale barrel sets as shown in Figures 1 and 2 from a full-scale system.

The combined HRT of both NBCRs and SBCRs for removal of nitrate and sulphate to BDL ranged from 12 to 22 days during the test. It is possible that an N/SBCR with a comparable HRT range would behave similarly to the BCR-in-series configuration which was tested.

Future testing at a larger, pilot scale is anticipated. However, simultaneously conducted bench-scale tests may allow the refinement of what appear to be significant design features such as the “ideal” biochar and limestone proportions, and the kinetic effects of temperature on microbial activity.

5 REFERENCES

- Interstate Technology Regulatory Council (ITRC), 2013. Biochemical Reactors for Mining-Influenced Water. Accessed April, 2017.
- Reynolds, Tom D. and Paul A., 1982. Unit Operations and Processes in Environmental Engineering. Second Edition. Boston, MA: PWS Publishing Company. ISBN 978-0-534-94884-9
- Xu, Shengnan, Dinesh Adhikari, Rixiang Huang, Hua Zhang, Yuanzhi Tang, Eric E. Roden, and Yu Yang, 2016. Biochar-Facilitated Microbial Reduction of Hematite. Environ. Sci. Technol., DOI: 10.1021/acs.est.5b05517 • Publication Date (Web): 02 Feb 2016

Impact of Calcium Hydroxide on the Equipment and Process of Oil Sands Tailings Treatment

K. Rahal

FLSmidth, Midvale, Utah, U.S.A.

J. Fox and J. Leikam

Graymont, Salt Lake City, Utah, U.S.A.

M. Tate

Graymont, Toledo, Ohio, U.S.A.

N. Romaniuk

Romaniuk Consulting, Edmonton, Alberta, Canada

ABSTRACT: Fluid fine tailings (FFT) from oil sands mining operations have proven difficult to dewater and reclaim. Complex water chemistry, clay particles, and residual bitumen in tailings slurry are obstacles for efficient and economic dewatering.

This study focuses on how hydrated lime addition affects the dewatering process for FFT. The addition of hydrated lime to the FFT results in two beneficial modifications of the clay particles. At pH above 11, soluble calcium exchanges with sodium at the surface of the clay. At pH above 12, silica and alumina in the clay become soluble and chemically react with calcium to form cementitious compounds. Combining these effects results in treated tailings that are much more efficiently dewatered.

This paper will compare the settling in simulated thickeners of FFT with lime to traditional flocculent addition. This paper will also present the subsequent impact of filtration rate and area on the filter costs.

1 INTRODUCTION

1.1 Problem Statement

Athabasca oil sand tailings have proven difficult to treat and dewater. A tailings slurry containing process water, sand, clay, and a small amount of residual bitumen is produced as a byproduct of the bitumen extraction process (Kasperski 1992). Fine clay particles segregate from these tailings and collect in ponds. These fine tailings, called fluid fine tailings (FFT), settle to approximately 30%-35% solids (Beier et al. 2009) over several years but have not consolidated further over decades of storage.

The use of flocculants has been examined to improve settling and dewatering by creating large flocs of fine clay particles in FFT. Limitations in the percentage of solids achieved and increases in the plasticity index of FFT treated with flocculants have made these treated tailings difficult to reclaim as landforms.

Though many technologies have been explored, finding a technology which is technically and economically feasible for creating landforms with treated FFT has been difficult (BCG 2010).

Both Hi Rate and Hi Density thickeners are used in the oil sands industry. However, slow settling rates increase the size and cost of the thickeners. In addition, relatively low underflow densities still leave significant amounts of water in the tailings. Filtration could be used to facilitate further dewatering of flocculated MFT. However, filtered tailings has been seen in the past as a cost-prohibitive process for larger throughput oil sands mines due to slow filtration times, low cake densities, and the subsequent impact on CAPEX and OPEX.

As low capacities have prevented the use of filters has high throughput mines, FLSmidth has invested in developing larger filter technologies to handle increased throughputs. FLSmidth has commissioned and operated the “colossal” 2 by 4 meters high pressure filter press, which currently has the highest capacity of any operational pressure filter. FLSmidth is also currently developing

a 3 by 5 meters high pressure filter press in cooperation with an industrial partner. Due to these advances in capacity, the authors feel it warrants investigating the impact of calcium hydroxide on the filtration rates of oil sand tailings.

The use of hydrated lime as a coagulant, with and without flocculants, in pressure filtration will be investigated in this work. The benefits of adding hydrated lime before and/or after thickening to increase the percent solids fed to the pressure filtration process will be explored. This work focuses on exploring the use of hydrated lime to improve pressure filtration dewatering, cycle time, filter cake strength development and capital cost.

1.2 Coagulation vs Flocculation, what is the difference?

Coagulation and flocculation are often used synonymously but are quite different (Drew 1994). Coagulation is the addition of a destabilizing agent to reduce the electrostatic repulsion of suspended particles by cation exchange or chemical reactions (Tate et al. 2017). Treatment of oil sands tailings with several coagulants, including lime, gypsum, alum, carbon dioxide, and sulfuric acid has been explored (Matthews et al. 2002) with some challenges and success. Flocculation is used to increase the settling rate of fine particles by using large organic polymers to capture suspended solids and form large agglomerates called flocs. Trapping the fine particles in flocs increases their density and allows for rapid settling. The effectiveness of the polymer is dependent on a number of factors including its type (anionic, cationic or nonionic), molecular weight, degree of ionization and mixing procedure. Some studies have investigated the use of both cationic and anionic polymers to enhance flocculation by bridging and charge neutralization (Lu et al 2016).

1.3 Surface Chemistry

How the additive interacts with particles is the key difference between coagulants and flocculants. Coagulants such as hydrated lime or gypsum can alter the surface chemistry of the particles in two ways:

Cation Exchange - Cations, such as sodium or magnesium, can be replaced by soluble calcium cations on the surface of clay particles. As seen in drinking water softening systems, this cation exchange is potentially reversible if the sodium concentration of the water surrounding the particle is high.

Chemical Modification – A coagulant can also destabilize particles by chemically reacting with them. It is well established in soil stabilization applications that as the pH is increased to 12.5, phyllosilicates can dissolve into their alumina and silica constituents which react with soluble calcium and water to form cementitious calcium aluminates and silicates. These reactions form stronger bonds that are more difficult to reverse.

Flocculants instead, interact by adsorbing particles onto the surface of a long-chained polymer. Since like charged particles repel each other, the properly charged flocculant can effectively neutralize the opposite charge which helps with agglomeration. While this does generate larger particles, the floc structure is weak and easily degrades and breaks apart during transportation and high shear mixing.

1.4 Mixing

One significant difference between coagulants and flocculants is how they can be mixed. Coagulants perform better when they are rapidly dispersed with intense, high shear mixing. Flocculants, on the other hand, require gentle agitation to capture particles with the polymer and form dense flocs that settle rapidly. Intense mixing can breakdown the long chains of polymer-based flocculants which makes them less effective. The presence of sand can also make the formation and retention of flocs difficult for polymer-based flocculants.

1.5 Hydrated lime as a coagulant in oil sands tailings treatment

Calcium hydroxide (the chemical name for hydrated lime) has been found to be an effective coagulant in a variety of applications including soil stabilization. In oil sands tailings treatment,

the water chemistry as well as the oil sands tailings characteristics impact how hydrated lime performs as a coagulant. Current work suggests that hydrated lime can be an effective coagulant when treating oil sands tailings but the method of addition and presence of bicarbonates must be considered. Hydrated lime can modify the surface of clays by cation exchange or chemical reactions. Besides potential coagulation benefits, hydrated lime can also benefit process water chemistry and turbidity.

1.5.1 Bicarbonate Role in Calcium Level of Release Water

Process water chemistry plays an important role in oil sands bitumen extraction and tailings treatment. Bicarbonate is an effective buffer used in many industries including the oil sands extraction process. Hydrated lime appears to react preferentially with calcium and sodium bicarbonates to precipitate calcium carbonate and increase pH of process water by creating sodium hydroxide, decreasing ionic conductivity (Tate et al 2016). Other forms of calcium, such as gypsum and calcium chloride, behave differently in a bicarbonate environment because their calcium is partially soluble in oil sands process water where they slightly lower pH and form stable complexes with the bicarbonates. When lime is used soluble calcium levels in tailings process water drop until the bicarbonates are largely depleted at a pH of approximately 11.5. Cation exchange is not seen with the hydrated lime treated oil sands FFT samples until this pH is reached. With gypsum and calcium chloride treated FFT cation exchange occurs at lower pH levels, but results in the addition of new chloride and sulfate anions that increases the ionic conductivity of the process water compared to lime. Another key advantage of hydrated lime is that the soluble calcium levels seen at high pH levels gradually are reduced by the absorption of carbonates into the process water. Treated process water appears to not only reduce in soluble calcium but also lowers in pH while restoring some bicarbonate back to the process water (Tate et al 2017).

1.5.2 Cation Exchange vs Clay Surface Changes via Pozzolanic Reactions

There are three steps that the process takes when adding calcium hydroxide. The first is calcium's preferential reaction with the bicarbonate species in the water. The second step occurs once soluble calcium is available after the bicarbonates have precipitated. At a pH of 11.5 or greater, soluble calcium will begin to displace sodium on the surface of clays through a cation exchange reaction. This removes some of the attraction of the clay particles to water and improves the settling of the tailings. The final step is the pozzolanic reaction which is a cementitious reaction that alters the surface of the clays and binds them to one another.

1.5.3 Effect on Complete Chemistry on Release Water

The benefits of hydrated lime can extend beyond the coagulation of clays in FFT. Lime is used regularly in water treatment processes to raise the pH of the water which allows for the removal of impurities and precipitation of many metals at elevated pH. Calcium's properties also allow for the precipitation of many anionic species, such as carbonates, sulfates, and fluorides. Lime is also used in water softening processes to precipitate calcium and magnesium. This results in an improved water chemistry that makes additional treatments easier. Meanwhile a higher pH will prevent acidic corrosion on dewatering equipment.

1.5.4 Improvement in Particle Size

Settling rate experiments were conducted to test lime's compatibility with current polymers to understand how coagulation with lime could improve thickening processes. It was discovered that the polymers had a more difficulty flocculating the ultrafine particles that were suspended in the tube. When hydrated lime was added those smaller particles became larger particles, which provides nearly complete fines capture and a more rapid flocculation. Improvements were seen in all three phases of the thickener: Before the polymer was added, in the resulting supernatant (if there were sufficient supernatant clays to analyze), and the underflow. Because of these improvements such as settling speed, the rate at which the underflow can be removed can be increased allowing

for more throughput and smaller thickeners. The increased clarity of the water will result in less accumulation of ultrafine particles and shorter residence times.

1.5.5 Turbidity

The most noticeable detail during the settling rate tests was the tremendous enhancement of the turbidity of the overflow water. When lime was added up to the point where the system reached a pH of 11 the process water had suspended ultrafine particles that clouded the water and accumulation of these particles should be avoided. But when sufficient amounts of hydrated lime were added to achieve a pH above 11.5, there were significant improvements in the water clarity. Despite having comparable total solids, the turbidity of some of the cylinders without lime were about 5 or 6 times more turbid than water that had optimal amounts of lime introduced; all while lowering the level of calcium from the previous levels. Removing the ultrafine particles results in high quality recycle water for tailings dilution water or extraction, which could improve the efficiency of the future dewatering process, such as thickening.

2 EXPERIMENTAL

2.1 Mixing Methods

Laboratory test results suggest that dry hydrated lime is not effective unless it is slurried in water prior to addition to the oil sands tailings. Results have shown that lime slurries must have low (less than 5%) solids content to be effective. When calcium hydroxide is added into the FFT it is imperative that the mixing be carried out in a specific fashion. If the lime slurry is too concentrated it can do one of two things, first, localized high concentrations of lime will result in extreme modifications of a small portion of clays while the majority of the mixture will remain unchanged. Second, undispersed clumps of hydrated lime form a physical barrier that limits the dissolution and availability of soluble calcium in the system. If dispersed well enough, the mixture will require minimal mixing to achieve maximum effect. Lowering requirements for labor, size, or capital cost to operate mixing equipment and dewatering equipment by improving throughput.

2.1.1 Percent Solids of Hydrated Lime Slurry

The first experiment was to determine the optimal lime slurry concentration by mixing the same amount of lime in various slurry concentrations and then blending the lime slurry with FFT. 4000 ppm $\text{Ca}(\text{OH})_2$ was added to 200 g FFT in slurries consisting of 1%, 5%, 10%, 20%, 30%, and 100% calcium hydroxide solids. After being thoroughly dispersed, 150 g of the mixture was then poured into the pressure filter for dewatering. An empty beaker was tared and analyzed every five minutes for the total filtrate generated during dewatering. Figure 1 shows how the slurry concentration affected the effectiveness of pressure filtration. In more dilute experiments, lime was able to disperse more effectively which facilitates better coagulation as demonstrated by a faster filtration rate.

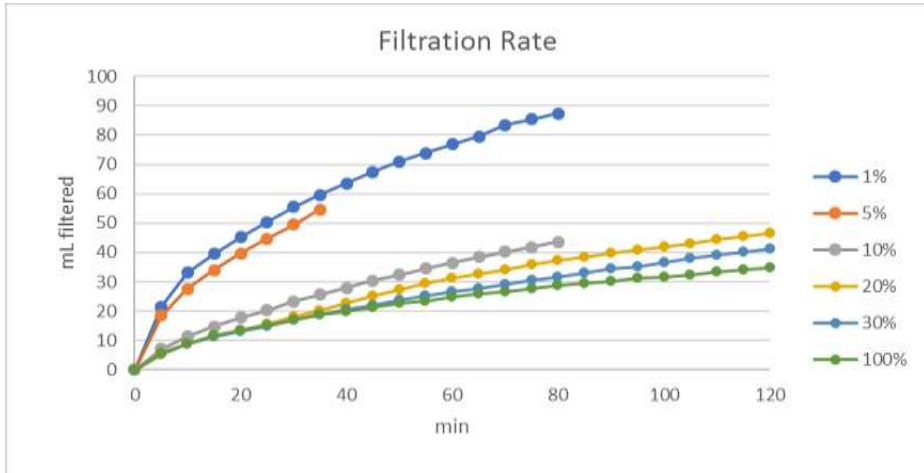


Figure 1. Filtration of FFT mixtures containing 4000 ppm hydrated lime added in various slurry concentrations (% mass of hydrated lime in water).

2.1.2 *Mixing Time Required*

The effect of mixing was demonstrated by comparing two different extremes of mixing. The first was mixed with 4000 ppm hydrated lime for 2 minutes with a glass stir rod relatively leisurely to display minimal mixing while an identical mixture was mixed with equal amounts of lime instead mixed with an overhead mixer on high RPM for 5 minutes to illustrate intensive high shear mixing. Figure 2 demonstrates that if the lime is thoroughly dispersed throughout the mixture, then any further mixing is unnecessary.

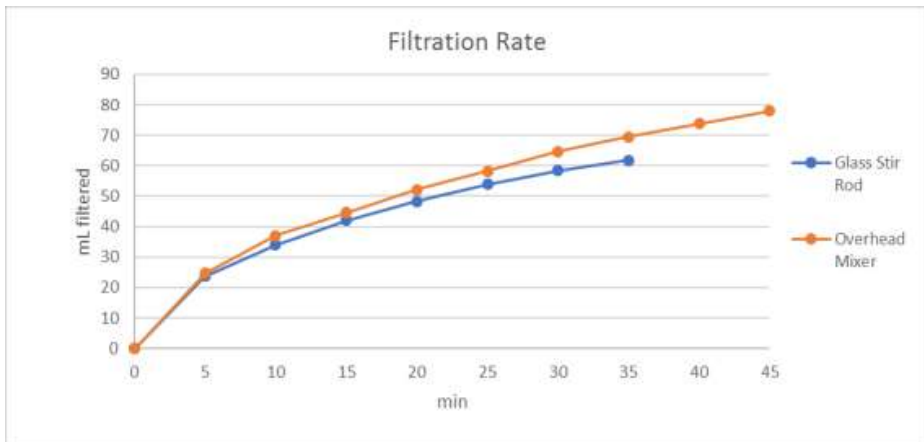


Figure 2. A comparison of the effect of minimal versus intensive mixing on the filtration rates of a 5% by mass of hydrated lime in water slurry with FFT. Minimal mixing was achieved using a glass stir rod for 2 minutes and intensive mixing was achieved using an overhead mixer at high RPM for 5 minutes.

2.2 Thickener Simulation Experiments

Thickening is an industrial process that has a lot of potential to improve dewatering in the oil sands industry when performed appropriately. A series of tests were set up to determine a multitude of settling parameters such as total settling after 30 min, initial speed of settling, turbidity, chemistry of the water, and particle size. FFT was diluted to 3% solids by weight into 1000 mL graduated cylinders using simulated process water. Various amounts of lime were added based upon the wet tailings mass and thoroughly mixed. 250 g/tonne of solids of a flocculating polymer was then added and carefully mixed, taking care to minimize shearing the polymer. The total settling after 30 minutes was intended to show the long-term capability to settle, whereas the time to reach 700 mL on the graduated cylinder was noted to show the initial speed of the settling. Table 1 displays the experimental results for lime pretreated to flocculation of FFT.

Table 1. Settling characteristics of flocculated lime treated FFT (diluted to 3% mass with simulated process water)

ppm of Lime	Time to settle to 700 mL (s)	Mud Line at 30 min (mL)
0	Not Observed*	155
750	8	190
900	5	245
1000	3	245
1250	4	275

*A clear mud line was not noticed until the flocculated particles had settled well below 700 mL.

Water samples of the supernatant were analyzed for water chemistry. Table 2 shows trends in dissolved ions with lime dose, initially calcium levels drop as it precipitates as calcium carbonate due to the rising pH. As more lime is added the equilibrium shifts toward soluble calcium. The results indicate that a particular lime dosage is required in order to achieve a desired concentration of calcium. Ca^{2+} , Na^+ , K^+ , SO_4^{2-} , Mg^{2+} , and Al^{3+} were analyzed on a PerkinElmer Optima 7300 ICP-OES while Cl^- and CO_3^{2-} were measured on a Thermo Fisher Dionex 2100 ion chromatographer.

Table 2. Water chemistry of supernatant water from settling test of flocculated lime treated FFT (diluted to 3% mass with simulated process water)

ppm of Lime	Ca^{2+}	Na^+	K^+	SO_4^{2-}	Mg^{2+}	Al^{3+}	Cl^-	CO_3^{2-}	HCO_3^{1-}	pH
	mg/L	mg/L	mg/L	mg/L	mg/L	mg/L	mg/L	mg/L	mg/L	
0	31	263	7	99	12	1	90	31	498	9.09
750	11	232	4	78	1	1	90	65	6	11.35
900	16	261	8	81	1	2	89	22	1	11.60
1,000	31	246	7	96	1	0	90	18	1	11.70
1,250	93	279	8	78	1	1	90	17	1	11.80

While performing this test it was noticed that there was vast improvement in water clarity. The experimental results suggest that coagulation of the finest particle with lime allows the polymer flocculant to capture all the particles, which results in rapid settling and the enhanced water clarity. Various samples were taken and treated with heptane to remove residual bitumen. The heptane was decanted and the particle size of the clays were analyzed. Table 3 shows the particle size of the solids through the settling experiment. The particle size before the flocculant was added was measured to demonstrate the effect of lime coagulation on the FFT solids. The supernatant solids demonstrate the sizes of particles not captured by flocculation, whereas the underflow solids show

the size of particles in the flocs. Particle size was analyzed on a Cilas 1190 dynamic laser diffraction particle size analyzer. Figure 3 is an illustration of how increased lime dosage increases water turbidity.

Table 3. Effect of lime coagulation on FFT particle size of unflocculated slurry, supernatant, and underflow post flocculation and settling

ppm of Lime	Before Polymer Addition		Supernatant		Underflow		Turbidity A at 750 nm
	D50 (μm)	D90 (μm)	D50 (μm)	D90 (μm)	D50 (μm)	D90 (μm)	
0	8	25	4	12	19	41	1.230
750	10	33	1	3	41	96	1.031
900	11	40	n/a*	n/a*	43	111	0.246
1000	15	49	n/a*	n/a*	38	87	0.120
1250	12	69	n/a*	n/a*	32	79	0.053

*Supernatant was clear and did not contain enough solids to analyze

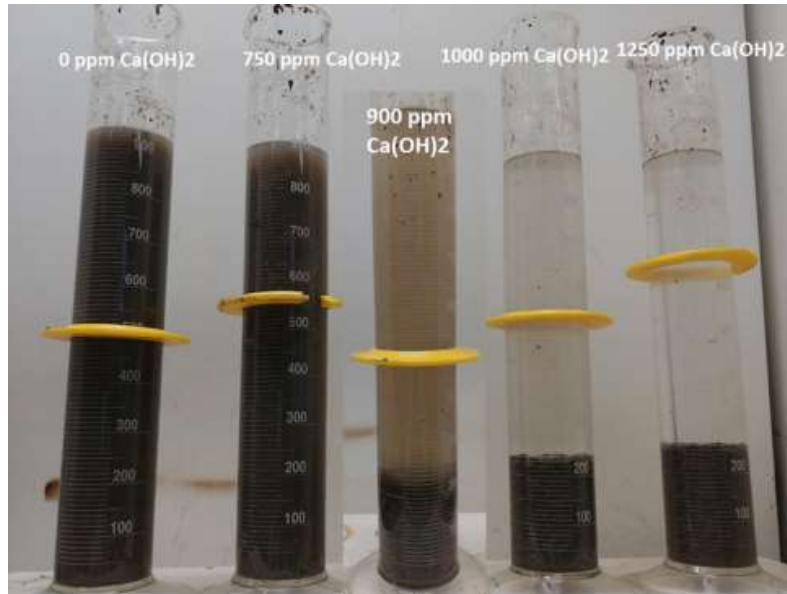


Figure 3. An illustration of the settling rate experiments showing side by side the improvement of the clarity of the water with increasing lime dose before flocculation of FFT (diluted to 3% mass with simulated process water).

2.2.1 Thickening Rate Experiments

Flocculant screening presents a qualitative and quantitative comparison for a range of flocculants typically effective in similar processes. Typical screen procedures were used to evaluate the effect of lime as a coagulant pretreatment to polymer flocculation. Observations made during flocculant screening include flocculant charge, flocculant molecular weight, floc structure, settling rate, supernatant clarity and general settling characteristics.

Flocculant solution is added drop wise to 250-mL graduated cylinders that contain slurry at a solids concentration that facilitates flocculant dispersion, while providing a qualitative comparison of floc structure and supernatant clarity. Settling rates measured through designated elevation intervals generate settling rate curves for quantitative comparison.

Static 5-L cylinder batch tests verify the initial settling velocity noted in flux testing, as well as other thickening sizing criteria. A 5-L cylinder diminishes sidewall effects.

To conduct the 5-L static test, the desired flocculant dose is added to the slurry using a mixing plunger. The mixing plunger adds flocculant to the slurry during mixing in the cylinder. This methodology simulates the mixing intensity and residence time typical in FLSmidth E-DUC® feed well systems. Mixing stops after flocculant addition and measurements of interface height over time are noted. The test runs through the initial settling time until the drop-in interface height ceases.

Wilhelm-Naide methodology provides data correlation of the static test results. The correlated results, using this method, represent unit area sizing for high rate thickeners designed to operate at an average effective bed depth of 1-m. The static test results also establish preliminary criteria for the design of high density and paste thickener as well which operate at bed depths greater than 1-m.

Testing was conducted with following feed mixtures:

- Flocculant only (considered the baseline test)
- Lime only (2000 ppm)
- Flocculant and lime

The results for settling velocity are shown in Table 4.

Table 4. Settling velocity for polymer flocculant, hydrated lime, and a combination of the additives after thickening tests.

Condition	Settling Velocity (m/hr)
Flocculant	47.95
2000 ppm Calcium Hydroxide	0.02
Flocculant & 2000 ppm Calcium Hydroxide	53.53

2.3 Filtration Experiments

FLSmidth conducted pressure filtration tests using a bench-scale filtration testing unit. The bench-scale testing unit can simulate FLSmidth’s recessed chamber configuration allowing for various feed solids concentrations, pressure profiles and cake thicknesses.

The recessed chamber test begins by pumping feed slurry at 125 psi into the double-sided chamber. FLSmidth records filtrate production and the resulting pressure profile with respect to time while the chamber fills. When the filtrate flow subsides, the cake consolidation portion of the test is complete. Cake blow was not used in this testing.

FLSmidth calculates the full-scale filtration rate using the form time, a standard mechanical time, a standard pump time, and the cake blow data for standard filter press testing. Full-scale filtration rates may vary depending on the size, pumping rate, and configuration, and degree of automation of the filter press and are reported as maximum instantaneous.

Testing was conducted with following feed mixtures:

- Flocculant only (typical of what an existing operation would experience)
- Lime only (4000 ppm)
- Flocculant and lime

Filtration performance is often measured in terms of filtration rate, which combines filter cycle times and cake densities. The test results for filter rates are shown in Table 5.

Table 5. Filtration rate for FFT treated with polymer flocculant, hydrated lime, and a combination of the additives after thickening tests.

Feed Mixture	Filtration Rate (kg/m ² /hr)
Flocculant only	1.727
4000 ppm calcium hydroxide	3.811
Flocculant and 4000 ppm calcium hydroxide	4.094

3 DISCUSSION

3.1 *Effects of Coagulation on Thickener Performance*

Pretreating oil sands tailings with a coagulant such as lime before entering the thickening process has been shown to increase thickener performance in lab scale experiments. The particle size data shows that by treating the mixture with lime the FFT particles, most likely clays, increase in D50 by 50 to 88% before the flocculant was added. The data measured for the settling test supernatant also shows that the smallest of the particles remain dispersed after flocculation; however, the coagulation demonstrated by lime improves the ability of the flocculant to bind and force to settle superfine particles, which results in high water clarity as the turbidity decreases by at least a factor of 5. Low turbidity decreases the amount of ultrafine clays in recycle water for tailings dilution and bitumen extraction, which will decrease the concentration of fine particles and improve future tailings treatment and bitumen extraction. By lowering the turbidity of the water, it removes the need of any clarifier systems which can lead to significant long term operations and maintenance savings.

3.2 *Speed of Settling*

The results show that the calcium hydroxide by itself does not increase settling rates, but when combined with the flocculant, the settling velocity increases by 11% over flocculant alone. This increase was not enough to affect the size of the thickener but merits further investigation into obtaining an economically optimal blend of flocculant and calcium hydroxide.

The test results also showed that the thickener underflow density remained between 41-43% solids for the conditions tested. Further testing of flocculant and calcium hydroxide mixtures might yield higher densities that would be beneficial to treatment of the underflow with a filtration process.

3.3 *Impact of Lime Coagulation on Recycled Process Water Quality*

High concentration of soluble calcium is a chief concern for the oil sands process water, especially when recycled to the extraction process. Dissolved calcium has been shown to hinder the extraction of bitumen when concentrations are above about 30 mg/L. By adding lime in the manner in which it is proposed, the soluble calcium levels will be able to be controlled and even lowered by the introduction of lime. During the first additions of lime the calcium levels were lower than the process water or FFT calcium levels were initially. Although the chemistry looks better around the 750-ppm range, the settling and clarity of the water suggest a slightly higher dosage. The dosage should be thoroughly examined as it can change depending on chemistry of the clays or the water used. While the pH of 12 may appear daunting, lime is used in a multitude of industries at that elevated pH. Soil stabilization and waste water treatment facilities use lime at saturated levels. With lime, the elevated pH levels are only temporary, lime treated water was shown to act as a carbon sink and will lower the pH in a matter of days while precipitation of soluble calcium as calcium carbonate. Lime's water treatment properties are not limited to calcium. It can be used to precipitate many other cationic and anionic solutes as well as improve dewatering and settling. Lime's water treatment properties alongside its clay coagulating capabilities make it the optimal coagulant for the oil sands tailings treatment for optimizing equipment efficiency and achieving dewatering requirements.

3.4 *Dosage of Lime*

In a series of experiments, it was determined that optimal lime dosages are dependent on multiple factors such as: bicarbonate concentration in the water, solids content, and pH. When performing pressure filtration, 4000 ppm $\text{Ca}(\text{OH})_2$ based on the total mass of the FFT was determined to be the optimal dosage on a majority of the FFT types tested. The reason for this is once the pH rises to a level above 12, pozzolanic reactions begin to dominate the system making cementitious compounds which dewater more readily than reactions that depend solely on cation exchange [Tate et. Al 2017]. As for the settling rate tests, the dosages were more dependent on the bicarbonate

concentration in the water. Because of the variances in different process waters, the optimal dosage varies from 700 to 1000 ppm $\text{Ca}(\text{OH})_2$ based on the total mass of the system when diluted to 3% solids.

3.5 Pressure Filtration

The results show that the use of 4000 ppm of calcium hydroxide increased the filtration rate by 121% over the base case of just flocculant addition in the thickener. The combination of flocculant and calcium hydroxide led to an increase in filtration rate of 137% versus just flocculant, an additional 16-point increase over just lime. This increase in filtration rates correspond to 56% and 58% decreases in quantity of filters for lime and flocculant/lime additions, respectively. This correlates to an equivalent reduction in filter CAPEX and OPEX. This indicates the potential for further testing to determine the impact of further lime addition on filtration cycle times.

The different levels of calcium hydroxide used in the thickening and filtration testing shows that a 2-stage addition approach is feasible if the optimal calcium hydroxide addition rate for the thickening step of dewatering is lower than the optimal for filtration.

4 CONCLUSION

Adding calcium hydroxide to the dewatering process allows the dewatering equipment to become more efficient and less expensive. More efficient equipment increases throughput of tailings, which may decrease capital expenditures as smaller or fewer thickeners would be required. Because lime is relatively inexpensive compared to other additives, there are potential savings in operating expenditures. Quick dispersion and lower residence time increases the thickener efficiency and usefulness in making dense underflow faster allowing for fewer or smaller, less intrusive thickeners.

By adding lime before the flocculant, it was shown that the ultrafine particles were captured. This is crucial as current methods have been unable to capture the troublesome finest particles. By capturing these particles, the water removal process and equipment can work more efficiently thus more economically. In addition to the improvements in water removal, the water sent back to the extraction process will be of higher quality, with lower total suspended solids and controllable soluble calcium levels, which should improve bitumen extraction performance.

Low capacity pressure filtration hasn't had the capacity to handle the throughput of the oil sands industry. With hydrated lime used as a coagulant above a pH of 12, the effects are more permanent, and have been shown to withstand the pressures of a pressure filter. This permanent effect allows for the pressure filters to work at more optimal rates than they would without treatment or with flocculant alone. As a result of increased efficiency in the pressure filtration and thickener, the amount of pressure filters required would be reduced by almost 60%. This paper shows that further improvements in filtration rates in future studies and larger capacity filters in development may provide an economical solution to the oils sands tailings reclamation issues.

Hydrated lime as a coagulant demonstrates compelling potential to provide inexpensive improvements to many areas of the tailings management and water purification such as water purification, thickening settling velocity, and overflow water clarity.

REFERENCES

- Rogers, C. D. F. and S. Glendinning, S. 1996. Modification of Clay Soils Using Lime. Lime Stabilisation, Proceedings of the seminar held at Loughborough University Civil & Building Engineering Department on 25 September, 1996, Thomas Telford. 99-1142.
- Lane, S. (1983). Lime Coagulation and Stabilization of Total Oil Sands Tailings. Petroleum Society of CIM, 83(34), 33rd ser.
- Richard J. et al. (2002) MANAGEMENT OF OIL SANDS TAILINGS, Petroleum Science and Technology, 20:9-10, 1025-1046, DOI: 10.1081/LFT-120003695
- Little, D.L., 1999. Evaluation of Structural Properties of Lime Stabilized Soils and Aggregates – Volume 1: Summary of Findings, National Lime Association, 1- 97.

- Caughill, D.L., Morgenstern, N.R., & Scott, J.D. 1993. Geotechnics of Non-Segregating Oil Sand Tailings, *Canadian Geotechnical Journal*, 30, 5, 801-811.
- Beier, N., M. Alostaz and D. Segó, 2009. Natural dewatering strategies for oil sands fine tailings. IN: *Tailings and Mine Waste '09*, Banff, Alberta. University of Alberta, Department of Civil & Environmental Engineering, Edmonton, Alberta.
- Kasperski, K.L. 1992. A Review of Properties and Treatment of Oil Sands Tailings, *AOSTRA Journal of Research*, 8, 11.
- Tate, M.J., Leikam, J., Fox, J., and Romaniuk, N., 2017, Use of Calcium Hydroxide as a Coagulant to Improve Oil Sands Tailings Treatment, *Tailings & Mining Waste Conference 2017*, Banff, Alberta, Canada.
- Tate, M., Leikam, J., Romaniuk, N., Ozum, B., & Scott, J.D. 2016. Understanding the Impact of Calcium Compound Addition on Oil Sands Water Chemistry, *Tailings & Mining Waste Conference 2016*, Keystone, CO, USA.
- Matthews, J.G., Shaw, W.H., Mackinnon, M.D., and Cuddy, R.G. 2002. Development of Composite Tailings Technology at Syncrude. *International Journal of Surface Mining, Reclamation and Environment*. Vol. 16, No. 1, pp. 24-39.
- Drew, 1994, *Principles of Industrial Water Treatment*, Ashland Chemical Company, Boonton, New Jersey pp 280-293.
- Lu, Q., Yan, B., Xie, L.Huang, J., and Zeng, H., 2016. A two-step flocculation process on oil sands tailings treatment using oppositely charged polymer flocculants, *Science of the Total Environment*, 565, 369-375.

Minimization, Treatment, and Monitoring of Acid Waters Generated in the Prometida Mine Waste Dump

C. Del Castillo Macedo

Buenaventura Company of Mine, Lima, Peru.

Abstract: Orcopampa mine has been working in various different techniques to minimize the acid water generation in its mine waste stockpiles, to treat effectively acid water, to implement new and innovative treatment systems. This will make possible to have an effluent that has an adequate quality to comply Peruvian environmental legislation so that the communities in agricultural, livestock and fish farming activities can reuse it. The main purpose of these projects is to obtain economic, environmental and social benefits to achieve sustainability for mining activities.

1 INTRODUCTION

Unit mining the Orcopampa is committed to having optimal management of water resources, by focusing on improving its treatment systems. Thus, Orcopampa recirculate as much water as possible and minimizes the generation of acidic waters, especially in mine waste stockpiles since these features acid with high concentration of heavy metals significantly raise treatment costs and shedding volumes.

Works for minimizing the generation of acid water, allows optimizing treatment systems, obtaining an effluent, which, added to other technological improvements, can be reused by the communities in agriculture and livestock. This improves significantly the relations of the company with the community, building trust and cooperation between the two parts and bringing sustainability to the mining activity. The economic benefits are also very significant, because this considerably decreases the volume of acid water to treat and the generation and disposal of sludge. Implementation of reactive treatment systems and monitoring water quality are very important to track efficiency.

2 OBJECTIVES

There were three objectives to this study:

- To present the work that Orcopampa mine is doing to minimize the generation of acid water in mining waste stockpiles;
- To show the effectiveness of the new treatment systems that the Orcopampa mine has implemented to ensure the quality of their effluent so that it can be reused; and
- To present the economic, social, and environmental benefits of minimization of acid water in mine waste stockpiles.

3 DESCRIPTION OF PROJECT

The project that Orcopampa mine has been implementing is covering the Prometida mine waste stockpile (raincoat), where materials from underground exploitation of gold and silver are stored. There are also acid water treatment systems, and the mine has a reactive treatment system that works as a final filter, ensuring that effluents have similar characteristics to the natural water of

the Chilcaymarca River, which is the main body of water within the area of influence of the mining activity.

The mine does constant monitoring of water generated by the activities described above, in order to comply with the quality demanded by the Peruvian environmental regulations for mining activities.

Then describes each of the activities and innovations that Orcopampa has been doing to optimize their water resources management:

- Rain Coat in the mining waste dump Prometida (MWD-Prometida).
- Acid water treatment system.
- Reactive treatment system.

3.1 Rain Coat in Prometida mine waste stockpile.

The water generated in the mining component have high heavy metal concentrations and acidic characteristics. Table 1 shows physico-chemical characterization obtained by the realization of environmental monitoring.

Table 1. Characterization physical chemistry

Description	pH	E.C. (uS/Cm)	Total metals				
			Cu mg/L	Fe mg/L	Pb mg/L	Zn mg/L	Mn mg/L
Prometida stockpile (without raincoat)	2.33	3225	1.03	216.40	0.151	2.036	17.79

As shown in Table 1, the characteristics of these waters make hard their treatment due to they require the use of a large amount of chemical material and big sedimentation structures (ponds), in addition to demand longer working time of the people, resulting in considerable economic investment.

Orcopampa mine had to look for controls to minimize costs in water treatment, that began by applying rain coat, which is a control based on covering the Prometida mine waste stockpile with waterproof materials. Those can be geomembranes or other types of plastics, in order to prevent the rainwater to infiltrate the dump and generate acid water. By the implementation of this control, we can collect the rainwater through channels and discharge them directly to a natural water body (river); this discharge will not have negative effects since they are rainwater that were not exposed to materials that can alter their physico-chemical properties.

The behavior of the Prometida mine waste stockpile without the application of the raincoat is shown in Figure 1 and the behavior with the application of the raincoat is shown in Figure 2.

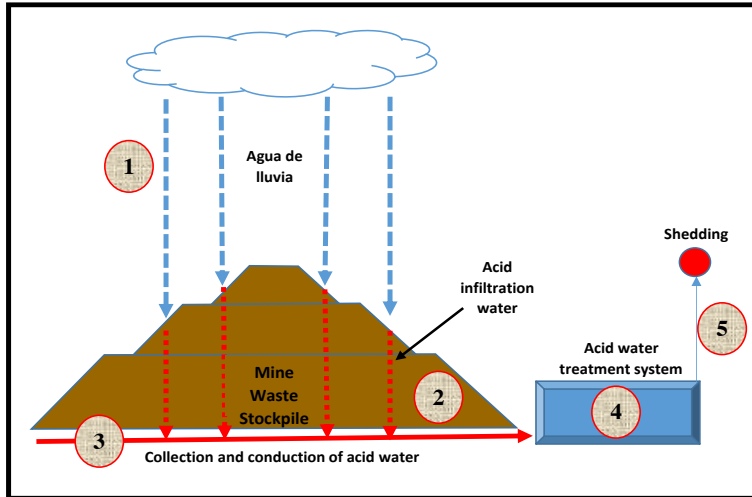


Figure 1. Behavior of the water in the mine waste stockpile without raincoat

The behavior of the mining waste Prometida without coating (raincoat) is given in the following ways:

1. The rainwater falling on the mine waste dump, changing its physico-chemical characteristics.
2. Rainwater seep into the dump, increasing contact time, acidifying to pH 2.3 (average levels) and leaching the components of the rocks and material, such as pyrite, sulphide, and others that make it contain high concentration of heavy metals that require aggressive treatment in order to comply with the quality that the Peruvian environmental regulations required.
3. Acid water generated in the mining waste dump are captured by the underdrain system and driven towards the acid water treatment system.
4. In the acid water treatment system, it applies calcium oxide to raise the pH and flocculants to accelerate sedimentation.
5. Finally, the treated water is poured into a natural water body (river), complying with the quality parameters required by law.

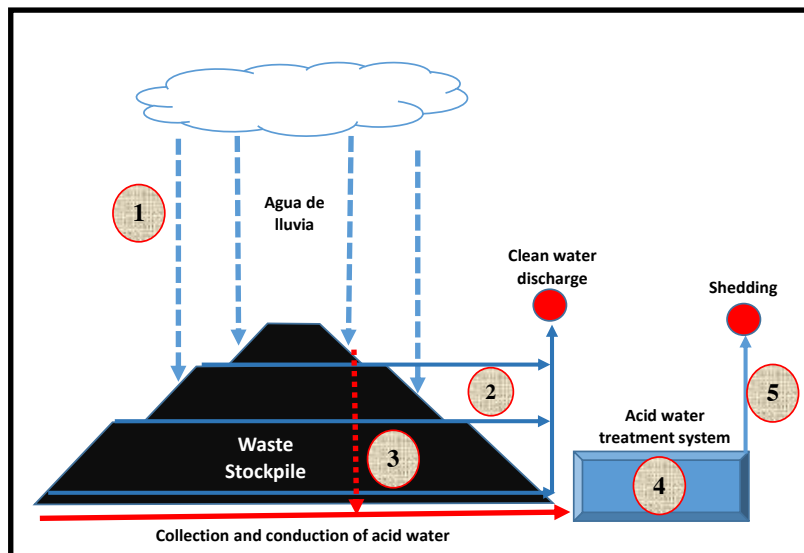


Figure 2. Behavior of the Prometida mine waste stockpile with raincoat

The behavior of the Prometida mine waste stockpile coated (raincoat) is given in the following ways:

1. Rainwater falls on the geomembrane used to cover the surface of the mine waste stockpile and this prevents water from contact with rocks and material, so its physico-chemical characteristics remain equal.
2. Rainwater are capture and derive without any contact to a natural water body by channels, and these not cause any impact on the environment due to they are clean water.
3. In some cases, a small amount of water can infiltrate and generate acidic waters that will be treat as in the figure 1. This can be avoid making a proper stick between the geomembrane and perform ongoing maintenance if holes appear due to wind and dust action.

In some mine waste stockpile, there are underground water with acidic characteristics, which cannot be captured or minimized by the rain coat, since this is a control for surface water and not underground water. To avoid this risk, mine waste stockpile should be built in areas that do not count with the presence of underground water or excavation does not reach to cut underground water.

4. Water that cannot be capture by the raincoat should be treat in the same manner indicated in the description of Figure 1.
5. Similarly, the shedding of the treated water must be does in the same way as in Figure 1.

The implementation of this control ensures a smaller volume of water treatment, achieving decrease up to 85% of the total flow.

3.11 Acid water treatment system:

The Orcopampa's acid water treatment system is a conventional one, in which applies calcium oxide to raise the pH of the water and flocculants to accelerate the agglomeration of the particles and to facilitate their sedimentation to finally obtain a clarified water. Figure 3 shows the flow of the treatment system.

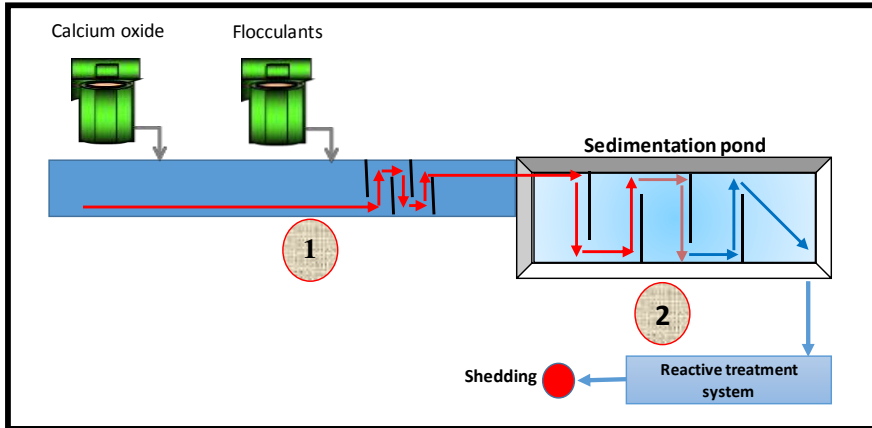


Figure 3. Acid water treatment system

Then describes the system of acid water treatment:

1. The water collected in the mine waste stockpile is discharged on a channel where is add calcium oxide to raise pH, then flocculants for the agglomeration of the particles, this is accelerated by the implementation of cells that allow a greater turbulence and making the mixture uniform.
2. Uniform water are discharged in a sedimentation pond, which also has cells but of larger size, with the purpose of offering to the pond a longer sedimentation time, the results are greater in the first cells, obtaining a clearer flow while it is approaching to the end of the pond. Finally gets a clarified water that is discharge to a treatment system reactive, which functions as a final.

3.21 Reactive treatment system:

The waters coming from the active acid water treatment systems are not optimal in quality by which require a last system of treatment to meet the parameters established by law. This system of treatment is different from passive treatment systems, which are based on the construction of ponds and sown with species of plants that facilitate precipitation of heavy metals and can be absorbed, in some cases, by the same plants.

Orcopampa mine has done scientific research to implement a system that is more optimal than conventional ones, so has achieved the implementation of a reactive treatment system. Its operation is based on simulating the conditions of natural wetlands, where are various species of plants and have a substrate that allows its self-sustainability, forming an ecosystem for the habitat of different species of animals.

The reactive treatment system that Orcopampa mine has been implementing is based on the construction of ponds, placing different types of substrates and planting different varieties of plants; its intention is that the treated water comply with the quality required by law to be able to be reused in agricultural activities by the community.

Figure 4 shows the conventional system which Orcopampa mine had before starting investigations to improve the functioning of the wetland. Figure 5 shows the reactive treatment system that the mining unit has been implementing as a result of the investigations.

Figure 4. Configuration of conventional wetland

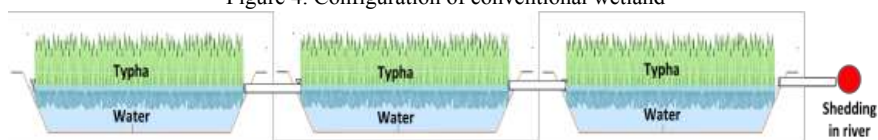


Figure 4. Configuration of conventional wetland

Then describes the process of conventional wetland.

The wetland consists of three continuous ponds in which was plant just one species of Typha. This system provides longer residence time to settle certain amount of heavy metals, but this was not enough to get optimum quality so it cannot be reused for irrigation or livestock activities, so the water is discharged into a body of water (river).

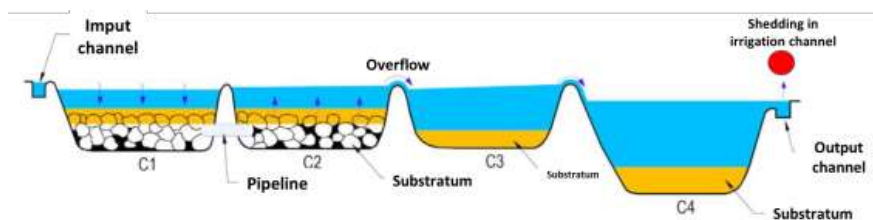


Figure 5. Configuration of the reactive treatment system.

Then described the reactive treatment system that Orcopampa mine is implementing:

Unlike the conventional system shown in Figure 4, this system has a substrate that is made of various types of organic material such as compost, bokashi and guano, which are combine with limestone and volcanic soil. This combination allows a rapid proliferation of plant species and facilitates the cationic and anionic exchange to accelerate the process of sedimentation and reuse of some metals and compounds by plants and bacteria that develop quickly in the new system.

1. Environment C1 and C2: the substrate of these environments is based on the application of biomass, organic debris, volcanic rock and limestone; these environments favor the absorption of potentially dangerous compounds by the characteristic of its substrate.
2. Environments C3 and C4: the substrate of these environments is based on the application of biomass, organic debris and limestone. They are environments due to their substrate characteristics become environments reductive, stimulating the growth of microbial favoring the removal of compounds such as sulphates.
3. Vegetation in the system is diverse; this favors the absorption of various compounds at a time through the roots, stems and leaves. The species that are mention before are shown in Figure 6.

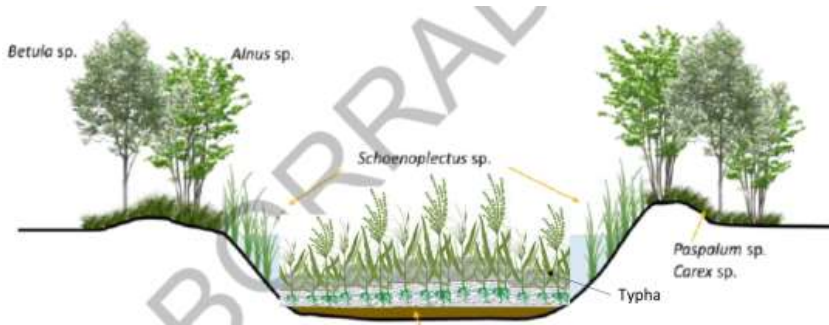


Figure 6. Plant Species

The plant species favors the absorption of dangerous compounds and accelerate the evaporation.

4. Once that the water goes through all the system this is discharged to a community channel, which finally is used for agriculture and livestock activities.

Table 2 shows the results of monitoring from the generation of acid water in Prometida mine waste stockpile, his treatment in the acid water treatment system and finally the reactive treatment system.

Table 2. Results of monitory

Description of Sample	pH	SO4 (mg/L)	E.C. (uS/Cm)	Total metals				
				Cu mg/L	Fe mg/L	Pb mg/L	Zn mg/L	Mn mg/L
Prometida – Mine waste stockpile	2.33	1,345	3,225	1.03	216.40	0.151	2.036	17.79
Acid water treatment system	7.86	912.19	1,803	0.22	1.29	<0.002	0.045	1.47
Reactive treatment system	7.07	350	945	0.002	0.23	<0.002	0.012	0.15

As shown in Table 2, the results of monitoring of the water generated in the mining waste dump are critical and need to be treat to raise its pH and minimize the concentration of heavy metals.

The characteristics of the treated water in acid water treatment system improve significantly, but still are not optimal in order to be reused for agricultural and livestock activities.

Finally, the water treated in the reactive treatment system that Orcopampa mine is implementing achieves the quality standards that the Peruvian environmental regulation requires to be reused in activities of irrigation and livestock.

4 BENEFITS

Water management from Orcopampa mine has several benefits, which are the following:

4.1 Environmental benefits.

- The implementation of the raincoat in the mine waste stockpile, allows that the natural rainwater is not affected by the contact with acidity generator material, thus it can be discharged directly into a natural water body, allowing a quick recharge of the body, which gives as a result the increase of water availability.
- The implementation of raincoat eliminates the possibility of generating dust, which is normally controlled by the use of water cisterns, increasing operations costs.

- Acid water treatment systems, allows the improvement of waters that have been impacted by the contact with acidity generator materials.
- Implementation a of reactive treatment system, allows ensuring that water complies with the strictest quality parameters so that it can be reused in other activities such as agriculture and thus avoid that the resource be poured without any value added.

4.2 *Social Benefits*

- The implementation of raincoat in mine waste stockpiles is an important environmental control that is appreciated by communities, which is a constant source of conflicts for mining companies. It can also be an important point to be exposed in internship and show the commitment that the companies have in caring for the environment.
- The implementation of reactive treatment system, allows having a water of the same or better characteristics as a natural water body, which can be used by communities in their daily activities such as agriculture, livestock or fish farming. This allows that the mining companies have good relations, giving the mining companies social sustainability for the development of its activities.

4.3 *Economic benefits*

- The implementation of raincoat in Prometida mine waste stockpile minimizes the costs of acid water treatment by decreasing in the flow to be treated. In the case of Orcopampa mine, initially spent a total of USD 45,000 for treating water generated in a 3-hectare dump. With the implementation of the raincoat, it achieved to decrease more the 85% of the flow, which means a saving of USD 38,250 that can be reinvested in other activities that the company creates convenient.
- The implementation of reactive treatment system, allows eliminating points of shedding into natural water bodies, which must be paid for the right of shedding (in Peru). Previously, the Orcopampa mine used to pay an amount of USD 135,000 annually, an amount that is saved and reinvested in the implementation of new environmental controls and research for new processes, which will allow the company have a better environmental management.

5 CONCLUSIONS

- The management of water resources in the Orcopampa mine is based on minimizing the generation of impacted water on mine waste dumps, tailings dumps, and others that may affect its natural characteristics.
- The mentioned environmental controls allow the company to count with several environmental and social benefits that provided sustainability to the development of their activities.
- Environmental controls that are implemented in the Orcopampa mine, allow us to have economic benefits, achieving savings of USD 173,250 annually that are reinvested in activities that generate a higher benefit to our operations.
- Environmental controls that are implemented are innovative controls that can be applied in any mining operation (operative and inoperative components), as well as they can also be applied wholly or partly.

5. PHOTOS



Photo 1: Prometida mine waste stockpile without rain coat



Photo 2: Prometida mine waste stockpile with rain coat (partially)



Photo 3: Acid water treatment system's sedimentation pond



Photo 4: Implementation process (reactive treatment system)



Photo 5: Reactive treatment system

Mitigation and Treatment Options for Selenium Control in Minesite Runoff

D.A. Jackson

Carollo Engineers, Inc., Costa Mesa, CA

ABSTRACT: This paper reviews recent progress in selenium control technologies and presents a basic methodology for developing water treatment plans that will help address the selenium control challenges at mine sites in a cost-effective manner. The method starts with understanding the mine site water - selenium balance and minimizing the requirement for “active” treatment (use of mechanical systems), which tends to be more cost-intensive than best management practices and certain other “passive” and “hybrid” mitigation measures. A wide range of passive and active treatment methods are surveyed and the methods that are ready for practical application, such as biological denitrification are described and compared on the basis of configuration, operational requirements, scalability and implementation challenges.

1 BACKGROUND

Selenium in stormwater runoff and contact water is a prominent current issue for coal and phosphate mining operations in West Virginia, Idaho, western Canada and an emerging issue for many other mining projects across North America. Selenium is liberated from waste rock during mining operations and is considered to have deleterious effects on certain aquatic organisms during their reproductive stage, at concentrations as low as 1 or 2 ppb. Runoff from mining operations can often have Se concentrations in excess of 100 ppb. Selenium is commonly associated with coal deposits, present in both the coal itself and in sedimentary rock overburden. Management of selenium can have major cost and permitting implications for a project and water management plans need to carefully consider the constraints associated with selenium control.

Selenium is located immediately beneath sulfur on the periodic table and behaves similarly in a mining context. It leeches out of waste rock dumps in a manner similar to acid rock drainage and in the process is oxidized to selenite and selenate, becoming bioavailable. The flux of free water in the dumps provides the oxygen for these processes and transports the mobilized selenium oxides out of the dump and into watersheds. Selenite is amenable to removal by various precipitation processes whereas options for removal of the fully oxidized selenate (the more common species in runoff) are much more limited.

2 UNDERSTANDING THE PROBLEM – WATER BALANCE, MINE PLANNING AND THE ENVIRONMENTAL CONTEXT

The water - selenium management plan for a mine site should be developed in concert with the mine plan. The potential costs associated with water and selenium management (projected to be

in excess of \$100 million for some coal mine sites) are of such a magnitude that accommodations in the mine plan to moderate these costs need to be considered. A thorough hydrologic / hydrogeological understanding of the mine site is fundamental and can be used in concert with variants of the mine plan to develop year-by-year water balances with seasonal water flows and selenium and nitrate concentrations for each affected catchment and watershed. Understanding groundwater flows on the mine site at a detailed level is important. Infiltration from rock dumps, drainage channels and ponds can bypass the runoff collection and treatment systems and has been noted as contributing to significant selenium levels in creeks in dry “no flow” conditions.

A geochemical model that relates mine activity (principally the volume of exposed waste rock) to the amount of Se release allows one to test different mine plan / water management scenarios. Predicting Se loading from waste rock varies with dump area, depth, volume, location and is site specific. It is generally agreed that there is a delay between waste rock placement and Se release – somewhere between 1 and 3 years. Site specific hydrology data and contaminant sampling data may be inserted into a model such as GoldSim® to predict selenium release over the mine life. Unfortunately, there is little data available on how the rate of selenium release changes through the decades of mine life and afterward. Consequently, these forecasts entail significant uncertainties and will have to be tuned as the mine operation proceeds.

The regulatory context for selenium discharge from mine sites is complex and evolving. In 2016, the USEPA promulgated a new "Aquatic Life Ambient Water Quality Criterion for Selenium in Freshwater" which for the first time includes tissue based as well as water quality objectives. In Canada, a new Coal Mining Effluent Regulation (CMER) is expected soon. It will remove this subsector from the Metal Mining Effluent Regulation (MMER) and may include stringent limits on selenium. Concurrently, water quality guidelines for Se are being developed or adopted by CCME and the Provinces of British Columbia and Alberta. The MMER is understood not to apply after mine operations are ceased, rendering the site under the jurisdiction of the Fisheries Act with its ambiguous prohibition on “deleterious substances”. An environmental assessment process (and / or the application of any of the mentioned regulations and guidelines) may result in site water quality performance objectives for a mine site that could include multiple in-stream Se effluent concentration targets for certain sampling points in various affected catchments or watersheds. Despite the regulatory uncertainty, some means must be found to establish effluent selenium targets for design purposes. If necessary, a range of values can be investigated. The time dimension of effluent selenium limits is a major consideration. A 10 ppb limit on a 30-day rolling average basis is much less onerous than a 10 ppb “not to exceed” grab sample basis, since the former allows some flexibility to adapt to changing site water flows and concentrations and will typically result in a reduced treatment plant size compared to the “not to exceed” basis.

During the operating phase of mines that employ blasting, nitrate is usually present with selenium and in concentrations that are typically orders of magnitude greater. The nitrate is predominantly derived from the use of explosives in the mining operations and therefore will diminish rapidly when operations cease, whereas selenium release will persist for many years or decades. Nitrate concentration is often the primary size-determining variable for selenium treatment systems because of the fact that (as explained below) most of the nitrate must be removed before selenium removal can be effected. Therefore, in situations where selenium discharge targets require active treatment, regulatory requirements relating to nitrate may not be of great consequence for treatment system costs. In contrast, any requirement to provide removal of sulfate as well as selenium and nitrate can have huge implications for the cost of treatment, as discussed in Section 5.

Mines that are located at the highest elevations of watersheds (a common situation for mines in the Western Cordillera) have a more challenging selenium management situation since the dilution capabilities of local watercourses will be low or non-existent. This location factor can easily make the difference between needing active treatment or not.

3 MINIMIZING THE PROBLEM WITH BEST MANAGEMENT PRACTICES AND WATER MANAGEMENT DESIGN

The cost of selenium and water management can be moderated by minimizing the volumes of incident rainwater, surface water and groundwater that could be exposed to contaminant sources

(principally waste rock) and subsequently requires treatment. Selenium contamination that will require active treatment for removal is to be particularly avoided to the extent possible due to the high capital and operating costs of this type of treatment compared to primary treatment (sedimentation optionally assisted by chemical addition).

Figure 1 is a simplified depiction of water / selenium interaction on a mine site and the means by which the requirement for active treatment of selenium may be minimized. Clean water diversion (structures to avoid contact between clean runoff and groundwater with waste rock) is well established and widely practiced. Where diversion around a valley-located waste rock dump is impractical, capturing upslope runoff and pipelining it through the dump may be. Clean water diversion combined with partial or full rock dump covers can dramatically reduce the water flux through rock dumps and consequently the release of selenium. Of course, rock dump covering, while excellent from the viewpoint of leachate control, entails geotechnical, logistical and material handling challenges that may limit its applicability to a given site.

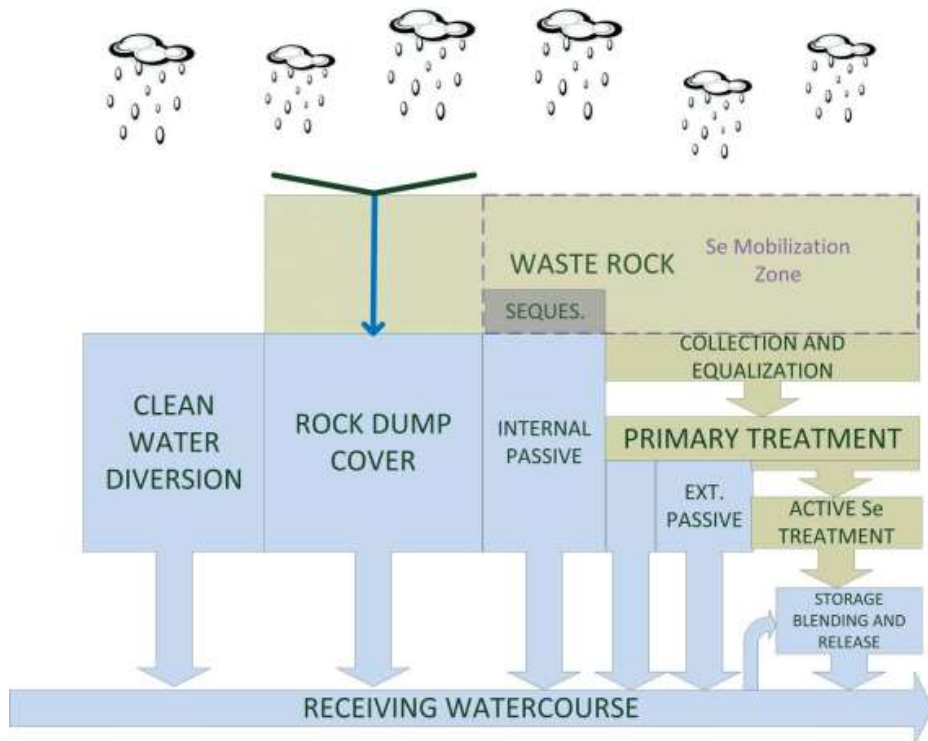


Figure 1. Simplified Depiction of Selenium Control Measures at a Mine Site

Any selenium-bearing waste rock that experiences a flux of water in an aerobic environment will tend to leach selenium. The levels of selenium mobilization for some affected waters may be such that primary treatment (sedimentation optionally assisted by chemical treatment) may meet discharge standards. Storage, blending and timed release may also help maximize the volume of water that may be released without selenium treatment. In other cases, some form of selenium removal is required. This can include internal passive, external passive and active treatment methods. While internal passive systems are typically constructed with considerable equalization / storage capacity, external passive and active systems are very sensitive to peak flows and it is necessary to optimize equalization capacities and discharge strategies to moderate capital costs for these more expensive facilities. For example, it is typically cost-prohibitive to treat the peak flow during the freshet; and the selection of an appropriate treatment design flow rate depends on

the interaction between the water balance, the engineered water management facilities (ponds and pumping systems), and the permitted discharge criteria.

Modelling has shown that ‘active’ water management –storing Se rich water and releasing during higher flow events - can be beneficial. Conversely, storage and release of ‘clean’ water during low flow periods can provide some benefit. Generally, the period immediately following the start of freshet is challenging to control (high flow and relatively high concentration). In a “top of watershed” setting, Se rich runoff from the mine site may increase before the flows in receiving creeks swell, resulting in temporarily higher Se concentrations in the creeks. In these situations, having storage capacity available in the sedimentation ponds at the start of the freshet can help avoid selenium discharge exceedances.

4 INTERNAL AND PASSIVE TREATMENT OPTIONS

It is not practical to totally eliminate water - waste rock contact at a mine site. For example, recently produced waste rock cannot be immediately covered and covering may be economically nonviable in many circumstances. In these cases, it may be possible to condition the contact water within the rock dump or pit lakes prior to release of the contact water into the environment. One promising general approach is to establish a saturated zone at a strategic location within a rock dump where reducing conditions will be maintained and where selenium mobilization through oxidation can be prevented or reversed. Variants of this approach include “in-pit subaqueous sequestration”, “saturated toe zone” (Claridge et al, 2011) and “saturated pit backfill” (Martin, 2013). These systems would be designed such that essentially all contact water within a rock dump would have to traverse the saturated zone before release to the environment. The saturated zone (essentially a buried pond) would be much smaller than the total volume of the contributing rock dumps. Field testing of the concept (Martin, 2013) showed that an annualized average hydraulic residence time of 145 days was more than adequate to reduce both selenium and nitrate to very low levels. The data suggested that considerably smaller hydraulic residence times might also be effective. More recently, evidence of in-situ denitrification and selenium bioremoval in unsaturated waste rock seepage has been noted (Stockwell et al, 2018). Many questions remain regarding the practicalities of design and long term performance of the concept, however, this internal, passive method for selenium control deserves further investigation.

A related approach uses a pit lake (Fig. 3) to establish reducing conditions at depth and remove selenium through reduction / precipitation (Martin et al, 2015). For all of these methods, it is necessary to avoid flooding the saturated zones with large fluxes of oxygenated water. Consequently, “post first flush” diversion techniques may be required during the freshet and some active management of the water facilities is required. Addition of chemical to control the redox conditions may be a more practical option with a pit lake than a submerged waste rock system because a pit lake will likely have point source inlets to which chemical can be added proportioned to flow, redox condition or other measurable variables.

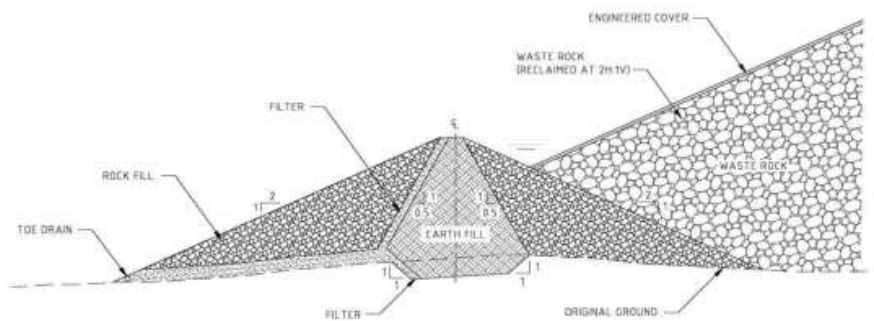


Figure 2. Simplified Depiction of a Saturated Toe Zone Impoundment

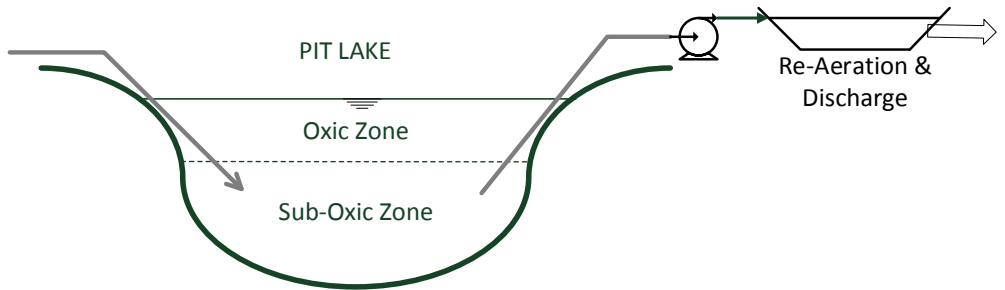


Figure 3. Simplified Depiction of a Pit Lake for Selenium Control

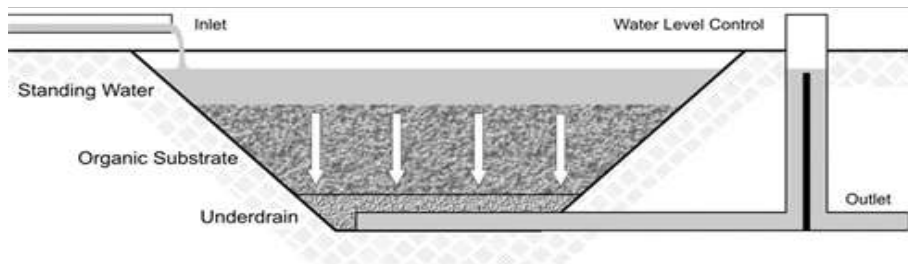


Figure 4. Simplified Depiction of an In-Ground Biochemical Reactor (BCR)

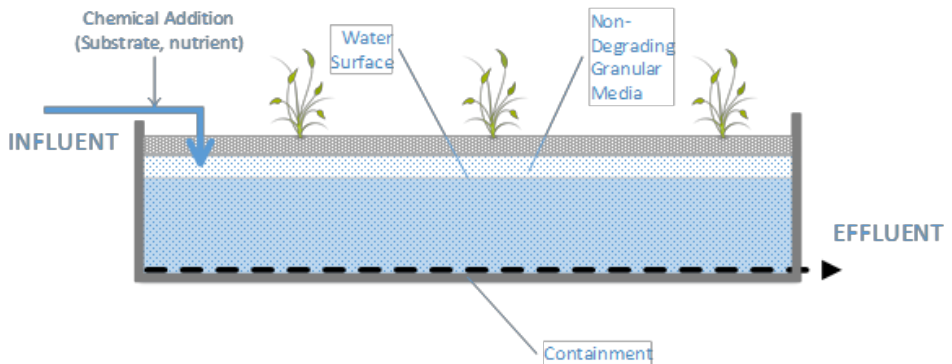


Figure 5. Simplified Depiction of a Semi-Passive In-Ground Packed Bed Reactor (PBR)

Other “external” passive methods have been applied to rock dump leachate and runoff to remove selenium and nitrate that has already mobilized. Wetlands have been employed but often require an impractically large area and are subject to seasonal changes that affect performance. An alternative passive system with better environmental control is the biochemical reactor (BCR). These are in-ground basins filled with specific mixtures and layering of organic media such as manure and peat. They are typically operated as upflow or downflow saturated biofilters, with the organic matter providing reducing conditions and the carbon source for biological denitrification and selenium reduction. Hydraulic residence times are on the order of several days. While effective at controlling nitrate and selenium, concerns with BCRs have included cold temperature performance, the release of soluble organic matter / nutrients and the long term performance of the systems once organic media are depleted. The scalability of the technology is also in question, as the vast majority of installations have been on the order of 45 m³/hr (200 USgpm) or less (Sandy,

2013) and the technology by nature exhibits relatively weak economies of scale. So far, BCRs are demonstrated to be appropriate for moderate flow applications in temperate regions, such as central Appalachia, although larger BCR systems have been built more recently.

A final passive option that overcomes some of the limitations of the BCR is the Packed Bed Reactor or PBR as depicted in Figure 5. This is similar to a BCR except that non-consumable media is used, typically gravel, coal screenings or some other granular material that can support a biofilm but is essentially inert. This method will typically require the addition of carbon source such as acetic acid to maintain appropriate redox conditions. As such, it is sometimes called a "hybrid" system with attributes of both passive and active systems. Work by duPreez et al (2018) to compare the performance of BCRs and PBRs on mine contact water containing both nitrate and selenium showed that the PBR could achieve higher levels of selenium removal (up to 96% compared with 89% for the BCR). The PBR achieved 91% removal at an HRT of 24 hours compared with more than 3 days for the BCR to achieve a similar level of performance. In addition, the PBR showed lower levels of residual nutrients. In summary, PBRs have the potential to be a more compact, controllable and efficient alternative to BCRs.

5 ACTIVE TREATMENT OPTIONS

This section addresses “active” methods that can be employed to remove nitrate and selenium from contact water. These are distinguished from the passive methods described above in that they are mechanical in nature and can be operated to respond to changing treatment conditions. Active selenium removal methods are many and varied. Several technology survey articles and reports have been prepared that compare and contrast available methods. The most comprehensive survey and the one most relevant to the mining industry was prepared by the North American Metals Council (NAMC, 2010) and subsequently updated (NAMC, 2013 and Sandy, 2013). It is understood that a further update may be forthcoming in 2019.

In comparison with more established selenium removal applications such as treatment of flue gas desulfurization (FGD) water, Mining Influenced Water (MIW) applications in Canada and the mountain states are characterized by high flows, low temperatures, relatively low selenium concentrations and stringent effluent discharge limits. For these applications, the methods that have been implemented to date for large scale mining runoff applications are almost exclusively based on attached growth biological treatment. Fundamentally, this is because selenate, being the dominant species encountered, is resistant to chemical precipitation methods and must be reduced before it can be removed. Chemical reduction of selenate is difficult and expensive, however, certain bacteria that are also responsible for denitrification have enzymatic mechanisms that can accomplish this task relatively easily.

5.1 Systems Based on Biological Reduction

Attached growth biological treatment systems use a media as a support structure and surface for the growth of a biofilm (complex colony of microorganisms) including the facultative heterotrophs that reduce nitrate to nitrogen gas and reduce selenate and selenite to elemental selenium. The insoluble selenium is precipitated to combine (and be removed) with the biological solids (biosolids, or sludge) that is a byproduct of any biological treatment process. The reduction process requires an electron donor supplied from organic sources such as acetic acid, methanol or molasses. The stoichiometric ratio of electron donor to electron acceptors (nitrate and selenate) must be carefully controlled to maintain appropriate oxidation-reduction (redox) conditions.

The redox profile for biological reduction reactions is well established. Important features of this profile relevant to selenium removal are as follows:

- a) Nitrate reduction (denitrification) must be largely complete before selenate can be reduced.
- b) Selenate reduction occurs at redox values of approximately 112 to 450 mV (2 to 8 pE), in the anaerobic region.
- c) More strongly negative redox encourages perchlorate reduction (if present) and sulfate reduction, producing hydrogen sulfide.

In MIWs, nitrate content will typically be several orders of magnitude greater than the selenium concentration so that variations in nitrate concentration can have a major influence on biological selenium reduction. MIWs also typically contain sulfate and conversion to H₂S is possible, however, this is undesirable from the viewpoint of odor and biotoxicity. Although sulfate can theoretically be removed with biological reduction, in practice, the cost of incremental electron donor, the complexities of handling H₂S production and biotoxicity concerns often render this impractical. If sulfate removal is required, substantial additional physical-chemical treatment facilities may be required.

5.2 Comparing Available Biological Reduction Systems

Three types of attached growth biological systems have been applied to selenium removal applications, namely Static Bed Biofilters (SBBs), Fluidized Bed Reactors (FBRs), and Moving Bed Bioreactors (MBBRs). They are chiefly distinguished by media type and motion (or lack thereof) within the reactors. In all three technologies, selenium will accumulate within, and be removed with, biosolids, however there are major differences in how this removal is effected. In terms of level of experience in industrial scale selenium treatment applications, SBB would be first, followed by FBR and finally MBBR.

Figure 6 is a simplified comparative schematic of how the three technologies would be implemented in a typical mine setting. It is clear that much of the infrastructure will be common to the three systems. For example, primary treatment, equalization and filtration will be required regardless of the system selected in order to moderate flows and the levels of suspended particulate in the runoff. All systems require the addition of a carbon source and nutrients to support the biological process and all generate biosolids that must be properly disposed of. Although other methods may be considered, the schematics assume that the biosolids (which will contain nearly all of the selenium) will be dewatered to produce a “dry cake” sludge product for disposal at a secure landfill, to minimize the opportunity for selenium remobilization. Consequently, biosolids thickening and dewatering equipment is common to the three systems. It is also likely that the systems will require aerobic biological post-treatment to both consume residual soluble organic matter and increase dissolved oxygen levels. Finally, these systems typically do not guarantee performance for temperatures below about 10C so heating may be required, depending on local seasonal conditions. Since heat fuels represent a high cost, heat integration is included to minimize this cost.

The SBB employs a media that (at least in normal operation) remains immobile. In contrast, the media in both the FBR and MBBR are in constant motion. In the case of the FBR, as represented by the Envirogen FBR™ process, a media consisting of sand or activated carbon is fluidized (kept in suspension) by the vertical flow of water in the cylindrical reactor. A variable recycle is employed to maintain a relatively constant velocity and bed expansion. In the MBBR process, the media consists of plastic “biomass carriers” approx. 1 – 3 cm in diameter that are shaped to provide a large surface area for biofilm growth. The biomass carriers are kept in suspension by fluid motion induced by a low speed impeller.

The SBB process is a semi-continuous flow through process whereby the bioreactor serves to accumulate and store biosolids as well as effect the biochemical reactions. For example, GE's ABMet™ process which has several full scale installations for treatment of selenium in MIW, is a conventional downflow activated carbon biofilter with periodic degassing and backwash. In a manner very similar to the common Biological Aerated Filter (BAF) process, the bioreactor must be periodically taken off-line and backwashed to strip out the accumulated biomass. The backwash must be thickened and dewatered.

The FBR and MBBR systems are flow-through, steady state processes with a continuous entrainment of biological solids in the treated effluent stream, requiring unit operations downstream of the reactors to remove solids from the full process flow. These solids must be separated from the effluent, thickened and dewatered. In this respect, they differ from the SBB which discharges biosolids only in the backwash mode. In normal operation, effluent from the SBB does not require a subsequent solids removal step. Given the turbulent nature and media collisions within the FBR and MBBR, the effluents may contain very fine particulate (including colloidal fractions) that is difficult to separate with conventional solids separation equipment and more advanced equipment such as ultrafiltration may be required to consistently achieve very low selenium target values (5 ppb or less).

Another area of difference is the semi-batch nature of SBB operation compared with flow-through steady state operation of the FBR and MBBR. Each SBB biofilter will be backwashed on a regular basis (perhaps daily). Each backwash dramatically changes the biomass content and therefore the microbial population of the reactor. A freshly backwashed reactor may be less efficient and require its effluent to be reprocessed in a “ripe” reactor for a period of time. There is also a question as to whether the steady state nature of the FBR and MBBR allows them to adapt more precisely and consistently to the particular characteristics of the influent. In the FBR and MBBR systems, there is a vigorous biomass control, a relatively constant sludge age (average residence time of biomass) and a high intensity of activity due to the high mass transfer kinetics (particularly so for the FBR). Gases generated in the process (which could include N₂, H₂S or even methane) are quickly stripped out of the systems and do not accumulate. In the SBB system, there will be noticeable changes in the microbe assembly between backwash cycles. Also, gases will tend to accumulate between backwashes and could cause channeling or episodic release (bubbling) both of which could affect performance. In cases of high nitrate loading, gas purging cycles may be required in addition to the normal backwash cycles.

The requirement to heat effluent is a major cost factor. Any substantial differences between the processes in tolerance for low temperatures would be a significant consideration. Indications are that FBR and SBB systems can perform at temperatures below 10C, however comparative data is scarce.

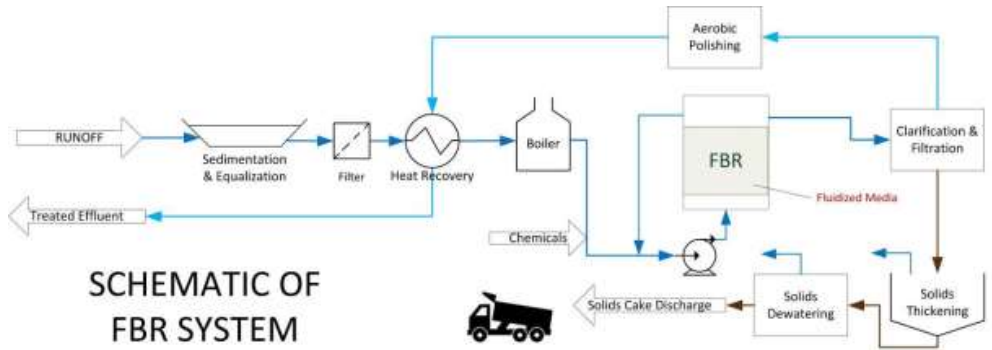
Hydraulic Retention Time (HRT) is an important variable for all three technologies. Excessive HRT can shift the redox toward a more negative region. Insufficient HRT can result in incomplete reduction. Since flows can vary dramatically seasonally at mine sites, the ability to adapt to changing flows is an important consideration. The SBB system addresses flow variations by employing multiple parallel modules, which can be used on an “as required” basis but with some serious constraints, namely that several weeks of acclimation would be required for the addition of a bioreactor, so that it must be done on a planned basis and not in response to short term runoff conditions. Similarly, once a bioreactor is taken offline and idled for several weeks, it cannot be immediately brought back online.

The FBR maintains a constant HRT for each bioreactor and a dedicated recycle flow is adjusted as required to maintain this, however long term operation at low flows would require modules to be shut down. Based on experience in other applications, MBBRs are expected to be tolerant of wide variations in flow, however, there is limited practical experience in selenium applications to support this supposition.

The foregoing discussion illustrates that the FBR and MBBR have a lot of similarities. The FBR is among the most volume-efficient bioreactor types available and can be expected to require less HRT than the SBB or MBBR for a given application. For FBR and MBBR, the principal tradeoff is between the reactor size and the mechanical and operational simplicity. Due to its simplicity, the MBBR may be more amenable to implementation in a distributed treatment scenario, where smaller plants are located at several sites, provided that a workable solids collection system can be developed.

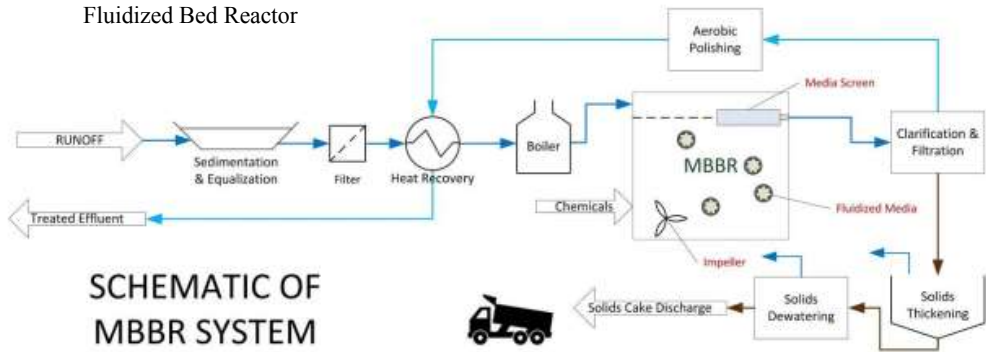
5.3 Comparative Costs of Active Treatment Systems

Current cost data for active selenium treatment systems is scarce, however, indicative costs for the three types of active treatments systems described herein can be estimated based on cost data included in the update to the major NAMC study (Sandy, 2013). The capital costs for a 3800 m³/day (700 USgpm) treatment facility were estimated to be between \$25 million and \$37 million, with MBBR having the lowest cost and SBB the highest. Operating costs were estimated to be between \$1.7 million/yr and \$2.0 million/yr for all three technologies. These estimates are out of date (probably high) and need to be revised in the light of technological advances and operational experience but provide an indication of how expensive active treatment can be. Also, no conclusions can be drawn regarding which technology would be most cost-effective for a particular application. Economies of scale can be expected to vary between the technologies and the ranking of costs could be different at higher flow rates. Each case would need to be investigated in detail to select the most cost-effective technology.



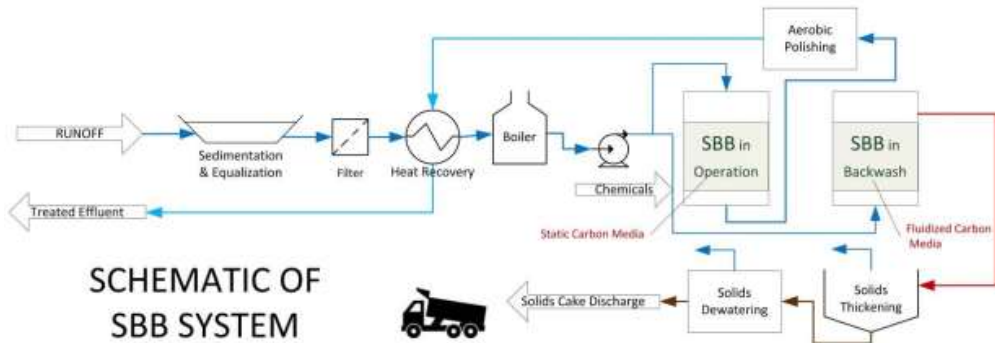
SCHEMATIC OF FBR SYSTEM

Fluidized Bed Reactor



SCHEMATIC OF MBBR SYSTEM

Moving Bed Bioreactor



SCHEMATIC OF SBB SYSTEM

Static Bed Bioreactor

Figure 6. Process Schematics for Several Active Treatment Systems for Selenium Removal.

6 CONCLUSIONS

A range of options is available for selenium control at mine sites. The cost of active selenium treatment is such that methods to minimize the volume of contact water requiring active treatment should be investigated and employed where practical. These methods include well-established practices such as clean water diversion, known effective but potentially costly methods such as

waste rock covers and novel passive and hybrid methods where the costs and long term performance are not well understood.

At the present time, for large scale (greater than 1500 m³/day) treatment of mine runoff in cold climates, biological reduction is the preferred treatment approach. Three types of such systems are currently available, namely Fluidized Bed Reactors (FBR), Static Bed Biofilters (SBBs) and Moving Bed Bioreactors. All of these technologies are being actively adapted for selenium treatment and unit costs are declining as operating experience accumulates. The systems exhibit significant differences with respect to solids management, scalability, and operational requirements that could be significant factors in making selections for a given application.

Semi-passive or "hybrid" systems such as the Packed Bed Reactor are developing technologies that offer an interesting and potentially cost-effective compromise between active and passive systems.

REFERENCES

- Claridge F, Funk W, Martin L., 2011 The Evolution of Mine Waste Management Practices in Western Canada WorleyParsons Canada Services Ltd.
- du Preez, Henlo, et al. 2018 Case Study for Passive and Hybrid Mine Water Treatment to Reduce Selenium Load. Presentation at NAMC-Selenium Working Group Meeting, June 13, 2018, Vancouver, BC, Canada
- Martin, A.J. et al, 2011. Biogeochemical Mechanisms of Selenium Exchange between Water and Sediments in Two Contrasting Lentic Environments Environ. Sci. Technol. 2011, 45, 2605-2612
- Martin, A. 2013 Assessment of Selenium Attenuation in Saturated Pit Backfill. Presentation at NAMC-Selenium Working Group Meeting, June 20, 2013, Vancouver, BC, Canada
- Martin, A.J. et al, 2015, In Situ Attenuation of Selenium in Coal Mine Flooded Pits. Proceedings, 10th International Conference on Acid Rock Drainage, Santiago Chile April, 2015
- North American Metals Council (NAMC) 2010 Review of Available Technologies for the Removal of Selenium from Water.
- North American Metals Council (NAMC), 2013 Review of Available Technologies for the Removal of Selenium from Water - Addendum.
- Sandy, T 2013. NAMC Whitepaper Report Addendum. Presentation at NAMC-Selenium Working Group Meeting, June 20, 2013, Vancouver, BC, Canada
- Stockwell, J and Martin, A.J. Nitrogen Isotope Enrichment as Evidence of In-situ Denitrification and Selenium Bioremoval in Unsaturated Mine Waste Rock Seepage. Presentation at NAMC-Selenium Working Group Meeting, June 13, 2018, Vancouver, BC, Canada

Passive Arsenic and Manganese Removal in Neutral Mining Influenced Water

T. Wildeman

Professor Emeritus of Chemistry and Geochemistry, Colorado School of Mines, United States

F. Vasconcelos

HidroGeo, Rua Rio Grande do Norte, 1.164 – Sala 501 Belo Horizonte/MG – CEP 30.130-131

ABSTRACT: Waters from three adits related to gold mining in Brasil are circum-neutral yet contain significant concentrations of arsenic and manganese. It is known that with passive treatment Mn can be removed using a limestone bed and As can be removed using lateritic material. However, the question is can these substrates significantly remove the other contaminant? Proof of principle experiments were conducted to answer this question. Limestone effectively removed Mn and this was catalyzed by the algae. However, As was minimally removed. Algae did enhance As removal. It appears that the arsenic is being removed by sorption onto the manganese oxyhydroxides. With laterite, As was effectively removed. However, algae impeded As removal to environmental limits. Manganese was somewhat removed by lateritic soil and again removal was enhanced by algae. High concentrations of As did not affect Mn removal. These results imply that a two stage system is necessary for treatment with laterite in the first stage because it can remove some of the manganese.

1 INTRODUCTION

Arsenic (As) and manganese (Mn) are two constituents of concern (COC) that can persist in mining influenced water (MIW) even when that water is circum-neutral. As a consequence, these two COCs are difficult to remove. In three waters from Brasil, both manganese and arsenic persist. The usual methods of passive treatment for these two COCs are quite different. So, the question is can either of these methods remove both As and Mn to concentrations below the regulatory limits. That is the question that this study strived to answer.

1.1 Arsenic

In MIW, the concentration of arsenic is closely related to the concentration of iron and the pH (Bednar, et al. 2006). In acid rock water where the pH is 3 or less, Fe(III) is soluble and Fe(II) can have a significant concentration. As the pH is raised and Fe(III) precipitates as ferric oxyhydroxide, As becomes adsorbed and is significantly removed from the water. However, under some circumstances, all of the arsenic is not removed and the result is water with a minimal concentration of Fe and a concentration of arsenic that can be considerably higher than the public drinking water concentration of 0.010 mg/L.

In a situation where active removal of arsenic is used, addition of an Fe(III) salt and precipitation of ferric oxyhydroxide is the usual method of treatment. However, in passive treatment where active addition of a reactant is not used and natural geochemical processes are relied upon for removal, treatment is more problematic. Nevertheless, passive treatment is more economical than active processes (Gusek, 1995) and so methods of passive removal of arsenic have been attempted with varying levels of success. For acid rock drainage, where the addition of alkalinity is essential, sulfate reducing bioreactors (SRB) are a passive treatment method of choice. In this reducing environment arsenic will be removed as a sulfide, either realgar or or-

piment. However, where arsenic is present in water treated by SRBs, the concentration level of As in the effluent appears to be removed only to a concentration of around 0.20 mg/L (Wilde- man, Filipek, & Gusek, 1994).

Attempts have been made to boost removal by the addition of a source of iron such as mag- netite or zero valent iron. This has met with some success in proof-of-principle tests and bench- scale studies but has not been attempted in a full-scale system (Pinto et al., 2001). If one is dealing with a neutral MIW with a significant As concentration the question is can a passive system be set up that mimics the absorption of arsenic by ferric oxyhydroxide that is used for active treatment? In the state of Minas Gerais in Brasil, where there is considerable waste from iron mining, the idea of using some type of material that has considerable Fe₂O₃ in some form to treat As is appealing. In this paper, this form of Fe₂O₃ is called laterite. Preliminary experi- ments have found this method for removal of As is feasible. However, the question of whether such material would remove both As and Mn is not known.

1.2 Manganese

Mn is a difficult COC to remove from MIW. MnS is quite soluble and removal by oxidation to MnO₂ is slow even in neutral water so, for active treatment, the pH has to be raised to between 10 and 11 to effect reasonable removal (Stumm & Morgan, 1996). For passive treatment, re- moval of manganese has been extensively studied because it is a persistent regulated contami- nant in neutral coal mine drainages (Rose et al., 2003). Clayton et al. (1999) studied the passive removal of Mn from MIW and found that two components, algae and limestone, are particularly effective in the removal of Mn. These results were also found for coal mine waters where the “go to” passive treatment option for manganese is an open limestone channel (Rose, et al., 2003, Denholm et al., 2008). However, such an open limestone system has not been tested for the removal of As.

1.3 The Waters to be Treated

Minas Gerais has long been a gold mining region in Brasil. Arsenic is often a signature COC in waters issuing from these gold mining operations (Pinto et al., 2001). Water chemistries in mg/L in three gold mining operations close to Belo Horizonte, MG are given in Table 1. The regulatory limits are for Minas Gerais waters. All analyses were performed at the Colorado School of Mines (CSM) by ICP-AES. Co, Cr, Cu, Pb, and Se are below the regulatory limits in all three waters. The Grande/Velha water had interesting chemistry. When it was shipped from Brasil it had concentrations of 11.0 and 0.71 mg/L of dissolved Fe and As. However, with a pH of 7.1, the iron rapidly oxidized and precipitated as iron oxyhydroxide. As a result, when ex- periments started the Fe was below detection limits and As was 0.030 mg/L. This change at- tests to the efficacy of arsenic removal by absorption onto iron oxyhydroxide precipitates.

Table 1. Dissolved water chemistry of three Minas Gerais gold mine along with Clear Creek water and the water regulations. All concentrations except pH are in mg/L.

Water	Bilcaho	Bela Fama	Grande/Velha	Clear Creek	Reg. Limit
pH	6.78	6.30	7.08	6.9	
Al*	0.029	0.029	0.055	0.050	0.100
As	2.09	0.024	0.030	BDL*	0.010
Fe	0.009	0.049	0.003	BDL*	0.300
Mn	0.14	0.13	5.0	0.003	0.100
Ni	0.007	0.007	0.003	0.002	0.025
SO ₄ ⁼	295	29	3400	78	250
Zn	0.016	0.014	0.045	0.072	0.180

*All concentrations except pH are in mg/L . BDL is below detection limits

2 MATERIALS AND METHODS

2.1 Materials

Mine waters were sent from Brasil for analysis and eventual use in the laboratory proof-of-principle experiments. However, to conserve the mine waters, Clear Creek water (CCW) in Golden, Colorado was used for the initial experiments. As noted in Table 1, CCW is close in chemistry to the Brazilian waters. In particular, sulfate is the dominant anion in all of the waters. Atomic emission standards of As and Mn were used to spike waters to concentrations that were higher than would be normally seen in natural waters.

The laterite chosen was consolidated so that 20 to 10 mesh particles could be used. High calcium limestone from Colorado Lien north of Fort Collins, Colorado was used and it also was sized from 20 to 10 mesh. Common algae were selected from streams around Golden, Colorado. The algae were gathered from 3 different places so that a diverse ecosystem could be assured.

2.2 Methods

Experiments were conducted in 500 mL Erlenmeyer flasks that could be loosely covered so that they would be in equilibrium with air. Ten grams of substrate were added to 100 mL of water that was spiked with As and/or Mn. For samples that contained algae, 10 mL of the collected mix that was kept in CCW on a laboratory window sill were added.

All experiments were conducted for at least 7 days so that an estimate of the residence time for removal in a passive treatment structure could be made. Water samples for analysis were taken at 1 and 4 hours and then the samples were moved to a laboratory window sill so that the algae could grow. Then, samples were taken at 1, 4, and 7 or 8 days. If there was considerable evaporation from sitting in the sun, 25 mL of unspiked water were added at various intervals. A blank sample, which was spiked with As and/or Mn but did not contain the substrate or algae was made to be able to monitor evaporation and possible precipitate formation. Table 2 gives the specifications for each experiment. Each experiment was developed to answer certain questions. These questions along with the results are covered in the next section.

Table 2. Details on each experiment.

Experiment	Materials	Constituents	Duration
One	Limestone	2, 5, 10 mg/L As	34 days
Two	Limestone and Algae	2, 5, 10 mg/L As	27 days
Three	Laterite	2, 5, 10 mg/L As	8 days
	Laterite and Algae	15 mg/L Mn	
Four	Laterite	Bicahlo water	8 days
	Laterite and Algae	Grande/Vehla water	
Five	Limestone	5 and 10 mg/L Mn	7 days
	Limestone and Algae	0.50 mg/L As	

3 RESULTS AND DISCUSSION

3.1 Experiment One

The first experiment was designed to answer the questions of whether limestone can remove As and if removal does occur, is it aided by algae? The results are presented in Figure 1 that is a diagram of arsenic removal with time. Note that the y-axis is on a log scale and that the x-axis shows the sampling times and is not to scale. A minimal amount of arsenic is being removed

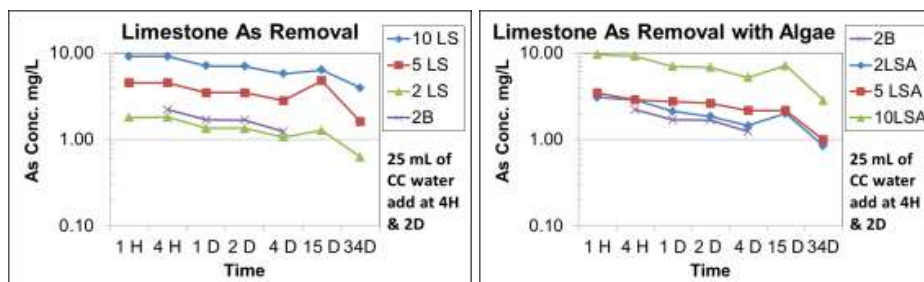


Figure 1. Arsenic concentrations at various time intervals using limestone and limestone with algae.

and algae does not aid in the removal. Sample 2B is CCW spiked with 2 mg/L of As with no limestone. It shows the trend of what would happen with no limestone. The concentration trends in the other flasks with 2, 5, and 10 mg/L are the same as in 2B. This shows that any As removal is basically minimal and accidental.

3.2 Experiment Two

The second experiment was designed to answer the questions of whether the laterite can adsorb As to the regulatory limit concentration of 0.010 mg/L. The questions of how rapidly As is absorbed and how algae would affect removal were also important. The results of the experiment are given in Figure 2. Again the y-axis is a log scale and the x-axis shows the sampling times intervals and is not to scale. Removal by laterite is impressive; a 2 mg/L concentration of As is reduced to the regulatory limit in one day. Even a 10 mg/L concentration of As is reduced to 0.010 mg/L in 4 days. If a passive treatment structure using this waste iron mining product can be made it would be quite effective. The experiment was run for 27 days and in that time no arsenic was released from the laterite.

The results where algae are present with laterite show that removal of As is slower and not as complete as when there is not algae. It also appears that at 27 days some of the As in the flasks containing algae is released back into solution.

3.3 Experiment Three

With the positive results in experiment two, the next question to answer was how will the presence of manganese affect the removal of arsenic by laterite? Also, experiment three tested the question of how well laterite will remove Mn. To answer these questions experiment two was repeated, however, to each flask was added 15 mg/L of Mn. The results of the experiment are given in Figures 3 and 4. Again, the figures are designed in the same manner as the previous figures.

For As removal, the results are a nice duplicate of experiment two. Arsenic is removed within one or two days to the regulatory limit of 0.010 mg/L. When algae are present, removal is slower and does not reach the regulatory limit. Also, it appears that by eight days, some arsenic

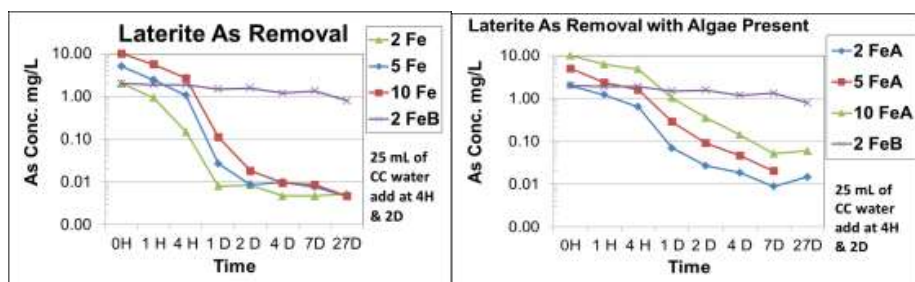


Figure 2. Arsenic concentrations at various time intervals using laterite and laterite with algae.

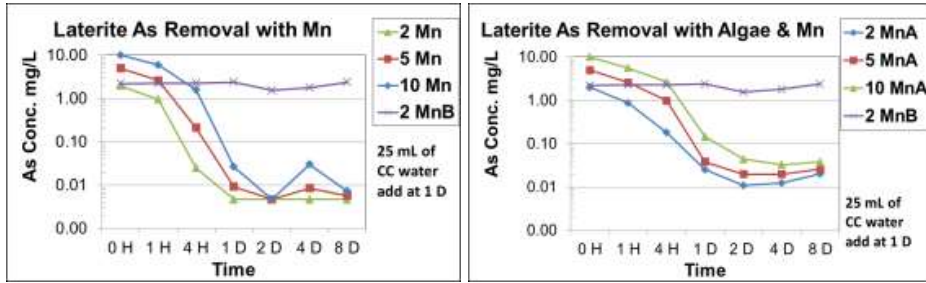


Figure 3. Arsenic concentrations at various time intervals using laterite and laterite with algae in the presence of 15 mg/L of manganese.

is released when algae are present. All flasks started with 15 mg/L of Mn. This concentration of Mn is much higher than any of the mine waters delineated in Table 1. It is apparent that As removal by the laterite is independent of high concentrations of Mn in the water.

Manganese removal by laterite when As is present is shown in Figure 4. Manganese removal is the same in the three flasks that do not have algae but the regulatory limit of 0.10 mg/L is not reached within eight days. For the three flasks with algae, removal is also the same; however, in this case the limit of 0.100 mg/L is almost reached after 8 days. The catalytic effect of algae is obvious (Clayton, et al., 1999). However, the rate of Mn removal was slow. Analysis of the concentration trends would put the half-life of Mn removal at between 2 and 4 days. Finally, as manganese is removed from solution, the removal of arsenic is not affected.

The results of experiments two and three show that arsenic can be effectively removed from CCW at a rapid rate using lateritic material. The removal is not affected by high concentrations of manganese. However, the presence of algae does impair the removal of arsenic. Manganese can also be removed in a laterite system. However, the decrease in concentration, even though it can be catalyzed by algae, is too slow to warrant its use as a passive treatment tool for Mn.

3.4 Experiment Four

With successful results in experiments two and three, experiment four evaluated the laterite system on two of the mine drainages from Brasil. The Bilchao water was chosen because of its high As concentration. The Grande/Vehlo water has high Mn concentration as well as a very high concentration of sulfate. Sulfate is a ubiquitous COC in mine waters and whether such a high concentration of SO_4^- would affect removal is of interest. Duplicate samples were studied. During this experiment, no extra water was added, so a blank of only Bilchao water was also run to show evaporation.

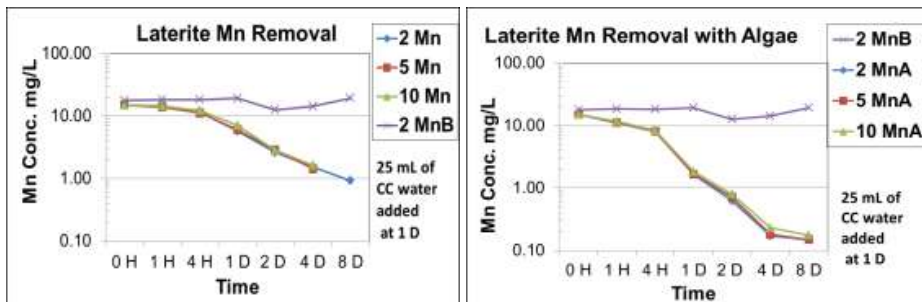


Figure 4. Manganese concentrations at various time intervals using laterite and laterite with algae.

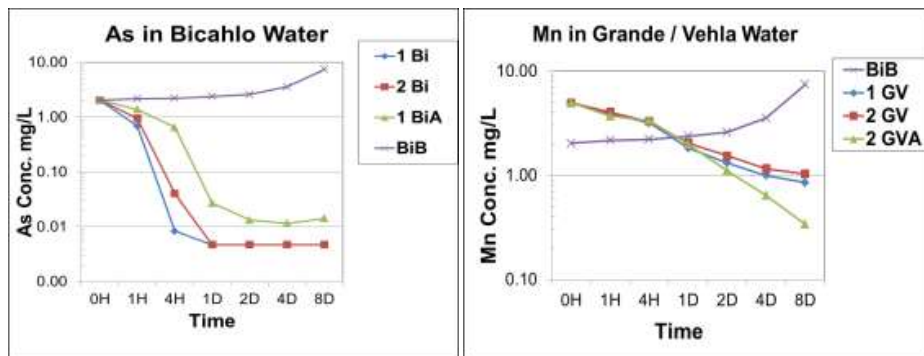


Figure 5. Concentrations of As in Bilchahlo water and Mn in Grande/Vehlo water in a laterite removal system. BIB is a sample of Bilchahlo water with no laterite used to show evaporation during the experiment.

For arsenic in the Bilchahlo water, the results are excellent and consistent with previous experiments. After the first day, the concentrations of As in the duplicates were below the detection limit of 0.005 mg/L. Again when algae were present, the regulatory limit of 0.010 mg/L was not reached and As appeared to be released on day eight. For the Grande/Vehlo water the results were the same. In particular, even though the initial concentration of As was 0.030 mg/L, when algae was present, the concentration of As in Grande/Vehlo water never reached the 0.010 mg/L limit.

For manganese in the Grande/Vehlo water, removal was consistent with what was seen in experiment three. Mn was removed, and algae catalyzed the removal. However, the decrease in concentration was slow and did not reach the 0.10 mg/L limit at the end of eight days. In the Bilchahlo water, Mn was below the regulatory limit after the first hour. So, in a laterite system if manganese is below the limit of 0.10 mg/L, it appears to be the case that release of Mn should not be expected. Such an observation is important because Mn is still mobile in neutral MIW and can be released in a passive treatment system (Blumenstein et al., 2008).

In this experiment, no extra water was added to the system and the concentration of As in BIB shows that there was considerable evaporation over the course of eight days. Even with this loss of water the concentration of sulfate and calcium stayed constant. It appears that considerable gypsum was precipitated during the course of the experiment. This precipitation of gypsum did not affect the As and Mn removal. So, high concentrations of sulfate do not influence the removal mechanisms for laterite removal of As and Mn.

3.5 Experiment Five

Finally, because manganese removal with laterite is ineffective, the removal of Mn with As by limestone was studied in experiment five. Because only minor amounts of arsenic were

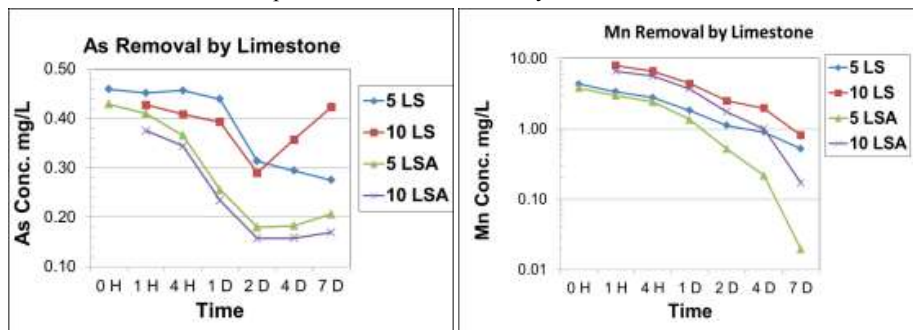


Figure 6. Arsenic and manganese removal by limestone.

removed in experiment 1 when no manganese was in CCW, the parameters for this experiment are changed. The concentrations of Mn are 5 and 10 mg/L and the concentration of arsenic is 0.50 mg/L in all samples. The results are presented in Figure 6. Notice that the y-axis for As removal is a linear scale.

For arsenic, removal is so poor that a compressed y-axis is used to show the results. All As concentrations started at 0.50 mg/L. Arsenic removal appears to cease after about 2 days even though, as seen in Figure 6, manganese removal continues. Also, unlike the other experiments, arsenic removal is best in the flasks that contained algae. This suggests that arsenic removal is tied to the removal of manganese. Also, the apparent leveling off of arsenic removal after 2 days may be because at that time, manganese and arsenic concentrations are roughly comparable. This effect is best seen in 10 LSA plots. Assuming that the reasons for these trends in arsenic concentrations are analyzed correctly, then, the cause for removal of arsenic is because of sorption into the manganese oxide that is being formed from the oxidation and precipitation of higher oxidation states of manganese oxyhydroxide. This suggests that little of the arsenic is being removed by the limestone. Indeed, in experiment one it was found that very little arsenic was removed by limestone.

Manganese removal follows the classic pattern of that described by Clayton et al., (1999). Manganese removal by formation of higher oxidation states of manganese oxyhydroxides is catalyzed by algae and limestone. This is seen where removal in the flasks that contain algae is much more effective. However, even though this is a preferred method of manganese removal, it is not very rapid. To reach the regulatory manganese concentration of 0.10 mg/L takes 7 days. This attests to the idea that removal of manganese by passive treatment methods is difficult.

4 CONCLUSIONS

For these neutral mine waters that contain both manganese and arsenic the results are clear.

1. For arsenic, removal by laterite or some other material that contains a high concentration of Fe_2O_3 is promising.
2. For manganese, the accepted method of removal by an open limestone channel catalyzed by common algae is the system of choice.
3. Removal of arsenic in a laterite system is independent of the manganese concentration. The minimal amount of As removal that occurs in a limestone system is slightly dependent on manganese concentration.
4. Algae is a detriment to the removal of arsenic in a laterite system.
5. Because some manganese is removed by a laterite system, in the design of a passive treatment system that is to remove both COCs, the laterite system would be the first component. Because algae are detrimental to arsenic removal, the laterite system should be designed as a subsurface flow structure.

In the best of circumstances, these results could be used to design a pilot system to see if indeed passive treatment of arsenic and manganese could be done by a laterite / limestone structure.

REFERENCES

- Bednar, A.J., Garbarino, J.R., Ranville, J.R., & T.R. Wildeman, 2005. Effects of iron on arsenic speciation and redox chemistry in acid mine water. *Journal of Geochemical Exploration* 85: 55–62.
- Blumenstein, E.P., Volberding, J., & Gusek, J.J., 2008. Designing a Biochemical Reactor for Selenium and Thallium Removal, from Bench Scale Testing Through Pilot Construction. In: *Proceedings of 24th Annual Meeting of American Society for Surface Mining and Reclamation*: 148-179.
- Gusek, J.J. 1995. Passive treatment of acid rock drainage: What is the potential bottom line?, *Mining Engineering* (March): pp 250-253.
- Clayton, L.A., Bolis, J.L., Wildeman, T.R., & Updegraff, D.M., 1999: A case study of the aerobic and anaerobic removal of manganese by wetland processes. In L.H. Filipek & G.S. Plumlee (eds.). *The environmental geochemistry of mineral deposits, Part B*. Reviews in Economic Geology, v. 6B, Society of Economic Geologists. 515-526.

- Denholm, C., Danehy, T., Busler, S., Dolence, R., & Dunn, M., 2008. Sustainable Passive Treatment of Mine Drainage: Demonstration of Manganese Resource Recovery. In: *Proceedings of 24th Annual Meeting of American Society for Surface Mining and Reclamation*: 1058-1078.
- Pinto, A. P., Wildeman, T. R., & Gusek, J. J., 2001: Remediation properties of materials to treat acid mine drainage water at a gold mine operation in Brazil. In: *Proceedings of 18th Annual Meeting of American Society for Surface Mining and Reclamation*: 585-591.
- Rose, A.W., Shah, P.J. & Means, B. 2003. Case Studies of Limestone-Bed Passive Systems for Manganese Removal from Acid Mine Drainage. In: *Proceedings of 20th Annual Meeting of American Society for Surface Mining and Reclamation*: 585-591.
- Stumm, W. and Morgan, J.J., 1996: *Aquatic chemistry*, 3rd ed. Wiley Interscience.
- Wildeman T. R., Filipek, L. H. & Gusek, J. J. 1994. Proof-of-Principle Studies for Passive Treatment of Acid Rock Drainage and Mill Tailing solutions from a Gold Operation in Nevada. In *Proceedings of the International Land Reclamation and Mine Drainage Conference*, U.S. Bureau of Mines Special Publication SP 06B-94.Vol. 2: 87-394.

Pile Scale Models for Acid Rock Drainage Prediction and Their Application

L. Ma, C. Huang, and Z-S Liu

National Research Council Canada, Vancouver, BC, Canada

K.A. Morin

Minesite Drainage Assessment Group, Surrey, BC, Canada

ABSTRACT: In this paper, we developed pile scale models that include major mechanisms for acid rock drainage process, such air flow, water flow, oxygen transport and consumption, geochemical production, and also heat transfer. Furthermore, the governing equations for these mechanisms are integrated in commercial software COMSOL with fully coupling features. This enables the proposed models to reasonably reflect the evolutions of oxygen concentration and temperature profile monitored inside the waste rock pile. We applied the proposed models to the main full-scale waste rock pile at the Equity Silver mine, Canada. The comparison between simulation results and monitoring data is provided; good agreement on the seasonal O₂ concentration fluctuation is observed. The changes of air convective pathway and oxygen supply due to the impact of a cover system are discussed; this helps us gain insights in the acid rock drainage processes.

1 INTRODUCTION

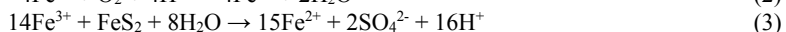
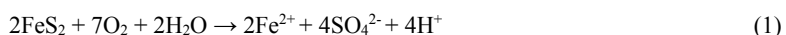
During the extracting process of hard rock mines, large amounts of waste rock are generated from open pits and underground operations. Most of the waste rock is placed in surface dumps, which are usually exposed to the open environment. In addition, significant amounts of waste rocks are also produced by major civil constructions such as highways, railways, airports and hydroelectric structures. When the waste rocks contain sulphide minerals, such as pyrite, pyrrhotite, sphalerite, galena, arsenopyrite, chalcopyrite, tetrahedrite, and molybdenite etc., they are identified to have strong acid generation potentials. As sulphide minerals interact with ambient oxygen and water, they gradually oxidize and release sulfate ions, proton and metal ions. Then those oxidation products are flushed by groundwater, releasing associated metals and metalloids into the surrounding environment. The acid rock drainage may under certain conditions have severe impacts on streams, rivers and aquatic life for decades or even hundreds years.

Currently acid rock drainage from sulphide bearing waste rock dumps is identified as one of the most serious environmental liabilities to the mine site owners or local governments. Most sulphide bearing waste rock dumps require perpetual treatment of seepage and runoff from the dumps. This requires substantial operating costs for labor, power, chemicals and maintenance. The cost of maintaining waste rock dumps is among the highest in the waste management facilities. Security bonds are often requested to provide assurance that these funds would be available over a long-term time. As a result, prediction of acid rock drainage production becomes important and essential for determining peak acid production rates, the duration of peak rates and the decline in acid production over time. Also a good prediction requires revision and calibration based on the historical data.

In order to predict acid rock drainage, extensive research has focused on studying integrated processes within waste rock and understanding the fundamental processes over the past several decades. For example, Davis and Ritchie (1986), Lefebvre, (1994), (2001) implemented mathematical modeling to compute the oxygen loss and heat production in the waste rock pile, which is based on reaction core model that considers pyrite oxidation as a function of temperature, oxygen concentration and pyrite mass fraction relative to the original pyrite concentration. In this paper, we proposed new pile scale models with fully coupled features to simulate the transport behaviors of reactant (oxygen) and product (proton) within the regime of waste rock piles. The purpose of this study is to evaluate the total acid rock reaction rate in the waste rock pile and investigate how the cover system impacts it.

2 PILE SCALE MODEL

Acid rock drainage is considered to originate from geochemical reactions on the waste rock surface contacting with water and air. The oxidation reactions of the pyrite can be summarized as



Here the transport of reactants to and the removal of reaction products from among finer waste rocks are the keys to determine local geochemical reaction rate and also to estimate the total amount of acid generation in the entire waste rock pile, as those finer rocks have much larger effective surface area than coarse ones. Pile scale mass models are developed in this section to study the water flow, air flow, oxygen and proton transport, and also heat transfer in the finer portions of waste rock pile. The governing equations for these pile scale models are illustrated below. In addition, the coupling relationship between each model is illustrated in Figure 1. More details about the water film model mentioned here can be found in another author's publication (Ma et al. 2018).

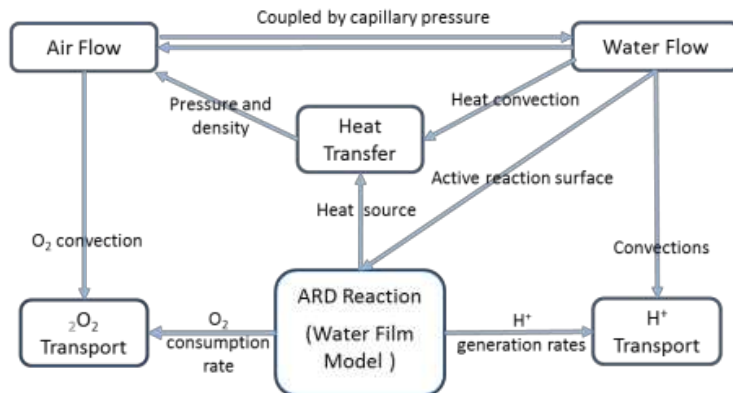


Figure 1. Couplings in Pile Scale Transport Models

2.1 Water and air flow

To describe the pattern of water and air flow in the finer portions of waste rock pile, two phase Darcy's law was applied to consider the capillary effects from both of air and water pressures. Here the saturation of each phase S_α is defined as the fraction of the pore space occupied by a given fluid:

$$S_\alpha = \frac{\theta_\alpha}{\phi} \quad (4)$$

where θ_α is the volume content for phase α and ϕ is the porosity. It is obvious that the sum of the air and water saturations must be equal to one:

$$S_a + S_w = 1 \quad (5)$$

In addition, the definition of effective saturation for phase α is also given as follow,

$$S_{e\alpha} = \frac{S_\alpha - S_\alpha^{\min}}{S_\alpha^{\max} - S_\alpha^{\min}} \quad (6)$$

The capillary pressure in the pore is defined as the pressure difference between water and air. At the Darcy scale, the capillary pressure is commonly assumed to be a function of the water saturation:

$$p_c = p_a - p_w = p_c [S_{ew}] \quad (7)$$

The relationship between capillary pressure and water saturation is called the water retention equation, and van Genuchten (1980) introduced a very well-known form for this equation as follows:

$$p_c [S_{ew}] = p_g \left((S_{ew})^{-1/m_g} - 1 \right)^{1/n_g} \quad (8)$$

where p_g is defined as entry capillary pressure. The exponents m_g and n_g are related to the pore size distribution.

By applying the Darcy's law, the velocities of air and water inside the pile can be determined:

$$\mathbf{q}_\alpha = -\frac{k_\alpha [S_\alpha]}{\mu_\alpha} (\nabla p_\alpha - \rho_\alpha \mathbf{g}) = -K_\alpha [S_\alpha] \nabla H_\alpha \quad (9)$$

where k_α and K_α are permeability and conductivity tensors, which depend on the saturation of the phase α . H_α is the fluid potential.

The permeability for unsaturated condition k_α in Eq.(18) is completely different from that for saturated condition $k_{s\alpha}$ in the porous structure. If $m_g = 1 - 1/n_g$, the relative permeability functions of water and air phases in the waste rock pile can also be deduced from the water saturation as below:

$$k_a [S_a] = k_{sa} k_{ra} [S_{ew}] = k_{sa} (1 - S_{ew})^\kappa \left(1 - (S_{ew})^{1/m_g} \right)^{2m_g} \quad (10)$$

$$k_w [S_w] = k_{sw} k_{rw} [S_{ew}] = k_{sw} (S_{ew})^\kappa \left(1 - \left(1 - (S_{ew})^{1/m_g} \right)^{m_g} \right)^2 \quad (11)$$

In the waste rock pile, the water density ρ_w for Darcy's equation is considered as constant and also the air density ρ_a can be estimated by:

$$\rho_a [p, T] = \frac{p_a}{RT} \quad (12)$$

where $R = 8.31447 \text{ J}/(\text{mol} \cdot \text{K})$ is the universal gas constant.

2.2 Proton and O₂ transport

To investigate the transport of proton related to acid rock drainage processes inside waste rock pile, a general species transport equation is adopted as below:

$$\frac{\partial}{\partial t} (\theta_w C_{H^+}) - \nabla \cdot (\theta_w D_{H^+} \nabla C_{H^+}) + \nabla \cdot (\mathbf{q}_w C_{H^+}) = Q_{H^+} \quad (13)$$

where C_{H^+} and D_{H^+} are the concentration and diffusion coefficient for proton, \mathbf{q}_w is the vector of matrix flow, and Q_{H^+} (sink or source term) means generation or consumption rate. Similarly, the supply of oxygen, concentration C_{O_2} to geochemical reactions can be calculated as below:

$$\frac{\partial}{\partial t} (\theta_a C_{O_2}) - \nabla \cdot (D_{O_2} \nabla C_{O_2}) + \nabla \cdot (\mathbf{q}_a C_{O_2}) = Q_{O_2} \quad (14)$$

2.3 Heat transfer

To consider the effect of reactive heat and cycle of ambient temperature on acid rock drainage processes, the equation for heat transfer in the waste rock pile is also included:

$$c_p \rho \frac{\partial T}{\partial t} + c_w \rho_w \nabla T \cdot \mathbf{q}_w - \nabla \cdot (k \nabla T) = Q_h \tag{15}$$

where c_p is the specific heat capacity. Q_h denotes the heat generation rate from geochemical reactions. The effective mass density ρ and the effective thermal conductivity k are defined as:

$$c_p \rho = \phi \rho_w S_w c_w + (1 - \phi) \rho_s c_s \tag{16}$$

$$k = k_{dry} + \sqrt{S_w} (k_{wet} - k_{dry}) \tag{17}$$

where c_w and c_s are heat capacities for water and solid (waste rock particles), and k_{dry} and k_{wet} are the heat conductivities for waste rocks in dry and wet conditions respectively.

3 MODEL VALIDATION

To validate the proposed pile scale transport models, the waste rock pile of Equity Silver mine from the central of British Columbia, Canada was simulated and the calculation results were compared with monitoring data to investigate the main controlling mechanisms in acid rock drainage.

There is approximately 80 million tons of waste rock at the Equity Silver mine, covering an area of approximately 1.4 km². The waste rock dumps have been producing acid rock drainage also with metal ions since the early 1980s (O’Kane et al, 1995; Aziz and Ferguson, 1997; Morin et al., 2010, 2012). To minimize acid rock drainage, a till/soil cover was constructed over the main dump during 1990-1994, with about 1m thickness for preventing the infiltration of ambient water and oxygen into the dump. Historical site records indicate the average annual precipitation is about 600 mm, with approximate 60% of the precipitation occurring as snow generally from November to April. Snow starts to melt in April. Rainy season starts from late April and ceases by the end of June. In the study, the data of precipitation and ambient temperature from 1991 to 2001 (total 10 years) obtained from Environment Canada are adopted as the boundary conditions for the simulation, as shown in Figure 2.

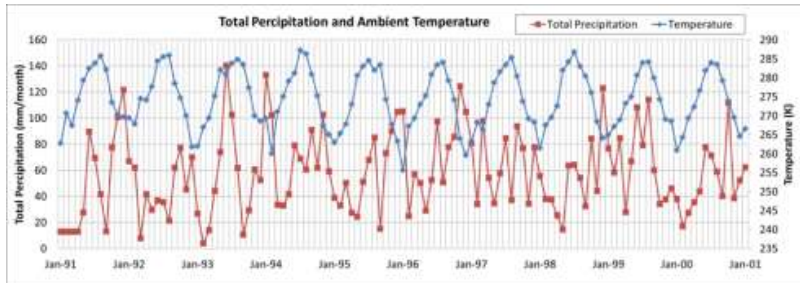


Figure 2. Precipitation and Ambient Temperature

For simplification, a 2-D cross section from the waste rock pile is simulated in this study. The schematic of the cross section is in Figure 3 with detail geometry information. An onsite monitoring probe is installed at 17m depth on the symmetric axis (the left side of the 2-D section), which is approximately considered as the center of the waste rock pile. According to historical reports, all of the waste rocks were piled up on a bedrock slope (water impermeable). The height of the pile is around 50 m and the width is about 1000 m.

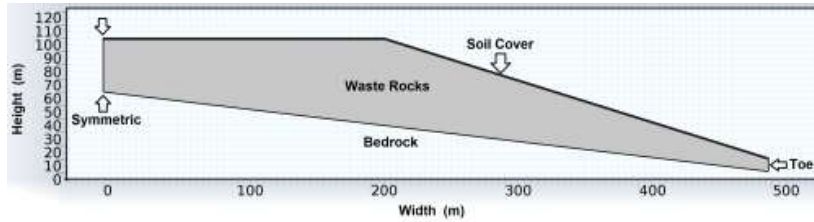


Figure 3. Schematic of the 2D cross section

Regarding the initial status for simulation, a transient simulation without the effect of cover system was performed from Jan 1991 to Jan 1994 to get the reactants and products fully distributed within the waste rock pile. Starting from Jan 1994, the effect of till/soil cover was included in the simulation, which is consistent to the completion time for the real cover installation; then the calculation continued until Jan 2001 to simulate seven years for the scenario of the waste rock dump with the till/soil cover. The parameters for the modeling are listed in Table 1.

Table 1. Parameters for modeling

Property	Units	Values
Effective air permeability (waste rock)	m ²	5.10e-12
Effective air permeability (cover)	m ²	5.02e-9
Entry capillary pressure	Pa	653
Van Genuchten <i>m</i> parameter (cover)	-	0.6
Van Genuchten <i>m</i> parameter (waste rock)	-	0.3
Van Genuchten <i>n</i> parameter (cover)	-	2.5
Van Genuchten <i>n</i> parameter (waste rock)	-	1.43
Hydraulic conductivity of water phase	m/s	0.0001
Thermal conductivity of dry rock	W/m °C	0.5
Thermal conductivity of wet rock	W/m °C	3
Oxygen diffusion coefficient	m ² /s	1.76e-5
Proton diffusion coefficient	m ² /s	9e-9
Heat capacity of water	J/Kg/K	4181.3
Heat capacity of rock	J/Kg/K	1139

As the competition of oxygen consumption and oxygen supply is directly related to acid generation rate, we tried to analyze the oxygen concentrations in the pile to understand the limiting factors in acid rock drainage. It is interesting that the historical monitoring data (oxygen concentration) from the probe has annual fluctuations. This “respiration” phenomenon is believed to be the results of annual cycle of ambient temperature, as temperature change has the same frequency. The change of ambient temperature significantly impacts the air density on the pile surfaces thus may influence the air flow pathway and also oxygen supply inside the full-scale waste rock pile.

Figure 4 shows the comparison of oxygen concentration at the probe between measurement and simulation. It should be addressed again that the effect of cover is applied to the model starting from Jan 1994 for the simulation, while the real full-scale cover onsite was installed during 1990 to 1994. The simulation before Jan 1994 was just the initialization stage to achieve relative stable stage of acid generation and storage in the pile. Starting from Jan 1994, the simulated oxygen concentration shows a similar fluctuation pattern to that observed from measurement: higher concentration in winter time and lower concentration in summer time. Measurements are missing from winter 1996 to spring 1997, but we believe that the oxygen

concentration rose during this period based on its historical trend. Another observation is that the simulated oxygen concentration on average decreased during the first several years after the installation of the cover, while the site monitoring also showed a similar downwards trend.

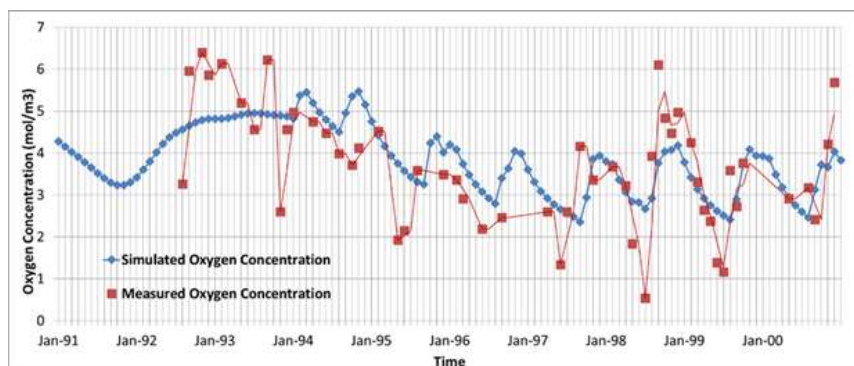


Figure 4. Comparison of O₂ concentration between simulation and measurement

The explanation for the lower O₂ concentration status after the installation of cover system is that the cover changed the air flow pathways in the waste rock pile. Figure 5 top shows the oxygen concentration and the air flow driven by convection in Dec 1993, right before the cover installation in the simulation. It indicates that the fresh air came into the waste rock pile through the right bottom toe and most eventually escaped from the top of the pile. Figure 5 bottom illustrates the air flow pathway in Dec 1996. The results indicate that the low permeability of the cover blocked the main air flow outlet on the top side and the air had to circulate within the waste rock pile and went out through the toe, which significantly increased the length of air pathway compared with uncovered status. Generally, longer air flow pathway indicates insufficient oxygen supply and lower oxygen concentration status. In addition, oxygen is not able to diffuse through the top surface in outflow conditions (uncovered), while the air circulation scenario (covered) makes it possible for oxygen diffusion through the top surface, especially for heavier air conditions in winter time. As a result, O₂ concentration in the pile starts to have annual cycle with seasonal temperature fluctuation.

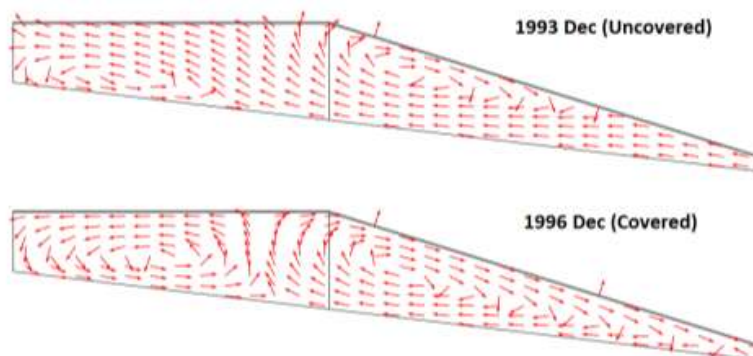


Figure 5 Simulated airflow pathway in the pile

In addition, the total amount of acid generated rate from the geochemical reactions within the 2D cross section is illustrated in Figure 6, which indicates a similar downward trend like oxy-

gen concentration shown above. The decrease trend of total acid generation rate is also reflected by the real consumption of lime to neutralize the acidities in the water treatment facility.

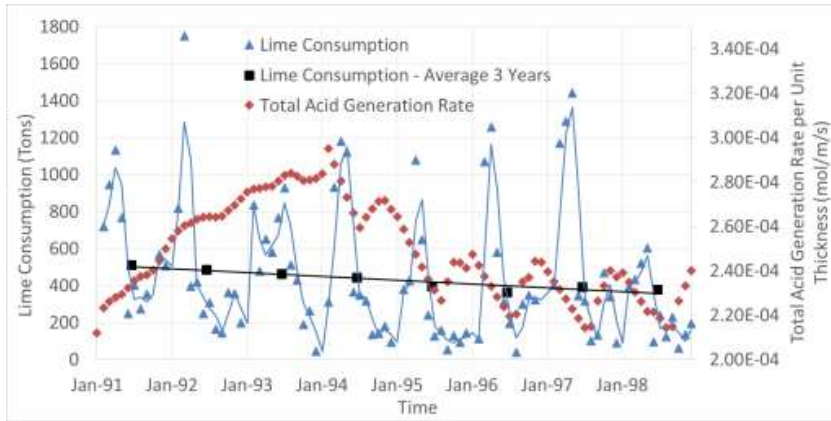


Figure 6. Lime consumption vs total acid generation rate

Note that there are still a lot of unknowns at the site, such as waste rock pile construction history, rock size distribution, underground water flow pattern and rate, rain infiltration rate, water content distribution, and microbial activities inside the waste rock pile. The unknowns are either due to lack of characterization data or difficult to measure on site. Therefore it's difficult to exactly match the models against the monitoring data. But matching with the trend of the monitoring data can still reveal the controlling mechanisms to the acid rock drainage generation processes.

4 CONCLUSIONS

To gain a comprehensive understanding of the physical and geochemical processes involved in acid rock drainage generation process, a set of mathematical models are coupled to simulate the transport of reactants and products in the waste rock piles. The full-scale waste rock pile from Equity Silver mine is used to validate the proposed model. The observations from the simulation results are generally consistent with the monitoring data, which reveals the air flow pathway in the waste rock pile. Through analyzing the simulation data, the function of the cover system for the waste rock pile was investigated and discussed in this paper. The proposed models are capable of capturing the main acid rock drainage geochemical and physical mechanisms. Therefore, these models can be an effective tool to optimize waste rock pile configurations and evaluate the design of cover systems to reduce acid rock drainage generation.

ACKNOWLEDGEMENTS

The authors gratefully acknowledge Mr. Mike Aziz and Mr. Cody Meints from Goldcorp Inc. for valuable historical monitoring data and also Mr. Mike O’Kane and Dr. Lindsay Tallon from M.A. O’Kane Consultants Inc. for technical discussions and constructive comments.

REFERENCES

- Aziz, M. L., Ferguson, K. D., Equity Silver Mine - Integrated case study. *In: Proceedings of the Fourth International Conference on Acid Rock Drainage*, Vancouver, Canada, May 31-June 6 1997.
- Davis, G.B., Ritchie, A.I.M., A model of oxidation in pyritic mine wastes: part I equations and approximate solution, *Applied Mathematical Modeling*, 10 (1986). pp. 314-322.
- Lefebvre, R., Hockley, D., Smolensky, J., Gelinas, P., Multiphase transfer processes in waste rock piles producing acid mine drainage 1: Conceptual model and system characterization, *Journal of Contaminant Hydrology*, 52 (2001a), pp. 137-164.
- Lefebvre, R., Hockley, D., Smolensky, J., Lamontagne, A., Multiphase transfer processes in waste rock piles producing acid mine drainage 2. Applications of numerical, *Journal of Contaminant Hydrology*, 52 (2001b) pp. 165-186.
- Ma, L., Huang, C, Liu, Z S, Morin, K, Aziz, M, Meints, C (submitted) 2018. A Water Film Model for Understanding Acid Rock Drainage and Metal Leaching in Sulphide Waste Rock Dumps.
- Morin, K.A., N.M. Hutt, and Aziz. M.L., 2010. Twenty-Three Years of Monitoring Minesite-Drainage Chemistry, During Operation and After Closure: The Equity Silver Minesite, British Columbia, Canada. *MDAG Internet Case Study #35*, www.mdag.com/case_studies/cs35.html
- Morin, K.A., N.M. Hutt, and M. Aziz. 2012. Case studies of thousands of water analyses through decades of monitoring: selected observations from three minesites in British Columbia, Canada. *In: Proceedings of the 2012 International Conference on Acid Rock Drainage*, Ottawa, Canada, May 22-24.
- O’Kane, M., Wilson, G.W., Barbour, S.L., Swanson, D.A., Aspects on the Performance of the Till Cover System at Equity Silver Mines LTD. *In: Conference on Mining and the Environment*, Sudbury, Ontario, May 28-June 1 1995.
- van Genuchten, M.T., A closed-form equation for predicting the hydraulic conductivity of unsaturated soils, *Soil science society of America journal*, 44 (1980), pp.892-898.

Understanding Mineralogical Composition, Weathering, and Alteration to Manage ML/ARD in a Base-Metal Tailings Storage Facility

J. Durocher and L. Robertson

Klohn Crippen Berger Ltd., Sudbury, ON, Canada

ABSTRACT: Assessing the geochemical behaviour of tailings storage facilities (TSFs), with respect to the management of environmental impacts, is considered a standard state of practice in the mining industry. Standard practices for screening level and detailed testing, used to characterize the metal leaching and acid generating potential of tailings, often focusses on bulk behaviour by analyzing the total elemental composition, performing acid base accounting, as well as short and long-term leachate tests. Although its recommended, less emphasis is placed on detailed mineralogical assessments which provide significant insight into the processes that control metal leaching and acid rock drainage (ML/ARD). The geochemical behaviour of a TSF is governed by the tailings minerals and their interaction with the surrounding environment. Weathering and alteration of tailings minerals, is initially governed by the reactivity of primary minerals (i.e. minerals deposited initially within a TSF). Primary minerals alter and release trace elements to pore water often resulting in the formation of several stages of secondary minerals (i.e. minerals that form post deposition). Metal(oid) attenuation through secondary minerals limits porewater and seepage concentrations by a complex series of mineral oxidation, dissolution-precipitation, coprecipitation, solid solution substitution and adsorption/desorption reactions. Changes to tailings management practices during operations through closure (e.g. saturation and the phreatic surface, pond level, or impermeable and vegetative covers, etc.) are important to consider for long term ML/ARD management as these minerals are only stable under the specific conditions. Minerals and mineral alteration reactions at the mineral-water interface are responsible for the composition of porewater and seepage, yet little effort focuses on understanding the solid phase forms that are responsible for balancing metal(oid)s and non-metals in solution. In this study, the mineralogical and chemical composition of tailings, tailings porewater, and seepage water, from a conventional acid generating, base-metal TSF were assessed to evaluate the rate and degree of tailings alteration as well as the potential changes to porewater and seepage water over time. Observations indicate mineral weathering and alteration is observed throughout the tailings profiles, resulting in specific alteration zones (oxidized, partially oxidized, and unoxidized tailings) that vary in thickness in variably aged tailings depositional areas within the TSF. Distinct porewater and seepage water suggests buffering and metal(oid) attenuation, through primary and secondary mineral reactions, are controlling water quality and the degree of alteration is related to water quality.

1 INTRODUCTION

Mine tailings are among the largest volume of mining wastes worldwide and many tailings storage facilities (TSFs) containing sulphide-bearing tailings are mineralogically and geochemically unstable. Sulphide-bearing tailings inevitably alter through rate determined geochemical processes that depend on the surrounding conditions (e.g. tailings mineralogical and chemical

composition, hydrology, and climate; pore gas content and level saturation, as well as, contacting solution pH, Eh, temperature, pressure and chemical makeup). These complex mineral alteration processes lead to surface and pore water leachates with varying pH, from the release and mobilization of acidity balanced by neutralization reactions, and increased concentrations of metal-, metalloid- and anionic-species. The reactions occur at the micro-scale mineral-fluid interface throughout a tailings storage facility (TSF) and can often result in porewater and seepage concentrations above regulatory discharge limits.

The most commonly known process occurring in sulphide-bearing tailings is the oxidation and subsequent dissolution of sulphide minerals that leads to the development of metal leaching and acid rock drainage (ML/ARD). Sulphide oxidation processes have been documented by many including: Lowson (1982), Evangelou (1995), Nordstrom (1997), Alpers (1999), Jambor (2003), Blowes (2003) and Lottermoser (2007); among many others. Sulphide oxidation reactions coupled with neutralization reactions, which occur from the weathering and dissolution of silicate, carbonate and oxide minerals, control the chemical composition of pore and seepage water by forming (or adsorbing to) secondary minerals.

Assessing the geochemical behaviour of tailings storage facilities, with respect to the management of environmental impacts, is considered a standard state of practice in the mining industry. Several guidance documents, including the Prediction Manual for Sulphidic Geologic Materials (Price, 2009), and the Gard Guide (INAP, 2009) recommend identifying and characterizing tailings material to be deposited, exposed or disturbed by mining, milling, and concentrating practices. Price recommends tailings facilities be characterized to understand the systems hydrogeochemistry and to predict the potential current and future impacts to effluents and drainage quality under site specific conditions (e.g. climate, temperature, pressure, degree of aeration, hydrology, and hydrogeology).

Understanding the hydrogeochemistry and predicting the short- and long-term drainage chemistry of a mine site requires a great deal of site specific information, as well as extensive material sampling plans, analytical methods and calculations. Screening level and detailed testing, used in the characterization of ML/ARD, often focusses on bulk material behaviour by analyzing the total elemental composition, performing acid base accounting, and short and long-term leachate tests. Short- and long-term water quality impacts are predicted using scaled calculations and modeling that often do not account for rate determined processes, as well as equilibrium, solubility reactions or the changing conditions (e.g. climate, pH, Eh, hydrology) within the TSF over time.

Minerals and mineral alteration mechanisms are responsible for the composition of pore water and seepage, yet little effort focuses on understanding the solid phase forms that are responsible for balancing metal(loid)s and non-metals in solution. This paper demonstrates how mineralogical identification, and primary and secondary mineralogy relate to the evolution of tailings porewater and seepage composition and in a sulphidic and variably aged base-metal TSF.

2 APPROACH AND METHODOLOGY

2.1 Approach

An investigation was conducted at an ageing Canadian base metal TSF to understand the evolution of tailings mineralogy as it relates to porewater and seepage water quality. Geochemical changes along the seepage flow pathway was evident from several areas within the TSF that ranged in depositional age (i.e. 1900's to present) and seepage from the TSF often exceeded regulatory guidelines. Secondary minerals had been previously observed in the form of amorphous sludge at the base of ponds and reservoirs, crystalline hardpans found throughout the

stratigraphy, and crystalline and amorphous minerals where seepage emerged from the dam. The change in mineralogy observed and the composition and characteristics of the emergent seepage warranted a detailed investigation into their relationship as minerals can give an indication of the type and scale of geochemical processes occurring within a TSF.

2.2 Methodology

Tailings material was sampled and tested from 48 boreholes, drilled to a maximum depth of 22 m, at 10 individual tailings disposal areas (Disposal Areas A to J)¹. Tailings cores were collected using sonic drilling methods and field characterization including Munsell colour and field tests including paste pH, paste oxidation-reduction potential (ORP), paste electrical conductivity (EC) and paste total dissolved (TDS) were performed on the cored material at a minimum of 1 ft intervals prior to sampling. Paste measurements were performed immediately after mixing, 10 g of material with 10 mL of deionized water, for 30 seconds.

Bulk solid tailings samples were collected in sample bags at 30 cm intervals and placed in coolers prior to being processed in the lab. Approximately 1200 tailings samples were subsampled for various analytical methods including: recommended static testing and single batch extractions, as well as, additional mineralogical assessments through microscopy, X-Ray diffraction (XRD) and scanning electron microscopy (SEM).

2.2.1 Static Geochemical Testing

Static testing, as recommended by leading guidance documents, was performed on selected bulk tailings samples (unseparated and non-crushed). Testing included major and trace element analysis, acid base accounting (ABA), and non-sequential extractions.

The concentration of major and trace elements was measured by digesting tailings subsamples in a mixture of 4 strong acids (hydrochloric, nitric, perchloric and hydrofluoric acids). The concentration of recoverable elements (i.e. those dissolved in the digestion) were measured with Inductively Coupled Plasma-Mass or Atomic Emission Spectrometers (ICP-MS or ICP-AES).

Acid-base Accounting was performed at a commercial accredited lab and included a fizz test, paste pH, Acid Potential (AP, as kg of calcite (CaCO_3) per tonne equivalent), Neutralization Potential (NP, as kgCaCO_3 per tonne equivalent), total sulphur (T-S, weight (wt.) % S), total sulphate (T-SO_4^{2-} , wt.% S), total insoluble-sulphur (T-S_{insol}, wt.% S) and a calculation of the total sulphide (T-S₂, wt.% S) content of the material. In addition, the total carbon (T-C, wt.% C), total organic and inorganic carbon (TIC, wt.% C), and the total carbonate (T-CO_3^{2-}) content of the material was also measured. Acid potential (AP) calculations assumed that the concentration of sulphur measured in the sample occurs as pyrite (FeS_2) and that pyrite reacts to produce acidity (i.e. 1 wt.% S produces 31 kg CaCO_3 equivalents of acidity). NP was measured by adding a known volume of hydrochloric acid (HCl) to a known mass of sample. The volume of HCl added to the sample is based on the results of a fizz test. The addition of hydrochloric acid (HCl) is followed by a back titration with sodium hydroxide (NaOH). The amount of acid consumed by the sample is then calculated as a kg CaCO_3 equivalent per tonne (kg CaCO_3/t) to provide an indication of the total NP of the sample. The resulting AP, NNP and NPR calculations allowed for the classification of materials into three ARD risk categories: Potentially Acid Generating (PAG) if the NPR is less than 1, not-Potentially Acid Generating (NPAG) if the NPR is greater than 2, and Uncertain (U) if the NPR is between 1 and 2.

¹ Disposal Areas A-J are areas that contain variably aged tailings. Disposal area A was active between 1936 and 1960; area B was active between 1945-1980; areas C to F were progressively active between 1960 to 1990; and disposal areas G to J have been collectively active since 1985.

Single batch extraction tests, including shake flask extraction (SFE), and modified SFE tests, measured the short-term metal leaching potential under varying solutions to understand the soluble phases from tailings at specific depths. Soluble phases may include secondary surface coatings or sorbed species as well as soluble primary or secondary minerals, including pre- and post-depositional oxidation products. Shake Flask Extraction (SFE) and a modified SFE tests were used to identify elements readily released from samples by water of varying pH (solution 1 was deionized (DI) water with a pH of 5.5 and solution 2 was HCl acidified DI water to pH 2.2). The tests were performed to provide an indication of the ML potential of soluble phases from selected tailings samples under low and sub-neutral pH conditions. In the test, the sample was placed in a flask with the solution at a 3:1 water to solid ratio by weight and shaken end over end for twenty-four (24) hours. Following the agitation, the sample was left to settle for a limited time and the supernatant was removed, filtered, and the pH, and electrical conductivity (EC), TDS, TSS, Conductivity, Acidity and Alkalinity, Chloride, Carbonate and Sulphate content were measured. The chemical composition of the supernatant was also measured for dissolved metals and metalloids by ICP-MS analysis.

2.2.2 Mineralogical Testing

Tailings samples were observed at various magnifications and imaged using an Olympus SZX16 research high-class stereo microscope equipped with an Olympus SDF PLAPO 2X PFC lens and a Martin microscope MM99 adapter (S/N 3961) attached to a Sony Cybershot, digital camera. Samples were divided into subsamples for additional mineralogical testing.

The mineralogical analyses were performed on selected samples by first separating the tailings in each sample by grain size using a riffle splitter. Separated samples were then crushed using a mortar and pestle and the powdered samples were prepared as smear mounts prior to being placed in a Phillips PW 1729 X-ray Diffractometer. The mounted samples were subjected to Co K α radiation at 40 kV and 30 mA and resulting X-ray diffraction patterns were recorded over a scan range of 10 – 60 2 θ degrees with a step size of 0.02 2 θ degrees and a dwell time of 4 seconds per step.

A separate set of sub-samples was prepared in fused epoxy disks and sputter coated with carbon to a thickness of 15 μ m and scanned using a JEOL JSM-6400 scanning electron microscope (SEM). Chemical analyses were completed at 20 keV with a paired EDS system from INCA X-sight by Oxford. Effort was made to reduce material oxidation, though it could not be completely prevented. Semi-quantitative calibration methods were employed (i.e., beam and vacuum stabilization). Standard reference materials were used to calibrate the SEM prior to analysis, however, were not used throughout the analyses. Results should be viewed as semi-qualitative (i.e., the chemical composition of areas analyzed are approximate and should not be relied upon as actual concentrations). Point analyses produced X-Ray spectra resulting in elemental atomic % concentrations for elements with an atomic mass greater than that of O. The resulting atomic concentrations were used to calculate atomic ratios of the elements present and theoretical chemical formulae, where O was assigned to each element based on an assumed valence state. The resulting M-S and M-O (where M = metal, S = sulphur and O = oxygen) atomic ratios and possible mineral formulae were used to identify secondary amorphous phases.

2.2.3 TSF Surface and Pore Water Monitoring

Monthly water monitoring was conducted at various locations throughout the studied TSF, for a period of three (3) years, to understand the chemical composition of surface and tailings pore water as well as to support ongoing ML/ARD assessments. Seepage water was collected from passive dam toe seeps and engineered drains, pipes, and, culverts and ponded water in upstream reservoirs and downstream seepage collection ponds, and, pore water extracted from select

monitoring wells were also monitored throughout the study period. For simplicity, the average chemical composition of surface, pore and seepage water is presented here.

3 RESULTS AND DISCUSSION

3.1 *Field and Standard Testing*

To assess the evolution of sulphide oxidation and measure the resulting alteration products in tailings, for various depositional areas, and within an ageing base-metal TSF (depositional areas ranging in age from 0 to 90 years), were targeted for chemical and mineralogical analysis. The evolution of secondary minerals and ageing is evident from the selected areas of study (ranging in age from 10 to 90 years). The tailings profiles within and among these depositional areas show distinct groupings of alteration zones; oxidized, partially oxidized, and unoxidized (Figure 3-1). These classifications were selected based on sample physical appearance (colour), visible mineralogical composition, and paste measurements.

The upper oxidized zone was defined as encompassing material that has undergone extensive mineral alteration resulting in little to no primary sulphides. This zone contained extensive secondary minerals and was approximately 4 m thick in the older tailings disposal areas and 1.5 m thick in the younger tailings disposal areas. The underlying partially oxidized zone varied in thickness from 5 m in older disposal areas to 3 m in younger disposal areas and was characterized by material containing both primary and secondary minerals. The unoxidized zone was dominated by primary minerals that have not sustained visible alteration and occurred at depths of 10 m and 5 m below surface, in older and younger tailings disposal areas, respectively.

Paste measurements performed in the field provided an indication of contact water pH from soluble phases. Paste pH increases with depth throughout the alteration zones and were typically more acidic (pH 2-4) in oxidized zone material when compared to sub-neutral paste pH values (pH 4-6) from the unoxidized zone material (Figure 1). Surface and near surface samples, collected from revegetated Disposal Areas B, E and F resulted in sub neutral paste pH values near the surface due to the addition of lime but deeper samples followed similar pH trends as similarly aged samples. Results generally indicate that younger disposal areas have slightly higher paste pH values and relatively lower oxidation reduction potential (ORP) for samples from comparable depths and alteration zones suggesting the degree of sulphide oxidation is lower and/or neutralization reactions are greater compared to older disposal areas.

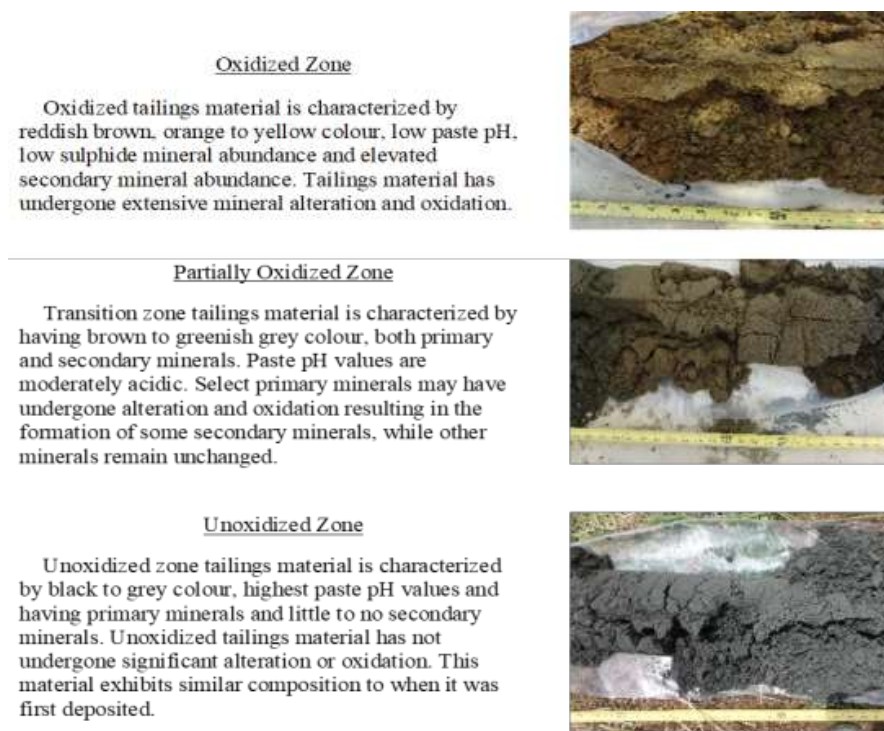


Figure 1. Physical Characteristics of Tailings from a Base-Metal TSF Grouped by Alteration Zone.

Concentrations of iron and sulphur in the solid phase also varied with depth with Fe concentrations being generally lower, and more variable, in the shallow depths of older TSF disposal areas (Figure 2). Similarly, sulphur and calcium were depleted near the surface and increased with depth. The relationship between paste pH and oxidation-reduction potential (ORP) indicate shallow oxidized zones are acidic and oxidizing whereas unoxidized zones are characterized by a sub-neutral paste pH and are less oxidizing resulting in the trends observed in iron, sulphur and other metal(oid) concentrations with depth and alteration zone. The relationship between iron and sulphur in the solid phase chemical analysis also indicates iron phases include sulphur, and likely occur as primary sulphides and secondary sulphates.

Acid base accounting was performed on select samples and compared to historical results for unaltered tailings material. Results for the studied TSFs indicated the total sulphur content varies depending on the alteration zone, depositional area and pyrrhotite management practices over time. Sulphur content was found to be relatively low in relatively younger depositional areas whereas older areas contained up to four times the sulphur from the varying pyrrhotite content. Neutralization potential (carbonate NP and total NP) was less than the acid generating potential indicating the tailings deposited within the TSF have a high potential to produce acid (PAG-tailings). Samples collected from the oxidized zone and some from the partially oxidized zone across the areas examined were further classified in this study as currently acid generating paste on their paste pH.

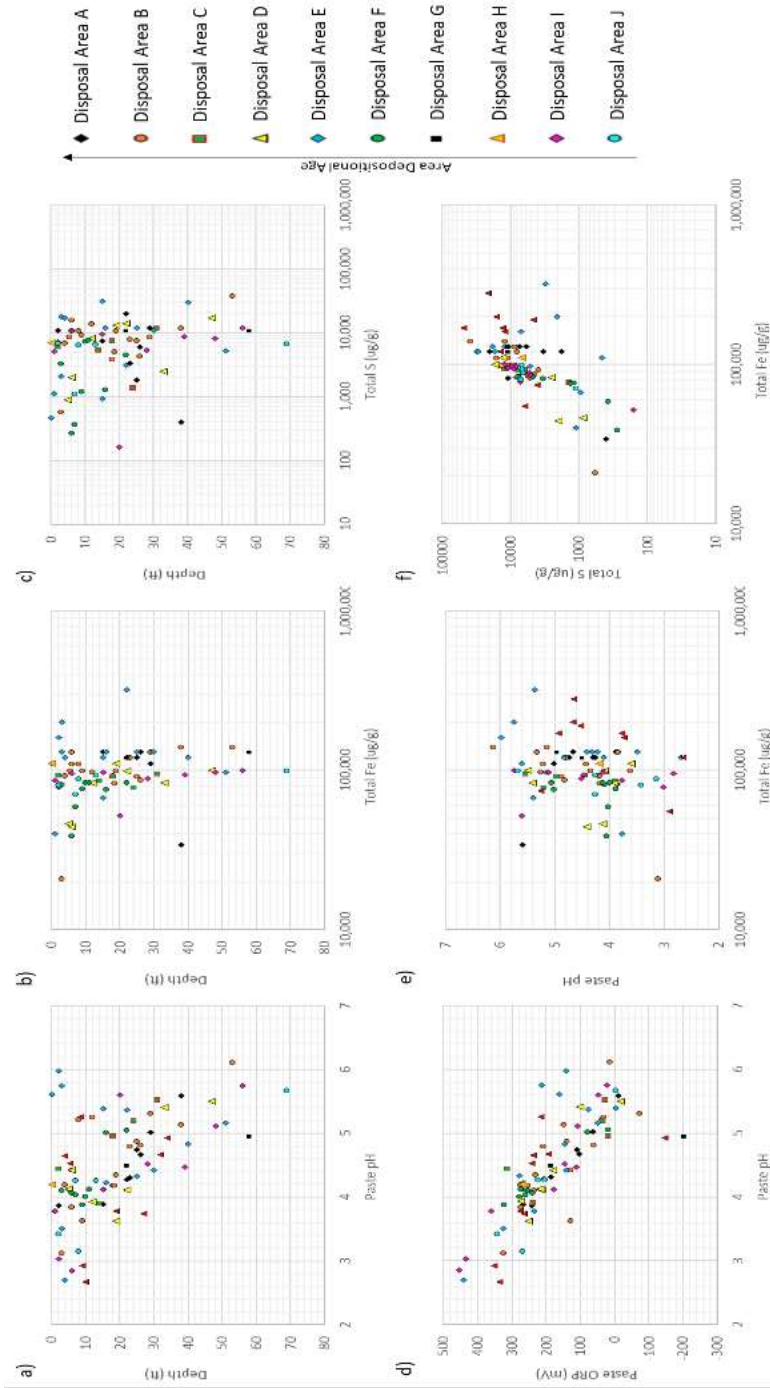


Figure 2. Select Solid Phase Results (a-f) showing the Chemical Composition of Tailings Collected at Various Depths from Various Disposal Areas. Paste measurements were performed using deionized water and were measured in the field. Total iron and sulphur concentrations were determined via acid digestion and ICP-MS/OES. Results are shown for samples collected from various TSF Disposal Areas and various depths.

The mobilization of metal(oid)s were assessed in the single batch extraction tests performed on tailings samples from the various depths and locations (Figure 3). Solutions used in the extractions included deionized water and acidified water to represent varying degrees of acidic surface and less acidic pore waters. The leachate tests performed on various samples collected at depth and with water resulted in slightly higher pH values when compared to the leachate test performed with the acidic solution on the same subset of samples. Similar concentrations of sulphate, Ca, Mg and mobile elements such as Ni, Pb, and Cr were solubilized in both tests; however, concentrations of mobilized sulphate, Fe, Ca, Mg, Cr, Pb and Ni were generally higher in samples collected from the younger disposal areas. When leachates were normalized to the chemical composition of the solid sample, trends were observed suggesting extraction results are a function of the presence of soluble secondary phases produced by mineral alteration processes.

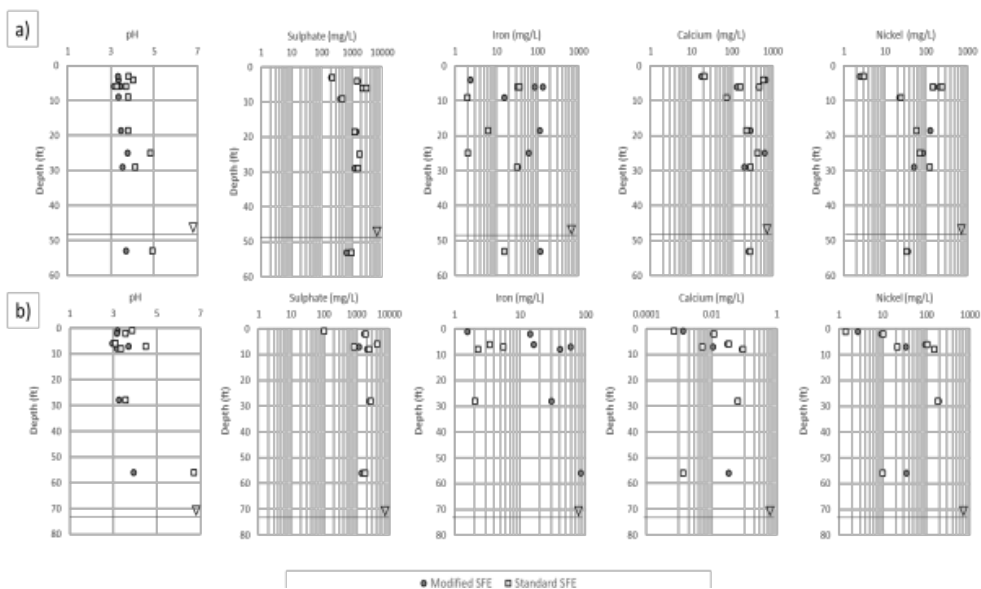


Figure 3. Single Batch Extraction Results for Selected Parameters using Deionized Water (DI) and Acidified DI (HCl to pH 2.2) Leached Tailings from Various Depths and Two Depositional Areas (B and J) Standard SFE included a 24 hour 3:1 leach using deionized water and the modified SFE included the same but used acidified DI to pH 2.2. a) represents an older disposal area, Area B, deposited between 1945 and 1979. b) represents a younger disposal area, Area J, actively deposited since 1985. Results are shown for samples collected from TSF dam crest drilled bore holes to offer comparable locations within the individual disposal areas, note the respective phreatic surface as indicated. The chemical composition of porewater, extracted from shallow and deep horizons below the phreatic surface, is not included in the above figure for simplicity but can be seen in Figure 4 for comparison.

The chemical composition of porewaters, extracted from shallow horizons below the phreatic surface in wells installed in the sampled bore holes, and extraction tests performed on the solid samples (collected from the well screen interval), were compared. Results show single batch extraction tests, performed with DI water (SFE initial pH 5.5) and acidified DI water (Mod SFE initial pH 2.2), reflect the different final pH results between the two tests (Area B: SFE final pH 4.9 and Mod SFE final pH 3.7; Area J: SFE final pH 6.7 and Mod SFE final pH 3.9) for the same sample indicating the differences in solubility products and neutralization reactions under the conditions of the two tests. Similar trends were observed among the disposal areas investi-

gated (not shown) where lower pH values in both tests were observed in samples from older depositional areas. Single batch extraction tests under neutral pH reflected similar pH values to the extracted porewater to younger disposal areas (Area B: porewater pH 6.2 and Area J: porewater pH 6.5). The chemical composition of single batch leachates however, did not well represent the pore water composition that was collected from the same depth (Figure 4). The final pH in the acidic extraction tests better reflected seepage water in older areas (Area B: seepage pH 3.2 and Area J: seepage pH 6.1) In addition, the extraction tests which are sometimes used to evaluate flushing events from heavy rainfall also did not reflect surface water runoff which is characterized by significantly lower pH and higher metal(oid)s content (not shown).

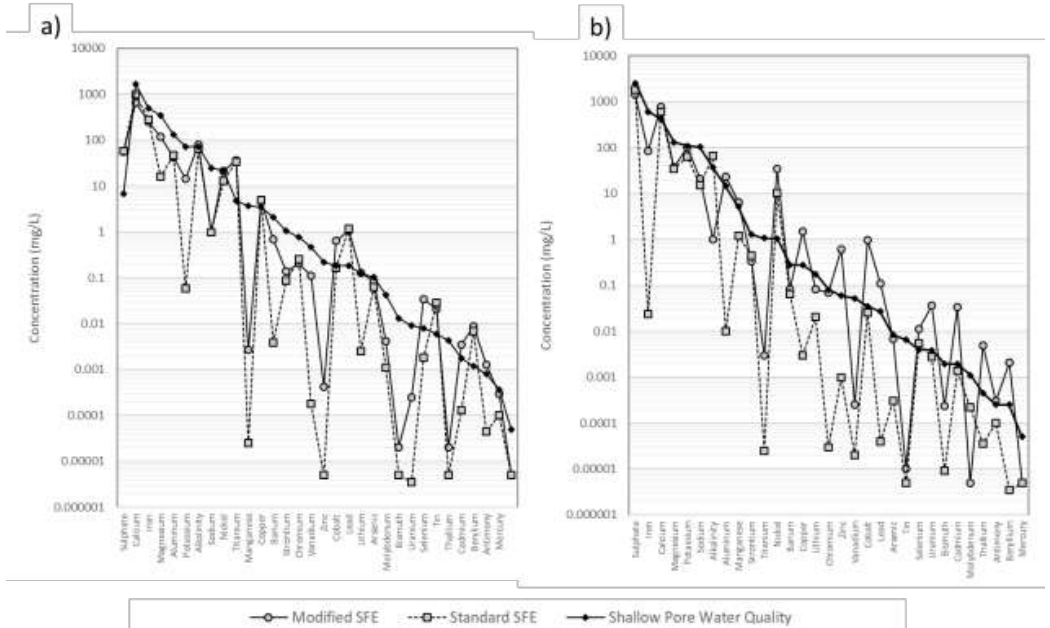


Figure 4. Chemical Composition Results for Single Batch Leachate Extraction Tests using Deionized Water (DI) and Acidified DI (HCl to pH 2.2) Leached Tailings and Pore Waters Collected from the Same Depth for Selected Parameters from Two Depositional Areas (B and J). Standard SFE included a 24 hour 3:1 leach using deionized water and the Modified SFE included the same but used acidified DI to pH 2.2. a) represents Disposal Area B, deposited between 1945 and 1979. b) represents Disposal Area J, actively deposited since 1985. Results are shown for samples collected from TSF dam crest drilled bore holes to offer comparable locations within the individual disposal areas, note the depth of a) and b) differ but are within 2 ft of the phreatic surface.

3.2 Mineralogy

The tailings studied were produced from massive and disseminated sulphide deposits, containing monoclinic (magnetic) and hexacubic pyrrhotite (FeS), pentlandite (Ni₃Fe₇S₂), chalcopyrite (CuFeS₂), and pyrite (FeS₂), minor amounts of cobaltite (CoAsS), sphalerite (ZnS), and galena (PbS). The ore deposits gangue minerals included quartz (SiO₂), albite (NaAlSi₃O₈), biotite (K(Mg,Fe)₃AlSi₃O₁₀(OH,F)₂) various pyroxenes (XY(Si,Al)₂O₆, where X = Al, Fe or Cr; and, Y = Ca or Na) and amphiboles (A₀₋₁B₂C₅T₈O₂₂(OH,F)₂, where A = Na or K; B = Na, Ca, Mg, Fe²⁺, Mn, or Li; C = Mg, Fe²⁺, Al, or Fe³⁺; and, T = Si or Al) and trace clay alteration minerals (variable formulae).

The resulting tailings mineralogy is typical of the base-metal deposit with pyrite and pyrrhotite as the primary sulphides. Tailings samples subjected to XRD analysis resulted in a mineralogical composition containing silicate minerals (albite, biotite, clinocllore, pyroxenes, amphiboles, feldspars and quartz), sulphates (jarosite, schwertmannite, and gypsum), oxides and hydroxides (wuestuite, hematite, maghemite, magnetite and ferrihydrite), and sulphides (chalcocopyrite, chalcocite, covellite pyrite, pyrrhotite and marcarsite); whereby the relative abundance of silicate, oxide and hydroxide, sulphate and sulphide minerals varied with alteration zone and the area's tailings depositional age (Figure 5)

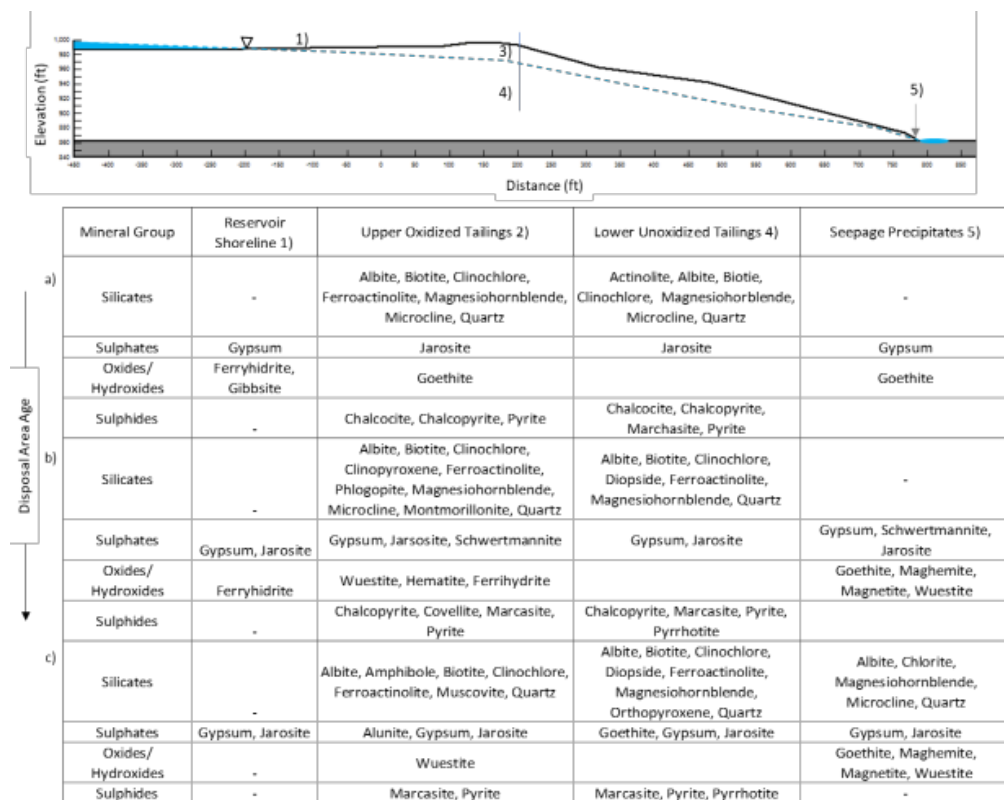


Figure 5. Minerals Identified by XRD from Various Locations within a Base-Metal TSF Upper: Typical cross section through a TSF area showing the upstream reservoir, exiting seepage water and a downstream seepage collection pond. The blue dashed line represents the phreatic surface to which underlying tailings remain saturated and less oxidized. Below: XRD results for tailings samples collected from various locations 1-5 (in upper). A to C) represents three areas within the TSF of different depositional ages (youngest to oldest).

Tailings material from the oxidized zone with the contact paste pH values ranging from 2.6 – 4 contained both primary silicates and secondary mineral phases. Secondary sulphate minerals were present across oxidized tailings material including gypsum (CaSO₄), jarosite [KFe³⁺₃(SO₄)₂(OH)₆], goethite [α -Fe³⁺O(OH)], and schwertmannite [Fe³⁺₁₆(OH,SO₄)₁₂-13O₁₆ 10-12H₂O). Hematite (Fe₂O₃), was the dominant oxide in the oxidized tailings material. The presence of secondary sulphates and oxides formed from the weathering of sulphide minerals, and the absence of sulphide minerals within this alteration zone suggests that the majority of the sulphide grains were dissolved, presumably through abiotic and biotic oxidation processes.

The material in the partially oxidized zone with a contact paste pH ranging from 3.6 - 5.3 is composed of silicates, with both sulphates and/or oxides and sulphides suggesting primary sulphides are partially reacted and secondary phases have formed as a result of these processes. The tailings material in the unoxidized zone is composed of primary minerals including silicates, and sulphides with no measurable secondary sulphate and/or oxide minerals. The presence of dominating sulphide minerals within this zone suggests that either sulphides have not yet been completely dissolved or they have been re-precipitated through an increase in abiotic and biotic reductive dissolution processes.

SEM investigations showed primary and secondary minerals in relatively undisturbed arrangements and textures (Figure 6). SEM investigations also showed amorphous to crystalline secondary phases with different morphologies including massive to globular grains and coatings.

The minerals associated with the the TSF contain trace elements including Ag, As, Bi, Cd, Co, Cr, Fe, Hg, In, Mn, Mo, Ni, Pb, Sb, Se, Sn, Ti, Tl, V, and Zn associated with their crystallographic structures. Secondary phases contained variable trace element content ranging up to 1 wt% of the total composition. Trace metals (e.g. Ni, Pb and Cr) were often associated with secondary jarosite, likely from co-precipitation reactions, and to a lesser extent ferrihydrite, likely from adsorption, and rarely in goethite. Relatively lower concentrations of trace metals associated with goethite can likely be attributed to desorption processes as ferrihydrite aged to goethite. Feldspars were observed altering to clay minerals (likely providing NP), and micro- to nano- sized metal bearing particles were present as residual primary or secondary metal-sulphides and -oxides.

3.3 TSF Surface and Porewater Monitoring

The chemical composition of contact surface water, tailings pore, and seepage water (averaged from a period of 3 years) varied depending on the locations sampled and surrounding physiochemical conditions, as a result of the tailing age and mineralogical composition (primary and secondary minerals).

In general results indicate that pore waters evolve as they progress from the shallow porewaters in dam crests towards the toe and becoming seepage (Figure 7). Reservoirs (where results were available) contained similar pH, ORP and concentrations of iron and sulphate (among other parameters) likely from similar processes and solubility constraints, however, pore and seepage waters differed. Effluents from the disposal areas throughout the TSF studied were characterized by lower pH and elevated metal(oids) when compared to their upstream pore water counterparts and older depositional areas produced lower pH and higher effluent concentrations in comparison to the more recently deposited areas. Flooded and revegetated dispositional areas (Areas B, E, and F) reflected only slightly better water quality but similar characteristics are however present at depth where similar processes are occurring resulting in similar chemical compositions.

Results show the concentrations of iron and sulphate (among others not shown) are related to their relative primary mineral reactions, soluble phase mobility and the pH and Eh (Eh is a temperature dependent function of ORP) of the solution. Statistical analysis of the combined results of this study show mineral alteration reactions with depth along the profile control pore water concentrations and water quality results confirmed the lowest pore water and seepage pH occur at the toe, providing an indication of the progression of ARD reactions with depth and distance.

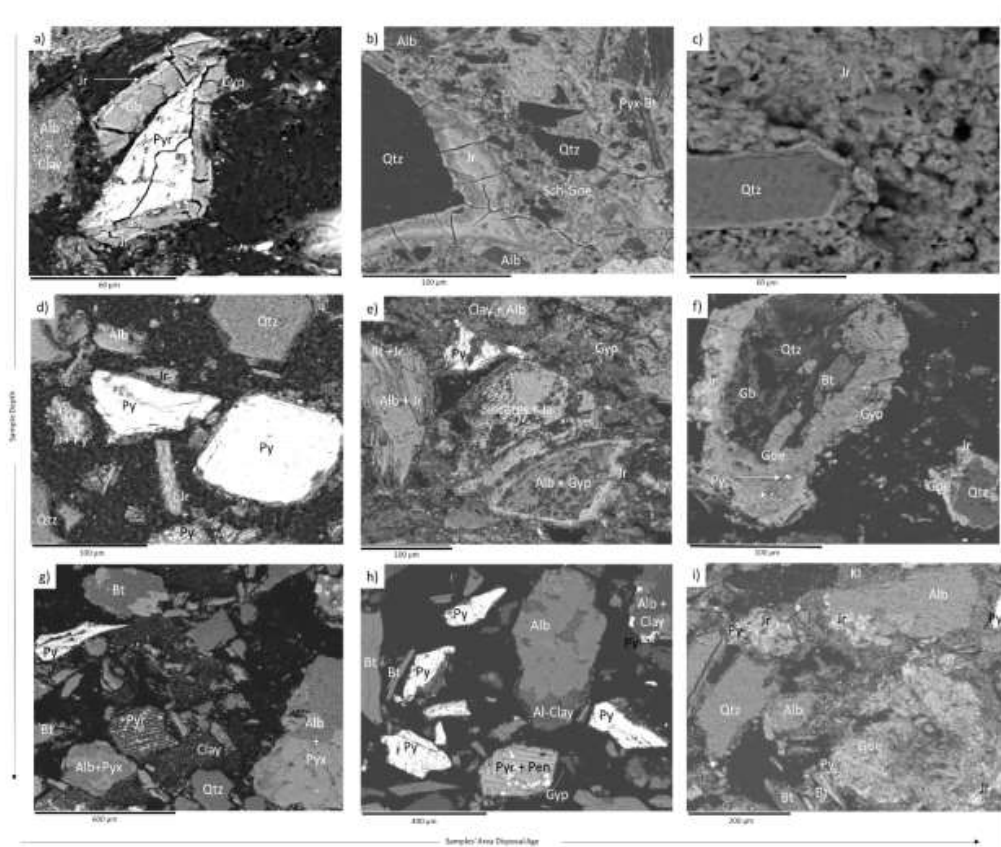


Figure 6. Scanning Electron Microscope (SEM) Backscatter Images of Selected Tailings Samples Organized by Depositional Age and Depth. a) Area I (0.3-0.6 m): fractured pyrite (Py) and primary albite (Alb) altering to clay minerals. Sample shows extensive dissolution and alteration. Secondary reaction products gypsum (Gyp), jarosite (Jr) and goethite (Goe) forming on altered pyrite surface; b) Area G (0.2-0.5 m): hardpan cemented tailings grains (Qtz = quartz, Pyx = pyroxene, Bt = biotite, and Alb = Albite). Cement composed of secondary iron minerals (Sch = schwertmannite and Goe = goethite); c) Area F (0.3-0.6 m): No evidence of silicate minerals remaining with the exception of quartz (Qtz) and complete replacement by secondary amorphous schwertmannite (Sch) to crystalline jarosite (Jr); d) Area H (3.7-3.9 m): fractured pyrite and silicate minerals (albite and quartz) with secondary jarosite and trace gypsum forming on and around pyrite; e) Area D (3.7-3.9 m): altered pyrite surrounded by fragmented silicates altered to secondary clays, and secondary jarosite and gypsum filling pore spaces and coating mineral grains; f) Area B (4.8-5.1 m): increased presence of secondary iron and gypsum coating primary grains, little silicates remaining; g) Area J (7.3-7.6 m): primary tailings minerals showing little evidence of alteration with the exception of some silicates altering to clay minerals and minor fractures in primary sulphides. Pyrrhotite (Pyr) is present at depth and is partially reacted however little secondary iron minerals and gypsum are present and reaction products were likely lost to porewaters; h) Area G (12-12.3 m): primary sulphides show increased fracturing, dissolution rims and are coated with secondary clay and iron sulphates minerals; and i) Area A (11.2-11.5 m): primary tailings minerals including various silicates and iron sulphides show increased weathering and alteration. Secondary gypsum, goethite and jarosite are observed coating primary grains and infilling pore spaces.

Geochemistry

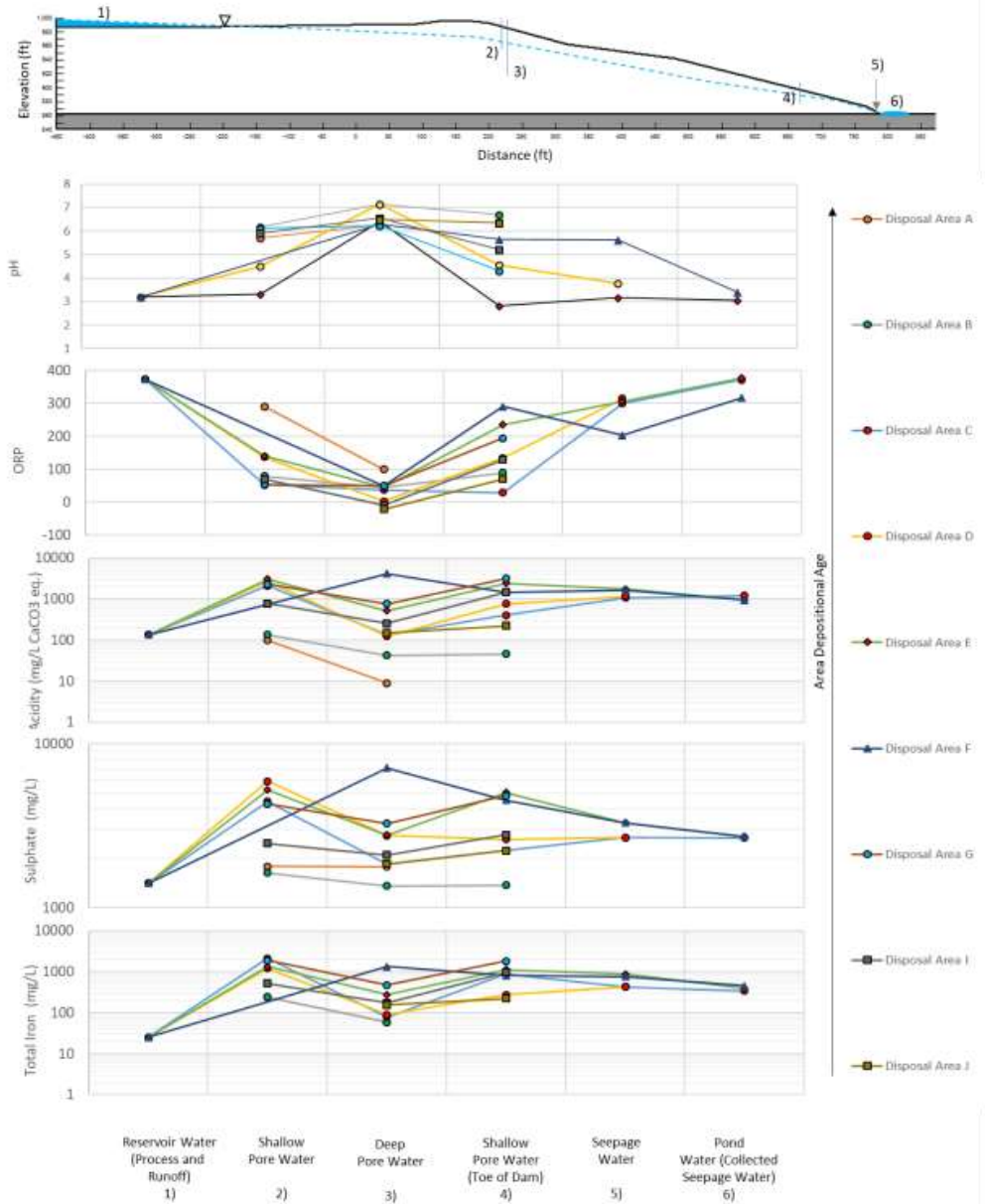


Figure 7. Chemical composition of Surface, Pore and Seepage Water of Selected Disposal Areas within the Studied TSF. Upper: Typical cross section through a TSF showing the upstream reservoir, exiting seepage water and a downstream seepage collection pond. The blue dashed line represents the phreatic surface to which underlying tailings remain saturated and less oxidized. Below: Water Quality results for various locations 1-5 (in upper). Refer to 1. for disposal area details.

4 CONCLUSION

The oxidation of pyrrhotite, pyrite and other primary sulphide minerals was evident in the oxidized and partially oxidized zones of all areas investigated, however, the degree of alteration and resulting alteration products varied with depth and age of the deposited tailings material. Subsequent sulphide oxidation produced lowered pH solutions that depended on the availability of neutralizing minerals and contained elevated metal(oids) that depended on their mobilities.

The concentration of metal(oids) were not well represented by recommended single batch extraction tests when compared to the chemical composition of pore waters. The chemical composition of pore and seepage waters were controlled by the reactions between primary and secondary minerals and the mobility of the elements released depended on the pH, Eh, temperature, pressure, the chemical composition of the solution, and the composition of the minerals within the system which varied by location (e.g. age, depth and distance). Secondary minerals were associated with trace elements indicating metal attenuation mechanism including incorporation into secondary mineral structures and adsorption were occurring, however, evidence suggests that ageing secondary phases can promote their re-release to surrounding pore waters under certain conditions.

The mineralogy and hydrogeochemistry of the sulphide-bearing TSF, in particular the concentrations of H⁺ (acidity), and dissolved metal(oid)s, were controlled by a series of pH-buffering reactions. The resulting acidic to sub-neutral surface and porewaters, containing elevated metal(oid)s, reacted with surrounding gangue minerals of the TSF, in a complex set of thermodynamic equilibrium reactions. Neutralization reactions generally occurred from the weathering and dissolution of carbonate, silicate and oxide species (aqueous and mineral) resulting in the precipitation of specific secondary minerals at specific pH ranges. Secondary minerals that form, as a product of these reactions, were the primary mechanisms of metal attenuation controlling surface and pore water concentrations.

This study demonstrates some of the mineralogical mechanisms controlling the movement of dissolved metals through several TSF profiles in variably aged base-metal tailings. Understanding the type and properties of individual mineral phases and identifying the stages of the many potential reaction pathways, is an essential component of drainage chemistry predictions.

5 REFERENCES

- Alpers Boorman, R.S., and Watson, D.M. 1976. "Chemical processes in abandoned sulphide tailings dumps and environmental implications for North Eastern New Brunswick". *Canadian Inst. Min. Bulletin.*, Vol 69, pp. 86-96.
- Blowes, D. W., Ptacek, C. J., Jambor, J. L. and Weisener, C. G. 2003. "The geochemistry of acid mine drainage". 9.05. In *Treatise on Geochemistry*, Ed. Sherwood, B., Holland, H.D., and Lollar K.K.T Vol. 9. pp. 149-204
- Broughton, L.M., Robertson, A.M., 1992. Acid rock drainage from mines – where we are now, IMM minerals. In: *Metals and Environment Conference*, Manchester, UK.
- Evangelou, V.P. 1995. Pyrite oxidation and its control: solution chemistry, surface chemistry, acid mine drainage (AMD), molecular oxidation mechanisms, microbial role, kinetic, control, ameliorates and limitations. *Microencapsulation*. CRC Press, Boca Raton, FL.
- Evangelou, V.P., and Zhang, Y.L. 1995 A review: pyrite oxidation mechanisms and acid mine drainage prevention. *Environmental Science and Technology*. 25(2) 141-199
- Hammerstrom, J.M., Seal, R.R., Meier, A.L., Kornfeld, J.M., 2005. Secondary Sulphate Minerals Associated with Acid Drainage in the Eastern US: Recycling of metals and acidity in surficial environments. *Chemical Geology*, Vol 215., pp. 407-431.
- Johnson, R.H., Blowes, D.W., Robertson, W.D., and Jambor, J.L. 2000. "The hydrogeochemistry of the Nickel Rim mine tailings impoundment, Sudbury, Ontario". *Contaminant Hydrology*. Vol. 41. pp. 49-80.
- Lottermoser, B.G., 2007., *Sulfidic Mine Wastes*. In *Mine Wastes-Characterization, Treatment, Environmental Impacts.*, Second Ed. Springer.

- Lowson, R.T. (1982) Aqueous oxidation of pyrite by molecular oxygen. *Chem.Rev.* Vol 82. 461-497
- McGregor, R.G.; Blowes, D.W.; Jambor, J.L.; Robertson, W.D. 1998a. "Mobilization and attenuation of heavy metals within a nickel mine tailings impoundment near Sudbury, Ontario, Canada". *Environmental Geology*, Vol. 36, pp. 305-319.
- McGregor, R.G.; Blowes, D.W.; Jambor, J.L.; Robertson, W.D. 1998b. "The solid-phase controls on the mobility of heavy metals at the Copper Cliff tailings area, Sudbury, Ontario, Canada". *J. Contaminant Hydrology*, Vol.33, pp. 247-271.
- Nordstrom D.K. and Alpers C.N. (1999) Geochemistry of acid mine waters In *The Environmental Geochemistry of Mineral Deposits*. Ed: G.S.Plumlee and M.J.Lodsdon. Society of Economic Geologists Inc., Littleton, D.C. Vol 6A. pp. 133-157
- Nordstrom, D.K. and Southam, G. (1997) Geomicrobiology of sulfide mineral oxidation. In *Geomicrobiology : Interactions between Microbes and Minerals*. Ed J.F.Banfield and K.H.Nelson. Mineralogical Society of America, Washington, DC. Vol 35. pp 361-385... Also check if the type width is 150 mm and the page length is 240 mm.

A New Safe and Sustainable Approach for Constructing Ballast Layers for Waste Containment Facility Liner Systems

C. Cilliers

Jones & Wagener, Johannesburg, Gauteng, South Africa

M. Briers

HUESKER Inc., Charlotte, NC, United States of America

ABSTRACT: Ballast layers are used to protect a containment facilities primary liner against U.V. radiation and thermal expansion whilst also ensuring intimate contact between the liner and underlying layers. Traditional ballast solutions comprise soil layers (typically enhanced with additives such as cement or bentonite) or concrete. The existing solutions require mechanical plant to drive above the primary liner during installation and research has shown that such operations significantly increase the risk of damage (leakage) to the lining system. A flexible geosynthetic mattress ballast (GBL) layer has been developed to provide the required performance characteristics of the ballast layer, whilst mitigating damage during installation above the primary liner. Further advantages of the GBL include potential re-use of waste, which has large environmental advantages, including lower carbon footprints and zero reduction in the available storage space of the facility. Practical aspects from a case history will also be presented.

1 INTRODUCTION

The development of geosynthetics continues to grow each day. New applications of geosynthetics are being found that form from overlaps of existing functions such as protection, separation, filtration and drainage. One such new application was developed and continues to show promise after it was implemented in a tailings storage facility back in 2015. This is the application of the Geosynthetic Ballast Layer (GBL): A new product that was developed to reduce the damage caused during conventional ballast installation processes.

The GBL is an “innovative geotextile containment system utilizing state-of-the-art weaving technology, which provides a tubular system interconnected into a singular geosynthetic mattress configuration which is filled with waste product (Huesker, 2016, p. 19)” and becomes the main ballasting medium. For the case study discussed, this material is industrial mineral waste which is pumped to the facility in the form of slurry. However, in other applications the filling material could range from sand to concrete.

A further optimization is the addition of a non-woven geotextile stitched to the exposed side slope layers to counter UV degradation of the underlying woven geotextile. This optimization was included

as part of the case study project as the ballast layers on the side slope take longer to be covered by the waste body due to the filling process.

A further potential advantage of the GBL relates to sustainability and this topic is introduced and discussed in more detail within this paper. The main advantage is that the site waste product for which the waste containment facility is being constructed is also used to create the ballast layer itself (as part of a geosynthetic/waste composite structure), which has large advantages in terms of sustainability for site operations. It is also worth highlighting that site owners can consider carbon off-setting as part of their operations (this subject is not dealt with further in this paper).

2 PREVIOUS RESEARCH

At Landfill 2015, the GBL was first introduced (Cilliers, 2015). The idea behind the ballast layer was to create a protecting layer above the primary geomembrane of a waste facility without using conventional methods of placing a typical ballast layer with large construction plant. Nosko and Touze-Foltz (2000) found that placing the ballast layer in this way was the largest contributing factor to leakage due to damage of the primary liner.

The GBL would need to fulfil all the features of the conventional ballast layer mainly: protecting the primary geomembrane from mechanical and UV damage, applying a confining stress to ensure intimate contact between the primary geomembrane and the underlying clay layers and ensure that no folds, due to thermal expansion, are entombed in the primary liner during installation.

Huesker have a long history of manufacturing Soiltain dewatering tubes made from woven geotextiles. Huesker also have a product range named Incomat, which effectively is a geotextile formwork that acts as a surface sealing system while protecting against erosion, mechanical damage and buoyancy, forces being traditionally filled with concrete (Huesker, 2016). Huesker and Jones & Wagener worked together to create a GBL prototype based on the concepts of the Soiltain dewatering tubes and Incomat products. The GBL concept was then discussed and offered as an alternative to a Client who was in the early stages of constructing an industrial waste facility. The facility was planned to have a Class-A liner system (South African Norms and Standards, 2013) with a conventional cement stabilized sand ballast layer. The Client agreed to start with site based trials to see if the GBL would be able to perform the required functions of the conventional ballast layer (CBL).

The trials were carried out both on the side slope of an earlier phase of the waste facility and on the horizontal surface of a filled waste facility to mimic the basin of the new facility.

The results were sufficiently successful to adapt the design to use the GBL as the entire ballast layer in the new facility. The trials also resulted in essential information such as expected shrinkage during filling which is later used to size the overlaps on the ballast layer panel layout. The trial also provided an indication of the difficulty of operations involved to fill the bags. The results of the trial were presented at the Landfill 2015 conference.

This paper continues to present information of the practical elements experienced from the end of the trial stage, throughout the manufacturing process, to the commencement of installation at site and also introduces a comparison between the GBL and CBL in relation to sustainability.

3 SUSTAINABILITY

The term sustainability can be defined as “development that meets the needs of the present without compromising the ability of future generations to meet their own needs” (Brundtland, 1987). One of the main indicators of sustainability is CO₂ emissions.

Sustainable low carbon construction targets are being set by several countries, through governments and/or funding bodies (e.g. Asian Development Bank). The construction industry’s drive for sustainable practices are focused on reducing CO₂, because CO₂ reduction contributes to national

targets for reducing overall greenhouse gas emissions (Koerner, 2016). Carbon foot printing techniques are used to establish the embodied carbon for a solution over set life cycle boundaries. A key component of any such assessment is the embodied carbon of the materials used within the construction solution.

Appropriate geosynthetic solutions can improve the sustainability credentials of a construction project (WRAP) compared to more traditional construction solutions. Following recent research in Europe (Raja et al, 2015), the accuracy and repeatability of assessing the embodied carbon of geosynthetics is improving.

The relevant European Union harmonized conditions (EU No 305/2011, 2011) relate to the Construction Products Regulation (CPR) and provide a common technical language to assess the performance of construction products and ensures that reliable information is available to professionals, public authorities, and consumers, so they can compare the performance of products from different manufacturers in different countries trading within the European Union. Clause 55 of the CPR states: “The basic requirement for construction works on sustainable use of natural resources should notably take into account the recyclability of construction works, their materials and parts after demolition, the durability of construction works and the use of environmentally compatible raw and secondary materials in construction works”.

Clause 56 of the CPR states ‘For the assessment of the sustainable use of resources and of the impact of construction works on the environment, Environmental Product Declarations (EPD) should be used when available’.

HUESKER has undertaken detailed analysis of its CO₂ emissions through its EPD certificates (EPDs, 2014 & 2016), which provide a full life cycle analysis (LCA), including carbon usage, assuming a cradle-to-gate model. The embodied carbon can now be accurately calculated for certain geosynthetic products and solutions.

The GBL solution was compared against the CBL. The CBL considered comprised a 300mm thick (compacted thickness) cement stabilized sand layer. The sand is sourced and screened on-site to reach a uniform grading size. The purpose of this example is to carry out an Embodied Carbon comparison of the two solutions and is based on an example calculation carried out for a site in South Africa assuming a 1ha area of site and is based on a cradle-to-end of construction comparison (EC values for production, transport to site and construction). Common activities for both the geosynthetic and traditional ballast solutions can be omitted, as they cancel each other out with respect to comparison and this helps simplify the analysis. It is highlighted that the activities accounted for in this case study are by no means exhaustive, and a more rigorous study may include country specific values for South Africa and a more detailed breakdown of construction activities on site. Nevertheless, the exercise remains valid and provides a clear overview and comparison of the two construction techniques in terms of carbon emissions.

Table 1 provides a summary of the input parameters to allow comparison of the two ballast solutions (i.e. CBL and GBL) in terms of EC. The value chosen for the geosynthetic EC value was 3.0 kgCO₂e/kg (Table 2), which is based on an averaged value from the combined EPD certificates of HUESKER, taking into consideration the amount of raw material used in the GBL (i.e. ~650 g/m² for the 3-layer material). This approach is conservative because the majority of the GBL used is a lighter weight two-layer material, which does not include the sacrificial nonwoven upper geotextile layer. Therefore, the overall EC value of the GBL is likely to be lower for many of the future projects. It is worth highlighting that the study by Raja et al (2015) highlights the significance of geosynthetic weight in terms of sustainability as the embodied carbon of the raw polymer accounts for approximately 80% of the final EC for a geosynthetic product at the gate (i.e. cradle-to-gate). Therefore, in order to achieve the optimum sustainability from a geosynthetic based construction solution, the geosynthetics must be used appropriately in design and also the polymer used efficiently in producing a material that can achieve the design criteria (Koerner, 2016).

The EC values for the cement stabilized sand to form the CBL are taken from published literature (Hammond et al, 2011) and then multiplied by the amount of material required to form the CBL (Table 2).

As the EC values for the GBL are cradle-to-gate (i.e. to the point of manufacture and ready for delivery from production plant) additional values for transport to site are required (Table 3). The calculation of the EC for transport (Equation 1) considers the distance travelled and the emissions of the transport mode. For this comparison it has been assumed that the cement was sourced locally within South Africa and the site is 300km from the cement production factory. For the road transport (both within Europe, where applicable, and South Africa), a 20t rigid Heavy Goods Vehicle was assumed with a fuel consumption of 3.33km/liter (U.K. Department for Transport, 2012) and CO2 emissions for diesel of 2.60 kgCO2 per liter of fuel (Defra, 2013). Values may differ for other Countries and reference made to the local guidelines/publications, if available.

$$C = (\beta (2D/\alpha))/1000Q \quad [1]$$

C= Total CO2 emissions per ton (tCO2/t),
 D= distance of transportation (km)
 α= Fuel consumption of rigid HGV
 Q= Quantity of material (tons)
 β= CO2 emissions per liter of fuel.

Table 1 – Input values for EC calculation

Property	Value	Units
Input data for Cradle to Gate		
Area	10,000	m ²
GBL mass per unit area (unfilled)	0.65	kg/m ²
GBL cradle to gate EC value (Raja et al 2015)	3.00	kgCO ₂ e/kg
CBL mass per unit area	2000	kg/m ³
Cement stabilized soil (8% cement) cradle to gate EC value (based on Hammond and Jones, 2011)	0.084	kgCO ₂ e/kg
Additional Data for cradle-site		
GBL Transport Distance (road)	675	km
GBL Transport Distance (sea)	16,000	km
Sand Transport Distance (on site)	0	km
Cement Transport Distance	300	km
α= Fuel consumption of rigid HGV	3.33	km/l
β = CO ₂ emissions per litre of fuel HGV	2.60	kgCO ₂ /litre
α _s = Fuel consumption of ship*	45	Km/l (per container)
β _s = CO ₂ emissions per ton-km – Ship**	0.01	kgCO ₂ /ton-km
Additional Data for cradle-end-of-construction		
Sand Layer thickness	300	mm
Compaction effort	1000	m ² /hour
Compaction Plant Fuel Usage	16.0	litres /hour
β = CO ₂ emissions per litre of fuel	2.60	kgCO ₂ /litre

* https://en.wikipedia.org/wiki/Energy_efficiency_in_transportation

** http://people.exeter.ac.uk/TWDavies/energy_conversion/Calculaion%20of%20CO2%20emissions%20from%20fuels.htm

Table 2 - Calculated EC values

GBL mass	6.5	t	CBL mass	6000	t
			Cement mass (based on 8% cement ratio)	520	t
Geosynthetics Embodied Carbon	Total	19.5	tCO ₂ e	CBL Total Embodied Carbon	504 tCO ₂ e

Table 3 - Calculated transport emissions

Distance	675	km	Distance (for cement)	300	km
Truckloads road	1		Truckloads	1	
Distance sea	16000	Km			
Container sea	1				
GBL transport emissions	1.162	tCO ₂ e	CBL transport emissions	0.468	tCO ₂ e

The construction plant emissions in this case account for the main carbon producing aspects of the construction. For the GBL the construction emissions are considered to be zero because any emissions produced due to the movement and positioning of the rolls of GBL with construction plant are vastly offset by the direct pumping of waste from the processing plant into the geosynthetic material to form the GBL. For the CBL, the construction emissions to spread and compact the CBL are calculated (Table 4).

Table 4 - Construction emissions

CBL Number of layers	1		GBL Number of layers	1	
Time for 1 compaction pass (full area)	10.00	hrs			
Number of passes / layer	4				
compaction time	40	hrs			
Fuel consumed	640	l			
CBL compaction emissions	1.66	tCO ₂ e	Total for geosynthetic construction	0	tCO ₂ e

Table 5 provides a summary of the total Embodied Carbon emissions including the material, transport and construction totals. It is clear that the majority of the EC emissions are produced during the production of the material used to form the ballast layer. For the CBL, if the sand had been sourced off-site the EC emissions for transport could also have been high, due to the bulk volume of the sand. The use of the waste product to fill the geosynthetic for this case study has a huge advantage from a sustainability point of view. Although not discussed as part of this paper, further research on the advantages of carbon off-setting, related to the use of waste to form the ballast layer would also be highly interesting.

Table 5 – Total calculated Embodied Carbon emissions

Solution	Embodied Carbon emissions (tCO ₂ e)			
	Embodied	Transport	Construction	Total
CBL	504	0.468	1.66	506.3
GBL	19.5	1.162	0	20.7

4 PRACTICAL ASPECTS

Due to the nature of the GBL, in its current form, it needs to be manufactured to size. Therefore a panel layout needs to be agreed upon between all parties. This panel layout becomes the official plan from which the material list is generated. The material list is formed from two sections: basin and side slope. Each panel has a corresponding number and length. The panels are also placed in a specific sequence such that the delivery schedule of the panels can be matched to the construction schedule if required. It is also important to note for side slope panels that additional length was added before and after the required length of side slope to cater for anchorage and toe support.

Knowing the method of installation before manufacturing also assists in packaging the bags such that deployment is carried out efficiently and correctly on site, this is assisted by printing suitable labels on the GBL panels. This helps specifically for the side slopes where the non-woven geotextile needs to face upwards as well as a certain length be placed at the top of the crest for anchorage.

Strict adherence to the setting out of the facility during the earthworks stage is required to ensure that deviations between panels manufactured to size and the as-built dimensions of the facility are compatible. The consequence of incompatibility is that the panels will not cover the full footprint of the liner at installation stage and additional panels will need to be supplied leaving some primary geomembrane exposed unless a temporary sacrificial cover layer is used.

Filling of the GBL with mineral waste slurry has commenced now that the installation is complete. It was estimated that it would take up to 5 months from when the first ballast layer is installed to when the first ballast layer is filled with slurry (the actual period turned out to be 24 months). Therefore the ballast bags needed to be suitably held down against wind uplift during this period.

Giroud, Pelte and Bathurst (1995) published equations to calculate the size and spacing of sand bags to suitably restrain geomembranes against wind uplift. The equations consider wind speed, altitude and suction factors that differ for the location of the geosynthetic whether it be placed on the basin, side slope or crest. These equations have been used to size the spacing for the ballast layer and are considered conservative as the ballast layer is more permeable than geomembrane and shouldn't experience as much suction from the wind.

The results of the equations indicate that the following spacing is required for temporary ballasting with sand bags:

- 1.25m spacing on the side slopes
- 1.80m spacing on the basin

While this spacing may seem conservative, the wind speeds in the location of the site during the autumn season are very high and previous facilities constructed during this time have had significant blow-outs of geomembrane which need to be replaced. The spacing is only used as a guideline; the spacing of the bags also need to consider the overlaps and ensuring that the ends of the layers where the wind could get below the layer are suitably sealed.

It was also essential to ensure that both the rope that holds the sandbags in place and the actual bags used are manufactured from UV resistant material. The first few sheets that were installed with the above bag spacing and are illustrated in Figure 1.

With any application of geosynthetics, veneer stability should always be assessed to ensure there is little risk of slippage. In terms of this installation, the GBL is being installed on textured geomembrane. Koerner and Narejo (2005) states that the expected residual friction angle between a woven geotextile and a textured geomembrane is in the range of 18°. On a 1[v]:3[h] slope of 18.4°, some slippage would be expected if no additional anchorage takes place at the crest. However, the intention is to securely anchor the GBL at the crest as illustrated in Figure 2. The ballast layer is placed in the same anchor trench as the geomembrane which ensures no sliding on the top surface of the geomembrane. This is then followed by a cement stabilized layer that will further anchor the ballast bag to the crest while completing the final ballasting functions as the slurry within the bags will not be able to extend beyond the full service level of the facility.



Figure 1: The geosynthetic ballast layer installed on the side slope and suitably ballasted with UV resistant sand bags and rope. The GBL is white due to the exposed non-woven geotextile being stitched to the underlying black woven geotextiles.

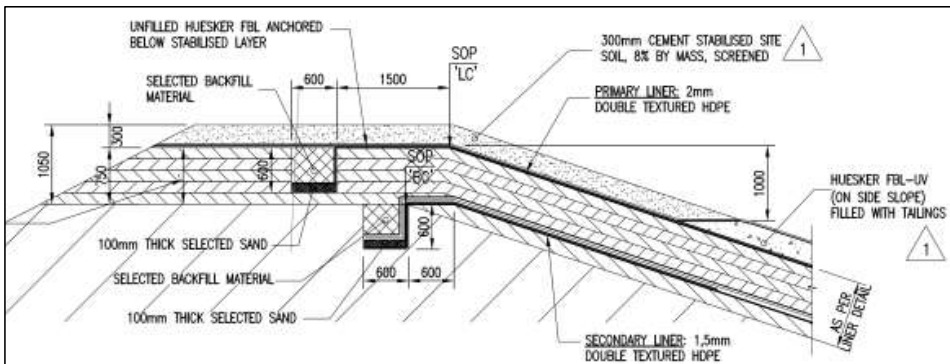


Figure 2: Anchorage detail of GBL at the crest



Figure 3: Construction of the cement stabilized soil perimeter cap. The GBL in the basin does not have a white non-woven geotextile stitched to the surface, as these will be filled first.

In order to fill the ballast bags, a pump point has been installed at the low points of the basin. During filling of the bag, there is continuous flow of liquid being generated from the dewatering process which drains to these low points. The liquid pools at the low point and will eventually need to be pumped out to another waste facility. Therefore these low points needed to be in place before the pumping of slurry into the ballast layer commenced.

Figure 4 illustrates the detail of the pumping low point. While the Concrete Canvas product may not be financially viable to use as a ballast layer over large areas, it provides convenience in the form of providing a good hardened surface for pumping activities which is easy to install and also does not pose significant threat to the primary geomembrane during installation.

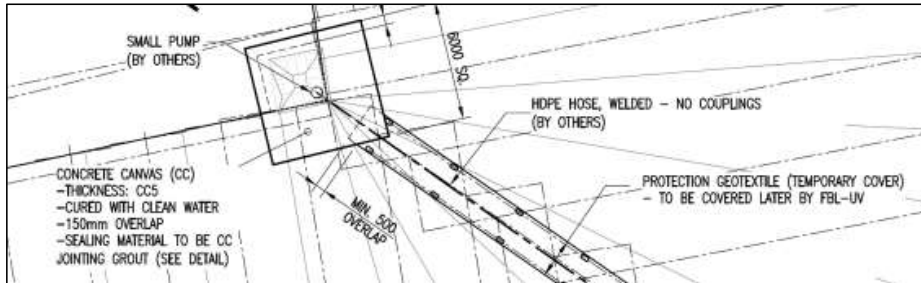


Figure 4: Pumping point detail at low spot of basin

5 OPERATIONAL ANALYSIS

The site trial of the ballast mattress took place on top of a smooth geomembrane on the side slope of an existing facility. From this trial, the estimated shrinkage of 26% was used to design the panel layout, taking into account the size of overlaps required. However, it is assumed that the shrinkage would be less on a textured geomembrane as there should be more resistance to the ballast moving on top of the geomembrane. This, however, leads to a conservative estimate of ballast material required.

During the same site trial, the ballast mattress was relatively easy to fill on the side slopes, however, the horizontal layers appeared challenging to fill completely. By making small changes to the entry position of the inlet and the pressure at which the slurry was pumped into the ballast mattress, it was effectively filled with solid tailings. Afterwards it was decided to control the pumping using a pressure regulator during installation (Cilliers, 2015).

The operations that will be required to fill all the ballast bags is expected to be a long process. There is approximately 38 000m² coverage of ballast layer on the side slope and similar on the basin. This results in approximately 490 ballast layer sheets that need to be filled. Assuming a production rate of one sheet a day this is approximately 22 to 24 months' worth of daily operations.

As the intention of using a GBL is to prevent damaging the primary liner, the filling operation is being carried out carefully and under supervision. While the non-woven geomembrane added for additional UV protection is considered to be sacrificial, the effect of solar radiation on the ballast bag is visually evident as shown in Figure 5, where at the time the trial ballast panel on the side slope had been in place for 12 months. Samples of this geotextile have been taken for testing and reporting on the degradation of the cover layer will be discussed in a future paper.



Figure 5: UV degradation evident on non-woven sacrificial geotextile cover on side slope ballast layers.

6 INITIAL FILLING EXPERIENCE

Filling of the first few GBLs has commenced in the basin. The Client is currently optimizing the form of manifold to use to fill the bags – see Figure 6. The manifold is formed by a perpendicular base HDPE pipe with 5 HDPE off-shoots each entering one of the tubes of the GBL. Slurry is then pumped through the manifold from the plant. The addition of a ventilation pipe at the end of the manifold has assisted in air flow during the filling process. Initially, a ball valve was added to each off-shoot pipe to control the flow. However, these were in the process of being removed as they did not serve a function during filling.

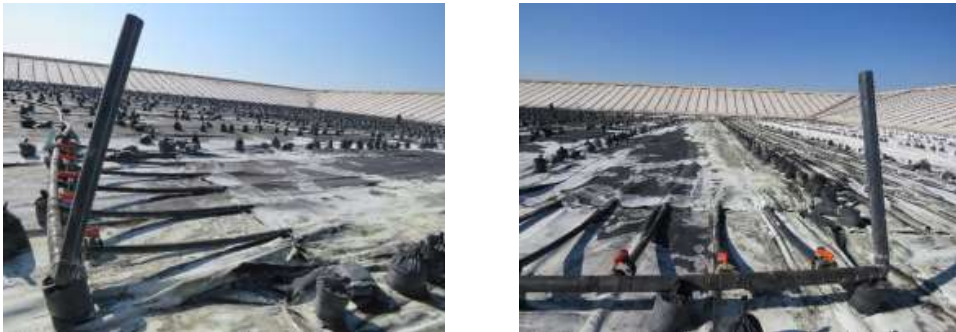


Figure 6: Optimized manifold showing ventilation pipe

One of the difficulties is ensuring that the entire bag is filled over the 50m length in the basin. During filling, the entire bag fills with liquid so it is difficult to observe where the solids are settling and whether the entire bag is full of solids. In some cases, the solids settled near the entrance by the manifold. In other cases, the solids settled near the end of the bag and in others the full bag was successfully filled as shown in Figure 7. The result is that the manifold can not be left unattended during the filling process and requires constant monitoring.



Figure 7: Successfully filled GBL on the basin

Other difficulties include removing all the sand bags as they interfere with the filling process. Any liquid above the ballast bags also interferes with the initial filling of the bag with liquid therefore it is essential to ensure that all excess liquid reports to the low point where the pump pad is located.

No GBL bags on the side slope have yet been filled, however, the lessons learnt in terms of optimizing the manifold and ensuring even filling of the bag will likely lead to an easier process – gravity filling on slopes. The sand bags were also placed on the sides of the GBL on the side slopes, therefore should be less of an interference during filling.

7 COST CONSIDERATIONS

In the Landfill paper (Cilliers, 2015), the costs of various ballast layer alternatives were presented. When comparing the costs of storage savings per m^3 , the cost of the geosynthetic ballast layer did compare favorably to the alternatives. However, it must be noted that this was based on a specific exchange rate at the time ($€1 = R 14.35$). As the GBL was the only international product in the comparison, its cost is influenced by exchange rate fluctuations. With current rates, there would be an approximate cost increase of 10% that would need to be considered when comparing to alternatives.

8 CONCLUSIONS

The GBL is an exciting new application of geosynthetics in lined facilities. It shows promise in providing all the essential services of a ballast layer while significantly decreasing the risk of damage to the entity it ultimately aims to protect, the primary geomembrane.

The filling process has commenced and some early challenges include optimizing the manifold used to fill the bags as well as ensuring an even distribution of solids over the length of the bag. These challenges are expected for an operations-intensive alternative and should not be a deterrent for future applications of the GBL.

In terms of sustainability the use of the GBL for the case study highlights a very large saving (i.e. >2300%) in Embodied Carbon emissions compared to the CBL. The main reason for this is the use of the waste product on site to form the ballast layer within the geosynthetic. Other advantages not discussed in this paper, but worth highlighting, include the saving in void space of the waste cell i.e. the CBL would have taken up 0.3m of space which is now filled with the same waste product that will be placed in the cell when construction is complete.

For this project the total storage capacity was increased by 3% to 4% or 150,000m³. There is also the monetary and time saving for installing the GBL compared to conventional layers. The site owner/operator can now also potentially off-set carbon and/or gain carbon credits due to re-using the waste as part of the construction. This subject requires further research into the local South African guidelines on carbon credits and off-setting to see if there would be a potential further advantage.

This paper and the case study discussed, highlights the importance of considering several factors when selecting the optimum ballast layer, including but not restricted to: project sustainability improvement, greater use of waste products, increased void space for waste depositing and overall project cost savings. The suitability of using the GBL compared to CBL should be assessed on a project-by-project basis.

REFERENCES

- Brundtland, G. (1987). *Our common future: The World Commission on Environment and Development*. Oxford University Press, Oxford, UK.
- Colliers C. (2015). The use of geosynthetics in the installation of ballast layers. Proceedings of the 2015 Landfill Conference, September 2015, Tulbagh, Western Cape, South Africa.
- DEFRA. (2013). *Guidelines to Defra's GHG conversion factors for company reporting*. Department for Environment, Food and Rural Affairs, London, UK.
- Environmental Product Declaration Number EPD-HUE-20140085-IAB1-EN, Huesker Synthetic GmbH, 2014. Institute Construction and Environment e.V. (IBU), Germany.
- Environmental Product Declaration Number EPD-HUE-20160015-IAC1-DE, Huesker Synthetic GmbH, 2016. Institute Construction and Environment e.V. (IBU), Germany.
- Environmental Product Declaration Number EPD-HUE-20160014-IAC1-DE, Huesker Synthetic GmbH, 2016. Institute Construction and Environment e.V. (IBU), Germany.
- Giroud, J.P., Pelte, T. and Bathurst, R.J., 1995, Uplift of Geomembranes by Wind, *Geosynthetics International*, 2, (6), pp. 897-952.
- Hammond, G.P. & Jones, C.I. (2011). *Inventory of (Embodied) Carbon & Energy (ICE) V2.0*. Department of Mechanical Engineering, University of Bath, UK
- Huesker. (2016). *Geosynthetic Ingenuity in Mining*. Gescher, Germany, Huesker Synthetic GmbH.
- Huesker. (2017). *Incomat® Geosynthetic Concrete Mattress System for Hydraulic Engineering*. Gescher, Germany, Huesker Synthetic GmbH.
- Koerner, R. M., (2016). *Geotextiles: From design to applications*, 1st ed., Woodhead Publishing, Sawston, Cambridge, U.K.
- Koerner, GR and Narejo, D. Direct shear database of geosynthetic-to-geosynthetic and geosynthetic-to-soil interfaces. GRI Report 30. Geosynthetic Research Institute, Pennsylvania, USA.
- Nosko V. and Touze-Foltz N., (2000). Geomembrane liner failure: modelling of its influence on contaminant transfer. Proceedings of the Second European Geosynthetics Conference, Patron Editore, Bologna, Italy, pp 557-560.
- Raja, J., Dixon, N., Fowmes, G., Frost, M., Assinder, P. (2015). Sustainable Construction Solutions Using Geosynthetics: Obtaining Reliable Embodied Carbon Values, *Geosynthetics International* 22 (5) pp 393-401.
- Regulation (EU) No 305/2011, (2011). Harmonised conditions for the marketing of construction products, European Parliament.
- RSA (Republic of South Africa) (2013c) National Environmental Management: Waste Act (59/2008): National norms and standards for disposal of waste to landfill. Government Gazette 36784 No.R. 636 of 23 August 2013.
- U.K. Department for Transport. (2012) Fuel consumption by HGV vehicle type in Great Britain, 1993 to 2010. Table RFS0141. Domestic road freight activity (RFS01). Available from: <https://www.gov.uk/government/statistical-data-sets/rfs01-goodslifted-and-distance-hauled>.
- WRAP Project MRF116 (2010). *Sustainable Geosystems in Civil Engineering Applications*. Waste and Resources Action Programme, Banbury, UK.

Critical Strength of High Peel Strength Geosynthetic Clay Liners at Low Normal Stresses

S. Ghazizadeh and C. Bareither

Colorado State University, Fort Collins, Colorado, USA

ABSTRACT: The use of Geosynthetic clay liners (GCLs) in containment applications including slopes can expose them to shear and normal stresses that must be resisted internally and at the interface between the GCL and the adjacent soil or geosynthetic layer. Needle-punched reinforced GCLs (NP GCLs) with high peel strength are designed for high σ_n applications; however, they may also be used in low σ_n applications. To evaluate the internal and interface shear behavior of high peel strength NP GCLs at low σ_n , a series of displacement-controlled internal and interface direct shear tests were performed with $\sigma_n \leq 500$ kPa on three NP GCLs with different peel strength. Consistent increase in the internal shear strength of NP GCLs was observed with increasing peel strength; however, no significant increase in the interface shear strength between the NP GCLs and textured geomembrane (GMX) was observed with increase in peel strength.

1 INTRODUCTION

Geosynthetic clay liners (GCLs) are hydraulic barriers consisting of a layer of bentonite clay encapsulated between two geotextile layers, or adhered to a geomembrane (ASTM D 4439). The use of GCLs in barrier systems of containment applications such as heap leach pads, municipal solid waste systems, etc. has been increased due to the low hydraulic conductivity, acceptable mechanical behavior, ease of installation, and economic advantages (Guyonnet et al. 2009, Fox & Stark 2015). In these applications, GCLs can be exposed to high shear (τ) and normal stresses (σ_n) (Lupo 2010) that needs to be resisted internally within the GCL, and at the interface between the GCL and the adjacent soil or geosynthetic layer. The design of GCLs for liner and cover systems of containment applications is based on the critical strength (τ_{cr}) which is the minimum value of the GCL internal strength and the interface shear strength between the GCL and adjacent geosynthetic layer. Internal shear strength of GCLs are enhanced via processes called stitched-bonding and needle-punching (Fox & Stark 2015) considering the low internal shear strength of the hydrated sodium bentonite (Mesri & Olson 1970). In the needle-punching process, a series of fibers from the top non-woven geotextile are punched through the bentonite layer and entangled into the lower woven or non-woven carrier geotextile.

To express the extent of needle-punching in a NP GCL, manufacturers use an index strength parameter called peel strength. Peel strength (PS) is defined as the average tensile force per specimen width required for peeling apart the carrier and cover geotextile of NP GCLs in a tensile test (ASTM D6496/6496M). Considering that the internal shear strength of a NP GCL increases with an increase in the peel strength (Athanasopoulos & Yuan 2011; Fox & Stark 2015; Bareither et al. 2018), high peel strength NP GCLs (e.g. $PS \geq 2600$ N/m) are designed for high stress applications such as heap leach facilities where the applied normal stress can be as high 4 MPa (Lupo 2010). Despite that, high peel strength NP GCLs can also be exposed to low

σ_n . For example, NP GCLs are often subjected to low σ_n with the intent of enabling the option for future expansion/higher stress.

The objective of this study was: (i) evaluate the τ_{cr} of high PS NP GCLs in low σ_n applications, and (ii) evaluate the effect of PS on τ_{cr} of NP GCL/GMX composite system. To address these objectives, a series of displacement-controlled internal and interface direct shear tests have been performed at $\sigma_n \leq 500$ kPa on a textured geomembrane (GMX) and multiple NP GCLs that have different PS. The τ_{cr} of composite systems were determined via comparing the peak internal and peak interface shear strength of NP GCLs. Then, τ_{cr} of the high PS NP GCL/GMX composite system was compared to the τ_{cr} of composite systems containing NP GCLs with lower PS to evaluate the effect of PS on τ_{cr} of NP GCL/GMX composite system.

2 BACKGROUND

Extensive research has been performed in the past to evaluate the internal and interface shear strength of GCLs. Displacement-controlled internal shear tests (DC-IN) have been performed to evaluate the peak (τ_p) and large-displacement (τ_{ld}) shear strength of GCLs with respect to GCL reinforcement type, hydration and consolidation procedure, specimen size, peel strength, applied σ_n , displacement rate during shear, elevated temperature, hydration with non-standard solutions, etc. (Gilbert et al. 1996; Fox et al. 1998; Olsta & Swan 2001; Zornberg et al. 2005; Athanassopoulos & Yuan 2011; Fox & Ross 2011; Bacas et al. 2013; Fox & Stark 2015; Bareither et al. 2018). In displacement-controlled interface shear tests (DC-IF) between GCLs and geomembranes, previous researchers investigated the effect of bentonite extrusion, progressive failure, displacement rate, geomembrane and geotextile characteristics, elevated temperature, etc. (Triplett & Fox 2001; Chiu & Fox 2004; Fox & Kim 2008; McCartney et al. 2009; Fox & Ross 2011; Hanson et al. 2015; Thielmann et al. 2016).

In liner systems of containment applications, GCLs are almost always used in combination with GMX. Therefore, evaluation of the τ_{cr} of composite GCL/GMX systems is important for the stability and integrity of liner systems. So far, either the internal shear strength of NP GCLs or the interface shear strength between a NP GCL and a geomembrane has been evaluated in most of the previous studies. Therefore, evaluation of the shear behavior of composite GCL/geomembrane system has received very limited attention. Fox & Ross (2011) performed a series of DC-IN and DC-IF tests, and reported the change in failure mechanism from interface failure between the GCL and the textured geomembrane (GMX) to internal failure within the GCL with increase in the σ_n . Similarly, Thielmann et al. (2016) performed DC-IF tests, and reported the transition of the failure mode from interface failure between the GCL and the geomembrane to partial interface/internal failure, and eventually to complete internal failure within the GCL with increase in σ_n . Despite providing valuable information, NP GCLs tested in these studies had $PS \leq 2300$ N/m. Therefore, the shear behavior of composite systems including a high PS NP GCL and GMX, especially at low σ_n , have not been fully understood.

3 MATERIAL

3.1 Geosynthetic clay liners

Characteristics of GCLs used in this study that includes general properties, geotextile properties, reinforcement fibers properties, and bentonite properties are tabulated in Table 1. All GCLs tested in this study were commercially-available products. The general GCL properties are reported by the manufacturer; whereas geotextile properties, reinforcement fibers properties, and bentonite properties were measured as a part of this study.

To characterize the geotextile properties, reinforcement fibers properties, and bentonite properties, ten 76.2-mm-square specimens were cut from different locations of each GCL rolls. Geotextiles mass per area was measured according to the ASTM D5261, and bentonite mass per area was measured using ASTM D5993 (Table 1).

The number of fiber bundles was counted on two sides of 76.2-mm-square GCL specimens to compute the average number of fiber bundles per 1centimeter in machine direction (MD) and

cross-machine direction (CMD). Dot plots of the number of fiber bundles per 1 centimeter in MD and CMD based on 20 measurements on GCL-1, GCL-2, and GCL-3 are shown in Fig. 1, and the average values are in Table 1. With an increase in the specimen peel strength, average number of fiber bundles per centimeter increased by up to 45%. This increase was due to higher intensity needle-punching during the manufacturing process of the high-peel strength GCL.

Table 1. Characteristics and properties of geosynthetic clay liners used in this study.

Category	Properties	GCL-1	GCL-2	GCL-3
General properties	Peel strength (N/m) ^a	980	2180	3850
	Heat Treatment Method	NHT	NHT	NHT
	Polymer Type	PP	PP	PP
Geotextile Properties	Carrier geotextile type	NW	W	NW
	Cover geotextile type	NW	NW	NW
	Carrier geotextile mass/area (g/m ²) ^b	260	130	360
	Cover geotextile mass/area (g/m ²) ^b	230	230	280
Reinforcement fibers properties	No. of fiber bundles per 1 cm, MD ^c	2.83	2.97	3.75
	No. of fiber bundles per 1 cm, CMD ^c	2.69	3.08	3.89
	Fiber bundle thickness (mm) ^c	0.84	0.96	1.09
Bentonite properties	Bentonite Type	Granular	Granular	Granular
	Bentonite mass per area (g/m ²) ^d	4220	4910	5570

NOTE: HT = Heat treated; NHT = Non-heat treated; W = woven; NW = non-woven; MD = Machine Direction; CMD = Cross-Machine Direction

^a Reported by manufacturers based on ASTM D6496/6496M

^b Based on ASTM D5261

^c Average value based on 20 measurements

^d Based on ASTM D5993

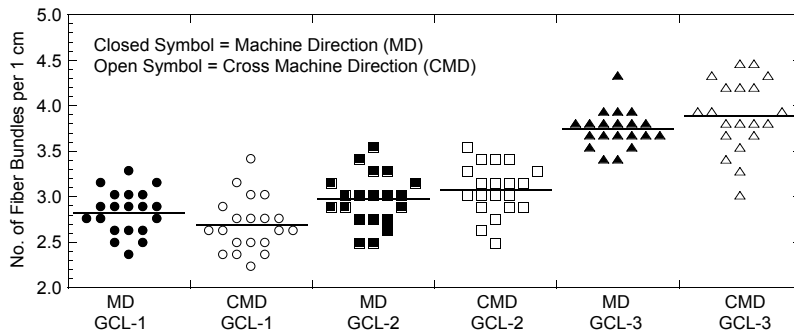


Figure 1. Dot plots of the number of fiber bundles per 1 cm in machine direction (MD) and cross-machine direction (CMD) based on 20 measurements on GCL-1, GCL-2, and GCL-3.

To estimate the average thickness of fiber bundles, a single fiber bundle was chosen randomly from two sides (parallel to MD and CMD) of the 76.2 m-square-specimens and the thickness of the fiber bundle was estimated using a digital stereoscopic microscope (Dino-lite v2). Dot plots of the fiber bundle thickness based on 20 measurements on GCL-1, GCL-2, and GCL-3 are in Figure 2, and the average values are in Table 1. The increase in the average fiber bundle thickness with increase in the specimen peel strength is attributed to high number of mono-filament fibers in fiber bundles due to the high mass per area of the cover geotextiles in high peel strength GCLs.

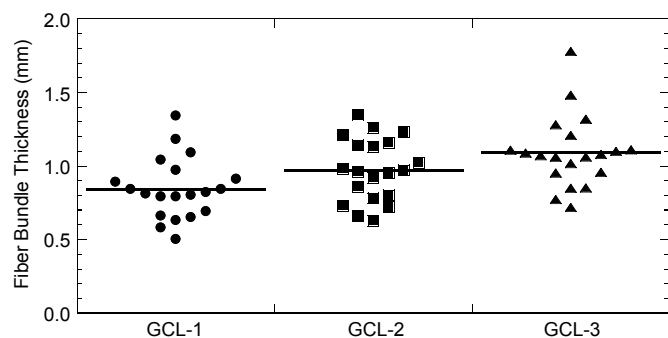


Figure 2. Dot plots of the fiber-bundle thickness of GCL-1, GCL-2, and GCL-3.

3.2 Textured geomembrane

The geomembrane used in all DC-IF tests was a textured linear-low density polyethylene (LLDPE) microspike geomembrane with the nominal thickness = 1.5 mm, average spike height = 0.51 mm, spike spacing = 3 mm in machine direction (MD) and = 7 mm in cross-machine direction (CMD). This GMX had characteristics of a typical GMX used in high σ_n containment applications such as heap leaching facilities (Thiel et al. 2004).

4 EXPERIMENTAL PROCEDURE

Displacement-controlled internal and interface direct shear tests were performed with a displacement-controlled direct shear apparatus. The design details and verification of the apparatus as well as the results of preliminary experiments has been discussed in Bareither et al. (2018). All DC-IN and DC-IF experiments were performed on 150 mm by 150 mm GCL specimens; however, in DC-IF tests, longer GMX was cut in the direction of shear. In this study, 150-mm-squared specimens were used instead of the conventional 300-mm-squared specimens; however, the verification for use of the smaller size specimens has been described in Olsta and Swan (2001) and Bareither et al. (2018).

In both DC-IN and DC-IF tests, GCL and GMX specimens aligned with their machine direction in the direction of shear. A two-stage hydration and consolidation procedure was performed according to Fox et al. (1998) and Bareither et al. (2018). In hydration stage, GCL specimens were placed between two perforated PVC plates than transferred to a plastic bin full of de-ionized water. Specimens were hydrated for 48-hr with $\sigma_n = 20$ kPa. Hydration procedure was similar for all GCLs prepared for DC-IN and DC-IF tests. At the end of hydration, specimens were transferred to the direct shear box to start consolidation. In DC-IN tests, specimens were sandwiched between two pyramid tooth plates for consolidation and shearing whereas in interface shear tests, GCL specimens were placed between a single pyramid tooth plate and a GMX contacting the cover geotextile of the GCL. The pyramid tooth plates were designed based on Allen & Fox (2007) and were used as the Geosynthetic gripping system. Consolidation of GCL and GCL/GMX test specimens was conducted in the direct shear box under an initial $\sigma_n = 20$ kPa. The σ_n was doubled every 4-6 hr to obtain the target normal stress for shearing (σ_{n-s}). After reaching σ_{n-s} , test specimens equilibrated in the shear box under σ_{n-s} for at least 24 hr. All internal and interface direct shear tests were conducted at room temperature (≈ 20 °C) and at a horizontal displacement rate of 0.1 mm/min to a horizontal displacement (δ_h) ≈ 70 mm.

5 RESULTS

A summary of the DC-IN and DC-IF shear tests are in Table 2 and Table 3, respectively. The summary of DC-IN tests includes σ_{n-s} , peak shear strength (τ_p), secant friction angle at peak

shear strength (ϕ_{s-p}), area-corrected normal stress (AC σ_{n-s}) at horizontal displacement (δ_h) = 70 mm, and area-corrected large-displacement shear strength at δ_h = 70 mm (AC τ_{70}). The summary of the DC-IF tests includes σ_{n-s} , τ_p , ϕ_{s-p} , large-displacement shear strength at δ_h = 70 mm (τ_{70}), and the post-peak strength reduction ratio (τ_{70}/τ_p).

In DC-IN experiments, fibers are gradually pulled out of the carrier geotextile as δ_h increases. However, before reaching the peak shear strength, needle-punched fibers are still in contact with the carrier geotextile. Therefore, despite the offset between the top and bottom shear platen, area correction was not performed in analysis of the peak shear strength of NP GCLs in DC-IN tests. However, after reaching the peak shear strength in DC-IN tests, reinforcement fibers are gradually pulled out of the carrier geotextile, and the process of fiber-disentanglement continues with increase in δ_h . Therefore, area correction was needed in the analysis of the large-displacement shear strength of NP GCLs in DC-IN tests. In DC-IF tests, the shearing area between the GMX and GCLs remains constant with δ_h ; therefore, area correction was not needed in the analysis of the peak or large-displacement shear strength. Further discussions about the area correction of specimens during the shear is in Bareither et al. (2018).

Table 2. Summary of displacement-controlled internal shear tests (DC-IN).

Test Type	GCL	σ_{n-s} (kPa)	τ_p (kPa)	ϕ_{s-p} (°)	AC σ_{n-s} (kPa)	AC τ_{70} (kPa)
DC-IN	GCL-1	100	141	54.7	335.4	42.9
		300	233.7	37.9	1006.2	72.8
		500	295.5	30.6	1676.9	143.9
	GCL-2	100	164.2	58.7	335.4	30.8
		300	293.3	44.4	1006.2	93.9
		500	416.2	39.8	1676.9	154.9
	GCL-3 ^a	80	199.7	-	-	-
		160	279.5	-	-	-
		250	294.2	-	-	-
		500	462	-	-	-

Notes: σ_{n-s} = shearing normal stress; τ_p = peak shear strength; ϕ_{s-p} = secant friction angle at peak shear strength; AC σ_{n-s} = area-corrected shearing normal stress at δ_h = 70 mm; AC τ_{70} = area-corrected large-displacement shear strength at δ_h = 70 mm

^a Internal shear failure did not occur in DC-IN experiments on GCL-3. Therefore, ϕ_{s-p} , AC σ_{n-s} , and AC τ_{70} were not defined for GCL-3.

Table 3. Summary of displacement-controlled interface shear tests (DC-IF).

Test Type ^a	GCL	σ_{n-s} (kPa) ^b	τ_p (kPa) ^c	ϕ_{s-p} (°) ^d	τ_{70} (kPa) ^e	τ_{70}/τ_p	
DC-IF	GCL-1	100	115.8	49.2	43.9	0.38	
		300	208.1	34.7	82.9	0.40	
		500	284.1	29.6	116.6	0.41	
	GCL-2	100	93.4	93.4	43	55.4	0.59
		300	249.1	249.1	39.7	104.3	0.42
		500	328.5	328.5	33.3	134.4	0.40
	GCL-3	100	119.8	119.8	50.1	65.4	0.56
		300	277.6	277.6	42.8	115.7	0.42
		500	337.3	337.3	34	133.5	0.40

Notes: σ_{n-s} = shearing normal stress; τ_p = peak shear strength; ϕ_{s-p} = secant friction angle at peak shear strength; τ_{70} = large-displacement shear strength at δ_h = 70 mm

5.1 Displacement-controlled internal shear tests

Relationship between the shear stress (τ) and δ_h in DC-IN tests on GCL-1, GCL-2, and GCL-3 are shown in Figures 3a-3c respectively. The τ - δ_h relationship for GCL-1 and GCL-2 is a typical of τ - δ_h relationship reported for NP GCLs (Gilbert et al. 1996; Fox et al. 1998; Zornberg et al. 2005; Fox & Stark 2015; Bareither et al. 2018). Both GCL-1 and GCL-2 experienced a defined peak shear strength followed by the displacement-softening behavior. The displacement softening behavior in NP GCLs is attributed to reduced internal shear resistance due to fiber-bundle disentanglement, tensile rupture within the reinforcement fibers, or a combination of both (Fox et al. 1998; Fox & Stark 2015; Bareither et al. 2018). The behavior observed in Figure 3b as well as post-shear inspection of GCL-1 and GCL-2 specimens, revealed no sign of slippage in the gripping system or geotextile elongation/tearing, which indicated the successful internal shearing of GCL-1 and GCL-2 specimens.

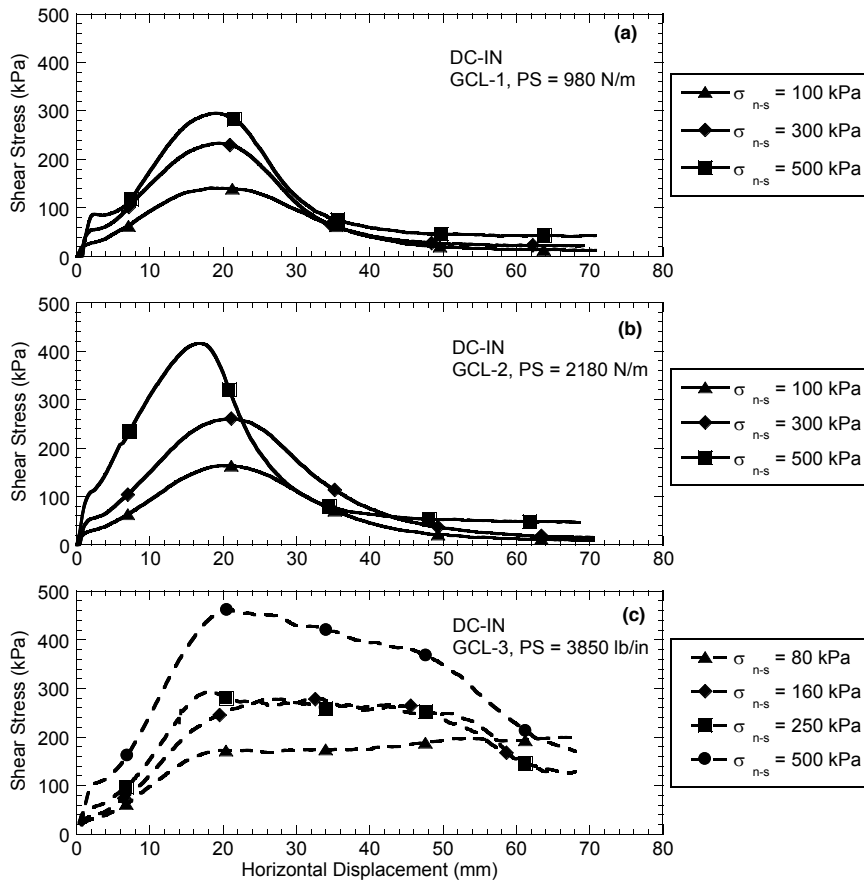


Figure 3. Relationship between shear stress (τ) versus horizontal displacement (δ_h) for DC-IN shear tests on (a) GCL-1, (b) GCL-2, and (c) GCL-3.

In contrast to the τ - δ_h behavior observed in DC-IN tests on GCL-1 and GCL-2, no defined peak and displacement softening behavior was observed for the high PS GCL-3 specimens (Figure 3Figure c). This irregularity in τ - δ_h relationship in Figure 3c is indicative of stress localization and unsuccessful internal shear failure (Fox & Stark 2015). The dashed lines are used in Figure 3c instead of solid lines to emphasize the unsuccessful shearing of GCL-3 in the DC-IN tests.

Pictures taken from GCL-3 specimens after DC-IN tests at $\sigma_{n-s} = 80$ kPa and $\sigma_{n-s} = 500$ kPa are shown in Figures 4a and 4b, respectively. Contrary to the post-shear observations of GCL-1 and GCL-2, no sign of internal shear failure (i.e., fiber bundles disentanglement or fiber rupture) was observed for GCL-3. In contrast, a combination of geotextile tearing, geotextile elongation, specimen necking, and geotextile separation were observed with different observations at different σ_{n-s} . For example, at $\sigma_{n-s} = 80$ kPa (Figure 4a), the DC-IN test resulted in slippage of the carrier geotextile over the pyramid tooth plate that resulted in carrier geotextile tearing as well as tensile elongation of geotextile around the clamping system. At $\sigma_{n-s} = 500$ kPa no slippage or relative displacement between the pyramid tooth plates and GCL was observed; however, tensile rupture of carrier and cover geotextiles was observed. The pictures in Figures 4a and 4b are examples of shear behavior at the low and high σ_{n-s} used in this study (i.e., 80 kPa and 500 kPa). However, similar unsuccessful shear behavior was also observed at $\sigma_{n-s} = 160$ and 250 kPa.

Unsuccessful internal shear failure of high peel strength NP GCLs at low σ_{n-s} has been reported previously (ASTM D 6243; Fox et al. 1998; Fox & Ross 2011; Fox & Stark 2015; Bareither et al. 2018). In general, internal failure of NP GCLs occurs if the applied shear stress can fully mobilize the maximum internal shear resistance of the reinforcement fibers. The inability of transferring the applied shear stress to the internal region of GCL-3 was not due to inefficiency of the gripping system used in this study (i.e., pyramid tooth plates) considering that the gripping system used in this study surpassed requirements mentioned in ASTM D6243. Therefore, the unsuccessful DC-IN tests on GCL-3 was attributed to the low tensile strength of carrier and cover geotextiles in GCL-3 relative to the internal shear strength of GCL-3 that caused tensile failure of geotextiles before mobilizing the maximum internal shear resistance of reinforcement fibers. Due to this physical limitation, internal failure of GCL-3 was not feasible at the experimental conditions of this study.



Figure 4. Post-shear pictures of GCL-3 from DC-IN tests at (a) $\sigma_{n-s} = 80$ kPa and (b) $\sigma_{n-s} = 500$ kPa.

Mohr-coulomb strength envelopes of GCL-1 and GCL-2 are shown in Figure 5a for the τ_p and in Figure 5b for AC τ_{70} . The τ_p envelopes were developed based on nominal shear and normal stresses as described previously. The maximum shear stress (τ_{max}) during the DC-IN tests

on GCL-3 is also included in Figure 5a for comparison. However, large-displacement shear strength of GCL-3 was not included in Figure 5b as internal failure of GCL-3 was not achieved. The shear strength parameters (i.e., cohesion, c_p , and friction angle, ϕ_p) for GCL-1 and GCL-2 were calculated using linear strength envelopes that yielded $c_p = 102$ kPa and $\phi_p = 21^\circ$ for GCL-1, and $c_p = 107$ kPa and $\phi_p = 32^\circ$ for GCL-2. Thus, an increase in PS from 980 N/m (GCL-1) to 2180 N/m (GCL-2) resulted in increased ϕ_p and an overall increase in internal shear strength.

In Figure 5b the large-displacement shear strength of GCL-1 and GCL-2 was based on the AC τ_{70} and AC σ_{n-s} . A linear strength envelope was regressed through both data sets, which yielded $c_{LD} = 0$ and $\phi_{LD} = 5^\circ$. Peak and the large displacement shear strength parameters of GCL-1 and GCL-2 were comparable to strength parameters of NP GCLs with comparable peel strength in Fox & Ross (2011) and Athanassopoulos & Yuan (2011).

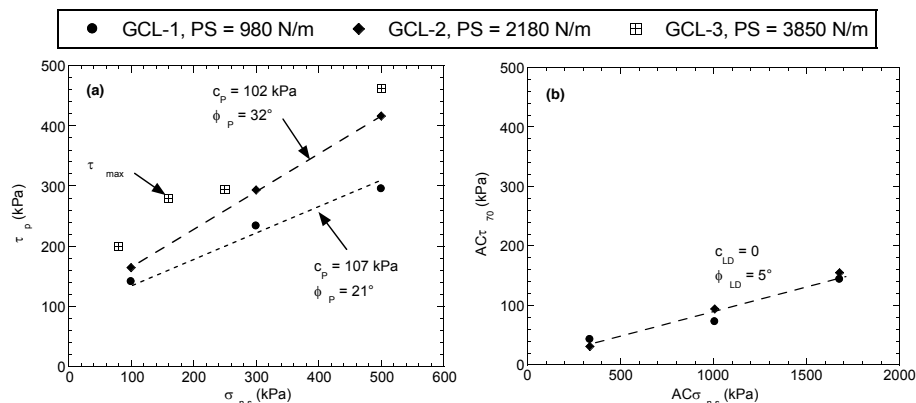


Figure 5. Relationships of (a) τ_p versus σ_{n-s} , and (b) area-corrected shear strength at $\delta_h = 70$ mm ($AC\tau_{70}$) versus $AC\sigma_{n-s}$ for GCL-1 and GCL-2. The maximum shear stress measured in DC-IN tests (τ_{max}) on GCL-3 was included for comparison. Mohr-Coulomb strength parameters (c = cohesion and ϕ = friction angle) were obtained from DC-IN tests on GCL-1 and GCL-2 via least squares regression.

5.2 Displacement-controlled interface shear tests

Relationships between τ and δ_h for DC-IF shear tests on GCL-1, GCL-2, and GCL-3 are shown in Figure 6. In all DC-IF tests, specimens experienced peak and displacement-softening behavior. However, different τ - δ_h relationships and post-peak strength reductions were observed for the different NP GCLs and σ_{n-s} . The differences in the shear behavior of specimens are indicative of different failure mechanisms during DC-IF experiments.

Failure mechanisms in DC-IF tests were investigated on post-shear specimens. Post-shear pictures of GCL-1 specimens in DC-IF tests are shown in Figures 7c and 7d at $\sigma_{n-s} = 100$ kPa and 500 kPa, respectively. In all DC-IF tests on GCL-1, specimens experienced considerable internal shear deformation and there observable fiber-bundle disentanglement from the carrier geotextile. Similar internal shear deformation was also observed in DC-IF tests on GCL-1 at $\sigma_{n-s} = 300$ kPa. In DC-IF experiments on GCL-1, the mobilized interface shear force between the GCL-1 and the GMX was high enough to disentangle some fiber bundles out of the carrier geotextile considering the low internal shear resistance of the GCL. However, despite experiencing internal shear deformation, slippage at GCL-1-GMX interface also occurred as signs of GMX spikes shearing the top geotextile were also observed. Therefore, the failure mechanism of GCL-1 in DC-IF tests was a combination of internal failure and interface failure. Considering the partial internal/interface failure mode, the post-peak strength reduction is due to the decrease in both internal and interface shear resistance of the GCL-1. Decrease in the interface shear resistance was attributed to damage to the geotextile and GMX asperities during shear, whereas decrease in the internal resistance was due to disentanglement of some reinforcement

fiber bundles. Partial interface/internal failure of NP GCLs in DC-IF tests have also been reported in Fox & Ross (2011), Fox & Stark (2015), and Thielmann et al. (2016).

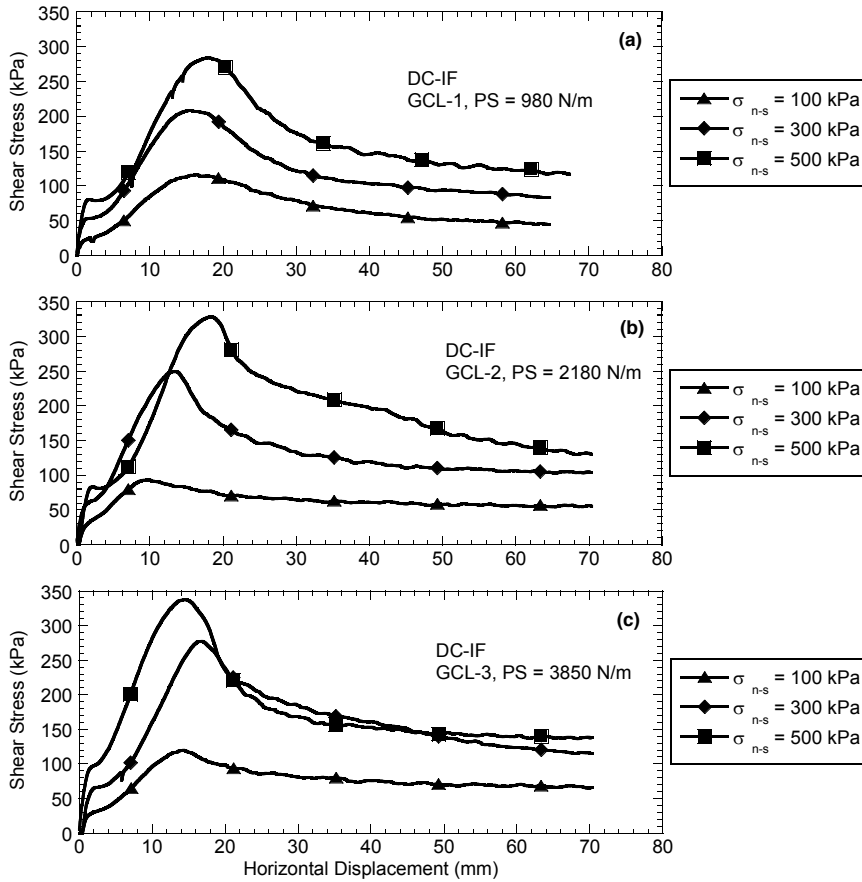


Figure 6. Relationship between shear stress (τ) versus horizontal displacement (δ_h) for displacement-controlled interface (DC-IF) shear tests on (a) GCL-1, (b) GCL-2, and (c) GCL-3.

Post-shear pictures of GCL-2 specimens in DC-IF tests are shown in Figures 7c and 7d. In DC-IF tests on GCL-2 at $\sigma_{n-s} = 100$ kPa, the mobilized interface shear force between GCL-2 and GMX was not high enough to cause disentanglement or rupture of reinforcement fibers. Therefore, although there was minimal internal shear deformation identified as inclination of fiber-bundles in the direction of the shear, horizontal deformation of GCL-2 in DC-IF test at $\sigma_{n-s} = 100$ kPa was mostly attributed to the slippage between the GCL and GMX. In this case, the failure mode was complete interface failure, and post-peak strength reduction was only due to damage along the surface of the geotextile and GMX spikes. Increase in the σ_{n-s} from 100 to 300 kPa in DC-IF tests on GCL-2 did not result in a change in failure mode, and complete interface failure was also observed at $\sigma_{n-s} = 300$ kPa. With further increase in the σ_{n-s} to 500 kPa (Fig. 7d), the mobilized shear force was high enough to disentangle some reinforcement fiber bundles from the geotextile; and therefore, the failure mode transitioned from complete interface to partial interface/internal failure. Despite experiencing partial interface/internal failure, GCL-2 specimens had lesser internal shear deformation than GCL-1 at $\sigma_{n-s} = 500$ kPa (Fig. 7d vs. Fig. 7b). The lesser degree of internal shear deformation of GCL-2 in comparison to GCL-1 was attributed to the higher peel strength and higher internal shear resistance of GCL-2.



Figure 7. Post shear pictures of GCLs after DC-IF tests on (a) GCL-1 at $\sigma_{n-s} = 100$ kPa, (b) GCL-1 at $\sigma_{n-s} = 500$ kPa, (c) GCL-2 at $\sigma_{n-s} = 100$ kPa (d) GCL-2 at $\sigma_{n-s} = 500$ kPa, (e) GCL-3 at $\sigma_{n-s} = 100$ kPa, and (f) GCL-3 at $\sigma_{n-s} = 500$ kPa

Finally, pictures of the high peel strength GCL-3 after DC-IF tests at $\sigma_{n-s} = 100$ and 500 kPa are shown in Figures 7e and 7f, respectively. In experiments on GCL-3, the mobilized shear force at the GCL/GMX interface was not sufficient to induce internal failure at any σ_{n-s} used in this study. Although minimal internal shear deformation was observed at $\sigma_{n-s} = 500$ kPa (Fig. 7f), no sign of fiber bundle disentanglement or fiber rupture was observed. Therefore, the high peel strength GCL-3 specimens experienced complete interface shear failure. The different failure mode of the GCL-3 was due to the higher peel strength of GCL-3.

5.3 Critical strength of NP GCL/GMX composite system

Comparison between the peak shear strength in DC-IN experiments (τ_p -IN) and the peak shear strength in DC-IF (τ_p -IF) experiments are shown in Figure 8a, 8b, and 8c for GCL-1, GCL-2, and GCL-3, respectively. In Figure 8c, the maximum shear stress during the DC-IN tests (τ_{\max} -IN) is used instead of τ_p -IN for GCL-3 since the internal failure of GCL-3 did not occur during DC-IN tests. The comparison between τ_p -IN (τ_{\max} -IN of GCL-3) and τ_p -IF is important for identifying the critical shear strength (τ_{cr}) of the composite GCL/GMX system. For the experimental condition of this study, τ_p -IF was always lower than the τ_p -IN (or τ_{\max} -IN of GCL-3) regardless of the PS; therefore, τ_{cr} of NP GCL/GMX composite systems was always controlled by the interface shear strength between the NP GCL and the GMX. Considering the partial interface/internal failure mode and high internal shear deformation of GCL-1, values of τ_p -IN and τ_p -IF for GCL-1 are very close to each other (Fig. 8a). The ϕ_p determined for the DC-IF tests on GCL-1, which corresponds to τ_{cr} , was 21°, which is identical to the ϕ_p determined for the DC-IN tests in Fig. 5a. However, the c_p for the DC-IN tests was higher (107 kPa) relative to the DC-IF tests (77 kPa), which corresponded to additional shear resistance from the needle-punched reinforcement fibers.

For GCL-2 and GCL-3, the difference between the τ_p -IN (τ_{\max} -IN of GCL-3) and τ_p -IF increased with an increase in peel strength (Figs. 8b and 8c). The ϕ_p determined for the DC-IF tests on GCL-2 was 30° and c_p was 48 kPa, which were both lower than the internal shear strength parameters determined from the DC-IN tests (Fig. 5a). In Figure 8c, the highest difference between the τ_p -IN and τ_p -IF would have been expected had GCL-3 specimens reached internal failure. However, τ_p and ϕ_p of GCL-2 and the high PS GCL-3 were quite comparable, which implies that these two GCL/GMX composite systems had comparable internal shear resistance. Therefore, the increase in the peel strength of NP GCLs may not necessarily contribute to the τ_{cr} of the NP GCL/GMX composite system at low σ_{n-s} .

6 CONCLUSION

A series of displacement-controlled internal and interface direct shear tests were performed on multiple needle-punched (NP) GCLs with different peel strength to evaluate the critical strength (τ_{cr}) of a high peel strength NP GCL/GMX composite system at low normal stress (σ_n) and to evaluate the effect of PS on the interface shear behavior of NP GCL/GMX composite systems. The following conclusion has been drawn from the results of this study.

- In displacement-controlled internal shear strength experiments, an increase in peel strength resulted in an increase in the internal peak shear strength of NP GCLs.
- Successful internal shear failure of NP GCLs occurs when tensile strength of the carrier and cover geotextiles surpass the internal shear strength of NP GCLs. This allows shear stress to be effectively transferred to the internal region of the NP GCL. Therefore, in very high peel strength NP GCLs (e.g., 3850 N/m in this study), internal shear failure may not be feasible at low σ_n as failure will occur within the carrier and/or cover geotextiles.
- Different failure modes were observed in the interface direct shear tests as a function of NP GCL peel strength and σ_n . Low peel strength GCLs experienced partial interface/internal failure regardless of the σ_n . However, the failure mode was always interface failure in experiments on high peel strength GCLs. An increase in σ_n transitioned the failure mode from complete interface failure to partial interface/internal failure in experiments on the medium peel strength (2180 N/m) NP GCL and at the σ_n used in this study.
- For the experimental conditions of this study, τ_{cr} of NP GCL/GMX composite systems was always controlled by the interface shear strength between the GCL and the GMX regardless of the NP GCL peel strength. Also, an increase in peel strength for the two NP GCLs with higher peel strength did not contribute to an increase in τ_{cr} of the NP GCL/GMX composite system.

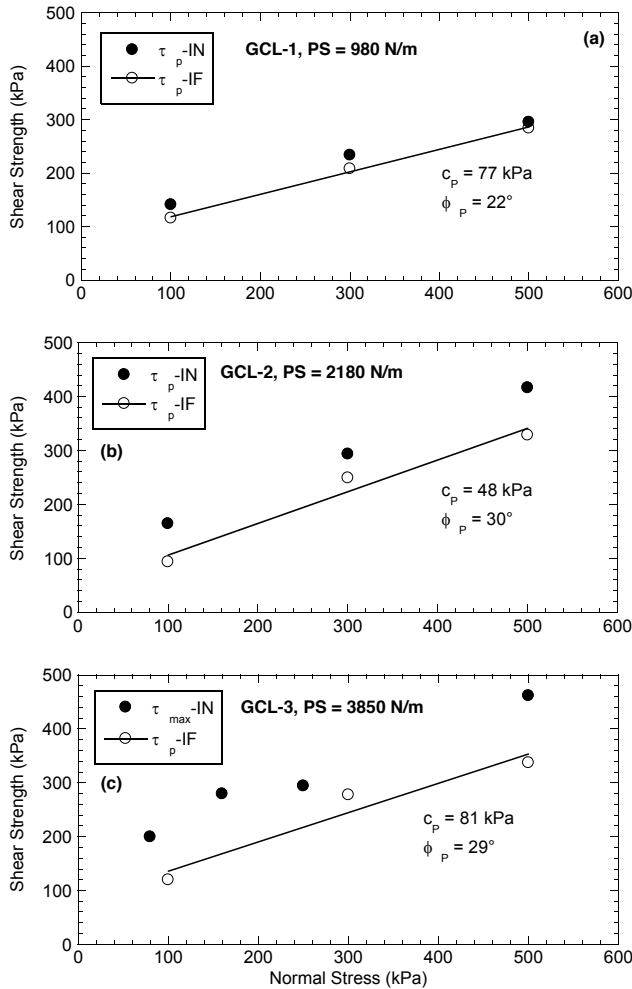


Figure 81. Relationships between peak shear strength (τ_p) and normal stress from internal and interface direct shear tests on (a) GCL-1, (b) GCL-2, and (c) GCL-3. The maximum shear strength (τ_{max}) measured in the internal direct shear tests on GCL-3 was used instead of τ_p since internal failure of GCL-3 was not achieved in the internal shear tests.

7 REFERENCES

- Allen, J. M. and Fox, P. J. 2007. Pyramid-tooth gripping surface for GCL shear testing. *Geosynthetics 2007*, North American Geosynthetics Society, Washington, DC, (CD-ROM).
- ASTM D4439 2015. Standard Terminology for Geosynthetics, Annual Book of ASTM Standards, ASTM D4439-15, *ASTM International*, West Conshohocken, PA, USA.
- ASTM D5261 2010. Standard Test Method For Measuring Mass Per Unit Area Of Geotextiles. D5261, *ASTM International*, West Conshohocken, PA, USA.
- ASTM D5993 2014. Standard Test Method For Measuring Mass Per Unit Area Of Geosynthetic Clay Liners. D5993, *ASTM International*, West Conshohocken, PA, USA.
- ASTM D6243 2009. Standard Test Method for Determining the Internal and Interface Shear Resistance of Geosynthetic Clay Liner by the Direct Shear Method, D6243, *ASTM International*, West Conshohock-

- en, Pennsylvania, USA.
- ASTM D6496/6496M 2015. Standard Test Method For Determining Average Bonding Peel Strength Between Top and Bottom Layers of Needle-Punched Geosynthetic Clay Liners. D6496/6496M, *ASTM International*, West Conshohocken, PA, USA.
- Athanassopoulos, C. & Yuan, Z. 2011. Correlation between needle punch-reinforced geosynthetic clay liner peel strength and internal shear strength. *Geo-Frontiers 2011: Advances in Geotechnical Engineering: 1922-1930*. Dallas, Texas, USA.
- Bacas, B. M., Blanco-Fernandez, E., & Cañizal, J. 2013. Comparison of the adhesion and shear tensile strength of needle-punched GCLs, *Geotextiles and Geomembranes* (41): 17-25.
- Bareither, C. A., Soleimanian, M., & Ghazizadeh, S. 2018. Direct shear testing of GCLs at elevated temperature and in a non-standard solution. *Geosynthetics International*, (25(3)), 350-368.
- Bouazza, A. & Bowders, J.J. 2010. Geosynthetic Clay Liners for Waste Containment Facilities, *CRC Pres: 239*. Boca Raton, FL, USA.
- Chiu, P., & Fox, P. J. 2004. Internal and interface shear strengths of unreinforced and needle-punched geosynthetic clay liners. *Geosynthetics International* 11(3): 176-199.
- Fox, P. J. & Kim, R. H. 2008. Effect of progressive failure on measured shear strength of geomembrane/GCL interface, *Journal of Geotechnical and Geoenvironmental Engineering* 134(4): 459-469.
- Fox, P. J. & Ross, J. D. 2011. Relationship between GCL internal and GMX/GCL interface shear strengths, *Journal of Geotechnical and Geoenvironmental Engineering* 137(8): 743-753.
- Fox, P. J. & Stark, T. D. 2004. State-of-the-art report: GCL shear strength and its measurement, *Geosynthetics International* 11(3): 141-175.
- Fox, P. J., & Stark, T. D. 2015. State-of-the-art report: GCL shear strength and its measurement—ten-year update, *Geosynthetics International* 22(1): 3-47.
- Fox, P. J., Rowland, M. G., & Scheithe, J. R. 1998. Internal shear strength of three geosynthetic clay liners. *Journal of Geotechnical and Geoenvironmental Engineering* 124(10): 933-944.
- Gilbert, R. B., Fernandez, F. & Horsfield, D. W. 1996. Shear strength of reinforced geosynthetic clay liner, *Journal of Geotechnical Engineering* 122(4): 259-266.
- Guyonnet, D., Touze-Foltz, N., Norotte, V., Pothier, C., Didier, G., Gailhanou, H., & Warmont, F. 2009. Performance-based indicators for controlling geosynthetic clay liners in landfill applications. *Geotextiles and Geomembranes* 27(5): 321-331.
- Hanson, J. L., Chrysovergis, T. S., Yesiller, N., & Manheim, D. 2015. Temperature and moisture effects on GCL and textured geomembrane interface shear strength, *Geosynthetics International* 22(1): 110-124.
- Lupo, J. F. 2010. Liner system design for heap leach pads. *Geotextiles and Geomembranes* 28(2): 163-173.
- McCartney, J. S., Zornberg, J. G., & Swan Jr, R. H. 2009. Analysis of a large database of GCL-geomembrane interface shear strength results. *Journal of Geotechnical and Geoenvironmental Engineering* 135(2): 209-223.
- Mesri, G. & Olson, R. E. 1970. Shear strength of montmorillonite, *Géotechnique* 20(3): 261-270.
- Olsta, J. T. & Swan, R. H. 2001. Internal shear strength of a geosynthetic clay liner at high normal loads, *Tailings and Mine Waste: 197-200*. Colorado State University, Fort Collins, CO, USA.
- Thielmann, S. S., Fox, P. J., & Athanassopoulos, C. 2016. Shear strength of GMX/GCL composite liner under high normal stress, *Journal of Geotechnical and Geoenvironmental Engineering* 142(5): 1-11.
- Thiel, R., & Smith, M. E. 2004. State of the practice review of heap leach pad design issues. *Geotextiles and Geomembranes* 22(6): 555-568.
- Triplet, E. J. & Fox, P. J. 2001. Shear strength of HDPE geomembrane/geosynthetic clay liner interfaces, *Journal of Geotechnical and Geoenvironmental Engineering* 127(6): 543-552.
- Zornberg, J. G., McCartney, J. S., & Swan, R. H. Jr. 2005. Analysis of a large database of GCL internal shear strength results, *Journal of Geotechnical and Geoenvironmental Engineering* 131 (3): 367-380.

Geotextile Dewatering of Acid Mine Drainage Precipitates

K.J. Westhaver, K. Zimmermann, N. Devaere and D.R. Latulippe
McMaster University, Hamilton, Ontario, Canada

R. Mafi and E. Ausch
Canadian General-Tower Ltd., Cambridge, Ontario, Canada

ABSTRACT: Acid mine drainage (AMD) is a major ongoing concern for the mining industry due to the potential environmental effects on receiving water bodies and inhibition of mine site reclamation strategies. Treatment of AMD results in the production of metal hydroxide precipitates which require on-site storage or further processing. A pre-disposal precipitate dewatering process can minimize the land use requirements and handling costs associated with these activities. In this study, we investigated the efficacy of thin-film dewatering filters –incorporating well-defined slit-pore geometries– to treat AMD precipitates from a nickel-copper mine. We first conducted a high-throughput screen of cationic and anionic polymer flocculants using the LUMiFuge: an analytical centrifuge that measures real-time stability behaviour. The results provide new insights into the importance of pore geometry, porosity, and polymer performance on filter cake development. They indicate that the thin-film dewatering filters can outperform conventional dewatering textiles with respect to key dewatering performance metrics.

1 INTRODUCTION

Canada is one of the world's largest producers of base and precious metals. In 2016, the extraction and processing of economic minerals contributed over \$50 billion to the country's national gross domestic product (GDP) and was responsible for the employment of approximately 600,000 people (MAC 2017). However, mining operations produce large volumes of hazardous wastes that can pose a significant threat to the environment and human health. Therefore, the treatment and disposal of mine waste in a responsible manner is critical to maintaining the health and overall quality of life of Canadians, as well as the continued growth of the economy.

The two most prevalent waste materials produced by base and precious metal mining operations are mine tailings and waste rock. 'Mine tailings' refers to the fine particulate matter left over after extractive processes have been used to remove valuable constituents from ore. 'Waste rock' refers to the broken rock or overburden –ranging in size from fine sand to large boulders– removed from the ground along with the ore which contains minerals in concentrations too low for economic recovery. The ever-growing inventory of mine waste presents a major ongoing concern for the mining industry due to the potential environmental effects on receiving water bodies and inhibition of mine site reclamation strategies associated with Acid Mine Drainage (AMD). Mine tailings and waste rock contain sulphide minerals –such as pyrite– which readily react with atmospheric oxygen and water to form AMD. These effluents contain elevated concentrations of toxic substances such as: cyanides, arsenic, heavy metals, and other by-products of ore extraction. These substances can cause widespread damage to surrounding ecosystems (Sithole 2015). The Kam Kotia Mine –located in Timmins, Ontario– is a notable example of the environmental and economic impacts of AMD. At this copper mine, a 'killzone' was created in

which nearly all vegetation was destroyed as AMD flowed through the groundwater and ultimately contaminated a nearby river. Despite entering closure in the 1970s, AMD production onsite persists and is expected to continue for the indefinite future. The estimated cost to fully remediate the Kam Kotia Mine is \$40.8 million (Hamblin & Kord 2003). Across Canada, it is estimated that as much as \$5 billion will be required to remediate all existing AMD sites (EM-CBC, 2000).

Conventional treatment options for AMD begin with the addition of an alkali –such as lime or caustic soda– to raise the pH (Barakat, 2011). The targeted pH is typically between 9.5 and 11 to precipitate metals out of solution as metal hydroxides (Aubé 2004). The metal hydroxide suspension is pumped to settling ponds wherein the metal hydroxides are removed. Polymer flocculants or coagulants may also be added to the process to agglomerate the solids into larger particles and improve the separation efficacy. To maintain the capacity of the AMD treatment system, the material which accumulates at the bottom of the ponds –referred to in this work as AMD precipitates– is removed periodically via dredging and subsequently sent for disposal in on-site engineered ‘ponds’ or transported to off-site processing facilities. The AMD precipitates produced by conventional pond treatment systems are typically 5% solids by weight (MEND 1997). Therefore, a pre-disposal precipitate dewatering process should be applied to reduce the overall volume of material and thus minimize the land use requirements and handling costs.

Sludge dewatering is commonly performed via non-mechanical methods such as: sludge drying beds and sedimentation basins. Sludge dewatering is also done via advanced mechanical systems such as: scroll decanter centrifuges, filter presses, and screw thickeners. Geotextile dewatering is a promising alternative to both methods. It uses less land than the non-mechanical methods and requires less capital and operating expenditures than the mechanical technologies. In this process, sludge is hydraulically pumped into an enclosed tube –or series of tubes– made from an engineered dewatering fabric. The pumping pressure forces the free water out through the pores of the fabric while keeping the solids contained within. As dewatering proceeds, a filter cake develops on the inner surface of the tube which contributes to the retention of fine particles. In contrast to the conventional sludge dewatering methods, geotextile tubes are economical, simple to use, easily transported, and can be fabricated in site specific sizes. These benefits make them particularly attractive for nomadic or transitory applications (Maurer et al. 2012).

This paper explores the efficacy of thin-film dewatering filters –incorporating well-defined slit-pore geometries– to treat AMD precipitates from a nickel-copper mine in Ontario, Canada. A high-throughput screen of cationic and anionic polymer flocculants was performed to identify the best one to use in lab-scale constant pressure filtration tests. A full-factorial design-of-experiments was employed to evaluate the effects of slit-pore dimensions and spacing on dewatering performance in terms of: dewatering rate, extent of dewatering, and solids retention.

2 EXPERIMENTAL

2.1 AMD precipitates

The AMD precipitate material tested in this study was obtained from a nickel-copper mine in Ontario, Canada. The sample was acquired from the polishing reservoir of the onsite lime treatment system using an Ekman dredge. The solids content of the sample was 6.1% which was determined via the standard 2540 B method (Clescerl et al. 1999). The density was 1.05 g/mL. Particle size analysis of the sample was performed via focused beam reflectance measurement (FBRM) using a Particle Track G400 instrument (Mettler Toledo). This method of particle sizing was selected for use in this study as it is capable of analysing high solids content materials. FBRM does not require the suspension to be kinetically stable as external mixing can be applied during measurement acquisition to prevent settling. Based on this analysis, the AMD precipitates consisted of particles ranging in size from 1 to 85 μm , while the median chord length observed was 12.32 μm .

2.2 Woven textile

To establish a baseline performance of geotextile dewatering technologies for the treatment of AMD precipitates, lab-scale dewatering tests were performed using a commercial woven dewatering textile constructed of multifilament, high-tenacity, polypropylene yarns. As reported by the manufacturer, the apparent opening size (AOS) was 430 μm , while the O50 and O95 pore opening sizes were 80 and 195 μm respectively. The woven textile samples used for the dewatering performance tests were circular discs 85 mm in diameter.

2.3 Thin-film dewatering filters

Dewatering performance tests were carried out using four thin-film dewatering filters, made from Kapton® HN general-purpose polyimide, with a nominal thickness of 127 μm . Each filter was manufactured using solid-state laser cutting techniques to possess an array of slit pores 100 μm in width. Each filter had a unique combination of pore-to-pore spacing and aspect ratio defined by a two-factor design-of-experiments (DOE) framework. ‘Pore-to-pore spacing’ refers to the distance between adjacent pores measured edge-to-edge in both the machine and cross machine directions. ‘Aspect ratio’ refers to the relative ratio between the length and width of the slit pores. The naming of each filter is based on the format ‘100×YYY_Z’ where: 100 is the pore width, YYY is the pore length, and Z is the pore-to-pore spacing. For example, the ‘100×1500_4mm’ filter possesses: a pore width of 100 μm , a slit-pore length of 1500 μm , and pore-to-pore spacing of 4 mm. The ‘100×1500_4mm’ filter has an aspect ratio of 15:1. Table 1 presents the technical details for the four thin-film dewatering filters, while Figure 1 includes representative images of the slit pores obtained using a Keyence VHX Digital Microscope.

Table 1. Technical details for the thin-film dewatering filters evaluated in this study.

Filter ID	Pore-to-pore spacing (mm)	Aspect ratio (length:width)	Porosity (%)
100x5000_1mm	1	50:1	8.81
100x1500_1mm	1	15:1	6.03
100x5000_4mm	4	50:1	0.88
100x1500_4mm	4	15:1	0.69

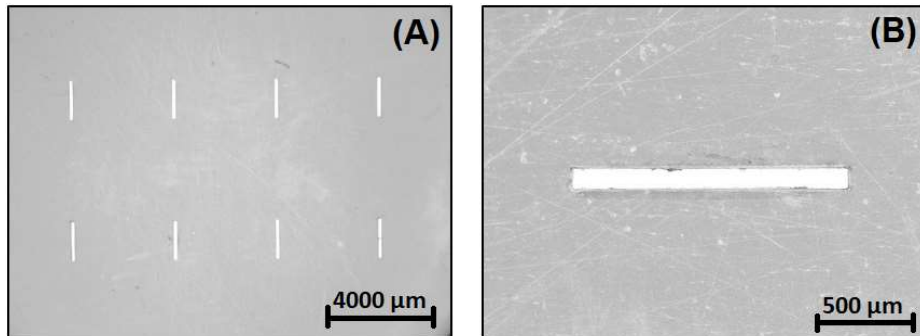


Figure 1. Images captured using the Keyence VHX Digital Microscope of the ‘100x1500_4mm’ filter at 30× (Panel A) and 200× (Panel B) magnification.

2.4 Polymer flocculants

A total of seven polyacrylamide flocculants were evaluated in this study for use as pre-treatment additives for the geotextile dewatering of AMD precipitates. Of the seven flocculants, four were cationic and three were anionic. The selection of appropriate polymers was performed such that those selected possessed a wide variety of properties as shown in Table 2.

Table 2. Technical details for the seven polymer flocculants employed in this work

Polymer ID	Charge	Charge density	Molecular weight
C1	+	Very high	High
C2	+	Low	Very high
C3	+	Medium	High
C4	+	High	Very high
A1	-	Medium	High
A2	-	High	Extremely high
A3	-	Medium	Very high

These polymers were supplied from the manufacturer either in dry or emulsion form. In both cases, 10 mM sodium phosphate monobasic buffer was used to produce a 0.3% by weight polymer emulsion. 40 g of the buffer was placed on a magnetic stir plate and stirred at 600 rpm using a cylindrical magnetic stir bar. The required amount of stock polymer was then added to the buffer via a weigh boat for dry polymers or a micropipette for emulsion polymers. The stir rate was immediately reduced to 400 rpm. After 10 min, a further 40 g of buffer was added, and the solution was stirred for an additional 10 min at 400 rpm. Stirring was then turned off; the polymer emulsion was let stand for 30 min before use. In all cases, the polymer emulsions were used within 24 hrs.

2.5 Polymer screening

High-throughput polymer screening was conducted using the LUMiFuge analytical centrifuge. The seven polymers were assessed in duplicate at four doses: 1, 2, 4, and 8 kg of polymer per tonne of total suspended solids (kg/TTS).

To begin, 8 mL samples of the AMD precipitates were placed into four wells of a standard flat-bottom 6-well microplate. A magnetic stir rod was placed in each well, and the microplate was positioned on a custom-built stand having an integrated ‘tumble stirrer’ (V&P Scientific). The four samples were mixed at 60 rpm while an appropriate quantity of polymer was added to each. After 10 sec, the stir rate was reduced to 40 rpm, and mixing was continued for an additional 110 sec. Duplicate 1.5 mL samples from each well were transferred to LUMiFuge sample vials via a positive displacement pipette. The analytical centrifugation test was performed at 500 rpm for a total of 12 min, with transmission measurements taken every 15 sec.

To compare the dewatering rate for each polymer-dose combination, the transmission profiles produced by the LUMiFuge were analyzed to track the position of the ‘solids front’ as a function of time. The ‘solids front’ for each profile was defined as the location at which the measured transmission was 50% of the maximum transmission recorded. The solids front positions were used to estimate the volume of the solids fraction. This was done using a linear regression of sample volume and horizontal position generated using sample vials filled with known quantities of deionized water.

2.6 Pressure filtration test (PFT)

Lab-scale constant pressure filtration tests (PFTs) were performed using the system shown in Figure 2. The cylindrical suspension cell was constructed of clear acrylic with a 1.5 L capacity. The bottom flange of the cell was designed to house a porous polypropylene disc (Scientific Commodities Inc.) with pore openings 200 μm in size. The porous disc served as a support for the dewatering fabrics. A nitrogen cylinder (Air Liquide) was used in conjunction with a CGA 580 regulator to apply a pressure of 35 kPa to the suspension cell. This was done to represent a common pumping pressure in industrial applications of the geotextile dewatering technology. An electronic balance was connected to a PC using METTLER TOLEDO BalanceLink software to record the mass of filtrate collected over time.

To begin the PFT, a drill-operated mixing rod was used to thoroughly mix the bulk AMD precipitate sample. A 500 g aliquot was transferred from the bulk sample to a glass beaker. For the PFTs performed using a cationic or anionic polymer, the aliquot was stirred using a pitched-

blade overhead mixer at 300 rpm while a syringe was used to deliver the appropriate quantity of polymer. After 10 sec, the mixing speed was reduced to 190 rpm and mixing was performed for an additional 110 sec. Once the mixing time elapsed, the AMD precipitates were immediately transferred to the suspension cell which was then pressurized to 35 kPa by the nitrogen gas supply. As dewatering proceeded, the filtrate was collected in sequential 45 g fractions identified as F1, F2, F3, and F4. The PFT was performed until 'breakthrough', which occurred when the filter cake dried to the point that a crack formed causing a loss of pressure. After dewatering, the solids content (SC) of the retained filter cake was determined using the standard 2540 B method, while the total suspended solids (TSS) of each filtrate fraction was found using method 2540 D (Clescerl et al. 1999).

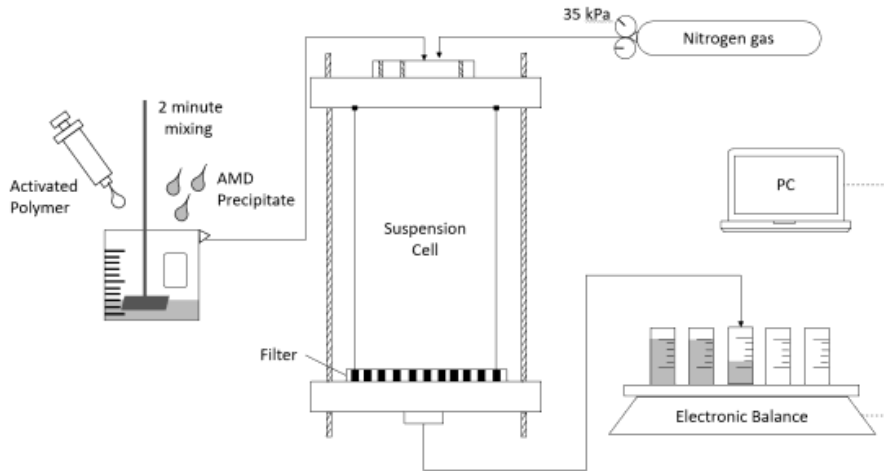


Figure 2. Schematic of the lab-scale PFT system.

3 RESULTS AND DISCUSSION

3.1 High-throughput polymer screening via LUMiFuge

The panels in Figure 3 display the solids volume vs. time curves from the LUMiFuge analysis of the polymer flocculants with the AMD precipitates. Cationic polymers were found to be effective flocculants in that the rate of dewatering increased incrementally with increasing quantities of cationic polymer. For the low polymer dose conditions of 1 to 2 kg/TTS, the increase in the rate of dewatering relative to the 'no polymer' condition was slight. The polymers which displayed the best flocculation performance at these doses possessed 'high' or 'very high' charge density and 'high' or 'very high' molecular weight. When the polymer dose was increased to 4 kg/TTS, the rate of dewatering was significantly increased. The observed relationship between relative solids volume and time became nonlinear: indicating a fundamental change in the separation behaviour of the AMD precipitates. A further increase in the rate of dewatering was observed for all cationic polymers with an increase in dose to 8 kg/TTS. Ultimately, 4 kg/TTS of Polymer C3 was identified as the optimum cationic polymer-dose combination as this condition combines excellent polymer performance and industrial practicality in terms of treatment costs. As reported in Table 2, Polymer C3 possessed a combination of 'medium' charge density and 'high' molecular weight.

The three anionic polymers produced only minor improvements in dewatering rate with increasing dose. The lone exception to this observation was Polymer A1 at an 8 kg/TTS dose which, while able to significantly increase the rate of dewatering, was deemed impractical due to the excessive quantities of polymer required. Polymer A3 at a 4 kg/TTS dose was selected as

an optimum anionic polymer. It was used in the PFTs to directly compare the performance of anionic and cationic polymers for the geotextile dewatering of AMD precipitates. Polymer A3 possessed a combination of ‘medium’ charge density and ‘very high’ molecular weight.

The best flocculation conditions were further evaluated using FBRM to assess the change in particle aggregation. As shown by the chord length distributions for the as-received and treated samples of AMD precipitates in Figure 4, neither polymer-dose combination resulted in a meaningful aggregation of the AMD precipitate particles.

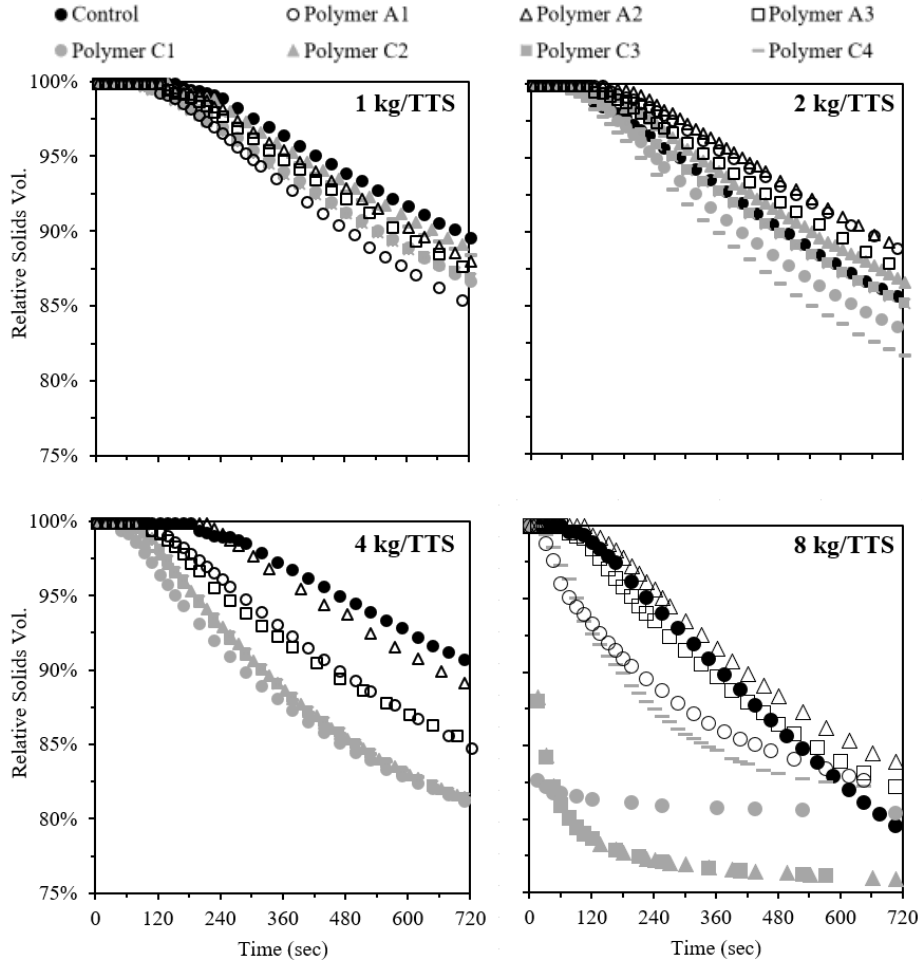


Figure 3. LUMiFuge stability analysis results for AMD precipitates treated with four cationic and three anionic polymers at four different doses.

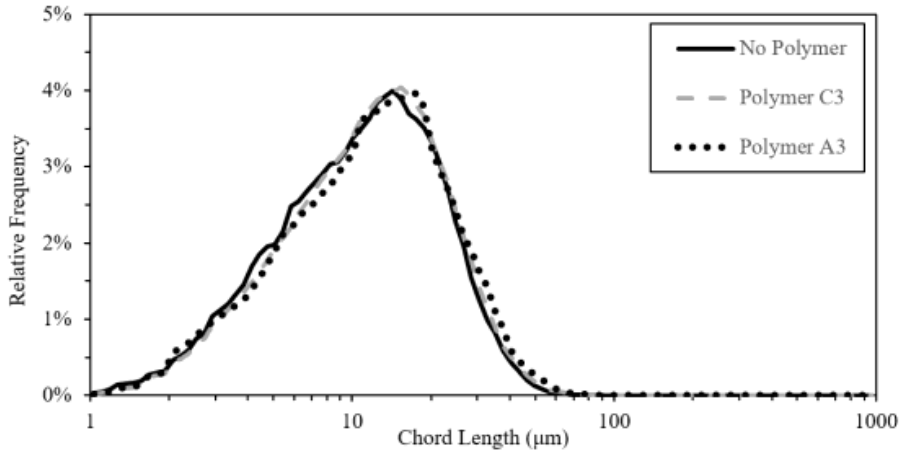


Figure 4. FBRM results depicting the impact of polymer addition on the chord length distribution of AMD precipitates. Results are shown for the as-received sample as well as AMD precipitates treated with polymers C3 and A3 at a 4 kg/TTS dose.

3.2 Pressure filtration test (PFT)

3.2.1 Dewatering performance of conventional woven fabrics

The results from the duplicate PFTs performed using the woven textile for untreated AMD precipitates and those treated with 4 kg/TTS of Polymers C3 and A3 are shown in Figure 5. Panel A of Figure 5 includes mass of filtrate vs. time curves which illustrate the rate of dewatering achieved at an applied pressure of 35 kPa. Overall, geotextile dewatering of AMD precipitates using conventional engineered dewatering fabrics was shown to be a slow process. Without polymer pre-treatment, the woven textile employed in this work required an average of 200 ± 20 min to reach breakthrough. The application of a polymer pre-treatment step using Polymer C3 was only able to reduce the required dewatering time to 190 ± 10 min while Polymer A3 reached breakthrough in 196 ± 9 min. Therefore, neither the cationic nor the anionic polymer were able to improve the rate of dewatering to a degree that would justify the additional operating cost associated with their use.

Despite requiring an extended period to perform dewatering, the woven textile was able to significantly increase the solids content of the AMD precipitates. Panel B of Figure 5 presents the SC of the filter cake after dewatering; the error bars represent the observed range above and below the average across duplicate tests. Without polymer pre-treatment the average SC was $18.5 \pm 0.6\%$. The use of Polymer C3 and Polymer A3 yielded SC values of $17.0 \pm 0.8\%$ and $17.0 \pm 0.2\%$ respectively. Dewatering efficiency (DE) is a useful indicator of dewatering capacity. DE is defined as the relative increase in the SC of the feed achieved during the dewatering process as shown in Equation 2 (Moo-Young et al. 2002):

$$DE (\%) = (SC_{\text{final}} - SC_{\text{initial}}) / SC_{\text{initial}} \times 100 \quad (2)$$

The SC values reported above for the woven textile correspond to DEs of: 203% without polymer pre-treatment, 179% using Polymer C3, and 179% using Polymer A3. Despite the significant difference in separation performance between cationic and anionic polymers observed in the LUMiFuge results, both polymer-dose combinations yielded the same DE. Furthermore, the use of either polymer type was shown to decrease the dewatering capacity of the woven textile relative to the 'no polymer' condition.

Panel C of Figure 5 presents the average filtrate TSS measured for each of the four sequential 45 g filtrate fractions collected; the error bars represent the range above and below the average across duplicate tests. Without polymer pre-treatment, the woven textile yielded an average filtrate TSS of 4200 ± 200 mg/L for F1, 97 ± 0 mg/L for F2, 16 ± 1 mg/L for F3, and 40

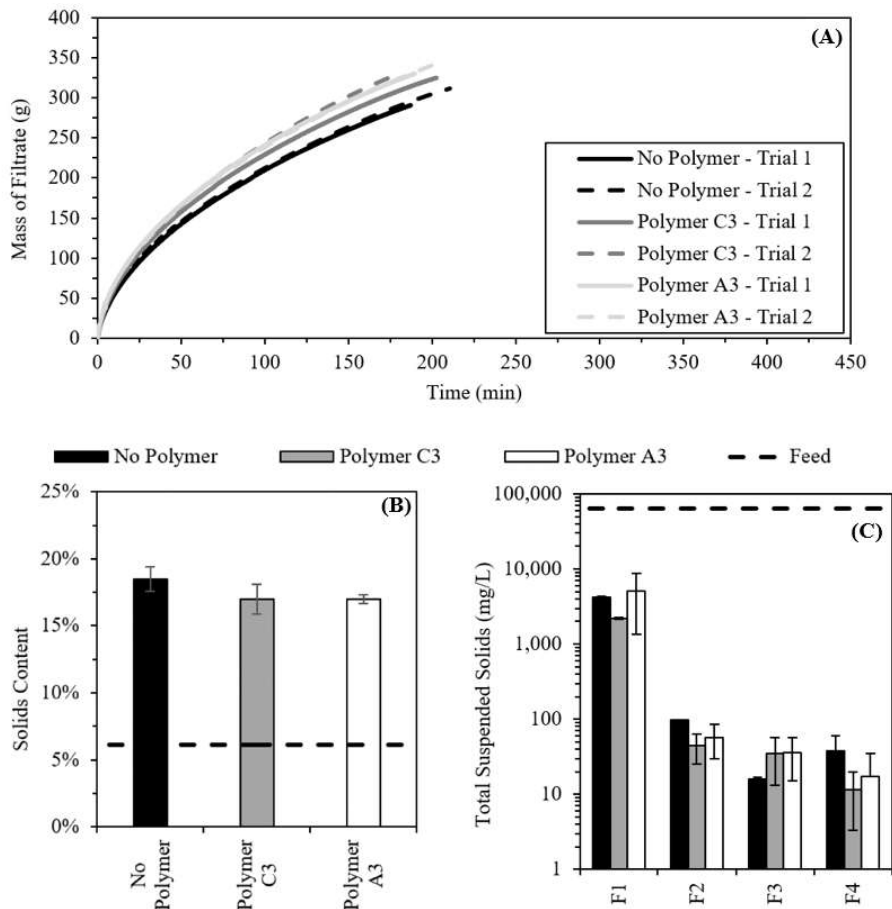


Figure 5. PFT results for the woven textile without polymer pre-treatment, with a 4 kg/TTS dose of Polymer C3, and with a 4 kg/TTS of Polymer A3. Panel A presents the mass of filtrate vs. time curves, Panel B presents the SC of the material retained within the suspension cell after dewatering, and Panel C presents the total suspended solids of the four filtrate fractions.

± 20 mg/L for F4. The dramatic decrease in filtrate TSS suggests that, over time, an effective filter cake was developed on the surface of the woven textile which served as the dominant mechanism by which solids were retained. For context, the ‘daily concentration limit’ of TSS for effluent originating from metal mining operations in Ontario, Canada is 30 mg/L as per O Reg 560/94. Therefore, the woven textile was able to meet the discharge limit after sufficient filter cake development without the use of polymer flocculants. Filtration efficiency (FE) is a metric used to index the solids retention capacity of a dewatering fabric when assessing the viability of dewatering with geotextile tubes; higher FE values indicate a greater capacity to retain solids. FE is calculated from the filtrate TSS and feed total solids (TS) as shown in Equation 3 (Moo-Young et al. 2002):

$$FE (\%) = (TS_{\text{feed}} - TSS_{\text{final}}) / TS_{\text{feed}} \times 100 \tag{3}$$

The range of TSS values reported above for the woven textile –without polymer pre-treatment– correspond to FEs of 93.4% for F1 and 99.9% for F4. Therefore, the woven textile was able to retain nearly all the suspended solids present in the AMD precipitates after the filter cake was

established. The use of a cationic polymer to pre-treat the AMD precipitates was shown to provide a modest improvement in FE during the initial stages of dewatering. Specifically, a 4 kg/TTS dose of Polymer C3 increased the average FE calculated for F1 from 93.4% to 96.6%. The FEs calculated for F2, F3, and F4 were comparable to the 'no polymer' condition. Conversely, pre-treating with Polymer A3 yielded a FE of only 92.0 % for F1. Hence, the cationic polymer provided a slight improvement in solids retention during the earliest stages of dewatering; while no improvement was observed for the anionic polymer. After the establishment of the filter cake, the woven textile displayed excellent solids retention with or without polymer pre-treatment.

3.2.2 Dewatering performance of the thin-film dewatering filters

Figure 6 presents the results of the PFTs performed using the thin-film dewatering filters for unmodified AMD precipitates. Panel A of Figure 6 includes the mass of filtrate vs. time curves for each filter. These results indicate that a negative correlation exists between the time required to reach breakthrough (BT) and filter porosity. For example, the '100x1500_4mm' filter, having a porosity of only 0.69%, required 425 min to dewater the 500 g sample. Conversely, the '100x5000_1mm' filter, having a porosity of 8.81%, required only 138 min. Therefore, by increasing the aspect ratio of the slit-pores from 15:1 to 50:1 and reducing the pore-to-pore spacing from 4 mm to 1 mm, the BT time was reduced by 70%. The power regression of the BT times versus porosity (P) for the treatment of AMD precipitates is presented as Equation 4:

$$BT \text{ (min)} = 327.55(P)^{-0.382} \quad (4)$$

The coefficient of determination was 0.95. As previously discussed, the woven textile required 200 ± 20 min to reach breakthrough. This result falls between the 173 min required by the '100x1500_1mm' filter with a porosity of 6.03% and the 299 min required by the '100x5000_4mm' filter with a porosity of 0.88%. Therefore, although not reported by the manufacturer, the effective porosity of the woven textile is estimated to be 3.64% using Equation 4.

Filter porosity was also shown to impact DE. Panel B of Figure 6 presents the SC of the material retained within the suspension cell at the end of the PFT for each of the thin-film filters without polymer pre-treatment. The measured SC values for the two highest porosity filters, '100x5000_1mm' and '100x1500_1mm', were 19.6% and 18.1% which correspond to DEs of 221% and 197%, respectively. Conversely, the two lowest porosity filters, '100x5000_4mm' and '100x1500_4mm', yielded DEs of only 179% and 189% respectively. Therefore, increasing the porosity of a thin-film filter using longer and more densely spaced pores, not only increases the rate at which dewatering occurs, but also provides a modest improvement to the extent of dewatering achieved.

Panel C of Figure 6 presents the TSS of the four sequential filtrate fractions collected using the thin-film dewatering filters. Although increasing filter porosity results in greater solids passthrough during the initial stages of the dewatering process, excellent solids retention is achieved irrespective of filter porosity once a stable filter cake is established. For example, the '100x1500_4mm' filter yielded a TSS of 4027 mg/L for F1; a value which corresponds to a FE of 93.7%. However, FE quickly improved to 99.9% for F2. Conversely, the '100x5000_1mm' filter yielded a TSS of: 41,547 mg/L for F1, 50,580 mg/L for F2, 18,767 mg/L for F3, and finally, 40 mg/L for F4. These values correspond to FEs of: 26.5%, 17.5%, 63.1%, and 99.9% respectively. Hence, a stable filter cake was not established on the surface of this filter until after the collection of 135 g of filtrate in F1-3. However, according to Panel A of Figure 6, this cake development period corresponds to only the first 5 min of dewatering, indicating that excellent solids retention was achieved for the majority of the PFT. Therefore, for full-scale applications where large volumes of AMD precipitates are to be dewatered, the period of reduced solids retention during cake layer development is expected to be limited to the initial filling of the dewatering tube. Thus, while the cake layer is important to dewatering performance, the time required to develop a stable filter cake is expected to be negligible in the overall operating life of the dewatering textile.

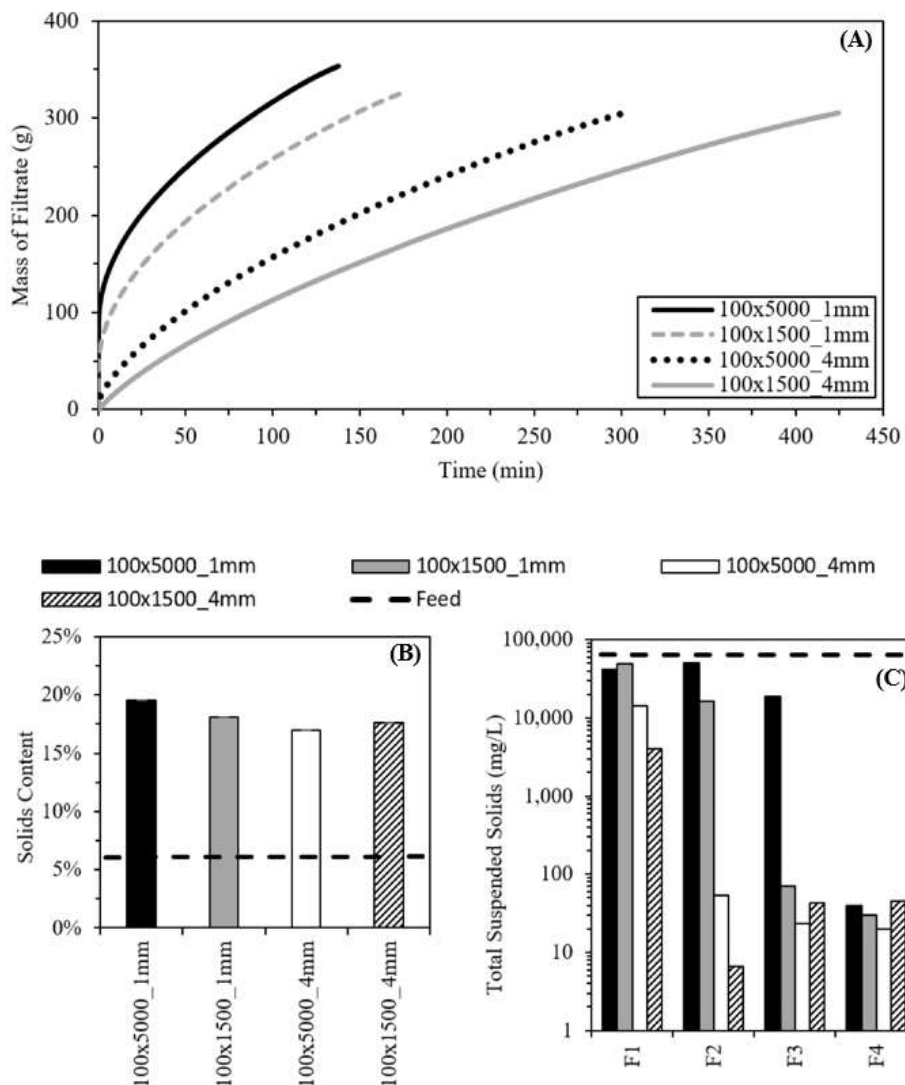


Figure 6. PFT results for the four thin-film dewatering filters without polymer pre-treatment. Panel A presents the mass of filtrate vs. time curves, Panel B presents the SC of the material retained within the suspension cell after dewatering, and Panel C presents the total suspended solids of the four filtrate fractions.

3.2.3 Improving solids retention of thin-film dewatering filters using polymer flocculants

Additional PFTs were performed to determine if polymer pre-treatment can be applied to promote a more rapid filter cake development for the high porosity thin-film dewatering filters. Figure 7 presents the average TSS for the sequential filtrate fractions collected using the ‘100x5000_1mm’ and ‘100x1500_1mm’ filters in combination with 4 kg/TTS doses of Polymer C3 and Polymer A3. Once again, the error bars represent the observed range above and below the average TSS result for duplicate tests. The obtained results indicate that a stable filter cake was established significantly earlier in the PFT for the high porosity thin-film dewatering filters when polymer pre-treatment of the AMD precipitates was employed.

As previously discussed, the ‘100x5000_1mm’ filter did not develop a filter cake capable of retaining the AMD precipitate particles prior to the collection of 135 g of filtrate without polymer pre-treatment. However, applying a 4 kg/TTS dose of either Polymer C3 or Polymer A3 significantly reduced filtrate TSS during the initial stages of dewatering. Specifically, Polymer C3 resulted in 36%, 84% and 99% reductions in TSS for F1, F2, and F3 respectively. Polymer A3 produced decreases of 19%, 95%, and 99% in TSS compared to the no-polymer trials for F1, F2, and F3 respectively. Similar observations can be made for the ‘100x1500_1mm’ filter which displayed poor solids retention for the first two filtrate fractions without polymer pre-treatment. In this case, Polymer C3 yielded reductions of 41% and 99% for F1 and F2. In the same case, Polymer A3 produced decreases of 46% and 99% for F1 and F2. Therefore, filter cake development was shown to occur significantly earlier in the dewatering process for the high porosity thin-film dewatering filters when either the cationic or the anionic polymer were used to pre-treat the AMD precipitates.

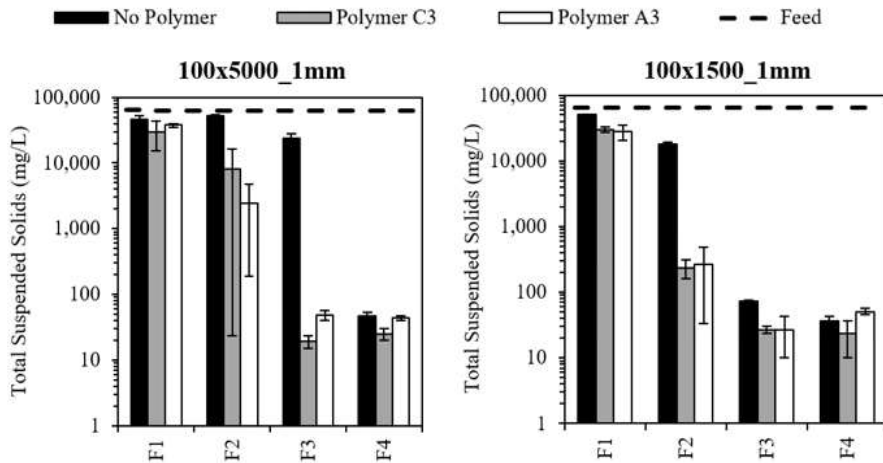


Figure 7. Filtrate TSS results for the ‘100x5000_1mm’ and ‘100x1500_1mm’ filter with two high-porosity thin-film dewatering filters without polymer addition, with a 4 kg/TTS dose of Polymer C3, and with a 4 kg/TTS dose of Polymer A3.

4 CONCLUSIONS

In this study, we investigated the efficacy of microfabricated thin-film dewatering filters for treating AMD precipitates through the performance of lab-scale PFTs. The effects of optimized polymer pre-treatment and the pore geometry, as well as total porosity of the filters, were studied. The dewatering rate, solids retention, and extent of dewatering results were compared to those for a commercially available woven dewatering textile. A review of the key findings from this research is given below:

- A LUMiFuge analytical centrifuge was used to screen four cationic and three anionic polymers. The cationic polymers significantly increased the rate of dewatering of AMD precipitates, while the use of the three anionic polymers yielded minimal benefit.
- The woven textile was able to retain 99.9 % of the suspended solids after filter cake development and increase the solids content of the AMD precipitates by up to 203%. However, permeability was low, resulting in a slow dewatering process. The use of polymer pre-treatment did not provide a meaningful improvement in dewatering rate, but cationic polymers did provide a slight improvement in the rate of filter cake development.
- The PFT results for the thin-film dewatering filters demonstrated that the use of closely spaced, elongated pores –which results in a high porosity– significantly improved the rate of

dewatering and provided moderate improvements in dewatering efficiency relative to conventional engineered dewatering fabrics. Furthermore, although increasing porosity was shown to delay filter cake development, excellent solids retention was achieved irrespective of porosity once a stable filter cake was established.

- Cationic and anionic polymers significantly increased the rate of filter cake development for the high porosity, thin-film dewatering filters; minimizing solids passthrough during the initial stages of dewatering.

Overall, this work provides new insights into the importance of pore geometry, porosity, and polymer performance on filter cake development. The dewatering of AMD precipitates is an important and often overlooked facet of mine waste management. The results presented herein indicate that the use of high-porosity dewatering fabrics incorporating slit-pore geometries is a viable method of performing AMD precipitate dewatering in a manner that is both environmentally and economically responsible.

REFERENCES

- Aubé, Bernard 2004. *The Science of Treating Acid Mine Drainage and Smelter Effluents*. Québec: EnvirAubé.
- Clescerl, L.S., Greenberg, A.E. & Eaton, A.D. (ed.) 1999. *Standard methods for the examination of water and wastewater*. 20th ed. Washington (DC): American Public Health Association.
- Moncur, M.C. 2006. Acid Mine Drainage: Past, Present...Future?. *Wat on Earth*.
- Hamblin, C.D & Kord, M.G. 2003. The Rehabilitation of Ontario's Kam Kotia Mine: an Abandoned Acid Generating Tailings Site. Proceedings of the Sudbury 2003 Conference on Mining and the Environment III. Sudbury (ON): Ministry of Northern Development and Mines & B.H. Martin Consultants Ltd.
- Barakat, M.A. 2011. New trends in removing heavy metals from industrial wastewater. *Arabian Journal of Chemistry* 4(4): 361-377.
- Maurer, B.W., Gustafson, A.C., Bhatia, S.K. & Palomino, A.M. 2012. Geotextile dewatering of flocculated, fiber reinforced fly-ash slurry. *Fuel* 97: 411-417
- MEND 1997. Characterization and Stability of Acid Mine Drainage Treatment Sludges. Mine Environment Neutral Drainage Program. Project 3.42.2a
- Moo-Young, H.K., Gaffney, D.A. & Mo, X. 2002. Testing procedures to assess the viability of dewatering with geotextile tubes. *Geotextiles and Geomembranes* 20(5): 289-303.
- Sithole, N.T. 2015. *Removal of heavy metals from aqueous acidic mineral effluents by reductive precipitation*. Master's thesis, University of Johannesburg, South Africa.
- MAC 2017. Facts and Figures 2017. The Mining Association of Canada. <<http://www.mining.ca/>> (accessed June 2018).
- EMCBC 2000. Acid Mine Drainage: Mining & Water Pollution Issues in BC. Environment Mining Council of BC. <<http://www.miningwatch.ca/>> (accessed June 2018).

Lessons Learned on the Performance of Multi-Linear Drainage Geocomposites for Mining Applications

P. Saunier

AFITEX-TEXEL, Vancouver, BC, Canada

E. Blond

Eric Blond Consultant, Montréal, QC, Canada

ABSTRACT: Tailings dewatering is a permanent concern for responsible mining companies. Soft and wet tailings can generally lead to stability issues in retaining ponds or dams, excessive environmental footprint because of their high water content and therefore a high volume to storage, and finally can increase the total process costs to a level that can eventually break the fragile equilibrium of the operation. This situation has become among the key issues to be solved, with higher environmental pressures and regulation authorities, as well as a market struggling since almost a decade. Traditional drainage geocomposites are commonly used in applications where the flow to be drained is average, the loads on the product are in the order of 500 kPa and the fines content of the soil to be drained is low. This paper presents a review of laboratory evaluations conducted on Multi-Linear Drainage Geocomposites (MLDG) to assess their applicability in tailings dewatering. Three studies were conducted. First, transmissivity tests were performed under very high normal loads, up to 2MPa, to reflect normal loads actually experienced in tailings and dams. Long-term flow tests were then conducted during 90 days. In addition, filtration tests modeling the mechanisms involved in the deposition of tailings in a slurry form were performed, using a modified version of ASTM D5101. A scale test has been conducted in Morocco accordingly. All these tests were found to be conclusive and confirmed the applicability of MLDG for tailings dewatering applications. A case study of a recent project in Canada will be presented as well.

1 INTRODUCTION

Management of tailings is one of the major operational and environmental challenges faced by the mining industry. Indeed, the consolidation rate of the high water-content tailings is generally limited by their high physical stability and low hydraulic conductivity. Extended laboratory work conducted in the last 7 years has shown that the use of Multi-Linear Drainage Geocomposites can accelerate the dewatering rate of tailings. Further to these laboratory evaluations, a full scale test was performed in Morocco and demonstrated the good functioning of a range of drainage's geocomposites for a better recovery of the water from the dikes and a good stability of the walls of proceed phosphate water flotation basins.

Multi-Linear Drainage Geocomposites (MLDG) have been used for decades in civil and environmental applications. This paper presents a series of studies conducted to assess their performance in mining applications.

- The MLDG used in this study is described on Figure 1. It includes the following components:
- A non-woven geotextile, which acts as a filter. This layer is typically selected with consideration to the gradation and properties of the overlying material, with opening sized ranging from 44 μ m to 200 μ m or more.

- A series of corrugated, perforated polypropylene tubes. The number of tubes per unit width can be adjusted to fit specific project's needs. These tubes provide most of the drainage capability of the product.
- Another non-woven geotextile, which is selected as a cushion, to protect the underlying geomembrane from puncture when exposed to coarse, angular gravels. This layer may also provide a secondary drainage medium.

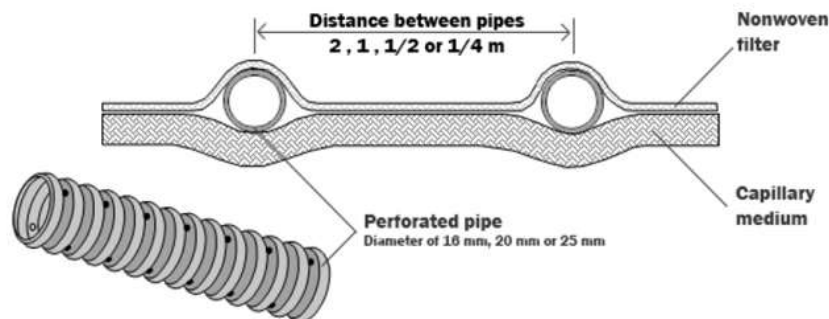


Figure 1 Multi-Linear drainage geocomposite

2 LABORATORY STUDY

2.1 Long-Term Flow Test – for heap leach pad applications

2.1.1 Concept of the experiment

Heap leach pads (HLPs) are among the world's largest man-made structures. The ore is typically staked at heights in the range of 40 to 70 meters, by successive 5 to 10 meters lifts (Breitenbach et al. 2005). Thiel and Smith (2004) even report heap leach pads 150 m and 230 m high in South America. Heap leaching is a mineral processing technology where large piles of crushed rock are leached with various chemical solutions that extract valuable minerals. This technique is used for copper, gold, nickel and uranium. The mined ore is crushed and heaped on a lined impermeable pad and irrigated with a leaching solution for an extended period of time (weeks, months or years). As the solution gradually percolates through the ore heap, it dissolves the valuable mineral, producing what is known as a 'pregnant solution'. This solution is collected at the base of the heap leach pad where a drainage base of crushed rock and embedded perforated pipes is installed above the liner system and below the ore heap. The importance of this drainage base cannot be overemphasized. This layer has to:

- Protect the geomembrane liner against puncture,
- Allow efficient removal of the ore-bearing solution from beneath the heap, and
- Ensure stability of the structure by maintaining a low hydraulic head, while preserving a high friction angle of liner interfaces.

In terms of structure, heap leach pads essentially consist in a liner and a drainage system, which are designed to permit recovery of the pregnant solution leaching through the ore. Considerations are also given to the global stability of the system, which may be affected by the performance of the drainage systems as well.

Filtration application in HLPs and more generally with mine residues may be challenging for geotextiles. First, the high seepage forces and suspended particles that must be filtered can lead to the blinding or clogging of the geotextile filter. Second, circulation of the pregnant solution can lead to chemical clogging (Faure, 2004; Fourie et al. 2010; Legge et al. 2009).

Long-term flow tests were conducted in SAGEOS laboratories in Canada to observe the performance of DTPG when subjected to acid circulation at a concentration representative of those

used in the mining industry during 3 months. To run this test, 10 test cells (0.1m x 0.2m) were designed to replicate field conditions prevailing on the MLDG (Figure 2). The filter used was a polyester filter with a filtration opening size of 120 µm (per CGSB 148.1 n°10). The MLDG was installed at in the bottom of the cell, and then covered with by one kilogram of crushed copper ore with an average grade of 3% Cu from a Chilean copper mine (Lomas Bayas). The ore was covered by a geo-spacer to facilitate uniform infiltration of the solution. This latter component was then covered by a closed-cell foam pad, compressed by a rigid plate, in order to seal the system while applying a nominal stress of 100 kPa.

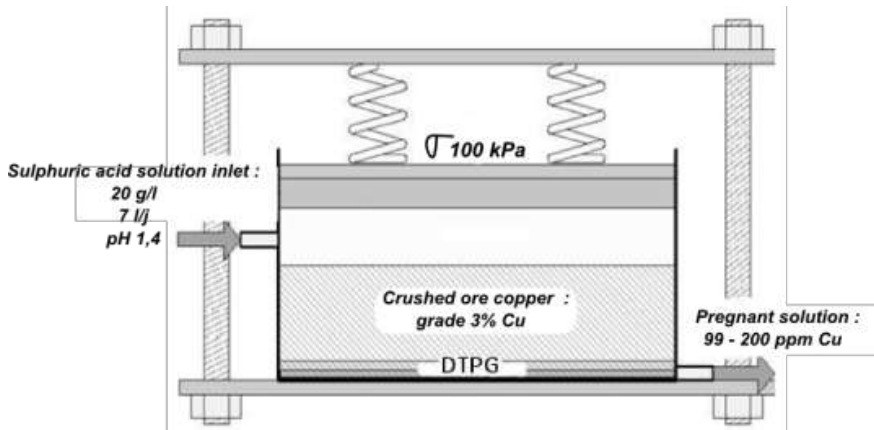


Figure 2 Cross-section of an experimental leaching cell. During 90 days, acid leachate percolates through the ore then the MLDG

An average daily flow of 15 L/h/m of the 20 g/l sulphuric acid solution with a pH of 1.4 was recirculated during 90 days through each cell.

The solution was injected through the geo-spacer, in order to flow downward through the ore, then the MLDG, to eventually be drained out by the perforated tube. During the testing period, the solution was replaced 3 times to avoid excessive copper concentration and facilitate control of the pH, which was maintained to approximately 1.4.

The representativity of the extraction process modelled at the laboratory scale was assessed by monitoring periodically the copper concentration of the sulphuric acid. The observations are reported on Table 1.

Table 1 Copper concentration in the leaching solution during experiment

Days of leaching	Copper concentration (ppm)	Copper recovered (g / kg of ore)
20	267.5	2.40
40	120	1.08
60	122.5	1.10
80	111.5	1.00
90	99	0.89

These observations confirmed that the chemical reaction which is expected to take place in a leach pad was actually taking place at the laboratory scale.

2.1.2 Flow rate

The flow rate was monitored to determine the evolution of the hydraulic properties i.e. to observe a possible clogging of the system. Results are expressed as an 'equivalent flow rate under a hydrostatic head of 5 mm'. This value does not have any significance by itself and cannot be related to the in-plane transmissivity of the geocomposite nor the permeability of the filter. However, it can be used as an indicator of the clogging of any component of the system, such as:

- Blinding or clogging of the filter;
- Clogging or collapse of the drainage media.
- Overall degradation of the product, i.e. chemical dissolution or any other issue

Figure 3 shows a typical flow rate curve as it has been monitored over time for each of the cells that were tested.

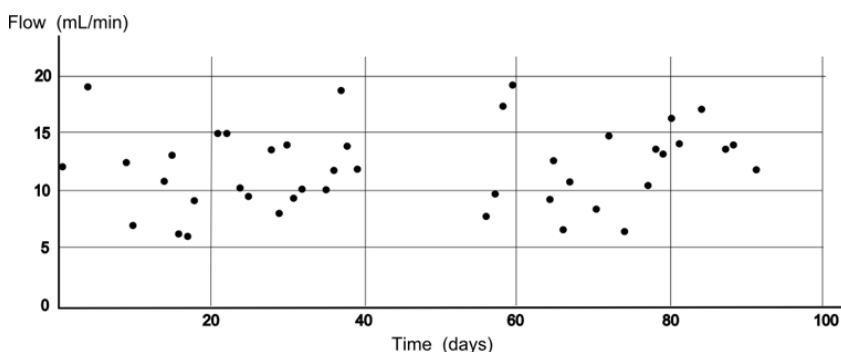


Figure 3 Typical flow rate under a hydraulic head of 5 mm.

From Figure 3, it is possible to observe that the flow rate remained relatively constant over time, which suggests that no clogging did occur and that the MLDG maintained its functionality over the duration of the test, or 90 days.

2.1.3 Observation of the geocomposite at the end of the test

After 3 months of continuous flow in the conditions described above, cells were dismantled to permit visual inspection of the geocomposites. Once observed that the integrity of the drainage pipe and perforated pipe had been fully maintained, three observations were made during these inspections:

- Quantity of particles retained on the upper geotextile (filter), making sure to remove the particles that were on top of the geotextile but not the embedded ones;
- Quantity of particles retained on the lower geotextile as well as trapped between the two geotextiles;
- Quantity of particles retained into the pipe.

A quantity of 80 g/m² of particles in average was observed into the upper geotextile, while only 10g/m² were found on the lower geotextile. On the other hand, the perforated drainage pipe was found to be completely free of particles.

Following these observations, permittivity tests were conducted on the filters. The tests were conducted with a hydraulic head of 10 mm to avoid excessive pressure that could have washed out the embedded particles. With these conditions, a reduction in permittivity in the range of 10% was observed, confirming the visual observation of a geotextile looking almost 'clean' on its inner side, compared to the outside, as can be seen on Figure 4.



Figure 4 external and internal view of the geocomposite after 3 months of percolation of sulphuric acid

2.2 Behavior under high compressive load

Compressive load on the drainage layer can reach 2 MPa (Thiel and Smith, 2004; Castillo, 2005). For traditional planar geocomposites involving a planar drainage core (such as biplanar or triplanar geonet), it has been shown by several authors that the hydraulic properties of these geosynthetics are adversely affected by such high compression stresses. Creep resistance is indeed a component that is taken in consideration in the selection of such products, and can be evaluated with ASTM standard D7341. However, Saunier et al. (2010) have shown that the particular structure of MLDG is favorable to the development of an arching effect around the pipe. This statement was made following the observation that transmissivity is not affected by compression stress, nor by time. Their results are reported on Figure 5.

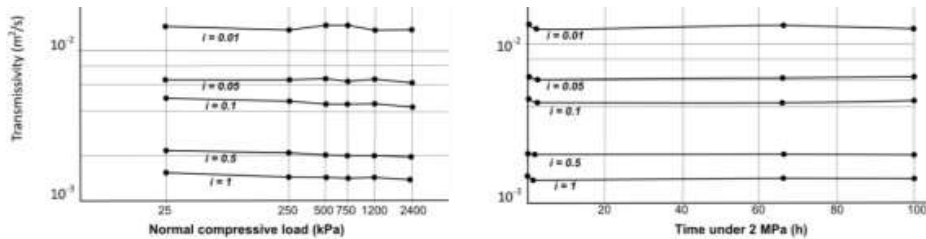


Figure 5 Transmissivity under different loads up to 2 Mpa and 100 h (i = hydraulic gradient) (after Saunier et al, 2010)

2.3 Filtration Compatibility with tailings

Tailings are conveyed to their storage facility in a slurry form. Slurries are highly challenging materials for geotextile filtration as the presence of a high concentration of fines segregated from the soil may create a cake on the surface of the geotextile, and reduce its permeability thus endanger the efficiency of the system and the geotechnical stability of the facility.

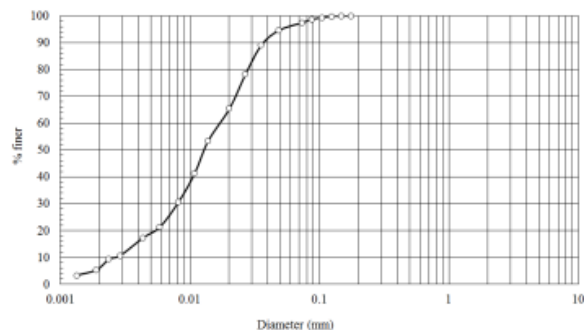
To assess the filtration behavior of the geotextile used as a filter in the MLDG, a modified gradient ratio test was developed to model the mechanisms prevailing at the time the slurry is deposited on the geotextile filter. The following hypotheses were considered to develop the experiment:

- First, the slurry reaches the geotextile with a solid / water ratio of 72% water / 28% solid – for the particular case that was analyzed.
- In the early stage of the slurry / geotextile interaction, the water head will be similar to the height of the slurry, and the system will settle.

- Eventually, more material will reach the deposit, and increase the water head, and eventually hydraulic gradient prevailing in the vicinity of the interface.

Considering these hypothesis, a testing strategy was developed, using a testing apparatus conforming to ASTM D5101, modified in order to model the above described scenario.

A slurry was prepared to the prescribed solid / water ratio, using the tailing which particle size distribution is presented on Figure 6-a. To initiate the test, this slurry was deposited in a liquid form (Figure 6-b) on the surface of the geotextile filter, selected for its filtration opening size of 60-70 μm (per CGSB 148.1 n°10). This led to a total head of about 300 mm above the geotextile.



(a) Gradation



(b) consistency for deposition

Figure 6 Gradation of the tailing

A valve located downstream the geotextile was opened immediately to initiate the test, by connecting the downstream section of the test cell to a container with a free surface maintained at a height of 150 mm above the geotextile. Given that, the initial conditions prevailing were a water (slurry) head of about 300 mm upstream the geotextile, and 150 mm downstream. A 'slurry head' of 150 mm was thus applied on the geotextile filter, initiating a flow through the geotextile at the same time the slurry was settling. Hydraulic head were monitored under the geotextile, at distances of 25 and 75mm and above the slurry, as well as the flow rate. This stage, combining a falling head and sedimentation of the tailing, was maintained until stabilization of the upstream head to 150 mm = same as the downstream head. During that stage, the soil / geotextile interface developed its structure in a fashion similar to what is likely to be taking place on-site.

After stabilization, the upper portion of the test cell was closed, and the standard gradient ratio test was initiated using the standard apparatus (Figure 7), using a hydraulic gradient of 1.0. During the test, the same hydraulic head were monitored, under the geotextile, at distances of 25 and 75mm and above the soil/slurry, as well as the flow rate.



Figure 7 Set-up of the filtration test (Gradient Ratio, ASTM D5101)

As there is no precise limit differentiating a ‘soil’ from a ‘slurry’ during the deposition stage, it was not possible to determine a flow length in the porous media, thus to calculate a permeability of a soil, geotextile, or obviously the slurry. It was thus decided to determine a ‘permittivity’ of the entire system, by dividing the flow rate by the total water head. This value was considered to be a sufficient indicator to observe a trend, i.e. an increase or a reduction of permeability over time. It is also a convenient way to normalize the flow rate to the water head, to analyze the geotextile interface behavior during the slurry deposition stage of the test.

Results and observations are presented in Figures 8 to 10.



(a) after 5 minutes (b) after 15 minutes (c) after 2 h 45 min (d) after 66 hours
 Figure 8 Settlement of the slurry during the first stage of the test

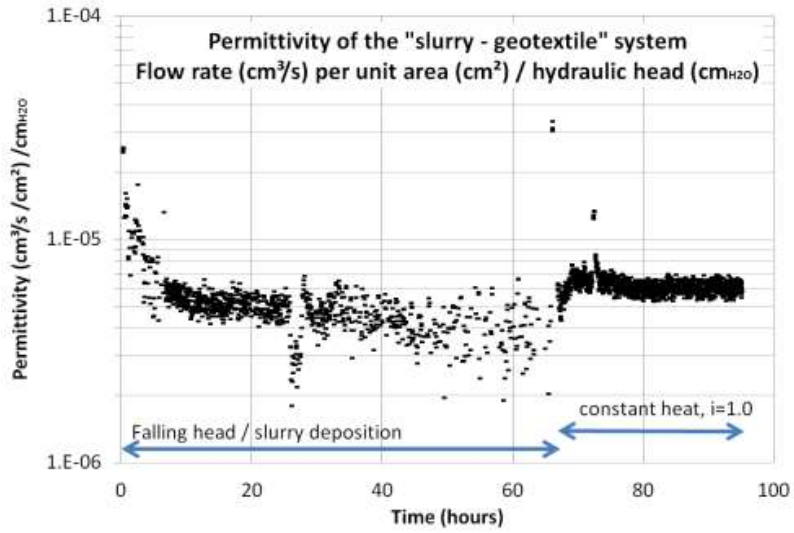


Figure 9 Permittivity versus time

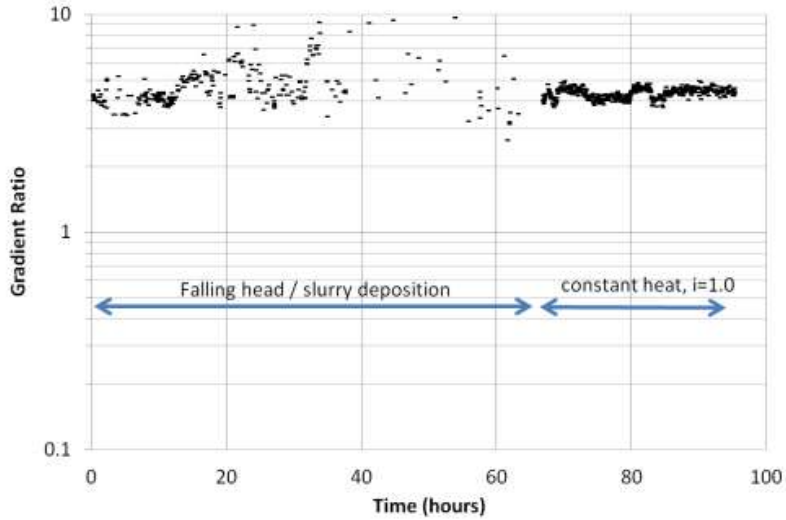


Figure 10 Gradient ratio versus time

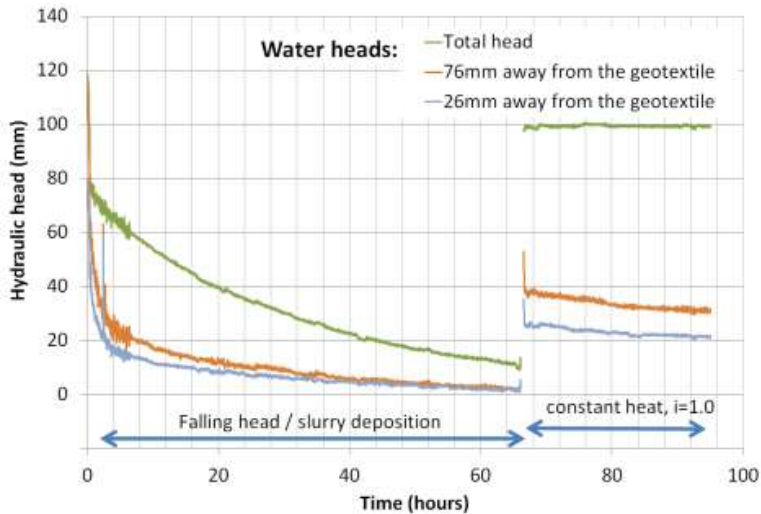


Figure 11 Water head versus time

The following observations were made:

- The 'permittivity' of the system, calculated by dividing the flow rate per unit area at a given time by the total hydraulic head, first decreased to reflect the accumulation of soil particles at the surface of the geotextile (Figure 9). It eventually stabilized to remain constant until the end of the first part of the test (sedimentation). After full settlement / deposition of the soil particles, the second phase of the test was initiated with the constant head test, and the permittivity stayed at the same level as what was measured before. It was thus concluded that the permittivity of the system was stable over time, thus that no clogging mechanism develops as the water flows through the system.

In order to estimate the permeability of the tailing / geotextile system, the permittivity can be multiplied by the height of soil after deposition (measured from the outside of the cell, i.e. on Figure 8-d). A value of $6.10 \cdot 10^{-5}$ cm/s was determined, which was reported to be similar to the permeability of the tailing as documented by the owner.

With a permeability of the system similar to the permeability of the native material and no decrease of permeability over time, the system was considered to be stable.

- Gradient ratio values of approximately 3 were observed and remained stable through the duration of the test (Figure 10). Although 3 is on the upper bound of what is usually considered acceptable, it has to be analyzed considering two factors:
 - o First, the soil was not compacted but installed in a slurry form. As a consequence, the arrangement of sedimented particles is likely to be more compact in the vicinity of the filter, where the water has the highest potential for being evacuated and let the soil arrange itself in a compact structure, by opposition to a slurry.
 - o Second, it does not evolve through time, which indicates that the permeability of the tailing / geotextile interface does not decrease faster than the permeability of the tailing, measured at a distance of the interface.

As a consequence, the gradient ratios were considered as reflecting a stable behavior of the geotextile / tailing interface, despite the value of 3, which is considered as reflecting clogging in ASTM D5101.

- Analysis of the evolution of the water heads (Figure 11) shows that more than half of the head loss occurs between the top of the soil and the piezometer located at a distance of 76mm from the geotextile, i.e. on the very top of the sedimented slurry. This observation can be explained by the sedimentation process, which favors segregation of the particles

with the coarser particles settling first. As a consequence, the gradation of the soil progresses, with a decreasing concentration of coarser particles, as the distance to the geotextile increases. This mechanism favors creation of a very fine grained layer on the top of the soil surface, which exhibits a lower permeability, thus a higher head loss on the upper layer, as observed on Figure 11.

Overall, the observations made with this test led to the conclusion that the tested geotextile, with a FOS of 70 μ m (as measured per CGSB 148.1 n°10) has offered a good filtration performance of the tailing with the particle size distribution shown on Figure 6-a, prepared as a 28% solid / 72% water slurry, during both sedimentation and filtration under a hydraulic gradient of 1.0.

3 LARGE SCALE EXPERIMENTATION

Phosphate mining at the OCP Mrah laundromat (Morocco) leads to the production of 24,000 m of sludge every day. This sludge contains between 70 and 80% water. A significant portion of this water cannot be recycled in the mining operation, but is lost because of:

- Evaporation due to strong sunshine and high temperature, especially in summer;
- Seepage into the underlying soil, potentially polluting the environment;
- Too slow sedimentation of the solid component of the slurry, water staying trapped by the electrochemical interactions with the solid particles.

The mining company decided to build a large scale test pad, to assess the performance of MLDG as a drainage component in the bottom of a sedimentation basin. The MLDG described on Figure 1 was used as the single drainage media, in direct contact with the slurry – that is, with no granular cover. Each mini-pipe of the MLDG was connected to its related main collector with connectors designed specifically for the MLDG.

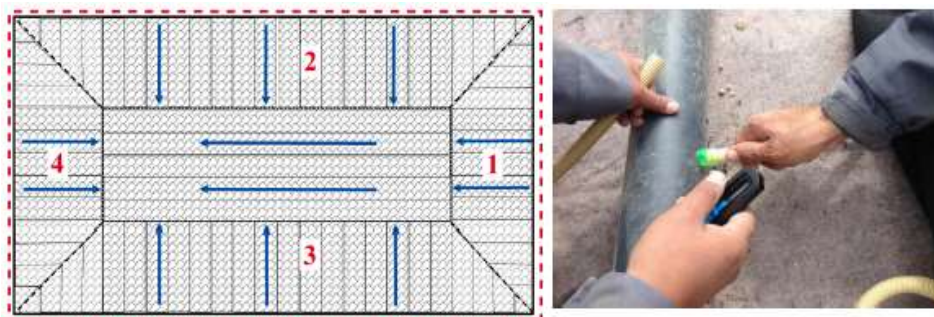


Figure 12: orientation of the MLDG and connection using connectors (photo courtesy Afitex-Textel)

The performance of the MLDG was compared to the one of a control basin, built using the traditional method, involving a granular drainage layer. The performance requirements set by the owner for the drainage component was as follow:

- Retention of solid particles in the basin;
- Free circulation of water toward, and into the drain;
- Capacity to transport water in its plane over a long distance (100 m).
- Minimize loss of water by infiltration into the soil – i.e. by waterproofing.
- Resist normal operating conditions, such as UV immediately after installation and before the first fill, and exposure to chemicals.

Photos of the structure are presented on Figures 13 and 14.

The quantity of recovered filtrate is a key performance factor which was monitored in both the control and the test basin. The use of MLDG led to about 20% more water recovery compared to the traditional solution. Furthermore, the filtration and drainage performance of the MLDG was found satisfactory in both the slopes and the floor of the basin. However, a flow of water could be observed more than two months after the owner stopped feeding the basin with sludge, which suggests that consolidation was still ongoing.

Presence of soil particles was observed in the filtrate samples recovered at the outlet of the test pond to assess its potential for subsequent reuse in the phosphate treatment process. Percentage of impurities below 1% were typically measured, which was considered by the OCP acceptable for phosphate's washing operations.



Figure 13: multi-linear drainage geocomposite used in a slurry dewatering facility (photo courtesy Afitex-
Texel)



Figure 14: Slurry dewatering facility (photo courtesy Afitec-Textel)



Figure 15: system in operation – Collected water from the bottom on the test pond

4 CONCLUSION

The behavior of Multi-Linear Drainage Geocomposite (MLDG) as a pregnant solution collection layer in heap-leach pads was investigated considering existing and genuine laboratory work. The following observations were made:

- No evidence of clogging could be detected after 90 days of circulation of a 20 g/l sulphuric acid through a copper ore and the MLDG. As a consequence, it was concluded that the exceptional chemical composition of the pregnant solution is not likely to affect the performance of DTPG with respect to its filtration and drainage efficiency.
- High normal loads do not affect the transmissivity of MLDG as demonstrated by Saunier et al.
- A geotextile filter typically used for the filtration of fine-grained materials in MLDG, with a FOS of 70 μm as measured per CGSB 148.1 n°10, has offered an excellent filtration performance after receiving a slurry with a soil / water ratio of 28% solid / 72% water.

Based on these observations, Multi-Linear Drainage Geocomposites should be considered promising solutions for heap leach applications as well as other applications involving potentially harsh chemical conditions as well as very fine grained materials, including tailings.

For dewatering applications, the use of Multi-Linear Drainage Geocomposites in a tailing dewatering facility was evaluated in the lab, as well as on a large-scale test pad. Observations made on the large scale test showed several advantages associated to the use of MLDG compared to granular solutions:

- Slopes are protected from erosion and instability thanks to the presence of a continuous layer of geosynthetic.
- The filtrate recovered downstream had a percentage of impurity of less than 1%, which makes it reusable in the process.

Overall, the use of a MLDG was found to generate interesting opportunities for both mining applications considered, that is, heap leach pads and dewatering.

5 REFERENCES

- Arab, R., Cherifi, F. and Loudjani, F. (2009). Landfill drainage with geocomposites, Colloque International Sols Non Saturés et Environnement, Tlemcen, Algeria.
- ASTM D 3895. Standard Test Method for Oxidative-Induction Time of Polyolefins by Differential Scanning Calorimetry, American Society for Testing and Materials, West Conshohocken, Pennsylvania, USA.
- ASTM D5101, Standard Test Method for Measuring the Filtration Compatibility of Soil-Geotextile Systems, American Society for Testing and Materials, West Conshohocken, Pennsylvania, USA.
- Blond, E., Bouthot, M., Vermeersch, O.G. and Mlynarek, J. (2003). Selection of protective cushions for geomembrane puncture protection, 56th Annual Canadian Geotechnical Conference, Winnipeg, Manitoba, Canada.
- Blond, Fourmont, Saunier (2013) Biological clogging resistance of tubular drainage geocomposites in leachate collection layers, proceedings of Geosynthetics'2013, Long Beach, California
- Saunier, P., Ragen, W. and Blond, E. (2009). Assessment of the Resistance of DTPG to high compressive loads, Proceedings of 9th International Conference on Geosynthetics, 2010, Brazil, 3: 1131.
- Tair A., Riot M., Gendrin P. and Chamini J. (2017). Pilot Tests for the Use of AFITEX Geocomposites in Sludge Basins of Mea Processing Units, Proceedings of 2017 GeoAfrica Conference, 2017, Morocco

Vertical Expansion of a 41-m High Geosynthetic Reinforced Soil Slope

F. Herrera, L. Chahua, and E. Murrugarra
Knight Piésold Consultores S.A., Lima, Lima, Peru

D. Reaño
Minera La Zanja S.R.L., Lima, Lima, Peru

ABSTRACT: The Pampa Verde waste dump expansion is highly driven by the following constraints: (1) relatively limited options for laterally extending the existing buttress; (2) the need to satisfy both static and seismic stability; (3) the need to properly select high-strength reinforcement products; (4) the importance of conducting material-specific tests to characterize the soil-geosynthetic interaction; and (5) the complex geometry of the overall system, particularly its global stability. The existing facility is stabilized by a geosynthetic-reinforced toe buttress that includes a compacted earth fill, with a slope of 2.1H:1V, overlying an mechanically stabilized earth wall (MSE or reinforced soil). The MSE structure involves upper and lower MSE wall sections with a horizontal step in between. The upper section is a geogrid-reinforced wall, while the lower section is a Terramesh system involving gabions reinforced with geogrids. The overall design approach involves the design of a geosynthetic-reinforced soil slope (RSS) that would use geogrids of high tensile capacity. The design guidelines for the proposed RSS are those outlined by the US Federal Highway Administration (FHWA-NHI-10-024). A key aspect of the proposed design is the proper evaluation of the soil vs. geosynthetic interface; a total of five geogrid products were considered for possible use in the construction of the geosynthetic-reinforced slope at the Pampa Verde project.

1 INTRODUCTION

1.1 Project Location

The La Zanja mining project, owned by Minera La Zanja S.R.L. (Minera La Zanja), is located in the district of Pulán, province of Santa Cruz de Succhabamba, in the department of Cajamarca, Peru, at an altitude that varies between 2,800 and 3,800 meters above sea level (masl).

The Pampa Verde waste dump is located south-southwest of the Pampa Verde pit and comprises a total area of approximately 188,525 m², after vertical expansion (effective area that does not include perimeter access, diversion channels and cut and fill slopes).

1.2 Background

The Pampa Verde waste dump was designed by Knight Piésold Consultores S.A. (Knight Piésold), considering that inside it would be encapsulated an unsuitable material stockpile.

In December 2013, the construction of the containment dike of the Pampa Verde waste dump was finalized, consisting of a 29-m high compacted earth fill, with a slope of 2.1H:1V, overlying a mechanically stabilized earth wall (MSE or reinforced soil). The MSE structure involves upper and lower MSE wall sections with a horizontal step in between; the upper section is a geogrid-reinforced wall, while the lower section is a Terramesh system involving gabions

reinforced with geogrids. Figure 1 shows an aerial overview of current conditions at the waste dump and Figure 2 shows an overview of the existing MSE structure and detail of the existing reinforced toe buttress.



Figure 1. Caption of the overview of the Pampa Verde Waste Dump.

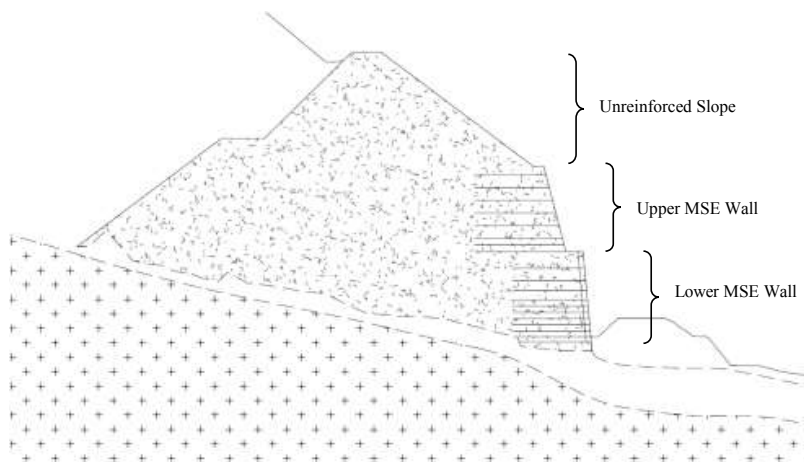


Figure 2. Cross section of the existing geogrid- reinforced toe buttress.

During the operation of the waste dump and the unsuitable material stockpile, several changes occurred, mainly due to the properties of the stored materials. Initially the Pampa Verde waste dump was designed to store siliceous rock, but in practice, up to four different types of materials were stored: argillic, advanced argillic, massive silica and moderate silica.

Because of the above, Minera La Zanja requested Knight Piésold to redesign the Pampa Verde waste dump in order to implement the necessary measures to ensure its physical stability, which made necessary the determination of the materials properties through a geotechnical investigations. As a result of the redesign of the Pampa Verde waste dump, Knight Piésold developed a loading plan to conform the four types of the materials identified.

In order to increase the storage capacity, Minera La Zanja requested the design of a vertical expansion of the waste dump to raise its elevation approximately 15 to 20 meters. The overall approach for stabilization of the vertical expansion involves the design and construction of a reinforced soil slope in front of the existing reinforced toe buttress. The raising of the Pampa Verde waste dump will allow for an additional storage capacity of 0.94 million cubic meters, compared to its initial configuration.

2 AREA CHARACTERIZATION

2.1 *Local Geology*

At the local level, in the area of the La Zanja project outcrops mainly pyroclastic volcanic rocks and spills of the Lama formations of the Lower Tertiary and volcanic rocks of the Porculla formation of the Middle Tertiary. The rocks of the Huambo formation of the Upper Tertiary, appear to the northwest, outside the limits of the project area.

2.2 *Geotechnical Investigation*

2.2.1 *Background*

The first geotechnical investigation was carried out between August 16 and October 11, 2010, in order to determine the geotechnical characteristics of the foundation surfaces where the Pampa Verde waste dump and associated structures would be constructed. The field works consisted of 6 drilling holes, 46 test pits, tests with dynamic penetrometer of conical tip (DPL) and geological-geotechnical mapping. The second geotechnical investigation was carried out in June 2013 and consisted of 6 drilling holes, 9 test pits and 4 in-situ density tests were carried out by the water replacement method. The third geotechnical investigation was carried out between June 5 and 25, 2014, in order to characterize the materials that were being stored in the deposit. 2 drilling holes, 12 test pits (sampling for large-scale grainsize tests) and 8 in-situ density tests were carried out by the water replacement method, in the advanced argillic and argillic materials.

In November 2014, an additional geotechnical investigation was carried out, in order to characterize the advanced argillic and argillic materials that had been conformed. 2 test pits, 2 large scale grainsize tests and 7 in-situ density tests were developed by the water replacement method. Between April and June 2017, a geotechnical investigation was carried out with the specific objective of designing the raising of the Pampa Verde waste dump, having characterized the stored materials and the foundation at the site of the projected reinforced soil slope.

2.2.2 *Fieldworks*

The field geotechnical investigation consisted of the execution of 7 drilling holes and 23 test pits. The vertical geotechnical drilling reached variable depths between 15.0 m and 90.0 m, in which Standard Penetration Tests (SPT) and Large Penetration Test (LPT) were performed as well as in-situ permeability tests, Lefranc (in soils) and Lugeon (in rocks). In the test pits, which reached variable depths between 0.8 m and 5.6 m, 6 large scale grainsize tests and 6 in-situ density tests were carried out by the water replacement method; in addition, detailed records were taken of the stratigraphy of the materials found; in-situ tests and sampling of disturbed and undisturbed samples were carried out for the laboratory tests.

Georys Ingenieros S.A.C. (Georys) conducted geophysical prospecting tests consisting of 14 measures of surface waves in multichannel arrays by the Multichannel Analysis of Surface Waves (MASW) method, 9 readings by the Microtremor Array Measurement (MAM) method and 3 lines MASW 2D. In order to monitor the water level in the unsuitable material stockpile and the Pampa Verde waste dump, 6 Casagrande piezometers were installed.

2.2.3 Laboratory Tests

Laboratory tests were developed in order to determine the materials properties, including the existing rock in the foundation. In order to evaluate the potential for generating acid drainage, geochemical tests were carried out using the Sobek Modified Method (ABAM), in the laboratory of ALS Environmental Chemex (Peru). There were also carried out laboratory tests of the geogrid and geogrid vs. soil interface tests (ASTM D 5321) in the TRI Environmental Inc. (TRI), in Texas, USA, whose results are presented in Section 4.

2.3 Design Earthquake

There are three seismic hazard studies developed for the specific location of the La Zanja project, the last one of June 2017 prepared by ZER Geosystem Peru S.A.C. (ZER Geosystem), which included the characterization of the seismogenic sources near the site of study, the elaboration of the seismic model based on the Ground Motion Prediction Equation (GMPE), the evaluation of the seismic hazard through the probabilistic and deterministic methodologies, seismic disaggregation analysis and the generation of five synthetic accelerograms adjusted to the Uniform Hazard Spectrum of the site.

The results of the probabilistic seismic hazard are presented in Table 1 for a soil type 'B', accordingly to the International Building Code (IBC). To evaluate the physical stability of structures for the storage of mining waste, it is recommended to use as a design earthquake that corresponds to a return period of 1 in 100 years, during the operating period, a criterion that is accepted worldwide for the design of this type of structures. Accordingly to the "Environmental Guide for the Slope Stability of Solid Mine Waste Deposits" of the Ministry of Energy and Mines of Peru (MINEM), the seismic coefficient can vary from 1/2 to 2/3 of the peak horizontal acceleration of the soil, that is, from 0.07 to 0.10. For the purposes of the seismic design (pseudo-static analysis) of the Pampa Verde waste dump rising, 0.12 was used with conservative criteria, for operating conditions.

Table 1. Seismic accelerations for different return periods (Seismic Hazard Study 2017).

Return period (Years)	Maximum seismic ground acceleration ⁽¹⁾ a (g)
100	0.143
250	0.205
500	0.262
1,000	0.331
2,500	0.435
5,000	0.530
10,000	0.637

1. Peak Ground Acceleration (PGA), considering rock terrain conditions for an average cut-off wave velocity equivalent to 760 m/s.

3 PAMPA VERDE WASTE DUMP VERTICAL EXTENSION

3.1 Design Criteria

The design criteria used have been proposed by Knight Piésold accordingly to international standards and national requirements for this type of structure, which were accepted by Minera La Zanja, as presented in Table 2.

Table 2. Design criteria.

Description		Value
Additional storage capacity		0.94 Mm ³ (maximum possible capacity)
Lift height		10 m
Slope lift		1.4H:1V
General slope of the waste dump pile		2.5H:1V
Peak ground acceleration (return period of 100 years)		0.23 g
Magnitude of the seismic event (return period of 100 years)		8.0
Seismic coefficient		0.12
Minimum safety factor - Waste dump (operating period)	Static condition	1.3
	Seismic condition	1.0
Minimum safety factor - Reinforced soil slope	Static condition	1.3
	Seismic condition	1.1
Global Analysis - External		
Minimum safety factor - Reinforced soil slope	Static condition	1.3 – 1.5
	Seismic condition	1.125
Slip analysis - Internal		

3.2 Project constraints

The project constraints are as follows:

1. Limited options for laterally extending the existing buttress to avoid encroaching on existing mining facilities;
2. The need to satisfy both static and seismic stability;
3. The need to properly select high-strength reinforcement products;
4. The importance of conducting material-specific tests to characterize the soil-geogrid interaction; and
5. The complex geometry of the overall system, particularly its global stability.

3.3 Reinforced Soil Slope Design

3.3.1 General

In order to increase the storage capacity of the Pampa Verde waste dump, it was proposed to vertically extend the containment dike by a soil reinforced slope with uniaxial geogrids. The crest of the reinforced soil slope will have 10.0 m width, an upstream slope of 2H:1V and will be supported on the existing containment dike, while the downstream slope will be 1H:1V. The total height of the reinforced slope will reach 41 m. At the foot of the reinforced soil slope, it was proposed to conform a reinforcement embankment with a slope of 2H:1V. The waste material inside the deposit will be formed with a general slope of 2.5H:1V, in 10 m height lifts, with 1.4H:1V slope, having to maintain berms of 11 m width between the waste material lifts. The additional volume to be stored will be 941 900 m³.

3.3.2 Slopes Geometry

The section for the analysis has been considered one that runs longitudinally through the Pampa Verde waste dump, considered the most critical because it covers the largest amount of waste material and the steepest slope downstream of the existing dike (where the haul road passes). Likewise, the general slope of the projected reinforced slope has been considered. The locations of the section that was analyzed is shown in Figure 3.

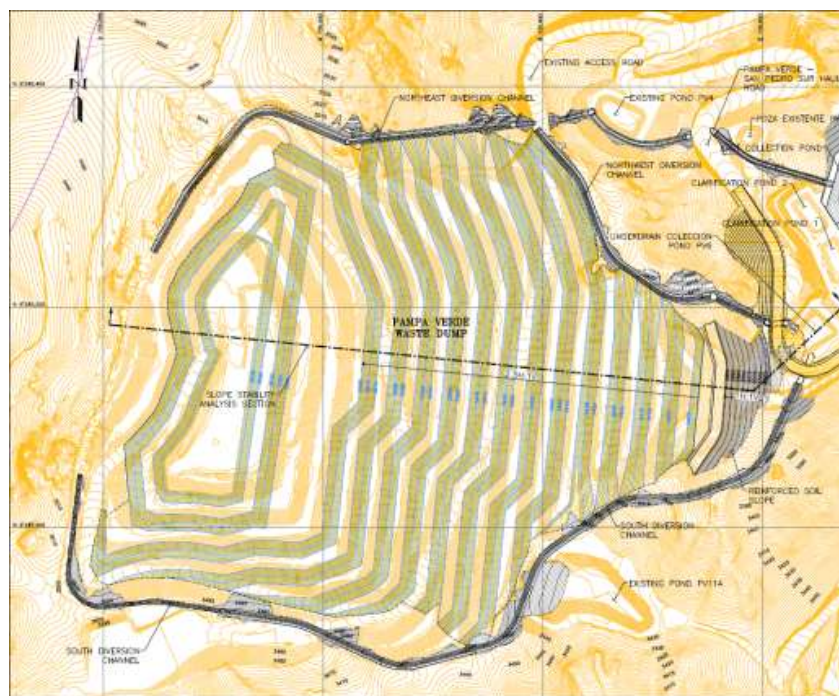


Figure 3. Section location for the slope stability analysis.

3.3.3 Materials Properties

For the geotechnical characterization of the materials involved in the slopes stability analysis, the results of the geotechnical investigation developed for the Pampa Verde mine waste design and also the results of the previous geotechnical investigations (2010, 2013 and 2014) were used. The properties of the different materials that intervene in the slopes stability analysis are presented in Table 3.

Table 3. Geotechnical properties of materials for the slope stability analysis.

Material type	Unit weight (kN/m ³)	Cohesion (kPa)	Friction angle (Degrees)	Undrained shear resistance (kPa)
Rocky basement ⁽¹⁾		Impenetrable material (bedrock)		
Residual soil ⁽¹⁾	21.0	50	29	-
Soil liner ⁽¹⁾	19.0	0	22	-
Anthropogenic fill ⁽¹⁾	19.0	0	33	-
Unsuitable material stockpile contain- ment dike ⁽¹⁾	19.0	0	35	-
Unsuitable material – fine dense ⁽²⁾	17.0	-	-	55
Unsuitable material stockpile contain- ment dike without QA ⁽¹⁾	19.0	0	32	-
Unsuitable material – coarse medium dense ⁽¹⁾	18.0	0	30	-
Unsuitable material – coarse loose (mixed) ⁽¹⁾	18.0	0	28	-
Waste material – silica ⁽¹⁾	21.0	0	37	-

Material type	Unit weight (kN/m ³)	Cohesion (kPa)	Friction angle (Degrees)	Undrained shear resistance (kPa)
Waste material – argillic ⁽¹⁾	20.0	0	31	-
Waste material – advanced argillic ⁽¹⁾	20.0	0	30	-
Mixed waste material – silica and argillic ⁽¹⁾	19.0	0	35	-
Mixed waste material – advanced argillic, argillic and unsuitable ⁽¹⁾	20.0	0	30	-
Reinforced soil slope fill material ⁽¹⁾	20.0	0	36	-
Reinforced soil slope fill material (projected) ⁽¹⁾	20.5	0	35	-
Randomfill and transition material ⁽³⁾	20.5	0	36	-
Gabions ⁽³⁾	21.0	0	33	-
Mud ⁽³⁾	15.0	-	-	9
Waste material (projected) ^(1,3)	21.0	0	33	-
Rock fill	21.0	0	40	-

1. Effective parameters obtained from field geotechnical investigation and laboratory tests, carried out in 2013, 2014 and 2017.

2. Effective parameters obtained from Standard Penetration Tests (SPT) and "back analysis".

3. Effective parameters based on the experience of Knight Piésold in similar materials.

4. The foundation of the waste consists mainly of residual soil and/or rock outcrops. The unsuitable materials stored in the deposit, which will be encapsulated by the waste material, have been considered as the weakest.

3.3.4 Piezometric Level Conditions

The piezometric level was defined based on the records of the piezometers installed in the 7 drilling holes of the geotechnical investigation carried out in June 2017. Two piezometric levels were considered:

- Variable depth between 26.4 and 36.8 m with respect to the existing ground level. This piezometric level appears due to the moisture of the material discharged and to the leaks that have occurred inside the existing waste material deposit.
- Depth variable between 38.0 and 75.2 m with respect to the existing ground level. This level is close to the foundation level of the deposit.

3.3.5 Geogrids Pullout Analysis

The computer program RESSA version 3.0, which belongs to the set of programs of Adama Engineering Inc., has been used. The program allows to develop the stability analysis considering the type of translational failure through the interaction between the geogrid and the soil. It has been used the results of the laboratory tests of the interface soil vs. uniaxial geogrid and geogrid performance. The design allowable tension of the uniaxial geogrids was 230 kN/m. The geogrids pullout analyzes were performed under static and earthquake conditions (pseudo-static analysis). The results of the geogrids pullout analyzes show a minimum static factor of safety of 1.51 and a minimum pseudo-estatic factor of safety of 1.16.

3.3.6 Waste Dump Facility Stability Analysis

The slope stability analyses associated with the vertical extension of the Pampa Verde waste dump were developed using the computer program SLOPE/W[®] version 7.23, for static and earthquake conditions (pseudo-static analysis). The following cases were analyzed:

- Global failure of the downstream slope. Failures through the body of the reinforced soil slope and the current and projected waste dump.
- Local failure downstream of the toe of the waste dump. Failures through the soil reinforced slope with uniaxial geogrids.
- Global failure of the upstream slope. Failures in the slopes of the existing and projected waste material.

The geotechnical model is shown in Figure 4 and the results of the slope stability analyzes of the Pampa Verde waste dump are presented in Table 4.

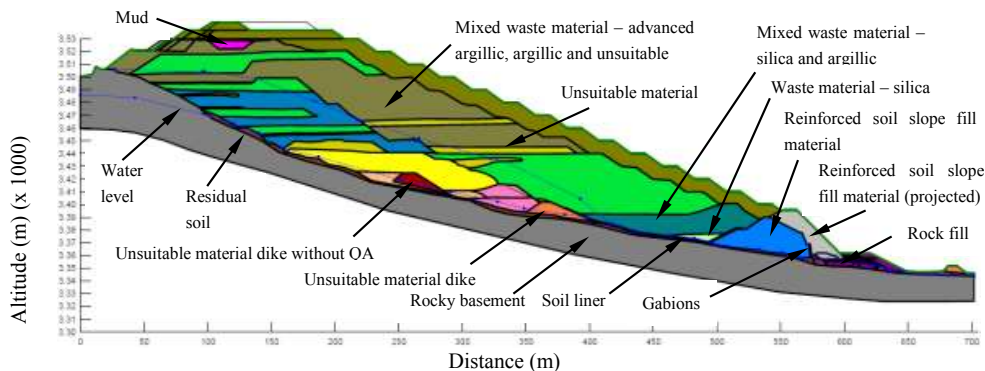


Figure 4. Section location for slope stability analysis.

Table 4. Results of the slope stability analyzes.

Failure type	Location	Static factor of safety	Pseudo-elastic factor of safety
Global	Downstream slope	1.34	1.00
	Upstream slope	1.46	1.07
Local	Downstream slope	1.39	1.12

4 UNIAXIAL GEOGRIDS EVALUATION

4.1 Testing Methods and Criteria

The obtained results would not be valid in the case there was not an appropriate interaction between the geogrids and the soil to be used in the construction of the geogrid-reinforced slope, so a proper selection of geogrids is particularly relevant in this project, mainly due to the following aspects:

- The structure is relatively high, which leads to the selection of geosynthetic products of high tensile strength.
- Direct shear is a relevant mode of failure for the configuration of this project. Consequently, interface shear strength between soil and geogrids should be properly characterized, not only for pullout evaluation, but also for wedge analyses.
- Because of the potential contact between the geogrid reinforcements and acidic fill materials, chemical degradation considerations are more relevant than for conventional retaining structures.

A proper evaluation of the soil vs. geogrid interface starts with the establishment of the testing conditions used for determination of the interface properties between uniaxial geogrids and the backfill material. The interface testing program was developed in the TRI Environmental Inc. (TRI) geotechnical and geosynthetics testing laboratory, located in Austin, Texas.

The conditions and characteristics of the soil direct shear and soil vs. geogrid interface shear tests conducted at TRI considered the following conditions:

- The need to conduct soil direct shear tests (in addition to the soil vs. geogrid interface shear tests) to properly define the soil vs. geogrid coefficient of interactions. This determination is significant to account for possible differences between the tested soil and backfill soil ultimately used during construction.
- The need to conduct tests under submerged conditions and comparatively small displacement rates (0.1 mm/min) to minimize the possible generation of pore water pressures. This approach was adopted after evaluating the effect of the displacement rate in the test results.
- The need to adopt test approach “B”, under ASTM D 6637, of the soil vs. geogrid interface testing method, which was found to be more consistent with the approach used for determination of soil shear strength and better account for corrections (e.g. area correction) in the interpretation of test results.

4.2 Geogrids Considered in the Testing Program

A total of five geogrid products were considered for possible use in the construction of the geogrid-reinforced slope at the Pampa Verde project; for the purposes of this paper, we are going to refer to the geogrids as “Geogrid 1” to “Geogrid 5”. The polymers used in the manufacturing process and key results from wide-width tensile tests (ASTM D 6637, Method B) are summarized in Table 5.

Table 5. Geogrids properties.

Geogrid type	Fibers type	Ultimate tensile strength (kN/m)	Ultimate elongation (%)	Unit tension (kN/m)	Tensile strain (%)	Secant stiffness (kN/m)
Geogrid 1	Polyester (PET)	389	9.4	180	5	3,600
Geogrid 2	Polyester (PET)	360	11.7	122	5	2,440
Geogrid 3	Polyester (PET)	302	12.8	77.1	5	1,542
Geogrid 4	Polyvinyl Alcohol (PVA)	364	5.44	312	5	6,240
Geogrid 5	Polyester (PET)	457	11.7	176	5	3,520

The preliminary design considered an admissible tensile strength (design tensile strength) of 230 kN/m, which was the basis for the identification of the five geogrid products. It should be noted that the allowable tensile strength is defined as the ultimate tensile strength penalized by a series of reduction factors (construction damage, degradation, creep); the reduction factors for each geogrid are different and established by certified documentation provided by the manufacturers. Table 6 summarizes the ultimate tensile strength as reported in tests conducted at TRI, the reduction factors and the predicted allowable tensile strength.

Table 6. Geogrids tensile strengths.

Geogrid type	Ultimate tensile strength (kN/m)	Reduction factor	Allowable tensile strength (kN/m)
Geogrid 1	389	1.76	221
Geogrid 2	360	1.57	229
Geogrid 3	302	2.73	111
Geogrid 4	364	1.49	244
Geogrid 5	457	1.68	268

As shown in Table 6, Geogrid 1 and Geogrid 2 led to an admissible tensile strength that is slightly below the 230 kN/m originally considered in the preliminary design. Geogrid 3 resulted in an admissible tensile strength that is significantly below 230 kN/m. Finally, Geogrid 4 and Geogrid 5 satisfied the admissible tensile strength considered in the preliminary design.

Two other considerations are also important for the Pampa Verde dike raising:

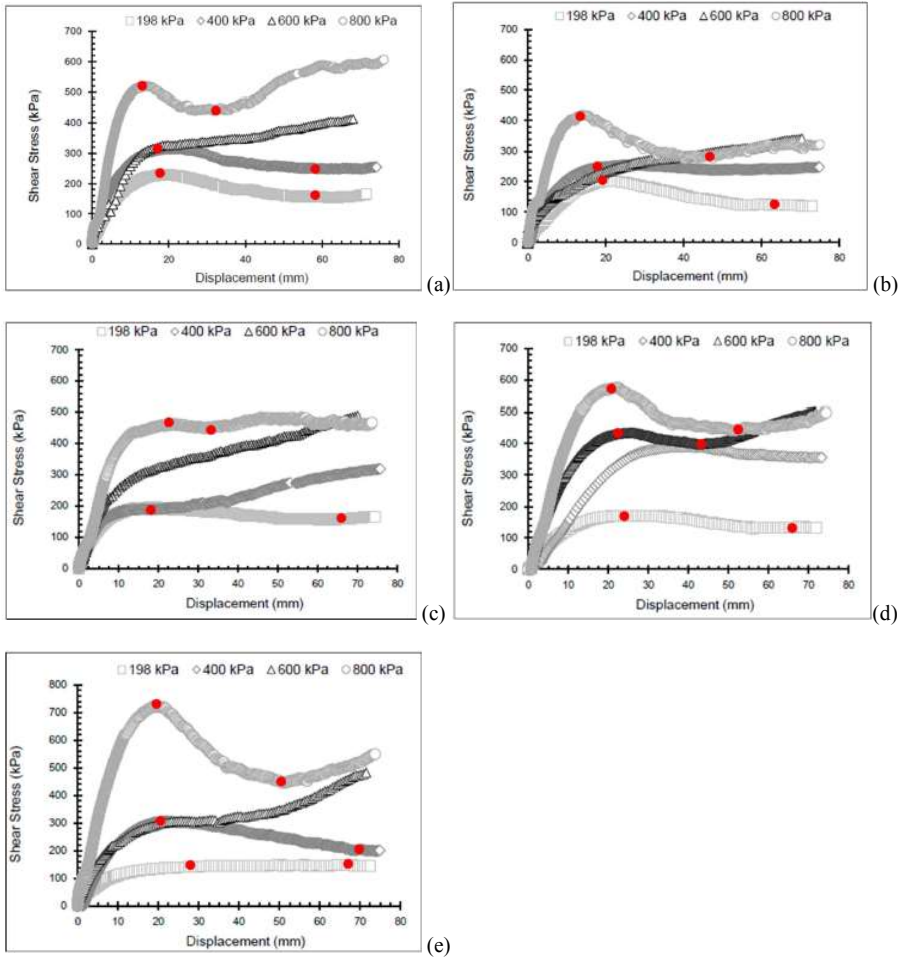
- Compatibility of soil and geogrid strains: As will be discussed in Section 4.4, the soil peak shear strength is found to occur at a shear strain of approximately 5%. Consequently, the unit tension at a strain of 5% will lead to enhanced performance. This is because although the tensile capacity of geogrids may continue to develop beyond a 5% strain, the soil shear strength would have already been achieved. Therefore, a relevant parameter to consider in the comparison of the different products is the secant stiffness at a tensile strain of 5%. With a secant stiffness of 6,240 kN/m, Geogrid 4 is the product that provides the best compatibility of displacements with the backfill soil. Geogrid 1 and Geogrid 5 provide a secant stiffness of about 3,500 kN/m. Finally, Geogrid 2 and Geogrid 3 provide a secant stiffness under 2,500 kN/m.
- Chemical resistance to acid soil environments: An important aspect to consider in the selection process, which is directly related to the raw polymeric material used in geogrid manufacturing, relates to the chemical resistance of the products. While polyester (PET) is susceptible to chemical degradation in basic environments (pH over 10) and acidic environments (pH below 2), polyvinyl alcohol (PVA) offers comparatively high chemical resistance in both highly basic and acid environments. While the actual borrow source of fill material may not be precisely defined, there is concern that the fill used in the geogrid-reinforced slope may possibly involve a comparatively acid environment. Consequently, polymeric materials such as PP, HDPE and PVA will provide better chemical resistance than PET. Among the geogrids considered in this project, the Geogrid 4 is the only product manufactured using a polymer that resists acid environments (PVA); all other products are manufactured using PET, as this material allows manufacturing of the high-strength geogrids required for this project. No PP or HDPE products have been identified that satisfy the tensile strength requirements for this project.

4.3 Soil Direct Shear Testing

Soil direct shear tests (ASTM D3080) were conducted using samples sieved to a maximum particle size of $\frac{3}{4}$ ". Tests were conducted at four different confining pressures (198, 400, 600, and 800 kPa). Tests were conducted under submerged conditions (with container flooded one hour prior to shearing initiation). Conditioning of the soil specimen involved application of the normal stress for a period of 15 minutes before shearing. The shearing displacement rate was 0.1 mm/min, which was deemed adequate to minimize the development of pore water pressures. The bottom half of the direct shear box had dimensions of 457 x 305 mm and was sheared against a smaller stationary container (top half with dimensions of 305 x 305 mm). Consequently, no area correction was considered in the interpretation of the results. This setup is consistent with ASTM D5321 used for interface shear testing. Shear testing typically took approximately 13 hours because of the comparatively small shear displacement rate. The test conducted at a normal stress of 800 kPa required use of a smaller box (203 x 203 mm) to achieve the target normal stress.

4.4 Soil vs. Geogrid Interface Shear Testing

Figure 5 (a) to (e) shows the shear stress versus displacement results obtained for the four soil vs. geogrid interface shear tests conducted using each one of the tested geogrid (Geogrid 1 to Geogrid 5, respectively).



Figures 5 (a) to (e): Interface shear stress vs. displacement response using Geogrid 1 to Geogrid 5, respectively.

Determination of the peak and residual shear strength values required careful interpretation. Accordingly, only the results indicated with “red dots” were considered in the determination of the shear strength parameters. For Geogrid 1, the peak interface shear strength was characterized by an interface friction angle of 26.0 degrees and an adhesion intercept of 134 kPa. The interface residual shear strength was characterized by an interface friction angle of 24.7 degrees and a cohesion intercept of 89 kPa. The coefficient of interaction for the peak interface shear strength was characterized by a frictional coefficient of 0.84 and an adhesion coefficient of 11.75. In addition, the coefficient of interaction for the residual interface shear strength was characterized by a frictional coefficient of 0.99 and an adhesion coefficient of 44.68.

For Geogrid 2, the peak interface shear strength was characterized by an interface friction angle of 20.4 degrees and an adhesion intercept of 115 kPa. The interface residual shear strength was characterized by an interface friction angle of 14.9 degrees and a cohesion intercept of 70 kPa. The coefficient of interaction for the peak interface shear strength was characterized by a frictional coefficient of 0.64 and an adhesion coefficient of 10.11. In addition, the coefficient of interaction for the residual interface shear strength was characterized by a frictional coefficient of 0.57 and an adhesion coefficient of 35.05.

For Geogrid 3, the peak interface shear strength was characterized by an interface friction angle of 24.2 degrees and an adhesion intercept of 100 kPa. The interface residual shear strength was characterized by an interface friction angle of 24.5 degrees and a cohesion intercept of 77 kPa. The coefficient of interaction for the peak interface shear strength was characterized by a frictional coefficient of 0.78 and an adhesion coefficient of 8.80. In addition, the coefficient of interaction for the residual interface shear strength was characterized by a frictional coefficient of 0.98 and an adhesion coefficient of 38.79.

For Geogrid 4, the peak interface shear strength was characterized by an interface friction angle of 33.8 degrees and an adhesion intercept of 37 kPa. The interface residual shear strength was characterized by an interface friction angle of 28.6 degrees and a cohesion intercept of 33 kPa. The coefficient of interaction for the peak interface shear strength was characterized by a frictional coefficient of 1.16 and an adhesion coefficient of 3.23. In addition, the coefficient of interaction for the residual interface shear strength was characterized by a frictional coefficient of 1.18 and an adhesion coefficient of 16.96.

For Geogrid 5, results of the test conducted at a normal stress of 800 kPa were observed to affect the estimated friction angle significantly. Nonetheless, they were considered in the interpretation of the results. The peak interface shear strength was characterized by an interface friction angle of 41.0 degrees and an adhesion intercept of 0.00 kPa. However, obtaining this comparatively high interface friction angle was highly influenced by the 800 kPa test. The interface residual shear strength was characterized by an interface friction angle of 28.1 degrees and a cohesion intercept of 15.4 kPa. The coefficient of interaction for the peak interface shear strength was characterized by a frictional coefficient of 1.50 and an adhesion coefficient of 0.00. In addition, the coefficient of interaction for the residual interface shear strength was characterized by a frictional coefficient of 1.16 and an adhesion coefficient of 7.76.

Figure 6 summarizes the peak interface shear strength results for all five soil vs. geogrid interfaces; the peak interface shear strength envelopes for the Geogrid 4 and Geogrid 5 (as well as the soil shear strength envelope) are represented by somewhat thicker lines. Figure 7 summarizes the residual interface shear strength results for all five soil vs. geogrid interfaces; the residual interface shear strength envelopes for the Geogrid 4 and Geogrid 5 (as well as the soil shear strength envelope) are represented by somewhat thicker lines in this figure as well.

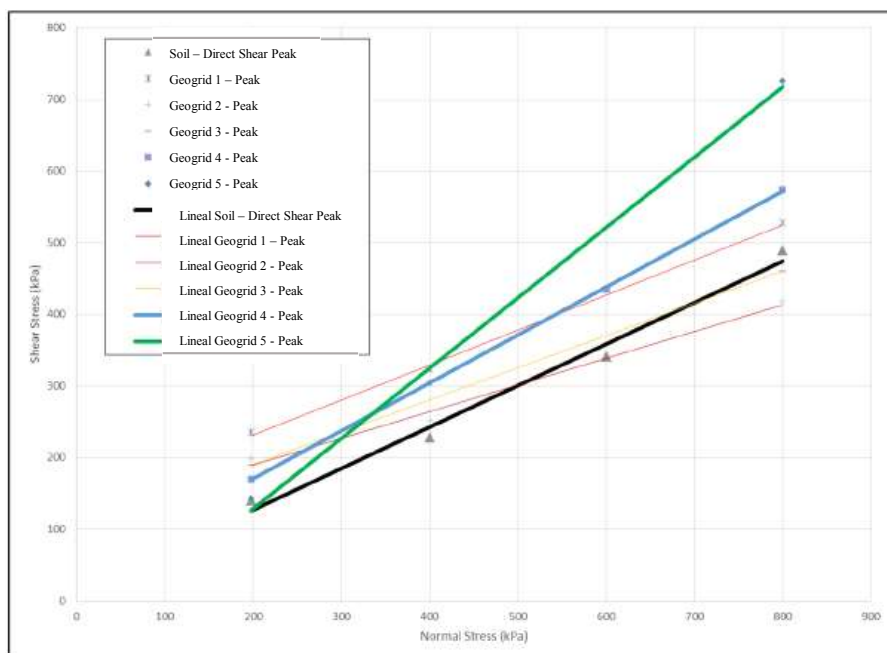


Figure 6. Summary of peak interface shear strength envelopes.

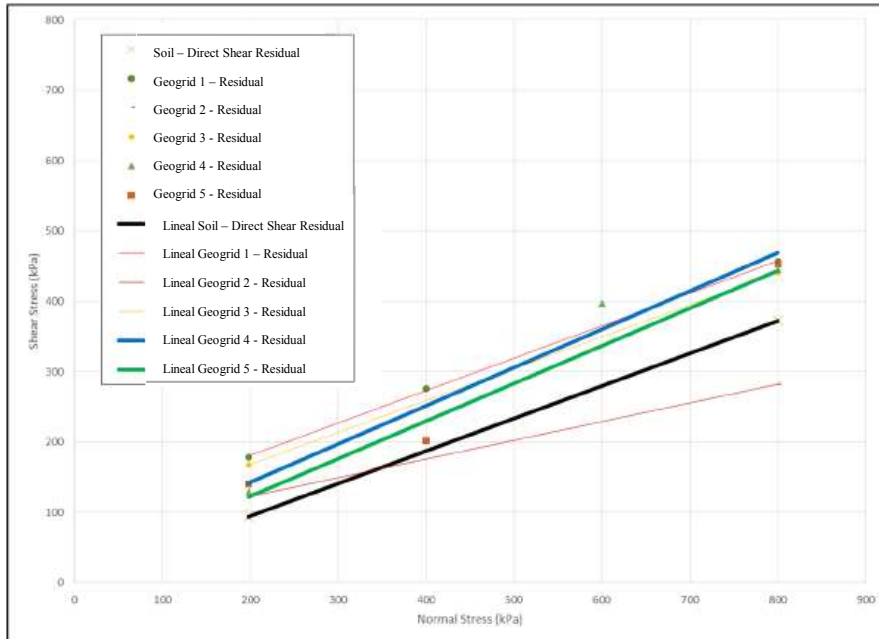


Figure 7. Summary of residual interface shear strength envelopes.

In the comparison of the different products, the most relevant parameters to assess, in relation to their interface shear strength characteristics, are the interface friction angle or the frictional coefficient of the interface shear strength. The highest interface coefficient for the peak interface shear strength was that of the Geogrid 5 (frictional coefficient of 1.50), followed by the interface coefficient for the Geogrid 4 (frictional coefficient of 1.16). In addition, the highest interface coefficient for the residual interface shear strength was that of the Geogrid 4 (frictional coefficient of 1.18), followed by the interface coefficient for the Geogrid 5 (frictional coefficient of 1.16). Overall, Geogrid 4 and Geogrid 5 were the products that provided the highest interface shear strength performance; Geogrid 1 was also observed to provide good interface shear response. In contrast, Geogrid 2 and Geogrid 3 produced comparatively low interface shear strength results.

4.5 Selection of the Reinforcement Geogrid

The proper selection of the geogrid to be used to mechanically stabilize the geogrid reinforced slope requires assessment of numerous factors. To objectively evaluate these various considerations, a value engineering approach, often used by the FHWA to assess the merits of different alternative retaining structures, was adopted. Specifically, the following factors were identified as relevant for the different geogrid products being considered as alternatives:

- Soil vs. geogrid interface shear strength properties.
- Deformation compatibility.
- Performance in acid environments.
- Documented manufacturing quality control and reduction factors.
- Anticipated quality of technical support during the final stages of design and installation.
- Tradition in the use of the geogrid product in geoenvironmental applications.

The tensile strength requirement was not adopted as a factor, as the allowable tensile strength was a minimum requirement for consideration of all five geogrid products. Additionally, cost

was not considered among the factors for selection and consequently only technical considerations were weighed in this evaluation.

Because all factors do not carry the same relevance, weighted ratings (WR) ranging from 1 to 3 were assigned for each selection factor. Accordingly, a WR of 3 was assigned to interface properties, a WR of 2 was assigned to performance in acid environments and to manufacturing QC, and a WR of 1 was assigned to the remaining selection factors. The selection factors are shown in Table 8.

For each geogrid reinforcement considered, qualitative ratings (QR) ranging from 1 to 4 were subsequently assigned based on the merit of each geogrid for each selection factor. The selected QR values are also shown in Table 8. Finally, the weighted ratings were obtained by multiplying the WR by the QR, as summarized in Table 8. A final score for each geogrid alternative is also shown in Table 7.

Table 7. Geogrids evaluation matrix.

Evaluation criteria	Interface properties	Deformation compatibility	Performance in acid environments	QC Documentation	Technical support in project	Tradition in geo-environmental applications	Weighted total score
Weighted level	3	1	2	2	1	1	
Geogrid 1	3	2	2	1	2	2	21
Geogrid 2	1	2	2	3	2	2	19
Geogrid 3	1	2	2	3	1	2	18
Geogrid 4	4	4	4	4	4	4	40
Geogrid 5	4	3	2	3	4	2	31

1. The individual score refers to the qualification of each supplier, where 1 means that the product is well below the evaluation criteria and 4 means that the product is adequate.
2. The weighting assigned to each criterion is based on the experience of Knight Piésold and the geotechnical design reviewer of the vertical expansion of the Pampa Verde waste dump.

As presented in this evaluation, Geogrid 4 was found to be the most appropriate geogrid alternative, with an aggregated score of 40. Geogrid 5 and Geogrid 1 were identified as somewhat distant second-rate alternatives, with aggregated scores of 31 and 21, respectively. Finally, Geogrid 2 and Geogrid 3 were identified as the least appropriate alternatives, with aggregated scores of 19 and 18, respectively.

It is recommended to select Geogrid 4 as geogrid reinforcement for the reinforced soil slope designed to stabilize the Pampa Verde waste dump. This selection is supported by the various considerations summarized in the value engineering approach documented in Table 7.

5 CONCLUSIONS AND RECOMMENDATIONS

The following are the conclusions and recommendations derived from the engineering of the vertical extension design of the Pampa Verde waste dump:

- The slope stability analyses indicate that the new configuration of the Pampa Verde waste dump will remain stable for static and earthquake conditions.
- Five different types of geogrids were evaluated. The results of the laboratory tests indicated that, according to their mechanical properties (resistance and deformation), it was recommended to use the Geogrid 4, whose raw material is polyvinyl alcohol (PVA).
- The Senior geotechnical design reviewer of the vertical expansion of the Pampa Verde waste dump considered particularly robust the efforts involved in the geotechnical characterization and engineering evaluations conducted by Knight Piésold. Complementing such efforts with the selection of an appropriate geogrid product is expected to lead to a safe and well performing vertical expansion of the Pampa Verde waste dump.

- Perform the laboratory tests of the geogrid that will be used in the construction of the reinforced soil slope, in the event that a geogrid different from the recommended one is used, in order to review the slope stability analyzes and verify the design of the reinforcement.

6 REFERENCES

- Koerner, R.M., 1998, *Designing with Geosynthetics, 4th Edition, Prentice Hall Inc.*, New Jersey.
- National Highway Institute, November 2019, "*Design and Construction of Mechanically Stabilized Earth Walls and Reinforced Soil Slopes*"
- TRI/Environmental, Inc., 1998, *Interface Friction/Direct Shear Testing & Slope Stability Issues Short Course, June 25-26*. Austin, Texas.

High Resolution Estimates of Tailings Facility Evaporation Using Landsat Data

J. Keller

GeoSystems Analysis, Inc., Hood River, OR, USA

J. Hendrickx

SoilHydrology Associates, LLC, Los Lunas, NM, USA

M. Milczarek

GeoSystems Analysis, Inc., Tucson, AZ, USA

F. Partey

Robinson Nevada Mining Company, Ely, NV, USA

M. Geddis

KGHM, Tucson, AZ, USA

ABSTRACT: A three-temperature (3T) energy balance model was developed to predict monthly distributed actual evaporation (AE) from a large TSF in Nevada, USA for the period of 1996 through 2015. The 3T energy balance model uses Landsat surface reflectance and temperature data to predict the AE as a relative fraction of local weather station estimated potential evaporation on 30 m centers (pixels). Additionally, Landsat reflectance data were used to develop a site specific algorithm to estimate the TSF footprint on six month time intervals. Estimated monthly AE ranged from over 150 mm/month during the summer months, to less than 20 mm/day during the winter months. Estimated TSF evaporation increased over time from an annual maximum of 60 l/s to greater than 350 l/s due to the increase in the evaporative surface of the TSF. Landsat based estimates of the TSF surface area were in agreement with storage curve tailings area estimates and also provided a high resolution estimate of the tailings footprint over time.

1 INTRODUCTION

Evaporation is often the largest unknown component of a tailings storage facility (TSF) water budget, which can result in significant errors about the rate and sources of tailings seepage and other losses. Potential evaporation (PE) can be estimated using weather station measurements; however, PE assumes a continuous water supply and cannot account for the variable nature of TSF operations. Actual evaporation (AE) rates depend on factors such as: climate; tailings moisture content, texture and water holding capacity; and solution salinity. Most TSFs have a large surface area which allows spatial and temporal estimates of AE using satellite data and an energy balance energy model. Specifically, biweekly Landsat datasets can be used to estimate AE from land surfaces with 30 x 30 m resolution. Satellite based energy balance models have been previously used to estimate evapotranspiration from irrigated agricultural and riparian habitat areas (i.e. METRIC and SEBAL, see Allen et al, 2011). However, these model applications are generally labor intensive and costly. Landsat data also can be used to determine the growth of the TSF over time.

A three-temperature (3T) energy balance model was developed to predict monthly AE from a large TSF in Nevada, USA for the period of 1996 (start of operations) through 2015. The site is located in a semi-arid climate with an average December temperature (coldest month) of -4 °C and an average July temperature (warmest month) of 20 °C. The tailings embankment is constructed using centerline raise methods with cyclone underflow sand deposition. Cyclone deposition typically occurs during the summer (May to September) with whole tailings deposition from the perimeter of the facility from October to April.

The 3T energy balance model predicts the AE as a relative fraction of nearby weather station estimated PE, using Landsat surface reflectance and temperature data on 30 m centers (pixels). The local weather station calculated PE is then used to predict the daily changes in AE at each pixel during the periods between each Landsat data event. Additionally, Landsat reflectance data were used to develop a site specific algorithm to estimate the TSF footprint every six months.

2 METHODS

AE estimates were based on calculations using a 3T model based on the physics of the full energy balance (Qiu and Zhao, 2010) as determined from local weather and data from Landsat 5, 7, and 8 satellite imagery. A total of 157 images, evenly distributed over the period 1996-2015, were selected for processing and input into the 3T model. A summary of the methodology of the energy balance approach used is provided below.

At the TSF where tailings exist under dry and wet conditions, evaporation can be estimated by:

$$LE = R_n - G - H \quad (1)$$

where LE is the latent heat flux in watts per square meter (W/m^2), R_n is the net radiation (W/m^2), G is the soil heat flux (W/m^2), and H is the sensible heat flux (W/m^2).

The R_n at satellite overpass is the sum of the net short wave radiation (R_{ns}) and the net longwave radiation (R_{nl}).

$$R_n = R_{ns} + R_{nl} \quad (2)$$

$$R_{ns} = (1 - \alpha)R_s \quad (3)$$

where α is the albedo (unitless) that varies for most pixels from 0.18 to 0.30 and R_s is the incoming solar radiation (W/m^2). The net longwave radiation (R_{nl}) equals:

$$R_{nl} = R_{lin} - R_{lout} - (1 - e_o) R_{lout} \quad (4)$$

$$R_{lin} = e_a \sigma T_{swet}^4 = 0.85 (-\ln \tau_{sw})^{0.09} \sigma T_{swet}^4 \quad (5)$$

$$R_{lout} = e_o \sigma T_s^4 \quad (6)$$

where R_{in} and R_{out} are the incoming and outgoing longwave radiation, respectively (W/m^2), e_o is the broadband surface emissivity (unitless), e_a is the effective atmospheric emissivity (unitless), σ is the Stefan-Boltzmann constant ($5.67 \times 10^{-8} W/m^2/K^4$), τ_{sw} is the broadband atmospheric transmissivity for short-wave radiation (unitless), T_s is the surface temperature in Kelvin (K) as calculated from the thermal band, T_{swet} is the surface temperature of the coldest non-ponded pixels. Qiu and Zhao (2010) assume an average value of $e_o = 0.925$ and use the simple function $e_a = 0.92 \times 10^{-5} T_a^2$ for the estimation of the emissivity values.

The G (W/m^2) was estimated using an empirical equation for soils with no or little vegetation (leaf area index less than 0.5) (Allen et al., 2011).

$$G = R_n \times \left\{ 1.80 \frac{T_s - 273.15}{R_n} + 0.084 \right\} \quad (7)$$

where T_s is the surface temperature (K).

The H (W/m^2) was estimated from:

$$H = (R_{nd} - G_d) \frac{T_s - T_{swet}}{T_{sd} - T_{swet}} \quad (8)$$

where R_{nd} is the net radiation of a reference dry soil surface without evaporation (W/m^2), G_d is the soil heat flux in dry soil (W/m^2), T_{sd} is the temperature of a reference dry soil surface (K).

The instantaneous evaporation (E_{inst}) in millimeters per hour (mm/hr) at the time of the satellite overpass is calculated as:

$$E_{inst} = 3600 \frac{LE}{L} \quad (9)$$

where 3600 is the time conversion from seconds to hours, and L is the latent heat of vaporization (at 20°C about 2.45×10^6 Joules per kilogram (J/kg)).

E_{inst} was extrapolated to daily evaporation values using the hourly standardized reference evapotranspiration for a short crop (ET_{Oinst}) (ASCE-EWRI, 2005) to calculate the Reference ET Fraction ($EToF$), defined as:

$$EToF = \frac{E_{inst}}{ET_{Oinst}} \tag{10}$$

$EToF$ was then applied to the daily reference evapotranspiration (ET_{Odaily}) to calculate daily evaporation (E_{daily}):

$$E_{daily} = EToF \times ET_{Odaily} \tag{11}$$

where ET_{Odaily} is the daily reference ET_o in millimeters per day (mm/day).

ET_{Odaily} and ET_{Oinst} were calculated from a series of consistent hourly meteorological measurements of air temperature, air relative humidity, wind speed, and incoming solar radiation available from a nearby weather station. The weather station environment is similar to the TSF, located approximately 40 km southeast of the TSF and at a similar elevation.

The Landsat data processing using the 3T model produced 30 m by 30 m areal predictions of the actual monthly evaporation for the period from 1996-2015. The aerially distributed monthly evaporation rates were then summarized to yield monthly evaporation volumes from the TSF.

The boundary of the TSF between 1996 and 2015 was estimated on an approximate six month time interval using Landsat reflectance data and application of a site-specific processing algorithm. The boundary between the TSF embankment and impoundment area was based on the location of the cyclone header pipe visible in aerial photographs. Estimated TSF areas were validated against aerial photographs and area estimates from the TSF annual monitoring report.

3 RESULTS

The estimated monthly average AE depths and rates from 1996 through 2015 are provided in Figure 1 and Figure 2, respectively. To delineate AE from the actively wetted embankment areas, predicted AE was separated into impoundment and embankment areas. Examples of the predicted growth of the TSF and the spatially distributed AE in the winter and summer of 1997, 2005 and 2015 are provided in Figure 3.

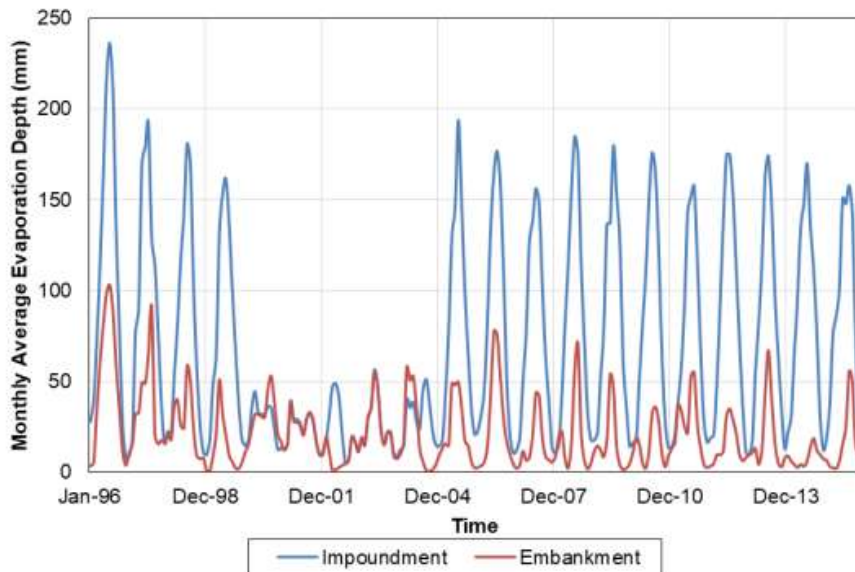


Figure 1. Estimated monthly evaporation depth.

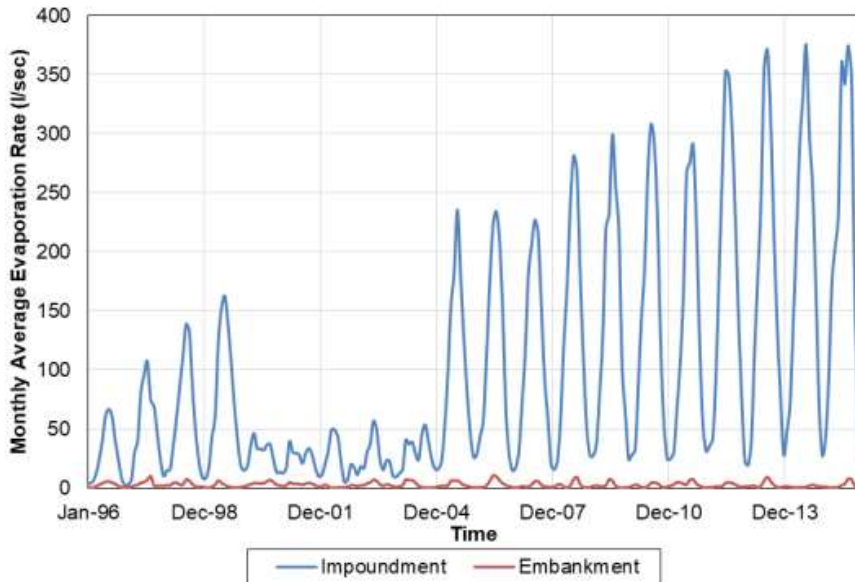


Figure 2. Estimated monthly evaporation rate.

Mining operations were suspended between July 1999 and September 2004, resulting in decreased AE due to water no longer being directed onto the TSF surface as part of the tailings slurry (Figure 1 and 2). Tailings deposition resumed October 2004 with the restart of mining and estimated AE increased (Figure 1 and 2).

Estimated monthly impoundment AE rates were in excess of 150 mm/month during the summer months when solar energy and evaporative demand is at its peak, to less than 20 mm/month during the winter months when evaporative demand is at its minimum (Figure 1). Due to the increase in the evaporative surface of the TSF, estimated TSF impoundment AE volume rates increased over time from an annual maximum of 60 l/s in 1996 to 350 l/s or greater after 2012 (Figure 2, Figure 3).

Greater AE depths were estimated for the impoundment than the embankment due to the higher moisture retaining characteristics of the finer grained impoundment tailings and presence of wet/ponded conditions in the decant pond area (Figure 1 through 3). Additionally, water was added to the embankment only during the summer cyclone period. The greater impoundment AE depth and surface area compared to the embankment resulted in considerably greater estimated AE rates from the impoundment (Figure 2).

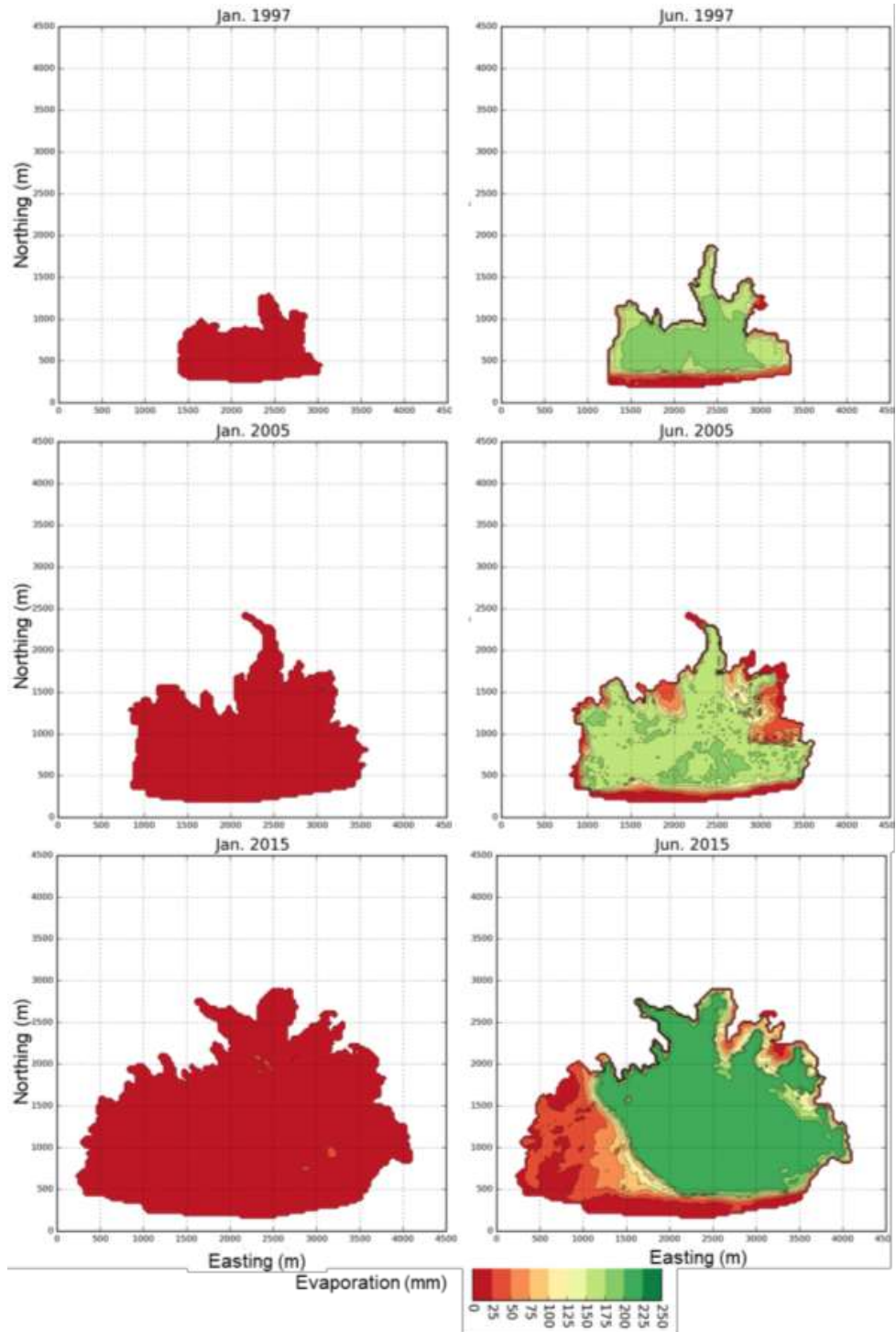


Figure 3. Example distributed evaporation from the TSF.

TSF areas estimated from Landsat reflectance data were also used to predict the tailings depth distribution (Figure 4). Tailings material thickness was estimated annually as the difference between the pre-mining surface topography and survey points near the embankment and northern perimeter of the TSF. In addition, the biweekly AE data allowed us to understand the progression of the tailing placement, such that tailing material estimates (i.e. underflow, overflow, mixed and slime tailings) could be made. These data were then used to develop a distributed seepage model based on tailing material properties and a predicted water balance using site specific data and the AE model. To validate the Landsat TSF area estimates, they were compared to mine annual report storage curve estimates and showed good agreement (Figure 5). The TSF had a rapid growth progression early-on during operations between 1996 and 1999 as the embankment grew and the basin was filled in with tailings.

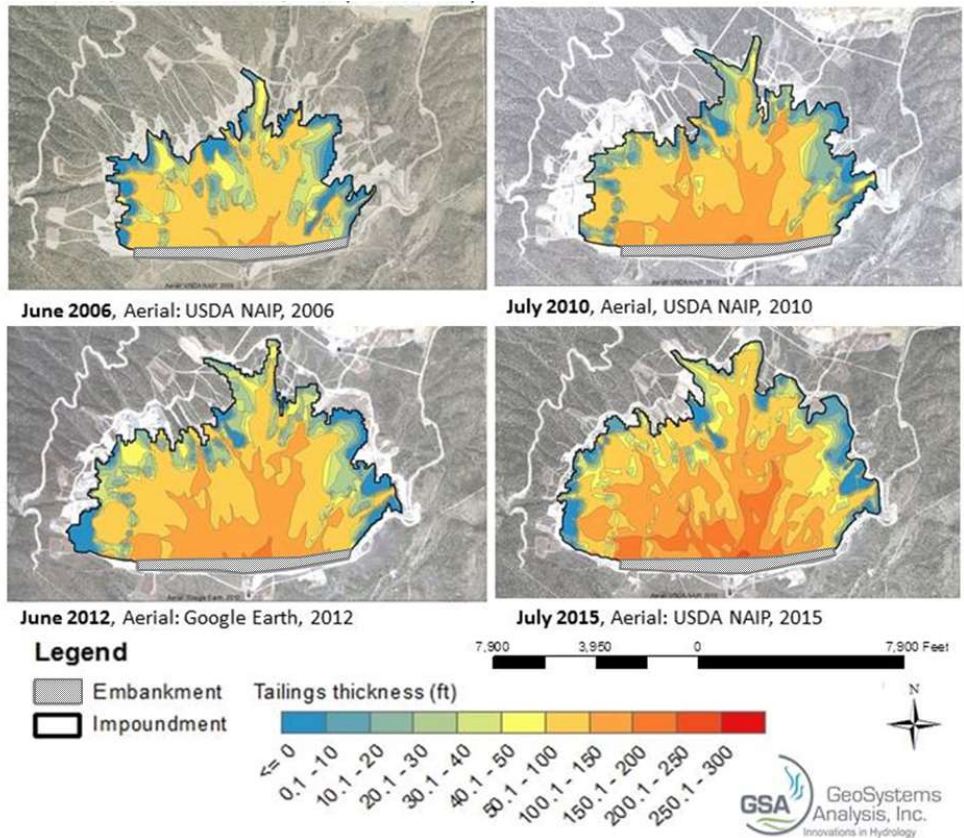


Figure 4. Estimated tailings depth distribution.

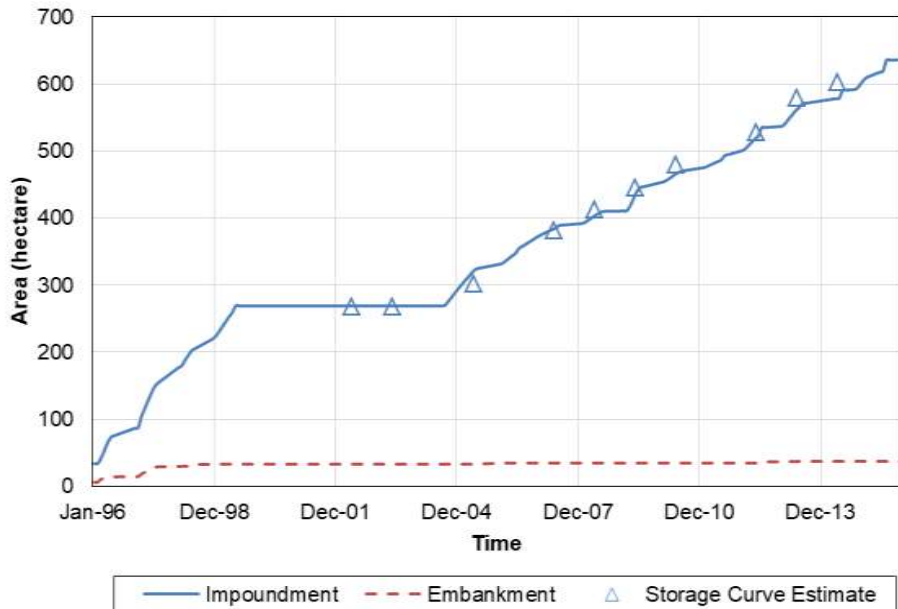


Figure 5. Estimated TSF embankment and impoundment areas.

4 CONCLUSIONS

The 3T model provides a cost-effective and accurate method to calculate high resolution spatial and temporal estimates of TSF AE, and it also captures seasonal changes in AE and surface ponding. Estimated monthly AE ranged from over 150 mm/month during the summer months, to less than 20 mm/day during the winter months. Estimated TSF evaporation increased over time from an annual maximum of 60 l/s to greater than 350 l/s due to the increase in the evaporative surface of the TSF. Landsat based 3T model estimates of the TSF surface area were in good agreement with storage curve tailings area estimates, and also provided a high resolution estimate of the tailings footprint distribution over time. Additional benefits to the method include the ability to predict tailings depth and the progression of tailings placement over time which can then be used to prepare estimates of tailings material types and a distributed seepage model.

5 ACKNOWLEDGEMENTS

The authors thank Robinson Nevada Mining Company for granting permission to publish this work.

6 REFERENCES

- Allen RG, Irmak A, Trezza R, Hendrickx JMH, Bastiaanssen WGM, Kjaersgaard J (2011) Satellite-based ET estimation in agriculture using SEBAL and METRIC, *Hydrologic Processes*, 25, 4011–4027.
- ASCE-EWRI (2005) *The ASCE standardized reference evapotranspiration equation.*, pp. 59 with six appendices, Environmental and Water Resources Institute, American Society of Civil Engineers, Reston, Virginia.

Qiu GY, Zhao M (2010) Remotely monitoring evaporation rate and soil water status using thermal imaging and "three-temperatures model (3T Model)" under field-scale conditions, *Journal of Environmental Monitoring*, 12(3):716-723.

Satellite-based Repeat Surveying of Tailings: A Cost-effective Alternative to Aerial Surveying

G. Mitchell and J. Turner

PhotoSat Information Ltd., Vancouver, BC, Canada

Jon Engels

Tailpro Consulting, Santiago, Chile

ABSTRACT: Satellite surveying of tailings storage facilities (TSFs) has become part of the operational management of many mines. Large TSFs can now be surveyed within a few days of the satellite pass. Twice-monthly updates, even for mines exceeding 200 km², have become routine. This allows an ongoing record of the state of the TSF and its surroundings. Monitoring tailings consolidation, the remaining capacity of the dam and deposition locations, thickness and beach slope are all common measurements. Regular surveys leads to a database that can be used to attest compliance with operating plans and licenses over time. PhotoSat has completed over 900 surveys of mines worldwide. This paper discusses the implementation of satellite surveying at a large oil sands mine and the ongoing surveying that has been done since 2013. Some commentary about the advantages and disadvantages of satellite surveying over ground and aerial surveying methods is offered. Satellite surveying is a feasible and lower-cost alternative to aerial surveying. Some current limitations may be overcome with data from satellites that will become operational in the coming years.

1 INTRODUCTION

The quality and availability of commercial optical satellite images has evolved dramatically over the past decades. Very-high-resolution photos captured from satellites now routinely replace airborne photogrammetry for surveying the topography of the Earth's surface (e.g., Barbarella et al., 2017). Building upon PhotoSat experience with over 900 mine surveys worldwide, this paper discusses satellite surveying for TSF's specifically as compared to alternatives and some specific derivatives that were developed for TSF surveying. Having proved itself in tailings surveying, satellite surveying is now recurrently used to survey all of the operating areas of mines (e.g., Lomond & Turner, 2014; Schmidt et al., 2015; Fig. 1).

2 EVOLUTION OF MINE SURVEYING WITH OPTICAL SATELLITE IMAGERY

Topographic survey grids produced using photogrammetry and stereo photographs taken from airplanes has been around since the 1930s. Commercial satellite imagery has been available since the 1970s but very-high-resolution stereo satellite data (pixel size < 1 m) only became available in the late 1990s. When processed with classical photogrammetry, survey grids derived from this satellite imagery typically had vertical accuracy limited to between 1.5-m and 3-m (Kayadibi, 2009). Such accuracy is not sufficient for mine volume measurements.

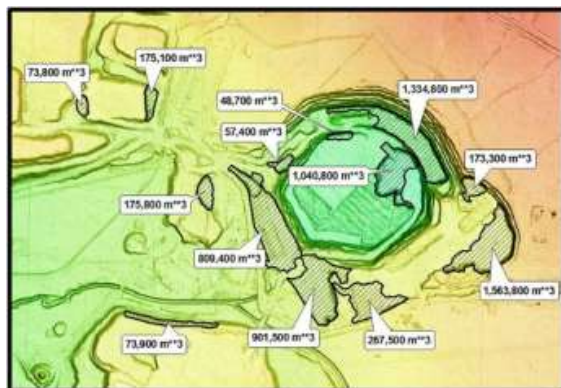


Figure 1. Mine satellite surveying produced in 2010: volumetrics of Penasquito Gold Mine, Mexico.

In the 2000s, PhotoSat started working on adapting and implementing seismic image processing algorithms to use with stereo satellite images. By 2009, vertical accuracy better than 50 cm was achieved on a survey of a large mine site (Mitchell & MacNabb, 2010).

These new algorithms achieved an accuracy level suitable for operational use at mines and by mid-2010 several large mining corporations had adopted optical satellite surveying. The new algorithms came at a cost – they are exceptionally processing-intensive and require an iterative approach. In 2010 the processing time for a mine site might be weeks.

To deal with this PhotoSat developed software that could be executed in a massively parallel processing environment. During the 2010's, systems with tens of thousands of processing cores at a cost of a few dollars per core became available.

Today the current processing time for a normal mine is a few days. For some mines, surveys of the TSF are delivered within hours of the satellite pass, with the remaining parts of the mine delivered a few days later.

Twice-monthly or monthly repeat-surveying at several mines worldwide allowed PhotoSat to accumulate a large amount of data on distortions in specific satellite camera systems. This data was used to develop systematic correction processes to further improve the accuracy of the surveys. This modelling was possible because at most mines the satellite images cover huge areas – much larger than the operational area of the mine. The survey areas include all the operating parts of the mine (pit, tailings, stockpiles etc.) however large areas outside these remain unchanged during the few days between surveys. Cataloging apparent changes allowed a library of corrections to be developed for each satellite camera. Applying these corrections allows satellite surveys to achieve vertical accuracy better than 15 cm.

3 GROUND VS. AERIAL VS. SATELLITE SURVEYING OF TAILINGS

3.1 Vertical accuracy

Tailings beaches are large and flat. In the flat to gently sloping surfaces of tailings, small vertical measurement errors can result in large errors in the derived volume measurements. Similarly, sufficient vertical accuracy for beach slope measurement is essential if consolidation models or remaining capacity measurements are to be useable or relevant.

“Sufficient” vertical accuracy varies based on the size of the TSF and the reporting regime that is being complied with. For Oil Sands mines the COSIA (Canadian Oil Sands Innovation Alliance) provides engineering level guidelines for TSF measurements which require vertical accuracy to be better than 15 cm RMSE (Ansah-Sam et al., 2015). This accuracy level requirement appears to be similar to that adopted by many mining corporations around the world.

Suncor surveyors compared the accuracy of ground surveying, airborne LiDAR, aerial photogrammetry (using drones), and satellite surveying, over a one-year period (Lomond & Turner, 2014). All methods were shown to be able to attain accuracy better than 15 cm in areas where good data could be collected. Ground surveying was however unsafe in parts of the TSF area and measurements from LASER scanners positioned on safely accessible points were rejected due to reduced accuracy and the time required to obtain even partial coverage.

PhotoSat conducted an extensive series of accuracy tests on the existing commercially available satellites. These are published in the public domain and can be found at <https://www.photosat.ca/surveying/satellite-surveying-accuracy-studies/>.

3.2 Safety and logistics

For safety reasons most mines restrict access to TSF areas. Many mine tailings beaches are too soft to safely walk or drive on. As a general rule less people in the area reduces risk and increases safety.

Satellite surveys offer an attractive improvement to safety since no human access to the TSF area, or anywhere on the mine site is required. Furthermore, due to the large areal coverage of satellite photos, existing surveys of infrastructure and monuments away from the tailings storage facility (TSF) can be used as ground control. There is no need for new targets to be installed and surveyed anywhere on the mine site.

Alternative methods such as ground surveying or drones require that personnel come within close proximity of the TSF. Drones require “in sight” operation and are usually controlled from a nearby area (but still on the mine site). In recent years drone mounted GPS receivers and a base station at the operator location offer the possibility of eliminating the need for new ground targets to be installed on the TSF surface however common practice is for new ground targets to be installed and surveyed using ground surveying for each drone survey. Additional safety rules apply to other personnel at the site during a drone operation. Most commonly other personnel are required to keep the drone flight area clear or remain in their vehicles while the drone is in the air.

Drones need to be insured for accidents and liability, and, for these reasons the drone operator is often a contractor with a valid Special Flying Operations Certificate granted by a national agency. Most countries require special authorization and diligent communication between the drone operator and air traffic controllers. On mine sites the drone operator is also required to be trained in and comply with the mine safety regulations and to be supervised while on-site.

Data collection with manned aircraft (aerial LiDAR) can produce excellent results with good accuracy and resolution. However, logistics and cost of scheduling flights plus the long times required for processing the data make twice monthly LiDAR flights impractical for TSF surveys.

3.3 Spatial coverage and survey duration

Satellite surveys of operating mines typically cover 25-100 km² however some mines cover over 200 km². In most cases a single satellite photo will cover the entire mine operating area. Surveys of TSF, which typically cover 5-20 km², can thus be delivered within 24 hours of the satellite pass.

Since the entire survey is derived from a single satellite image, accuracy level is consistent across the site. In addition, the methodology results in a consistent level of accuracy and quality from one month to the next.

At the Suncor Millennium mine satellite surveys cover not only the TSF but the entire 270 km² mine lease area (Fig. 2). Satellite photos are available for QC checking a few hours after each satellite pass. After an image set passes QC Suncor engineers are informed that a new survey grid for the TSF is being processed for delivery within 24 hours.

Different mine engineering departments work with different software and thus require different data file formats. To avoid data management issues and to speed up operational use, the deliverables are provided in the formats and coordinate systems that the engineers directly work with.

Drone photogrammetry typically requires multiple flights taking hours or days to capture 100's (or 1000's) of photos to cover the TSF with sufficient overlap between photos. A fixed-wing drone can acquire a few km² in a day (usually less than 2 km²). Capturing different parts of the TSF at different moments is not ideal due to the ongoing deposition in different parts of the TSF.

Data collection with manned aircrafts (airborne LiDAR) is fast but involves complex logistics. Ground resolution achieved by aerial surveying is similar to or better than that of satellite surveying, but the latter is significantly faster and more cost-effective.

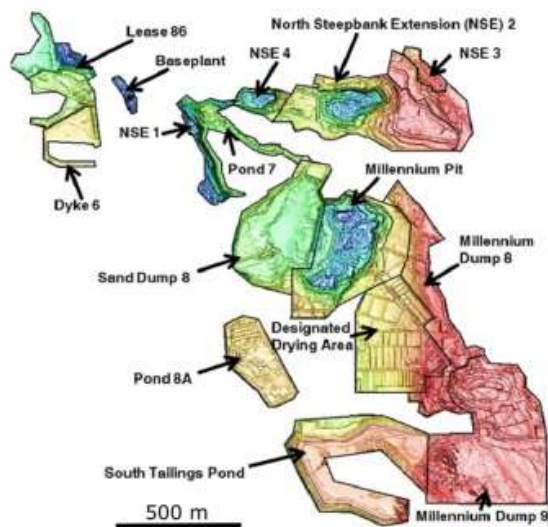


Figure 2. Suncor Millennium Mine survey areas. Different functional areas are surveyed at different intervals and delivered in different formats. (Lomond et al 2014)

3.4 Survey density

For volume measurements, a dense array of points is necessary. A common density for practical use is about one elevation value per sq. meter. Higher elevation point density seems attractive and is available from drones, LiDAR and satellite surveying however the higher point density can make the data files sizes too large for practical use.

The cost and time to acquire a 1m ground sampling distance using ground based RTK GPS/GNSS is prohibitive. Ground-based LASER scanning can provide this density if multiple set-ups are used however this is time consuming and does not work well on large, flat, TSF surfaces due to the low incidence angles further away from the LASER. Drone photogrammetry can provide the highest ground sampling distance but at the cost of very long data acquisition and processing times.

3.5 Survey Frequency

If cost was not a factor, the ideal survey frequency of TSFs at some mines would be weekly or even daily. At the Suncor Millennium mine, the TSF surveying frequency is twice monthly. To achieve this four satellites are deployed simultaneously. If cloud obscures the site during one satellite pass, a different satellite will make another attempt later the same day or on subsequent days. Tasking multiple satellites increases the number of opportunities for good photos to be taken. Since this does not impact the cost it is common practice.

Both satellite, LiDAR and drone surveys are impacted by weather. If cloud obscures the site, no satellite images can be acquired and the capture will be delayed until the next satellite pass. Drones can fly below the cloud but are impacted by strong winds. The northern Alberta winter

can mean months of very low (battery freezing) temperatures, which limits flying times for drones to a few minutes per flight. Short daylight periods in winter also limit drone access.

4 WATER BODY DELINEATION

Determining the edges of the ponds is challenging using the human eye because the transition between wet tailings and silty water in the pond is often unclear (Fig. 3). To the eye, the suspended silt has the same color as the tailings. This problem is compounded when matching 100's of photos because sun glint and the lack of features can make it impossible to match the images along the shoreline, resulting in large vertical errors.

Optical satellite cameras include detectors that record not only visible light but also infrared wavelengths. Water has very high absorption in the infrared with the result that silty water and a wet beach have distinct spectral signatures in the combined visible and infrared wavelengths. This forms the basis for a reliable and repeatable method for determining the edge of the tailings ponds.

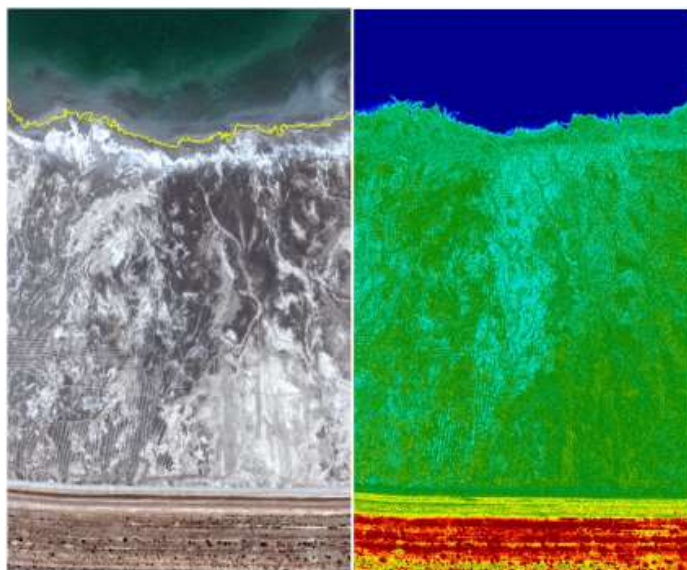


Figure 3. Multispectral processing of satellite photos for TSF pond delineation. Note the difficulty in precisely determining the water edge in the original photo (on the left) and the sharp contrast between water and land in the processed image (on the right). The yellow line superimposed on the original (left) satellite photo was automatically derived from the processed image.

5 TAILINGS BEACH MEASUREMENTS

Common measurements for TSF performance monitoring include: 1) freeboard and current available storage volume; 2) volume of recent deposits; 3) size and location of ponds; 4) beach length and slope.

These measurements require an accurate and repeatable determination of the edge of the pond and high density, accurate, elevation measurements on the beach. Measuring and monitoring tailings beach slopes and the thicknesses of the pours over time (Figure 4) enables verification of TSF capacity models. As an example the Sierra Gorda TSF in Chile has been surveyed monthly or bi-monthly since November 2016. The evolution of the beach profile up to April 2018 is shown in Figure 5. Being able to accurately track the pour thickness as a new spigot system was tested allowed this project to be validated (Engels et al., 2018).

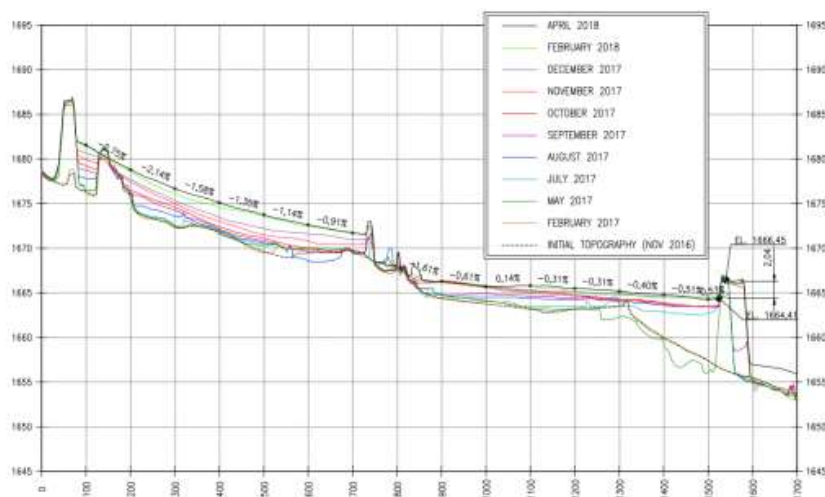


Figure 4. Multi-temporal beach profiles from satellite surveying of the Sierra Gorda, Chile (Engels et al., 2018)

6 FUTURE SATELLITE SURVEYING

There are currently many commercially available satellites in orbit from which elevation surveys with various levels of vertical accuracy can be produced. High accuracy algorithms and validation have been done for many of these however only a few are in current use.

PhotoSat can produce satellite surveys accurate to better than 15 cm RMSE in elevation from three satellites: WorldView-1, WorldView-2 and WorldView-3. The fourth satellite of this constellation (WorldView-4) has been in orbit for over two years, however at the time of writing it is not in use commercially for mine site surveying. PhotoSat expects to start using WorldView-4 data for commercial TSF surveys in late 2018.

There are eight additional satellites with suitable high accuracy cameras scheduled for launch by 2020. These will greatly improve the photo collection capacity, providing at least daily survey opportunities for most of the world’s mine sites.

There are many industry reports about currently available “small sat’s” and a promise of a tsunami of future launches is envisioned. These offer the possibility of very low cost and almost continuous satellite coverage anywhere in the world. At present, the optical technology in these satellites does not provide sufficient elevation accuracy to be of use for TSF surveying.

The rise of “big data” has driven the demand and further lowered the cost of commercially available computer power by several orders of magnitude. PhotoSat transitioned its algorithms for some application to the Amazon servers in early 2015. This allows processing to be scaled and will allow the processing systems to expand to exploit the availability of the new satellites.

It is plausible that satellite surveying could be used to regularly survey every large TSF on the planet within the next 5 years.

7 CONCLUSION

The fact that satellite surveying 1) improves safety (reduces field-work requirements and liability), 2) has progressed to an accuracy level suitable for common operational measurements at

TSFs, and 3) provides fast, consistent surveys of entire TSF areas, makes it an attractive alternative to other technologies.

It is now routine to use satellite surveying for measurements of pond size and location, beach slope and length, volumes deposited, and current TSF capacity. Improvements in processing times have led to the adoption of satellite surveying for monthly or twice-monthly surveying. In the next few years, additional satellites and improved resolution will allow for more recurrent (possibly daily) and detailed surveying.

REFERENCES

- Ansah-Sam, M., Binczyk, T., Dobek, C., Geremew, A., Guo, C., Mimura, W. & Weerakone, S. 2015. Guidelines for tailings deposit sampling and measuring tools. Canadian Oilsands Innovation Alliance (COSIA).
- Engels, J., Gonzalez, H., Aedo, G. & McPhail, G.I. 2018. Implementation of spigot discharge systems for high-density tailings at Sierra Gorda Sociedad Contractual Minera, Chile. in RJ Jewell & AB Fourie (eds), *Proceedings of the 21st International Seminar on Paste and Thickened Tailings*, Australian Centre for Geomechanics, Perth, pp. 389-400.
- Kayadibi, O. 2009. Recent advances in satellite technologies using to generate the Digital Elevation Model (DEM), *Proceedings of the 4th International Conference on Recent Advances in Space Technologies*, Istanbul, Turkey, IEEE, pp. 380–385.
- Lomond, P. & Turner, J. 2014. Mapping and Monitoring for Suncor's Oil Sands Tailings Reduction Operation process using GPS surveying and PhotoSat satellite topography. 2014 Trimble Dimensions user conference, Las Vegas.
- Mitchell, G. & MacNabb, K. 2010. High resolution stereo satellite elevation mapping accuracy assessment, *Proceedings of the 2010 Annual ASPRS Conference*, San Diego, California, pp. 26–30.
- Schmidt, B., Malgesini, M, Turner, J. & Reinson, J. 2015. Satellite monitoring of a large tailings storage facility, *Proceedings of the Tailings and Mine Waste 2015*, Vancouver, BC.

Design of a Centerline Method Tailings Dam using Mine Waste Rockfill in Perú

P.W. Ridlen, T.F. Kerr, G. Dominquez, J-B. Varnier
Knight Piésold, Denver, Colorado, USA

J. Toro
Hudbay Minerals, Toronto, Ontario, USA

ABSTRACT: The Constancia tailings facility, located in the Peruvian Andes, was designed to store more than 450 million tonnes of copper tailings in an area of relatively high seismicity and seasonally high rainfall. The tailings dam, currently more than 100 meters high, is constructed of compacted rockfill sourced from glacial outwash, quarried sandstone, and open-pit waste rock, and will ultimately be raised to a height greater than 170 meters. The dam comprises an initial downstream-method rockfill embankment with sloping upstream core and chimney drain, with subsequent conversion to a centerline-method, supported by an upstream rockfill platform to provide support to the vertical section of core and filter/drain zones. This paper provides a summary of the design analyses and describes observations made during construction and operation. Site-specific deterministic and probabilistic seismic hazard analyses, seepage, slope stability, and deformation analyses performed to predict the long-term engineering behavior of the dam and impounded tailings are described.

1 INTRODUCTION AND PROJECT SETTING

1.1 Project Description

The Constancia open-pit copper mine, owned and operated by Hudbay Perú SAC, is located in southern Perú, approximately 100 kilometers (km) south of Cusco, at elevations ranging from 3900 to 4500 meters above sea level (masl). The Constancia deposit is a porphyry copper-molybdenum system, emplaced in multiple phases of monzonites and monzonite porphyry. Milling rates are in the range of 80,000 to 90,000 tonnes per day (tpd). The original mine plan considered 525 million tonnes (Mt) of ore and 538 Mt of waste rock to be produced over a 17-year life of mine (additional reserves have since been added but are not considered in this paper). The process plant employs a conventional grinding and flotation circuit, from which tailings are pumped approximately 5.3 km through a high-density polyethylene tailings delivery line and spigotted into a partially-lined Tailings Management Facility (TMF). Figure 1 shows the layout of the TMF, processing plant, open pit, and other facilities at the site.

In the TMF, tailings are contained by an arcuately-shaped, cross-valley tailings dam with multiple small saddle dams, all constructed of rockfill, that will have a crest length of 4.1 km at design height. The TMF design was developed by Knight Piésold of Denver, Colorado, USA, to store approximately 290 million cubic meters of tailings at a maximum dam height of 170 meters (m), corresponding to a crest elevation of 4160 masl. Construction of the TMF was initiated in 2013, and the facility was placed into operations in late 2014, with full production achieved in early 2015. Since then, the dam has been incrementally raised to a height of 107 m as of December 2017. Prefeasibility designs have been prepared to raise the ultimate height to 200 m (crest elevation 4190 masl) to accommodate additional reserves, and final design studies for expansion are in progress.

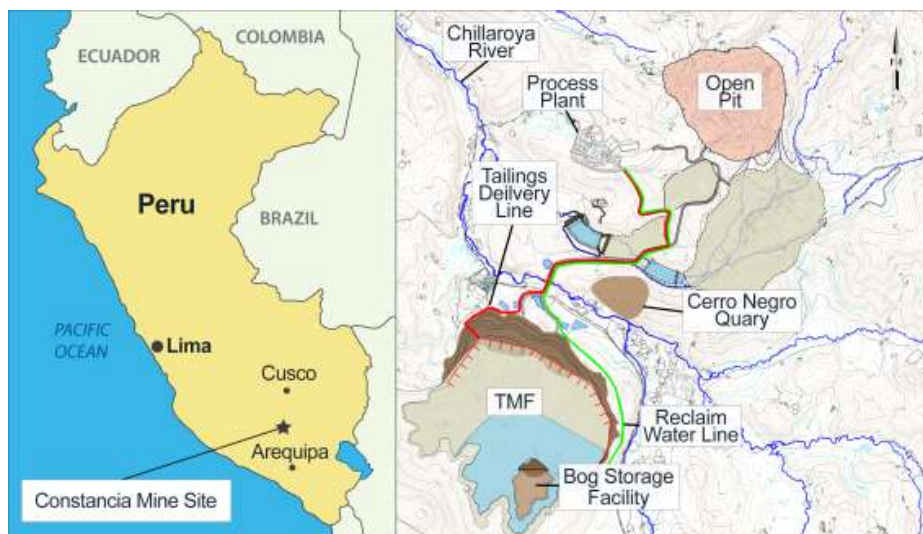


Figure 1. Location of site and general plan view on the Constancia Mine.



Figure 2. Aerial drone photograph of the Constancia TMF in June 2018.

1.2 Geologic Setting

The site is located within the eastern cordillera of the Andes mountains. Geomorphology is characterized by moderate relief, influenced by lithologic trends, structural features, and glacial erosion, with low rolling hills approximately 400 to 500 m high. Dissolution surfaces and karst are found where limestone dominates the rock mass but are absent at the TMF site. The Chillaroya river, a tributary of the Apurimac River within the Amazon watershed, flows from southeast to northwest just north of the TMF and captures drainage from the TMF and vicinity.

The oldest rocks in the area are sandstones and mudstones of the Lower Cretaceous-age Chillaroya Formation, overlain discordantly by limestones, calc-arenites, and conglomerates of the Arcurquina and Ferrobamba formations of Upper Cretaceous age. These formations were intruded by Oligocene-age dioritic/granodioritic plutons of the Andahuaylas-Yauri Batholith, and several monzonitic stocks and dikes intrude and cross-cut the sedimentary lithologies. The intrusives have been exposed to extensive weathering, leading to a deep oxidation profile.

Bedrock beneath the TMF comprises diorite/granodiorite of the Apurimac Batholith and sandstone of the Chillaroya formation. The degree of weathering is highly variable with compe-

tent rock exposed in some areas, but also with frequent exposure of moderate-to-soft rock overlain by low-to-moderately plastic soils. Diorite is exposed over most of the TMF basin and below the western portion of the TMF embankment, while sandstone is exposed in the northeastern portion of the basin and the east half of the dam. The diorite exhibits significant weathering to several meters depth beneath the west abutment of the dam, requiring deep stripping in some areas to reach competent rock for the dam foundation. Structural features in the TMF area correspond to stratification, faulting and fracturing systems of the sedimentary rock strata formed by the magmatic intrusions. Three fault systems were identified near the TMF, which were investigated by trenching and considered to be inactive in recent geologic time.

Quaternary deposits of alluvium and bog partially cover bedrock in the valley bottoms of the TMF area. The alluvium, which is typically non-plastic, was eroded from the weathered diorite, carried downslope and deposited in the valley bottoms. Bog deposits, consisting of organic-rich soils or peat, are several meters deep in many valleys. The bog deposits are highly compressible and have low strength, so the bog and loose alluvium deposits were removed from under the embankment and geomembrane-lined areas and placed into designated bog disposal areas.

1.3 Climate and Hydrologic Setting

Climate at the site is humid and seasonably cool with well-defined rainy and dry seasons. Average daily maximum temperatures range from 13 to 16 degrees Celsius and average daily minimum temperatures range from -11 to 0 degrees Celsius. Virtually all precipitation occurs during the wet season, which is defined from October to April of each year. Climatological data for use in the designs were based on data from multiple climatological stations located in the region, supplemented by data from a single on-site station, and a regression analysis was used to correlate on-site precipitation data with outlying stations. Estimates for the design 24-hour storm events were calculated using a theoretical Extreme Type I Gumbel probability distribution on precipitation data from approximately 48 years of historical records. The probable maximum precipitation (PMP) was estimated according to the World Meteorological Organization (WMO, 1973) methodology for all stations with 24-hour maximum precipitation records greater than 10 years. The resulting design data and parameters are provided in Table 1.

Table 1. Summary of Climatological and Hydrological Design Data

Description	Design Value	Description	Design Value
Annual average precipitation	1,000 mm	Annual maximum precipitation	1,353 mm
Annual minimum precipitation	590 mm	Average wet season precipitation	932 mm
Average dry season precipitation	72 mm	100-year/24-hour storm precipitation	92 mm
PMP/24-hour storm precipitation	263 mm	Potential annual evaporation	961 mm
Annual evaporation from natural ground	480 mm	Evaporation from dry tailing	455 mm
Evaporation from wet tailing	865 mm	Evaporation from waste area	296 mm
Evaporation from water surfaces	673 mm		

1.4 Seismicity and Seismic Hazard

The site is located within a seismically-active region of Perú, where the Nazca Plate subducts under the South American Plate at a rate of about 80 millimeters/year. The region experiences earthquakes associated with the subduction zone and crustal faulting within the continental intraplate zone. Deterministic seismic hazard analyses and probabilistic seismic hazard analyses (PSHA) were performed originally by Alva (2013) and updated by GeoPentech (2018). Maximum credible earthquake (MCE) scenarios were developed for each of three categories of seismic sources: subduction interface (SDI), deep intraslab (DIS), and shallow crustal (SCS). MCE scenarios and resulting peak horizontal ground accelerations for 84th-percentile ground motions are summarized in Table 2. The PSHA results were used to select operating basis earthquake ground motions for the TMF and maximum design earthquakes for non-critical structures, and to inform the deterministic analyses. The MCE response spectrum for the DIS and SCS scenarios fell mostly between the uniform hazard spectra for 2475-year and 5000-year probabilistic ground motions. The 10,000 peak ground acceleration (PGA) is about 0.8g, and the return period for PGA of 0.6g (corresponding to the MCE) is approximately 2475 years.

Table 2. MCE Scenarios

Source Category	Moment Magnitude	Distance (km)	PGA	Ground Motion Models used
Subduction Interface	9.0	250	0.09g	Abrahamson et al. (2016), Zhao et al. (2006), Atkinson & Boore (2003, 2008)
Deep Intraslab	7.75	100	0.59g	Abrahamson et al. (2016), Zhao et al. (2006)
Shallow Crustal	6.75	1.5	0.62g	NGA-West2 (Boore et al. 2014)

2 EMBANKMENT DESIGN

2.1 Design Criteria

Design criteria, developed jointly by Hudbay and Knight Piésold, generally followed the Canadian Dam Association (CDA) dam safety guidelines, with consideration to other international guidelines. Dam consequence classification of Very High was considered realistic for this facility, considering the relatively low population at risk and the lack of critical infrastructure in the downstream area, but the more conservative Extreme consequence category was used for design, given the height of the dam, the perceived cultural and environmental value of the surrounding area, and the potential for reputational impact on the owner. The design earthquake and design storm deserve special discussions provided in this section, as follows.

Selection of the design earthquake was guided by CDA (2007, 2013), ANCOLD (2012), ICOLD (2010, 2016), and the experience of the designers and Independent Professional Review Board (IPRB). For extreme hazard dams, CDA (2013) recommends the MCE or 10,000-year earthquake. ANCOLD (2012) recommends the 10,000-year earthquake during operations and the MCE for post-closure. ICOLD (2016) recommends either the MCE or an earthquake with a “long return period, for example 10,000 years” and that “deterministically-evaluated earthquakes may be more appropriate in locations with relatively frequent earthquakes that occur on well-identified sources, for example near plate boundaries.” Because the Constancia site is in an area of frequent seismic activity with relatively short recurrence intervals between large magnitude events, the PGA estimated for a 10,000-year earthquake exceeds the PGA estimated for the 84th-percentile MCE, although the MCE ground motions at longer periods for crustal sources are higher than the 10,000-year uniform hazard spectrum. The 84th percentile MCE was ultimately selected as the appropriate design earthquake.

Once the dam reaches final height, a permanent spillway designed for the PMP will be constructed into natural ground near the left abutment. However, during operations, the TMF will have no spillway. As a result, the design storm criteria during operations were developed using a probabilistic water balance to maintain sufficient volume above the tailings surface to contain the volume of water corresponding to an annual exceedance probability (AEP) of 0.1% (i.e., 1:1000 years), which is consistent with recommendations for extreme-consequence, non-release dams described in ANCOLD (2012). The raise sequence of the dam was planned to maintain a minimum of 2 m of freeboard above the 0.1% water surface elevation at all times. Further discussion of the water balance method and application are provided in Section 2.6.

2.2 Geometric Design and Embankment Zonation

Plan view of the TMF is shown in Figure 1. The main dam crosses two valleys separated by a central ridge, creating separate basins in the initial years of operation. A repository for bog and other unsuitable material removed from the valleys within the TMF footprint during construction is in the southern end of the east basin and will eventually be inundated by water and tailings. The reclaim pond is maintained at the southern end of the east basin, which is fully geomembrane-lined. The geomembrane liner is a 2-mm linear low-density polyethylene (LLDPE) with double-sided texturing. Only a portion of the west basin is lined.

The maximum section, depicted in Figure 3, is in the west valley. The embankment is comprised of the zones and materials summarized in Table 3. The width of the core (Zone A) ranges from a maximum of about 24 m at the base of the maximum section to 4 m wide in the vertical section (i.e., centerline-raised portion). Zone B (filter/drain) is 2 m wide for the entire dam height was designed to meet both piping criteria (to filter Zone A) and permeability criteria.

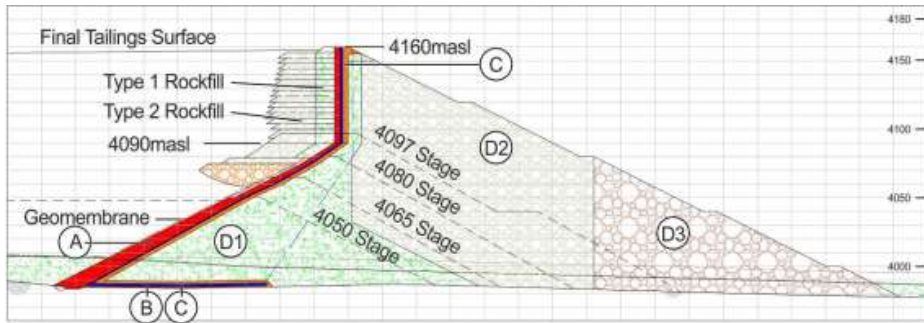


Figure 3. Typical cross-section of TMF embankment at maximum section.

Zone C (transition/coarse filter) is 4 m wide for the entire dam height, and its gradation was designed to meet only piping criteria (to filter Zone B material). A drainage blanket of Zone B/Zone C material was placed beneath the upstream portion of the dam to collect upward seepage from the foundation and seepage through the core. This drainage blanket directs seepage toward a central collection drain of coarse gravel in the bottom of the two main valleys, which empty into two sump, from which water is pumped and returned to the process circuit.

The downstream shell comprises three zones: D1, D2, and D3. Zone D1 was used to construct the starter dam and provides transition between Zone C and Zone D2 in the vertical core section. The maximum allowable fines content of 20% for Zone D1 is higher than normal for good-quality rockfill but was allowed since Zone D1 is well-compacted and located deep in the dam's interior. Most of the material placed in this zone had fines content of less than 15% based on quality control testing. Zone D2 comprises the greatest percentage of dam volume and is described in the following paragraphs. To date, no Zone D3 material has been placed.

Initially, Zone D2 material was sourced from a sandstone quarry (Cerro Negro), hauled in 40-tonne trucks and compacted with 19-tonne rollers. Then, once open-pit mining started, Zone D2 material was sourced from non-acid-generating waste rock—mostly unaltered limestone/sandstone—and delivered and compacted with 240-tonne mine trucks. Extensive testing has been performed on the Zone D2 material during construction and operation, including 1-m diameter triaxial tests and companion six-inch diameter triaxial tests.

A key feature of the design is the upstream rockfill zone (Type 1 and Type 2 Rockfill), which provides support for the vertical core section. A crest detail showing the upstream rockfill zone is shown in Figure 4, and a photograph of construction is provided in Figure 5. The initial lifts of this zone—referred to as the “Initial Working Platform”—were placed over tailings, but once the initial working platform was built, subsequent lifts are placed on compacted rockfill, using 0.5-m to 1.0-m lift thicknesses, with compaction provided either by a 190-tonne roller or loaded haul trucks. Thus, the design concept and construction sequence produce a compacted rockfill zone that is fully supported on the upstream slope of the downstream-method starter dam. By starting the Initial Working Platform construction when the tailings surface is about 20 m below the conversion from downstream construction to centerline construction, the initial rockfill lifts displace into the soft tailings and form a stable working surface for subsequent lifts.

2.3 Material Characterization

Material properties were developed during design based on field and laboratory investigations of materials deemed representative at the time. However, borrow-source investigations were limited due to access restrictions related to land ownership during project development. As a result, the Observational Method (Peck, 1969) was applied, and supplemental investigations and laboratory testing were performed during construction and operation to confirm or update the design parameters, based on actual materials. Table 4 presents selected geotechnical parameters for the primary materials of interest. The following sections provide discussion of the embankment materials and tailings material characterizations.

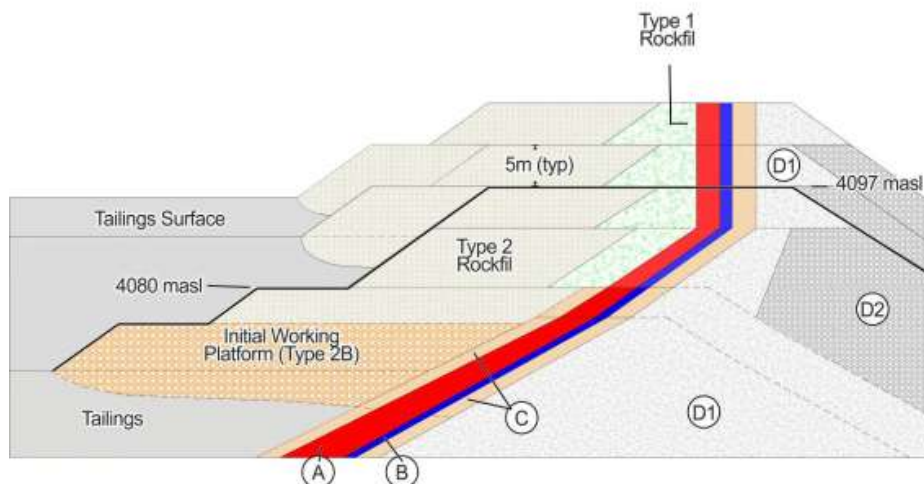


Figure 4: Crest detail showing upstream rockfill platform.



Figure 5: Construction of initial working platform.

2.3.1 Embankment Materials

The stability and performance of the TMF dam is largely dependent on the Zone D2 and Zone D3 materials, which comprise about 70 percent of the embankment volume, and to a lesser degree on the Zone D1 materials. By nature of the geologic development of the ore body, the waste rock is highly variable, based on the lithology and type of thermal alteration. The primary rock types to be used in dam construction are unaltered sedimentary formations (limestone/sandstone) and monzonite. The monzonite materials are altered as typical to porphyry development—argillic, phyllic, propylitic, potassic, and silicic—although not all alteration types are suitable for dam construction, depending on their potential for acid generation (the design considered that only non-acid generating materials would be placed downstream of the core).

Most of the Zone D2 material to date was sourced from fresh limestone waste rock, sandstone from the Cerro Negro quarry, and a small amount of argillically-altered monzonite. A laboratory testing program on samples of the Zone D2 materials selected during construction was performed, comprising large-scale (1000-mm diameter) triaxial testing performed at the IDIEM laboratory at the University of Chile in Santiago and medium-scale (150-mm diameter) triaxial testing at the Knight Piésold laboratory in Denver, Colorado. Samples were prepared using the

parallel gradation technique described by Lowe (1964) and by Frossard et al. (2012) to match representative gradations measured on in-place materials (associated with large-diameter water replacement density tests). Extensive characterization of index and engineering properties were performed on each sample.

Table 3. Embankment Zone Materials and Specifications.

Zone	Description	Borrow Source	Max. Particle Size	Fines* Content	Loose Lift Thickness	Compaction
A	Clay Core	Glacial Till/Out wash	6 inch (152 mm)	25-85%	200 mm (8 inch)	95% of ASTM D 1557
B	Fine Filter/Drain	Wash plant	3 inch (76 mm)	0-5%**	500 mm (19 inch)	4 passes of roller or tamped
C	Coarse Filter/Transition	Screened quarried rock	4 inch (102 mm)	0-10%†	500 mm (19 inch)	95% of ASTM D 1557
D1	Structural Fill	Glacial Outwash, Quarry	12 inch (300 mm)	0-20%	500 mm (19 inch)	95% of ASTM D 1557
D2	Structural Rockfill	Quarry or Waste Rock	24 inch (600 mm)	0-8%††	1000 mm (39 inch)	Method specification/test fills
D3	Thick-Lift Structural Rockfill	Waste Rock	1200 mm	0-5%	2000 mm (68 inch)	Method specification/test fills
Type 1, 1A Rockfill	Upstream Platform	Waste Rock	24 inch (600 mm)	0-20%	500 mm (19 inch)	Method specification
Type 2, 2A, 2B Rockfill	Upstream Platform	Waste Rock	24 inch (600 mm)	0-10%†	1000 mm (39 inch)	Method specification/test fills

*Fines content defined as percent passing 0.075 mm (No. 200 sieve)

**Zone B: <10% of tests within 30-test running average allowed to have fines content between 5%-8%.

†Zone C: <10% of tests within a 30-test running average allowed to have fines content between 10-15%.

Within the downstream-raised section, Zone C was allowed to have up to 20% fines content.

††Zone D2: <10% of tests within 30-test running average allowed with fines content between 8-12%.

Laboratory testing results on the limestone waste rock material are shown in Figure 6 in the stress-dependent framework of Leps (1970). The triangular symbols represent peak shear strengths for specimens prepared to relatively high density (relative density, D_R , of approximately 75%) with a relatively coarse gradation (less than 10% percent passing No. 200 sieve in field-scale samples). The blue best-fit line in Figure 6 passing through the triangle symbols is parallel to the Leps (1970) lines and slightly higher than the “Low Leps” relationship, supporting the use of the Low Leps relationship in design. The diamond symbols represent “lower-quality” rockfill specimens, which were prepared either to a relatively low density ($D_R \approx 33\%$) and with a coarse gradation, or to a relatively high density ($D_R \approx 75\%$) with a finer gradation (approximately 20% passing No. 200 sieve). The resulting best-fit line is approximately 3 degrees lower than the “higher quality” material, but higher than the “lower limit” proposed by Linero et al. (2007).

The lower-strength relationship was used in optimization studies to evaluate the potential for increasing lift thickness, which lowers the relative density, or to consider uses for other lower-quality rockfill scenarios. All medium-scale results presented in Figure 6 were adjusted for maximum particle size based on the Frossard et al. (2012) method. The comparison between the large-scale results from IDIEM was favorable to the corresponding size-adjusted medium-scale results, which validated the use of the Frossard method.

Conventional laboratory testing was also performed on the core, filter/drain, and transition materials. Table 4 provides a summary of the most relevant material properties for each embankment materials used in the various geotechnical analyses described in Section 2.4.

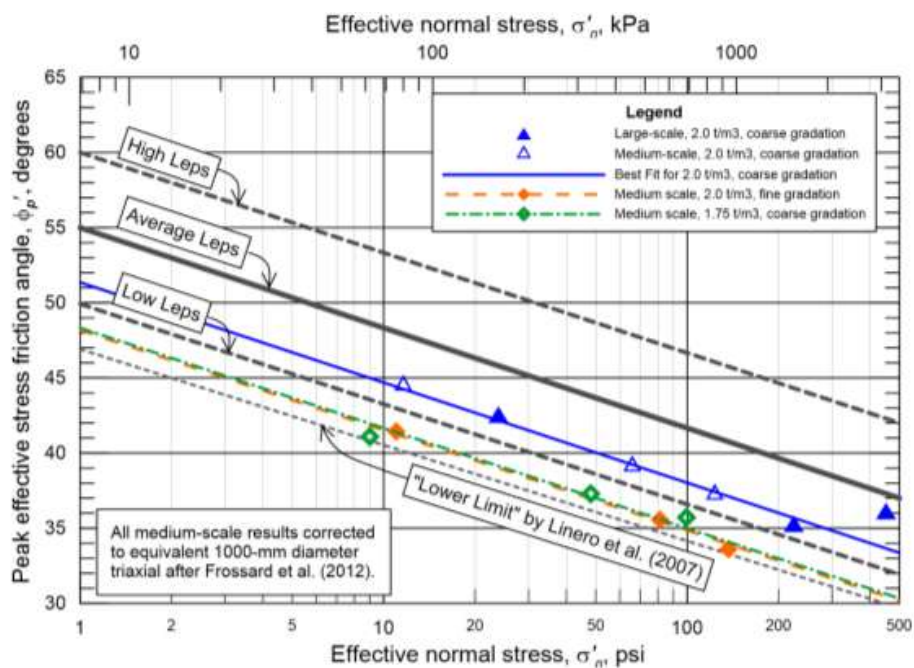


Figure 6. Shear strength characterization of the Zone D2 rockfill material.

2.3.2 Tailings

Two prototype tailings samples were selected during design from bench-scale metallurgical testing of core samples and were subjected to index property tests, triaxial strength and permeability tests, settling and sedimentation tests, and seepage-induced consolidation tests (SICT). These idealized materials exhibited 100% by weight passing the No. 50 sieve and 70% passing the No. 200 sieve. During operations, index property testing has been regularly performed on whole tailings samples from the tailings thickener underflow, which demonstrate a range of 88% to 100% passing No. 50 sieve and 50% to 80% passing No. 200 sieve, indicating the prototype materials were generally on the fine side of the range of tailings produced by the milling operation.

The key parameters for tailings characterization are the drained shear strength, undrained yield shear strength, liquefaction susceptibility, residual (post-liquefaction) undrained shear strength, permeability, and in situ density. Strength and permeability characteristics used in design are summarized in Table 4. The tailings were assumed to completely liquefy during the design earthquake. The relationship between in situ density and effective stress was developed using CONDES software (Gjerapic and Znidarcic, 2007), which was used to forecast the average tailings density over time, ranging from 1.2 tonnes/cubic meter (t/m^3) after one year to 1.55 t/m^3 after 16.5 years. Bathymetric surveying results over the first 3 years of operations indicate the actual average density is approximately 1.39 t/m^3 , just slightly lower than the value of 1.42 t/m^3 indicated by the consolidation model, but within the usual range of uncertainty.

A confirmatory laboratory and field investigation was performed to characterize the tailings after about 3 years of operations. The field investigation relied mostly on cone penetration testing (CPT), supplemented with vane shear and limited drilling and sampling. Interpretation of the CPT data supported the assumed yield undrained shear strength ratio of 0.22 and supported raising the residual (post-liquefaction) undrained shear strength ratio from 0.04 to 0.05.

2.4 Geotechnical Analyses

Geotechnical analyses to support the design included two-dimensional seepage analyses using SEEP/W, limit-equilibrium slope-stability analyses using SLOPE/W, simplified dynamic-

deformation analyses, and advanced dynamic analyses using the FLAC software. Key material properties used in the analyses are summarized in Table 4.

Table 4. Selected Material Properties for Geotechnical Analyses

Material	Unit Weight (kN/m ³)	Permeability (cm/s)	Porosity	Shear Strength Parameters	Constitutive Model in FLAC	G _{max} @ 1atm (MPa)
Tailings	1240	3x10 ⁻⁶	0.549	φ _B =29°, c=0 s _w /σ' _v (yield) = 0.22 s _w /σ' _v (liq) = 0.04	UBCSand*	49
Zone A	2160	4x10 ⁻⁷	0.212	φ _B =25°, c=0	UBCHyst**	120
Zone B	2060	5x10 ⁻²	0.228	φ _B =38°, c=0	UBCHyst	242
Zone C	2160		0.193	Leps High	UBCHyst	346
Zone D1	2160	1x10 ⁻⁴	0.193	Leps High	UBCHyst	346
Zone D2	2160	1x10 ⁻¹	0.193	Leps Average	UBCHyst	242
Zone D3	2160	1x10 ⁻¹	0.193	Leps Low	UBCHyst	242
Type 1/2 Rockfill	2160	1x10 ⁻¹	0.193	Leps Average	UBCHyst	242
Alluvium	1340	1x10 ⁻⁴	0.504	φ _B =29°, c=0	Mohr-Coulomb	77
Foundation (weathered rock)	2630	1x10 ⁻⁴	0.100	φ _B =36°, c=0	Mohr-Coulomb	650
Foundation (sound rock)	2630	1x10 ⁻⁴	0.100	Not Applicable	Elastic	650

*Beaty & Byrne (1998), **Naasgaard (2011)

2.4.1 Seepage and Stability Analyses

In the seepage analyses, boundary conditions for intermediate height cases were conservatively applied to represent a fully-submerged condition for the entire tailings impoundment (i.e., no exposed beach), with total head values set to the water elevations predicted by the water balance for flood conditions. For final height (end of operations), the edge of the saturated zone was set 250 m upstream from the crest, representing a minimum pond setback requirement to be incorporated at closure. The geomembrane liner on the upstream face of the dam and in the bottom of the tailings basin was conservatively omitted to allow flow through the foundation and the low-permeability core. The outlet of the drain layer into the central drain (i.e., flow perpendicular to the plane of the mesh) was ignored, another conservative assumption. A drainage sump located about 20 m beyond the ultimate downstream toe was modeled as a zero-pressure head. Review nodes were applied along the crest, downstream slope, and downstream toe area of the TMF embankment, allowing the model to iterate and estimate a conservative phreatic surface within the downstream shell, which is shown on Figure 7.

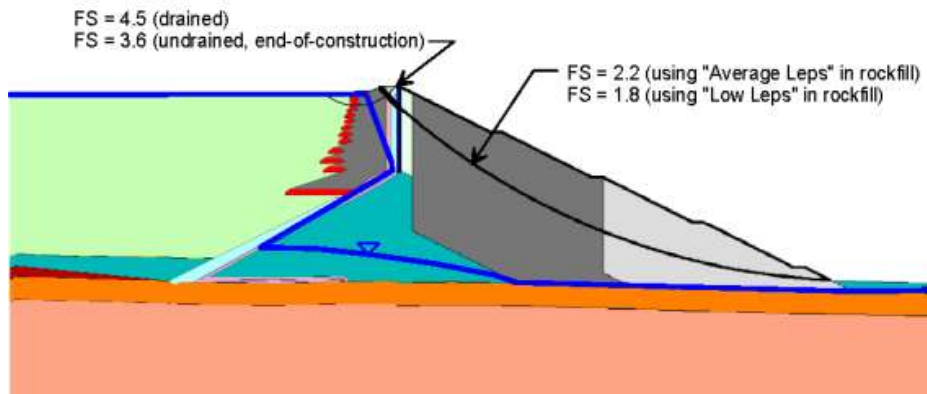


Figure 7. Critical shear surfaces and factors of safety from limit-equilibrium analyses.

Limit-equilibrium slope stability analyses were performed according to the Spencer (1967) method of slices. Model geometry and pore pressure conditions were imported from the SEEP/W output into SLOPE/W for the slope stability analyses. Minimum acceptable factor of safety (FS) values, based on CDA (2013), were 1.5 for long-term loading conditions, 1.3 for the end-of-construction conditions, and 1.2 for post-earthquake loading conditions. For long-term (steady-state) conditions, the minimum FS of 1.5 was applied to a conservative strength characterization in the rockfill (Low Leps relationship) and a minimum FS of 1.8 was used for "average" strength characterization. Figure 7 illustrates the calculated factors of safety for the downstream slope along with the phreatic surface predicted by seepage analyses. The resulting calculated factors of safety are well above the minima, allowing for future optimization of the design.

For design of the Initial Working Platform, an end-of-construction analysis was used to estimate the penetration of rockfill into soft tailings by varying the thickness of the platform to obtain a computed FS = 1.0 at the upstream edge while using undrained strengths in the tailings. The width of setback for additional lifts was then varied to achieve a minimum FS = 1.3 for a "global" failure mode on the upstream slope of the platform. A "safe operating zone" for the loaded haul trucks was established by applying a concentrated load to the platform to represent the truck weight and varying the distance from the upstream edge to achieve the minimum FS.

Simplified deformation analyses were performed using Makdisi and Seed (1978), Bray and Travasarou (2007), and Swaisgood (2014) to confirm the design would perform satisfactorily during the design earthquake. The results were compared to the numerical analyses described in the following section.

2.4.2 Dynamic Deformation Analyses

Seismic deformation analyses of the dam were performed using the explicit finite-difference software FLAC 8.0. The model mesh was set up to consider eight construction stages. These stages were subjected to gravity (static) loading incrementally, which allowed stresses and deformations to come to equilibrium after each stage was added. A seepage analysis was performed for each stage with the objective of obtaining a pore pressure distribution similar to the pore pressure distribution estimated by the SEEP/W model. Material properties used in the analyses are summarized in Table 4.

Seven spectrally-matched acceleration time histories were developed for use in the seismic deformation analysis and applied to the base of the model. The largest amount of deformation was obtained with SCS time history based on the 2009 L'Aquila earthquake in Italy. Displacements induced by this controlling MCE ground motion are presented in Figure 8. The FLAC model indicated a maximum total displacement of 1 m and maximum vertical displacement of 0.9m, which is caused primarily by an upstream rotation of the top portion of the upstream rockfill platform into the liquefied tailings. The downstream shell exhibits a slight downstream horizontal movement with very little to no vertical deformation. The model results indicate no significant damage to the core and filter, and no significant loss of freeboard during the MCE.

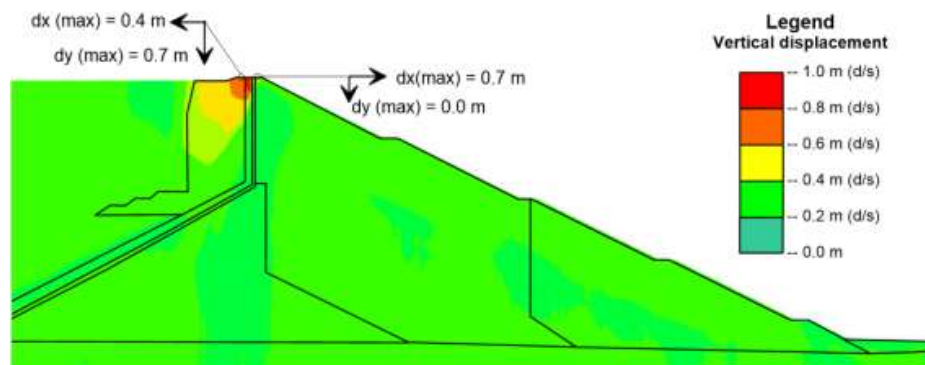


Figure 8. Results of FLAC dynamic deformation analyses for the controlling MCE

3 WATER BALANCE ANALYSES

Probabilistic water balance analyses, generally following the approach described in Truby et al. (2010), were developed cooperatively between Knight Piésold and Hudbay. The site-wide water balance model applies the 48-year precipitation record using to the Indexed Sequential Method (House & Ungvari, 1983) through a customized GoldSim® model that considers the complex interactions among the natural hydrologic conditions and the various systems in operation at the mine. Statistical analysis is performed on the multiple outcomes to estimate the water volumes corresponding to various AEPs. The construction sequence for raising the dam is planned to maintain at all times an empty volume that could safely store the 0.1 percent AEP water volume, plus an additional 2 m of freeboard. The water balance is updated by Hudbay technical services staff on at least a monthly basis to provide ongoing guidance for operation of various pumping systems, when to discharge and when to collect (harvest) water from runoff or pit dewatering efforts. Figure 9 shows historical and predicted volumes corresponding to the crest elevation, tailings surface elevation, and water surface elevations for average, 1 percent AEP and 0.1 percent AEP conditions.

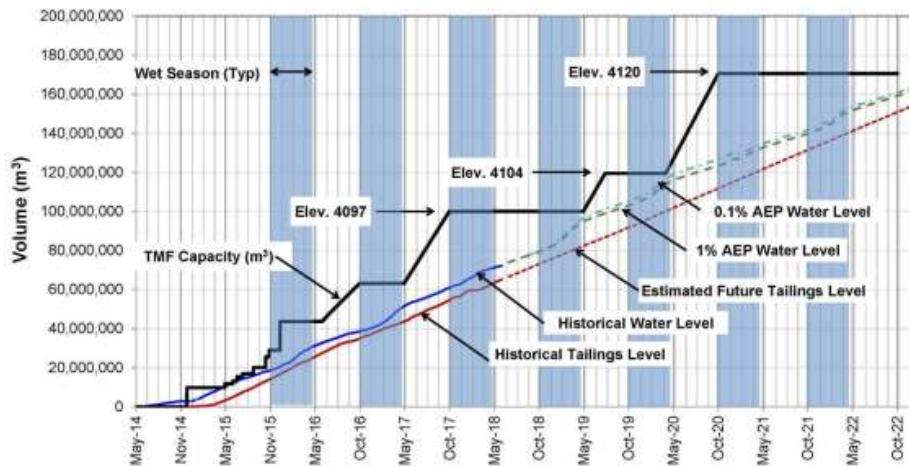


Figure 9. Probabilistic water balance projections.

4 SUMMARY

The Constancia tailings dam is a successful application of the Observational Method resulting in a robust, cost-effective design that has overcome several technical challenges. The use of compacted mine waste rock to construct to significant height a dam inherently resistant to liquefaction and stable under the expected high earthquake load is a best practice that is perhaps underappreciated with the modern emphasis on reduction of risk by new technologies such as filtering. The design philosophy of making appropriately conservative assumptions using relatively limited data, combined with reasonably conservative design criteria (such as factors of safety higher than the minimum required) provides flexibility in the design that allows optimization based on actual conditions realized during construction and operation. Regular involvement of an experienced Engineer of Record in construction and operations, combined with the oversight of an independent review board, reduces risk associated with dam stability and safe operation and maximizes the investment made by mine owners. Integration of multiple disciplines—mine planning, construction services, tailings operation, water balance, and geotechnical engineering, and environmental/permitting services—has made the Constancia project an exceptional case history.

5 REFERENCES

- Abrahamson, N.A., Gregor, N., & Addo, K. 2016. BC Hydro Ground Motion Prediction Equations for Subduction Earthquakes. *Earthquake Spectra*, 32(1): 23–44.
- ANCOLD (Australian National Committee on Large Dams). 2012. “Guidelines on Tailings Dam Design, Construction, and Operation,” May.
- Alva Hurtado Ingenieros E.I.R.L. 2013. *Estudio de Peligro Sismico, Informe Final, Mina Constancia, Chumbivilcas, Cuzco*, 33 pp. plus appendices.
- Atkinson, G. & Boore, D. 2003. “Empirical ground-motion relationships for subduction-zone earthquakes and application to Cascadia & other regions.” *Bull. Seismological Soc. America*, 93: 1703–1729.
- Atkinson, G. & Boore, D. 2008. “Erratum to empirical ground-motion relationships for subduction-zone earthquakes and their application...” *Bull. of Seismological Soc. of America*, 98: 2567–2569.
- Boore, D., Stewart, J., Seyhan, E., and Atkinson, G.M. 2014. NGA-West2 Equations for Predicting PGA, PGV, PSA for Shallow Crustal Earthquakes, *Earthquake Spectra*, 30(3): 1057-1085.
- Beatty, M., and Byrne, P. 1998. “An effective stress model for predicting liquefaction behaviour of sand.” *Geotechnical Earthquake Engineering and Soil Dynamics, GSP 75*: 766-777.
- Bray, J., and Travasarou, T. 2007. “Simplified procedure for estimating earthquake-induced deviatoric slope displacements.” *Journal of Geotechnical and Geoenvironmental Engineering*, 133(4): 381–392.
- CDA (Canadian Dam Association). 2007. “Dam Safety Guidelines,” Edmonton, Alberta, Canada.
- CDA. 2013. “2007 Dam Safety Guidelines, 2013 Edition” Edmonton, Alberta, Canada.
- Frossard, E., Hu, W., Dano, C., Hicher, P.Y. 2012.) “Rockfill shear strength evaluation: a rational method based on size effects.” *Géotechnique*, No. 62: 415–428.
- Gjerapic, G., and Znidarcic, D. 2007. “A Mass-Conservative Numerical Solution for Finite Strain Consolidation During Continuous Soil Deposition.” *Proceedings Geo-Denver2007*, Vol. GSP157.
- House, P. & Ungvari, J. 1983. “Indexed sequential modeling of hydropower system operation.” *Proceedings of Water Power 32: Int’l Conf. on Hydropower*, Vol. 2, Knoxville, Tennessee: 1046-1055.
- ICOLD (International Commission on Large Dams). 2016. “Bulletin 72: Selecting seismic parameters for large dams guidelines, 2010 edition.” International Commission on Large Dams, Paris, 37 pp.
- ICOLD, 2016. “Bulletin 148: Selecting seismic parameters for large dams guidelines.” Commission Internationale des Grands Barrages/International Commission on Large Dams, Paris, 75 pp.
- Truby, S., Kunkel, J., and Lishnevsky, V. 2010. “A priori and posterior probabilities in operational water balances for tailing storage facilities.” *Tailings and Mine Waste 2010*, pp. 131-164.
- Leps, T. 1970. “Review of Shearing Strength of Rockfill”, *Journal of the Soil Mechanics and Foundations Division*, 96(4): 1159-1170.
- Linero, S., Palma, C. and Apablaza, R. 2007. “Geotechnical characterization of waste material in very high dumps with large scale triaxial testing”, *Int’l Sym. Rock Slope Stability*, Perth, Aus., pp. 59-76.
- Lowe, J. 1964. “Shear strength of coarse embankment dam materials.” *8th International Congress on large dams*, ICOLD, Edinburgh, Scotland, pp. 745-761.
- Makdisi, F., and Seed, H. 1978. “Simplified procedure for estimating dam and embankment earthquake-induced deformations.” *Journal of Geotechnical Engineering*, 104(7): 849–867.
- Naesgaard, E. 2011. “A hybrid effective stress–total stress procedure for analyzing soil embankments subjected to potential liquefaction and flow.” PhD dissertation, University of British Columbia.
- Peck, R.B., 1969. “Advantages and Limitations of the Observational Method in Applied Soil Mechanics.” Ninth Rankine Lecture, *Geotechnique*, 19(2): 171 – 187.
- Spencer, E. 1967. “A Method of Analysis for the Stability of Embankments Assuming Parallel Interslice Forces,” *Geotechnique*, 17(1): 11-26.
- Swaigood, J. R. 2014. “Behavior of embankment dams during earthquake,” *Journal of Dam Safety, Association of State Dam Safety Officials (ASDSO)*, 12(2): 35-44.
- World Meteorological Organization (WMO) 1973. A Manual for Estimation of Probable Maximum Precipitation, Operational Hydrology Report No. 1, WMO - No. 332, Geneva, Switzerland.
- Zhao, J, Zhang, J, Asano, A, Ohno, Y, Oouchi, T, Takahashi, T, Ogawa, H, Irikura, K, Thio, H, Somerville, P, & Fukushima, Y. 2006. “Attenuation relations of strong ground motion in Japan using site classification based on predominant period.” *Bull. Seismological Society of America* No. 96, 898–913.

ACKNOWLEDGEMENTS

The authors recognize the contributions of the IPRB: Dr. Leslie Smith, Dr. Iain Bruce, Mr. James Swaisgood, and (previously) Dr. Gabriel Fernandez. The authors also thank Hudbay’s management, including Mr. Alan Hair, Mr. Cashel Meagher, and Sr. Javier del Rio, who have supported the technical excellence making this world-class facility possible.

Direct Extraction Lithium Processes: The Challenges of Spent Brine Disposal

I. Ezama and C. de los Hoyos
SRK Consulting, Salta, Salta, Argentina

P. Cortegoso and T. Braun
SRK Consulting, Denver, Colorado, USA

ABSTRACT: The significant role of lithium in the continued development and expansion of renewable and clean energy has led to an increase in the demand for projects involving the extraction of lithium from shallow brines, particularly in the ‘lithium triangle’ – Salar de Atacama in Chile, Salar de Uyuni in Bolivia and Salar de Hombre Muerto in Argentina – to be developed.

In line with increased demand, several companies have developed direct extraction processes and new technology to recover the lithium contained in brine. These direct extraction processes have emerged as an alternative to the conventional processes that are based on increasing the concentration of lithium through solar evaporation in evaporation ponds. The advantages of direct extraction processes include lower costs, shorter ramp-up periods and reduced dependence on climate.

However, management of spent brine tailings can be a significant issue if planning is inadequate. Direct extraction processes generate large amounts of spent brine (brine with a reduced lithium concentration), which may potentially affect the lithium-rich brine concentration. To prevent tailings disposal from affecting the lithium-rich brine, diligent engineering design is required. A key aspect in achieving cost-efficient direct extraction processes is providing solutions that avoid extensive use of liner in the disposal ponds or high operational costs.

This paper showcases recent experience with spent brine tailings management at projects in the lithium triangle, and experience in brine potash projects, which are similar in terms of mining methodology.

1 INTRODUCTION

Lithium is an important chemical element with many end-uses, but it is most commonly known for its powerful electrochemical properties that are harnessed in the form of efficient, lightweight lithium-ion batteries. This critical commodity keeps our world charged and connected, and has a significant role to play in the continued development and expansion of renewable, clean energy to power our world. As global demand for lithium increases, new projects and/ or increased production is required.

Lithium was traditionally extracted from minerals in igneous rocks such as pegmatites (mainly spodumene), clay minerals (mainly hectorite), and from naturally-enriched brines hosted within Salars (salt lakes) in hyper-arid regions. Following the increased demand for the mineral, projects involving the extraction of lithium from shallow brines, particularly in the ‘lithium triangle’ – Salar de Atacama in Chile, Salar de Uyuni in Bolivia and Salar de Hombre Muerto in Argentina – have gained interest from a market perspective, becoming the preferred alternative lithium source. The investor’s preference for lithium brines is based on the environmental, logistical and cost advantages during initial prospecting, exploration and development of the project. Additionally, important by-products such as potassium (K), boron (B) and sulphate (SO_4^{2-}) can be extracted from these brines and commercialised.

The increased market interest has also driven the technical evolution of the extraction process. Direct extraction technologies are an alternative to the conventional production processes. The conventional process is based on increasing the concentration of lithium through solar evaporation in evaporation ponds. The main advantage of direct extraction processes is the shorter period between extraction commencing and the first lithium carbonate (Li_2CO_3) batch being produced (almost immediate), compared with the time required to obtain a highly concentrated brine to feed to the process plant in a conventional extraction process (2 to 3 years, depending on factors such as initial concentration, final concentration requirements and climate). Other advantages of direct extraction processes include lower capital costs and reduced dependence on climate.

A generic flowchart of the two extraction alternatives is presented in Figure 1 and Figure 2, which show indicative ranges of lithium ion (Li^+) concentration and brine/water amounts based on a unit value intake. In conventional extraction methodology, most of the water in the raw brine is evaporated before the brine arrives at the final process plant. In contrast, direct extraction methodologies do not result in significantly reduced brine/ water volumes. This difference has a significant impact on the amount of spent brine disposal volumes.

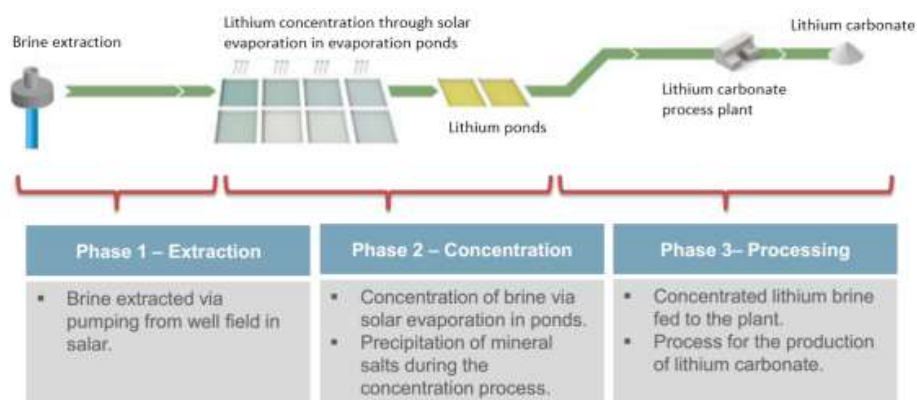


Figure 1. Conventional solar evaporation process flowchart – from Lithium Americas 2017.

Innovative & Low Cost Direct Extraction Process

Direct Extraction Process is simple, efficient, low-cost and more environmentally friendly than conventional evaporation process

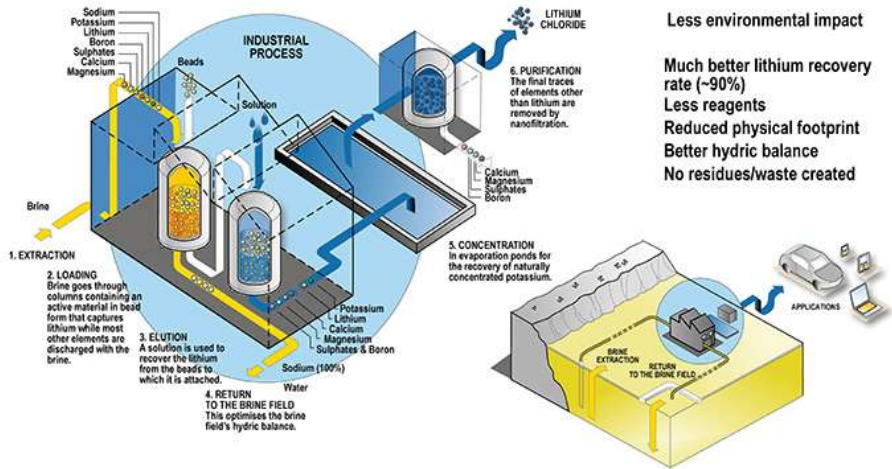


Figure 2. Direct extraction process flowchart – from article in business.gov.au

The specific details of brine lithium mining projects, and the risks and implications of the spent brine disposal are addressed in the following sections. Recent experience in the management of spent brine tailings at projects in the lithium triangle is also presented. In a wide sense, the presented concepts can be applied to a wide variety of brine projects, i.e. both conventional evaporation and direct extraction processes for lithium (Li), potassium (K), boron (Bo), sulphate (SO₄²⁻) and others.

2 BRINE RESOURCES – DYNAMIC RESOURCE

Economic concentrations of lithium-bearing brines occur in Salars (salt lakes) in select arid regions around the world. These brines account for over half of global lithium production in 2017 (USGS, 2017). Brines are unique amongst mineral deposits because the valuable elements are contained in a mobile environment, and the brine composition and grade have a temporal component, before and during extraction. Because each Salar can exhibit highly variable characteristics, there are no ‘rules of thumb’ for evaluating and classifying resources. The chemical and hydrogeological complexity of closed evaporite basins makes the exploration, evaluation, and reporting of Mineral Resources for lithium brines challenging.

Lithium mining from highly enriched brines is significantly different to classic hard-rock mining, given the fluid nature of the resource host (i.e. the brine). Classic mining is exempt from issues related to the fluid nature of the resource host, with the resource in solution, such as the potential for lithium concentration variation across time.

Given the nature of this type of project, brine resource and reserve estimation requires the application of specialised hydrogeological knowledge, i.e. hypersaline solution theories for groundwater dynamics modelling, and chemical processing engineering, i.e. brine processing for high-purity Li₂CO₃ extraction. In line with this, the hydrogeologist becomes the mining engineer, and the chemical engineer becomes the process mining engineer (Braun et al., 2016).

Brine extraction for surface processing and recovery of potash, lithium and industrial salt requires the application of traditional hydrogeological theories of hypersaline solutions. Such brines present additional technical challenges in comparison to fresh water, due to the effects of density (e.g. 1.2 g/cm³), density-driven multi- chemical composition flow on a large scale, and interaction between brines and fresh water over the course of the production period. Surface processing

facilities require estimation of brine composition over time. Therefore, the hydrogeologist is tasked with balancing extraction rates from multiple production wells, locating the production wells in space (and time), predicting chemical composition of the pre- pumping and extracted brines and monitoring depletion of a ‘dynamic’ resource. Each of these parameters can have a significant impact on project economics.

Parameters such as effective porosity, permeability (‘hydraulic conductivity’ adjusted by density and dynamic viscosity), anisotropy, aquifer configuration (extent, thickness and heterogeneity), and wellfield efficiency are key in the estimation of resources and reserves for brine extraction projects. During the pre-feasibility and feasibility stages, an accurately built numerical groundwater model is required to develop a production plan (Braun et al., 2016).

3 SPENT BRINE DISPOSAL MANAGEMENT

Direct extraction processes generate large amounts of spent brine (brine with a reduced Li⁺ concentration), which may potentially affect the concentration of lithium-rich brine. From an environmental point of view, the disposal of spent brine usually does not present major challenges because the chemical characteristics of the spent brine are usually similar to the initial resources; however, the mobile nature of highly enriched brines may turn the disposal of spent brine into a real challenge, given the potential effects of this additional flow source over the ‘dynamic’ resource.

Two usual strategies are considered for disposal of spent brine under direct extraction process:

- 1) ReInjection of spent brine back into the basin
- 2) Disposal in evaporation ponds.

Each one of these strategies has its own benefits and drawbacks and, in order to prevent negative impacts on the resources (i.e. dilution), adequate planning with respect to the spent brine management should be undertaken as part of the early stages of the project planning development.

3.1 *Spent brine reinjection*

Pumping (reinjecting) spent brine back into the basin is the traditional solution considered for the conventional evaporation process. The brine is returned to its original environment, with no impacts on the surface.

In this regard, the pumping solution is ideal. However, with large volumes of spent brine, it is likely that lithium-rich brine concentrations may become affected over time. As stated earlier, the valuable minerals in shallow brines are contained in a mobile environment, and the brine composition and grade have a temporal component, before and during extraction, driven by multi- chemical composition flow, and interaction between brines and fresh water over the course of the production period.

The inclusion of reinjection in the hydrodynamics (in addition to the rich brine hosted in the Salar and the fresh water sources) adds another source of dilution. This extra source needs to be balanced when considering the production wells (i.e. setting extraction rates, and locations over time), and when predicting chemical composition of the brines and forecasting depletion of a ‘dynamic’ resource. The extra source, i.e. the spent brine inflow, can have a significant impact on project economics, which is potentially negative if not properly considered.

High costs may also be an issue when volumes of spent brine are considerable. Capital expenditure for an alternative like this is mainly linked to the installation of pipelines and feed wells to appropriate positions (and depths). Operational costs are mainly driven by energy consumption involved in forcing brine into a saturated basin.

With the increase in volumes, strategies for controlling dilution may lead to increasing capital expenditure in the development of the discharge points. On the other hand, energy costs that are related to flow rates of the discharge and the characteristics of the aquifer, will also increase. Moreover, the discharge strategy should be included from early stages (pre-feasibility and feasibility) in the accurately built numerical groundwater model required to develop the production plan (and estimate resources and reserves), which will increase the complexity of the design.

Therefore, as this option is still viable, it should be considered as part of a holistic approach, from early stages of the project development, as it will be an important component of development

of the extraction plan. Moreover, it will be an additional element in the development of a commercial-scale brine extraction project, to be considered with similar concepts to the ones mentioned in Braun et al., 2016 and Houston et al, 2011.

3.2 *Disposing in evaporation ponds*

Disposal of spent brine in evaporation ponds seems counter-intuitive considering that a key aspect of the cost efficient direct extraction processes is providing an alternative solution that avoids the need for expansive evaporation ponds, and in particular the use of an impermeable liner – a major cost component in conventional evaporation processes. However, if seepage is not controlled (no lining is used), spent brine tailings can have a significant impact on the mineral-rich brine.

Nonetheless, taking advantage of the brine's characteristics and the environment hosting the brines, a holistic solution can be developed. This is solved by undertaking a design that balances evaporation, crystallisation and seepage to keep the recycled brine inflow to the basin at a controlled rate (and potentially at an increased mineral concentration – similar to the raw brine concentration), while developing a hybrid evaporation pond-salt stack using the reject material.

While this solution has an impact over the surface (salt landforms are developed), the mineralogical contents do not differ from the original ones in the environment, as there are no considerable additions (in terms of chemical components).

In addition, the risk of lithium-rich brine concentrations becoming diluted on time are reduced by two related aspects considered in this type of design concept, namely:

- 1) A reduction in the inflow rate
- 2) A potential increase in the mineral content of the spent brine, with a similar order of magnitude to the one in the raw brine hosted in the Salar.

Costs to be considered in the development of evaporation disposal strategy should include, among others, land to be commissioned by the salt stack (area will be related to production and climatic conditions), earthworks for containment structures, and pipelines for disposal lines. The availability of land, and the earthworks required for the containment structures, will be the critical costs.

In return, while the discharge strategy needs to be kept in mind from the early stages of the project (pre-feasibility and feasibility), it will not be necessary to include seepage in the numerical groundwater model required to develop the production plan. This reduces the complexity (and uncertainties) of the production plan design, and the requirement for iterations, allowing for a more robust estimation of the resources and reserves.

Therefore, when adequately developed from early stages of the project, this option will allow the production plan development problem to be decoupled from the brine disposal problem.

4 SHOWCASE OF DISPOSAL DESIGN STRATEGY

During the past few years, SRK has been involved in the development of a series of brine projects around the world, and particularly in the Lithium Triangle.

As part of the services provided, SRK has developed an in-house methodology to manage spent brine disposal through a holistic evaporation-stacking disposal strategy.

To showcase the magnitude of the disposal volumes, 'average' values for direct extraction projects are presented for the following design parameters:

- 1) Lithium production rate: 25ktpa Li_2CO_3
- 2) Average raw brine concentration: 400–700 mg/l Li
- 3) Overall efficiency: ~50%
- 4) Spent brine disposal rate: 1,500–3,000 m^3/hr of brine
- 5) Brine evaporation rates in the lithium triangle: 4–8 mm/day.

With the objective of achieving an economically feasible design with minimum impact over the 'dynamic' resource, the starting point for the disposal design was the study of the basin flow conditions and mineral concentrations. This considers the nature of the basin (mature - halite dominant and immature - clastic dominant, as per Houston et al., 2011), aquifer geometry, porosity, brine grades, and location of the fresh water inflows. In particular, because the disposal strategy is to keep spent brine near the surface, the availability of low conductivity zones that can be

used as a ‘natural’ liner will be of interest. As these aspects are also part of the requirements for evaluating brine prospects, only minor complementary studies need to be considered to complete this.

Closely related to this first assessment is the extraction plan. While this is the main aspect in the development of a brine prospect, and the objective is to avoid interaction between disposal and extraction, the knowledge developed during this stage can be of great value for the selection of the disposal site. In other words, the extraction plan will provide a holistic view of all aspects considered in the basin data review, which will support the site selection.

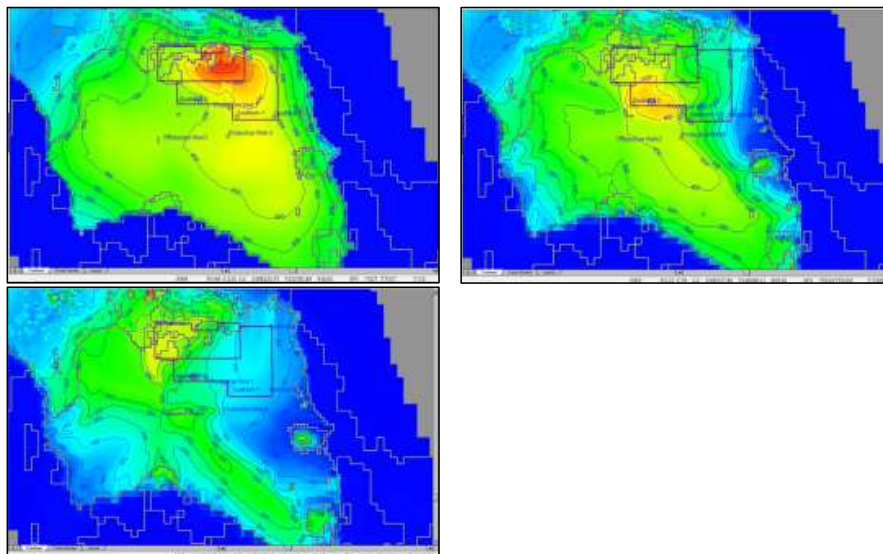


Figure 3. Li^+ concentration evolution through production for a project in the lithium triangle -situation before production start and after 20 and 100 years of production – SRK Consulting (2016b)

Once a site-wide study of the potential disposal areas has been completed, and the benefits and disadvantages in terms of potential impact over the resource are identified, specific engineering and management aspects related to disposal can be considered. Among them, critical aspects will be the disposal area sizing, and the decision for tolerance/ allowance for seepage and infiltration (quantity and quality). The required area of disposal is linked to the evaporation capacity of the site and the expected spent brine flow, and the tolerance/allowance for seepage and infiltration. The brine storage volume (and level) is to be kept at minimum, both to avoid increasing earthworks (for storing/ retaining the increased brine volumes), and to maintain a low water head (main driver for infiltration). For a project such as the example used here, and depending on the Li^+ concentration in the spent brine, an area between 500 ha and 1000 ha should be considered to achieve the objectives.

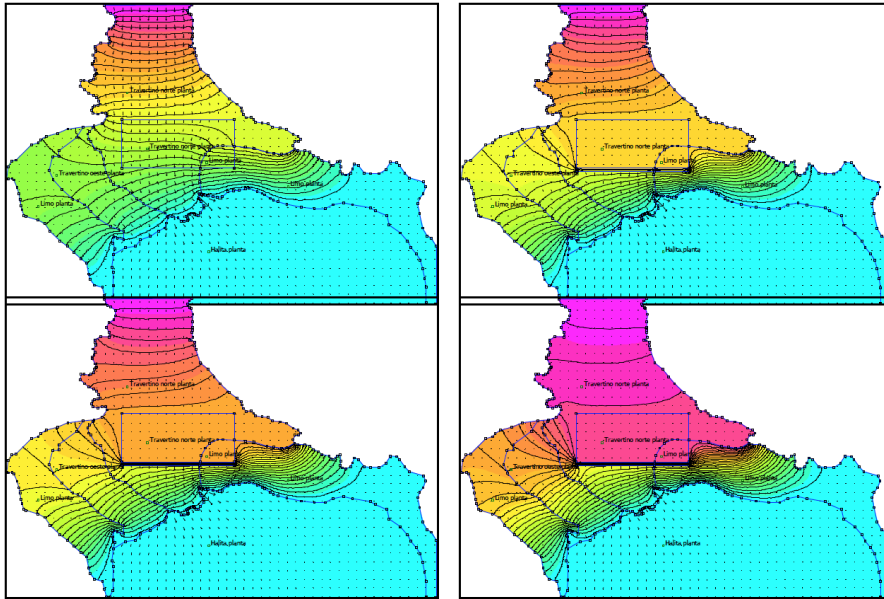


Figure 4. Recharge flow evolution over time for a project in the lithium triangle. Situation before production start and after 1, 5 and 20 years of production – internal database, SRK.

Given the areal requirements, reduction of the earthworks through the life span of the project should also be considered. The economic and financial impact of diligent engineering of the disposal facility can be significant, given the length of the facility’s perimeter. Aspects to consider include topographical characteristics of the area and the availability of local materials.

The selected area is to be assessed by undertaking an integrated mass balance to understand the evolution of the evaporation pond-salt stack hybrid disposal, focusing on reducing earthworks, and/or delaying them, while controlling seepage (quality and quantity). To do this, a design that achieves balance between evaporation, crystallisation and seepage should be undertaken, to maintain inflow of the recycled brine to the basin at a controlled rate (and potentially at an increased mineral concentration – similar to the raw brine concentration), while developing a hybrid evaporation pond-salt stack using the reject material.

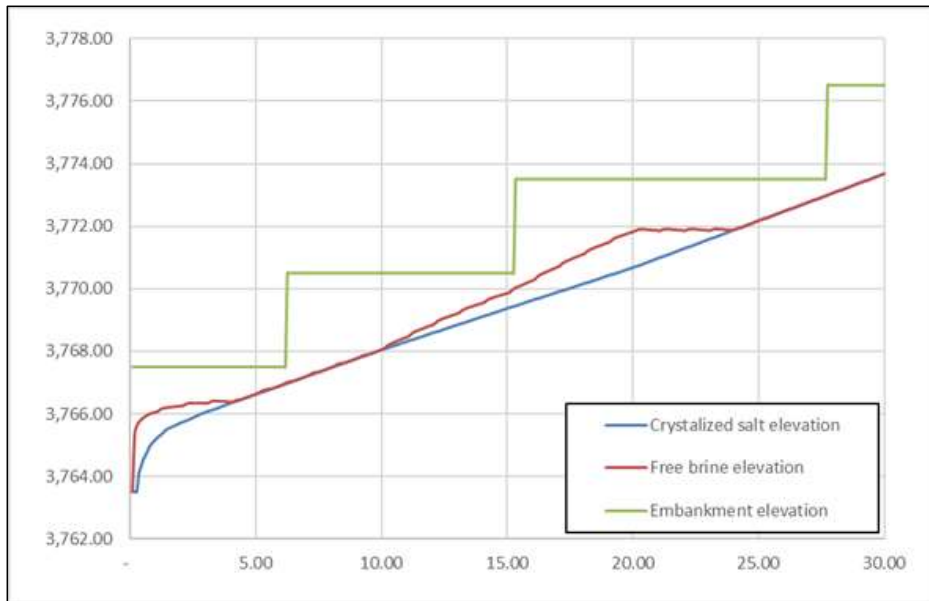


Figure 5. Brine storage level, crystallized salt elevation and embankment raising evolution over time for a project in the lithium triangle – internal database, SRK.

In terms of earthworks reduction by using local material, taking advantage of the crystallised salt, can reduce development costings significantly. However, a good understanding of the specific characteristics of this material when used for structural purposes is needed, i.e. being rock, it can dissolve, creep and have significant permeability; interaction with the disposal facility, as a whole, should be studied.

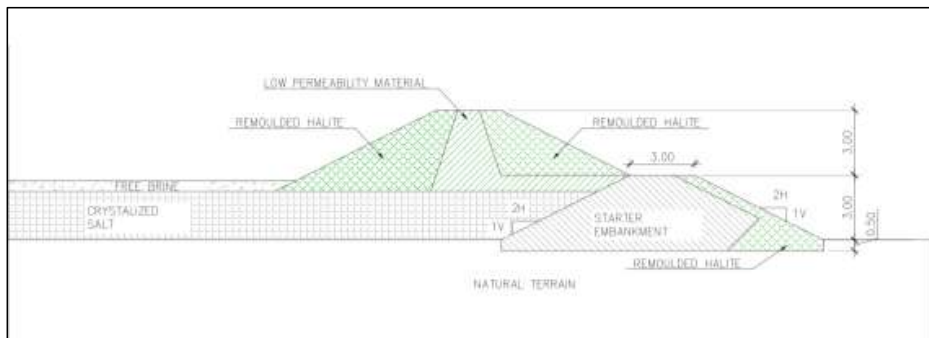


Figure 6. Typical cross section of a evaporation pond-salt stack for a project in the lithium triangle – internal database, SRK.

Finally, distance to, and difference in elevation from, the process plant will affect the sizing of the disposal pipelines and energy consumption.

Assessment of CCBE Performance with Climate Change: Case Study of the Lorraine Mine Site

G. Hotton, E. Bresson, B. Bussière and I. Demers

RIME – Research Institute on Mines and Environment, Université du Québec en Abitibi-Témiscamingue, Rouyn-Noranda, QC, Canada

P. Thomas

RIME – Research Institute on Mines and Environment, Polytechnique Montreal, Montreal, QC, Canada

R. Philippe,

Ouranos Inc., Montreal, QC, Canada

ABSTRACT: Significant changes in temperature and precipitation are projected in the coming decades across Canada as a result of climate change (CC). Notably, the frequency and duration of drought events are expected to increase. The performance of oxygen barriers such as covers with capillary barrier effects (CCBE), used to control acid mine drainage (AMD) generation, could be affected by these changes. Drought events could cause a desaturation of the moisture-retaining layer leading to an increase of the oxygen flux through the cover and AMD generation. The Lorraine mine site in Quebec was generating AMD but was rehabilitated with a CCBE in 1999. The site was used to investigate the effect of CC on the cover performance. A numerical model was developed based on meteorological and hydrogeological data and predictive simulations were performed to estimate the impact of CC on the long-term performance of the Lorraine CCBE.

1 INTRODUCTION

Mining operations generate large amounts of waste rocks and tailings that can have significant impacts on the environment if they are not properly managed. Acid mine drainage (AMD), formed when sulfide minerals contained in the mine wastes are exposed to water and oxygen, is one of the main issues faced by the mining industry (Aubertin et al., 2002, 2016). AMD can alter groundwater and surface water quality with low pH, and high concentrations of soluble metal and suspended solids (Aubertin et al., 2002). Moreover, AMD and water acidification could continue for hundreds of years after mine closure (Bussière et al., 2001). Efficient management of mine wastes is therefore a critical issue for the reclamation of closed and operating mine sites.

Preventive measures limiting environmental impacts must be taken to inhibit oxidation reaction of sulfide minerals from wastes that are potentially acid generating. Layered cover systems such as covers with capillary barrier effects (CCBE) are efficient reclamation methods to prevent acid generation. These covers are made of several types of soils with various hydrogeotechnical characteristics to limit infiltration of water and/or oxygen to the underlying tailings. A CCBE was constructed in 1999 at the Lorraine mine site, located 45 km east of Ville-Marie (Quebec, Canada; see Fig. 1). This cover was designed using laboratory and field testing, as well as numerical simulations. At that time, only the average historical precipitation rate was taken into account as climate data to define the top boundary conditions and design the cover system (Nastev and Aubertin, 2000).

However, significant changes in temperature and precipitation are expected across Quebec by the end of the 21st century (Desjarlais et al., 2010) and more intense drought events will have to be considered in design criteria (Guay et al., 2015).

The objective of this research was to investigate how CCBE performance could be impacted by climate change based on the case study of the Lorraine mine site. Preliminary results are presented in this paper. First, the cover system of Lorraine is described. Second, the methodology used for the numerical simulations and model validation are presented. Climate change expected for this region of Quebec and a simplified approach to simulate CC are described. Finally, preliminary results regarding the influence of the simplified CC scenario on the performance of the cover are discussed.



Figure 1. Location of Lorraine mine site (blue triangle) and meteorological stations used in this study (green cross). The Quebec province is in white and the region of Abitibi-Témiscamingue is surrounded in red (adapted from Ministry of Energy and Natural Resources, 2006).

2 LORRAINE MINING SITE

2.1 Background and Reclamation Strategy

The polymetallic deposit of Lorraine was discovered in 1961 and was exploited between 1964 and 1968 for copper, nickel, gold and silver (Lavergne, 1985).

The Lorraine mine generated almost 600 000 tonnes of tailings during the operation. The tailings area covered 15.5 ha before the reclamation with a thickness of a few centimetres north of the site up to 6 m to the south. The tailings were disposed of in a shallow valley which was connected to the nearby Lett creek to the south. The tailings pond was surrounded by two retention dikes to the south and west that modified the groundwater flow pattern. The water table increased to the surface, submerging the tailings in the northern part of the site and the tailings in the central and southern zone remained, however, unsaturated (Nastev and Aubertin, 2000).

The tailings composition is characterized by 10 % sulfide minerals, mainly pyrrhotite and traces of pyrite and chalcopyrite and the absence of carbonate minerals (Bernier, 1996). The acid generation potential of Lorraine tailings was evaluated using static tests; the net neutralizing potential (NNP) for the Lorraine site can be as low as -200 kgCaCO₃ eq/t (Bernier, 1996).

The tailings impoundment was abandoned during thirty years without environmental consideration at the end of the operation of Lorraine mine in 1968. Tailings were exposed to oxygen and water and sulfide oxidation occurred, mostly in the unsaturated zone. An oxidation front between 15 and 120 cm was formed, and acidic leachate was observed at the bottom of dikes. Starting in 1994, the Ministry of Energy and Natural Resources (MERN) conducted characterization field studies on the Lorraine site. At that time, measured pHs were between 2.2 and 2.6 and chemical analyses indicated high sulfate (3730 to 9190 mg/l) and metal concentrations (Cu

from 0.135 to 0.804 mg/l; Fe from 838 to 3200 mg/l; Ni from 0.21 to 9.5 mg/l; Zn from 0.19 to 1 mg/l) (Entraco, 1996).

MERN started reclamation of the Lorraine site in 1997 based on the preliminary study of Aubertin (1996). A CCBE was built as an oxygen barrier and three dolomitic and one limestone drains located at the final effluents were used as passive treatment systems. The present study focuses on the CCBE performance; more information about limestone and dolomitic drains can be found in Bussi re et al. (2009) and Potvin (2009).

2.2 CCBE and Materials Characteristics

The concept of the CCBE was developed in the 1980's (Nicholson et al., 1989; Aubertin et al. 1995, 1999). It relies on materials unsaturated properties to create a barrier against gas migration and water infiltration (Aubertin et al., 1995). A CCBE is usually composed of a fine-grained material layer placed between two layers of coarser materials. The contrast in unsaturated hydraulic properties creates capillary barrier effects which help maintaining a high degree of saturation at all time in the fine-grained layer, also called the moisture-retaining layer (MRL).

The construction of the CCBE at Lorraine site began in the summer of 1998 and ended in the spring of 1999. The cover was made of three layers, from bottom to top: a 0.3 m sandy layer acting as capillary break layer, 0.5 m of silt used as MRL, and 0.3 m of a sand and gravel protection layer (Aubertin, 1996; Nastev and Aubertin, 2000).

The Lorraine MRL is made of non-plastic inorganic silt (ML) and the sand used as the bottom capillary break layer is a uniform sand with low proportion of silt (SP-SM) according to USCS classification (ASTM D2487). The sand of the protection layer has similar properties as the capillary break layer. The main physical and hydrogeological properties of these materials are summarized in Table 1. More information about design, construction and material characterization of the CCBE can be found in Nastev and Aubertin (2000) and Dagenais (2005).

Table 1. Properties of silty and sandy materials used in the Lorraine CCBE (adapted from Dagenais et al., 2001).

Properties	Silt	Sand
D ₁₀ (mm)	0.001 to 0.0021	0.06 to 0.15
Cu	5.1 to 7.1	2.5 to 3.3
Gs	2.76	2.7
Saturated hydraulic conductivity (m/s)	2x10 ⁻⁸ to 1x10 ⁻⁷ (n from 0.42 to 0.48)	7x10 ⁻⁵ (n=0.38)
Air entry value (m of water)	2.9 to 5 (n from 0.38 to 0.46)	0.25 (n=0.38)

2.3 Instrumentation and Performance Monitoring

The instrumentation of the cover was carried out in 1999 and measurements were performed until 2011. The selection of the probes and their position in the cover (Figs 2 and 3) were based on laboratory and field studies (Aubertin et al., 1997; 1999; Bussi re, 1999; Maqsoud et al., 2007). 20 monitoring stations were initially installed along 3 instrumentation lines (Lines A, B, C; Fig. 3). An equipment update was completed in 2008 to replace the inefficient probes and to add five new stations (stations D) at the south of the site (Fig. 3).

The volumetric water content (θ) and the matrix suction (Ψ) were monitored. θ was measured for lines A, B and C using time domain reflectometry method (TDR) (Topp et al., 1980). For D stations, θ was measured with Ech2O probes which use the frequency domain (FD) (Robinson and Dean 1993; Hilhorst and Dirksen 1994). Ψ were measured with Irrrometer Watermark (WM) granular matrix sensors (White and Zegelin, 1995).

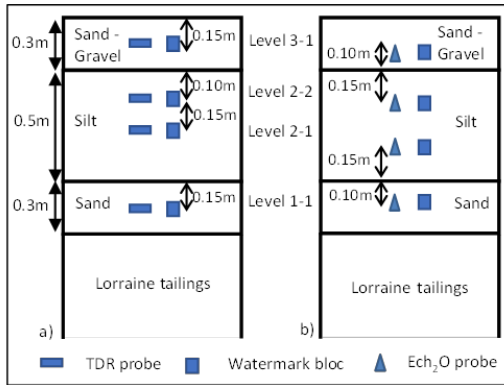


Figure 2. Configuration of the Lorraine CCBE and location of the probes for monitoring stations at a) lines A, B and C and b) line D (adapted from Dagenais et al., 2001 and Maqsoud and Bussi re, 2008).

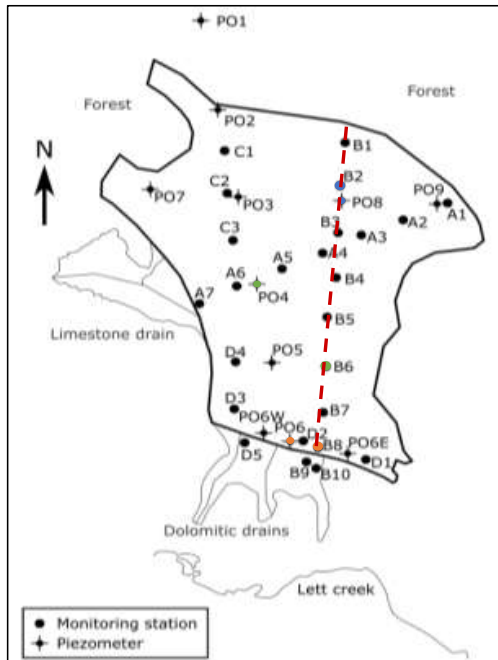


Figure 3. Location of monitoring stations and piezometers at the Lorraine site. Highlighted stations are studied in more detail in this study and the red dashed line represents the cross-section used in the numerical model (adapted from Dagenais et al., 2001 and Maqsoud and Bussi re, 2008).

θ and Ψ were measured between 4 and 8 times per year between 1999 and 2008 (Bussi re et al., 2009) and daily measurements were performed at D stations from 2008 to 2011 (Maqsoud et al., 2012). The database for this study contains more than 48 000 measurements of θ and Ψ . 11 piezometers were also installed on the Lorraine site to measure piezometric levels in the tailings ponds (Fig. 3) (Maqsoud and Bussi re, 2008). Piezometric levels were measured during the summer on a monthly basis between 1999 and 2009 and daily measurements were carried out for the PO3, PO4 and PO6 piezometers between 2009 and 2011 in order to better identify the fluctuations of the piezometric level (Maqsoud et al., 2012). Table 2 summarizes the type of probes and the frequency of measurements for the different monitoring stations and piezometers.

Several studies were carried out to evaluate the Lorraine CCBE performance since its construction (Dagenais, 2005; Bussi re et al., 2009; Maqsoud et al., 2012). These studies indicate that the degree of saturation in the MRL remains above 85 %. Ψ measurements in the MRL were mostly below the air entry value of the silt, i.e., less than 20 kPa during the 10 years following the CCBE installation (Bussi re et al., 2009). θ and Ψ measurements over the years indicate that capillary barrier effects are well developed from the centre of the tailings pond to the south. The MRL in the northern part of the site is below the water table and is consequently fully saturated at all time.

Table 2. Type of probes and frequency of θ , Ψ and piezometric level measurements for the different monitoring stations and piezometers.

Station	Probes		Period	Frequency
	θ	Ψ		
A, B and C	TDR	WM	1999 – 2008	4 to 8 times/year
D	Ech ₂ O	WM	2008 – 2011	Daily
Piezometer	Probes		Period	Frequency
PO1 to 9	Manual		1999 – 2009	4 to 6 times/year
PO3, 4 and 6	Automatic		2009 – 2011	Daily

3 NUMERICAL MODEL

One of the main objective of this study was to validate a numerical model with the data gathered from 1999 to 2012 and to make long term predictions using boundary conditions that represent, at least partially, future CC.

3.1 SEEP/W 2018

SEEP/W 2018 (Geo-Slope International Ltd., 2017) was used to simulate the hydrogeological behaviour of the Lorraine CCBE. SEEP/W is a Finite Element Model (FEM) and can simulate the movement of liquid water or water vapour through saturated and unsaturated porous media (Geo-Slope International Ltd. 2017). Previous works have demonstrated the capacity of SEEP/W to simulate similar conditions; good correlation between simulated results and laboratory or field measurements was observed by Bussi re et al. (2003), Dagenais (2005), Aubertin et al., (2009), Pabst (2011), Kalonji-Kabambi et al. (2017).

3.2 Numerical Model Geometry

The numerical model built with SEEP/W simulates a cross section along the B transect (Fig. 3). The section crosses the tailings pond from the southern dike to the submerged zone at the northwest. The numerical model geometry is based on the previous work of Dagenais (2005). Figure 4 shows the geometry of the model in the dyke area (a) and in the flooded area (b). The Lorraine site is 352 m long but the model was shortened to simulate a section of 125 m long to

simplify the numerical model and reduce the calculation time. The proposed model is appropriate to evaluate the vulnerability of the CCBE to CC since the desaturation could essentially be present close to the dyke. Lorraine tailings are 4.5 m thick. The dyke is made of waste rock and is 4 m high, 15 m long at the bottom and 5 m long at the top. The drain material is placed on the downstream side of the dyke.

The mesh is made of a total of 37,379 quadrilateral and triangular elements. The mesh density is higher in the cover layers than in the tailings to improve the precision of the calculations in this critical zone.

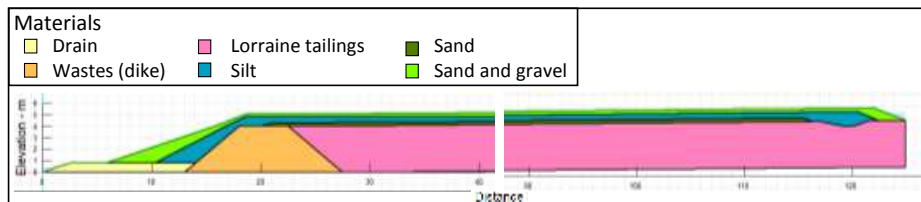


Figure 4. Numerical model of Lorraine site CCBE with SEEP/W a) south dike sector b) north-east limit of the cover.

3.3 Material Properties of Numerical Model

Each material is defined in SEEP/W by assigning a water retention curve (WRC) and a permeability function (k_a). The van Genuchten (1980) method was used in this study to describe the water retention curve; permeability functions and WRCs are shown in Figure 5. The drain material properties were obtained from the SEEP/W library and corresponded to a uniform sand. The other material properties were defined using field and laboratory tests (Table 3; Dagenais, 2005).

Table 3. Material properties used in numerical simulations (adapted from Dagenais, 2005).

Materials	k_{sat} (m/s)	θ_s	θ_r	α (/cm)	n_v
Drain	1×10^{-4}	0.34	0.07	-	-
Wastes (dike)	7×10^{-4}	0.42	0.1	0.011	2.9
Lorraine tailings	1×10^{-6}	0.41	0.13	0.0039	2.1
Silt	3×10^{-8}	0.38	0.05	0.0014	1.7
Sand	8×10^{-5}	0.36	0.03	0.03	4
Sand and gravel	9×10^{-4}	0.33	0.07	0.08	2.5

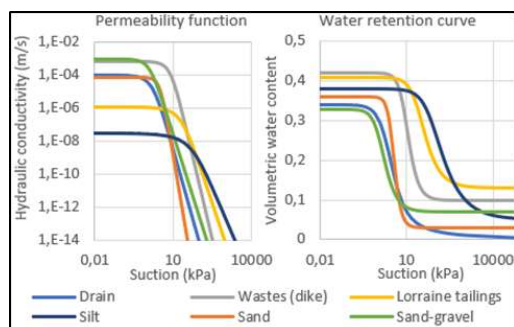


Figure 5. Permeability functions and WRCs of materials used in the numerical simulation.

3.4 Climate Conditions

3.4.1 Historical Climate Data

Most of the climate data (temperature, precipitation, speed and direction of the wind) used for the numerical simulations of the Lorraine site were obtained from Environment and Climate Change Canada's meteorological stations of Latulipe and Angliers which are respectively 10 km and 30 km north-east of the site (Fig. 1). Measurements from more distant stations such as Remigny, Earlton, Rouyn-Noranda and Val-d'Or were also used to complete missing data in the dataset (Fig. 1). A complete data set from 1999 to 2007 was established with daily net recharge and daily mean temperatures (Fig. 6).

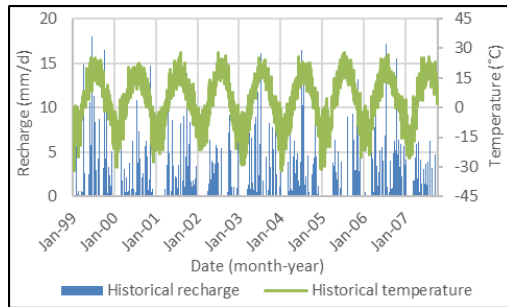


Figure 6. Daily net recharge in mm/d and mean temperature in °C from 1999 to 2007.

Data of temperature and precipitation (rain and snow) were used to estimate infiltration (INF) (Eq. 1 and 2) and evapotranspiration (EVT) (Eq. 3 to 5). The net recharge (NR) was then calculated from INF and EVT values (Eq. 6 and 7) and was applied as top boundary conditions for the simulations with historical climate. Equations 1 to 7 are calculated for each day of the dataset (d). This approach was taken for another mine site in Quebec (Richelieu Hydrogéologie Inc., 2010).

$$\begin{aligned} \text{If } T > 0^{\circ}\text{C}; \quad \text{INF} &= ((\text{SG}_{d-1} - \text{SG}_d) / 2 + P) / 2.25 \text{ (mm)} & [1] \\ \text{If } T < 0^{\circ}\text{C}; \quad \text{INF} &= 0 \text{ mm} & [2] \end{aligned}$$

$$\begin{aligned} \text{If } T > 10^{\circ}\text{C}; \quad \text{EVT} &= 2 \text{ mm} & [3] \\ \text{If } T > 15^{\circ}\text{C}; \quad \text{EVT} &= 4 \text{ mm} & [4] \\ \text{If } T < 10^{\circ}\text{C}; \quad \text{EVT} &= 0 \text{ mm} & [5] \end{aligned}$$

$$\begin{aligned} \text{If } \text{INF} - \text{EVT} < 0; \quad \text{NR} &= 0 \text{ mm} & [6] \\ \text{If } \text{INF} - \text{EVT} > 0; \quad \text{NR} &= \text{INF} - \text{EVT} \text{ (mm)} & [7] \end{aligned}$$

With T the temperature in Celsius degree; SG_{d-1} the snow on ground in cm for d-1; SG_d the snow on ground for d; P the daily liquid precipitation in mm, 2.25 value is used as a correction factor for the run-off.

3.4.2 Climate Data with CC

In Quebec, south of the 50th parallel, where the region of Abitibi-Témiscamingue is located, mean temperatures and precipitations are projected to increase by the end of the century, as well as extreme precipitation and severe drought events (Plummer et al., 2006; Desjarlais et al.,

2010; Guay et al., 2015). More drastic drought events could affect CCBE effectiveness that depends mainly on the degree of saturation in the MRL.

A two-month period without precipitation is currently used in the design of reclamation system to simulate extreme drought events (Bussi re et al., 2003; Broda et al., 2014). This criterion is representative of current extreme conditions in the Abitibi-T miscamingue region of Quebec, but it is not based on a systematic analysis of historical meteorological data. A research work is underway to propose a new drought index that could be used for long term predictions of CCBE performance that integrate CC (see Bresson et al., 2018; in prep.).

The simplified climate change scenario (SCCS) proposed in this study is based on recent studies (Ouranos, 2015; Ethier, 2018). The SCCS consists in a period of 74 days without precipitation, i.e., a 20 % longer period than current dry spells, and with total annual precipitation 20 % higher than the historical climate. The recharge associated to this scenario compared to the historical climate is showed in Figure 7 for a one-year period.

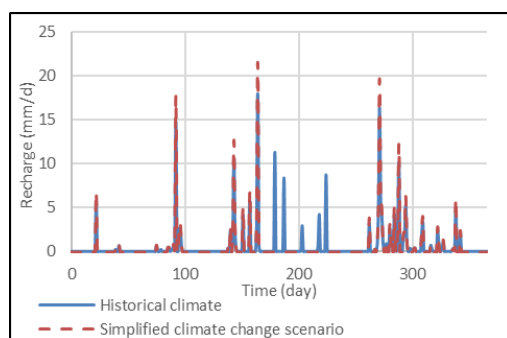


Figure 7. Recharge rate in mm/d imposed in the model for the historical climate and for the SCCS for one year. Day 0 corresponds to January 1st.

3.5 Other Boundary Conditions

The tailings pond foundation is composed of till which can be considered as impermeable. Hence, an impermeable boundary condition is applied at the bottom of the numerical model. A pressure head of 0 m is applied at the exit of the drain which represents the final effluent. The cover is bordered by a small body of water at the north-west limit, so a pressure head of 0 m is also applied at the surface.

4 PRELIMINARY NUMERICAL RESULTS

4.1 Numerical Model Validation

Initial conditions were simulated under steady state conditions with a 0 m head at the exit of the drain.

The model was then validated comparing field data with simulated data. Figure 8 compares piezometer measurements from 1999 to 2003 with simulated piezometric heads. The location of the three piezometers (PO4, PO6 and PO8) is indicated in Figure. 3. Figure 9 shows the predicted volumetric water content and the field measurements from 1999 to 2004 in the MRL at B6 station located in the unsaturated zone, close to the dyke. The numerical simulations generally show good agreement with measured values. This validation indicates that the model can reproduce the hydrogeological behaviour of the Lorraine CCBE exposed to natural conditions.

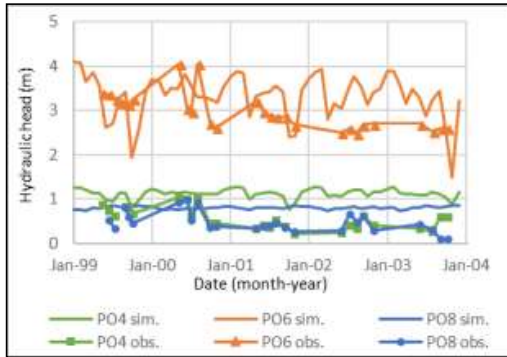


Figure 9. Observed (obs.) vs. simulated (sim.) piezometric heads from CCBE surface at 3 observation wells (PO4, PO6 and PO8) from May 14th 1999 to October 9th 2003.

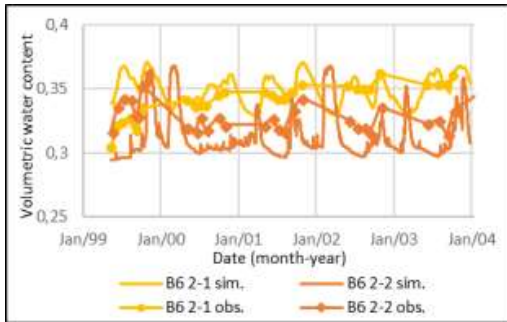


Figure 8. Observed (obs.) vs. simulated (sim.) volumetric water contents at levels 2-2 and 2-1 in the MRL at the monitoring station B6 from May 14th 1999 to January 1st 2004.

4.2 Simulations with SCCS

The piezometric levels simulated with the SCCS present only slight differences with those simulated with historical climate data (Fig. 10). Hydraulic heads are slightly influenced by SCCS both in the northern part of the site (PO4 and PO8) and the southern part which is unsaturated (PO6). Hydraulic head simulated at PO8 location with SCCS indicates an average of the piezometric level at approximately 0.73 m below the surface while the average for the current climate is slightly higher, close to 0.80 m below the surface. At PO4 and PO6, higher differences between simulation with current climate and with SCCS are observed for the drought events periods. A decrease of the hydraulic head is notable each year when the 74 days without precipitation are applied (Fig. 10).

Few minor differences are also observed in terms of volumetric water contents. The differences between historical climate data and SCCS are smaller than 0.04, which indicate that the modification of the top boundary conditions with the SCCS did not affect significantly the degree of saturation in the MRL.

Additional numerical analyses are currently ongoing to confirm these results by including a parametric study and top boundary conditions adapted to more realistic climate change.

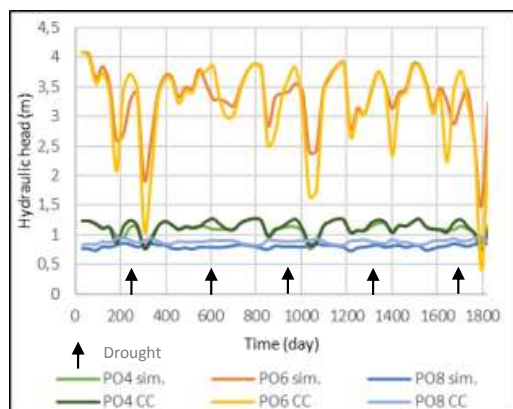


Figure 10. Piezometric levels from CCBE surface simulated with historical climate (sim.) vs. SCCS at 3 observations wells (PO4, 6 and 8) for a period of 5 years.

5 CONCLUSION

Hydrogeological modelling is an effective method to assess the performance of cover systems such as CCBE. Climate conditions can be applied in such models as top boundary conditions and the influence of climate change on CCBE performance can therefore be evaluated.

The case study of the Lorraine mine site allows the validation of a numerical model using field data (climate conditions, piezometric levels and volumetric water contents). A simplified climate change scenario was applied in this work by simulating a period of 74 consecutive days without precipitation and increasing rainfall by 20 % (except during the dry period) compared to the observed historical climate. No major impact on the performance of the cover system was found. It is important to note that the climate change scenario tested here is idealized and simplified.

As next steps, climate projections will be defined by global climate models and will be used to obtain more realistic climate conditions, adapted to the Lorraine mine site. Extreme boundary conditions will be proposed by the development of a drought index, leading to the assessment of the CCBE performance according to these new parameters (see Bresson et al., 2018; in prep.).

ACKNOWLEDGMENTS

This work was funded by the *Fonds de recherche du Québec – Nature et technologies* (FRQNT) and the Research Institute on Mines and the Environment (RIME) UQAT-Polytechnique (www.irme.ca/en). The authors would like to thank also the Ministry of Energy and Natural Resources of Quebec (MERN), and Ouranos Inc. for their support.

REFERENCES

- Aubertin, M. 1996. *Recouvrement multicouche pour le parc à résidus du site minier Lorraine*. Report submitted to MRNQ (SDM-R-96-23). 30 p.
- Aubertin, M., Chapuis, R., Aachib, M., Bussière, B., Ricard, J. and Tremblay, L. 1995. *Évaluation en laboratoire de barrières sèches construites à partir de résidus miniers*. École Polytechnique de Montréal, QC, Canada, NEDEM/MEND Projet 2.22.2a, 199p.

- Aubertin, M., Bussière, B., Barbera, J.M., Chapuis, R.P., Monzon, M. and Aachib, M. 1997. Construction and instrumentation of in situ test plots to evaluate covers built with clean tailings. *4th International Conference on Acid Rock Drainage*, Vancouver, BC, Canada, Vol. 2, 715-730.
- Aubertin, M., Bussière, B., Monzon, M., Joanes, A.M., Gagnon, D., Barbera, J.-M., Aachib, M., Bedard, C., Chapuis, R.P. and Bernier, L. 1999. *Étude sur les barrières sèches construites à partir des résidus miniers. - Phase II : Essais en place*. Research report Projet CDT P1899, NEDEM/MEND 2.22.2c, 331p.
- Aubertin, M., Bussière and B., Bernier, L. 2002. Environnement et gestion des résidus miniers [CD-ROM]. *Les Presses Internationales Polytechnique de Montréal*, QC, Canada.
- Aubertin, M., Cifuentes, E., Apithy, S., Bussière, B., Molson, J. and Chapuis, R.P. 2009. Analyses of water diversion along inclined covers with capillary barrier effects. *Canadian Geotechnical Journal*, 46(10), 1146-1164.
- Aubertin, M., Bussière, B., Pabst, T., James, M. and Mbonimpa, M. 2016. Review of the reclamation techniques for acid-generating mine wastes upon closure of disposal sites. *Geo-Chicago 2016* (pp. 343-358).
- Bernier, L. 1996. *Rapport d'analyses minéralogiques sur 7 échantillons de résidus miniers, Mine Lorraine, Témiscamingue, Québec*. Géoberex Recherche, 14 p.
- Bresson, É., Demers, I., Roy, P., Pabst, T. and Chavailleaz, Y. 2018. Effectiveness of oxygen barriers under climate change: definition of a drought index. *Tailings and Mine Waste '18 Conference, Keystone, Colorado, USA, Sept.30-Oct.2, 2018*.
- Broda, S., Aubertin, M., Blessent, D., Maqsood, A. and Bussière, B. 2014. Simulating the variation of the phreatic surface level to assess reclamation techniques for an acidic tailings impoundment - A field-scale study. *GeoRegina 2014: 67th CGS Conference*, Regina, SK, Canada. 7p.
- Bussière, B. 1999. *Étude du comportement hydrique de couvertures avec effets de barrières capillaires inclinées à l'aide de modélisations physiques et numériques*. Ph. D. Thesis, Department of Civil, Geological and Mining Engineering, École Polytechnique de Montréal, QC, Canada.
- Bussière, B., Aubertin, M. and Julien, M. 2001. Couvertures avec effets de barrière capillaire pour limiter le drainage minier acide, aspects théoriques et pratiques. *Vecteur Environnement*, 34(3), 37-50.
- Bussière, B., Aubertin, M. and Chapuis, R.P. 2003. The behavior of inclined covers used as oxygen barriers. *Canadian Geotechnical Journal*, 40(3), 512-535.
- Bussière, B., Potvin, R., Dagenais, A. M., Aubertin, M., Maqsood, A. and Cyr, J. 2009. Restauration du site minier Lorraine, Latulipe, Québec : Résultats de 10 ans de suivi. *Déchets Sciences Et Techniques*, 54, 49-64.
- Dagenais, A.M., Aubertin, M., Bussière, B., Bernier, L. and Cyr, J. 2001. Monitoring at the Lorraine mine site: a follow up on the remediation plan. In 2001 *National Association of Abandoned Mine Land Programs Annual Conference*: Land Reborn: Tolls for the 21st Century, Athens, OH, USA, Proceedings on CD-Rom.
- Dagenais, A.M. 2005. *Techniques de contrôle du drainage minier acide basées sur les effets capillaires*. Ph. D. Thesis, Department of Civil, Geological and Mining Engineering, École Polytechnique de Montréal, QC, Canada.
- Desjarlais, C., Allard, M., Bélanger, D., Blondlot, A., Bouffard, A., Bourque, A., Chaumont, D., Gosselin, P., Houle, D., Larrivée, C., Lease, N., Pham, A.T., Roy, R., Savard, J.P., Turcotte, R. and Villeneuve, C. 2010. *Savoir s'adapter aux changements climatiques*. Ouranos, Montréal, QC, Canada, 128p.
- Ethier, M. P., Bussière, B., Broda, S. and Aubertin, M. 2018. Three-dimensional hydrogeological modeling to assess the elevated-water-table technique for controlling acid generation from an abandoned tailings site in Quebec, Canada. *Hydrogeology Journal*, 1-19.
- Entraco Inc. 1996. *Conception d'un programme de restauration du site minier Lorraine*. Final report. 70p.
- Geo-Slope International Ltd. 2017. *Heat and mass transfer modeling with GeoStudio 2018*. Calgary, AB, Canada.
- Guay, C., Minville, M. and Braun, M. 2015. A global portrait of hydrological changes at the 2050 horizon for the province of Québec. *Canadian Water Resources*, 40(3), 285-302.
- Hilhorst M.A. and Dirksen C. 1994. Dielectric water content sensors: Time domain versus frequency domain. p. 23-33. *Symposium on TDR in Environmental, Infrastructure and Mining Applications*. Northwestern Univ., Evanston, IL. Sept. 1994. Special Publication. SP 19-94. U.S. Dep. of Interior Bureau of Mines, U.S. Gov. Print. Office, Washington, DC, USA.
- Kabambi, A.K., Bussière, B. and Demers, I. 2017. Hydrogeological Behaviour of Covers with Capillary Barrier Effects Made of Mining Materials. *Geotechnical and Geological Engineering*, 35(3), 1199-1220.
- Lavergne, C. 1985. *Gîtes minéraux à tonnage évalué et production minérale du Québec*. Ministère de l'Énergie et des Ressources. DV 85-08, 76 pp.

- Maqsoud, A. and Bussière, B. 2008. Mise à jour de l'instrumentation du site Lorraine. Report of URSTM submitted to MRNF, 12 pp.
- Maqsoud, A., Bussière, B., Mbonimpa, M., Aubertin, M., and Wilson, W.G. 2007. Instrumentation and monitoring of covers used to control Acid Mine drainage. *Mining Industry Conference, CIM*, Montreal, QC, Canada, CD-ROM.
- Maqsoud, A., Bussière, B., Aubertin and M., Cyr, J. 2012. Transient hydrogeological behaviour of the Lorraine CCBE (Québec, Canada). *GESRIM 2012: International Congress on the Management of the Mining Wastes and Closed Mines*, 3-6 Avril 2012, Marrakech, Morocco.
- Nastev, M. and Aubertin, M. 2000. Hydrogeological modelling for the reclamation work at the Lorraine mine site Québec. *53rd Canadian Geotechnical Conference and 1st joint IAHCNC and CGS Ground-water Specialty Conference*, Montreal, QC, Canada, pp. 311-318.
- Nicholson, R.V., Gillham, R.W.M. Cherry, J.A. and Reardon. E.J. 1989. Reduction of acid generation in mine tailings through the use of moisture-retaining cover layers as oxygen barriers. *Canadian Geotechnical Journal*, vol. 26, pp.1-8.
- Ouranos 2015. *Vers l'adaptation. Synthèse des connaissances sur les changements climatiques au Québec. Partie I : Evolution climatique au Québec*. Edition 2015. Montreal, QC, Canada, 114 p.
- Pabst, T. 2011. *Etude expérimentale et numérique du comportement hydro-géochimique de recouvrement placé sur des résidus sulfureux partiellement oxydés*. Doctoral Thesis, Department of Civil, Geological and Mining Engineering, École Polytechnique de Montréal, QC, Canada.
- Plummer, D. A., Caya, D., Frigon, A., Côté, H., Giguère, M., Paquin, D., Biner, S., Harvery, R. and De Elia, R. 2006. Climate and climate change over North America as simulated by the Canadian RCM. *Journal of Climate*, 19(13), 3112-3132.
- Potvin, R. 2009. *Évaluation à différentes échelles de la performance de systèmes de traitement passif pour des effluents fortement contaminés par le drainage minier acide*. Doctoral thesis, Université du Québec en Abitibi-Témiscamingue, QC, Canada.
- Richelieu Hydrogéologie Inc., 2010. *Étude hydrogéologique, Site Manitou, Val-d'Or (Québec)*. Unpublished report.
- Robinson, M., Dean, T.J. 1993. Measurement of near surface soil water content using a capacitance probe. *Hydrological Processes*, 7, 77-86.
- Topp, G.C., Davis, J.L. and Annan, A.P. 1980. Electromagnetic determination of soil water content: measurement in coaxial transmission lines. *Water Resources Research*, vol. 16, pp. 574-582.
- Van Genuchten, M.Th. 1980. A closed-form equation for predicting the hydraulic conductivity of unsaturated soils. *Soil Science Society of America Journal*, 44(5): 892-898.
- White, I. and Zegelin, S.J. 1995. *Electric and dielectric methods for monitoring soil-water content. Handbook of vadoze zone characterization and monitoring*. Wilson, L.G., Everett, L.G. et Cullen, S.J. éditeurs. CRC Press, Boca Raton, FL, USA.

Closure of Abandoned and Derelict Asbestos Mines: Design, Construction and Monitoring

R. Mayne and W. Naidoo
SRK Consulting, Johannesburg, South Africa

X. Adams
SRK Consulting, Cape Town, South Africa

ABSTRACT: Historically, many mines in South Africa did not implement closure plans once resources were depleted. This has resulted in approximately 6 000 ownerless and derelict mines across the country for which the South African government now has closure responsibility. These include mines for almost all minerals exploited in South Africa. As these abandoned operations often represent a significant Health, Safety and Environmental risk, the authorities have instituted a program of rehabilitation activities to affect closure. Given the health risks such as asbestosis and mesothelioma associated with asbestos, the authorities have focused attention initially on the rehabilitation of defunct asbestos mines.

The design of rehabilitation and closure measures for these asbestos mines involved a multi-disciplinary team to assist with the identification of site specific risks for which remedial measures are required. Mitigation of risks was the driver for the conceptual design, and ultimately the final design of closure. This included preventing the mobilization of loose fibers from mining waste. The majority of mines are located in steep terrain, requiring particular attention to erosion protection and other water related damage. The integration of technical disciplines was thus key to closure designs and required geotechnical, environmental and civil engineering, hydrological, geological and other scientific inputs.

This paper describes the thought processes followed to realize the above-mentioned designs, at the same time discussing these designs. Establishing closure concepts in a site specific context and the utilization of these concepts to develop detailed design is described. Specific phases followed throughout the decision making and engineering process are discussed to illustrate how practical closure of the abandoned and derelict asbestos mines was achieved.

1 INTRODUCTION

Given the long history of mining in South Africa, as well as changes in industry development and specific mineral demands worldwide, some mines have not implemented environmental closure after operation. This has resulted in there being approximately 6 000 ownerless and derelict mines across the country for which the Department of Mineral Resources (DMR) has inherited closure responsibility. Mining for all manner of minerals was carried out at these mines.

To mitigate significant Health, Safety and Environmental risk, the Department of Mineral Resources (DMR) instituted a program to affect closure. This program has been in place for some 33 years and has evolved to address specific closure related challenges. Given health risks such as asbestosis, mesothelioma, lung cancer and pleural plaques due to exposure to asbestos fibers, the DMR has focused its attention on the rehabilitation of historical asbestos (but not limited to) mines primarily in the Northern Cape, Mpumalanga and Limpopo Provinces of South Africa. The closure of certain of these operations is being facilitated by Mintek, a national mineral research organization, who is the appointed implementation agent.

SRK Consulting (South Africa) (Pty) Ltd (SRK) was appointed by Mintek in the last quarter of 2013, to provide engineering and design services for mine rehabilitation projects for several of these asbestos mines. By mid-2016, closure measures had successfully been implemented for some of the sites in the Northern Cape, Mpumalanga and Limpopo Provinces. This paper will focus on case studies from the Limpopo province only.

Utilizing an internal non-negotiable Health and Safety requirement, based on the South African Asbestos Regulations of the Occupational Health and Safety Act of 1993, SRK has deployed a multidisciplinary team to assist with the identification of site specific risks for which remedial measures are required.

Mitigation of on-site risks informs the conceptual design and ultimately the final design of remedial measures. This includes the preventing of loose fibers present on surface where mining and processing activities took place from being mobilized. Similarly efforts are targeted at reducing the potential mobilization of fibers in the rock matrix in which asbestos was contained. The closure activities also include sealing of the means of ingress and egress from the workings. The majority of the abandoned mines are located in steep terrain, requiring protection from erosion and other water related damage in the closure design.

Being set within the South African context, this paper aims to take the reader through the thought processes relevant to the project. It also aims to illustrate the progressive development in the design evolution from the commencement of the project to the current applications taking place.

2 BACKGROUND

During the mid-1980s, asbestos was described as being one of the most widely used minerals known to man, as well as being one of the oldest minerals utilized in various applications. Asbestos was reportedly used more than 200 years ago in China, Egypt and Greece and its name is derived from the Greek for ‘inextinguishable flame’. One of its earliest applications was that it was a virtually indestructible wick for oil lamps (Hart 1988). Asbestos was utilized in various applications in the construction and industrial process, due to its many characteristics, which included its high tensile strength, resistance to heat and fire as well as its basic durability and versatility.

In the South African context, asbestos ore is unique within the mineral rich country. Asbestos occurs in the country in six types of asbestiform minerals, although only three of these types were mined and milled on a commercial scale (crocidolite, amosite and chrysotile). While asbestos was used locally in South Africa, the majority was exported worldwide (James I. Phillip, David Rees, Jill Murray and John C.A. Davies 2012).

Asbestos mining in South Africa began in earnest in the 1930s and it attracted multitude of large and small companies and even individuals such as farmers exploiting the mineral on their farm properties at a small scale (Hart 1988). Legislation in South Africa banning the use of all types of asbestos came into effect in 2008, which was a few years after the last asbestos producing mine stopped production in 2001 and closed in 2002. The mining of asbestos left a legacy of disease and environmental contamination through mining activities and the transport of asbestos and asbestos containing products (James I. Phillip, David Rees, Jill Murray and John C.A. Davies 2012).

3 LEGISLATION

Although South Africa has a long history of mining, it was the 1991 Minerals Act (Act 50 of 1991) that formally required operations to undertake rehabilitation activities. This was undertaken through the inclusion of the requirement that the rehabilitation of the surface of land concerned in any prospecting or mining operation, shall be carried out by the holder. The holder of the permit/authorization must restore the surface of the land to its natural state or predetermined land use that complies with the concept of sustainable development. The management of environmental impacts during prospecting or mining must proceed in accordance with an approved environmental management program (EMP) based on an environmental impact assessment. En-

vironmental management shall be done as an integral part of and simultaneously with prospecting or mining operations. The holder must, furthermore, make financial provision for the execution of his/her EMP and provide the then Department of Minerals and Energy (DME) with the necessary financial guarantees (Department of Minerals and Energy, 2011).

The holder of such prospecting permit or mining authorization remains liable for complying with the relevant provisions of the Act until a certificate in terms of section 12 of the Act has been issued to the effect that the said provisions have been complied with. Where a mine has been closed in terms of this section and the mine residue deposits rehabilitated, a certificate will be issued to the mine (Department of Minerals and Energy, 2011).

In the case of derelict and/or ownerless asbestos mines, Government, in the absence of a legally responsible person and subject to the availability of funds, acts in the interest of a community and the environment by addressing the pollution emanating from such mines (Department of Minerals and Energy, 2011).

The need to rehabilitate derelict and/or ownerless asbestos mines as a matter of extreme urgency was identified in 1986 after it became internationally accepted that asbestos fibers pose a serious health risk to humans as a cause of lung-related diseases such as lung cancer, asbestosis and mesothelioma when inhaled. Steps were taken in 1986 to rehabilitate the most critical asbestos pollution sources (Department of Minerals and Energy, 2011).

4 DESIGN PHILOSOPHY

SRK used the Standard Protocol and Guidelines for the rehabilitation of Derelict/Ownerless Asbestos Mine Residue Deposits in South Africa, compiled by the old Department of Minerals and Energy (DME), as basic guidance in the design process. However, because of the widespread distribution and microscopic nature of asbestos fiber contamination, achieving the objectives described within the standard protocol, was challenging, and not practically achievable or accurately quantifiable.

SRK therefore adopted a more pragmatic approach, when applying design criteria to the individual sites. Our initial criteria were slightly modified to incorporate client specific requirements. However, further development of a consistent design criteria and definition of the level of remediation necessary to obtain “adequate closure” may still be required as performance of the remedial measures evolves.

SRKs primary objective when designing remedial works was to provide mitigation measures to limit the potential mobilization of asbestos by the pathways listed below:

- Wind;
- Water;
- Animal and human foot-traffic; and
- Vehicular traffic.

Our approach to achieving the primary objective is described below.

4.1 *Limiting erosion to prevent mobilization of asbestos material*

4.1.1 *Cover design (Rock Cladding)*

Erosion rates are controlled by various factors which include, but are not limited to, soil type, precipitation intensity, slope angle and length, vegetation cover and the amount of surface armor from rock fragments that serve to dissipate raindrop energy and related runoff velocities (Milczarek et.al, 2011). Due to time and budgetary constraints, extensive erosion modelling was not done.

Various mitigations are considered in the design of a cover material. These include, but again are not limited to, gabion basket/reno mattress combinations; stabilized soil crete cover; concrete and rock paving; rock cladding; the application of shotcrete/gunite; the installation and vegetation of a geofabric (such as hessian sheets); the installation, fill and vegetation of geocells; application of foams to bind asbestos fibers insitu such as formaldehyde or polyurethane foam; application of a binding primer or resin or the application and vegetation of topsoil.

The application of topsoil and establishment of indigenous vegetation is the preferred rehabilitation measure by the DMR (DMR, 2011). As asbestos fibers are, for the most part, unable to migrate through soil, this proves to be an effective containment cover medium. Establishment of vegetation, however, may prove difficult due to dry and arid conditions at some rehabilitation sites.

Rock cladding has been proven to be effective on moderately steep slopes or areas where vegetation is not effective or difficult to establish (M. Smith, 2004). Table 1 below contains the considerations in the design of a rock cladding layer and their relevance in application to these projects.

Table 1. Considerations during design of a rock armouring layer to a tailings storage facility.

Consideration	Response
Volume of material	Uncontaminated material to be obtained on site (i.e. material that is not asbestos-bearing)
Particle size distribution	Large volumes of material available on many sites Highly variable particle size of material on site Required particle size calculated by Shield’s law and “Du Boys type” equations: $\tau_{cr} = 0.056(\rho_s - \rho)gD_{50}$ The critical shear stress applied by a storm event of a 100 year return period is determined and used in the calculation of a minimum D_{50} to withstand erosion/sediment transport.
Geochemical considerations	As asbestos itself is chemically inert, this consideration applies to other elements found within the residue deposits

Final design of rock and soil cover layer:

- 300 mm layer is considered the minimum practical thickness of rock and soil placement;
- Fine rock material reduces the quantity of material eroded by rainfall by approximately 60% to 90% when the in-situ surface is appropriately compacted;
- Addition of a rock only armouring layer inhibits the velocity of raindrops and prevents formation of rills and gullies; and
- The layer structure of this rock cladding layer is depicted in Figure 1 below.

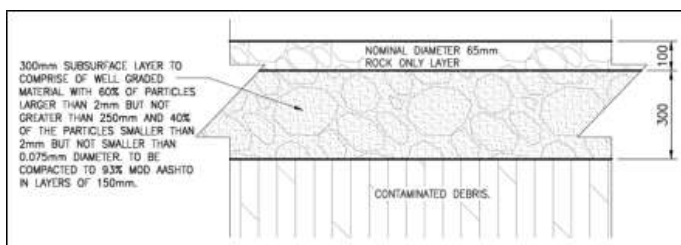


Figure 1. Layer structure of rock cladding

4.1.2 Stormwater control

The installation of stormwater control structures on rehabilitated asbestos dumps are intended to divert upstream runoff from the residue deposits and reduce erosion, limiting the risk of asbestos fiber exposure. Stormwater control measures may include gabions, reno mattresses, contour walls, retaining walls, storm water diversion channels, berms/ bunds and energy dissipators. Similar stormwater management approaches are needed to safeguard remedial cladding.

As such, stormwater runoff is always quantified as accurately as possible to ensure that stormwater management features are adequately sized/specified.

Where deposits are found near watercourses or within flood plains, these must be relocated to prevent mobilisation of asbestos fibers, further contamination of the watercourse and excessive erosion by the movement of water. The relocation, however, is dependent on the volume and nature of material, and following a cost-benefit analysis, in-situ remediation with sufficient flood protection measures installed may be carried out.

4.2 Providing a facility that is stable over the design life

A Factor of Safety of 1.5 is generally applied for civil engineering works where slopes are to remain stable over the design life of a structure. Following the methodology used by Silva, Lambe and Marr (2008), SRK determines the required Factor of Safety by first determining the level of engineering predicated by the level of investigation, testing, analyses and documentation, construction and operation and monitoring.

A resultant factor of safety is then determined based on the level of engineering determined as well as an annual probability of failure (a maximum of 10^{-3}). This is then applied in the design and analyses of all rehabilitation measures, slope stability analyses and slope stabilisation measures.

4.3 Addressing health and safety hazards by closure of open shafts and adits

Closure of adits and decline shafts are carried out in a safe and responsible manner. In the selection of a closure methods, various alternatives with corresponding implications were considered.

Typical methods of closure include, backfill, fencing, closure by gabion wall, rock and mortar structure and casting of a monolithic concrete capping, amongst others. A combination of these methods may also be used.

Shafts and adits located in areas inaccessible by vehicle can be closed by the installation of rock-filled gabion basket walls as the materials used are practical to transport at high elevations and difficult terrain.

At sites where access provision to the shafts and adits and transport of materials is easier, the closure is executed by backfill and sealing with a 1 m thick rock and mortar wall as illustrated in Figure 2.

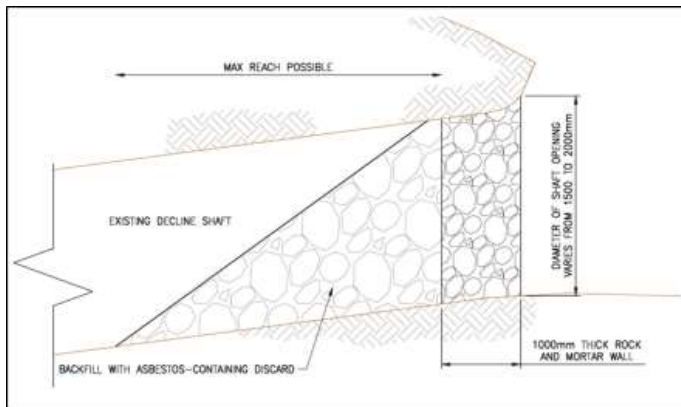


Figure 2. Declined shaft closure

4.4 Integration into the natural landscape

Use of uncontaminated natural materials (obtained on site where possible), installation of gabion baskets, reno mattresses, benching and sloping to allow integration into the natural environment as much as possible while still maintaining operational and structural integrity.

4.5 Providing a cost effective solution

Cost benefit analyses are conducted during the consideration of all alternatives for rehabilitation measures implemented.

By the installation of rock cladding, a much greater resistance to erosion is provided an additional safeguard against erosion. Extensive irrigation to ensure the establishment of vegetation is also avoided thereby reducing expenditure, and the need for fencing is negated as livestock will not be attracted to the areas to graze (i.e. establishing vegetation).

4.6 Providing a facility that is self-sustainable/requires minimal maintenance over the design life

A variety of materials are included in the design of the engineering solutions contributing to the rehabilitation of the proposed sites. All materials have their own inherent lifespan and, regardless of design, may ultimately deteriorate due to exposure to the natural elements and various other factors. Taking this into account, all rehabilitation measures are designed to require minimal to no maintenance to bolster future sustainability.

To evaluate the success of the rehabilitation, the containment of asbestos fibers being the primary objective, must be monitored. The performance and durability of the cover material may provide an indicative measure of success, bearing the following in mind:

- A protective treatment for a slope surface takes a number of years to show its true value and thus the efficiency of a protective treatment cannot be assessed on the basis of its performance in a single wet season;
- Based on previous studies completed by Blight and Amponsah-Dacosta (2004), the efficiency of rock cladding on tailings dams is highly variable although successful in many instances. Their experiment conducted at Doornkop illustrated an average erosion rate of 164 tons/ha/annum on a conventionally grassed test panel whereas a 300 mm rock cladded panel subjected to the same conditions displayed an average erosion rate of only 66.75 tons/ha/annum; and
- The sites to which rock cladding has been installed/applied as a cover medium may be monitored into the future and the efficiency, in terms of erosion resistance and containment of asbestos fibers, evaluated over a period of time spanning several wet seasons.

5 PROJECT DESIGN APPROACH

At inception of the Rehabilitation & Closure projects, the “Standard Protocol & Guidelines for the Rehabilitation of Derelict/Ownerless Asbestos Mine Residue Deposits in South Africa” document by the DME was provided to SRK to aid with design and implementation. As mentioned before, this document provides a generic overview of design and implementation strategies of typical scenarios encountered in the rehabilitation of Asbestos Mine Residues. The document does not, however, provide sufficient detail of specific rehabilitation and the analysis/design there-of.

SRK opted to use the document as a guideline and supplement where shortfalls were encountered. When investigating and analysing each mining site and its localized technical setting, design engineers undertook to concentrate and place importance on four factors, namely;

- Asbestos Source Characteristics;
- Asbestos Source Stability;
- Potential Vectors; and
- Receptors.

It is SRK's opinion that if these factors are investigated and assessed with due diligence and measures are put into place to mitigate the negative impacts identified, the desired outcome (retarding mobilization of fibers) is achieved. As is the case with most construction projects, there are time constraints placed on remediation of each of the mining sites. This means that investigations, analysis and design often occur concurrently to meet deadlines.

The process is phased. The phased approach is an industry standard (Government Gazette No. 39480) which demonstrates that the Engineer pays due diligence, applies his/her mind and evolves his/her design strategy from start to finish. The phased approach is described in the sub-sections below.

5.1 Inception

During the Inception Phase, SRK was provided with site coordinates and emphasis was placed on investigating and determining the nature of the mining site and its inherent characteristics. This involves problem definition specifically relating to aspects such as site access, access control, contamination and extent, subsidence, presence of adits, vertical shafts or inclined shafts, discard rock dumps, asbestos tailings deposits, asbestos mill sweepings, mining structures, drainage line and river contamination, distributed asbestos bearing rock, soil and vegetation contamination and secondary offsite contamination.

This phase involves visiting the site with a team of capable professionals to visually identify preliminary elements and parameters for consideration in the design, and undertaking a baseline air quality assessment as is mandatory in the Health and Safety legislation (Government Notice R155). A land survey of the site is also done, along with the identification of all elements to be included in the scope of the project.

A range of possible solutions and options to the elements identified are compiled and a high-level cost estimate is generated to ringfence envisaged construction costs. A draft closure concept is then presented and after discussions with the client, a preliminary scope is agreed for works going forward.

Recommendations are made by the engineers on additional investigations that may be required, such as horticultural and vegetative investigations, quantitative and qualitative testing of discard material to identify asbestos type and content, and geotechnical investigations.

The closure concept is then finalised and fundamentally serves as a scoping document, (with high-level costing) for works going forward.

5.2 Preliminary design

During the Preliminary Design Phase, investigations recommended in the Inception Phase, commence, and option analysis is undertaken assuming likely outcomes of the investigations taking place concurrently. SRK also screens out various options in order to begin converging on options that support the design objectives. Preliminary design on all the elements identified and stated in the Closure Concept is undertaken and a preliminary cost estimate is generated, based on selected options and design solutions.

5.3 Detailed Design

At commencement of the Detailed Design Phase, results of testing conducted during the Preliminary Design Phase are obtained and optimization done. Final design solution options are selected by testing each option in terms of Construction Cost vs Practicality vs Competent Design Parameters. The detail design and detailed construction drawings are produced and submitted to the client for review, and thereafter used for procurement and appointment of a Contractor.

5.4 Procurement Documentation

During this phase, the engineer and the principal consultant meet with sub-consultants and prepare specifications and preambles for the works which include construction specifications, specialist specifications, detailed schedules of quantities, contract documentation and enquiry documents. These documents are submitted to the Client for review and thereafter the Client undertakes the procurement services in isolation and appoints a Contractor.

All construction works required to be executed are laid out within the procurement documentation as well as variations that applied to the Standardized Specifications. The contractors are required to comply with these specifications during the contributing process to achieve the required project outcomes.

5.5 Contract Administration & Inspection

Once a contractor has been appointed by the client, the construction phase commences. The engineer is appointed and conducts site monitoring and contract administration throughout the duration of the construction contract. The client reserves the environmental, health and safety monitoring which is undertaken and conducted on an independent basis and mandates the appointed engineer to monitor and quantify works in terms of ongoing construction requirements, engineering requirements, contract requirements, measurement and certification of the works and quality assurance. Supervision of the works occurs once a month in some instances. If specific milestones are met, this occurs once every two weeks, and equates to Level 1 periodic construction monitoring (Government Gazette No. 39480). Supervision, monitoring and measurement of the works does not require frequent visits as the nature of the works are not skilled labor intensive, and requirements are placed on the contractor to supply weekly updates, information such as daily site diaries, survey data and photographic evidence of quality and progress of the works to the Engineer. The client also conducts site supervision and monitoring at different intervals to the engineer, in an attempt to ensure continuity.

5.6 Closeout

At the end of the contract, closeout procedures such as inspection, verification and rectification of the defects, management of guarantees and warranties, management of as-built drawings, manage and issue payment valuations and certificates, issue completion certificates and the preparation and issue of the project closeout report is completed.

6 CASE STUDIES

6.1 Mahlatjane rehabilitation

6.1.1 Introduction

Near the village of Mafefe in the Limpopo Province, an asbestos waste rock dump adjoins the D4050 road to the southeast. The Mahlatjane asbestos waste rock dump facility appears to have been previously rehabilitated, by the placement of a soil and rock cover over the asbestos waste. Visual evidence suggests that no storm water control measures were included in the previous rehabilitation efforts as erosion and scouring is evident on the facility.

The site is bordered by the Mahlatsane River, a non-perennial water course, which flows along the eastern toe of the facility. An access road is located along the western edge of the dump. This access road slopes in a northerly direction towards the asphalt road providing an apparent preferential flow path with visual evidence suggesting that water causes ground erosion across the waste area.

6.1.2 Project Components

6.1.2.1 Cover material

Sporadic instances of exposed asbestos fibers were observed on site, particularly along the dump perimeter. This consisted of small bundles of loose clumped fibers as well as bound within the banded ironstone host rock matrix. Observations indicate that this is due to uneven cover on the waste, either due to poor cover placement or to erosion removing the cover.

6.1.2.2 Flood protection

The waste rock dump facility is situated within the 1:100 year return period flood plain of the Mahlatsane River. Observations on site indicated that there had been some erosion at the toe adjacent to the road and the river, with vertical slopes arising from washout of both cover and asbestos containing waste. Erosion protection was thus required to remedy this situation. SRK therefore recommended that flood protection measures be built to ensure that erosion of the toe of the asbestos residue deposit, due to a storm event, does not occur.

6.1.3 Design

6.1.3.1 Cover material

In areas where asbestos fibers had resurfaced, cover material consisting of 300 mm of topsoil and indigenous vegetation was applied. To prevent future erosion of the cover, stormwater diversion berms were strategically constructed.

6.1.3.2 Flood protection

Various erosion protection alternatives were considered including the use of vegetated hyson cells, installation of geo-textiles, loffelstein blocks, reno mattress lining and gabion baskets.

The flow depths and velocity profiles used in the design of erosion protection measures were obtained from the simulation of a 100 year return period storm event in a simulation model. A velocity profile is shown in figure 3. The shear force exerted by the water on the gabion baskets was determined, following which the inclusion of concrete cut-off beams intermittently along the length of the gabion basket installation was deemed necessary. An example of a flood protection gabion basket is shown in figure 4.

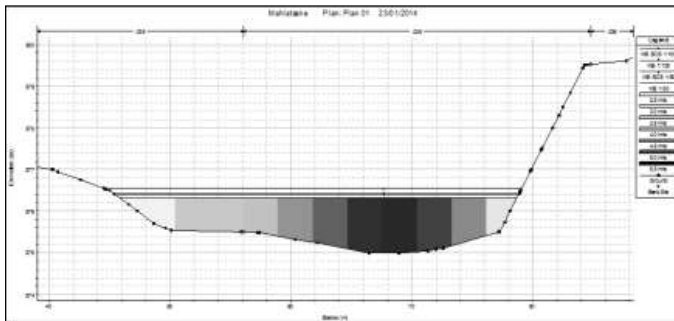


Figure 3. Velocity profile of the Mahlatsane River for a 100 year return period storm event

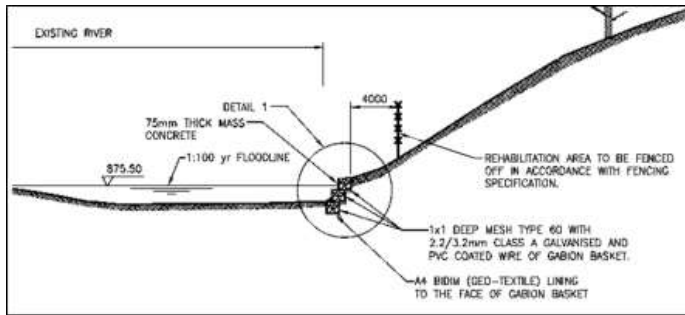


Figure 4. Gabion basket flood protection measures

6.1.4 Stormwater erosion protection

Channel improvements were designed to protect the rock waste dump from flood hazards by safely routing and discharging storm water into the non-perennial Mahlatsane River.

Following hydrologic and hydraulic analysis, a reno mattress lined channel with weirs placed at regular intervals to dissipate energy was designed. A cross section of the channel is included in Figure 5.

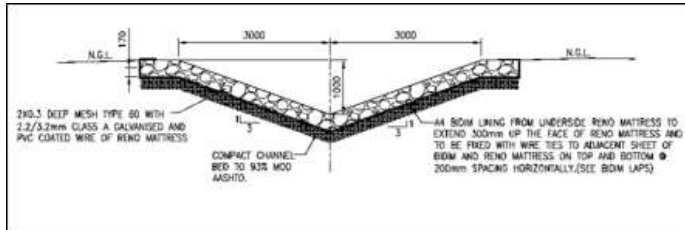


Figure 5. Cross Section of Reno Mattress lined channel

6.4.1 Construction

Following appointment of a contractor, the entire rehabilitation project was completed within a five month period. During the construction period, Level 1 construction monitoring was carried out for quality assurance and contract administration. Selected project outcomes are illustrated in Figure 6 below. In order for the Contractor to have completed the project a final site inspection commenced after the Defects Liability Period of one year. During this final inspection all structures (gabion walls, reno mattress channel, and slopes) were adequate and deemed stable.



Figure 6. Construction progress during the rehabilitation project

6.2 *Buisvlei North*

6.2.1 *Introduction*

Buisvlei farm, located near Prieska in the Northern Cape, is host to a derelict asbestos mining facility which consists of a number of open shafts and adits, as well as accompanying waste rock dumps and residue deposits. There are remnants of previous closure measures on site, such as concrete capping of what appears to be an abandoned vertical shaft, but no evidence of any further rehabilitation work.

The general topography of the site is moderately steep and all the identified residue deposits, adits and shafts are located on the slopes of the naturally steep hills within the large valley with the gradient reaching a maximum of approximately 40° in some areas. A non-perennial stream runs through the affected portion of the site in a north-westerly to south-easterly direction. The site is vegetated with local shrubs, a few trees and has limited ground cover.

6.2.2 *Project Components*

The components included within the scope of the rehabilitation project are listed as follows:

6.2.2.1 *Closure of adits and shafts*

The adits and shafts impact the environment aesthetically due to the lack of vegetation, creating a contrast with the natural biodiversity. These areas are topographically distinct to the surrounding landscape and impact on the aesthetics of the site. The adits may also serve as a source of airborne asbestos as asbestos tailings were historically used to form a flat, working surface near the entrance, although these have not been conclusively identified on site.

6.2.2.2 *Remediation of residue deposits*

The residue deposits/ dumps identified on site contain banded ironstone rock (possibly the result of tunnel creation), asbestos bearing rock with seams of fiber (asbestos ore with no economic value), clumps of asbestos and loose but congealed fibers.

The asbestos residue deposits are at extremely steep angles; some even possibly at the angle of repose and therefore pose a possible hazard from a slope stability perspective. This may also contribute to the further migration of asbestos contaminated waste / asbestos bearing rock into the environment by means of rock fall and the formation of colluvium. The stability may require detailed assessment through sampling, modelling and analysis.

6.2.2.3 Prevention of fiber transport by/into nearby watercourses

There are three watercourses on the Buisvlei site - two non-perennial streams and a river on the Southern portion of the site. Traces of asbestos fiber were visually identified within the flow-path of the stream running through the site that borders the large residue deposit.

6.2.3 Design

6.2.3.1 Remediation of residue deposits

The two largest residue deposits appear to consist of a variety of material including fine semi-processed fiber; matrix bound asbestos fiber and asbestos-bearing waste rock. The rehabilitation of these two deposits is proposed as in-situ rehabilitation to avoid the possible mobilization of fine fibers by relocation and due to the large volume of material contained with each deposit estimated to contain more than 20 000 m³ of residue each.

The perimeter slopes of the two dumps are steep (isolated areas at an angle up to 43°) with flat crests (similar to a plateaux). Erosion protection and slope stability measures were required at the perimeter. The selected cover material could easily be placed on the surface of the deposit following a regrading and compaction exercise. Following extensive confirmatory slope stability analysis, hydraulic and hydrologic analysis and floodline determination, SRK designed a gabion wall structure to retain material while also providing erosion and flood protection. A typical section of the gabion wall structure is illustrated in Figure 7.

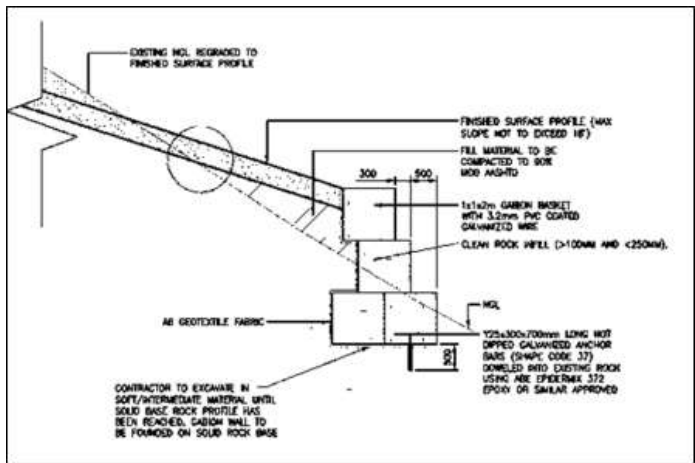


Figure 7. Typical section of gabion wall structure

6.2.3.2 Closure of adits and shaft

Closure of all adits, shafts and sub-vertical workings were designed and included the following activities:

- Clearing, grubbing and preparation of entrance to shafts and adits for construction works.
- Exclusion of bats as per Bat Management Specification supplied in the contract documentation.
- Backfilling of adits with asbestos residue to as great a depth as possible.
- Construction of one metre thick rock and mortar wall to entrance using class 1 mortar.

6.2.3.3 Prevention of fiber transport by/into nearby watercourses

By adequately containing the fibers within the residue deposits and constructing the gabion wall structure along the toe of the residue deposit, further contamination of watercourses by these sources was prevented.

6.2.4 Construction

Following the appointment of a contractor, the construction commenced in early 2015 and construction was completed within 13 months. During the final inspection, one year since the project was completed the permanent works did not manifest any defects and were deemed to be in the condition required.

7 CONCLUSIONS

Understanding the industry approaches, standards and guidelines available can provide benefits in terms of efficiency, practicality and project planning. The availability of literature and the multi-disciplinary work place experience gained by SRK over the years, provided our client with the required services for these particular projects. The approach taken by SRK in terms of planning, offered our client the opportunity to holistically understand the design and costing implication (be it high-level initially) at a very early stage in the projects.

Moreover, in taking the process developed, SRK was able to meet very strict/tight deliverable deadlines set by our client, as well as provide savings in terms of efficiency and cost for future projects. In developing the technical specifications, SRK provided measures to ensure that the contractors and the client utilised appropriate measures set to ensure good industry practices and their resultant benefits in mitigating potential future risks associated with these rehabilitated sites.

REFERENCES

- Blight, G. E. (2009) *Geotechnical Engineering for Mine Waste Storage Facilities*. CRC Press
- Blight, G. E. and Amponsah-Dacosta, F. (2004) *Erosional stability of tailings dam slopes, Ground Water Bioengineering for Erosion Control*. Barker, D. et al (eds), Science Publishers Inc, USA
- Chadwick, A. Morfett, J. Borthwick, M. (2008) *Hydraulics in Civil and Environmental Engineering. Fourth Edition*. Spon Press, Cornwall, UK.
- Craig, R.F. (2004) *Soil Mechanics*. 7th Edition. Spon Press, Cornwall, UK.
- DMR. (2011) *Standard Protocol and guidelines for the rehabilitation of derelict/ownerless asbestos mine residue deposits in South Africa*, Department of Minerals and Energy, South Africa.
- Government Gazette No. 39480 (12 December 2014), Guideline for Services and Processes for Estimating Fees for Persons Registered in terms of the Engineering Profession Act, 2000, (Act No. 46 of 2000), Guideline Scope of Services, Vol 594, pp 11-16
- Government Gazette No. 39480 (12 December 2014), Guideline for Services and Processes for Estimating Fees for Persons Registered in terms of the Engineering Profession Act, 2000, (Act No. 46 of 2000), Guideline Scope of Services, Vol 594, p 15
- Government Notice R155, Occupational Health and Safety Act (1993), Asbestos Regulations, 2001, (Clause 7)
- Milczarek et al. (2011) *Characterization and Selection of Waste Rock Borrow Material for Use as Rock Armor to reduce Tailing Impoundment Side-Slope Erosion, Proceedings Tailings and Mine Waste 2011*, Vancouver
- Silva, F. Lambe, T.W. Marr, W.A. (2008) *Probability and Risk of Slope Failure*. Journal of Geotechnical Engineering. Vol. 134 (12) p.1691-1695
- Smith, M. (2004) *Rock cladding of tailings dams*, Civil Engineering, August
- Wates, J.A. & Rykaart, E.M. (1994) *Design of soil covers for control of infiltration*, The First Conference on Environmental Management Technology and Development Proceedings, South Africa

Effectiveness of Oxygen Barriers under Climate Change: Definition of a Drought Index

É. Bresson and I. Demers

Université du Québec en Abitibi-Témiscamingue, Rouyn-Noranda, Quebec, Canada

RIME - Research Institute on Mines and the Environment, Rouyn-Noranda, Quebec, Canada

Y. Chavaillaz

Concordia University, Montreal, Quebec, Canada

Ouranos Inc, Montréal, Quebec Canada

P. Roy

Ouranos Inc, Montréal, Quebec Canada

T. Pabst

Polytechnique-Montréal, Montréal, Quebec, Canada

RIME - Research Institute on Mines and the Environment, Montréal, Quebec, Canada

ABSTRACT: Reclamation methods for mine waste storage sites do not always consider climate changes in their design. For region with a humid climate, an oxygen barrier cover is often used for reclamation to control acid mine drainage generation. These barriers are usually very sensitive to in situ water balance, but climate models predict an intensification of droughts during summer periods by 2100 in the studied areas. This could increase the risk of desaturation of tailings and/or cover systems, thus reducing the performance of reclamation.

Existing drought indices can be poorly adapted to mining purposes and drought features currently used for the assessment of long-term performance of reclamation methods are mostly arbitrary. Here, we propose a new drought index designed based on two different oxygen barrier techniques. It considers water balance, accumulation of precipitation before each drought, and duration of drought. Climate projections are used to evaluate index evolution by 2100.

1 INTRODUCTION

1.1 Climate Changes (CC) in Quebec

The province of Quebec is located in the eastern part of Canada and encompasses a large area from 45N to 62N and 65W to 80W as shown on Figure 1. The climate varies substantially over the spatial domain, ranging from humid continental, oceanic, polar to subarctic climate, with significant seasonal contrasts. For example, mean temperatures North to South are comprised between -25 and -8°C in winter and between 3 and 20°C in summer (Desjarlais et al. 2010). Precipitation is typically more abundant in the South than in the North. Abitibi-Témiscamingue, a major mining region, is located in the western part of Quebec as shown on Figure 1, and characterized by a humid continental climate, with significant annual temperature variations.

A global warming was reported for the late-20th century in the Quebec province, inducing a shortening of the freezing season (Yagouti et al. 2008, Diffenbaugh & Scherer 2011, Romero-Lankao et al. 2014). The deep permafrost temperature increased by 1.1°C between 1994 and 2007 (Allard et al. 2008). The number of events with intense precipitation increased significantly from the mid-20th to the early 21st century (Peterson & Baringer 2009). The total number of days with low precipitation also increased in the recent past (1960-2005; Vincent & Mekis 2006).

By the end of the 21st century, mean temperatures are projected to increase in the province of Quebec, especially in winter (Plummer et al. 2006, Christensen et al. 2007). An increase in mean precipitation is also projected, mainly in Northern Quebec (Desjarlais et al. 2010). Both mean values and extreme events are expected to increase according to climatic projections. The changes in the distribution of temperatures will increase the frequency of hot day events during summer (i.e. the 90th percentile part of the distribution). A lengthening of the periods without precipitation

is also projected, as well as more frequent heavy precipitation events (i.e. the 90^e percentile part of the distribution; Mailhot et al. 2007).

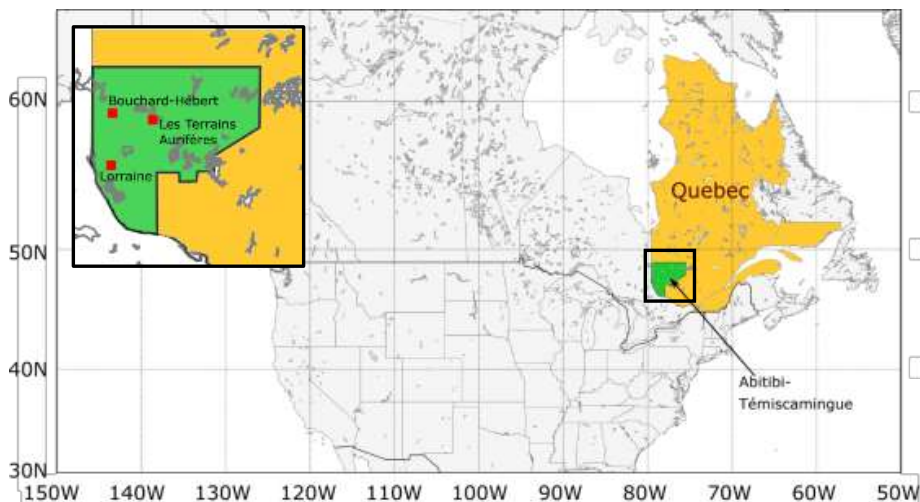
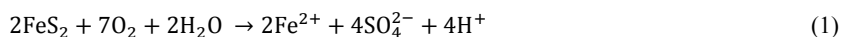


Figure 1. North America map. The province of Quebec is highlighted in yellow and the Abitibi-Témiscamingue region in green. Zoom for the Abitibi-Témiscamingue region in the black box.

1.1 Vulnerability of Mine Site Reclamation to CC

Mining operations generate large volumes of solid wastes (tailings and waste rock) that are usually disposed of in surface management facilities (Bussière 2007). An adequate reclamation of the mine waste disposal sites is required to ensure their long-term geochemical and geotechnical stability. The main geochemical issue with mine wastes is acid mine drainage (AMD) which can be generated when sulfide bearing mine wastes are exposed to water and oxygen (Eq. 1; e.g. Ritcey 1989, Evangelou 1995, Morin & Hutt 1997). AMD is characterized by a low pH, and high concentration of sulfates and dissolved metals (Jambor 1994, Ritchie 1994; Monterroso & Macias 1998, Nordstrom 2000, Blowes et al. 2014). The main objective of most reclamation methods is to prevent AMD generation by controlling oxygen and/or water supply.



In a humid climate, such as in Abitibi-Témiscamingue, oxygen barriers can be an effective solution to control oxygen diffusion into the tailings and prevent AMD generation (SRK 1989, MEND 2001, Aubertin et al. 2016). The performance of such reclamation methods usually rely on maintaining a high degree of saturation (i.e. $S_r \geq 85\%$) in the tailings, or in the cover system. Oxygen diffusion is thus reduced by approximately 10 000 times in water (or nearly saturated medium) compared to diffusion in air (Collin & Rasmuson 1988). Climate and water balance observations are therefore an essential part of the reclamation design and performance assessment. Reclamation needs to remain effective for the whole lifetime of the mine waste disposal area (which could be indefinite; Vick 2001) and, consequently, climate changes could have an impact on future performance.

1.2 Objectives of the Research

Changes in dry periods are expected in the Abitibi-Témiscamingue region by the end of the century (Lemmen et al. 2007, Desjarlais et al. 2010, IPCC 2014). The saturation in the tailings and/or cover material could then decrease below the critical 85% threshold, and alter the reclamation effectiveness. A precise description of dry periods, including their duration, severity and frequency, is therefore required to tackle the adverse effects of climate change. Some drought indices have been defined in literature but mainly for agricultural, meteorological and hydrological purposes. The features of such indices might not consider the characteristics of the oxygen barriers.

The main objective of this study is to define a drought index that specifically takes into account the specificities of oxygen barriers used to control AMD generation from mine wastes. In order to reach this objective, an overview of the existing drought index is first presented (section 2). The two main types of oxygen barriers that could be affected by prolonged drought period are then described (section 3) and a drought index adapted to mine wastes reclamation is described in section 4.

2 OVERVIEW OF EXISTING DROUGHT INDICES

The Intergovernmental Panel on Climate Change (IPCC) defines a drought as: “A period of abnormally dry weather long enough to cause a serious hydrological imbalance.” (IPCC 2014). Three types of droughts are usually specified in the literature depending on the studied topic: 1) the meteorological drought is a period with an abnormal deficit of precipitation. Evapotranspiration can increase with a precipitation deficit and high temperatures, and can influence soil moisture; 2) the agricultural (or soil moisture) drought, linked to crop production during the growing period, is controlled by precipitation and soil moisture deficit; and 3) hydrological drought corresponds to a deficit of precipitation, and a decrease of soil moisture and groundwater level. The history of soil moisture and groundwater storage (e.g. previous dry period) can also have an impact on the hydrological balance.

Indices were developed for each type of drought and take into account the inputs involved (i.e. precipitation, temperature and soil moisture) and drought characteristics, which can include: severity, duration, surface coverage and frequency (Dracup et al. 1980). The existing drought indices can be used for short term forecasts and long-term climatic evolution (Heim 2002, Dai 2011, WMO & GWP 2016).

The Consecutive Dry Days (CDD) index is defined as the maximum of days without precipitation during a given period (Frich et al. 2002, Alexander et al. 2006, Tebaldi et al. 2006). Typically, the CDD is calculated considering maximum consecutive days with precipitation not exceeding 1 mm day^{-1} on a yearly basis (Hennessy et al. 1999). The Standard Precipitation Index (SPI; McKee et al. 1993, Lloyd-Hughes & Saunders 2002) is based on a precipitation probabilistic approach and only requires the precipitation as input parameter. It can be applied for various time scale (i.e. 3, 6, 9, 12 or 24 months). As a consequence, it also considers the cumulative effect of precipitation deficit. The SPI is normalized and can be used either in arid or humid climate. The relevance of the SPI is limited, because the temperature is not taken into account, and it does not account for evapotranspiration. The Standardized Precipitation Evapotranspiration Index (SPEI) build on the SPI and includes a temperature component based on a simplified water balance calculation (Vicente-Serrano et al. 2010). This index has a time step from 1 to 48 months and complete temperature and precipitation datasets are required. The longer the series, the more robust are the results. The Palmer Drought Severity Index (PDSI; Palmer 1965) is a widely used index based on monthly precipitation, monthly temperature and soil moisture (or water content). It was first developed for the management of agriculture droughts in the USA. Complete temperature and precipitation datasets are also required for this index.

The existing drought indices have several advantages. Nevertheless, they require a complete and/or dataset available for a long period while in Quebec, meteorological surface station data have an inhomogeneous and low spatial distribution. Moreover, the existing drought indices use one or more variables (i.e. precipitation, temperature and soil moisture). The two oxygen barrier

covers described hereafter highlight which variables are important for this topic and have to be taken into account for the development of an adapted drought index.

3 OXYGEN BARRIER

Two types of oxygen barrier are presented in the paper: an elevated water table (EWT) with a monolayer cover, and a cover with capillary barrier effects (CCBE).

3.1 Elevated Water Table

The objective of an EWT with a monolayer cover is to keep the reactive tailings underneath close to saturation by maintaining the water table high enough in the tailings storage facility as shown on Figure 2 (Aubertin et al. 1999). A layer of coarse material can be added on the top to prevent evapotranspiration and improve infiltration, thus modifying the water balance by increasing the percolation (Ouanguwra et al. 2009). A fine material could also be used as cover to enhance the capillary rise capacity of the system and further control oxygen diffusion (Demers et al. 2008).

The performance of the EWT technique depends on the degree of saturation in the tailings. However, it can be difficult to maintain the level of the water table high enough during long, severe and frequent drought periods. The degree of saturation in the reactive tailings could then decrease and the oxygen diffusion increase, leading to AMD generation.

An ETW with a monolayer was implemented for a large part of the Manitou site with Goldex non-reactive tailing as monolayer cover (reclamation started in 2008; Ethier et al. 2018). The Doyon-Westwood site reclamation method is a EWT with a monolayer cover made of fine desulfurized tailings (MEND 1996, Orava et al. 1997, Dagenais et al. 2005, Ouanguwra 2007, Demers et al. 2008, Ouanguwra et al. 2009). The AMD generation of one tailings pond of the Aldermac site, one of the most problematic abandoned mine in the region, is controlled by an ETW with a monolayer (Maqsoud et al. 2013, 2015). The *in situ* monitoring present a good performance of the reclamation designs implemented in the different sites (Ouanguwra et al. 2009, Ethier et al. 2018).

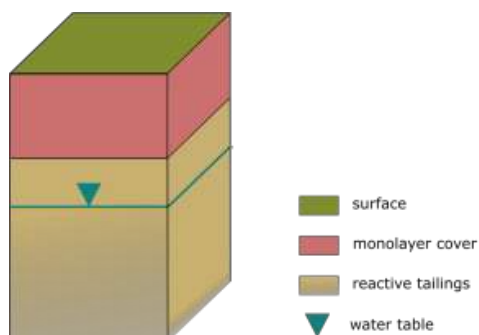


Figure 2. Schematic representation of the EWT with a monolayer cover (adapted from MEND, 1996). The depth of the water table should not exceed a critical value (typically between the interface and the air entry value of the tailings; Ouanguwra et al. 2009, Ethier et al. 2018). The monolayer cover can be made of either a fine or a coarse material.

3.2 Cover with Capillary Barrier Effects

A CCBE is typically made of 3 to 5 (and more) layers of different materials as shown on Figure 3 (Aubertin 1996, Nastev & Aubertin 2000). The objective is to create an oxygen barrier by maintaining one of these layers nearly saturated. A CCBE can be efficient even when the water table

is relatively deep. The five main layers of a CCBE are: a superficial layer (coverage of the reclamation site), a protective layer (protection against biological intrusion), a draining layer (prevention of water accumulation), a low permeability layer (water retention and oxygen diffusion barrier) and a support layer (capillary barrier). CCBE layers can have more than one function in practice. The performance of CCBE is based on a phenomenon called capillary barrier effect that can develop when a fine grain material overlay a coarse layer above the water table. The finer material retains water due to capillary forces. Oxygen diffusion is therefore restricted and oxygen flux that reaches the reactive tailings placed underneath the cover is controlled.

The CCBE structure can be affected by its environment. The water retained in the low permeability layer could be vulnerable to long and frequent droughts. Moreover warmer temperature could increase the soil evapotranspiration and lead to a desaturation of the layer. The oxygen could thus diffuse more rapidly to the reactive tailings and contribute to AMD generation.

In the Abitibi-Témiscamingue region, CCBE covers are implemented in several mining sites: for example, the gold mine *Les Terrains Aurifères* (Bussière et al. 2006), the abandoned polymetallic site of Lorraine (Aubertin 1996, Bussière et al. 2009), the mine Bouchard-Hébert (Bernier et al. 2005). The location of these mines is shown on Figure 1, and a summary of the CCBE covers is presented in Table 1. The CCBE layers material and thickness depend on the features of the mining site tailings. The reclamation sites are instrumented with water content probes to monitor the water content in the low permeability layer and assess the effectiveness of the CCBE (Dagenais et al. 2005).

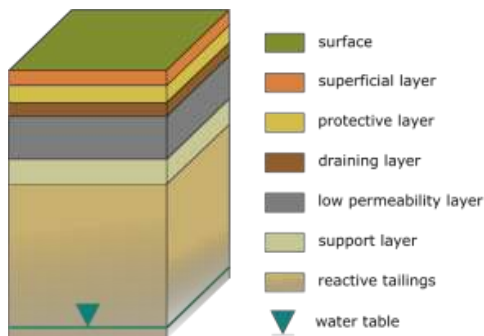


Figure 3. Schematic representation of a CCBE (adapted from Aubertin et al. 2002). In this case, the CCBE is composed of five layers (superficial, protective, draining, low permeability and support layers). The water table is located deep below the tailings surface.

Table 1. Characteristics of three mines with a CCBE cover in the Abitibi-Témiscamingue region.

Name	Les Terrains Aurifères	Lorraine	Bouchard-Hébert
Location	Malartic	Latulipe	Rouyn-Noranda
Construction	1995–1996	1998–1999	2005–2007
Area (ha)	≈ 70	≈ 15	≈ 70
CCBE structure*	0.3 m of sand 0.8 m of silt/tailings 0.5 m of sand	0.3 m of sand and gravel 0.5 m of clay 0.3 m of sand	0.3 m of sand and gravel 0.6 m of clay 0.4 m of sand

*From top to bottom.

4 DROUGHT INDEX

4.1 *Parameters of the New Index Adapted to Oxygen Barrier Design*

Both reclamation methods presented above (EWT and CCBE) are vulnerable to long and intense droughts. If the tailings or the CCBE become unsaturated, the oxygen barrier will become less efficient and AMD can be generated. The soil moisture of the cover material or the tailings plays a significant role in the oxygen barrier performance.

Meteorological surface stations have an inhomogeneous and low spatial distribution over the Quebec province. Therefore, it can be difficult to collect enough meteorological data for a robust drought index calculation, such as CDD, SPI, SPEI and PDSI. The snowmelt, the runoff and the impact of vegetation are not considered in these indices in order to have a coherent and simple metric. Some features should be taken into account and integrated into a new drought index that would be applicable in long-term scenario performance predictions of mine waste reclamation in order to encompass tailings reclamation design limitations. The main parameters to consider are precipitation and evapotranspiration. The duration of a dry period is another important point to integrate in the new index for these reclamation methods, as numerical modeling shown that the performance of a CCBE can be affected at different degree by a prolonged period without precipitation (Aubertin et al. 1996, Bussi re et al. 2003, Pabst et al. 2017). The index should consider also the absence of water refill in the soil between frequent dry periods.

4.2 *Methodology to Develop the New Drought Index*

A three-step method is proposed to select periods of drought and assess their characteristics.

A first selection allows the definition of dry months and provide a sub-dataset used in the second step of the method. Soil is frozen and/or covered by snow in western Quebec during winter, usually oxygen diffusion is considered negligible in frozen soils. The reclamation methods efficiency is therefore not addressed for the frozen period. The trends in eastern Canada for future climate seem to indicate a decrease in the length of the cold season (Plummer et al. 2006). The calculation of the drought index considers the whole non-frozen period throughout a year (i.e. all days with a 7-days running mean temperature above 5 C). Time steps need to be selected from monthly data considered as dry. A month is considered dry if the surface water balance (i.e. the monthly mean difference between precipitation and evapotranspiration) is under a given threshold. This threshold corresponds to tails of monthly mean distributions from observation datasets available for the region of study.

Second, a duration index is estimated with the number of consecutive dry days during months considered as dry in the first step of the selection method as shown on Figure 4. A day is defined as dry when the daily precipitation stays below 1 mm. The duration of all the periods with more than two consecutive dry days is computed. The frequency of a dry period can also be calculated from this point.

Then, the severity of periods of consecutive dry days within a dry month is influenced by the soil moisture history. The surface water balance of months prior to a drought period is thus taken into account. The severity index is proportional to the inverse of the integral of the daily precipitation over 30 days preceding the first day of the dry period as shown on Figure 4. The more positive the water balance of previous months is, the lower the severity of the drought event.

Finally, the new drought index is a function of the duration, frequency and severity of the dry periods. The calculations are performed first with the reference climate and then with the projected climate in order to estimate the evolution of the drought index by 2100 regarding the reference climate.

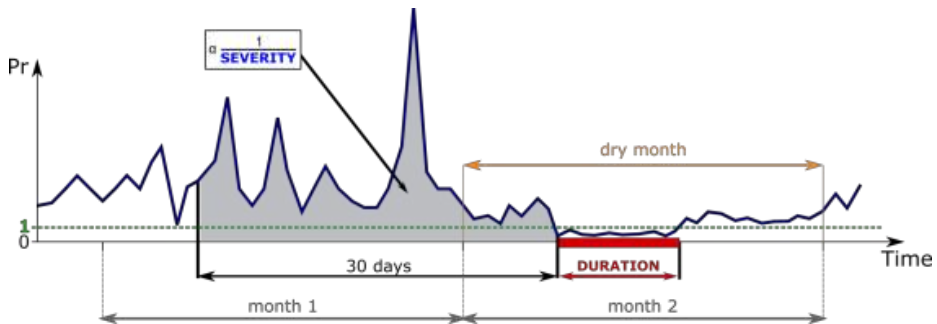


Figure 4: Schematic representation of the calculation for the duration and severity index for dry periods. For a dry month (here month 2), the duration of a dry event is the number of consecutive days with a daily precipitation under the 1 mm day^{-1} threshold (green dotted line). The severity is estimated with the inverse of the integral of the daily precipitation for the 30 days preceding the first dry day (blue area).

4.3 Application

For past and current periods, the calculation is performed using meteorological surface observation datasets close to the mine sites and using reanalysis when no data is available. Simulations of the Representative Concentration Pathways (RCP; Moss et al. 2010) 4.5 and 8.5 scenarios from several models which participated in the Coupled Model Intercomparison Project Phase 5 (CMIP5; Taylor et al. 2012) are used for the index computation up to 2100. A statistical quantile-quantile mapping bias correction is used to ensure that climate models outputs are coherent with the observations (Grenier et al. 2015).

The performance monitoring of an oxygen barrier design can be modelled with the 2018 version of SEEP/W (GEO-SLOPE International Ltd. 2017). This software can simulate the oxygen diffusion in an overlay structure. Climate parameters (e.g. precipitation and temperature) can be introduced in the boundary conditions. The past and current meteorological parameters with the soil characteristics are used as inputs for oxygen diffusion model calibration. The drought index evolution can be applied to a representative year of projected climate and then be used to define boundary conditions in long term simulations.

5 CONCLUSIONS

The reclamation methods of mine tailings implemented in the Abitibi-Témiscamingue region such as oxygen barrier are vulnerable to drought. The features of droughts (frequency, severity and duration) are projected to change by 2100. In literature, several drought indices are used but mainly for meteorological, hydrological and agricultural purposes. In this paper, a new drought index is defined taking into account the characteristics of two types of oxygen barriers: 1) elevated water table with a monolayer cover, and 2) cover with capillary barrier effects. This index is well adapted to oxygen barrier vulnerabilities and specificities like drought duration and soil refill of water between two dry periods.

The calculation of the drought index will be performed for two sites: 1) Doyon-Westwood where an elevated water table combined with a monolayer cover is planned to reclaim tailings impoundments; and 2) Lorraine where a cover with capillary barrier effects was built in 1999 to control AMD generation from sulphidic tailings (Hotton et al. 2018). Numerical simulations of these two oxygen barrier covers with reference climate and future climate, and the integration of the drought index evolution will provide an estimation of the performance of these oxygen barriers methods by 2100.

The described new drought index can be calculated for other mine sites with an oxygen barrier in a humid climate, and therefore can provide guidelines for mining companies and governments about oxygen barriers designs.

ACKNOWLEDGMENTS

This work is funded by the *Fonds de recherche du Québec – Nature et technologies* (FRQNT), Mines Canadian Malartic and IAMGOLD. The authors would like to thank also the Research Institute on Mines and Environment (RIME; www.irme.ca/en/) and Ouranos Inc. for their support.

REFERENCES

- Alexander, L.V., Zhang, X., Peterson, T.C., Caesar, J., Gleason, B., Klein Tank, A.M.G., Haylock, M., Collins, D., Trewin, B., Rahimzadeh, F., Tagipour, A., Kumar, K.R., Revadekar, J., Griffiths, G., Vincent, L., Stephenson, D.B., Burn, J., Aguilar, E., Brunet, M., Taylor, M., New, M., Zhai, P., Rusticucci, M. & Vazquez-Aguirre, J.L. 2006: Global observed changes in daily climate extremes of temperature and precipitation. *Journal of Geophysical Research – Atmospheres*, 111, D05109.
- Allard, M., Sarrasin, D. & Marchildon, C. 2008. Evidences of impacts of climate warming on permafrost in Nunavik, *Symposium sur l'environnement et les mines Rouyn-Noranda*, p. 16.
- Aubertin, M. 1996. Recouvrement multicouche pour le parc à résidus du site minier Lorraine. *Rapport soumis au MRNQ* (SDM-R-96-23). 30 p.
- Aubertin, M., Bussière, B., Monzon, M., Joanes, A.-M., Gagnon, D., Barbera, J.-M., Achib, M., Bedard, C., Chapuis, R.P. & Bernier, L. 1999. Étude sur les barrières sèches construites à partir des résidus miniers. - Phase II : Essais en place. *Research report*. Project CDT P1899, NEDEM/MEND 2.22.2c, 331p.
- Aubertin, M., Bussière, B. & Bernier, L. 2002. Environnement et gestion des résidus miniers. *Presses Internationales de Polytechnique*, Corporation de l'École Polytechnique de Montréal, Montréal.
- Aubertin, M., Bussière, B., Pabst, T., James, M. & Mbonimpa, M. 2016. Review of the reclamation techniques for acid-generating mine wastes upon closure of disposal sites. *Geo-Chicago 2016* (pp. 343–358).
- Bernier, L., Bédard, C., Lemieux, J. & Latour, F. 2005. Plan de fermeture et restauration du parc à résidus miniers de la mine Bouchard-Hébert. *Symposium 2005 sur l'environnement et les mines*, Rouyn-Noranda, Institut canadien des mines, de la métallurgie et du pétrole (ICM), [on CDROM].
- Blowes, D.W., Ptacek, C.J., Jambor, J.L., Weisener, C.G., Paktunc, D., Gould, W.D. & Johnson, D.B. 2014. The geochemistry of acid mine drainage. In: Holland, Turekian (Eds.), *Treatise on Geochemistry*, second ed. vol. 11, pp. 131–190.
- Bussière, B., Maqsood, A., Aubertin, M., Martschuk, J., McMullen, J. & Julien, M. 2003, May. Results from the monitoring program at the LTA site: hydraulic behavior of the cover. *105th Annual General Meeting of CIM-ICM*, Montréal, Québec pp. 4–7.
- Bussière, B. 2007. Colloquium 2004: Hydrogeotechnical properties of hard rock tailings from metal mines and emerging geoenvironmental disposal approaches. *Canadian Geotechnical Journal*, 44(9), 1019–1052.
- Bussière, B., Maqsood, A., Aubertin, M., Martschuk, J., McMullen, J. & Julien, M. 2006. Cover performance at the LTA site, Malartic, Québec, Canada. *CIM Bulletin*, september/october, 20, 1–16.
- Bussière, B., Potvin, R., Dagenais, A. M., Aubertin, M., Maqsood, A. & Cyr, J. 2009. Restauration du site minier Lorraine, Latulipe, Québec: Résultats de 10 ans de suivi. *Déchets Sci Et Tech*, 54, 49–64.
- Christensen, J.H., Hewitson, B., Busuioic, A., Chen, A., Gao, S., Held, I., Jones, R., Kolli, R.K., Kwon, W.-T., Laprise, R., Magana Rueda, V., Mearns, L., Menendez, C.G., Räisänen, J., Rinke, A., Sarr, A. & Whetton, P. 2007. « Regional Climate Projections », in *Climate Change 2007 : The Physical Science Basis, Contribution of Working Group I to the Forth Assessment Report of the Intergovernmental Panel on Climate Change*, S. Salomon, D. Qin, M. Manning, Z. Chen, M. Marquis, K.B. Averyt, M. Tignot et H.L. Miller (éd.), Cambridge University Press, Cambridge et New York, p. 847–940.
- Collin, M. & Rasmuson, A. 1988. A comparison of gas diffusivity models for unsaturated porous media. *Soil Sci Soc Am J* 52:1559–1565
- Dagenais, A. M., Aubertin, M., Bussière, B. & Cyr, J. 2005. Performance of the Lorraine mine site cover to limit oxygen migration. *SME Transaction*, 318, 190–200.
- Dai, A. 2011. Drought under global warming: a review. *Wiley Interdisciplinary Reviews: Climate Change*, 2(1), 45–65.

- Demers, I., Bussière, B., Benzaazoua, M., Mbonimpa, M. & Blier, A. 2008. Column test investigation on the performance of monolayer covers made of desulphurized tailings to prevent acid mine drainage. *Mineral Engineering*, 21: 317–329.
- Desjarlais, C., Allard, M., Belanger, D., Blondlot, A., Bouffard, A., Bourque, A., Chaumont, D., Gosselin, P., Houle, D., Larrivière, C., Lease, N., Pham, A.T., Roy, R., Savard, J.-P., Turcotte, R. & Villeneuve, C. 2010. *Savoir s'adapter aux changements climatiques*. Bibliothèque nationale du Québec, Montreal, p. 128.
- Diffenbaugh, N.S. & Scherer, M. 2011. Observational and model evidence of global emergence of permanent, unprecedented heat in the 20th and 21st centuries. *Climatic Change*, 107(3-4), 615–624.
- Dracup, J.A., Lee, K.S. & Paulson E.G. 1980. On the definition of droughts. *Water Resources Research* 16, 297–302.
- Ethier, M.P., Bussière, B., Broda, S. & Aubertin, M. 2018. Three-dimensional hydrogeological modeling to assess the elevated-water-table technique for controlling acid generation from an abandoned tailings site in Quebec, Canada. *Hydrogeol J.* <https://doi.org/10.1007/s10040-017-1713-y>
- Evangélow, V.P. 1995. Pyrite Oxidation and Its Control. *CRC Press*.
- Frich, P., Alexander, L.V., Della-Marta, P.M., Gleason, B., Haylock, M., Klein Tank, A.M.G. & Peterson, T. 2002. Observed coherent changes in climatic extremes during the second half of the twentieth century. *Climate Research*, 19(3), 193–212.
- GEO-SLOPE International Ltd. 2017. Heat and mass transfer modeling with GeoStudio 2018. Calgary, Alberta, Canada.
- Grenier, P., R. de Elia, & D. Chaumont, 2015: Chances of Short-Term Cooling Estimated from a Selection of CMIP5-Based Climate Scenarios during 2006–35 over Canada. *J. Climate*, 28, 3232–3249, <https://doi.org/10.1175/JCLI-D-14-00224.1>
- Heim Jr, R.R. 2002. A review of twentieth-century drought indices used in the United States. *Bulletin of the American Meteorological Society*, 83(8), 1149–1165.
- Hennessy, K.J., Suppiah, R. & Page, C.M. 1999. “Australian Rainfall Changes, 1910-1995.” *Australian Meteorological Magazine* 48 (1): 1–13.
- Hotton, G., Bresson, É., Bussière, B., Demers, I., Pabst, T. & Roy, P. 2018. Assessment of CCBEs performance with climate change: case study of the Lorraine mine site. *Tailings and Mine Waste '18 Conference, Keystone, Colorado, USA*.
- IPCC. 2014. Climate Change 2014: Impacts, Adaptation, and Vulnerability. Part A: Global and Sectoral Aspects. Contribution of Working Group II to the Fifth Assessment Report of the Intergovernmental Panel on Climate Change Cambridge University Press ed, New York, p. 1132.
- Jambor, J.L. 1994. Chapter 3, Mineralogy of sulfide-rich tailings and their oxidation products. In *Short Course Handbook on Environmental Geochemistry of Sulfide Mine-Wastes*. Edited by D.W. Blowes and J.L. Jambor.
- Lemmen, D.S., Warren, F.J., Lacroix, J. & Bush, E. 2008. From Impacts to Adaptation: *Canada in a Changing Climate 2007*, in: Canada, N.R. (Ed.). Government of Canada, Ottawa, p. 448.
- Lloyd- Hughes, B. and Saunders, M.A. 2002. A drought climatology for Europe. *International journal of climatology*, 22(13), 1571–1592.
- Mailhot, A., Duchesne, S., Caya, D. & Talbot, G. 2007. Assessment of future change in intensity–duration–frequency (IDF) curves for Southern Quebec using the Canadian Regional Climate Model (CRCM). *Journal of hydrology*, 347(1), 197–210.
- Maqsoud, A., Mbonimpa, M., Bussière, B. & Dionne, J. 2013. Restauration du site minier abandonné Aldermac : résultats préliminaires du suivi de la nappe surélevée. *Canadian Geotechnical Conference, GeoMontreal, QC, Canada*.
- Maqsoud, A., Mbonimpa, M., Bussière, B. & Benzaazoua, M. 2015. The hydrochemical behaviour of the aldermac abandoned mine site after its rehabilitation. *Canadian Geotechnical Conference, GeoQuébec, QC, Canada*.
- McKee, T.B., Doesken, N.J. & Kleist, J. 1993. The relationship of drought frequency and duration to time scales. *8th Conference on Applied Climatology* (Vol. 17, No. 22, pp. 179–183). Boston, MA: American Meteorological Society.
- MEND. 1996. Review of use of an elevated water table as a method to control and reduce acidic drainage from tailings, Mine Environment Neutral Drainage Report 2.17.1. Canada Centre for Mineral and Energy Technology, Ottawa, Canada.

- MEND. 2001. Manual report 5.4.2, Volume 1: Summary, Volume 2: Sampling and Analysis, Volume 3: Prediction, Volume 4: Prevention and Control, Volume 5: Treatment, Volume 6: Monitoring. Canada Centre for Mineral and Energy Technology, Ottawa, Canada.
- Monterroso, C. & Macias, F. 1998. Drainage waters affected by pyrite oxidation in a coal mine in Galicia (NW Spain): composition and mineral stability. *Science of the total environment*, 216(1-2), 121–132.
- Morin, K.A. & Hutt, N.M. 1997. Environmental Geochemistry of Minesite Drainage. *Practical Theory and Case Studies*. MDAG Publishing.
- Moss, R.H., Edmonds, J.E., Hibbard, K.A., Manning, M.R., Rose, S.K., van Vuuren, D.P., Carter, T.R., Emori, S., Kainuma, M., Kram, T., Meehl, G.A., Mitchell, J.F.B., Nakicenovic, N., Riahi, K., Smith, S.J., Stouffer, R.J., Thomson, A.M., Weyant, J.P. & Wilbanks, T.J. 2010. The next generation of scenarios for climate change research and assessment. *Nature*, 463(7282), pp.747–756.
- Nastev M. & Aubertin M. 2000. Hydrogeological modelling for the reclamation work at the Lorraine mine site Quebec, *1st Joint IAH-CNC-CGS Groundwater Specialty Conference*, Montreal, Quebec, pp. 311–318.
- Nordstrom, D.K. 2000. Advances in the hydrogeochemistry and microbiology of acid mine waters. *International Geology Review*, 42(6), 499–515.
- Orava, D.A, Tremblay, G.A., Tibble, A. & Nicholson, R. 1997. Prevention of acid rock drainage through the application of in-pit disposal and elevated water table concepts, *4th ICARD*. Vancouver, Canada, Vol.3, p.973–983. Washington, DC: US Department of Commerce, Weather Bureau.
- Ouangrawa, M. 2007. Étude expérimentale et analyse numérique des facteurs qui influencent le comportement hydro-géochimique des résidus miniers sulfureux partiellement saturés. *Ph.D. Thesis*, Department of Civil, Geological & Mining Engineering, École Polytechnique Montréal.
- Ouangrawa, M., Molson, J., Aubertin, M., Bussière, B. & Zagury, G.J. 2009. Reactive transport modelling of mine tailings columns with capillarity-induced high water saturation for preventing sulphide oxidation. *Applied Geochemistry*, 24: 1312–1323.
- Pabst, T., Aubertin, M., Bussière, B. & Molson, J. 2017. Experimental and numerical evaluation of single-layer covers placed on acid-generating tailings. *Geotech Geol Eng* 35: 1421–1438. <https://doi.org/10.1007/s10706-017-0185-0>
- Palmer, W.C. 1965. *Meteorological drought* (Vol. 30).
- Peterson, T.C. & Baringer, M.O. 2009. State of the climate in 2008. *Bulletin of the American Meteorological Society*, 90(8), S1–S196.
- Plummer, D.A., Caya, D., Frigon, A., Côté, H., Giguère, M., Paquin, D., Biner, S., Harvey, R. & De Elia, R. 2006. Climate and climate change over North America as simulated by the Canadian RCM. *Journal of Climate* 19, 3112–3132.
- Ritcey, G.M. 1989. Tailings Management, Problems and Solutions in the Mining Industries. *Elsevier*.
- Ritchie, A.I.M. 1994. Rates of mechanisms that govern pollutant generation from pyritic wastes. In *Environmental Geochemistry of Sulfide Oxidation*. December 20, 1993, 108–122. DOI:10.1021/bk-1994-0550.ch009
- Romero-Lankao, P., Smith, J.B., Davidson, D.J., Diffenbaugh, N.S., Kinney, P.L., Kirshen, P., Kovacs, P. & Villers-Ruiz, L. 2014. North America. In: *Climate Change 2014: Impacts, Adaptation, and Vulnerability. Part B: Regional Aspects. Contribution of Working Group II to the Fifth Assessment Report of the Intergovernmental Panel on Climate Change*. Cambridge University Press, Cambridge, United Kingdom and New York, NY, USA, pp. 1439–1498.
- Seneviratne, S.I., Nicholls, N., Easterling, D., Goodess, C.M., Kanae, S., Kossin, J., Luo, Y., Marengo, J., McInnes, K., Rahimi, M., Reichstein, M., Sorteberg, A., Vera, C. & Zhang, X. 2012. *Changes in climate extremes and their impacts on the natural physical environment*. In: *Managing the Risks of Extreme Events and Disasters to Advance Climate Change Adaptation*. A Special Report of Working Groups I and II of the Intergovernmental Panel on Climate Change. Cambridge University Press, Cambridge, United Kingdom and New York, NY, USA, pp. 109–230.
- SRK (Steffen, Robertson & Kirsten), 1989. *Draft Acid Rock Technical Guide*. BC AMD Task Force, Vol. 1.
- Taylor, K.E., Stouffer, R.J., & Meehl G.A. 2012. An overview of CMIP5 and the experiment design. *Bulletin of the American Meteorological Society*, 93(4), 485–498
- Tebaldi, C., Hayhoe, K., Arblaster, J.M. & Meehl, G.A. 2006. Going to the extremes. An intercomparison of model-simulated historical and future changes in extreme events. *Climatic Change*, 79(3-4), 185–211.

- Vicente-Serrano, S. M., Beguería, S. & López-Moreno, J.I. 2010. A multiscalar drought index sensitive to global warming: the standardized precipitation evapotranspiration index. *Journal of climate*, 23(7), 1696–1718.
- Vick, S.G. 2001. Stability aspects of long-term closure for sulphide tailings. In: *Safe Tailings Dams Constructions*, Gaellivare, Sweden, 12p.
- Vincent, L. A. & Mekis, E. 2006. Changes in daily and extreme temperature and precipitation indices for Canada over the twentieth century. *Atmosphere-Ocean*, 44(2), 177–193.
- World Meteorological Organization (WMO) and Global Water Partnership (GWP). 2016: *Handbook of Drought Indicators and Indices* (M. Svoboda and B.A. Fuchs). Integrated Drought Management Programme (IDMP), Integrated Drought Management Tools and Guidelines Series 2. Geneva.
- Yagouti, A., Boulet, G., Vincent, L., Vescovi, L. & Mekis, E. 2008. Observed changes in daily temperature and precipitation indices for southern Québec, 1960–2005. *Atmosphere-Ocean*, 46(2), 243–256.

Evaluation of Physical Parameters in Environmental Desulfurization by Flotation for Production of Reclamation Cover-suitable Desulfurized Tailings

J. Guimond-Rousson, I. Demers, and C. Rocard

Research Institute on Mines and Environment, University of Quebec in Abitibi-Témiscamingue, Rouyn-Noranda, Quebec, Canada

ABSTRACT: Environmental desulfurization is a process that can be integrated at the end of ore processing to produce sulfide-lean tailings that can then be reused for on-site construction purposes. Very few studies focused on the hydrodynamic aspects of flotation, and on how these parameters may affect the desulfurized tailings physical properties. The present project investigated the influence of residence time and slurry density on the residual sulfide (S) content and on the particle size distribution of the desulfurized tailings. A reduction of residence time increased the %S in the tailings and decreased S recovery to the concentrate. With a 25% solids feed, the flotation tailings were coarser than the feed, while with a feed at 20 and 15% solids, the tailings were finer. Empirical models to estimate the saturated hydraulic conductivity and water retention curve were used to compare the desulfurized tailings to typical cover materials used in mine site reclamation.

1 INTRODUCTION

1.1 Previous work

Environmental desulfurization was proposed as a part of “integrated mine waste management”, an approach that focuses on the optimization of material fluxes within the mining and waste management processes to ultimately reduce the environmental impacts of mining operations (e.g. Bois et al. 2005; Benzaazoua et al. 2000, 2008; Hesketh et al. 2010). The main objective of environmental desulfurization is the removal of most of the reactive fraction of a mine waste stream to produce unreactive tailings and a concentrated reactive fraction, with a much lower mass than the initial waste stream (Humber, 1995; Leppinen et al., 1997; Benzaazoua et al., 2000). In the case of acid generating tailings, sulfide minerals are the reactive fraction that needs to be removed. Environmental desulfurization was studied by several authors at the laboratory scale (e.g. McLaughlin and Stuparyk, 1994; Humber, 1995; Leppinen et al., 1997; Benzaazoua et al., 2000; Yalcin et al., 2004). It was found that froth flotation of bulk sulfides was the most efficient technique to desulfurize tailings (Humber, 1995; Benzaazoua et al., 2000). Being successful in the laboratory, some authors performed desulfurization in pilot plant, and in the plant (McLaughlin and Robertson, 1994).

Three mechanisms are considered to be involved in mineral recovery by flotation: i) attachment of hydrophobic particles to air bubbles (real flotation); ii) hydraulic entrainment of particles by water that reaches the froth zone; iii) physical entrapment of particles between slurry and air bubbles. In the case of real flotation, recovery is defined by three steps: collision between the air bubble and the solid particle, then adhesion of the particle to the bubble, and pos-

sibly detachment of the particle from the air bubble. The probability of recovery is therefore defined as (Yoon, 2000):

$$P = P_c P_a (1 - P_d) \quad (1)$$

Where P is the probability of recovery, P_c is the probability of collision, P_a is the probability of adhesion, and P_d is the probability of detachment. Collision is influenced by particle and bubble sizes and hydrodynamic conditions. Adhesion is influenced by hydrophobicity of particles. Detachment is a function of particle mass as well as hydrophobicity (Yoon, 2000).

The “integrated mine waste management” approach suggests to use desulfurized tailings as cover material in tailings pond reclamation to prevent acid mine drainage generation. Several cover types are available (MEND, 2004); however in a humid climate (such as the one in Canada) oxygen barriers are considered the most efficient to prevent AMD production. An oxygen barrier can be created by submerging the sulfide tailings under water (Davé et al., 1997), or by keeping at least part of the cover material nearly water saturated (Nicholson et al., 1989). The use of desulfurized tailings as oxygen barrier cover material was investigated in the laboratory where desulfurized tailings were used as the moisture-retaining layer in covers with capillary barrier effect (CCBE) (Bussière et al., 1997; Benzaazoua et al., 1998; Bussière et al., 2004), and as monolayer covers combined with an elevated water table (Dubchuk et al. 2013; Demers et al. 2009). Numerical modelling work was performed to simulate the performance of covers made of desulfurized tailings (Mbonimpa et al., 2003; Romano et al., 2003; Demers et al. 2010). Results indicated that low sulfide tailings are chemically suitable as cover material, and that residual sulfide content of desulfurized tailings can contribute to the reduction of oxygen flux by consuming part of the oxygen that migrates through the cover. Prior work was mainly focused on physicochemical aspects of flotation, but no studies were performed on the effect of desulfurization on tailings hydrogeological properties. Those properties, and more specifically particle size distribution, may be altered by the desulfurization process and ultimately affect the performance of cover systems made of desulfurized tailings. A recent experiment performed by the research team revealed that desulfurization of tailings from 17%S to below 2%S yielded a desulfurized material coarser than the original tailings (Demers et al. 2013). The suitability of this desulfurized material for oxygen barrier cover application is then questionable.

1.2 Objective of the work

Ultimately, the research strives to integrate mineral processing and environmental management to improve and optimize tailings management to ultimately ease site reclamation, though environmental desulfurization as a mean to produce material with the adequate hydrogeological properties to be used in mine site reclamation. A major objective is to study the effect of environmental desulfurization by flotation on the tailings hydrogeological properties. The present project investigated the influence of residence time and slurry density during desulfurization in a laboratory flotation column, on the residual sulfide (S) content and on the particle size distribution of the desulfurized tailings.

2 MATERIALS AND METHODS

2.1 Characterization methods

Tailings from Westwood mine (Iamgold Corp.) were transported to RIME laboratory as slurry in barrels. The tailings were kept submerged in process water until tested to prevent oxidation. Flotation tests were performed in two steps: rougher and scavenger steps. The focus of environmental desulfurization being on the S content of the tailings, no cleaner step was done on the concentrate. Solids were transferred into clean barrels and tap water was added to reduce slurry density to reach the desired % solids. Results presented in this paper were obtained in the scavenger flotation, therefore the initial feed represents the tails from the rougher step. Detailed characterization was performed on the feed to the scavenger flotation. An initial tailings sample was collected, dried and analyzed for specific gravity (helium pycnometer), and particle size distribution (Malvern Mastersizer laser particle size analyzer). Acid-base accounting was also

performed to obtain the neutralization potential and an induction furnace to obtain total sulfur and carbon content.

During the flotation tests, samples of feed, tailings and concentrate were collected every 12 to 16 minutes, which represents the residence time in the flotation circuit. The samples were filtered using a vacuum filter, then a portion was dried rapidly and sent to the induction furnace to get a rapid evaluation of the sulfur content. Later, the samples were homogenized and analyzed for particle size distribution using the Malvern Mastersizer laser particle size analyzer.

2.2 Flotation tests methods

Figure 1 presents a schematic view of the flotation circuit used in this project. It is composed of a distribution tank where the slurry density is set to the desired value. For this project, slurry density was a parameter that varied between 15 and 25% solids. A test was done at 10% solids without success, and over 25% solids settlement in the pumps and pipes was observed. The distribution tank feeds the first conditioner where activator CuSO_4 was added at a dosage of 300 g/t for rougher and 50 g/t for scavenger flotation. Reagents are added by dosing pumps. The slurry is transferred by gravity to the second conditioner where collector Kax-51 is added at a dosage of 300 g/t for rougher and 50g/t for scavenger. Frother (MIBC, 50 g/t) is added in the collector conditioner. Natural pH was selected for the material in this project, therefore no pH modifier were used. Nevertheless, pH and Eh were monitored by sensors in the distribution tank, in both conditioner, and in the tailings tank.

The conditioned slurry is transferred in the flotation column using a variable speed pump, initially set at 1.34 l/min. This value was modified from 1.17 l/min to 1.50 l/min during the test. Air is introduced in the column at a constant rate of 3.9 l/min and passes through a porous plate to generate bubbles. The column is 4 m high and has an inner diameter of 7.62 cm, which corresponds to a volume of approximately 19 liters. Froth level was set at 20 cm from the top of the column. Wash water was not used in this project. A control system regulates the operation of the flotation column circuit. The concentrate is collected in a specific tank, while tailings are also stored in tanks.

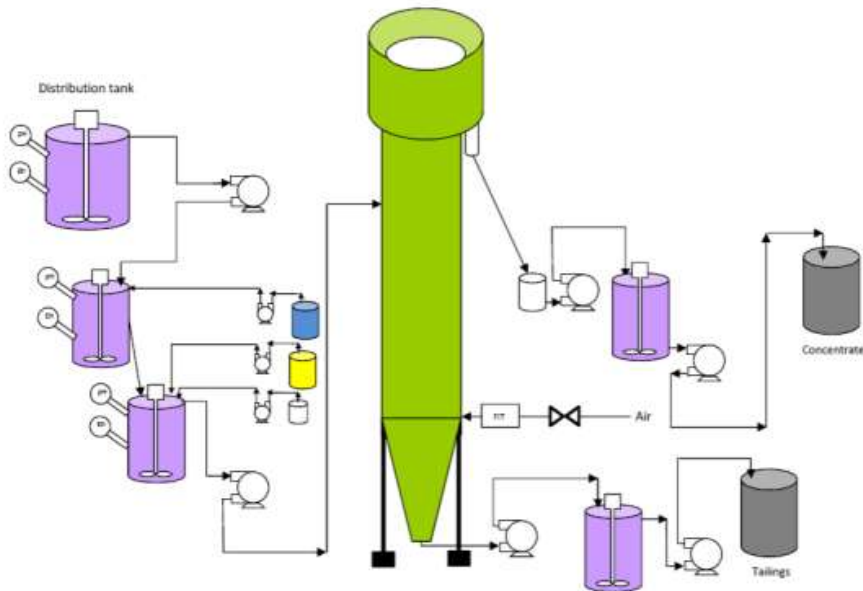


Figure 1. Schematic view of the flotation column circuit used in this project

Flotation was performed over several days. On the first day, the rougher step was done to produce tailings with 0.4% S. Since the target S content in the desulfurized tailings was below 0.3%, a scavenger step was performed. Three days were required to test the slurry density and residence time effect on the tailings properties: day 1 with feed at 20% solids; day 2 with feed at 15% solids; and day 3 with feed at 25% solids. For the 15% solids test day, residence time was varied by changing the slurry feed rate to the column. Approximately one hour was allowed for the system to stabilize between each feed rate modification. Samples were taken regularly to establish the mass balance. Table 1 presents tested variable values corresponding to the samples collected.

Table 1: Description of the tested parameter values during scavenger flotation tests

Samples	Slurry density (% solids)	Slurry feed rate (l/min)	Residence time (min)
#1 to #4	20	1.34	14
#5 to #8	15	1.34	14
#9 to #12	15	1.50	12
#13 to #16	15	1.17	16
#17 to #20	15	1.34	14
#20 to #24	25	1.34	14

3 RESULTS

3.1 Initial characterization

Westwood tailings used as feed for the complete desulfurization tests contained 5% S, however this project was performed in the scavenger step, where the feed was tailings from the rougher step. The scavenger feed contained 0.49% S and 0.18% C, which correspond to an acidification potential of 15.4 kg CaCO₃/t. Neutralization potential was evaluated at 15.7 kg CaCO₃/t. The acid-base accounting results indicated that the scavenger feed is considered as potentially acid-generating because its net neutralization potential (NNP) is below -20 kg CaCO₃/t and its ratio of NP/AP is below 3 (Price et al. 1997). These results confirmed the need to perform the scavenger step to produce tailings that are non-acid generating. The low neutralization potential is not sufficient to neutralize the potential acid produced by the residual S. According to the ratio NP/AP, to reach a ratio of 3 the S content in the tailings should be approximately 0.17%.

Scavenger feed particle size distribution is presented in Figure 2. Most of the particles are within the range 10-100 µm, which respond usually well to separation by flotation (Tortorelli et al. 1997). Almost 90% of all particles are below 80 µm, and D₁₀ (diameter where 10% of particles are finer) is 4.1 µm. Coefficients of uniformity (C_u) and of conformity (C_c) are 6.73 and 1.01, respectively.

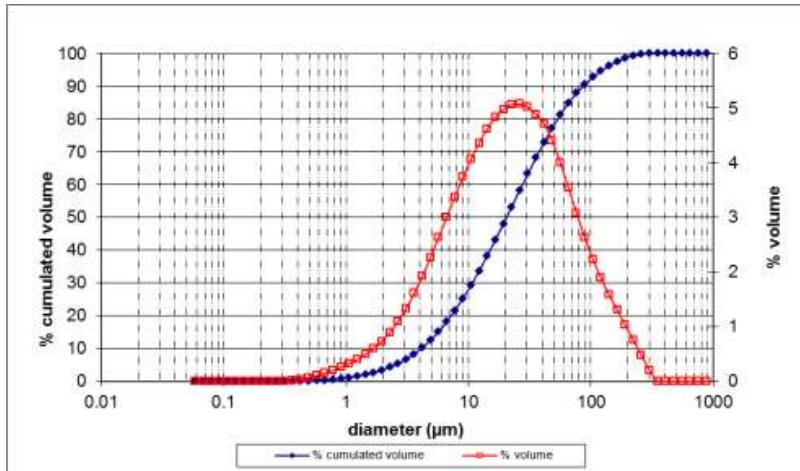


Figure 2. Particle size distribution of scavenger feed

3.2 Flotation results

Complete flotation results obtained during the three days of scavenger flotation are presented continuously in Figure 3. Vertical lines indicate changes in parameter settings. The feed grade had an average of 0.40% S, however a decreasing trend was observed. This decrease was attributed to the mixing of the slurry barrels before feeding the distribution tank. S content in the tails was generally below 0.15%, which meets the target of 0.17% S determined from the NP/AP ratio criterion to produce a non-acid-generating tailings. Concentrate grade fluctuated somewhat more compared to feed and tails grade. Oscillations between 16 and 31% S were observed, with the highest concentrate grades obtained at the end of the flotation test.

Figure 4 presents the recovery throughout the test. Above 60% recovery of S was achieved in the concentrate. The mass recovery to the concentrate was very low, 1 to 2%, which is expected for environmental desulfurization. The objective of desulfurization is to remove most of the sulfides from the tailings and concentrate these sulfides in a low volume or mass fraction. Such a high mass recovery to the tails was possible because the calculation was done for the scavenger step only.

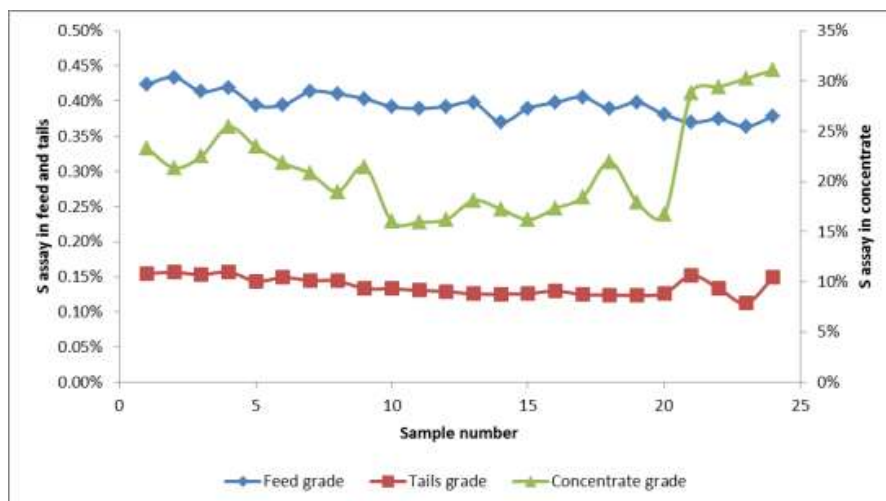


Figure 3. Sulfur content in feed, tails and concentrate from the scavenger flotation test

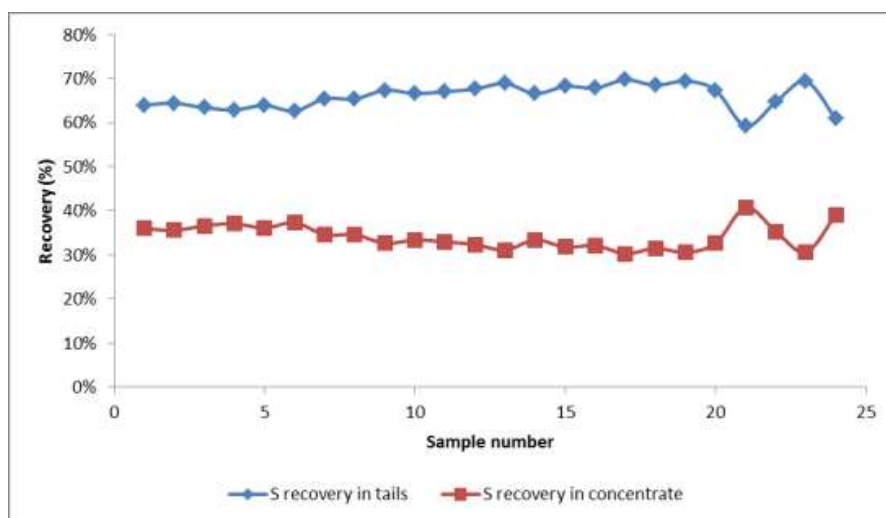


Figure 4. Sulfur recovery in concentrate and tails from the scavenger flotation test

3.2.1 Effect of residence time on desulfurization

Samples representing the three different residence time in the flotation column were extracted and compared. Figure 5 shows that the S content in the flotation tails varies between 0.13% and 0.15%, with the highest value at a residence time of 14 minutes. A trend is more evident for S recovery to the tails, which increases from 66.5% to 70.2% with an increase in residence time from 12 to 16 minutes. For environmental desulfurization, the lowest S content and the highest S recovery in the concentrate are targeted. In this sense, the flotation with a residence time of 16

minutes in the column provides the minimal values for grade in tails, and maximal value for recovery.

Particle size distributions for the samples representing the three residence times were compared and showed no difference between each other. It appears that residence time has an effect on the partition of S during the process, but not on the size of particles being separated.

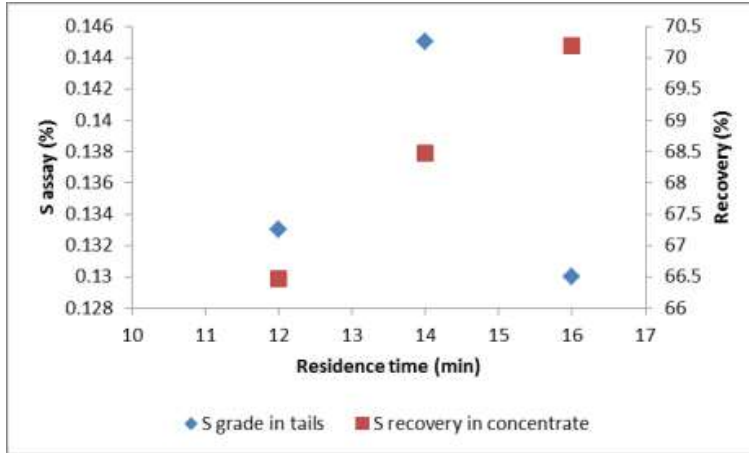


Figure 5: S grade in tails and recovery in concentrate for the tested residence time in the flotation column

3.2.2 Effect of slurry density on desulfurization

Figure 6 presents the effect of slurry density on S content in the tails and on its recovery in the concentrate. As seen with the test on residence time variation, the slurry density had a minimal impact on S content, with no particular trend. However, S recovery decreased with increasing slurry density. The addition of solid particles in the column, which replaced water but did not change the amount of gas, reduced the probability of particle-gas bubble collision, which affected the recovery. A lower slurry density is therefore desired for a better recovery.

Particle size distribution of the tails samples are presented in Figure 7. Compared to the feed, tails produced with 15% and 20% solids are finer, while tails produced at 25% solids are coarser. Feed D_{50} was 20 μm , while after desulfurization it became 18 μm for 15% and 20% solids, and 25 μm for 25% solids. Likewise, feed D_{80} was 55 μm and became 45 and 46 μm for 15% solids and 20% solids, respectively, and for 25% solids D_{80} was 80 μm .

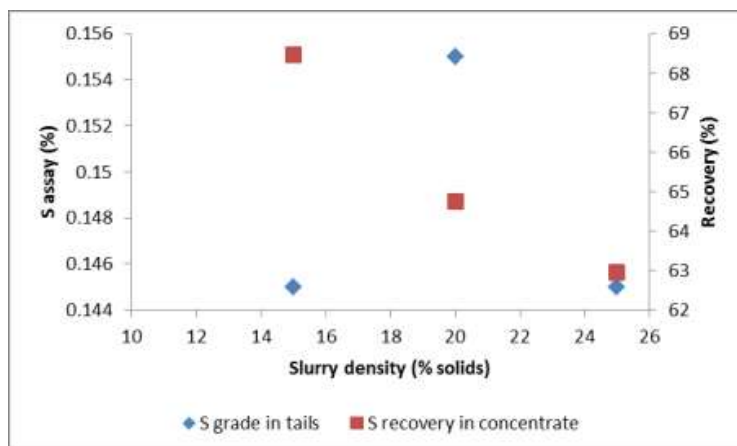


Figure 6. S grade in tails and recovery in concentrate for the tested slurry density in the flotation column

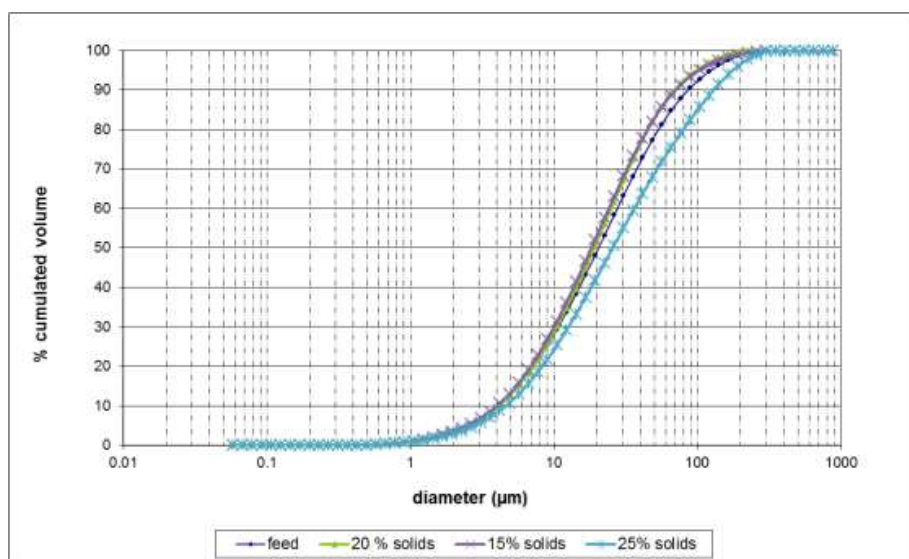


Figure 7. Particle size distribution of feed material and desulfurized tailings at different slurry density

4 DISCUSSION

Results showed that residence time had no visible impact on particle size distribution of the desulfurized tailings, but an increase in slurry density made the desulfurized tailings coarser than the feed. It appears that finer particles were recovered preferentially at higher slurry density. For production reasons, it could be desirable to desulfurized at higher slurry density to increase throughput, however it is necessary to verify if the desulfurized tailings can still be used as efficient cover material.

Preliminary evaluation of hydrogeological properties can be achieved with simple empirical models. For saturated hydraulic conductivity (k_{sat}), Kozeny-Carman modified equation (see equations 2 and 3) (Aubertin et al 1996) can be applied using particle size distribution data.

$$k_{\text{sat}} = C_H D_{10}^2 \quad (2)$$

$$C_H = 1962 \frac{e^{5.16}}{(1+e)} C_U^{1/3} \quad (3)$$

Assuming a void index of 0.8 (typical of slurry deposited tailings, Bussi re 2007), for 15% solids the calculated k_{sat} is 5.20×10^{-5} cm/s. For 25% solids, the calculated k_{sat} is 7.56×10^{-5} cm/s. The values are quite similar. The reason is that the value of D_{10} in the equation has a considerable impact on the k_{sat} value, and both tailings at 15% solids and 25% solids have very close values of D_{10} . Typical values of k_{sat} for cover material range between 10^{-4} to 10^{-5} cm/s, therefore both materials produced would be suitable in terms of k_{sat} .

Preliminary estimation of the soil-water characteristic curve (SWCC) was obtained using the modified Kovacs model (Aubertin et al. 2003). Using again particle size distribution data and a void index of 0.8, the estimated SWCC are presented in Figure 8. Both SWCC have the same shape, only the point of inflection where drainage starts, the air-entry value (AEV), is different, which shifts the 15% solids material towards higher suction values. Indeed, the AEV estimated is 200 cm for the 25% solids material and 300 cm for the 15% solids material. Values obtained from cover applications are in the range of 200 to 500 cm (Demers et al. 2017). The difference warrants a more detailed investigation using laboratory measurements to better evaluate the SWCC and AEV. Nevertheless, the difference observed in the AEV should be considered when designing the desulfurization circuit, particularly when choosing the desired slurry density.

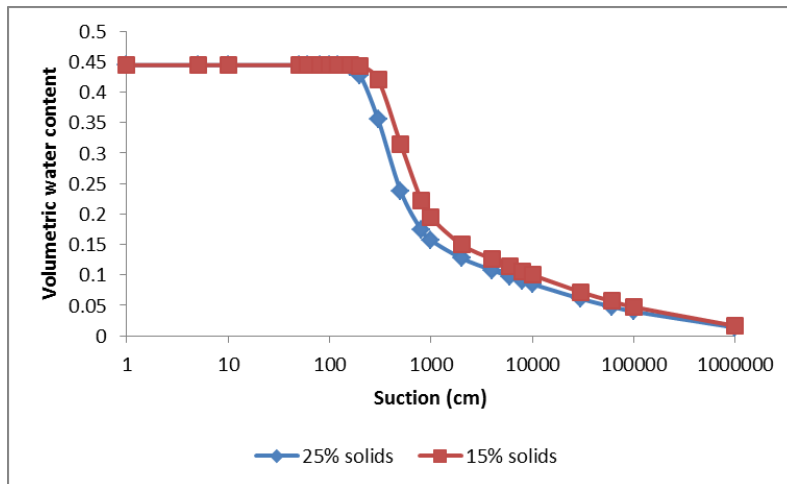


Figure 8. Soil-water characteristic curves for tailings desulfurized at 15% solids and 25% solids

5 CONCLUSION

Desulfurization is now recognized as an integrated mine waste management method to reduce the environmental impact of mine waste by removing the sulfide minerals from tailings. The sulfide-lean, or desulfurized tailings, are suggested as material to be reused as a replacement of natural fine soil in reclamation cover scenarios. The hydrogeological properties of desulfurized tailings should therefore be similar to those of materials used in cover applications.

Desulfurization of tailings was performed in a flotation column to investigate the effect of residence time and slurry density on desulfurization performance to produce sulfide-lean tailings and also on the tailings particle size distribution.

Results showed that residence time had no visible impact on particle size distribution of the desulfurized tailings, but an increase in slurry density made the desulfurized tailings coarser than the feed. Using empirical relationships, saturated hydraulic conductivity, soil-water characteristic curve and air-entry value were estimated for tailings desulfurized at 15% solids and at 25% solids. Saturated hydraulic conductivity in the range of 10-5 cm/s were obtained, as well as AEV of 200 and 300 cm. These parameters correspond to values seen in natural materials used as cover.

Further investigations are suggested to evaluate more precisely the soil-water characteristic curve and air-entry value, since these parameters are crucial to understand the hydrogeotechnical behavior of the materials. Other hydrodynamic parameters during flotation are also under investigation, such as air flowrate and froth thickness, to identify the most significant parameters that affect particle size distribution of the desulfurized tailings.

ACKNOWLEDGEMENTS

The authors would like to acknowledge the implication of UQAT laboratory personnel: Tony Grondin, Annie-Claude Drouin, Mathieu Doire, Joël Beauregard. Financial support was provided by Fond de recherche du Québec – Nature et technologies (FRQNT) and Iamgold corporation.

REFERENCES

- Aubertin, M., Bussière, B., and Chapuis, R.P. 1996. Hydraulic conductivity of homogenized tailings from hard rock mines. *Canadian Geotechnical Journal*, 33(3): 470-482
- Aubertin, M., Mbonimpa, M., Bussière, B., Chapuis, R.P. 2003. A model to predict the water retention curve from basic geotechnical properties. *Canadian Geotechnical Journal* 40(6): 1104-1122
- Bois, D., Benzaazoua, M., Bussière, B., Kongolo, M. and Poirier, P. 2005. A feasibility study on the use of desulphurized tailings to control acid mine drainage. *CIM Bulletin*, 98(1087):74.
- Benzaazoua, M., Bussière, B., Nicholson, R.V. and Bernier, L., 1998. Geochemical behavior of multi layered cover made of desulphurized mine tailings. *Tailings and Mine Waste* 98, Fort Collins, pp. 389-398.
- Benzaazoua, M., Bussière, B., Kongolo, M., McLaughlin, J. and Marion, P. 2000. Environmental desulphurization of four canadian mine tailings using froth flotation. *International Journal of Mineral Processing*, 60: 57-74.
- Benzaazoua, M., Bussière, B., Aubertin, M., Demers, I., Fried, E. et Blier, A. 2008. Integrated mine tailings by combining environmental desulphurization and cemented paste backfill: application to Mine Doyon, Québec, Canada. *Minerals Engineering*, 21: 330-340.
- Bussière, B. 2007. Colloquium 2004: Hydrogeotechnical properties of hard rock tailings from metal mines and emerging geoenvironmental disposal approaches. *Canadian Geotechnical Journal*, 44(9): 1019-1052
- Bussière, B., Nicholson, R.V., Aubertin, M. and Servant, S. 1997. Effectiveness of covers built with desulphurized tailings: column test investigation, *4th International Conference on Acid Rock Drainage*, Vancouver, BC, pp. 763-778.
- Bussière, B., Benzaazoua, M., Aubertin, M. and Mbonimpa, M. 2004. A laboratory study of covers made of low sulphide tailings to prevent acid mine drainage. *Environmental Geology*, 45: 609-622.
- Davé, N.K., Lim, T.P., Horne, D., Boucher, Y. and Stuparyk, R., 1997. Water cover on reactive tailings and wasterock: Laboratory studies of oxidation and metal release characteristics. *4th International Conference on Acid Rock Drainage*, Vancouver, pp. 779-794.
- Demers, I., Bussière, B., Mbonimpa, M., Benzaazoua, M., 2009. Oxygen diffusion and consumption in low-sulphide tailings covers. *Canadian Geotechnical Journal*, 46: 454-469.

- Demers, I., Bussière, B., Benzaazoua, M., Mbonimpa, M., 2010. Preliminary optimization of a single-layer cover made of desulfurized tailings: application to the Doyon Mine tailings impoundment. *SME transactions*, vol. 326, p. 21-33.
- Demers, I., Villeneuve, M., Kalonji-Kabambi, A., 2013. *Désulfuration de résidus de la mine Laronde aux fins d'évaluation du comportement hydrogéologique d'une CEBC faite essentiellement de matériaux miniers*. Rapport URSTM, projet PU-2013-03-786.
- Demers, I., Huo-Kang, J. and Mbonimpa, M., 2017. Variability of material properties used for covers to prevent acid mine drainage. *Canadian Geotechnical Conference GeoOttawa 2017*, Ottawa, Canada, 1-4 oct.
- Dobchuk, B., Nichol, C., Wilson, G.W., Aubertin, M., 2013. Evaluation of a single-layer desulphurized tailings cover. *Canadian Geotechnical Journal*, 50(7), 777-792.
- Hesketh, A.H., Broadhurst, J.L., Harrison, S.T.L., 2010. Mitigating the generation of acid mine drainage from copper sulfide tailings. *Minerals Engineering*, 23: 225-229.
- Humber, A.J. 1995. Separation of sulphide minerals from mill tailings, Sudbury 95, *Conference on mining and the environment*, Sudbury, Ontario, pp. 149-158.
- Leppinen, J.O., Salonsaari, P. and Palosaari, V. 1997. Flotation in acid mine drainage control: beneficial of concentrate. *Canadian Metallurgical Quarterly*, 36(4): 225-230.
- Mbonimpa, M., Aubertin, M., Aachib, M. and Bussière, B., 2003. Diffusion and consumption of oxygen in unsaturated cover materials. *Canadian Geotechnical Journal*, 40: 916-932
- McLaughlin, J. and Robertson, G., 1994. Test production of low sulphur rock tailings at Inco's Clarabelle mill. *26th annual meeting of the Canadian Mineral Processors*, Ottawa, Canada.
- McLaughlin, J. and Stuparyk, R., 1994. Evaluation of low sulphur rock tailings production at Inco's Clarabelle mill. *Innovation in Mineral Processing*, Sudbury, Ontario.
- MEND, 2004. *Design, Construction and Performance Monitoring of Cover Systems for Waste Rock and Tailings*, MEND report 2.21.4, Canmet, Ottawa, Canada.
- Nicholson, R.V., Gillham, R.W., Cherry, J.A. and Reardon, E.J., 1989. Reduction of acid generation through the use of moisture-retaining cover layers as oxygen barriers. *Canadian Geotechnical Journal*, 26: 1-8.
- Price, W.A., Morin, K., and Hutt, N. 1997. Guideline for the prediction of acid rock drainage and metal leaching for mines in British Columbia: Part II - Recommended procedures for static and kinetic testing. *4th International Conference on Acid Rock Drainage*, Vancouver, BC, pp. 15-30.
- Romano, C.G., Mayer, K.U., Jones, D.R., Ellerbroek, D.A. and Blowes, D.W., 2003. Effectiveness of various cover scenarios on the rate of sulfide oxidation of mine tailings. *Journal of Hydrology*, 271: 171-187.
- Tortorelli, J.P., Craven, J., Toguri, J., Dobby, G. et Agar, G. 1997. The effect of external gas/slurry contact on the flotation of fine particles. *Minerals engineering*, 10(10), 1127-1138.
- Yalcin, T., Papadakis, M., Hmidi, N. and Hilscher, B., 2004. Desulphurization of Placer Dome's Musselwhite mine gold cyanidation tailings. *CIM Bulletin*, 97(1084).
- Yoon, R.-H. 2000. The role of hydrodynamic and surface forces in bubble-particle interaction. *International Journal of Mineral Processing*, 58(1-4), 129-143.

Mine Waste Remediation as a Stepping Stone for New Contractors in Emerging Economies

X. Adams and B. Engelsman

SRK Consulting, Cape Town, Western Cape, South Africa

R. Mayne

SRK Consulting, Johannesburg, Gauteng, South Africa

ABSTRACT: In emerging markets many small construction contractors have difficulty entering the large construction project market, even when local content is encouraged. Such contractors suffer from a lack of training and experience that would allow them to win projects. That training is often unaffordable, in many cases due to historical discrimination. In contrast to typical construction projects, remediation of certain types of mining waste, such as asbestos waste, is less complex and thus requires less training and thus an opportunity for newer contractors.

In South Africa, a current project to remediate mining waste at derelict asbestos mines has provided such opportunities and is described in this paper as a case study. Experience on that project has identified successes, but also challenges particularly in administrative and financial management as well as health and safety. This paper concludes that a framework which includes sizing of projects, training and mentorship, might address these challenges.

1 INTRODUCTION

1.1 Barriers to Entry into large-scale construction in South Africa

Barriers to entry in a marketplace are problematic, not only for individuals, but also on a societal level. For individuals, these barriers entrench any disadvantages that are the result of circumstance thus blocking off opportunities for personal economic growth. In an economy, the arrival of new competitors into a market place improves competition (OECD 2007). A competitive market is generally advantageous at all levels of the economy, from small scale projects to large industries. It therefore follows that barriers to entry matter not only for very small businesses, or employees, but also for businesses attempting to expand from smaller to larger projects.

In any economy, barriers to entry exist for market newcomers. However, in South Africa barriers to entry also arise from disparities among people, particularly in education, and in many cases due to historical inequalities. In the construction sector, similar barriers to entry exist as for other industries (Gruneberg and Ive 2000) but one barrier imposed by clients is particularly limiting. Clients generally insist that contractors have experience on projects of a similar nature, size and complexity thereby limiting upward growth for construction firms (De Valance, 2012).

In South Africa, the Construction Industry Development Board (CIDB) has attempted to address the problem of experience by creating a stepped grading system. The CIDB is a public entity established by an Act of parliament and is tasked with building a regulatory and development framework in which capabilities can be expanded in the industry in an effort to develop globally competitive standards (CIDB, 2018a).

In the CIDB grading system, successfully completing a job of a certain size qualifies a contractor for a project of a larger size. The grading system also includes requirements for staff skill levels depending on the size of the project (CIDB, 2018b) The Department of Public Works in South Africa, in partnership with the CIDB, also provides a framework for contractor

development that includes approaches such as encouraging joint ventures between large contractors and developing contractors (DPW, 2011)

1.2 Mine Waste Remediation as an opportunity

Mine closure, including mine waste remediation, provides a large economic opportunity because it is a large and growing industry. In South Africa, derelict and ownerless mines alone number nearly 6000, and many active mines still exist (DMR, 2009). Of these, many include waste rock dumps and tailings facilities. The most common type of mine waste remediation in South Africa involves capping the waste in place, which presents a particular opportunity to new contractors because it is relatively simple from a construction point of view. Technical simplicity can allow contractors to focus on other aspects of the operation that present challenges.

Capping in place is simple because it involves relatively simple construction tasks. The first step is to reshape the waste if necessary. Thereafter a cover is placed over the waste such as a liner, rock cladding, a well-graded fill, a geotextile, soil or some combination of these. Thereafter, stormwater controls are constructed and vegetation planted (except in rock cladding) to manage long-term erosion and improve aesthetics. These activities involve mostly bulk earthworks with relatively wide tolerances on final levels compared to the tight tolerances required on other projects such as infrastructure development.

It must be noted that capping in place can be more complex particularly where groundwater contamination exists or other facilities are present. However, even in these cases the basic closure can be separated out as a large but simple construction project. Furthermore, in South Africa, a large number of derelict mines do not have a groundwater pollution problem because they are asbestos mines and asbestos does not migrate in groundwater.

1.3 This paper

In South Africa, a project is underway to remediate mining waste at derelict asbestos mines. The project has provided opportunities to relatively new contractors. SRK Consulting has been part of a team designing and overseeing construction activities at these mines for the last six years. After a number of years, experience on such projects has led to the identification of opportunities, but also challenges, and these will be discussed herein.

2 OBJECTIVE

The objective of this paper are to:

1. Assess whether mine waste remediation did provide a stepping stone for junior contractors using case studies.
2. Identify any challenges and opportunities associated with such an approach.
3. Recommend improvements to the stepping stone concept based on the above.

3 METHODOLOGY

A case study approach was adopted due to difficulty in obtaining confidential business information from Contractors and the Employer. Two emerging construction contractors and their work at three different mine waste remediation projects were selected as case studies. The selection was based on the size of the project, the availability of information and the fact that both contractors were relatively inexperienced at the outset. One of the Contractors also went on to remediate another mine, providing invaluable information on progress over time for this paper.

It is necessary to define what is meant by success in order to evaluate whether these projects did provide a stepping stone for emerging contractors. The following was selected as criteria for success:

1. Adequate performance on the project:
 - o Remediation met engineering design criteria;

- No endangering of health and safety.
- 2. Adequate business performance for the contractor (i.e. sound financial outcomes).
 - Improved skill and marketability for the contractor in the form of additional experience to assist in winning future projects;

Many of these items could not be measured directly – some were confidential business information and others were difficult to quantify. Consequently the following indicators were selected:

1. Adequate performance on the project
 - Engineer reviews;
 - Final completion certificates certifying adequate performance;
2. Health and safety observations (Note that SRK Consulting was not the direct health and safety agent and thus does not have full access to these data).
3. Adequate business performance for the Contractor (i.e. sound financial outcomes):
 - Tender pricing versus pricing by a professional quantity surveyor;
 - Anecdotal evidence of financial problems.
4. Improved skill and marketability of the Contractor:
 - It is assumed that if the Contractor performed adequately they would benefit from having a project to add to their list of experience and would have learnt by experience (i.e. indicator same as for 1);
 - Anecdotal evidence of improved skill in the Contractor's workforce.

4 CASE STUDIES

Over the last six years, the authors have been part of a team of engineers providing design and construction monitoring services to close abandoned asbestos mines. The primary aim of the overall project is to remediate mining waste deposits and other major sources of asbestos. Another aim, not addressed in this paper, but noted here for completeness, is to close adits, shafts and other remnants of mining. The methods of closure typically involved reshaping and capping in line with the guidelines for asbestos mine waste remediation in South Africa (DMR 2011).

Although not an explicit objective, a number of relatively inexperienced Contractors have been given opportunities on the project. No information was provided to the engineering team on the contractors selected for the work and their level of experience. However, it was clear that the contractors were, in many cases inexperienced, which should become clear from the case studies.

4.1 Site A, Contractor A, Relocation and capping of semi-processed waste at Site A

Site A was a derelict asbestos mine with very basic mining infrastructure and operations currently used by the local community for grazing. The exact date that mining ended is unknown, but discussions with locals indicated that mining ceased in the 1950s. This matches with the remains on site, which appear to indicate that mining in the area was artisanal – there is no indication of old roads, and hand-held hammers appear to have been used to separate the asbestos from the host rock so that it could be carried down the mountains on donkeys. Consequently, the mining waste was composed of material similar to that shown in Figure 1, as opposed to milled fiber common in more modern operations. Another indication that this was an artisanal mining setting, was that waste deposits were strewn across the site, most lying directly below adits on steep, densely vegetated slopes. In one case, the toe of the waste material extended into a non-perennial stream, prompting concerns of waste mobilizing off-site.

The closure plan for Site A included removal of asbestos waste from the steep slopes, particularly the slope adjacent to the watercourse. The waste would then be concentrated in a central deposit located in a more accessible area which was flatter and further away from the community. A cross-section of the design of that deposit is shown in Figure 2. The waste was covered with a well-graded mixture of material excavated from the central deposit footprint. The central deposit was designed with benches as well as subsurface drains and a protective gabion wall toe.



Figure 1. Rock waste including asbestos seams (left) and semi-processed asbestos waste with fibers separated from rock typically with hammers (right)

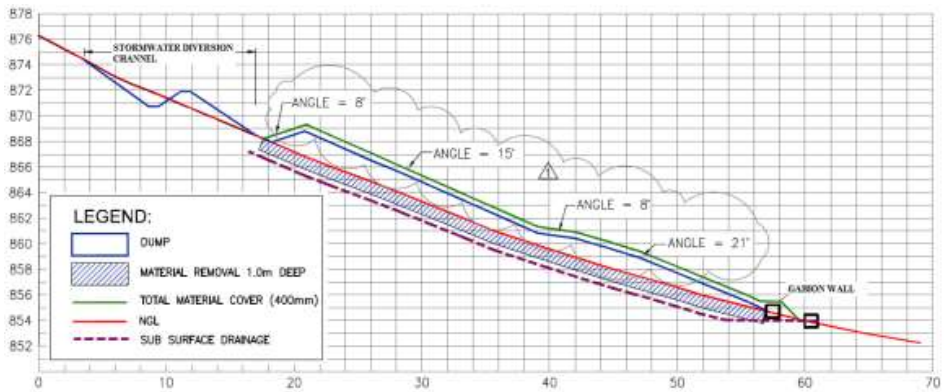


Figure 2. Cross-section showing the design of the central waste deposit at Site A



Figure 3. Construction of the central dump and the gabion wall of the central dump at Site A

The contractor employed to carry out the design was a relatively inexperienced earthworks contractor, mostly with road building experience, and will be referred to in this paper as Contractor A. The Contractor was overseen by the engineers from a distance, with monthly site visits to assess progress and quality.

Contractor A struggled to begin the work at Site A. The first item to be addressed, as per the contract was the submission of mandatory documentation. Once those documents were submitted, access to the site would be granted and work would begin. The contract stipulated that the documents were to be submitted within 7 calendar days and should include proof of insurance, proof of a guarantee, a program and a health and safety plan. The Contractor took 26 calendar days to submit the correct documentation. This indicated poor contract management, and possibly a poor understanding of the contract, and indeed throughout the project, documentation was submitted late and with errors.

On the technical aspects, the contractor completed some elements of the work very well, but did not entirely succeed in implementing the design. Figure 3 shows the central dump and the gabion wall at the toe of the dump under construction.

The Contractor carried out one portion of the work very well for an unexpected reason. A member of the community arrived with a business card indicating that he could build gabions and pour concrete slabs. This community member, with his team of young men from the community built all of the gabions to the required standard and suggested improvements which they conducted at no additional cost.

One particular technical failure was related to remediation of a steep slopes from which material was removed. Early in the work, Contractor A removed semi-processed waste mixed with rock from a particular steep slope by machine. After removal, the slope was inaccessible by machine because the exposed finer underlying material provided insufficient traction for vehicles. Without machine access, the Contractor failed to adequately cover and revegetate the slope although in time, vegetation began to grow naturally.

Technical work was concluded at Site A, when it was agreed by the engineers and the client that the contractor could not perform any better. The work was then deemed adequate, if not to specification, and the project was closed.

Financially, it was apparent that the Contractor struggled. The tendered price for the work was approximately half a million dollars (note that all prices are stated in US dollars and that the exchange rate on 10 June 18 was used to convert all prices). In comparison, the estimated cost by a professional quantity surveyor was just under \$ 900 000. At a particular point in the project, the Contractor requested early payment for the gravel capping layer that had not yet been procured to site, and supplied receipts for the gravel. The gravel in question was about forty percent more expensive than the contractor's price in the contract, and the Contractor incurred a substantial loss on the gravel. Later in the Works, the Contractor failed to obtain a dump truck as well as other equipment and materials timeously suggesting a potential cash flow problem. Finally, at the end of the project Contractor A was penalized \$ 50 000 for finishing late. Based on these facts, particularly the fact that the Contractor was eventually paid about 50% of what the professional quantity surveyor estimated, and the fact that Construction as a competitive industry does not have margins in the region of 50%, it is probable that the Contractor lost money on this particular project.

Health and safety was a priority on the project, but certain occurrences gave cause for concern. Two of the major actions to protect health and safety on asbestos projects are the use of protective masks to mitigate inhalation of asbestos, and dust control to mitigate asbestos being mobilized by wind. At the beginning of the project, the health and safety officer was unsure of the type of mask required which was very concerning, but this was fortunately quickly resolved. Dust control was also a concern as, on a number of occasions, the water truck used for dust control remained at the laydown area due to disputes with the operator. Payment was withheld for this aspect and it appeared to resolve thereafter.

4.2 Case Study 2: Contractor B, Remediation by reshaping and capping at Site B

Site B was an asbestos mine in a very arid area of the country. The date that mining ceased was unknown, but the larger scale of the workings and more structured adits suggested a higher level of mechanization than at Site A. The site included 21 separate waste dumps, some of which

comprised mostly of waste rock with some asbestos seams and some of which included concentrated loose asbestos fibers. A non-perennial stream bounded one of the deposits containing loose, processed fibers.

The closure plan involved reshaping the deposits and covering them with rock cladding. A gabion wall was also specified along the toe of the deposit for flood protection from erosion. The design is shown in cross-section in Figure 4, and in reality, after construction of the gabion wall in Figure 5.

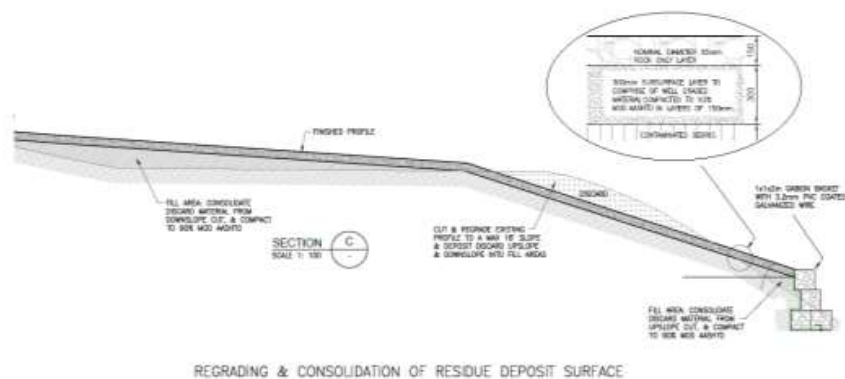


Figure 4. Cross-section showing the design of the central waste deposit at Site B



Figure 5. A waste deposit at Site B with gabion wall constructed.

No background information was provided to the Engineers on the Contractor selected for the work, but it was once again clear that the Contractor was inexperienced. The Contractor was overseen by the engineers from a distance, with monthly site visits to assess progress and quality.

On the technical aspects, the Contractor completed the job to a satisfactory standard, but appeared to struggle with administration, health and safety and in particular, finances. The con-

tractor struggled to submit initial documentation, such as insurances, timeously and received site access 62 calendar days late when the correct documents were finally submitted. Safety was also concerning especially when no work could proceed on the day that engineers visited the site because no personal protective equipment was available. Safety preparedness did improve over the course of the project, possibly due to the withholding of payment for safety management or due to constant reminders.

The financial setting was that the tendered price was \$ 1.2 million dollars, which was 67% of the \$ 1.8 million estimated by a professional quantity surveyor. This suggested that the contractor had underpriced, and indeed it was later discovered that the Contractor had underpriced his rock import by at least thirty percent, resulting in a substantial loss. The Contractor also failed to submit legitimate claims within contractual time limits thus forgoing additional revenue by being months late on their administration. The Contractor paid approximately a hundred thousand dollars in penalties for finishing late. By the end of the job, the contractor only managed to claim 0.8 Million for the above reasons.

Based on the above, and typical profit margins in the construction industry, it is unlikely that the Contractor profited at all from this project. They did however, stay in business and won another contract a few years later, which is the subject of the 3rd case study.

4.3 Case Study 3: Contractor B, Remediation by reshaping and capping at Site C

A few years after completion at Site B in 2016, Contractor B was awarded another tender at Site C. Site C was a large, commercial asbestos mine. The exact date that mining ceased is unknown, but mining in the area continued to as late as the 1980's (CSMI 2008). Site C included a number of waste deposits with some large deposits containing a mixture of rock and the more hazardous, loose fibers. The closure design for the deposits once again included reshaping and capping with a well graded material, and finally a protective rock-cladding layer. The project is ongoing at the time of writing, with little of the construction yet in place. However, some information on Contractor B's progress is already available.

The client took a different approach at Site C than on the previous projects. A resident engineer was stationed full time at the site. Training courses were included as mandatory for obtaining site access. Training courses included asbestos safety training, construction skills and construction management skills and were mandated for both the contractor and all local laborers. The objective was to provide locals with saleable skills and better equip the contractor for their work.

The contractor's performance was poor at the outset, but did show improvement with time. The Contractor began 49 days late, once again due to not providing the correct documentation to gain access to the works in time. This was very poor performance, but an improvement on the 62 days at Site B.

Financially, the Contractor appeared to be in a better position with their tendered price totaling slightly more than the estimation by a professional quantity surveyor. This suggests that they might have adequately priced for the job, and probably due to lessons learnt on the previous project.

From a safety perspective, the Contractor performed well. A survey of four engineers working with the Contractors, indicated that safety was of a high standard, and no major concerns directly related to the Contractor had occurred.

New problems on the site included volatile community relations, which have delayed the contractor considerably. In addition, water has been difficult to obtain which appears to be due to political issues at the supplier. This in turn has caused major safety concerns.

5 DISCUSSION

Based on the experiences communicated above, as well as at other sites remediated over six years, one particular conclusion is unavoidable: Major barriers to entry exist for emerging contractors at any level above the job of a laborer in the construction industry, and these barriers are in addition to the initial problem of winning projects. Good performance on large projects is actually very complicated and multifaceted, with challenges ranging from financial to social to

safety and technical. Furthermore, such projects are underpinned by large tender documents strewn with complex sets of standards and laws that are complex to navigate. Some key points on the technical, financial and health and safety issues inherent in these projects are discussed below, followed by a discussion on how the overall challenges encountered could be overcome.

5.1 Technical construction challenges and opportunities

Technical challenges on the site related to site specific settings rather than the complexity of the work itself. In general, the challenges were overcome by the contractors themselves, which was expected as construction is their core business. However, engineers did mention that technical challenges were largely reduced and the quality of construction improved where a full time resident engineer was employed. This indicates that the employment of a resident engineer might provide an opportunity for skills development, not least because of the more immediate and continuous feedback available to the contractor. Ready access to guidance from the resident engineer is also an obvious advantage.

Another approach to improving technical work could be that the joint ventures (as proposed by the CIDB) might also provide additional technical development for emerging contractors. However, larger companies might be hesitant to train competitors. On the case studies described, the client was hesitant to mandate joint ventures having experienced problems with the approach previously. To avoid this employing or contracting of an experienced individual, specifically tasked with mentoring, could be considered. There would be great benefit in doing so at tender stage.

5.2 Health and safety challenges and opportunities

At the sites described, it wasn't entirely clear why health and safety challenges occurred, especially as the engineering team was completely separate from the health and safety team. However, it was observed that contractors were at first unaware of the level of risk and how to address it. Withholding payments, constantly reminding contractors and informing them personally of some of the risks did appear to help. Contractor B, on their second project, performed much better possibly due to lessons learnt on the first project, and possibly due to the mandatory training courses which made workers at all levels aware of health and safety issues.

Another challenge with health and safety was the volatile community and the workers from the community. These people lived in the area and had been exposed to the risk for years. Perhaps, they did not distinguish between the lower, but significant, risks of living nearby and the higher risks when material was disturbed in their immediate vicinity. Furthermore, it was obvious that the community faced many other, much more immediate challenges, such as poverty and possibly more common illnesses typical in rural areas (e.g. Tuberculosis, HIV). To fully understand this issue is outside the typical engineering responsibilities, however, it has been identified by engineers as a major challenge.

Opportunities to ensure health and safety appear to be the actions already undertaken – providing information and enforcing standards and training. However, it would be useful if further research is done in the social sciences to provide guidelines on how to deal with communities for whom asbestos and workplace health and safety are only one of a host of much more pressing issues in their daily lives.

5.3 Financial challenges and opportunities

Inexperienced Contractors struggle to price correctly, and may take on too much financial risk when tendering. This is particularly clear when comparing their pricing to that of a professional quantity surveyor as shown in Figure 6 and then noting the anecdotal evidence of financial struggles described above in the case studies.

Pricing of tenders occurs before any involvement with engineers and thus it is difficult to assist contractors at this stage, and there is an obvious conflict of interest.

One option to assist in better pricing, similar to what was discussed in 5.2, is requiring a partnership between an established contractor and a newer contractor in the tender documenta-

tion or requiring explicit appointment of a mentor, with the mentor to counter-sign the tender documentation.

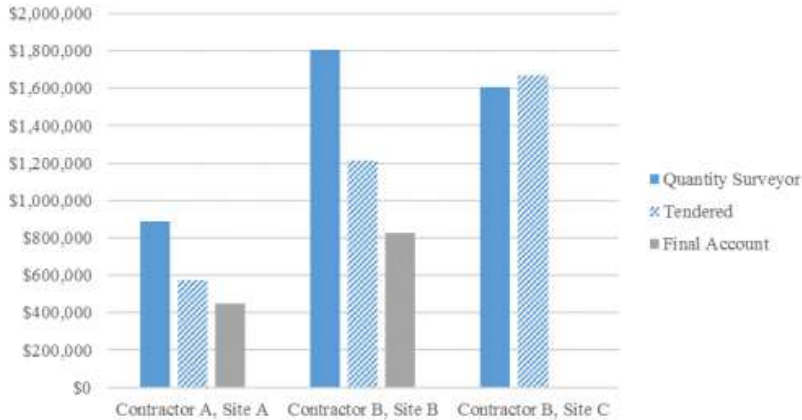


Figure 6. Pricing by professional quantity surveyors compared to tendered values and final accounts

Another approach is to carefully split projects such that manageable sizes and complexity of projects are let. Over time, contractors could apply for larger and larger jobs as their experience grows. This approach is also essentially the system proposed by the CIDB grading discussed in Section 1.1, but it would be a refinement of that grading with lower levels added. It would also involve splitting projects to specifically to allow for it. In fact, the opportunities identified for technical performance and health and safety could also be incorporated to cover all aspects which is the subject of the next section (Section 5.4).

5.4 All aspects

On consideration of the projects already conducted, the challenges encountered, and what worked well, a framework seemed like the next obvious step for improvement. One idea for that framework is based on approaches from the CIDB, as well as project experience, and additional ideas from engineers (Note that this is just a preliminary example to provide guidance for further debate, not a rigorous framework). Figure 7 provides a graphical example of that framework using the example of the asbestos mines already encountered (i.e. hazardous conditions, dispersed waste).

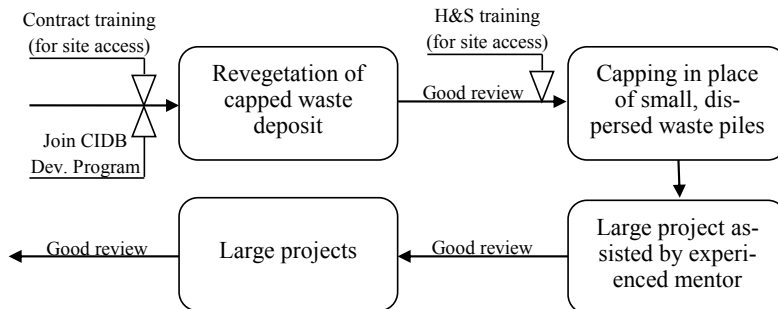


Figure 7. Preliminary example system of contractor development on asbestos mine remediation projects

Essentially the example in Figure 7 involves compartmentalizing some small defined but independent portions of remediation projects, particularly for first time contractors (first time in the sense of working on large remediation jobs, not in the sense of technical experience). These contractors can then learn and demonstrate their abilities before qualifying to bid for an entire site. Small independent portions could be something like burying of easily accessible dispersed material on site. The technical work is very simple, which would allow the contractor to instead focus on management, safety and documentation. Other examples could be demolition of easily accessible buildings or placement of soils and final revegetation.

In concert with the above stepped approach, training courses in contract management could be specified as part of the contract as an explicit requirement before site access is granted. Furthermore, retaining a resident engineer on site or using the mentorship approach could also add value.

Implementing a framework, like the above-described, does increase work for designers, and during tender compilation and during construction monitoring. However, if the aim is to empower emerging contractors, and not risk either the project's success or the viability of the contractors business, then something more is required than the current approach. The above system is a very early idea of what that "something more" could be, and warrants further development by a multidisciplinary team such that the multidisciplinary challenges of both projects, and emerging contractors, can be addressed.

6 CONCLUSION AND RECOMMENDATIONS

The case studies showed that mine waste remediation, using the approaches described in the case studies, was a stepping stone for some contractors. However it was a risky stepping stone, and it appears to have helped some emerging contractors to move into larger more complex markets and provided experience and training to them. However, it has also placed large financial strain on those contractors, and caused potential health and safety risks. That said, the aim of assisting newcomers in a market to overcome barriers to entry is an important one, especially in an economy dominated by inequality.

It is recommended that programs to assist new contractors continue, but that these programs be designed to adequately address the risks incurred by contractors when they take on these new, but challenging opportunities. Based on the case studies, a promising option to increase these stepping stones is a framework that includes oversight, mentorship and mandatory training. The system should also include compartmentalizing small projects out of larger projects, such that contractors can first work on these and learn the administration and formal contracting aspects of the work. The framework should be designed with rigorous, multidisciplinary research and piloting to address the multidisciplinary problems that contractors actually face.

REFERENCES

- CIDB, 2018a, About the cidb, *Construction Industry Development Board*, South Africa, <http://www.cidb.org.za/AboutUs/Pages/default.aspx>, accessed on 14 June 2018.
- CIDB, 2018b, Grading Designation Calculator, *Construction Industry Development Board*, South Africa, <https://registers.cidb.org.za/PublicContractors/GradingDesignationCalc>, accessed on 14 June 2018.
- CSMI, 2008, The Future of Penge - Prospects for People and the Environment, written for the Asbestos Relief Trust by the Centre for Sustainability in Mining and Industry, Johannesburg, South Africa.
- DPW, 2011, National Contractor Development Programme – Summary Framework, Produced by the Department of Public Works, South Africa and the Construction Industry Development Board, South Africa.
- DMR. (2009) The National Strategy for the Management of Derelict and Ownerless Mines in South Africa, Department of Minerals and Energy, South Africa.
- DMR. (2011) Standard Protocol and guidelines for the rehabilitation of derelict/ownerless asbestos mine residue deposits in South Africa, Department of Minerals and Energy, South Africa.
- L. Gruneberg, Stephen & Ive, Graham. (2000). The Economics of the Modern Construction Firm. 10.1057/9780230510432.
- OECD (2007), Competition and Barriers to Entry, *January 2007 Policy Brief*, Organisation for Econom-

ic Co-operation and Development, Paris, France.
Valence, Gerard. (2012). The Significance of Barriers to Entry in the Construction Industry. *Australasian Journal of Construction Economics and Building*. 7. 29. 10.5130/ajceb.v7i1.2975.

Monitoring a Cover Performance Test Section on a Uranium Mill Tailings Management Cell

M.M. Davis

Stantec Consulting Services Inc., Colorado, USA

C.H. Benson

University of Virginia, Virginia, USA

E.F. Redente

Redente Ecological Consultants Inc., Colorado, USA

H.R. Roberts

Consultant for Energy Fuels Resources (USA) Inc., Colorado, USA

ABSTRACT: Reclamation of an inactive uranium tailings management cell was initiated in 2016 at the White Mesa Uranium Mill Facility located in southeastern Utah, USA. Reclamation activities through 2017 included placement of the first phase of a monolithic water balance cover and construction of a cover performance test section. The test section was constructed as a design-build project during reclamation cover construction using procedures adopted from the test section installation instructions developed by the United States Environmental Protection Agency's ("EPA") Alternative Cover Assessment Program ("ACAP"). The test section is being monitored to assess the performance of the reclamation cover system for the tailings management cells. This paper summarizes the reclamation cover design and construction, describes the test section monitoring through 2017, provides an interpretation of the monitoring data to date, and compares the measured water balance with predictions made during design. The monitoring data include meteorological and water balance and vegetation surveys. Acceptable cover performance will be demonstrated after monitoring is complete (approximately 7 years) and after the applicable regulatory agencies have confirmed that all performance criteria have been met.

1 INTRODUCTION

Energy Fuels Resources (USA) Inc. ("EFRI") commenced reclamation of an inactive tailings management cell in 2016 at the EFRI White Mesa Uranium Mill located in southeastern Utah, USA. EFRI facilities at the site consist of a uranium processing mill and five lined tailings/process solution evaporation cells within an approximately 156-ha restricted area located just south of the Mill.

Reclamation activities since 2016 included placement of the first phase of reclamation cover on an inactive tailings management cell and construction of a cover performance test section within the cover on the cell. The test section is being monitored to assess the hydrologic performance of the reclamation cover for the tailings management cells and will be used in a regulatory determination on approval of the cover design.

This paper presents an overview of the reclamation cover and test section design, background on the site and regulatory framework, and summarizes test section hydrologic and vegetation monitoring through 2017.

2 BACKGROUND

The Mill was constructed in the late 1970s and has a capacity of approximately 1,800 dry metric tonnes per day. The Mill has been operating since 1980 on a campaign basis and is the only operating conventional uranium mill in the United States. Operations have been placed on standby during various periods as market conditions warrant. Since the early 1990s, the Mill has processed alternate feed materials when not processing conventional ores. Alternate feed materials are uranium-bearing materials other than conventionally mined uranium ores. An alternate feed circuit was installed in 2009 to process select alternate feed materials simultaneously with conventional ores. The Mill has processed over five million tons of ore and alternate feeds since inception.

The tailings management/process solution cells were constructed starting in 1978 with the most recent cell constructed in 2010. The cells are located south of the Mill and comprise the following:

- Cell 1 – 22 hectares (55 acres), used for evaporation of process solutions;
- Cell 2 – 26 hectares (65 acres), inactive tailings management cell, reclamation in progress;
- Cell 3 – 28 hectares (70 acres), used for storage of barren tailings sands, currently only receiving mill waste and is partially reclaimed;
- Cell 4A – 16 hectares (40 acres), used for storage of barren tailings sands and evaporation of process solutions; and
- Cell 4B – 16 hectares (40 acres), used for evaporation of process solutions.

The site is regulated by the Utah Department of Environmental Quality (“UDEQ”) under a radioactive materials license and groundwater discharge permit. EFRI and UDEQ completed an agreement in 2017 to define the commitments and schedule for reclamation of Cell 2. The agreement stated that the Cell 2 cover presented in the approved reclamation plan would be placed in two phases (Phase 1 and Phase 2) and acceptable cover performance would be demonstrated via a 7-year performance monitoring program that follows principles in NUREG/CR-7028 (Benson et al. 2011). EFRI committed to completing the Phase 1 cover placement on Cell 2 and constructing a cover performance test section by the end of 2017.

Cell 2 Phase 1 cover placement commenced in April 2016 and was completed in April 2017. The test section was constructed within the Cell 2 cover in the fall of 2016 (concurrently with the Phase 1 cover placement). The test section was seeded immediately following construction. Phase 2 cover construction will commence after the 7-year monitoring period is complete and UDEQ approves that the test section monitoring results demonstrate acceptable cover performance.

3 MONITORING REQUIREMENTS

Per EFRI’s agreement with UDEQ, the test section is required to be monitored for percolation and vegetative cover performance. EFRI initiated test section monitoring immediately after construction in 2016. Required test section calibration monitoring began on January 1, 2018 and will be conducted for two years. Official performance monitoring is required to commence after calibration monitoring ends (i.e. January 1, 2020) and continue for five years.

The percolation rate from the base of the test section lysimeter will be used as the performance parameter for the cover system. The cover design will be considered to have performed adequately if the average annual percolation rate is 2.3 mm/yr or less over the official performance monitoring time period.

The vegetation component of the cover will be considered successful if (1) a minimum vegetation cover of 40% and (2) acceptable vegetation diversity are met for the test section by the end of the 5-year official performance monitoring time period.

As part of Cell 2 reclamation, EFRI is also conducting settlement monitoring of the Phase 1 cover surface and monitoring of water levels in the tailings. Settlement and dewatering data will

be evaluated after the cover performance monitoring is complete. The evaluation will determine if sufficient settlement has occurred to facilitate Phase 2 cover placement and minimize maintenance of the final cover surface. Decreasing trends in settlement followed by a maximum of 0.1 feet of cumulative settlement over 12 months (for at least 90% of the settlement monuments) will be considered acceptable to proceed with placement of the Phase 2 Cell 2 cover after the 7-year performance monitoring time period.

4 COVER AND TEST SECTION DESIGN

The cover system is a monolithic water balance cover designed to minimize percolation, meet the radon emanation standard, minimize maintenance over the short- and long-term, and promote sustainability. The design reclamation cover thickness for the tailings management cells ranges from 9.5 to 10.5 feet. The minimum design cover thickness of 9.5 feet was used for the lysimeter area of the test section to evaluate the lower bound reclamation cover thickness for the tailings management cells. The remaining area within the test section was constructed to the full-depth Cell 2 cover profile (10.5 feet). The cover profile within the lysimeter is shown on Figure 1. The reclamation cover contains the following layers, listed in order from top to bottom:

- Layer 4 – 0.15 meters (0.5 feet) thick Erosion Protection Layer (topsoil-gravel admixture)
- Layer 3 – 1.07 meters (3.5 feet) thick Growth Medium Layer (loam to sandy clay)
- Layer 2 – 0.91 to 1.22 meters (3.0 to 4.0 feet) thick Compacted Cover (highly compacted loam to sandy clay)
- Layer 1 – 0.76 meters (2.5 feet) thick (minimum) Interim Fill Layer (loam to sandy clay)

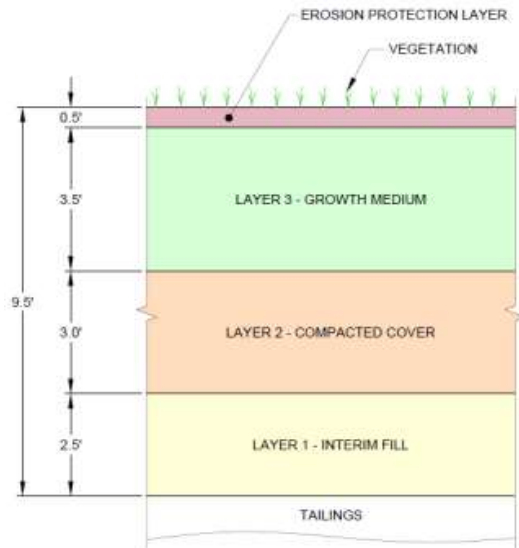


Figure 1. Cover profile within test section lysimeter.

Layer 1 was placed in stages as interim cover on Cell 2 from 1991 through 2008. Phase 1 cover construction initiated in 2016 and completed in 2017 included placement of (1) additional

interim cover to achieve design grades prior to placement of cover Layer 2, and (2) the entirety of Layer 2. Phase 2 cover construction will include placement of Layers 3 and 4.

The test section is located in the southeast corner of Cell 2. The test section was constructed as a design-build project during reclamation cover construction using procedures adopted from the test section installation instructions developed by the EPA’s ACAP (Benson et al., 1999, 2001). The test section is approximately 100 feet by 100 feet with a 32-foot by 64-foot lysimeter centered within the test section. The longer side of the lysimeter is oriented parallel to the cover slope. The lysimeter collects percolation from the base of the cover, surface runoff, and interflow from the textural interface between the interim fill (Layer 1) and compacted cover (Layer 2). Sensors monitor hydrologic state variables (temperature and water content) within the cover. Percolation rate, lateral drainage, runoff, internal state conditions, and meteorological data are recorded continuously using a data logger located near the southern edge of the test section. The sensors and data acquisition system used for monitoring the test section are maintained and recalibrated annually. An evaluation of data quality is conducted monthly for measurements from all sensors. Annual surveys are conducted to evaluate the test section vegetation.

5 TEST SECTION HYDROLOGIC MONITORING

Hydrologic data were collected from the test section for the period September 9, 2016 to December 31, 2017. The data represent the first full calendar year (2017) of monitoring. A summary of the water balance is in Table 1.

Table 1. Cell 2 Test Section Water Balance for 2016 and 2017.

Water Balance Quantity (mm)	2016*	2017
Precipitation	60	223
Runoff	0	0
Lateral Flow	0	0
Change Storage	17	39
Evapotranspiration	35	325
Percolation	0.0	0.6

*Partial year, monitoring began on September 9, 2016.

Comparisons between 1) average daily precipitation and daily air temperature measured on-site, and 2) long-term historical averages reported by the National Weather Service (“NWS”) at the Blanding station, are shown in Figures 2 and 3, respectively. The average air temperatures measured at the test section generally fall within the long-term high and low temperatures recorded at the Blanding station. The on-site precipitation generally follows the historical precipitation trend through mid-summer. In contrast, late summer and fall were drier than normal, with only 6.5 mm of precipitation recorded between September 1, 2017 and December 31, 2017. Consequently, the 2017 annual precipitation is substantially below the long-term average annual precipitation at the Blanding station (223 vs. 355 mm).

The long-term average precipitation record does not exhibit the same seasonality or variability inherent in the actual precipitation record. Smoothing associated with long-term temporal averaging makes the long-term precipitation record smoother and more gradually varying compared to actual records. When a daily precipitation record is averaged over very long periods of time, the number of days with non-zero precipitation diminishes (in the limit, the number of non-zero precipitation days tends to zero). The number of days with large precipitation events diminishes as well. For this reason, long-term precipitation records are not recommended for use in simulating the hydrology of covers (Albright et al. 2010), but are useful for comparative analyses.

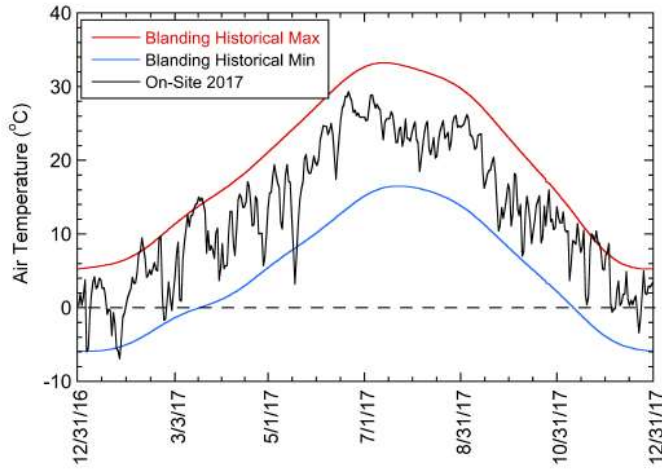


Figure 2. Comparison of on-site air temperature data to historical data from the Blanding NWS station.

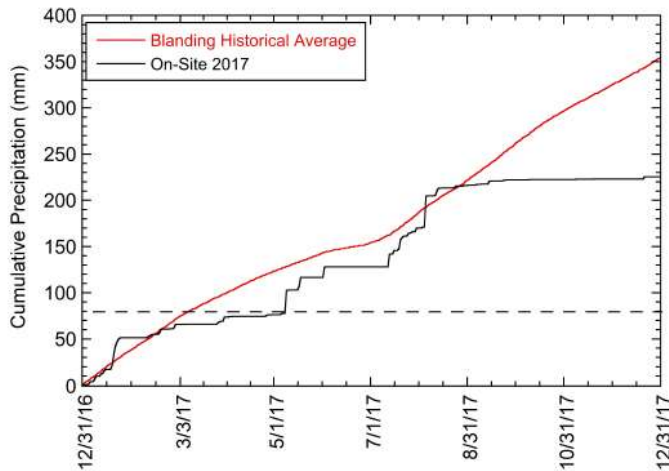


Figure 3. Comparison of on-site cumulative precipitation data to historical data from the Blanding NWS station.

Cumulative precipitation and potential evapotranspiration (“PET”) computed using the FAO method (Allen et al. 1988) are shown in Figure 4 for 2017. Annual ET far exceeds precipitation, indicating an excess of energy for evaporation and transpiration relative to the amount of water to manage. During late fall to mid-winter, however, the rate of precipitation exceeds PET. Soil water storage accumulates during this period, as illustrated in the water balance graph (Figure 5).

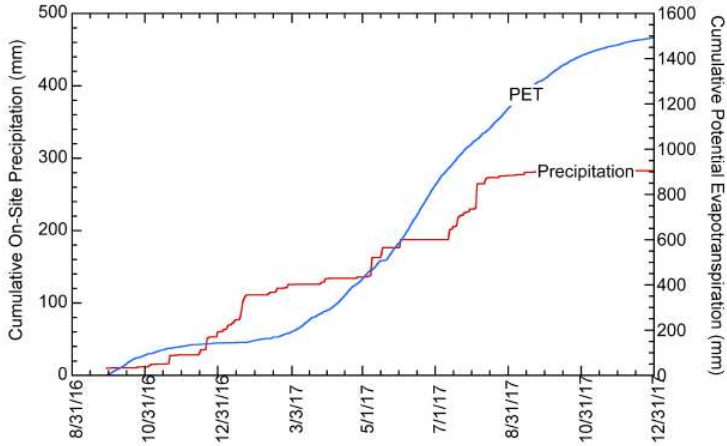


Figure 4. PET on-site during 2017.

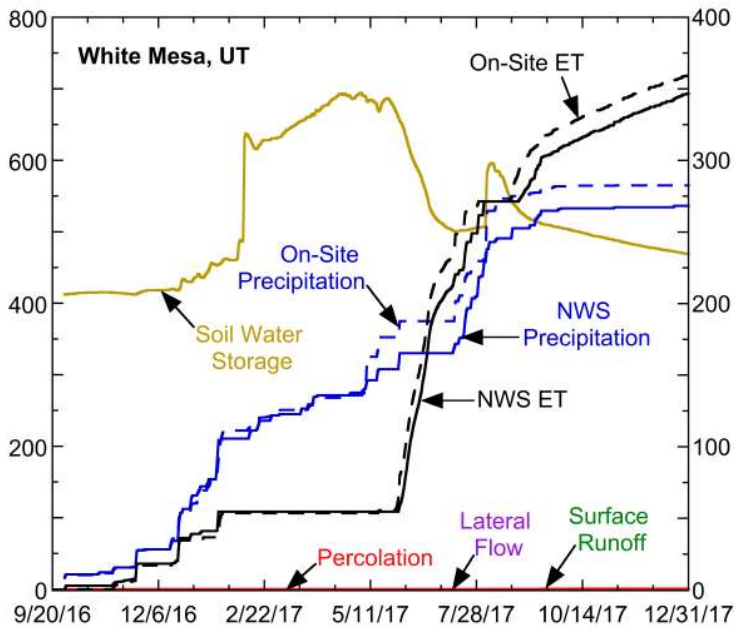


Figure 5. Water balance graph for test section through end of 2017.

Cumulative quantities are shown in Figure 5 for each of the water balance fluxes (precipitation, evapotranspiration, runoff, lateral flow, and percolation) as a function of time. Percolation is the flux from the base of the cover that is captured by the geocomposite drain in the base of the lysimeter and would normally flow into the tailings. Lateral flow is the flux of liquid occurring laterally at the interface between the growth medium and the compacted layer and is captured by a collection point at the downslope edge of the lysimeter. Soil water storage (total water stored in the cover per unit surface area) is also shown as function of time in Figure

5. Soil water storage is computed by integrating the water content measurements over the volume of the test section at a given point in time.

Each of the water balance quantities is measured directly except for evapotranspiration (“ET”), which is computed as the residual of the daily water balance. ET was calculated as 325 mm in 2017 for the site, which is more than 100% of total precipitation due to carry over of snow accumulated at the end of 2016. Computed cumulative annual ET is in excellent agreement with the generalized relationship between annual ET, PET, and precipitation for water balance covers and natural watersheds, as shown in Figure 6. Annual PET in Figure 6 was computed using the on-site meteorological data with the FAO method described in Allen et al. (1998) and shown in Figure 4.

The seasonal trends in the water balance shown in Figure 5 are consistent with expectations for a water balance cover in a semi-arid climate. Soil water storage gradually accumulated during the fall of 2016 and through April 2017 due to infiltration of precipitation, snow melt, and rain on snow. Accumulation of soil water storage accelerated in late January and early February as air temperatures above freezing persisted (Figure 7), resulting in snowmelt and infiltration. Soil temperatures above freezing were present throughout the entire winter period (Figure 7), allowing water re-distribution throughout the profile in response to infiltration. The wetting front moved rapidly through the test section due to the heavy infiltration that occurred in late January and early February 2017 (Figure 8), with water contents increasing in every layer of the cover. Water contents in the growth medium diminished later in the spring and summer due to evapotranspiration. In contrast, water contents in the compacted layer increased slightly until early September, and then became relatively constant. Water contents in the interim layer spiked soon after the infiltration from snow melt, then diminished modestly, and subsequently climbed very slowly until early September. Since the end of September, water contents in each layer decreased slightly or remained essentially constant (Figure 8).

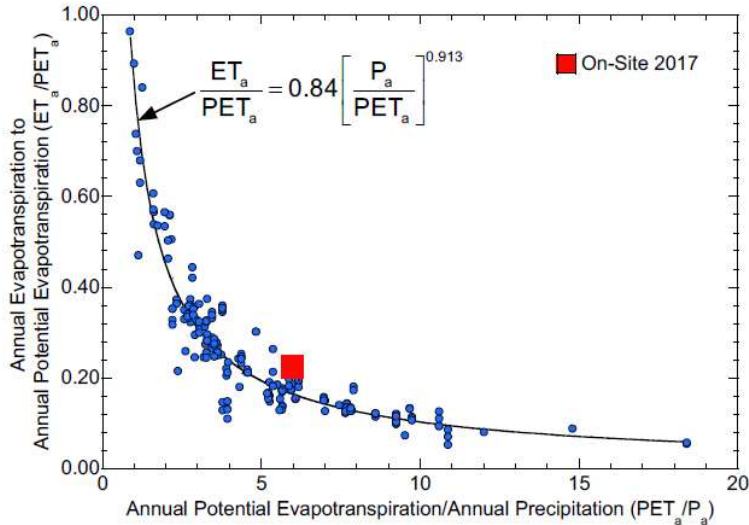


Figure 6. Relationship between annual precipitation (“Pa”), annual potential evapotranspiration (“PETa”), and annual evapotranspiration (“Eta”) for test section at White Mesa (red square) and from ACAP and other international studies (solid blue circles) reported by Apiwantragoon et al. (2014).

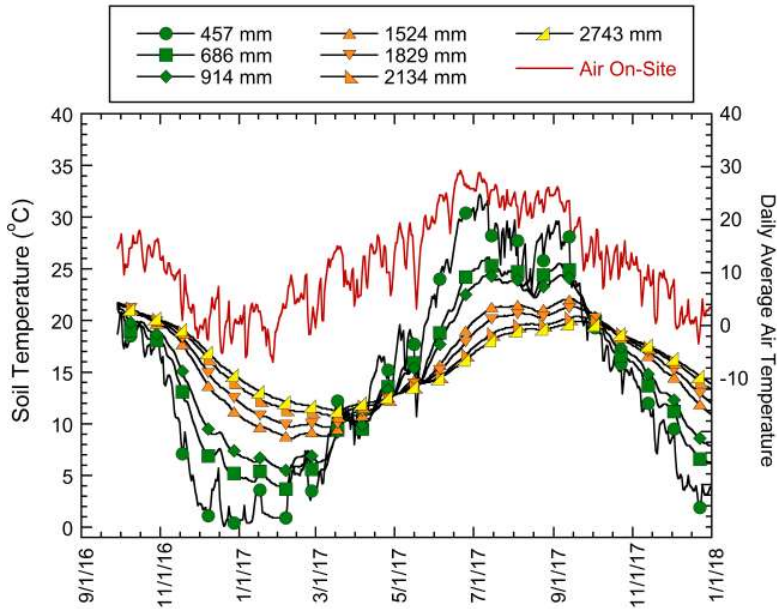


Figure 7. Daily average air temperature and daily average soil temperature at various depths in the test section (green = growth medium, orange = compacted layer, yellow = interim layer).

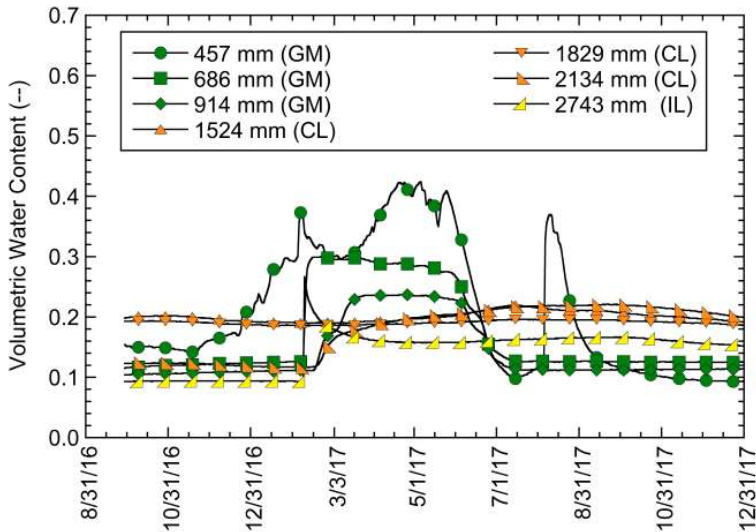


Figure 8. Daily average water content at various depths in the test section (green = growth medium (“GM”), orange = compacted layer (“CL”), yellow = interim layer (“IL”)).

Percolation began on July 14, 2017, approximately five weeks after the soil water storage began to diminish and immediately preceding an increase in storage associated with a heavy precipitation event (Figure 9). The initiation of percolation likely corresponds to moisture reaching the base of the lysimeter during the first year of wetting, and is consistent with the

gradual increase in water contents at depth evident in Figure 8. The onset of percolation is likely not due to the short-term increase in storage in late July, as this increase in storage occurred approximately two weeks after the onset of percolation and was associated with large increases in water content only near the surface of the cover (Figure 8). In subsequent years, percolation likely will initiate around the time when soil water storage reaches a peak.

Annual percolation from the test section for 2017 (0.6 mm, Table 1) is shown in Figure 10 along with data compiled from USEPA's ACAP and other data sources, as reported by Apiwantragoon et al. (2014). Data from the test section fall in the middle of the data reported by Apiwantragoon et al. (2014) for the bin corresponding to annual precipitation between 0 to 250 mm/yr.

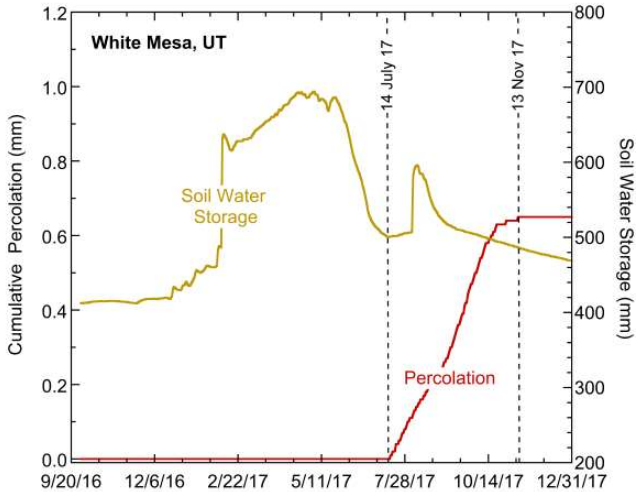


Figure 9. Soil water storage and cumulative percolation over time for the test section.

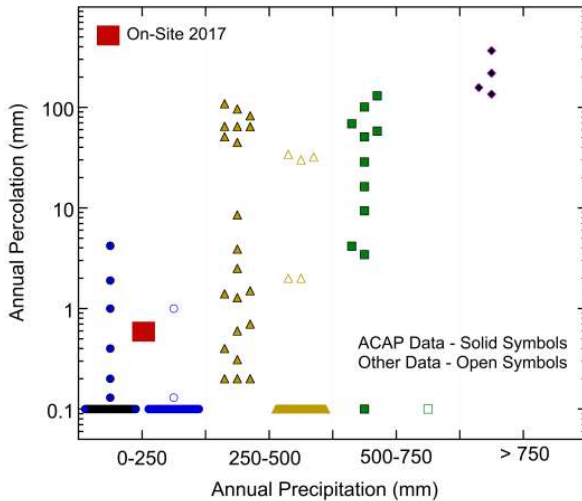


Figure 10. Annual percolation for the test section at White Mesa in context of data from other sites in ACAP and other international studies as reported by Apiwantragoon et al. (2014).

6 TEST SECTION VEGETATION INSPECTION

Inspections of the plant development status on the test section were made in July and November 2017. The presence of seedlings in July 2017 indicated good germination and seedling emergence in the spring of 2017. Active plant growth continued until a lack of precipitation in June and July caused most seedlings to go dormant. A survey of the site, including a 100-foot transect to estimate plant cover, showed plant cover of perennial species to be about 10%. Considering the dry conditions that existed in June and July, this plant cover of perennial species met expectations for first year plant growth. In comparison, first year plant growth at the Monticello lysimeter study that was seeded in 2000 showed plant cover of perennial species to be 5.5% during the first growing season and 12.2% after two growing seasons (Waugh et al., 2008). A second inspection of the site on November 2017 showed that additional plant growth did occur between July and November and cover of perennial species was slightly greater than the 10% observed in July. The most encouraging observation that was made in both July and November was the presence of many fourwing saltbush seedlings and substantial growth that they exhibited under low moisture conditions.

In July, the site was dominated by two annual broadleaf weeds. Weed control was recommended to remove the weeds to eliminate this source of seed and reduce the occurrence of these species in 2018. Hand pulling of the weeds was determined to be an effective control measure and designated plants were removed from the site one week following the July inspection. The November inspection of the area showed that the weed removal was successful and very few weed species were present.

Following the inspections in July and November 2017, seeding of the test section was deemed successful. Although low precipitation in the summer limited plant growth, the outlook for future years is that plant cover of the seeded species will eventually reach approximately 40% as a maximum sustainable cover for this environment. This maximum cover should be achieved in approximately seven (7) years unless consecutive years of drought occur and the trajectory for plant cover development is delayed.

7 SUMMARY CONCLUSIONS

Hydrology of the test section during 2017 was consistent with expectations for a water balance cover in a semi-arid environment. Evapotranspiration comprised essentially all of the water balance of the cover. Annual runoff and annual lateral flow were less than 1 mm and annual percolation was 0.6 mm. A good comparison was obtained between the measured percolation for the test section and percolation rates reported in the literature for water balance covers in similar climates. The 2017 calibration monitoring results indicate the cover can meet the required average annual percolation rate of 2.3 mm/yr or less over the official performance monitoring period.

The seeding of the test section was successful with measured plant cover of approximately 10% in 2017. Plant cover is expected to continue to increase and to meet the minimum vegetation cover of 40% by the end of the official performance time period.

Phase 2 reclamation cover will be placed after the 7-year monitoring period and regulatory acceptance of the performance monitoring results. The cover design would then be used for reclamation of the remaining tailings management cells.

REFERENCES

- Albright, W., Benson, C., and Waugh, W., 2010). *Water Balance Covers for Waste Containment: Principles and Practice*, ASCE Press, Reston, VA, 158 p.
- Allen, R., Pereira, L., Raes, D., and Smith, M., 1998. *Crop Evapotranspiration Guidelines for Computing Crop Water Requirements*. FAO Irrigation and Drainage Paper 56, Food and Agricultural Organization of the United Nations, Rome.
- Apiwantragoon, P., Benson, C., and Albright, W., 2014. *Field Hydrology of Water Balance Covers for Waste Containment*, J. Geotechnical and Geoenvironmental Eng., 04014101-1-20.

- Benson, C., T. Abichou, X. Wang, G. Gee, and W. Albright, 1999. Test Section Installation Instructions – Alternative Cover Assessment Program, Geotechnics Report 99-3, Geological Engineering, University of Wisconsin-Madison.
- Benson, C., Abichou, T., Albright, W., Gee, G., and Roesler, A. 2001. Field Evaluation of Alternative Earthen Final Covers, *International J. Phytoremediation*, 3(1), 1-21.
- Benson, C., Albright, W., Fratta, D., Tinjum, J., Kucukkirca, E., Lee, S., Scalia, J., Schlicht, P., and Wang, X., 2011. Engineered Covers for Waste Containment: Changes in Engineering Properties and Implications for Long-Term Performance Assessment. NUREG/CR-7028, prepared for the U.S. Nuclear Regulatory Commission, Washington, D.C., December.
- Waugh, W. J., M. K. Kastens, L. R. L. Sheader, C. H. Benson, W. H. Albright, and P. S. Mushovic, 2008. Monitoring the performance of an alternative landfill cover at the Monticello, Utah, Uranium Mill Tailings Disposal Site. *Proceedings of the Waste Management 2008 Symposium*. Phoenix, AZ.

Remediation Design of a Uranium Mill Tailings Pond

Y. Koitzsch, S. Metzker and A. Mühl
CDM Smith Consult, Leipzig, Saxony, Germany

U. Barnekow and M. Speer
Wismut, Chemnitz, Saxony, Germany

ABSTRACT: The remediation of the East German uranium mining sites, which were operated and used until 1990, started in 1991 and was funded by the German Federal Government. However, most of the numerous (often privately owned) abandoned uranium mining sites, distributed all over Saxony, were not included. In 2003 the Federal Government and the Free State of Saxony agreed to jointly fund the remediation of those abandoned mining sites of high priority. Wismut's department for Project Management of Wismut's Abandoned Saxonian Mining Sites was given the responsibility for the project management. The Dänkritz 2 uranium mill tailings pond is one of the abandoned sites. Mill tailings were discharged at the Dänkritz 2 tailings pond during the 1950s surrounded by a 12 m high autostable tailings dam, which was reshaped during the 1960s to improve geotechnical stability. Dynamic stability calculations, applying the finite element program PLAXIS, were carried out by CDM Smith as part of the remediation design. The results indicated the maximum credible earthquake would cause instability of the dam. In addition, soft fine-grained tailings needed to be stabilized to place a multi-layer type surface cover. Wismut, Division Engineering/Radiation Protection designed the tailings remediation project. Geotechnical analyses were carried out by CDM Smith as part of the remediation design. Wismut applied for planning approval of the project in August 2015. To date the approval is expected for summer 2018. The project duration was estimated to five years with overall costs of approximately EUR 11.2 million. The present paper will particularly focus on the advanced constitutive models used for the slope stability analyses of the embankment under dynamic loads and of the stability of the fine-grained tailings during interim cover placement.

1 INTRODUCTION

In Eastern Germany uranium mining lasted from 1945 until 1990. In total ca. 216,300 t of uranium were produced. The remediation of the uranium mining sites, operated and used until 1990 by the Soviet-German Wismut company, started in 1991 under responsibility of the newly founded Wismut GmbH funded by the German Federal Government. However, most of the numerous (often privately owned) abandoned uranium mining sites distributed throughout Saxony, were not included. In 2003 the Federal Government and the Free State of Saxony agreed to jointly fund the remediation of those abandoned mining sites of high priority. Wismut's department for Project

Management of Wismut's Abandoned Saxonian Mining Sites was given the responsibility for the project management. The Dänkriz 2 uranium mill tailings pond is one of the abandoned sites of high priority. The radiological, environmental and geotechnical site assessment proved that remediation of the Dänkriz 2 site was required. Wismut's Division Engineering/Radiation Protection designed the tailings remediation project and applied for the respective planning approval in August 2015. Wismut applied for planning approval of the project in August 2015. To date the approval is expected for summer 2018. The project duration was estimated to five years with overall costs of approximately EUR 11.2 million.. The remediation includes water collection and treatment during remediation, interim covering of sandy and soft fine-grained tailings, dam reshaping, re-contouring of the pond area enhancing tailings consolidation by using vertical drains, placement of a multi-layer type final cover and revegetation.

Geotechnical analyses were carried out by CDM Smith as part of the remediation design with the following aim:

- Prove static and seismic stability of the ring dam.
- Investigate settlements due to consolidation of the tailings, under the load of the overlying re-contouring layer and surface cover, to ensure the functionality for the planned runoff diversion system in the final state.
- Prove stability of the interim cover on the fine-grained tailings during placement under the load of the construction equipment.

2 SITE CHARACTERIZATION

The uranium mill tailings pond, Dänkriz 2, is located in Germany, approximately 8 km northwest of the city center of Zwickau (Saxony). The pond has an extension of ca. 250 m from east to west and ca. 400 m from north to south. Its area represents approximately 10.5 ha. The tailings pond is located in a former gravel quarry. Between 1955 and 1958 uranium mill tailings from soda-alkaline leaching were discharged into the abandoned open pit. Once the discharge of the tailings exceeded the pit capacity, the coarser particles were piled up to a surrounding ring dam. The heights of this ring dam range between 2 m and a maximum of 14 m. Slopes of the ring dam show a gradient between 1:2.5 and 1:3 (vertical to horizontal). The basin surrounded by the ring dam is now filled with tailings at thicknesses between < 2 m and 12 m. In total about 820,000 m³ tailings are currently contained in the impoundment, which is partly covered with a supernatant water layer up to a depth of 2 m. Figure 1 shows an aerial view of the Dänkriz 2 tailings pond in 2015.

The geogenic subsurface strata of the tailings pond Dänkriz 2 consists of the Upper Permian, bedrock which has a weathered zone of approximately 30 m thickness. The upper 2 m of the weathered zone includes 10 to 15% impermeable kaolinite. The Upper Permian is covered by tertiary gravels. On the eastern and southern side of the tailings pond a silt layer with a thickness of 3 m is enclosed in these gravels. The tertiary gravels were extracted during the working process of the gravel quarry so that there are just 2 to 10 m left.



Figure 1. Areal view on the Dänkritz 2 tailings pond in 2015 (view from north-west to south-east)

3 STABILITY FOR THE RING DAM

The seismic design was performed in accordance with the European standard Eurocode 8. Furthermore, for the seismic design of the remediation the ponds as sedimentation basins, considering the German standard for the design of dam structures (DIN 19700-15). The representative safe-shutdown earthquake was derived in an expert seismological opinion for the respective Wismut locations from an analysis of historical events in the immediate vicinity of these locations and it corresponds to the progress of an earthquake that occurred in the North Italian region of Friuli in May 1976.

In order to analyze slope stability under the influence of earthquakes, fully dynamic calculations were carried out. This method allows for development of acceleration curves (accelerograms) from local expert seismological opinions. The calculations were completed applying a horizontal and a vertical acceleration of the safe-shutdown earthquake as a seismic input motion corresponding to the accelerogram on the base of a Finite Element Model. The calculations were repeated while reducing the parameters $\tan\phi'$ and c' until a continuous sliding surface, characterizing a slope failure, could be observed by analyzing plastic failure points. The factor of safety for the slope was determined by the ratio of shear strength, at this accordingly observed failure, to the available shear strength using Fellenius's law (Fellenius 1936). The slope stability was analyzed considering both, drained and undrained conditions.

Figure 2 shows the numerical model for the slope on the eastern side of the ring dam. It is an extract of the numerical cross section 1 – 1', which is about 540 m long. In the numerical model the layer thickness of the underground is about 30 m. The bottom of the model implies the bedrock. The lower model boundary was coupled with a prescribed displacement on which the motion signal corresponding to the accelerogram was applied.

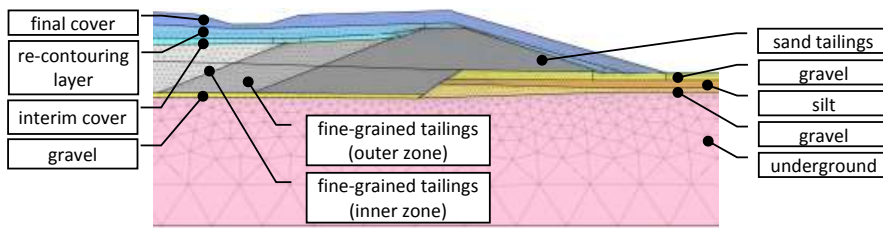


Figure 2. Extract of the numerical cross section 1 – 1', eastern side of the ring dam (showing the final state), not at scale

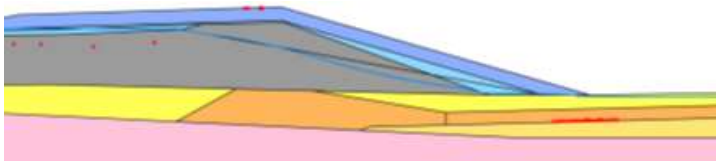
Soils have been modeled using the hardening soil model with small strain stiffness (HSsmall). The HSsmall model is based on the Hardening Soil model (Schanz 1999), extended with an elastic overlay model to take into account the high stiffness at small strain levels (Benz 2007; Benz et al. 2006). Brinkgreve et al. 2007 give an extended overview of the derivation of the hysteretic damping from the small-strain stiffness formulation in the HSsmall model. Here the dependency of the damping ratio from $\gamma_{0.7}$ and the G_0/G_{ur} ratio is shown due to varying $\gamma_{0.7}$ in a range of $1 \cdot 10^{-4}$ to $3 \cdot 10^{-4}$ and the G_0/G_{ur} ratio in a range of 2.5 to 10. Decreasing the value of $\gamma_{0.7}$ increases material damping and the ratio of G_0/G_{ur} (adequate to E_0/E_{ur}) and results in an increase of material damping.

In addition, according to Brinkgreve et al. (2007), Rayleigh-damping was postulated in the dynamic calculations while these damping parameters were set constant for all layers, which satisfied the requirements of simplification.

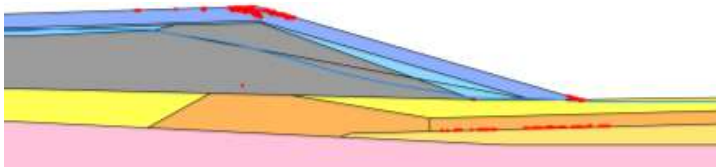
The history of the development of the tailings pond was modeled in order to generate the initial stress state. The ring dam did not show sufficient stability under seismic loading in this state. For this reason the slope of the dam was flattened and a multi-layer type surface cover was added to reduce the quantity of seepage water, which also had a positive impact on the stability of the slope. This multi-layer type surface cover consists from bottom to top of a 0.5 m thick sealing layer (hydraulic conductivity $k_f \leq 5 \cdot 10^{-9}$ m/s), an 0.3 m thick drainage layer (with a grain size distribution granting suffusion stability) and a 1.5 m thick storage and recultivation layer made of mixed-grained soil. Figure 3 shows an example of the potential failure mechanism in the static load case for the remediated southern slope of the ring dam of the Dänkritz 2 tailings pond. The calculated global factor of safety is $\eta_{min} = 1.71$. When applying horizontal and vertical acceleration of the safe-shutdown earthquake no continuous sliding surface could be observed by analyzing plastic failure points (refer Figure 4a) under provided shear strength. Due to reducing shear strength by 1.1 the calculation model showed an increase in failure points with a tendency towards a continuous sliding surface at the time step 6.6s (refer Figure 4b). Thus, sufficient stability of the ring dam, under seismic loading due to an earthquake, could be proven for the final state with a global factor of safety of $\eta_{min} > 1.10$.



Figure 3. Concentration of deviatoric strain characterizing potential failure kinematics of the southern slope in the static load case (final state)



(a)



(b)

Figure 4. Development of plastic points due to reduction of shear strength (final state, crucial time step at 6.6 sec.): (a) plastic points due to seismic loading; (b) plastic points due to seismic loading, shear parameters reduced by 1.1

4 PLACEMENT OF A MULTI-LAYER TYPE FINAL COVER

4.1 Modeling of consolidation

The behavior of the soft fine-grained tailings is undrained. When the material is loaded by the multi-layer type surface cover an immediate increase in pore pressure occurs. This excess pore pressure dissipates very slowly from the fine-grained tailings due to its low permeability. As the water drains from the material, change in volume occurs causing settlement (consolidation settlement). After placing the final cover layer with its water drainage system no more work for regulation shall be done. That means the cover has to be built with a higher level and a pre-defined contour that takes into account the settlement due to the consolidation process. While the interim cover has to be built from the ring dam towards the center of the pond, the re-contouring layers can be placed beginning from the center of the pond towards the ring dam, allowing the material in the center to consolidate more quickly. In addition, the dissipation of pore water pressure will

be enhanced by means of vertical wick drains. The calculation has to consider all these conditions and the model should place Wismut into a position to design the re-contouring work in the right sequence and time, so that the final cover is correctly contoured and the water drainage system is working after completion of consolidation.

A three-dimensional finite element calculation using advanced constitutive soil models for the simulation of the non-linear and time-dependent behavior of tailings has been carried out. The placement of the layers has been modeled by splitting the sequence into calculation phases. The vertical drains and the geogrid have been modeled by means of structure elements. The vertical drains ended two meters above the bottom of the tailings to prevent drainage into the underground. The software PLAXIS was used to implement an undrained effective stress analysis, using effective strength parameters to model the material's undrained shear strength. The width of the modeled sections corresponds to the grid of the vertical drains using the symmetric conditions. Figure 5 is an illustration of a section from the calculation model.

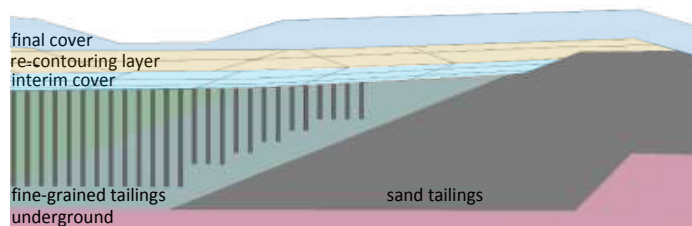


Figure 5. Section used for calculation (cutout — east side of Section 1 – 1')

The Soft Soil Model was used for this calculation. The model parameters have been derived from standard odometer tests conducted by Wismut. Based on of these tests Wismut provided the void-ratio-stress and the void ratio-permeability relations. Furthermore, the depth-dependent, undrained cohesion was measured along profiles by in-situ shear vane testing.

The surface settling process and consolidation tailings material due to discharge were verified analytically using a one-dimensional column model and a finite element column model to model the initial stress state of the tailings as close to reality as possible. The void ratio-depth profiles obtained were compared with one another in Figure 6 except for the material of the inner zone of the fine-grained tailings. The void ratios measured in 2014, for depths down to 2m, are shown here as a reference. Finally, the tailings in the three-dimensional finite element model were divided into layers measuring one meter while the void ratio, the specific unit weight and the permeability were postulated in terms of depth here from the calculation of the initial state on the column model.

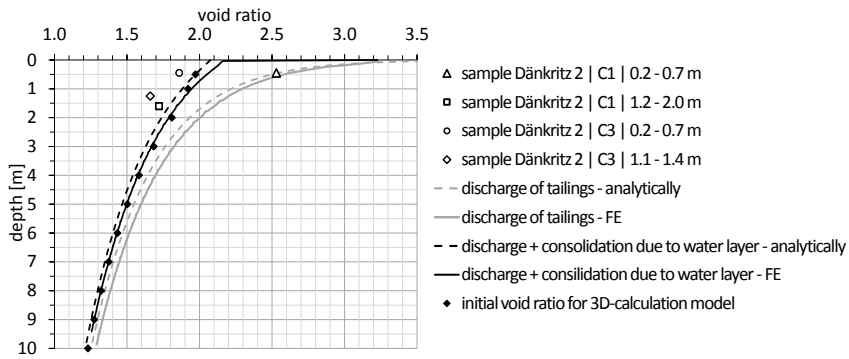


Figure 6. Void ratio depth profile of the inner zone of the fine-grained tailings due simulation of discharge of tailings

Consolidation was calculated taking into account the intermediate construction intervals (placement of interim cover, re-contouring layer and final cover). The modeled sequences followed this procedure with the aim to prove that the major portion of settlement due to consolidation will be completed at the end of the re-contouring work. This was essential for the strategy of the construction sequences and construction time.

With completion of the re-contouring layer a maximum settlement of 0.7 m was calculated in the center of the pond. The increase of contouring material for compensating this settlement was calculated at approximately 34,500 m³. The additional load of this material was considered in the calculation. Figure 7 shows the progression of the final cover surface after completing the consolidation except for the eastern side of the tailings pond. Position 0.0 m represents the center of the tailing pond. At position 90.0 m the ring dam begins. For the final layer a total settlement of 1.3 m was calculated at the time step approximately 21 months after completing final covering. This settlement still ensured the functionality for the planned surface-runoff diversion system and for the drainage system.

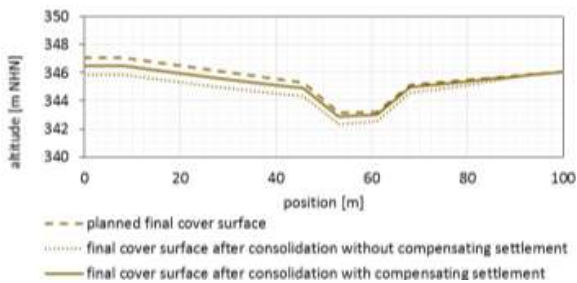


Figure 7. Progression of the final cover surface after completing the consolidation

4.2 Stability of the construction equipment

To ensure stability during construction a geogrid will be laid out on the surface of the tailings. The stability analysis was intended to confirm sufficient load-bearing capacity of the geogrid.

This was done pursuant to Eurocode 7 for the ultimate limit state due to the failure of the ground while applying the finite-element method with factored loads. Stability is defined as proven if the finite element model converges in the calculation. The geogrid was designed for the tensile stress resulting in the calculation, which uses factored loads.

The stability of construction equipment on the interim cover was analyzed by using a three-dimensional finite element model (Figure 8), where the tailings were divided into layers measuring one meter while the void ratio, the specific unit weight and the permeability were postulated in terms of depth as calculated for the initial state in the column model. In addition, vertical wick drains were modeled with a triangular grid spacing of 1.25 m and a depth of 8 m including a geogrid on the surface of the tailings. The interim cover has been modeled with its three successively placed layers of thicknesses of 0.3 m (first layer), 0.5 m (second layer) and 0.7 m (third layer).

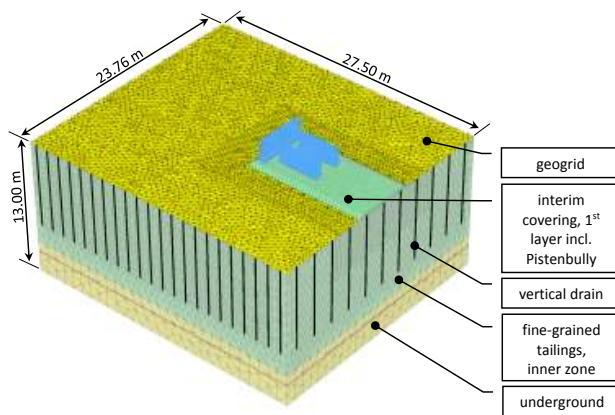


Figure 8. Calculation model for analyzing the stability of the construction equipment on interim cover

The Soft Soil Model parameters from the consolidation model were used. Figure 9 shows the distribution of the undrained shear strength resulting in the calculation model based on the effective strength parameters. It shows an excellent fit with the very low values measured due to in situ shear vane tests in the upper 3 m of the tailings, which are relevant for the stability.

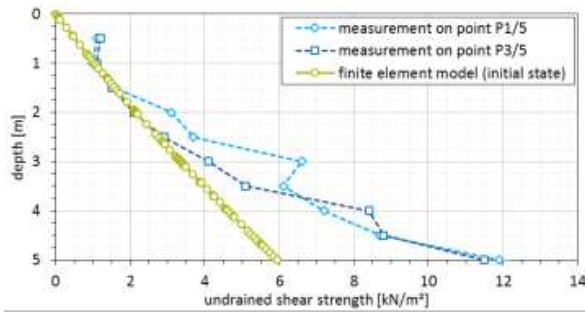


Figure 9. Progression of depth of the undrained shear strength in the fine tailings

An axial tensile stiffness of 700 kN/m was postulated in finite element modeling for the geogrid design on the surface of the tailings. This value is guided by the SS40 geogrid from Tensar International Limited (2003) that has a resistance to tension of 14 kN/m at a 2% strain in the longitudinal and transverse direction of the grid.

The analysis was carried out with the aim to prove the stability of a Pistenbully 300 (Moor caterpillar) and a CAT D3K2 chain dozer. In addition, a stack of soil material was placed in front of the Pistenbully or Dozer considered to impose a surface load of 20 kN/m. Figure 10 shows the Pistenbully, placing the first interim cover layer elsewhere on Wismut’s Culmitzsch tailings pond, and the geometry postulated in the numerical calculation.

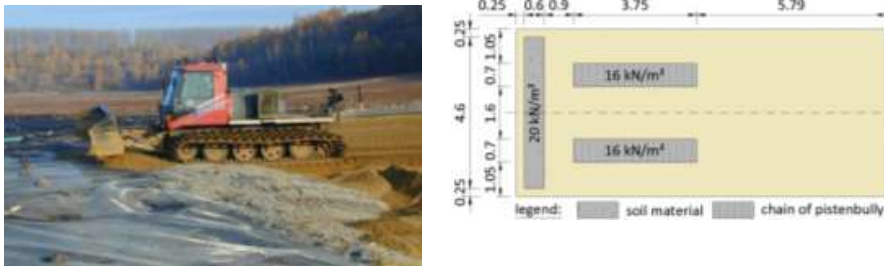


Figure 10. Pistenbully 300 and designed load

The assumption made in the calculations was that the entire geogrid and vertical wick drains had been placed at the beginning of building the 1st layer of interim cover material. Then, the 1st layer was consolidated before building the 2nd layer, which was included in the calculation with a consolidation time of 60 days. The finished 2nd layer of the interim cover was also consolidated for 60 days in the calculation before building the 3rd layer. The illustration of the excess pore water pressure shown in Figure 11 indicates the effectiveness of vertical wick drains during building up the 3rd layer of the interim cover.

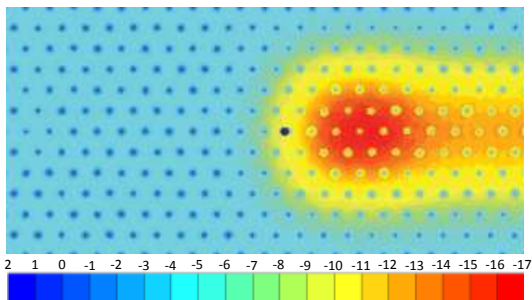


Figure 11. Excess pore water pressure in kN/m² during building up the 3rd layer of the interim cover (horizontal cross section at 1 m depth below tailing surface)

As expected, the maximum tensile stress N_d in the geogrid resulted from the build-up of the 1st layer of the interim cover ($N_d \approx 11$ kN/m). The ground deformation showed a failure behavior at the 1st layer of the interim cover, but the calculation converged under factored loads and the analysis of the deviatoric strain (Figure 12) indicated reserves in resistance. The safety of equipment of the equipment could be proven.

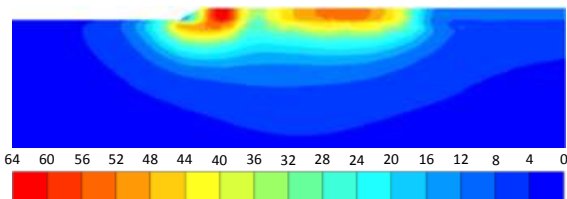


Figure 12. Deviatoric strain (10^{-3} m) due to Build-up of the 1st layer of the interim cover (vertical cross section at chain of Pistenbully)

5 CONCLUSION

The Dänkritz 2 uranium mill tailings pond is one of the abandoned uranium mining sites in Eastern Germany of high priority. The radiological, environmental and geotechnical site assessment proved that the site required remediation. Wismut’s department for Project Management Saxonian Abandoned Wismut Mining Sites was given the responsibility to manage the project. Wismut’s Division Engineering/Radiation Protection designed the tailings remediation project and applied for the respective planning approval in August 2015. To date the approval is expected for summer 2018. The project duration was estimated to five years with overall costs of approximately EUR 11.2 million. The remediation included water collection and treatment during remediation, interim covering of sandy and of soft fine grained tailings, dam reshaping, re-contouring of the pond area enhancing tailings consolidation by using vertical wick drains, placement of a multi-layer type final cover and revegetation. Geotechnical analyses were carried out by CDM Smith as part of the remediation design.

In order to analyze the stability of the ring dam under seismic loading CDM Smith performed a fully dynamic calculation using finite element models. Soils have been modelled

using the hardening soil model with small strain stiffness, which implements a hysteretic damping. A Rayleigh damping was additionally defined. The calculations were made applying a horizontal and a vertical acceleration of the safe-shutdown earthquake. The factor of safety was determined by repeating the calculations while reducing the shear strength parameters and analyzing the development of plastic failure in the system. The ring dam did not show sufficient stability under seismic loading due to an earthquake in its actual state. For this reason the slope of the dam was profiled. Additionally, a multi-layer type surface cover was provided to reduce the quantity of seepage water which had a positive impact on the stability of the slope. Sufficient stability of the ring dam under seismic loading could be proven for the final state with a global factor of safety of $\eta_{min} > 1.10$.

In order to place Wismut into a position to design the re-contouring work in the right sequence and time, such that the final cover lies in correct contour and the water drainage system is working after completion of consolidation of the tailings, CDM Smith carried out a three-dimensional finite element calculation using advanced constitutive soil models for the simulation of the non-linear and time-dependent behaviour of the tailings. The parameters used for the soil model have been calibrated in one-dimensional models based on results from laboratory and field investigations. The modelled sequences followed the procedure of the construction with the aim to prove that the major portion of settlement due to consolidation will be completed at the end of the re-contouring works. This was essential for the design strategy of the construction sequences and construction time. For the final state a total settlement of 1.3 m was calculated at the time step approximately 21 months after completing the final surface cover. This settlement still ensured the functionality of the planned surface runoff diversion system and the drainage system within the surface cover.

It is necessary to prevent any ground failure when using construction equipment for successive placement of the interim cover on the tailings. This is accomplished by installing an underlying geogrid. The aim of the stability analysis carried out by CDM Smith was to prove sufficient load-bearing capacity of the geogrid. This was done pursuant to Eurocode 7 while applying the finite-element method with factored loads. Stability has been proven as the finite element model converged in the calculation. The geogrid was designed for the tensile stress resulting in the calculation, using factored loads.

REFERENCES

- Benz, T 2007. 'Small Strain stiffness of soils and its numerical consequences', PhD thesis. Stuttgart: University of Stuttgart.
- Brinkgreve, RBJ, Kappert, MH & Bonnier, PG 2007. 'Hysteretic damping in a small-strain stiffness model', in GN Pande & S Pietruszczak (eds). *Numerical Models in Geomechanics*. London: Taylor & Francis Group.
- Fellenius, WKA (1936), 'Calculation of the Stability of Earth Dams', in *Transactions of the Second Congress on Large Dams*. Washington DC, 4, pp. 445–462.

Repurposing Mine Sites – A Win for Owners, Colorado, and the Environment

R.L. Almon

Ireland Stapleton Pryor & Pascoe, PC, Denver, Colorado, United States of America

S.L. Borden

LT Environmental, Inc., Arvada, Colorado, United States of America

ABSTRACT: The United States Environmental Protection Agency (USEPA) recently developed an agency initiative to address legacy contamination from Mine-Scarred Lands (MSLs). The intent is to repurpose abandoned or inactive mines to the benefit of owners, the public, and the environment. Several repurposed Colorado MSL sites, and sites currently planned for repurposing, are reaping financial, social, and environmental benefits for Colorado, all with encouragement from USEPA, the State of Colorado, and increasingly sophisticated private funding sources. Remarkably, benefits of MSL repurposing are not due to mine reopening for traditional ore extraction. Rather, benefits are due to the strategic repurposing of MSLs for use as residential development and commercial destinations. MSL repurposing requires the best engineering, environmental, and legal teamwork; controlling mine waste releases to the environment; partnering with regulators and the local community; negotiating regulatory liability protections; and strategically positioning MSL sites to attract and keep both public and private funding.

1 ACCOMPLISHING THE REPURPOSE OF MINE-SCARRED LANDS

MSL repurposing requires teamwork between property owners and engineers, environmental consultants, and legal counsel. The goal is to control mine waste releases to the environment; establish partnerships with regulators and the local community; negotiate regulatory liability protections to spur development; and strategically position MSL sites to attract both public and private funding. This paper provides a model for understating the regulatory MSL framework and how to develop partnerships with the stakeholders to permit and fund the repurposing of MSL sites.

QUICK READ - WHAT ARE MINE -SCARRED LANDS?

- USEPA defines MSLs as, “lands, associated waters, and surrounding watersheds where extraction, beneficiation, or processing of ores and minerals ...has occurred.”
- USEPA has identified the remediation of MSL waste as potentially CERCLA enforceable.
- In Colorado, the primary contaminant sources at or originating from MSLs have been identified by the USEPA as:
 - Abandoned surface and underground mines
 - Waste rock and spent ore piles
 - Abandoned tailings, tailings piles, and disposal ponds
 - Abandoned smelters
 - Acid or alkaline mine drainage
 - Water bodies and watersheds impacted by mine drainage

2 A SHORT HISTORY OF SUPERFUND AND THE MSL INITIATIVE

In 1980, Congress passed the Comprehensive Environmental Response, Compensation, and Liability Act (CERCLA, 42 United States Code [U.S.C.] 9601), which is more commonly referred to as “Superfund.” CERCLA was an emergency federal regulation stemming from the discovery and subsequent legal battles of “Love Canal,” the infamous toxic dumping ground that became the epicenter of the nation’s largest environmental and human health disaster to date. Under CERCLA, USEPA has the authority to identify those parties legally responsible, known as Potentially Responsible Parties (PRPs), for hazardous substance releases, such as the contaminants inherent to Colorado’s historic mining industry, and compel them to remediate. If PRPs cannot be identified, USEPA can conduct necessary remediation using money contained in the Superfund. The liability structure of CERCLA is imposing, placing blame on any person or entity within the chain of title (past or present), generators of hazardous waste, and transporters of hazardous waste to any facility later deemed a CERCLA site.

While the intent of CERCLA was noble, it chilled the ability of MSL sites to be reopened or repurposed due to liability concerns and the inability of owners to obtain financing for redevelopment costs related to construction, or worse, USEPA-compelled remediation. Consequently, the primary barrier to MSL repurposing became the inability of projects to obtain and keep funding, as private sources of financing were unwilling to risk becoming a PRP. However, on January 11, 2002, Congress passed the Small Business Liability Relief and Brownfields Revitalization Act (Public Law 107-118; H.R. 2869). With the passing of this amendment to CERCLA, traditionally referred to as the “Brownfields Amendments,” this all changed and led to the Brownfields MSL Initiative which provides funds to empower cleanup and revitalization of MSLs and encourages stakeholder cooperation.

The MSL Initiative recognized that across the United States property owners were attempting to repurpose MSLs, but without a roadmap that allowed for securing necessary private sector funding. With the passage of the Brownfields Amendments, federal agencies with jurisdiction over MSLs recognized the opportunity to better coordinate repurposing efforts, including a model for forming public-private funding partnerships.

QUICK READ - WHAT IS THE MINE-SCARRED LANDS INITIATIVE?

- The Initiative is an, “interagency partnership designed to explore approaches to mine-scarred lands cleanup and community revitalization.”
- Initiative partners include the U.S. Army Corps of Engineers, U.S. Department of Agriculture, U.S. Department of Housing and Urban Development, U.S. Department of the Interior, U.S. Environmental Protection Agency, and the Appalachian Regional Commission.
- Lessons-learned from the Initiative’s demonstration projects can be used as a model for developing partnerships with the regulatory, financial, legal, environmental, and engineering stakeholders.

3 CERCLA AND COLORADO MSL SUCCESS STORIES

Given our historic mining industry, Colorado is ripe with opportunities for MSL redevelopments. We’ve worked with owners of portions of the California Gulch Superfund site in the City of Leadville to return the old mining site to reuse by following prescribed waste management practices, cooperating with local governments to support residential reuse, and coordination with USEPA and CDPHE to remove certain Operable Units from the Superfund program. De-listing of this property from CERCLA allowed the owner to access additional grant money for redevelopment activities typically denied at CERCLA-listed sites. Residential and commercial development is well on its way on this former CERCLA site, generating local jobs, tax revenue, and much-needed additional housing in the Leadville/Interstate-70 corridor. Dreams are also being realized at the Central City, Clear Creek Superfund site where the property owners are working to revitalize the Idaho Springs mining town, showcase the historic ARGO Mine operations, and plan for residential and commercial development in harmony with the old waste rock piles left behind by long-ago miners. And after many years of remedial

design and negotiation with USEPA and CDPHE, the former Eagle Mine Superfund site in Minturn was showcased by the Trump Administration's new "Superfund Task Force" as having the "greatest expected redevelopment and commercial potential." USEPA's renewed focus on accelerating work and progress at Superfund sites to successfully return them to productive reuse signals a new horizon for MSLS and increased opportunities and economic benefits for our communities and private sector investors. The USEPA's Administration is now focusing on redevelopment training for its career regulators, seeking out interested investors to highlight potential developments, and providing the tools and resources needed to work hand-in-hand with developers to reuse these MSLS sites.

4 THE REAL CHALLENGE TO MSLS REPURPOSING: FUNDING

In our experience and contrary to conventional wisdom, it is not fear of legal risk or environmental regulation that prevent MSLS repurposing. While the potential for liability and compliance with applicable regulations must always be considered, from initial vision to final realization, it is the inability of owners to obtain and keep funding that thwarts their efforts. Throughout the repurposing process, the legal and technical teams need to know that the most daunting challenge faced by owners is securing financing. Since few owners have the financial resources to buy, assess, remediate, and redevelop MSLS, it is critically important to understand how owners obtain funding and to retain funding through the life of the project.

If our readers take away only one new idea, it is that throughout the MSLS project life-cycle: *funding is key*. In our over 65-years of combined experience in the repurposing of MSLS and other contaminated properties, it is the unintentional consequences of poorly thought out legal, environmental, or engineering advice that kills the ability of owners to obtain *and keep* funding.

QUICK READ - THE MOST IMPORTANT TAKE-AWAYS?

- Funding is key, funding is key, funding is key.
- Assuming that an MSLS project is otherwise viable, it is the unintentional consequences of poor legal or technical advice that typically kills the ability of owners to obtain and keep funding.
- Time is money in the world of MSLS repurposing. When owners cannot get to project completion in a time frame suitable to their specific business model, typically due to poor upfront communication and management between the legal and technical teams, they will often walk away from a deal even if funding may be available in the future.
- Use of the regulatorily-approved MSLS Initiative model can aid owners when they approach private lending sources. Private lending sources can have some assurance that the regulatory community understands the need to work with all stakeholders, and will not act punitively.

5 PRIVATE SOURCES OF FUNDING

Partnering with the private sector is key, as the private sector is usually the only stakeholder with the financial capital needed to fill the gaps between public funding (discussed below) and final MSLS repurposing. The potential sources of private money are too many to enumerate here, but in general can include commercial banks, insurance companies, savings and loan associations, pension funds, trusts, and hard-money lenders.

Lending decisions made by private funding sources are influenced by wide-ranging, and often unique-to-the-organization sensitivities. While these funding sources analyze and dissect the usual data attendant on any loan application (credit rating, loan to value, etc.), the additional lending criteria for MSLS or other impacted properties universally revolve around the risk of unforeseen construction costs and scheduling delays due to poorly managed and/or implemented legal and technical requirements.

CERCLA imposes "strict, joint, and several" liability on all parties in a property's chain-of-title. Consequently, when CERCLA was first passed, nearly all private sources of funding of commercial or industrial repurposing, including MSLS, began to view every site as the next

Love Canal. While the 2002 passage of the Brownfield Amendments alleviated much of the risk, many private lenders remain sensitive to becoming a PRP. When the legal, environmental, and engineering teams do not communicate often and early, the likelihood of a private lending source pulling financing sky-rockets due to the risk of becoming a PRP or having an owner default on the loan.

QUICK READ – PRIVATE FUNDING

- Typically, only the private sector has the necessary financial resources to fill the gaps between public sources of funding and final MSL repurposing.
- Private funding can include contribution toward conservation easements, open space, trails, and natural areas—which ultimately draws additional funding for residential and commercial development.

6 PUBLIC SOURCES OF FUNDING

To close the gap when private funding isn't enough, which is often the case, there are many public funding mechanisms available for MSL projects. Not only can they supplement the initial site assessment costs prior to incurring larger capital expenses, they generate public interest in the project and can lead to additional investment. Property owners should evaluate: Community Development Block Grants, which provide federal funding for community-based revitalization; the Oil and Public Safety (OPS) Brownfield Redevelopment Fund to cover petroleum tank removal and remediation costs; USEPA and State Brownfields Cleanup and Assessment Grants; Tax Increment Financing, Tax Credit, and Metro District options; and access to the state and federal revolving loan funds for maximum capitalization.

7 FINANCIAL DEAL KILLERS: UNDERSTAND THE TRANSACTION

In our experience, the primary financial deal killers for MSL repurposing result from failure to understand the nature of the specific real estate transaction. Without this fundamental focus, consultants will miss the pain thresholds and non-negotiables for financiers; ignore the necessary profit margins needed to accomplish the repurpose; fail to consider non-regulatory funding, permitting or zoning requirements; or inadvertently re-plot existing MSL boundaries without regard to financial and legal considerations. While we typically think of burdensome regulations as deal-killers on these contaminated sites, it's the unintended consequences of non-strategic MSL assessments that can really kill the deal. Not only should consultants be aware of the real estate transaction terms, applying their expertise to strategic assessment and sampling will provide stakeholders with an understanding of what, when, and by whom, sampling results should be managed. It's not regulations that kill, it's the timing and threat of getting stuck in a regulatory abyss that takes too long for an owner or developer to withstand.

8 REGULATORY CULTURE CHANGES = OPPORTUNITIES

With the dawn of a new Federal Administration comes opportunity to approach these MSL projects differently. While past regulators were beginning to understand that private sector progress in revitalizing MSLs requires full agency cooperation and support—know this: it's not your Mother's Superfund Site anymore. In 2017, USEPA created a Superfund Task Force to better address environmental liability concerns and to encourage third-party clean-up and reuse at Superfund sites. The result: flexibility, cooperation, and the willingness to execute site-specific agreements more beneficial to the prospective buyer or owner. The agency's clear intent is to foster reuse of MSLs and other Brownfields sites. The result is a win-win-win for communities, the environment, and the developer. And don't discount that the agencies appreciate a little positive PR, too. As we experienced here in Colorado at the Gold King Mine site, the USEPA suffers just as much when a project goes sideways. The goal is to seek out and court a champion at the USEPA—one who understands your objectives, has regulatory

oversight over your MSL project, and the technical expertise to get it done. A successful MSL project requires legal, environmental, and engineering teams to work together and share and use the same data; and for property owners and developers to share land-use plans with the agencies as they evolve. The successful developers work to embrace the agencies' input rather than shy away from it. Time is money.

9 CONCLUSION

It's a new era for impacted mining properties and those interested in leveraging resources to bring life back to Colorado's historic mining towns. The technical environmental considerations are the same, but the legal hurdles are now diminished and the market is embracing public-private partnerships to repurpose MSL sites. With the right team in cooperation with the regulatory agencies, there is now a clear roadmap to success. Lastly, it's imperative to get your local community involved and in support of your plans. Stakeholders seek to retain their community "feel" but are eager to repurpose underutilized or abandoned lands to benefit their residents. The result: a *win-win-win* for all.

Soil Health & Biotic Soils via 5 Fundamentals for Sustainable and Cost Effective Mine Rehabilitation

M.D. Robeson

Profile Products, Fort Collins, CO, USA

A. Jung

Western GeoSystems, Golden, CO, USA

ABSTRACT: Successful rehabilitation, reclamation or closure of massive soil and vegetation disturbances from mining requires a comprehensive approach starting with a proper soil foundation. Those overseeing rehabilitation efforts must assimilate five fundamental considerations starting with a healthy soil in order to obtain a successful outcome. Healthy soil is a key component of long term erosion control and sustainable vegetation and ultimate reclamation. The costs and logistical challenges of importing biologically active healthy topsoil to most mine sites can be enormous. As such, the development of a newer class of hydraulically applied materials referred to generally as Biotic Soil Technologies (BST) have been created in an effort to help rebuild the upper layers of soil and ultimately generate healthy soils for long term erosion control and sustainable vegetation. This paper will describe the 5 fundamentals as applied on a mine site while trying to understand and determine if BST are actually impacting soil health.

1 INTRODUCTION

1.1 Five Fundamentals

Successful restoration of disturbed mine sites requires a comprehensive and holistic approach. Those overseeing mine reclamation efforts must integrate several considerations supported by proper planning and execution.

Employing creative methodologies to develop a suitable growing layer from less than desirable soils or substrates can only be accomplished by first understanding the make-up of the soil or substrate through comprehensive soil testing for agronomic potential and limitations. Soil testing, interpretation of the test results, and incorporation of prescriptive remedies to improve soils should be the first fundamental of any reclamation or revegetation project. It is difficult to predict potential project success without a proper understanding of soils or substrates considered for use as growing media to establish vegetation.

Prior to conducting and interpreting soil tests, it is important to understand relevant soil testing methods for reclamation and/or vegetation establishment projects. Further, it is important to properly collect and label soil samples prior to sending them to a reputable and experienced laboratory. Consistency in testing methods allows for simplified and more rapid evaluations of the results. There are various ways to extract measurable soil characteristics and analyze samples, but rarely do varying soil testing methods produce identical results. Relevant testing protocol and methodologies for erosion control projects that require vegetative establishment are described in detail in a technical primer for Soil Testing and Interpretation (Profile Products Technical Document, 2015). This publication also provides optimal ranges for various soil parameters and values where deficiencies or excesses may compromise or limit vegetative establishment.

The second fundamental requires an assessment of suitable plant species for achieving sustainable growth and effective erosion control – while meeting the collective post-reclamation expectations of owners, their consultants, the installer and relevant regulatory agencies. Soil

properties, climate, moisture regimes, slope aspect, maintenance, future land use and a host of other considerations contribute to proper species selection.

Once soil and agronomic considerations have been addressed, the third fundamental is to analyze site conditions to assess necessary erosion and sediment control measures. Site conditions, such as slope lengths, gradients and aspects and channel flow hydraulics must be examined and proper controls selected. Quantifiable performance attributes such as erosion control effectiveness, functional longevity and ability to facilitate growth establishment as well as cost effectiveness must be factored into determination of suitable products and/or techniques.

The fourth fundamental entails proper installation practices critical to the success of the rehabilitation program. Detailed guidelines must be developed and combined with onsite supervision to assure proper installation.

Finally, once reclamation measures have been installed, all active sites should be routinely inspected and maintained after each significant precipitation or other potentially damaging event – the fifth fundamental.

The Five Fundamentals are neither novel nor revolutionary advancements or methodologies for successful mined land rehabilitation, but rather the assimilation of time proven design considerations combined with proper execution and implementation in the field. Using these fundamentals must begin by building a healthy soil.

1.2 Soil Health

Healthy soils provide the capacity for a living ecosystem that sustains plants, animals and humans through nutrient cycling, filtering and buffering along with biodiversity. Once the soils are on the path to becoming healthy, sustainable vegetation can occur leading to reclamation. Key elements of healthy soils are: minerals; organic matter; biological activity; water and air as shown in Figure 1.

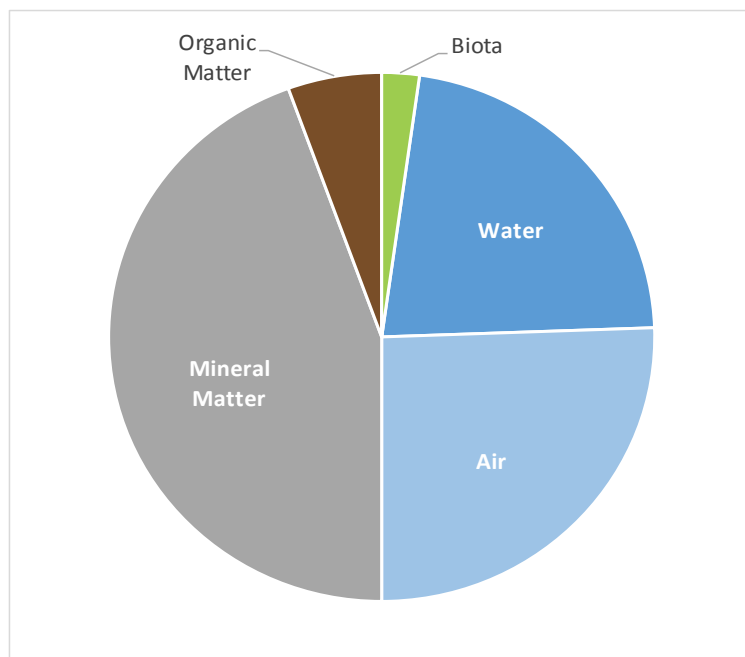


Figure 1. Key Element of Healthy Soil

Minerals, water and air are typically things that are unable to be managed due to the fact that site designers prefer to rely on existing soils and the natural rainfall conditions. As such, from a

design standpoint, the two key parameters that can be managed for improved soil health are organic matter and biological activity.

Organic Matter (OM) is largely made up of carbon that originated from living organisms and dead material, mostly derived from biological processes. OM is where soil carbon is stored and is directly derived from biomass of microbial communities (bacterial, fungal and protozoan) in the soil, as well as from plant roots and detritus, and biomass-containing amendments such as wood fiber, manure, mulch, crop residue, etc. Organic matter is of profound importance for soil function greatly impacting its physical, biological and chemical properties. OM acts as a long term carbon sink and as a slow-release pool for nutrients contributing to cation exchange capacity, nutrient cycling, soil aggregation and water holding capacity. It can also contain nutrients in its molecular structure providing energy to plant and soil microbial communities.

As soil biota decompose organic matter, nutrients are released and become available to plants. Some of the very small particles of well decomposed organic materials become bound to fine soil mineral particles and can become protected from further biological activity inside very small soil aggregates, leading to stabilized soil organic matter. Stabilized organic matter contributes to soil function in numerous ways, including those related to soil structure such as its capacity to store water and thus provide drought resistance. (Cornell University, 2017).

It is widely accepted that soils capable of supporting sustainable vegetation should contain at least 3-5% organic matter. Realistically, in practice, most construction soils offer less than 1% organic matter which is almost always insufficient to support sustainable vegetation. It is also important to also understand the stormwater management benefit of organic matter in soils. Depending upon soil type, for every 1% increase in organic matter, the soil can capture and hold between 16,500 and 27,000 gallons of water per acre (154,461 - 252,755 L per hectare)

Given that most mined sites have less than 1% OM, a major practical issue arises in how this shortfall can be bridged. Traditional options are by importing copious quantities of topsoil, compost, peat, and manure or sources of fibers such as wood chips, saw dust and more. It is suggested instead that a paradigm shift be considered, where a process is initiated to develop organic matter onsite rather than importing it.

One vexing issue facing successful restoration of disturbed sites is lack of available topsoil to create viable environments for establishing sustainable vegetation. In markets such as residential and commercial construction, energy development, mining, landfilling, and other construction related activities, it is recommended that the contractor remove or strip onsite topsoil or suitable overburden and stockpile them for future use. Unfortunately, this is not always a standard practice and even if topsoil stockpiles are constructed, after a few weeks only the very top of the pile (that receives sunlight, air and water) actually remains biologically active. Lower levels of the stockpile would be better termed top dirt. Further, a lot of topsoil simply is lost during the stripping and handling process while its composition is forever changed, never to be as viable as when in its former condition in a natural environment.

When onsite topsoil is not readily available the standard approach has been to locate nearby soil borrow areas and truck in suitable cover material prior to revegetation or restoration. This technique is often cost prohibitive and rarely will this material be truly viable "topsoil". One way to enforce quality of replacement soil is to include very specific specifications for its composition, required depths and quality assurance from load to load. Rarely are comprehensive soil specifications included into project designs, thus many construction sites will have need of prescribed amounts of supplemental organic matter and soil amendments to create a sustainable growing medium. Such applications may be perceived to be expensive, but cost savings can be substantial versus expensive imported topsoil, subsoil and even compost.

Compost is generally regarded as the next best alternative to topsoil, but is plagued by many of the same issues as soils – availability and proximity to project sites, cost and consistent quality. The composting process requires careful inputs of carbon- and nitrogen-based organic matter such as green waste and animal waste, along with sufficient moisture in an oxygenated environment conducive to aerobic decomposition. Both US EPA and the US Composting Council (USCC) have gone to great lengths to encourage and prescribe testing and specifications for Class A or exceptional quality compost for use in erosion control and landscaping applications. The USCC has developed a Seal of Testing Assurance (STA) program to certify that compost products have been sampled and tested in accordance with certain methods taken from the Test

Methods for the Examination of Compost and Composting (TMECC) Manual (US Composting Council, 2001).

Failure to produce and/or utilize STA vetted Class A compost could result in material that is high in pathogens, phyto-toxins, free nitrogen, contaminants, heavy metals, fecal coliform (*Escherichia coli*) and *Salmonella* sp. as well as other pollutants can have disastrous consequences for erosion control projects and stormwater quality.

Clearly the process for obtaining topsoil for a mine site can be difficult and likely very costly, especially when it comes to bringing in topsoil or compost.

2 BIOTIC SOIL TECHNOLOGIES

In the absence of adequate and/or cost effective sources of topsoil, new techniques have been developed to treat and revive depleted soils to render them more capable of accelerating and sustaining vegetative growth. Essentially, on-site soils can be modified and/or blended to improve their physical and biological properties. Beyond that, agronomic amendments such as those used to increase organic matter and fertility can be added to effectively engineer marginal soils into productive and sustainable growth media. Biotic soil technology (BST) can effectively complement or replace topsoil – thus reducing quantity requirements and costs while improving project success. BST contain a variety of components that can be grouped into three sub-categories as described below.

2.1 Base Fiber Components

- These are typically bark, wood or straw fibers that are phyto-sanitized to provide organic matter, erosion resistance and high moisture retention free while of weed seeds and pathogens.

2.2 Common Soil Building Components

- Biochar is short for Biological Charcoal and these stable, porous particles demonstrate a high Cation Exchange Capacity (CEC) which measures a material or soil's ability to hold water and nutrients. Biochar also acts as habitat, analogous to a coral reef for beneficial bacteria and fungi to colonize.
- Porous ceramic particles from calcined illite clay improve infiltration while also increasing moisture and nutrient retention. These particles also provide a very high cation exchange capacity and habitat for microorganisms.
- Beneficial Bacteria colonize “fresh” substrates and are essential for soil processes, Nitrogen fixation, aggregation of soil particles, and maintenance of soil nutrients.
- Endomycorrhizae are a symbiotic association of fungi with plant root hairs to facilitate nutrient and water uptake which improves drought, disease and salinity resistance
- Humic acid is the principal component of humic substances, which are the major organic constituents of soil (humus) and peat produced by biodegradation of dead organic matter.
- Sphagnum peat moss is a growth medium that promotes nutrient maintenance, increases water retention and releases humic acid.
- Seaweed extracts are a natural source of cytokinins – which are plant growth substances (phyto-hormones) that promote cell division or cytokinesis in plant roots and shoots.

2.3 Performance Enhancing Additives

- Cross-linked polysaccharide biopolymers or flocculants increase water-holding capacity, viscosity, bond strength, erosion resistance and flow of the hydraulic slurry through equipment and some can serve as a food source for included bacteria

Biotic soil technology also contain components that increase the water and nutrient holding capacity of soils while, creating a more suitable environment for growth of beneficial microorganisms that promote faster seed germination and vegetation establishment. BSTs are typically

mixed with water and hydraulically- applied as a uniform slurry using standard hydraulic seeding and mulching equipment; offering the distinct advantage of also placing seed, fertilizer and other soil amendments in one convenient application.

Although BSTs offer a moderate level of erosion protection, they are normally covered with higher performing hydraulically-applied, rolled or other erosion control techniques. For example, a combination of a BST and Flexible Growth Medium™ (FGM) erosion control matrix applied at standard areal rates can absorb and retain over 11,000 gallons per acre (107,000 L/hectare) of water. Unlike field harvested topsoil, sub-soil and compost; these materials are manufactured under controlled factory conditions with specific formulations that ensure product quality, consistency, and performance.

Upon application, BST will not match topsoil when considering physical properties such as depth, volume, texture, sieve analysis and possibly organic matter. The initial input of organic material from the BST and the overlying erosion control materials is sufficient to allow germination and vegetative development in the first few growing seasons. Concurrently, additional organic matter is developed as vegetation becomes established and nutrient cycling commences. BST therefore foster the development of topsoil on deficient substrates within the rhizosphere – the region of soil where plant roots are concentrated and the soil’s chemistry and microbiology are influenced by their growth, respiration, and nutrient exchange. This process in turn promotes faster seed germination and provides long term nutrient cycling that enhances sustainable vegetation establishment. In the end, BST offer an ideal place for plants to get started and provide the necessary components to build a healthy soil over time by accelerating the nutrient cycle.

3 INTEGRATION OF 5 FUNDAMENTALS WITH BST FOR SOIL HEALTH

With the ultimate goal of land reclamation and sustainable vegetation, the afore discussed techniques and concepts were put into practice on a mine site and monitored to determine if these techniques were actually improving soil health, leading to sustainable vegetation and ultimate reclamation.

For 13 years, an abandoned mine in the southeast of the United States sat partially barren as shown in Figure 2.



Figure 2. Abandoned Mine Site in Southeastern USA

The mining company had worked to revegetate and obtain reclamation release of a 5-acre portion of the site near a water body several times over the years with traditional seeding operations. Every time the site experienced a typical rain event for the region, significant erosion took place, seeds were washed away which prevented the mine from obtaining the project reclamation release. Further, the small amount of vegetation that was able to establish struggled to succeed. In November of 2015, the mining company had reached the point in time where they had to close out the project site and obtain the reclamation release from the regional authority and a 4th failed attempt at revegetation was not an option.

Knowing that the ultimate goal for this site was reclamation and seamless integration into the surrounding landscape, a team was brought in to assess the project site using the 5 fundamentals for reclamation in an effort to improve soil health and get the project headed towards sustainable vegetation and ultimate reclamation.

Utilizing these fundamentals and the selected materials and products determined from this process led to improved soil health and sustainable vegetation which will lead to full reclamation for this mine site as shown in Figure 3.



Figure 3. Sustainable Vegetation Heading Towards Full Reclamation at the Mine Site

Based on the soil health discussion earlier that organic matter and biological activity are the two key items to manage for soil health, the design team decided to monitor these values over time on this site in an effort to determine if soil health was actually improving, to determine if this project had sustainable vegetation and was on the path to reclamation. Of course, along the way, hoping to satisfy the regional authority and obtain reclamation release. Site photos documenting the installation that took place in March 2016 along with regional authority inspections that took place in August 2016 are shown in Figure 4 below.



Figure 4. Regraded Site in March 2016 (left), Regional Authority Inspection of Site in August 2016, Reclamation Release Approved (in 5 months) and Sustainable Vegetation Heading Towards Full Reclamation (right)

As shown in Figure 4, the site was regraded and the selected materials and products were installed in April of 2016. In early June 2016, Tropical Storm Colin hit the project site and dumped 5 inches of rain in a 36-hour period. The site was inspected by the design engineer and he said, “The site did remarkably well with no erosion, rills, gullies or ditches forming (not even small rills). The ProGanics, Flexterra and soil amendments stayed in place after the event and the project area benefited from the overall design. The water clarity in the lake was clear and the site withstood a significant storm event.” By September 1, 2016, the project was approved for reclamation release by the regional authority. An interesting note about this project and timing was that one day after the project was released by the regional authority, hurricane Hermine hit the area and dropped 6-10 inches of rain in a 24-hour period. The site held up great and there were no issues to report.

In regards to soil health, values of organic matter, soil respiration (an indicator of biological activity), along with total biological counts were monitored from project initiation in March 2016 to September 2017 to provide validation and reclamation release. As can be observed in Figures 5 and 6, the key parameters of organic matter and biological activity have increased significantly over the 18-month testing period from start of installation in March 2016 to September 2017, a clear indicator that sustainable vegetation has been achieved and reclamation is under way.

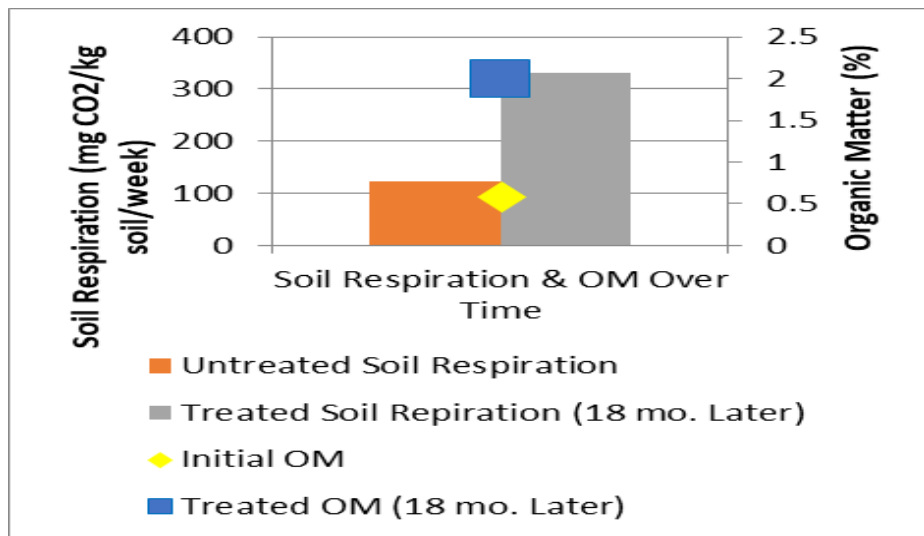


Figure 5. Soil Respiration (Increase of 271%) and Organic Matter (Increase of 333%) Over Time

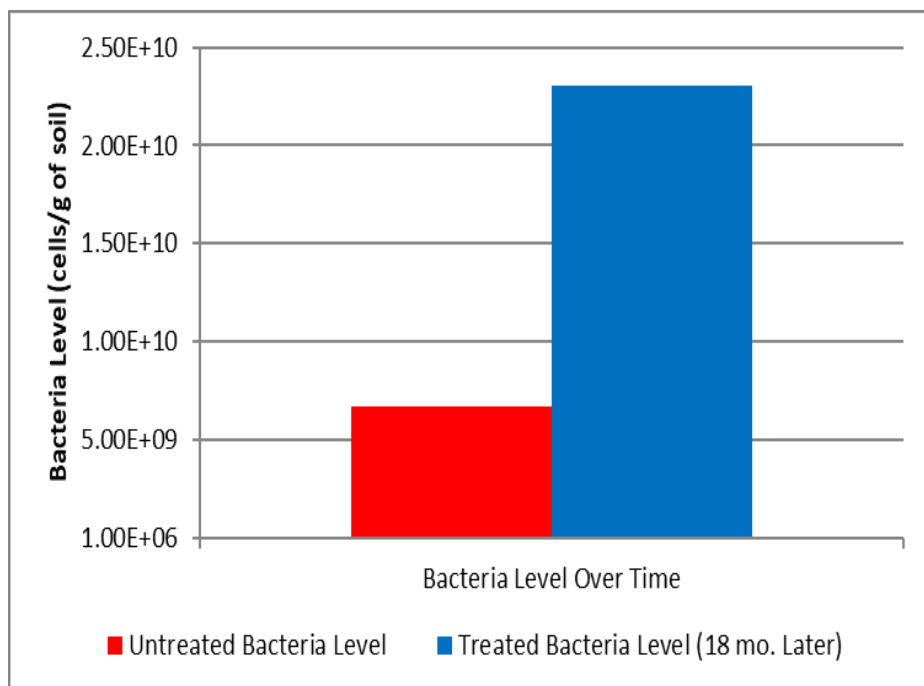


Figure 6. Bacteria Level Over Time: 345 % Increase

4 CONCLUSIONS

The mine project demonstrated within this paper utilizes the 5 fundamentals and takes a full evaluation of soil health from start to finish. The use of BST on this project as part of the solution was critical to the mine rehabilitation success. In this project, the owners recognized excellent results with significant savings over traditional topsoil, compost or other methods of increasing organic matter content. As such, it is clear that the ultimate goal for this site of reclamation and seamless integration into the surrounding landscape is well on its way, proven by reclamation release and tracked soil health data parameters that demonstrate a project following the Five Fundamentals in conjunction with Biotic Soil Technology can lead to sustainable vegetation and eventually full reclamation of mine sites.

5 REFERENCES

- Profile, 2015. Soil Testing and Interpretation. pp 1-4. USA.
- Schindelbeck, R.R., Ristow, A.J., Kurtz K.S., Fennell, L.F., van Es, H.M, 2017. Cornell University Comprehensive Assessment of Soil Health Laboratory Soil Health Manual Series, USA
- US EPA, 1990. Analytic procedures used in US EPA Report SW-846. Test Methods for Evaluating Solid Waste, 3rd Edition. USA
- US Composting Council, 2001. Test Methods for the Examination of Composting and Compost. Sample Collection and Laboratory Preparation. 02.01 Field Sampling of Compost Materials. US Composting Council. pp 1 -24. USA

Synergy between Operation and Closure of the Orcopampa Mine

A.B. Fernandez Canchos

Company of Minas Buenaventura S.A.A., Lima, Lima, Peru

ABSTRACT: The mining activity generates positive economic and social aspects in the area of social influence, by creating local job and tax collection, but generates social changes that result in conflicts as well. The social conflicts are generated mainly by the lack of consultation and community involvement, lack of information, profit expectations, environmental concerns, land use, sale of land and financial compensation for complaints and disputes (miningfacts.org, 2018)¹.

In Peru and in the Orcopampa mine, there are delays because of the negotiations about the sale of land for the construction of the components. This report seeks alternatives through efficient and eco-efficient methodologies by reusing areas already impacted and thereby achieving the continuity of the project without generating social conflicts (Van Hoof, 2015)². The approach of this report is to define a methodology focused on long-term strategies, determining the time of sale of land, permitting, construction, operation, closure and costs (Ruiz, 2015)³.

The approach was to create a "committee" named "strategic planning", which was composed of a multidisciplinary team. The committee identified the strengths and weaknesses of the planning process of the distribution of the principal components and develop a long-term matrix with the needs of construction, operation and closure. From the opportunities identified, the report develops the synergy between the closure of the tailings deposit and the unloading of sterile mine material.

The best alternative identified by the "committee" was the closure of the tailings deposit with waste rock using a method called 'overloading', avoiding the construction of another deposit. The environmental benefits are: (1) reduction of the volume and consolidation of tailings, reduction of the infiltration, and separation of the solution for its treatment in the processing plant in the medium term.

Thus, this report describes the approach to find the most efficient alternatives regarding the planning of the components of the mine, using appropriate methodologies for managing the given resources and the environment, as well as the synergy of operation and mine closure.

1 INTRODUCTION

1.1 Background

Lack of planning over the years has generated several problems which we have been adapting or getting used to. Since its inception the human species has exploited the various resources that nature has put at their disposal. In a long period extending from its origins to the Neolithic period, about 8,000 years ago, humans lived as hunter-gatherer clustered in small groups making a very

¹ <http://www.miningfacts.org/Comunidades/Ocasionala-la-mineria-conflictos-sociales/>

² Van Hoof. (2015) Course: Industrial Ecology. ESAN University.

³ Ruiz. (2015) Course: Environmental Trends and their implications for the business in Peru. ESAN University.

extensive use of their environment. The traces left behind in nature were very superficial. The abandonment of nomadic life gave rise to agriculture and the domestication of the first animals and plant species. The relationship with the natural environment changed dramatically. Humans discovered that they could modify their environment to their advantages and reach a level of well-being hitherto unknown. Large areas to create fields were plowed and through the economic and demographic explosion caused by the development of agriculture the basis for the creation of the first organized societies was given. (UNED, 2018)⁴.

Since then great progress was made, but over a very long period the available technology made the intensive exploitation of the natural resources impossible. Consequently, their impact on the natural environment was very limited. In this period the problem of poor planning for the development of a city or a project was virtually unknown because human activities were integrated into natural cycles, and the byproducts of human activity were absorbed smoothly by natural ecosystems. However, as problems arose when the lack of planning in collecting waste in emerging urban centers lead to pests and epidemics that had a tremendous impact on the population (UNED, 2018).

In the late eighteenth century at the beginning of the Industrial Revolution, thanks to the development of science and technology, new industries emerged and trade developed in an extraordinary way. The result was an authentic demographic and economic explosion, that manifested itself in the unstoppable development of urbanization. It was then when the first measures were taken to technically deal with the emerging problems of waste, which nowadays is generated with such a pace and is of such a nature, because of new production processes being implemented, that it can no longer be assimilated by natural cycles as before. But from the twentieth century on, especially in the second third, with the expansion of the economy based on consumption, the culture of ‘use and throw-away’, as well as the extraordinary technical advances achieved, the problem started to become critical and began to generate serious environmental impacts (UNED, 2018).

Buenaventura’s Orcopampa Mine is an underground mining operation that extracts and processes gold and silver minerals and which currently has been in operation for over 50 years. The mine is located between the districts of Orcopampa and Chilcaymarca in the province of Castilla, which forms part of the region of Arequipa, Peru. When the mining operations began in the Orcopampa Mine, environmental legislations were non-existent; only in 1992 the first regulation for environmental protection was passed, which lead to adjustments of environmental management. However, an adjustment process towards the understanding and application occurred during this decade and the following one. On the other hand, tools for environmental strategies did not exist. The purpose of environmental management is to define and develop a management system that includes suitable tools for the administration of resources and therefore the environment.

1.2 Issue

The lack of strategic environmental tools during the design and monitoring process of a project with suitable managerial alternatives for the resource management and, consequently, the environment.

1.3 Objectives

General objective:

- Implement a strategic environmental tool for managing resources and the environment.

Specific objectives:

- Develop a strategic long-term plan.
- Design mining components considering the proper management of resources, cost savings and environmental protection.

⁴ <http://www2.uned.es/biblioteca/rsu/pagina1.htm>

1.4 *Scope*

The right tools for environmental management in resource management can be applied in all types of industries with the main objective being the economic profitability achieved by good management of inputs and assets, distribution of components as well as the reduction and the recycling of waste. Furthermore, through these tools synergies with other stakeholders to reduce the cost of inputs and/or treatment of waste generated can be accomplished, not only achieving savings and environmental management, but also social responsibility towards the community.

2 METHODS OF SOLUTION

2.1 *Long-term strategic plan.*

Steps:

Good strategic planning is of major importance when it comes to a mining project; considering this step, the responsibility is not only up to the planning area and/or the operational areas, on the contrary, it is up to all the areas that are involved in the decision-making in the value chain, support and strategies. Therefore, the responsible persons and members of the "committee" will be in charge of the processes according Figure 1.

After defining the members of the "committee", which would be responsible for the processes, the steps and scope for the strategy to be use should be determined. Figure 2 presents the strategy to use be used; this strategy needs to be represented by a matrix called "Strategic Planning" (See Figure 3).

Figure 3 represents the matrix for strategic planning. It needs to be mentioned, that this matrix is a methodology that brings together the plans of all the areas or processes in general and which should be updated on a biweekly or monthly basis depending on the project's needs, although this is not restrictive. Nevertheless, each responsible of an area or process should review his plans with his team members beforehand, in order to avoid lengthy conversations and monologues. In case there were any observations, that cannot be rectified by the person in charge during the meeting, suggestions by the committee members will be made accordingly, which need to be reviewed and solved by the responsible area and returned to the head of the committee in order to update the matrix before the next meeting.

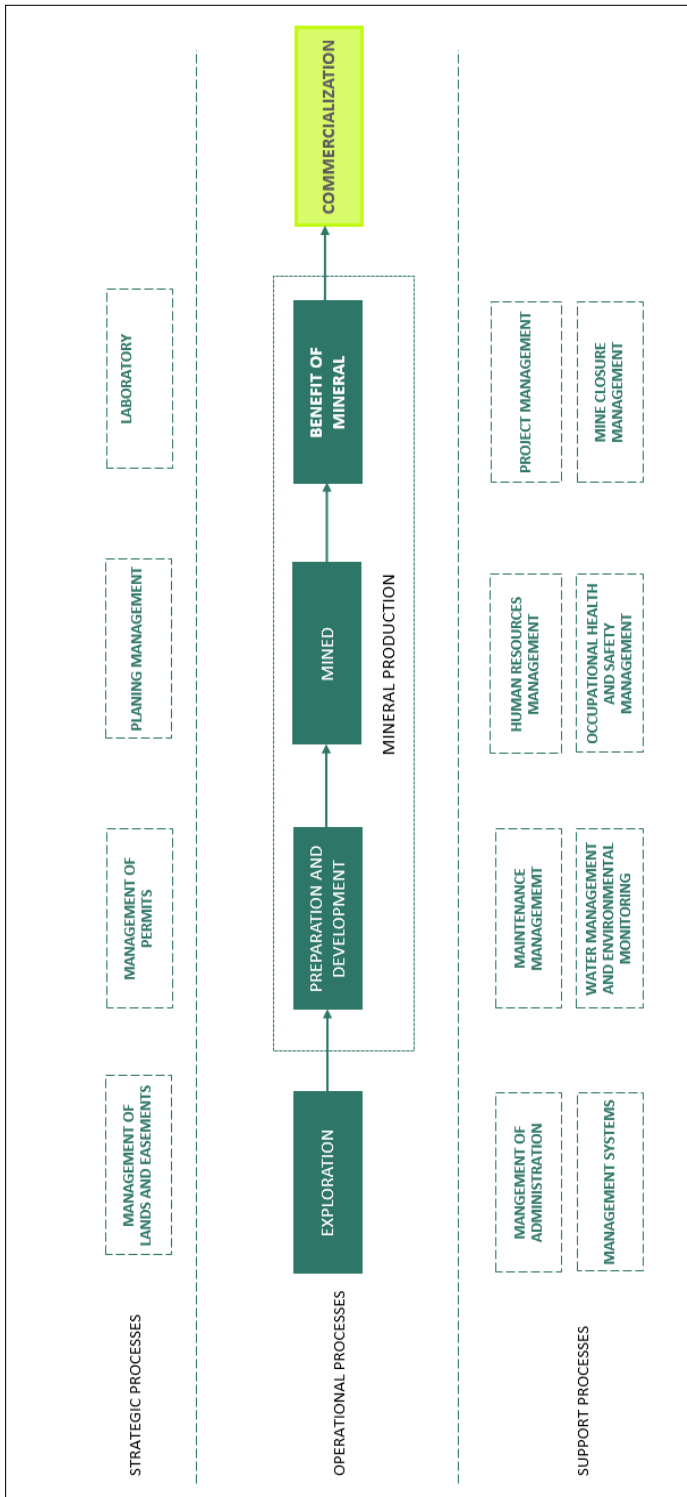


Figure 1. Identified processes.
Own source

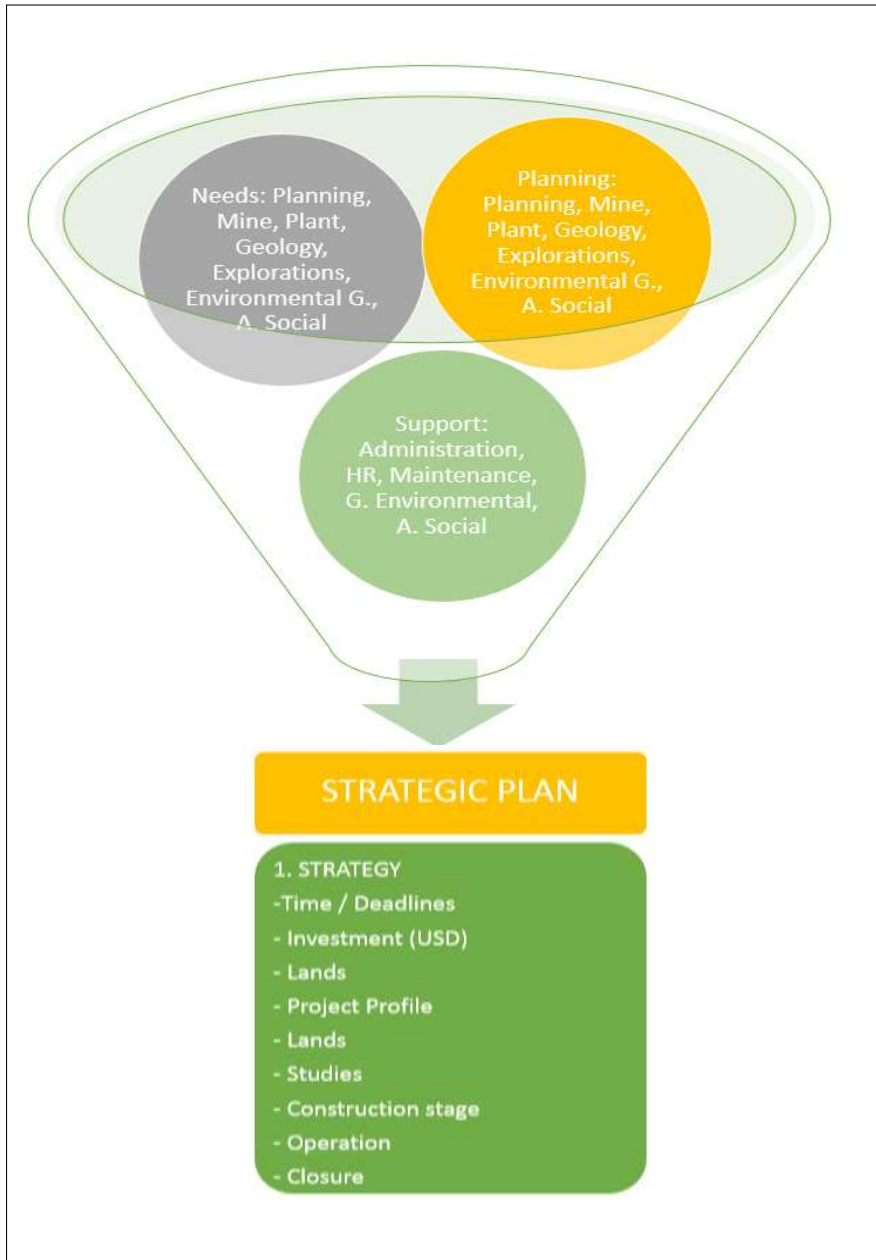


Figure 2. Strategy conceptualization.
Own source

TASK NAME	RESPONSIBLE	DURATION	START	END
▲ RELIEF HANDLING				
▲ RELAYER 1				
OPERATION				
▲ ALTERNATIVE RECREATION - RELAYER 1				
DETAILED ENGINEERING				
ENVIRONMENTAL MANAGEMENT INSTRUMENT				
AUTHORIZATION OF CONSTRUCTION / OPERATION				
CONSTRUCTION				
OPERATION				
▲ ALTERNATIVE - RELAYER 2				
SERVITUDE				
DETAILED ENGINEERING				
AUTHORIZATION OF CONSTRUCTION				
CONSTRUCTION				
AUTHORIZATION OF OPERATION				
OPERATION				
▲ ALTERNATIVE - RELAYER 3				
SERVITUDE				
DETAILED ENGINEERING				
ENVIRONMENTAL MANAGEMENT INSTRUMENT				
AUTHORIZATION OF CONSTRUCTION				
CONSTRUCTION				
AUTHORIZATION OF OPERATION				
OPERATION				
OPERACIÓN / FUNCIONAMIENTO				

Figure 3. Example of a strategic planning matrix
Own source

The figure above shows, that not all alternatives have the same tasks. That depends on the task and every responsible has to indicate the task's characteristics in function of time, capacity, constraints, among others.

2.2 *Component design with appropriate resource management, cost savings and environmental protection.*

When alternatives of different components are developed, the opportunities to be more efficient and eco-efficient need to be detected.

3 RESULTS

3.1 *Long-term strategic plan.*

As part of the activities a strategic plan with an A0 format was designed; the lead time of the following processes was obtained:

- Tailings Management
- Handling of mine waste
- Increasing of resources
- Program for mining ventilation
- Underground mining
- Others

To implement the tool of environmental strategy, the support of all the responsible persons forming the "Committee", a multidisciplinary team, was given. The "Committee" of strategic long-term planning tried to reach the communication of all responsible people in an effective meeting. Conversations about details were not part of the meeting, those were rather reviewed by the teams and their respective leaders as part of their daily tasks. In Orcopampa it was decided, that these meetings would take place every third Saturday of the month. The mine manager was involved as the president of the "Committee".

The following table shows a summary of the tailings and waste rock management which was determined by the before mentioned matrix, as well as the "Committee". It is important to mention, that the names for this work have been changed and the necessary summary was placed to be able to transmit and accomplish with the objective N° 2. It is clear, that in order to determine these dates, deadlines for land, permits, construction and others were set. It is worth mentioning, that there were changes during the development of the strategic planning matrix: At the beginning, optimistic and possible dates were set for the deadlines (based on historical data), but this lead to continuous errors, so that the initial dates were modified to more pessimistic dates, reaching an improved planification and compliance of the deadlines.

Table 1. Summary of the Strategic Planning Matrix; Should N° 6 or 7 be executed?

No.	Tailings and mine waste	Functioning	
		Start	End
1	tailing 1	Execution	30/11/2019
2	Alternative tailing regrowing 1	01/12/2019	05/23/2021
3	Alternative tailing 2	05/24/2021	10/28/2031
4	Close tailing with mine waste	Execution	08/31/2018
5	Mine waste deposit 1	01/09/2018	10/05/2019
6	Close tailing 2nd stage	06/10/2019	07/01/2022
	Close tailing 3rd stage	02/07/2022	22/12/2027
7	Mine waste deposit 2 (build)	06/10/2019	06/29/2022

Own source

From the alternatives for the discharge of waste material, alternative N°6 was chosen as the best one, anticipating the investment for the closure of the tailings pond and thus avoiding further disturbance of further areas. The closure envisages putting mine waste over the tailings pond and recover part of the solution trapped between the particles. This allows an appropriate closure of the deposit and leads to further economic, social and environmental advantages.

Alternative 7 would lead to the disturbance of more land by generation of discharges, among others. Furthermore, it is important to note that the reduction of the volume of solution trapped within the tailing reduces environmental impacts by infiltrations, compacts the tailings and separates the solution. Figure 5 and 6 depicts the items that were used to reach a better efficiency regarding the tailings pond's closure with mine waste. Moreover, the alternatives for replacing the construction of another deposit is being presents (See Figure 7).



Figure 4. Should N° 6 or 7 be executed?

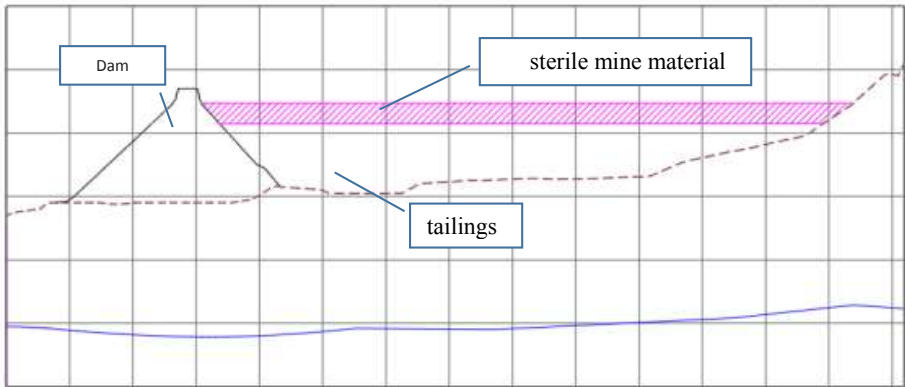


Figure 5. Alternative 4: Close tailing 1st stage - View profile

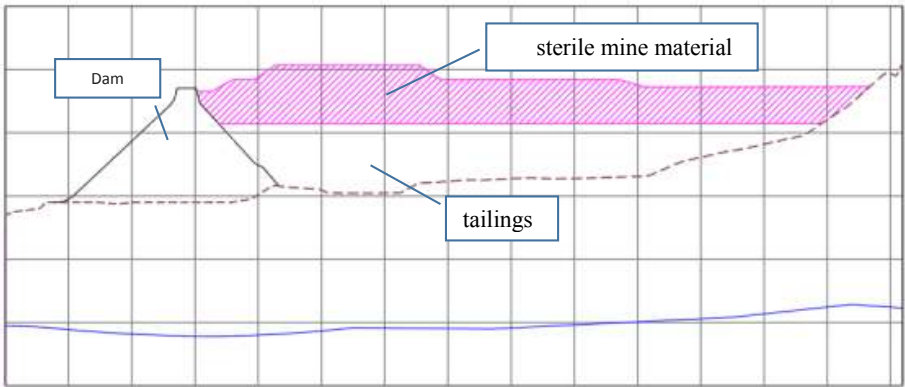


Figure 6. Alternative 6: Close tailing 2nd stage - View profile

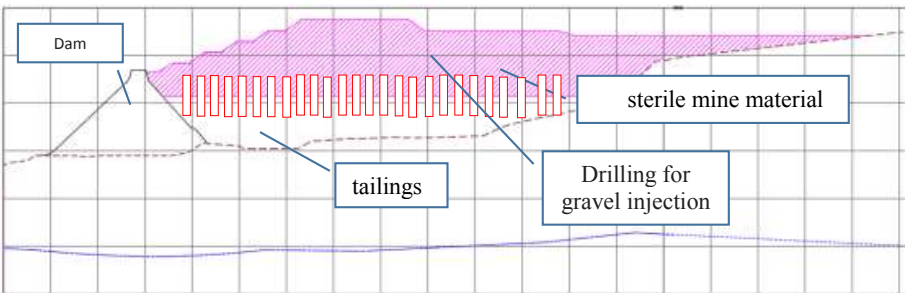


Figure 7. Alternative 6: Close tailing 3rd stage - View profile

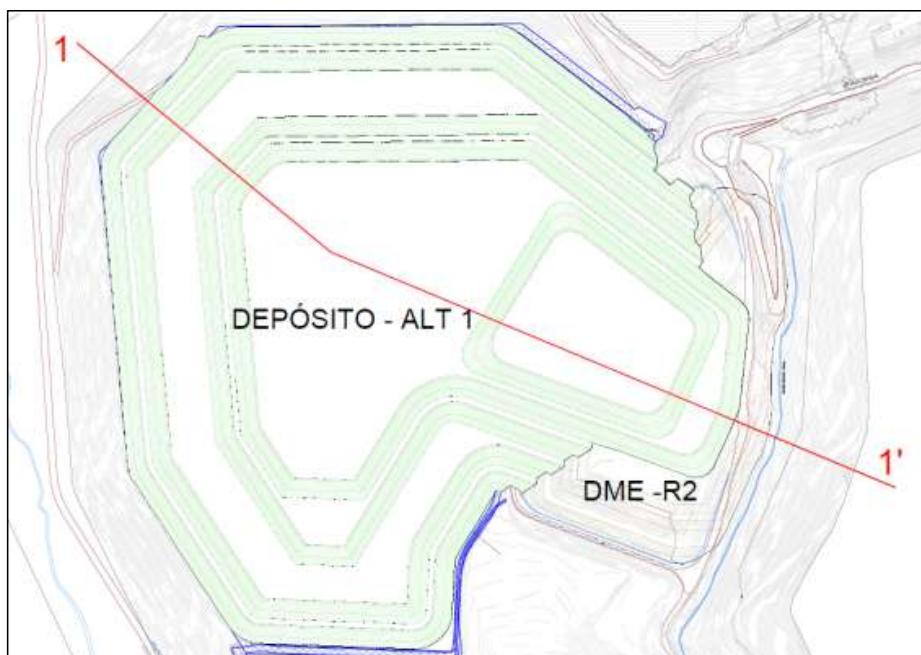


Figure 8. Alternative 6: Close tailing 3rd stage - View plant

Finally, it needs to be mentioned, that the best alternative obtained through the "Strategic Planning Committee" has been elaborated in detail. On the other hand, this alternative is not necessarily a good alternative for the environment, but as it is a good economic alternative a point of balance needs to be found. The goal is to modify the conventional through other alternatives with economic, social, technical and environmental benefits, seeking cost saving and corporate responsibility.

4 CONCLUSIONS

- The implementation of a strategic environmental tool for the management of environment and resources is feasible having the support of all those responsible for operational processes and strategic support.
- The development of a long-term strategic plan needs the communication of all the responsible people in an effective meeting. Any details have to be reviewed by the responsible team.
- If there is no continuity and compliance with the scheduled dates of the meeting, strategic planning is bound to fail.
- During the development of a strategic plan, optimistic dates and deadlines should not be set, on the contrary, the dates rather have to be set in a pessimistic manner and according to historical data. It is recommended to have two matrices: a real one and a pessimistic one.
- During the development of the matrix, opportunities are being detected; it is recommended to conduct an analysis of the alternatives which considers economic, environmental and social aspects.
- The best alternative must be suitable for the operation and if the process was chosen correctly, it will lead to notable social and environmental benefits.

5 REFERENCES

- Mattos. (2018). Closing engineering of tailings DME R2 R4- -R4A. AUSENCO. Lima Peru.
Recovered:
<http://www.uned.es/biblioteca/rsu/pagina1.htm>
- Recovered:
<http://www.miningfacts.org/Comunidades/Ocasiona-la-mineria-conflictos-sociales/>
- MINAM. (2014) Sixth Report National Solid Waste Management Municipal Municipal No 2013. Scope and Lima, Peru
- Ruiz. (2015). Course: Environmental Trends and their implications for the business in Peru. ESAN University. Lima Peru.
- Saker. (2015). Course. Corporate Environmental estartegia. ESAN University. Lima Peru.
- Van Hoof. (2015). Course: Industrial Ecology. ESAN University. Lima Peru.

Thermal Cover Design for Mine Waste Facilities in Cold Regions

C.W. Stevens

SRK Consulting (U.S.) Inc., Anchorage, Alaska, USA

T. Shapka-Fels and M. Rykaart

SRK Consulting (Canada) Inc., Vancouver, British Columbia, Canada

ABSTRACT: Thermal covers have been widely adopted in northern Canada for freeze encapsulation of potentially reactive mine waste to limit acid rock drainage. A better understanding of the predicted and observed thermal performance of these cover systems is needed to improve design and gain regulatory and public acceptance of the strategy for long-term closure. This paper describes the design and dominant heat transfer mechanisms that impact thermal performance of thermal conduction, latent heat, and air convection covers. Thermal model results for each cover type is compared to demonstrate major differences in short and long-term thermal performance. Review of Canadian mining projects that have adopted the freeze encapsulation strategy indicate that the most common design is the thermal conduction cover which is generally performing as expected under contemporary climates. Thermal covers for freeze encapsulation of mine waste remain a viable approach for closure of some mine waste facilities located in cold regions.

1 INTRODUCTION

Thermal covers have been widely adopted for freeze encapsulation of potentially reactive mine waste rock and tailings. The covers are constructed over potentially acid-generating (PAG) waste to limit the depth of seasonal thaw to non-acid-generating (NAG) cover material, and to promote ground cooling that sustains a perennially frozen condition of the waste. Freezeback of the PAG waste can limit geochemical and biochemical oxidation of sulfides by reducing surface water infiltration and availability of in situ pore water within the waste material. It has also been argued that freezeback may limit oxygen supply and biological activity that contribute to the sulfide oxidation (MEND 1996).

Thermal covers have been previously referred to as an “insulating cover” (MEND 1993, MEND 1996, Pham 2013), however, this nomenclature is misleading as few covers are specifically designed to restrict heat transfer using a material of high thermal resistance. The term “thermal cover” is more appropriate to describe cover function and its dependency on the thermal regime.

This paper describes the three main thermal cover designs and the dominant mechanisms of heat transfer for each. Numerical thermal modeling results are provided to compare thermal performance of the different covers based on an equivalent cover thickness and surface climate. A review of Canadian projects and mines that have adopted thermal covers as part of the closure strategy are also summarized, followed by a description of guiding principles for cover design.

2 THERMAL COVER FUNCTION AND DESIGN

Mine waste cover systems are designed to perform specific functions that allow for the management of acid rock drainage (ARD) to the extent that the site closure objectives can be met. The primary function of a thermal cover is to limit seasonal thaw (i.e. the active layer) to the depth of the NAG cover material and to decrease the gain and/or increase the loss of heat from the underlying PAG waste. The net annual loss of heat results in perennially frozen PAG waste and establishment of the top of permafrost into the cover (Figure 1a).

Figure 1b shows near surface ground temperature and the corresponding active layer depth; i.e. the uppermost portion of the thermal cover that seasonally thaws. The active layer begins to thaw in the spring as ambient air and ground surface temperature warm above 0°C. Freezeback is typically in early winter depending on the site climate and heat in the ground. Year-to-year variability in active layer thickness caused by annual difference in heat transfer with the atmosphere and the ground can be expected.

There are three basic thermal cover designs; thermal conduction covers constructed of geochemically suitable run-of-mine (ROM)/run-of-quarry (ROQ) rock or overburden (typically sand and gravel), latent heat covers that incorporate a material of relatively high moisture content, and air convection covers that consist of poorly graded ROM/ROQ rock to achieve a high air permeability of the material (Figure 1c). A fourth cover type is based on the use of passive thermosyphons installed below a layer of insulation to cool the ground. However, this design has limited application for large mine waste facilities due to the relatively small effective freeze radius around a thermosyphon evaporator pipe and the related cost of these systems.

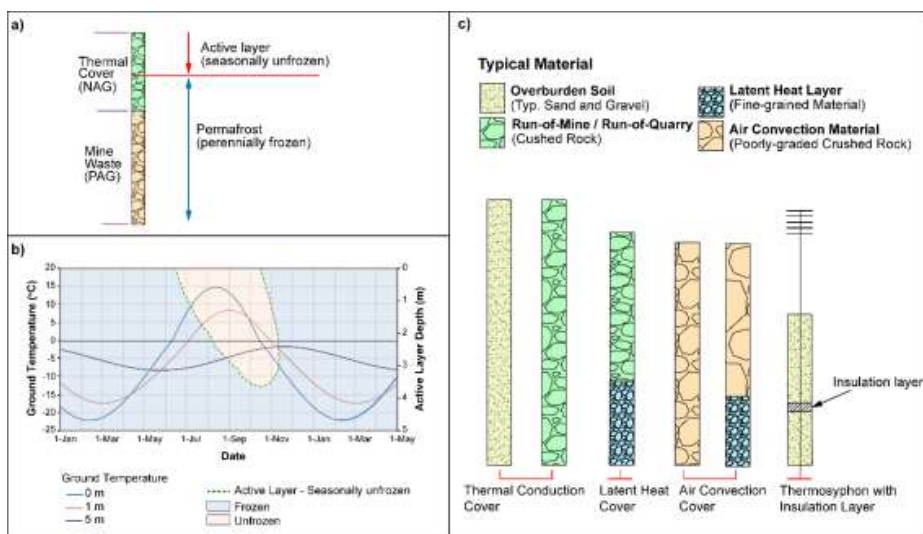


Figure 1. a) Schematic diagram of a thermal cover, b) typical progression of active layer and near surface ground temperatures for one year, and c) basic types of thermal covers.

3 DOMINANT MECHANISM OF HEAT TRANSFER

The dominant mechanism(s) of heat transfer for each cover is a function of the thermophysical properties of the cover material and the applied thermal boundaries. There are three heat transfer mechanisms that impact cover design and performance: thermal conduction through solids and liquids, convection in fluids (liquid or air), and radiation from the particles.

Johansen (1975) evaluated heat transfer mechanisms for various granular material as a function of the d_{10} particle size and the degree of saturation. Figure 2 shows the theoretical and experimental limits of the mechanisms for heat transfer. At a low saturation for silt and clay, the moisture content gradient may allow for vapor diffusion due to the differences in relative humidity of the air within the soil pores, with thermally redistributed moisture at higher material saturation. Thermal conduction dominates the heat transfer through the material as a material becomes progressively coarser or saturated, until reaching a high saturation and grain size that thermal convection can effectively occur within the pore space. Convection in sand and gravel at relatively high saturation is caused by thermally related gradients in the water density that allow for natural convection within the pore space or the advection of heat from the movement of water through the material (Figure 2). Gravel or larger material with a relatively high air-saturation (low moisture) may allow for differences in air density that result in natural air convection or cross-pore radiation through air-filled pores due to the transfer of electromagnetic energy from a warmer to colder particle.

Thermal conduction is often regarded as the most common means of heat transfer; however, other mechanisms exist and should be considered depending on the physical properties and expected thermal boundary conditions applied to the cover material.

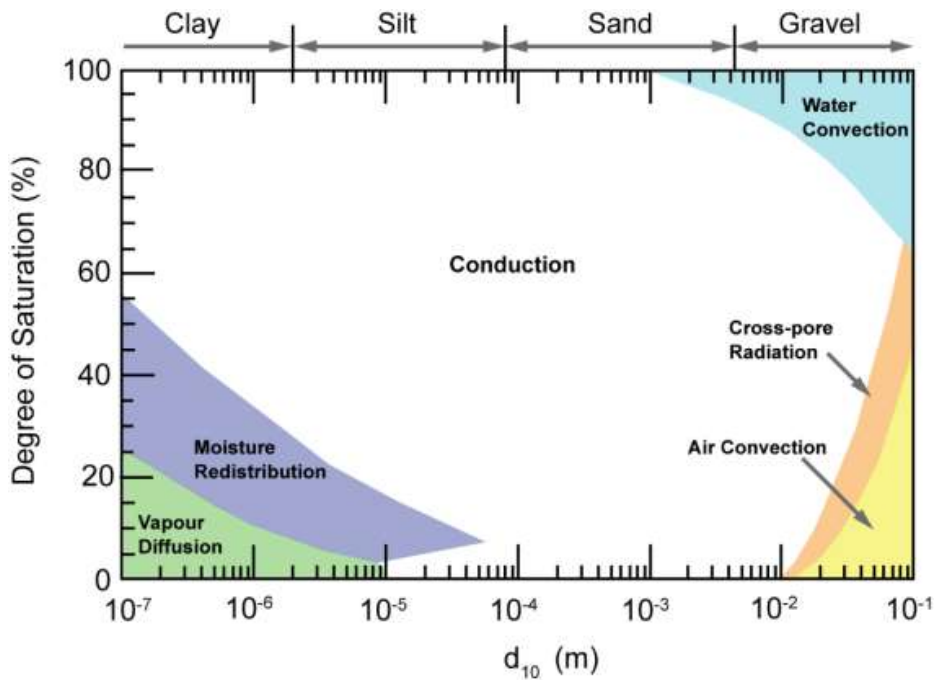


Figure 2. Heat transfer mechanisms for soils based on d_{10} particle size and degree of saturation (modified from Johansen 1975).

3.1 Thermal Conduction Cover

Thermal conduction covers are constructed of a single layer of geochemically suitable ROM/ROQ rock or coarse-grained overburden sand and gravel (Figure 1c). The material is typically well-drained, poorly to moderately graded crushed or blasted rock, but natural overburden may also be suitable. The degree of saturation of the ROM/ROQ rock is typically less than 30% depending on the physical properties of the material and site conditions.

Thermal conduction is the dominant mechanism for heat transfer through thermal conduction covers, i.e. most of the transfer of thermal energy by molecular vibration between particles. Air convection may still occur with the thermal conduction cover due to the coarse nature of some types of rock fill material due to the low fines content. The low moisture content of the cover material reduces the heat capacity and less energy is required to raise the temperature of the material. The low moisture content also results in a low latent heat requirement, and therefore less energy is required for phase change of liquid water or ice within the cover material.

3.2 Latent Heat Cover

A latent heat cover commonly consists of a double-layer cover constructed of ROM/ROQ material with an underlying soil of relatively high moisture content, referred to as the latent heat layer (Figure 1c). The dominant mechanism of heat transfer for a latent heat cover is thermal conduction. However, heat transfer and the advancement of the thawing front is greatly controlled by the moisture content within the latent heat layer. A significantly greater amount of latent heat energy (334 kJ kg^{-1} of water) is required to change phase of the pore ice to liquid water within this layer. The latent heat energy requirement consequently delays advancement of thaw into the cover. The elevated heat capacity of the high moisture layer also increases the energy requirement to raise the sensible heat component of the material. These effects reduce active layer depth and warming of the underlying waste.

3.3 Air Convection Cover

An air convection cover is constructed of highly porous, poorly graded material with a low fines content (Figure 1c) to allow for density-driven instability of the air column within the cover material that results in air displacement; i.e. the temperature gradient causes an air density difference that allows for the circulation of the air in the pore space and mass transfer of heat.

During the thawing season (summer), the cool air remains at the base of the cover and reversal in the air density gradient halts the natural air convection process. Thermal conduction becomes the dominant mechanism for heat transfer during this period. The active layer depth for a natural air convection system is dependent upon the low thermal conductivity resulting from the very low moisture content of the well-drained porous ROM/ROQ rock. During the freezing season (winter), the heat transfer by natural convection is more efficient than thermal conduction taking place in summer. The imbalance in heat transfer between freezing and thawing season results in more rapid freezeback and colder waste temperatures than would be achieved from conductive heat transfer alone. Pham (2013) previously evaluated natural air convection for design of thermal covers.

4 THERMAL PERFORMANCE MODELING

Thermal cover performance is routinely evaluated using numerical thermal modeling which considers site-specific factors including: contemporary and long-term climate, waste and cover material thermal and geochemical properties, and operational placement/management of waste material. Where exothermal reactions from the oxidation of sulfides are expected, heat generation should be considered to fully evaluate performance of the thermal cover. The objectives of the models and basis for evaluating thermal performance include the timing of waste freezeback, cover active layer depth, and the short- and long-term thermal regime.

4.1 Model Setup

SVHeat and SVAir finite element models with FlexPDE version 6.35 solver was used to show major differences in thermal performance of each cover type and sensitivity to key input parameters for some of the covers. The hypothetical model cases are based on site-specific information to provide credibility to the model results, yet were not completed for a specific mine project.

The model domain consisted of a one-dimensional model based on an 80-m section of waste covered with a 5.0-m-thick cover. The model results were evaluated on the basis of active layer

depth, although additional evaluation criteria are often used during design (see Section 6.1). For simplicity, heat generation from the mine waste and geometric effects of the waste facility were not considered in the models.

4.1.1 *Boundary Conditions*

The thermal boundary applied to the uppermost surface of the model was defined by a sinusoidal air temperature wave corrected to ground surface temperature using average thawing and freezing n-factors for exposed crushed rock and gravel. The n-factors act as a constant offset to summarize heat transfer between the cover surface and the atmosphere. The surface boundary was defined as:

$$T = \max\left(nf * \left[MAAT + (C_A * t) + Amp * \sin\left(\frac{2\pi+(t+P)}{365}\right)\right], nt * \left[MAAT + (C_A * t) + Amp * \sin\left(\frac{2\pi+(t+P)}{365}\right)\right]\right) \tag{1}$$

where *T* is the surface ground temperature (°C), *MAAT* is the mean annual air temperature (°C), *Amp* is the air temperature amplitude (°C), *C_A* is the air climate change factor (°C d⁻¹), *t* is time (days), *P* is the phase of the sine wave (°), and *nf* and *nt* are the respective surface freezing and thawing n-factors. Climate change is considered in Equation 1 using the air climate change factor which allows for a daily increase in the model. Table 1 summarizes input values applied to Equation 1.

Table 1. Surface boundary conditions.

Model Parameter	Value
Mean annual air temperature (<i>MAAT</i>)	-10.7°C
Air temperature amplitude (<i>Amp</i>)	21.0°C
Climate change factor (<i>C_A</i>)	0.000203
Surface, Thawing n-factor (<i>nt</i>)	1.52
Surface, Freezing n-factor (<i>nf</i>)	0.86

A geothermal heat flux of 2.11 kJ/(m·day·°C) is applied to the lower boundary of the model which was calculated from the average geothermal gradient (0.018°C m⁻¹) and the thermal conductivity of the mine waste rock. The initial conditions were defined by each material region in the model and assumed to be -1°C to represent an average material temperature for waste placed during operation. The average waste rock temperature applied to the model is conservative when compared to the colder waste rock temperature measured at the Diavik Mine North Country Waste Rock Facility. The cover material was specified as a constant initial temperature of 0°C. Initial conditions used in cover design should agree with site-specific conditions.

4.1.2 *Thermal Properties*

Table 2 provides a summary of the thermal properties applied to the models. The thermal conductivity and heat capacity were calculated in accordance with Cote & Konrad (2005) and make use of typical index properties of the material based on laboratory measurements and experience. Thermal properties for mine cover design should be based on the physical and thermal properties of materials intended to be used for construction of the cover system, as discussed in Section 6.

The waste rock and ROQ material used for the rock fill of thermal covers were assumed to have the same thermal properties. The tailings thermal properties were based on physical samples of tailings. Tailings process water was assumed to not have an appreciable level of dissolved ions which contribute to a freezing point depression, and no allowance was made in the model. In some cases, the inclusion of a freezing point depression in the model may be warranted by the mine

waste and pore water chemistry. The latent heat material was based on a fine-grained material with 40, 60, and 80% saturation (Table 2). The tailings and latent heat material included an unfrozen water content curve based on published values for similar material. Crushed rock for the air convection material was assumed to be selected material with a d_{10} of 75 mm. Intrinsic air permeability was calculated to be of $5.6E-07$ using the Chapuis equation modified version of the Kozeny-Carman equation (Chapuis 2004).

Table 2. Material thermal properties applied to thermal models.

Material	Degree of Saturation (%)	Porosity	Thermal Conductivity $\text{kJ}/(\text{m}\cdot\text{day}\cdot^{\circ}\text{C})$		Volumetric Heat Capacity $\text{kJ}/(\text{m}^3\cdot^{\circ}\text{C})$	
			Unfrozen	Frozen	Unfrozen	Frozen
ROQ / Waste Rock Material	30	0.30	104	117	1697	1509
Tailings	100	0.55	123	232	3502	2350
Latent Heat Material 1	40	0.40	81	92	2109	1942
Latent Heat Material 2	60	0.40	100	131	2445	2109
Latent Heat Material 3	80	0.40	115	172	2779	2277
Air Convection Material	5	0.43	59	54	1367	1367

4.2 Model Results

Figure 3 shows the estimated active layer depth for thermal conduction, latent heat, and air convection covers of an equivalent thickness and applied surface boundary condition. The active layer depth is observed in the models to decrease over the first five to six years following cover construction due to cooling (heat loss) that occurs as a new thermal equilibrium within the cover and underlying waste is established. Over the long term, the active layer depth increases in response to the climate warming applied to the upper surface of the model.

A large difference in short- and long-term performance of the covers exists when comparing active layer depth for a thermal conduction cover placed over waste rock versus tailings due to the difference in heat transfer through the waste material (Figure 3a). The results demonstrate the importance of completing thermal modeling that is specific to the mine site and material type. The difference in active layer depth between the conduction covers placed over waste rock and tailings is 0.9 m for model year 10 and 2.6 m for year 75. The active layer is shown to be maintained long-term for the thermal conduction cover placed over tailings due to the combined effects of thermal properties and latent heat requirements in the higher moisture content tailings. Greater heat transfer that contributes to ground warming takes place in the low moisture content rock fill used in the thermal conduction cover and underlying waste rock, resulting in a more rapid advancement of the thawing front (Figure 3a).

Figure 3b shows the impact of changes in active layer depth for a thermal conduction cover constructed over waste rock as a function of variation in the applied n-factor which changes the ground surface temperature applied to the uppermost surface of the model. As expected, warmer ground surface temperatures result in greater active layer depth over time.

Figure 3c shows the active layer depth for a latent heat cover modeled with 3.0 m of ROQ rock underlain by a 2.0 m thick latent heat layer. The active layer depth and rate of change over time due to increasing air temperature is less for the latent heat cover (Figure 3c) when compared to a thermal conduction cover (Figure 3b). The results show the effectiveness of the latent heat requirements to reduce seasonal advancement of the thawing front into the relatively high moisture content layer located at the base of the cover. Figure 3c shows sensitivity of active layer depth to change in volumetric water content for a soil porosity of 0.4 and an initial saturation of 40%, 60%, and 80%. Seasonal thaw depth is estimated to increase as the water content and latent heat requirements decrease. The change in water content also modifies the frozen and unfrozen thermal conductivity and heat capacity of the materials.

The predicted performance of an air convection cover with and without a basal latent heat layer is shown in Figure 3d. The air convection cover generally performs better over the first 50 years when compared to the thermal conduction cover (Figure 3b) and latent heat cover (Figure 3c). The addition of a 2.0-m-thick latent heat layer below the poorly graded air convection material results in a 0.4-m decrease in thaw depth by model year 75. However, the active layer depth increases at a relatively high rate over time once the thaw penetrates the underlying latent heat layer located below the air convection cover material. This behavior is shown in the model results for an air convection cover with a 2.5-m-thick basal latent heat layer (Figure 3d), and represents an important attribute of cover performance to consider.

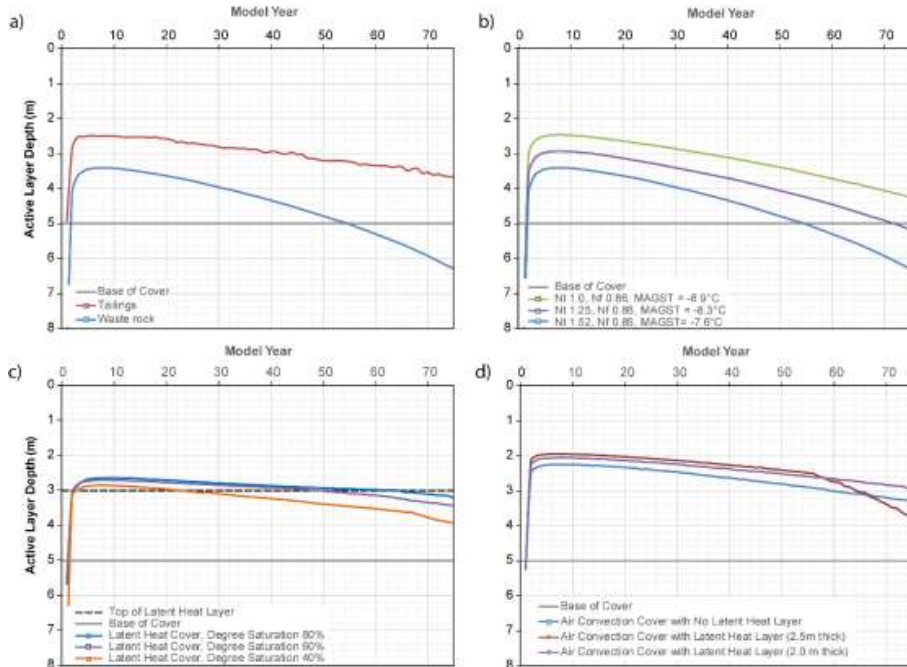


Figure 3. Estimated active layer depth for a) thermal conduction covers underlain by waste rock and tailings, b) thermal conduction covers with varying ground surface temperature, c) latent heat covers with varying material saturation, and d) air convection covers with and without a latent heat layer.

5 REVIEW OF THERMAL COVERS IN CANADA

Canadian mining projects that use thermal covers for closure of mine waste rock facilities were reviewed to compare differences in general climate and geographic applicability, design procedure and specifications. The covers were reviewed using the most recent publicly available information.

5.1 Review Summary

Thermal covers have been constructed, or are proposed to be implemented, at a minimum of eight mines in Nunavut and Northwest Territories for the closure of waste rock facilities (Figure 4). Climate change was considered in the design process in varying degrees for each of the covers reviewed. The geographic coverage ranges from high latitude sites in the Canadian Arctic (i.e. Nanisivik) to lower latitude sites located along the southern margin of the continuous zone of

permafrost (i.e. Snap Lake), covering a MAAT range of approximately -8 to -15°C. While continuous permafrost is not a limiting factor for thermal covers, continuous permafrost is presently within regions that maintain colder air temperatures.

Each cover has been designed to consider site-specific factors, which include, but are not limited to: waste material properties and reactivity, availability of construction material, material placement history, facility design, and stage of project. Thermal cover thickness is also dependent on cover type and design, which is specific to the individual mine waste facilities. Care must be taken to consider these factors when directly comparing cover thicknesses between projects.

The reviewed thermal covers for waste rock storage areas (WRSAs) ranged from 2.2 m to 5.0 m in thickness. Figure 5 demonstrates the trend and variability of cover thickness, compared to MAAT, latitude, and cover type. Cover thickness is generally greater at southerly sites which exhibit warmer MAAT and longer periods of seasonal thaw. Northerly sites located at higher latitudes generally exhibit colder MAAT, and shorter periods of thaw, thus requiring less cover material to maintain the active layer within the cover. At some sites, the current active layer depth for the WRSAs were found to exceed the cover thickness due to ongoing placement of material and ground thermal conditions, which are currently in thermal disequilibrium with the surface conditions. Over time and with limited heat generation from the waste rock, the net heat loss from the waste rock is expected to lead to decreased active layer depth as the thermal regime shift to colder conditions. This decrease has been observed at several of the Canadian sites and is consistent with numerical modeling results shown in Section 4.2.

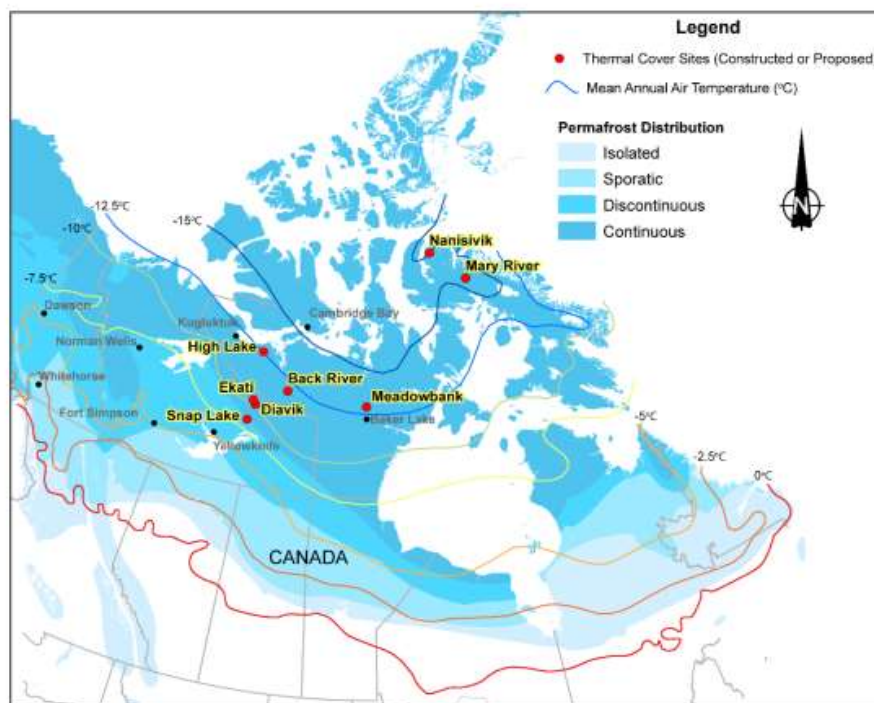


Figure 4. Thermal covers constructed or proposed for closure of waste rock facilities in Canada.

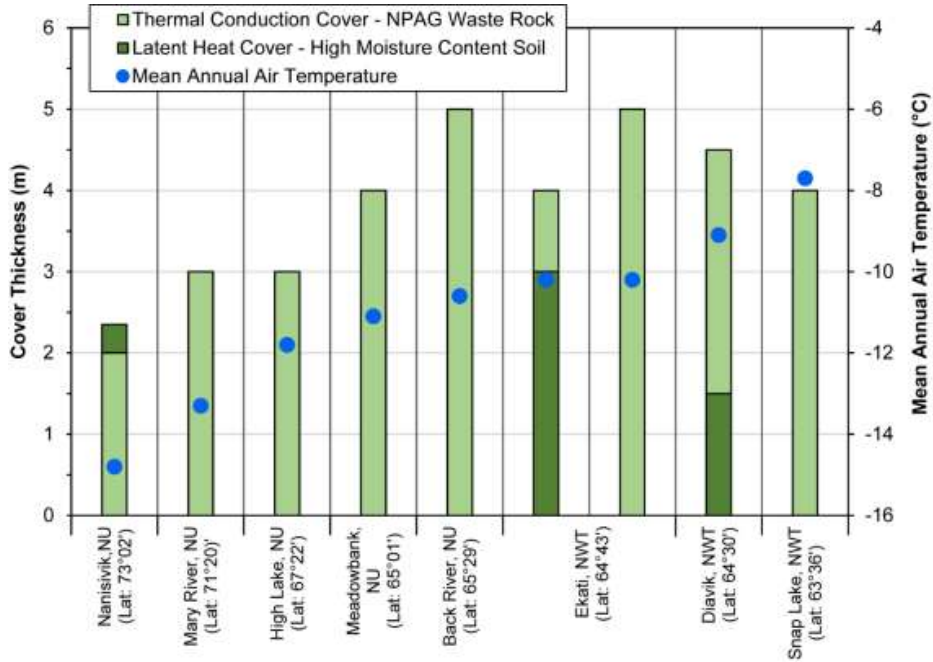


Figure 5. Summary of thermal conduction covers and latent heat covers for waste rock facilities in Canada.

Figure 6 shows maximum annual ground temperature and active layer depth measured at the Nanisivik Mine West Open Pit Waste rock cover, and clearly illustrates establishment of the active layer following cover construction. The Nanisivik zinc-lead mine, located in Nunavut on Baffin Island operated between 1976 and 2002, with full-scale mine reclamation beginning in 2004. As part of site closure, test and full-scale thermal covers were constructed (BGC 2004). MAAT at the site is -14.9°C (BGC 2018).

The West Open Pit Waste rock cover, constructed in 2006, consists of a minimum thickness of 2.0 m of granular shale overlain by 0.35 m of armor material consisting of sand, gravel, and cobbles. The waste rock used to backfill the pit has frozen back and the permafrost table has vertically aggraded into the cover (Figure 6). Net annual loss of heat from the underlying permafrost has resulting in the decrease in active layer depth between 2009 and 2014.

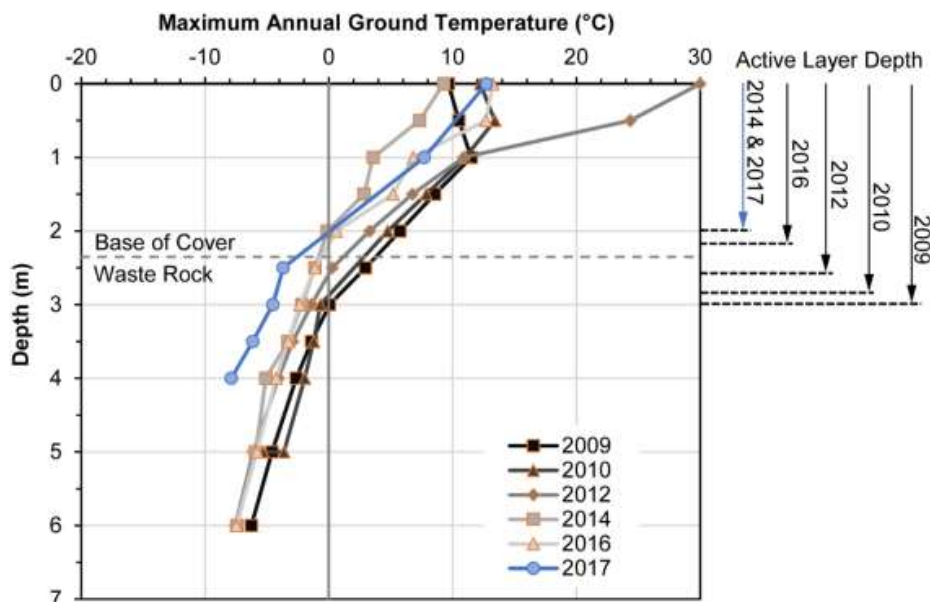


Figure 6. Measured ground temperature from mid-August and estimated active layer depth for the Nanisivik West Open Pit Waste Rock Thermal Cover. Ground temperature data reproduced from BGC (2018).

6 GUIDING PRINCIPLES FOR COVER DESIGN

6.1 Suitability

Adequate long-term performance of thermal covers is largely dependent on site climatic conditions. Selection of this as the preferred closure strategy will require an appropriately conservative and rigorous design and monitoring approach to demonstrate that the required design criteria can be met, considering relevant climate change predictions. The authors are of the opinion that thermal covers are best suited for areas well within the continuous permafrost regions of Canada.

6.2 Thermal Modeling

The current accepted practice for evaluating the thermal performance of a thermal cover is based on numerical modeling. The models are typically based on a finite element approach and account for present-day and future climate. Future climate should be assessed using best practice approaches which represents a clear understanding of the uncertainty and bias of the information (Rykaart et al. 2016). The authors view is that prediction of thermal cover performance should be modeled to the year 2100, given the current uncertainty and variability in climate change model outputs beyond this point. This limitation in the analysis tools should however be carefully considered when evaluating the long-term performance.

Performance criteria for evaluating the model results in the context of the closure objectives should be developed and consider:

- Evolution of the thermal regime, such as the aggradation of permafrost
- Short- and long-term active layer depth
- Sensitivity of cover performance to key inputs to model

One-dimensional numerical models may not be appropriate in all cases to estimate cover performance due to the complex geometry of the waste facility. For example, greater active layer depth may occur beneath side slopes where greater accumulation of snow occurs or within south-facing slopes that receive greater solar insolation from incoming shortwave radiation. Two-dimensional models should be used to account for geometric effects and where possible boundary conditions modified to meet surface conditions. Thermal models should be calibrated with site-specific ground temperature measurements.

Thermal properties and freezing characteristics for the waste and cover materials can be reasonably estimated using laboratory measurements of the physical index properties, and should be measured where possible to verify estimates and define heterogeneity from material placement. For air convection covers, the intrinsic air permeability and thermal conductivity of the material exert the greatest control on the estimated heat transfer whereas the predicted heat transfer for a latent heat layer is sensitive to differences in moisture content of the material. Sensitivity analysis for key model inputs and boundary conditions should be performed to understand the potential variability in thermal conditions over time. Thermal covers designed for tailings versus waste rock facilities should be independently evaluated due to the significant different thermal properties and heat transfer through the underlying waste, as shown in Figure 3a. Engineering judgement must also be used to evaluate the model results in the context of the model assumptions and the closure objectives.

6.3 Trial Covers

Trial covers have been constructed to confirm performance of the cover system at the project site. The contemporary conditions observed from trial covers does not unequivocally equate to the long-term performance as time is necessary for the ground thermal regime to adjust to a new equilibrium following waste placement and cover construction. Additionally, inherent differences that exist for trial cover construction when compared to full-scale covers may materially affect the inferred performance. Therefore, although trial covers can offer useful insight, the authors do not believe that trial covers should be a prerequisite, and if a trial cover is proposed it should be intentionally designed to verify:

- Construction methods and materials
- In situ physical and thermal properties of the cover material
- Thermal surface boundary conditions
- Seasonal thaw depth
- Time-dependent changes to the cover which impact thermal performance

6.4 Construction Quality Assurance and Quality Control

Construction quality assurance (QA) and quality control (QC) should be clearly defined to ensure cover construction meets the design specifications and conditions used in thermal modeling to predict long-term performance. If field conditions are found to not be within the allowable limits of the design, additional thermal modeling may be warranted to verify acceptable performance will be achieved.

The type and level of construction QA/QC that is required largely depends on the cover type, method of construction, and site-specific constraints, such as timing of material placement and construction materials. At a minimum, the QA/QC program should verify that key parameters controlling heat flow, as specified by the design are met. For example, a performance latent heat cover is controlled by the amount of latent heat required to change phase of the pore ice to liquid water. The performance of this type of thermal cover relies on the ability to achieve and retain the required moisture content. A design specification should therefore ensure physical moisture conditions will be met, maintained, and confirmed during construction.

6.5 Monitoring

A suitable monitoring program should be developed to adequately characterize conditions within the cover and underlying mine waste. The monitoring frequency and period are determined by the design and closure objectives for the site. At a minimum, ground temperature cables should be installed to monitor the ground thermal regime and active layer depth, with site locations selected to capture the expected variability in ground thermal conditions. For covers that include a latent heat layer, continuous moisture content profile monitoring may be necessary. Long-term site-specific climate measurements are also required to confirm climate change predictions.

The monitoring period will be site-specific, but is likely to be in the decadal scale. The period should focus on establishing two key elements: agreement with the modeling progression independent of the climate change predictions, and confirmation that the climate change predictions are reasonable.

7 DISCUSSION AND CONCLUSIONS

Thermal covers for freeze encapsulation of mine waste remain a viable approach for closure of some mine waste facilities located in cold regions. The primary function of a thermal cover is to limit geochemical and biochemical oxidation of sulfides by reducing surface water infiltration and availability of in situ pore water. To achieve these conditions, the cover system is designed to maintain seasonal thaw within the NAG cover material and contribute to the frozen condition of the underlying PAG waste.

The dominant heat transfer mechanism(s) for each cover is a function of the thermophysical properties of the cover material and the applied thermal boundaries. Numerical thermal modeling is the currently accepted approach to demonstrate adequate thermal performance of the design for the current and long-term climate conditions. Thermal analyses were carried out in this paper to show relative differences in active layer depth based on typical cover materials under an equivalent cover thickness and climate. The results show reduced active layer depth and improved performance are achieved with a latent heat and air convection cover design when compared to thermal conduction covers. Thermal conduction covers remain a suitable design, but require greater cover thickness to achieve the same performance. Thermal covers are sensitive to key physical parameters that should be considered during cover design and construction to ensure adequate performance.

A comprehensive understanding of the geochemical properties of the waste is required to determine if sulfide oxidation is expected to significantly contribute to heat generation and impact freezeback. For simplicity, heat generation was not addressed in this paper. Freeze encapsulation and performance of the thermal cover is dependent upon proper waste management during operation. It is imperative that the waste be managed on site through an effective plan which aims to limit sulfide oxidation during placement, as heat generation during operation could exclude the future use of the freeze strategy for closure. Waste management plans may specify segregation or blending, a maximum annual lift thickness for placement of waste to achieve annual freezeback, and other mitigation to limit heat generation prior to cover placement.

A review of thermal covers for waste rock facilities in Canada has indicated that thermal conduction covers are the most common. Where constructed, these covers are described to be adequately performing under the contemporary climate. The continuation of thermal cover monitoring will improve prediction of long-term performance through better definition of the physical and thermal conditions over time. Climate change presents unique challenges for cover function and public acceptance, but are no more or less vulnerable to poor performance when compared to alternative types of covers, as suitability of the cover system must be assessed individually for each site.

REFERENCES

- BGC Engineering Inc. (BGC). 2004. Nanisivik mine closure studies engineering design of surface reclamation covers (Water License Part G, Item 4). Report submitted to Canzinc Ltd.
- BGC Engineering Inc. (BGC). 2018. Nanisivik Mine, Nunavut 2017 annual geotechnical inspection. Report submitted to NYRSTAR.
- Chapuis, R.P. 2004. Predicting the saturated hydraulic conductivity of sand and gravel using effective diameter and void ratio. *Canadian Geotechnical Journal*. 41: 787–795.
- Cote, J. & Konrad, J.-M. 2005. A Generalized thermal conductivity model for soils and construction materials. *Canadian Geotechnical Journal*. 42: 443–458.
- Johansen, O. 1975. Thermal conductivity of soils. Ph.D. thesis, University of Trondheim, Trondheim, Norway. CRREL Draft English Translation 637, US Army Corps of Engineers, Cold Regions Research and Engineering Laboratory, Hanover, N.H. p. 291.
- MEND. 1993. Preventing AMD by disposing of reactive tailings in permafrost, MEND Project 6.1. Technical report.
- MEND. 1996. Acid mine drainage in permafrost regions: Issues, control strategies and research requirements, MEND Project 1.61.2. Technical report submitted to Department of Indian and Northern Affairs Canada.
- Pham, H.N. 2013. Heat transfer in waste-rock piles constructed in a continuous permafrost region. PhD Dissertation. Department of Civil and Environmental Engineering. University of Alberta. 376 p.
- Rykaart, M., Munoz, V., & Stevens, C.W. 2016. Climate change for the engineer: standardized procedure for climate change integration into engineering design. Saskatchewan Mining Association Environmental Forum. October 18–20. p. 10.

Update on Tailings Dam Safety and Regulation in the United States

C.F. Cobb

Alaska Department of Natural Resources, Anchorage, Alaska, USA

ABSTRACT: Attention to the safety of mine tailings dams was invigorated after two, high-profile international incidents in 2014 and 2015. Government agencies and organizations around the world began to review and update guidance for tailings disposal and regulation. In the United States, Montana led the nation with revised mine reclamation laws. Alaska followed with the publication of draft guidelines for regulating tailings dams under existing state statutes and regulations. At the national level, the Association of State Dam Safety Officials (ASDSO) published a resolution to support states that regulate tailings dams and chartered a new committee to address tailings dam regulation at the state level. Most significantly, the U.S. Environmental Protection Agency promoted rules for financial assurance requirements for hardrock mines under CERCLA 108(b), then in its final decision, did not adopt those rules. These state and national efforts to address the risk of tailings dam failures are reviewed.

1 UNITED STATES

Arguably the most significant, national, regulatory action related to mining within the last four decades was largely unrelated to the international tailings dam incidents in 2014 and 2015, but developed from the Comprehensive Environmental Response, Compensation and Liability Act of 1980 (CERCLA) also known as Superfund. However, the regulatory action was directly aimed at the hardrock mining industry and driven by perceptions of the history of that industry, aggravated by the recent failure incidents. The action of the U.S. Environmental Protection Agency (EPA) in 2017 was the publication of draft regulations to meet the requirements of Section 108(b) of CERCLA. The “proposed rule” required financial guarantees to reduce the risk of the cost to taxpayers for contingencies at currently operating, hardrock mines, regardless of the specific history or characteristics of a particular mine. The final decision of the EPA was not to adopt those regulations. The following is a synopsis of the Federal Register (FR) Volume 83, Number 35 published on February 21, 2018 which summarizes thirty-two and a half, triple columned pages of 9-point font typeset and includes select excerpts and editorial commentary believed to be noteworthy for those interested in the hardrock mining industry, and perhaps other industries potentially subject to 108(b). All things considered, your tax dollars are working for the economy for a change.

The publication of the “final action” begins with a summary statement of the EPA decision not to issue final regulations on the proposed rule, effective March 23, 2018 and includes contact information for the EPA. This is followed by a table of contents that includes seven main sections.

Section I, *Executive Summary* includes key information and statements necessary to understand the full scope of the issue including the history to the action leading the EPA to declare, “The Agency has determined that final regulations are not appropriate.” The following statements are noteworthy:

EPA has analyzed the need for financial responsibility based on risk of taxpayer funded cleanups at hardrock mining facilities operating under *modern management practices and modern environmental regulations*, i.e., the type of facilities to which financial responsibility regulations would apply. That risk is identified by examining the management of hazardous substances at such facilities, as well as by examining federal and state regulatory controls on that management and federal and state financial responsibility requirements. With that focus, the record demonstrates that, in the context of CERCLA section 108(b), *the degree and duration of risk associated with the modern production, transportation, treatment, storage or disposal of hazardous substances* by the hardrock mining industry does not present a level of risk of taxpayer funded response actions that warrant imposition of financial responsibility requirements for this sector.

The first italics emphasize a point of interest developed further in this paper and the second italics identify a buzzline that recurs throughout the rulemaking. CERCLA 108(b) required the EPA to develop financial responsibility requirements for certain classes of facilities not limited to the hardrock mining industry. In 2009, the FR reported EPA’s decision to identify the hardrock mining industry as the first class of facilities used for developing the respective regulations. The EPA would consider legacy mines and other factors that did not contribute to risk, without considering “modern” mining practices or the reduction in risk from other federal and state regulatory programs. The Executive Summary does not report what compelled the EPA to get around to publishing the proposed rule eight years later in January 2017 (that is covered later in this synopsis). The proposed rule included two goals:

- providing funds to address CERCLA liabilities at sites
- creating incentives for sound practices that will minimize the likelihood of need for a future CERCLA response

The Executive Summary does report, “the EPA now believes those goals have been met” after adequate consideration was given to “improved mining practices at modern mines” and state and federal regulatory programs. This represents a success story for the mining industry, state and federal regulatory programs, such organizations as Tailings & Mine Waste, the United States Society on Dams (USSD), the Association of State Dam Safety Officials (ASDSO), the Federal Emergency Management Agency (FEMA) and the giants who built the modern standard of care in mining represented by Andy Robertson, “Nordie” Morgenstern, John Nelson, Steve Vick, Dirk Van Zyl, Ward Wilson, the inimitable Jack Caldwell and many others. However, in taking the final action, the EPA effectively emphasizes the burden of the risk reduction carried by the individuals and representatives within these groups. Consequently, it is incumbent upon us to drill down (all puns intended) further into the FR to understand the value of the final action.

On a tangent to this paper, the Executive Summary states the value of the risk at less than \$16 million per year, while the “projected costs to industry” from the proposed rule was between \$111 million and \$171 million per year. Those assuaged by the final decision are mentioned including state and federal regulators and others who opposed the rule. The fact that no financial instruments were available to meet the requirements of 108(b) is also mentioned. Back on point for this paper, EPA states their decision on the final action was based on the record and:

...information submitted by commenters on three key points, which in combination demonstrate significantly reduced risk at current hardrock mining operations:

- (1) The reduction in risks due to the requirements of existing federal and state mining programs and voluntary protective practices of current hardrock mining owners and operators,
- (2) the reduced costs to the taxpayer resulting from effective hardrock mining programs, enforcement actions, and owner or operator responses, including financial assurance requirements pursuant to these other programs, and
- (3) the resulting reduction in the risk of the need for federally financed response actions at hardrock mines.

The record thus evaluated also supports EPA's determination that federal and state regulation and practices at modern facilities reduce the risks posed by operating facilities...

The EPA also mentions potential concerns from the proposed rule including disruption and preemption of existing state and federal requirements, problems with financial responsibility requirements of 108(b), and problems with "tailoring financial responsibility to a specific level of risk." The EPA concludes the Executive Summary with the reservation of their authority and the epitaph:

Thus, there are no regulatory provisions associated with this final action.

The twenty-eight words, fourteen numbers, five abbreviations and two dates has to be a federal record for succinctness, but must carry a lot of weight in Section II, *Authorities*. Section III, *Background Information* is a bit more wordy but includes some noteworthy material as we reach another layer in the borehole. In the first subsection, EPA explains the basis of their authority under CERCLA is to:

undertake removal or remedial actions in response to any release or threatened release into the environment of 'hazardous substances' or, in some circumstances, any other 'pollutant or contaminant.'

The EPA describes "removal actions" from CERCLA 101; CERCLA 111 is referenced for the "Superfund Trust Fund" for funding such actions; CERCLA 106 gives EPA the big stick to "compel action"; and:

CERCLA section 107 imposes liability for response costs on a variety of parties...so long as the costs incurred are 'not inconsistent with the national contingency plan,' (NCP)...[and] imposes liability for natural resource damages and health assessment costs... regardless of whether an owner or operator has provided evidence of financial responsibility under section 108(b).

The NCP published in 1990 is described briefly and EPA makes a distinction between "response actions" under the NCP due to certain risks and the risks to be covered by the "financial responsibilities" required by CERCLA 108(b). EPA goes on to describe the parts of 108(b) that compelled them to write such regulations for "owners and operators of facilities (in addition to those under Subtitle C of the Solid Waste Disposal Act and other federal law)" and to develop a "priority notice" effectively targeting their determination of the first to feel the object of their rulemaking.

The second subsection is a history of the rulemaking and a split spoon sampler is needed to classify an important stratum in our investigation. In 2003, EPA conducted the "120 Day Study" of the Superfund program and in 2005 published an action plan to address the 100 recommendations of the study. One of those recommendations was to determine if "action under 108(b) was appropriate." A number of additional studies occurred over the following years. In one of those studies:

The Agency attempted to exclude historic practices and legacy contamination resulting from such practices by using 1990 as a date to distinguish between modern and legacy practices. The Agency stated that it used 1990 because by that date most of the regulations under [the Resources Conservation and Recovery Act (RCRA)] relating to management of hazardous waste had been promulgated.

EPA claims consistency with other studies on hazardous wastes but notes its determination in 1986 to exclude from provisions of RCRA the "solid waste from the beneficiation of ores and minerals [because they] do not present sufficient risk to warrant regulation under Subtitle C of RCRA..." The EPA mentions this to suggest that 1990 is not a hard date to herald in "the advent of modern regulation or mining." They also mention "commenters" who suggest the "mid-1990s" for the rise of "modern mining regulation."

The third part of the Background Information gets us below the water table in a discussion about the legal action compelling the EPA to act. A lawsuit filed by the Sierra Club in 2008 led to a court decision in February 2009 ordering the EPA to publish the Priority Notice required by

108(b). The EPA's pace in accomplishing that endeavor attracted another lawsuit in August 2014 demanding Section 108(b) financial responsibility rules for four industries:

- hardrock mining
- chemical manufacturing
- petroleum and coal products manufacturing
- electric power generation, transmission, and distribution

As we drill on down through the overburden without additional sampling, the EPA reaches the bedrock conclusion that hardrock mining represented the “type of risk” to put them at the top of the priority list and the 108(b) coring. The proposed rule was published on January 11, 2017 in the Code of Federal Regulations (40 CFR Part 320) and limited to address “current hardrock mining operations” for various reasons.

The more than twenty-one pages in Section IV, *Statutory and Record Support for this Final Rulemaking* may seem like a lot of waste rock, but it contains low-grade and high-grade ore and some valuable nuggets of information. In the first subsection, the EPA interprets the statutes and lays out its thought processes for figuring out how to solve the statutory demand of financial responsibility “consistent with the degree and duration of risk associated with the production, transportation, treatment, storage or disposal of hazardous substances” (the buzzline) without doing “precise” risk assessments. Lacking any statutory direction, the EPA took a number of things into consideration including “the existence of state and federal regulations and financial responsibility requirements” and “Congressional intent.” Interestingly, EPA indicates consideration of “potentially duplicative Federal financial responsibility requirements...[and] state laws before imposing federal financial responsibility requirements...” as consistent with Congressional intent. EPA also didn't believe Congress intended for them to “disrupt existing state programs that are already successfully regulating industrial operations to minimize risk...” The EPA also considers “modern conditions [including] state and federal programs” with respective financial assurance requirements for currently operating facilities and “appropriate standards of care.” EPA describes the additional considerations already reviewed here in the Executive Summary and deflects specific responses to comments on the proposed rule because the final rule does not promulgate any regulations. That is a nugget with collector's value.

The EPA evaluates the administrative record in the second subsection of Section IV which is low grade ore for the risk assessment sensitive borehole loggers and includes gold and pyrite. The EPA relied on three primary reports for their evaluation:

- Evidence Report
- Releases Report
- Practices Report

See the FR for the specific references. They also relied on “the reduction of risk as the result of federal and state financial assurance requirements” and the history of Superfund payments at “modern mining facilities.”

Under the subheading *Reports of Risks Posed by Hardrock Mining Facilities*, the EPA reverses previous conclusions drawn from the Evidence Report because hardrock mining “shares characteristics related to the potential release” of nasties by bad actors at other Superfund sites and re-concludes the Evidence Report does not support the previous conclusion, and that had nothing to do anyway with the “degree and duration of risk” at “operating mines under modern environmental regulations”. Interestingly, the Evidence Report compared 24 operating facilities on the National Priorities List called “post-1980 historical sites” with a history of releases to facilities operating in 2009. EPA states:

...the report conflates risks posed by the historical facilities to risks posed by the 2009 facilities by comparing mining practices and contaminants of concern released at the facilities...[but] does not take into account the fact that by 2009, practices at mining facilities were already heavily regulated.

EPA continues to excoriate the Evidence Report for mixing up historic releases with permitted releases and the “mere presence of hazardous substances” and “a receptor”, with risk thrown into the cuttings. EPA emphatically states:

Rather, the primary determinant of risk is how current operations at the mine are conducted, including the current regulatory regime under which they operate. As documented in this final action, it is in this respect that most of the historic examples discussed in the proposed rule differ from the modern mines that would actually be subject to its requirements.

Maybe all that needs to go through the mill and a flotation circuit to extract the value, but it effectively reflects the efforts of the hardrock mining industry to distance itself from those historical operations.

A garnet of information is the EPA's conclusions on the Releases Report which was "intended" to drive a wedge into the reduced risk of regulated, modern mines. EPA said the limitations of the Release Report caused it to fail to support any 108(b) actions. The Practices Report is another gem. That report "purports to present information on the potential for future releases at operating hardrock mining facilities." EPA concludes that none of the reports "provide an appropriate basis for the identification of risk" and do not support the proposed rule for 108(b) action. (The references are on page 7563 of the cited FR if you still really want them.)

The next ore body in the deep hole, *Federal and State Regulatory Requirements* reviews hardrock mining under the Clean Water Act, the Clean Air Act and RCRA, as well as federal land management laws and other regulatory requirements. EPA determined these regulatory authorities did "reduce the risk" of federal spending on response actions. A statistic of curiosity states out of 354 operating facilities, the majority are after gold, iron, copper, phosphate and uranium, and half are goldmines. EPA pointed out that the proposed rule tried to distinguish between CERCLA "liabilities" and existing state and federal mine reclamation financial assurance requirements, as well as "technical engineering" required under state and federal permits. EPA "acknowledges" these other programs are "critical to understand 'the degree and duration of risk...'" buzzline as well as the risk to taxpayers. EPA adds value with their conclusion that the risks covered by the existing regulatory programs are the same as intended by the proposed rule and gives credit for being persuaded by the commenters from those state and federal agencies. EPA quoted the distinguished comment of the U.S. Forest Service speaking to everyone's fears:

The outcome is that EPA is attempting to regulate that which is already regulated.

Subsection IV.B concludes with a discussion on the risks of Superfund payments at hardrock mines and notes that \$4 billion dollars was Superfund money out of \$12.9 billion spent at 243 historical mining and mineral processing facilities (without mentioning where the other \$8.9 billion came from). EPA again credits "modern regulations" for the "degree and duration of risk" buzzline caused by the hardrock mining industry to the taxpayer to be insufficient to "warrant imposition" of the proposed rule and reviews background information, case studies and federal and state experiences with hardrock mining that supports the conclusion.

One man's interest is another man's boredom; drilling can be monotonous but you must log every layer. Still in Section IV, EPA addresses comments from supporters and opponents of the proposed rule. Supporters of the proposed rule were popular and included dozens of environmental groups, individual citizens, indigenous people organizations and four mass mailing campaigns. The specter of indefinite water treatment was raised among other concerns. EPA recognized such legacy situations and responded:

Modern regulation of both process discharges and runoff, as well as reclamation requirements to control sources of contamination, significantly address those risks...residual risk does not change EPA's conclusion that it is not appropriate to issue final section 108(b) requirements for current hardrock mining operations.

This layer of the FR was a bit more than one side of one page thick.

Opponents of the proposed rule garnered more than eleven FR pages of comments from the EPA. Opponents included federal and state regulatory agencies, the Interstate Mining Compact Commission, mining companies and trade associations. Opponents challenged the proposed rule on several fronts, as represented in the following excerpt from the table of contents:

- 1) Comments Regarding Appropriateness of Information Used

- (a) Use of Information Not Relevant to the Mines To Be Regulated Under the Rule
 - (b) Use of Data That Did Not Directly Demonstrate Risk at Current Hardrock Mining Operations
- 2) Comments That EPA Failed To Consider Relevant Information
- (a) Comments Providing Information on the Role of Federal and State Programs and Protective Mining Practices in Reducing Risks at Current Hardrock Mining Operations
 - (i) Examples of Federal Programs
 - (ii) Examples of State Programs
 - (b) Comments Providing Information on Reduced Costs to the Taxpayer Resulting From Effective Hardrock Mining Programs and Owner or Operator Responses

Notably, EPA agrees that the mining industry has raised the bar and the risks are not the same now as they were when many of the legacy mines were operating. Credit is given to modern engineering controls “such as surface water containment structures, engineered storage facilities, water treatment, impermeable liners, and leak detection and recovery systems.” The rise of these technologies is again discussed in a debate on the year when “modern” methods began, 1980 a point of challenge. EPA wisely observes there is no “particular date” that distinguishes the old from the new and progresses to “current applicable regulatory schemes as ‘current’ operations.” In effect, EPA agrees that mining has come of age and modern mining practices and regulatory “regimes” reduce risks from hardrock mining. Regulatory programs are reviewed including the U.S. Bureau of Land Management, U.S. Forest Service, Nevada, New Mexico, Alaska (the *Guidelines for Cooperation with the Alaska Dam Safety Program* discussed in this update were mentioned as providing “further safeguards” for dams), Colorado, and Montana (the 2015 mine reclamation law amendment is also discussed in this update). The EPA addressed comments on state programs and “agreed...the proposed rule did not adequately consider the protectiveness and financial assurance requirements of current state regulatory programs in assessing ‘the degree and duration of risk’” buzzline, the risk to taxpayers, and “based this final decision in part upon its more comprehensive consideration of those existing programs.” The EPA discusses “Protective Mining Practices” including commenter provided and project specific examples of state and federal reclamation requirements, corporate volunteer programs, engineering designs of tailings dams, waste rock and water management systems, monitoring, maintenance, correction actions, communication plans and other “environmental protection controls.” (The things we do.) Notable again:

EPA acknowledges that the requirements of current federal and state programs can reduce risk at hardrock mining facilities, and that when determining the need for section 108(b) requirements for hardrock mining facilities at proposal, EPA did not adequately consider their impact... EPA agrees with commenters opposing the proposed rule that those reductions in risk should be considered...[is] convinced ... that the rulemaking record supporting requirements under section 108(b) for currently operating facilities was incomplete in not adequately considering the risk reductions currently obtained by other Federal and state regulatory programs.

EPA adds the qualifier:

While...the risk of a release is never totally eliminated by the requirements of other programs, this residual risk does not change EPA’s conclusion that it is not appropriate to issue final section 108(b) requirements for current hardrock mining operations.

Section IV continues with the discussion of the reduced cost to taxpayers from the current state of the practice in hardrock mining. Very few cases of mining facilities that cost the taxpayers were noted and the \$ 4 billion of Superfund money spent at legacy mines and historical mining practices did not reflect “relative risks” from modern operating mines. Continuous improvement in mining

operations and regulatory programs are mentioned. Section IV finally concludes with a discussion on the lack of availability in the financial world for the types of instruments Section 108(b) would require. A poison pill to these requirements is described under Section VI.

Section V is a brief discussion of EPA’s decision not to publish Subparts A through C of the proposed rule which they could, but since they were not publishing any regulations they wanted to avoid “potential confusion.”

Section VI describes obstacles in the development and implementation of the proposed rule including:

- 1) the potential disruption of state, tribal, and local mining programs
- 2) the determination of a financial responsibility amount
- 3) the economic impacts of the proposed rule
- 4) the availability of instruments
- 5) identifying the facility for purposes of the rule

Each of these obstacles are addressed. The poison pill is in the fourth item; Section 108(c)(2) of CERCLA allows claims against the “guarantor” of the financial instruments, effectively dooming any chance that a third-party angel would put money on the table.

Section VII, *Statutory and Executive Order Reviews* is well beyond the ore body and concludes the FR most notably by stating the final action is:

A significant regulatory action that was submitted to the Office of Management and Budget (OMB) for review, because it may raise novel legal or policy issues... although it is not economically significant. Any changes made in response to OMB recommendations have been documented in the docket. EPA prepared an economic analysis for the proposed rule, but that analysis is not relevant for this final rulemaking because no regulatory provisions are being finalized.

End of boring (puns still intended).

A footnote on the epitaph: As a result of EPA’s final action, on May 16, 2018, certain environmental organizations filed a Petition for Review of the decision with the U.S. Court of Appeals, District of Columbia Circuit. As of June 15, 2018, fourteen states filed a Motion to Intervene because of those state’s interests in the final action.

The following sections reflect examples of “modern mining regulations” in a review of three new regulatory actions that occurred since 2015, independent from any federal incentives. A revised mine reclamation law in Montana, draft revisions of dam safety guidelines in Alaska, and ASDSO committee efforts are reviewed.

2 MONTANA

In 2015, the 64th legislature of the Great State of Montana unanimously advanced Senate Bill 409 amending Chapter 4, *Reclamation* of Title 82, *Minerals, Oil and Gas* of the *Montana Annotated Code* (MAC).

SB409 was promoted by the mining industry in Montana in the wake of the misfortune at their neighbors to the north. The Montana Mining 2015/2016 magazine described the new law as “the most rigorous and cutting-edge regulation in the western states and possibly the world on tailing storage facilities associated with current and future mine operations” (DEL, 2016). The act codified terminology and practices related to engineering, design, operation, monitoring, maintenance, reclamation and financial responsibility for tailings storage facilities and other aspects of mines.

The following items are based on personal contacts except as noted and any misrepresentations of the opinions described are the sole responsibility of the writer. Five perspectives on the new law were elicited:

- The common perspective of someone who cares about the environment, with technical credentials to understand the potential impacts of the mine operations and the implications of the statute: According to Dr. Dave Chambers of the Center for Science in Public Participation headquartered in Bozeman, Montana, the new statute is generally pretty

good. He likes the design criteria for extreme earthquake and hydrology events and the requirement for an independent engineering review panel. He is concerned that some of the exemptions may exclude projects that should also be regulated. In any case, “safety should be made the primary consideration, especially over cost, but even over environmental and social impacts.”

- The unique perspective of the regulator who is charged with the task of measuring up the operation to see if it meets the standard of care set by the legislators: According to Charles Freshman with the Hard Rock Mining Bureau of the Montana Department of Environmental Quality, the independent review panel is making decisions previously made by the regulator in certain cases; questions from the state are not always addressed by the panel if the subject is not defined within their scope of work for the project. However, it is nice to have specific information in the statute, that previously would have required an outside reference such as Canadian Dam Association guidelines.
- The exclusive perspective of a trusted colleague who shares all of these perspectives and more, including the 2017 Regional Award of Merit from ASDSO for promoting dam safety in the western United States: Michele Lemieux, manager of the Montana Dam Safety Program, said the new law seems to be very helpful. It raised the standard of care in Montana. The design criteria in law eliminates arguments on what must be evaluated. However, the requirement for an independent review panel is great and allows the engineer some flexibility if the panel approves of the deviation from the law on a technical detail.
- The seemingly rarefied air of the mining industry, which was panned from the Montana Mining 2015/2016 magazine: Mark Thompson, president of Montana Mining Association and Manager of Environmental Affairs at Montana Resources brings it down to earth: “SB409 is the advent of a new era of mining in Montana, where industry proposes standards progressive in concept, comprehensive in scope and definitive in responsible management of tailings storage facilities.”
- The purely subjective perspective of the professional critic holding the pen, whose candid opinions are included in commentary in the following review of select components of SB409 that were adopted into law.

The Montana Legislature is commended for the clear statement of intent in 82-2-301 of the MAC that:

(b) tailings storage facilities are designed, operated, monitored, and closed in a manner that:

- (i) meets state-of-practice engineering design standards;
- (ii) uses applicable, appropriate, and current technologies and techniques as are practicable given site-specific conditions and concerns; and
- (iii) provides protection of human health and the environment; and

(c) the regulation of tailings storage facilities is not prescriptive in detail but allows for adaptive management using evolving best engineering practices based on the recommendations of qualified, experienced engineers.

This may be the most focused statute on tailings storage facilities in the United States and clearly represents the legislature’s understanding of the risk identified incidentally by the EPA as a state responsibility to mitigate. Further, because it was advanced by the mining industry shows that industry is willing to do what it takes to do the job right, but needs the flexibility to adapt to the site-specific conditions where strictly enforced, prescriptive government regulations may not be the best approach to minimize risk.

Section 82-4-303, *Definitions* introduces some new ones including:

Certification

Engineer of record

Independent review engineer

Material deviation
 Maximum credible earthquake
 Observational method
 Panel
 Practicable
 Professional engineer
 Qualified engineer
 Tailings storage facility

The definition of certification will continue a debate addressed by the Affiliate Member Advisory Committee of ASDSO (i.e., the consultant world) in two white papers dated 2012 and 2013 regarding concerns about that very word in regulation and the respective legal morass it represents for engineers (ASDSO, 2013). However, the Montana statutes may have anticipated those concerns to some extent because in the definition, certification “does not constitute a warranty or guarantee...” Montana was ahead of the pack in defining the Engineer of Record (EOR); more recently, the Geoprofessional Business Association developed draft recommendations on EORs and “designers of record (DORs)” for mine tailings dams and is in the process of completing their trade publication as of the submittal date for this paper. Independent review engineers may be a regulator’s love/hate relationship; they bring tremendous value and credibility to a project, but managing the course of an independent ship presents many dilemmas for regulators, for example, confidentiality, the liability for the engineering advice, etc. A notable and poignant definition is the observational method; it is a modern, abbreviated take on the traditional definition of the geotechnical engineering masters, Terzaghi and Peck. Practicable is a good definition to have; the Montana definition includes consideration of cost, which may explain the comment above about cost versus safety. Tailings storage facility is defined appropriately comprehensive and reflects the exemptions mentioned by the concerned party above:

- (a) "Tailings storage facility" means a facility that temporarily or permanently stores tailings, including the impoundment, embankment, tailings distribution works, reclaim water works, monitoring devices, storm water diversions, and other ancillary structures.
- (b) The term does not include a facility that:
 - (i) stores 50 acre-feet or less of free water or process solution;
 - (ii) is wholly contained below surrounding grade with no man-made structures retaining tailings, water, or process solution or underground mines that use tailings as backfill; or
 - (iii) stores dry stack or filtered tailings.

Duties of the EOR are further defined in the MAC and includes a restriction on the EOR from employment with the “operator or permit applicant” which seems to deflect responsibility from the owner who has been held liable for dams since the advent of the written code, almost 4000 years ago (Hammurabi, 1760, B. C.). The EOR has a duty to report unsafe conditions and the legislature appeared to offer the EOR a parachute off the project, because if a “Dear John” letter is sent, the operator has 90 days to find another one or they must shut down the tailings deposition, i.e. the mill and probably the mine.

Other interesting aspects of SB409 include minimum factors of safety “against slope instability” and requirements for seismic evaluations for the “1-in-10,000 year event or the maximum credible earthquake, whichever is larger” (even though the definition of MCE indicates it is the “most severe that could be expected at a site.”) A “list of quantitative performance parameters” is required and includes such features as “embankment crest width, embankment slope, beach width...” which appear to reflect design criteria more than “performance parameters.” SB409 goes on to include a comprehensive list of expectations for technical evaluations and content which represents the minimum standard of care in Montana for a modern mining operation and a nation-leading example of modern mine regulation.

3 ALASKA

When your neighbor’s house is burning, you don’t ignore it; but if there is nothing you can do about it, then you do your best to ensure that the flying embers that land on your roof do not set your house on fire. Alaska shares a border with British Columbia and their fish swim together in the sea. After Quesnel Lake and the Fraser River took the load in 2014 and the news reports flowed towards the common water, the “transboundary mines” of B.C. and coastal Alaska became a great source of concern to the people who depend on the sea for the sustenance of life. Other mines and mine prospects in Alaska were also under the microscope of the “scrutineers” (Tangen, 2018) of all varieties including state and federal regulatory agencies, native villages and corporations, federal court cases, private investigations, environmental non-government organizations (NGOs) and the media. Not to mention the mining companies themselves, boring and coring away, trying to identify just how big those Motherlodes in Alaska really are, and figuring out how to get it. Similar to Montana, the Alaska Mining Association was quick to react by providing information about Alaska’s mines, and host training and educational workshops at annual and regional conferences. The Alaska Dam Safety Program in the Alaska Department of Natural Resources regulates tailings dams and reviewed the operating projects to ensure that the conditions that triggered the calamity upon our neighbors did not lurk in the foundations of the tailings dams in Alaska. The state regulations were reviewed with respect to tailings dams and compared with British Columbia. The *Guidelines for Cooperation with the Alaska Dam Safety Program* (the ADSP Guidelines) were revised to include specific discussions on tailings dams and dams at mines and the applicability of the existing statutes and regulations. These revisions were published draft in July 2017.

The ADSP Guidelines include an interactive table of contents that allows the reader to review the outline and move back and forth between the content and the table. The outline tells the story as seen here at the first level for all chapters except Chapter 15 which lists the third. The emphasis indicates sections that include significant revisions since the 2005 edition.

- 1 WELCOME TO THE ALASKA DAM SAFETY PROGRAM
- 2 BASIS FOR REGULATION OF ALASKA DAMS
- 3 CERTIFICATES OF APPROVAL
- 4 FIVE STAGES IN THE REGULATORY LIFE OF A DAM
- 6 DESIGNING A DAM IN ALASKA
- 7 CONSTRUCTING THE DAM
- 8 OPERATIONS AND MAINTENANCE PROGRAM
- 9 EMERGENCY ACTION PLANNING
- 10 INSPECTIONS
- 11 *CONDITION ASSESSMENT*
- 12 PERFORMANCE AND INCIDENT REPORTING
- 13 *RISK REDUCTION, REMEDIAL INVESTIGATIONS, AND DECISION MAKING*
- 14 CLOSURE
- 15 *DAMS AT MINES AND TAILINGS STORAGE FACILITIES*
 - 15.1 *Technical Services Team*
 - 15.1.1 *Owner’s Technical Services Team Manager*
 - 15.1.2 *Engineers of Record and Other Professionals*
 - 15.1.3 *Independent Engineering Review Board*
 - 15.2 *Quality and Change Management*
 - 15.3 *Design, Construction, Operation, and Closure*

15.3.1 Design

15.3.2 Construction

15.3.3 Operation

15.3.4 Closure

15.4 Post-Closure Financial Assurance for Permanent Mine Features

16 REFERENCES

With the bureaucratic cross-section showing the depth of interest in dams from a modern, regulatory perspective, an additional borehole is not required. Without belaboring content, three notable layers represent modern concepts related to tailings dams. The Alaska Dam Safety Program advocates for a team approach as described in Section 15.1 lead by a responsible person employed by the owner to coordinate the safe design, construction and operation of the highly technical and complex systems that are used to manage waste rock, tailings, and water. Section 15.3.4 of the ADSP Guidelines introduces a unique perspective on the closure of tailings dams in terms of potential energy, entropy and risk. The simplified concept shown here in Figure 1 illustrates how a dry closure immediately reduces the potential energy and risk at closure, with the post-closure risk dependent on the basis of the design and the maintenance requirements in closure. Only if a dam meets the “Best Approach”, could abandonment be considered. If “Poor Approach” describes the dam, mitigation is required. For the “Minimum Approach”, post-closure financial assurance is required to provide for operation, monitoring, inspection, and maintenance for an indefinite period of time. Note that a marginal design is represented by meeting the minimum standard of care. In this case, Section 15.4 describes a method of providing financial assurance based on the *Mine Reclamation Trust Fund* established by the Alaska legislature in 2004 “for the purpose of protecting the public interest in reclaiming mine sites in the state” including “maintenance of dams and other permanent features...control and treatment of acid rock drainage...protection and treatment of surface water and groundwater...[and] long term site management...” This essentially addresses the residual risk that EPA acknowledges exists at some facilities, but defers to the modern state or federal regulatory programs to mitigate.

The ADSP Guidelines are available for download at the website for the Alaska Dam Safety Program at

<http://dnr.alaska.gov/mlw/water/dams/>

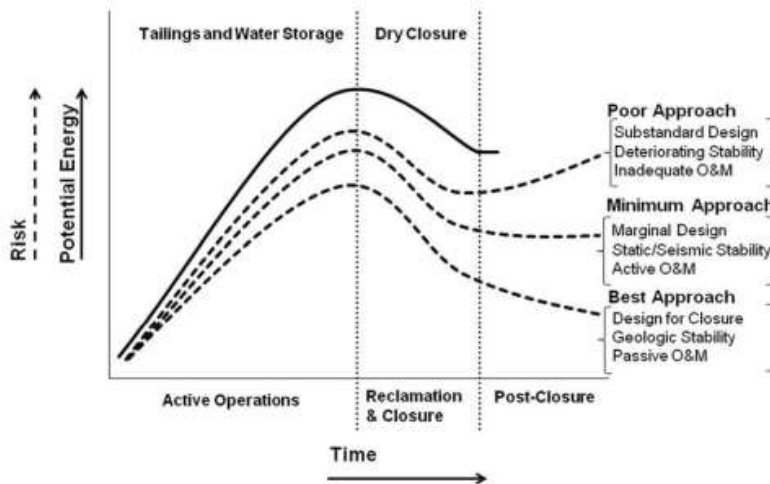


Figure 15-3. System Energy and Risk

Notes:

1. Not to scale.
2. Geologic stability implies acceptable performance under chronic and acute loadings throughout a predicted, localized, geomorphological succession.

Figure 1. Excerpt from *Guidelines for Cooperation with the Alaska Dam Safety Program* (2017)

4 ASSOCIATION OF STATE DAM SAFETY OFFICIALS

As an indirect result of the first National Dam Safety Act of 1972, state officials organized ASDSO in the early 1980s. By 1987, “State Representatives” of ASDSO and others developed and published the *Model State Dam Safety Program* (FEMA, 2007). The model program makes recommendations for statutes and regulations applicable to all types of dams and includes the generic definition which begins:

“Dam” means any artificial barrier, including appurtenant works, with the ability to impound water, wastewater, or *liquid borne materials* (emphasis added) and which [includes qualifiers]

In January 2016, the ASDSO Board of Directors authorized the formation of a Tailings Dam Working Group which developed the *Issue Brief: Tailings Dam Safety in the States* (ASDSO, 2016). This brief reviewed tailings dams and the states that include mining and regulate tailings dams. At the Dam Safety 2016 annual conference in September, State Representatives unanimously passed resolution 1-2016 signed by President Jim Pawloski of the mining state of Michigan, committing the resources of ASDSO to help support states that regulate mine tailings dams. In June 2017, the Board of Directors chartered a Tailings Dam Regulatory Committee which first met at Dam Safety 2017 in San Antonio, Texas. That inaugural meeting led to the recruitment of the current committee roster that includes members from state and federal agencies, trade associations, and engineering and environmental professionals. One of the key efforts of the committee so far was to conduct a gap analysis of the publications of the National Dam Safety Program with respect to “tailings dams, dams at mines, coal waste dams, coal combustion residue (CCR) dams, similar facilities or tailings dam closure” (ASDSO, 2018). Of the 22 publications reviewed including the website of the National Dam Safety Program, the committee found that the high level publications, such as the *Federal Guidelines for Dam Safety* first published in 1979

(FEMA, 2004) and the *Model State Dam Safety Program* are “broadly applicable to tailings dams, etc.” while only four specifically mention or address tailings dams etc. even though all but one of the other publications were considered broadly applicable (with qualifications for tailings dams) such as *Earthquake Analysis and Design of Dams* (FEMA, 2005) or *Evaluation and Monitoring for Seepage and Internal Erosion* (FEMA, 2015). The committee concludes:

The apparent gaps described herein may be due to the disproportion between the total number of dams in the nation compared to tailings dams etc. causing the relative popularity of water dams to appear to skew the emphasis.

The Chairman presented the findings of the gap analysis to the National Dam Safety Review Board in July 2018.

5 CONCLUSIONS

The EPA clearly placed the burden of risk reduction on the state and federal agencies that regulate mining in its final action on the proposed rules for CERCLA 108(b). The EPA discussed the advent of “modern mining and modern regulation” with respect to air and water quality, reclamation, and existing state and federal financial assurance requirements, which can be described as born in the 1980s and raised in the 90s. A gap analysis of the FR shows dam safety barely getting noticed for providing “further safeguards.” The mining and financial industries learned the hard way the value of the tailings dam.

If the souls from West Virginia are remembered, the birth of modern dam safety was closer to 1972 and the modern dam safety regulation teenager came of age in 1987 with the publication of the *Model State Dam Safety Program*. These years track closely with the advent of the modern design and regulation of solid and hazardous waste. But the solid and hazardous waste industries set the standard of care in the design, construction, and monitoring of containment facilities, while the 80,000 water dams in the country caused the standard of care for dams to be more focused on water and hydroelectric dams, as represented by the publications of the National Dam Safety Program and numerous other state and federal regulations. Tailings storage facilities and dams represent the most diverse fusion of water and solid waste containment, with the potential for water treatment challenges thrown in for good measure, and always water management challenges, especially during operations.

While Congress clearly intended for dam safety concepts to apply to the mining industry, the Bevill Amendment in the Solid Waste Amendment Act of 1980 demonstrated Congress’s recognition of the limited and regional diversity of mining and mine waste disposal when it exempted mine waste from the provisions of RCRA (EPA, 2003). This exemption left mine waste management technology in a regulatory backwater that was drafting in the wake of the other industries as the real value of exceeding the minimum standard of care in waste management was recognized by mine operators, and the competitors raised the bar on themselves. Nevertheless, the body of work of the National Dam Safety Program and the regulatory programs over solid and hazardous waste management represents the growth of the “modern” standard of care where the regulation of tailings dams and mine waste management needs to be at the state level, with the gaps filled in. Until this occurs, tailings dam safety represents a risk profile generally overlooked by the parental National Dam Safety Program and EPA, but acutely apparent to the federal and state dam safety programs and hardrock mining bureaus that are on their own apart from the support of cooperative mining companies and volunteer organizations, if tailings dams are even regulated.

The modern regulatory approach of Montana was to incorporate dam safety concepts into the mine reclamation law. The modern regulatory approach of Alaska was to discuss the nuances of tailings dams and dams at mines in the context of the existing dam safety regulations in draft guidelines, while the industry resolves complex technical issues of interest to regulators, such as tailings dams in closure. Volunteers in the USSD, ASDSO, Tailings & Mine Waste and many other organizations continue to collaborate on modern engineering and modern regulation and bring together state and federal regulatory agencies, mining companies, engineers and environmental professionals to advance the conversation on safe tailings dams in the nation and promote uniform guidelines. In fact, these are the very professionals who raised the standard of

care and reduced the risks associated with tailings dams and hardrock mines over the course of time that the EPA was talking about in its final decision.

Regulators struggle with the pace of the advancements to find the appropriate level of regulatory “scrutiny” to help mitigate the risks that threaten public safety and the environment. Mine operators struggle with a regulatory “regime” that is a patchwork quilt of obligations. Everyone struggles with rapidly changing technology, inadequate staffing and budget battles. Consistency is an ambition. EPA’s consideration of modern mining and regulation to be “current applicable regulatory schemes as ‘current’ operations” was wise in contrast to the way things used to be done, even in the 90s. The pace of technology, the demand for continuous improvement and the risk that hides between the borings and in the stretches of time requires an eternal vigilance to the same degree that men have been driven to mine for iron and gold since days long forgot. Only then will the risk be mitigated to the extent necessary for a social license to mine to be renewed.

6 REFERENCES

- ADNR 2017. *Guidelines for Cooperation with the Alaska Dam Safety Program* (draft revision), Alaska Department of Natural Resources, July 2017
- ASDSO 2013. *White Paper on Engineering Certification*, ASDSO Affiliate Member Advisory Committee, Association of State Dam Safety Officials dated 2012 and 2013
- ASDSO 2016. *Issue Brief on Tailings Dam Safety in the States*, Association of State Dam Safety Officials, 2016
- ASDSO 2018. *Gap analysis of the National Dam Safety Program with respect to tailings dams, etc.*, Report to Board of Directors, Tailings Dam Regulatory Committee, Association of State Dam Safety Officials, May 14, 2018 (unpublished)
- DEL 2016. *Progressive legislation ushers in new era of mining*, Montana Mining 2015-2016, DEL Communications Inc., 2016
- EPA 2003. *EPA and Hardrock Mining: A Source Book for Industry in the Northwest and Alaska*, U.S. Environmental Protection Agency, January 2003
- EPA 2018. *Federal Register*, Volume 83 Number 35, U.S. Environmental Protection Agency, February 21, 2018
- FEMA 2005. *Earthquake Analysis and Design of Dams*, FEMA 65, Federal Emergency Management Agency, 2005
- FEMA 2007. *National Dam Safety Program Model State Dam Safety Program*, Federal Emergency Management Agency, July 2007
- FEMA 2015. *Evaluation and Monitoring for Seepage and Internal Erosion*, FEMA P-1032, Federal Emergency Management Agency, 2015
- FEMA 2004. *Federal Guidelines for Dam Safety*, FEMA 93, Interagency Committee on Dam Safety, Federal Emergency Management Agency, 1979, reprinted April 2004
- Montana 2015. *Montana Annotated Code*, Title 82, Chapter 4, 2015
- Hammurabi 1760 BC. Section 53, Code of Hammurabi, 1760 BC
- Tangen, J. P. 2018. *Cheechakos keep coming into the country*, North of 60 Mining News, May 24, 2018

Assessment of Design and Operating Practices on the Risks Associated with Waste Rock Stockpiles

L. Piciacchia, B. Lavoie, J. Mosquera, and Z. Bouazza

BBA Inc., Mine Waste Management and Environment, Montréal, Québec, Canada

ABSTRACT: The risks associated with the construction, operation and closure of a Waste Rock Facility (WRF) can be significant. This paper demonstrates the impacts that design, construction and operation can have on the overall risk associated with such facilities. This paper first looks at a facility and its current ongoing operation. This is followed by an evaluation of risk for the proposed LOM configuration, with and without mitigating measures with respect to design, construction and operation. The risks associated with current operations as well as the configuration at closure carried with it a level of risk which the operator found inappropriate. Design, construction and operating recommendations were which reduced risks to acceptable levels. This paper relates the findings of this case study.

1 INTRODUCTION

The construction of waste rock facilities (WRF) is a requirement for most mines and they should provide adequate capacity for the waste rock storage over the life of the mine (LOM). As such, WRFs can be classified as high risk due to deficient design criteria, uncontrolled construction and operating techniques. In order for WRFs to be safely managed both during operations and at closure, risk-based design, carefully planned construction and operating practices are necessary. Risk-based design and assessment are also fundamental managing tools for mine operators used to estimate the likelihood of slope instability in waste rock piles and to account for the multiple variables associated with large mining operations. This paper presents the risk assessment and classification of ten (10) waste rock piles of a large WRF using the Commonwealth Scientific and Industrial Research Organization-CSIRO (Hawley et al., 2017).

In the CISRO method, a series of multi-factor matrices and ratings are applied to the regional parameters, the state of the foundations, the quality of the deposited materials, the mass and the geometry, the analysis of stability, the construction and the performance of each waste rock pile. The evaluations of these factors yield two indices: the Engineering Geology Index (EGI) and the Design and Performance Index (DPI). The combination of these two indices leads to different risk levels that range from very low to very high.

The CISRO method was applied to current and at closure configurations of waste rock piles as they were proposed by the mine operators. Then, a second risk classification of the waste rock piles was conducted assuming the implementation of the design, construction and operational recommendations provided by the authors. The results of the comparative classification and the recommendations for the proposed configuration are presented in this paper.

2 METHODOLOGY

2.1 CSIRO Mine Waste Rock Classification Method

The risk assessment and classification of a WRF was conducted following the CSIRO Mine Waste Rock Classification Method (Hawley et al, 2017). This classification is based on the assessment and scoring of twenty two (22) factors such as seismicity, chemical stability of the waste rock and the height of the dumps. The factors are divided into seven (7) groupings, namely the regional parameters, the state of the foundations, the quality of the deposited materials, the mass and the geometry, stability analysis, construction method and the waste stockpile performance. Each factor is assigned a rating (numerical value) and each rating has qualitative and quantitative ranges pertaining specific constituents and analyses of the waste rock pile. The weight allocated for the ratings of each factor yields two indices: the Engineering Geology Index (EGI) and the Design Performance Index (DPI).

The EGI is the sum of the scores of factors of three groups: regional setting, foundation conditions, and material quality. The DPI is the sum of the factors of four groups: geometry and mass, stability analysis, construction and performance. The sum of the numerical values of EGI DPI results in the Waste and Stockpile Stability Rating (WSR). The WSR is a value ranging between 0 and 100. A pile with a rating WRS of 100 will be considered very low risk while a WRS of less than 20 is associated with a very high risk. The WSR score is then assigned a Waste Hazard Class (WHC). The WHC range from class I to class V. For example, Class I represents a waste rock pile with very low hazard, class III represents a moderate hazard and class V is a waste rock pile with very high hazard. The risk level can also be represented graphically in the form of a matrix whose input parameters are the EGI and DPI indexes as shown in table 1.

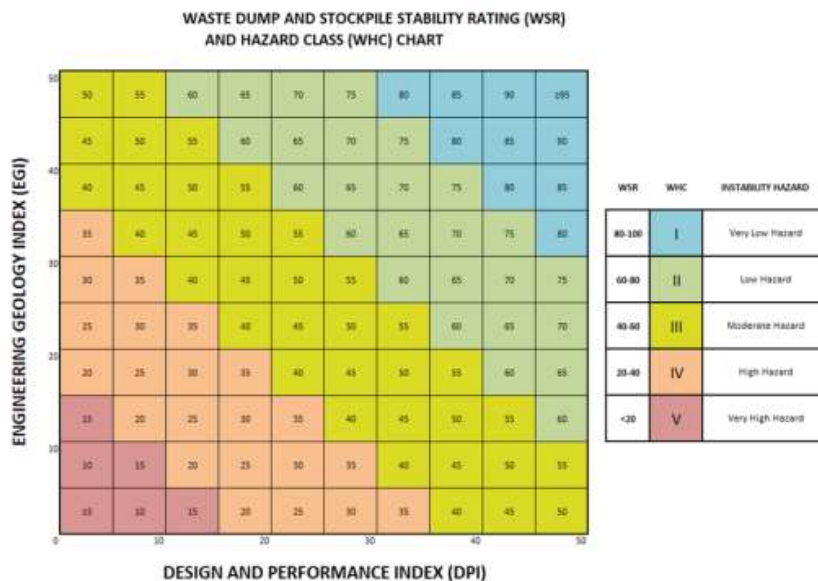


Figure 1. Classification Matrix and Rating System CSIRO method Hawley et al., (2017)

2.2 Risk classification method for current and LOM configurations

The CSIRO waste rock pile risk classification method was applied to 10 waste rock piles of a large WRF. The ratings of all factors were based on detailed analysis of existing data for each

waste rock pile. The data analyzed included site topography and regional setting assessment, the waste rock piles volume according to mine plan, the gradation and material quality (coarse, fine, mixed), the waste rock piles geometry (overall and benches slopes and heights), geotechnical reports, and field observations. The method of construction, operation and management practices of the WRF were also analyzed. The rating classification also took into consideration the results of 2D and 3D static and pseudo static slope stability analyses of current and LOM configurations of the WRF assuming that the volumes, geometries and the operation and construction practices of the waste rock piles remained unchanged throughout the LOM and followed the mine plan (Piciacchia et al., 2018)

The results of the EGI and the DPI for current and LOM of each waste rock pile for the current and LOM configurations are presented in table 1. The results of WSR and WHC of each waste rock pile are presented in table 2.

Table 1. EGI and the DPI of current and LOM configurations of proposed by the mine operators

Waste rock pile ID	EGI		DPI	
	Current Configuration	LOM Configuration	Current Configuration	LOM Configuration
WRP6	31	31	-0.5	-1
WRP13	31	31	3.5	2.5
WRP15	31	31	18.5	19
WRP18	31	31	19.5	20.5
WRP19	32.5	32.5	26	25
WRP24	32.5	32.5	25	25
WRP42	31	31	21.5	20.5
WRP53	31	31	2.5	3
WRP54	31	31	25	24
WRP60	31	31	22.5	21.5

Table 2. Waste rock pile stability rating (WSR) and waste rock hazard class

Waste rock pile ID	WSR		WHC		Risk Level	
	Current Configuration	LOM Configuration	Current Configuration	LOM Configuration	Current Configuration	LOM Configuration
WRP6	30.5	30	IV	IV	High	High
WRP13	34.5	33.5	IV	IV	High	High
WRP15	49.5	50	III	III	Moderate	Moderate
WRP18	50.5	51.5	III	III	Moderate	Moderate
WRP19	58.5	57.5	III	III	Moderate	Moderate
WRP24	57.5	57.5	III	III	Moderate	Moderate
WRP42	52.5	51.5	III	III	Moderate	Moderate
WRP53	33.5	34	IV	IV	High	High
WRP54	56	55	III	III	Moderate	Moderate
WRP60	53.5	52.5	III	III	Moderate	Moderate

As shown in table 1, the minimum and maximum EGI are respectively 31 and 32.5 on a maximum possible 50 points. The EGI is primarily influenced by factors that are common to the entire site such as precipitation, groundwater level, and chemical stability of the materials. The difference between the EGI is therefore mainly due to the slope and the shape of the foundation, which explains the small variation between the EGI of the piles studied.

The design performance index (DPI) varied significantly between waste rock piles. The DPI ranges between -0.5 and 26 for the current configuration and between -1 and 24 for the LOM configuration. The variations are largely attributable to the Stability Performance factor, the bench heights and overall slope associated with each waste rock pile. Overall, risk can be mitigated by focusing on DPI more so than EGI where little design or operation control is possible. Good operating practices and approaches as proposed by Vides et al., (2018), can be used to positively affect DPI and therefore reduce risk.

As shown in table 2, seven (7) waste rock piles obtained a moderate risk level classification for current conditions and at closure. A moderate risk classification generally indicates that one or more variables could cause failure if not carefully controlled. A high risk level classification was obtained for three (3) rock piles, namely, WRP6, WRP13 and WRP53 for current conditions and at closure. The waste rock piles with high risk level also represent piles that had experienced failures in the past or that have geometry concerns such as steep overall slopes and poor drainage behavior due to the type of waste rock with which they were constructed. In general, waste rock piles that experience failures, obtain low rating in the Stability Performance factor (ranges from -15 to 15 or very poor to very good, respectively). The Stability Performance factor has a very important relative weight in the overall classification, and waste rock piles with a history of failures are strongly penalized.

2.3 Risk classification method for the proposed configuration

In order to assess the impact of implementing design, construction and operational modifications on the risk classification of the to the current and LOM configurations, a third classification procedure was conducted on idealized waste rock piles that were assumed to follow specific design, construction and operational criteria and recommendations.

2.3.1 Design criteria for the proposed configuration

The main design criteria for the proposed configuration were the (local-individual benches) and at closure (global) factors of safety (FS) required by the regulation. According to common regulations, the factor of safety for individual benches should equal to or greater than 1.2. The FS for the closure configuration should be equal to or greater than 1.5.

The factor of safety of a waste rock pile depends on the material of construction (coarse vs. fine waste rock piles), the geometry of the pile and the angle of repose of the material that makes up the pile. According to Piciacchia et al. (2018), the overall angle of deposition (β) of a waste rock pile (constructed in descending fashion) is equal to the angle of internal friction (ϕ) of the material. As such, the factor of safety (FS) of waste rock piles is in equilibrium (FS=1). The current and LOM configurations of the case study showed overall angles β of 35 to 37 degrees for coarse grain waste rock piles and 30-32 degrees for fine grain waste rock.

In order to increase the minimum local and at closure factors of safety, it became necessary to design the waste rock pile with a flatter overall slopes. In the case of coarse waste rock piles, the final overall slope was determined to be 26 degrees, Piciacchia et al., (2018). In the case of fine waste rock piles, the overall slope angle was set to 22 degrees rather than 30-32 degrees for the current configuration.

Another design recommendation was the construction of a stabilization buttress at the foot of the existing waste rock piles. The stabilization buttress was designed to have one to three benches, depending on topography and waste rock pile height. The stabilization buttress was designed to have bench widths of 35m and the heights of 50m. The internal slopes of the buttress were similar to those observed in existing waste rock piles 1.3H: 1V. Its construction was recommended to be carried in a combination of ascending and free dumping construction techniques. Static and pseudo-static slope stability analyses (3D and 2D) were conducted on the proposed configuration and compliance of the regulations for operational and long term factors of safety was achieved.

2.4 Construction and operational recommendations for the proposed configuration

The main construction and operational recommendations made for the proposed configuration were: material segregation during operation, assessment of the advancement rate, preparation of deposition plans, and elaboration of an operation, maintenance and safety manual, Vides et al, (2018), Piciacchia et al., (2018).

2.4.1.1 *Material segregation during operation*

Material types entering the WRF can vary over time. Given the marked difference between the angle of internal friction of fine and coarse waste rock, it was recommended to deposit these materials in separate stockpiles. Experience has shown that at times (i.e. during a push-back on a pit wall) larger quantities of fine grained waste will likely be generated. If these materials are placed over the face of a coarse grained waste, which are also free draining, water levels within the stockpile will rise. The rising water levels can initiate a failure, particularly in the finer material. From a design point of view designing a facility with an angle of internal friction of 38 degrees is far different than with one at 30 degrees. In order to properly design a WRF and ensure reliability of such a design it is far better to reduce material property variability, which would be accomplished by separating the coarse and fine fractions.

2.4.1.2 *Rate of advancement*

The stability of a waste rock pile is influenced by several parameters such as the geometry of the pile, the quality of the materials, the climatic conditions and the materials of the foundations. However, several cases of historical failures show that they are closely related to the height and rate of advance of the pile. During deposition of waste rock, it is important to evenly distribute the materials on the ridge, which allows to reduce the pressure on the materials constituting the heap already in place and to reduce the risks of instabilities. Controlling this parameter reduces short term or operational risk of instability. In general, rates of advancement 1 and 3m per meter of crest per day were recommended based on the height of each waste rock pile at the time of the deposition and on the geotechnical properties of the foundation and the size distribution of the waste rock, Vides et al. (2018).

2.4.1.3 *Deposition plans*

WRF are complex structures whose operating criteria change over time, including the quantity and quality of materials to be managed at a specific time. In addition, the construction of these complex structures must be harmonized with all other mining and engineering activities. As such, waste rock deposition plans are essential management tools that help mining operators evaluate and prioritize, in a predetermined frequency, the construction needs according to the waste rock piles exploitation rates and the mine plan. It was recommended to the mine operators to prepare three series waste rock deposition plans for the short (year 1 and 2), medium (year 5), long term (year 10, and mine life) planning of the WRF. The deposition plans must respect the wastewater management plan and be adjusted according to changes and operational requirements.

2.4.1.4 *Operation and Management and Safety Manual*

The Operation and Management and Safety (OMS) manual allows for the clarification of individual responsibilities, decision-making processes, guidelines for design and possible modifications, instrumentation, monitoring and the development of environmental protection measures and emergency plans for the WRF. Operational guidelines must take into account both long-term and short-term operational needs. The operating manual is a master document that standardizes the operating procedures at the mine and should be updated to include any changes in the operation. Although the OMS manual does not have an impact on the IDP rating by itself, it is the good practices documented in it that will have a direct impact in the overall performance of the WRF overtime.

3 RESULTS AND DISCUSSION

The results of the risk classification for the proposed configuration are presented in tables 3 to 5

Table 3. Comparison of EGI and DPI for all configurations

Waste rock Pile ID	EGI			DPI		
	Current Configuration	LOM Configuration	Proposed Configuration	Current Configuration	LOM Configuration	Proposed Configuration
WRP6	31	31	32.5	-0.5	-1	25
WRP13	31	31	32.5	3.5	2.5	24
WRP15	31	31	34	18.5	19	26
WRP18	31	31	32.5	19.5	20.5	28.5
WRP19	32.5	32.5	34	26	25	26.5
WRP24	32.5	32.5	34	25	25	30
WRP42	31	31	32.5	21.5	20.5	25
WRP53	31	31	32.5	2.5	3	25
WRP54	31	31	32.5	25	24	30
WRP60	31	31	34	22.5	21.5	24.5

Table 4. Comparison of WSR and waste rock hazard class for all configurations

Waste rock Pile ID	WSR			WHC		
	Current Configuration	LOM Configuration	Proposed Configuration	Current Configuration	LOM Configuration	Proposed Configuration
WRP6	30.5	30	57.5	IV	IV	III
WR13	34.5	33.5	56.5	IV	IV	III
WRP15	49.5	50	60	III	III	II
WRP18	50.5	51.5	61	III	III	II
WRP19	58.5	57.5	60.5	III	III	II
WRP24	57.5	57.5	64	III	III	II
WRP42	52.5	51.5	57.5	III	III	III
WRP53	33.5	34	57.5	IV	IV	III
WRP54	56	55	62.5	III	III	II
WRP60	53.5	52.5	58.5	III	III	III

Table 5. Comparison of Risk Level Classification for all configurations

Waste rock Pile ID	DPI		Risk Level	
	LOM Configuration	Proposed Configuration	LOM Configuration	Proposed Configuration
WRP6	-1	25	High	Moderate
WR13	2.5	24	High	Moderate
WRP15	19	26	Moderate	Low
WRP18	20.5	28.5	Moderate	Low
WRP19	25	26.5	Moderate	Low
WRP24	25	30	Moderate	Low
WRP42	20.5	25	Moderate	Moderate
WRP53	3	25	High	Moderate
WRP54	24	30	Moderate	Low
WRP60	21.5	24.5	Moderate	Moderate

As shown in table 3, the EGI is slightly modified with values varying between 32.5 and 34. The improvement in EGI is attributed to an increase in the rating of material quality, associated to the recommendation of segregation of materials.

The DPI is the index with the greatest variation from current and LOM configuration. As shown in tables 4 and 5, the geometry modifications, the flattening of the waste rock pile overall slope and the increase in local and global factors of safety from 1 to 1.2 and 1.5, as well as the operating and construction recommendations are attributed to the increase in the DPI which varies between 24 and 30, and represents an average increase of 8 points compared to current operations. Three factors directly impacting DPI rating were analyzed for the waste rock piles

for the LOM and Proposed configurations; the results of the comparison are presented in figures 2 and 3.

Figure 2. Rating of Design Performance Index Factors - Life of Mine Configuration

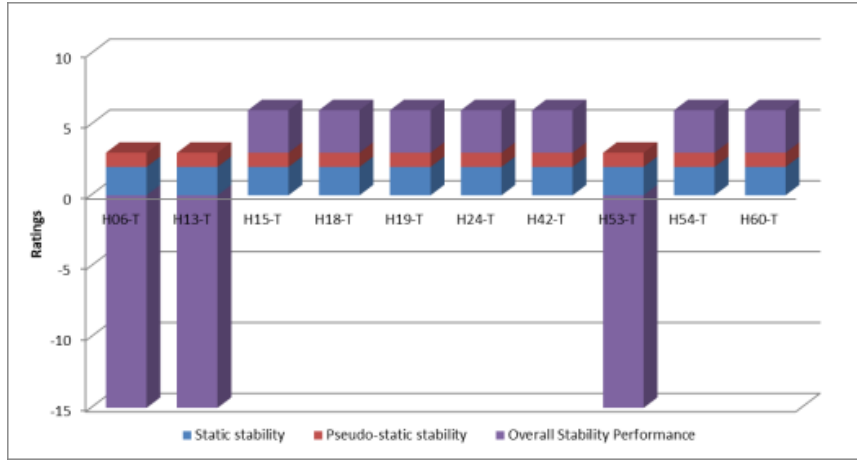
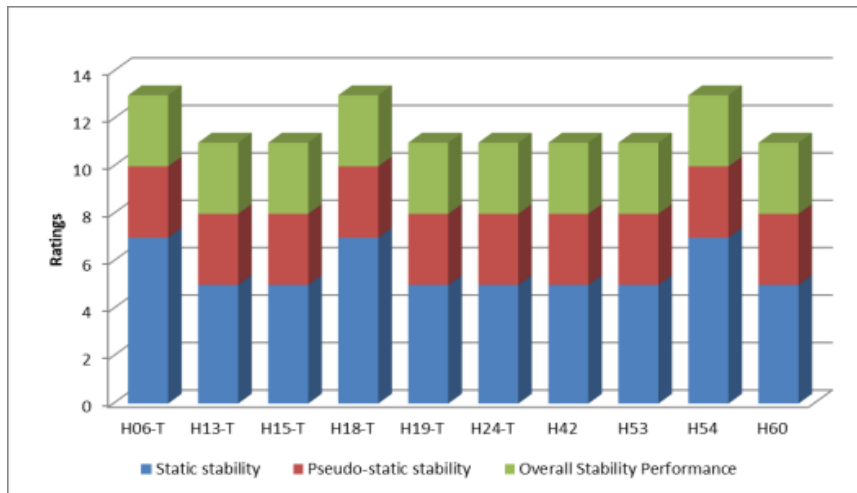


Figure 3. Rating of Design Performance Index Factors – Proposed Configuration



As shown in the two figures, three waste rock piles, namely, WRP6, WRP13 and WRP53 went from High risk to Moderate risk which is a significant gain. Waste rock piles WRP42 and WRP60 remained in the moderate risk category which is explained by the fact that the stability rating of current and LOM configurations is on average 51 and therefore would require an average increase of 9 points in order to access the category at low risk (60 to 80 points). This is an increase that is too large to be fully met by improvements in geometric factors, stability analysis and construction.

4 CONCLUSIONS

The CSIRO Mine Waste Rock Classification Methodology was selected and adapted for application to 10 waste rock piles of a large WRF. While the initial configuration proposed by the

mine operators would contain more than 30% of the waste rock piles in high risk category, the proposed configuration would ensure that none of the piles would be classified as such. In addition, if the recommendations are followed, 50% of stockpiles would be classified as low risk. It has been demonstrated that the implementation of the design, construction and operation recommendations in the current and LOM configurations of the WRF would result in reduced risk in 80% of waste rock piles and compliance with the regulations.

REFERENCES

- Hawley, M. Cunning, J. 2017. Guidelines for Mine Waste Dump and Stockpile Design, Piciacchia, L., Marefat, V., and Mosquera, J., 2018. The use of 3D models and analysis in support of waste stockpile design and operations. BBA Inc., Montreal, Quebec, Canada.
- Piciacchia, L., Marefat, V., and Vides J.A. 2018. Practical Nomograms for Waste Rock Piles Design on Competent Foundations. BBA Inc., Montreal, Quebec, Canada.
- Piciacchia, L., Vides, J.A., and Mosquera, J., 2018. Mine Waste rock design, construction, and operation as engineered structures.
- Vides, J.A, Piciacchia, L., and Marefat, V. 2018. Guidance for the safe and optimized operation of waste rock facilities. BBA Inc., Montreal, Quebec, Canada

Risk Informed Design of a Large Scale, Lined Tailings Storage Facility

L.I. Boshoff and R.W. McNeill

SRK Consulting, Pietermaritzburg, KwaZulu Natal, South Africa

M. Boroko

Anglo American Platinum, Mototolo JV Concentrator, Lydenburg, Mpumalanga, South Africa

ABSTRACT: Changing legislation, ongoing changes in general mining practices and availability of suitable sites amidst the renewed international interest in static liquefaction risks of tailings is augmenting the traditional views of what risk informed tailings design and management for the future holds. The Maresburg TSF in South Africa, is a good example of a new tailings facility designed within this changing paradigm. Unique challenges were imposed on the original conceptual design, following changes in legislation within the South African mining context. Updates to the traditionally acceptable risk management strategies were also required, following risk trends in tailings and further highlighted and confirmed by the major tailings dam failures that occurred at Mt Polley (British Columbia) and Samarco (Brazil). This paper provides insight into how financial, environmental, technical and site specific risks were managed as part of the design and construction process to ensure a fit for purpose, risk informed design and execution phase could be realized.

1 INTRODUCTION

1.1 The risks and cost of Tailings management

Tailings - the part of the mining business, as it stands today, we all love to hate and some of us, hate to love. It is one of the end products of mining nobody really wants and this unfortunate trend is gaining more and more momentum as time goes by. Why? Well, some of the greatest risks we face in this industry can be associated with tailings and waste facilities. Risk to human life and the environment has always been associated with different perceptions of how serious the risk is or how critical a consequence of it occurring would be. However, regular Joe, and even not so regular Joe, is becoming increasingly intolerant of these risks. Risk is something one can become complacent of, especially when no failure events occur over a long period of time or if past failures had consequences deemed insignificant. We assess, avoid or mitigate risk as far as possible, but who, how and when do we decide that “we have done enough”? To what degree do we tempt fate?

The last two larger failures experienced at Mt Polley in British Columbia, and Samarco in Brazil have renewed or fueled current perceptions of the high risk of tailings facilities to human life and the environment, and quite rightly – rattled the cage. These recent events initiated a lot of work in the review and update to management, design and operating standards of tailings facilities since they occurred and this is still ongoing.

However, recognized experts in the field, such as Dr Andrew Robertson (Principal of Robertson GeoConsultants Inc. and co-founder of SRK Consulting) regularly speaks and spoke about the current risk trend associated with tailings, even prior to the recent failure events so fresh in our minds. His research and predictions speak about data trending of the past and the fact that every 30 years the risk associated with tailings can be said to increase by at least 20 fold (Robertson,

2011). Why? It is because we are milling finer, we are increasing throughput rates and volume and therefore increasing the volume of tailings that needs a temporary or permanent home. This results in tailings structures that are required to ever increase in area and height, and in this instance – bigger is not necessarily better. We need to bring balance to the force, Dr Robertson notes several ways-either to do so:

- Assessing and avoiding risk where possible, or
- implementing new innovations and better technologies,
- ensuring better investigation and characterization and analyses,
- better and more robust design,
- increased vigilance in construction, operation and monitoring,
- rapid response to unexpected behaviour,
- seamless and effective emergency preparedness and response plans,
- check, check and checking again.

All of the above sound great, logical, but they come at a cost. Avoiding risk altogether usually has the highest cost and most operations try to find a happy medium between avoidance and management of the risks. However, the fact remains that statistics do not lie and we need to take note and change the way we perceive and manage the real increasing risks in tailings and become more pro-active. Fortunately, the point and perception of “we have now done enough”, is shifting. The tide is turning and many in industry are acknowledging the benefit and necessity of respecting the statistics. There is wider recognition of the importance of continued and more in-depth search for the gaps in the current status quo of our knowledge, risk avoidance measures and strategies when designing tailings facilities, monitoring and management systems. The secret, however, remains to get the balance right, and this may remain an issue of perception and often result in moral dilemmas.

1.2 Maresburg TSF

The Maresburg TSF site is located approximately 23 kilometres (km) south of the town of Steelport, in the Limpopo Province, South Africa, and approximately 3 km due east of the existing operational Helena TSF and the operational Mototolo JV concentrator plant as shown in Figure 1.



Figure 1. Helena TSF and Maresburg TSF site location and main features.

The current Helena TSF servicing the Mototolo JV operation is expected to reach its maximum allowable storage capacity, in June 2019. However, the maximum allowable design annual rate

of rise (6.0 metres per annum) was predicted to be prior to this date, which would necessitate a decrease in deposition rates. The new replacement TSF – Mareesburg – therefore needed to be developed and commissioned timeously to service the Mototolo JV operation and prevent production throughput cuts.

The Mareesburg site features a range of very deeply eroded drainage channels draining from the high ground in the east towards the more gently sloping areas in the west. The western boundary of the site is constrained by the presence of the Mareesburg stream and property boundaries to the north and south with very steep terrain in the east. The site is underlain by relatively shallow bedrock in the east with variable thickness of transported fine colluvium soils in the west and talus materials overlying residual material towards the west high ground. The majority of the site is strewn with cobbles and boulders originating from the steep talus slopes in the east.

The Mareesburg TSF was designed as a hillside development with an 8 metre high starter dam wall located along the low lying western portion of the site. Deposition is planned to occur in an easterly direction (upslope) and systematically build height using upstream hydro-cyclone deposition methods. To enable full utilization of the approved 118 Ha footprint the TSF will ultimately grow to 115 m in height and is planned to provide capacity for disposal of 97.6 million tonnes of platinum tailings.

1.3 The South African context

Along with global trends, a recent shift in the South African legislation (in 2015, shortly before the feasibility design of the Mareesburg TSF commenced) had changed the landscape of mine waste and tailings management for the South African mining industry. The current legislation necessitates the majority of new mine tailings facilities to include some form of geomembrane basal liner. This is contrary to historic requirements, which were based on site specific environmental risk considerations and fit for purpose design to prevent pollution of water resources.

Although geomembrane lined waste facilities are not “new”, the application of such technologies in the mining context does impose many technical challenges to the design, development and operation of large scale tailings facilities. With increasing scale, the risk of the facility increases and the introduction of a liner complicates matters even further. Add onto this the real concerns around static liquefaction and the stability of specifically upstream raised structures, difficult site conditions and you have a significant design challenge.

Historically the “go to” most cost effective design to opt for on most occasions was the upstream TSF concept. This design concept always worked well given the South African sunny climate, ample wide open spaces and typical gold and platinum tailings characteristics. Upstream developments are known to be more risky to implement than the downstream or centerline construction approach. Based on the trends, it was therefore known that this design option would increasingly come under scrutiny and become more difficult to design and operate safely. Suitable sites are also become harder to secure. The increased risk profile of these facilities requires the application of new and innovative solutions to improve robustness of the design and operational management of these type of facilities.

A further concern at the time of designing the Mareesburg TSF, was the uncertainty surrounding how the new legislation would be interpreted and implemented by the local regulatory authorities and how this could impact on how “innovative” one could be.

2 NAVIGATING A RISKY LANDSCAPE

The Mareesburg TSF was one of the first under a new South African legislative framework. The feasibility design was completed in 2016, in the aftermath of the Mt Polley and Samarco disasters. Everyone was concerned, all involved wanted to do the right thing and essentially implement what Dr Robertson was talking about. The team was invested in coming up with and delivering a cost effective yet risk informed design solution – a difficult balance to strike. The necessary structures were put in place from both the client side and the design team side to make sure the correct support and scrutiny was provided to help ensure these objectives were realized.

At the time of compiling this paper, commissioning was looming and only time would tell if the efforts had paid off. The section aims to highlight some of the main areas of risk and design challenges related thereto.

2.1 *Environmental and Social risks – the biggest bone of contention*

By far the most vulnerable to the consequences of something going drastically wrong (or even a little wrong) on a tailings facility, is the downstream community and the environment.

The Mareesburg TSF site is located in a beautiful, appealing landscape where Giraffe and Eland antelope and the odd head of cattle, and surely leopard, roam at will (Fig. 2 refers). The nearby Mareesburg Stream flows immediately to the west of the tailing site and would be impacted by potential groundwater pollution plumes emanating from the TSF should no controls be put in place or prove ineffective.



Figure 2. Mareesburg TSF site – Environmental considerations.

Although there are limited local communities residing immediately downstream of the Mareesburg TSF, the wider valley is populated with Chrome and Platinum mining operations and essential infrastructure. Heritage impact assessments identified several historic grave sites on and around the site. Ironically, on this occasion, those that had already come to pass from this world, proved to become of the highest social risks to the project. The sensitivity of the matter required lengthy processes to resolve next of kin compensation and to obtain exhumation approval and grave relocation arrangements. This eventually necessitated design changes at the last hour to temporarily accommodate social concerns and avoid impacting on these sites for as long as possible until all issues could be resolved.

2.2 *Inherent risk considerations*

Inherent risks, common to all tailings projects, only differing in scale and complexity depending on the nature of the development and the nature of the site, are worth a mention. Inherent risks can be introduced by nature (i.e. existing site conditions, geometry and general setting), the scale and complexity of systems and interdependencies as well as risks introduced with time over the planned life of the facility. The key inherent risks that specifically influenced the Mareesburg TSF design are as follows:

- Challenging ground conditions where the existing soils and landforms increased the complexity of design and construction, specifically when assuming basin preparations for the placement of a lining would be required.
- Site morphology that complicated the management of risks associated with site surface water run-off control during potential extreme rainfall events.
- Seismic risks that always requires evaluation.
- The scale of the new Mareesburg TSF introduced inherent risk in terms of stability and scale of potential environmental impacts (e.g. 115 m high facility, compared to the 65 m high Helena TSF).

- Further risk was introduced to the design concept in that it would be interdependent on co-disposal with the Helena TSF during the first few years to ensure the rate of rise of the facility remained at an acceptable level. Alternatively, a much larger starter dam wall would be required to manage rates of rise on the Mareesburg site, potentially limiting feasibility of the design.
- If the full approved height and footprint area is maximized, the period over which the facility is planned to be in service is more than 40 years. With time, risk can change and evolve. Changes in tailings material properties, operational practices or changes in processing needs can lead to a progressive digression from the original design intent. This should be anticipated and planned for in the present to ensure any risks introduced with time are recognized and managed adequately by future generations.

2.3 Regulatory induced technical and financial risk

Under the new legislative framework within South Africa, mine waste is now considered as a “general waste” that needs to be treated in line with the prescribed norms and standards of the “Waste Act”. The Mototolo JV concentrator tailings classifies as Type 3 waste and by regulation requires that the TSF be lined to ensure minimum barrier permeability characterization in compliance to a prescribed Class ‘C’ barrier system. Any alternative configuration proposed would have to be proven as equivalent or superior to the minimum requirements. Figure 4 provides the minimum required configuration for a Class C barrier for a typical Type 3 waste application. In terms of the Mareesburg site had several implications, some technical and some financial. Financial risks included:

- As no suitable clay materials were available on site (Fig. 3) – importing of suitable materials would require an additional ZAR212.4 million.
- Inclusion of an under-liner herringbone sub-surface drainage layer to protect the composite liner would have increased the capital costs by ZAR26.9 million.
- Inclusion of an above-liner finger drainage system - considering the footprint area in question would result in an additional cost of approximately ZAR52.1 million.
- The inclusion of the geomembrane liner on the TSF footprint would require an additional ZAR102.4 million.

If only considering the impact of these requirements on the cost to the project, the new regulations caused the estimated cost of the facility to increase between two or three fold from the original pre-feasibility study phase estimated costs. This threatened the viability of the entire operation if alternative, more cost effective design solutions for the replacement TSF could not be tabled and accepted by the authorities. The inability to obtain approval of the design would also jeopardize the approval of the water use license for all future operations within this area.

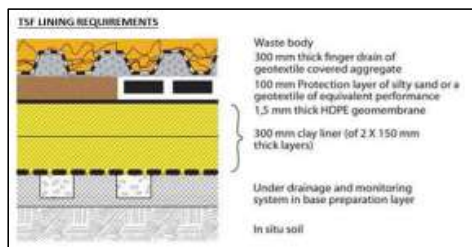


Figure 3. Minimum requirement of a Class C barrier system applicable to typical mine tailings.

As with any mining project, the environment may be negatively impacted but the project will also impact positively on the livelihood of many local communities. Should the project feasibility be threatened by high costs, the potential positive impact on the community is also nullified.

Technical implications introduced by these regulations were:

- Interface friction angles between the geotextiles and HDPE geomembranes, clays and or GCL interfaces are generally lower than that of the tailings materials. The introduction of these interfaces within the base of the facility was not ideal, given site geometry, and introduces additional stability concerns that would need to be designed out.

- The introduction of a barrier system would increase the complexity of the design, construction and operation of the design significantly – increasing inherent risks as noted in Section 2.2 above.
- The reliance on effective drainage design would be even more crucial to ensure sufficient capacity is provided to dewater the tailings body over time and to ensure development of elevated phreatic levels within the tailings during operational phase can be controlled.

Considering the above cost and technical implications, the main challenge remained to deliver a risk informed design that could adequately mitigate, reduce or even avoid the negative impacts whilst also ensuring project feasibility to realize the positive impacts.

3 RISK INFORMED DESIGN

The design process included rigorous review and engagement processes between the design consultant team, owner’s team as well as an independent technical review board consisting of highly experienced individuals. The aim of the structured approach for engagement and review was to ensure several perspectives were gained during the evaluation of potential risks and resulting engineering designs proposed to manage these risks. The authors consider the implementation of such review processes as a vital component of “risk informed design” and believe it is a sound risk reduction management strategy. Considering some of the onerous risks and challenges highlighted in Section 2 of this paper, this section provides a summary of selected design solutions tabled and approved for implementation. Risk management strategies included as part of the surveillance monitoring design is also discussed.

3.1 Barrier system design and risk

Alternative barrier design configurations were proposed and motivated to the authorities. Considering the site specific characteristics and constrains, alternatives had to be devised to provide a more cost effective, simplified design that would realize reduced technical risk whilst also delivering equivalent or better environmental protection. The main differences in the design to the minimum requirements and motivations tabled for each requested change are summarized in Table 1.

Table 1. Alternatives proposed to minimum required components of a Class C barrier system.

Minimum Requirement	Function	Proposed alternative	Motivation
Finger drains/Over liner drainage	Evacuation of all seepage water reporting to the liner interface to limit seepage plumes that could develop via defects in these locations.	Equivalent over liner drainage provided only within specific “transition” zones where the tailings permeability is expected to be in excess of 1×10^{-8} m/s	Where fine tailings reside further from the TSF crest would effectively act as an inverted barrier zone with low seepage volumes reporting to interface (Barrier Zone A vs B refer, Fig. 4).
1.5 mm HDPE geomembrane	Main seepage prevention control	2 mm dual textured HDPE.	<ul style="list-style-type: none"> - To ensure similar or better hydraulic equivalence* due to replacement of the 300 mm clay barrier zone of more permeable tailings. - From literature review (Lupo, 2008) 2 mm HDPE geomembrane will provide benefits in terms of longevity under high imposed loads, strength and puncture resistance and will perform better considering the anticipated site and construction conditions. - Dual textured HDPE improves interface friction.

Minimum Requirement	Function	Proposed alternative	Motivation
300 mm Clay liner	Additional seepage protection and bedding layer to HDPE	300 mm of fine tailings will be used instead of clay.	Geochemical and mineralogical analyses proven that when dried tailings is used in this setting, mobilization of harmful components is not considered a risk.**
Under drainage and monitoring system	Required if permanent groundwater levels are < 2 m below barrier system.	Omitted. Fiber optic cable monitoring included as part of design to detect seepage.	From hydrogeological investigation the permanent Groundwater table levels would not impact the barrier system, the underdrainage component as per the minimum requirements has been omitted from the proposed system

*Replacement of the minimum required 1500 μm (1.5 mm) and 300 mm compacted clay barrier with a 2000 μm (2 mm) thick HDPE geomembrane was proposed to provide equivalent/better barrier protection than the minimum requirements based on the theoretical principle of “hydraulic equivalence”.

** The chrome concentration measured in the sample exceeded the Total Concentration Threshold (TCT0) value of 4.6% and the concentrations of arsenic, copper and nickel exceeded their respective TCT0. However, all Leachable Concentrations were below the Leachable Threshold Concentrations (LCT) prescribed by the regulations for all metals and anions.

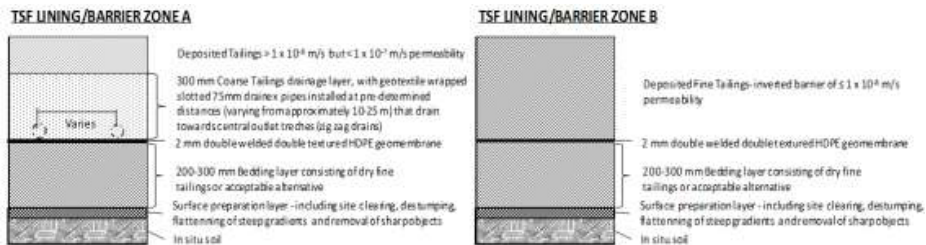


Figure 4. Barrier Zone A and B presented to authorities.

Although there were exceedances of Total Threshold Concentrations (TCT0) for the fine tailings, the implication of the LCT levels being acceptable was that the use of the fine tailings as a bedding layer could be motivated not to represent a significant environmental risk and had benefits over imported materials supported by the following:

- Chemicals present in the tailings are not readily environmentally available, especially if not source of seepage flow is present.
- Metals present in the tailings are not mobile.
- Homogeneity of material for bedding is superior to other sources.
- Tailings should not be considered a waste in this context.

Despite there being no metal mobilization, the analyses did however indicate that the concentrations of nitrates and Total Dissolved Solids (TDS) are elevated against the LCT values. Based on leach test and liquor analysis results, seepage from the Maresburg TSF is likely to have impacts on the quality of groundwater underlying the TSF footprint or surrounding surface watercourses if not contained.

Hydrogeological and surface seepage simulations showed that, irrespective of the barrier system being in place and even when applying a strict construction quality assurance plan, expected defects in the geomembrane would still result in a pollution plume reaching the Maresburg stream during the life of the facility and post closure. The concentrations of these elements during life of mine and post closure are likely to exceed the applicable WUL, discharge and/or drinking water limits used for precautionary screening. To manage this risk, the design and implementation of a secondary interception system will be required to intercept any pollution plumes that occur. The design therefore has made allowance for the implementation of such interception systems in the operational phases as and when surveillance monitoring detects and confirms the formation and location of such plumes (Section 3.4 refers).

The alternative design configurations ultimately translated in savings of approximately ZAR317.0 million. In addition to the optimised configuration, the facility was designed to be

developed in a phased manner upslope, reducing the upfront capital expenditure. Although associated with its own unique challenges, the phased development would allow an opportunity to reduce or spread capital costs over a longer period whilst limiting possible damage to the geomembrane with time. The concept would result in lining only being exposed for less than 2 years before active tailings deposition cover the lined area whilst the next phase is being prepared.

3.2 Seepage, drainage and stability design aspects

Seepage flow, drainage design and stability considerations are interdependent components of the design. Risk based design criteria required viable estimates of the saturated and unsaturated hydraulic behaviour of the tailings materials be made for active deposition and post closure phases. This would then be applied to stability modelling.

Common methods of estimating drainage, seepage and phreatic surface development in tailings impoundments consider contributions from the pool and average atmospheric inputs at the tailings surface. However, detailed deposition sequences, rainfall and evaporation fluxes and the hydraulic behaviour of the material are often called for to satisfy risk based design criteria and to optimize water use (Lorentz, 2017). As part of the Mareesburg TSF design a 2D soil-water physics finite element model was developed to simulate the hydraulic behaviour during cyclone deposition for the typical deposition criteria, daily atmospheric inputs, drain placement and base liner conditions. This detailed technical analysis allowed optimisation of the drainage designs and helped provide confirmation of the robustness of the chosen drainage configuration in satisfying the stability criteria for various adverse scenarios simulated. For lined facilities this type of modelling is considered to be especially valuable.

In order to simulate the phreatic conditions that may develop in the Mareesburg TSF the existing Helena TSF was first simulated (Fig. 5a) as the phreatic surface position, fluxes to drains and hydraulic gradients could be compared to the actuals observed. Once satisfactory performance of the Helena TSF 2D model was obtained, the Mareesburg TSF design was simulated on the same principles (Fig 5b).

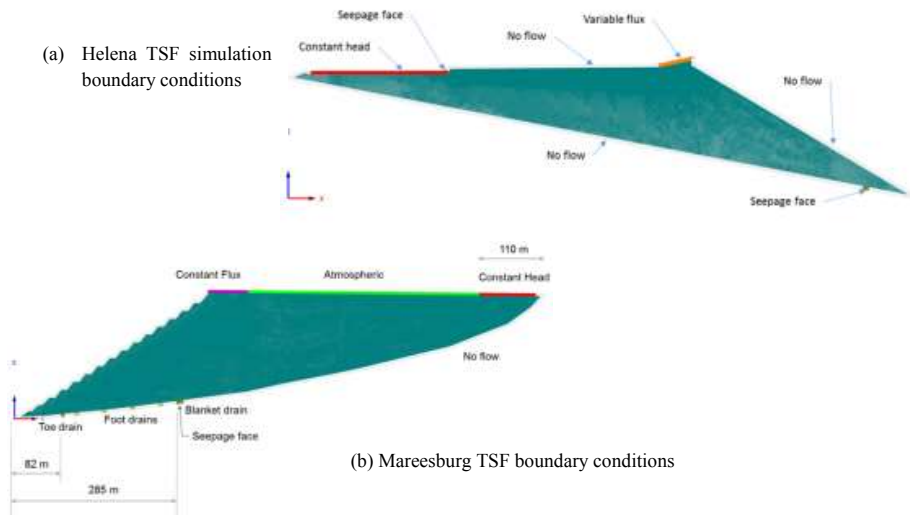


Figure 5. 2D-finite element model boundary conditions for simulating hydraulic behaviour estimations.

The hydraulic properties of the Helena tailings were measured using in-situ double ring infiltrometer, tension infiltrometer and Guelph permeameter tests on site and supplemented with constant head laboratory tests on undisturbed samples. Review of piezocone test information was also

completed to provide further estimates on hydraulic conductivity, in-situ observations of the phreatic surface levels and to determine effective vertical hydraulic gradients. Observations of fluxes from the tailings dam drains were extracted from mine records, although some seepage was considered unaccounted for via basal drainage and other seepage observed on site. The simulation modelling included the rainfall and potential evaporation drivers as well as slurry water inputs.

The 2D simulations of the phreatic surface of the Helena TSF dam compared favorably to the observed levels. The simulated fluxes from the drains ranged from 120 m³/day to 425 m³/day, whereas observed values ranged between 184 m³/day and 272 m³/day. The higher simulated peak values were considered feasible due to the observed seepage from ungauged sources.

With the model performing satisfactorily, illustrative scenarios of the proposed Maresburg TSF design were performed at various development stages (Fig. 6a to 6d).

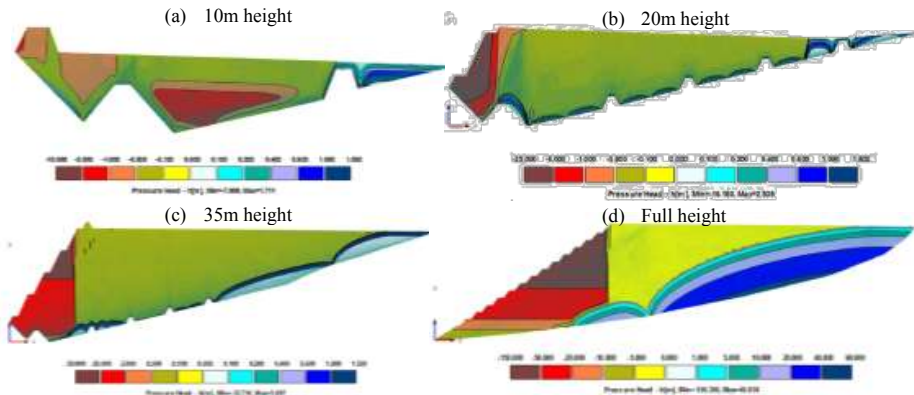


Figure 6. 2D-finite element simulations of development phases assuming footprint drain inefficiency.

The main risks identified for the Maresburg TSF design with respect to drainage and ultimately stability, was the reliance of the design on the performance of the over liner footprint drain configuration located between the toe drain and first main blanket drain (Fig. 5b). The purpose of the footprint drainage features was two-fold in that:

1. They would reduce hydraulic pressure on the liner within the transition zone of the coarse underflow tailings wedge to the finer grained overflow tailings beach.
2. They would increase the extent of the de-saturated tailings prism and in so doing, guard against the risk of mobilization of undrained shear strength and/or possible static or cyclic flow liquefaction of tailings – this behaviour would be limited to materials residing within or close to saturated zone.

Further simulations proved robustness of the design during early phases of development prior to main blank drains, further upslope, became effective. Scenarios simulated for where drainage layers between the main drain drainage piping were removed still proved to be effective in drawing down the phreatic levels sufficiently to satisfy the stability concerns.

Stability design criteria applied aimed at avoiding the risk of large scale slope failure under the following loading conditions:

- Static (Drained and Undrained strength conditions)
- Pseudo static (Application of a seismic coefficient)
- Dynamic (post-earthquake conditions assuming cyclic loading induces flow liquefaction in susceptible layers)
- Static liquefaction (assuming loose liquefiable tailings subject to sufficient trigger event/s to mobilize the liquefied shear strength of the tailings)

Efficient drainage and effective desaturation of the majority of the outer edge of the facility was paramount to ensure stability under all the aforementioned loading conditions (Fig. 7 refers).

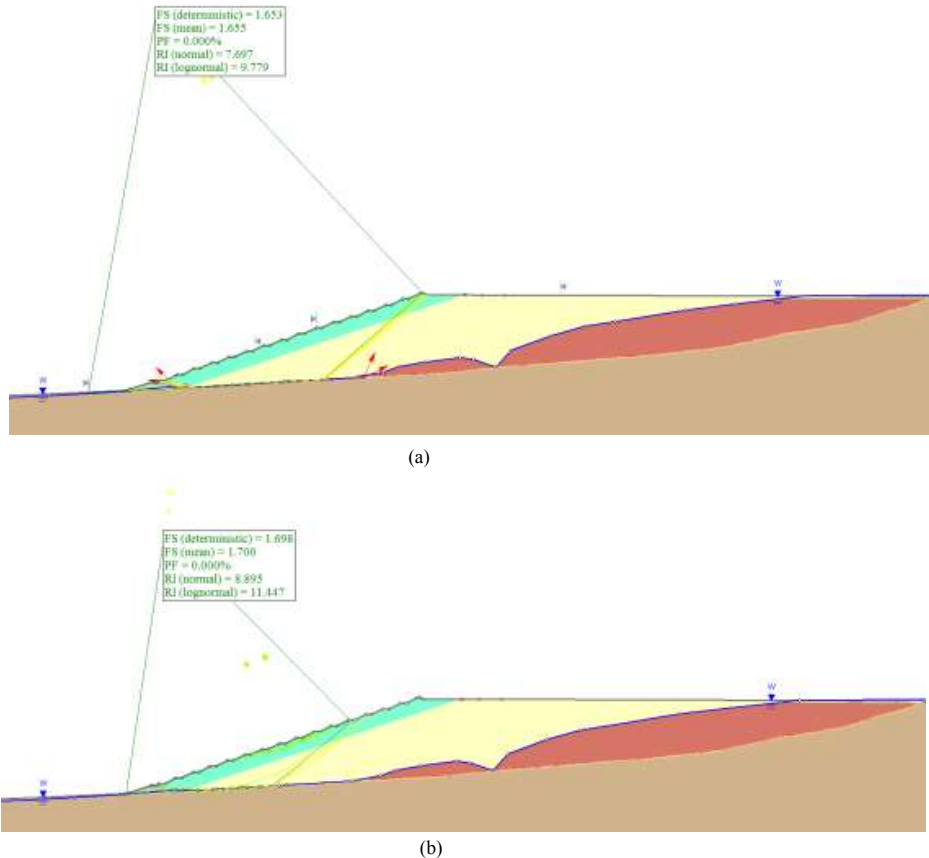


Figure 7. Limit equilibrium stability check at 115m height – Liquefied shear strength below water table applied using (a) Path search - (b) Block search methods

The HDPE liner interface with the tailings bedding materials was also considered a vulnerable aspect of the design, especially as the facility sits on sloping ground.

The risk associated with the interface was mitigated by way of the textured liner, and the passive resistance provided to sliding along this interface by the starter dam inner slope configuration and the addition of 1.5m high “stability” bund walls within the western footprint area. To ensure the critical failure surface with the smallest Factor of Safety was identified, stability assessments were run using both a global path and block search methodology to focus the failure surface search along the weaker HDPE/tailings interface. Further robustness of the design was ensured by applying conservative strength parameter choices to cater for statistical variation and uncertainties in this regard.

In the spirit of “check, check and checking again” the drainage design was reviewed and model simulations expanded during the detail design and construction phase using the finally prepared basin gradients, results from large scale column tests on site and additional laboratory testing verification. These tests were completed to confirm filter material specification criteria and compatibility of all sourced materials with each other and the planned tailings to be deposited over the drainage infrastructure. As noted above (Fig. 5a to 5d refer) several modelled scenarios were evaluated where the installed drainage was modelled to function and/or fail to various degrees. The resulting impact on the developed phreatic levels and stability associated with these conditions at various stages of development were evaluated. The third party review instigated some of the additional modelling work, which was useful, as this improved understanding of the risks,

how they could develop over time and what conditions, when picked up during surveillance monitoring, may solicit cause for concern or further mitigation actions. It was also decided by the project team to add additional redundancy to the system where it was considered that some uncertainty exists surrounding the finite element modelling of transient conditions during the early depositional phases during a high initial rate of construction. Drainage infrastructure, being a relatively inexpensive yet essential component, has the ability to provide significant benefit in terms of risk reduction when compared to the overall financial impact on the project.

3.3 Water management

A common inherent risk on all tailings dam sites that require careful consideration is the risk associated with surface water management. Firstly, from an environmental perspective to ensure clean and dirty water sources are separated and secondly, to protect and prevent damage to the tailings dam itself (erosion, overtopping etc.). A lapse in management of surface water (process or stormwater) is one of the most common failure modes that could give rise to progressive failure and potential static liquefaction.

Challenges with regards this aspect on the Maresburg TSF site are related to the general site morphology (steepness of the eastern, northern and southern perimeter) and the phased manner in which the facility will be developed (Figure 8 refers).

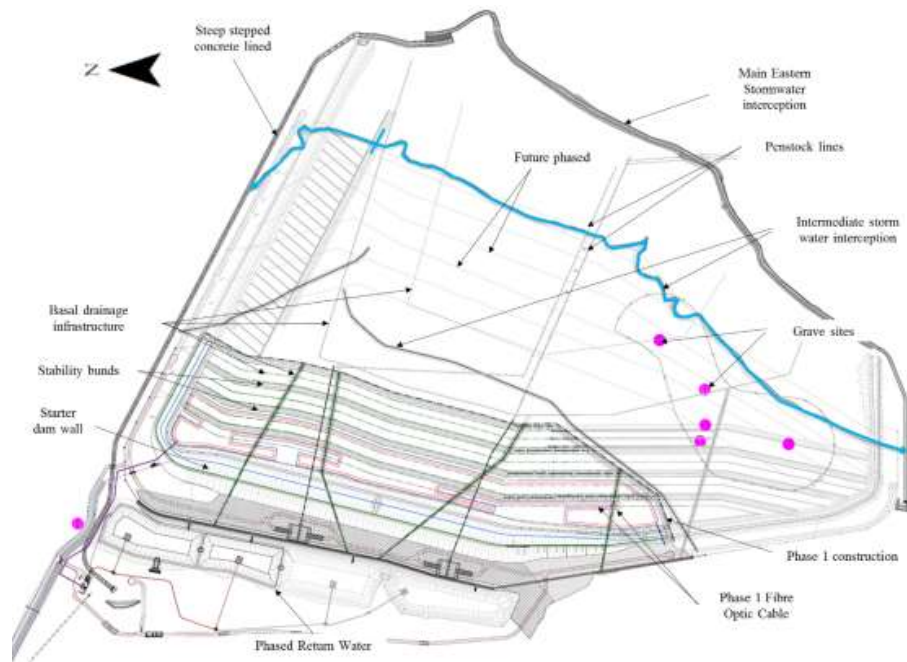


Figure 8. Maresburg TSF layout showing catchment, first development phases, water management infrastructure and grave site locations.

Construction of the clean stormwater diversion in the east was associated with extreme challenging conditions to access and construct. The gradient within the north and south was steep and necessitated the construction of a large stepped concrete channel to ensure flow velocities of the 1:100 year (24hr) flood event could be dissipated sufficiently. Although design standards indicated diversion structures be designed for a 1:100 year (24hr) flood event, the location of the diversion trench with potentially unstable talus slopes above, raised concern with regards the risk of instability and blockage of this feature by sheet wash and natural morphological processes.

Constrained access would make maintenance and clearing of these areas challenging. Storm events exceeding the 1:100 year (24hr) event, combined with potential blockage of the channel would result in stormwater bypassing this feature and flooding the TSF area.

Extra precautions were deemed required to manage this risk and prevent possible damage to developed areas prepared for placement of geomembrane or excessive water collecting in the operational pool areas and potential overtopping. Bolstering the design included construction of two intermediate cut off channels downslope of the main eastern cut off trench, one temporary (shifted upslope every 18 months) and the other, located along the toe of the steep ground (that would be operational for at least 15 years) (Fig. 8 refers). Penstock decant capacity and configuration was also optimised to ensure six active penstock towers were able to decant collected surface water from the TSF surface at any given time. The duration to decant the resulting PMP, assuming no storm water diversions were in place, would be 2.5 days. This is significantly faster than the historically accepted design standard of 7 days.

3.4 Monitoring and Management

It makes a lot of sense to match management and surveillance to the increasing risk and increasingly catastrophic consequence of the gargantuan structures we seek to build. A step change in risk has met with a step change in surveillance requirements. Furthermore, tailings dams are dynamic and continually evolving structures, and will essentially be expected to last “forever”. Case history experience shows that many tailings dam failure modes give advanced warning signs that, if properly monitored and interpreted, can afford opportunity to implement preventative measures. An effective surveillance program and is a risk informed designs’ last defense. Assumptions made now, may well not hold true for 40 years and beyond. This necessitates the evolution of the facility, processes and the environmental conditions to be tracked, to flag risks introduced with time and possible digression from the original design intent or performance. Proper dam safety surveillance requires more than just monitoring equipment and data. It also requires an understanding of how to manage all risks. It requires commitment, adequate resources and support, awareness, interpretive imagination, and clarity of communication among all responsible parties (Martin et al, undated reference). Some advances in the “conventional” surveillance methods, especially within the South African context, that will be applied to the Maresburg TSF facility are highlighted below.

3.4.1 Real time pore pressure monitoring

Real time pore pressure monitoring has not been applied widely in the South Africa until quite recently (although it has been around for a while). The risk of “sudden” excess pore pressure build-up – one of the main precursors to static liquefaction has always been managed by cautious design and limiting the rate of construction of upstream tailings deposits to suit the expected material behaviour. In addition, stringent operational and surveillance requirements have long been the accepted standard means of managing other potential liquefaction triggers. However, again considering known trends, it is becoming increasingly clear that all aspects of tailings design and management have to become even more robust to prevent repeat incidents like the Fundão TSF failure. We literally do not only need more eyes on the ground, but also “in” the ground.

As part of the Maresburg TSF surveillance monitoring, the implementation of a vibrating wire piezometer (VWP) network will form an essential component of surveillance. The network is planned to allow monitoring and assessment of the hydraulic performance of the drainage components, phreatic surface development and to monitor pore pressures in key locations. Where variance to anticipated or assumed design parameters/performance is noted it could flag an increased risk of triggering flow liquefaction given sufficient trigger events and this would necessitate development of mitigation measures.

3.4.2 Fibre Optic Cable installation: Seepage and strain levels

Considering the potential technical risks introduced by the lining requirements and also other inherent environmental risks posed by the Maresburg TSF (should the integrity of the lining and/or the facility be compromised by movement or possible construction defects) it made sense to make optimum use of available and emerging technology to maximize value from tailings dam surveillance. With increasing technological advances there has been a progressively widespread

application of Fibre optic cable (FOC) in water dam safety programs. It is currently an emergent technology for tailings dams' surveillance. Specific benefits of FOC technology include the measurement of multiple parameters, continuously over the entire length of an installed cable. Multiple cable installation allows even more comprehensive, essentially continuous instrumentation coverage compared to the traditional "point source" monitoring of typical tailings dams' instrumentation networks (such as piezometers), greatly increasing the likelihood of early detection of anomalous behaviour. Data can be gathered, recorded, transmitted, and interpreted in real time, enabling much faster response to any concerning behaviour, and enhancing the benefits of surveillance.

The conceptual scheme for FOC emplacement within the starter facilities is to place a network of cables on top and below the geomembrane liner, for measurement of any developing strains or temperature fluxes. The strain measurements can be used to determine if unacceptably high strains are developing along the tailings-liner interface, largely governing dam stability. The tailings-liner interface strain response can provide indicators to situations where stabilizing mitigation design changes would need to be considered. Strain levels that could induce defects (tensile failure) within the geomembrane can be monitored. In conjunction with strain measurements, temperature flux, indicative of seepage flow, can monitor the efficacy of the liner and underdrainage system put in place and flag location of any developing seepage loss via the membrane/barrier system.

The FOC has been included as a research and development initiative and all learnings gained from the design, installation, operation and interpretation of data gathered is intended to further advance application of this technology to other TSF sites that might benefit from such monitoring. Reflection and review of the installation process, success/failures in data collection and interpretations and the lessons learnt during the application of the FOC technology to the Mareesburg TSF site will be required. The authors expect there to be opportunity to capture and share these learnings at similar forums in future.

4 CONCLUSIONS

The Mareesburg TSF design provided opportunities to embody a needed shift change in risk based design. Needed updates to the traditionally acceptable risk management strategies were challenged, to ensure the design and operation of this facility was truly risk informed, following risk trends and recent learnings gained from failures events across the globe. This paper provides some insight into how financial, environmental, technical and site specific risks were managed and balanced to allow implementation of a fit for purpose, risk informed design. The authors are hopeful that the effort put in upfront into the enhancement of how this facility will be monitored from inception could bridge gaps in current knowledge and help in gaining a better understanding of the risks we face and how best to manage them for the future.

ACKNOWLEDGEMENT

The sharing of site specific data provided as part of this paper was made possible by Anglo American Platinum and the relevant operation. The authors would like to thank all affiliated parties and all SRK colleagues forming part of the design team involved in the design and execution phases of the Mareesburg TSF.

REFERENCES

Robertson. A 2011. Mine Waste Management in the 21st Century Challenges & Solutions Beyond Incremental Changes, *Key Note Address Tailings & Mine Waste*, Vancouver B.C., <http://www.infomine.com/library/publications/docs/Robertson2011c.pdf>

- Bowker, L. N. & Chambers D.M. 2015. The risk, public liability, & economics of tailings storage facility failures. *Associates Science & Research In The Public Interest, 15 Cove Meadow Rd Stonington, Maine, 04681*
- Martin T.E. & Davies, M.P. Undated. Development and review of surveillance programs for Tailings Dams, *AGRA Earth & Environmental Limited, Burnaby B.C.*
- Lorentz S.A. 2017 Tailings Water Hydraulics Analyses for Risk Based Design, – In: Wolkersdorfer, C.; Sartz, L.; Sillanpää, M. & Häkkinen, A.: *Mine Water & Circular Economy (Vol I)*. – p. 282 – 288; Lappeenranta, Finland (Lappeenranta University of Technology).

Risk Management by Tailings Storage Facility Dam Classification

C. Johns

Tetra Tech Canada Inc., Kelowna, British Columbia., Canada

D. Hasanloo

Tetra Tech Canada Inc., Vancouver, British Columbia, Canada

ABSTRACT: Tailings storage facility dam classification can be a useful tool for risk identification and management, for operational control and forecasting, and for comparison of design or remediation options. The Canadian Dam Association (CDA) guidelines include a framework for dam classification that can be used to establish design requirements and are a regulatory requirement in some jurisdictions.

The CDA framework for dam classification includes the following key elements: failure mode identification, dam breach analysis and inundation mapping, and an assessment of dam failure consequences. Consequences considered include potential loss of life, economic impact and infrastructure damage, and environmental impact.

A mine tailings storage facility in the southern interior of British Columbia, Canada was classified under this framework based on a multidisciplinary workshop undertaken to identify potential failure modes, a dam breach and inundation study to identify the extent of potential impact, and an assessment of the dam failure consequences. The dam breach study was completed using a combination of empirical methods and two-dimensional finite element modelling of the flood wave. The critical failure mode was assessed to be failure of a surface water diversion during a flood event and the subsequent cascade failure of tailings retaining embankments. The outcome of the study provided not only a dam classification and identification of key risks, but also recommended actions to mitigate risk and potentially reduce the level of dam classification.

1 INTRODUCTION

There has been a heightened interest in identifying and managing tailings dam risks over the last several years due to reaction and impact of recent failures in British Columbia, Brazil, and elsewhere.

Classification of tailings dams is a useful exercise (Kirkham, 2002) that can support:

- Risk identification and management,
- Selection of design and operational controls,
- Comparison of design or remediation options,
- Establishment of design parameters, operating constraints, and monitoring requirements, and
- Adoption of appropriate regulations and license requirements.

It is generally undertaken as an interdisciplinary technical exercise by specialist consultants with close involvement of the mine management and technical team. As the perceived risk associated with a tailings dam increases, greater effort and more stringent design requirements can be specified. The classification of tailings dams typically follows the same general proto-

cols that are associated with water storage dam classification, and adopt risk management techniques that are widely applied (Figure 1-1).

The process is often driven by regulators and although the protocols and language describing the process, elements, and outcomes varies between jurisdictions, the key elements are the same.

The process generally involves a system to rank the potential hazard of the dam based on consequences of a dam failure to the environment, economic losses, and human life (CDA, 2013, FEMA, 1998, ANCOLD, 2012). The outcome of the dam classification (described as hazard potential classification under FEMA) can be used in the design, operation, and closure phases to identify the appropriate level of effort and attention required to adequately manage risk.

The classification outcome is not intended to assess the actual condition of a dam, but instead is based on potential failure outcomes. Well-engineered tailings dams that are fully instrumented and adequately monitored, can still retain the most severe risk ranking due to the potential impact in the event of a failure.

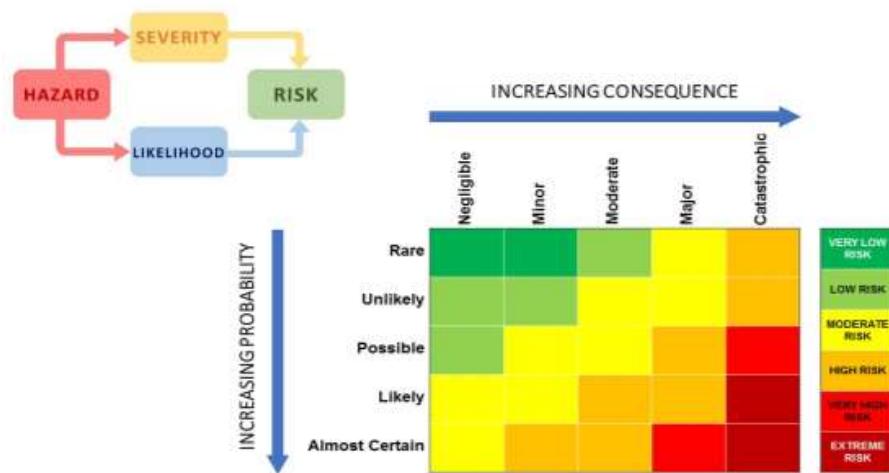


Figure 1-1: Hazard and risk relationships for consequence determination

2 DAM CLASSIFICATION FRAMEWORK

Application of the CDA dam classification framework (CDA, 2013) involves the following key elements:

- Failure mode identification,
- Dam breach analysis and inundation mapping, and
- Assessment of dam failure consequence.

The level of effort and the methods selected to undertake each step should match the expected level of risk. The CDA guidelines recommend a preliminary assessment be initially undertaken using conservative assumptions, and that more advanced methods can be subsequently applied to provide greater accuracy and technical support to the adopted classification, if required.

The failure mode identification step involves adequate characterization of system elements, identification of external and internal hazards, and consideration of credible failure modes that may occur independently or in combination. Existing risk mitigation measures should be considered in the assessment. Development of a ‘bow-tie’ diagram (Figure 2-1) can be effective to

help organize and communicate hazards, controls, and consequences. Low probability events should be included in the assessment.

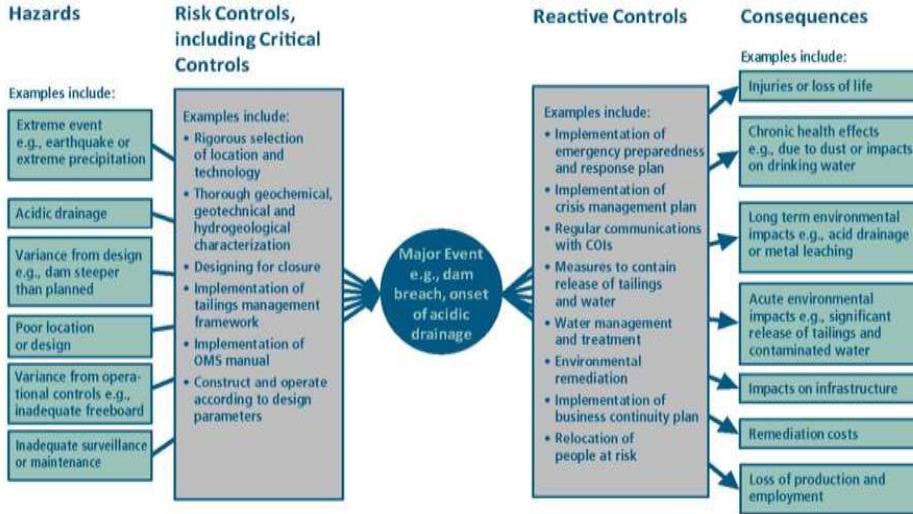


Figure 2-1: Typical ‘Bow-tie’ diagram summarizing hazards, risk controls, and consequences (from MAC, 2017)

The use of empirical correlations is common for preliminary assessment of tailings dam breach and inundation assessment (Rico, 2008, Small, 2017). More advanced assessment by deterministic modelling requires advanced techniques, adequate characterization of existing and expected conditions, and significant assumptions.

A federal dam classification system developed by an interagency task group in the United States is summarized in Figure 2-2. This framework was developed to provide a simple system in language that could be readily understood by the public (FEMA, 1998).

Hazard Potential Classification	Loss of Human Life	Economic, Environmental, Lifeline Losses
Low	None expected	Low and generally limited to owner
Significant	None expected	Yes
High	Probable. One or more expected	Yes (but not necessary for this classification)

Figure 2-2: Hazard potential classification system for dams (FEMA, 1998)

Under the CDA framework, the selection of the dam class is based on the most conservative outcome under the assessment of incremental losses under the following categories: Loss of life, environmental and cultural values, and infrastructure and economics. Figure 2-3 provides a summary of the CDA dam classification framework as presented in CDA, 2013. A separate CDA technical bulletin describing the application of the Dam Safety Guidelines to mining dams was prepared that defined mining dams as structures designed to retain solids and/or contaminated liquids (CDA, 2014). This bulletin provides considerations that are unique to mining dam safety and classification, including slurry flow as part of dam breach and inundation, environmental impact, and impact to mining company reputation and shareholder value (CDA, 2014).

Dam Class	Population at Risk [note 1]	Incremental Losses		
		Loss of Life [note 2]	Environmental and Cultural Values	Infrastructure and Economics
Low	None	0	Minimal short-term loss No long-term loss	Low economic losses; area contains limited infrastructure or services
Significant	Temporary only	Unspecified	No significant loss or only deterioration of fish or wildlife habitat Loss of marginal habitat only Restoration or compensation in kind highly possible	Losses to recreational facilities, seasonal work-places, and infrequently used transportation routes
High	Permanent	10 or fewer	Significant loss or deterioration of <i>important</i> fish or wildlife habitat Restoration or compensation in kind highly possible	High economic losses affecting infrastructure, public transportation and commercial facilities
Very High	Permanent	100 or fewer	Significant loss or deterioration of <i>critical</i> fish or wildlife habitat Restoration or compensation in kind possible but impractical	Very high economic losses affecting important infrastructure or services (e.g. highway, industrial facilities, storage facilities for dangerous substances)
Extreme	Permanent	More than 100	Major loss of <i>critical</i> fish or wildlife habitat Restoration or compensation in kind impossible	Extreme losses affecting critical infrastructure or services (e.g. hospital, major industrial complex, major storage facilities for dangerous substances)

Note 1. Definitions for population at risk:
 None—There is no identifiable population at risk, so there is no possibility of loss of life other than through unforeseeable misadventure.
 Temporary—People are only temporarily in the dam-breach inundation zone (e.g., seasonal cottage use, passing through on transportation routes, participating in recreational activities).
 Permanent—The population at risk is ordinarily located in the dam-breach inundation zone (e.g., as permanent residents); three consequence classes (high, very high, extreme) are proposed to allow for more detailed estimates of potential loss of life (to assist in decision-making if the appropriate analysis is carried out).

Note 2. Implications for loss of life:
 Unspecified—The appropriate level of safety required at a dam where people are temporarily at risk depends on the number of people, the exposure time, the nature of their activity, and other conditions. A higher class could be appropriate, depending on the requirements. However, the design flood requirement, for example, might not be higher if the temporary population is not likely to be present during the flood season.

Figure 2-3: Dam classification criteria (CDA 2013)

Several areas of the dam classification process are not well established, as evidenced by active updates to CDA mining dam guidance that are in progress. These updates to guidance are to include dam breach assessment methods, environmental consequence classification, and de-classification requirements (i.e., conversion to a non-dam).

3 DAM CLASSIFICATION CASE STUDY

When the CDA dam classification process was applied to Nicola Mining's Merritt Tailings Storage Facility (TSF), the significant risks were identified and their potential impact was characterized. The process permitted identification of mitigation measures that have resulted in an improved dam management outcome for the mine and stakeholders.

3.1 *Setting*

The Merritt TSF was constructed as a valley-type TSF approximately 65 km southwest of Kamloops in the southern interior of British Columbia (Figure 3-1). The climate is semiarid, with a mean annual precipitation of approximately 330 mm and annual evaporation of approximately 600 mm. The valley slopes are covered with a thin veneer of glacial till and alluvium. The site is located in an area of moderate earthquake risk, well inland from the coastal high seismic hazard zone. Thick glaciofluvial deposits of dense silty sand and gravel line the valley bottom. The community of Lower Nicola is between 2 km and 4 km south (downgradient) of the TSF.

The current operational situation is not uncommon for sites with a long history. There is a relatively large area of inactive old tailings and a relatively small subset of the facility that the current owners have permitted for active tailings storage. The historical Craigmont Copper Mine was an open pit operation that produced the majority of the tailings stored in the current facility between 1962 and 1982. A tailings retreatment project to produce magnetite for the coal industry was subsequently operated in the tailings area from 1985 until 2012. This process involved gravity separation of magnetite from a re-slurried mixture of tailings, which was then pumped back to the tailings area into new storage cells. These cells were built using a combination of cyclone separated sand tailings and granular soils to construct the embankments. The embankments were raised by a combination of centerline and upstream methods to a height of between 10 m and 30 m. The Merritt TSF is comprised of five cells including the Huldra Tailings Facility (HTF), Upper Tailings Facility (UTF), West Tailings Facility (WTF), Expanded Tailings Facility (ETF) and the Lower Tailings Facility (LTF). The alignment of Merritt TSF structures at the time of the study is shown on Figure 3-1. The HTF is the most recent and the only active facility, and was constructed as a geomembrane-lined cell within the UTF.

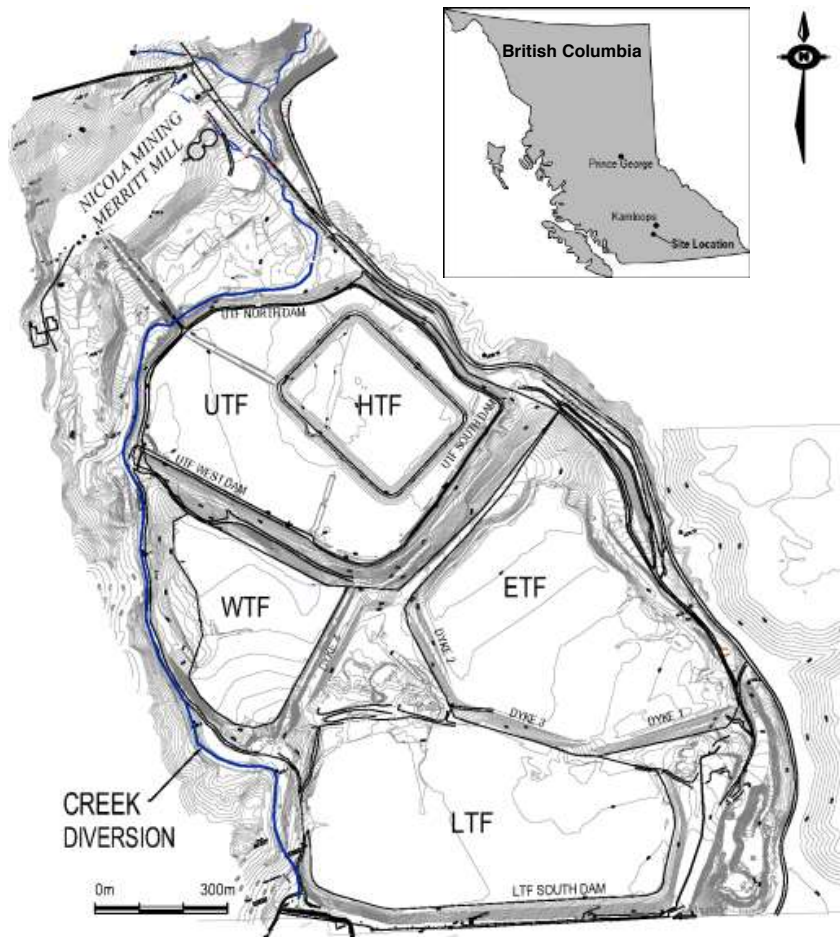


Figure 3-1: Merritt TSF site plan with location plan inset

3.2 Hazards and Failure Mode Identification

The dam classification process was initiated with a facility status review, and the following available information was compiled:

- Dam construction and operation information, including construction materials and methods, geometry of containment and water management structures, and tailings production and capacity data for each cell,
- Geotechnical parameters, including geometry and material properties at critical sections, and groundwater levels,
- Hydrological and hydrotechnical parameters, including climate information, catchment area, extreme storm event magnitudes, freeboard, and surface water management system capacity,
- Site environmental characteristics, including distribution of any identified contaminated soil and water, location and character of potential receiving environment, and potential pathways for impact.



Figure 3-2: Photographs of Merritt TSF (A) creek diversion and (B) LTF embankment

A workshop was held with specialists in geotechnical, hydrotechnical, tailings, and dam engineering to identify hazards and credible failure modes. Consideration was given to both sunny day and rainy day failure events that included dam instability, overtopping, and contaminated seepage. Each component of the system and storage area was reviewed and potential failure modes documented. Hazards were assessed with consideration of adverse elements, uncertainty, and mitigating factors, and the information compiled in a table with preliminary risk ranking.

It was determined that the main risks for the Merritt TSF at that time were related to management of storm event inflow from the catchment upstream of the TSF during ‘rainy day’ events. Failure modes associated with geotechnical instability were considered to have less impact due to the partially saturated condition of the inactive tailings and the regional setting.

In a typical year, it had been observed that the creek diversion only flowed during the spring runoff period (Figure 3-2). The diversion around the Merritt TSF was reportedly designed for a 1:200 year flood event, and the possibility of a failure of the diversion into the WTF during an extreme storm event was considered credible by the workshop team.

Further, with consideration of the nature of WTF embankment construction and the capacity of the WTF and the LTF, it was determined that the diversion failure could result in a cascade type failure of the WTF and the LTF.

3.3 Dam Breach and Inundation Study

To provide a basis for assessment of impact of the significant failure modes, a dam breach and inundation study was undertaken (Hasanloo et al, 2017).

Figure 3-3 shows a plan view of the area downstream of Merritt TSF and includes the extent of the dam breach study boundary. The boundary was selected to include areas that could be significantly impacted in the event of a dam breach. The model geometry was generated from a combination of LiDAR data near the mine site and National Topographic System map data further downstream.

Flood wave routing was carried out using a two-dimensional model (FLO-2D software) to simulate unconfined overland non-Newtonian viscous flow of the tailings and flood water. The modelling was undertaken to calculate the extent of inundation and the maximum flooding depth. Several assumptions were required to support the assessment, including breach characteristics, the volume of tailings released, and the density of the released slurry. At the time of the assignment, a 1:1000 year flood event was adopted for the model to be consistent with regulations and with the design event for a ‘Significant’ dam under CDA guidelines. Regulations for tailings dams in British Columbia are now more stringent, and require consideration of a design flood calculated as 1/3 between 1:975 year event and the Probable Maximum Flood for a ‘Significant’ dam classification (HSRC, 2016).



Figure 3-3: Merritt TSF dam breach and inundation study area

3.4 Flood Hazard Assessment and Dam Classification

The results of the inundation study were used to assess the potential impact of a dam failure on loss of life, environment and cultural values, and infrastructure and economics as per the process summarized on Figure 2-3. In accordance with the CDA dam classification protocol, the incremental impact of a potential failure of the Merritt TSF above the baseline flood event impact was considered.

The potential Loss of Life was established using a method that involved estimation of a Fatality Rate applied to the Population at Risk.

The following definitions are relevant to the process:

- Population at Risk: The number of people who would experience consequences,
- Fatality Rate: Expected fatalities estimated to result from dam failure,
- Loss of Life: Estimated by Fatality Rate multiplied by Population at Risk.

The Fatality Rate was calculated using methods consistent with those described by the US Bureau of Reclamation and related to the magnitude of the flood depth and the flood velocity (USBR, 2015). GIS tools were used to link the spatial distribution of the Fatality Rate with the physical distribution of the Population at Risk.

Downstream infrastructure that was potentially impacted included housing, roads, and a provincial highway. Despite the benign tailings geochemistry, it was determined that there was potential environmental impact on surface water quality that could deteriorate fish habitat downstream of the Merritt TSF.

The estimated impact of the baseline 1:1000 year flood event, assuming the Merritt TSF was not present, was damage to housing and local roads, but no loss of life was expected.

It was determined that the 24 hour, 1000 year flood event could not be contained within the diversion, and that it had enough volume to overtop the WTF dam. Further, it was assessed that there was inadequate capacity within the LTF, and that the flood velocity associated with a WTF failure had sufficient velocity to erode LTF tailings.

For the specific scenario of a cascade WTF and LTF failure and the assumptions adopted in the model, it was recommended that the dam classification be increased from ‘Significant’ to ‘High’. This was based primarily on the potential for loss of life in the residential area downstream of the dam, as summarized in the following list of potential impacts with corresponding classification in brackets:

- Loss of Life of 10 or fewer (High),
- Significant loss or deterioration to fish and wildlife habitat, restoration highly possible (Significant to High), and
- No major Incremental Losses to Secondary Highway System, but significant incremental damage to infrastructure (Significant).

3.5 Facility Upgrades for Risk Mitigation

In response to the identification of hazards and risk presented as part of the dam classification, Nicola Mining adopted measures to mitigate risk and change the credible failure modes. It was recognized that the diversion performance represents a significant amount of risk, and there was high value in the adequate design and construction of diversion geometry and erosion protection measures. The importance of diversion inspection and maintenance was also highlighted.

It was also determined that earthworks to remove a portion of an internal embankment at the WTF would eliminate the possibility of the cascade failure. The removal of the WTF embankment also reduced the volume of water associated with the LTF failure, and thus increased the slurry density of the displaced tailings and reduced the expected inundation extent.

Merritt TSF design assessment and construction upgrade measures are in progress. The partial removal of the internal embankment has resulted in a reduction in the potential for Loss of Life associated with a failure of the Merritt TSF. Figure 3-4 provides a comparison of model outcomes for the maximum 1:1000 year flood event depth for:

- A cascade failure of both the WTF and the LTF (left), and
- A failure of the LTF only (right).

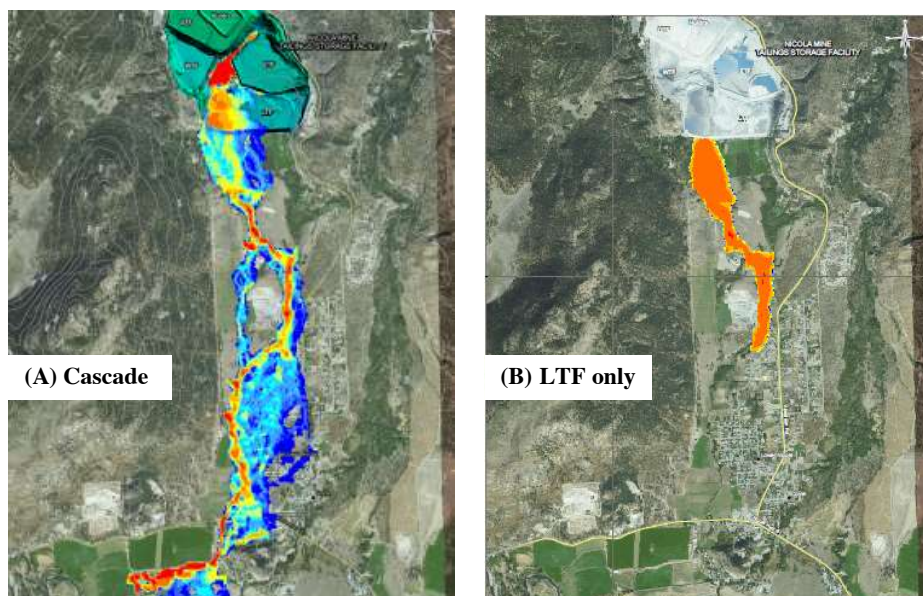


Figure 3-4: Merritt TSF inundation maximum flow depth for (A) cascade failure (before upgrades) and (B) indicative LTF failure only (post upgrades)

At the Merritt TSF, additional measures to improve water management and advance the inactive ‘lower’ tailings areas (LTF, WTF, and ETF) towards closure and de-licensing are in progress. These measures include construction of a spillway on the LTF, and placement of cover on the exposed tailings surfaces.

Preliminary interpretation of these changes suggests a reduction in dam classification to ‘Significant’ is appropriate.

Geotechnical investigation and assessment of the tailings and the embankments is planned for 2018 that will improve the technical understanding of embankment stability and better characterize the potential failure modes.

The dam classification should be updated in future with consideration of proposed TSF closure earthworks that will improve water management and potentially further reduce the extent and character of inundation associated with a dam failure. Future consideration should also be given to any changes in downstream developments that may impact the consequence classification of the hazards (ICOLD, 2013).

4 SUMMARY AND CONCLUSIONS

The dam classification process is an important procedure that can highlight hazards and risks associated with a tailings storage facility and indicate methods to mitigate and manage risk.

The dam classification process varies across jurisdictions, but generally includes hazard identification and a system to rank the potential hazards based on the consequences of a dam failure. The CDA dam classification process was applied to a tailings storage facility in the southern interior of British Columbia, and the critical elements that controlled risk were identified. Further, the process enabled the facility owner to identify mitigating action that reduced risk associated with the facility.

The dam classification at every tailings storage facility should be reviewed periodically to address potential changes in the facility construction and operation, and potential changes in the environment upstream and downstream of the site.

5 ACKNOWLEDGEMENTS

The authors thank Nicola Mining Inc. for the opportunity to present the project information in this paper. We are grateful for document formatting support provided by Brenda Ingwersen and Anisha Navaratnam's assistance with figure preparation.

6 REFERENCES

- Alaska Department of Natural Resources, 2017. Draft Revision of *Guidelines for Cooperation with the Alaska Dam Safety Program*. Prepared by Dam Safety and Construction Unit, Water Resources Section, Division of Mining, Land and Water.
- ANCOLD, 2012. *Guidelines on Tailings Dams, Planning, Design, Construction, Operation and Closure*. British Columbia Ministry of Forest, Lands and Natural Resources, 2015. *Downstream Consequence of Failure Classification Interpretation Guideline for Dam Safety Officers*.
- British Columbia Ministry of Energy and Mines, 2016. *Health, Safety and Reclamation Code for Mines in British Columbia*, Guidance Document, Version 1.0, July 2016.
- CDA Guidelines, 2014. *Application of Dam Safety Guidelines to Mining Dams*.
- CDA Guidelines, 2013. *Dam Safety Guidelines*.
- Federal Emergency Management Agency (FEMA), 1998. Federal Guidelines for Dam Safety: Hazard Potential Classification System for Dams. Originally Prepared by the Interagency Committee on Dam Safety, FEMA, U.S. Department of Homeland Security, October 1998, reprinted 2004.
- FLO-2D Software Inc. 2012. FLO-2D Reference Manual, Version 2012.
- Hasanloo, D, Johns, C, Sinclair J, Creba, C, and Patrick B, 2017. Dam Break Assessment and Classification of a Tailings Storage Facility in Interior British Columbia. *Proceedings of the CDA 2017 Annual Conference*, Kelowna, BC, Oct 16-18, 2017.
- ICOLD, 2013. Sustainable Design and Post-Closure Performance of Tailings Dams, Bulletin 153.
- Kirkham, A, 2002. Incremental Consequence Classification Methods, Tools and Challenges. *Proceedings of the CDA 2002 Annual Conference*, Victoria, BC, Oct 6-10, 2002.
- Mining Association of Canada, 2017. A Guide to the Management of Tailings Facilities. 3rd Edition, October 2017.
- MacDonald, T.C. and J.L. Monopolis, 1984. Breaching Characteristics of Dam Failures, *Journal of Hydraulic Engineering* 110 (5), May.
- Rico, M., Benito, G., Diez-Herrero, A. 2008. Floods from Tailings Dam Failures, *Journal of Hazardous Materials* 154 (1-3): 79-87.
- Small, A, James, M, and Mohammad, A., 2017. Advancing the State of Practice for Tailings Dam Breach Assessment Using Empirical Correlations, *Proceedings of the CDA 2017 Annual Conference*, Kelowna, BC, Oct 16-18, 2017.
- U.S. Bureau of Reclamation (USBR), 2015. RCEM - Reclamation Consequence Estimating Methodology, Interim Guidelines for Estimating Life Loss for Dam Safety Risk Analysis, U.S. Department of the Interior, July 2015.
- USBR, 1988. *Downstream Hazard Classification Guidelines*. ACER Technical Memorandum No. 11. December 1988.

Tailings Facility Performance: 2017 & 2018

C. Strachan

Stantec Consulting Services Inc., Fort Collins CO, USA

J.A. Caldwell

Robertson Geoconsultants, Vancouver BC, Canada

ABSTRACT: This paper is a continuation of a series of papers over the past few years from events and documents of the preceding year that affect the principles and practice of tailings facility design, construction, operation, management, and closure. These events and documents comprise information on tailings facility incidents, published descriptions of technology developments, and updated or new tailings management guidelines.

The information reviewed for 2017 and 2018 include: tailings facility incidents in Africa, Australia, the Americas, Europe, and southeast Asia; a guidance documents issued by the Association of Professional Engineers and Geologists, British Columbia about site characterization for dams and in particular tailings facilities; an updated tailings guidance document issued by the Mining Association of Canada, a guidance document issued by the United Nations; recent conference proceedings on mine water management pertaining to tailings facilities.

1 INTRODUCTION

This paper is a continuation of a series of papers that have been prepared to summarize events and documents of the preceding year that affect the principles and practice of tailings facility design, construction, operation, management, and closure (Caldwell, 2016, 2017, and previous years). These events and documents comprise information on tailings facility incidents, published descriptions of technology developments, and updated or new tailings management guidelines.

2 RECENT EVENTS

Figure 1 summarizes the history of documented tailings impoundment or tailings dam incidents from 1900 through the second quarter of 2018. This figure has been modified for 2017 and 2018 information, from Strachan and Goodwin (2015) and Strachan and Van (2018). The tailings data set are limited to mill process tailings (or tailing) or coal processing residues. Coal ash impoundments, heap leach facilities, and waste rock storage facilities were not included in this summary.

The term “incidents” is used to be consistent with earlier publications documenting water-storage dam and tailings dam events (USCOLD, 1976, 1988, 1994). Incidents include failures (indicating breach of the dam and loss of process water or tailings), accidents (indicating repairs made to the dam with little or no loss of process water or tailings), and groundwater issues (indicating seepage or groundwater impact issues that were inconsistent with design intent).

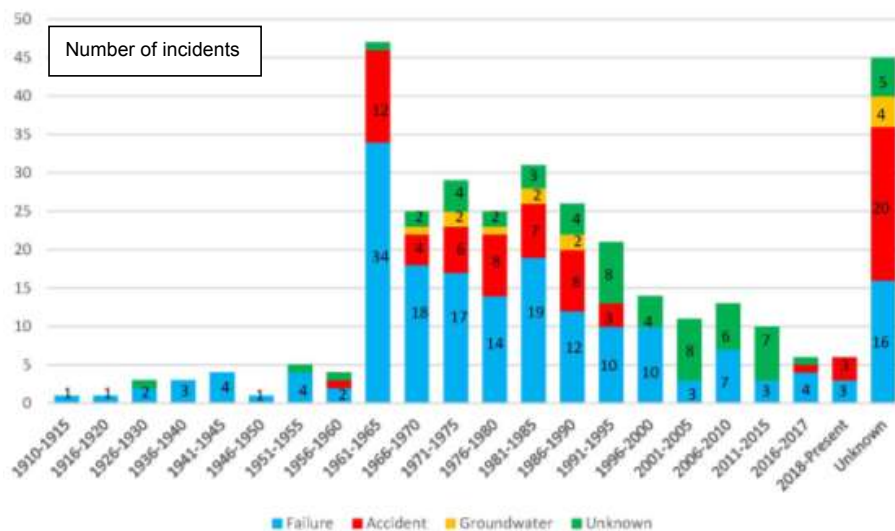


Figure 1. Tailings dam incident history.

The number of incidents is presented five-year increments through 2015. There is a general decreasing trend in incidents from the 1961-1965 period through 2015. The 2016-2018 period totals 12 incidents, which presents an increase in incidents during the 2016-2020 period. The number of failures during these five-year periods has gradually decreased from the 1961-1965 period, but since 2001 has remained between 3 to 7 failures during each five-year period. The key item from Figure 1 is that the number of incidents (both failures and accidents) has not decreased to zero, despite our knowledge of dam behavior and current technological capabilities.

Table 1 below summarizes the eight incidents that are discussed below. The incident data presented below are based on available information at the present time, and do not reflect the opinions or interpretations of the authors.

Table 1. Reported incidents, second half 2017 through first half 2018.

Name	Date	Location	Incident Type	Status	Probable Cause
Kokoya	Sep 27, 2017	Liberia	Failure	Active	Piping
Hernic	Dec 29, 2017	South Africa	Accident	Active	Overtopping
Peñarroya	Feb 15, 2018	Spain	Failure	Inactive	Overtopping
Alunorte	Feb 17, 2018	Brazil	Accident	Active	Overtopping
Minera Lincuna	Mar 5, 2018	Peru	Failure	Active	Slope stability
Bong Mieu	Mar 16, 2018	Vietnam	Failure	Active	Slope stability
Cadia Valley	Mar 16, 2018	Australia	Accident	Active	Slope stability
Cieneguita	Jun 4, 2018	Mexico	Failure	Active	Slope stability

2.1 Kokova (Liberia)

A release of slurry containing cyanide was reported on September 27, 2017 from the Kokova Gold Mine in Liberia. The mine is operated by MNG Gold Liberia, a company registered in Turkey. The release reached nearby Sig Creek and surrounding wetlands, potentially affecting surface water and groundwater. The reported cause of the release was a rupture in a section of the geomembrane liner within the tailings impoundment. The estimated volume of slurry released was approximately 11,000 m³. The Liberia Environmental Protection Agency;

Ministry of Land, Mines, and Energy; Ministry of Internal Affairs; and National Public Health Institute were involved with follow-up work.

The sources of information are *The News* (a Liberian newspaper) and Bowker and Associates, Science & Research In the Public Interest.

2.2 *Hernic (South Africa)*

A tailings release occurred at the Hernic Ferrichrome processing facility in South Africa (used for recovery of chrome and platinum). The facility is associated with the Dilokong chrome mine, owned by Jubilee Metals Group PLC. The volume of released tailings was not reported, but was contained within a former open-pit mine area on mine property. The release was through a v-shaped failure of a side wall (embankment), and was repaired the same day of the release.

The sources of information are *Alliance News* (a London newspaper) and <miningreview.com>.

2.3 *Peñarroya (Spain)*

A tailings release from a reported dam breach reached the nearby Brandelos River in southwest Spain. The volume of release was not reported. The facility is part of an old copper/gold mining complex operated by Mining and Metallurgical Society of Peñarroya and Río Tinto Patiño. Following the release, a complaint was filed with the European Parliament about the release as well as environmental issues in the area.

The source of information is <mining.com>.

2.4 *Alunorte (Brazil)*

A waste spill from a holding basins at the Norske Hydro Alunorte bauxite and aluminum refining plant followed heavy precipitation in the area. The site in the Para State of Brazil, near the mouth of the Amazon River. The facility is operated by Norske Hydro, a Norwegian company. The affected holding basin was geomembrane-lined, and appeared to be overtopped, with no damage to the geomembrane. The waste spill volume was not reported, but flowed into nearby areas.

The source of information is <news.mongabay.com>.

2.5 *Minera Lincuna (Peru)*

A tailings release occurred from a dam failure in the Ancash Region of Peru. The estimated release volume was approximately 50,000 m³ into the Sipchoc Basin and the Rio Santa. The operator is Minera Lincuna SA.

The source of information is <elcomercio.pe>.

2.6 *Bong Mieu (Vietnam)*

A tailings dam breach from the Bong Mieu gold mine in Tam Lanh Town, Quang Nam Province in Vietnam released tailings into the Que Phuong River. The volume of release is not reported. The Bong Mieu Gold Mining Limited Company had operated the mine, but the company had closed and the site was taken over by 6666 Mineral Industry Joint Stock Company. The location of the tailings dam breach was located and sealed with sand bags two days after the breach.

The source of information is <e.vnexpress.net>.

2.7 *Cadia Valley (Australia)*

At Newcrest Mining's Cadia Valley Mine in NSW Australia, the embankment between the northern and southern tailings impoundments experienced a partial failure, releasing tailings from the northern impoundment into the southern impoundment. There was no external release

of tailings. The volume of tailings released between impoundments is not reported. The cause of the partial embankment failure appears to be slope instability, perhaps due to seismic activity two days before the event.

The source of information is *Sydney Morning Herald* <smh.com.au/national/nsw/>.

2.8 Cieneguita (Mexico)

A tailings embankment failure at the Cieneguita Mine in Mexico released approximately 250,000 m³ of tailings, which migrated up to 29 km downstream along the course of the Cañitas River. The mine is operated by Minera Rio Tinto (Cluster Minero de Chihuahua A.C.). Fatalities were reported. Cracks in the embankment were reported prior to the failure.

The sources of information are *The London Free Press*, WISE Uranium Project, and Bowker and Associates, Science & Research In the Public Interest.

3 NEW DOCUMENTS

New guidelines and documents of interest are summarized below.

3.1 MAC Guidelines

The Mining Association of Canada (MAC) released two documents in November 2017: (1) a third edition of *A Guide to the Management of Tailings Facilities*, and (2) *Maintenance and Surveillance Manual for Tailings and Water Management Facilities*.

The third edition of the Guide includes updates based on a standard of zero failure for mining facilities. The third edition includes technical components critical to the physical and chemical stability of tailings facilities and consideration of Best Available Technology and Best Available/Applicable Practices. The third edition also discusses management components of a mine life cycle, including change management, critical controls for risk management, and performance evaluation.

These guidelines are available at <www.mining.ca/tailings-management>.

3.2 MEND Document

A new summary of current tailings management technologies is documented in the *Study of Tailings Management Technologies* for the Mine Environmental Neutral Drainage (MEND) Program (KCB, 2017). The focus of the document is comparison of slurried, thickened/paste, and filtered tailings facilities.

3.3 UNEP Document

A 2017 document published by the United Nations Environment Programme (UNEP) focused on recent tailings impoundment failures (UNEP, 2017). In addition to better management of tailings impoundments and minimization of human error, recommendations include setting “zero tolerance” for dam breaches, making human and environmental safety a higher priority, and a developing an UNEP stakeholder forum to develop stronger international regulations.

4 CONCLUSIONS

The recent incidents described above indicate that tailings effective management involves issues beyond embankment slope stability, including managing process water and excess water from precipitation, monitoring performance with inspection and instrumentation, and notifying management personnel of observed problems. The recent documents listed above also outline observation, communication, and notification issues critical to effective and safe tailings management. While stronger regulations may improve performance in countries where there are not current regulations or mining companies are not adhering to international standards of

practice, tailings dam incidents still occur in countries with comprehensive mining and dam safety regulations.

Methods to reduce the number of tailings dam incidents involve basic physical and operational issues, as well as personnel training and communication issues. These are summarized below.

- Managing tailings impoundments in a manner that (1) minimizes ponded water within the impoundment, (2) maintains ponded water away from the tailings dams, and (3) effectively accommodates excess process water or precipitation with dam freeboard or emergency spillways.
- Operating tailings facilities to optimize tailings densities through consolidation and drainage or by compaction or mechanical methods. Alternative process water reduction methods the milling process (such as thickening or filtration) also increase residual tailings densities, and may have lower capital and operating costs through the entire mine life cycle (including closure and post-closure periods).
- Educating personnel involved with tailings facility operation, monitoring, and management to recognize proper tailings dam performance and best management practices, and know established procedures to notify the appropriate personnel and take action when unforeseen conditions are observed.

Accepted geotechnical engineering practice includes standards for slope stability and factors of safety, and acceptable pore pressures under dilatant or compressive tailings behavior. Other engineering concepts may need to be considered, such as the risks associated with the facility, the robustness of the design, and the resilience of the facility performance (Robertson and van Zyl, 2016; Davidson, 2017).

The tailings incidents listed in this report are not acceptable, and the goal for the mining industry is to have no tailings impoundment failures.

REFERENCES

- Caldwell, J. A. 2016. 2015 Tailings Failures and Successes, *Tailings and Mine Waste '16*, Keystone, Colorado, Colorado State University, October 2-5, pp 757-764.
- Caldwell, J. A. 2017. Tailings History: 2016 & 2017, *Tailings and Mine Waste '17*, Banff, Alberta, University of Alberta Geotechnical Center, 5-8 November, pp 87-91.
- Canadian Dam Association (CDA) 2013. *Dam Safety Guidelines, 2007 (Revised 2013)*. CDA.
- Davidson, R. R. 2017. The State of Mining Geotechnics, *Tailings and Mine Waste '17*, Banff, Alberta, University of Alberta Geotechnical Center, 5-8 November, pp 44-52.
- International Commission on Large Dams, Committee on Mine & Industrial Tailings Dams (ICOLD) 1989. Tailings Dam Safety, Guidelines, *Bulletin 79*. Paris: ICOLD.
- International Commission on Large Dams, Committee on Design Flood (ICOLD) 1992. Selection of Design Flood, Current Methods, *Bulletin 82*. Paris: ICOLD.
- Klohn Krippen Berger (KCB), 2017. Study of Tailings Management Technologies, MEND Report 2.50.1, sponsored by the Mine Environmental Neutral Drainage (MEND) Program and the Mining Association of Canada, September.
- McKenna, G., R. An, E. Scordo, and J. McGreevy 2013. Toward effective closure planning: From progressive reclamation to sustainable mining, *Tailings and Mine Waste '13*, Banff, Alberta: University of Alberta, November 3-6, pp 615-626.
- Robertson, A. MacG, and D. van Zyl, 2016. Risk, Resilience and Robustness of Mine Waste Facilities, Strachan, C. L., and S. Goodwin 2015. Conclusions from Evaluation of Tailings Dam Incidents, *Proceedings*, USSD Annual Meeting, Miami, April 30 – May 2.
- Strachan, C. L., and S. Goodwin 2015. The Role of Water Management in Tailings Dam Incidents, *Tailings and Mine Waste 2015*, Vancouver, British Columbia, October 26-28, pp 329-342.
- Strachan, C. L., and B. Van 2018. Conclusions from Evaluation of Tailings Dam Incidents, *Proceedings*, USSD Annual Meeting, Miami, April 30 – May 2.
- U.N. Environment and GRID-Arendal (UNEP) 2017. *Mine Tailings Storage: Safety Is No Accident*, United Nations Environment Programme, November.

- U.S. Committee on Large Dams, Committee on Failures and Accidents to Large Dams (USCOLD) 1976. *Lessons from Dam Incidents USA*, ASCE/USCOLD.
- U.S. Committee on Large Dams, Committee on Dam Safety (USCOLD) 1988. *Lessons from Dam Incidents USA II*, ASCE.
- U.S. Committee on Large Dams, Committee on Tailings Dams (USCOLD) 1994. *Tailings Dam Incidents*. Denver: U.S Committee on Large Dams.

A Geotechnical Monitoring System to Support Implementation of the Observational Method at Teck Highland Valley Copper

G. Afriyie, B. Bale, and C. Anderson

Teck Highland Valley Copper Partnership, Logan Lake, British Columbia, Canada

ABSTRACT: The Observational Method of design is a useful tool in the effective risk management of dam design and construction. This Method is used for the design and construction of the L-L dam which is classified as an *Extreme* consequence dam. The successful implementation of this design approach is critically dependent on the ability to measure predicted design parameters to actual conditions. Teck Highland Valley Copper Partnership (THVCP) has a robust Geotechnical Monitoring System and formalized review process in place, to ensure the effective monitoring of the design parameters against actual conditions. As part of continuous improvement at THVCP and implementation of Best Available Technologies (BAT), instrument capacity has been increased at the different dam domains and several upgrade initiatives have been undertaken at the L-L dam. The monitoring program and these initiatives have been effective towards using the Observational Method at the L-L dam and are considered to be an example of appropriate stewardship of an *Extreme* consequence dam.

1 INTRODUCTION

Recent failures of major tailings dams worldwide have increased scrutiny on dam owners, dam designers and regulators, to provide assurance for the safety of these structures. With an estimated of 3,500 active tailings dams worldwide (Davies, 2002) and increasing demand for mining products from anticipated growth in population (Kesler, 2000), the inventory of tailings dams could increase in the coming years.

It is essential for tailings dam owners to use effective risk management tools to best allow the construction and maintenance of tailings dams meet the intent for which the dam was designed. Design engineers use the Conventional or Observational Method of design to inform the construction of various structures (Szatis-Nossan, 2006). The main difference between the two approaches is that the Observational Method allows for design changes to be made as the long term construction progresses and establishes a predefined framework for risk management (Powderham, 2015). To effectively use the framework which compares predicted key design parameters to measured parameters, a robust monitoring program to measure and document actual performance parameters is required.

The Observational Method of design is used as the design basis for the Highland Tailings Storage Facility (HTSF) whose main dam is the L-L dam at the Teck Highland Valley Copper Partnership (THVCP) mine. The application of this method of design for this *Extreme* Consequence dam (CDA, 2007) is effective due to:

- a robust dam monitoring program at the site level,
- early notification of undesirable observations or measurements to the Engineer of Record (EoR),
- a formalized review procedure at the site level,

- frequent, routine review of all available data by the EoR.

Over the 41 year operation of this tailings dam, the monitoring program and associated actions as listed above have proven to be effective towards the implementation of the Observational Method and is considered to be an example of appropriate stewardship of an *Extreme* consequence dam.

The Highland Valley Copper (HVC) Mine, as shown in Figure 1a, has the largest hydraulic sand tailings dam in Canada and one of the largest in the world. Classified as an *Extreme* consequence dam, the L-L dam as shown in Figure 1b is the main dam forming the active HTSF. The dam is currently 169 m high, 3 km wide, and constructed of cycloned sand with a till core.



Figure 1a Location of The Highland Valley Copper Mine



Figure 1b Site Overview Map of THVCP

2 OBSERVATIONAL METHOD

The formulation and development of a systemic procedure for the use of the observational approach in design is attributed to Terzaghi (Terzaghi & Peck, 1967; Peck, 1969), with a formalized framework for implementing the Observational Method of design by Peck (Peck, 1969). The Observational Method has been used successfully by engineers in the design and construction of tunnels, dam embankments, cofferdams, building foundation, and tunnels (Powderham, 2004; Peck, 1969).

2.1 The Framework, Advantages and Limitations of the Observational Method

There are eight formal steps in the Observational Method (Peck, 1969). These steps are:

- a. Exploration sufficient to establish at least the general nature, pattern and properties of the deposits, but not necessarily in detail
- b. Assessment of the most probable conditions and the most unfavourable conceivable from these conditions
- c. Establishment of the design based on a working hypothesis of behaviour anticipated under the most probable conditions
- d. Selection of quantities to be observed as construction proceeds and calculation of their anticipated values on the basis of the working hypothesis
- e. Calculation of values of the same quantities under the most unfavourable conditions compatible with the available data concerning the subsurface conditions
- f. Selection in advance of a course of action or modification of design for every foreseeable significant deviation of the observational findings from those predicted on the basis of the working hypothesis
- g. Measurement of quantities to be observed and evaluation of actual conditions
- h. Modification of design to suit actual conditions.

The successful implementation of this design approach is critically dependent on step 'g' which measures predicted parameters to actual conditions. To diligently carry out this step it is essential to ensure:

- well defined parameters of measurement
- a robust monitoring program
- formal procedure for data verification and review
- effective communication between the design engineer and construction team

The application of the method provides many benefits if applied correctly. These benefits include, cost savings due to optimization of the design through construction, a strong connection of the design to construction, higher quality of data available to measure performance, and assurance of acceptable safety (Spross, 2014; Powderham, 2004; Peck, 1969).

Like every design approach the Observational Method has its limitations. One key limitation of the Method is inability to apply to projects that cannot adapt to changes (Peck, 1969).

2.2 Application of the Observational Method to the L-L dam

The Observational Method implemented on the L-L dam, which is an *Extreme* consequence dam, has been undertaken in accordance with the 8 steps as described by Peck (Peck, 1969). The first step was extensive characterization of the subsurface conditions including drilling, geophysical surveys, in-situ testing and retrieval of samples for laboratory analysis for a detailed understanding of the foundation conditions at the L-L dam.

From this data set the Most Likely Case (MLC) design parameters and Reasonable Worst Case (RWC) design parameters are interpreted for design. The MLC and RWC parameters are used in the design models with key parameters like deformation and pore water pressure predicted for each case. For the RWC conditions, suitable contingency plans are provided as part of the design to mitigate these conditions during construction of the dam. The key parameters are measured during construction and deviations from the MLC behaviours are identified with sufficient time to change the design or implement another contingency.

The monitoring program at the L-L dam is part of a Trigger Alert Response Plan (TARP). The TARP identifies deviation from the MLC parameters and is also tied to the dam Emergency Response Plan. The TARP developed for the geotechnical monitoring systems are reviewed annually and updated based on dam performance. At the site level, a robust monitoring program, a formalized review process for verification and analysis of data as well as an effective reporting procedure to communicate with the EoR is in place. This ensures proper measurement, monitoring and documentation of actual measurements in comparison to the predicted design parameters (TARP) and initiates changes to the design or implementation of contingencies per the Observational Method.

3 GEOTECHNICAL MONITORING OF THE L-L DAM

As previously discussed, the Observational Method is critically reliant on a robust monitoring program. At the site level, a robust geotechnical monitoring program has been designed together with the EoR for the L-L dam. This monitoring program has also been reviewed by both external engineers independent of the EoR through Dam Safety Reviews as well as continually by the External Independent Tailings Review Board (ITRB) - both of which confirm that the monitoring program is “robust”. The program is designed primarily to ensure that actual dam performance parameters can be measured and documented appropriately to support the Observational Method of design adopted for the dam. Data collected from the monitoring program undergoes rigorous review to analyze instrument trends in comparison to predicted design parameters.

3.1 L-L Dam Monitoring Program

Dam performance monitoring is done through the use of geotechnical monitoring systems and visual surveillance. Formally trained THVCP personnel who are involved in the monitoring program of the L-L dam are well informed on the Observational Method and the TARP established for the geotechnical monitoring systems. Monitoring and reporting on the L-L dam is undertaken by the Tailings and Water Department at THVCP.

The geotechnical monitoring systems or instrumentation at the L-L dam are made up of piezometers (standpipes, and vibrating wire piezometers) and inclinometers (standard inclinometers, ShapeAccelArray and In-Place-Inclinometers).

There are over 150 active piezometers across the entire length of the dam. These instruments are divided into 4 groups and monitored on a weekly basis; hence, each instrument is read on a monthly frequency during normal operation of the dam. The 4 groups are created such that each weekly reading gives an indication of piezometric elevations across all of the different domains of the L-L dam.

In addition to the piezometers, there are 30 inclinometers located at different domains of the dam. The inclinometers are read on a monthly frequency during normal operation. Similar to the piezometers, the inclinometers are divided into 4 groups such that movement and piezometric elevations can be correlated on a weekly basis across the different domains.

During construction sentinel instruments are selected and the monitoring frequency increased depending on the construction activity. The frequency for construction is typically daily to weekly for piezometers depending on the relative location to the activity and its screened unit. For inclinometers, the increased frequency is typically weekly for construction.

Each piezometer and inclinometer has alerts defined for monitoring both pore water pressure and deformation respectively. For the inclinometers, the deformation alerts are defined for the different foundation units. In efficiently monitoring these alerts, THVCP has an e-mail automated notification system as part of the monitoring program. The notification system helps in the quick identification of alerts and reporting to the EoR for action.

In addition to the geotechnical monitoring systems, visual surveillance is conducted on a daily frequency on the L-L dam by qualified THVCP personnel. The record from the surveillance is in the form of digital forms and photos. These records help in correlating physical observations to instrument interpretation as well as detect physical defects.

This robust monitoring program allows for dam performance to be monitored effectively, using installed instruments to detect and document trends for piezometric elevations as well as dam movement. The visual surveillance in addition detects any physical changes to the dam components.

This program as designed by THVCP is adequate to ensure that predictions as laid out in the Observational Method framework are adequately monitored against to ensure the successful application of the method.

3.2 Review Process for Dam Monitoring

As discussed earlier, the application of the Observational Method is reliant on the quality of data measured and formal process for data verification, review and documentation. THVCP utilizes a 5 step quality control (QC) and quality assurance (QA) process as shown in Figure 2. Upon completion of instrument readings, THVCP's dam inspectors conduct the initial review/processing of instrumentation data to ensure that readings taken from the field are of acceptable quality. Second, a geotechnical engineer reviews the data for trends and compares actual measurements to the design prediction targets as provided by the EoR.

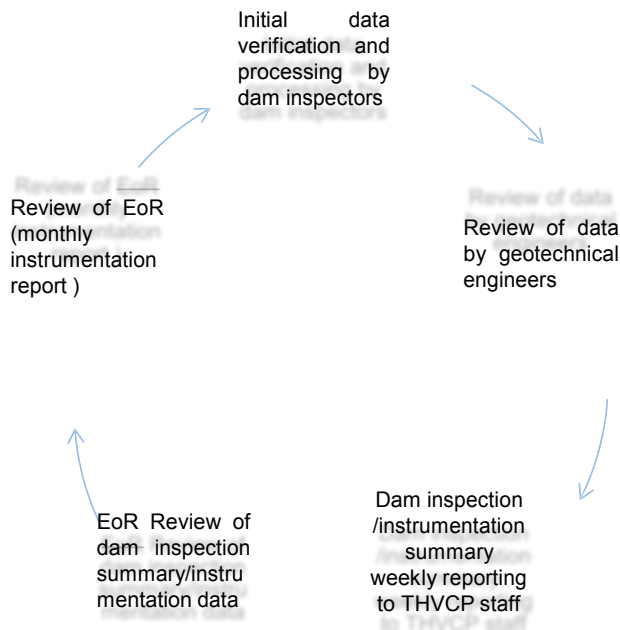


Figure 2 Routine QC/QA process for data verification and interpretation at THVCP

Instrument trends, visual observations and key performance indicators (KPI) are compiled for presentation to senior staff of the Tailings and Water Department including the Qualified Person (QP) for the L-L dam on a weekly basis. This allows for the QP and all staff to review and provide feedback on dam performance parameters. The weekly KPIs include a dashboard showing the weekly inclinometer trends at a glance across all the domains, conformance to deposition planning into the HTSF impoundment, construction activities on the L-L dam and operating levels of various water storage facilities on site. This weekly meeting condenses the overall performance of the L-L dam into a 2 hour review. The minutes from the meeting in the form of a PowerPoint slide deck are then sent to the EoR for review and comments within 24 hours. This ensures that the EoR is particularly aware of weekly observations and instrumentation trends at the L-L dam.

During the site review, if instrument trends should exceed predicted design parameters, THVCP reports this to the EoR within 24 hours of the observation. The EoR in turn provides a monitoring memo to THVCP discussing the causes of the exceedance and any recommended actions in the form of a Monitoring Review Memo (MRM).

In addition to the weekly review undertaken by the EoR, the verified instrument data are provided to the EoR for processing and analysis. A Routine Monthly Review (RMR) memo is then issued to THVCP discussing instrument trends, causes of observed trends, recommendations and action items. The RMR is then reviewed by THVCP at a monthly instrumentation meeting and feedback is provided to the EoR.

This combination of site-based quality control and interpretation, combined with external interpretation is considered to be appropriate for a dam of this importance.

4 THVCP MONITORING UPGRADES

As part of continuous improvement and implementation of Best Available Technologies (BAT). THVCP has undertaken several projects over the past few years to improve dam performance monitoring in support of the Observational Method. These projects include upgrades to the visual surveillance and geotechnical monitoring system/instruments.

4.1 Geotechnical Monitoring System upgrades

The geotechnical monitoring systems/instruments at the L-L dam have also undergone significant upgrades to improve on reporting and documentation of information retrieved from the instruments. About 35% of instruments have been installed over the last few years to increase capacity as well as provide redundancy for monitoring of key foundation units. Redundancy has been provided by installing multiple instruments within the same foundation units to improve resiliency across the entire dam. The objectives of the upgrade to the system were mainly to improve access to data through real time monitoring, identify and automate reporting of threshold exceedances as defined by the TARP, as well as improve analysis of instrument trends by collecting continuous data.

In achieving the aforementioned objectives, existing standpipes were converted to vibrating wire piezometers and in-place-inclinometers were deployed into standard inclinometers for monitoring critical foundation units. The standpipes were converted by defining tip elevations within the standpipes and dropping vibrating wire piezometers into the standpipes. The vibrating wire piezometers were then connected to telemetry units to transmit data to the e-mail notification system. All historic data for the different standpipes from manual dips were also imported into the e-mail notification system to have the full history of the instrument for comparing trends. Due to bends within some of the standpipes, vibrating wire piezometers could not be installed. For these instruments, a field app has been created to allow for data to be sent to the e-mail notification system directly when data is manually taken.

For standard inclinometers, discrete zones of movements were identified based on historic data for In-Place-Inclinometers (IPI) to be installed for continuous monitoring of the discrete

zones. These IPIs were then connected to telemetry units to transmit data to the e-mail notification system. These IPIs are removed annually for manual reading of the full inclinometer depth to be taken. This helps to get data for other foundation units and serves as a check for the IPI readings.

Real time monitoring on the L-L dam is highly beneficial to the Observational Method. This allows for easy access to data and monitoring of data trends for dam performance during construction. The real time notification system has also improved the identification and automatic reporting of threshold exceedances or alerts. The system transmits an e-mail to select personnel when alert values are exceeded for piezometers or inclinometers. In addition to this, continuous data is collected for each instrument. This allows for easy review and optimization of construction using the Observational Method. This initiative has also reduced the workload on dam monitors in manually reading instruments and reduced the risk of repetitive strain that could result from manually reading these instruments.

4.2 Dam surveillance upgrades (visual)

The previous visual surveillance process consisted mainly of paper forms and photos. In upgrading this aspect of monitoring, the forms were digitally produced via a Geographic Information System (GIS) based platform to allow these forms to be operated electronically. The forms are operated using tablets or cell phones. The purpose of the upgrade was to improve data management for the visual surveillance, improving ease with logging and tracking observed issues, and real time monitoring of visual surveillance.

Data management and reporting is one of the key steps for the successful implementation of the Observational Method. The upgrade allows data to be categorized by date, dam components, observations and deficiencies. The electronic forms improve the ease of searching and reporting on observations as opposed to searching for information from scanned reports.

One of the advantages of the observational approach is the ability to review observations and make the proper adjustments during construction. These observations and the actions taken have to be tracked and documented appropriately. The electronic forms data categorizes action items which can be easily accessed and tracked for completion. This makes it easy as a site to demonstrate to key stakeholders the implementation of the Observational Method and actions arising from key field observations.

The electronic forms also allow for real time monitoring of visual surveillance. This allows dam monitors to escalate potential issues via e-mail to select personnel for actions to be taken. This allows for quick reporting of observations to THVCP management and the EoR. The e-mail is transmitted with coordinates of the identified issues for reviewers to quickly check on escalated items.

5 CONCLUSION

The application of the Observational Method is appropriate for dams. It is particularly useful for dams of *Extreme* consequence and can enable cost savings due to the ability to optimize construction during design, a stronger connection of design to construction allowing a team based approach for risk management between contractor and designer, and increased safety during construction due to ongoing monitoring for changes to performance of a structure under construction. Also, it improves continuous understanding of soil/structure interactions as a result of the continuous measurement of key performance parameters as well as provides case history data for future design and construction through formal documentation (Spross, 2014; Powderham, 2004; Nicholson et al., 1999; Powderham, 1994; Terzaghi and Peck, 1967; Peck, 1969).

Although the benefits above make the application of the method attractive for applicable projects especially tailings dam where the construction of the dam spans multiple years, it is essential to note that the successful application of the method on any tailings dam is heavily reliant on monitoring instrumentation and interpretation. A good network of geotechnical

monitoring systems, frequent routine dam inspections, early notification of undesirable observations or measurements, formalized review procedure at the site level and frequent, routine review of all available data by the EoR are essential parts of the Observational Method.

In striving for best practices in dam safety, dam owners who use the Observational Method should increase instrument capacity across all dam domains to ensure dam resiliency, monitor instruments weekly to verify predicted design parameters and have a formalized QC/QA process at the site level with the EoR for data interpretation/discussion to ensure successful use of the Observational Method as a risk management tool.

REFERENCES

- Canadian Dam Association (2007). Dam Safety Guidelines. www.cda.ca
- Davies, M. P. (2002). Tailings impoundment failures: are geotechnical engineers listening. *Geotechnical News*, September, 2002, 31-36.
- Kesler, S. E. (2007). Mineral supply and demand into the 21st century. In *Proceedings for a workshop on deposit modeling, mineral resource assessment, and their role in sustainable development*. Circular (Vol. 1294, pp. 55-62).
- Peck, R. B. (1969). Advantages and limitations of the observational method in applied soil mechanics. *Geotechnique*, 19 (2), 171-187.
- Powderham, A. (1994). An overview of the observational method: development in cut and cover and bored tunnelling projects. *Geotechnique*, 44 (4), 619-636.
- Powderham, A. (2004). *The observational method-learning from projects*.
- Spross, J. (2014). *A critical review of the observational method* (Unpublished doctoral dissertation). KTH Royal Institute of Technology.
- Szavits-Nossan, A. (2006). Observations on the observational method. In *Xiii. danube-european conference on geotechnical engineering*.
- Terzaghi, K., Peck, R. B., & Mesri, G. (1996). *Soil mechanics in engineering practice*. John Wiley & Sons.

Comparing CPT and Vs Liquefaction Triggering Methods for Mine Tailings

R. Moghaddam, Y. Mao, and S. Kam
Golder, Mississauga, Ontario, Canada

ABSTRACT: To assess the liquefaction potential of soft ground such as deposited mine tailings, the small-strain shear modulus (G_{\max}) is required in analytical procedures for estimating dynamic ground response. G_{\max} is directly related to the shear wave velocity (V_s), which can be measured in the field. This paper examines the use of V_s as a field index of liquefaction resistance. Liquefaction methods based on V_s have the advantage that they do not consider soil characteristics, such as fines content, which might be of concerns with regards to liquefaction assessment of non-plastic fine-grained tailings. This paper presents the results of liquefaction assessment for two mine tailings using a CPT-based method in comparison with V_s -based method in a case study. In this study, the in-situ shear wave velocity was directly measured using a seismic cone penetrometer.

1 INTRODUCTION

The ‘simplified procedure’ which was originally developed by Seed and Idriss (1971) is the common practice for predicting liquefaction potential of soils induced by earthquakes. In this procedure, the cyclic resistance ratio (CRR) of the soil is compared with a parameter representing the seismic loading on the soil, called cyclic stress ratio (CSR).

The procedures based on the Standard Penetration Test (SPT), Cone Penetration Test (CPT), and small-strain shear-wave velocity (V_s) measurements have been developed to estimate the CRR of the soil as described in a report by the National Research Council (1985) and a summary report from the 1996 National Center for Earthquake Engineering Research (NCEER) and 1998 NCEER/National Science Foundation (NSF) workshops on evaluation of liquefaction resistance of soils by Youd et al. (2001). The peak horizontal acceleration of at ground surface is required to estimate the CSR in this procedure.

As stated by Youd et al. (2001), SPTs and CPTs are generally preferred (for assessment of liquefaction resistance) because of the more extensive databases and past experience. Although this might be a fact for natural soils, there are limited site calibrated data for mine tailings. The use of these procedures to assess the liquefaction potential of deposited mine tailings may not be appropriate. The limitation on the simplified method when applied to mine tailings has been noted by some authors (e.g., James et al. 2011).

Deposited mine tailings are usually classified as soft ground (e.g., Site Class E or F - $V_s < 375$ m/s) based on the National Building Code of Canada (NBCC). To assess the liquefaction potential of these tailings deposits, the small-strain shear modulus (G_{\max}) is required in analytical procedures (i.e., one-dimensional ground response analysis) for estimating the peak ground acceleration and as a result the CSR in the simplified procedure. G_{\max} is directly related to the shear wave velocity (V_s), which can be measured in the field. In addition, the use of V_s as a

field index of liquefaction resistance is soundly based because both V_s and cyclic resistance ratio are similarly, but not proportionally, influenced by void ratio, effective confining stresses, stress history, and geologic age. Liquefaction methods based on V_s have the advantage that they do not consider soil characteristics, such as fines content, which might be of concerns with regards to liquefaction assessment of non-plastic fine-grained tailings, as most of these methods are based on empirical relationships for natural soil deposits.

This paper presents the results of CRR estimation for tailings deposited in two mine sites using the CPT-based methods developed by Robertson and Canal (2015) and Boulanger and Idriss (2015) in comparison with the V_s -based method by Andrus et al. (2004). The in-situ shear wave velocity was directly measured using a seismic cone penetrometer (SCPT) while obtaining the CPT data.

2 METHODOLOGY

The shear wave velocity-based method of CRR calculation presented in Andrus et al. (2004), which is a modification to Youd et al. (2001), was used in this paper. As described by Andrus et al. (2004), the traditional procedures for correcting penetration resistance, V_s should be corrected to a reference overburden stress by Equation 1 (Sykora 1987, Robertson et al. 1992):

$$V_{s1} = V_s \quad C_{vs} = V_s \left(\frac{P_a}{\sigma'_v} \right)^{0.25} \tag{1}$$

where V_{s1} is stress-corrected shear-wave velocity, P_a is a reference stress of 100 kPa, and σ'_v is initial effective overburden stress in kPa. The CRR is then defined by Equation 2, which is an empirical relationship developed by Andrus and Stokoe (2000) for magnitude 7.5 earthquakes and un-cemented soils of Holocene age with case history data.

$$CRR = MSF \left[0.022 \left(\frac{K_{a1} V_{s1}}{100} \right)^2 + 2.8 \left(\frac{1}{V_{s1}^* - (K_{a1} V_{s1})} - \frac{1}{V_{s1}^*} \right) \right] K_{a2} \tag{2}$$

where MSF is the magnitude scaling factor (i.e., MSF=1 for M7.5), K_{a1} is a factor to correct for high V_{s1} values caused by aging, K_{a2} is a factor to correct for influence of age on CRR, and V_{s1}^* is the limiting upper value of V_{s1} for liquefaction occurrence. Andrus and Stokoe (2000) suggested the following relationship for estimating V_{s1}^* :

$$V_{s1}^* = 215 \text{ m/s for } FC < 5\% \tag{3a}$$

$$V_{s1}^* = 215 - 0.5(FC - 5) \text{ m/s for } 5\% < FC < 35\% \tag{3b}$$

$$V_{s1}^* = 200 \text{ m/s for } FC > 35\% \tag{3c}$$

where FC is average fines content in percent by mass. In this study, K_{a1} and K_{a2} were considered to be 1 as none of these factors were applicable for young deposited tailings and FC was estimated based on the particle size distribution curves of the samples obtained during the investigation.

3 SITE DESCRIPTION

3.1 Site A

The Site A is located in Northern Ontario, Canada. The tailings facility at this site is contained by a series of engineered, low permeability dams. The perimeter dams were constructed in 1996, raised in 2000 and again in 2005.

The tailings facility capacity was expanded in 2010 with the commencement of thickened

tailings disposal, from a series of starter berms constructed on the deposited tailings beach upstream of the perimeter dams. The berms have since been stage raised with the upstream method of construction.

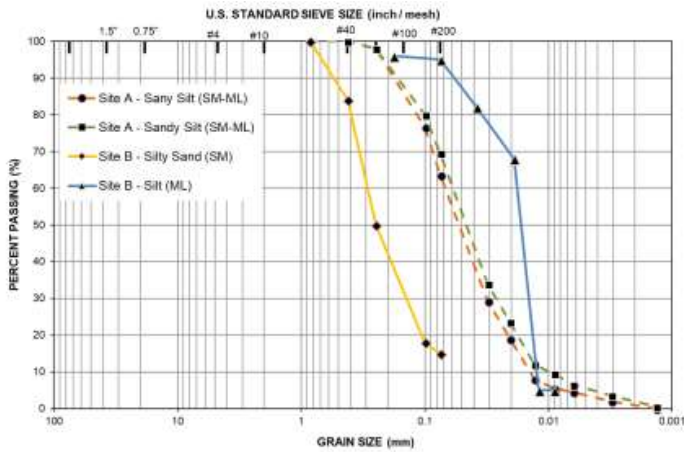
Mill tailings slurry has a typical solids content of about 50% prior to entering the thickened tailings plant. The slurry is thickened to between 65 and 68% solids in a tailings thickening plant located at the west end of the tailings facility before being discharged. About 75% of the processing water is reclaimed from the tailings pond.

The tailings are non-plastic with a gradation ranges from silt sand (SM) to sandy silt (ML), as shown on Figure 1. The specific gravity of the tailings is 3.25. CPT profiles were obtained through the deposited thickened tailings and the underlying slurry tailings.

3.2 Site B

Site B is a closed Tailings Management Area (TMA) in northern Ontario. The facility was decommissioned from 1991 to 1995 to accommodate a water cover over the impounded tailings. The TMA uses a shallow water cover to maintain tailings saturation to mitigate long-term environmental impacts. The main site activities are effluent treatment, environmental monitoring, routine surveillance and maintenance, and reporting to regulatory agencies.

The Site B TMA has a number of perimeter containment dam structures within an undulating bedrock basin, as well as internal dykes. The internal dykes were constructed over the tailings beach and/or historical waste rock dykes during operation, to maintain a water cover in each cell for closure. The SCPT data were obtained during a recent site investigation. The tailings samples obtained along the SCPT profiles during the drilling program of the investigation indicate that the tailings are non-plastic with a gradation ranging from silt (ML) to silty sand/sand (SM-SP), as shown on Figure 1. The specific gravity of the tailings is 2.72.



Contractive – Sensitive (CCS); (2) Clay-like – Contractive (CC); (3) Clay-like – Dilative (CD); (4) Transitional – Contractive (TC); (5) Transitional – Dilative (TD); (6) Sand-like – Contractive (SC); and (7) Sand-like – Dilative (SD). The groups that capture soils that are in transition from sand-like to clay-like ($32 < IB < 22$) are called transitional.

Idriss and Boulanger (2008) suggested that sand-like soils are susceptible to cyclic liquefaction, but clay-like soils are not. They also suggested that fine-grained soils transition from behavior that is more fundamentally like sands to behavior that is more fundamentally like clays over a fairly narrow range of Plasticity Index (PI). Sand-like soils tend to have $PI < 10\%$ and clay-like soils tend to have $PI > 18\%$ (Bray and Sancio 2006).

As described by Robertson (2016), the transition from more sand-like to more clay-like behavior is conceptually similar to the transition in the Unified Soil Classification System (USCS) from coarse-grained (non-plastic) to fine-grained (plastic) soils, although some low-plastic or non-plastic fine-grained soils (e.g., silt and low-plasticity clay) can behave more sand-like, as suggested by Idriss and Boulanger (2008). Note that the contractive fine-grained non-plastic tailings might be classified as CCS or TC.

Likewise, the transition from saturated soils that are more sand-like to more clay-like typically corresponds to a response that transitions from one that is predominately drained under most static loading to a response that is predominately undrained under most static loading, although the rate of loading also has a major role.

4.1 Site A Tailings Profile

Figure 2 shows the corrected cone resistance (qt), sleeve friction (fs) and SBT classification with depth at the representative SCPT profile for Site A. The SCPT profile consists of two distinct tailings units classified based on the SBT Chart: (1) a top unit of sand-like contractive (SC) tailings from the ground surface to a depth of 10 mbgs corresponding to the stage of thickened tailings deposition; and (2) a bottom sand-like dilative (SD) unit from a depth of 10 mbgs to 20 mbgs with multiple sand-like contractive (SC) interlayers. In other words, the slurry tailings shows both SD and SC types of behavior. This unit corresponds to the stage of slurry tailings deposition. Both SC and SD tailings are non-plastic with fines content ranges between 5% and 15% based on the sample obtained at this location.

4.2 Site B Tailings Profile

Figure 3 shows the corrected cone resistance (qt), sleeve friction (fs) and SBT classification with depth at the representative SCPT profile for Site B. The SCPT profile consists of two distinct tailings units classified based on the SBT Chart: (1) a top unit of sand-like contractive (SC) tailings from a depth of 13 mbgs to 18 mbgs; and (2) a bottom fine-grained tailings unit from a depth of 18 mbgs to 25 mbgs that exhibits a range of behavior from clay-like contractive (CC) to clay-like contractive – sensitive (CCS). Note that the CC and CCS tailings are non-plastic with 100% fines content (i.e., < 75 microns). The SC tailings are also non-plastic with fines content ranging between 5% and 15% based on the samples obtained at this location. These two tailings types are located at the foundation of the internal dyke, which has to be drilled out during the CPT investigation.

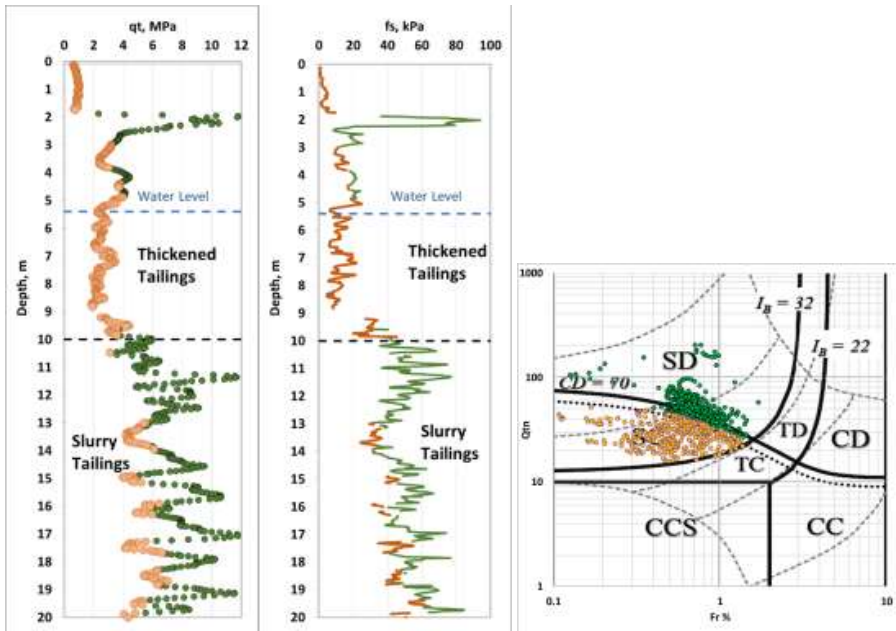


Figure 2. Site A tailings profile and SBT classification.

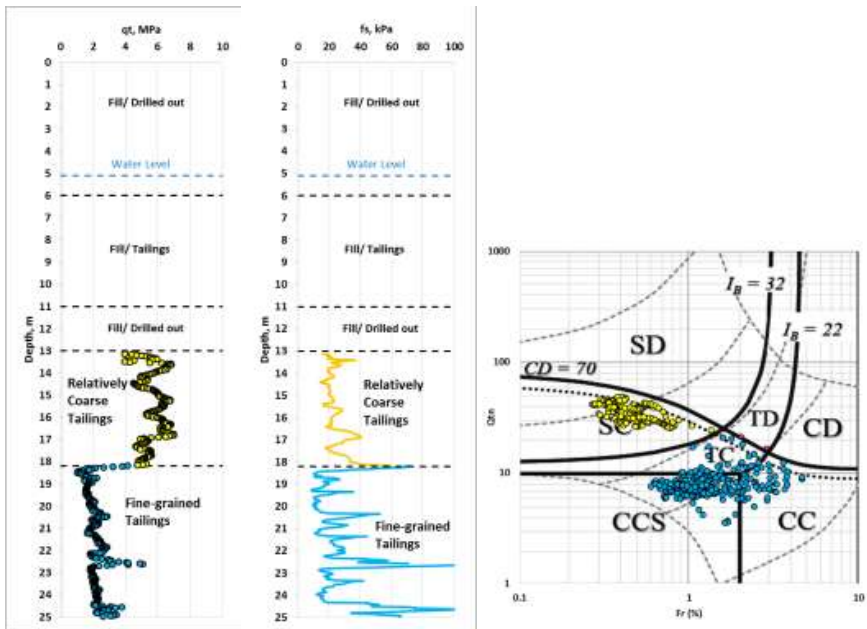


Figure 3. Site B tailings profile and SBT classification.

5 SHEAR WAVE-BASED CRR RESULTS

5.1 Site A CRR Estimation

Figure 4 shows the field V_s and V_{s1} calculated based on Equation 1 for Site A. The field V_s ranges between 163 m/s and 229 m/s. For the thickened tailings (SC) below the water level, the average field V_s is 173 m/s while the average field V_s for the slurry tailings (SD) is about 209 m/s. In contrast, the V_{s1} value is estimated to be between 163 m/s and 197 m/s. In addition, the V_{s1} value was also calculated based on the CPT data using an equation proposed by Robertson (2015). The CPT-based V_{s1} values were found to correlate well with the field V_{s1} values of the slurry tailings but they are lower than the field V_{s1} values for the thickened tailings.

The V_s -based CRR values for Site A are also presented in Figure 4 along with the CPT-based CRR values. It is apparent that the V_s -based CRR values are generally higher than those of the CPT-based method except for a section between 9 mbgs and 12 mbgs, where the values are matched. The apparent discrepancy will be discussed in Section 6.

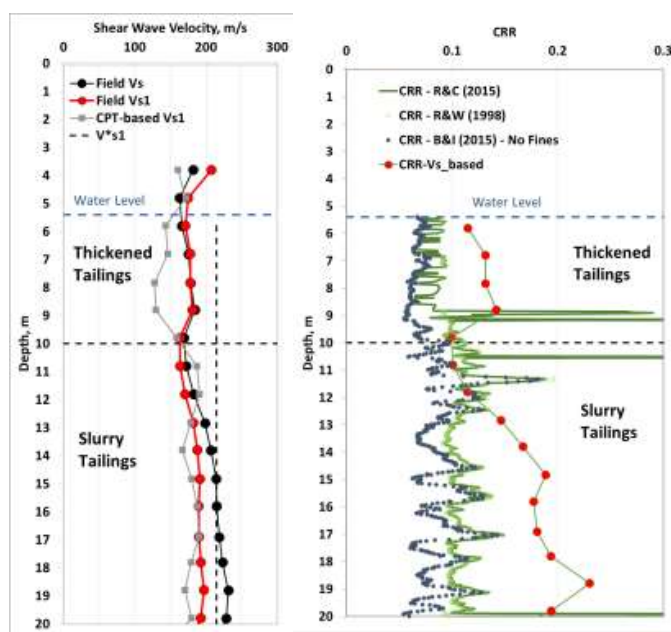


Figure 4: Site A – Shear wave velocity and estimated CRR values (MSF=1 for M7.5).

5.2 Site B CRR Estimation

Figure 5 shows the field V_s and V_{s1} calculated based on Equation 1 for Site B. The field V_s ranges between 167 m/s and 295 m/s. For the relatively coarse tailings (SC) unit below the water level, the average field V_s is 194 m/s while the average field V_s for the fine-grained tailings (CCS-CS) is about 280 m/s. In contrast, the V_{s1} value is estimated to be between 148 m/s and 243 m/s. The V_{s1} value for fine-grained tailings was observed to be higher than the V_{s1}^* value. In addition, the CPT-based V_{s1} values correlate well to some extent with the field V_{s1} values for coarse tailings but they are significantly higher than the field V_{s1} values for fine-grained tailings.

The V_s -based CRR values for Site B are also presented in Figure 5 along with the CPT-based CRR values. It is apparent that the V_s -based CRR values are slightly higher than those obtained for the CPT-based method for relatively coarse tailings (SC). However, the V_s -based CRR values for fine-grained tailings are not estimated as the V_{s1} values exceed the upper

limit (V_{s1}^*) value. The CPT-based CRR values for fine-grained tailings based on Robertson and Wride (1998) and Robertson and Cabal (2015) are also shown on Figure 5. The apparent differences are discussed in Section 6.2.

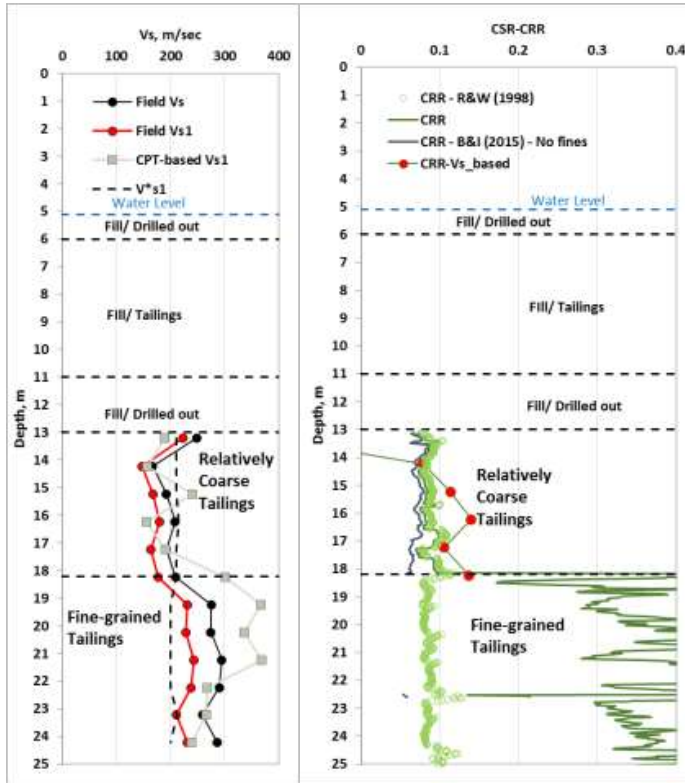


Figure 5: Site B - Shear wave velocity and estimated CRR values (MSF=1 for M7.5).

6 INTERPRETATION AND DISCUSSION

6.1 Effect of Fines on CRR

The CPT-based CRR values estimated for sand-like tailings (SC and SD) in this study were based on Robertson and Wride (1998) and Robertson and Cabal (2015). These two methods include a fines correction factor for sands. However, James et al. (2011) stated that sand-like hard rock tailings tend to behave similar to clean sands with respect to their shear strength and penetration resistance and applying the correction factor for fines content can result in an overestimation of the CRR values. A CPT-based method developed by Boulanger and Idriss (2015) was used to estimate the CRR values ignoring effect of fines content, as shown on Figures 4 and 5. It is apparent that applying a fines correction factor increases the CRR values. Having said that a comparison between the CPT-based CRR values and Vs-based CRR values for sand-like tailings (SC and SD) shows that the Vs-based values are equal or higher than the CPT-based values even if we consider applying a fines content factor.

6.2 CRR for Fine-grained Tailings

It was observed that the CPT-based CRR values based on Robertson and Cabal (2015) for the CCS and CC tailings are significantly higher than the CPT-based CRR values based on Robertson and Wride (1998) as these materials were considered as sand-like type in 1998. In contrast, the CPT-based method developed by Boulanger and Idriss (2015) does not provide any CRR values for these types of material (i.e., CCS-CS).

The CPT-based method based on Robertson and Cabal (2015) has been developed for natural soils rather than tailings. All soils with I_B values > 22 are considered clay-like soils with PIs more than 10%, as described in Section 4. However, fine-grained tailings (CCS-CC) are non-plastic and do not exhibit clay like behavior. Therefore, CPT-based CRR values for “clay-like” tailings are overestimated. The V_s -based method did not provide any values for these materials considering liquefaction resistant as the V_{s1} values exceed the upper limit ($V_{s1}^* = 215$). To better understand the cyclic response of clay-like soils, Youd et al. (2001) suggested laboratory testing.

6.3 V_s versus Cone Resistance

The field V_s values for the fine-grained tailings (CCS-CC) were observed to be higher than the values for the coarse tailings (SC) for Site B. However, both q_t and f_s of the fine-grained tailings are lower than those of the coarse tailings. It is believed that the higher V_s of fine-grained tailings are related to the higher stiffness rather than the shear strength (i.e., cone resistance). Closely packed fine particles may indeed allow better transmission of shear wave. Although the V_s -based method suggests that cyclic liquefaction due to stiffness loss might not occur for fine-grained tailings, flow liquefaction might be of concerns for these materials due to loss of shear strength from pore pressure buildups.

6.4 V_s Measurements

V_s is influenced by degree of saturation in tailings. If V_s measurements are made when the groundwater table is low and a higher water table is possible, values of V_s above the water table may be too high due to negative pore-water pressures. Negative pore pressures can be particularly significant in silty soils. This effect should be considered in the estimation of for correcting V_s to V_{s1} (Andrus et al., 2004). Accordingly, the interpretation of V_s -based CRR should consider likely changes in the groundwater conditions.

The calculated V_s profiles and the measured V_s profiles can differ substantially as evident in Figure 5. As G_{max} is a parameter used to generate the ground acceleration profile in a one-dimensional ground response model, the use of field V_s should be encouraged as a means to improve accuracy of CSR estimates.

7 CONCLUSIONS

The CRR calculation for tailings with different mechanical properties was investigated in this paper based on the SCPT profiles obtained at two mine sites. It was observed that for the test cases examined the V_s -based CRR values are higher than the CPT-based CRR values for sand-like tailings. For fine-grained tailings in this study, no V_s -based CRR was estimated as the field V_{s1} was estimated to be higher than V_{s1}^* that can be considered to be non-liquefiable based on the case histories provided by Andrus et al. (2004). As such the use of V_s -based CRR should be cautioned.

The CPT-based CRR values might be significantly different depends if fine-grained tailings are considered to be sand-like or clay-like. Youd et al. (2001) suggests that samples need to be retrieved for fine-grained soils and to be tested in laboratory to investigate the response of these materials. The current state of practice to evaluate cyclic liquefaction of soils is based on the empirical relationship developed based on mainly natural soils case histories. To address cyclic

liquefaction of tailings, site-calibrated SCPT data should be used. Field measurement of V_s is recommended to improve accuracy of ground response modelling.

8 REFERENCES

- Andrus, R. D., Piratheepan, P., Ellis, B. S., Zhang, J., and Juang, C. H. (2004). "Comparing liquefaction evaluation methods using penetration- V_s relationships." *Soil Dyn. Earthquake Eng.*, 24(9–10), 713–721.
- Boulanger, R.W. and Idriss, I.M. 2008. Soil Liquefaction during Earthquake. EERI Publication, Monograph MNO-12, Earthquake Engineering Research Institute, Oakland.
- Bray, J. D., & Sancio, R. B. 2006. Assessment of the liquefaction susceptibility of fine-grained soils. *J. Geotech. Geoenviron. Eng.*, 132, 1165-1177.
- James, M., Aubertin, M., Wijewickreme, D. and Wilson G.W. 2011. A laboratory investigation of the dynamic properties of tailings, *Canadian Geotechnical Journal*, 48: 1587-1600.
- Robertson, P. K. 2016. Cone penetration test (CPT)-based soil behaviour type (SBT) classification system — an update. *Can. Geotech. J.* 00: 1–18-2016-0044.
- Robertson, P. K. 2015. Comparing CPT and V_s Liquefaction Triggering Methods. *Journal of Geotechnical and Geoenvironmental Engineering*, © ASCE, ISSN 1090-0241/04015037(10).
- Robertson, P. K. and Cabal, K. L. 2015. Guide to cone penetration testing for geotechnical engineering, Gregg Drilling and Testing Inc. 6th Edition.
- Robertson, P. K., and Wride, C. E. 1998. "Evaluating cyclic liquefaction potential using the cone penetration test." *Can. Geotech. J.*, Ottawa, 35(3), 442–459.
- Robertson, P. K., Woeller, D. J., and Finn, W. D. L., 1992. Seismic Cone Penetration Test for evaluating liquefaction potential under cyclic loading, *Can. Geotech. J.* 29 (4), 686–695.
- Seed, H.B. and Idriss, I.M. 1971. "Simplified Procedure for Evaluating Soil Liquefaction Potential" *J. Soil Mechanics and Foundations Div.*, ASCE 107:SM9, 1249-1274, 1971.
- Sykora, D. W., 1987. Creation of a data base of seismic shear wave velocities for correlation analysis, Geotechnical Laboratory Miscellaneous Paper GL-87-26, U.S. Army Engineer Waterways Experiment Station, Vicksburg, MS.
- Youd, T.L., Idriss, I.M., Andrus, R.D., Arango, I., Castro, G., Christian, J.T., Dobry, R., Liam, Finn, W.D., Harder, L.F. J., Hynes, M.E., Ishihara, K., Koester, J.P., Liao, S.S.C., Marcuson, W.F., Martin, G.R., Mitchell, J.K., Moriwaki, Y., Power, M.S., Robertson, P.K., Seed, R.B., and Stokoe, K.H. 2001. Liquefaction resistance of soils: Summary report from the 1996 NCEER and 1998 NCEER/NSF workshops on evaluation of liquefaction resistance of soils. ASCE, *Journal of Geotechnical and Geoenvironmental Engineering*, 127:817-833.

EGT – Innovative Fine Granular Material Sampling Technique

J.-F. St-Laurent

SRK Consulting Canada, Montréal, Québec, Canada

ABSTRACT: The properties of cohesionless soils are known to depend on numerous factors. High-quality in-situ tests or laboratory assays of truly undisturbed cohesionless soils are needed to determine their geomechanical behaviour under certain critical situations. However, current sampling methods as developed over the years can have an impact on soil properties. Indirect and in-situ sampling methods have therefore been developed to evaluate the geotechnical properties of soil deposits. These in-situ measurements are paired with geotechnical properties by using empirical correlations, which need to be validated with highly accurate samples of the undisturbed soil's in-situ density. This paper introduces a new highly efficient sampling technique that provides reliable samples of fine saturated granular material that may be considered as undisturbed. EGT sampling technique stabilizes fine-grained granular material by using a thermal fluidizing gelatin. A comparative assessment of the geotechnical behaviour shows that the proposed stabilization method preserves the geotechnical behaviour of subsamples.

1 INTRODUCTION

It is known that both static and cyclic shear strengths of cohesionless soils are highly influenced by numerous characteristics such as grain-to-grain configuration, the mineral precipitation at grain contacts, stress-strain history, and other properties. To evaluate the in-situ strength and deformation characteristics of cohesionless soils, high quality in-situ tests or laboratory assays on undisturbed soil samples must be conducted. Numerous sampling methods have been developed through the years to collect reliable samples for testing. Studies agree that sampling damages the “brittle” structure of cohesionless soils. As shown by Cuccovillo and Coop (1999), Vaid et al. (1999), Hoeg et al. (2000), and da Fonseca and Pineda (2017) the sampling method may impact the sample behavior by causing (i) water content variations, (ii) changes in void ratio, (iii) chemical constituent variations, and (iv) particle or constituent movements and mix and/or segregation.

In-situ and indirect methods as well as empirical correlation were developed to assess and determine the “intact” geotechnical properties of soil deposits as well as the liquefaction potential. However, as shown by Konrad (1990) those empirical correlations need to be validated with a highly accurate measurement of undisturbed soil/sample in-situ density. Moreover, as presented by Taylor et al. (2012), relying on high quality samples to capture the natural soil fabric has an effect on the cyclic and monotonic stiffness and strength characteristics and is of great interest, while tested soils tend to deviate from the initial dataset used to develop the empirical relations used to assess the liquefaction potential; as is the case with tailings.

Considerable efforts have been made in the past to develop and refine sampling techniques to obtain and maintain high quality samples for laboratory testing. Numerous studies have indicated that in-situ ground freezing using a large diameter tube sampler is probably the technique with the least disturbance potential. This technique allows us to increase the soil in-situ strength by freezing the inter-granular water. Hofmann et al. (2000) and Konrad & Pouliot (1997) have shown that care has to be taken while using this technique to limit sample disturbance. However, it is realistic to believe that pore water density variation associated to the freezing or thawing process will affect sample geo-mechanical behavior; even if the freezing rate is low and thaw is progressively applied in the laboratory under in-situ stress conditions. Taylor et al. (2012) has shown that the new Gel-Push sampler has great promise with some very good sand samples recovered from a site in New Zealand. However, it seems that the Gel-Push sampler design and procedure could be improved to enable sampling of loose sandy soils with a $V_s < 150$ m/s which are prone to densifying during the sampling procedure, as might be the situation with cyclone tailings beaches.

2 HIGH QUALITY SAMPLING – IDEALIZED

As presented by da Fonseca and Pineda (2017), truly undisturbed samples of sand can only be obtained if the in-situ sand structure is preserved before sampling. However, the typical nine stage soil sampling process represents a potential source of disturbance (Taylor et al., 2012) as schematically shown in Figure 1.

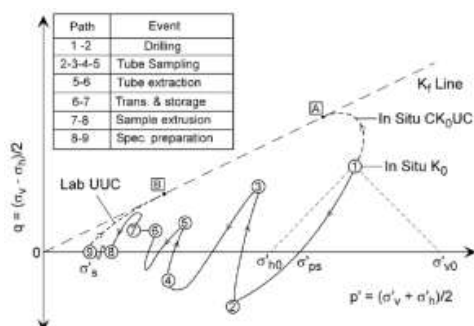


Figure 1. Schematic hypothetical stress path during each stage from tube sampling through testing for a low OCR clay material (Ladd and DeGroot, 2003).

Based on the above, the idealized sampling approach will therefore allow us to get a sample that has not be subjected to any of the following; (i) stress relief during the drilling, (ii) stress variation, shearing, compression or dilatancy/relaxation or vibration during the insertion and extraction of the sampler as well as during the storage, transport, manipulation and trimming to fit into the apparatus, (iii) the water content and void ratio variation will be null as fine particles are lost during all nine stages of sampling. In addition to these, the best possible sampling techniques will minimise both the disturbance due to shearing the soil, and the effect of loss of confining stress on the soil stiffness and strength (Taylor et al., 2012).

The object of this paper is to introduce a new and promising sampling technique that has the potential to be extremely efficient at obtaining undisturbed samples of saturated fine granular material, such as loose sandy soil or cycloned tailings. As with the Gel-Push sampler, this technique uses gel during the sampling procedure. However, instead of using a gel to lubricate and reduce friction between the sample and the tube (Taylor et al. (2012)), the gel is stabilizing and stiffening the material as if it were frozen. However, compared to the in-situ water freezing method the proposed stabilization procedure is without any pore fluid density variation. Labora-

tory testing has shown that stabilizing, manipulating and trimming samples can be achieved without impacting the sample's mechanical behavior. This technique is referred to as EGT sampling ("Échantillonnage par Gel Thermo-fluidifiant" which loosely translates to "Sampling using Gelatin"). The EGT sampling technique and proposed procedure should allow us to limit the influence of points (i) to (iii) listed above and therefore greatly increase the sample quality.

3 LABORATORY DEVELOPMENT OF THE EGT SAMPLING METHOD

As mentioned above, the EGT sampling method allows stabilizing and stiffening of fine, cohesionless material without any sample or pore fluid density variation. The solidification/stabilization process is achieved by using a solution of gelatin.

3.1 Gelatin description and characteristics

Gelatin is a purified protein, derived from the selective hydrolysis of collagen, the largest organic component of the bones and skins of mammals. Gelatin can either be produced through an acid process or an alkaline process, A-type gelatin or B-type gelatin respectively. The most well-known property of gelatin is its ability to form an elastic gel resulting in a unique sequence of hydrogenous bridge formation between amino acids (Ward and Coutts, 1977). Gelatin solution at most temperatures and concentrations displays Newtonian rheological properties and its viscosity characteristics are related to the solution's concentration and temperature, i.e. viscosity increases with concentration and decreasing temperature. The rigidity of elastic gelatin gels increases with maturation time, reaching equilibrium after approximately 18 hours (Figures 2 and 3). Gelatin gel strength depends on the concentration, structure and molecular weight of the gelatin product used.

The proposed approach consists of replacing the sample pore water with the gelatin solution (i.e. water immiscible solution) by injection. The gelatin solution's change of state from liquid to an elastic gel is a progressive phenomenon that can be observed and identified through the solution's dynamic viscosity increasing as the solution's temperature decreases (Figures 4 and 5). In addition to the ability to form an elastic gel as above described, the other key characteristic of the gel is that hydrogenous bridges, at the origin of the elastic gel, can be dissolved. Stabilized samples can be washed of the elastic gel by: (i) increasing the sample temperature to 70°C, (ii) injecting 70°C deaerate distilled and chemically neutral water under a low injection gradient (1 kPa/10 cm), (iii) injection of a 70°C low vapor pressure deaerated alkaline solution at a pH of 10.5, and (iv) sample saturation with deaerated distilled and chemically neutral water prior to testing.

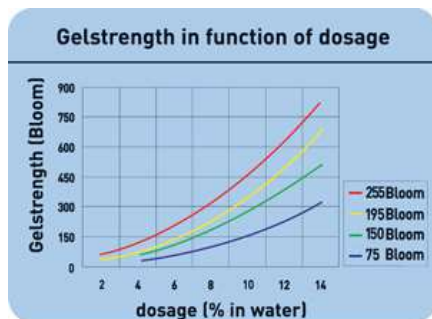


Figure 2. Gelatin gel strength vs solution's concentration (www.gelatin.com)

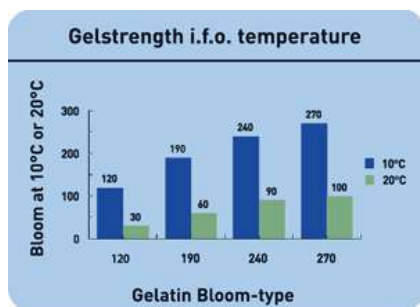


Figure 3. Gelatin gel strength vs gel's temperature (www.gelatin.com)

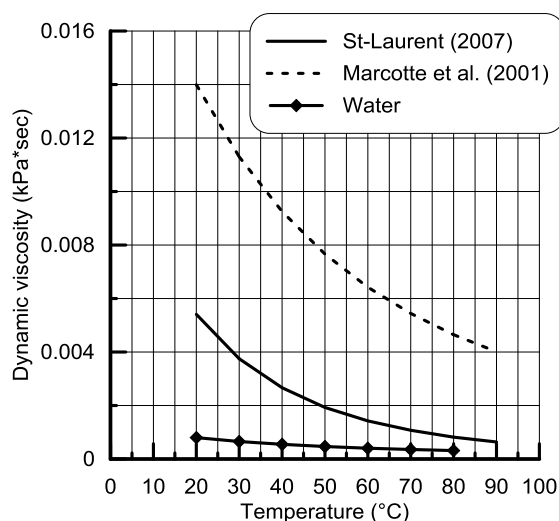


Figure 4. Gelatin solutions and water's dynamic viscosity vs temperature (St-Laurent, 2007)

3.2 Laboratory testing program

To establish the viability of the proposed stabilization technique, uniform rounded Ottawa sand material was used to perform laboratory triaxial assays. To obtain uniform and highly similar samples, an underwater pluviation technique was used to build the sample directly in triaxial apparatus and consolidated to the desired void ratio. Firstly, the impact of the gelatin solution as a sample saturation fluid was studied. Then, the geomechanical impact of gelatin washing and the water re-saturation process were looked at. Finally, triaxial testing was used to establish if the stabilized samples could be manipulated and trimmed without geomechanical behavior modification (Robichaud, 2003). The laboratory program consisted of performing 15 undrained triaxial tests and the sample behavior was studied in q - p' , q - ϵ_a and Δu - ϵ_a domains.

Five (5) reference samples were used to establish the standard geotechnical behavior of the Ottawa sand that was used. Four (4) samples were built as described above and saturated with a 70°C gelatin solution. The gelatin solution percolation was performed under a low hydraulic gradient (1 kPa/10 cm). A horizontal constraint (σ_3) of 150 to 240 kPa and a porous back pressure of 180 to 190 kPa were applied to maintain the grain-to-grain original configuration and to limit the fluid injection impact on the sample's geotechnical behavior. Once the gelatin saturation was completed, the sample's temperature was decreased to 10°C for 16 to 18 hours. Then, the stabilized sample's temperature was increased back to 70°C to allow the gelatin gel to convert

into a viscous solution that then behaved as the sample's saturation fluid. The sample's temperature was maintained at 70°C during triaxial testing. Three (3) samples were stabilized, washed and saturated back with water as previously described. Finally, two (2) sub-samples (50 mm in diameter and height) were obtained from stabilized samples 100 mm in diameter and height. The manipulating and trimming work was performed as quickly as possible to limit gelatin oxidation.

As can be seen in Figure 6, stabilized sand samples could be manipulated as if it were stiff clay. Recovered smaller samples were then installed into the triaxial apparatus, washed and saturated back with deaerated distilled and chemically neutral water.



Figure 5. Stabilized Ottawa sand sample cut as stiff clay (Robichaud, 2003)

3.3 Laboratory testing results

Results obtained from the five reference samples allowed us to establish an average friction angle of 31.15° for the Ottawa sand. Reference samples showed a contractive behavior up to ~0.75% of axial deformation and then showed dilatancy behavior.

As shown in Figure 7, samples having gelatin solution as saturation fluid do have a lower friction angle (29.44°). Knowing that the gelatin injection was achieved under a low hydraulic gradient and assuming that such injection gradient could not lead to particle rearrangement under the applied confining pressure used during the injection process, it is therefore believed that the gelatin solution acts as a grain-to-grain lubricator. This is directly in line with the conclusions of Khamehchiyan et al. (2007). These results and observations confirmed that stabilized samples should be washed of the gelatin solution and saturated back with water prior to testing.

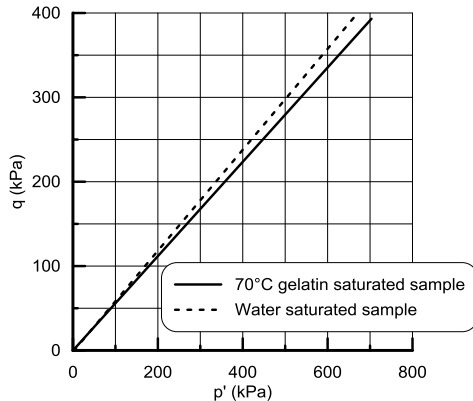


Figure 6. Impact of 70°C gelatin on the Ottawa soil friction angle (modified from Robichaud, 2003).

As can be observed in Figure 7, the initial stiffness of both types of samples (washed and reference) are similar. As shown in Figure 8, the q-p' behavior of washed samples against reference samples are highly comparable, suggesting that both sample's friction angles are similar. Both sample's stress-strain behaviors are similar as well. At the end of the contractile phase ($\epsilon_a \sim 0.5\%$) or dilatancy phase ($\epsilon_a \sim 2.3\%$) both samples showed identical q values. The observed divergence in the $\Delta u - \epsilon_a$ domain is believed to be associated with a lower saturation degree in washed samples. Also, observed divergence between results is associated with the washed sample's longer consolidation period and saturation degree. The performed testing program demonstrates that the washing methodology developed allows samples to retrieve their initial friction angle and geotechnical behavior.

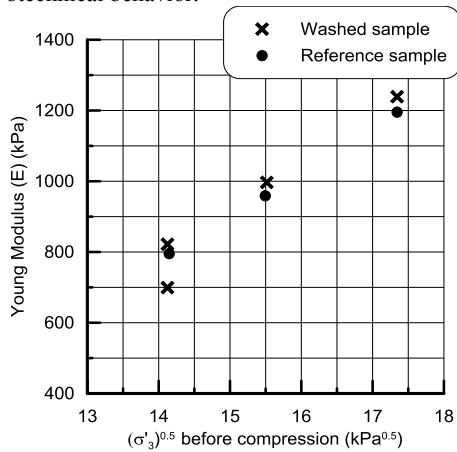


Figure 7. Young modulus of washed and reference sample in compression phase (modified from Robichaud, 2003)

As shown in Figure 8, the trimming and washing process did not significantly affect the sub-sample behavior; sub-sample and reference sample's q-p' curves are similar. Figure 8 suggests that the stress-strain behavior of sub-samples is not affected when compared to the reference sample. However, when comparing the q- ϵ_a sub-sample behavior to the washed sample behavior, a significant divergence is observed. It is assumed that the observed divergence is related to the overall system saturation, which may differ between tests. In addition, the consolidation time is longer for sub-samples, and therefore may have impacted the sample's behavior. Similar behavior divergence is observed in the $\Delta u - \epsilon_a$ domain, which tends to endorse the above noted assumption. Additional testing should be performed to validate this assumption. Even though divergence is observed, it should be noted that sample stiffnesses are similar. This suggests that grain-to-grain configuration has been maintained throughout the manipulation process.

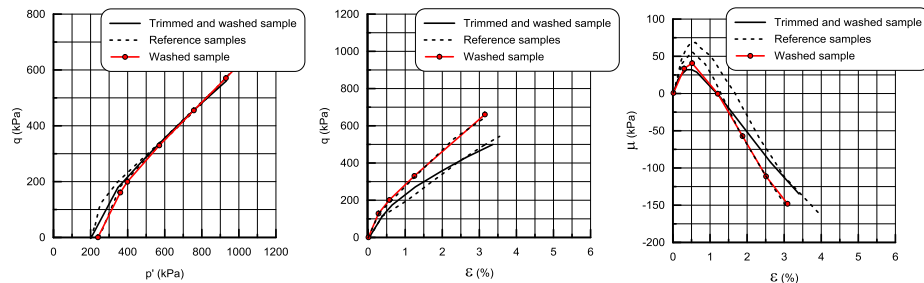


Figure 8. Behavior of washed vs reference vs trimmed samples (modified from Robichaud, 2003).

4 BOREHOLE INJECTION MODELLING

Laboratory testing showed the viability of using gelatin as a stabilization method to maintain cohesionless soil geotechnical behavior. However, injecting such a hot and highly viscous fluid into temperate soil presents numerous challenges. A numerical model was then developed to simulate the gelatin solution injection into a porous media, such as fine grain sand or coarse tailings. The finite element software FlexPDE was used to establish and predict the gelatin flow pattern and the amount of material to be stabilized under the specific injection process and site conditions. Spherical or axisymmetric flow created by an injection was simplified through a 1D radial numerical model.

One of the key soil parameters that governs the fluid flow is the hydraulic conductivity. Saturated soil hydraulic conductivity is characterized by the soil's physical characteristics and by porous fluid, as defined by Equation 1 where K is the saturated hydraulic conductivity, κ is the soil intrinsic permeability, ρ_f is the fluid density, g is the gravity and η is the fluid's dynamic viscosity.

$$K = (\kappa \cdot \rho_f \cdot g) / \eta \quad (1)$$

As can be seen, the fluid's dynamic viscosity governs the soil hydraulic conductivity and consequently how the fluid flows within the soil. As previously shown in Figure 5, the dynamic viscosity of the gelatin solution is higher than water's and is drastically impacted by its own temperature.

Most of the time hydrogeologists assume that both the fluid and soil temperatures are similar. However, as mentioned above, gelatin solution should be injected at about 70°C. Therefore, the fluid and solid thermal non-equilibrium model (Kim and Jang, 2002) should be used to model the gelatin solution injection. This thermal model allows determination of the fluid temperature variation through time, which establishes the soil hydraulic conductivity variation through time (i.e. dynamic viscosity variation).

Gelatin solution is immiscible with water. Therefore, considering that the mass conservation principle can be applied, and assuming that the soil porosity is constant as well as uniform through time and space, and that the injected fluid is non-compressible, the amount of gelatin mass injected and transported through the soil by the advection process can be represented by the mass flux principle (Gelhar and Axness, 1983). Therefore, an advanced and unified thermo fluid-mass flow numerical model using a total of 11 equations was developed. The developed numerical model allows us to predict the gelatin solution distribution through time and space and establish the amount of soil to be stabilized using a specific injection gradient and both initial and boundary conditions.

As shown in Figure 9, the developed numerical model allows the prediction of the stabilized bulb dimensions under laboratory conditions with acceptable precision. Most of the time, the numerical model was under estimating the stabilized sample size by 5 to 15 %. It is judged that such precision is appropriate for the intended application. Observed divergence between the numerical model and laboratory data is associated with the soil's intrinsic conductivity, storage and transmissivity coefficients estimation, and to the limited depth of injection in the current laboratory injection apparatus.

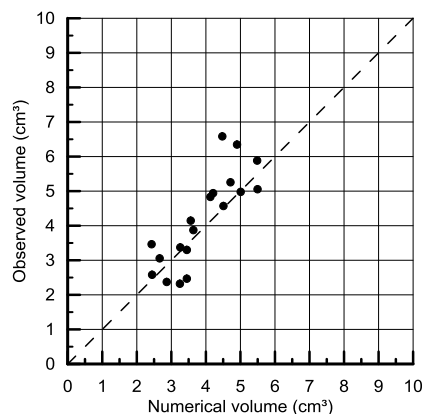


Figure 9. Predicted stabilized injection bulb size vs laboratory observed bulb size (modified from St-Laurent, 2007).

5 DISCUSSION AND CONCLUSION

The developed numerical model, using the non-thermal equilibrium model between the fluid and the soil, as well as mass and flow equations, allows us to predict the amount of material to be stabilized through a controlled gelatin injection process. Laboratory testing demonstrated that manipulation of a stabilized fine granular sand sample as if it was a stiff clay material is possible and that larger stabilized samples could be trimmed and cut without any difficulties. Undrained triaxial testing programs showed that the developed washing process allows the cleaning of the gelatin solution from the stabilized sand samples without impacting the sample's geotechnical behaviour.

Based on the above observations and investigations, it appears that the proposed EGT sampling technique tends to be highly efficient in obtaining high quality undisturbed saturated samples in an efficient, cheap and simple approach.

The proposed method has been developed with the consideration that most drilling contractors are equipped to perform injections into boreholes. In order to implement the EGT sampling method, only an additional heating/mixing system is required. To obtain the best possible results the following field procedure is proposed:

1. At the depth of desired sampling, cylindrical injection of 70°C water under a low hydraulic gradient is achieved prior to gelatin injection. Injection rate must be established based on field conditions to ensure that the soil structure is not affected by fluid flow pressure. As optional quality control, thermistor strings can be used to record surrounding soil temperature to decide when the water injection should stop.
2. During the hot gelatin injection process, within the pre-heated soil mass, injection pressure must be recorded to monitor the fluid state of change - as the pressure increases it means that the fluid viscosity increases. Soil temperature recording may be used as quality control as well. Injection pressure must be limited to a fraction of the effective overburden pressure to reduce the risk of disturbance (i.e. 10%).
3. After the required 18 hours of maturation, a second borehole is completed next to the initial one where the injection is administered to sample material that will not have seen any stress release.
4. It is recommended that a large diameter sampler or the Gel-Push sampler be used to recover the stabilized material.
5. Recovered samples are transported to the laboratory for testing after they have been trimmed, washed of the gelatin and saturated back with deaerated chemically neutral distilled water.

6 ACKNOWLEDGEMENTS

The writers would like to acknowledge the contribution of several individuals to this paper, especially Simon Robichaud, François Gilbert for laboratory support, Marc Lebeau for his support during the numerical model development as well Professors Jean-Marie Konrad and Denis Leboeuf for the research grant. Thanks to Aaron Fultz and Gabi Green for their paper review and editing.

REFERENCES

- Cuccovillo, T. and Coop, M.R. 1990. On the Mechanics of Structured Sands, *Géotechnique* 49 (6): 741-760.
- da Fonseca, A. V., Pineda, J. 2017. Getting High-quality Samples in “Sensitive” Soils for Advanced Laboratory Tests. *Innovative Infrastructure Solutions*, 2(1), 34.
- Gelhar, L.W., Axness, C.L. 1983 Three-dimensional Stochastic Analysis of Macrodispersion in Aquifers. *Water Resources Research* 19(1): 161-180.
- Hoeg, K. (ASCE), Duvik, P. and Sandbaekken, G. 2000. Strength of Undisturbed versus Reconstituted Silt and Silty Sand Specimen. *Journal of Geotechnical and Geoenvironmental Engineering* 126: 606-617.
- Hofmann, B.A., Segoo, D.C. (ASCE) and Robertson, P.K. (ASCE). 2000. In-situ Ground Freezing to Obtain Undisturbed Samples of Loose Sands. *Journal of Geotechnical and Geoenvironmental Engineering* 126: 979-989.
- Khamehchiyan, M., Charkhabi A.H., and Tajik, M. Effects of Crude Oil Contamination on Geotechnical Properties of Clayey and Sandy Soils. *Engineering Geology* 89.3-4 2007: 220-229.
- Kim, S.J. and Jang, S.P. 2002. Effect of the Darcy Number, the Prandtl Number and the Reynolds number on Local Thermal Non-equilibrium. *International Journal of Heat and Mass Transfer* 45:3885-3896.
- Konrad, J-M. 1990. Sampling of Saturated and Unsaturated Sands by Freezing. *Geotechnical Testing Journal* 13 (2): 88-96.
- Konrad, J-M. and Pouliot, N. 1997. Ultimate State of Reconstituted and Intact Samples of Deltaic Sand. *Canadian Geotechnical Journal* 34 (5): 737-748.
- Ladd C.C. and DeGroot D.J. 2003. Recommended Practice for Soft Ground Site Characterization: Arthur Casagrande Lecture. 12th Panamerican Conference on Soil Mechanics and Geotechnical Engineering. Massachusetts Institute of Technology, Cambridge, MA USA.
- Marcotte, M., Taherian Hoshahil, A.R. and Ramaswamy, H.S. 2001. Rheological Properties of Selected Hydrocolloids as a Function of Concentration and Temperature. *Food Research International* 34: 695-703.
- Robichaud, S. 2003. L'échantillonnage non remanié des sables au Gel Thermo-fluidifiant. Mémoire de maîtrise, Université Laval.
- St-Laurent, J-F. 2007. Développement d'un Modèle Numérique Thermo-hydrigue Advectionnel pour l'optimisation de la Technique d'échantillonnage des Sables Pulvérulents par gel Thermo-fluidifiant (EGT). Mémoire de maîtrise, Université Laval.
- Taylor, M. L., Cubrinovski, M., and Haycock, I. 2012. Application of New Gel-Push Sampling Procedure to Obtain High Quality Laboratory Test Data for Advanced Geotechnical Analyses. In April 2012 New Zealand Society for Earthquake Engineering Conference. Christchurch, New Zealand, NZSEE.
- Vaid, Y.P., Sivathayalan, S. and Stedman, D. 1999. Influence of Specimen Reconstitution Method on the Undrained Response of Sand. *Geotechnical Testing Journal* 22 (3): 187-195.
- Ward, A.G. and Courts, A. 1977. *The Science and Technology of Gelatin*. Edited by A.G. Ward, A. Courts. Academic Press London; New York. 1977.

Geotechnical and Structural Monitoring System Deployment for the Spillway of a Dam at Padcal Mine in the Philippines

V. Le Borgne, A. Cosentino, S.-É. Thivierge and J.-M. Br  h  
GKM Consultants, Sainte-Julie, Qu  bec, Canada

The Padcal Mine in the Philippines has been in service for over 50 years. To complete the most recent life-extension projects of the mine, the owner has been upgrading the most recently built tailing dam. It is a concrete gravity dam, the largest of its kind in a tailings facility in the world. To ensure long term reliability of the dam, a major instrumentation system has been installed to provide real-time structural data. Instruments include in-place inclinometers, joint meters across concrete blocks, piezometers within the dam and extensometers. In-place inclinometers were installed in the already-built concrete structure between the spillway and a gallery. Multipoint extensometers were installed through the existing structure into the soil underneath the dam. This being an already-existing dam under expansion, retrofitting the existing structure with new instruments was met significant hurdles. In this case study, we present the methods developed to tackle these challenges.

1 INTRODUCTION

The Padcal mine, a gold and copper mine located in the Benguet province in the Philippines, has been in service for decades. It has proven reserves of 216 million lbs of copper and 627 000 oz of gold. It employs 2000 people locally and has been at the centre of the economic development of the region. Though there are still significant reserves and more exploration to be done, the mountainous landscape and heavy rainfalls of the region limit the mine operator's flexibility with regard to tailings storage. It appears that this will be the main factor limiting the lifespan of this mine.

The challenges of maintaining a large tailings system of this type in this landscape was abruptly brought to public attention in 2012. The mine was faced with significant challenges when an acid waste drainage tunnel under penstock 3 ruptured (Catholic Bishops Conference of the Philippines 2012). The mine operator claims that this was a "force majeure" event caused by heavier than usual rainfalls (Caluza 2013). An estimated 20 million metric ton of tailings escaped through punctured roof of the tunnel (Dinglasaz 2013). The leak led to a significant increase in heavy metals levels downstream and ecological damage to the creek (Dinglasaz 2013). It also damaged one of the offset dikes of the tailings, lowering its capacity for future operations. The leak was plugged with a large concrete boulder that gave sufficient time for the team to backfill the tunnel. Because this section of the tailings was compromised, there was an increased risk of further failures due to damage to the existing dams. To limit the risks that future heavy rainfalls could pose, a new concrete gravity dam with three 12-meter spillways was designed and built (Dinglasaz 2013). As of 2014, the first sections of the dams and a first spillway was put in service, designed to accommodate up to 1500 mm of rain. A satellite image of the dam in 2014 before the opening of the first spillways is shown in Figure 1 (a). Over the following years, two more spillways were built and the top of the dam was raised, as shown in Figure 1 (b).

This ambitious project requires a significant amount of instrumentation for close monitoring during construction, operation and for future maintenance. Several types of instruments were selected and installed: piezometers, temperature probes, in-place inclinometers (IPI), strain gages, multi-point borehole extensometers (MPBX), 3D jointmeters and weir monitors. Our involvement in the project came in after construction had begun and existing structures had to be retrofitted to accommodate a complex instrumentation plan. A brief overview of all instruments will be given. More attention will be devoted to inclinometer casing, IPIs, MPBX and jointmeters. The unique situations encountered in this project will be discussed, as well as the novel approaches deployed to tackle them. Adding embedded instrumentation to an existing structure poses difficulties that are otherwise uncommon, such as drilling through galleries. However, the fact that the dam was still under expansion allowed for creative and novel instrumentation installations.

In this project, we provided the instruments themselves, installation services and training. Installation of the instruments took place over several missions in from 2016 to 2018. Many instruments, such as piezometers and thermistor strings, were installed by the local staff after training, while more complex instruments such as MPBX were installed during one of these missions. All instruments except manual inclinometer surveys were intended to be read by data loggers provided and installed during the final mission.

2 INSTALLATION

2.1 Context

A satellite image of the dam (google) from 2018 is shown in Figure 1 (b). It can be seen that, as of 2018, the three spillways are built, and that water is flowing in spillway 3.



Figure 1 Padcal mine concrete dam. (a) The dam in early 2014. Two of the three spillways were completed. (b) The dam in 2018. The three spillways are seen, with water overflow going down spillway 3.

2.2 Inclinometer casing

Inclinometer probes are a frequently used instrument in structures such as dam to follow long term deformation of the structure (Dunnicliff 1993). Six inclinometer casing boreholes were drilled in the structure, from which manual readings are taken using a Geokon GK-604D probe. Manual inclinometer probes allow for low-cost, long-term monitoring, but are slow and do not provide real-time information on the structure.

The boreholes were drilled from the top of the structure down into the gallery, and then down again through the floor of the gallery. In theory, these boreholes should have been drilled before the gallery roof was built, but delays in the work schedule and availability of instrumentation specialists delayed this installation.

In this project, the casing had to be inserted from the top of the dam, down into the gallery, where another worker would align the casing inside the borehole for final installation. This was the only way to accommodate the 3m casing length. This operation is illustrated in Figure 2.



Figure 2 View from inside the gallery where inclinometer casing is being installed. The casing is slid through the roof of the gallery after which a worker will go and insert in the borehole in the floor of the gallery.

2.3 IPI

Tiltmeters are often used in large structures such as dams to follow long term health. Due to their rigidity, some failure modes will register a tilt of the structure (FERC 2018) (Dunnicliff 1993). This tilt can be measured with tiltmeters installed on the surface after construction but we took advantage of the fact the structure was being extended to embed single-point in-place inclinometers in the structure. The selected IPI (Geokon 6300, vibrating wire) is commonly used in inclinometer boreholes as a permanently installed chain of sensors (Dunnicliff 1993).

Installation was conducted after the first layer of blocks above the gallery had been poured but before the top of the dam was erected. The IPI casing was installed and held in-place with the IPI inside until the new concrete form was poured. After the installation, the tubing was protruding approximately 3 m above the current level of concrete as shown in Figure 3 (a). It was securely attached until the new form was poured because impacts or stormy weather could have bent or broken the casing and the instrument inside.

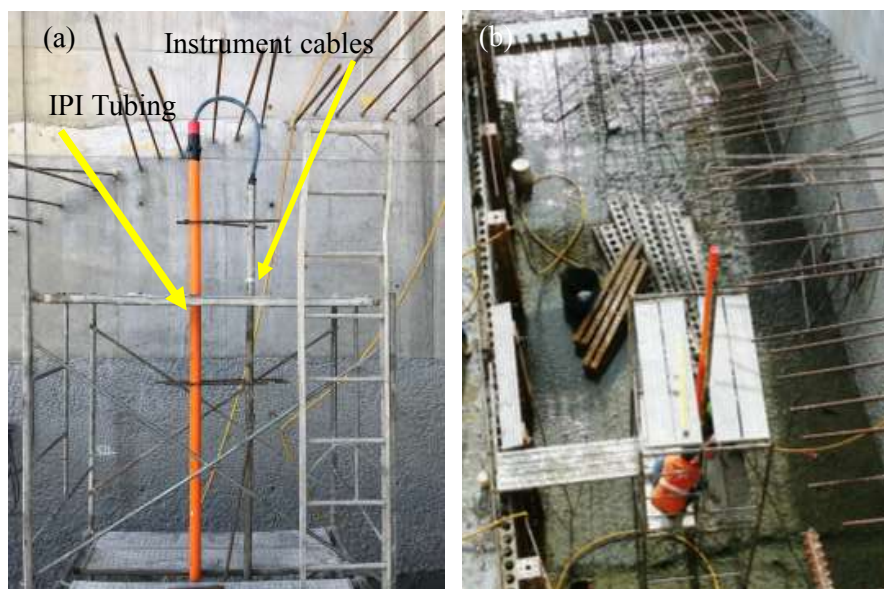


Figure 3 (a) IPI casing sticking out after instrument installation. (b) IPI casing sticking in the in-use spillway

It was originally planned that the inclinometer casing would be installed from the roof of the gallery and installed pushing up. However, the low availability of hardware such as metal plates and anchors to hold the tubing in place forced a different installation. Tubing was installed in a shallow borehole from the top of the block with its bottom resting on the bottom of the borehole without having broken through inside the gallery, preventing insertion of the instrument from the inside of the gallery. Additionally, it was discovered on-site that the IPI's themselves were too long to be manipulated and inserted from the bottom up and would have had to be inserted from the top in any case. Temporary scaffolding was built to access the top of the casings to insert the IPI's inside the casing. This can be seen in Figure 3 (b) where the casing is sticking outside the water in the spillway.

The three permanently embedded IPIs allow for real-time monitoring of the angle of top of the dam, as opposed to the manual readings which have a long turnaround and no real-time capabilities.

2.4 MPBX

MPBX are commonly used to follow either settlement or uplift in structures such as dams (Dunnicliff 2013). Just like for inclinometer casing, most boreholes had to be drilled from the top of the structure, into a gallery and then down to the bottom of the dam at more than 45 m from the top of the dam. The MPBX head was intended to be installed recessed in the floor of the gallery. A few others were installed through the dam sidestepping the gallery and with the head located at the top of the structure.

Borehole drilling for MPBX was very similar to drilling for inclinometer casing installation but the silty soil at the foundation of the dam would close up quickly after drilling, giving a window shorter than an hour for the insertion of the lowest MPBX anchor. In normal conditions, drilling casing is available and inserted to keep the borehole intact until instruments are installed but it was unavailable in the region. Despite this difficulty, the bottom anchors of all MPBX but one were installed at the intended depth. For this single MPBX, the head stuck out above the floor of the gallery, and a concrete form was poured to protect and solidly anchor the head to the structure within the gallery.

A typical installation of these instruments, as described in the manufacturer’s manual, requires that there be a larger recess bored at the top of the borehole to easily connect the anchor rods to the head and remove the suspenders. The larger drilling bit was not available on site, but it was possible to make the best of this unique situation. The MPBX heads were left sticking out of the boreholes, held in place with its bladder anchor, knowing that they would be fully encased in a new concrete block. This unique opportunity helps reduce costs and installation time with respect to the standard installation of MPBX.

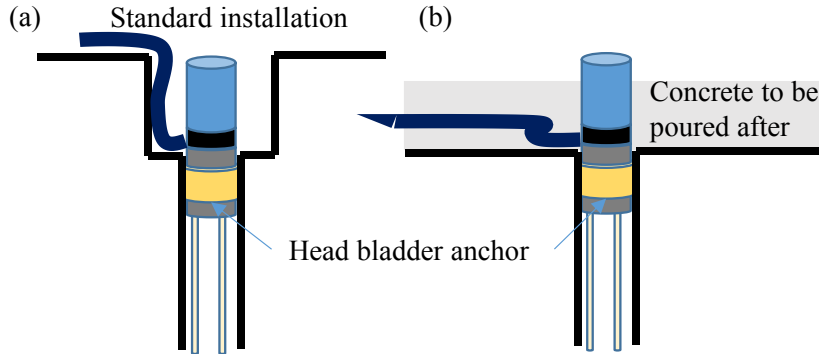


Figure 4 (a) Standard MPBX head installation. (b) Modified MPBX head installation

Figure 5 shows the final installation of an MPBX head before it is encased fully in concrete. Because the MPBX was to be installed directly in the boreholes without casing, bladder type anchors for the rods were used. These anchors provide direct contact with soil and/or rock and preclude the need for grouting. The system is designed in such a way that each anchor can be inflated sequentially to anchor locally each rod. In addition using bladder anchors, the MPBX were grouted in place to limit water circulation along the inside of the boreholes. The bladder anchors were inflated only after the grout had set. This double approach ensures the most reliable



Figure 5 (a) MPBX head sticking out from the floor of the gallery (b) MPBX head after being encased in concrete

long term measurements with anchors stronger than simple groutable anchors and the benefits of a watertight grout-filled borehole.

Another minor hurdle that was that there were no clear indications of where rebar were in the concrete blocks. No ground penetrating radar or other methods were available on-site. Whenever a rebar was hit during the drilling of a borehole, the drilling rig had to be moved to start a new borehole.

2.5 3D jointmeters

The 3D jointmeters are attached directly to the structure. They are potentiometer sensors that allow for direct measurement of the position of each sensor. The Pico-tec jointmeters used in this project are faster and easier to install than traditional jointmeters as there is only a rod and a single 3D reading point rather than three instruments installed perpendicular to each other in a standard 3D assembly as compared in Figure 5. A typical assembly (b) requires installation and commissioning of three different instruments in various configurations and the installation of supports and right-angle metal plates. This is time-consuming and measurement points are a bit spaced out. As shown in (a), this novel jointmeter has a single rod that is read by an internal 3D assembly of potentiometer sensors. This simple design allows for more compact and more localized installations.

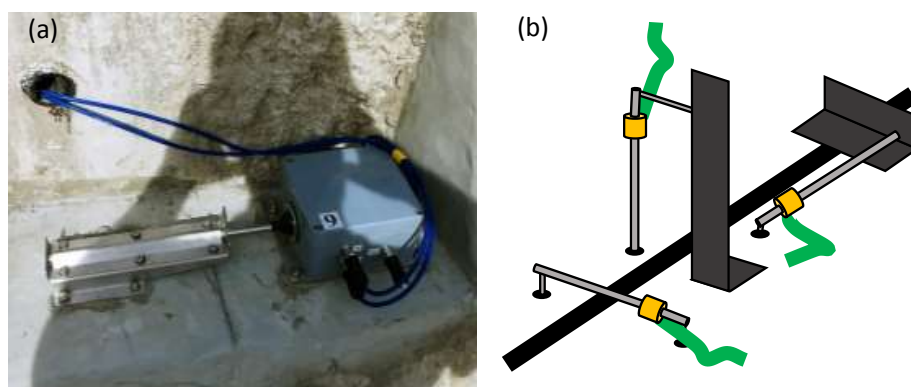


Figure 5 (a) Pico-tec jointmeter (b) traditional 3D jointmeter

Because the entire structure is accessible during construction, installation of these instruments on nearly all blocks was greatly facilitated when compared to other dam monitoring projects, where we are required to go in and install instruments on an already-built dam. This complete coverage of the structures gives a complete image of the mechanical of the dam for the consulting firm to follow short and long-term behavior of the dam.

2.6 Other instruments

Geokon vibrating wire piezometers were installed in the core and under the dam, with cables running out to the side of the dam. Thermistor strings were installed at selected levels to follow concrete curing. They are also used to detect changes in temperatures that could indicate water ingress. Vibrating wire strain gages (Geokon 4200) were embedded in the concrete blocks.

2.7 Data logging

The instruments discussed in this project are vibrating wire-based instruments with the exception of thermistor strings and 3D jointmeters. All were directly integrated in Campbell Scientific-based data loggers. All instruments were installed with sufficient lead cable that the cables could be

routed to a data logger. Though splicing cables is always possible, it adds a weak point that is not compatible with the long term requirements of dam monitoring.

As is often the case in remote projects, hardware that is taken for granted in other parts of the world can be hard to come by. A large number of the instrument cables were intended to run through the main gallery and held and protected by cable trays or clamps. However, this type of hardware was not readily available so bits of rebar were fixed in drilled holes in the concrete and the cables attached to the rebar with tape or cable ties.

The data logging system was fully centralized as shown in Figure 6. All multiplexers and data loggers are located in a single room. This approach increases the manpower requirements for and cost of cabling itself, but it's a troubleshooting is greatly simplified when working from a single location.



Figure 6 Data logging system where all instruments are connected

3 CONCLUSIONS

The instrumentation program designed for the extension of the Padcal mine's concrete gravity dam was met with unique challenges. Installing and commissioning instrumentation in a regular dam poses difficulties not found in other projects, but adding instruments to a dam currently under expansion provided new opportunities for creative solutions. It was possible to take advantage of the future concrete pours to install embedded tiltmeters rather than to install them only at the top of the structure. It was also possible to install MPBX in a more time-efficient manner by not recessing the MPBX head in the borehole and protecting it until the concrete forms were poured. It was also an opportunity to install a novel type of 3D jointmeters that are much easier and simpler to install than traditional 3D jointmeters. This monitoring system will help the mine operator take full advantage of the new structure and will contribute to its maintenance and operations for decades to come.

REFERENCES

- Catholic Bishops Conference of the Philippines – National Secretariat for Social Action. 2012. The Philex Mine Tailings Spills of 2012: An Independent Fact-Finding Mission Report. September
- Caluza, D. 2013. Pangilinan: Philex not required to clean up San Roque dam. *INQUIRER.NET*. June 29 2013.
- Dinglasan, R. R. No stranger to mine spills, Philex still wants rehab of aging tailings pond. *GMA New*, February 11 2013
- Dunncliff. 1993. Geotechnical instrumentation for monitoring field performance. *John Wiley and Sons*. New York City.
- FERC. Engineering Guidelines for the Evaluation of Hydropower Projects. *Federal Energy Regulatory Commission*, Chapter 3.
- FERC. Engineering Guidelines for the Evaluation of Hydropower Projects. *Federal Energy Regulatory Commission*, Chapter 9.

Magnetometric Resistivity as an Effective Tool for Leakage Detection and Monitoring

M. Jessop, V. Kofoed, and K. Wall

Willowstick Technologies, LLC; 132 East 13065 South, Draper, Utah 84020, USA

A. Revil

Univ. Grenoble Alpes, Univ. Savoie Mont Blanc, CNRS, IRD, ISTerre, 38000 Grenoble, France

A. Jardani

Université de Rouen, M2C, UMR 6143, CNRS, Mont Saint Aignan, France

ABSTRACT: The injection of a low frequency electrical current in the ground generates a magnetic field that can be measured at the ground surface. The map of this field can be used to determine the position of the current paths. Conductive current paths can be associated with preferential flow paths under certain conditions. We developed simple strategies to invert the magnetic field in terms of current paths. A case study, from a tailings impoundment at a Zinc Mine in Tennessee, is presented. Several preferential paths of electric current were identified and interpreted as channelized seepage paths where water flowed out of the impoundment. One in particular identified the source and path of a spring down-gradient of the impoundment (referred to as the “Big Seep”) that appeared decades ago without any explanation. This method has been shown to be an effective tool to model preferential seepage flow paths and assist in targeting remedial works.

1 INTRODUCTION

Detecting preferential seepage paths is an important goal of hydrogeophysics, a field of science devoted to the development of minimally invasive techniques to image the flow of ground water in the subsurface of the Earth. The direct current (DC) conductivity/resistivity method is a well-known geophysical technique able to image the electrical conductivity distribution of the ground and this method is widely used in hydrogeophysics (e.g., Revil et al., 2012) but lacks resolution to identify preferential ground water flowpaths. A less known method is the Magnetometric Resistivity (MMR) method. With MMR, a low-frequency electrical current (frequency < 1 kHz) is injected in the ground, between two electrodes A and B and the resulting magnetic field is measured. This method was initially proposed by Jakosky (1933) and then refined by Stefanescu & Nabighian (1962) and Nabighian (1991a, b) with the purpose of determining the electrical conductivity of the Earth (Edwards, 1974).

We use here MMR in a very different way. Acosta & Worthington (1983) pointed out the sensitivity of MMR to current that is concentrated within a conductive anomaly. We inject the current between two electrodes A and B and our goal is to use MMR to visualize directly the current path in the ground in area of high conduction paths rather than to reconstruct the conductivity field.

2 BACKGROUND

We first describe how a MMR survey can be performed done using the sketch shown in Figure 1. The fictitious site is composed of a waste rock dump and a tailings pond. The tailings pond provides storage for tailings, waste water and drainage from the mine. Drainage through the waste rock has usually higher contaminant concentrations than the tailings water. It follows that it is preferable to collect and treat drainage from the waste rock dump before flowing into the tailings pond. MMR can be used to identify preferential drainage flow paths bypassing the waste rock dump drainage collection trench to the tailings pond.

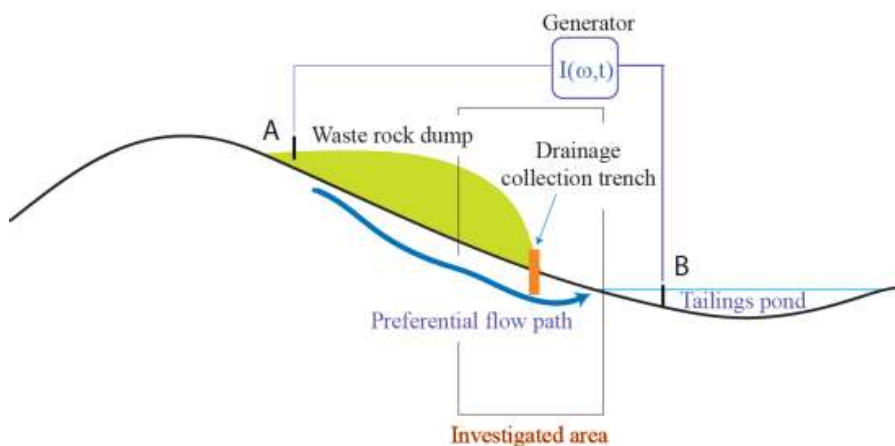


Figure 1. Sketch of the geometry of the energizing electrodes A and B to map a preferential ground water flow path passing a mine waste rock dump drainage collection trench to the tailings pond. The A and B current electrodes are located up-gradient and down-gradient of the drainage collection trench, respectively. An Alternative Current (AC) electrical current with a frequency of 380 hertz is applied to these two electrodes. As the electric current flow between A and B, it generates a magnetic field measured at the ground surface. This field is used to identify the location of preferential electric current flow paths. By identifying the electrically conductive flow paths between the strategically placed electrodes A and B, preferential flow paths bypassing the drainage collection trench into the tailings pond can be identified. The investigated area corresponds to the zone where the three components of the magnetic fields are recorded at the ground surface of the Earth.

Since these flow paths are characterized by highly mineralized pore water, they are more conductive than the background porous material. By identifying preferential electric current flow paths, the MMR method has the potential to identify these drainage paths. This requires however to place the energizing electrodes A and B in strategic positions up-gradient and down-gradient of the drainage collection trench (Fig. 1). An AC electric current with a specific signature frequency can be applied to the paired (A, B) electrodes. The electric current flowing between a bipole current electrodes (A, B) generates a magnetic field at the same frequency. At each station of the survey, the 3 components of the magnetic field are recorded at the ground surface in the survey area between electrodes A and B with a 3 components flux gate magnetometer. The coil magnetometer can repeat measurements within a standard deviation of about 2 pT.

In order to provide the very best interpretation of the data as possible, measurement stations influenced by conductive culture can be filtered out before modeling or interpretation. The recorded magnetic field must also be corrected using the predicted magnetic field model based on a current distribution in an electrically homogeneous subsurface. This causes the concentration of electric current due to changes in subsurface conductivity (such as preferential groundwater flow paths) to stand out much better. By dividing the observed magnetic field map by the predicted magnetic field map, a ratio response map is created which corrects for the electrode effect and shows areas of anomalous electric current flow—greater or lesser than predicted. Next the ratio response map is iteratively inverted to determine the distribution of the electric current flow in 3D.



Figure 2. Aerial photo of a tailings impoundment at a zinc mine, located in Tennessee, with the locations of the settling pond, Big Seep, 2016 Sinkhole and Main Sinkhole labeled.

3 FIELD APPLICATION

At a Zinc Mine in Tennessee, two sinkholes appeared within the confines of a tailings impoundment, leading to a citation for the mine owners. Additionally, water down-gradient of the tailings impoundment drains to a centralized area called the “Big Seep” that appeared decades ago without any explanation (see Fig. 2). A dye test confirmed that water from a nearby settling pond was also connected to the Big Seep, but the owners did not know how they were connected. The owners needed to know if the sinkholes posed a risk to the integrity of the impoundment, and they also wanted to know the source of water to the Big Seep.

A MMR (magnetometric) survey investigation was conducted by Willowstick to understand the cause of the sinkholes and to identify the source of the “Big Seep”. Four different energizing configurations were utilized to investigate the areas of concern. The survey configurations are shown in Figure 3.

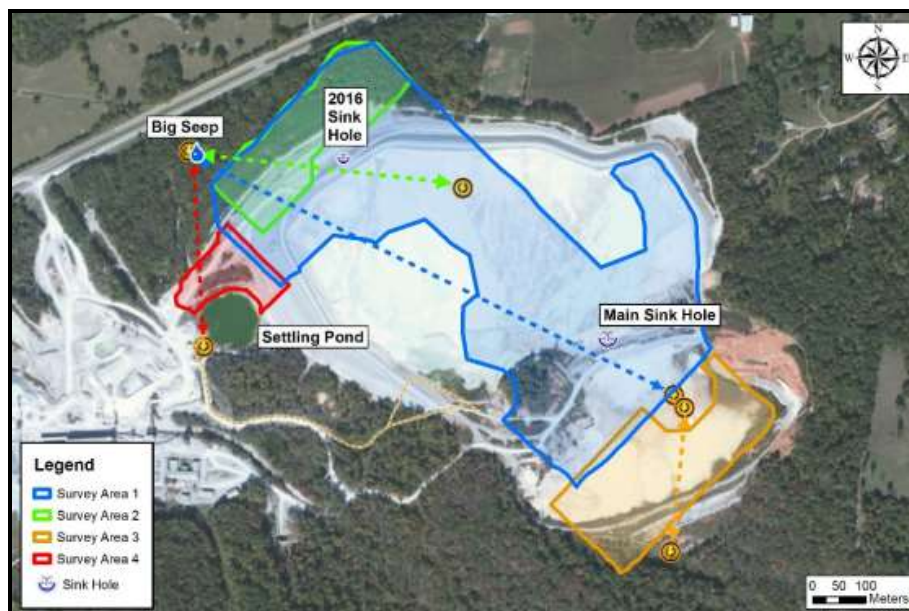


Figure 3. Survey configurations for the Magnetometric Resistivity investigation. There were four independent surveys completed and the outlines are shown. The yellow circles with the lightning symbols represents the electrodes used for each investigation. Each survey had a circuit wire (not shown) which connected the electrodes, and it was placed away from the study area for each survey. Measurement points were collected within the study area.

Figure 4 shows slices from the electric current density (ECD) model (for each survey or energizing setup) which indicate the channelized flow paths and patterns leading out of the tailings impoundment for Surveys 1, 3 and 4 (ECD model slices at elevations 297, 320 and 305 meters, respectively). The green shading highlights areas where electric current density is more concentrated than predicted, and the dark purple shading identifies areas where electric current is less concentrated. The yellow dashed arrows denote the center of dominant flow paths of electric current interpreted as preferential seepage flow paths. As water seeps out of the impoundment in channelized paths, it can carry with it tailings and other earthen materials and cause sinkholes that can compromise the integrity of the impoundment. The preferential electric current flow paths are located directly below the noted sinkholes, suggesting that the geophysical method has successfully identified preferential seepage flow paths out of the impoundment.

The investigation also showed two electric current flow paths, interpreted as preferential seepage flow paths, going towards the “Big Seep,” one from the settling pond and the other from the tailings impoundment. These two paths merge before moving toward the “Big Seep”. With this information, a targeted remediation plan was created saving the owners a significant amount of time and money. This method has been shown to be an effective tool to model preferential seepage flow paths and assist in design of targeted remedial works.

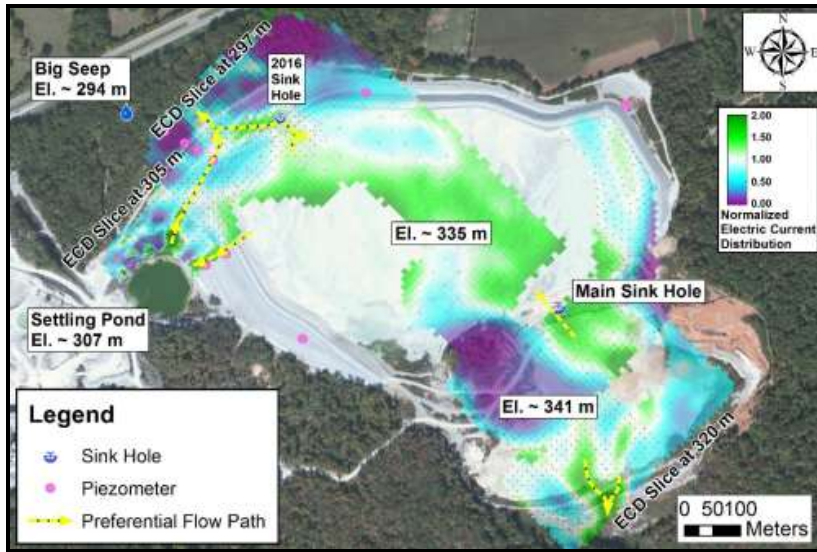


Figure 4. Inversion slices from the electric current density (ECD) model which shows the electric current flow paths and patterns out of the tailings impoundment for Surveys 1, 3 and 4 (ECD model slices at elevations 297, 320 and 305 meters, respectively). The green shading highlights areas where electric current density is more concentrated than predicted, and the dark purple shading identifies areas where electric current is less concentrated. The yellow dashed arrows denote the center of dominant flow paths of electric current interpreted as preferential seepage flow paths.

4 CONCLUSION

Magnetometric resistivity consists in measuring the magnetic field associated with the injection of an alternating current in the ground. Under some conditions, the current follows the preferential ground water flow paths. A case study shows two electric current flow paths, interpreted as preferential seepage flow paths, one from the settling pond and the other from the tailings impoundment. With this information, an effective remediation plan was developed.

REFERENCES

- Acosta, J. E. & Worthington, M. H., 1983. A borehole magnetometric resistivity experiment. *Geophysical Prospecting* 31: 800-809.
- Edwards, R. N., 1974. The magnetometric resistivity method and its application to the mapping of a fault. *Canadian Journal of Earth Sciences*, **11**, NRC Research Press, Ottawa, 1136-1156.
- Jakosky, J. J., 1933, *Method and Apparatus for Determining Underground Structure*. US Patent No. 1906271.
- Nabighian M. N., 1991a. Investigations in Geophysics no. 3: Electromagnetic Methods in Applied Geophysics. volume 1, Theory. SEG, Tulsa.
- Nabighian M. N., 1991b. Investigations in Geophysics no. 3, Electromagnetic Methods in Applied Geophysics volume 2. Application, part A and B. SEG, Tulsa.
- Revil A., Karaoulis M., Johnson T., & Kemna A., 2012. Review: Some low-frequency electrical methods for subsurface characterization and monitoring in hydrogeology. *Hydrogeology Journal* 20(4): 617-658, doi:10.1007/s10040-011-0819-x.
- Stefanescu, S. & Nabighian, M., 1962. Uber magnetische storfelder als folge senkrechter schichtungen im gleichstrom. *Revue de Géologie et de Géographie, Académie de la République Populaire Roumaine* 6: 139-155.

Non-Invasive Geophysics for Active Mining Sites

S. Calendine and D. Rucker

Hydrogeophysics, Tucson, Arizona, USA

ABSTRACT: Non-invasive subsurface geophysical technologies are being applied within active mine sites in new and innovative ways to improve safety, aid production, and manage environmental challenges. The majority of contemporary subsurface investigative techniques rely on invasive and extensive drilling programs, which use point source information to infer the broader picture. Geophysical methods, on the other hand, offer a robust alternative that provides improved targeting options to enhance drilling programs. Geophysical methods can be applied over many stages of the mine lifecycle; including exploration, preconstruction investigations and characterization, heap characterization for permeability analysis in leaching operations, injection monitoring for enhanced recovery, and environmental characterization for seepage, acid rock drainage, and plume delineation. In addition, these surveys can provide a high-resolution, spatially-continuous study that when repeated in the same area using the same technique, presents a temporal component assessing subsurface changes over time. This paper gives an overview of geophysical applications applied specifically to solve problems associated with tailings and waste. We show how methods are applied to characterization, monitoring, conceptual site model development, siting of facilities, and how it could be used to monitor stabilization efforts.

1 INTRODUCTION

Historically, the primary role of geophysics in the mining industry was in the exploration for economically viable resources. As geophysics progressed, an expanding range of technologies and methods were developed and improved upon. Equally, as geophysical methods and purveyors of geophysical services became more prolific, applications for geophysical technologies began to develop. Currently, geophysical technologies are no longer limited to exploration and are now playing new and important roles within a diverse set of industries including mining. More importantly, geophysics can be applied throughout the entire mining life cycle. For example, in the production of metals such as copper, gold, and silver, geophysical methods are used to enhance the heap leaching process and improve metal recovery. A geophysical technology known as electrical resistivity tomography (ERT) can be used to assess adverse hydraulic processes in heaps such as pooling, preferential flow, and compaction (Rucker et al., 2009). Others have applied ERT to tailings facilities to investigate internal flow and transport within oil sands (Booterbaugh et al., 2015), acid mine drainage from metal mines (Placencia-Gómez et al., 2010; Benyassine et al., 2017), and to map underlying bedrock (Grangeia et al., 2011).

The fundamentals of ERT are based on the technology's ability to map contrasts in electrical resistivity (or its converse, conductivity) as it relates to the heterogeneity of soils, rocks, and the distribution of moisture and ionic solutions. Given the broad ability of ERT to easily characterize imposed fluids in the earth's subsurface, mining facilities are a perfect environment to apply geophysical studies for numerous subsurface site challenges. These studies can help understand the unique internal structure of tailings and waste rock and the influence that structure has on solution behavior within them. The ERT method affords a holistic approach, providing a means of spatially characterizing the subsurface to determine areas of

potential leakage, weaknesses in dams, or plume mapping. Now, hydrological processes that were once invisible, unknown, and poorly understood can be mapped, thus allowing mining operators to target potential areas of concern for corrective actions.

In this paper, we give an overview of ERT and provide examples for usage on tailings facilities. These examples include tailings characterization, plume mapping, dam investigations, seepage characterization, and facility siting. We also discuss the potential for ERT to be used to monitor stabilization efforts for increasing structural support or for reduced permeability. We draw several of our examples from work on leach pads, which is another mining-based rock pile with hydraulic issues.

2 ELECTRICAL RESISTIVITY OVERVIEW

The relationship between the electrical resistivity, current and the electrical potential is governed by Ohm's law (Loke et al. 2013). To calculate the potential in a continuous medium, the form of Ohm's Law as given by Poisson's equation is normally used. The potential due to a point current source located at \mathbf{x} is given by

$$\nabla \cdot \left[\frac{1}{\rho(x, y, z)} \nabla \phi(x, y, z) \right] = - \frac{\partial j_c}{\partial t} \delta(\mathbf{x}_s) \quad (1)$$

where ρ is the resistivity, ϕ is the potential and j_c is the charge density. The potential at any point on the surface or within the medium can be calculated if the resistivity distribution is known. This is the forward problem, and we specifically separate it from the inverse problem discussed below. Analytical methods can be used for simple structures such as a cylinder or sphere in a homogeneous medium. For modeling of field data, the finite-difference, finite-element, or finite volume methods are more commonly used. These methods discretize the subsurface into a large number of cells. By using a sufficiently fine mesh and the proper boundary conditions, an accurate solution for the potential over complex distributions of resistivity can be obtained.

The purpose of the resistivity method is to calculate the electrical resistivity of the subsurface, which is an unknown quantity. The measurements for the resistivity survey are made by passing a current into the ground through two current electrodes (usually metal stakes), and measuring the difference in the resulting voltage at two potential electrodes. In its most basic form, the resistivity meter has a current source and voltage measuring circuitry that are connected by cables to a minimum of four electrodes. The basic data from a resistivity survey are the positions of the current and potential electrodes, the current (I) injected into the ground and the resulting voltage difference (ΔV) between the potential electrodes. The current and voltage measurements are then converted into an apparent resistivity (ρ_a) value by using the following formula

$$\rho_a = k \frac{\Delta V}{I}, \quad (2)$$

where k is the geometric factor that depends on the configuration of the current and potential electrodes (Loke et al., 2013). Different arrangements of the current and potential electrodes (or arrays) have been devised over the years (e.g., Cabbage et al., 2017).

Equation 2 represents the simplest form of the inverse problem and assumes that the earth is homogeneous for each combination of current and potential measurements. For more complicated problems, inversion relies on a methodology to back calculate the resistivity that gave rise to the measured potential measurements. Starting from a simple initial model (usually a homogeneous half-space), a non-linear optimization method is used to iteratively change the resistivity of the model cells to minimize the difference between the measured and calculated apparent resistivity values. The inversion problem is frequently ill-posed and ill-constrained due to incomplete, inconsistent and noisy data (Loke et al., 2013).

Smoothness or other constraints are usually incorporated to stabilize the inversion procedure to avoid numerical artifacts. We call this type of calculation tomography, hence giving rise to the term ERT.

An example of an ERT section is provided in Figure 1, where low resistivity is typical of wet ore and high resistivity is indicative of drier conditions. The data were collected with a Schlumberger array and inverted using RES2DINV. The section shows coherency in both low and high resistivity targets, where both compacted and wet zones are identified (and summarily confirmed through drilling). Other interpretations were made based on hydrological principles, understanding stacking methodologies, and discussing the history of the facility with the mining superintendent.

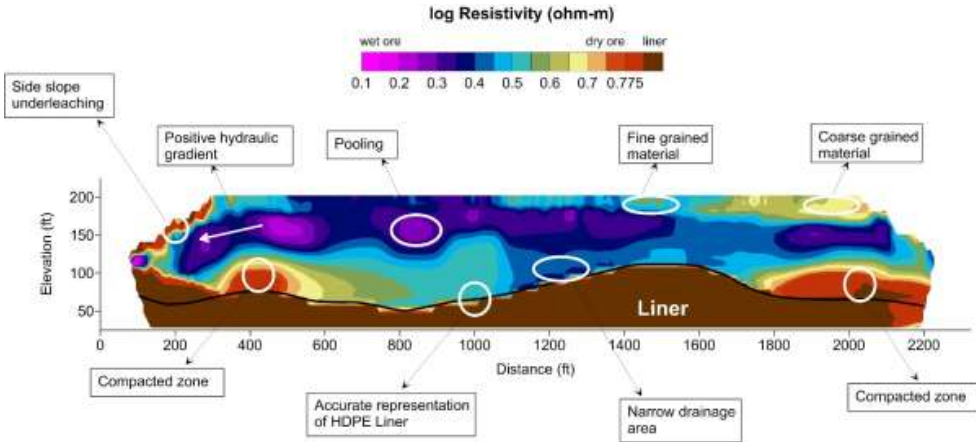


Figure 1. Example of ERT applied to a rock pile with an underliner.

3 TAILINGS CHARACTERIZATION

Tailings and waste rock piles are extremely heterogeneous systems, comprising various features at different scales. Characteristics of these piles can vary greatly with respect to rubblized and processed content, grain and rock size, rock type, large-scale structural design, and stacking strategies. In every case, no two tailings piles are the same and will differ in mineralogy, morphology, and chemical characteristics. To understand the influence of these factors, it is critical to characterize the structure and the relevant material distribution within tailings piles (Dawood et al., 2009).

Electrical resistivity affords a dynamic approach to tailings characterization and understanding of the properties that dictate solution movement by providing a means of spatially characterizing their unique structure. For instance, mapping the permeability of tailings piles can expose areas of high moisture, which may be a consequence of preferential flow or perched aquifers within the structure. Whereas dry resistive areas may be the result of compacted areas or zones that no longer allow water to drain effectively.

An example of these types of conductive and resistive targets can again be seen in Figure 2. We used electrical resistivity to discover large conductive anomalies that are responsible for creating seeps on the margins of a waste rock pile. The conductive anomalies represent saturated material as dark blue and purple targets while a more resistive, less saturated zone sits below the upper conductive areas at the center of the profile, represented by variations of olive green.

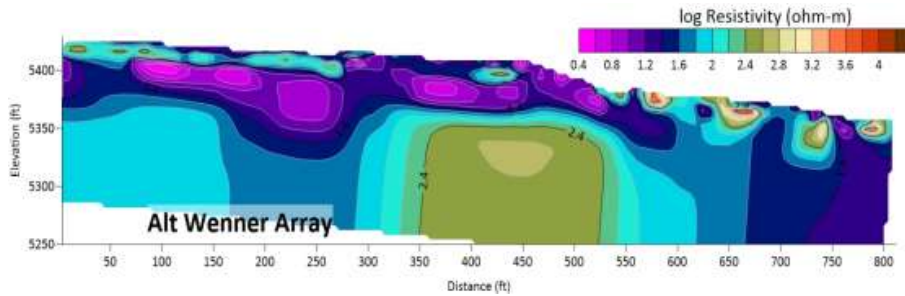


Figure 2. Example of electrical resistivity across a waste rock pile with seepage issues.

4 STRUCTURAL MAPPING AND FACILITIES SITING

As the flow of both surface and groundwater domains provide the main pathways of mine pollutants to the environment, it is essential that the geological materials that control them are well understood (Howett et al., 2015). Towards this end, mapping the subsurface becomes an important step in siting new facilities to minimize damage. Several have used surface geophysics and ERT to help site these facilities and establish background conditions prior to construction (Bauman et al., 2014; Pettifer et al., 2017).

In our work, we have used ERT extensively to map structure beneath potential locations for tailings facilities. In Figure 3, we present two sections that were acquired within a mile of each other to investigate subsurface conditions. The top section (Line 1) was acquired across a single sedimentary rock formation and the resistivity is shown to be fairly uniform at high values. Given that moisture would dramatically reduce the resistivity, it is likely that the formation is fairly competent with low fracture-based porosity to hold moisture. In Line 2, the ERT line crosses several formations of varying sedimentary, igneous, and metamorphic complexes. These data show that geological boundaries can extend deeply into the subsurface, thus allowing a means for contaminants to transport more easily to groundwater. Formation 2, in particular, is rather conductive, hinting at the fact that it could be fractured and holding some moisture. These fractures too could act as conduits. Therefore, we would recommend further exploration near Line 1 and abandon the consideration of siting the facility at Line 2.

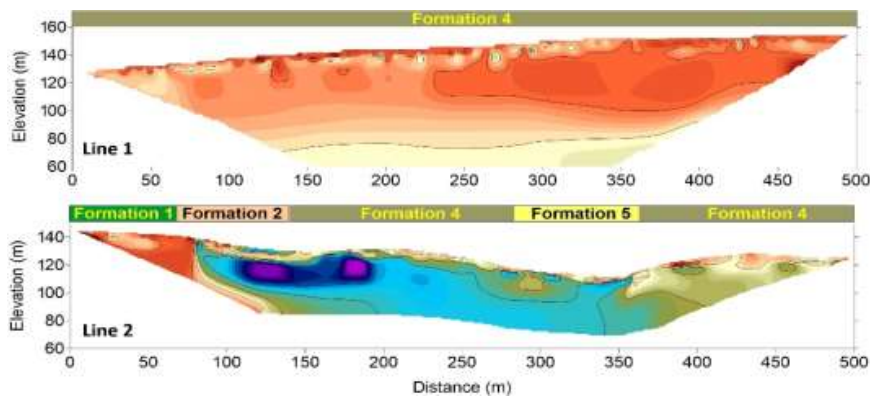


Figure 3. Example of ERT applied to structural mapping for siting facilities

5 LEAKAGE AND SEEPAGE CHARACTERIZATION

While it is valuable to understand properties that dictate solution movement and the distribution of solution within tailings piles, it is equally important to understand where that solution may go beyond the impoundment boundaries. Thus, the long term stability and environmental performance of these structures is critical to their long-term management and cost. The primary impact on these structures is atmospheric water or ground water that intrudes into tailings piles leading to the formation of acid creating the problem of acid rock drainage (ARD). Fundamentally, ARD challenges are related to the flow of water through tailings and it becomes critically important to be able to evaluate water movement and distribution in these piles (Dawood et al., 2009).

These structures are uniquely constructed and are commonly placed in areas where the geology forms natural depressions or boundaries to contain the large quantities of waste. However, the very geological and environmental conditions pursued to build tailings structures can also lead to the development of subsurface seepage pathways that progress beyond the impoundment confines. This is because geological depressions and valleys are commonly associated with faults and other related geological structures that can carry tailings solutions off site through natural subsurface pathways. Locating these pathways can prove exceedingly difficult and costly, especially when using invasive measures such as drilling and potholing.

While ERT serves as a valuable characterization application to understand the internal hydrodynamic structure of tailings piles, it can also be used to track and delineate the extent of seepage pathways beyond impoundment boundaries. Both applications have the distinct advantages of imaging through the entire tailings pile, tailings dam or impoundment and its contact with basement geology to understand fluid movement. When tracking seepage, ERT arrays are arranged perpendicular to suspected subsurface solution pathways and moved outward from the source toward known ‘outfalls’, creating a linear series of 2D profiles mapping fluid infiltration through natural geologic conduits. This methodology is used to determine both the direction and depth of seepage pathways. Figure 4 shows a series of ERT arrays used to track solution emanating from a tailings pile.

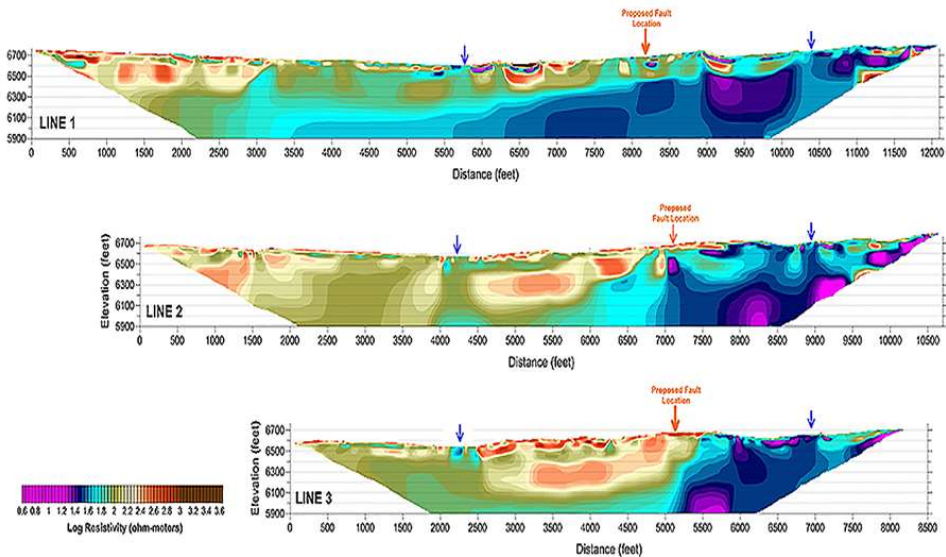


Figure 4. Example of ERT arrays down gradient of a tailings dam.

Additionally, ERT can be used to track leaking or flowing water into tailings and waste rock through covers. Tailings piles are always under the influence of seasonal and diurnal cycles that affect internal temperature, moisture, and solution movement. When combined with natural atmospheric precipitation and groundwater fluctuations, understanding water infiltration can be challenging without the use of more holistic measure such as ERT. Covers are designed to absorb some precipitation and allow the rest to run off in an effort to keep the contaminant material beneath dry and reduce future impacts to the environment. In Figure 5, a series of ERT arrays were used to understand seasonal changes occurring in waste rock and the integrity of an earthen cover over a pile.

In the Figure 5 example, the operator monitoring the mine waste was unsure whether the cover was effective based on long-term treatment of drain down waters and atypical water level fluctuations. The ERT survey revealed limited weak spots where the cover was compromised. The weak areas appear as low resistivity anomalies punctuating the resistive cover, whereas the waste is significantly more conductive when compared to the resistive cover and weak areas. This example demonstrates that potential seep migration pathways into the waste are not likely coming through the cover and, in fact, the cover is intact and working as designed. The source of water entering the pile is likely groundwater and not surface rainfall.

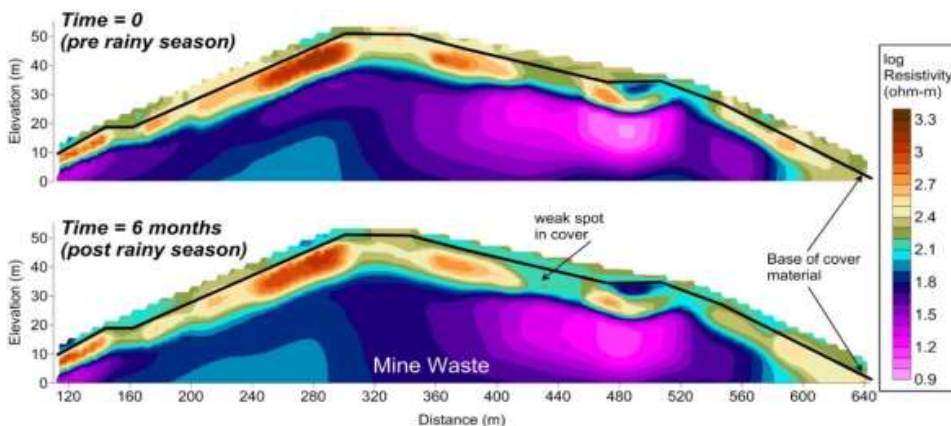


Figure 5. Example of two ERT surveys acquired 6 months apart over a covered tailings pile.

6 PLUME MAPPING

Geophysical methods have increasingly demonstrated their potential to delineate areas contaminated with potentially harmful elements and compounds and acidic seepage from mine waste sites (Placencia-Gómez et al., 2010). ERT is a highly promising tool for investigating the internal structure of mine wastes that are controlled by water and oxygen fluxes responsible for sulfide oxidation and possible generation of ARD (Chouteau et al. 2005). ARD is comprised of highly ionic porewater, providing a strong target for ERT relative to the typical resistive host rock. Vanhala et al. (2004) provides more proof of the power of ERT to map ARD.

In our example, provided in Figure 6, an ERT line was placed adjacent to a tailings facility to investigate the extent of contamination to the subsurface. Line C shows a strong conductive anomaly of around 10 ohm-m, with a center of mass around 33 ft below ground surface. This would seem to be an extreme environmental hazard, but fortunately, the plume was truncated as shown in Lines A and B, placed at incremental distances from Line C. These sections become more resistive owing to the decreased mine impacted waters flowing from the tailings facility. The ERT data were then used to site an environmental monitoring well and a pumping well for reducing contamination and tracking the progress.

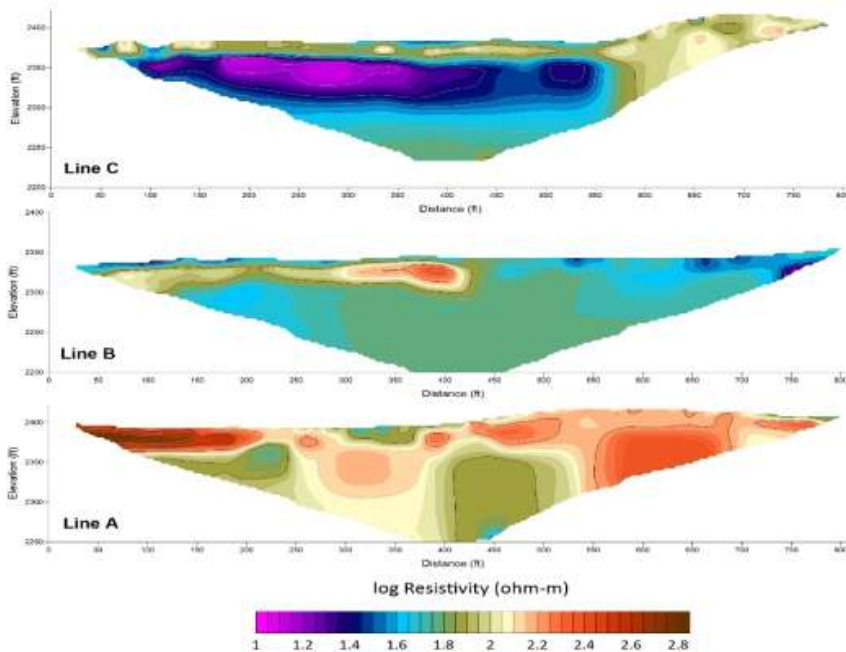


Figure 6. Example of ERT applied to mapping ARD plumes adjacent to a tailings facility.

7 STABILIZATION MONITORING

Under certain scenarios, it is necessary to stabilize a tailings facility, as Cline et al. (2016) showed with the use of grout injection. In their work, the grout was used to strengthen the zone of overbank deposits, on which their tailings were built, thus it was a critical element to improving the geomechanical stability of the facility. The overbank deposits have low shear strength and could liquefy during a seismic event. In other work, Kim et al. (2003) used iron as a reducing agent to geochemically stabilize tailings from arsenic contamination. Mohamed et al. (2003) used a fly ash based cement with aluminum to hydro-mechanically stabilize tailings, which reduced permeability and increased strength.

In each of these examples, the stabilizer needs to mix with existing material. An efficient means of mixing could be through injection, which would ensure depth penetration of the stabilizer. To optimize delivery of the stabilizer, one would need information on penetration and ERT can be an excellent tool for monitoring events in time. The ERT would be collected over a series of snapshots, with the data being compared to a baseline event prior to injection. In our work (Rucker, 2014; Rucker et al., 2014; Rucker et al., 2015) we have used ERT extensively to track injections into rockpiles and heaps to understand fluid propagation and movement. The data are then used to develop upscaled well fields and ensure adequate coverage.

An example of injection monitoring is shown in Figure 7. In this example, we placed electrodes for the ERT monitoring survey on the surface of the rockpile as well as within boreholes to increase resolution. We then acquired ERT data on 168 electrodes with a pole-pole array, taking a snapshot every 25 minutes.

The data show the injected solution to be nearly symmetric about the injection well extending out to a radius of about 58ft. Having this information allows placement of other injection wells at optimized distances to ensure complete coverage of the injected solution.

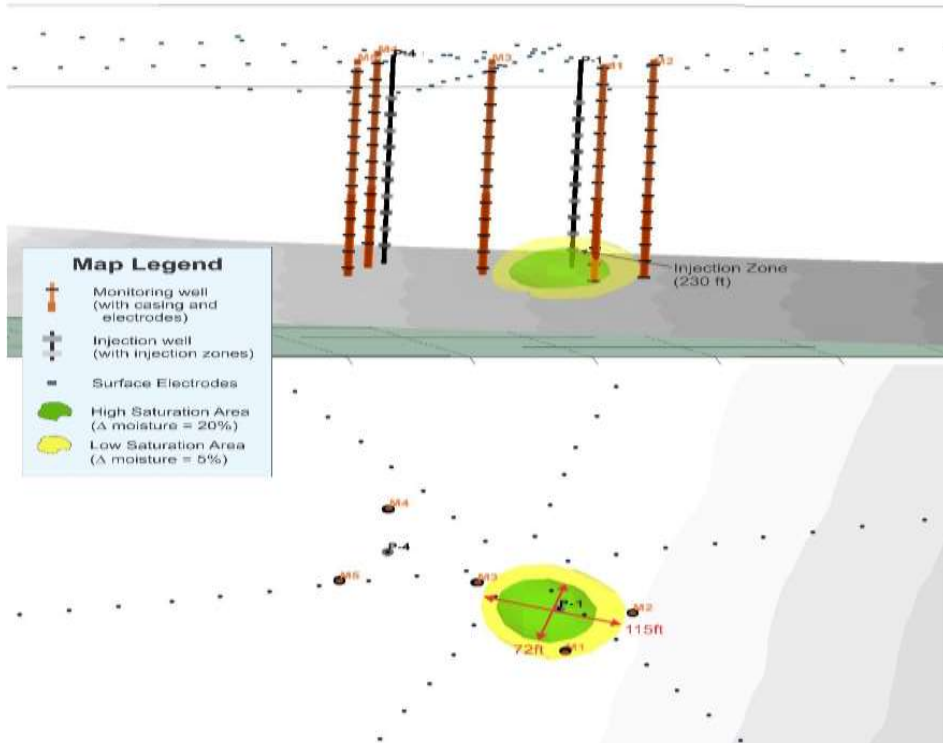


Figure 7. Example of time lapse ERT applied to injection monitoring.

8 CONCLUSION

Electrical resistivity methods afford a dynamic approach to tailings characterization and understanding of the properties that dictate solution movement, providing a means of spatially characterizing their unique substructure. ERT methods have been successfully used to map the subsurface of tailings piles for spatial distribution of pore water content, monitoring fluid infiltration through geologic materials, delineating preferential groundwater flow pathways, and determining structural integrity. These innovations have allowed broader assessment of large-scale hydraulic processes, helping tailings managers gain holistic information to highlight areas where potential challenges may exist. This allows for proactive mitigation of tailings managements challenges.

REFERENCES

- Bauman, P., Parker, D., Pankratow, L. and Hume, K., 2014, March. Geophysical Methods As an Aid to Planning, Monitoring, and Abandoning Tailings Facilities in the Alberta Oil Sands. In Symposium on the Application of Geophysics to Engineering and Environmental Problems 2014 (pp. 94-94). Society of Exploration Geophysicists and Environment and Engineering Geophysical Society.
- Benyassine, E.M., Lachhab, A., Dekayir, A., Parisot, J.C. and Rouai, M., 2017. An Application of Electrical Resistivity Tomography to Investigate Heavy Metals Pathways. *Journal of Environmental and Engineering Geophysics*, 22(4), pp.315-324.
- Booterbaugh, A.P., Bentley, L.R. and Mendoza, C.A., 2015. Geophysical characterization of an undrained dyke containing an oil sands tailings pond, Alberta, Canada. *Journal of Environmental and Engineering Geophysics*, 20(4), pp.303-317.
- Chouteau, M., Poisson, J., Aubertin, M., and Campos, D., 2005. Internal structure and preferential flow of a waste rock pile from geophysical surveys. In: Proceedings of the symposium for the application of geophysics to environmental and engineering problems, SAGEEP 2005. Environmental and Engineering Geophysical Society, pp 289-297.
- Cline, D.J., Crouse, P.E., DeDen, M.F. and Zimmer, T.R., 2016. Engineering and reclamation of the Holden Legacy Mine—advancing the state-of-practice for mine closure. Mine Closure 2016, Perth, Australia.
- Cubbage, B., Noonan, G.E. and Rucker, D.F., 2017. A Modified Wenner Array for Efficient Use of Eight-Channel Resistivity Meters. *Pure and Applied Geophysics*, 174(7), pp.2705-2718.
- Dawood, I., Aubertin, M., Intissar, R., Chouteau, M., 2011. A combined hydrogeological–geophysical approach to evaluate unsaturated flow in a large waste rock pile. Pan-AM CGS Getechnical Conference Montreal, Canada.
- Grangeia, C., Ávila, P., Matias, M. and Da Silva, E.F., 2011. Mine tailings integrated investigations: the case of Rio tailings (Panasqueira Mine, Central Portugal). *Engineering Geology*, 123(4), pp.359-372.
- Howett, P.J., Salonen, V.P., Hyttinen, O.S.M., Korkka-Niemi, K.I. and Moreau, J., 2015. A hydrostratigraphical approach to support environmentally safe siting of a mining waste facility at Rautuvaara, Finland. *Bulletin of the Geological Society of Finland*.
- Kim, J.Y., Davis, A.P. and Kim, K.W., 2003. Stabilization of available arsenic in highly contaminated mine tailings using iron. *Environmental science & technology*, 37(1), pp.189-195.
- Loke, M.H., Chambers, J.E., Rucker, D.F., Kuras, O. and Wilkinson, P.B., 2013. Recent developments in the direct-current geoelectrical imaging method. *Journal of Applied Geophysics*, 95, pp.135-156.
- Mohamed, A., Hossein, M. and Hassani, F., 2002. Hydro-mechanical evaluation of stabilized mine tailings. *Environmental Geology*, 41(7), pp.749-759.
- Pettifer, G., Richards, G., Jenke, G. and Lester, N., 2017, March. Characterisation of a fractured rock aquifer system by 2d/3d resistivity surveying and modelling around a disused mining pit proposed for mine tailings disposal. In Symposium on the Application of Geophysics to Engineering and Environmental Problems 2017, pp. 232-237.
- Placencia-Gómez, E., Parviainen, A., Hokkanen, T. and Loukola-Ruskeeniemi, K., 2010. Integrated geophysical and geochemical study on AMD generation at the Haveri Au–Cu mine tailings, SW Finland. *Environmental Earth Sciences*, 61(7), pp.1435-1447.
- Rucker, D.F., Schindler, A., Levitt, M.T. and Glaser, D.R., 2009. Three-dimensional electrical resistivity imaging of a gold heap. *Hydrometallurgy*, 98(3-4), pp.267-275.
- Rucker, D.F., 2015. Deep Well Rinsing of a Copper Oxide Heap. *Hydrometallurgy* 153, 145-153.
- Rucker, D.F., 2014. Investigating Motion Blur and Temporal Aliasing from Time-Lapse Electrical Resistivity. *Journal of Applied Geophysics* 111(1), 1-13.
- Rucker, D.F., N. Crook, J. Winterton, M. McNeill, C.A. Baldyga, G. Noonan, and J.B. Fink, 2014. Real-Time Electrical Monitoring of Reagent Delivery during a Subsurface Amendment Experiment. *Near Surface Geophysics* 12 (1), 151-163.
- Vanhala, H., Räisänen, M.L., Huotari, T., Valjus, T., Lehtimäki, J. and Suppala, I., 2004, September. Characterizing tailings impoundment at the closed Hammaslahti Cu-Zn mine, Finland. In Near Surface 2004-10th EAGE European Meeting of Environmental and Engineering Geophysics.

Site Characterization throughout the Tailings Facility Life Cycle

M. Malgesini and L. Aubone

Golder, Denver, CO, USA

R. Hunsaker and W. Boyd

Goldcorp-Minera Peñasquito, Zacatecas, Mexico

ABSTRACT: Since operations began at the Goldcorp Minera Peñasquito Tailings Facility in 2009, major design changes have been required to adapt to increased reserves, increased mill throughput, and challenges associated with operating an 110,000 tonne per day facility. Originally designed as a 3-sided, centerline raise, cyclone sand dam with an ultimate perimeter length of approximately 11 kilometers and a maximum height of approximately 115 meters, the facility design, construction, and operation has transitioned to a buttressed, centerline raise rockfill dam with a cyclone sand transition zone separating the tailings and rockfill. This paper provides a case study summarizing the history of the design changes and the detailed site characterization studies that have enabled the successful adaptive management of the facility as it has been constructed and operated.

1 INTRODUCTION

The life cycle of a tailings facility is rarely discrete or linear and tailings facilities are often required to adapt and evolve to change. Change may result from increasing mine reserves, new process technology, construction strategy, or any number of things not predictable at the time of the initial mine and tailings facility conception. The life cycle of a tailings facility can also extend for many decades, during which time the facility continues to be constructed and operated. This requirement makes tailings facilities unique when compared to other types of containment structures, such as water resource or hydroelectric dams that are designed and constructed to the final configuration at the beginning of a project. The inevitable outcome of this life cycle is that change must be managed in order to control risks.

Ongoing site characterization throughout the life of a tailings facility is one way to manage many of the risks introduced by change. Site characterization is required to define the conditions of the site as they relate to the design, construction, and operation of a tailings facility. Site characterization is a standard component of project development, and there are many guidelines to help define the requirements for site characterization as the project progresses from concept and planning, to design, and into initial construction. Most site characterization studies are conducted throughout the initial planning and design stages of the project and these studies are typically tailored to the specific configuration identified at project conception. As the life of the tailings facility progresses and changes are introduced, it is imperative to update and advance the site characterization to reflect these changes.

This paper presents a case study demonstrating the importance of ongoing site characterization at the Goldcorp Minera Peñasquito tailings facility that have been required in response to changes to the facility design, construction and operation since the initial construction phase.

2 MINERA PEÑASQUITO PROJECT AND TAILINGS FACILITY OVERVIEW

The Minera Penasquito Mine is a large scale open pit polymetallic operation, located about 780 kilometers northwest of Mexico City. Peñasquito produces gold, silver, lead and zinc and is a major contributor to Goldcorp’s revenue and growth plans. Ore is extracted by using standard shovel mining techniques and trucked to either the heap leach, which processes oxide ore; or the plant that processes sulphide ore using a high pressure grinding roll circuit. The processing capacity of the sulphide plant is approximately 130,000 tonnes per day. Tailings from the sulphide plant are sent via slurry pipeline to two cyclone stations where sand sized particles are separated from the whole tailings for future use in construction of the perimeter dams. The remainder of the whole tailings and cyclone overflow are pumped to the crest of the dam and discharged uniformly around the perimeter of the facility. Free water from the discharged tailings is recovered from an internal water reclaim pond and pumped back to the mill for re-use.

The Penasquito tailings facility consists of an 11-kilometer long, 3-sided, centerline raise rockfill and cyclone sand dam. Rockfill is used to create a buttress and the downstream shell for the facility, cyclone sand is used in construction as a transition zone separating the tailings beach from rockfill.

As of June 2018, the tailings facility has a maximum height of approximately 80 meters, and stores approximately 284 million tonnes of tailings that have been produced since 2010. The life of mine plan for the tailings facility is to continue raising the dam to a maximum height of approximately 150 meters, which will provide a total storage capacity of at least 807 million tonnes. An aerial view of the Penasquito tailings facility from March 2018 is provided in Figure 1.

The Penasquito tailings facility has gone through a number of configuration changes as each phase of the project has evolved. Changes have been in response to changes in mine plan, construction strategy, and operation. Looking forward, continued evolution of the facility is anticipated and future raises have been planned to accommodate change, including the opportunity to capitalize on alternative tailings management initiatives, such as those currently being evaluated with the Goldcorp Ecotails project.

Throughout each of the changes that have occurred, it has been critical to review, advance and update the site characterization.



Figure 1. Penasquito Tailings Facility March 2018

3 PEÑASQUITO TAILINGS FACILITY LIFE CYCLE SITE CHARACTERIZATION

3.1 Site Characterization for Planning and Concept Phase

During the initial planning and concept phase for the Penasquito mine, a site characterization was conducted that included a typical geologic reconnaissance, and a limited field program to identify geologic features, bedrock type and depth, soil profiles, material properties, and groundwater levels in the immediate proximity of the proposed tailings facility site. This initial site characterization was done to support an initial alternatives assessment as well as a conceptual configuration for the tailings facility.

The initial site characterization included nine boreholes and seven test pits located within the general vicinity of the proposed tailings facility site. The initial site characterization and geologic reconnaissance identified that the site conditions generally consisted of heterogeneous alluvial deposits consisting of gravels, sands, silts and clays, overlying bedrock.

Based upon the mine plan, site characterization and desired tailings management strategy, the tailings facility was conceptualized as a cyclone sand dam with out slopes defined as three horizontal to one vertical (3H: 1V). The tailings facility was initially planned to accommodate tailings throughput from the mill at 50,000 tonnes per day and an ultimate capacity of on the order of 200 to 300 million tonnes. The facility was planned to be constructed in stages, sequenced based upon an initial 2-year starter facility at the western limit of the property. As tailings were deposited, the facility would expand by sequentially raising west dam, and raising and extending the north, and south dams to the east as illustrated in Figure 2. The eastern limit of the facility would be provided by the 2-percent grade of the native topography.

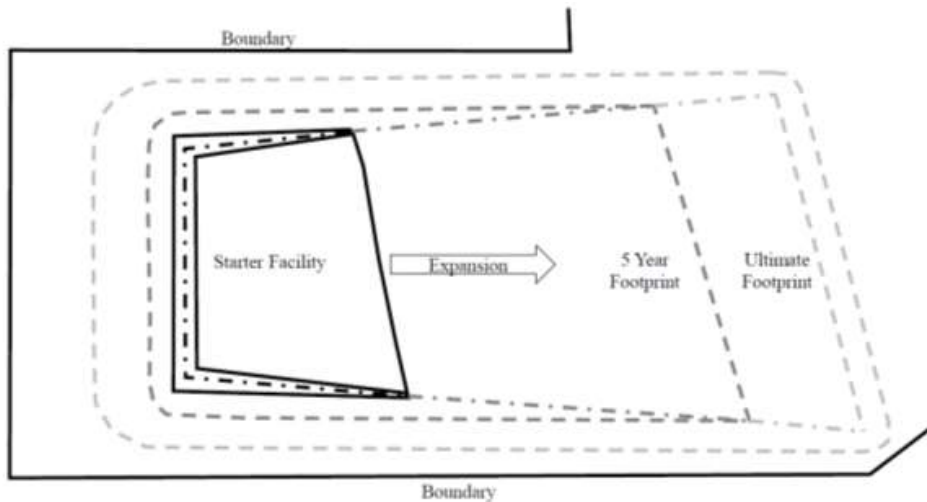


Figure 2. Penasquito Tailings Facility Conceptual Development Plan

3.2 Site Characterization for Design Phase

The site characterization carried out during the design phase of the Penasquito tailings facility consisted of 40 boreholes, 66 test pits, and review of core logs from 80 condemnation core holes advanced by the mine. The site characterization for the facility at the design phase was focused on further characterization of foundation material properties, and identifying construction materials that could be used during construction of the starter facility.

During this phase of site characterization, additional information was obtained to support increased definition regarding the variability of the subsurface materials, including the identification of felsite tuff materials that were encountered along the south side of the tailings facility,

cemented zones of sand and gravel within the alluvium, and cemented conglomerate zones overlying the bedrock. The variability in the depth to bedrock and depth to groundwater levels was also further defined during the design phase of the site characterization.

Groundwater was typically encountered near or below the bedrock elevation underlying the site. Based on this site characterization, the key issues for design of the tailings facility were in regards to: (1) the properties of heterogeneous alluvial materials, felsite tuff, and how these materials would respond to the loading induced by the cyclone sand dam with a rate of rise of approximately 2.5 meters per year; and (2) response of the foundation soils to potential wetting and loading of alluvium from potential seepage through the liner. A detailed laboratory testing program was conducted to evaluate these issues. Based upon this characterization the tailings facility design was completed and passed onto initial construction phase. Figure 3 provides a photographic representation of the types of geologic materials encountered within the vicinity of the tailings facility.

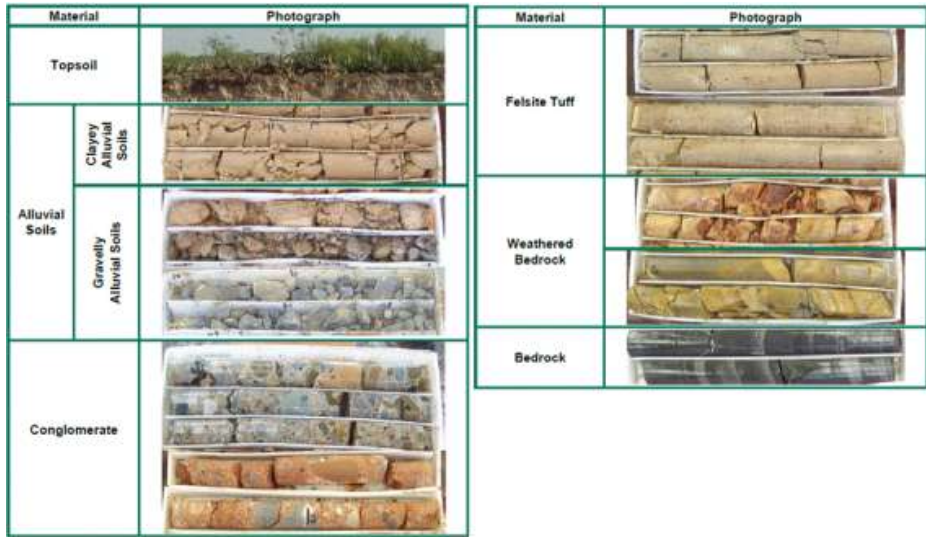


Figure 3. Geologic Materials Underlying Penasquito tailings facility

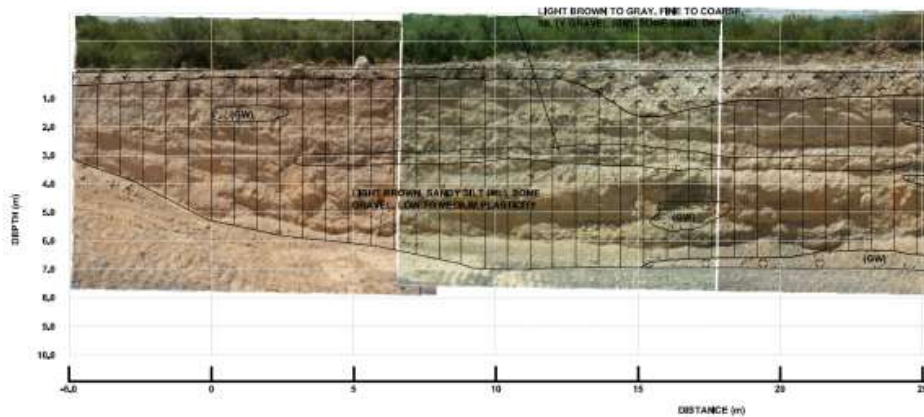


Figure 4. Test Trench for Soil Liner Borrow Source Site Investigation

3.3 Site Characterization for Initial Construction Phase

Following completion of the initial detailed design of the tailings starter facility, the mine plan for the project changed such that the planned mill throughput more than doubled to 130,000 tonnes per day, and the total capacity of the tailings facility was increased to approximately 807 million tonnes. This change required additional evaluations for configuration of the facility (which was restricted by property boundary), including an evaluation of the rate of rise (which would double to nearly 5 meters per year), and evaluations on the constructability of the starter dams and sand dam construction during operation.

To evaluate constructability of starter facility, additional site investigations had to be conducted to assess additional borrow materials that would be required, including identification of sufficient quality and quantity of soil liner materials. To evaluate potential borrow sources for soil liner, 11 large scale test trenches, measuring 6 to 12 meters deep by approximately 50 meters long were advanced to evaluate consistency of material properties of potential clay liner borrow materials that had been identified within the future limits of the tailings facility. A photograph of a typical test trench completed to during the clay liner borrow characterizations study is provided in Figure 4.

The site characterization performed between the detailed design and initial construction phase identified that sufficient borrow materials were available or could be processed from the alluvium; however, the timeline for construction of the starter facility was such that a 2-year facility could not be constructed in the time allowed. This assessment led to a reduction in the starter facility life such that it would be constructed with a 1-year capacity (rather than two as originally planned), thus increasing the risk of not being able to ramp up and construct of the cyclone sand dam raises sufficiently to maintain the increased rate of rise of the facility.

3.4 Site Characterization for Operations and Ongoing Construction – Adapting to Changes

The Penasquito tailings starter facility was constructed in 2008 and operations began in late 2009. Upon commencement of operations, it became apparent that the challenges associated with raising the tailings facility at 5 meters per year via a centerline raise, cyclone sand dam methods were too significant to overcome and a design change was needed. The design change included a rockfill buttress, which was used to raise the downstream portion of the starter dam, and a transition zone of cyclone sand placed between the rockfill buttress and the deposited tailings. This configuration allowed for a significant reduction in the requirements for producing and placing cyclone sand. The buttress was designed to extend the life of the facility by 2 years, during which time cyclone sand production and construction could be improved and the facility would revert back to be constructed as a cyclone sand dam. The rockfill buttress was designed with 1.75H: 1V downstream slope that was constructed on dry native alluvial soils (water table was near or below the bedrock contact). The buttress was to be a temporary condition that would be incorporated into the cyclone sand dam as dam was raised. The site characterization completed during the design and initial construction stages indicated that the foundation materials were suitable to support this configuration on a temporary basis, while maintaining a minimum required factor of safety of 1.5. However, as operations continued over the following year, a decision was made that the dam would not revert to a traditional cyclone sand dam, thus limiting the maximum height of facility to that which could be supported by the rockfill buttress assuming centerline raise methods of construction.

The decision that the tailings facility would not revert to a traditional sand dam, along with additional tailings storage capacity and water savings needs, required that alternative tailings management strategies and expansion plans be developed. To support these alternatives, additional site characterizations were conducted. The key focus areas of these site characterizations included: evaluation of deposited tailings to confirm material properties defined during the initial planning and design phases; and evaluation of the response of the foundation materials as compared to properties and conditions identified during the design phase. The additional site characterizations suggested that the concept to continue raising the existing tailings facility was possible using centerline raise methods, provided that the existing dams were buttressed. Based upon these findings, a feasibility study was conducted to further evaluate continued raising of

the existing TSF. This feasibility study was completed and approved, and Stage 1 of the Tailings Facility Centerline Raise Project has been ongoing since 2017.

The tailings facility centerline raise project would not have been feasible without completing the detailed investigations that were carried out in 2014 and 2015 to evaluate the material properties of the in-place cyclone sand and deposited tailings making up the tailings beach. This site investigation consisted of 55 Cone Penetration Test soundings with pore pressure dissipation tests. These soundings provided information regarding the in situ relative density and hydraulic conductivity with depth, and with horizontal distance from the dam centerline. This investigation also included advancing 12 boreholes and installing a series of vibrating wire piezometer arrays. Boreholes were used to collect samples and to calibrate material properties as interpreted from the Cone Penetration Test soundings. Vibrating wire piezometer arrays were used to monitor the phreatic surface within the tailings beach extending from the crest of the dam.

Additional investigations of the foundation materials below the tailings facility was also conducted during this period. This site characterization campaign consisted of installing 15 additional boreholes, with vibrating wire piezometers, around the perimeter of the tailings facility. These vibrating wire piezometers were intended to monitor groundwater levels and pore pressure response as the tailings dam was raised. Groundwater levels were observed to be rising around the facility, resulting wetting of the alluvial soils. Samples collected during this site characterization campaign were subjected to laboratory testing to further characterize the potential for pore pressure response, and to further characterize the drained and undrained strength of the foundation soils. A key finding of this program was the uncertainty with respect to the potential for undrained conditions occurring below the tailings facility. If undrained conditions were to develop, this would result in a lower than acceptable factor of safety. This uncertainty regarding the potential drained versus undrained response, derived from material behavior observed from laboratory scale testing indicating the potential for an undrained response as compared to the field scale response.



Figure 5. Penasquito tailings facility under construction June 2018

The findings of these site characterization campaigns provided sufficient information to demonstrate that the in situ beach and cyclone sand properties, as well as the foundation material properties, were adequate to continue raising and expanding the dam. The configuration for the future dam raises included additional rockfill buttresses to provide for an adequate factor of safety against undrained conditions. A detailed monitoring and instrumentation plan was developed to monitor the conditions of the beach and foundation materials as the facility would continue to be raised. Figure 5 provides a typical photo of the configuration of the tailings facility being constructed as of June 2018.

Stage 1 of the Peñasquito tailings facility centerline raise project expansion was started in mid-2017 with construction of the initial buttress. The initial buttress was instrumented with a series of vibrating wire piezometers, settlement plates, and inclinometers to evaluate the response to the foundation to buttress loading. Assessments following each of the four lifts (5 meters each) of the buttress fill construction indicated a near fully drained response in the alluvial materials, and partially drained response in the felsite tuff materials underlying the facility. The responses that were observed indicated that pore pressures generation and dissipation could be managed within the planned rate of construction of the facility to prevent an undrained condition within the foundation materials. As of June 2018, a campaign to install additional geotechnical instrumentation with and below the tailings facility is ongoing. Future campaigns to re-assess the tailings beach properties are planned in the next phases of construction and operation.

3.5 Future Site Characterization to Support Potential Tailings Management Alternatives

Goldcorp is committed to continually improving the way that tailings are managed on their sites. For the Peñasquito tailings facility, this means continuing to evaluate alternative methods for tailings management and continuing to evaluate ways to optimize the management of the existing tailings facility as operations progress and future raises are executed. Site characterization to support new alternatives and improvements is a critical part of this strategy

3.6 Closure and Post-Closure Phases

While not discussed in detail in this case study, site characterization for closure is key a component of the tailings facility life cycle. For the Peñasquito tailings facility, site characterization has been undertaken and future work is planned to support various closure concepts and cover designs, including the potential to incorporate various land form closure design concepts.

4 SUMMARY

The history of the Minera Peñasquito tailings facility demonstrates the importance of ongoing site characterization through the facility life cycle. The changes in configuration and design criteria that have occurred throughout the history of this facility have required that the site characterization be continually advanced and improved in order to support the assessment of alternatives and to make decisions related to the ongoing operation and development of the facility.

Throughout this process, Goldcorp has relied upon and supported the role of Engineer of Record in the development of the facility. Goldcorp has also implemented a Tailings Review Board since 2016, which has been instrumental in guiding development of site characterization recommendations and assessments. Additionally, Goldcorp has implemented a Tailings Stewardship Program for all of their facilities that provides an additional level of third party review and guidance. These best practices of third party review and Engineer of Record engagement have ensured that adequate site characterization has continued as the tailings facility has been designed, constructed, and operated.

Assessing Mine Site or Tailings Facility Water Management Risks by Integrating Tailings Deposition and Water Balance Modeling

K. Patterson, M. Liew and R.W. Chambers

Klohn Crippen Berger Ltd., Vancouver, British Columbia, Canada

ABSTRACT: Design and management of tailings storage facilities (TSF) should take a risk-based approach. Water management is key when assessing mine site and tailings facility dam safety, environment and society risks. To understand the water management risks and help identify potential critical controls, site-wide or (at least) TSF water balance modeling should be completed in conjunction with tailings deposition planning because their inputs and outputs are interdependent.

This paper presents two workflows options and several case histories of assessing water management risks for mines sites and/or TSFs by integrating tailings deposition planning and water balance modeling. The workflow should be selected based on the risk(s) being assessed. Case study risks were either quantified; mitigated through design, tailings deposition or water management; or identified as requiring monitoring (potentially as a critical control).

1 INTRODUCTION

Mine site water management can often be “reactive” rather than “proactive”. This reactive behavior and lack of a combined long-term tailings placement and site-wide water management strategy can lead to increased risk for the project by increasing the likelihood and/or potential consequence of unwanted events, such as a dam failure, an unscheduled release of impacted water to the environment or a shutdown of the ore processing due to lack of water supply.

To avoid unwanted events, a risk-based approach is recommended for the design and management of tailings storage facilities (TSFs) (MAC 2017). As part of a risk-based approach, long-term planning through integrated tailings deposition modeling and water balance modeling can help mine owners better understand, mitigate, identify critical controls (i.e. site-specific and governance level risk controls, and associated performance measures, that would significantly or reduce the likelihood of the occurrence of an unwanted event or condition that poses unacceptable risk) and monitor water management risks surrounding mine sites and TSFs.

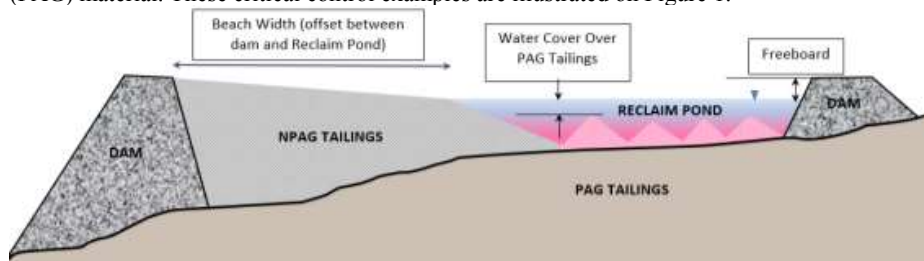
For proposed mines, assessing the water management risks can allow for mitigation through design or planning. For operating mines, assessing the water management risks can help identify critical controls that should be implemented and monitored as part of the TSF’s Operation, Maintenance and Surveillance (OMS) manual.

To understand water management risks and help identify potential critical controls for TSFs, site-wide or (at least) TSF water balance modeling should be completed in conjunction with tailings deposition planning because their inputs and outputs are interdependent.

This paper presents two workflows options and several case histories of assessing water management risks for mines sites and/or TSFs by integrating tailings deposition planning and water balance modeling. The workflow should be selected based on the risk(s) being assessed.

2 ASSESSING WATER MANAGEMENT RISK

A risk-based tailings management strategy requires risks to be identified through systematic evaluations, such as risk assessments (e.g. Failure Modes and Effects Assessment (FMEA)). Key risks may be identified as requiring a critical control, for example: maintaining a beach width for geotechnical stability, or maintaining a water cover over Potentially Acid Generating (PAG) material. These critical control examples are illustrated on Figure 1.



Note: NPAG – Non-Potentially Acid Generating; PAG – Potentially Acid Generating

Figure 1. Illustration of Critical Controls for Mitigating Dam Safety and Environmental Risks

Once risks are identified, assessment of certain water management risks can be done with the integration of tailings deposition and water balance modeling, examples are included in Table 1.

Table 1. Examples of Risks that can be Assessed with Integrated Tailings Deposition and Water Balance Modeling

Risk	How Risk can be Assessed with the Results from Integrated Tailings Deposition and Water Balance Modeling
<p>Dam Safety</p> <p>For example:</p> <ul style="list-style-type: none"> • Potential for overtopping dam failure due to inadequate storage and freeboard during the Inflow Design Flood (IDF) (Note 1). • Potential for piping or erosional dam failure due to water ponding adjacent to susceptible materials. 	<ul style="list-style-type: none"> • Estimate location and level of operating reclaim pond and predicted IDF pond for assessments of geotechnical (stability, piping, etc.), overtopping, and erosion (wind-wave). • Estimate location and level of operating reclaim pond and predicted IDF pond to identify critical controls and/or confirm compliance with potential Quantitative Performance Objectives (QPOs) (MEM 2016), such as beach width or freeboard.
<p>Water Supply</p> <p>For example:</p> <ul style="list-style-type: none"> • Reliability of water supply for downstream users. • Potential for shutdown of ore processing due to lack of water supply. 	<ul style="list-style-type: none"> • Estimate makeup water demand rates under a variety of scenarios (e.g. climatic). • Estimate availability of water for downstream environment and users under a variety of scenarios (e.g. climatic) and the probability of not meeting environmental or social requirements. Note, this may be considered a critical control. • Estimate availability for water reclaim to the ore processing facility under a variety of scenarios (e.g. climatic) and the probability of not meeting processing requirements. • Size backup water management structure (e.g. dams) to manage flood and drought conditions for dam safety, environment and ore processing.
<p>Environmental</p> <p>For example:</p> <ul style="list-style-type: none"> • Potential for desaturation of potentially PAG tailings leading to Acid Rock Drainage/Metal Leaching (ARD/ML) resulting in poor water 	<ul style="list-style-type: none"> • Size water treatment plants and estimate probability of those water treatment plants not meeting required flow rates during a variety of flood events and durations. • Estimate the Environmental Design Flood (EDF) (Note 2) required to meet downstream water quality guidelines. The tailings deposition and water balance assessments

<p>quality that requires management.</p> <ul style="list-style-type: none"> • Release of tailings sediments and process water into the environment. 	<p>would be combined with a water quality model to estimate this. Integrating water quality modeling with tailings deposition and water balance modeling is not the focus of this paper but is an important tool in assessing environmental risk.</p>
<p>Operational /Constructability For example:</p> <ul style="list-style-type: none"> • Inadequate distribution or reclaim systems or management plans leading to operational issues. 	<ul style="list-style-type: none"> • Determine the location of operating reclaim pond for planning construction and placement of operational facilities (e.g. pumps). • Determine spigot locations to achieve desired tailings beach configuration and pond volume for infrastructure planning.

Note 1: Inflow Design Flood (IDF) is defined as the flood into the impoundment resulting from the design hydrologic event (MEM 2016), also defined as the maximum flood that a dam is able to withstand (CDA 2007).

Note 2: Environmental Design Flood (EDF) is defined as the hydrological event that is to be managed without release of untreated water to the environment (MEM 2016).

3 WATER BALANCE AND TAILINGS DEPOSITION INTEGRATION

3.1 Approach

GoldSim dynamic simulation software (by GoldSim Technology Group) can be used for TSF water balance modeling. While a spreadsheet may suffice for a simple TSF water balance, GoldSim is preferred for more complex models because of its dynamic simulation capability that allows users to model varying timesteps (ranging from seconds/days to thousands of years) and provides a user-friendly interface that allows for better model conceptualization. It also has specialized modules that support water quality modeling and probabilistic (Monte Carlo).

Muck3D design software (by MineBridge) can be used for three-dimensional tailings deposition modeling. Users can specify tailings properties such as dry density, production rate, and tailings deposition slopes; and choose from a range options to estimate the reclaim pond volume or depth depending on what the deposition strategy is.

Figure 2 illustrates a typical TSF water balance conceptualization including the key flows that would be programmed into GoldSim. An example of a Muck3D output is included in Figure 3, which illustrates a simplified deposition run that predicts the pond volume/depth/area and the tailings beach width.

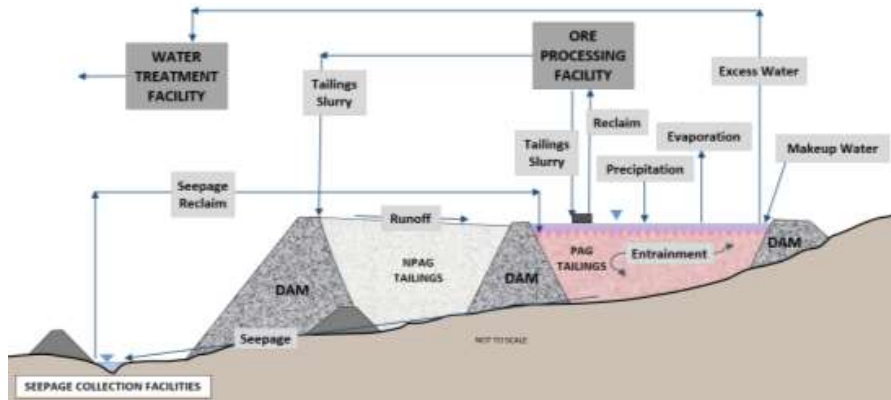
Key interdependencies between a TSF water balance and tailings deposition are shown on Figure 4.

The parameter that is potentially an input and output in both tailings deposition and water balance assessments is the operating reclaim pond volume. The stage of the project (e.g. design, operations) and objectives of the tailings management strategy dictates how the two assessments are integrated and the number of iterations between the two. The two general workflow options are described below.

3.1.1 Workflow 1 - Pond size determined by performance objectives (e.g. maintain a minimum water cover for PAG tailings, maintain a minimum pond depth for reclaim barge)

- Step 1: Tailings Deposition - complete tailings deposition to estimate the pond properties (e.g. volume, area, depth, water cover).
- Step 2: Water Balance - input pond properties and catchment delineations from Step 1 into water balance model.
- Step 3: Repeat for each timestep.

Water balance results include estimates of inflows or outflows required to achieve the pond volume to meet performance objectives (e.g. estimate makeup water requirements or water treatment rates to maintain a minimum water cover or pond depth).



Note: NPAG – Non-Potentially Acid Generating; PAG – Potentially Acid Generating

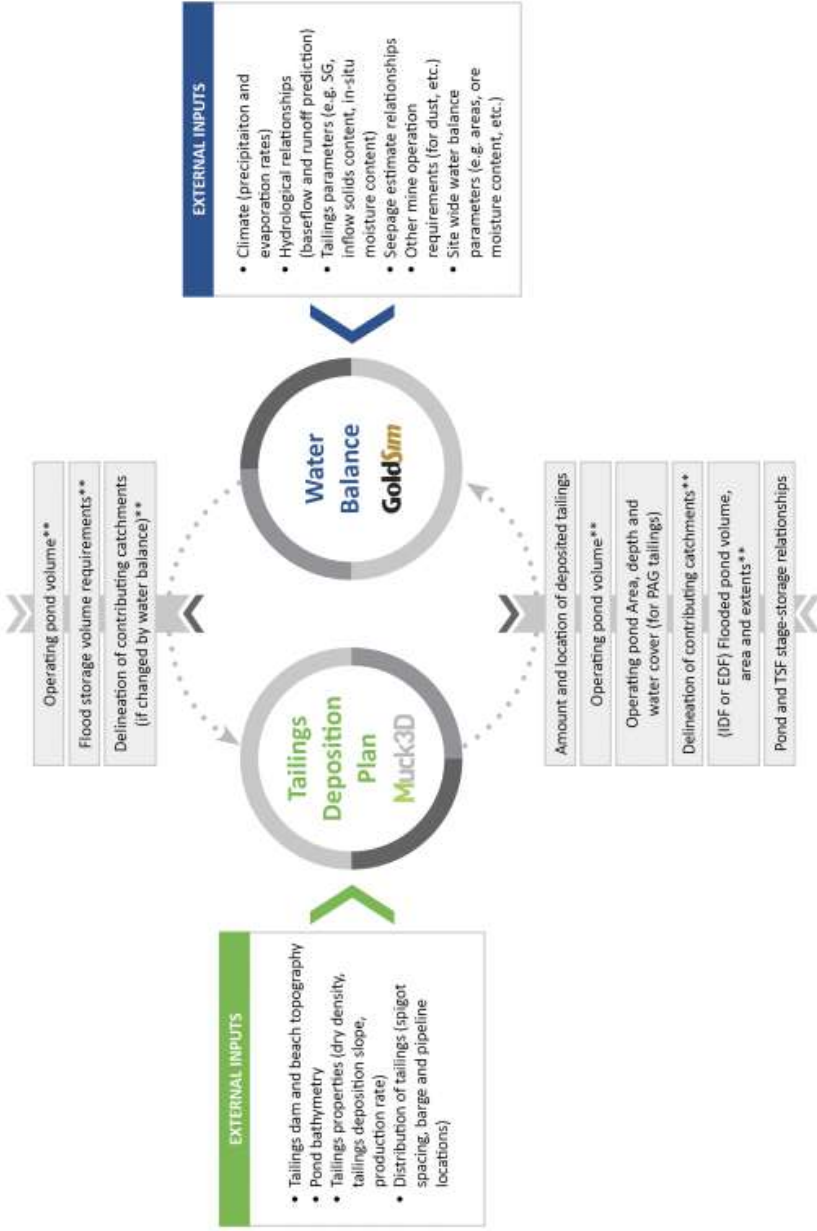
Figure 2. Typical TSF Water Balance Conceptualization Schematic



Figure 3. Tailings Deposition Modeling in Muck3D (MineBridge 2018b)

3.1.2 Workflow 2 - Pond size determined by water balance inflows/outflows

- Step 1: Tailings Deposition - complete tailings deposition with an approximate operating reclaim pond volume.
- Step 2: Water Balance - input pond properties (e.g. volume, area, depth, water cover), catchment delineations, and any other necessary parameters (e.g. stage-storage relationships) from Step 1 into the water balance model to estimate the predicted pond volume for that particular timestep.
- Step 3: Tailings Deposition Iteration: repeat Step 1 if the pond volume from Step 1 and Step 2 are significantly different. Input pond volume from water balance model (Step 2) into the tailings deposition to update the original assumption (from Step 1).
- Step 4: Water Balance Iteration: repeat Step 2.
- Step 5: Repeat for each timestep. The pond volume in Step 1 of the next timestep should be the pond volume estimated from Step 4 of the previous timestep.



Notes: ** denotes interdependencies; PAG – Potentially Acid Generating

Figure 4. Tailings Deposition and Water Balance Modeling Interdependencies

Workflow 2 is a brute-force approach and can be time-consuming unless careful consideration is given to original pond estimates, timestep length and error tolerance. The iterations can be automated with additional programming linkages between GoldSim and Muck3D if the tailings deposition plan has simple geometry (Cooper et al. 2018).

This workflow is preferred for operating TSFs that calibrate to historical conditions. In these cases, the Step 1 pond volume estimate is based on existing conditions measured from bathymetric surveys. Operating TSFs also allow for calibration to tailings deposition slopes and measured flows.

3.2 *Managing Uncertainties*

As with any modeling, the usual disclaimers apply: “model outputs are only as good as the inputs” and “no model can accurately simulate or predict reality, but the results can be useful and informative”. In order for a model to be useful, confirming the objectives and proper conceptualization of the system is the crucial first step. For example, the conceptualization presented in Figure 1 may not fit an intended purpose for another project and thus should be adjusted to suit. As well, all model inputs have varying degrees of uncertainty; typical input parameters that have uncertainty are:

- tailings properties (e.g. incoming solids content; dry density; consolidation; tailings deposition slopes; hydraulic conductivity, which would affect seepage rates);
- climate (e.g. seasonal variability; short- and long-duration storm events; inter-annual variability; climate change); and
- hydrology (e.g. contributions to baseflow and surface flow; runoff coefficient).

Managing the uncertainty of these inputs can be completed by taking a conservative approach (e.g. choosing a conservative value for each parameter) or a stochastic (Monte Carlo) approach, where input parameters are assigned a probability distribution, and potentially thousands of computational runs are completed to determine the range and likelihood of outcomes. A conservative approach is often simpler, easier to understand and easier to communicate results. However, conservatism on top of conservatism can result in unrealistic results and a poor understanding of the likelihood in the risk equation ($\text{Risk} = \text{Likelihood} \times \text{Consequence}$).

A stochastic approach, although more complex with more challenging results to communicate, will give a better understanding of the overall risk profile. Monte Carlo simulation can be programmed into GoldSim for water balance modeling, however, uncertainties associated with tailings deposition would need to be incorporated through sensitivities.

4 PROJECT EXAMPLES

Several project examples of how the integration of tailings deposition and water balance modeling have been used to assess water management risks for mines sites and/or TSFs are provided in this section. Each project has been summarized by the following categories: stage of the project, purpose of the assessment, key risks, key uncertainties, site climate, water balance climate scenarios, methodology, and conclusions. The Köppen–Geiger Climate Classification (Ruben & Kottek 2010) was used to classify the project site’s climate in a systematic way. The classification is notated by an acronym where the first letter represents the major climate type which can be subdivided into sub-climate types (represented by subsequent letters) based on precipitation and temperature.

4.1 Example 1 – Site-Wide Water Balance to Estimate Downstream Impacts in Tropical Climate

Item	Description
Stage of Project	Proposed Mine in Design and Permitting Phase
Purpose of Assessment	<p>To complete a predictive site-wide water balance model and tailings/waste rock deposition plan with the following objectives:</p> <ul style="list-style-type: none"> • Develop a management plan that maintains saturation of PAG tailings with a water cover. • Estimate water usage, impacts on downstream flows and required dry seasons storage. • Estimate flood storage requirements for dam safety.
Key Risks	<ul style="list-style-type: none"> • Potential for desaturation of PAG tailings leading to ARD/ML resulting in poor water quality. • Potential for inadequate water supply for ore processing and downstream users. • Potential for dam overtopping and/or geotechnical instability due to inadequate tailings and reclaim pond management.
Key Uncertainties or Project Constraints	Limited climate data record and quality of climate data for assessment.
Site Climate based on Köppen–Geiger Classification	Af, Tropical rainforest climate, hot and wet throughout the year.
Water Balance Climate Scenarios	<ul style="list-style-type: none"> • Average monthly climate. • Synthetic climate, hydrology relationship and runoff/streamflow generator for use in stochastic Monte Carlo simulations. Details on the synthetic climate/hydrology module is included in Patterson (2016).
Methodology	<p>A variation of Workflow 2 (Section 3.1.2) was used for this project. The proposed project, located in the tropical jungle, is in the headwaters of a river system that supplies downstream populations and ecosystems. The mine facilities include a Water Storage Dam and a TSF adjacent to each other, therefore, the staging of the dams is dependent on each other (i.e. the Water Storage Dam crest elevation is required to be higher than the tailings surface). Iterations between the tailings/waste rock staging and site-wide water balance were completed for each year of the mine life to estimate:</p> <ul style="list-style-type: none"> • water storage required for dry periods in the Water Storage Dam (to supply adequate flows downstream and to the ore processing facility) and the TSF (to maintain saturation of PAG materials); and • flood storage allowance required for the Water Storage Dam and the TSF. <p>Deposition modeling was used to estimate the preferred pond water volumes to maintain saturation of PAG waste rock deposited within the TSF and the tailings surface elevations. Pond volumes, areas and stage-storage curves were inputs into the site-wide water balance, which was used to estimate the water storage requirements for dry periods and flood storage allowance requirements. A synthetic climate generator was developed in GoldSim to predict a range of possible climate scenarios and was used to assess the risk and estimate the probability of meeting the project's minimum release requirements for downstream users (Callow et. al. 2016). The water balance model was coupled with a predictive water quality model within GoldSim, to estimate the water quality (not the focus of this paper).</p>
Conclusions	<p>This approach was successful for assessing the water management risks for the project and informing the client on preferred tailings deposition and water management strategies that would decrease the risk of the overall project. It also identified during what climate scenarios there is an increased risk of ore processing shutdown or not meeting downstream requirements. The results may be used to identify critical controls and would be used as a predictive tool for dry season planning and developing mitigation strategies.</p>

4.2 *Example 2 - Site-Wide Water Balance for Flood Management Sizing in Cold, Wet Climate*

Item	Description
Stage of Project	Proposed Mine in Design and Permitting Phase
Purpose of Assessment	<p>To complete a predictive site-wide water balance model and tailings/waste rock deposition plan with the following objectives:</p> <ul style="list-style-type: none"> • Develop a management plan that maintains saturation of PAG tailings with a water cover. • Estimate design flow rate for the water treatment plant. • Estimate TSF flood management and site-wide storage requirements for dam safety.
Key Risks	<ul style="list-style-type: none"> • Potential for desaturation of PAG tailings leading to ARD/ML resulting in poor water quality. • Potential for inadequate water treatment capacity during wet periods. • Potential for dam overtopping, piping, erosion and/or geotechnical instability due to inadequate tailings and reclaim pond management (including geohazard management such as avalanches and rock slides).
Key Uncertainties or Project Constraints	<p>Limited climate data record. Precipitation variability spatially and orographically. Water inflows (e.g. glacial melts) and water losses (e.g. seepage). Steep terrain limiting the TSF configuration.</p>
Site Climate based on Köppen–Geiger Classification	Dfc, boreal climate, long cold winters, and short mild summers.
Water Balance Climate Scenarios	<p>Average monthly climate. Wet year assessment by running multiple iterations in GoldSim, each including a 200-year wet year at a different stage in the mine life to assess the impact of wet conditions on inter-annual flood management.</p>
Methodology	<p>Workflow 1 (Section 3.1.1) was used for this project. The proposed project is located in headwaters of snowy, coastal mountains that feed into salmon spawning rivers many kilometers downstream. The mine facilities include open pits, waste rock facilities, and a water storage dam for storage of contact water at one location; and a TSF at another location. Tailings deposition modeling was completed to estimate pond volume requirements for PAG tailings saturation and estimate design flow rate for the reclaim system. Results were incorporated into a site-wide water balance model that was used to estimate the design flow rate for the water treatment plant. The design flow rate for the water treatment plant included contingency for wet years and uncertainties around the input parameters. Results were also used to size the storage volumes and freeboard requirements (QPOs) required for flood management within the TSF and water storage facilities.</p>
Conclusions	<p>This approach was successful for assessing the water management risks for the project, including appropriate sizing for flood storage and design flow rate for the water treatment facility. The results may be used to identify critical controls for flood management.</p>

4.3 Example 3 - PAG TSF in Semi-Arid Environment

Item	Description
Stage of Project	Proposed Tailings Facility Alternatives in Design and Permitting Phase
Purpose of Assessment	<p>To complete a predictive TSF water balance model and tailings deposition plan for several alternatives with the following objectives:</p> <ul style="list-style-type: none"> • Develop a management plan that maintains saturation of PAG tailings with a water cover. • Estimate water losses, such as evaporation and dust management; and estimate makeup water requirements for maintaining PAG tailings saturated and for ore processing. • Estimate flood storage requirements for dam safety.
Key Risks	<ul style="list-style-type: none"> • Potential for desaturation of PAG tailings leading to ARD/ML resulting in poor water quality. • Potential for high makeup water demands due to losses. • Potential for dam overtopping, piping, erosion and/or geotechnical instability due to inadequate tailings and reclaim pond management.
Key Uncertainties or Project Constraints	Water loss processes (e.g. beach evaporation)
Site Climate based on Köppen–Geiger Classification	BWh, subtropical desert/ low-latitude arid hot climate.
Water Balance Climate Scenarios	<p>Average monthly climate. Historical climate dataset.</p>
Methodology	<p>Workflow 1 (Section 3.1.1) was used for this project. The project is located in a semi-arid region with limited water supply and sensitive downstream receptors. Tailings deposition modeling was completed for several TSF alternatives and sites for input into an alternatives assessment. The layout configurations were designed to maintain saturation of PAG tailings by subaqueous deposition in a pond but also to minimize evaporative losses (i.e. minimize pond area). Tailings deposition dictated the pond volume required to maintain PAG tailings saturation with water cover. Results were incorporated into TSF water balance models for start-up, operations and closure. Key results from the water balance were used to estimate available water to be reclaimed for ore processing, makeup water requirements and water treatment rates.</p>
Conclusions	<p>This approach was successful for assessing the water management risks for the project, including what alternatives would result in the higher water losses and require the larger makeup water quantities. The results were used in a multi-criteria analysis during the alternatives assessment.</p>

4.4 Example 4 - PAG TSF in Tropical Monsoon Region

Item	Description
Stage of Project	Proposed Tailings Facility in Design Phase
Purpose of Assessment	To complete a predictive TSF water balance model and tailings deposition plan with the following objectives: <ul style="list-style-type: none"> •Estimate required pond volumes to maintain water cover over PAG tailings during start-up, operations and post-closure.
Key Risks	<ul style="list-style-type: none"> •Potential for desaturation of PAG tailings leading to ARD/ML resulting in poor water quality. •Potential for dam overtopping, piping, erosion and/or geotechnical instability due to inadequate tailings and reclaim pond management.
Key Uncertainties or Project Constraints	Limited climate data record and quality of climate data for assessment. Underwater tailings deposition slopes.
Site Climate based on Köppen–Geiger Classification	Af, tropical rainforest climate, hot and wet throughout the year.
Water Balance Climate Scenarios	Average monthly climate. Historical climate dataset. Synthetic climate generation, details included in Patterson & Wang (2017). Workflow 2 (Section 3.1.2) was used for this project.
Methodology	<p>The proposed project is located in a wet, equatorial region but is also influenced by seasonal monsoons. PAG tailings are proposed to be deposited subaqueously into a pond contained by a ring dyke. The purpose of the assessment was to estimate the pond volume required for start-up and to determine the deposition strategy to achieve subaqueous deposition under a variety of climate conditions. Due to the interconnections of the tailings deposition required to maintain water cover and the water balance, Workflow 2 was required.</p> <p>A Monte Carlo synthetic climate generator was developed in the GoldSim water balance model to assess the results based on a variety of climate conditions (see Patterson & Wang 2017 for details on the synthetic climate generator).</p> <p>From an operability standpoint, it is beneficial to deposit the tailings from one location as long as possible. However, because of the expected steep deposition slopes of the PAG tailings, the deposition point is required to move at some frequency to maintain a water cover.</p> <p>Tailings deposition modeling was completed to estimate pond volume requirements for start-up conditions (i.e. enough water cover for three months of PAG tailings deposition). Results were incorporated into the water balance with the synthetic climate generator. The minimum predicted pond volume within a certain confidence interval was then used in the next timestep of the tailings deposition plan. These steps for each timestep continued for the proposed mine life.</p>
Conclusions	This approach was successful for assessing the water management risks for the project, including the required period for water collection within the pond prior to start-up.

4.5 Example 5 - Operating TSF in Cold, Wet Climate

Item	Description
Stage of Project	Operating Tailings Storage Facility
Purpose of Assessment	<p>To complete a calibrated TSF water balance model and tailings deposition surface and use as a starting point for a predictive TSF water balance model and tailings deposition plan with the following objectives:</p> <ul style="list-style-type: none"> • Calibrate and understand the pond capacity and flood storage requirements. • Develop a tailings deposition plan for future TSF expansion and closure.
Key Risks	<ul style="list-style-type: none"> • Potential for dam overtopping, piping, erosion and/or geotechnical instability due to inadequate tailings and reclaim pond management. • Potential for environmental impacts caused by a potential release of water downstream.
Key Uncertainties or Project Constraints	<p>Historical water flows for water balance calibration. Expanding TSF with limitations on footprint.</p>
Site Climate based on Köppen–Geiger Classification	Dfc, boreal climate, long cold winters, and short mild summers.
Water Balance Climate Scenarios	<p>Average monthly climate. Historical climate dataset. Wet year assessment to determine the impact of wet conditions on inter-annual flood management.</p>
Methodology	<p>Workflow 2 (Section 3.1.2) was used for this project. The operating TSF is located in a plateau situated between two mountain ranges. The long-term plan for the TSF is to increase the TSF storage capacity by stacking cycloned tailings on the existing tailings beach to minimize the volume of tailings deposited in the pond. The proposed cycloned tailings stacks would include several construction stages and numerous spigot points. The design also requires the reclaim pond to have a minimum setback from the dam crest and cycloned tailings stack for construction and geotechnical stability. The water balance setup included calibration to historical or existing site conditions and flows. Water balance and tailings deposition modeling were completed iteratively at defined timesteps (ranging from a few months to a year), starting with tailings deposition modeling for the first timestep on top of the existing TSF surface LiDAR and bathymetry. Following the initial calibration and predictive integrated water balance and tailings deposition models were completed, the assessment is repeated every year. The models are verified and recalibrated with LiDAR and bathymetric surveys, measured flows, and settling and consolidation tests to confirm tailings properties. Results of the tailings deposition and water balance modeling are used for the ongoing planning of spigot locations and sequencing of the construction for the cycloned tailings stacks and earthfill dams. Predicted pond water levels from the water balance, minimum freeboard and beach width requirements were incorporated in OMS manual as critical controls for the TSF. The continuous planning, implementation and monitoring of tailings deposition and water inflows and outflows and update of the water balance is part of the facility's tailings management strategy.</p>
Conclusions	This approach was successful for assessing the water management risks for the project. It is used to calibrate to historical data, identify and update critical controls and as a tool for tailings spigot location planning.

5 CONCLUSION

The integration of tailings deposition and water balance modeling is dependent the specifics of the project, objectives, risk being assessed and uncertainties present, and should be based on a good conceptual understanding of the system. Tailings deposition and water balance integration allows for better calibration and prediction of the tailings and pond development in the TSF.

Integrating long-term planning for tailings deposition and mine site-wide water balance is recommended for use in a risk-based approach to tailings facility design and management. The integration approach presented in this paper can help mine owners better understand, mitigate, identify critical controls and monitor the water management risks surrounding mine sites and TSFs.

REFERENCES

- Callow, I.P., Meynink W.J.C., Patterson K.B., Gancho E.G. Altobano M.C., & Tupas. S.M.Y. 2016. "Sustainable Water Management Planning for Minerals Development in the Philippines," in Proceedings of the 5th International Congress on Water Management in Mining. Santiago: May 18 to 20, 2016.
- Canadian Dam Association (CDA). 2007. Technical Bulletin: Hydrotechnical Considerations for Dam Safety.
- Cooper, C., Grobler, J., & Reyes, M.P. 2018. "3D Deposition and Water Balance Modeling with Muk3D and GoldSim", in proceedings of Mine Water Solutions 2018. Vancouver: June 12-16, 2018.
- GoldSim Technology Group. 2017. *GoldSim Version 12*. [computer software].
<http://www.minebridgesoftware.com/muck3d/gallery/>
- Mining Association of Canada (MAC). 2017. "A Guide to the Management of Tailings Facilities" Third Edition. October.
- Ministry of Energy & Mines (MEM). 2016. "Revisions to Part 10 of the Health, Safety and Reclamation Code Effective as of July 20, 2016". Victoria, BC. Accessed July 5, 2018.
http://www2.gov.bc.ca/assets/gov/farming-natural-resources-and-industry/mineral-exploration-mining/documents/health-and-safety/code-review/hsrc_code_part_10_revisions_effective_july_20_2016.pdf
- Minebridge Software Inc. 2018a. *Muck3D Version 2018.1.4*. [computer software]
- Minebridge Software Inc. 2018b. "Muck3D Gallery Examples". Canada. Accessed July 5, 2018.
<http://www.minebridgesoftware.com/muck3d/gallery/>
- Patterson, K. B. 2016. "Synthetic precipitation and streamflow generation for a mine water balance in the tropics," in Proceedings of the 5th International Congress on Water Management in Mining. Santiago: May 18 to 20, 2016.
- Patterson, K. & Wang, C. 2017. "Generating Synthetic Climate Data for Design that Match Natural Trends," in Proceedings of the Canadian Dam Association 2017 Annual Conference. Kelowna: October 16 to 18, 2017.
- Rubel, F., & Kottek, M. 2010: Observed and projected climate shifts 1901- 2100 depicted by world maps of the Köppen- Geiger climate classification. Meteorol. Z., 19, 135- 141. DOI: 10.1127/0941- 2948/2010/0430.

Geochemical Behavior of Different Waste Rock Configurations from the Lac Tio Mine: Comparison between Column Tests and Experimental Waste Rock Pile Results

B. Poaty, B. Plante, B. Bussière and M. Benzaazoua,
*Université du Québec en Abitibi-Témiscamingue, Research Institute on Mines and Environment (RIME),
Rouyn-Noranda, Québec, Canada. Corr. Author: poap01@uqat.ca*

T. Pabst and V. Martin
Polytechnique Montréal, Research Institute on Mines and Environment, Montreal, Québec, Canada

M. Thériault
Lac Tio mine, Rio Tinto Fer et Titane, Havre-Saint-Pierre, Québec, Canada

P. Nadeau
Rio Tinto Iron and Titanium, Sorel-Tracy, Québec, Canada

ABSTRACT: Waste rocks are extracted from mines to access the orebody and are usually stored at the surface in large piles. Certain minerals within the waste rocks may react when exposed to surface environmental conditions, generating contaminated mine drainage. A novel management method using inclined compacted benches was proposed to control water infiltration and minimize contamination in waste rock piles. The proposed configuration is based on a flow control layer made of fine-grained, compacted non-reactive materials that contribute to divert water towards the exterior of the pile, made of non-reactive waste rock. An experimental waste rock pile was constructed at the Lac Tio mine (near Havre-Saint-Pierre, Québec, Canada) to assess the performance of this approach under field conditions. A compacted layer made of sand and crushed non-reactive waste rock was used as the flow control layer at the pile surface. Column tests were carried out in the laboratory to understand the performance of the system under controlled conditions. Results suggest that a well-designed flow control layer could be effective to control infiltration and reduce water contamination. This novel waste rock management method could be applied to other mine sites.

1 INTRODUCTION

Mining operations generate different mine wastes, such as waste rock and tailings. Exposure of tailings and waste rocks to atmospheric conditions causes some of the minerals within the wastes to react with air and water, which will modify the quality of mine drainage waters circulating through waste rock piles and tailings ponds. The oxidation of sulfide minerals such as pyrite generates acidity and releases sulfate and metal ions to the drainage waters. In the absence of neutralizing minerals, these phenomena can result in the development of acid mine drainage (AMD) conditions (e.g. Blowes *et al.* 2014). In the presence of sufficient neutralizing minerals, the pH may remain around neutrality, but metal concentrations may be higher than permitted, resulting in contaminated neutral drainage (CND) conditions (e.g. Nicholson, 2004; Plante *et al.* 2011).

It is essential to predict the geochemical behavior of waste rocks in order to choose a management method minimizing the contamination of their drainage waters. Measures to prevent water contamination can be adopted by planning the construction of the waste rock piles in order to limit water infiltration and promote the flow of infiltrated water to non-reactive areas or out of the pile (Aubertin *et al.*, 2005, 2009, 2013; Fala *et al.* 2005; Aubertin, 2013).

Theoretically, it is possible to minimize the infiltration of water into the piles, hence the production of contaminated drainage, by using inclined layers of fine and compacted material during the construction of the waste rock piles (e.g., Aubertin, 2013; Fala *et al.*, 2005), which are called flow control layers (FCL). These layers have the necessary hydrogeological properties

(e.g., hydraulic conductivity) to limit the percolation of water within the pile and direct the infiltrated water towards the outside of the piles (e.g., Aubertin *et al.*, 2005; Rohde and Williams, 2009). This management of the materials favors the establishment of capillary barrier effects between the layer of fine and dense material of the FCL and the looser waste rocks (Broda *et al.*, 2013, 2017; Dawood and Aubertin, 2009; Fala *et al.*, 2005). The FCL allows water diversion over a distance which depends on its hydrogeological properties, thickness, and angle (Aubertin *et al.*, 2005; Aubertin, 2013).

A novel management method using inclined compacted benches was proposed to control water infiltration and minimize contamination in waste rock piles. The proposed configuration is based on a flow control layer made of fine-grained, compacted non-reactive materials that contribute to divert water towards the exterior of the pile, made of non-reactive waste rock. An experimental waste rock pile was constructed at the Lac Tio mine (near Havre-Saint-Pierre, Quebec, Canada) to assess the performance of this approach under field conditions. A compacted layer made of sand and crushed non-reactive waste rock was used as the flow control layer at the pile surface. Column tests were carried out in the laboratory to understand the performance of the system under controlled conditions. Results suggest that a well-designed flow control layer could be effective to control infiltration and reduce water contamination. This novel waste rock management method could be applied to other mine sites.

2 STUDY SITE, TEST PILE DESIGN AND CONSTRUCTION

The Lac Tio mine was chosen as the construction site of a test pile because the waste rocks from this site have been extensively characterized in previous studies. Indeed, several mineralogical, geochemical, and hydrogeological characterization studies have been carried out on the Lac Tio mine waste rocks, which enabled to understand the mechanisms of Ni-CND generation from the Lac Tio mine waste rocks (e.g., Bussière *et al.*, 2008, 2011; Demers *et al.*, 2011; Pepin *et al.*, 2008; Plante *et al.*, 2010, 2011; Peregoedova *et al.*, 2013).

This mine is located 43 km northeast of Havre-Saint-Pierre, on the north shore of the Saint Lawrence river in Quebec, Canada. It is a Rio Tinto Fer et Titane-owned open-pit mine in operation since 1950 extracting a hematite-ilmenite ore (Fe_2O_3 and FeTiO_3 respectively) commonly called hemo-ilmenite. The Lac Tio deposit is a wide band of hemo-ilmenite embedded within an anorthositic complex. The cut-off grade of ore conveyed to the processing plant varied during the operation period and is presently approximately 76% of hemo-ilmenite, below which the extracted material is considered to be waste rocks of no economic value and stored in the waste rock piles. Some waste rock piles generate a contaminated nickel effluent that, if not treated, is occasionally above 0.50 mg/L, an environmental standard prescribed in Directive 019 of the Quebec province (Plante 2010; Bussière *et al.* 2011).

A test pile measuring 60 m × 35 m × 7 m, with a slope of 5% (Fig. 1) was built by push-dumping at the Lac Tio mine site. At the base of this test pile, six 10 m x 10 m lysimeters (lys 1 to lys 6) were installed to collect the water that percolates down these locations (Martin *et al.*, 2017). The dimensions of the experimental pile are based on previous studies (Broda *et al.*, 2017).

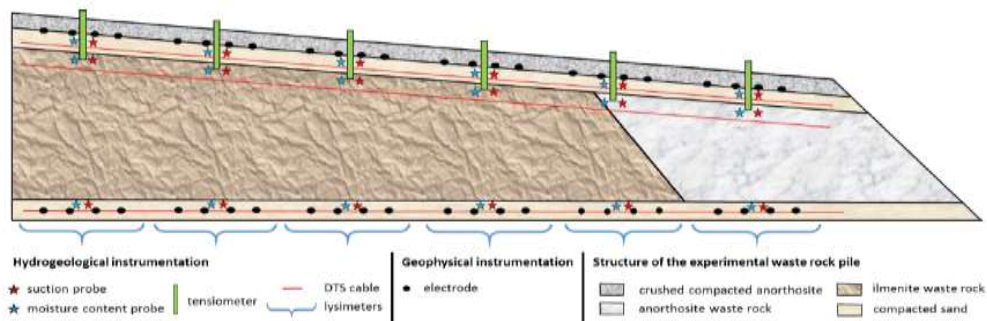


Figure 1. Design of the experimental waste rock pile, showing instrumentation location (Not to scale; Dimech *et al.* 2017)

The first 50 m of the waste rock pile consist of hemo-ilmenite waste rocks (> 5% hemo-ilmenite) while the last 10 m is made of anorthositic waste rocks (<5% hemo-ilmenite and <0.1% sulfur). The pile was covered with a 0.5 m layer of compacted sand. The sand layer was covered by a 0.25 m thick layer of compacted, crushed anorthosite (sieved to <10 mm) (Martin *et al.*, 2017). These two layers together constitute the FCL of the experimental pile.

The monitoring of the water distribution throughout the pile is carried out by instrumenting the experimental pile with multiple hydrogeological and geophysical sensors (for more information, see the papers of Martin *et al.*, 2017 and Dimech *et al.*, 2017). The design of the experimental waste rock pile and instrumentation locations are shown in Figure 1. The anorthositic waste rock was sampled from the crushed anorthosite used in the FCL of the test pile at the Lac Tio mine site. Similarly, the hemo-ilmenite (<50 mm) waste rocks were sampled from the materials used in the construction of the test pile. The hemo-ilmenite samples were stored in three 170 liters barrels while the crushed anorthosite was stored in four plastic buckets (20 liters), hermetically sealed and transported to the URSTM-UQAT laboratory. Each type of waste rock was homogenized manually using a shovel. The sampled materials were subjected to a physicochemical, chemical, and mineralogical characterization.

The volumes of leachate collected from each lysimeter were recorded daily using tipping bucket flow meters during the unfrozen months of 3 years (2015, 2016, 2017). The analyses of pH values, electrical conductivity (EC) and redox potential (Eh) of the leachates were carried out in the field. The values of acidity, alkalinity and concentrations of the chemical species present in the collected leachates were measured in the laboratory.

3 COLUMNS TESTS

Since the internal structure of the experimental pile consists of hemo-ilmenite waste rocks (from lysimeter 1 to lysimeter 5) and anorthosite waste rock (lysimeter 6), it is necessary to study the geochemical behavior of these two types of materials. Therefore, four (4) columns were set up in the laboratory as shown in Figure 2: two control columns each one filled with a single type of materials (anorthosite or hemo-ilmenite) and two mixed columns filled with both types of materials. The characteristics of the columns (Co HI, Co Anor, Co AI, Co Sandwich) are presented in Table 1.

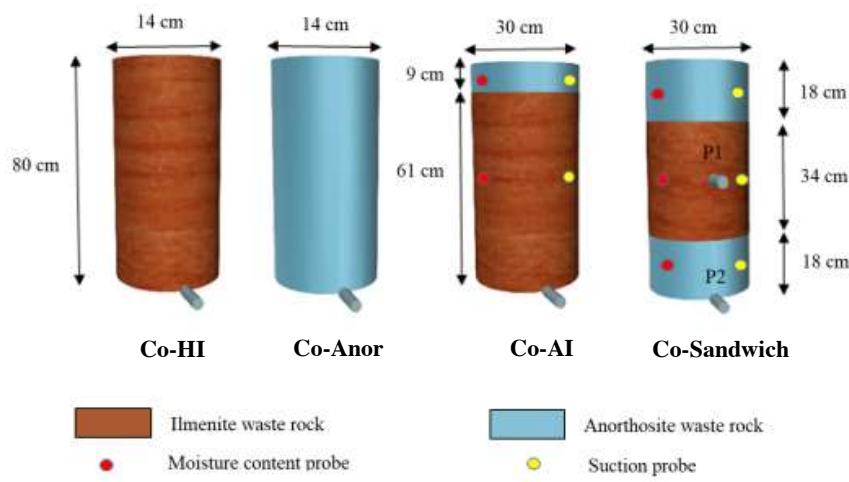


Figure 2. Configuration of the laboratory column set up

The hemo-ilmenite and anorthosite columns (respectively, Co-HI and Co-Anor) consist of a 1m-high, 14 cm internal diameter (ID) PVC (polyvinyl chloride) tube. These columns were respectively filled with 36.1 kg of hemo-ilmenite (Co-HI) and 23.0 kg of anorthosite (Co-Anor; Fig. 2 and Table 1). The other two columns consist of 80 cm-high, 30 cm ID PVC tubes. One of these two columns, called "AI Column" (Co-AI) was filled with a 61 cm thick layer of hemo-ilmenite, topped by a 9 cm anorthosite layer. The second column, called the "Sandwich column" (Co-Sandwich), was filled with a 34 cm thick layer of hemo-ilmenite positioned between two 18 cm anorthosite layers (Fig. 2). A funnel-shaped lysimeter, covered with a geotextile for retaining fine particles and connected to a 12 mm ID tube for water sampling, was installed at a height of 20 cm (at the center of the hemo-ilmenite layer) of the Co-Sandwich (labelled port 1, or P1; Fig. 2). Leachate collection ports were also installed at the bottom of each of the four columns. A geotextile filter was placed at the base of all four columns to retain the fine particles.

Table 1. Features of the columns and volumes of rinse water.

Column names		Co HI	Co Anor	Co-AI	Co-Sandwich
Column dimensions	Diameter (cm)	14	14	30	30
	Height (cm)	91	91.5	80	80
Hemo-ilmenite layer:	Number of layers of this type	1	0	1	1
	Thickness (cm)	80	-	61	34
	Porosity n (unitless)	0.4	-	0.36	0.38
	Initial water content (%)	1.3			
Anorthosite layer:	Number of layers of this type	0	1	1	2
	Thickness (cm)	-	80	9	18
	Porosity n	-	0.35	0.29	0.3
	Initial water content (%)	1.3			
Volume of rinse water (L)	Normal rainfall	1.8	1.8	8.4	8.4
	Low rainfall	0.9	0.9	4.2	4.2
	High rainfall	4	0.9	12	12

The columns were flushed every 14 days. The volumes of water were representative of monthly rainfalls in the Havre-Saint-Pierre area (Table 1). Higher and lower rainfall conditions were also simulated by halving or doubling the normal volume of deionized water. The volume of rinse water used during the various column tests are shown in Table 1. In the case of columns filled with mixed materials (Co-AI and Co-Sandwich), the normal volume of deionized water could not be doubled due to the limited capacity of the columns, so it was increased by approximately 1.5 times instead (12 liters instead of 8.4 liters; Table 1). The rinse water was left in contact with the materials for approximately 3 hours before opening the bottom valve and enabling the leachate to drain. The columns were left exposed to ambient air to dry in between flushes. These column tests were performed for a total of 38 cycles (over 500 days).

4 RESULTS AND INTERPRETATION

The following will present the preliminary results from the materials characterization, as well as from the geochemical monitoring of the test pile lysimeters and laboratory column tests.

4.1 Material characterization

The materials that were sampled during the construction of the test pile and those that were used for the setting up of the columns were subjected to a chemical characterization by X-ray fluorescence (XRF) analysis. The chemical characterization by XRF analysis of more than 20 elements was carried out on 27 samples ($n = 27$) from the experimental pile and those of the columns. Only the elements of interest are presented in Table 2, where it could be seen that the chemical composition of the hemo-ilmenite waste rocks from the experimental pile and those of the columns are nearly identical. The anorthositic waste rock sampled contains less than 0.1% sulfur and a low hemo-ilmenite content, in agreement with what was targeted for the test pile construction. The mineralized waste rock sampled contains more than 30% iron and 14% Ti, suggesting a high hemo-ilmenite (HI) content (over 40% ilmenite). As for the hydrological properties of the materials used in the FCL of the experimental pile, they have been detailed in the papers of Bréard Lanoix *et al.*, 2017, Martin *et al.*, 2017, and Dubuc *et al.*, 2017.

Table 2. Chemical characterization of samples from the experimental waste rock pile (mean values of 27 samples) and columns.

	HI waste rock (test pile)	HI waste rock (columns)	Anorthosite (test pile and column)
Fe (%)	31.1	30.5	2.9
Ti (%)	14.1	16.7	1.4
S (%)	0.40	0.33	0.003
Ni (mg/kg)	633	560	<100
Si (%)	7.8	7.6	24.7
Ca (%)	2.0	1.6	5.7
Al (%)	5.1	7.6	13.2

4.2 Test pile geochemistry results

The analysis of leachate samples collected from the lysimeters provided several geochemical parameters (pH, electrical conductivity, acidity, alkalinity, cations, anions, and dissolved metals). However, only key parameters such as pH, electrical conductivity, as well as nickel and sulfate concentrations (sulfide oxidation products) are presented here. Nickel and sulfate are presented in

terms of concentrations and cumulative loadings. The pH values (Fig. 3a) of all lysimeter leachates remain neutral within 6.5 and 7.5 throughout the monitoring period. However, the electrical conductivity values of the leachate from the lysimeter 6 are lower compared to those from lysimeters 1 to 5 (Fig. 3b). Figures 3c and 3d respectively show the trends of sulfate and nickel release in leachates collected from the six lysimeters of the test pile. During the three years of monitoring, the highest sulfate and nickel concentrations were measured in leachates from lysimeters 1, 2 and 3 (Figs 3c and 3d, respectively). In general, nickel and sulfate concentrations were higher in lysimeters 1 to 5 than in lysimeter 6, the latter being located in the anorthositic part of the test pile (Fig. 1). These preliminary results show that the water passing through the anorthosite waste rock is less contaminated. Although more work is needed to completely understand the main factors controlling the water quality in the test pile, the relative ratios of leaching water volume vs quantity of waste rocks over each lysimeter is probably one of the most significant parameters to focus on.

The cumulative nickel and sulfate loadings were estimated by multiplying the concentrations and volumes of collected leachates, divided by the estimated mass of waste rocks over each lysimeter. Figures 4a and b show the evolution of sulfate and nickel cumulative loadings from the lysimeters between the spring and autumn of 2016. The cumulative loadings show that less nickel and sulfate come out of lysimeter 6. Therefore, the lower concentrations obtained in the leachate from the lysimeter 6 are not related to a dilution caused by the higher volumes of leachate collected in this lysimeter. Indeed, lysimeter 6 systematically leaches more water than the other lysimeters; the distribution of water leaching out of the pile is described in more details in Martin *et al.*, 2017 and Dubuc *et al.*, 2017. Thus, the lower nickel and sulfate concentrations in the lysimeter 6 leachates are attributed to the low sulfide contents of the anorthosite (e.g., Bussière *et al.*, 2011; Plante *et al.*, 2010, 2011).

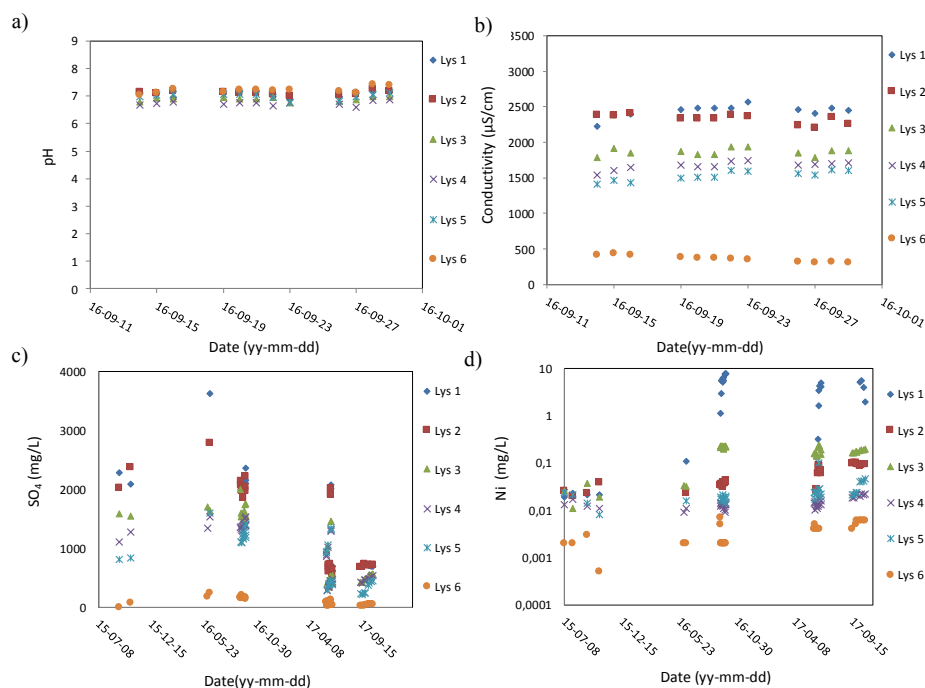


Figure 3. Evolution of the main geochemical parameters from lysimeters 1 to 6 over time

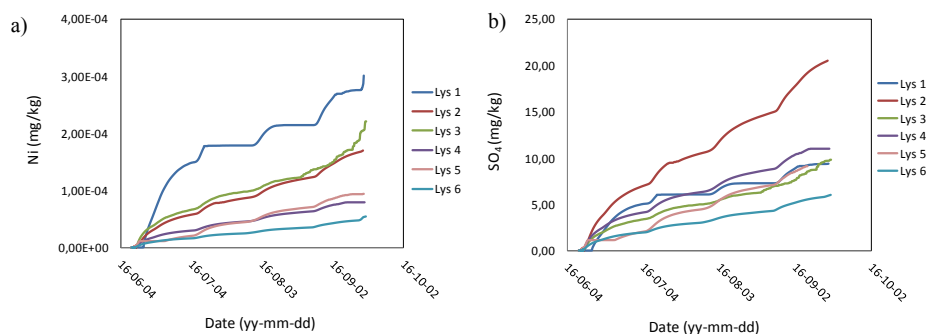


Figure 4. Nickel (a) and sulfate (b) cumulative loadings from lysimeters 1 to 6 during the 2016 season

4.3 Column test geochemistry results

The results of the column tests carried out to simulate the geochemical behavior of waste rocks of test pile are presented here. The column tests allow investigating the effect of an anorthosite layer placed above a hemo-ilmenite layer on the quality of the leachate (Co-AI), as well as the effect of an anorthosite layer underneath a hemo-ilmenite layer (Co-Sandwich). Port 1 of the Co-Sandwich enables to sample the water quality in the interstitial water of the hemo-ilmenite layer (sampling port 1 or P1), before that water passes through the underlying anorthosite layer (sampling port 2 or P2). Only the same key parameters as were shown for the experimental pile are presented here: pH, electrical conductivity, as well as nickel and sulfate concentrations and cumulative loadings.

The pH values measured in the leachates from the columns are presented in Figure 5a. The anorthosite control column (Co-Anor) showed the highest pH values ($\text{pH} \approx 8$), while the leachates from the control hemo-ilmenite column (Co-HI) had the lowest pH values ($\text{pH} \approx 6$). The pH values of leachate from the two other columns (Co-AI and Co-Sandwich) are between 6 and 8. The electrical conductivity values (Fig. 5b) of Co-Anor are the lowest, while those of the Co-HI and of P1 (in hemo-ilmenite) of Co-Sandwich are the highest.

Figures 5c and 5d respectively show that the lowest nickel and sulfate concentrations are released by Co-Anor and port 2 of Co-Sandwich. This demonstrates that the anorthosite waste rocks are the lowest reactive materials, consistent with their $<0.1\%$ sulfur content. This also demonstrates that although the overlying hemo-ilmenite does generate nickel in the leachates, this nickel is intercepted by the lower anorthosite layer, most probably by sorption phenomena, as it was demonstrated in previous studies (e.g., Bussi re *et al.*, 2011; Plante *et al.*, 2010, 2011).

When the columns were rinsed with a higher volume of water compared to normal flushes, the sulfate and nickel concentrations decreased by almost 50%, whereas when the volume of rinse water was halved compared to normal, the sulfate and nickel concentrations almost doubled. These results suggest that the relative liquid-solid ratios has a significant effect on the water quality, consistent with previous results obtained at different scales on the Lac Tio mine waste rocks (Plante *et al.*, 2014).

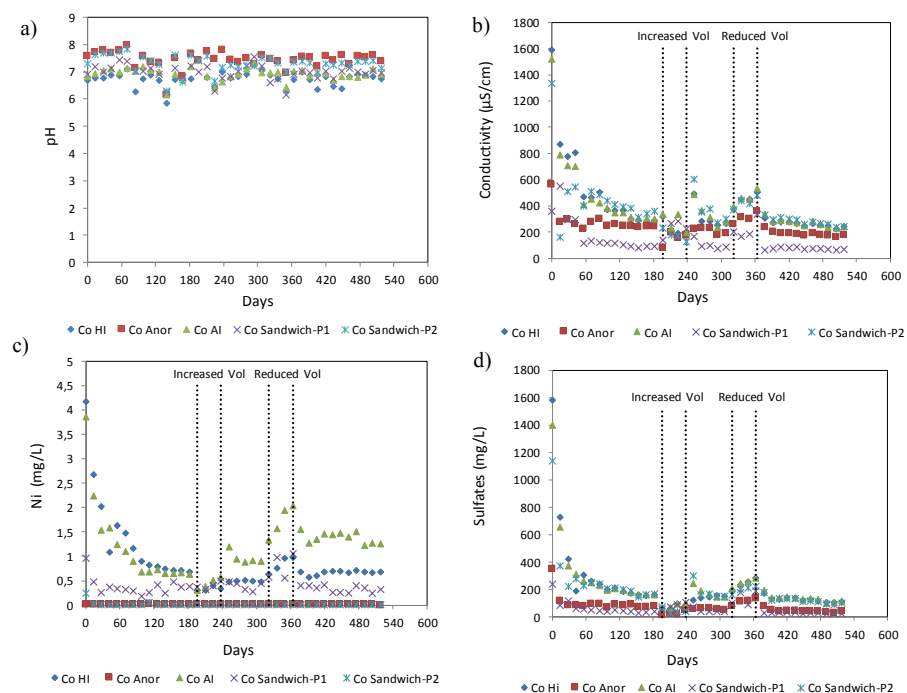


Figure 5. Evolution of geochemical parameters over time in the column tests

Figure 6 shows the evolution of nickel and sulfate cumulative loadings over time in the column leachates. Figure 6a shows that the nickel cumulative loadings from the leachates collected through port 1 of Co-Sandwich are the highest of all the columns, whereas those from the leachates collected through port 2 are the lowest (in fact, they are close to zero, because the Ni concentrations were systematically below the detection limit of 0.004 mg/L). This suggests that the Ni generated by the hemo-ilmenite layer was not influenced by the presence of an upper anorthosite layer. The results also demonstrate that the Ni generated by the hemo-ilmenite layer was removed from solution by the underlying anorthosite layer. In addition, the trends of the Ni cumulative loadings from the leachates of the hemo-ilmenite column (Co-HI) are the same as those from the leachate from the AI column (Co-AI) up to approximately on the 300th day. This also suggests that the presence of an upper anorthosite layer does not seem to significantly change the geochemical behavior of the underlying hemo-ilmenite. Figure 6a also shows two (2) significant changes in the slope of the cumulative nickel and sulfate values: a significant increase between 196 to 238 days (corresponding to the period where the leaching volumes were increased), and a plateau between 322 and 364 days (corresponding to the period where the leaching volumes were decreased). For the rest of the test where normal flush volumes were used, the slopes are similar. It is also noteworthy that these slope changes are not observed for the other columns. It appears that preferential flow paths seem to develop when the leaching volumes changed, leading to an increase of the fraction of the volume that was intercepted by P1 when the leaching volume was increased, and to a decrease when the leaching volume was halved.

Figure 6b shows the sulfate cumulative loadings over time in the leachates collected at the bottom of the columns. The Co-Sandwich P1 sulfate cumulative loadings show the same trends as those observed for nickel, namely a slope increase between 196 and 238 days and a plateau between 322 and 364 days, while the slopes of other columns do not show significant changes, consistent with the hypothetical preferential flow paths abovementioned.

In addition, the P1 slopes are slightly higher than those of the Co-HI column, suggesting that

the nickel and sulfate release rates are higher within the Co-AI column than in the Co-HI column. The reasons behind these differences need to be investigated further.

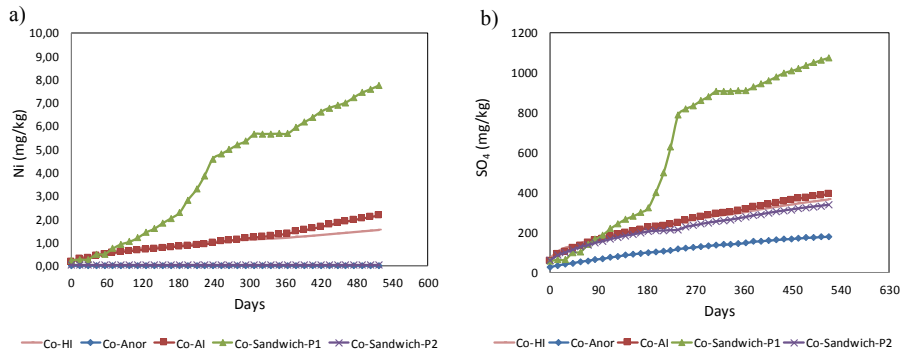


Figure 6. Cumulative nickel (a) and sulfate (b) loadings over time in the column tests

4.4 Comparison between laboratory and field scales

The results of nickel and sulfate concentrations from the experimental pile and laboratory columns differ. The sulfate concentrations in leachates from the column tests (up to 1500 mg/L) are lower than those from the test pile (up to about 3500 mg/L). Similarly, the nickel concentrations in leachates from the test pile (up to 8.8 mg/L) are higher than those obtained with the columns (<4.5 mg/L). In addition, the nickel cumulative loadings from leachates collected in the field in the 2016 season (up to 3×10^{-4} mg/kg) are higher than those from the column tests (up to 8 mg/kg). Finally, the sulfate cumulative loadings are lower in the 2016 field leachates (<25 mg/kg) than in the columns (up to 1100 mg/kg). Given the time period over which each scale is compared, the cumulative loadings can be used to estimate the release rates of nickel and sulfate by calculating the slope of the curves shown in Figures 4 and 6. The highest nickel release rates are estimated to approximately 0.012 mg/kg/day in the laboratory, while they are 3×10^{-6} mg/kg/day in the field. The highest sulfate release rates between the laboratory and the field are closer than for nickel, with approximately 1.0-1.6 mg/kg/day and 0.2 mg/kg/day, respectively.

The differences in nickel and sulfates release rates observed between the laboratory and field scales are related to several factors such as pH, liquid-solid ratio, precipitation of secondary minerals, temperature, grain size distributions, and surface phenomena (sorption, ion exchange, etc.) (Bussière *et al.*, 2011; Evans and Banwart, 2006; Plante *et al.*, 2014; Sapsford *et al.*, 2009). The contribution of these factors to the observed scale differences for nickel and sulfate are currently being studied further, including using numerical modeling and thermodynamical equilibrium calculations.

5 CONCLUSION AND FUTURE WORK

This study presents the preliminary results from an experimental test pile and those obtained from column tests in the laboratory. The results show that the use of anorthosite waste rock in a flow control layer allows controlling water infiltration and the generation of CND from hemo-ilmenite waste rock by favoring water circulation within anorthosite waste rock that is non CND-generating. The results of the experimental test pile suggest that this new approach to the construction of waste rock piles effectively enables to decrease the contamination of mine drainage.

Column test results show that the concentrations of nickel and sulfate leached out of the columns are closely linked to changes in leaching volume. They also show that an overlying anorthosite layer above CND-generating hemo-ilmenite waste rocks does not affect nickel and sulfate generation in the leachates. However, column tests results show that the nickel generated

from the hemo-ilmenite waste rocks is removed by an underlying anorthosite layer, thus suggesting that using successive benches constructed as in the experimental test pile described here would enable to intercept contaminated water and improve its quality.

As part of future work to be carried out, the material characterizations will be completed, and a 2D intermediate-scale test (approximately 2m³) will be set up in the laboratory in order to better understand the mechanisms for release and attenuation of contaminants from the Lac Tio mine waste rocks. Additional interpretations will also focus on the scale effects between laboratory and field results. This work will also include numerical modeling of the columns and of the intermediate scale test with MIN3P to understand the main factors of influence on the geochemical behavior of the Lac Tio mine waste rocks.

REFERENCES

- Aubertin, M. 2013. Waste rock disposal to improve the geotechnical and geochemical stability of piles. *In Proceedings of the world mining congress, Montreal, QC, Canada.*
- Aubertin, M., Fala, O., Molson, J., Gamache-Rochette, A., Lahmira, B., Martin, V., Lefebvre, R., Bussière, B., Chapuis, R. P. & Chouteau, M. 2005. Évaluation du comportement hydrogéologique et géochimique des haldes à stériles. *Proc. of the 2005 Symposium sur l'Environnement et les Mines, Rouyn-Noranda, QC, Canada.*
- Aubertin, M., Cifuentes, E., Aphy, S., Bussière, B., Molson, J. & Chapuis, R.P. 2009. Analyses of Water Diversion along Inclined Covers with Capillary Barrier Effects. *Canadian Geotechnical Journal* 46: 1146-1164.
- Aubertin, M., James, M., Maknoon, M. & Bussière, B. 2013. Recommandations pour améliorer le comportement hydrogéotechnique des haldes à stériles. *GeoMontreal 2013, Canadian Geotechnical Society, Montreal, QC, Canada.*
- Blowes, D.W., Ptacek, C.J., Jambor, J.L., Weisener, C.G., Paktunc, D., Gould, W.D. & Johnson, D.B. 2014. 11.5 - The Geochemistry of Acid Mine Drainage, in: Turekian, H.D.H.K. (Ed.), *Treatise on Geochemistry (Second Edition)*. Elsevier, Oxford, pp. 131-190.
- Bréard Lanoix, M.L., Pabst, T. & Aubertin, M. 2017. Characterization of the Hydrogeological Properties of a Sand Layer Placed on an Experimental Waste Rock Pile. *GeoOttawa 2017-70th Canadian Geotechnical Conference, Ottawa, ON, Canada.*
- Broda, S., Hirthe E., Blessent, D., Aubertin, M. & Graf, T. 2013. Using Random Discrete Fractures for Representing Preferential Flow in Waste Rock Piles with Compacted Layers. *GeoMontreal 2013, Canadian Geotechnical Society, Montreal, QC, Canada.*
- Broda, S., Aubertin, M., Blessent, D., Hirthe, E. & Graf, T. 2017. Improving control of contamination from waste rock piles. *Environmental Geotechnics* 4: 274-283.
- Bussière, B., Benzaazoua, M., Plante, B., Pepin, G., Aubertin, M. & Laflamme, D. 2008. Évaluation du comportement géochimique des stériles de la mine Tio, Havre-Saint-Pierre, Québec. *Proc. of the 2008 Symposium sur l'Environnement et les Mines, Rouyn-Noranda, QC, Canada.*
- Bussière, B., Demers, I., Dawood, I., Plante, B., Aubertin, M., Peregoedova, A., Pepin, G., Lessard, G., Intissar, R., & Benzaazoua, M. 2011. Comportement géochimique et hydrogéologique des stériles de la mine Lac Tio. *Proc. of the 2011 Symposium sur l'Environnement et les Mines, Rouyn-Noranda, QC, Canada.*
- Dawood, I. & Aubertin, M. 2009. A numerical investigation of the influence of internal structure on the unsaturated flow in a large waste rock pile. *62nd Canadian Geotechnical Conference, Halifax, Nova Scotia, Canada, CD-Rom.*
- Demers, I., Bussière, B. & Plante, B. 2011. Field retention tests to evaluate nickel retention on mine waste rock. *In Pan-Am CGS Geotechnical Conference, Toronto, ON, Canada.*
- Dimech, A., Chouteau, M., Chou, E. T.-K., Aubertin, M., Martin, V., Bussière, B. & Plante, B. 2017. Monitoring water infiltration in an experimental waste rock pile with time-lapse ERT and multi-parameter data collection. *Proc. of SAGEEP, Society of Exploration Geophysicists and Environment and Engineering Geophysical Society, pp. 195-203.*
- Dubuc, J., Pabst, T. & Aubertin, M. 2017. An assessment of the hydrogeological response of the flow control layer installed on the experimental waste rock pile at the lac Tio mine. *GeoOttawa 2017-70th Canadian Geotechnical Conference, Ottawa, ON, Canada.*
- Evans, K. & Banwart, S. 2006. Rate controls on the chemical weathering of natural polymineralic material. I. Dissolution behaviour of polymineralic assemblages determined using batch and unsaturated column experiments. *Applied Geochemistry* 21:352-376.
- Fala, O., Molson, J., Aubertin, M. & Bussière, B. 2005. Numerical modelling of flow and capillary barrier effects in unsaturated waste rock piles. *Mine water and the environment* 24:172-185.

- Martin, V., Plante, B., Bussière, B., Aubertin, M., Pabst, T., Chen, D., Bréard Lanoix, M.-L., Dubuc, J., Dimech, A. & Poaty, B. 2017. Controlling water infiltration in waste rock piles: Design, construction and monitoring of a large-scale in-situ pilot test pile. *GeoOttawa 2017-70th Canadian Geotechnical Conference, Ottawa, ON, Canada*.
- Nicholson, R. 2004. Overview of near neutral pH drainage and its mitigation: results of a MEND study. *MEND Ontario workshop, Sudbury, ON, Canada*.
- Pepin, G., Bussière, B., Aubertin, M., Benzaazoua, M. & Plante, B. 2008. Field Experimental Cells to Evaluate the Generation of Contaminated Neutral Drainage by Waste Rock at the Tio Mine, Quebec, Canada. *In Proc. of the 10th International Mine Water Assoc (IMWA) Congress on Mine Water and the Environment, Karlovy Vary, Czech Republic, pp. 309-312*.
- Peregoedova, A., Aubertin, M. & Bussière, B. 2013. Laboratory measurement and prediction of the saturated hydraulic conductivity of mine waste rock. *GeoMontreal 2013, Canadian Geotechnical Society, Montreal, QC, Canada*.
- Plante, B., Benzaazoua, M., Bussière, B., Biesinger, M. & Pratt, A. 2010. Study of Ni sorption onto Tio mine waste rock surfaces. *Applied Geochemistry 25:1830-1844*.
- Plante, B., Benzaazoua, M. & Bussière, B. 2011. Kinetic testing and sorption studies by modified weathering cells to characterize the potential to generate contaminated neutral drainage. *Mine water and the environment 30:22-37*.
- Plante, B., Bussière, B & Benzaazoua, M., 2014. Lab to field scale effects on contaminated neutral drainage prediction from the Tio mine waste rocks. *Journal of Geochemical Exploration 137:37-47*.
- Rohde, T. K., & Williams, D. J. 2009. Early hydrological monitoring of Cadia's instrumented trial waste rock dump. *Proc. of Securing the Future and 8th International Conference on Acid Rock Drainage (ICARD). SveMin/INAP*.
- Sapsford, D. J., Bowell, R., Dey, M. & Williams, K. P. 2009. Humidity cell tests for the prediction of acid rock drainage. *Minerals Engineering 22:25-36*.

How Plant Water Use Efficiency Can Inform Evapo-transpirative Cover Design

R. Murphy and J. Dillon

Cedar Creek Associates, Fort Collins, Colorado, USA

ABSTRACT: Optimizing to the minimum necessary thickness of evapo-transpirative cap and cover systems has large cost-saving implications on mining projects. Site specific challenges such as limited or unsuitable borrow sources can dictate the need for creative solutions when faced with insufficient volumes of cover material. Making informed decisions on a suitable cover thickness when volumes are limited is imperative. This is especially important in arid systems from a water balance standpoint, accounting for storage and drainage, and from a vegetation sustainability and suitability perspective. A Water Use Efficiency (WUE) concept was recently employed to evaluate if modeled plant available water (water partitioned to transpiration in cover system simulations) was sufficient to support a self-sustaining vegetation community on a Tailings Storage Facility (TSF) in Nevada with limited cover materials. WUE defines the volume of water required for a plant species or lifeform to produce one unit of biomass. This property relates to the physiology of plants (such as the pore water tensions enacted by plant roots), and can indicate drought tolerance. Sufficient literature exists to describe the WUE on the most common arid western plants, especially species commercially available for use in mine reclamation. Site specific demonstration data will be utilized to discuss the implications of applying the WUE concept, specifically how later-seral (lower vegetative cover and lower Leaf Area Index [LAI]) systems can actually extract significantly more water than early –seral (typically larger LAI) systems. WUE concepts can be used to quantify vegetation input parameters in existing models to better represent site specific, real world conditions, optimize seed mixes for site specific circumstances, and inform necessary cover thicknesses.

1 INTRODUCTION

Conducting unsaturated flow simulations of proposed Evaporation / Transpiration (ET) covers for mine waste and tailings is a vital part of the design process. The most successful covers achieve project goals with efficient costs. Site specific model parameterization must occur to create informative outcomes. Leaf Area Index (LAI) is typically used to partition meteoric water into transpiration and evaporation in cover system modeling. Meteoric water which is not allocated to evaporation or transpiration typically contributes to drainage or a change in storage. However, LAI for nativespecies in arid ecosystems is not a reliable parameter, as later-seral vegetation typically exhibits lower LAI values, despite an increased ability to transpire water. Scurlock et al. (2001) reviewed worldwide historical leaf area studies and reported mean LAI values for deserts ($1.31 + 0.85$), grasslands ($2.5 + 2.98$), and shrublands ($2.08 + 1.58$). In addition, practitioners typically use an undisturbed reference area in close proximity to the proposed ET cover to develop site specific LAI parameterization within the modeling environment. However, due to the anthropogenic soil profile, plant community assemblages found on ET co-

vers rarely match the undisturbed adjacent communities, especially in the early years following revegetation. The paper demonstrates an alternative approach to accounting for the transpiration parameter in unsaturated flow simulations on ET covers through the use of Water Use Efficiencies (WUE) specific to each plant. Water use efficiency is the amount of water used by a plant to produce one unit of biomass (dry weight).

2 IMPORTANCE OF DEFINING GOALS

Before considering an in-depth parameterization of vegetation modeling inputs, it is important to carefully consider the desired outcomes of the project. The purpose of vegetation on ET covers can be:

- to provide wind and water erosion control,
- to provide transpiration in an effort to limit percolation,
- to provide habitat or forage potential, or
- to be visual appeasing.

Whatever the goals may be, they should be well defined before designing a revegetation plan and characterizing the anticipated vegetation parameters.

3 CASE STUDY

3.1 *Background*

A mine in northern Nevada was planning for final closure of their large Tailings Storage Facility. Borrow materials were limited in the immediate vicinity and cost prohibitive to haul in from long distances. Local borrow materials are mostly quaternary alluviums with a minor coarse fragment component. The site receives arid land precipitation (generally less than 10 inches) in episodic and infrequent events, and is often very windy. Annual precipitation is extremely variable from year to year ranging from 5 to over 12 inches.

3.2 *Project Goals and Approach*

The primary objectives of vegetation establishment on the TSF ET cover is to provide sufficient transpiration to limit percolation, and prevent aeolian erosion of cover materials which could potentially expose the underlying tailings. Due to the limited volumes of TSF cover materials available onsite, a study was initiated to evaluate the potential use of a thinner cover system to support and sustain a plant community. With one of the goals pertaining to sustainability of plant communities, a more robust vegetation analysis was warranted to evaluate the Plant Available Water (PAW) in the thinner cover system during both average and below average precipitation years.

3.3 *Defining Plant Community Assemblages*

Vegetation sampling for the parameters of ground cover and current annual production was conducted on several reclamation plots which exhibited circumstances similar to those of the eventual TSF ET cover. For instance, these sites were composed of similar growth media and exhibited a similar soil profile depth and topography, aspect, and elevation. Effectively, these areas could serve as reclamation reference sites.

3.4 *Unsaturated Water Flow Modeling*

One-dimensional unsaturated flow models were developed to simulate a one foot thick alluvium ET cover systems over three different tailing types: a) the fine-textured low permeability slimes area; b) coarse-textured, high moderate permeability embankment and beach areas, and; c) mixed tailings of low moderate permeability. The models were developed using the numerical

code Hydrus, which simulates the flow of water and vapor in soils by incorporating the processes of precipitation, evaporation, plant transpiration, water storage in the soil, and drainage.

4 RESULTS

The goals for this project related to both percolation and vegetation sustainability. The following sections present information on both.

4.1 Percolation

Numerical ET cover system water balance models predicted annual average net percolation through a one foot thick alluvium cover placed on the TSF will be less than one percent of precipitation (less than 1 mm/yr). Sensitivity analysis indicates that reduced vegetation and increased alluvium Ksat may increase net percolation up to 1.5 percent of precipitation (4 mm/yr).

4.2 Vegetation

Based on average annual precipitation, the plant available water (PAW) calculated in the rooting profile was 11.74 cm annually. Then, select years representative of this annual average were utilized to extract and average the corresponding transpiration data predicted by the model. On an acreage basis, 11.74cm of PAW equates 474,705 liters of water available plant use during the average growing season. Water use efficiency is the amount of water used by a plant to produce one unit of biomass (dry weight). Essentially, water use efficiency describes how many milliliters of water are needed to produce 1 gram of plant biomass. These efficiencies vary significantly by species, age of plant, and environmental conditions. Table 1 displays list of water use efficiencies for common species to Nevada.

Table 1. Water Use Efficiencies of Common Reclamation Species in Nevada.

Type	Species	Water Use Efficiency
Grasses	Various	400-700
	Western Wheatgrass	1,127
	Crested Wheatgrass	858
	Cheatgrass	273
Forbs	Various	200-500
	Alfalfa	772
	Sweetclover	1,060
	Russian Thistle	297
Shrubs	Various	700-4,000
	Big Sagebrush	2,216
	Fourwing Saltbush	984

Vegetation sampling of reclamation reference areas were used to develop a projected plant community assemblage (composition) anticipated to inhabit the ET cover. Table 2 displays modeled PAW (474,705 liters) distributed by water use efficiencies on the projected plant community. The outcomes are presented as total plant production, including growth associated with previous year's stems and foliage. Sustaining previous root and shoot growth typically accounts for 70% of the production. The remaining production is referred to as current annual growth.

Table 2. Current Annual Growth Based on Water Use Efficiencies of Plant Available Water of a Project Shrub and Grass Co-Dominated Reclamation Community.

	Composition	WUE (milliliter:gram)	Plant Production	
			Total grams / acre	Total pounds / acre
Perennial Grasses	50%	1,000	237,352	523.3
Perennial Forbs	3%	300	14,241	104.7
Shrubs				
Big Sagebrush	20%	2,216	42,843	94.5
Fourwing Saltbush	20%	984	96,484	212.7
Annuals	7%	280	118,676	261.6
Total Plant Production				1046.5
Current Annual Growth				359.0

Ecological site descriptions for the tailings facility were referenced from the NRCS Soil Survey. The range in productivity (current annual growth) for soils in the vicinity of the tailings facility ranged from 366 pounds per acre in the steep uplands to 1,754 pounds per acre in the alluvial draws under normal precipitation conditions. Therefore, the modeled result of 359.0 pounds per acre of current annual growth is marginally below the anticipated range of production. When considering topographic factors on the flat ET cover compared with the NRCS Ecological Site Descriptions, the resulting production of the ET cover is well below expected conditions.

However, the modeling may be underrepresenting the amount of PAW. Due to the anticipated negligible loss of water from the cover due to percolation, the fate of the vast majority of soil water is currently modeled as evapotranspiration and a significant amount of that water is currently modeled as surface evaporation. Since evaporative processes are concurrent with transpiration, it is possible that the model is over allocating the evapotranspirative balance toward surface evaporation, and underestimating transpiration.

Current cover modeling reveals that vegetation growth in average years is likely to be slightly diminutive. The cover system is likely to display vegetative production below values observed on steep slopes in the project area, and significantly below values on flat or gently sloping terrain. These results indicate a more concerning situation in drought years, where it is unclear whether modeled plant available water will be capable of sustaining vegetation growth. Further studies must be completed to understand the full implications of these results.

5 CONCLUSIONS

With regard to the case study, the percolation goal was met, but vegetation sustainability analysis using water use efficiencies suggested that plant communities on the ET Cover may be susceptible to drought conditions and therefore, may not protect the surface of the ET Cover from wind and water erosion.

Overall, WUE concepts can be used to quantify vegetation input parameters in existing models to better represent site specific, real world conditions, optimize seed mixes for site specific circumstances, and inform necessary cover thicknesses

6 REFERENCES

- Romig, D., Munk, L., and T. Stein. 2006. Leaf Area and Root Density Measurements for Use in Cover Performance Evaluations on Semi-arid Reclaimed Mine Lands. 7th ICARD, March 26-30, 2006, St. Louis MO. Published by ASMR.
- Scurlock, J. M. O., G. P. Asner, and S. T. Gower. 2001. Worldwide historical estimates of leaf area index, 1932-2000. Prepared by the Oak Ridge National Laboratory. Oak Ridge, Tennessee.

Water Management

United States Department of Agriculture (USDA) - Natural Resources Conservation Service (NRCS).
2018. Custom Soil Resource Report. Web soil survey. Soil Survey Area: [Redacted].

Impact of Changes in Water Use Policy and Legislation on Mine Waste Water Management Infrastructure – A Case Study of In-Line Attenuation Ponds

W. Naidoo

SRK Consulting (South Africa) Pty Ltd, Johannesburg, Gauteng, South Africa

P. Janse van Rensburg

SRK Consulting (Australasia) Pty Ltd, Perth, Western Australia, Australia

ABSTRACT: South Africa is an arid country currently experiencing a drought. Consequently, protection of water resources and responsible water use in all sectors, including the mining industry, has been prioritized. New legislation requires stringent pollution control barriers in mine waste infrastructure. For compliance and to protect the underlying aquifer, the design of a new tailings dam required a barrier system which includes an HDPE liner. Paddock systems are traditionally constructed around South African tailings dams to manage runoff from embankment slopes. The requirement to install a barrier system renders the capital cost of these elements prohibitive. This paper presents a summary of the hydrological analysis, flood routing, and design of an in-line attenuation pond system that combines the functions of traditional paddocks and solution trenches. The solution is cost effective, limits evaporative and seepage losses and complies with legislation. The system was optimized by designing the in-line attenuation ponds to provide attenuation during storm events and conveyance during operational conditions.

1 INTRODUCTION AND SCOPE

Earth is made up of nearly 70 % water, with approximately 3 % of it being fresh water (USGS, 2016). Additionally, the extreme weather patterns and droughts being experienced all over the world are causing severe water stress. Protection of water resources is therefore essential to ensure safe human consumption as well as longevity of aquatic ecosystems. Many countries have imposed strict legislation regarding water resource protection in the mining industry. These are related to separation of clean and dirty water and prevention of groundwater and surface water pollution. These regulations pose new challenges in the design and construction of mine waste infrastructure such as tailings dams as innovative designs are required to ensure project feasibility without compromising safe functionality and operability. This paper presents a design challenge that resulted from changes in water use policy and promulgation of new legislation, and the development of a design solution to meet the requirements.

2 BACKGROUND

Tailings storage facilities (TSFs) in South Africa are predominantly constructed as upstream facilities with a drainage system, decant structure and conveyance, return water dam and associated stormwater management. The primary decant system typically consists of a centrally located penstock through which supernatant pond water is routed and conveyed by a gravity flow outfall pipeline into a solution trench. Most dams are designed to include a drainage system that consists of toe/heel drains, a blanket drain and a curtain drain. The drains collect seepage water and also discharge into the solution trench. The solution trench is an open channel that transports decant

water (from the penstocks) and seepage water (from the various seepage drains) to the return water system. It is common for upstream TSFs to be constructed and operated with stormwater management components known as paddocks to manage runoff from the outer TSF embankments. Paddocks are constructed along the perimeter of the facility between the TSF embankment and the solution trench. This is illustrated in the typical perimeter section in Figure 1.

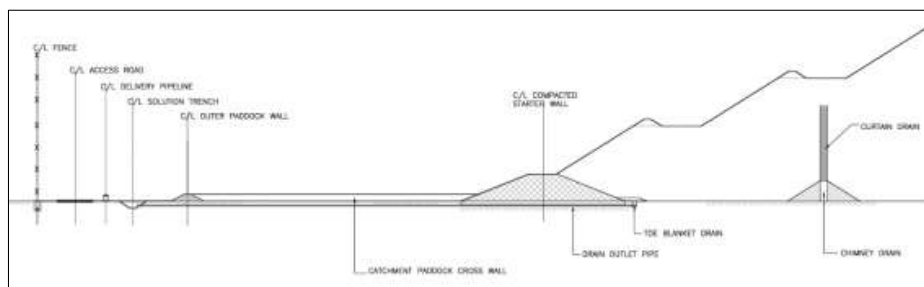


Figure 1. Typical perimeter section schematic through a traditional upstream TSF in South Africa (NTS)

The paddocks are designed to contain and store stormwater runoff from the embankment of the TSF for evaporation and/or seepage into the substrate. Additionally, the individual paddocks serve as intermediate silt traps to contain silt transported by embankment runoff or minor pipeline spills. The disadvantages of the traditional paddock system are as follows:

- i) Dirty runoff water can seep into the substrate; however, the contribution from this runoff water is considered far less than the water seeping through the base of the tailings dam into the substrate.
- ii) Stormwater runoff is lost and excluded from the water balance on the assumption that it is negligible.
- iii) A considerably expansive area around the footprint of the TSF is utilized.

As a result of the promulgation of legislation, the design and construction of new TSFs must include a pollution control barrier system that includes a high-density polyethylene (HDPE) liner. Interpretation of the legislation suggests that the requirement for a barrier system that includes an HDPE liner may extend to the paddocks, significantly increasing construction costs. A new approach to the design of the paddock and solution trench system of a typical South African TSF was therefore required.

The challenge was addressed by combining the function of two components of the TSF – the solution trench and the paddock system – to in-line attenuation ponds. This paper presents a case study of analysis and design of the in-line attenuation pond system for a new TSF.

2.1 Changes in legislation

The National Water Act (NWA) (Act No. 36 of 1998) states that “a person in control of land or occupying or using land and which causes, or is likely to cause pollution of a water resource, must take all reasonable measures to prevent any such pollution from occurring, continuing or recurring”. In addition, the subsequent clause states that reasonable measures shall be taken to comply with any prescribed waste standard or management practice to contain or prevent the movement of pollutants and remedy the effects of the pollution. Regulation 704 of the NWA also prescribes separation of clean and dirty water.

The additional legislation, promulgated in 2013, currently applicable to the design and construction of new TSFs includes Regulation 632 of the National Environmental Management: Waste Act of South Africa (Act No. 59 of 2008). This regulation details the requirements regarding the planning and management of residue stockpiles and residue deposits from prospecting, mining, exploration or production. The regulation states that waste must be classified based on contaminants and an appropriate pollution control barrier system installed as defined by the following regulations appended to the National Environmental Management: Waste Act (Act No. 59 of 2008):

- i) Regulation No. 634 - Waste Classification and Management Regulations
- ii) Regulation No. 635 - National norms and standards for the assessment of waste for landfill disposal
- iii) Regulation No. 636 - National norms and standards for disposal of waste to landfill.

In accordance with these regulations, waste may be classified as one of five types of waste (Type 0 to Type 4) by assessment of the concentration of contaminants contained in the waste material or potential leachate. A corresponding minimum treatment or engineered barrier control system is prescribed in Regulation No. 636 for each waste type (treatment or Class A to Class D). The requirement for a Class C barrier system applicable to a Type 3 waste (comparable to platinum tailings material) is illustrated in Figure 2.

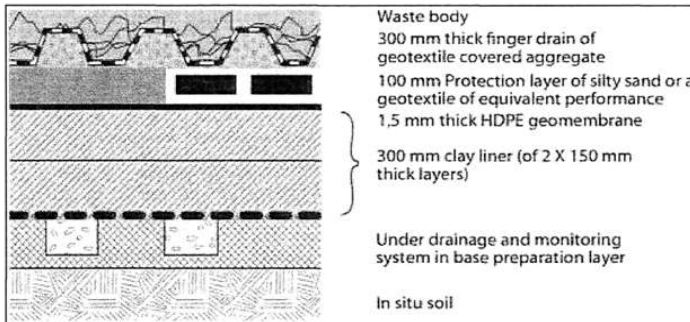


Figure 2. Class C pollution control barrier requirement

Interpretation of the legislation suggests that the requirement for an engineered pollution control barrier system, including the components illustrated in Figure 2, would extend to the construction of the traditional paddock system as the water contained in the paddocks is considered dirty water (i.e. contaminated runoff).

2.2 Overview of the requirements for a lined system

Large parts of South Africa are classified as arid by the Köppen Climate Classification system (Kottek, et al., 2006) and it is therefore considered the nation's collective responsibility to use water as efficiently as possible. This is further magnified by the events of February 2018 when South Africa declared a national disaster based on the drought afflicting parts of the country.

This requirement for responsible water use and protection of water resources extends to the mining industry and the design and operation of mine waste infrastructure. Therefore, in addition to the legislative requirements, changes in water use policy influenced the design objectives and requirements for the new lined system which were as follows:

- i) Maximize water return
- ii) Protect groundwater from pollution
- iii) Minimize cost in an already cost-sensitive environment.

3 CASE STUDY

3.1 Overview of the project

The TSF at a platinum mine located in the Limpopo Province of South Africa is approaching the end of its design life. Life of mine (LOM) is planned to proceed for at least another 20 years and therefore an alternate tailings disposal option was required. Following an extensive options analysis and risk assessment phase, construction of a second TSF was determined to be the best option for the mine. The second TSF was designed as an abutment to the existing facility with a footprint

constrained by the current surface lease area and environmental authorisation. A general arrangement of the planned facility is illustrated in Figure 3.

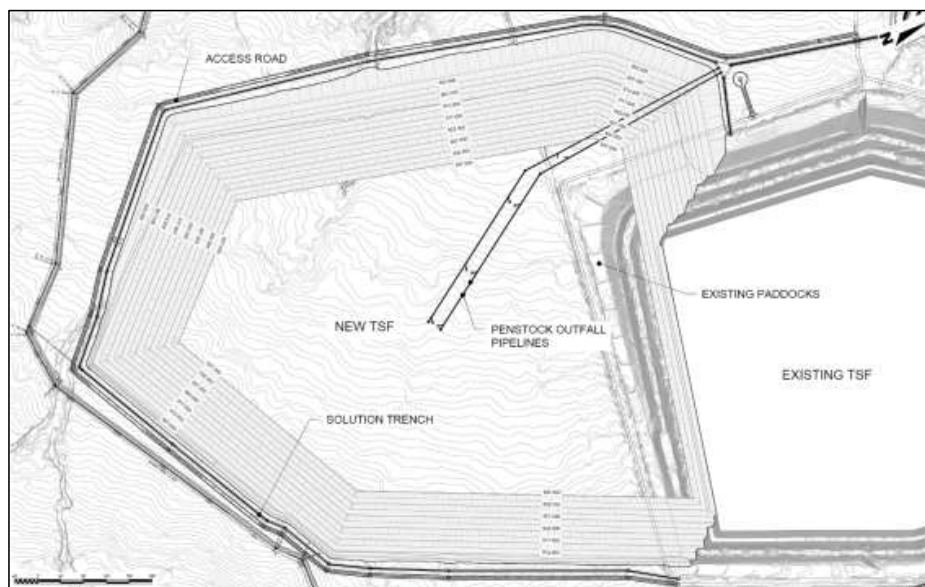


Figure 3. General layout of new TSF

In accordance with the applicable legislation, samples of the waste were obtained and tested to classify the waste type and subsequently the barrier system requirement. The resultant waste type classification (Type 3) prescribed the design of a pollution control barrier system that comprised a 1.5 mm thick single layer HDPE geomembrane over a 300 mm thick clay layer, an above and below liner drainage system and protection to the liner from damage (Class C). In addition, the local communities' main source of water in the area is groundwater and potential contamination of the groundwater may affect the community health and social well-being, further reinforcing the requirement for stringent pollution control.

Conveyance of the stormwater runoff from the eastern and southeastern flanks of the facility posed a challenge as the site is located within a valley and the abutment of the new facility to the existing facility prevents the possibility of open channel flow around the northern perimeter. The solution trench is therefore required to collect and convey the runoff generated by the TSF embankments in addition to the operational flow rate in a single direction for the length of the perimeter of the new facility. To provide the required hydraulic capacity for a storm event by means of a single conveyance feature was considered impractical and attenuation was deemed necessary.

The design and construction of the traditional paddock system was not considered feasible due to the surface area constraint, the increased cost of installing the pollution control barrier to the paddocks and the loss of runoff/ stormwater to evaporation which could otherwise be harvested. The design approach was therefore to develop a solution trench that combined the conveyance function of a traditional solution trench with the attenuation function of the traditional paddock system.

3.2 Design criteria and considerations

The design criteria were split into operational and storm event design criteria. Operational flow consists of flow from the seepage drains (above and below liner, blanket drain and toe drains) and water decanted from the supernatant pond by the penstock and outfall pipeline.

The storm event hydraulic capacity consists of stormwater (within the basin decanted by the penstock and runoff from the TSF embankments captured directly by the solution trench) in addition to the operational flow. The design storm event for stormwater conveyances in and around a mine is a 1 in 50-year 24-hour storm event in accordance with the recommendations by the Chamber of Mines (1996).

In addition to hydraulic capacity, practical design considerations include cleaning and maintenance and the limitation of a single flow path around the TSF towards the return water dam.

3.3 Hydrologic analysis

The catchment contributing to the solution trench was divided into five subcatchments, as indicated in Figure 4. During operation of the TSF, berms will be constructed on each bench/step-in containing stormwater runoff. Each berm will therefore act as an effective paddock attenuating runoff and enabling evaporation and infiltration into the dam. Runoff from the lowest bench only therefore contributes to the assessment of the in-line attenuation ponds. The respective catchment characteristics determined are summarized in Table 1.



Figure 4. Subcatchment areas

Table 1. Catchment characteristics

	Area (m ²)	Hydraulic length (m)	Average catchment slope (%)
Eastern	17,500	24.3	39
Southeastern	11,919	10.8	27
Southwestern	9,752	40.0	24
Western	44,560	67.5	28
Northern	6,100	71.0	28

The design storm (24-hour, 1 in 50-year annual exceedance probability (AEP)) depth was determined as 127 mm by fitting 98 years of daily data to a log-normal distribution. The Soil Conservation Service South Africa (SCS-SA) method of runoff estimation was used to determine stormflow runoff for each catchment as recommended by Smithers and Schulze (2002). No flow

and/or depth gauge records were available to calibrate the coefficients and runoff values from the slopes of the TSF embankment and therefore reasonable assumptions were made based on vegetation condition and soil type. A curve number of 75 was considered appropriate as the embankment slopes are designed to be well vegetated which will result in some infiltration despite the steep catchment slopes. The resultant runoff depth was determined as 69.1 mm.

Peak flow determinations would ideally be conducted using calibrated runoff models; however, limited hourly rainfall records are available in South Africa. The peak discharge was therefore estimated according to the South African National Roads Agency Limited (SANRAL) Drainage Manual (SANRAL, 2013) using SCS techniques based on the triangular unit hydrograph concept. The unit hydrograph represents the temporal distribution of stormflow for an incremental unit depth of stormflow, ΔQ , that occurs in a unit duration of time, ΔD . By assuming a time to peak of 3/8 of the total hydrograph duration, the peak discharge for a storm with a uniform temporal rainfall distribution is given by Equation 1.

$$q_p = \frac{0.2083 AQ}{D/2+L} \tag{1}$$

In Equation 1, q_p is the peak discharge in m^3/s , A is catchment area in km^2 , Q is the stormflow depth in mm, D is the effective storm duration in hours and L is the catchment lag in hours. The effective storm duration is related to the catchment response time (or the lag) and therefore the denominator of Equation 1 can be simplified to 1.83 L . The stormflow runoff volumes and peak discharge values estimated are summarized in Table 2.

Table 2. Catchment runoff volume and peak discharge

	Runoff volume (m^3)	Peak discharge (m^3/s)
Eastern	1,210	17.6
Southeastern	824	19.1
Southwestern	674	5.2
Western	3,081	16.8
Northern	422	2.2

Hydrographs for each subcatchment were generated using the method developed by Haan (1994) and are shown in Figure 5.

3.4 Hydraulic design

The solution trench was divided into attenuation ponds by including concrete walls at 100 m intervals along its alignment. The hydraulic design of the in-line attenuation ponds was divided into two components, i.e. the solution trench conveyance during normal operational conditions and the attenuation ponds for the storm condition. While the larger constraint is the storm event flow condition, the outlets between the attenuation ponds must be sized to allow unrestricted flow during the operational condition. The sizing of the solution trench channel and outlets was an iterative process described in the sections below.

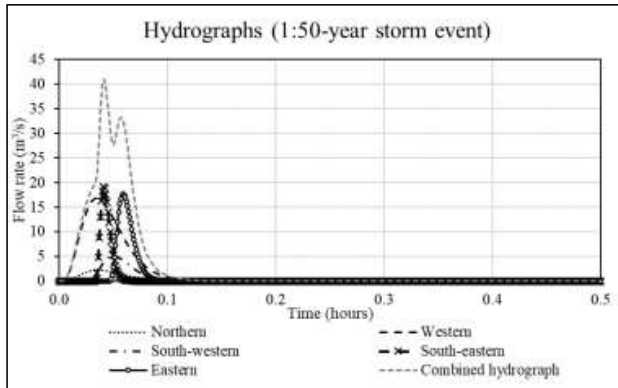


Figure 5. Hydrographs for each subcatchment

3.4.1 Operational conditions

The operational flow rate was quantified by considering the drain flows measured on the existing facility, outputs from the seepage model (for the above and below liner drain designs) and operational penstock decant flow rates estimated for the facility.

Under free surface flow conditions, the hydraulic capacity of the solution trench and outlets was determined by Manning's equation for open channel flow which is described by Equation 2.

$$Q = \frac{1}{n} \times A \times R^{\frac{2}{3}} \times \sqrt{S} \quad (2)$$

In Equation 2, Q represents the flow rate in m^3/s , A represents the cross-sectional flow area in m^2 , n represents the Manning's roughness coefficient of the channel surface in $\text{s}/\text{m}^{1/3}$, R the hydraulic radius in m and S the slope of the channel in m/m . The slope of the solution trench varies along the perimeter of the facility due to undulation of the natural topography and therefore the hydraulic capacity of the solution trench and outlets under free surface flow conditions is not constant.

The initial configuration selected for the system was a trapezoidal concrete solution trench, with a base width of 1.5 m and provision for four 200 mm nominal diameter PVC pipes to serve as outlets. As part of the iterative process and to facilitate cleaning and maintenance, the outlets included in the final design are two rectangular box-outs of 450 x 200 mm in the concrete wall of each pond at the invert level of the solution trench. The minimum capacity of the solution trench and rectangular outlets exceeds the maximum flow rate under operational conditions and was therefore deemed satisfactory for operational conditions.

3.4.2 Storm event conditions

During the design storm event with a 1 in 50-year AEP, the runoff generated on the slopes of the TSF is collected by the in-line attenuation pond system and attenuated, while the rate of discharge between ponds is controlled by the outlet. Based on the maximum head determined, the concrete walls that form the in-line attenuation ponds are sized to be 1.20 m high at intervals of 100 m, and the initial proposed solution trench is deemed acceptable as the dimensions enable maintenance and operation as well as 0.43 m of channel freeboard (as a minimum). A partial plan view of the in-line attenuation ponds is illustrated in Figure 6.

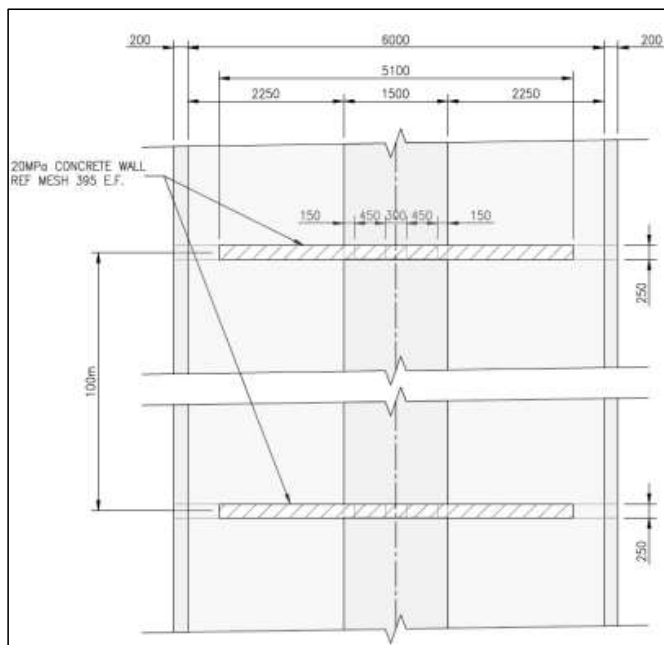


Figure 6. Partial plan view of in-line attenuation pond system

As a result of the location of the outlets at invert level, the outlets will be submerged after/ during a storm event and the orifice discharge formula described by Equation 3 is applicable to determine the rate of discharge.

$$Q = C_D \cdot A_o \sqrt{2gH} \quad (3)$$

In Equation 3, C_D represents the discharge coefficient, A_o is the cross-sectional area of the opening of the outlet in m^2 , g represents gravitational acceleration, H is the vertical height of water (head) at the outlet wall measured in m relative to the invert level of the outlet measured.

The range of the anticipated flow rates through the various compartments at the outlets using Equation 2 was determined as approximately $0.33 m^3/s$ (for the maximum head) and $0.24 m^3/s$ (for the minimum head). The area provided by two box-outs of 450×200 mm each provide sufficient control of the discharge rate resulting in the desired attenuation. A typical cross-section of a division wall within the solution trench forming an in-line attenuation pond is illustrated in Figure 7.

To ensure effective operation of the in-line attenuation pond system, any accumulated silt within the ponds must be cleared regularly and the outlets must be kept clean and clear of debris. To ensure that maintenance and cleaning is as easy to carry out as possible, the pipe outlets specified during the preliminary design were replaced with rectangular section outlets to enable the use of a broom during cleaning.

3.6 Construction and maintenance consideration

The walls that divide the solution trench into the attenuation ponds are designed for construction using 20 MPa reference mesh-reinforced concrete. The openings could be cast in a concrete wall as box-outs without difficulty. The openings were also sized to ensure ease of cleaning in the event of siltation or blockage by debris. Siltation of the ponds is anticipated over time and therefore an essential part of the operations and maintenance considerations will be the ongoing maintenance and care of the in-line attenuation ponds.

4 CONCLUSIONS

The impact of water stress caused by drought conditions and water scarcity is a growing concern across the world in all sectors, including the mining industry. Innovative solutions are therefore imperative to optimize the management of mine waste water.

To design optimized systems or structures for the collection, attenuation and conveyance of stormwater runoff from the embankments of TSFs in future, reducing the uncertainty in quantifying stormwater runoff rates and volumes is required.

The methods currently employed in determination of the stormwater runoff flow rates and volumes are sensitive to the selection of a series of runoff coefficients. These runoff coefficients are selected on the basis of land use, vegetation condition and soil type (characterised by hydrologic soil groups). The runoff coefficients which may be considered applicable to partially vegetated TSF embankments require calibration and/or validation.

Climate monitoring stations on site are currently maintained and operated by the operator on the facility. In addition to measurement of the rainfall depth, measurement of the stormwater volumes accumulated within the paddocks at facilities that use the traditional paddock system (or recording of the depths resulting in the in-line attenuation ponds) is recommended. Monitoring of water levels within the paddocks at existing TSFs and water facilities will enable calibration of the runoff coefficients resulting from the storm depth as measured.

Furthermore, the impact of drought and extreme weather patterns may affect the type and rate of establishment of vegetation. Many TSF embankments in South Africa are currently irrigated to suppress dust and encourage and sustain vegetation establishment. This practice may prove unsustainable in future due to the volumes of water consumed and alternate vegetation and/or erosion protection measures may be required, altering the stormwater runoff generation potential.

The in-line attenuation pond system optimizes the footprint of the facility, and reduces capital cost and water losses. Exclusion of a paddock system lined with the required pollution control barrier system resulted in a footprint that was reduced by approximately 8.5 Ha and an estimated capital cost saving of more than ZAR 10 million. Following construction, with effective maintenance, the efficacy of the in-line attenuation pond system can be evaluated and potentially applied to the design and construction of other facilities that are subject to similar constraints.

REFERENCES

- Chadwick, A., Morfett, J. & Borthwick, M., 2004. *Hydraulics in Civil and Environmental Engineering*. Fourth Edition ed. New York: Spon Press.
- Department of Water Affairs and Forestry, 1999. *Regulation No. 704 on Use of Water for Mining Related Activities Aimed at the Protection of Water Resources*, Pretoria: National Water Act, 1998 (Act No. 36 of 1998).
- Department of Environmental Affairs, 2013a. *Regulation No. 634: National Environmental Management: Waste Act (59/2008): Waste Classification and Management Regulations*. Government Gazette of the Republic of South Africa, 578(36784), pp. 3-21.
- Department of Environmental Affairs, 2013b. *Regulation No. 635: National Environmental Management: Waste Act (59/2008): National norms and standards for the assessment of waste for landfill disposal*. Government Gazette of the Republic of South Africa, 578(36784), pp. 22-33.
- Department of Environmental Affairs, 2013c. *Regulation No. 636: National Environmental Management: Waste Act (59/2008): National norms and standards for disposal of waste to landfill*. Government Gazette of South Africa, 578(36784), pp. 34-45.

- Department of Environmental Affairs, 2015a. *Regulation No. 632: National Environmental Management: Waste Act (59/2008): Regulations Regarding the Planning and Management of Residue*. Government Gazette of the Republic of South Africa, 601(39020), pp. 4-14.
- Department of Environmental Affairs, 2015b. *Regulation No. 633: National Environmental Management: Waste Act (59/2008): Amendments to the List of Waste Management Activities that have, or are likely to have, a Detrimental Effect on the Environment*. Government Gazette of the Republic of South Africa, 601(39020), pp. 15-16.
- Haan, Barfield & Haynes, 1994. *Design Hydrology and Sedimentology for Small Catchments*. London: Academic Press Inc.
- Kottek, M., J. Grieser, C. Beck, B. Rudolf, and F. Rubel, 2006: *World Map of the Köppen-Geiger climate classification updated*. Meteorol. Z., 15, 259-263. DOI: 10.1127/0941-2948/2006/0130.
- Parliament of the Republic of South Africa, 1998. *National Water Act (36 of 1998)*, Cape Town: Parliament of the RSA.
- SANRAL, 2013. *The Drainage Manual*. Sixth ed. Pretoria: The South African National Roads Agency SOC Ltd.
- Smithers, J. C. & Schulze, R. E., 2002. *Design Rainfall and Flood Estimation in South Africa*, Pietermaritzburg: Water Research Commission.
- SRK, 2017. *Marula Tailings Dam No. 2 – Preliminary Design Report – Engineering Analysis and Design of Tailings Dam*, Johannesburg: SRK Consulting (South Africa) (Pty) Ltd.
- The Chamber of Mines of South Africa, 1996. *Guidelines for Environmental Protection: The Engineering Design, Operation and Closure of Metalliferous, Diamond and Coal Residue Deposits*. Johannesburg: Chamber of Mines of South Africa.
- United States Geological Survey (USGS), 2016. *How much water is there on, in, and above the Earth?* [Online] Available at: <https://water.usgs.gov/edu/earthhowmuch.html> [Accessed 24 June 2018].

Improving Water Management in the Orcopampa Mine

J.C. Gabriel Espinoza

Compañía de Minas Buenaventura S.A.A., Lima, Lima, Perú

ABSTRACT: The Orcopampa mine, with over 50 years of operation, began when there was no environmental legislation in Peru. Years later, it adapted to the environmental laws that grew as the industry evolved. In 2014, Orcopampa started the “Improving Water Management” project which oversees the different mining processes: mine closure (temporary for mine waste stockpiles and permanent for tunnels using hermetic plugs) and water treatment (effluent treatment plants, re-use of filtration water to avoid fresh water consumption). The project aim is to create a synergy within these processes to obtain economic, social and environmental benefits.

1 INTRODUCTION

1.1 Background

The Orcopampa Mine from Compañía de Minas Buenaventura S.A.A. (CMBSAA) is an underground mine which extracts and process gold and silver ores. This mine is over 50 years old and is located in the districts of Orcopampa and Chilcaymarca, in the Castilla province of the Arequipa region, Peru.

When this mine came into operation, Peru did not have an environmental regulation for mining activities. During the decade of 1990’s the first environmental laws were created, starting with the Environmental Management and Adaptation Plans (PAMA, in its Spanish acronym), Orcopampa drafted and approved the PAMA for its operations. Years later, in 2003 Orcopampa obtained the approval of its first Environmental Impact Assessment (EIA), which has had several modifications since. Water management had a similar focus, aimed only at legislation compliance leaving aside possible synergies between water treatment (water treatment plants) and mine closure (temporary for mine stockpiles, permanent for tunnels, etc.).

In Orcopampa, effluents are treated in a water treatment system (pools, reservoirs, flow meter, instrumentation, etc.) similar to an acid water treatment plant, it uses the process of High Density Sludge. This allows Orcopampa to continuously dispose of the treated effluents with quality levels that comply with the Maximum Permissible Limits (MPL) according to the law (D.S. N° 010-2010-MINAM). During the last decade, Peruvian environmental legislation has evolved and has established strict levels, mainly, regarding Environmental Quality Standards (ECA) and Maximum Permissible Limits (MPL), this motivates and challenges the water and environmental management.

In 2014, a plan was drafted for the project “Improving Water Management in Orcopampa”, the aim was to integrate the different processes of water treatment – effluents in a single treatment plant for acid water using a wetland as a natural filter and reuse of filtered underground water to minimize fresh water consumption – and mine closure – temporary for mine waste stockpiles, permanent for tunnels to avoid effluents, etc. –.

The project aims to shift from the classic model of legislation compliance to an eco-efficiency model that provides added value to society and third parties. The main activities are

- Elimination of effluent sources, progressive mine closure and the final Mine Closure Plan
- Quality assurance of treated effluents
- Diminish fresh water consumption
- Reuse of treated industrial water

In order to eliminate sources of acid water, the construction of hermetic plugs was required. The most important site was the closure of the “Alberto Tunnel” which meant the removal of 15 Lt/s of mining effluents with concentrations of Pb, Zn and Mn that exceeded the Maximum Permissible Limits.

The quality assurance of treated effluents was carried out by employing different treatment methods. In our case, it meant the development of the Unified Plant with a capacity of 400 Lt/s. The decrease in fresh water consumption for the operation was met with the recirculation of water in different processes, which allowed the efficient use of water. Finally, the reuse of treated industrial water by the community in agriculture, fish farm, etc.

This project, Improving Water Management, will allow a solid and sustainable management of the water resource providing economic, environmental and social benefits.

1.2 Objectives

The aim for water management is to optimize the use and quality assurance of water treatment in the Orcopampa operations and mine closure, it benefits the Orcopampa and Chilcaymarca river or the reuse of industrial water by the communities.

Specific objectives

- Contribute with water availability in the Orcopampa and Chilcaymarca rivers
- Reach a higher efficiency in water use by the operation
- Provide treated water for use by the communities surrounding the mine
- Introduce eco-efficiency tools to improve environmental and economic standards

2 METHOD

2.1 Improving Water Management

Operations in the Orcopampa mine complied with legal requirements regarding water management. Diagram 1 and 2 – Legal Compliance Model



Source: CMBSAA

Diagram 1: Legal Compliance Model

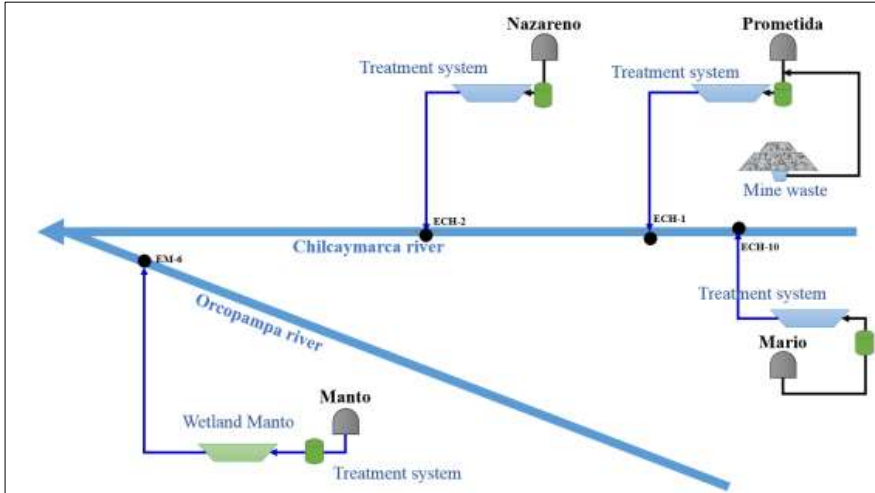
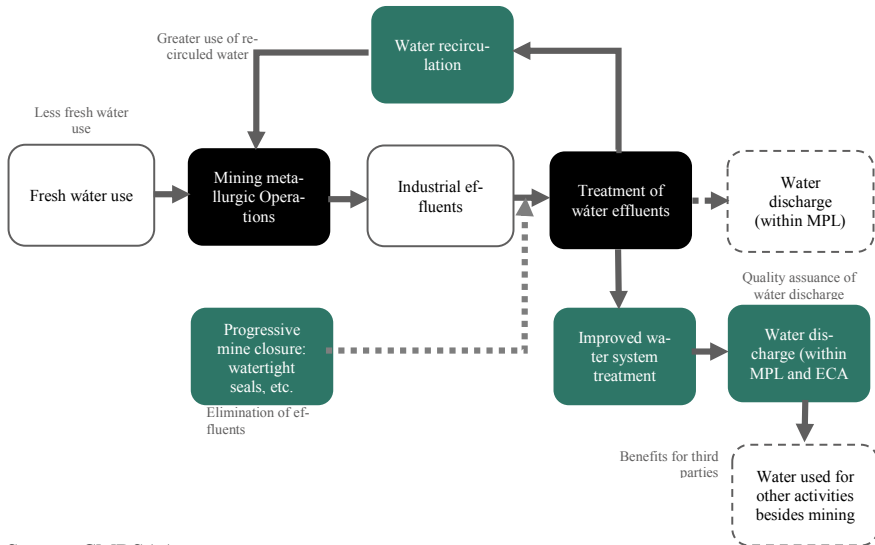


Diagram 2. Water Management – Legal Compliance

Since 2014 a new conceptual model was drafted to improve water management in Orcopampa [Diagram 3]. In addition to meeting all legal requirements, we established the elimination of effluent sources by promoting the progressive mine closure plan (tunnels and mine waste stock-piles), quality assurance of water discharge (improving water management) and the decrease of fresh water consumption by the operation (increase in recirculation from treated water).



Source: CMBSAA

Diagram 3: Conceptual Model of Improving Water Management in the Orcopampa Mine.

The implementation of this new model took into consideration different activities divided in 3 stages starting in 2014 and that will finish by 2020.

Table 1. Project schedule

Nº	Activities	2014	2015	2016	2017	2018	2019	2020
1	Stage I							
1.1	Location and construction of Wetland Pucará		█					
1.2	Progressive mine closure (mine adit level 3800 – Alberto Tunnel)			█				
2	Stage II							
2.1	Redirect treated effluents in STARI to wetland Pucará			█				
2.2	Operation of wetland Pucará				█	█	█	█
3	Stage III							
3.1	Covers for mine waste stockpiles (protection from rain)				█			
3.2	Detailed engineering of Industrial Water Treatment System (STARI)				█	█	█	█
3.2.1	Construction of Unified Plant						█	█
3.2.2	Improvement of Water Treatment Systems						█	█

Source: CMBSAA

3 PROJECT DEVELOPMENT

3.1 Stage I

- a. Location and construction of Wetland Pucará
 In order to build wetland Pucará, the efficiency of heavy metal removal had to be determined. Upon its evaluation, table 2 represents the results

Table 2. Efficiency of water treatment mechanisms

Parameters	Main removal mechanisms
Suspended solids	Sedimentation, precipitation and filtration.
DBO and DQO	Organic matter sedimentation, filtration, absorption, and microbial degradation (aerobic and anaerobic); mainly executed by bacteria that grows on plants or form part of biofilms in the wetland.
Nitrogen	Ammonification, nitrification, denitrification, volatilization, assimilation by plants and microorganisms.
Phosphorus	Absorption, precipitation (using aluminum, iron, calcium, etc.), adsorption, used by plants and microorganisms.
Pathogens	Sedimentation and filtration, natural death, death by ultraviolet radiation, antibiotic secretion from plant roots.
Heavy metals	Absorption in plant roots and sediment particles, precipitation and filtration.

Source: Brix, 1994; Champagne, 2007

Main advantages of wetlands (Kadlec & Wallace, 2009):

- Use natural energy.
- Lower construction and maintenance costs than conventional treatment systems.
- Low or no sludging
- Offers an added ecological and aesthetic value creating a unique ecosystem
- Can be integrated to different water treatment systems without odor.
- Does not require highly qualified personnel.

The disadvantages of wetlands:

- Requires big areas.
- The design requires highly qualified personnel.
- Probabilities of success are narrow

Treated effluents go through concrete canals to Wetland Pucará, after the process they will be disposed of through one station.

By the end of 2014, the construction of the artificial wetland of horizontal flow had started, a couple of kilometers downstream of the operations. The effluents of superficial flow are designed so the water is over the substrate and vegetation is partially underwater. This technology is characterized as an easy implementation and low cost. This mechanism of acid drainage treatment has had impulse in mining since the 1980's.



Photo 1. Wetland Pucará

Table 3. Investment costs in Chipmo.

Component	Investment (US\$)
Wetland Pucara	639,685.00

Source: CMBSAA

The Wetland Pucará created a new habitat for birds and other species. In addition the heavy metals removal is 61% on average. The results are presented in Table 4

Table 4. Removal efficiency of Wetland Pucará.

Parameters	Unit	Quality before Wet-land Pucará	Quality after Wet-land Pucará	Efficiency (%)	MPL	ECA
STS	mg/L	13.00	<5	81%	25	-
Aluminium total	mg/L	0.38	0.12	68%	-	5
Copper total	mg/L	0.01	0.00	50%	0.5	0.5
Iron total	mg/L	0.88	0.29	67%	-	5
Manganese total	mg/L	0.95	0.66	30%	-	0.2
Zinc total	mg/L	0.02	0.01	72%	1.2	2

Progressive mine closure (mine adit level 3800, Tunnel Alberto) Old mining sites in Orcopampa were located in Santa Rosa, Blancas, Tudela and Calera sectors. The Tunnel Alberto tunnel used to generate 15 lt/s of effluents with concentrations of Mn, Pb and Zn above MPL. This effluent was treated in a passive artificial wetland (Manto), which, after the process the effluents were

discharge comply with the MPL according to Peruvian regulation. Photo 2 demonstrates the closed mine located in Manto, this represented a decrease of water treatment of 15 lt/s.

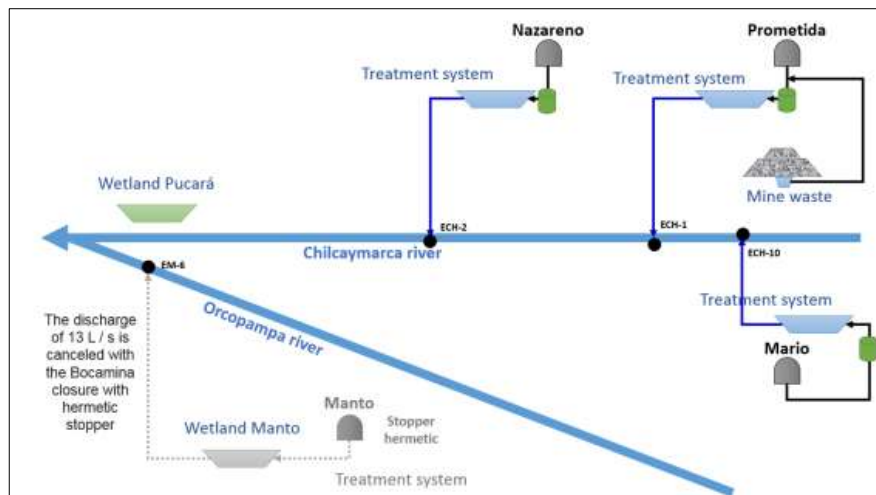


Diagram 4. Improving Water Management – Stage



Photo 2. Mine adit Tunnel Alberto, zero effluents.

Investments and reduced costs due to the elimination of effluents from Tunnel Albert are shown below.

Table 5. Investment costs in Manto.

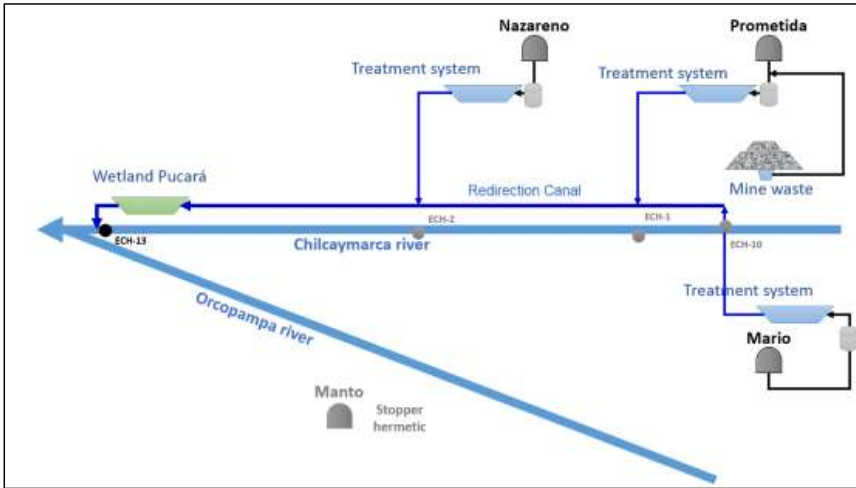
Component	Watertight seal construction for mine closure (US\$)	Reduced costs by Water Treatment Plant implementation (US\$)	Operation costs reduction (US\$/year)
Mine adit level 3800 effluent flow 15 L/s	395,853	750,000	75,400

Source: CMBSAA

3.2 Stage II

3.2.1 Divert effluents from Industrial Water Treatment Systems to Wetland Pucará.

The redirection of treated effluents from treatment systems in Prometida, Nazareno and Mario began on June 2016. Currently, stage II has concluded, as shown in Diagram 5, the flowchart summarises the current water treatment of effluents and redirection to Wetland Pucará.



Source: CMBSAA
Diagram 5. Improving Water Management – Stage II.

The goals met include the centralization of water disposal in one station and the elimination of 4 other disposal stations.

3.2.2 Operation of Wetland Pucará

Wetland Pucará came into operation in 2017 with several species such as typhas, water hyacinth and algae. The efficiency of Wetland Pucará presented satisfactory results shown in Table 6.

Table 6. Water quality at the beginning and end of Wetland Pucará

Parameters	Unit	Beginning	End	MPL	ECA
Temperature	°C	23.5	22	--	--
pH	pH	7.8	8.19	6-9	6.5-8.4
STS (Suspended Solids)	mg/L	13	<5	50.00	--
Aluminium Total	mg/L	0.38	0.12	--	5.00
Barium total	mg/L	0.028	0.024	--	0.70
Cobalt total	mg/L	0.016	0.011	--	0.05
Copper total	mg/L	0.006	0.003	0.50	0.20
Iron total	mg/L	0.88	0.29	--	1.00
Dissolved iron	mg/L	0.01	<0.01	2.00	--
Manganese total	mg/L	0.947	0.661	--	0.20
Lead total	mg/L	<0.01	<0.01	0.20	0.05
Zinc total	mg/L	0.018	0.005	1.50	2.00

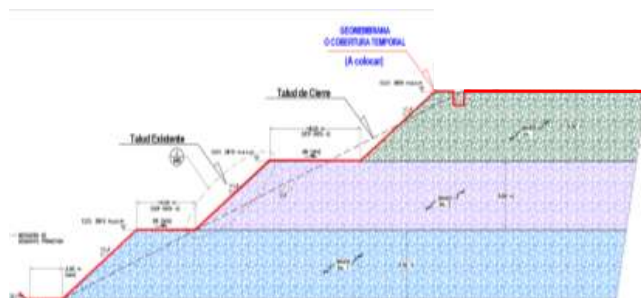
Source: CMBSAA

The results show a significant difference in suspended solids, copper, iron, manganese and zinc. Therefore, Wetland Pucará is an efficient water treatment system.

3.3 Stage III

3.3.1 Covers to protect mine waste stockpiles from rain (temporary closure)

Geomembranes were used to cover the stockpiles of mine waste located in Prometida. This prevented acid drainage from the deposit. This is able to partially eliminate an effluent that would need to be treated from this component.



Source: CMBSAA
Diagram 6. Design of the cover for the stockpile at Prometida

This decreased 0.57 lt/s of mine acid effluents with high concentrations of iron, copper, lead, zinc and manganese.



Photo 3. Geomembrane cover on stockpile at Prometida

3.3.2 Improving Treatment Systems and Implementation of a Unified Plant for Acid Water Treatment

The operation had to ensure the quality of effluents, according to law, they should be below MPL. Therefore, improvements are being introduced to the Industrial Water Treatment Systems at Nazareno and Prometida.

Currently these water treatment systems process water from the mine and any water with acidic pH while the water treatment system at Mario processes slightly alkaline water. Diagram 7 shows the process of water treatment. Diagram 7 shows the process of water treatment.

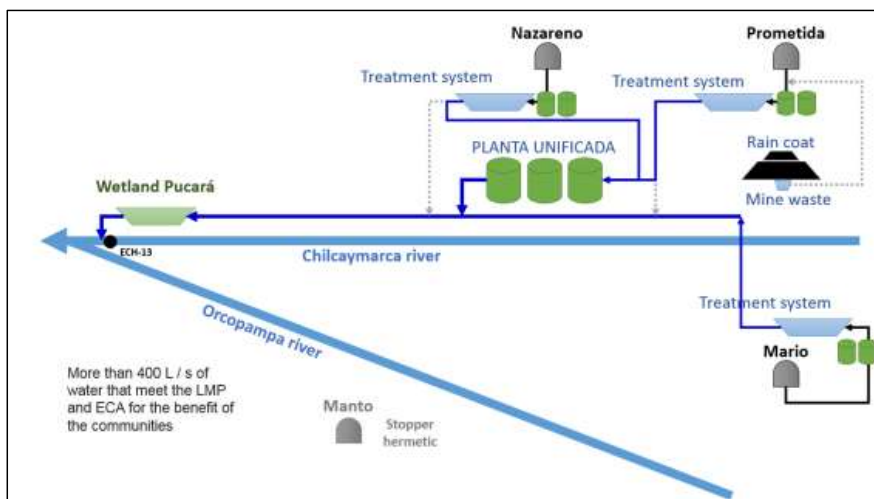


Source: CMBSAA
Diagram 7: Acid Water Treatment Process

3.3.3 Water Treatment System Design

Currently, the three treatment systems process a total of 250 lt/s, the treated effluents are below MPL.

The Improving Water Management project aimed to develop the existing treatment systems at Nazareno and Prometida and to construct a new unified plant with a capacity of 400 lt/s. This plant will process all effluents from Nazareno and Prometida, to later blend with the effluents from Mario and finally join Wetland Pucará.



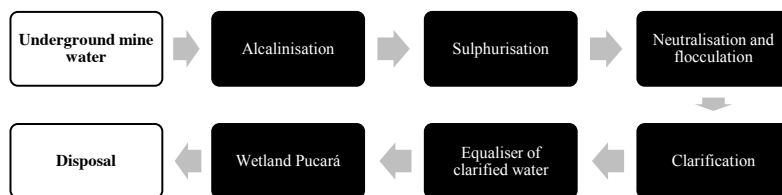
Source: CMBSAA
Diagram 8: Improving Water Management – Stage III

The new treatment process is based in the following theories: Alkalinisation: eliminates dissolved metals, pH elevates over 9.5, the result is precipitation of metallic hydroxides that separate due to sedimentation. Limestone is usually used for neutralisation.

Phase change:

- Sulphurisation
- Oxidation
- Coagulation and flocculation
- Total suspended solids (TSS)

We concluded that the improvement of the current water treatment systems and the implementation of a unified plant, require the methodology shown in Diagram 9.



Source: CMBSAA
Diagram 9: Process to implement a Unified Plant

4 RESULTS

4.1 Planned investment and savings

The project costs are detailed in Table 7, it shows the projected and executed expenses

Table 7. Water Treatment Plant Investment.

Alternative	Period 2014-2017 (US\$)	Period 2018-2025 (US\$)
Scenario 1: Legal compliance	3'983,165	7'164,934
Scenario 2: Improving Water Management	3'399,818	4,749,756
Savings	583,347	2'415,178

4.2 Decrease in Fresh Water Consumption

Actions are oriented to recycle water, promoting its use in mining and metallurgic operations. Recirculation circuits have been implemented in the underground mine and the processing plant. Recirculation has significantly decreased the consumption of fresh water during the last couple of years. Table 8 shows the benefits.

Table 8. Authorised and real consumption

Type of usage	Authorised mm ³ /year	Real consumption mm ³ /year
Mining, industrial and domestic	5,091.80	1,856.69

Source: CMBSAA

5 CONCLUSIONS

5.1 Social

- Water availability of 400 lt/s within MPL and ECA that can be used by local communities for agriculture and fish farms.
- Improved corporate image regarding water management.

- Decrease in complaints and conflicts with communities regarding responsible water management.

5.2 *Environmental*

- Creating a micro-ecosystem in Wetland Pucar for native and migratory species.
- Create a greater opportunity for water reuse within the operation.
- Fresh water consumption saving of 3,235.11mm³ per year.
- Elimination of 4 discharge points.
- Quality assurance and compliance of legal standards (MPL and ECA).

5.3 *Economic*

- Since the beginning of the project in 2014, the company has saved US\$ 583,347
- It has a projected saving of US\$ 2,415,178 for the period 2018 – 2028
- A decrease in operation costs

REFERENCES

- Brix, 1994, Functions of macrophytes in constructed wetlands
C. Boutin, A. M. Crolla, C. B. Kinsley and P. Champagne (2004) The Role of Plants in the Removal of Nutrients in a Constructed Wetland Treating Agricultural Wastewater
Wallace 2009, Treatment Wetlands 2nd Edition_0

Mine Tailings Drainage: A Bottoms Up Approach Using HDD Well Installation Methods

J. Gallagher and D. Bardsley

Directed Technologies Drilling, Bellafonte, Pennsylvania, USA

ABSTRACT: Mine tailings impoundments, when saturated, can represent the risk of contamination seepage to the surrounding watershed as well as significant physical risk in the event of structural failure. Dewatering the tailings is often a crucial step in the mine reclamation/remediation process, however conventional dewatering techniques may not always be applicable or cost effective.

This paper presents a case study where horizontal directional drilling (HDD) was used to install a gravity-fed dewatering well that was drilled underneath the embankment and then up through the floor of a tailings pond.

The HDD method provided several distinct advantages over other approaches; however, it also brought its own unique challenges, which were overcome in due course.

1 HISTORY OF HDD WELLS

1.1 Oilfield technology

Steering technology, allowing directional control of a sub-surface drilling bit, was initially developed for the oilfield in the early 20th century. Early applications involved strategically deviating from a vertical boring to exploit the geometry of a productive formation.

1.2 Trenchless utility installation

Then in the 1970s, HDD rigs were developed that entered the ground at a shallow angle (between 5-25 degrees off horizontal) for trenchless utility installation underneath roadways, rivers or other surface obstructions.

1.3 Groundwater remediation

Finally, in the 1980s the HDD method was used to install the first horizontal wells which were designed for extraction and remediation of contaminated groundwater. While the drilling and steering technology of HDD carried over from the utility industry, an important difference emerged since wells need to communicate with the surrounding aquifer. Variables such as screen design, drilling mud properties and other factors from the water well/environmental drilling industry now needed to be considered.

Additionally, because a well isn't just a conduit, but is providing access to the subsurface, the typical double-ended configuration of most HDD utility bores was not always necessary, and

often prohibitive due to site constraints. Thus, the so-called “blind” or “single-ended” borehole configuration has evolved within the niche corner of the HDD well industry.

Since the initial wells installed in the 1980s, HDD has been used for a wide range of different groundwater applications including environmental remediation, water supply and dewatering.

2 CALLAHAN MINE SITE BACKGROUND

The Callahan Mine site is located in Hancock County, Maine. Zinc-copper sulfide deposits were discovered in 1880 and the mine operated from the late 19th century until its closure in 1972. During the mine’s lifespan ore bodies containing zinc, copper, lead, arsenic and cadmium were discovered. The primary period of open pit mining occurred during 1968-1972.

The current site consists of a submerged open pit, three waste rock piles and the tailings impoundment. The tailings impoundment has a 21-acre footprint and contains 700,000 cubic yards of material.

In 2009, the federal Environmental Protection Agency (EPA) signed a record of decision (ROD) to clean up the site in collaboration with the Maine Department of Environmental Protection (MEDEP).

In 2010, along with some other remediation work, cap/cover and drainage of the tailings impoundment was split off from the Operable Unit 1 (OU1) ROD and rolled into a separate Operable Unit 3 (OU3).

The tailings impoundment was found to be leaching heavy metal contamination into the nearby watershed. It was also determined to be marginally unstable over long term static conditions. So, the tailings component of the OU3 remedy involved draining the water from within the impoundment, treating the effluent and finally installing a cap to limit future inundation of the tailings.

3 DEWATERING APPROACHES CONSIDERED

3.1 *Vertical dewatering wells*

Hydrological models of the tailings impoundment predicted that upwards of twenty vertical dewatering wells would need to be drilled into the tailings. There were two primary drawbacks that eventually ruled out vertical wells:

The first issue was that the wellhead infrastructure on the surface of the tailings would inhibit or at least severely complicate the excavation, regrading and cap/cover construction activities that were also planned as part of the OU3 remedy.

The second issue was that vertical dewatering wells would require pumps. Notwithstanding the ongoing operational costs of running the pump system, the remote nature of the site made the prospect of running a power drop to the vertical well field prohibitively costly and complex.

3.2 *Deep infiltration trench (“one pass”)*

While a deep, single-pass trench installation would conceptually have provided the best drainage, this approach faced the same issues as the vertical well approach; i.e. it would have required piping and power infrastructure on the surface of the impoundment. Additionally, the cost of installing a single-pass trench was several times that of drilling either vertical or horizontal wells.

3.3 *HDD dewatering well(s)*

A horizontal drainage well (or wells) was ultimately the approach that was selected. In contrast to the vertical wells or deep trenching approaches, a directionally drilled well (if installed at the proper elevations) would provide gravity powered drainage to a specific outlet point, eliminating the need for electrical power infrastructure. Further, the wellhead of the horizontal well

could be designed such that it would be in proximity to the eventual treatment system location, minimizing conveyance piping required.

Along with the facts that the surface of the impoundment would remain totally clear for grading/construction activities and the installation cost was comparable to vertical drilling, these factors ultimately made the HDD design the best technical and economical approach considered.

4 HDD WELL DESIGN

A bore profile for the HDD well was developed based on site logistical considerations and hydrogeologic modeling of the impoundment. The final well design consisted of a 991ft long well with 740ft of screen and 251ft of blank casing. The well would be installed in a single-ended



(blind) configuration parallel to the north/south axis of the tailings impoundment. The entry point at the northern end of the well was 24ft below the distal, southern end of the well, and the well screen was approximately 40-50ft below the surface of the tailings.

Figure 1. Plan view of bore profile for horizontal drainage well.

The bore path was designed to enter the native soil formation at a shallow angle so as to pass underneath the impoundment's embankment, and then trend upwards to penetrate into the tailings. The target path for the well screen ran along the bottom of the tailings until it terminated below grade.

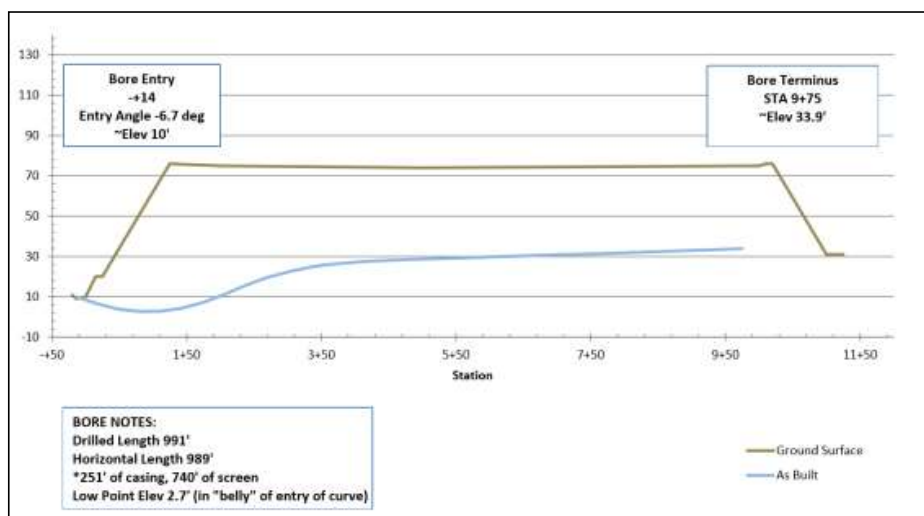


Figure 2. Cross sectional view of bore profile for horizontal drainage well.

5 PRINCIPAL CHALLENGES

Since the well path had been designed to meet certain project-specific criteria (gravity powered drainage, drilling under rather than through the dam embankment, etc.), drilling would require accurate and reliable steering controls.

While steerability is not a unique challenge for an HDD project, the fact that the well would be single-ended raised several technical concerns.

5.1 Single-ended vs double-ended HDD boring configurations

A double-ended HDD installation consists of both an entry and exit point of the borepath into and out of the subsurface. Typically, the well casing and screen material (or utility conduit, piping, or whatever is being installed) is pulled from the exit point back to the entry by the rig in tension. Reaming or hole opening tools can be positioned between the pull tooling and the well materials to ensure the borehole is clear and open.

A single-ended HDD installation, on the other hand, consists of just an entry point into the subsurface, therefore the well casing must be pushed into the open borehole from the entry by the rig in compression.

5.2 Challenges of long single-ended HDD installations

The compressive forces required to install well materials into a single-ended borehole increase with total length. Additionally, borehole stability becomes more and more of a concern as the bore length increases.

The horizontal drainage well designed to dewater this tailings impoundment was relatively long for a single-ended completion. Since leachate was expected to be corrosive, an inert well casing and screen material was required, but PVC or HDPE would not withstand the compressive forces required to push the casing into an open borehole. Furthermore, the non-cohesive nature of the tailings gave reason to suspect that it would be incredibly difficult to maintain borehole stability long enough to install well materials into an open hole, ie the borehole would collapse before or during well installation.

5.3 Hydrostatic head of the leachate

By design, the distal end of the well screen would be approximately 24ft higher in elevation than the wellhead so that impounded water would flow by gravity out of the tailings. However, the borehole would be subject to these same hydraulic forces prior to the installation of the well casing, which was the HDD equivalent of drilling into artesian conditions.

Concern was raised that the drilling fluid alone might not be able to hold back the flow of leachate during drilling operations, and the risk of an uncontrolled flowback situation had to be considered.

6 SOLUTIONS TO PRINCIPAL CHALLENGES

Two unique innovations were applied to the project in order to address the above issues and ensure a successful well installation.

6.1 Steerable knock-off bit assembly

To ensure that borehole collapse wouldn't interfere with well material placement and PVC could be used, a since patented steerable knock-off drill bit assembly was used.

The knock-off system uses a steerable, 12" nominal diameter detachable drill bit with 5" inside diameter drill pipe. The locating electronics have been moved from the conventional location behind the bit inside the drill pipe to a collar leaving the full inside diameter open.

Plastic well casing and screen can be pushed inside the smooth, machined interior of the drill pipe without the significant compressive forces incurred in an open borehole. Additionally, the steel drill pipe physically cases the borehole, eliminating concerns about borehole stability.

During well materials installation, the distal end of the well engages the knock-off bit's release mechanism, leaving the detachable bit in place as an anchor for the well, and the drill pipe (with locating collar) is removed leaving the well in place.



Figure 3. Steerable knock-off bit assembly.

6.2 Surface casing and wellhead controls

It was unknown what exactly would happen when the drill bit penetrated into the tailings. Obviously an uncontrolled flowback situation was completely untenable, so a physical engineering control was devised to give field crews a fail-safe way to close the borehole if necessary.

40 feet of 16" diameter surface casing was drilled and installed using angled auger boring methods. This conductor casing was cemented into place, and a removable flange fitting was installed at the surface. Once the cement had cured, the casing and flange assembly served as a kind of "blowout preventer". If uncontrolled flow conditions were encountered, the drill pipe could always be cut off, pushed into the casing and the flange closed.



Figure 4. Drilling through 16" diameter surface casing with removable flange

7 WELL DRILLING, INSTALLATION AND PERFORMANCE

Equipment mobilization and the initial drilling/installation of the surface casing was completed August 13, 2015. Because of the Gold King Mine release on the Animas river (August 5 2015), the EPA shut down all work on US mine sites for review and the project was delayed. Field work resumed on August 25 and was completed September 1.

As designed, 991 feet of schedule 80 PVC well materials (740 feet of screen) were installed at the target elevations.

A biodegradable drilling fluid was used to minimize the amount of development time needed. Well development consisted of flushing and high-velocity jetting of the well screen with fresh water and an enzyme solution specially formulated to break down the biopolymer.

After well development was complete, the well was gravity flowing at approximately 5gpm and the wellhead control valve was closed pending construction of the effluent treatment system.

In December of 2015 the bioreactor effluent treatment system was completed, and the dewatering well was allowed to flow. As of the most recent reporting period (March 2017), the system had treated approximately 1.48M gallons of effluent at an average flow rate of 2.22gpm, which is a higher flow than originally projected by the groundwater model.

Although the average flow rate has exceeded initial projections, water levels in the impoundment have not dropped as much as predicted by the model. Additional long-term data are likely needed to determine seasonality of groundwater levels.

8 CONCLUSION

This project demonstrated the viability of HDD methods for installing dewatering wells in tailings impoundments.

The approach kept the surface of the tailings completely clear of any wellhead infrastructure and provided a “passive” dewatering mechanism that requires no electricity to operate.

The patented steerable knock-off bit technology was instrumental in allowing for such a long, single-ended completion to be constructed with plastic well materials in a loose, unconsolidated formation such as mine tailings.

As always, site-specific conditions will ultimately dictate the best approach to tailings impoundment dewatering, but the Callahan Mine project suggests that installing drainage wells using HDD technology is worth considering.

REFERENCES

- Baker, P. & Peters, M. 2015. OU3 Final Remedial Design Basis of Design Report, Callahan Mine Superfund Site Brooksville Maine
- CIGB ICOLD. 2001. Bulletin 121 Tailings Dams, Risk of Dangerous Occurrences; Lessons learnt from practical experiences
- Crederre Associates LLP. 2017. March 8-9 2017 Performance Assessment Summary Report, Callahan Mine Superfund Site, Operable Unit 3 – TP-1 Performance Assessment Brooksville Maine
- Kaback, D. & Oakley, D. 1996. Horizontal Environmental Wells in the United States: A Catalogue. In Colorado Center for Environmental Management Report
- Lubrecht, M. et al. 2016. System and method for installing casing in a blind horizontal well. US Patent # 9,376,869

Operational Improvements through Installation of Seepage Cutoff Wall using Soil Mixing

I. Contreras and G.K. Bryant
Barr Engineering Co., Minneapolis, MN, USA

ABSTRACT: The Cross Delta Dike (CDD) at the Big Island Mine in Green River, Wyoming, was originally constructed by placing random fill over hydraulically deposited tailings and decahydrate (deca) deposits underlain by fractured bedrock. The 3500-foot-long dike was used as a haul route and to provide separation between the tailings disposal cell and reclaim water cell, improving reclaim water quality. Reclaim operations, which included removal and reprocessing of deca from the tailings disposal cells, are critical to facility operations. Development of safety and operational issues related to concentrated seepage as well as internal erosion and development of voids within the dike necessitated remedial action. These issues were expected to worsen, as future expansion would increase the head drop across the CDD. The authors performed a study and identified a seepage cutoff wall as the most appropriate option. Construction was performed using the Trench Remixing and Deep Wall (TRD) method. This paper describes the field investigation, laboratory testing, design, construction, and monitoring associated with the seepage cutoff wall. It also describes successful performance of the cutoff wall and benefits in terms of improved facility operations.

1 INTRODUCTION

Ciner (formerly OCI) owns and operates the Big Island Mine facility near Green River, Wyoming. Ciner mines trona at the site, and the ore extraction takes place underground while the processing plant and disposal facilities are located at the ground surface. The dams and earthen structures are used for storage, water retention, and evaporation.

An expected increase in production and operational issues with deca harvesting required seepage enhancement of the Cross Delta Dike (CDD). In addition, future construction would require upstream construction of the west side of the CDD which will impose additional loading on the CDD. As a result, a preliminary design for a seepage cutoff, consisting of heavy steel sheetpiling, was prepared in 2012 by Barr Engineering Co. (Barr). This option was considered feasible but required heavy steel sheets to penetrate hard deca layers. However, in 2014, further discussions identified the possibility of using soil-mix technology to build a seepage cutoff. A subsequent option study identified the Trench Remixing and Deep Wall (TRD) method as feasible and most appropriate to meet the project objectives. This paper describes the background, design process, construction, and monitoring of the seepage cutoff wall at the CDD.

2 BACKGROUND

The CDD is an earthen structure, approximately 3500 feet in length, which separates the Upper Delta tailings disposal basin from Pond 1, as shown in Figure 1. In general, water is stored for

evaporation in Pond 1, whereas the tailings delta is used for tailings storage. The dike was originally constructed to provide separation between the tailings disposal area and Pond 1 to filter the water before it enters Pond 1. This provides higher quality water in the Pond 1 basin. More recently, the CDD has also been used as a barrier to minimize pumping while transferring water up to Pond 4 and as a haul road during the deca harvest. The CDD was constructed directly on top of previously deposited tailings and deca deposits.



Figure 1. Cross Delta Dike Location

Water from the Upper Delta seeps through the CDD during dewatering of Pond 1. The differential head generated across the CDD (between the Upper Delta and Pond 1) promoted internal erosion of the tailings and uncontrolled dike fill. Furthermore, the dike subsurface included deposits of deca which are susceptible to dissolution. As a result, sinkholes and surface depressions were an issue, impacting the use of the CDD as a haul road and causing concern about overall CDD safety. Figure 2 illustrates a picture of the typical development of sinkholes at the CDD.



Figure 2. Sinkhole Developed on Cross Delta Dike

Operational issues related to seepage, piping development, voids, deca harvest, and dike stability during future upstream construction required attention to maintain safe operation and efficient deca harvesting. Construction of the seepage cutoff wall was necessary to address these issues and facilitate long-term operation and performance of the dike.

3 DESIGN

3.1 *Design objectives*

The objectives of the seepage cutoff wall project include the following:

- Create a barrier able to control/prevent piping and voids in the dike
- Provide a solution that allows use of a safer road
- Minimize seepage to improve the Pond 1 dewatering process
- Help preserve the quality of the deca harvested at Pond 1
- Promote movement of water from higher elevations into Pond 1
- Improve the overall stability of the Upper Delta

It was decided to develop the design of a low-permeability barrier including an area to temporarily store water upstream of the CDD to transfer the water to Pond 1. The concept involves building a soil-mix wall and inserting an intermediate barrier within the trench while the material is still fresh. Using this concept, the water upstream of the CDD is transferred to Pond 1 using a decant structure.

3.2 *Design issues*

The overall approach for design of the proposed wall involves creating a barrier (i.e. cutoff wall) with low permeability and adequate strength so that it can meet the project objectives while providing long-term durability. Many of these issues revolve around a proper mix design so that a robust wall can be built. During wall construction, while the mix is still fresh, the design should allow for the insertion of a secondary barrier within the soil mix. In this way, the final product would be sufficiently robust so that if the wall cracks or fails there is a second line of defense against seepage and piping. Additionally, the wall should be designed to withstand any potential

deformation resulting from the development of voids or deca dissolution. A review of the proposed cutoff construction identified the design/construction issues briefly discussed below:

- Permeability. The proposed wall should have low permeability to help control the seepage across the cutoff wall.
- Strength. The soil mix of the wall should be designed such that the wall is strong enough to provide adequate support for lateral pressure. Similarly, the composited section should be able to withstand any deformation and stresses resulting from the development of voids or ground loss resulting from deca dissolution.
- Set Time. Since the wall involves the insertion of a barrier while the soil mix is still fresh (i.e. vinyl sheet pile), the soil mix should have a set time long enough to allow this operation in the field.
- Durability. The soil mix should be designed to provide long-term wall durability.
- Presence of Deca in Mix. It is known that deca will be encountered during construction of the wall and deca will be part of the soil mix (soilcrete). However, the amount or proportion of deca is not constant along the wall alignment. Preliminary laboratory testing showed that deca has a major impact on the set time and strength.
- Depth of Wall. The depth of the wall is an important design feature; the previous design concept included placement of steel sheet piles driven down to refusal at bedrock level.
- Stability of Upper Delta. In the future, the south perimeter dike will be located in the Upper Delta. As a result, deformation of the cutoff wall induced by dike construction needs evaluation.

4 FIELD INVESTIGATIONS AND SUBSURFACE CONDITIONS

Several field investigations were conducted as a part of the CDD seepage cutoff wall project. The field investigations consisted of soil borings, CPT soundings, a geophysical seismic refraction survey along the entire dike alignment, and bulk sampling of the tailings and deca. These investigations were completed to gather subsurface information for design and construction. In addition, a laboratory testing program was developed. The main objective of the laboratory testing program was to explore how various mix designs would react with the presence of deca throughout the CDD, as well as to determine a baseline for soil-mix performance in terms of permeability, strength, set time, and durability.

In general, the field investigations identified stiff, sandy lean clay (fill) overlying a saturated mixture of lean clay (tailings) and deca. The deca was primarily observed as numerous inclusions or lenses, but in some cases the deca was well formed as a crystallized hard layer. The deca and tailings were underlain by native soils consisting of sandy lean clay, lean clay, and fat clay. Weathered mudstone bedrock was encountered at depth in all borings.

The seismic survey was used to delineate the depth of the native soils and bedrock at the foundation of the CDD. The seismic survey was also intended to identify zones of concentrated deca within the dike profile. The geophysical survey was completed using the Multi-Channel Analysis of Surface Waves (MASW) technique to acquire shear wave data.

5 ANALYSIS

The analyses conducted as part of the project evaluated seepage, slope stability, structural performance of the wall, and deformation. The parameters for the different materials included in the model were selected based on the results of the field investigation and laboratory testing.

Potential future conditions for the Upper Delta and Pond 1 were incorporated into the analyses. The plan for ultimate configuration of the South Interior Dike includes raising dam crests to an approximate elevation of 6290 feet using an upstream offset of approximately 105 feet between the South Interior Dike and the CDD. After simulating the initial conditions, the construction of the ultimate South Interior Dike configuration was modeled, including the filling of tailings. The simulations also included excavation of deca in Pond 1 down to an elevation of 6220 feet and dewatering to as low as 6217 feet.

A brief description of the seepage, deformation, stability, and structural analyses are discussed below.

5.1 Seepage Analysis

The main objective of the seepage analysis was to develop an understanding of the flow of water through the CDD and the proposed cutoff wall and how it relates to stability of the dike and wall. Special emphasis was placed on evaluating the parameters to model the most relevant hydrogeologic materials. Subsequently, simulations were made to predict the phreatic and pore-water pressure conditions under future scenarios.

A steady-state seepage analysis was performed for the CDD (Station 12+00) based on the planned cutoff wall. The analysis also incorporated the proposed future configuration of the Upper Delta to an ultimate crest elevation of 6290 feet. The seepage analysis is an important aspect of the modeling process because the model calculates seepage forces within the cutoff wall cross section. The model also determines a phreatic surface and allows for the prediction of pore-water pressures within the dike and at the wall; this helps in the wall and dike design. The seepage model was initially run for existing conditions with the cutoff wall and for future conditions in the Upper Delta to evaluate seepage gradients across the dike. Steady-state seepage simulations indicate a head differential of approximately 12 feet across the cutoff wall after completion (elevation of 6245 feet on the Upper Delta side of the wall and 6233 feet on the Pond 1 side).

5.2 Deformation Analysis

The main objective of the deformation analysis was to develop an understanding of the deformation, pore-water pressures, and stresses that will be generated on the dike and proposed wall due to hydraulic head differences and as a result of construction of the upstream dams on the Upper Delta. Special emphasis was made in the evaluation (estimation of parameters and boundary conditions) to model the most relevant materials while matching the model results to observed field performance. Coupled seepage-deformation models were created using the finite element method with GeoStudio software (SEEP/W and SIGMA/W).

Deformation analyses were conducted on a representative cross section (Station 12+00). The initial conditions were established by stepping the existing conditions model to equilibrium and incorporating the results of the seepage analysis under steady-state conditions. This initial state of the model reflects gravity loading based on seepage and displacement boundary conditions.

After simulating the initial conditions, the construction of the ultimate South Interior Dike configuration was modeled, including the filling of tailings. The resulting deformation, pore-water pressures, and stresses at select points within the cutoff wall were monitored during the staged modeling.

The ultimate proposed configuration of the South Interior Dike was modeled to predict the behavior of the stresses induced on the CDD cutoff wall. The behavior of the cutoff wall in response to the offset upstream dam construction was evaluated in terms of stresses, deformation, and pore-water pressures.

The results of the deformation analysis for CDD are interpreted in terms of the pore-water pressure, effective stress, and deformation. Based on the analysis and assumed conditions presented in Barr (2014), the total lateral deformation of the cutoff wall due to upstream dam construction is less than 0.5 inches. This deformation is sufficiently small to indicate that the wall should not be damaged or significantly altered by future development of the Upper Delta.

5.3 Stability Analysis

The main objective of the slope-stability analysis was to evaluate the safety of the dike and wall under different operating scenarios and construction, as well as long-term conditions. Special emphasis was placed on evaluating the impact of the groundwater flow on stability. The stability was also evaluated in relationship to the design issues previously identified.

The slope-stability analyses for the CDD and wall were performed using the same cross section as the seepage and deformation analyses. The configuration of the downstream slope of the CDD (Pond 1 side) was analyzed using a 3H:1V slope extending to the bottom of Pond 1. Analyses

were performed under different conditions utilizing undrained and drained soil parameters for stability.

Models were run to analyze a circular failure surface, as well as a wedge failure. To run a wedge analysis, stronger underlying layers were modeled as impenetrable (or “bedrock”). This forces the failure surface to truncate along the stronger layer and models the movement along the interface between the two layers. The wedge models analyzed the potential for fill and weaker native soils to move; therefore, the bedrock was set to impenetrable.

Slope-stability analyses were conducted for drained and undrained shear strength soil conditions. The drained condition generally applies to long-term, steady-state flow conditions. No excess pore-water pressure exists and, in many cases, the drained condition represents the most stable condition for dam construction. The undrained condition generally applies to short-term conditions, for example during or immediately after construction, where the soil mass and groundwater have not had time to come to equilibrium. As such, there is some strength reduction in those soils that are not permeable enough to freely drain as excess pore-water pressures will develop within those saturated soil masses (undrained response).

Slope-stability calculations of the CDD were completed using Undrained Strength Stability Analysis (USSA) and Effective Stress Stability Analysis (ESSA). The minimum recommended factor of safety for the ESSA is 1.5. The minimum recommended factor of safety for the USSA is 1.3.

All computed factor-of-safety values for USSA and ESSA conditions for CDD are greater than the recommended minimum values of 1.3 and 1.5. The results indicate that future offset upstream dam construction, cutoff wall construction, and the associated changes to the loading and pore-water pressures do not result in dike instability.

5.4 Structural Analysis

The main objective of the structural analysis was to evaluate the integrity and safety of the wall under different operating scenarios and construction conditions, as well as long-term conditions. Special emphasis was placed on evaluating the impact of the groundwater flow, soil stresses, and dissolution of deca layers on the structural stability of the wall. The stability was also evaluated in relationship to the design issues previously identified.

The structural analyses for the wall were performed under potential conditions of deca dissolution. Data from the laboratory testing on mixes was used in the analysis.

The sheet pile analysis assumed that 40-foot-long sheets would be installed at the top of the existing CDD (elevation 6252 feet) and extend approximately 2 feet into the native clay. Water elevation was assumed to be 6245 feet on the Upper Delta side of the wall and 6223 feet on the Pond 1 side.

Two different sheet pile models were made to check the loading on the sheet pile. The first model assumed 4 feet of settlement caused by deca dissolution on the CDD on the Pond 1 side. This would create a nominal 4-foot cantilever at the top of the 40-foot-deep wall in addition to the water pressure.

The second model assumed that a 12-foot void was created in the deca layer from an elevation of 6229 to 6217 on the Pond 1 side of the wall. The sheet pile flexural loading was checked assuming both a simple beam and fixed-end beam over the 12-foot span.

6 PLANS AND SPECIFICATIONS

A complete set of plans and specifications was developed for bidding and construction. The main design features of the cutoff wall included the following:

- The required maximum permeability of the cutoff wall was 1.0×10^{-6} cm/s.
- The unconfined compressive strength was established as 40 psi for a 10-point average with a single test minimum of 30 psi.
- The width of the cutoff wall was at least 18 inches.
- A secondary seepage barrier, consisting of vinyl sheet SG-325, was incorporated into the design. The set time of the mix was set to at least 18 hours to allow for vinyl sheet insertion.

- The cutoff wall was 3550 feet in length with variable depth but inserted into native soils at least 2 feet deep.
- Specifications included provisions for the process of demonstrating mixing, joint construction, and secondary barrier (i.e. vinyl) installation. Therefore, a test section prior to the beginning of cutoff wall installation was specified to provide the contractor with an opportunity to evaluate construction.

The plans and specifications were part of the bidding package. The TRD construction method was selected because it allowed for penetration through deca layers, adequate mixing, and installation of a secondary barrier.

7 CONSTRUCTION

The CDD seepage cutoff wall consists of a primary and secondary seepage barrier. The primary seepage barrier was the soil-mix wall and the secondary was vinyl sheet pile. The following describes the construction methods and equipment used for both of them.

7.1 Primary Cutoff - TRD

The primary seepage cutoff consisted of an approximately 21.6-inch-wide homogeneous soil mix wall. The barrier was installed using the TRD method. This involved cutting a vertical trench through the CDD to the design depth through the tailings and native materials while continuously adding fresh grout. The resulting soil mix (also referred to as soilcrete) formed the cutoff wall. The mixing process included vertically cycling back the excavated material that became incorporated in the soilcrete. The engineered fresh grout was prepared in an automated batch plant and pumped through the TRD to the bottom of the TRD cutter post (bottom of wall).

The primary seepage cutoff equipment consisted of a TRD (model TRD25-KM) mounted on a Kobelco 7055-2 crawler base. The TRD cutter post was installed in sections at a design depth below the ground surface, cutting a trench by rotating a chain with steel cutting teeth propagating outward—similar to a chainsaw. The intent of this method is to cut and mix subsurface materials and grout to form a homogeneous wall with no discontinuities. At locations where the design depth increased or decreased, cutter post sections were added or removed. Figure 3 shows a diagram and a photo of the TRD used at the CDD.

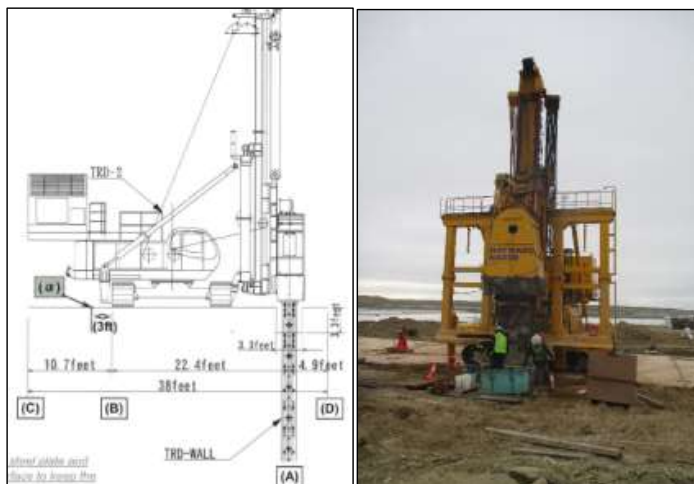


Figure 3. TRD Machine

The TRD was equipped with a Micro Motion grout monitoring system, which constantly monitored properties of the freshly mixed grout as it was delivered to the TRD from the batch plant. Properties measured include specific gravity of the grout, temperature of the grout, flow rate to the cutter post injection ports, and total volume of fluid passing through the monitoring equipment. This information was observed in real-time by the TRD operator.

7.2 Secondary Cutoff- Vinyl

The secondary seepage cutoff was constructed using vinyl sheet piling. This secondary barrier was inserted within the primary seepage cutoff and included interlocking connections, allowing for continuity of the secondary seepage cutoff. The vinyl sheet pile was installed before setting of the cementitious soil mix to achieve proper installation and contact between the two seepage cutoff elements.

The contractor used an ABI Mobilram system (model TM14/17 SL) to operate the pile hammer and mandrel. The mandrel setup was designed to support various lengths of sheet pile up to 50 feet. The ABI was mounted on tracks and progressed closely behind the TRD. The vinyl sheets were attached to the mandrel, interlocked to the preceding sheet, and then driven to depth. The mandrel was withdrawn when the vinyl sheet pile encountered the bottom of the trench, leaving the installed piling in place. The mandrel was manufactured by Crane Materials International (CMI). Figure 4 and Figure 5 show a diagram and a photo of the ABI machine and mandrel used by the contractor at the CDD seepage cutoff.



Figure 4. ABI Pile Driver



Figure 5. Mandrel

8 MONITORING

Monitoring instrumentation was installed along the alignment to track the impact of the new seepage cutoff. In the spring of 2015 (prior to cutoff wall construction), vibrating wire (VW) piezometers were installed at three locations upstream of the cutoff wall alignment at approximately Stations 11+46, 18+69, and 23+31. Once cutoff construction was complete (in July 2015), VW piezometers were installed downstream of the wall at similar stationing along the alignment (one at Station 11+46, two at Station 18+69, and one at Station 23+31). The combined upstream and downstream instrumentation provides data to monitor head differential across the dike and seepage cutoff. All piezometers installed featured nested sensors at various elevations to measure pore pressure in the tailings and the underlying fractured bedrock. In addition, one in-place inclinometer (IPI) was installed at Station 18+69 to monitor displacement post construction. The monitoring instrumentation layout is shown in Figure 6.

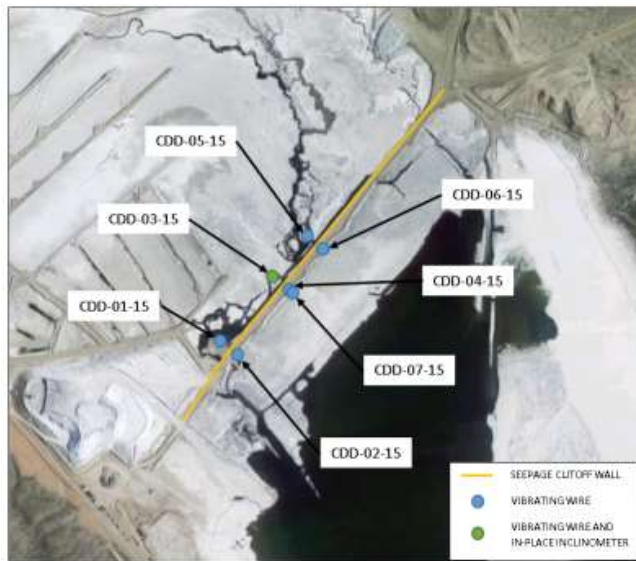


Figure 6. Cross Delta Dike Monitoring Instrumentation Layout

Figure 7 depicts a general cross-sectional layout of the VW piezometers installed along the seepage cutoff wall to monitor the performance of the wall.

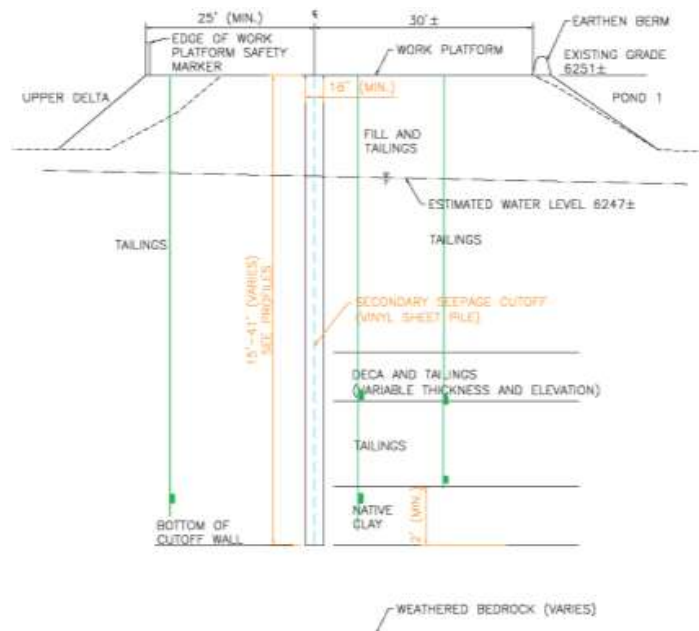


Figure 7. Typical Nested Vibrating Wire (VW) Piezometers at Cross Delta Dike Site (Not to Scale)

8.1 Performance Monitoring

The VW piezometers, installed in 2015 on either side of the seepage cutoff wall at Stations 11+46, 18+69, and 23+31, indicated a successful seepage cutoff at the CDD. The nested VW piezometers were installed specifically to evaluate the pore pressures and head differentials in specific layers. Figures 8 and 9 show the decrease in the total head downstream of the cutoff wall.

It can be seen from Figures 8 and 9 that the total head upstream of the wall construction remains fairly constant at about elevation 6247 to 6248 in piezometers 01A and 05A. After the installation of the cutoff wall, the total head in piezometers 2A/B and 6A/B (located downstream of the wall) started to decrease. By December 2015, the differential head across the wall was approximately 8 to 10 feet. Figures 8 shows the decrease of the total head downstream of the cutoff wall during two dewatering cycles of Pond 1 in 2016 and 2017. Based on these results, the seepage cutoff is performing as designed and intended.

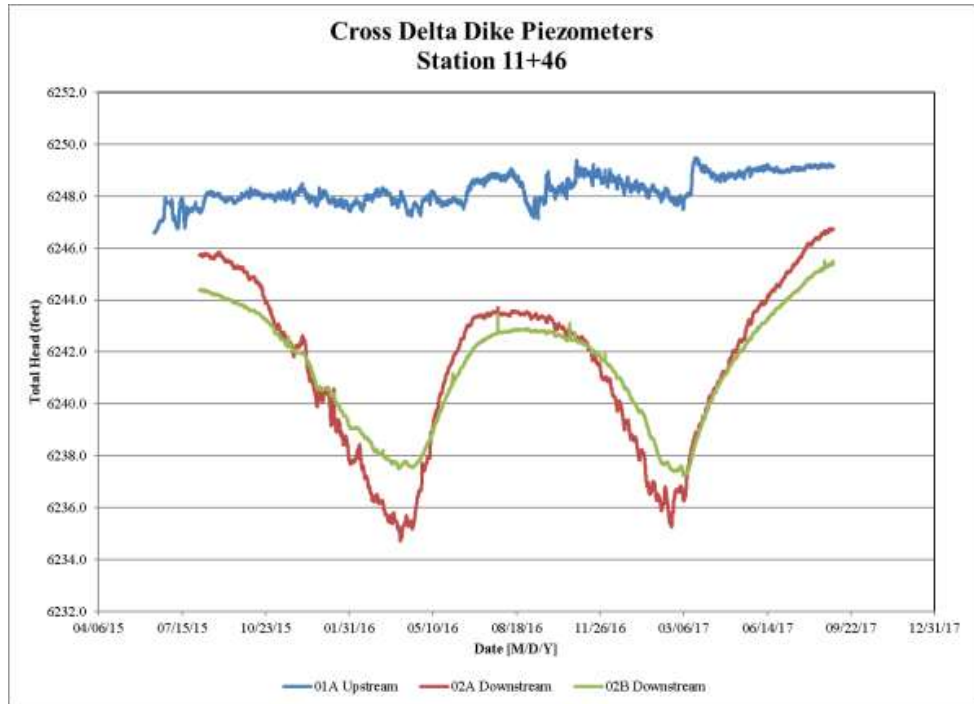


Figure 8. Total Head at Station 11+46

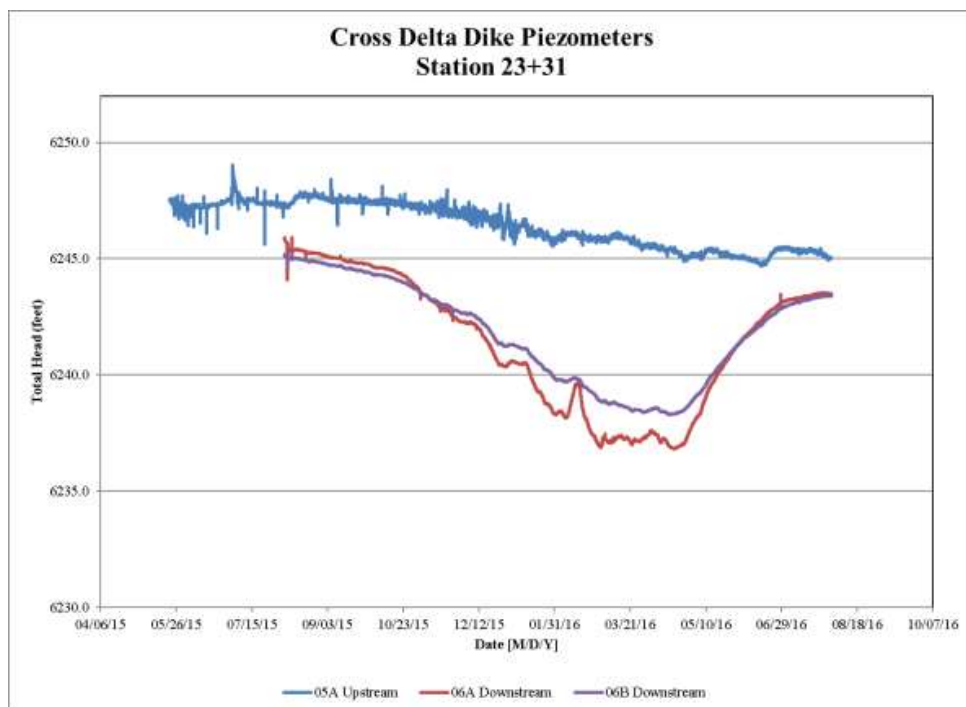


Figure 9. Total Head at Station 23+31

9 CONCLUSIONS

This paper presented the background, design process, construction, and monitoring of the seepage cutoff wall at the CDD. The objectives of the cutoff wall were to create a seepage barrier able to control and prevent piping, provide a safer road, and minimize seepage to improve Pond 1 dewatering while helping preserve the quality of the deca harvested at Pond 1. Finally, the barrier was intended to improve the overall stability of the upper dike.

The performance of the cutoff wall with more than three years of construction and deca harvesting campaigns has demonstrated that the objectives have been achieved. The monitoring dam further verifies the satisfactory performance of the cutoff wall.

10 REFERENCES

- Barr Engineering Co. 2012. "Sheetpile wall for Cross Delta Dike"
- Barr Engineering Co. 2014. "Cross Delta Dike Cutoff wall Design Report." October 2014.

Optimizing Tailings Deposition and Water Management for a Mine in Ontario, Canada

R. Couto and P. Merry

Golder Associates Ltd., Mississauga, ON, Canada

ABSTRACT: A mine in Ontario produces tailings that reports both as a slurry into a surface tailings impoundment area (TIA) and as cemented paste backfill into stopes underground. The TIA operates as a “zero-discharge” facility, retaining tailings and water via a series of zoned earthfill dams. Tailings are deposited along a non-water retaining dam, which relies on a minimum tailings beach development for seepage control. Excess pond water has developed over time, periodically inhibiting adequate beach development. Inflow sources include process water, underground mine dewatering, in addition to runoff from precipitation. To address this issue, water balance modelling combined with sensitivity analyses were conducted to determine the best “levers” to reduce the amount of water in the TIA. Variables included the water treatment rate, mine dewatering rate, percent tailings to surface versus underground, mill throughput rate and precipitation conditions. Pond accumulation results were correlated with the rate of rise in the TIA to identify which scenario(s) met the minimum beach development requirements. Results indicated that a reduction of water pumped to the TIA with additional site-wide water treatment capacity most influenced pond volume accumulation and ability to maintain tailings beach length.

1 INTRODUCTION

An underground and open pit mine in Ontario, Canada, processes ore at a rate that ranges between 7,000 and 8,000 tonnes per day. As of 2018, the projected mine life is until the year 2037, with a total production (since mine inception) of about 65 Mt of ore.

The elevation of the project site is about 350 m above sea level (masl) and is located on a raised plateau within an area of rugged hummocky terrain and modest to significant topographic relief. Elevation changes that range from 20 m to 50 m are common. Rock cliffs up to 30 m in height are present and the area is forested with numerous lakes and streams.

The mine produces tailings that report both as a slurry (44% solids) on surface into a conventional tailings impoundment area (TIA) and as cemented paste backfill (77% solids and 2 to 3% cement by mass) used to fill mined out stopes underground. The typical breakdown of tailings solids reporting to surface relative to the underground is about 60% to 40%. The TIA has historically operated as a “zero-discharge” facility and retains tailings and water via a series of zoned earthfill dams, raised in stages as storage requirements dictate, with the primary water retaining dam (Dam 1) lined with an HDPE geomembrane and raised by the downstream method of construction. Tailings are primarily deposited along a non-water retaining dam (Dam 2), which relies on a minimum tailings beach development for seepage control. Figure 1 provides a general schematic layout of the TIA. The slope of the tailings beach typically ranges from 0.8% to 1% based on data obtained from annual tailings beach and bathymetric surveys.

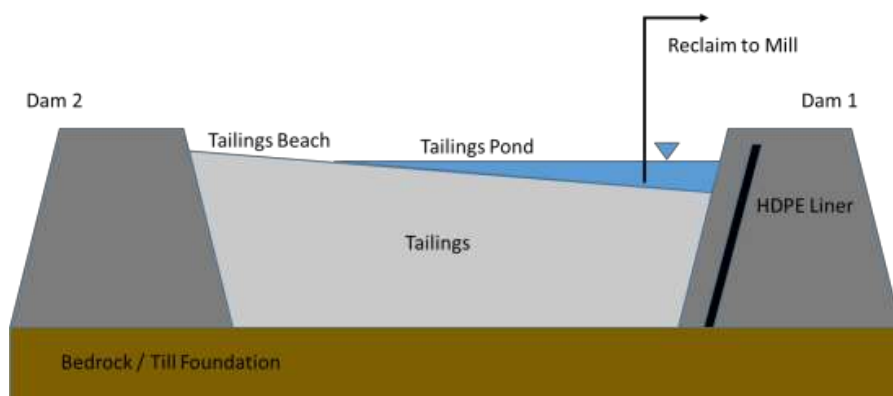


Figure 1. Schematic cross-section of the TIA

Excess tailings pond water has developed over time in the TIA, at an average annual rate of 200,000 m³ to 250,000 m³, at times inhibiting adequate beach development along Dam 2. Water inflow sources have included process water associated with the production of the slurry and paste tailings and water from underground mine dewatering, in addition to contributions from runoff due to precipitation. To address this issue, water balance modelling combined with sensitivity analyses were conducted to determine the best “levers” the site had at its disposal to reduce the amount of water in the tailings area while maintaining the minimum beach development requirements for Dam 2. To achieve this, estimated pond volume accumulation results were cross-referenced with the expected rate of rise of the tailings in the TIA and tailings deposition modelling was conducted to determine which scenario(s) met the minimum beach development requirements.

The remainder of this paper describes the general operation of the TIA, the design criteria and methodologies adopted for the water balance modelling and sensitivity analyses, and the results associated with those analyses. Deposition modelling results are generally discussed, though not shown due to confidentiality agreements.

2 DESCRIPTION OF TAILINGS FACILITY

The main components of the TIA consist of the following:

- Three (3) main dams (Dams 1, 2, and 3);
- An emergency spillway on Dam 1;
- A small saddle dam;
- A northern watershed diversion channel;
- A reclaim pump barge located upstream of Dam 1; and
- Seepage collection systems along the downstream toe of Dams 1 to 3.

The first stage of the TIA was completed in 2011 (Stage 1A), with the construction of the Dam 1 and Dam 2 starter dams. Subsequent raising of the dams have occurred in five additional stages between 2012 and 2018, to reach its ultimate dam crest elevation of 365 masl. Dams 1 and 2 are essentially designed as rock fill dams with an impervious upstream barrier. The impervious barrier for Dam 2 is a 60 mil HDPE liner on the starter dam only (Stage 1A) to an elevation of 338 masl. In subsequent construction stages the deposited tailings on the upstream face of Dam 2 acts as the seepage barrier. A 60 mil HDPE liner is provided for the entire up-

stream face of the Dams 1 and 3, which currently retain the water pond. The liner is connected to bedrock via a concrete plinth. The dams are founded on either competent overburden material such as till or bedrock. Dam 3 was initially constructed during the 2015 Stage 2B raise, and subsequently raised and extended to connect with Dam 2 in 2016. Containment to the south is provided by natural ground and a new water retaining saddle dam, constructed in 2018. The water that collects in the pond is removed with a pump barge located upstream of Dam 1. It can be recycled to the mill, or pumped to the mine water pond at the mill site. The emergency spillway is located on Dam 1 and is sized to convey the Inflow Design Flood (IDF), corresponding to the Probable Maximum Precipitation (PMP) event of 432 mm in 24 hrs.

3 SITE WATER MANAGEMENT

Figure 2 provides the general site water management strategy and flow logic on site. The TIA receives tailings and process water from the process plant as well as tailings overflow water from the paste backfill plant. TIA pond water is reclaimed back to the process plant to meet processing requirements. Fresh-water is pulled from a local river to the process plant for use in the acid wash circuit, reagent mixing, CIL compressors and lube skid cooling.

Underground mine water is pumped from the portal ramp and underground mine Sumps 1 and 2. Mine water pumped from the portal ramp and Sump 1 consists of clean contact water that infiltrates through the open pit and is pumped to the mine water pond for settling of solids prior to discharge to the environment. As of late 2016, mine water from Sump 2 is pumped to a moving bed biofilm reactor (MBBR) water treatment system (located in the paste plant) to treat for ammonia prior to discharge to the mine water pond. Any excess water from Sump 2 that can not be treated is pumped to TIA. Previous to the commissioning of the MBBR system, all contaminated underground mine water was pumped and stored in the TIA.

Run-off from the waste rock stockpile is considered to be clean contact water and is discharged directly to the environment.

The site currently plans to pump and treat water from their historical open pit, to gain access to mineralization beneath the pit, via a proposed submerged attached growth reactor (SAGR) treatment system which will be installed within the mine water pond during the spring of 2018. The SAGR system consists of biologically flooded rock media which will treat for ammonia through nitrification, and will be front ended by a system for the treatment of copper. Once the historical open pit has been dewatered, the plan is to then begin treatment of tailings pond water to reduce to the stress that the pond poses on the development of the tailings beach.

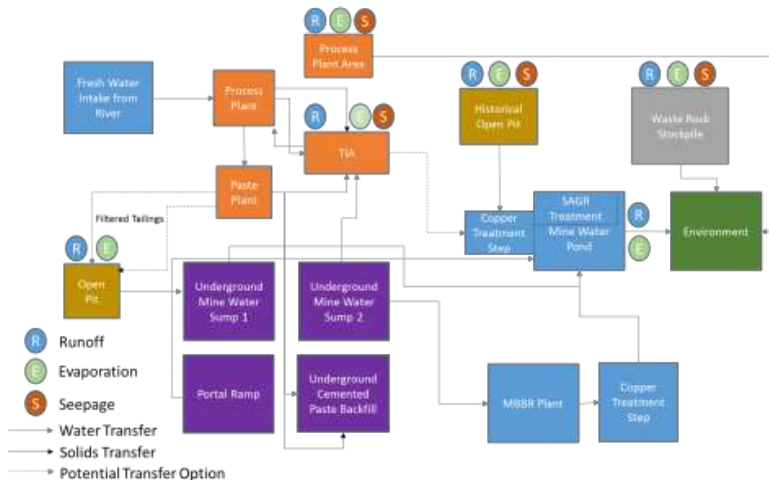


Figure 2. Site flow logic diagram

4 WATER BALANCE OPERATING DATA AND DESIGN CRITERIA

Table 1 below lists the operating data used in the water balance for TIA. Pertinent design criteria for the TIA, as it pertains to the water balance includes the ability to retain the Environmental Design Flood (EDF) at all times during operations, which corresponds to the 1:100 yr – 30-day spring run-off event (about 300,000 m³), and to maintain a minimum elevation difference of 0.8 m between the elevation of the tailings beach at the Dam 2 upstream toe and the tailings pond to prevent excessive dam seepage.

Temperature and precipitation data was obtained from a regional climate station (1950 to 2006 data). The mean evaporation data was also obtained from a separate regional climate station (1968 to 1993 data). Tables 2 and 3 provide the climate and storm return period data used in the water balance.

Table 1. Water balance operating data

Parameter	Base value used in water balance
Production rate	7500 tonnes / day
Mill availability	94%
Tailings to ore ratio	1.0
Percent tailings to TIA	60%
Percent tailings to underground backfill	40%
Slurry density of tailings prior to thickening (i.e. deposited to TIA)	44%
Slurry density of paste tailings to underground backfill	77%
Deposited void ratio of tailings on surface	1.10
Deposited void ratio of tailings to underground as backfill	0.65
Moisture content of the ore entering the mill	2.0%
Clean (fresh) make-up water from external source required in the mill	41 m ³ /hr (984 m ³ /day)
Percentage of the fresh water that reports to the TIA	50%
Water lost in the mill to evaporation and spillage – expressed as a percentage of total flow through the mill.	2%
Mine dewatering rate from Sump 2 (reporting to MBBR for treatment with any excess reporting to TIA)	1625 m ³ /day
Mine dewatering rate from Sump 1 to mine water pond	580 m ³ /day
Mine dewatering from Portal Ramp to mine water pond	30 m ³ /day
Mine water pond discharge	2000 m ³ /day
Treatment rate capacity (MBBR)	1500 m ³ /day

Table 2. Mean temperature, precipitation, and evaporation data

Month	Mean temperature (degrees Celsius)	Mean precipitation (mm)	Mean evaporation (mm)	
			Pan	Measured lake
January	-16.9	60.2	0.0	0.0
February	-14.5	47.5	0.0	0.0
March	-7.8	55.0	0.0	0.0
April	1.6	50.2	21.9	15.3
May	9.6	68.4	140.1	98.1
June	15.2	88.0	172.6	120.8
July	17.7	85.4	181.4	127.0
August	16.2	89.3	143.0	100.1
September	11.2	92.5	84.1	58.9
October	5.0	72.1	24.7	17.3
November	-3.0	67.5	0.0	0.0
December	-12.5	63.7	0.0	0.0
Annual	1.8	840.7	767.9	537.5

Table 3. Return period data for storm events

Annual return period (years)	Precipitation (mm)	Duration (hours)	30-day rain on snowmelt depth (mm)
2	43.8	24	232.7
5	63.1	24	290.4
10	75.9	24	328.7
25	92.1	24	377
50	104.1	24	412.8
100	116.0	24	448.4
1000	155.5	24	
Timmins storm	193.0	12	
PMP	431.9	24	

Source: AES 24-hr rainfall Intensity-Duration-Frequency values are from Environment Canada Timmins A Ontario Station (1955-2003). 30-day rain on snowmelt depth values are from Environment Canada Kirkland Lake, Ontario Station (data 1950 – 2006).

5 WATER BALANCE MODELLING

A deterministic water balance model for the site was developed using a series of linked excel spreadsheets in an attempt to capture all pertinent inflows and outflows to the site, with particular emphasis on determining the annual pond accumulation in the TIA under various input scenarios. The following sections describe the water balance methodology and setup.

5.1 Methodology and Model Setup

The general methodology undertaken in this study was to vary a total of four input variables, one at a time, to determine which would have the greatest affect on annual pond accumulations in the TIA under average precipitation and evaporation conditions, as well as the 1:100 year wet and 1:100 year dry years. The four input variables were the water treatment rate, the percentage of tailings solids reporting to underground backfill, the mine dewatering rate, and mill throughput rate. Each variable was assigned a base value based on average values of the data collected on site during the 2017 year to establish the “zero” point for the sensitivity analyses. For each subsequent model run, the base values were adjusted by a certain percentage based on a reasonably expected range determined by discussion and collaboration with on site staff. Note that the water treatment rate considered treatment of underground mine water only, as the SAGR system had not been commissioned at the time of this study. Table 4 provides the base value used for each variable and the range for which the each value was adjusted.

Table 4. Input data varied during water balance modelling

Variable	Unit	Base value	Modelled range
Water treatment rate (MBBR)	m ³ /day	1500	750 – 2000
Mine dewatering rate	m ³ /day	1625	1200 - 2000
Tailings to underground backfill	% (total)	40	20 - 60
Mill processing rate	tonnes/day	7500	7000 - 8000

5.2 Sensitivity Analysis Results – Annual Pond Accumulation

Figure 3 provides the results of the sensitivity analyses for each of the input variables expressed as a percent change relative to the base value under average precipitation and evaporation conditions. For reference the sensitivity analyses for treatment rate are provided for the 1:100 yr wet and 1:100 yr dry scenarios to provide a sense of the expected range of pond accumulation / deficit that the mine could expect in any given year. A point is also provided for the original

“do nothing” scenario in which the water treatment rate is set to 0 and all other base values are kept the same. In this case, the “do nothing” scenario would result in an annual pond accumulation of about 200,000 m³.

The water balance results typically indicate annual pond reductions based on the expected range of the input variables and show that the mine dewatering rate and the mine production rate have the greatest unit effect on the annual pond accumulation (steepest slope). However, these are factors that the mine has limited control over as the mine dewatering rate is dictated by groundwater conditions and the mine production rate is not expected to vary widely. The treatment rate, however, is a variable for which the mine has a greater amount of control, for which they can maximize the flow rate by controlling the incoming temperature and pH of the incoming feed.

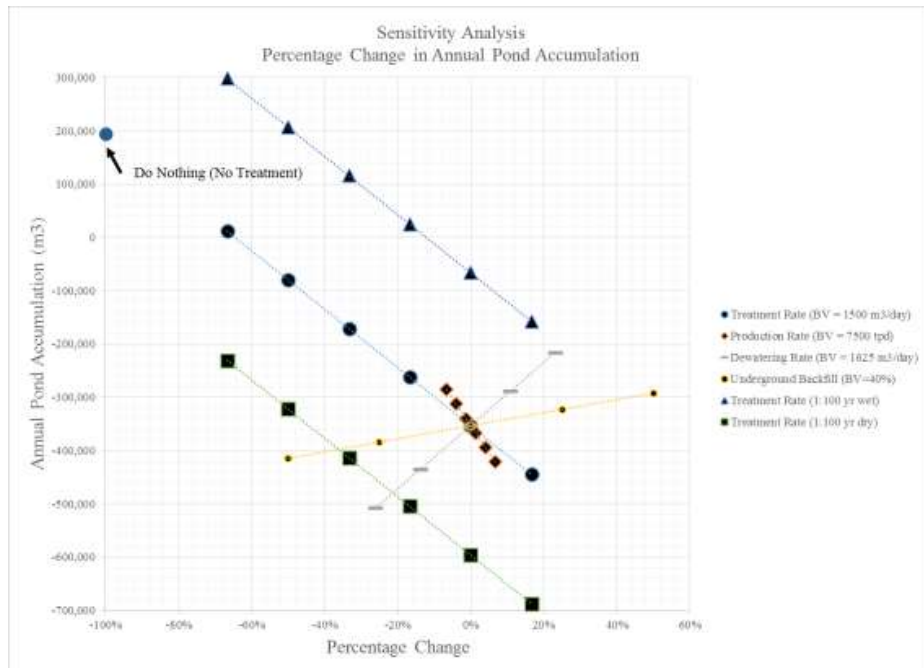


Figure 3. Sensitivity analysis results for annual pond accumulation in the TIA

6 RATE OF RISE AND REMAINING OPERATING LIFE OF THE TIA

The pond accumulation results shown in Figure 3 were then combined with the expected tailings volume deposited on surface for each scenario and correlated with the struck level capacity curve to determine the monthly and annual rate of rise for the TIA. Figure 4 provides a plot of the monthly rate of rise versus percent change for each scenario, while Figure 5 plots the annual rate of the rise of the tailings beach (at the upstream toe of Dam 2) and pond level against the struck level capacity curve for the TIA under average precipitation conditions taking into account base value scenario outlined in Table 4.

When considering the rate of rise for the TIA, which combines both the amount of water and the tailings reporting to the TIA, the factor which influences the rate of rise the most is the percent of tailings that report to surface versus underground backfill, which differs from the results shown on Figure 3 when only considering annual pond volume accumulations. However, reducing the amount of tailings reporting to surface can not necessarily be considered as the best “lever” to reduce pond volumes while also maintaining minimum beach level requirements, as a

certain amount of dry tailings solids is required annually to maintain the elevation difference between the tailings beach and the pond. Deposition modelling has shown that it may become difficult to maintain an adequate tailings beach if the percent of tailings reporting to surface decreases below 50% as the contribution of water from paste plant overflow to the rate of rise becomes greater than that of the accumulation of tailings solids.

The treatment rate and mine dewatering rates show similar, though inversely proportional, slopes. As mentioned in Section 5, the mine may have limited control over underground dewatering, therefore indicating that providing additional treatment rate capacity is the best way to control the rate of rise in the TIA, while reducing overall pond volume.

The analysis shown on Figure 5 attempts to determine the storage capacity timeline for the TIA, given the expected treatment rate beholden to a series of constraints as follows:

- The tailings pond should be maintained at a minimum volume of 500,000 m³ in order to meet reclaim (pond depth for pumping) and winter storage requirements;
- The maximum allowable water level for the TIA is 362.5 m in order to allow containment of the EDF; and
- The maximum tailings deposition elevation was set at 364 m.

Figure 5 implicitly assumes an “active” treatment phase from 2018 to about the end of 2020 that would reduce the total pond volume from 1.6 M-m³ down to 500,000 m³. From thereon after, the treatment rate would be re-calibrated to keep the tailings pond volume balance. The results indicate that under average precipitation conditions and an average annual rate of rise of 2.13 m, the TIA would have storage capacity for tailings to about the end of 2021 when the pond reaches an elevation of 362.5 m. These results were verified with 3D deposition models.

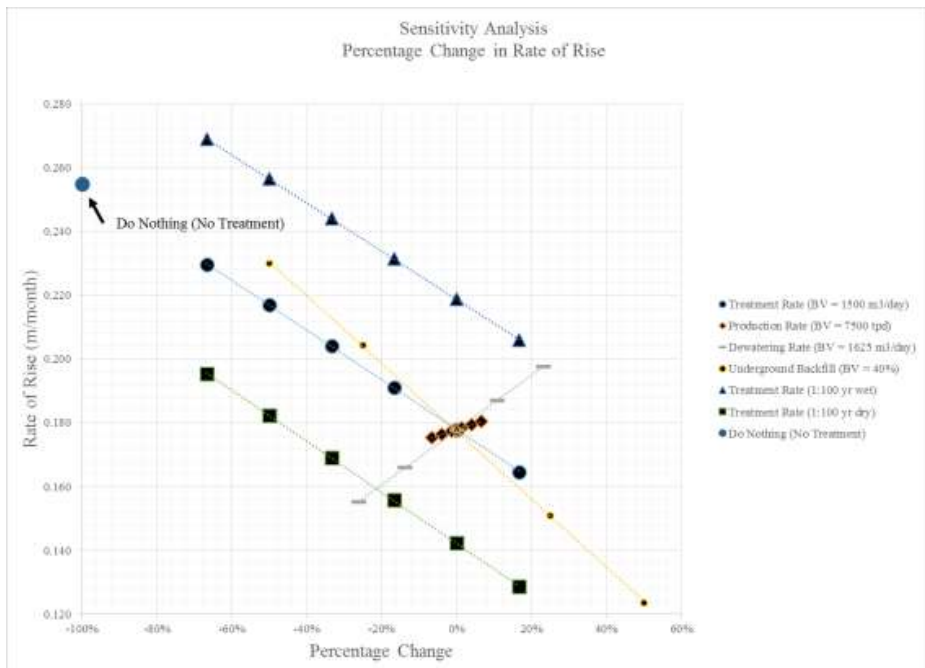


Figure 4. Sensitivity analysis results for monthly rate of rise for the TIA

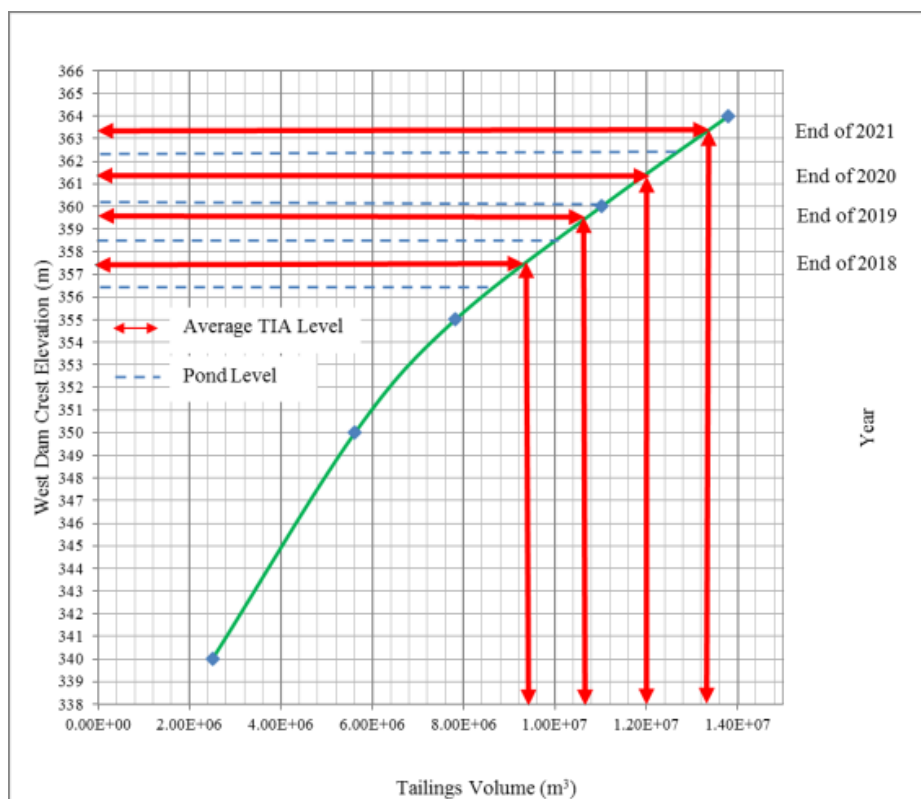


Figure 5 – TIA storage capacity timeline prediction based on struck level capacity curve

Figure 5 also indicates that a minimum 1 m difference between the tailings beach and the pond can be maintained throughout deposition. The results shown on Figure 5 can be reproduced for any of the various scenarios considered in the water balance. Figure 6 provides a summary of the approximate end of life timelines for the TIA under each of the scenarios run. Once again, the 1:100 yr wet and dry scenarios for the treatment rate are presented for reference. As noted, the timeline for the base value condition shown in Figure 6 agrees with the results shown in Figure 5 (i.e. end of 2021). Similar to Figure 4, varying the ratio of tailings to surface versus underground backfill has the largest affect on TIA timeline.

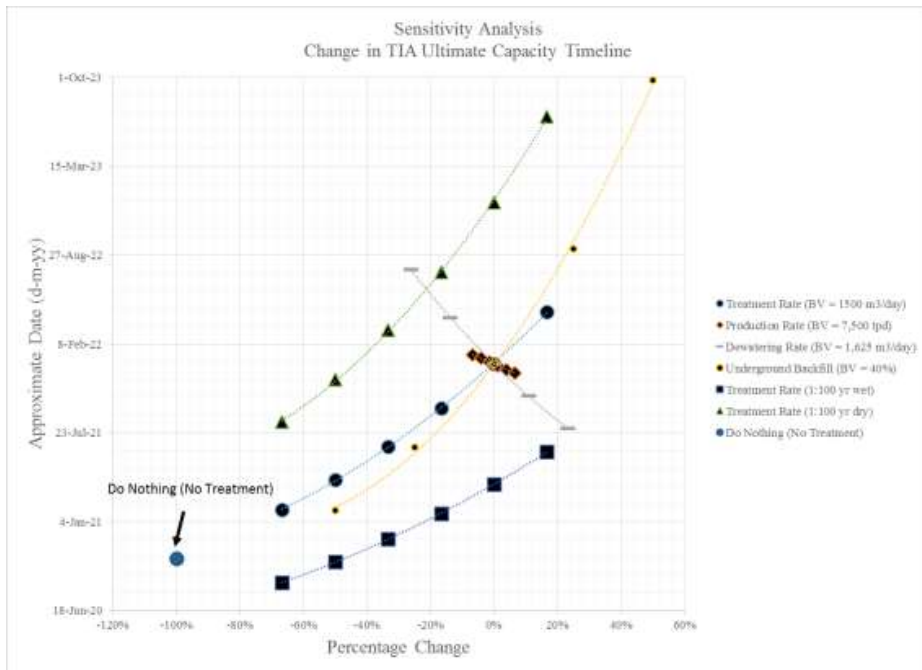


Figure 6 – Sensitivity analysis results for TIA storage capacity timeline

7 SUMMARY

This study sought to provide the mine site with guidance on a water management strategy that would both reduce pond volume in their TIA while still maintaining minimum beach requirements for seepage control along Dam 2. Various water balance scenarios were run by toggling a set of input parameters that were understood to affect both tailings and pond levels in the TIA. The results indicate that the treatment rate is the best “lever” that the site has for controlling the pond level in the TIA while consequently extending its ultimate lifespan. Deposition modelling confirmed that under the proposed water treatment and deposition strategy, the minimum tailings beach elevation differences between the tailings and the pond could be maintained.

The analyses described in this paper are considered to be site specific and will vary for each site depending on the climatic conditions, the geometry of the TIA, the mine production rate, the geotechnical and geochemical properties of the tailings and its supernatant, the slurry density of the tailings, and the method of deposition. Therefore, it is best to gain a good understanding of the site specific conditions that would drive the development of the TIA over time.

REFERENCES

- Environment Canada Amos, Quebec Station Climate Normals (1968 – 1993). http://climate.weather.gc.ca/historical_data/search_historic_data_e.html
- Environment Canada Kirkland Lake, Ontario Station Climate Normals (1950 – 2006). http://climate.weather.gc.ca/historical_data/search_historic_data_e.html

Author Index

Adams, X.	569, 607	Castro, G.J.I	221
Afriyie, G.	739	Castro, J.	365
Aghajanyan, A.	377	Catling, M.L.	277
Almon, R.L.	643	Chahua, L.	503
Anderson, C.	739	Chambers, R.W.	799
Arnipally, S.	77	Chavaillaz, Y.	583
Aubone, L.	791	Chilson, J.	17
Ausch, E.	477	Cilliers, C.	451
Bale, B.	739	Ciloglu, F.	221
Bardsley, D.	853	Cobb, C.F.	685
Bareither, C.A.	163, 463	Contreras, I.	861
Barnekow, U.	631	Cooke, R.	35
Barrero, A.	245	Cortegoso, P.	547
Beier, N.	95	Cosentino, A.	767
Bellwood, J.	277	Couto, R.	873
Benson, C.H.	619	Crystal, C.	209
Benzaazoua, M.	811	Davis, M.M.	619
Blond, E.	489	de los Hoyos, C.	547
Borden, S.L.	643	del Castillo Macedo, C.	399
Boroko, M.	63, 707	Demers, I.	557, 583, 595
Boshoff, L.	63, 707	Devaere, N.	477
Boswell, J.	51	Dillon, J.	823
Bouazza, Z.	699	Dinis, M.L.	139
Boxill, L.	277	Dominquez, G.	535
Boyd, W.	791	dos Santos, G.J.I.	27
Bradfield, L.R.	319	Durocher, J.	435
Braun, T.	547	Engels, J.	527
Br��h��, J.M.	767	Engelsman, B.	607
Bresson, ��.	557, 583	Ezama, I.	209, 547
Briers, M.	451	Farrell, I.	35
Bryant, G.K.	861	Fattore, G.	377
Burden, R.	77, 347	Fernandez Canchos, A.B.	659
Bussiere, B.	557, 811	Ferreira, A.M.	27
Caldwell, J.A.	733	Figueiredo, J.	139
Calendine, S.	781	Fityus, S.G.	319

Fiúza, A.	139	Kruger, W.	333
Foster, B.F.H.	151	Kurylo, J.	175
Fourie, A.	365	Latulippe, D.R.	477
Fox, J.	387	Lavoie, B.	699
Futuro, A.	139	Le Borgne, V.	767
Gabriel Espinoza, J.C.	841	Lei, X.	187
Gallagher, J.	853	Leikam, J.	387
Geddis, M.	519	Leite, A.	139
Genes, B.E.	221	Liew, M.	799
Ghazizadeh, S.	463	Lingwall, B.N.	151
Gilbert, J.	17	Liu, Z.-S.	427
Gipson, Jr., A.H.	17	Lizcano, A.	175, 245
Gjerapić, G.J.I.	201, 267	Luedke, P.	233
Góis, J.	139	Lundell, D.	117
Gomide, P.C.R.	27	Lupo, J.F.	3, 365
Gorakhki, M.H.	163	Ma, L.	427
Guimond-Rousson, J.	595	Mafi, R.	477
Gusek, J.J.	377	Malgesini, M.	791
Hasanloo, D.	721	Mao, Y.	747
Hendrickx, J.	519	Marefat, V.	43, 109, 301
Herrera, F.	503	Marthin, P.	117
Hockley, D.	127	Martin, V.	811
Hore, C.	209	Martins, D.	139
Hotton, G.	557	Martinson, R.	35
Huang, C.	427	Mayne, R.	569, 607
Hunsaker, R.	791	McNeill, R.W.	707
Hutchings, B.	17	Meintjes, H.A.C.	63, 287
Jackson, D.	409	Merry, P.	873
Jacobs, M.	163, 347	Metzker, S.	631
Janse van Rensburg, P.	829	Milczarek, M.	519
Jardani, A.	775	Mitchell, G.	527
Jessop, M.	775	Moghaddam, R.	747
Johns, C.	721	Moriarty, M.D.	151
Jokinen, K.	117	Morin, K.A.	427
Josselyn, L.P.	377	Morrison, K.F.	27
Jung, A.	649	Mosquera, J.	87, 109, 699
Kam, S.	747	Mühl, A.	631
Kaunda, R.B.	259	Murphy, R.	823
Keller, T.O.	221	Murrugarra, E.	503
Keller, J.	519	Nadeau, P.	811
Kerr, T.F.	535	Naidoo, W.	569, 829
Kofoed, V.	775	Ozum, B.	77
Koitzsch, Y.	631	Pabst, T.	583, 811

Parkhill, S.T.	151	Toro, J.	535
Partey, F.	519	Torrey López, C.T.	277
Patterson, K.	799	Töyrä, S.	117
Pedrosa, H.G.	27	Turner, J.	527
Perić, D.	201	Ulrich, B.	357
Philippe, R.	557	Ungerer, H.C.	333
Piciacchia, L.	43, 87, 109, 301, 699	Varnier, J-B.	535
Plante, B.	811	Vasconcelos, F.	419
Poaty, B.	811	Vides, J.A.	43, 87, 301
Quintero, S.	187	Vila, M.C.	139
Rahal, K.	387	Wall, K.	775
Reaño, D.	503	Westhaver, K.J.	477
Redente, E.F.	619	Wildeman, T.	419
Reid, D.	365	Williams, D.J.	9, 187, 347
Revil, A.	775	Wilson, G.W.	347
Ridlen, P.W.	535	Zhang, C.	187
Roberts, H.R.	619	Zheng, T.	95
Robertson, L.	435	Zimmermann, K.	477
Robeson, M.D.	649	Znidarčić, D.	201, 267
Rocard, C.	595		
Rogers, J.	357		
Romaniuk, N.	387		
Rourke, H.	127		
Roy, P.	583		
Rucker, D.	781		
Rykaart, M.	175, 233, 245, 671		
Saunier, P.	489		
Scalia, J.	163		
Scott, J.D.	77		
Shapka-Fels, T.	671		
Simmons, J.V.	319		
Smith, A.	287		
Sobkowicz, J.	51		
Speer, M.	631		
St-Laurent, J-F.	757		
Stevens, C.W.	233, 671		
Stowe, J.	35		
Strachan, C.L.	309, 733		
Tate, M.	387		
Taylor, J.	17		
Thériault, M.	811		
Thivierge, S.-É.	767		
Thomas, P.	557		

This is the twenty-second annual Tailings and Mine Waste Conference which is being hosted by Colorado State University of Fort Collins, Colorado and now alternating odd years with the University of Alberta and the University of British Columbia. The purpose of these conferences is to provide a forum for discussion and establishment of dialogue among all people in the mining industry and environmental community regarding tailings and mine waste.

This year's conference includes papers which present state-of-the-art on mine and mill tailings and mine waste, as well as current and future issues facing the mining and environmental communities. Matters dealing with technical capabilities and developments, design and operations of tailings, and environmental concerns are discussed.